



ICRDSET '21

**Proceedings of the
International Conference
on
Research and Development in
Science, Engineering and Technology**

organized by
St. Anne's
College of Engineering and Technology

in association with



**INSTITUTION'S
INNOVATION
COUNCIL**
(Ministry of Education Initiative)

**Proceedings of
International Conference on Research and Development
in Science, Engineering and Technology**

ICRDSET '21

05th March 2021

Organised by



**St. Anne's College of Engineering and Technology
Panruti, Cuddalore District – 607106.
Tamilnadu, India.**

PREFACE

Globalisation, privatisation and digitalization today have dramatically reshaped the education system in India and have created tremendous opportunities for internationalisation, especially transnational or cross-border education. Various educational institutions have partnered with foreign institutions to provide best form of education to the students. However, many challenges and obstacles are being faced in the strategic planning and the mechanics of bringing internationalization of the education system into action. We wish to discuss and deliberate on the dynamics of Internationalisation of Higher Education in the country and across borders.

St. Anne's College of Engineering and Technology feels proud in its consistent progress to introduce the First international Conference on Research and Development in Science, Engineering and Technology (ICRDSET '21) on 5th March, 2021. ICRDSET '21 aims to bring together leading academic scientists, researchers and research scholars to share and exchange their experiences and research results on various aspects of Science, Engineering and Technology. It also provides an interdisciplinary platform for policy makers, top managers, researchers, practitioners and educators to present and discuss the most recent innovations, trends, and concerns as well as practical challenges encountered and the solutions adopted in the fields of Science, Engineering and Technology. ICRDSET '21 assures to be both informative and stimulating with a wonderful array of keynote and contributions of eminent speakers from all over the world.

This conference is jointly organized by the Departments of Mechanical Engineering, Electrical and Electronics Engineering, Electronics and Communication Engineering, Computer Science and Engineering and Science and Humanities in association with Institution's Innovation Council (IIC), Indian Society for Technical Education (ISTE).

The proceedings of the conference are published with ISSN. It is believed that the research papers included in these proceedings will create a solid background for useful discussions during the conference and for further research. It is also hoped that these proceedings will provide valuable reference material and a source of information on academic achievements and current debate in Engineering and Technology education. After peer review, the editorial board selected 162 papers from the 200 papers submitted. The selected papers covered a wide range of topics: Advance Trends in Intelligent Materials, Recent Methods in Manufacturing, AI and Deep Learning, cyber security, IoT and Networking, 5G wireless Communication, Smart agriculture/health sector, Smart Grid technology, Renewable energy Engineering, New functional materials and Recent Advancements in Applied Mathematics.

All the presentations were much impressive with high level of professionalism, and in many cases original ideas and activities have been proposed and accomplished in various respect. Efforts taken by peer reviewers contributed to improve the quality of papers through constructive and critical comments; improvements and corrections to the authors are gratefully appreciated. We are very grateful to the International/National advisory committee, Session Chairs who selflessly contributed to the success of the conference. The organizing committee likes to congratulate all the authors for their interests and efforts. The committee thanks all the participants for their support in making the conference a great success.

Convener

Dr. Sr. S. Anita, M.Tech., Ph.D.

Professor and Head,

Department of Electronics and Communication Engineering,

St. Anne's College of Engineering and Technology.

ORGANISING COMMITTEE

CHIEF PATRON

Rev. Mother Reginal, SAT,
Superior General

PATRON

Rev. Sr. Dr. Y. Yesu Thangam, SAT,
Secretary
St. Anne's College of Engineering and Technology

ORGANIZING CHAIR

Dr. R. Arokiadass,
Principal
St. Anne's College of Engineering and Technology

ORGANIZING SECRETARY

Sr. Punitha Jilt, SAT,
Vice Principal and Head
Department of Computer Science and Engineering
St. Anne's College of Engineering and Technology

CONVENOR

Dr. Sr. S. Anita, SAT,
Professor and Head
Department of Electronics and Communication Engineering

STEERING COMMITTEE

Dr. D. Ommurugadasan,
Professor and Head
Department of Mechanical Engineering

Dr. A. John Peter,
Professor and Head
Department of Science and Humanities

Mr. V.C. Eugin Martin Raj,
Associate Professor and Head
Department of Electrical and Electronics Engineering

MESSAGE FROM CHIEF GUEST

A heartfelt congratulations is in order to the St. Anne's College of Engineering and Technology for organizing a conference on research and development in science, engineering and technology, particularly bringing together great minds in the field of science and engineering. The conference has all major research clusters covered in various tracks where the various scientific and engineering field come together to offer solutions to a better world.

In this challenging time while we are still facing the Covid-19 pandemic, it is encouraging to connect and interact with participants online. The presentations and discussions with every participant will definitely result in further development of the solutions presented here. I am confident in the fruitful outcome of this event, and I wish the organizers the best for the success of the conference.

Dr. Muhammad Rafiq Mirza Bin Julaihi

Swinburne University of Technology
Malaysia

MESSAGE FROM SECRETARY'S DESK

In this globalised and technological scenario, knowledge as power, quality education, super-fast communication systems, and higher-level jobs have been some of the concepts which direct the world. In this context, St. Anne's College of Engineering and Technology, a distinguished centre for modern learning, aims at character formation, excellence in teaching, learning, research and placement, empowerment of rural youth, and has grown in all directions with its Motto: To Build a Holistic Society. The commitment and continuous hard work of our Faculty instill originality and creativity in teaching, learning and research and one such fruit of their effort results in conducting an **International Conference on Research and Development in Science, Engineering and Technology 2021 (ICRDSET'21)** every year. I deem it a great joy to congratulate the Principal, organizers, committee members and all the Faculty and Non-teaching staff for their involvement and cooperation to conduct this ICRDSET. This International Conference, ICRDSET '21, provides ample opportunity to the Faculty, Industrialists and Students to exhibit their research articles, share and exchange their views and aspirations and learn novel methods and approach in their respective field. I congratulate all the eminent Faculty and erudite Scholars as well as the young Engineering Students from various Institutions who contributed for the Proceedings of the ICRDSET which comprises the articles with novel themes like Cloud, Soft and Green Computing, IoT and Networking, Smart Grid, Renewal Energy Systems, Computational Field Dynamics, Designing Tool and Cutting Materials, Composite Materials, Alternative Fuels, VLSI, Medical Signal Processing, Advanced Antennas, Environment Science, Crystalline Materials, Material Science and Chemistry, Mathematical Analysis and English Language Teaching Methodology. I wish and pray for the fruitful deliberation of this Conference. May the Lord Almighty inspire and enrich every participant to acquire more wisdom, insight and knowledge through this Conference!

Rev. Sr. Dr. Y. Yesu Thangam, S.A.T.

Secretary

St. Anne's College of Engineering and Technology

MESSAGE FROM PRINCIPAL

It gives me immense pleasure that St. Anne's College of Engineering and Technology is organizing an International Conference on Research and development in Science, Engineering and Technology on March 5th, 2021.

Research activities across all the Engineering fields pave the way for the industrial world to strive forward with huge advancements. St. Anne's CET provides an opportunity for sharing knowledge, innovative ideas and to have interaction intensively in the thrust areas of Mechanical, Electrical and Electronics, Electronics and Communication and Computer Science among researchers, academicians, industrialist and Scientists in various fields of Science, Engineering and Technology.

The eminent key note speakers will cover the reality of recent developments in research in their domain from different perspectives. The proceeding of the conference will help the next generation researchers to gain insight in their area of interest.

I congratulate the organizing team, staff members, students, participants from the host and other institutions for their efforts in organizing and participating in this conference and wish the conference all the success.

Dr. R. Arokiadass, M.E., Ph.D.,

Principal

St. Anne's College of Engineering and Technology

MESSAGE FROM VICE-PRINCIPAL

St. Anne's College of Engineering and Technology has borne the mantle of excellence, committed to ensure the students their own space to learn, grow and broaden their horizon of knowledge by indulging into diverse spheres of learning. In our endeavor to raise the standards of discourse, we continue to remain aware in order to meet with the changing needs of our stakeholders.

Research activities across all the engineering fields pave the way for the industrial world to strive forward with huge advancements. As an educational institution, encouragement and support to research can be provided by establishing a suitable platform for the research community, to interact with each other and to share the knowledge. Having this objective, an International Conference on Research and Development in Science, Engineering and Technology - 2021 has been planned to provide the learning experience to all the participants. The Conference aims to bring different ideologies under one roof and provide opportunities to exchange ideas face to face, to establish research relations and to find global partners for future collaboration.

Sessions on different domains, key note addresses from eminent professors and opportunity to network with the researchers will help the participants immensely in their research career. This proceeding of the conference has been documented with utmost care. I believe strongly that, this will stand as a great source of knowledge to all the researchers.

I would like to congratulate the organising team, staff, and the students for their contribution in successfully organising this event.

Sr. Punitha Jilt, SAT

Vice Principal and Head
Department of Computer Science and Engineering
St. Anne's College of Engineering and Technology

INDEX

Computer Science and Engineering

| | | |
|--------------|--|----|
| ICRDSET 5007 | An Effective Covid-19 Vaccine Distribution Plan Using Machine Learning Models <i>P.Dhivya, A.Bazilabanu</i> | 1 |
| ICRDSET 5008 | Enhanced Duck Traveler Optimization (EDTO) Algorithm with Multilevel Thresholding, Region of Interest and K-Means Clustering for Mammogram Image Segmentation to improving accuracy <i>A.Krishnaveni, R.Shankar, S.Duraisamy</i> | 6 |
| ICRDSET 5096 | Eyeblink Detection FOR Liveness Detection Using Deep Convolutional Neural Network <i>N.Nanthini, N.Puviarasan , P.Aruna</i> | 20 |
| ICRDSET 5102 | A Comparative Study on Liver Disease Prediction using Machine Learning Approach <i>S.Omprakash, R.Soumya</i> | 26 |
| ICRDSET 5016 | Construction of Question Answering System for Optimized Knowledge Graph <i>G.Kavitha, V.Khanna</i> | 31 |
| ICRDSET 5022 | Detection of Black Hole Attacks in Manets By Using Principle of Exclusion and Inclusion <i>G.Revathy</i> | 35 |
| ICRDSET 5042 | Heart Disease Prediction Using Machine Learning <i>L.Haripriya, Jayandrika</i> | 44 |
| ICRDSET 5044 | A New Technique for Image Compression Using Linear Algebra With Python Algorithm <i>S.Karthigai Selvam, S.Selvam</i> | 48 |
| ICRDSET 5050 | Mathematical Analysis and Wavelength Transformation process for secure data-hiding in images <i>Perepi Rajarajeswari</i> | 57 |
| ICRDSET 5059 | “An Automatic Attendance Monitoring System Using Python” <i>J.Narmatha, V.Krithika</i> | 63 |
| ICRDSET 5075 | A Novel Analysis on Outliers <i>S.Rajalakshmi, P.Madhubala</i> | 71 |

| | | |
|--------------|--|-----|
| ICRDSET 5082 | Modified Non-local Means Filtering Techniques to Remove Various Noise Types from MRI image <i>T.Anitha, T.Kalaiselvi</i> | 76 |
| ICRDSET 5101 | A novelty approach of exact string matching <i>Armstrong Joseph, C.R.Rene Robin</i> | 82 |
| ICRDSET 5103 | Understanding awareness regarding cyber security and preference for advanced protection among young netizens <i>Shaswat Shetty</i> | 89 |
| ICRDSET 5141 | An Intelligent Algorithm with Feature Selection for Thyroid Disease Classification And Dignosis Using Data Mining Techniques <i>S.Parimala, P.Senthil Vadivu</i> | 96 |
| ICRDSET 5012 | Automatic Product Billing Through Camera Using Artificial Intelligence and Edge Computing <i>S.Harivyas, M.Abishek, M.M.Pavithran</i> | 102 |
| ICRDSET 5018 | Mitigation Scheme Can Effectively Manage DDOS Attack in Cloud Computing / Prevention Technique of DDOS Attack In Cloud Computing <i>Manoj Kumar Dixit</i> | 109 |
| ICRDSET 5037 | Short Text Sentiment Classification with Word Embeddings using LSTM Approach- A Survey <i>M.Rajalakshmi, A.Senthil Kumar</i> | 116 |
| ICRDSET 5039 | Adoption of WhatsApp and Telegram in India <i>S.Karunkaran, M.Santhiya, E.Harsiny, B.Moviga, T.M.Nivedhitha</i> | 123 |
| ICRDSET 5045 | A New Discovery of The Network Navigation Using Datamining <i>S.Selvam</i> | 128 |
| ICRDSET 5089 | SIRD Model Simulation for Corona pandemic in Tamil Nadu <i>P.Ananthi, S.Jabeen Begum</i> | 134 |
| ICRDSET 5095 | Sentiment Analysis with Unsupervised Machine Learning and Natural Language Processing <i>Rahul Pandya, Suraj Moolya, Sujal Charak, Shivani Naik</i> | 141 |
| ICRDSET 5106 | Mango Image Feature Extraction for Quality Grading (A Pilot Study-1) <i>T.Kalaiselvi, A.Thahira Banu, K.Somasundaram, P.Veerakumar</i> | 150 |
| ICRDSET 5107 | Healthcare Management Using Big Data <i>S.Vishnu Prakash, A.Vibin Gowtham</i> | 154 |

| | | |
|--------------|---|-----|
| ICRDSET 5109 | Speech Recognition Using Python <i>K.Shobikaa, K.Santhiya, R.Suguna</i> | 159 |
| ICRDSET 5112 | Guarded Electronic Voting System Using Blockchain Technology <i>V.Parameshwari, M.Sajitha banu, A.Ramya</i> | 165 |
| ICRDSET 5115 | Diabetic Retinopathy Retinal Vessels Classification Using Deep Learning Techniques <i>Sr.Punitha Jilt, M.Aruna, R.Ashwini, M.R.Varsha</i> | 171 |
| ICRDSET 5116 | A Multi Tasking Agriculture Robot Using Internet Of Things And Raspberry Pi <i>V.Brittadevi</i> | 178 |
| ICRDSET 5121 | Attribute-Based Access Control with Data in Cloud Storage <i>S.Rajarajan, D.Hemalatha, K.Monisha, A.Thenaruvi</i> | 182 |
| ICRDSET 5123 | Preserving Sensitive Health Care Data in Distributed Cloud Using block-Chain Concept <i>S.Meena , V.Gayathri</i> | 186 |
| ICRDSET 5181 | IoT Based Automated Safety Industrial System <i>N.Kumar, K.Kamali, K.Sivasankari, E.Sowmiya</i> | 193 |
| ICRDSET 5128 | Deep Learning Based Identification of Novel Corona Virus Using Lung (Lus) <i>N.Kumar, J.Madhavan, G.Thirumalvalav, P.Praveen Kumar, P.JustinRaj</i> | 199 |
| ICRDSET 5132 | AI in Agriculture <i>S.B.Kapilyaswanth, R.Karthick, V.Mohanakrishnan, K.Nagaraj</i> | 204 |
| ICRDSET 5136 | Performance Analysis of Nature Inspired Optimization Algorithms For Virtual Machine Migration Problem In Cloud Environment <i>Deepak Kumar, Deepti Mehrotra, Vijay Anant Athavale, Suresh Chand Gupta</i> | 209 |
| ICRDSET 5139 | Automated Software Testing Using Genetic Algorithm <i>R.Hanusha, M.Manisha Koyarala, B.Vanitha, E.Indhuma</i> | 218 |
| ICRDSET 5140 | A Machine Learning Approach to Predict Air Quality in India <i>M.Rajkumar, P.Sharchandar, P.Julian Kennady, E.Indhuma</i> | 222 |
| ICRDSET 5142 | Execution of Cloud Computing Education in Current Scenario in The World Countries <i>S.Dharmaraj, P.Kavitha</i> | 228 |
| ICRDSET 5143 | Mobile Camera-Based Assistive Text and Product Label Reading Using Android for Blind Persons <i>S.Periya Nayaga Mary, S.Manavalan</i> | 237 |

| | | |
|--------------|--|-----|
| ICRDSET 5147 | Farmer Trade Using Android Application <i>J.Santhosh Kumar, M.Srinivasan, V.Tamil Selvan, S.Manavalan</i> | 242 |
| ICRDSET 5149 | The Impact of Big Data Analytics in Information Technology Sector <i>M.K.Ganeshan</i> | 246 |
| ICRDSET 5150 | Performance of A Knight Tour Parallel Algorithm on Multi-Core System Using Openmp <i>Vidyaathulasiraman, S.Vijayakumar</i> | 251 |
| ICRDSET 5151 | A Blockchain-Enabled Paradigm to Share Electronic Health Records Using IPFS <i>SagarLachure, Ashish Tiwari</i> | 256 |
| ICRDSET 5152 | Face Mask Detection and Person Identification <i>Sr.A.Punitha Jilt</i> | 260 |
| ICRDSET 5154 | Whale Optimized Adaptively Regularized Kernel Based Fuzzy C-Means for Multi-Objective Imagesegmentation <i>N.Parvin, P.Kavitha, D. Arul Pon Daniel</i> | 265 |
| ICRDSET 5155 | Fake User Identification on Social Networks <i>K.Abinaya, .Abirami, L.Anushiya, V.Brittadevi</i> | 272 |
| ICRDSET 5157 | Opinion Classification for Tourists Reviews Using Support Vector Machine. <i>G.Bharathi, G.Anandharaj</i> | 276 |
| ICRDSET 5160 | A Measurement Analysis of Website Attackers Using Onionbots <i>R.Ranjith Kumar, A.Pradeep, S.Ajith Kumar, D.Pauline Freeda</i> | 282 |
| ICRDSET 5161 | Secure Scheme for Medical Image Storage in Cloud <i>R.Sangeetha, K.Aswini, E.Kanniyammal, D.Pauline Freeda</i> | 287 |
| ICRDSET 5163 | A Subsystem for Network Traffic Analysis Using Deep Learning <i>G.Bhuvaneswari</i> | 292 |
| ICRDSET 5164 | Integrated Level Aggregation Method for the Identification of Apps in Top Charts <i>R.Jeeva, N.Muthukumaran</i> | 296 |
| ICRDSET 5167 | An Enhanced Hybrid Algorithm Using Levy Flight, Simulated Annealing And K-Means Algorithm for Clustering High Dimensional Datasets <i>R.Jensi</i> | 304 |

| | | |
|--------------|---|-----|
| ICRDSET 5170 | Integrity and Privacy Preserving of Data for Secure Cloud Storage Using Third Party Auditor <i>J.Lizy Pravarthana, S.Roja, G.Kaviya, Z.Asmathunnisa</i> | 313 |
| ICRDSET 5175 | Disdet: DODAG Information Solicitation Attack Detection in Ipv6 Based Low Power Lossy Networks <i>Arul Anitha, L.Arockiam</i> | 319 |
| ICRDSET 5126 | Integration of a chat bot With Education for The Smart learning <i>K.Kavitha, M.Monisha, R.Vishnupriya, V.Brittadevi</i> | 328 |
| ICRDSET 5195 | Computer-Aided Detection System for Mammogram Screening A Review Using Image Processing and Machine Learning Techniques <i>K.Poornambigai, K.Balasubramanian, K.Karthikeyan</i> | 332 |
| ICRDSET 5197 | Crop yield prediction based on phenotype applying time series analysis <i>S.Iniyan, R.Jebakumar</i> | 346 |

Electronics and Communication Engineering

| | | |
|--------------|---|-----|
| ICRDSET 5004 | Design of Low Power Capable Logic Circuit Using Adiabatic Performance <i>G.Ramachandran, T.Sheela, G.Sureshkumar,</i> | 351 |
| ICRDSET 5013 | An Effective Optimization Technique of Extracted Watermark Image Using Particle Swarm Optimisation <i>M.Selvaganapathy, R. Kayalvizhi</i> | 358 |
| ICRDSET 5014 | Tumble Gear based Smart Vehicle for physically challenged people <i>N.Nishavithri, M.Selvaganapathy</i> | 363 |
| ICRDSET 5034 | A Circular Shaped DGS for Coplanar Waveguide Transmission <i>L.Pavithra, V.Baranidharan, B. Ragavi</i> | 367 |
| ICRDSET 5035 | Resource Allocation Scheme Based on NOMA In OFDM <i>L.Pavithra, B.Ragavi, V.D.Nandhini</i> | 375 |
| ICRDSET 5036 | Design of dielectric coupled line resonator with Defected Ground Structure in Linear wave filter. <i>B.Ragavi, V.Baranidharan, L.Pavithra</i> | 382 |
| ICRDSET 5047 | Advanced Handwritten Signature identification system with use of HU's moment invariants <i>Jayesh Rane</i> | 390 |

| | | |
|--------------|---|-----|
| ICRDSET 5049 | Energy-Efficient Adaptive Encoding for Off-Chip Communication <i>V.Venkatesan, S.DuraiRaj, B. Arunkumar</i> | 395 |
| ICRDSET 5057 | Optimization and Simulation of Capacitive Pressure Sensor with Improved Parameters <i>G. Mohamammed Althaf, Kaustubh Kumar Shukla</i> | 402 |
| ICRDSET 5058 | Early Diagnosis of Parkinson's Disease using Convolutional Neural Network <i>S.Jothi, S.Anita, S.Sivakumar</i> | 410 |
| ICRDSET 5060 | Investigation of ZnO as substitute explicit materials in Sensor Innovation <i>Kaustubh Kumar Shukla, T.Muthumanickam, T.Sheela</i> | 416 |
| ICRDSET 5063 | Approaches on Different Power Management Techniques for IoT enabled 5G Communication – A Survey <i>Manikannan Govindasamy, P.Prabakaran, B.Theeban Chakkaravarthy</i> | 421 |
| ICRDSET 5065 | Design of low power Magnitude Comparator Using GDI Technique <i>M.Sahinipiriya, B.Mary Amala Jenni, D.Umamaheswari</i> | 427 |
| ICRDSET 5074 | Real Time Fabric Flaw Detector Using Arduino <i>A.Selvarasi</i> | 434 |
| ICRDSET 5076 | Smart Health Tracking Band – A Curator for Well Being <i>M.Pravin Savaridass, C.Praveen, J.Rakshith, N.Pavithra, N.Praveena, S.B.Kapil Yaswanth</i> | 441 |
| ICRDSET 5080 | Segmentation of Retinal Fundus Images for Global Eye Disease Diagnosis <i>T.Vijayan, M.Sangeetha</i> | 447 |
| ICRDSET 5085 | Monaural Speech Separation By means of Video Stream Digital image processing <i>B.Kalaiselvi, B.Karthik, T.Vijayan</i> | 452 |
| ICRDSET 5087 | Hybrid System Design of FSO- Tech and RF Signals In Spacial Communication <i>B.Mary Amala Jenni, D.Umamaheswari, M.Sahinipiriya</i> | 460 |
| ICRDSET 5088 | Raspberry Pi Based Automatic Vehicle Speed Detection Warning and Control System <i>B.Arunkumar, V.Venkatesan,S.Durai Raj</i> | 467 |
| ICRDSET 5097 | Safety System for Automobiles Through Vehicle –To-Vehicle Communication Using LiFi <i>S.Pavithra, S.Abirami, R.Sharmila, V.Thiyagarajan</i> | 474 |

| | | |
|--------------|--|-----|
| ICRDSET 5098 | Design and Implementation of Miniature U-slot Patch antenna for 5G Communication <i>S.Durai Raj, B.Arunkumar, V.Venkatesan</i> | 479 |
| ICRDSET 5125 | Smart Saline Monitoring Device using LoRa Technology <i>S.Balabasker, D.Umamaheswari, R.Radhakrishnan</i> | 485 |
| ICRDSET 5131 | A Survey On GPS Based Smart Speed Control For Electric Vehicle In Speed Restricted Zone <i>M.PheminaSelvi, R.Thenmozhi, M.Yuvarani, N.Helka, K.Priyanka</i> | 491 |
| ICRDSET 5135 | Home Automation for Paralyzed People Using Eye Blink Sensor <i>S.D.Sindhuja, G.Umamageshwari, K.Sabarinathani</i> | 500 |
| ICRDSET 5146 | Automatic Detection for Diabetic Retinopathy Using Deep learning in Modified AlexNet CNN Architecture <i>D.Umamaheswari, N.Nachammai</i> | 505 |
| ICRDSET 5148 | Design and Analysis of a Lab IP Spy Camera and Alarm System using Raspberry Pi and ATMEGA328P <i>S.Shameera, K.Nivetha, S.Meera, G.Sadiq Basha, B.Abitha</i> | 513 |
| ICRDSET 5158 | Integrated Technique for Data Integrity and Confidentiality <i>P.Shanmuga Priya, T.Helan Vidhya</i> | 518 |
| ICRDSET 5171 | Smart Irrigation Monitoring System Using Lora Technology <i>R.Radhakrishnan, S. Balabasker</i> | 522 |
| ICRDSET 5182 | A Source-Location Privacy in Wireless Sensor Networks Using Multi-Sinks <i>V.Dhivyapriya, J.Sumitha Josphine</i> | 529 |
| ICRDSET 5184 | IoT Based Automatic Ration Product Dispensing System <i>A.Uma Maheswari, A.Pavithra</i> | 536 |
| ICRDSET 5187 | Driver Drowsiness Detection and Alert System <i>J. Nisha, C.Sugapriya, B.Arunkumar</i> | 542 |
| ICRDSET 5188 | Intravenous Flow Monitoring System Using Lora Technology <i>M.Malini,D.Divya, R.Radhakrishnan</i> | 547 |
| ICRDSET 5189 | Reconfigurable H-Shaped Dielectric Resonator Antenna <i>M.Nandhini, S.Abitha, S.Durai Raj</i> | 552 |
| ICRDSET 5190 | Design of Low Power Hybrid Full Adder Using Xor/Xnor Circuit <i>S.Anandh, A.Punniyakodi, V.Venkatesan</i> | 557 |

| | | |
|--------------|---|-----|
| ICRDSET 5191 | Design And Analysis of RF LNA With Transistor Configurations <i>K.Priyadharshini, K.Nandhini, B.Mary Amala Jenni</i> | 564 |
| ICRDSET 5192 | Deep CNN Based Automated Diabetic Retinopathy Disease Identification System <i>M.Stephygrafi, R.Shalini, D.Umamaheswari</i> | 570 |
| ICRDSET 5193 | Design of 4:1 Multiplexer Based Adder Using Various Logic Techniques <i>P.Yuvarani, K.Raja, M.Sahinippiriya</i> | 577 |
| ICRDSET 5194 | Design and Implementation of Internet Controlled Switch Box <i>M.Selva, N.Rajadurai, S.Balabasker</i> | 585 |

Electrical and Electronics Engineering

| | | |
|--------------|---|-----|
| ICRDSET 5005 | Supervisory Control & Data Acquisition (SCADA) Systems in Power Stations <i>S.Kamalesh Kumar, S.Yogesh, R.Gowtham</i> | 589 |
| ICRDSET 5041 | PV Panel Cooling Using Stack Effect <i>Rajkumar, Ujjwal K Menon, Shahrooq Shahjahan, P.Sundaramoorthi</i> | 594 |
| ICRDSET 5046 | A Joint Optimal Algorithm Design for Envi-Economic Power Generation by Using Communicative Smart Grid <i>P.Madhumathi, K.Thenmalar, S.B.Kayalvizhi, S.Mutharasu</i> | 599 |
| ICRDSET 5053 | Effect of DC Ripple and Commutation on the Line Harmonics of Current-Controlled AC-DC Converters <i>V.Balaji</i> | 603 |
| ICRDSET 5054 | An Overview on Multiport DC-DC Converters for Integration and Energy Harvest from Renewable Energy Sources <i>C.R.Balamurugan, N.Ramadevi, T.Sengolrajan</i> | 612 |
| ICRDSET 5056 | Non-Linear Dynamical Forecasting of Electricity Demands <i>Justine Yasappan, Maria Wenisch, Arul Oli</i> | 618 |
| ICRDSET 5067 | Pesticide Spraying Device Using Raspberry Pi for Agricultural Application <i>M.Venkatesh, J.Rajesh</i> | 632 |
| ICRDSET 5073 | Design of 7 Level Multilevel Inverter with Reduced Switches <i>S.Shobana, M.Saranya, K.Thenmalar</i> | 642 |
| ICRDSET 5079 | Group Leader Optimisation Algorithm Based Optimal Reconfiguration of Distribution Feeder for Loss Reduction <i>K.Sriram, S.P.Mangaiyarkarasi</i> | 657 |

| | | |
|--------------|--|-----|
| ICRDSET 5090 | PV Based Switched Capacitor Converter for NPC Inverter in Grid Connected Applications <i>M.Meenalochani, A.Albert Martin Ruban, R.Santhiya</i> | 664 |
| ICRDSET 5093 | IOT Based Monitoring and Control of Distribution Transformer & Transmission Lines <i>S.R.Karthikeyan, J.Arokiaraj, R.Divyabharath, E.Ganesan, P.Gopinath</i> | 671 |
| ICRDSET 5100 | IoT Based Non Intrusive Power Monitoring and Energy Alert <i>R.Raghuraman, S.Saravanan, A.Arulvizhi, D.Venkatesan</i> | 674 |
| ICRDSET 5117 | Analysis of A 21 Level Inverter with Reduced Switch Count <i>A.Annai Theresa</i> | 679 |
| ICRDSET 5119 | Optimizing Combined Emission Economic Dispatch for Solar Integrated Power Systems <i>A.Richard Pravin, V.Dhivya, C.Gandhimathi, R.Vinothini</i> | 686 |
| ICRDSET 5120 | A Single Phase Bidirectional Electric Drive Reconstructed Onboard Converter For Electric Vehicles Applications <i>N.Rajeswari, A.Albert Martin Ruban, S.Nalini</i> | 695 |
| ICRDSET 5122 | Enhancing LVAD Device Performance Using BLDC Motor <i>V.Vasugi, M.Srividhya, G.Sasikala, V.Suganya</i> | 701 |
| ICRDSET 5134 | Voltage Reference Control for Standalone PV Systems <i>S.Subitha, S.Krishnan, M.Sidheswaran</i> | 707 |
| ICRDSET 5159 | A Review of Non Conventional Energy Systems and Energy Regulation Technologies <i>C.Dinakaran, T.Padmavathi, K.Sri Chandan</i> | 713 |
| ICRDSET 5165 | A Novel Design and Fabrication of Road Sweeper by using Photo-voltaic system <i>S.Prasanna, R.Amaresh, A.Mohamed Suhaib</i> | 723 |
| ICRDSET 5172 | Plant Growth Algorithm Based Load Forecasting of a Power System <i>J.Arul Martinal</i> | 728 |
| ICRDSET 5173 | Minimization of Reactive power in Power System using Group Leader Optimization Algorithm <i>M.Premaltaha</i> | 731 |
| ICRDSET 5177 | Advanced Embedded Design Based Power System Maximum Demand Prediction and Controller for Efficient Power Management by Using Proteus <i>J.Ramesh, J.Balaji</i> | 737 |

| | | |
|--------------|--|-----|
| ICRDSET 5178 | Optimal Design of Energy Saving for Single Phase Induction Motor <i>A.Sundara Pandiyan, K. Aruloli</i> | 748 |
| ICRDSET 5179 | Design and Implementaion of Solar Tracking System with Improvement of Voltage and Current Using Labview <i>V.Devi Priya, J.R.Lydia Jenifer, C.Jansi Sophia Mary</i> | 754 |
| ICRDSET 5183 | Grasshopper Optimization Algorithm for Multi-Fuel Power Dispatch <i>K.Karthikeyan, S.Ganesan, N. Jayakumar</i> | 760 |
| ICRDSET 5196 | Optimal Setting of FACTS Devices using BAT Optimization Algorithm for Congestion Management Problem in Deregulated Power System <i>M.Gnanaprakash, S.P.Mangaiyarkarasi</i> | 772 |

Mechanical Engineering

| | | |
|--------------|---|-----|
| ICRDSET 5010 | Behaviour Modelling of Composite Glass Fibre and Epoxy Matrix in different angles <i>K.Rajendran, S.Muthukumar</i> | 777 |
| ICRDSET 5023 | Experimental Investigation of the Correlation Between FDM Process Parameters and Dimensional Accuracy for Nylon Parts <i>C.R.Sanghani, V.R.Vaghani</i> | 784 |
| ICRDSET 5031 | Microstructural Investigations by Using Friction Stir Processing <i>Bazani Shaik, G.HarinathGowd, B.Durga Prasad</i> | 791 |
| ICRDSET 5032 | Design and Analysis of Internal Combustion Engine Manifold Using Cfd Analysis <i>P.Saravanan, S.Senthil, R.Rajappan</i> | 797 |
| ICRDSET 5033 | Investigating the Sliding Wear Characteristics Of Zamak 5 Alloy Under Dryand Wet Lubricating Conditions <i>S.Udhayakumar, K.Kalidas, P.T.Saravanakumar</i> | 808 |
| ICRDSET 5038 | Analysis and Performance Characteristics of Various Fluids Used in Cooling System of Electric Car Battery With Cfd Analysis Software <i>P.Saravanan, S.Senthil, R.Rajappan, P.Paramadayalan</i> | 814 |
| ICRDSET 5083 | Micro Hardness and Surface Analysis of Polysiloxane Coating on Alloy Steel Substrate <i>M.Sivamanikandan, R.Jayakumar, K.Venkatesh</i> | 826 |

| | | |
|--------------|---|-----|
| ICRDSET 5092 | Wear Simulation of Aluminum-Silicon Carbide Metal Matrix Composites <i>G.Hareesha, N.Chikkanna, Saleemsab Doddamani</i> | 833 |
| ICRDSET 5094 | Experimental Investigation of Edm For Surface Roughness and Mrr In Machining Of Aluminium 2024 <i>A.Aravintha raj, S.Arun, D.Aravindhan</i> | 841 |
| ICRDSET 5104 | Optimization of Injection Molding Process Parameters for Improvement of Tensile Strength Using the Taguchi Experimental Design <i>Tapas Chakraborty</i> | 848 |
| ICRDSET 5104 | A Review of Multifunctional Composite Materials with Their Applications <i>T.Elangovan, K.Saravanan</i> | 857 |
| ICRDSET 5130 | Patient Health Monitoring System in Ambulance for Accident Management Using Internet of Vehicles <i>N.Dhavaneeswaran, A.Thiyagarajan</i> | 866 |
| ICRDSET 5144 | Impact Behaviour of Nano Sic Reinforced Aa7075 Metal Matrix Composites, by Fe Simulation Tests <i>AnilKumar kallimani, N.Chikkanna, Thirtha Prasad Rukmangada</i> | 872 |
| ICRDSET 5156 | Smart Freezing Technique Using Thermoacoustic Energy <i>C.Kaviarasu, M.Barath, V.S.Kavinkumar, B.Santhosh</i> | 881 |
| ICRDSET 5168 | Data Analysis and Prediction Of Optimum Process Parameters For Cryo-Cooled Near-Dry Wedm Process <i>Boopathi Sampath, Sureshkumar Myilsamy</i> | 886 |
| ICRDSET 5176 | A Study of Electro Discharge Coating and Characteristics <i>K.Shanmuga Elango, K.Lakshminarasiman</i> | 894 |
| ICRDSET 5185 | Prediction Of Tool Life On Cnc Turning Of Auminium Alloy 6063 Using Tungsten Carbide Tools <i>R.Arokiadass, N.Kaviyaran Kumaran, P.Prakash, B.Balraj</i> | 901 |

Science and Humanities

| | | |
|--------------|--|-----|
| ICRDSET 5028 | A Comparative Account of Antioxidants Activity of Ethyl Acetate, Methanolic and Aquaous Extract of Leaves and Bark of <i>Baccaurea Ramiflora</i> (Lour.) by Synthesis of Gold Nanoparticles and Other Method <i>Mehebab Ali Khan, SK.Ismail, Md. Akhtarul Alam</i> | 908 |
|--------------|--|-----|

| | | |
|--------------|---|-----|
| ICRDSET 5040 | Correlation Studies in Fibre Reinforced Medium Strength Concrete <i>I.Regina Mary, T.Bhagavathy Pushpa</i> | 916 |
| ICRDSET 5043 | Study of Parametric Strength of Coconut Shell and Coir Fibres using Slump Test <i>Jyoti Prasad Ganthia, Paresh Biswal</i> | 922 |
| ICRDSET 5048 | Steady-State Analysis of an M=M=2 Queueing System Operating in A Multi-Phase Random Environment Subject to Disaster and Repair <i>D.Piriadarshani, S.Narasimhan</i> | 927 |
| ICRDSET 5051 | Conservation of Natural Aggregate by Identifying Alternatives in Coarse Aggregate <i>Anne Mary Janarthanan, Janardhanan Ganga Tulasi</i> | 930 |
| ICRDSET 5061 | Mind Mapping: The Best Selective Tool for Learning and Teaching <i>Ramu Yarlagadda, Mantri Venkata Raghu Ram</i> | 938 |
| ICRDSET 5066 | Analyses of Plant Diversity in a Sacred Grove of Ariyalur District, Tamil Nadu, India <i>G.Rajkumar, S.Ravipaul</i> | 944 |
| ICRDSET 5077 | A Review on Applications of AHP and Fuzzy AHP in Geographical Information System <i>G.Mahender Reddy, P.Kousalya</i> | 953 |
| ICRDSET 5108 | Preparation and Investigation on Phosphor Materials <i>A.John Peter</i> | 958 |
| ICRDSET 5111 | A Novel method for Biosynthesis of Cadmium Sulphide <i>J.Joaquine Arokia Mary</i> | 961 |
| ICRDSET 5113 | An Analysis of Obesity in School Children during the Pandemic COVID-19 using Plithogenic Single Valued Fuzzy Sets <i>S.P.Priyadharshini, F.Nirmala Irudayam</i> | 964 |
| ICRDSET 5114 | Tutoring Grammar in Professional Institutions <i>D.Sampath Kumar</i> | 969 |
| ICRDSET 5133 | Generalisation of Statistical Convergence in Cone Metric Space <i>Sonia Rani</i> | 971 |
| ICRDSET 5153 | Adsorption and Filtration Techniques on the Pollutants from Different Waste Water <i>S.Karthick, M.Mithunkumar, B.Akash, S.Gobinathan</i> | 978 |

| | | |
|--------------|---|-----|
| ICRDSET 5166 | Customer Service Automation among Small and Medium Enterprises: An Empirical Examination <i>K.B.Sridevi</i> | 985 |
| ICRDSET 5174 | Regular and Totally Regular Fuzzy Graphs <i>R.Viswalingam, V.Prakash</i> | 993 |

An Effective Covid-19 Vaccine Distribution Plan Using Machine Learning Models

¹P.Dhivya, ²Dr.A.Bazilabanu

¹Assistant Professor, Department of Computer Science and Engineering, Bannari Amman Institute of Technology, Erode, Tamilnadu, dhivyap@bitsathy.ac.in

²Professor, Department of Computer Science and Engineering, Bannari Amman Institute of Technology, Erode, Tamilnadu, bazilabanu@bitsathy.ac.in

Abstract

Corona Virus Disease 2019 (Covid-19) virus is a communicable disease. Currently most of the pharmacological researchers revealed the vaccine to prevent Covid-19 infection. However, the vaccine distribution has got many challenges like identification of distribution centre and providing preferences to the people based on the affected cases in a particular area including front line staff members. In the proposed work, researchers identified a novel machine learning model that can be used by the required authorities to vaccinate the people based on the prioritization of populations and corona affected cases recorded in a particular area. Researchers designed a novel COVA clustering algorithm by improving the pitfalls present in the K-Means Clustering. Areas present in the locations are identified as nodes. The proposed approach calculates the centroid of the cluster by considering both the distance and correlation between the nodes.

Keywords: Covid-19, Correlation, COVA clustering algorithm, K-Means Clustering.

1 Introduction

Corona Virus Disease 2019 (Covid-19) is caused by the coronavirus believed to be emerged from China during December 2019 [8]. Certain symptoms like cough, fever, shortness of breath or trouble in breathing, muscle or frame aches, sore throat, loss of flavour or scent, diarrhea, severe headache, new fatigue, nausea and congestion or runny nostril. It can be an intense, and a few instances lead to severe outcome like death [4]. Initial stage of the viral infection is tough to be identified through laboratory test. Receiving a Covid-19 vaccine can help and defend by using growing an antibody reaction for body [5]. The vaccine may prevent from receiving Covid-19. In receipt of vaccination perhaps protect the human beings, predominantly from the elevated hazards mentioned for the disease [3]. Physicians and other officials stay on the front line of the nation's battle towards this critical pandemic [18]. Healthcare personnel's race and ethnicity, underlying fitness conditions, occupation type, and activity putting can make a contribution to their hazard of acquiring Corona thereby facing severe outcomes [6]. By means of supplying crucial care to people infected with the virus, front line staff members have an extreme threat of being exposed to the atmosphere frequently [17]. Given the evidence of on-going Covid-19 persevered safety measures such as complete lock downs, work at home inside the community stays a country wide priority [7, 20]. However priority in vaccination needs to be provided by considering the boundless contributions provided by the people working in health care sectors and other essential government divisions.

Most of the applications which include genes information, text categorization, photograph retrieval and data retrieval include sizable amounts of multivariate records in phrases of times and attributes. This huge records quantity a way outpaces human's potential to apprehend and take care of it [9, 19]. Information mining challenge performs a vital position to discover patterns in such big volume of information. Its miles challenging for device learning to discover relevant and non-redundant information from the packages, which includes hundreds to thousands of attributes and greater multifaceted information acquire at a remarkable speed [10].

It involves routinely discovering natural grouping in records. In contrast to supervised getting to know (like predictive modelling), clustering algorithms best interpret the enter records and locate natural agencies or clusters in characteristic area [11]. A cluster is frequently an area of density in the characteristic space where examples from the domain (observations or rows of data) are in the direction of the cluster than other clusters. The cluster may additionally have a centre (the centroid) that is a sample or a point feature area and might have a boundary or extent [12]. Clustering may be beneficial as a facts analysis pastime so that you can examine greater approximately the hassle domain, so-called sample discovery or know-how discovery. Clustering can also be useful as a form of feature engineering, where existing and new examples may be mapped and categorized as belonging to one of the diagnosed clusters in the facts [13]. Most of the algorithms use similarity or distance measures between examples within the function area so as to find out dense areas of observations. As such, it's far regularly right practice to scale statistics previous to the usage of clustering algorithms [14].

2 Materials and Methods

In this work, researchers collected the data by considering the population census and corona affected people in the Tamilnadu state provision present in India. The collected data contains the number of districts in Tamilnadu, strength of the people in town/municipality and corona affected cases [1, 2]. The description of the dataset for few districts are given in the Table 1. The population census of selected district based on town/municipality and corona affected cases for all the districts in Tamilnadu are retrieved from the Kaggle repository [15].

Table 1: Sample Dataset Collection

| <i>District</i> | <i>Status</i> | <i>Population Census</i> | <i>Corona Affected cases</i> |
|-------------------|---------------------|--------------------------|------------------------------|
| <i>Ariyalur</i> | <i>Municipality</i> | <i>28902</i> | <i>1822</i> |
| <i>Ariyalur</i> | <i>Town</i> | <i>12688</i> | <i>2732</i> |
| <i>Coimbatore</i> | <i>Municipality</i> | <i>95924</i> | <i>19312</i> |
| <i>Coimbatore</i> | <i>Town</i> | <i>20122</i> | <i>28967</i> |
| <i>Cuddalore</i> | <i>Municipality</i> | <i>46678</i> | <i>9662</i> |
| <i>Cuddalore</i> | <i>Town</i> | <i>16289</i> | <i>14494</i> |
| <i>Dharmapuri</i> | <i>Municipality</i> | <i>68619</i> | <i>2414</i> |
| <i>Dharmapuri</i> | <i>Town</i> | <i>12705</i> | <i>3621</i> |
| <i>Dindigul</i> | <i>Municipality</i> | <i>207327</i> | <i>4092</i> |

A new COVA clustering model is applied to identify the distribution centre effectively. In this model clustering the areas to a particular centre was done. Based the Euclidean distance and severity of affected people, the areas in Tamilnadu is clustered effectively. After clustering the areas the distribution centre is identified for the both Town/Municipality. Then the correlation between the population census and corona affected cases is identified to prioritize the particular area in a cluster. The following workflow Figure.1 shows the COVA clustering model. The following formula (1) is used for identifying the distance where c and p represents the two points in a plane.

$$distance = \sqrt{\sum_{i=1}^n (c_i - p_i)^2} \quad (1)$$

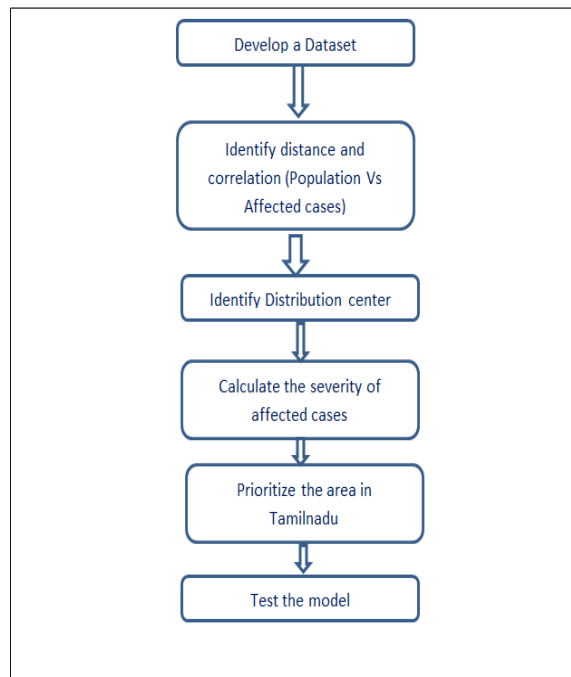


Figure 1: Working flow of COVA Clustering

3 Results and Discussion

Based on the distance and correlation between the population census and affected cases there are three distribution centre is identified initially [22]. The identification of the distribution centres varied randomly based on the facilities of frozen container with the government [16].

The following figure 2 shows the distribution of Population census in Tamilnadu and Figure 3 shows the clustering the areas in Tamilnadu. The correlation between Population and corona affected cases is identified using pair plot and Heat map shown in Figure.4. Prioritize the area in a particular cluster based on the following Equations 2. In that figure two variables exhibit positive correlation with the same magnitude because the population censuses and corona affected cases in a particular area is considered for correlation. Figure.5 shows the ranking of each area in Tamilnadu. After applying the COVA Clustering, prioritization of the areas are given in Figure.6.

$$f(x) = \sum_{n=1}^k \left(\text{Town/ Municipality} \left(\frac{\text{Population Census}}{\text{Corona Affected Cases}} \right) \right) \tag{2}$$

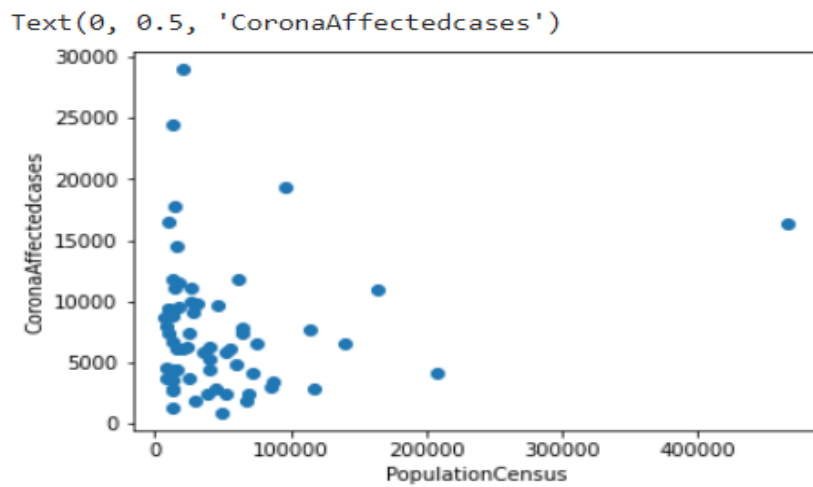


Figure 2: Distribution of data

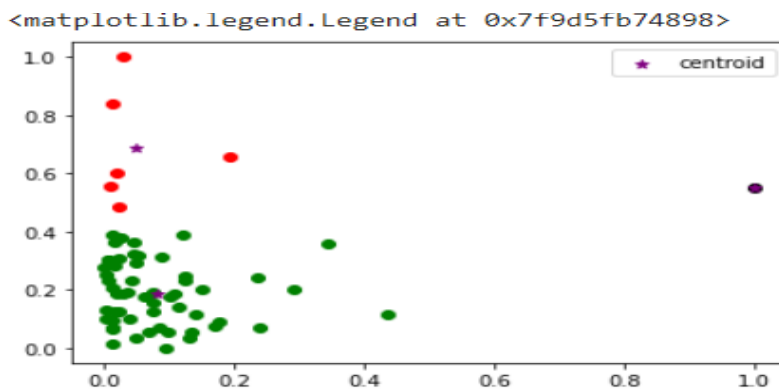


Figure 3: Identification of Distribution centre

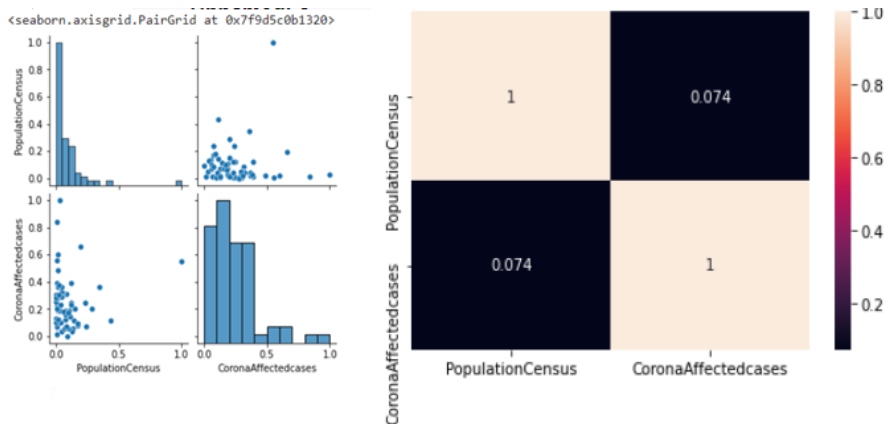


Figure 4: Correlation (Population Census Vs. Corona Affected Cases)

| | District | Status | PopulationCensus | ... | cluster | correlation | Rank |
|-----|--------------|--------|------------------|-----|---------|-------------|------|
| 0 | Ariyalur | M | 0.047919 | ... | 0 | 144.961327 | 10.0 |
| 1 | Ariyalur | T | 0.012619 | ... | 0 | 19.273605 | 32.0 |
| 2 | Coimbatore | M | 0.193837 | ... | 1 | 29.544983 | 30.0 |
| 3 | Coimbatore | T | 0.028804 | ... | 1 | 2.880389 | 52.0 |
| 4 | Cuddalore | M | 0.086621 | ... | 0 | 27.733828 | 31.0 |
| ... | ... | ... | ... | ... | ... | ... | ... |
| 57 | Vellore | T | 0.024896 | ... | 0 | 6.561228 | 46.0 |
| 58 | Viluppuram | M | 0.099311 | ... | 0 | 56.528140 | 22.0 |
| 59 | Viluppuram | T | 0.000000 | ... | 0 | 0.000000 | 62.0 |
| 60 | Virudhunagar | M | 0.175980 | ... | 0 | 189.865202 | 7.0 |
| 61 | Virudhunagar | T | 0.023139 | ... | 0 | 7.535713 | 45.0 |

[62 rows x 9 columns]

Figure 5: Ranking the areas in Tamilnadu

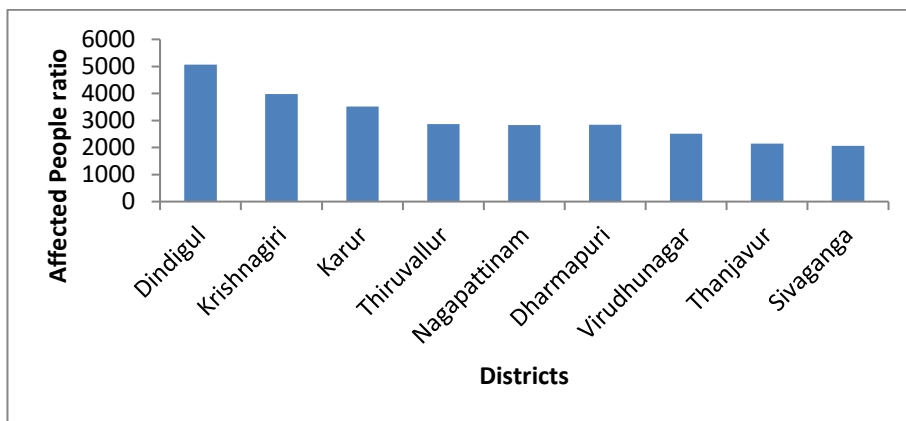


Figure 6: Prioritize the areas for Vaccine Distribution

4 Conclusion

Covid-19 Vaccine distribution has become a challenging one for any country. There are more challenging tasks like needs a separate frozen container at particular temperature .Based on the container availability, clustering the areas in Tamilnadu and identifying the distribution center using COVA Clustering model. The proposed algorithm uses the distance and correlation between the population census, affected cases and severity of affected people in a particular area. Finally, the ranking of the each district (Town/Municipality) is identified and prioritize the areas for vaccine distribution. The proposed model gives the accuracy of 93.4%.

References

- [1] <https://www.kaggle.com/sudalairajkumar/covid19-in-india>.
- [2] Tamil Population <https://www.kaggle.com/vaishnavivenkatesan/tamilnadu-population>.
- [3] Elaziz MA, Hosny KM, Salah A, Darwish MM, Lu S, Sahlol AT. New machine learning method for image-based diagnosis of COVID-19. *Plos one*. 2020 Jun 26;15(6):e0235187.
- [4] Ahmad A, Garhwal S, Ray SK, Kumar G, Malebary SJ, Barukab OM. The number of confirmed cases of covid-19 by using machine learning: Methods and challenges. *Archives of Computational Methods in Engineering*. 2020 Aug 4:1-9.
- [5] Wang P, Zheng X, Li J, Zhu B. Prediction of epidemic trends in COVID-19 with logistic model and machine learning technics. *Chaos, Solitons & Fractals*. 2020 Oct 1;139:110058.
- [6] Yadav M, Perumal M, Srinivas M. Analysis on novel coronavirus (COVID-19) using machine learning methods. *Chaos, Solitons & Fractals*. 2020 Oct 1;139:110050.
- [7] Lalmuanawma S, Hussain J, Chhakhuak L. Applications of machine learning and artificial intelligence for Covid-19 (SARS-CoV-2) pandemic: A review. *Chaos, Solitons & Fractals*. 2020 Jun 25:110059.
- [8] Khanday AM, Rabani ST, Khan QR, Rouf N, Din MM. Machine learning based approaches for detecting COVID-19 using clinical text data. *International Journal of Information Technology*. 2020 Sep;12(3):731-9.
- [9] Gupta A, Gharehgozli A. Developing a machine learning framework to determine the spread of COVID-19. Available at SSRN 3635211. 2020 Apr 25.
- [10] Kassani SH, Kassani PH, Wesolowski MJ, Schneider KA, Deters R. Automatic Detection of Coronavirus Disease (COVID-19) in X-ray and CT Images: A Machine Learning-Based Approach. *arXiv preprint arXiv:2004.10641*. 2020 Apr 22.
- [11] Sengupta S, Mugde S, Sharma G. Covid-19 pandemic data analysis and forecasting using machine learning algorithms. *medRxiv*. 2020 Jan 1.
- [12] Yan L, Zhang HT, Xiao Y, Wang M, Sun C, Liang J, Li S, Zhang M, Guo Y, Xiao Y, Tang X. Prediction of survival for severe Covid-19 patients with three clinical features: development of a machine learning-based prognostic model with clinical data in Wuhan. *medRxiv*. 2020 Jan 1.
- [13] Siddiqui MK, Morales-Menendez R, Gupta PK, Iqbal HM, Hussain F, Khatoon K, Ahmad S. Correlation between temperature and COVID-19 (suspected, confirmed and death) cases based on machine learning analysis. *J Pure Appl Microbiol*. 2020 May;14.
- [14] Debnath S, Barnaby DP, Coppa K, Makhnevich A, Kim EJ, Chatterjee S, Tóth V, Levy TJ, d Paradis M, Cohen SL, Hirsch JS. Machine learning to assist clinical decision-making during the COVID-19 pandemic. *Bioelectronic medicine*. 2020 Dec;6(1):1-8.
- [15] Punn NS, Sonbhadra SK, Agarwal S. COVID-19 Epidemic Analysis using Machine Learning. *EBADI A, Xi P, Tremblay S, Spencer B, Pall R, Wong A. Understanding the temporal evolution of COVID-19 research through machine learning and natural language processing. Scientometrics*. 2020 Nov 19:1-5. *ring and Deep Learning Algorithms*. *medRxiv*. 2020 Jan 1.
- [16] Kannan S, Subbaram K, Ali S, Kannan H. The role of artificial intelligence and machine learning techniques: Race for covid-19 vaccine. *Archives of Clinical Infectious Diseases*. 2020 Apr 30;15(2).
- [17] Prakash A, Muthya S, Arokiaswamy TP, Nair RS. Using machine learning to assess covid-19 risks. *medRxiv*. 2020 Jan 1.
- [18] Hussain L, Nguyen T, Li H, Abbasi AA, Lone KJ, Zhao Z, Zaib M, Chen A, Duong TQ. Machine-learning classification of texture features of portable chest X-ray accurately classifies COVID-19 lung infection. *BioMedical Engineering OnLine*. 2020 Dec;19(1):1-8.
- [19] Raza K. Artificial intelligence against COVID-19: A meta-analysis of current research. *Big Data Analytics and Artificial Intelligence Against COVID-19: Innovation Vision and Approach*. 2020:165-76.
- [20] Wang J. Mathematical models for COVID-19: Applications, limitations, and potentials. *Journal of public health and emergency*. 2020 Jun;4.
- [21] Roy AN, Jose J, Sunil A, Gautam N, Nathalia D, Suresh A. Prediction and Spread Visualization of Covid-19 Pandemic Using Machine Learning.
- [22] Ravi T. Classification of correlated subspaces using HoVer representation of Census Data. In 2011 international conference on emerging trends in electrical and computer technology 2011 Mar 23 (pp. 906-911). IEEE.

Enhanced Duck Traveler Optimization (EDTO) Algorithm with Multilevel Thresholding, Region of Interest and K-Means Clustering for Mammogram Image Segmentation to improving Accuracy

¹Krishnaveni A, ²Shankar R, ³Duraisamy S

Abstract

Research about breast cancer consciousness has discovered that social and strict issues imply that ladies don't get to health administrations, are reluctant to counsel male specialists despite the fact that their relatives particularly couldn't discuss with husbands also. Breast tumor analysis is rarely simple; it is particularly hard when the lady is in her age of 30's and has recently begun arranging a future for herself and her family. Hence, a new Meta heuristic Duck traveller optimization algorithm is used to segment the breast tumor to help the doctors to disease diagnosis. **Methods:** Selecting the best duck from given duck flock is an example of optimization. Optimizing the threshold values EDTO based multilevel thresholding (EDTO-MTH) algorithm is introduced to segmenting the cancer. Desired region of the breast is determined by using EDTO based Region Growing (EDTO-ROI) to highlighting the tumor region. To improving the segmentation results DTO with K-Means Clustering is proposed (EDTO-K means). **Results:** The performance results of EDTO are evaluated by using the quality metrics accuracy, precision, recall and f-measure. **Conclusion:** It is assessed that high mortality because of breast tumor in India would increment throughout the long term. Hence, these calculations discover a terrible requirement for starting essential and auxiliary counteraction measures for the control of breast tumor in our country.

Keywords: *Bio Inspired Algorithm, Enhanced Duck Traveller Optimization, Breast Tumor, Multilevel Thresholding, Region, Clustering, Segmentation, Accuracy*

1 Introduction

One lady gets determined to have breast disease like clockwork in India, and one lady bites the dust of breast malignant growth at regular intervals, making it the most predominant disease among Indian ladies. Ladies in India are for the most part analyzed at a later, further developed stage with helpless anticipation. Around 1 of every 28 ladies is relied upon to create bosom disease during their lifetime. By 2030, bosom disease will cause most passings among ladies in India than some other illness. Dr.Sanjeev Kanoria said the importance of self checking mammography for ladies to detect early signs of breast cancer. Cancer of breast with assessed 1.5 lakh (more than 10%, everything be equal) new cases during 2016, is the main disease generally. Image segmentation assumes a significant job and is a basic cycle in clinical pictures. An exact and normalized method for breast tumor division is a basic advance for checking and evaluating bosom malignant growth. Designing such an accurate and exact breast region segmentation technique remains a difficult issue in digital mammography. The most well-known manifestation of breast cancer is another lump or mass, yet different side effects are additionally conceivable. In 2019, an expected 2, 68,600 new instances of obtrusive breast cancer will be analyzed among ladies and roughly 2,670 cases will be analyzed in men. Roughly 41,760 ladies and 500 men are relied upon to bite from breast cancer in 2019.

1.1 Image Segmentation

Image Segmentation, the way toward portioning a computerized picture into different fragments, is probably the most established issue in computer vision. The reason for division is to rearrange or change the portrayal of a picture into some structure that is simpler and more important to dissect. All in all, the objective of picture division is to group pixels into striking picture districts, for example, locales relating to singular surfaces, object surfaces, or other common pieces of articles. The division is generally made by some homogeneity standard. Thus, there are numerous application fields for picture division, for example, object acknowledgment, impediment limit assessment, picture pressure, picture altering, and picture recovery. Much of the time, the nature of the division relies upon the picture. Various methodologies are reasonable for various sorts of pictures. Due to this picture subordinate trademark. It is unimaginable to expect to discover a division technique which is entirely appropriate for a wide assortment of pictures.

1.2 Image Thresholding

Thresholding is the easiest methodology of picture division. Initially, thresholding was utilized to make parallel pictures from a grayscale picture. During the thresholding method, every pixel in a picture is set apart as an article pixel. On the off chance that its worth is more noteworthy than some limit esteem, it will be treated as a forefront pixel. Else, it will be treated as foundation pixel. At long last, a double picture is made by setting every pixel

frontal area or foundation. Truth be told, thresholding is the most essential cycle in picture handling and PC vision. In any case, this two-level thresholding has numerous limitations in its applications. To all the more adequately find objects of interest portrayed in a picture, Multilevel Thresholding (MTH) techniques can be arranged into various gatherings as per the data the calculation controls, for example, histogram shape, entropy, spatial and object credits.

1.3 Computer Aided Diagnosis

Breast malignancy is one of the main sicknesses that mirrors an uncontrolled development of unusual cells in the breast. Because of the breast anomalies properties and the idea of the human visual insight, it is characteristic that, occasionally the anomalies are missed or miss ordered. Accordingly, pointless biopsies are taken. To alleviate this issue, Computer Aided Diagnosis (CAD) framework has arisen. Disease is a huge issue wherever on the planet. It is an affliction, which is deadly much of the time and has influenced the existences of numerous and will keep on influencing the existences of some more. A huge number of grandmas, moms, and little girls succumb to breast disease consistently. Malignancy is grouped by the different kinds of cell, and in excess of 200 sorts of tumors are known. Bosom malignant growth is a kind of disease created from the breast muscle, regularly it happens inside the milk channels or lobules providing the conduits with milk. Breast disease creates in the two people, albeit the previous is uncommon. In breast, typical cells develop and partition at a specific time yet if there should be an occurrence of the harmful cells, the cell development is nonstop and uncontrolled as demonstrated in Figure 1.

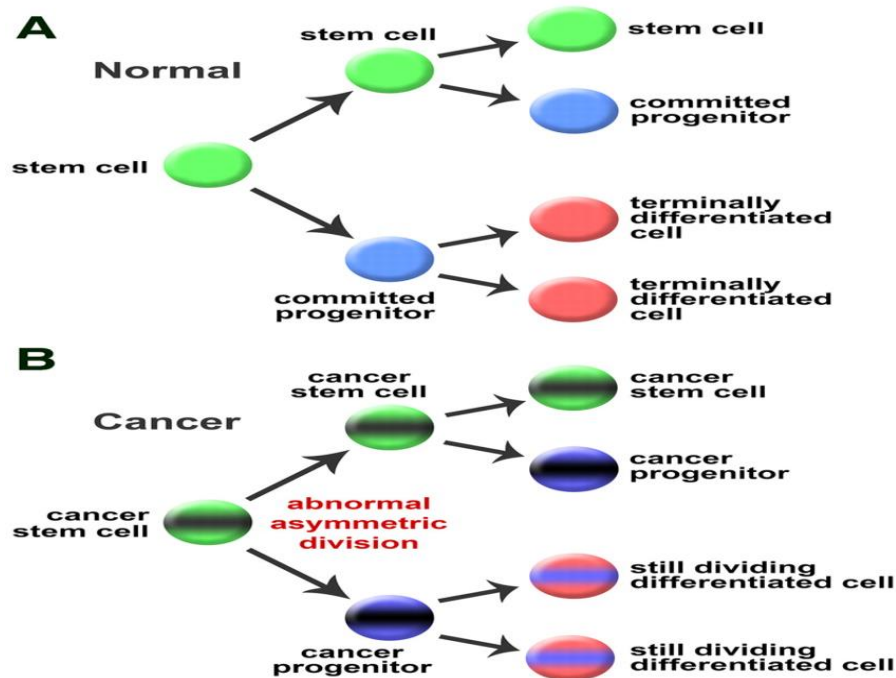


Figure 1: Normal cell vs Cancer cell

In India, the surveys say at the year of 2030, the breast cancer sufferer rate greater than before 2, 00,000.

1.4 Dataset (MIAS) & (DDSM)

In this research work, MIAS data set is utilized for the test reason. Absolutely, 322 breast pictures of typical, microcalcification, mass, generous and dangerous classes are accessible in MIAS information base. All pictures have a goal of 1024×1024 pixels and 8-bit precision (dark level). Normally, MIAS data set pictures contain foundation data, pectoral muscle, and different kinds of noises. It is important to eliminate every one of those undesirable data for better and right investigation and understanding of breast pictures. The data set additionally contains the data about variation from the norm areas. The areas of irregularities are provided by the MIAS for each picture thus, a ROI of size 256 x 256 pixels is removed from every unique picture.

The Digital Database for Screening Mammography (DDSM) is another asset for conceivable use by the mammographic picture investigation research local area. It is a collective exertion between Massachusetts General Hospital, Sandia National Laboratories and the University of South Florida Computer Science and Engineering Department. The information base contains roughly 2,500 investigations. Each examination incorporates two

pictures of each bosom, alongside some related patient data (age at season of study, ACR bosom thickness rating, nuance rating for anomalies, ACR catchphrase portrayal of variations from the norm) and picture data (scanner, spatial goal ...). Pictures containing dubious zones have related pixel-level "ground truth" data about the areas and sorts of dubious districts. Additionally gave are programming both to getting to the mammogram and truth pictures and for computing execution figures for computerized picture examination calculations.

1.5 Image Preprocessing

Pictures are by and large contaminated by noise. When all is said in done, unwanted things happens because of different reasons likes flawed instruments, issues with the information securing measure and meddling normal marvels. Besides, noise is presented by transmission blunders and pressure. The noise picture (Gonzalez and Woods 2002) is demonstrated and the Equation is given in the accompanying condition

$$g(a, b) = f(a, b) + n(a, b)$$

where

$f(a, b)$ – unique picture pixel

$n(a, b)$ - noise

$g(a, b)$ - resulting noisy pixel

Mammogram pictures are hard to decipher therefore, pre processing activity is fundamental to improve the picture quality. Pre processing plan is a significant advance in clinical picture investigation. Prior to applying any PC based robotized investigation; pre-preparing steps are regularly executed to improve the picture quality. The hidden standards behind pre-handling are to make a picture understood and to improve the differentiation of the picture. In pre-handling stage, the breast is apportioned to improve the quest for irregularities without unnecessary impact from the foundation of the mammogram and some sifting or editing is cultivated to improve the nature of the of the picture and to diminish commotion. Pre-handling gives quality improvement in representation and understanding of clinical pictures.

1.6 Image Enhancement

Picture improvement is a chief assignment in low level picture handling framework and one of the pre-preparing methods, which upgrades the quality (lucidity) of pictures for human discernment. The objective is to deliver an appropriate prepared picture for a specific application. The reason for the upgrade of mammogram picture is to create a solid portrayal of breast tissue structures by improving the differentiation and smothering the noise in picture.

1.7 Image Segmentation and ROI Selection

Picture division separates a picture into a few portions or locales wherein, each section is outwardly lucid. In this manner, picture division is characterized as a cycle, which partitions a picture into various districts or portions, with the end goal that, every area is homogeneous and makes it simpler to dissect them. The objective for division is to discover and name the vital part in a picture, which gives data about specific realities than the other piece of the picture. Therefore, certain areas of interest are disconnected from a genuine picture to separate those zones inside the picture and furthermore to help radiologists in conclusion. Picture division is broadly utilized in distant detecting, clinical imaging, and so forth Locales of interest are bit of breast pictures, which are utilized by radiologists to recognize irregularities like microcalcifications (considerate and threatening) and masses (kind and malignant). The programmed recognition of regions of interest is troublesome. Thus, in this exploration work, ROI picture is physically edited by utilizing irregularity area, which is accessible in the MIAS data set.

1.8 Feature Extraction

Highlight extraction is a significant segment that chooses execution of CAD. Highlight extraction is additionally called as depiction. Depiction manages the way toward extricating ascribes, which produce some quantitative data of interest, to separate one class of items from another. At the point when the info information utilized for control is unpredictable, at that point it is changed over into a bunch of features called include vector. It is the way toward gathering picture data, for example, shading, shape, and surface. Highlights contain the proper data of a picture and it is utilized in the picture handling task (for example looking, recovery, putting away).

1.9 Feature Selection

Now and then, the first list of capabilities contains repetitive and unessential subtleties. Highlight the feature choice is important to discover a subset of significant highlights by disposing of excess and unimportant features. This prompts the better grouping exactness. Highlight positioning and subset determination are the two sorts of highlight choice strategies.

1.10 Classification

As a rule, classification is the finishing up period of clinical picture preparing procedures, where every single anonymous example is named to be a category class. Classification task is done dependent on two phases specifically, preparing and testing stage. In the preparation stage, a preparation informational index is utilized to foresee the names of a class. In the testing stage, pictures are checked to recognize, regardless of whether it is has a place with the carcinogenic picture or non-malignant picture, with the assistance of the prepared classifier.

2 Related Work

As per Technopedia, A. Nayyar et al (2018) said a transformative calculation works through the choice cycle where the most un-fit individuals from the populace set are disposed of from the calculation, while the fit individuals are permitted to endure and proceed until a superior arrangement is resolved. In other words, Evolutionary calculations are a computational calculation that is propelled and copy organic cycles to take care of complex issues. There are different bio-propelled calculations at present in working however the normal thought behind every one of them is the same: give a populace of people, the characteristic cycle causes basic determination (natural selection), and this causes a spike in the wellness of the populace.

The creators S. Kotte et al (2018) in their paper proposed the utilization of multilevel picture division has been executed dependent on novel developmental calculation Improved Differential Search (IDS). The achievability of proposed approach/calculation has been tried on standard dark scale pictures. To check the viability of the proposed approach/calculation, all exploratory outcomes are dissected quantitatively and subjectively. The creators M. H. Ashraf et al (2018) incorporate another methodology, applied on the Mini-MIAS dataset of 322 pictures, including a pre-handling technique and inbuilt component extraction utilizing K-mean bunching for Speed-Up Robust Features (SURF) choice. The creators P. Kaur et al (2019) contemplated and demonstrated the breast disease is a critical purpose behind death in females. Early acknowledgment of this infection with the help of mammography decreases the passing rate. Profound learning (DL) is a methodology being used and mentioned by radiologist that helps them in making a precise conclusion and assists with improving result expectations. This paper incorporates another methodology, applied on the Mini-MIAS dataset of 322 pictures, including a pre-handling strategy and inbuilt component extraction utilizing K-mean bunching for Speed-Up Robust Features (SURF) determination. N. Shrivastava et al (2020) shows a blend of determination strategies for bit by bit assessment for Efficient Seeded Region Growing with upgraded execution to spot bosom disease. The creators Mehdy, Ng, Shair, Saleh, and Gomes (2017) in their paper have examined the use of fake neural organizations in bosom disease discovery. They have talked about various varieties of neural organization particularly the new pattern of half breed neural organizations like SOM display and have presumed that neural organizations when joined with different techniques can accomplish better precision, affectability and positive prescient worth. Wang, Nishikawa, and Yang (2017) built up a convolutional neural organization (CNN) to which the info comprised of huge picture window for modernized identification of bunched microcalcifications. They directed the trial on computerized and movie mammograms and assessed the location execution utilizing recipient trademark investigation.

3 Objective of the Research

Essential objective of this exploration work is to plan and build up the better CAD framework and to improve the classification accuracy of breast malignancy discovery and classification technique using Duck Traveller Optimization algorithm.

The objectives of this research work are,

- Demonstrate new pre-handling methods to improve the picture quality and choice of ROI
- Uses of wavelet families for highlight the features.
- Distinguishing proof and extraction of appropriate highlights from wavelet coefficients
- Finding the best feature subset utilizing EDTO
- Create microcalcification picture arrangement approach utilizing SAF & LDA Classifier

4 Proposed Work

Most ordinarily discovered malignant growth among ladies is breast disease. Generally 12% of ladies develop breast disease during their lifetime. It is the second noticeable lethal malignant growth among ladies. Breast disease finding is important during its underlying stage for the appropriate treatment of the patients to have useful existences for a broad period. A wide range of calculations are acquainted with improve the determination of breast malignancy, however many have less proficiency. In this work, we have proposed novel bio-inspired calculation including superb highlights of nature inspired to tackling complex optimization issue for instance breast disease segmentation and classification.

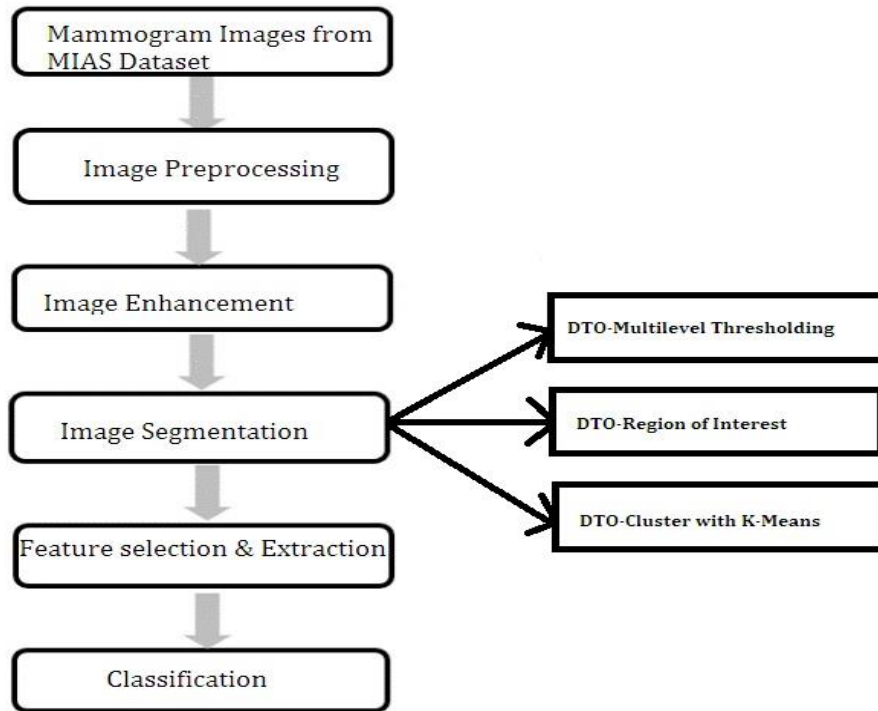


Figure 2 EDTO-MTH, EDTO-ROI & EDTO-Cluster with K-Means for Breast Cancer Segmentation

4.1 Duck Traveler Optimization (EDTO) Algorithm

The endurance is the fundamental aim of any multitude; accordingly the entirety of the people ought to pulled in towards the ducks in duck flock which has high grouping exactness and occupied outwards the ducks which has unessential regions. Every one of the practices of ducks is numerically communicated as follows:

$$D_g = + \sum_{x=1}^X Y - Y_x \quad (1)$$

$$DA_g = \frac{\sum_{x=1}^X V_x}{X} \quad (2)$$

In Eq. (1), D_g is the partition of g^{th} individual, Y is the current individual, Y_x shows the position y^{th} adjoining individual, and X is the quantity of adjoining people. In Eq. (2), DA_g is the adjustment of g^{th} individual, V_x is the velocity of x^{th} contiguous character.

$$C_g = \frac{\sum_{x=1}^X V_x}{X} - X \quad (3)$$

In Eq. (3), C_g is the cohesion of g^{th} individual. The accompanying condition shows the fascination of ducks towards a food source.

$$DA_g = \frac{\sum_{x=1}^X V_x}{X} \quad (4)$$

In Eq.(4), FS_g is the food wellspring of the g^{th} individual, Z^+ speaks to the location of the food source and Z represents the position of the current individual. Interruption outwards unessential element is determined as

follows:

$$IF_g = Z^- + Z \quad (5)$$

In Eq.(5), IF_g is the position of the irrelevant regions and Z^- is the location of irrelevant features. To refresh the situation of counterfeit ducks in the inquiry space and reproduce their movements, two vectors for example, step ΔZ and position (Z) are considered. ΔZ represents the path of the duck movements which is determined as,

$$\Delta Z_{iter + 1} = wD_g + awA_g + cwC_g + fFS_g + iIF_g + iw\Delta Z_{iter} \quad (6)$$

In Eq. (6), w means the partition weight, f is the food factor, aw is the alignment weight, i is the opponent factor, cw is the cohesion weight, iw is the inertia weight and $iter$ is the iteration counter. The position vectors are determined after the step vector estimation, which is given as follows:

$$Z_{iter + 1} = Z_{iter} + \Delta Z_{iter + 1} \quad (7)$$

Ducks wanted to sort out their development in the unique duck flock. Duck game plan is staggeringly languid in the static movement, in spite of the fact that it is exceptionally fit for battling the rival. In this way, the game plan coefficient is high and the congruity coefficient is extremely low in disclosure, while the course of action coefficient is little in the extraction cycle and the concordance coefficient is enormous.

On the off chance that there is no local answer for improve the disclosure of counterfeit ducks, an arbitrariness arrangement is accomplished utilizing Terrif Method (TF). Accordingly, the duck's in duck flock position is refreshed as,

$$Z_{iter + 1} = Z_{iter} + Terrif(s) * Z_{iter} \quad (8)$$

In Eq. (8), s means the size of the position vector.

$$Terrif(z) = 0.01 * \frac{rn1 * \sigma}{|rn2|^{1/\gamma}} \quad (9)$$

In Eq. (9), $rn1$ and $rn2$ are unsystematic numbers which is goes from 0 to 1 and γ is the unvarying value. σ is determined as,

$$\sigma = \left(\frac{\exists(1 + \gamma) * \sin\left(\frac{\pi\gamma}{2}\right)}{\exists\left(\frac{1+\gamma}{2}\right) * \gamma * 2^{\left(\frac{\gamma-1}{2}\right)}} \right) \quad (10)$$

In Eq. (10), $\exists(z) = (z - 1)!$



Figure 3 : searching the food source by duck flock

Duck Traveler Optimization (EDTO) Algorithm for Segmentation

Initialize the population of ducks $D_g (g = 1, 2, \dots, n)$

Initialize D_g with desired regions of input mammogram images

while the end condition is not satisfied

Call DTO-MTH/DTO-ROI/DTO-K Means to find the segmentation accuracy

Revise the food source and irrelevant regions

Revise aw, s, cw, f and i

Compute $DA_g, C_g, FS_g, Food$ and iIF_g using (1) to (5)

Revise neighboring radius

if a duck has at least one neighboring duck

```

Revise velocity vector using (6)
Revise position vector using (7)
else
Revise position vector using (8)
end if
According to the variable boundaries check and correct the new positions
end while

```

4.2 Enhanced Duck Traveler Optimization-Multilevel Thresholding (EDTO-MTH)

Duck Traveler Optimization algorithm is a new metaheuristic algorithm for breast cancer image segmentation and classification problem. The basic swam behavior of duck flock is identified as an inspiration to medical image processing. Screening mammography is the first aid for breast cancer prediction and early diagnosis method like duck identifying the siblings by using imprinting behavior and stack of intelligence. In DTO-MTH algorithm the first step is to calculate the total number of pixels in input mammogram from MIAS dataset. From the total count of pixels the objective value is obtained by using entropy method Kapur and class variance method Otsu method. Initialization positions $DP_i (i = 1; 2; \dots; n)$ with size n , velocities $DV_i (i = 1; 2; \dots; n)$, total number of iterations T_{max} , fitness function fn , c , C_1 , C_2 , C_3 , C_4 , C_5 , r_1 , r_2 , R , $t = 1$

```

2: Calculate objective function  $fn$  for each duck  $DP_i$ 
3: Find best duck  $DP_{best}$ 
4: while  $t \leq T_{max}$  do
5: for  $(i = 1 : i < n + 1)$  do
6: if  $(R < 0.5)$  then
7: Update position of current swimming duck as
 $DP_{nd}(t + 1) = DP_{best}(t) - C_1 \cdot j \cdot C_2 \cdot DP_{best}(t) - DP_{nd}(t) \cdot j$ 
8: else
9: Update velocity of current flying duck as
 $DV(t + 1) = C_3 \cdot DV(t) + C_4 \cdot r_2 \cdot (DP_{best}(t) - DP_{nd}(t)) + C_5 \cdot r_2 \cdot (DP_{Gbest} - DP_{nd}(t))$ 
10: Update position of current flying duck as
 $DP_{nd}(t + 1) = DP_{nd}(t) + DV(t + 1)$ 
11: end if
12: end for
13: Calculate objective function  $fn$  for each duck  $DP_i$ 
14: Update  $c$ ,  $C_1$ ,  $C_2$ ,  $R$ 
15: Find best duck  $DP_{best}$ 
16: Set  $DP_{Gbest} = DP_{best}$ 
17: Set  $t = t + 1$ 
18: end while
19: Return best duck  $DP_{Gbest}$ 

```

This technique is an augmentation of binarization and bi-level thresholding where different edges are utilized to delineate picture into the resultant picture. In the binarization strategy, just a single edge is utilized. In bi-level thresholding technique, two edges are utilized. Nonetheless, in posterizing technique different edges are utilized. Choice or figuring of the staggered edges is critical in picture division since appropriate division relies upon sufficiently registered limits. There are various strategies for processing the limits for a picture, for example,

- Maximizing the gray level variance
- Entropy similarity
- Measure of fuzziness

When all is said in done, thresholding techniques can be partitioned into parametric and nonparametric strategies. Utilizing parametric strategies, for example, a novel picture thresholding strategy dependent on Parzen window gauge, non managed picture division dependent on multi-objective enhancement, a staggered thresholding approach utilizing a cross breed ideal estimation calculation, and ideal multi-thresholding utilizing a mixture improvement approach, may include the arrangement of nonlinear conditions which increments of the computational multifaceted nature. Along these lines, the nonparametric strategies are presented for finding the edges by advancing some segregating criteria.

Among the referenced diverse thresholding criteria, the entropy is the most famous streamlining strategy. Utilizing the entropy of the histogram, Pun was the first to present another technique for dark level picture thresholding. Afterward, this technique was remedied and improved by Kapur et al.

Ideal limit determination for bi-level thresholding isn't computationally costly, while for staggered thresholding, processing in excess of scarcely any ideal edge esteems is a costly and tedious activity. The ideal limit esteems can be dictated by streamlining some model capacities characterized from the histogram of picture. The Kapur's strategy dependent on the entropy is utilized to perform staggered thresholding. The staggered thresholding issue is frequently treated as an issue of improvement of a goal work.

Two extensively utilized ideal thresholding techniques in particular entropy model (Kapur's) strategy and between-class (Otsu's) strategy are utilized. The ideal staggered thresholding issue can be arranged as a m-dimensional advancement issue, for assurance of m ideal limits for a given picture $[t_1, t_2 \dots, t_m]$, where the point is to augment the target work

$$f([t_1, t_2, \dots, t_m]) = H_0 + H_1 + H_2 + \dots + H_m$$

$$\begin{aligned} H_0 &= \sum_{i=0}^{t_1-1} \frac{P_i}{w_0} \ln \frac{P_i}{w_0}, & w_0 &= \sum_{i=0}^{t_1-1} P_i \\ H_1 &= - \sum_{i=t_1}^{t_2-1} \frac{P_i}{w_1} \ln \frac{P_i}{w_1}, & w_1 &= \sum_{i=t_1}^{t_2-1} P_i \\ H_2 &= - \sum_{i=t_2}^{t_3-1} \frac{P_i}{w_2} \ln \frac{P_i}{w_2}, & w_2 &= \sum_{i=t_2}^{t_3-1} P_i, \dots \dots \\ H_m &= - \sum_{i=t_m}^{L-1} \frac{P_i}{w_m} \ln \frac{P_i}{w_m}, & w_m &= \sum_{i=t_m}^{L-1} P_i. \end{aligned}$$

As Kapur based entropy measure strategy has been utilized in deciding if the ideal thresholding can furnish histogram-based picture division with acceptable wanted. The Kapur strategies have been demonstrated as a proficient strategy for bi-level thresholding in picture division. Be that as it may, when these strategies are reached out to staggered thresholding, the calculation time develops exponentially with the quantity of limits. It would restrain the staggered thresholding applications. To defeat the above issue the Kapur, DTO calculation for tackling staggered thresholding issue is to expand the Kapur's target work in a proficient way. The interest of discover/make the ideal arrangement by the scientist for creative picture division strategies are required.

4.3 Enhanced Duck Traveler Optimization-Region of Interest (EDTO-ROI)

Best Region selection using Self Seeking Duck Traveler Algorithm

```

If  $i_{max} > i_{final}$ 
Set  $D_g = D_1 = D_2 = \Phi$ ;
Initialize  $DP_{ij} = 1/n_i$ ;
arbitrary();
robustness();
greatest();
recompense();
reprimand();
Set  $D_g = \text{Pick\_greatest}()$ ;
Do {
 $D_1 = \text{Pick\_arbitrary}()$ ;
 $D_2 = \text{Pick\_arbitrary}()$ ;
If  $\text{robustness}(D_1) \geq \text{robustness}(D_2)$ 
{
recompense( $D_1$ );
reprimand( $D_2$ );
 $D_g = D_1$ ;
}
}
Else

```

```

{
recompense(D2);
reprimand(D1);
Dg= D2;
}
}while end condition is satisfied;
Return Dg;

```

$$D(k) = D(k - 1) + fk(k) - fl(k) - Df(k) - Dk(k);$$

Where $D(k)$ is the food forage stage of duck flock at end of the month k (when $k=1$, $D(k-1)$ is equal to D_0 , the initial food forage level); the forage level for the successive months $D(k-1)$ will be the preceding month's end of the day's food forage level. $fk(k)$ is the food capture and $fl(k)$ is the food loss rate during month k . $D(k)$ is the save food that might ultimately fall from the duck as a result of run over, during the month k . It is also important to take care of the feature that duck capacity should not be less than the lifeless storage space.

4.4 Enhanced Duck Traveler Optimization-K Means Clustering (EDTO-K Means)

Duck flock passes on every single person are unique. Everybody has their own style of composing. So attempting to make a calculation which perceives such a significant number of meta-heuristic could be extreme as well as every one of the criteria's are not to be completely fulfilled by the whole calculation. Thus we make such a framework which can adapt simply like the manner in which human mind learns. For example, experimentation strategy is considered. Here DCO is proposed from those previously mentioned thoughts.

Start to Initialization (Generate a **Duck Clusters** (DC))

DC = { $Z_j, j=1,2,\dots,DC_n$ };

$f > 1$;

For $f = 1:f_{max}$ value in DC do

Compute the value of $DC_{nj} = f(Z_j D C)$;

Minimization

Cluster C in the uphill order of DC;

Maximization

Cluster C in the downhill order of DC;

(i) Create a new populace $DC\emptyset$;

For each $Z_j, j=1,2,\dots, DC_n$ do

$d_i >$ set of sprinters (size of the position and the distance)

for each sprinter (individually) are relative to DC_i ,

(the standardize goal importance)

(ii) $DC\emptyset \succ DC\emptyset \vee d_i$ (add to population);

End of for

$C > DC\emptyset$ {the novel populace};

End of for

Return C, the CLUSTER size of the answer

Stop

5 Results and Discussion

In this research work, the efficiency of EDTO with different segmentation methods such as EDTO-MTH, EDTO-ROI and EDTO-K Means is tested in terms of accuracy, precision, recall and F-measure. MIAS and DDSM dataset is used for experimental purpose. The MIAS dataset consists of 322 sample mammogram images with combination of left and right breasts. The instance in breast cancer images having 1024*1024 pixels in Portable GreyMap (PGM) format. The breast cancer (MIAS) dataset and (DDSM) is available in the <https://www.mammoimage.org/databases/>

1) Accuracy

It measures the fraction of correct breast cancer predictions to the total number of instances evaluated. It is calculated as,

$$Accuracy = \frac{TP + TN}{TP + FP + TN + FN}$$

The accuracy value of EDTO with different methods for mammogram image segmentation is given in Table 1.
 Table 1: Accuracy of proposed EDTO with Datasets

| Segmentation Methods | MIAS | DDSM | Time (sec) |
|----------------------|-------|-------|------------|
| EDTO-MTH | 0.80 | 0.857 | 31.75 |
| EDTO-ROI | 0.832 | 0.896 | 16.25 |
| EDTO-K Means | 0.867 | 0.93 | 13.5 |

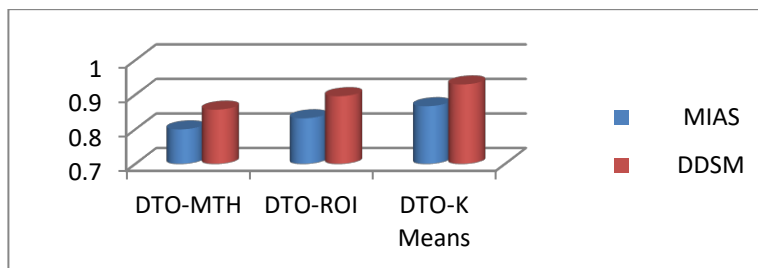


Figure 4 : Accuracy of EDTO-MTH, EDTO-ROI and EDTO-K Means with MIAS and DDSM Comparison

The accuracy of MIAS and DDSM with EDTO-MTH, EDTO-ROI and EDTO-K Means segmentation methods for breast cancer diagnosis is shown in Fig. 4. The accuracy of EDTO-K Means is 93% and greater than EDTO-MTH and EDTO-ROI method for breast cancer diagnosis. From Fig. 2, it is proved that the EDTO-K Means has better breast cancer diagnosis accuracy than other methods.

2) Precision

It is used to measure the positive patterns (i.e., presence of breast cancer) that are correctly predicted from the total predicted patterns in the positive class. It is calculated as,

$$Precision = \frac{TP}{TP + FP}$$

The precision value of EDTO-MTH, EDTO-ROI and EDTO-K Means with different methods for breast cancer diagnosis is shown in Table 2.

Table 2: Precision of proposed EDTO with Datasets

| Segmentation Methods | MIAS | DDSM | Time (sec) |
|----------------------|-------|-------|------------|
| EDTO-MTH | 0.804 | 0.89 | 85.6 |
| EDTO-ROI | 0.846 | 0.90 | 87.5 |
| EDTO-K Means | 0.875 | 0.937 | 78.2 |

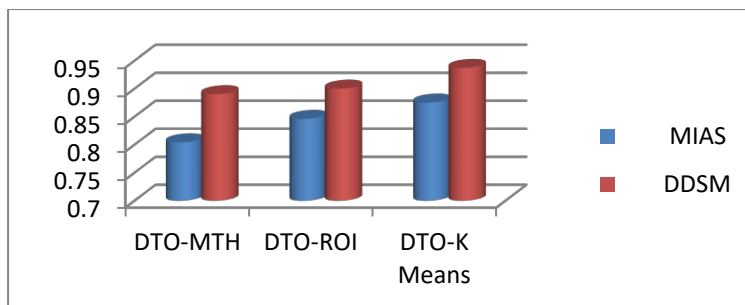


Figure 5 : Precision of EDTO-MTH, EDTO-ROI and EDTO-K Means with MIAS and DDSM Comparison

The precision of EDTO-MTH, EDTO-ROI, and EDTO-K Means methods for breast cancer diagnosis is shown in Fig. 5. The precision of DTO-K Means is 93.7% and greater than EDTO-MTH and EDTO-ROI method for breast cancer diagnosis. From Fig. 3, it is proved that the EDTO-K Means has better breast cancer diagnosis precision than other methods.

3) Recall

It is used to calculate the proportion of optimistic patterns with the intention of is properly off the record. It is designed as,

$$Recall = \frac{TP}{TN + TP}$$

The recall value of EDTO-MTH, EDTO-ROI and EDTO-K different methods for breast cancer diagnosis is shown in Table 3.

Table 3: Recall of proposed EDTO with Datasets

| Segmentation Methods | MIAS | DDSM | Time (sec) |
|----------------------|-------|-------|------------|
| EDTO-MTH | 0.816 | 0.833 | 27.5 |
| EDTO-ROI | 0.876 | 0.923 | 13.5 |
| EDTO-K Means | 0.90 | 0.937 | 12.1 |

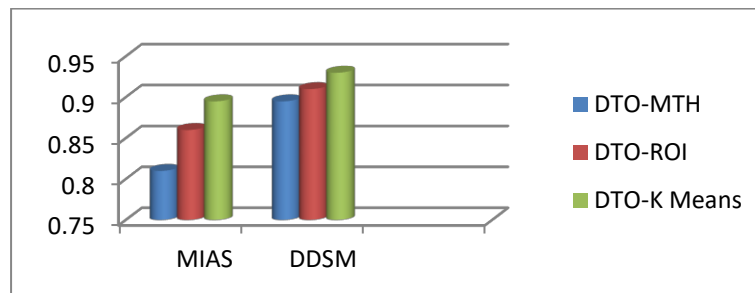


Figure 6 : Recall values of EDTO-MTH, EDTO-ROI and EDTO-K Means with MIAS and DDSM Comparison

The recall of EDTO-MTH, EDTO-ROI and EDTO-K methods for breast cancer diagnosis is shown in Fig. 6. The recall of EDTO-K Means is 93.7% and greater than EDTO-ROI and EDTO-MTH method for breast cancer diagnosis. From Fig. 6, it is proved that the EDTO-K Means has better breast cancer diagnosis recall than other methods.

4) F-Measure

It is the mean flanked by the precision and recall. It is intended as,

$$F - Measure = \frac{2 * Recall * Precision}{Recall + Precision}$$

The F-measure value of EDTO with different segmentation methods MTH, ROI, and K Means for breast cancer diagnosis is given in Table 4.

Table 4: Recall of proposed EDTO with Datasets

| Segmentation Methods | MIAS | DDSM | Time (sec) |
|----------------------|-------|-------|------------|
| EDTO-MTH | 0.81 | 0.895 | 23.8 |
| EDTO-ROI | 0.86 | 0.91 | 14.5 |
| EDTO-K Means | 0.895 | 0.93 | 11.9 |

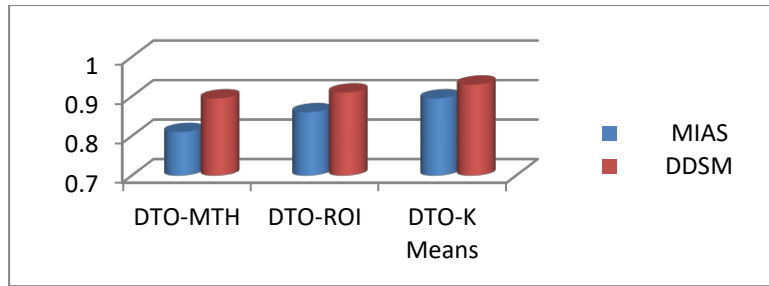


Figure 7 : Recall values of EDTO-MTH, EDTO-ROI and EDTO-K Means with MIAS and DDSM Comparison

F-measure of EDTO-MTH, EDTO-ROI and EDTO-K methods for breast cancer diagnosis is shown in Fig. 7. The F-measure of EDTO-K Means is 0.93% and greater than EDTO-ROI and EDTO-MTH method for breast cancer diagnosis. From Fig. 7, it is proved that the EDTO-K Means has better breast cancer diagnosis F-measure than other methods.

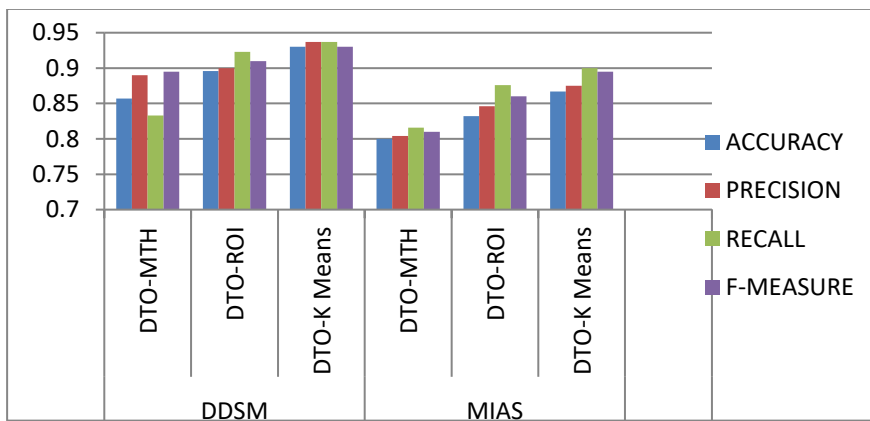


Figure 8 : The evaluation of accuracy, precision, recall and F-Measure values with DDSM and MIAS dataset

Performance evaluations of proposed segmentation methods of EDTO-MTH, EDTO-ROI and EDTO-K Means are shown in Fig.8. Four quality metrics are used to improving the performance of EDTO are accuracy, precision, recall and F-Measure with two different breast cancer datasets like MIAS and DDSM for breast cancer. DDSM dataset having high accuracy, high precision, high recall and high F-Measure better than MIAS dataset. Among EDTO-MTH, EDTO-ROI and EDTO-K Means the EDTO-K Means having the high accuracy values as well as high precision and high recall value. Hence we prove that the proposed novel Meta heuristic optimization algorithm EDTO has the high efficiency to performing breast cancer segmentation using K-Means algorithm.

The computational complexity of the DTO algorithm can be expressed as follow. For population n and iterations tmax, the time complexity will be defined as in the following

Initialization DPi(i = 1; 2; :::; n), DVi(i = 1; 2; :::; n), Tmax, c, C1, C2, C3, C4, C5, r1, r2, R, t = 1: O (1).

Calculate objective function fn for each duck DPi: O (n).

Finding best duck DPbest: O (n).

Updating position of current swimming duck: O (tmax_n).

Updating velocity of current flying duck: O (tmax_n).

Updating position of current flying duck: O (tmax_n).

Calculating objective function fn for each duck DPi:O (tmax).

Updating c, C1, C2, R: O (tmax).

Finding best duck DPbest: O (tmax).

Setting DPGbest = DPbest: O (tmax).

Setting t = t + 1: O (tmax).

Producing the best duck DPGbest: O (1)

From this analysis, the complexity of computations isO (tmax _ n) and O (tmax _ n _ d) with d dimension.

6 Conclusions

In this research work, EDTO is proposed to choose the most discriminative areas/pixels of MIAS and DDSM information for breast malignant growth conclusion. It takes care of absence of inner memory issue, untimely intermingling issue and arbitrary movement issue. A Terrif strategy (TS) is utilized in EDTO to refresh the development of the duck when there is no local arrangement. It improved the meaning of neighbourhood span utilized in EDTO, both while encouraging the development of ducks and saving time. The EDTO cycle is done to choose the most discriminative pixels/districts dependent on the division exactness of strategies, for example, MTH, ROI and K-Means dependent on EDTO. At last, they chose pixels are applied in MTH, ROI and K-Means segmentors to foresee the breast malignancy adequately. The test results show that the proposed EDTO-K Means strategy has better exactness, accuracy, review and F-measure for breast malignancy finding than different techniques. In future the extended version of EDTO is planned to develop for disease diagnosis in medical image processing.

Acknowledgement

“We thank MIAS and DDSM dataset” for allowing us to use sample images for experimental facilities.

References

- [1] S.Kotte, P.R.Kumar, S.K.Injeti, “An efficient approach for optimal multilevel thresholding selection for grey scale images based on improved differential search algorithm”, *Aim shams engineering journal* (2018) 9, 1043-1067
- [2] M.H.Ashraf, M.Radwa, M.E.Hussein, “Multilevel thresholding for image segmentation using an improved electromagnetism optimization algorithm”, *Int jou of int mm and AI*, volume: 5 Number: 4, (2018)
- [3] P.Kaur, G.Singh, K.Parminder, “Intellectual detection and validation of automated mammogram breast cancer images by multi-class SVM using deep learning classification”, *Info in med unlocked* 16 (2019) 100151
- [4] N.Shrivastava, J.Bharti, “Breast tumor detection in digital mammogram based on efficient seed region growing segmentation, *IETE Journal of research* (2020) DOI:10.1080/03772063.2019.1710583
- [5] P.S.Game, V.Vaze, M. Emmanuel, “Bio-inspired Optimization: metaheuristic algorithms for optimization” national conference on emerging trends, challenges and opportunities in data mining and information security (NTCOMIS) (2020).
- [6] A.Ibrahim, S.Mohammed, H.A.Ali, S.E.Hussein, “Breast cancer segmentation from thermal images based on chaotic salp swarm algorithm” *IEEE Access* (2020)
- [7] A.Krishnaveni, R.Shankar, S.Duraisamy, “A Survey on Nature Inspired Computing (NIC): Algorithms and Challenges”, *Global journal of computer science and technology: D Neural & Artificial Intelligence* volume 19 issue 3 version 1.0 Year (2019)
- [8] Krishnaveni A, Shankar R, Duraisamy S, “A Review on various image thresholding methods for mammogram image segmentation”, *Compliance engineering journal* volume 11, Issue:2 (2020)
- [9] A.Nayyar, S.Garg, D.Gupta, A.Khanna, “Evolutionary Computation-Theory and algorithms”, *Advances in swarm intelligence for optimizing problems in computer science*, chap.1 CRC Press, T&F group (2018)
- [10] A.Krishnaveni, R.Shankar, S.Duraisamy, “Duck Cluster optimization algorithm with k-means clustering for mammogram image segmentation” *Solid State Technology* volume 63 number 6 (2020)
- [11] A.Krishnaveni, R.Shankar, S.Duraisamy, “An Efficient Methodology for Breast Tumor Segmentation using Duck Traveler Optimization Algorithm”, *PalArch’s Journal of Archaeology of Egypt/Egyptology*, SCOPUS Indexed ISSN NO: 1567-214X Volume 17, Issue 9, (2020).
- [12] Sannasi S.R.C, Rajaguru H, “Comparison analysis of linear discriminants analysis and cuckoo search algorithm in the classification of breast cancer from digital mammograms” *A.P.J.Cancer prevention* volume 20 (2019)
- [13] S.Ahmed, A.Tarik Rashid, A.Rawan. Al-Rashid Agha, N.K. Al-Salihi, M.M Shamsaldin “Donkey and Smuggler Optimization Algorithm: A Collaborative Working Approach to Path Finding”, *Journal of Computational Design and Engineering* (2019).
- [14] He.L and Huang S, “An efficient krill herd algorithm for color image multilevel thresholding segmentation problem, *Applied Soft Computing Journal* (2020). <https://doi.org/10.1016/j.asoc.2020.106063>.
- [15] Priyadharshini S P and Grasiyas S J, “Image segmentation with optimization techniques *International Journal of Applied Research* 2(8): 284-287 (2016)

- [16] Krishnaveni Arumugam, Shankar Ramasamy, Duraisamy Subramani “Improved Duck and Traveler Optimization (IDTO) Algorithm: A Two-way efficient approach for breast tumor segmentation using multilevel thresholding”, European Journal of Molecular & Clinical Medicine ISSN 2515-8260 Volume 7, Issue 10, 2020

Appendix

A.1 Multilevel Thresholding (MTH)

Let us consider the real linear multilevel shown below. It has more than two threshold values and levels

$$f([t_1, t_2, \dots, t_m]) = H_0 + H_1 + H_2 + \dots + H_m$$

A.2 Region of Interest (ROI)

$$D(k) = D(k - 1) + fk(k) - fl(k) - Df(k) - Dk(k);$$

A.3 K-Means Clustering (K Means)

$$DC = \{Z_j, j = 1, 2, \dots, DCn\};$$

A.4 Enhanced Duck Traveler Optimization (EDTO)

$$D_g = + \sum_{x=1}^x Y - Y_x$$

Eyeblink Detection For Liveness Detection Using Deep Convolutional Neural Network

N.Nanthini¹, N.Puviarasan², P.Aruna³

^{1,3}Department of Computer Science and Engineering, Annamalai University,
Chidambaram, Tamilnadu, India
nanthini0294@gmail.com, arunapuvi@yahoo.co.in

²Department of Computer and Information Science, Annamalai University,
Chidambaram, Tamilnadu, India
npuvi2410@yahoo.in

Abstract

Spoofing attacks on biometric systems are one of the major disorders to their use for secure applications. In case of face recognition, it is not easy for the computer to detect whether the person is live or not. In this paper, we implemented a novel approach to detect face liveness using Deep Learning. Eye Blinking is an action represented by the image sequence which consists of images with close and open state. ROSE-YOUTU datasets for liveness detection is given as the neural network input for the model training and testing. We analyse the effects of different neurons activation function on the neural network with the accuracy of the eye blink detection. The experimental result shows that ReLU activation function has the more accuracy than Sigmoid and Tanh activation function for our liveness detection model.

Keywords: *Spoofing attacks, Liveness detection, eye blink detection, activation function.*

1 Introduction

Face recognition, has developed rapidly in recent years, as a biometric identification technology. It has been widely applied to attendance and security systems. But spoofing is a major cause for the failure of various face recognition systems [1-3]. In general, Face recognition system can't distinguish a face between live and not live state. A secure system needs liveness detection in order to protect against spoofing. Liveness detection is an emerging technique for digital fraudulent. It is categorized based on motion, texture and life sign [4].

Eye blinking is one among the types from life sign category. Blinking is an action which consists of sequences of open and close state of eyes. Machine learning methods only utilizes the basic feature of images. In order to perform with videos or large sequence of images deep learning is used. Deep learning has proven to be excellent in solving complex structures with high dimensional data. There are different deep learning approaches but CNN is widely used for image and face recognition. Convolutional Neural Network (CNN) is an artificial neural network that employs to extract and increase the number of features from the input data.

The main contribution of this paper is to obtain a powerful liveness detection algorithm with high accuracy. In this paper, a deep CNN architecture is developed by adding 2 different activation functions after the fully connected layer for training step.

The rest of this paper is organized as follows. Section 2 discusses the related works of liveness detection. Section 3 explains the methodology of CNN. Section 4 presents the proposed system in detail. Section 5 shows the experimental results. Section 6 provides the conclusions.

2 Related works

Lin sun et.al first introduced the eyeblink detection for the face liveness detection system using conditional random fields (CRF) which accommodate long range contextual dependencies among the observation sequence [5]. Pan et.al proposed an undirected conditional graphical framework for blinking image sequence and computed the local binary pattern descriptors extracted in scale space for scenic clues [6]. Singh and Arora proposed an eyeblinking and mouth movement combined technique for procuring maximum reliability during face liveness detection [7].

Kim et.al classified the open and closed eye images in different conditions using deep learning. They performs zero-center normalisation for the input images before give it to neural networks which uses mean values instead of pixel values [8]. Rehman et.al proposed an efficient approach for face liveness detection which utilizes continuous data randomization in the form of small mini-batches during training a deep CNN network [9]. Avinash et.al conducted a challenge and response method for real time liveness detection for security system [10]. Musab et.al developed a modified CNN architecture for face recognition by adding normalisation layer between 2 different layers. It improves the accuracy of the system [11]. Yu et.al proposed diffusion based kernel model which enhance the edges of the each frame in the video and extract the feature called Diffusion Kernel (DK) features. It reflects the inner correlation of face images in the video [12].

3 Methodology

Here we present eye blinking liveness detection approach to detect the biometric forgery in case of 2D photo masks using deep learning. When detection of smaller regions is the case, existing models such as VGG-16, VGG-19 suffers from overfitting. So in such scenarios CNN with necessary modification gives best results. CNN is very effective in areas such as image recognition and classification. CNN is a kind of feed-forward neural networks made up of many layers. It consists of neurons that have learnable weights and biases. Each neuron takes some inputs, performs convolution and optionally follows it with a non-linearity. The structure of CNN contains Convolutional, pooling, activation function, and fully Connected layers.

3.1 Convolutional Layer

Convolutional layer is the important building block of a Convolutional Neural Network that does most of the computational operations. The key purpose of this layer is to extract features from the input data which is an image. Convolutional layer preserves the spatial relationship between pixels by learning image features using small squares of input image. The input image is convoluted by employing a set of learnable neurons. The convolutional layer analyse every smaller square of the input image in depth and as far as possible to get the higher degree of feature extraction. This produces a feature map in the output image and then the feature maps are given as input data to the next layer.

3.2 Pooling Layer

Pooling layer is usually placed between convolutional layers. The output feature maps from the convolutional layer are given as inputs to the pooling layer. The input images are divided into a set of non-overlapping rectangles. Each region is down-sampled by a non-linear operation such as average, maximum and minimum. The pooling layer does not change the depth of the three-dimensional matrix in the neural network, it reduces the dimensionality of each feature map but continues to have the most important information, so as to reduce the parameters of the whole neural network and decrease the training time. This layer achieves better simplification, faster convergence, robust to translation and distortion.

3.3 Activation Function

In neural networks, activation functions are used to perform diverse computation between hidden layers and output layers. It computes the weighted sum of input and biases, of which is used to decide if a neuron can be dismissed or not. It manipulates the presented data through some gradient processing usually gradient descent and afterwards produces an output for the neural network that contains the parameters in the data.

3.4 Fully connected layer

Fully Connected Layer refers to that every filter in the previous layer is connected to every filter in the next layer. The output from the convolutional, pooling, and activation functions are embodiments of high-level features of the input image. The goal of using the fully connected layer is to employ these features for classifying the input image into various classes based on the training dataset. It is considered as final pooling layer feeding the features to a classifier that uses activation function. The sum of output probabilities from the Fully Connected Layer is 1.

4 Proposed work

In this section we present the proposed eye blink detection using deep convolutional neural network. The proposed Deep CNN architecture is shown in fig.1. The proposed model consisting of multiple convolution layers followed by pooling layer, flattening layer, two fully connected layers and a softmax layer. The Video input is converted into series of consecutive frames. Then the frames are given as input image to the CNN model. The proposed CNN model has 5 convolutional blocks with 10 convolutional layers. Block 1 has 2 convolutional layers with 32 filters, block 2 has 2 convolutional layers with 64 filters, block 3 has 2 convolutional layers with 128 filters, block 4 and 5 has 2 convolution layer with 512 filter. All the blocks have a max pooling layer after the last convolution layer with kernel size of 3x3 filter, stride of size 1 and activation function.

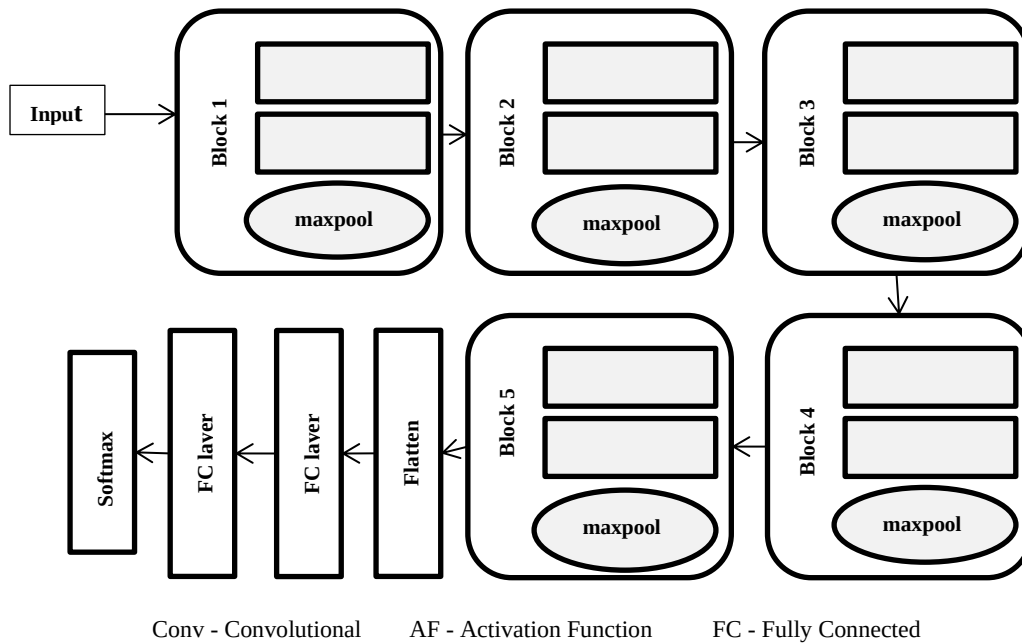


Figure 1: The proposed deep CNN Architecture for face liveness detection

The activation function in convolutional layers is to remove redundant data while conserving features and maps out these features by nonlinear functions, which is the necessary for the neural network to solve the complex nonlinear problem. In this proposed work, 3 kinds of activation functions have been applied to this model such as Sigmoid, Tanh and ReLU.

a) Sigmoid:

It is a nonlinear activation function which is also referred as logistic function. They are used for predicting probability based output and has been applied successfully in binary classification problems.

$$f(x) = \left(\frac{1}{1 + \exp^{-x}} \right)$$

b) Tanh

The Hyperbolic tangent function is a smoother function whose range lies between -1 to 1. When compared to sigmoid function, Tanh gives the better training performance on the multi-layer neural networks.

$$f(x) = \left(\frac{e^x - e^{-x}}{e^x + e^{-x}} \right)$$

c) ReLU

The rectified linear unit (ReLU) function is a faster function compared to Sigmoid and Tanh. It implements a threshold operation to each input element where values less than zero are set to 0 and eliminating the vanishing gradient problem.

$$f(x) = \max(0, x) = \begin{cases} x, & \text{if } x \geq 0 \\ 0, & \text{if } x < 0 \end{cases}$$

After the 5th block, the features are flattened to form 786944 feature values and fed to a fully connected layer having 4096 neurons consists a total of 32,485,761 trainable parameters. The number of neurons in the fully connected layers was also altered to fit the proposed model. The dense layer hidden neurons are changed from 4096 to 512 neurons in the first dense layer and to 128 neurons in the second dense layer respectively. Then classify 2 classes using Softmax layer. The final detection of open and closed eye images is performed based on the output of the Softmax layer.

5 Experimental results

5.1 Dataset:

For training phase, MRL Eye Dataset is used. It contains total of 84,898 images of both eye open and close state from 37 different persons. To obtain the eye images, the eye detector based HOG with SVM classifier is used. Fig.2 shows the sample eyes images of MRL eye dataset. For testing phase, ROSE-YOUTU database is used. It contains of 150 videos from 20 different persons of the categories with glass, without glass, photo imposters and video captures. The length of the one video clip is about 10 to 15 seconds with 30 frames per second.



Fig.2. Sample images of training dataset

5.2 Training and testing

The proposed model is trained for 100 epochs using randomly selected 5000 eye images from the training dataset. In training phase, the model has 32,485,761 trainable parameters with their weights are adjusted to 880,189 times for each epoch. For testing, a video input is given to the proposed model to classify the open and closed state of eye for the eyeblink detection. Fig.3. shows the detection of eyeblinking from the input video.



Fig.3. Screenshot of Eyeblink detection using proposed model

The performance of the proposed CNN is evaluated by using four metrics such as accuracy, precision, recall and F1score. The model saved its best accuracy with patience=10 for the given 3 activation functions Simoid, Tanh and ReLU.

The formulas for above mentioned metrics are given below,

$$Accuracy = \frac{TP+TN}{total\ no.\ of\ samples\ given} \quad (1)$$

$$Precision(pr) = \frac{TP}{TP+FP} \quad (2)$$

$$Recall(rc) = \frac{TP}{TP+FN} \quad (3)$$

$$F1score = \frac{pr \times rc}{pr+rc} \quad (4)$$

Where, TP (true positives) denotes the number of correct detections, TN (true negatives) denotes the number of wrong detection of eyes. FP (false positives) denotes the number missed eye, FN (false negatives) denotes the number of incorrect detection of eyes.

The average accuracy, precision, recall and F1score for the proposed model were 0.75, 0.76, 0.73 and 0.81. The results suggest the proposed model for eyeblink detection classify the classes with higher accuracy. The evaluation metrics for the proposed deep CNN model is shown in table 1.

Table1: Evaluation metrics proposed deep CNN model

| Evaluation metrics | Sigmoid | | Tanh | | ReLU | |
|--------------------|---------|-------|------|-------|------|-------|
| | open | Close | open | close | open | close |
| Precision | 0 | 0.49 | 0.84 | 0.86 | 0.95 | 0.99 |
| Recall | 0 | 1.0 | 0.81 | 0.84 | 0.99 | 0.94 |
| F1score | 0 | 0.66 | 0.83 | 0.83 | 0.97 | 0.96 |

The performance of the proposed system is evaluated by calculating the average of above evaluation metrics and accuracy. The proposed model is trained with epochs in the interval of 25. It is observed that the accuracy remains same for the epochs from 50. Table 2 shows the performance of various activation functions used in the proposed model and fig.4 shows its corresponding chart.

Table 2: Performances of various activation functions

| Activation function | Precision | Recall | F1score | Accuracy |
|---------------------|-----------|--------|---------|----------|
| Sigmoid | 0.49 | 0.99 | 0.66 | 0.48 |
| Tanh | 0.84 | 0.81 | 0.83 | 0.82 |
| ReLU | 0.94 | 0.93 | 0.95 | 0.96 |

From the above analysis, the accuracy for Sigmoid activation function is 48%, Tanh activation function is 82% and ReLU activation function is 96%. It is observed that, by using ReLU activation function for the proposed deep CNN model achieves the higher accuracy.

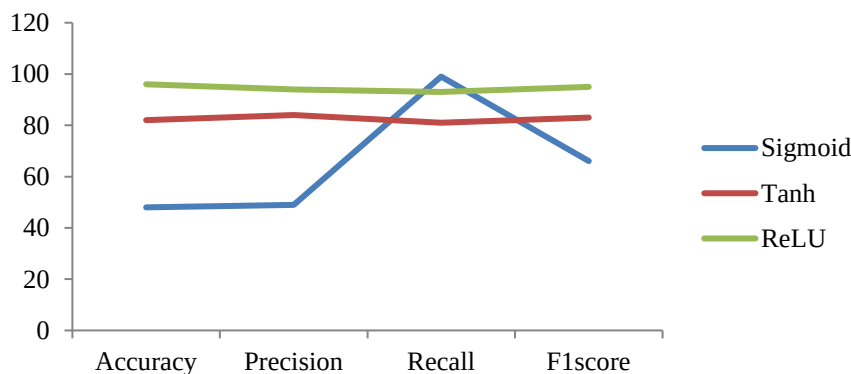


Figure 4: Performance of Proposed Deep CNN Model

6 Conclusion

This work proposed a deep CNN model for liveness detection using eyeblink detection. The performance of neurons in different activation function in the proposed model is evaluated by calculating the accuracy values. From the above experimental results of our proposed model, it is inferred that ReLU activation function results excellent and has more accuracy of 96% than Sigmoid and Tanh activation functions.

References

- [1] Md Rezwan Hasan, S M Hasan Mahmud and Xiang Yu Li, "Face Anti-Spoofing Using Texture-Based Techniques and Filtering Methods", journal of physics-conference series (IOP-2019), pp.1-10, 2019.
- [2] S.G Bhele and V.H Mankar, "A Review Paper on Face Recognition Techniques", International journal of research in computer science engineering and technology, vol.1, pp. 2278-323, 2012.
- [3] D.N Parmar and B. Mehta, "Face Recognition methods and applications", international journal of computer technology applications, vol.4, pp.84-86, 2013.
- [4] Klaus Kollreider, Hartwig Fronthaler, Maycel Isaac Faraj, and Josef Bigun, "Real-Time Face Detection and Motion Analysis With Application in "Liveness" Assessment", IEEE transactions on information forensics and security, vol. 2, issue. 3, pp. 548-558, 2007.
- [5] Lin Sun, Gang Pan, Zhaohui Wu, Shihong Lao, "Blinking-Based Live Face Detection Using Conditional Random Fields", International Conference (ICB 2007), pp. 252-260, 2007.
- [6] Gang Pan, Lin Sun, ZhaohuiWu, YuemingWang "Monocular camera-based face liveness detection by combining eyeblink and scene context", Telecommunication system, Springer, vol.47, pp. 215-225, 2011.
- [7] Manminder Singh, A.S. Arora "A robust anti-spoofing technique for face liveness detection with morphological operations", Optik, Elsevier, vol.139, pp.347-354, 2017.

- [8] Ki Wan Kim, Hyung Gil Hong, Gi Pyo Nam and Kang Ryoung Park "A Study of Deep CNN-Based Classification of Open and Closed Eyes Using a Visible Light Camera Sensor", *sensors*, MDPI, vol.17, pp.1-21, 2017.
- [9] Yasar Abbas Ur Rehman, Po. Lai Man, Mengyang Liu "LiveNet: Improving Features Generalization for Face Liveness Detection using Convolution Neural Networks", *Expert system with Applications*, Elsevier, vol.45, pp.1-25,2018.
- [10] Avinash Kumar Singh, Piyush Joshi, G. C. Nandi "Face Recognition with Liveness Detection using Eye and Mouth Movement", *International Conference on Signal Propagation and Computer Technology (ICSPCT)*, pp.592-597, 2014.
- [11] Musab Coşkun, Ayşegül Uçar, Özal Yıldırım, Yakup Demir "Face Recognition Based on Convolutional Neural Network", *international conference on modern electrical and energy systems(IEEE)*, vol.10, pp.2-5, 2017.
- [12] Changyong Yu, Chengtang Yao, Mingtao Pei, Yunde Jia "Diffusion-based kernel matrix model for face liveness detection", *image vision and computing*, Elsevier, vol.89, pp.88-94, 2019.

A Comparative Study on Liver Disease Prediction using Machine Learning Approach

Omprakash S¹, Soumya R²

¹ Assistant Professor, Department of Computer Science, Sankara College of Science and Commerce Saravanampatti, Coimbatore-35, Tamilnadu

² MPhil Research Scholar, Department of Computer Science, Sankara College of Science and Commerce Saravanampatti, Coimbatore-35, Tamilnadu

Abstract

Data mining makes use of algorithms to find out interesting information. Data mining tasks involve Classification, Clustering, Sequence discovery, forming Association rules, etc. Data mining techniques have been generally used in the procedure of disease identification, drug development etc. Few examples are the prediction of liver disease, prediction of heart disease, etc. The use of machine learning technique in early disease identification is very much supportive for medical practitioners and to medical-related people. Classification algorithms are widely used to accurately predict the item belongs to a particular class or not. Classification algorithms play a foremost role in determining the accurate prediction of diseases. Classification is of two types- binary classification or multiclass classification. In this era of advanced technologies, the use of machine learning approaches is highly appreciable and it takes the problem-solving method to a higher level. A comparison between different approaches is carried out here and it was found that the Random Forest approach is the best while using Weka Tool and Ensemble Bagged Tree is best while using the Matlab tool.

Keywords: *Classification, decision stump, J48, RepTree, LWL, RandomForest, IBK, Kstar, Quadratic SVM, Bagged Trees*

1 Introduction

The process of dredging the required data from the large database is called data mining and thus obtained information is used for predicting or analyzing the hidden facts. This technique is extensively used in various fields like health care, education, forecasting, stock prediction, financial prediction etc.

The liver is recognized to be the second-largest organ in the human body. The liver performs numerous fundamental functions such as immunity, digestion, a stash of supplements, protein creation, disposing of poisons from the body. The malfunction of the liver paves the way to serious health conditions [1].

The performance of the liver is tested by two types of tests such as imaging tests and liver function tests. Liver sickness occurs due to the following factors like stress, food habits, excess utilization of alcohol, drug ingestion, etc. Classification algorithms are functionally used in medical data sets for disease prediction and analysis.

2 Review of Literature

Nazmun Nahar and Ferdous Ara et al., [2] applied decision tree algorithms: J48, LMT, Random Tree, Random Forest, REPTree, Decision Stump, and Hoeffding Tree for the forecast of liver disease. From the analysis, it was discovered that the Decision Stump algorithm works effectively when compared to other algorithms and its accuracy rate is 70.67%.

Dr.S.Vijayarani, Mr.S.Dhayanand[3] has conducted a study on liver disease prediction using classification algorithms. The algorithms chosen are Naïve Bayes and support vector machine (SVM). Assessments of these algorithms were based on the performance factors like classification accuracy and execution time. From the results, it concludes that the SVM classifier is reflected as the best classification algorithm due to its highest classification accuracy values.

Dhamodharan S [4] has used data mining techniques in foretelling about the three major liver diseases such as Liver cancer, Cirrhosis, and Hepatitis. Naive Bayes and FT Tree algorithms were used for disease forecast. Comparison of these two algorithms was carried out based on the classification accuracy measure. From the experimental results, it was concluded that Naïve Bayes was the best algorithm.

M Banupriya, P Laura Juliet, P R Tamilselvi[5]proposed a system that includes the PSO feature selection methods for the Indian Liver Patient Dataset. They performed classification of the liver disease using algorithms such as J48, MLP, SVM, Random Forest, and Bayesnet Classification. It has been seen that Bayes net and J48 Classification delivers better results.

Rosalina A H, NoraZiah A [6] for hepatitis diagnosis used Support Vector Machine (SVM) and Wrapper Method. Pre-processing was done using wrapper methods to eliminate the noise features. Firstly SVM feature selection was executed to get better accuracy and to reduce noisy or irrelevant data. They have attained the target by combining Wrappers Method and SVM techniques.

Omar S. Soliman, Eman Abo Elhamd[7] have suggested a hybrid classification system for HCV diagnosis, by blending Modified Particle Swarm Optimization(PSO) algorithm and Least Squares Support Vector Machine (LS-SVM). Feature vectors were extracted using Principal Component Analysis(PCA) algorithm. Because the LS-SVM algorithm is responsive to the changes of values of its parameters, Modified-PSO Algorithm was used to explore the optimal values of LS-SVM parameters in less iteration. The anticipated system was executed and assessed on the benchmark HCV data set from the UCI repository of machine learning databases. From the investigational results, the planned system attained maximum classification accuracy.

3 Methodology

3.1 Dataset

The dataset named Indian Patient Liver Dataset,(IPLD) is collected from UCI Machine Learning Repository. This dataset contains five hundred and eighty-three instances with ten attributes. IPLD dataset is a mixed type dataset that comprises both nominal and numeric attributes.

This dataset encompasses 416 liver patient records and 167 non-liver patient records. This dataset was collected from Northeast of Andhra Pradesh, India. This dataset comprises details of 441 male patients and 142 female patients. Table 1 represents the attribute names and data types of the ten attributes.

Table 1:Dataset

| <i>Attribute Name</i> | <i>Datatype</i> |
|---------------------------------------|-----------------|
| Age | Numeric |
| Gender | Nominal |
| Total Bilirubin(TB) | Numeric |
| Direct Bilirubin(DB) | Numeric |
| Alkphos Alkaline Phosphate(Alk) | Numeric |
| SGPT Alamine Aminotransferase | Numeric |
| SGOT Aspartate Aminotransferase | Numeric |
| Total Proteins(TP) | Numeric |
| Albumin(ALB) | Numeric |
| Albumin and Globulin Ratio(A/G Ratio) | Numeric |

3.2 Weka

Weka is a data mining tool that is written in java and developed at Waikato. [9]WEKA is a very efficient data mining tool to categorize the accuracy by applying different algorithmic approaches and evaluate based on datasets. It is also used to perform clustering and association techniques. Here whole training set is first analyzed and later it is divided into two- 80% (training data)and 20%(test data).

Decision Tree [2]

J48: J48 is an advanced version of C4.5. The principle of this algorithm is to use the divide-and-conquer policy. It uses the pruning method to construct a tree. It is a common method that is used in information gain or entropy measure. Thus it is a tree structure with the root node, intermediate, and leaf nodes. Leaf node holds the decision and helps to achieve the result.

REP Tree: REP Tree is a speedy decision tree learner. It is used to construct a regression tree using entropy as the impurity measure and prunes using reduced-error pruning. It arranges values for numeric attributes.

Decision Stump: Decision stumps are decision trees with a single label. A stump has multiple layers. It stops after the first split. Decision stumps are used with large datasets. It is also used to make a simple yes/no decision model for smaller datasets.

Random Forests: Ensemble algorithms are a dominant class of machine learning algorithms that combine the predictions from multiple models. Random Forest is an expanded version of bagging for decision trees that can be used for classification or regression Random Forest is an improvement upon bagged decision trees that obstructs the greedy splitting algorithm during the construction of the tree so that split points can only be selected from a random subset of the input attributes.

Lazy Learning(Instance-based)

Locally Weighted Learning(LWL): Locally Weighted Learning is a class of function approximation techniques, where a prediction is carried out by using an approximated local model around the current value.

LWL is also termed *lazy learning* because the processing of the training data is reallocated until a query point needs to be retested.

This approach turns out LWL a very accurate function approximation method where it is effortless to append new training points. The performance measures include Kappa statistic, mean absolute error, root mean squared error, relative absolute error, root relative squared error.

Kstar: K* is an instance-based classifier It differs from other instance-based learners by using an entropy-based distance function. The performance measures include Kappa statistic, mean absolute error, root mean squared error, relative absolute error, root relative squared error.

IBK(instance-based): K-Nearest Neighbor Algorithm(KNN) is also known by the name IBK. The IBK algorithm does not create a model, but, it initiates a prediction for a test case. The IBK algorithm uses a distance measure to trace *k* “close” instances in the training data for each test instance and utilizes those elected instances to make a prediction. The performance measures include Kappa statistic, mean absolute error, root mean squared error, relative absolute error, root relative squared error.

3.3 Matlab

Algorithms used in Matlab are Quadratic SVM(Support Vector Machine) and Bagged Trees. Principal Component Analysis with 6 features is applied to both the approaches and the result is found out. The six features included are TB,ALK,SGPT,SGOT,TP,ALB.

Quadratic Support Vector Machine: A support vector machine (SVM) is a supervised learning algorithm used for many classification and regression problems, like image classification, speech recognition, text classification, signal processing medical applications, natural language processing [10].

Quadratic support vector machine [11] corresponds to solving a *quadratic* optimization problem to fit a hyper plane that minimizes the soft margin between the classes. Margin is the maximum distance.

Ensemble Bagged Trees: *Ensemble methods*, which blend several decision trees to produce better predictive performance than utilizing a single decision tree. The notion in the ensemble model is that a group of weak learners gather mutually to form a strong learner.

Bagging is an approach to diminish the variance in the prediction which is done by constructing supplementary data for training from the original dataset. Repeated groups of datasets are chosen and combined which result in numerous datasets. Boosting is an iterative procedure that adjusts the weight of an observation based on the last classification.

A Bagging classifier is an all-together estimator that mounts base classifiers each on random subsets of the original dataset and then coalesce their predictions to form a final prediction.

4 Findings

4.1 Accuracy

Classification Accuracy is the ratio of the number of correct predictions to the total number of input samples. It is found from table 2 that after testing Random forest shows the highest accuracy in the Decision tree classifier and LWL is the best classifier in instance-based after the split.

Table 2: Accuracy

| Classification Algorithm | Accuracy(before split) | Accuracy(after split) |
|--------------------------|------------------------|-----------------------|
| LWL | 71% | 72% |
| IBK | 99% | 54% |
| KSTAR | 100% | 61% |
| J48 | 87% | 72% |
| RANDOM FOREST | 100% | 73% |
| REP TREES | 73% | 71% |
| DECISION STUMP | 71% | 72% |

4.2 Mean Absolute Error (MAE)

MAE measures the average magnitude of the errors in a set of predictions, without considering their direction. It's the average over the test sample of the absolute differences between prediction and actual observation where all individual differences are equiweight.

$$\text{MAE} = \frac{1}{n} \sum |y_j - \hat{y}_j| \quad (1)$$

It is observed from Table 3 that the error rate is minimal for the Kstar algorithm and LWL before and after split respectively.

Table 3: Mean Absolute Error

| <i>Classification Algorithm</i> | <i>Accuracy(before split)</i> | <i>Accuracy(after split)</i> |
|---------------------------------|-------------------------------|------------------------------|
| LWL | 0.362 | 0.357 |
| IBK | 0.0051 | 0.4532 |
| KSTAR | 0.001 | 0.5569 |
| J48 | 0.1921 | 0.4047 |
| RANDOM FOREST | 0.1238 | 0.3457 |
| REP TREES | 0.3322 | 0.3467 |
| DECISION STUMP | 0.3699 | 0.3638 |

4.3 Accuracy (MATLAB)

It is observed from table 4 that Ensemble Bagged trees perform well even after PCA. So it is well suited to predict liver disease. Initially, all ten features were considered to train the set. The six features taken into considerations for PCA are: TB, ALK, SGPT, SGOT, TP, and ALB.

Table 4:Accuracy from Matlab

| <i>Classification algorithm</i> | <i>Accuracy</i> | <i>Accuracy(after PCA with 6 features)</i> |
|---------------------------------|-----------------|--|
| QSVM | 70% | 75% |
| ENSEMBLE BAGGED TREES | 75.6% | 76.3% |

5 Conclusion

An analysis of machine learning algorithms was conducted for liver disease prediction. When training data was divided to 80%split maximum accuracy was shown by LWL and Random Forest. When comparing the error rate KStar and LWL have shown less error rate. In the case of Mat lab algorithms, Ensemble Bagged trees were found to be best suited than Quadratic SVM. A combination of algorithms, dimensionality reduction techniques, can be implemented in the future to detect the sickness prediction. Fuzzy methods, Learning vector methods, etc approaches can be further implemented to improve the accuracy in the future.

References

- [1] Bendi Venkata Ramana, Surendra. Prasad Babu. M, Venkateswarlu. N.B, A Critical Study of Selected Classification Algorithms for Liver Disease Diagnosis, International Journal of Database Management Systems (IJDMS), Vol.3, No.2, May 2011 page no 101-114
- [2] Nazmun Nahar and Ferdous Ara, "Liver disease prediction by using different decision tree techniques", International Journal of Data Mining & Knowledge Management Process (IJDMP), Vol.8, No.2, March 2018.
- [3] Dr.S.Vijayarani, Mr.S.Dhayanand, "Liver disease prediction using SVM and Navies Bayes", International Journal of Science Engineering and Technology Research, Vol.4, Issue 4, April 2015.
- [4] Dhamodharan. S, Liver Disease Prediction Using Bayesian Classification, Special Issue, 4th National Conference on Advanced Computing, Applications & Technologies, May 2014, page no 1-3.
- [5] M. Banu Priya, P. Laura Juliet P.R. Tamilselvi," Performance Analysis of Liver Disease Prediction Using Machine Learning Algorithms", International Research Journal of Engineering and Technology, Vol.5, Issue 1, January 2018.
- [6] Rosalina. A.H, Noraziah. A. "Prediction of Hepatitis Prognosis Using Support Vector Machine and Wrapper Method", IEEE, (2010), 2209-22
- [7] Omar S.Soliman, Eman Abo Elhamd, "Classification of Hepatitis C Virus using Modified Particle Swarm Optimization and Least Squares Support Vector Machine", International Journal of Scientific & Engineering Research, Volume 5, Issue 3, March-2014 122.M. Young, The Technical Writer's Handbook. Mill Valley, CA: University Science, 1989.
- [8] R Kalaiselvi, G Santhoshini, "A Comparative Study on Predicting the Probability of Liver Disease" International Journal of Engineering Research & Technology (IJERT) ISSN: 2278-0181 Vol. 8, Issue 10, October-2019
- [9] S. S. Aksenova , 'Machine Learning with WEKA -WEKA Explorer Tutorial for WEKA Version 3.4', 2004.

- [10] Omprakash S, Ravichandran M. Ant Colony Optimization Based Support Vector Machine Towards Predicting Coronary Artery Disease. *International Journal of Recent Technology and Engineering*. 2019;7:210–215
- [11] Omprakash S, Ravichandran M. Prediction of Coronary Artery Disease Using Core Principal Component Analysis Based Support Vector Machine. *International Journal of Scientific & Technology Research*. 2019;8:791–798.
- [12] A. Ghosal, *Robotics: Fundamental Concepts and Analysis*. New Delhi: OxfordUniversity Press, 2006.
- [13] J.-P. Merlet, “Singularity configurations of parallel manipulators and Grassmanngeometry,” *International Journal of Robotics Research*, vol. 8, pp. 45–56, 1989.
- [14] B. Roth, “Screws, motors and wrenches that cannot be bought in a hardwarestore,” in *Robotics Research: The First International Symposium*, M. Brady and R. Paul(Eds.), pp. 679–693, 1984.
- [15] D. Sonavane, “Instantaneous kinematics of Stewart platforms using dual numbers,” M. E. thesis, Indian Institute of Science, Bangalore, India, Jan. 2002.
- [16] J. M. McCarthy, *Instantaneous kinematics of point and line trajectories*. PhDthesis, StanfordUniversity, 1979.

Construction of Question Answering System for Optimized Knowledge Graph

¹G. Kavitha, ²Dr. V. Khanna

¹Research Scholar, ²Professor

¹Department of Computer Science and Engineering

²Department of Information Technology

Bharath Institute of Higher Education and Research (BIHER)

Agaram Main Rd, Selaiyur, Chennai, Tamil Nadu, India

Mail id: ¹kavithag90@gmail.com, Mobile: ¹9047469800

Abstract

The success of search engine depends on user satisfaction of results for the given query. These results are based on the keywords given for search. The user can obtain a suitable answer for their enquiries only when the user and knowledge bases are linked. The aim is to provide the precise answer to the query by using knowledge base. To obtain precise answers directly, a question answering system is modified Optimize knowledge graph for RDF repository with Calculated Semantic weightage using optimized Knowledge Graphs and paths in a knowledge base.

Keywords: Artificial Intelligence Mark-up Language, Calculated Semantic Weightage, Optimized Knowledge Graphs Matching

1 Introduction

Question answering applications usually retrieve an answer from large database. These questions can be written natural language. Question answering system is an important tool in search engine optimization. Natural language Processing plays a vital role for resolving the question answering job. In recent years, the Natural Language Processing have been dominated by deep neural networks which fundamentally mimic the human brain. Thus have tendency to produce better results [6,7].

Recently, several approaches deploy different technologies to apprehend questions given in natural language text and after analysing the question. Simultaneously, the increasing amount of data makes more difficult for the search engine to produce appropriate results. The aim of a question answering (QA) system is to calculate the correct answers to the queries given in natural language, by using their knowledge base. Knowledge bases are usually organized in accurate triples (subject, predicate and object) with RDF standard. So, the main job of a QA system is to interpret a natural language question into a suitable SPARQL query in order to provides the correct answer [8].

In this paper, we focus answering question with Multilingualism, Source heterogeneity and Scalability. Multilingualism is the capability of a scheme to reply the same questions framed in different languages. Source heterogeneity is the ability to answer questions that might only be replied by resourcing to the grouping of organized datasets and information specified in free text documents. Scalability is the performance of a system in replying questions at a swelling pace.

2 Literature Survey

In this paper, QAS is developed that receives the question from the user and perform syntactic and semantic analyse using Natural Language Processing, considering pedagogical Ontologies. Then the system verify if the question is new or already answered. If it is answered it produce the results from the database else start to Finding the Answer Process through different agents. Till the answer is not found automatically, other tutors and learners subsidise in answering the question [1].

In this paper, the field of Question Answering is explained with respect to an learning environment. New framework is proposed based on a dynamic self-evolving Concept Network. The framework is built specifically for a particular subject [2].

In this paper, the algorithm is developed to answer recommender system. It consists of three steps. In first step, the system finds the similar cases in the past. Then in the second step, the system estimates the quality of answers. Finally, it considers both question similarity and answer estimated to obtain a final score. This will helps in producing best answer for user's question [3].

An open domain question answering system is proposed in this paper. There are number of attempts made in QAS to provide the solution. But this approach is a unique one that provides the answer for the given question by using web snippets. Two domains namely sports and agriculture are tried to check the results. It provides the estimated results for the given question [4].

To improve user satisfaction and the success of question answering systems, a user centred evaluation model is proposed. A schema is extracted based on a review and synthesis of existing user satisfaction and technology. This approach has great contribution on achievement of understanding of short domain questions in natural language. The experiments show that this method could be applied to QA system based on database. It will return answers with higher accuracy and without redundancy. The proposed user-centered evaluation model provides a framework for the design of question answering systems from the user's perspective and that it could help to increase user acceptance of QAS [5].

3 Existing System

Existing system composed of three layers: User layer, Answer Finding Layer and Database layer.

User layer: It acts as a interface to communicate with the learners and tutors. It suits with multiple platform.

Answer Finding Layer: This is the main layer of the proposed system, in which the question is received as input and the answer is generated as output. Different agents work together in 3 global phases in order to provide the right answer:

- 1) **Question Analysing:** Question Analysing where syntactic and semantic analysis is performed.
- 2) **Answer Generation:** To generate the answer, the Answer Generation Agent needs to collaborate with the Data Extraction agents and work on different data to extract the right components of the answer that matches user.
- 3) **Answer Validation:** Validation is performed before saving the Question/Answer to the Database.

Database layer: It contain the different databases to generate the answer.

Drawbacks of Existing System:

1. This system focuses on only question answering process in education system and not suited with other field.
2. Storing Database in the system makes it more complex to maintain and consumes more space.

4 Proposed System Architecture

The Fig.1 defines the suggested System Architecture. The detailed explanation is provided below. Firstly, this system has itemized questions and its response is stockpiled in database for reference.

If any user inputs are identical, the suggested system recognizes the question and the response from the database. Subsequently, the Tree-tagger parser alters the given question in the form of syntactic parsing to take the Noun, Verb, Adverb and Adjective. The projected work contemplates Noun, Verb, Adverb and Adjective to enhance the QA systems. The POS (Parts-of-Speech) checks for the resemblance matching with the nodes of the database built by KG.

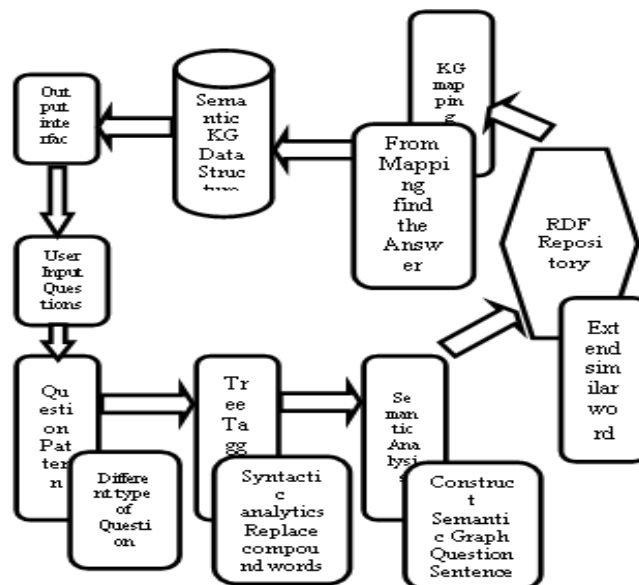


Figure 1: Proposed System Architecture

If the answer is mined from the Stored Data Structure, it shows the answer and stores the question as well as the answer in the database for future recovery. If the system flops, it sends the text to the user as “answer not

found". Based on question levels the user question is identified. Noun, verb, adverb and adjective phrase are extracted using Tree-Tagger Parsers.

Table 1: Parsing of Question

| Question | Question Parser Output | | | | | | | |
|-------------------------------------|------------------------|----------------------|-----|-------|----|-----|----|------|
| | VV | NN | VBZ | WN | IN | DT | JJ | WP |
| What is meant by "QA System" | | QA System | is | Meant | by | | | What |
| Define Abstract class | Define | Abstract class | | | | | | |
| Give the Definition of Interface | Give | Interface Definition | | | of | the | | |
| Explain Package | Explain | Package | | | | | | |
| What is the latest version in HTML? | | Version HTML | is | | in | the | | what |

Every question category is examined to represent the precise meaning by the learner. Tree Tagger parser aids to find the head chunk of Noun phrase and Verb phrase for the given question. Table 1 describes the Parsing of Question, For instance, question kind with "What" can be denoted in diverse forms. These forms of questions are commonly characterized as "What [NP] [do/does/did/AUX] [functional-words] [NP] [VP] X? The clarification of the question is derived by the parser.

5 Conclusion

The suggested technique allows e-learning users to deliver changes to the Question Answering Scheme. This ground-breaking method recognises the diverse patterns of the questions that have attained a more time efficiency. This technique also uses noun, verb, adverb and adjective for this Semantic Weightage Based Optimized Knowledge Graphs Matching over Knowledge Graphs and also focus on any domain specific Semantic Weightage Knowledge Graph that can be combined for improvement of e-learning applications.

6 Future Work

The success of the search depends on the keywords. Here regional languages are not considered in the keyword. In the future, the user's regional language also can be considered as a keyword of search and attain improved results.

References

- [1] Haarmann, Bastian, Claudio Martens, Henning Petzka, and Giulio Napolitano. "A Mighty Dataset for Stress-Testing Question Answering Systems." In *2018 IEEE 12th International Conference on Semantic Computing (ICSC)*, pp. 278-281. IEEE, 2018.
- [2] Agarwal, Abhishek, Nikhil Sachdeva, Raj Kamal Yadav, Vishaal Udandarao, Vrinda Mittal, Anubha Gupta, and Abhinav Mathur. "EDUQA: Educational Domain Question Answering System Using Conceptual Network Mapping." In *ICASSP 2019-2019 IEEE International Conference on Acoustics, Speech and Signal Processing (ICASSP)*, pp. 8137-8141. IEEE, 2019.
- [3] Yang, Shengqi, Fangqiu Han, Yinghui Wu, and Xifeng Yan. "Fast top-k search in knowledge graphs." In *2016 IEEE 32nd international conference on data engineering (ICDE)*, pp. 990-1001. IEEE, 2016.
- [4] Menaha, R., A. Udhaya Surya, K. Nandhini, and M. Ishwarya. "Question answering system using web snippets." In *2017 International Conference on I-SMAC (IoT in Social, Mobile, Analytics and Cloud)(I-SMAC)*, pp. 387-390. IEEE, 2017.
- [5] Mishra, Megha, V. K. Mishra, and H. R. Sharma. "Leveraging knowledge based question answer technology to address user-interactive short domain question in natural language." In *2012 2nd National Conference on Computational Intelligence and Signal Processing (CISP)*, pp. 86-90. IEEE, 2012.

- [6] Pudaruth, Sameerchand, Kajal Boodhoo, and Lushika Goolbudun. "An intelligent question answering system for ict." In *2016 International Conference on Electrical, Electronics, and Optimization Techniques (ICEEOT)*, pp. 2895-2899. IEEE, 2016.
- [7] G. Kavitha, Dr.V. Khanna, Scheme for Question Answering System By Using Optimized Knowledge Graphs , PalArch's Journal of Archaeology of Egypt / Egyptology: Vol. 17 No. 7 (2020): PalArch's Journal of Archaeology of Egypt/Egyptology
- [8] G. Kavitha, Dr.V. Khanna, Refine Search by Question Answering System by using Knowledge Graphs , PalArch's Journal of Archaeology of Egypt / Egyptology: Vol. 17 No. 7 (2020): PalArch's Journal of Archaeology of Egypt/Egyptology.

Detection of Black Hole Attacks in Manets By Using Principle of Exclusion and Inclusion

Dr G Revathy,
Erode Sengunthar Engineering College(Autonomous),
Erode, Tamilnadu.

Abstract

A mobile ad-hoc network (MANET) is a self-configuring network of mobile routers related by wireless links the amalgamation of which form an capricious topology. Black hole attack is a variety of attack in which a malevolent node deceives the source node and advertises itself for having the unswerving path. In this way the source node than establishes a route to malevolent node and sends its complete data packet to the malevolent node. By doing this, the malevolent node can divest the traffic from the source node. In this paper we have discussed about the loom for detecting black hole attack in MANET using neighborhood based method. This method can effectively detect black hole attack.

Keywords: AODV, black hole attack, neighbor set method, MANET, security, attack, throughput

1 Introduction

Mobile Ad-Hoc Networks are sovereign and decentralized wireless systems. MANETs consist of mobile nodes that are gratis in moving in and out in the network. Nodes are the systems or devices i.e. mobile phone, laptop, personal digital assistance, MP3 player and personal computer that are participating in the network and are mobile. These nodes can act as host/router or both at the same time. They can form random topologies depending on their connectivity with each other in the network. These nodes have the capability to configure themselves and because of their self configuration aptitude, they can be deployed urgently without the need of any infrastructure. Many routing protocols have been urbanized for MANETS, i.e. AODV, OLSR, DSR etc. Precautions in Mobile Ad-Hoc network is the most imperative concern for the basic functionality of network. The availability of network services, discretion and reliability of the data can be achieved by assuring that refuge issues have been met. MANETs often undergo from justification attacks because of its features like open medium, altering its topology vigorously, lack of central monitoring and administration, cooperative algorithms and no clear resistance mechanism. These factors have changed the battle field situation for the MANETs against the security threats. The MANETs work without a federal organization where the nodes communicate with each other on the basis of mutual trust. This characteristic makes MANETs more exposed to be browbeaten by an attacker inside the network.

Wireless links also makes the MANETs more predisposed to attacks, which make it easier for the attacker to go within the network and get admittance to the enduring communication. Mobile nodes present within the assortment of wireless link can eavesdrop and even partake in the network. MANET is very much popular due to the fact that these networks are dynamic, infrastructure less and scalable. Despite the fact of esteem of MANET, these networks are very much exposed to attacks. Wireless links also makes the MANET more inclined to attacks which make it easier for the aggressor to go within the network and get admittance to the constant communication. Security in Mobile Ad-Hoc Network is the most significant concern for the basic functionality of network. The accessibility of network services, confidentiality and reliability of the data can be achieved by assuring that protection issues have been met. MANETs often endure from security attacks because of its features like open medium, changing its topology dynamically, lack of central monitoring and management, cooperative algorithms and no clear defense mechanism. These factors have distorted the battle field situation for the MANETs against the security threats. The MANETs work without a federal management where the nodes communicate with each other on the basis of communal trust. This characteristic makes MANETs more vulnerable to be subjugated by an attacker inside the network. Wireless links also makes the MANETs more inclined to attacks, which make it easier for the attacker to go inside the network and get access to the ongoing communication [2, 5]. Mobile nodes present within the range of wireless link can overhear and even participate in the network. The routing protocols in MANET are broadly classified in three categories:

1. Pro-active (table-driven) routing protocols

2. Reactive (On demand) routing protocols
3. Hybrid routing protocols

We propose a neighbor set-based method. Our elucidation can be briefly elaborated as: Once the normal path innovation procedure in a routing protocol is completed, the source node sends a unique control packet to appeal the destination to send its current neighbor set. By comparing the received neighbor sets, the source node can determine whether there is a black hole attack in the network. To mitigate the bang of the black hole attack, we design a routing recovery protocol to establish the path to the correct destination.

AODV is reactive protocol, when a node wishes to start diffusion with another node in the network to which it has no route; AODV will provide topology information for the node [4]. AODV use control messages to find a route to the destination node in the network. There are three types of control messages in AODV which are discussed below.

Route Request Message (RREQ):

Source node that needs to converse with another node in the network transmits RREQ message. AODV floods RREQ message, using escalating ring technique. There is a time to live (TTL) value in every RREQ message, the value of TTL states the number of hops the RREQ should be transmitted.

Route Reply Message (RREP):

A node having a requested uniqueness or any intermediate node that has a route to the requested node generates a route reply RREP message back to the originator node.

Route Error Message (RERR):

Every node in the network keeps monitoring the link status to its neighbor's nodes during active routes. When the node detects a link crack in an active route, (RERR) message is generated by the node in order to notify other nodes that the link is down.

AODV is a reactive on-demand routing protocol which means a route flanked by two nodes will be resolute only when there is data to be transmitted. Each node's routing table only contains the next hop to a meticulous destination, so the information on the route to be traversed by a packet is disseminated along all the nodes on the path. Neighbor connectivity is conventional with periodic Hello Messages. Routes are found by flooding of route request (RREQ) messages (Fig. 1). As each node receives and retransmits the RREQ it records the preceding hop in its routing table. A unicast route reply (RREP) is sent back from the destination or any node with a route to the objective. Nodes route this RREP back to the source using the previous hop information recorded from the RREQ. On the way the RREPs previous hop information is recorded into each nodes routing table scenery up the final path to the destination. RREQs use hop counts and RREP use objective succession numbers (DSNs) so the sender can discriminate routes based on hop count and newness. Route maintenance is done using route error (RERR) messages. On sensing a broken link in an active route (failing to receive regular HELLO messages from a node), a RERR message is sent to its upstream neighbors that use it as the next hop in the broken route(s). Different kinds of attacks have been analyzed in MANET and their affect on the network. An attack occurs when an intruder tries to exploit vulnerabilities of a system. There are many types of attacks in MANET.

Generally vocalizations, these attacks can be confidential into two broad categories: passive and active attacks [3,6]. In passive attacks, the attackers characteristically involve eavesdropping of data, thus disclose the information of the position and move patterns of mobile nodes. This kind of attack is very difficult to distinguish, because the attacker infrequently exhibits abnormal activities. Active attacks, on the other hand, involve actions performed by intruder. The target of the attack can be either data traffic or routing traffic. The intruders may insert large dimensions of superfluous data packets into networks. They can also intentionally drop, corrupt and delay data packets passing through it.

External attackers are mainly external the networks who want to get entrée to the network and once they get entrée to the network they establish sending counterfeit packets, denial of service in regulate to disrupt the concert of the whole network. This attack is same, like the attacks that are made against wired network. These attacks can

be barred by implementing security measures such as firewall, where the access of unconstitutional person to the network can be mitigated.

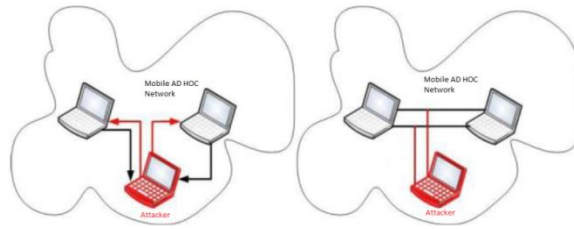


Figure 1: Active and Passive Attack in MANETs

While in internal attack the attacker wants to have normal access to the network as well as partake in the normal activities of the network. The attacker gain access in the network as new node either by compromising a current node in the network or by malevolent impersonation and start its malicious behavior. Internal attack is more severe attacks then external attacks.

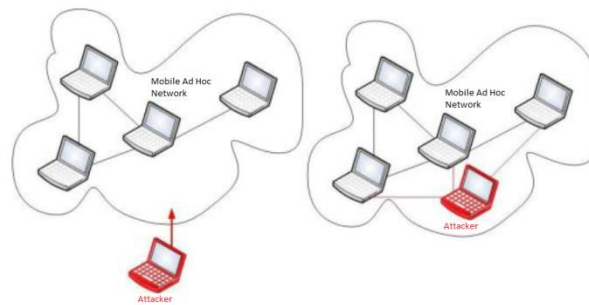


Figure 2: Black hole attack in AODV routing protocol

In black hole attack, a malevolent node uses its routing protocol in order to publicize itself for having the express path to the destination node or to the packet it wants to interrupt. This unreceptive node advertises its availability of fresh routes irrespective of checking its routing table. In this way attacker node will always have the availability in replying to the route request and thus intercept the data packet and retain it. In protocol based on flooding, the malicious node reply will be received by the requesting node before the reception of reply from actual node; hence a malicious and forged route is created. When this route is establish, now it's up to the node whether to drop all the packets or forward it to the unknown address. The method how malicious node fits in the data routes varies.

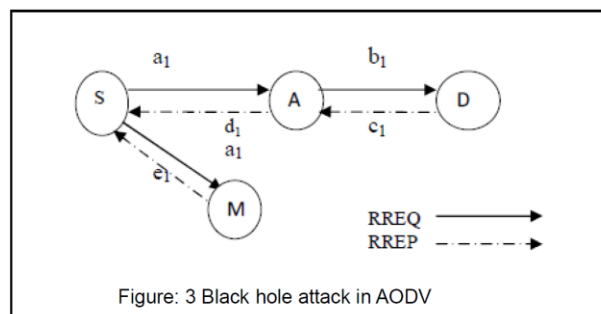
To detect this type of black hole attack, we have applied a neighborhood-based method. The solution can be elaborated as: Once the normal path discovery procedure in a routing protocol is finished, the source node sends a special control packet to request the destination to send its current neighbor set. By comparing the received neighbor sets, the source node can determine whether there is a black hole attack in the network. A black hole attack happens when a malicious node D'' intercepts the data traffic from the source node S to the destination node D [9]. D'' claims to have the IP address of D , thus leads S to form the path to D'' instead of D . Taking AODV for example, when the attacker D'' receives a route request (RREQ) packet, it generates a route reply (RREP) packet to reply back to S telling S that it is the destination node. When D'' is closer to the source node than the true destination D , a forged route is created between S and D'' instead of between S and D . In this case, all subsequent data traffic generated by S will go to the attacker D'' , instead of D . We notice that the attack may fail when D is closer to S than D'' . If the attacker D'' and D are close enough to become neighbors, it is easy for D to know that it is attacked. Two types of black hole attack can be described in AODV in order to distinguish the kind of black hole attack. Internal Black hole attack and External Black hole attack. In internal black hole attack there is an internal malicious node which fits in between the routes of given source and destination. As soon as it gets the chance this malicious node make itself an active data route element. At this stage it is now capable of conducting attack with the start of data transmission. This is an internal attack because node itself belongs to the data route. Internal attack is more vulnerable to defend against because of difficulty in detecting the internal misbehaving node. External attacks physically stay outside of the network and deny access to network traffic or creating

congestion in network or by disrupting the entire network. External attack can become a kind of internal attack when it take control of internal malicious node and control it to attack other nodes in MANET. External black hole attack can be summarized in following points.

1. Malicious node detects the active route and notes the destination address.
2. Malicious node sends a route reply packet (RREP) including the destination address field spoofed to an unknown destination address. Hop count value is set to lowest values and the sequence number is set to the highest value.
3. Malicious node send RREP to the nearest available node which belongs to the active route. This can also be send directly to the data source node if route is available.
4. The RREP received by the nearest available node to the malicious node will relayed via the established inverse route to the data of source node.
5. The new information received in the route reply will allow the source node to update its routing table.
6. New route selected by source node for selecting data.
7. The malicious node will drop now all the data to which it belong in the route.

2 Methodology

In AODV, Dst Seq is used to determine the freshness of routing information contained in the message from originating node. When generating a RREP message, a destination node compares its current sequence number and Dst_Seq in the RREQ packet plus one, and then selects the larger one as RREP's Dst_Seq. Upon receiving a number of RREP, a source node selects the one with greatest Dst_Seq in order to construct a route. To succeed in the black hole attack the attacker must generate its RREP with Dst_Seq greater than the Dst_Seq of the destination node. It is possible for the attacker to find out Dst_Seq of the destination node from the RREQ packet. In general, the attacker can set the value of its RREP's Dst Seq base on the received RREQ's Dst Seq. However, this RREQ's Dst Seq may not present the current Dst Seq of the destination node. Figure 2 shows an example of the black hole attack.



We use AODV protocol as the routing protocol in our method. Neighbor set is defined as all of the nodes that are within the radio transmission range of a node, due to the rapid movement of the nodes, the neighbor set of a node keeps changing and it is expected that the neighbor set changes faster when mobility increases. The chance that two mobile nodes have the same neighbor set at the same time is very small. So the neighbor set provides a good "identity" of a node, i.e., if the two neighbor sets received at the same time are different enough, we can conclude that they are generated by two different nodes.

Two processes are implemented to say that determining neighbor set of a node is a good identification for finding malicious node.

- In the first experiment, we measured the neighbor set difference of one node at different time instants t and $t + I$ under different moving speeds and system size (i.e., number of nodes in the system), where I means one second.
- In the second experiment, we examined the neighbor set difference of two different nodes, say node A and node B, at the same time. We measured the number of Nodes in the set of $((\{A's\ neighbor\ set\} \cup \{B's\ neighbor\ set\}) - (\{A's\ neighbor\ set\} \cap \{B's\ neighbor\ set\}))$.

Based on this neighbor set information, we design a method to deal with the black hole attack, which consists of two parts: detection and response.

Detection

In order to collect neighbor set information, we introduce two types of control packets in the detection phase:

requestneighborset(RQNS) and *replyneighborset*(RPNS).

The packet format of RQNS is as follows:

```
{srcaddr, destaddr, requestneighborseq#, nexthop }.
```

srcaddr is the IP address of the source node S

destaddr is the IP address of the destination D.

Each node is responsible for maintaining one counter: the sequence number of the RQNS, Each time a node sends a RQNS, requestneighborseq# increases by one. The sequence number in each node uniquely identifies the RQNS, which unicasts to the destination using the underlying AODV routing protocol. D or D' (malicious node), after receiving RQNS, replies a message RPNS.

The message format of RPNS is as follows:

```
{srcaddr, destaddr, requestneighborseq#, neighbor set}
```

The first three items, i.e., *srcaddr*, *destaddr*, *requestneighborseq#*, identify to which RQNS this RPNS corresponds. Neighbor set contains the current neighbor set of D or D'. This RPNS unicast back to S. There are two major steps.

Step 1: Collect neighbor set information.

By using AODV protocol, the source node S floods RREQ packets across the network to find a route to the destination node D. Now for each received RREP, S will unicast a RQNS packet, and the RQNS packet will go to either D or D', depending on the path contained in RREP.

After D or D' receives RQNS, it will generate a RPNS packet, which contains its current neighbor set, and unicast it back to S.

Step 2: Determine whether there exists a black hole attack

The source node S, after receiving more than one RPNS packet in a certain period will start comparing the received neighbor sets. The difference among the neighbor sets is defined as the union of the received neighbor sets minus the intersection of the neighbor sets. If the difference is larger than the predefined threshold value, S will know that the current network has black hole attacks and take some actions to respond to it. One concern is that what if D' first requests the neighbor set of D, and replies it to S? We think that it is difficult for D' to do so. Because D' claim D's address, D' has to use D's address to request D's neighbor set, (otherwise, D's neighbors can find that D' is a masquerader). But D will raise an alert to this request, because it uses the same address of D.

Response

We assume there exists a public key infrastructure, which S can use to authenticate D or D'. After S detects the black hole attack, it will use the cryptography-based method to authenticate D and D'. In this way, S can identify D, the true destination.

Once D is identified, S will send a *modifyrouteentry* control packet to D to form a correct path by modifying the routing entries of the intermediate nodes from S to D. We call this routing recovery protocol. The packet format of MRE is as follows:

```
{destaddr, correctpath }
```

destaddr is the IP address of D. *correctpath* is the hop by hop path from S to D.

S can get the information *correctpath* from the received RPNS's. After each node receives the MRE, it will modify its corresponding routing entry (identified by the IP address of D) to make its next hop on the path to D, instead of D'. After D receives MRE, a correct path has formed between S and D, which will make the traffic of S go to the correct destination.

Method to Add a Malicious Node

The main setback of black hole attack is to hinder the communication from source to destination. To add malicious nodes in AODV the following procedure has been implemented.

First we need to modify aodv.cc and aodv.h files:

In aodv.h:

```
bool malicious;
```

In aodv.cc:

```
malicious = false;
if(strcmp(argv[1], "hacker") == 0)
{
    malicious = true;
    return TCL_OK;
}
```

Next we need to modify the TCL file to set a malicious node:

```
$ns at 0.0 "[$mnode_(i) set ragent_] hacker"
```

```

if (malicious == true) {
    drop (p,DROP_RTR_ROUTE_LOOP);}

```

To protect MANETs from outside attacks, the routing protocols must fulfil certain set of requirements to guarantee the correct functioning of all the paths from source to destination. These are:

- Only the authorized nodes shall be able to execute route discovery processes
- Negligible exposure of network topology
- Early detection of distorted routing messages
- Avoiding formation of loops
- Avert redirection of data from shortest paths

Algorithm

Step1: Source node broadcasts RREQ to neighbours

Step2: Source node receives RREP from neighbours

Step3: Source node selects shortest and next shortest path based on the number of hops

Step4: Source node checks its routing table for single hop neighbouring nodes only

Step5: If the neighbour node is in its routing table then route data packet Else The node is malicious and sends false packets to that node

Step 6: Invoke the route discovery Inform all the neighbouring nodes about the stranger

Step 7: Add the status of stranger to the routing table of source node

Step 8: Again send packet to neighbouring node

Step 9: If step 5 repeats then broadcast the malicious node as black hole

Step 10: Update the routing table of source node after every broadcast

Step 11: Repeat step 4 to 10 until packet reaches the destination node correctly

Simulation Environment

We have implemented Black hole attack in an ns2 simulator. CBR (Constant Bit Rate) application has been implemented. The problem is investigated by means of collecting data, experiments and simulation which gives some results, these results are analyzed and decisions are made on their basis. The simulator which is used for simulation is ns2. Using ns2, we can implement your new protocol and compare its performance to TCP. To evaluate the performance of a protocol for an ad hoc network, it is necessary to analyze it under practical conditions, especially including the movement of mobile nodes. Simulation requires setting up traffic and mobility model for performance evaluation. Table 1 shows the parameters that have been used in performing simulation.

Table 1: Simulation Parameters

| Parameters | Value |
|------------------------|---------------------------------|
| Simulator | Ns-2.34 |
| Data packet size | 512 byte |
| Simulation time | 1000 sec |
| Environment size | 1000 x1000 |
| Number of nodes | 50 |
| Transmission range | 250m |
| Pause time | 2 s |
| Observation parameters | PDF, end-to-end delay, overhead |
| No. of malicious node | 1 |
| Traffic Type | CBR |
| Mobility | 60 m/s |
| Routing Protocols | AODV and IAODV |

3 Result

In a network when a node becomes malicious it grasps the IP address of the node and thereby claims to have the shortest path. The source in response ignores all other RREPs received from other nodes. By using neighborhood based method [3] we have implemented and tried to detect black hole attack in the network and represented how the routing tables changes on receiving RREQ and RREP.

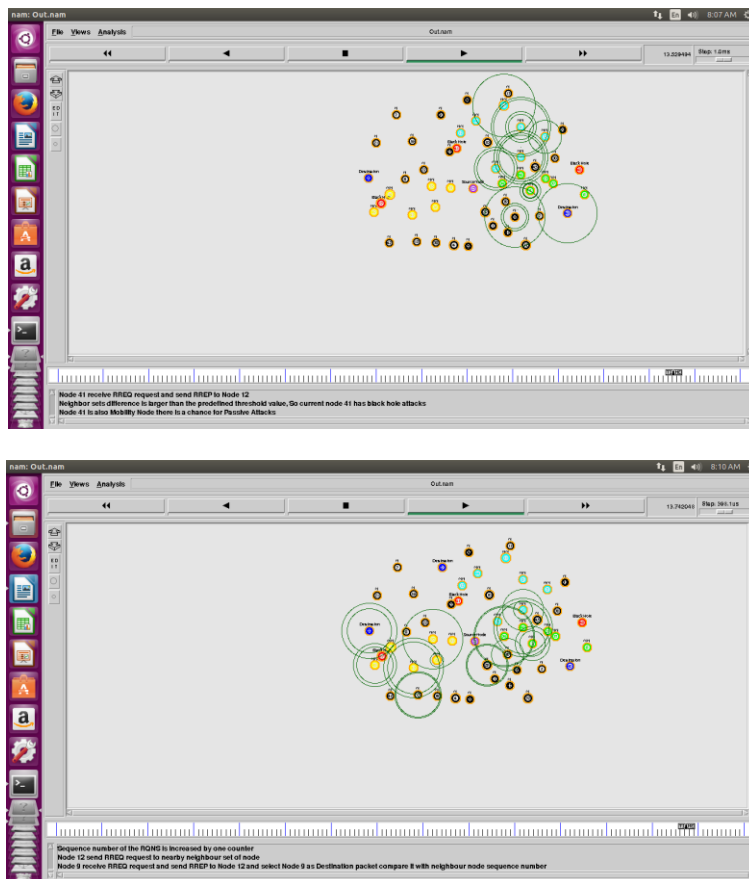


Figure 4: Simulation result

PDR (Packet delivery ratio)

It can be measured as the proportion of the received packets by the destination nodes to the packets sent by the source node. This assesses the capacity of the protocol to convey data packets to the destination in the vicinity of malicious nodes.

$$PDR = (\text{received packets} / \text{packets sent}) * 100$$

Energy Consumption

It gives the energy utilized by the node as a part of the network. It diminishes with black hole attacks of the fact that the packets transmitted between the source and destination gets dropped which prompts less transmission between the nodes.

Throughput

Throughput is characterized as the effective information or data packets transmitted per unit time. The parameter differs specifically with the number of packets received and is inverse proportional corresponding to the end to end delay. Accordingly, these two are the integral variables for the throughput.

$$\text{Throughput} = \Sigma \text{ received packets} / (\text{arrived timesendtime}) * \text{packet size} * \text{time} / 1000 \text{ in kbps.}$$

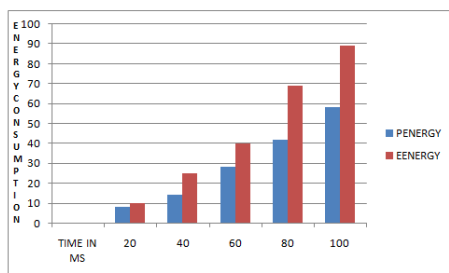


Figure 5: Energy consumption graph

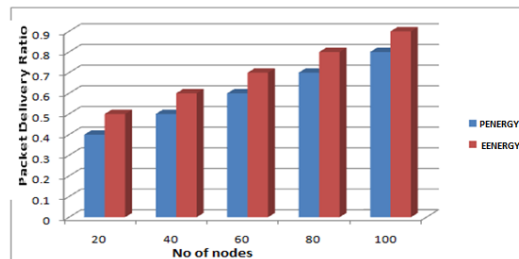


Figure 6 : Packet delivery ratio graph

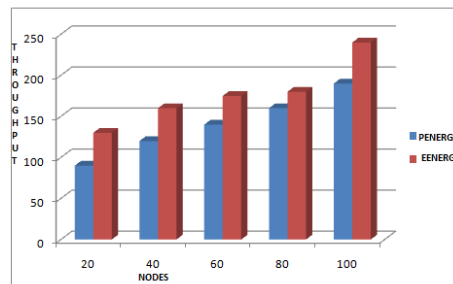


Figure 7: Throughput comparison graph

4 Conclusion

Black hole attack is one of the most important security problems in MANET. It is an attack that a malicious node impersonates a destination node by sending forged RREP to a source node that initiates route discovery, and consequently deprives data traffic from the source node. A neighbor set based approach has been used to detect black hole attack and a muting recovery protocol to mitigate the effect of black hole attacks methods could effectively and efficiently detect black hole attack without introducing much routing control overhead to the network. In the future, we would like to further explore whether there exists a non-cryptography based method to identify the true destination and the optimal detection.

References

- [1] Dr G.Revathy, Ms Anju, Parimalam and Imaya Kanishka, “Diabetic Detection Using Irish”, International Journal of Scientific Research in Engineering and Management (IJSREM), Volume: 04 Issue: 03 | Mar -2020 ISSN: 2582-3930
- [2] Dr.G.Revathy, N.S.Kavitha, K.Senthivadivu. D.Sathya and P.Logeshwari , “ Girl Child Safety using IoT Sensors and Tabu Search Optimization” International Journal of Recent Technology and Engineering (IJRTE) ISSN: 2277-3878 volume 8, January 2020.
- [3] Dr.G.Revathy, Dr.G.Saravanan, Dr.R.Madonna Arieth and Mr.M.Vengateshwaran, “
- [4] Magnify Qos with Tabu & Link Scheduling In Wmn” , International Journal of Recent Technology and Engineering (IJRTE) ISSN: 2277-3878, Volume-8, Issue-4, November 2019
- [5] Mrs G.Revathy , “Mounting Eminence of services in wireless mesh networks”, International journal of Research and Analytical reviews, sep 2018(ISSN 2349 5138)
- [6] Mrs.G.Revathy and Dr.K.Selvakumar, “ Sustain route by tabu and amplified qos by distributed scheduling in wmn”, International Journal of Recent trends in Enginnering and research (ISSN: 0973-7391).
- [7] Mrs.G.Revathy and Dr.K.Selvakumar, “Channel assignment using tabu search in wireless mesh networks”,Wireless personal communication ISSN NO 09296212.
- [8] Mrs.G.Revathy and Dr.K.Selvakumar,“Increasing quality of services in wireless mesh networks”, International journal of advanced research in computer engineering and technology, vol 7, issue 3, march 2018. ISSN 22781323

- [9] Mrs.G.Revathy and Dr.K.Selvakumar, “Escalating quality of services with channel assignment and traffic scheduling in wireless mesh networks”, Cluster computing, Jan 2018. ISSN no 13867857.
- [10] Mrs G.Revathy and Dr.K.Selvakumar, “Route maintenance using tabu search and priority scheduling in wireless mesh networks”, Journal of advanced research in dynamical and control systems, vol 9,sp-6, 2017. ISSN 1943023X

Heart Disease Prediction Using Machine Learning

¹HariPriya.L,²Jayandrika.K,³JanaSruthi.S.U, ⁴P.Dhivya ⁴Assitant Professor

^{1,2,3}II Year, Department of Computer Science and Engineering, Bannari Amman Institute of Technology, Sathyamangalam, Erode, Tamilnadu – 638401 ¹

hariPriya.cs19@bitsathy.ac.in, ² jayandrika.cs19@bitsathy.ac.in, ³ janasruthi.cs19@bitsathy.ac.in.

Abstract

Heart is an important organ in every living organism. Heart disease diagnosis and prediction should be done with perfection, whereas little mistakes can cause us many problems and even death related to heart disease and increasing day by day. To come out of this problem we need a prediction system to make awareness of these diseases. Machine learning is a part of artificial intelligence. It contains many algorithms which are useful to predict each and every event in natural happening. We can calculate the accuracy by using machine learning algorithms for prediction of heart disease. For this prediction algorithms such as k-nearest neighbor, decision tree, random forest, support vector machine and so many algorithms can be used to predict the accurate machine learning model by using the datasets which are available at the UIC repository. We can implement these algorithms in python programming anaconda or google colab notebook which is online software available at google platform. Google colab notebook is the best one for implementation because it contains many types of library, header files which are useful for predicting the accuracy. In this paper, we are going to predict whether the patient has heart disease or not by using four types of classification algorithms and by comparing those algorithms and find the highest accuracy model among them to predict the results.

Keywords: Heart disease, machine learning, UIC repository, algorithms, prediction.

1 Introduction

Heart is an important organ in the human body. It pumps blood to every part of our body. It supplies blood and nutrients to all parts of our body. Heart disease is the leading factor to cause death to humans in the world. Heart disease can be caused by smoking, by drinking too much alcohol, Stress, even obesity may cause us heart related problems. In the year of 2019, approximately from 12.1 million to 18.6 million people died by heart disease. According to the estimation of the World Health Organization (WHO), cardiovascular disease takes nearly 17.9 million people lives each year. So, it results in number one cause for death worldwide. Heart attack is one of the most common among the heart diseases. The symptoms of heart attack are lack of breathing for a while period, shoulder pain, over sweating, chest pain and also abdomen pains. It is easy to solve at the early stage of any kind of heart disease but we need to identify as earlier as possible when it takes long timing it may not be solved much easier they may become more complex to solve. Medical Organizations present in all over the world, gather the health and disease related data. Those data can be used for various machine learning techniques to predict heart disease. That's why, many algorithms can be used expertly to find the presence and absence of heart related diseases correctly.

2 Materials And Methods

In this project, we have collected the dataset from UCI machine learning repository which contains a variety of databases, domain theories and data generators. This dataset contains 14 features such as age, sex, cp, trestbps, chol, fbs, restecg, thalach, exang, oldpeak, slope, ca, thal, and target. First we have to preprocess the data which we have taken. Data preprocessing helps our data to make it suitable for the machine learning models. Its one of the most important steps to create a machine learning model which gives us best accuracy.

2.1 Data Preprocessing

Data preprocessing steps are a necessary part to create a machine learning model. The Steps involved are:

2.1.1 Importing Libraries:

To perform data preprocessing using python we need some libraries which are available predefined. These libraries are used to build a model which is good for doing specific things. Some of the libraries are pandas, numpy, matplotlib, seabornect..

2.1.2 Importing Datasets:

We have to import a dataset which we have taken from the UCI repository. The dataset should be in a different format but we have taken comma separated value files. To import a dataset in Google colab we have to upload the dataset in google drive, then copy the path of the dataset which we have uploaded and for anaconda we do not need to upload dataset because it is an offline tool.

2.1.3 Taking care of missing data in the datasets:

Sometimes, some data are missed in the dataset. This might cause a problem while training and testing the model. To overcome this type of problem, we can remove the particular row or column which has a null value, but this method is not 100% efficient. So to handle this, we can calculate mean value for a particular feature that contains null value and replace the resultant value with a missing value. Here, `isna()` function is used to identify the missing values.

2.1.4 Encoding Categorical Data:

After viewing the dataset I have need to convert the categorical values into dummy variables. Dummy variable is nothing but it contains only 0 and 1. Here 1 is used to identify that the presence of value whereas 0 is used for the other identification purpose. One hot encoder is one kind of method used to encode the categorical data in dataset.

2.1.5 Splitting the dataset into Training set and Test set:

In this step, we are splitting the dataset into two sets, which are train set and test set. In train set, Machine Learning Model gets trained, that is Machine Learning Model will attempt to understand the correlation. In the test set, the model is tested which means it checks how it can predict the heart disease accurately. A general rule for splitting the dataset is 80% of the dataset should be a training set and the remaining 20% of the dataset should be a test set.

2.1.6 Feature Scaling:

It is the final step in data preprocessing for dataset in Machine learning. It is one of the steps to specify the independent variable with specific range. It helps us to make the independent variable in dataset to not depend on any other variables.

3 Proposed Algorithm

Here, we are using the classification algorithm which is able to say that whether the person is suffering from heart disease is not. Here we have taken four different algorithms to find out which model is suitable for predicting the heart disease efficiently. The used algorithms are K Nearest Neighbor, Support vector machine, Decision Tree Classifier, Random Forest Classifier.

3.1 Classification:

There are three types of machine learning. They are supervised learning, unsupervised learning and reinforcement learning. Here we have used Classification. Classification is one of the supervised learning models which helps us to predict a label. Whereas Regression is used to predict continuous outcome values. It identifies the objects and separates them into categories. Classification can give us an output in the form of yes or no (1/0) type.

3.1.1 KnearestNeighbour:

The K nearest neighbour algorithm (KNN) is a non-parameter classification method in statistics. It divides the data into classes based on the data point distance. The data which are close to each other is considered that they are similar to each other in the same closet cluster. To find distance we will use the euclidean metric method mathematical formula is,

$$d(x, x') = \text{square root of } (x_1 - x_1')^2 + (x_n - x_n')^2 \quad (1)$$

3.1.2 Support Vector Machine:

Support vector machine (SVM) is a specific linear classifier which is based on the principle of Margin Maximization. It is helpful in high dimensional spaces which is the case where the number of dimensions is greater than the number of samples. It can be applicable for both linear and non-linear problems. Support Vectors are useful in maximizing the classifier's margin.

Mathematical expression for SVM optimization problem,

$$f(w) = \frac{1}{2} \|w\|^2, g(w, x + b) - 1, i = 1 \dots m \quad (1)$$

Whereas in function of lagrangian

$$L(w, b, a) = \frac{1}{2} \|w\|^2 - \sum m_i = 1 a_i [y_i (w \cdot x + b) - 1] \quad (2)$$

3.1.3 Decision Tree Classification:

Decision tree algorithm comes under the supervised machine learning algorithm. In this algorithm, the main aim is to develop the training model which can be used to calculate the value of the target variable by studying simple decision rules deduced from training data. It obeys the Sum of Product representation.

Entropy is a collection of information needed to express some kind of sample. The mathematical expression for this is,

$$\text{Entropy} = - \sum p_i * \log(p_i) \quad (1)$$

Gini Index is the measure of inequality samples. It values between 0 and 1. It is also known as Gini impurity. The index value 0 refers to perfectly homogeneous and 1 refers to maximal inequality among the elements. The mathematical expression is,

$$\text{Gini index} = 1 - \sum p_i^2 \quad (2)$$

3.1.4 Random Forest Classifier:

Random Forest algorithm is a one kind of supervised learning machine learning algorithm. It is one kind of flexible type algorithm it is easy to produce and it also does not need any kind of hyper-parameter tuning which produces great results. We can simply say that it builds multiple decision trees and combines them all together to result with stable prediction along great accurate values. The formula for classification we can use Gini index method of decision tree algorithm, the mathematical expression is ,

$$Gini = 1 - \sum p_i^2 \tag{1}$$

It is used to determine the node of branches by using class and probability. We can also use the entropy method to find the node of branches.

4 Step By Step Procedure



Figure 1: Flow Chart For Steps of Heart Disease Prediction

Here, the steps involved in predicting heart disease are shown in the form of a Flow Chart in Fig.(1). These are the following steps involved importing a dataset, training the data & testing the data, Algorithm preferred among them the best accurate producing model is considered as the final result.

5 Experiment Result

The training and testing accuracy obtained by above used algorithms are:

Table 1: Training and testing accuracy

| MODEL | TRAINING ACCURACY | TESTING ACCURACY |
|---------------------------------|-------------------|------------------|
| <i>K nearest neighbor</i> | 86.79% | 86.81% |
| <i>Support vector machine</i> | 93.40% | 87.91% |
| <i>Decision tree classifier</i> | 100% | 78.02% |
| <i>Random forest classifier</i> | 100% | 82.42% |

By comparing all the above algorithms, heart disease prediction using machine learning can be efficiently done by the Support Vector Machine (SVM) algorithm, which gives 87.91% testing accuracy.

6 Conclusion

In our day to day life, the number of death cases is increasing rapidly due to heart disease. So it is important to develop a model to predict heart disease wisely and precisely. Because of this, four classifications algorithms are compared and considered the algorithm with highest accuracy as the well efficient algorithm to predict heart disease. Here, Support Vector Machine (SVM) results in highest accuracy 93.40%.

7 Future Work

In future, we can try other performance measures and other machine learning techniques like XGBoost classifier, Logistic Regression, Naive Bayes and so on, for better heart disease prediction and its accuracy. This can help many medical organizations with a superior model which is used for early disease prediction.

References

- [1] Krishnan J Santhana and S Geetha, "Prediction of Heart Disease using Machine Learning Algorithms", *ICICT*, 2019.
- [2] A. Hazra, S. Mandal, A. Gupta and Mukherjee, "A Heart Disease Diagnosis and Prediction Using Machine Learning and Data Mining Techniques: A Review", *Advances in Computational Sciences and Technology*, 2017.
- [3] Saba Bashir, Usman Qamar, M.YounusJaved et al. "An Ensemble based Decision Support Framework for Intelligent Heart Disease Diagnosis" *International Conference on Information Society (i-Society 2014)*.
- [4] JafarAlzubi, Anand Nayyar, Akshay Kumar. "Machine Learning from Theory to Algorithms: An Overview", *Journal of Physics: Conference Series*, 2018
- [5] M. A. Jabbar, P. Chandra and B. L. Deekshatulu, "Prediction of risk score for heart disease using associative classification and hybrid feature subset selection", *Int. Conf. Intell. Syst. Des. Appl. ISDA*, pp. 628-634, 2012.
- [6] Haq AU, Li JP, Memon MH, Nazir S, Sun R. A hybrid intelligent system framework for the prediction of heart disease using machine learning algorithms. *Mobile Information Systems*. 2018 Dec 2;2018.
- [7] Nikhar S, Karandikar AM. Prediction of heart disease using machine learning algorithms. *International Journal of Advanced Engineering, Management and Science*. 2016;2(6):239484.
- [8] Sharma H, Rizvi MA. Prediction of heart disease using machine learning algorithms: A survey. *International Journal on Recent and Innovation Trends in Computing and Communication*. 2017 Aug;5(8):99-104.
- [9] Ramalingam VV, Dandapath A, Raja MK. Heart disease prediction using machine learning techniques: a survey. *International Journal of Engineering & Technology*. 2018;7(2.8):684-7.
- [10] Gavhane A, Kokkula G, Pandya I, Devadkar K. Prediction of heart disease using machine learning. In2018 *Second International Conference on Electronics, Communication and Aerospace Technology (ICECA) 2018 Mar 29* (pp. 1275-1278). IEEE.
- [11] Ramalingam VV, Dandapath A, Raja MK. Heart disease prediction using machine learning techniques: a survey. *International Journal of Engineering & Technology*. 2018;7(2.8):684-7.
- [12] Khourdifi Y, Bahaj M. Heart disease prediction and classification using machine learning algorithms optimized by particle swarm optimization and ant colony optimization. *International Journal of Intelligent Engineering & Systems*. 2019 Feb;12(1):242-52.
- [13] Patel J, TejalUpadhyay D, Patel S. Heart disease prediction using machine learning and data mining technique. *Heart Disease*. 2015 Sep;7(1):129-37.
- [14] Kanchan BD, Kishor MM. Study of machine learning algorithms for special disease prediction using principal of component analysis. In2016 *international conference on global trends in signal processing, information computing and communication (ICGTSPICC) 2016 Dec 22* (pp. 5-10). IEEE.
- [15] Chandna D. Diagnosis of heart disease using data mining algorithm. *International Journal of Computer Science and Information Technologies*. 2014;5(2):1678-80.
- [16] Krishnani D, Kumari A, Dewangan A, Singh A, Naik NS. Prediction of coronary heart disease using supervised machine learning algorithms. InTENCON 2019-2019 *IEEE Region 10 Conference (TENCON) 2019 Oct 17* (pp. 367-372). IEEE.
- [17] Dinesh KG, Arumugaraj K, Santhosh KD, Mareeswari V. Prediction of cardiovascular disease using machine learning algorithms. In2018 *International Conference on Current Trends towards Converging Technologies (ICCTCT) 2018 Mar 1* (pp. 1-7). IEEE.

A New Technique for Image Compression Using Linear Algebra With Python Algorithm

Dr.S.Karthigai Selvam¹ ,Assistant professor and Dr.S.Selvam , Head & Assistant Professor
 , Department of Mathematics,
 N.M.S.S.V.N. College, Madurai – 625 019, Tamil Nadu, India
 E-mail : s.karthic4@gmail.com,, E-mail : s.selvammphil@gmail.com

Abstract

In recent days, the data are transformed in the form of multimedia data such as images, graphics, audio and video. Multimedia data require a huge amount of storage capacity and transmission bandwidth. Consequently, data compression is used for reducing the data redundancy and serve more storage of data. In this paper, addresses the problem (demerits) of the lossy compression of images.

This proposed method is deals on SVD Power Method that overcomes the demerits of Python SVD function. In our experimental result shows superiority of proposed compression method over those of Python SVD function and some various compression techniques. In addition, the proposed method also provides different degrees of error flexibility, which give minimum of execution of time and a better image compression.

Keywords: *Image Compression, Singular Value Decomposition, MSE, Lossy image compression, PSNR.*

1 Introduction

The Singular Value Decomposition(SVD) is a generalization of the eigen-decomposition used to analyze rectangular matrices. It plays an important role for many exciting real-world applications such as Mathematical models, physical and biological processes, data mining , search engines to rank in huge databases, including the Web, image processing etc. The purpose of this paper is to present the SVD applied to the image compression.

The main idea of image compression is reducing the redundancy of the image and the transferring data in an efficient form. The image compression takes an important place in several domains like web designing, in fact, maximally reduce an image allows us to create websites faster and saves bandwidth users, it also reduces the bandwidth of the servers and thus save time and money. Here, we used two aspects: image size in pixels and its degree of compression. The main goal of such system is to reduce the storage quantity as much as possible while ensuring that the decoded image displayed in the monitor can be visually similar to the original image as much as it can be.

2 Existing Methods

In past few years, various image compression schemes and their applications in image processing have been proposed. In this section, a empirical review of few important contributions from the existing method is presented.

In general, there are two approaches for image compression: lossy or lossless[1,2]. A lossless compression is an image compression technique that allows no loss of data, and which retains the full information needed to reconstruct the original image. This type of compression is also known as entropy coding because of the fact that a compressed signal is generally more random than the original one and the patterns are removed when a signal is compressed. The lossless compression can be very useful for exact reconstruction of images. The compression ratio provided by this kind of methods is not sufficiently high to be truly used in image compression. Lossless image compression is particularly useful in image archiving as in the storage of legal or medical records. The lossless image compression methods include: Bit-plane coding, Huffman coding[3], Run-Length coding and Entropy coding.

Lossy compression is another type of image compression technique in which the original signal cannot be exactly reconstructed from the compressed data. The reason behind this is that much of the detail in an image can be discarded without greatly changing the appearance of the image. In lossy image compression, even a very fine detail of the images can be lost, but ultimately, the image size is drastically reduced.

Lossy image compressions are useful in many applications such as broadcast television, video conferencing, and facsimile transmission, in which a same amount of error is an acceptable trade-off for increased compression performance. Among methods for lossy compression, we find: Transform coding Fourier-related transform, Fractal compression[4], Discrete Cosine Transform[5,6] and Wavelet transform.

Generally, SVD is a lossy compression technique which achieves compression by using a smaller rank to approximate the original matrix representing an image. Furthermore, lossy compression yields good

compression ratio comparing with lossless compression while the lossless compression gives good quality of compressed images.

According to the state-of-the-art, there are several works suggested to use the SVD with other compression methods or with variation of SVD. Awwal et al.[7] presented new compression technique using SVD and the Wavelet Difference Reduction. The WDR used for further reduction. This technique has been tested with other techniques such as WDR and JPEG 2000 and gives a better result than these techniques. Furthermore, using WDR with SVD enhance the PSNR and compression ratio.

A technique based on Wavelet-SVD, which used a graph coloring technique in the quantization process, is presented in[8]. This technique worked well and enhanced the PSNR and compression ratio. The generated compression ratio by this work ranged between 50-60%, while the average PSNR ranged between 40-80db.

Ranade et al.[9] suggested a variation on SVD based image compression. This approach is a slight modification to the original SVD algorithm, which gives much better compression than the standard compression using SVD method. In addition, it performs substantially better than the SVD method. Typically, for any given compression quality, this approach needs about 30% fewer singular values and vectors to be retained.

The technique given by El Abbadi et al.[13], proposes to use SVD and MPQ-BTC, the input image is compressed by reducing the image matrix rank, by using the SVD process and then the result matrix compressed by using BTC. Following the some objective of image compression using SVD, the most problem is which K rank to use for giving a better image compression. For this reason, the method presented in El Asnaoui et al.[14], introduces two new approaches: The first one is an improvement of the Block Truncation Coding method that overcomes the disadvantages of the classical Block Truncation Coding, while the second one describes how to obtain a new rank of SVD method, which gives a better image compression.

3 Image Compression Technique Using SVD

The main intention of studying the SVD of an image (matrix of $m \times n$) is to create approximations of an image using the least amount of the terms of the diagonal matrix in the decomposition. This approximation of the matrix is the basis of image compression using SVD, since images can be viewed as matrices with each pixel being an element of a matrix.

The main concept of this section is to present two algorithms: The first one is the Python SVD function, while the second one describes how to obtain a new SVD using Block SVD Power Method.

3.1 Algorithm of Python SVD Function

We will use *numpy.linalg* library's *svd* function to compute svd of a matrix in python. The *svd* function returns *U,s,V* .

- *U* has left singular vectors in the columns
- *s* is rank 1 numpy array with singular values
- *V* has right singular vectors in the rows -equivalent to *V* transpose in traditional linear algebra literature

The reconstructed approximation of the original matrix is done using a subset of singular vectors as below in the *compress_svd* function . We use numpy array slicing to select *k* singular vectors and values. Instead of storing $m \times n$ values for the original image, we can now store $k(m+n)+k$ values.

```
reconst_matrix = np.dot(U[:, :k], np.dot(np.diag(s[:k]), V[:, k:]))
def compress_svd(image, k):
    """
    Perform svd decomposition and truncated (using k singular
    values/vectors) reconstruction
    returns
    -----
    reconstructed matrix reconst_matrix, array of singular values s
    """
    U, s, V = svd(image, full_matrices=False)
    reconst_matrix = np.dot(U[:, :k], np.dot(np.diag(s[:k]), V[:, k:]))
    return reconst_matrix, s
```

3.2 Algorithm of SVD Power Method

Input: A matrix $A \in (R)^{n \times m}$, a block-vector
 $V = V(0) \in R^{m \times s}$ and a tolerance *tol*

Output: An orthogonal matrices

$U = [u_1, u_2, \dots, u_s] \in R^{n \times s}$
 $V = [v_1, v_2, \dots, v_s] \in R^{m \times s}$
 and a positive diagonal matrix
 $\Sigma = \text{diag}(\alpha_1, \alpha_2, \dots, \alpha_s)$
 such that : $AV = U\Sigma$
 While ($err > tol$) do
 $AV = QR(\text{factorization } QR)$,
 $U \leftarrow Q(:, 1 : s)$
 (the s first vector colonne of Q)
 $ATU = QR$,
 $V \leftarrow Q(:, 1 : s)$ and $\Sigma \leftarrow R(1 : s, 1 : s)$
 $err = ||AV - U\Sigma||$
 End

3.3 Proposed Image Compression Technique

The contribution of this paper is the introduction of the concept of application of Block SVD Power Method to image compression, the main idea of image compression is reducing the redundancy of the image and the transferring data in an efficient form.

We propose our method to integrate the Block SVD Power Method and adopt it to create an algorithm that compress an image. Figure 1 shows the main pipeline of the proposed method.

When the SVD is applied to an image, it is not compressed, but the data take a form in which the first singular value has a large amount of the image information. With this, we can use only a few singular values to represent the image with slight differences from the original. The input image can be a color image with RGB color components or may be a grayscale image. Additionally, for creating new image with Python SVD function as indicated in the Fig. 1, we use :

$$I_{\text{comp}} = U(:, 1 : K) * \Sigma(1 : K, 1 : K) * (V(:, 1 : K))^T \tag{1}$$

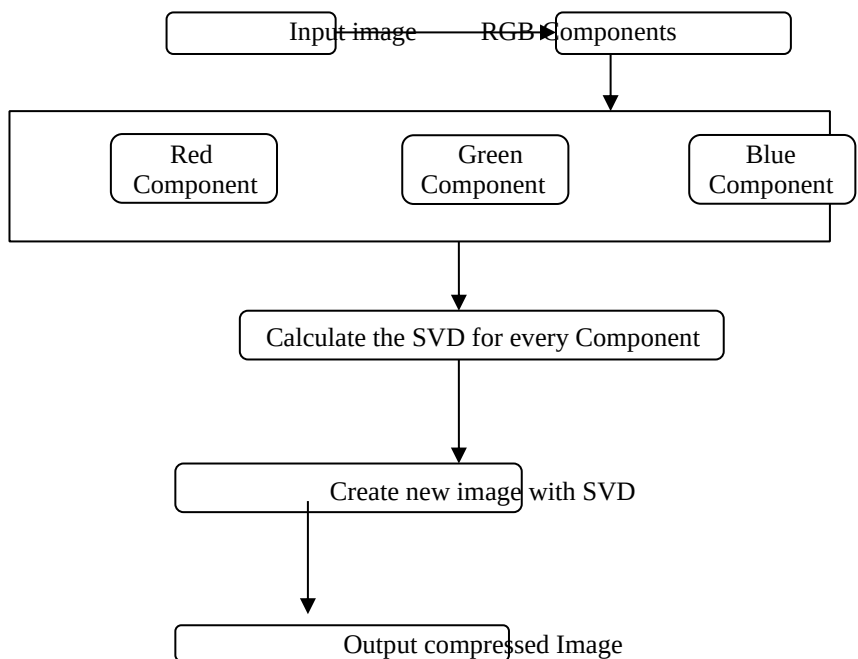


Fig. 1 New Architecture of Image pre-processing using SVD

In this paper is to set up a new algorithm for image compression that overcomes some inconveniences encountered in existing methods that use Python SVD function. Our modification consists of a computing the SVD for each component step, in which the entries in the image I are calculated using Block SVD Power Method obtained by [15] instead of Python SVD function[14] and keeps the K rank determined by (see Eq.5).

We suggesting an image compression based on Block SVD Power Method. Most of methods focus on other methods and other variation of SVD. Moreover, our method is novel, efficient for solving our problem. It is general and many other computer visions can benefit from using it. The results are clearly showing the superiority

of the proposed lossy image compression technique over those of Python SVD function and some different compression techniques.

4 Experimental Results

Main aim of our work is Image compression. Our experiments were performed on several images available on WANG Databases. Simulations were done in Python.

4.1 Measurement for comparison

To evaluate the performance of the proposed method, the quality of the image is estimated using several quality measurement variables like, Mean Square Error (MSE) and Peak Signal-to-Noise Ratio (PSNR). These variables are signal fidelity metrics and do not measure how viewers perceive visual quality of an image.

4.1.1 Measurement of Compression Ratio

The degree of data reduction obtained by a compression method can be evaluated using the compression ratio (Q_{comp}) defined by the formula:

$$Q_{comp} = \frac{\text{Size of Original image}}{\text{Size of Compressed image}} \quad (2)$$

4.1.2 Mean Square Error(MSE)

MSE, which for two $M * N$ monochrome images X and Y where one of the images is considered noisy approximation of the other and is defined as follows:

$$e_{MSE} = \frac{1}{MN} \sum_{i=0}^{M-1} \sum_{j=0}^{N-1} [X(i,j) - Y(i,j)]^2 \quad (3)$$

4.1.3 Peak Singal-to-Noise Ratio (PSNR)

PSNR is measured in decibels (dB), and is only meaningful for data encoded in terms of bits per sample bits per pixel. For example, an image with 8 bits per pixel contains integers from 0–255. PSNR is given by the following equation:

$$PSNR = 10 \log_{10} \frac{(2^B-1)^2}{e_{MSE}} \quad (4)$$

A high PSNR value indicates that there is less visual degradation in the compressed image.

4.2 Image Compression

We test our method, we develop a user interface. The method was applied to various and real images to demonstrate the performances of the proposed algorithm of image compression.

Here, we used 2 color images such as Giraffe and India Gate available in WANG Database and one in grayscale. Figures 4, 5, 6 and 7 show the test images and the resulting compressed images using Python SVD function [14] and the proposed compression method.

We recall that our goal is to approximate an image (matrix of $m \times n$) using the least amount of information. Thereby, to obtain a better quality of the compressed image using SVD, we use the K rank determined by El Asnaoui et al. [14]:

$$K = \frac{m \times n}{m+n+1} \quad (5)$$

Where m and n are the size of original image.



(a) Giraffe (b) India Gate (c) grayscale

Fig. 4 Original images

4.2.1 Analysis with Color Image

After rank $K = 438$, we obtain:



Fig. 5 Image compressed results obtained by: **a.** Python SVD function , **b.** Proposed method

Table 1 Image compression results for Giraffe.jpg, 1024×768 , 858Kb, by using:
Python SVD function Proposed method

| K | Q_{comp} | MSE | PSNR | Q_{comp} | MSE | PSNR |
|-----|------------|---------|---------|---------------|----------------|----------------|
| 25 | 9.8635 | 30.8213 | 30.7839 | 7.5023 | 46.8792 | 48.0017 |
| 50 | 9.4127 | 31.2231 | 32.8613 | 7.4123 | 47.2051 | 49.6834 |
| 75 | 8.8454 | 33.4624 | 34.9174 | 7.3923 | 48.2928 | 50.7678 |
| 100 | 8.2839 | 35.5016 | 36.9711 | 7.3722 | 49.3804 | 51.8522 |
| 125 | 8.0601 | 36.9601 | 38.5246 | 7.3628 | 50.2263 | 52.6677 |
| 150 | 7.8416 | 38.4162 | 40.0752 | 7.3532 | 51.0722 | 53.4831 |
| 175 | 7.7425 | 39.6034 | 41.4147 | 7.3538 | 51.3384 | 53.7384 |
| 200 | 7.6453 | 40.7905 | 42.7541 | 7.3543 | 51.6045 | 53.9934 |
| 225 | 7.5935 | 41.8770 | 43.9656 | 7.3481 | 52.7398 | 55.0594 |
| 250 | 7.5402 | 42.9643 | 45.1763 | 7.3419 | 53.8751 | 56.1254 |
| 275 | 7.5041 | 44.0238 | 46.3197 | 7.3371 | 55.0086 | 57.2463 |
| 300 | 7.4661 | 45.0832 | 47.4630 | 7.3323 | 56.1422 | 58.3672 |
| 325 | 7.4393 | 46.1445 | 48.5717 | 7.3312 | 57.4115 | 59.8254 |
| 350 | 7.4123 | 47.2051 | 49.6804 | 7.3301 | 58.6809 | 61.2833 |

| | | | | | | |
|-----|---------------|----------------|----------------|---------------|----------------|----------------|
| 375 | 7.3923 | 48.2943 | 50.7653 | 7.3283 | 60.5681 | 63.8087 |
| 400 | 7.3722 | 49.3834 | 51.8542 | 7.3264 | 62.4553 | 66.3341 |
| 425 | 7.3628 | 50.2573 | 52.6687 | 7.3234 | 66.6775 | 71.6270 |
| 438 | 7.3532 | 51.0722 | 53.4831 | 7.3203 | 70.8998 | 76.9199 |



Fig. 6 Image compressed results obtained by: **a.** Python SVD function , **b.** Proposed method
Table 2 Image compression results for IndiaGate.jpg, 1024×768 , 858Kb, by using:
Python SVD function Proposed method

| K | Q_{comp} | MSE | PSNR | Q_{comp} | MSE | PSNR |
|-----|------------|---------|---------|---------------|----------------|----------------|
| 25 | 9.5409 | 27.6201 | 33.9037 | 7.0768 | 43.7210 | 46.9405 |
| 50 | 9.2389 | 28.4011 | 35.1045 | 6.9845 | 44.5122 | 48.4405 |
| 75 | 8.6088 | 29.8450 | 36.2988 | 6.9623 | 46.1665 | 49.8235 |
| 100 | 7.9788 | 31.2889 | 37.4932 | 6.9401 | 47.8209 | 51.2066 |
| 125 | 7.7346 | 32.5600 | 38.5471 | 6.9317 | 49.2150 | 52.4031 |
| 150 | 7.4904 | 33.8312 | 39.6011 | 6.9234 | 50.6091 | 53.5996 |
| 175 | 7.3713 | 35.0760 | 40.6256 | 6.9227 | 51.0844 | 54.0164 |
| 200 | 7.2523 | 36.3209 | 41.6502 | 6.9221 | 51.5598 | 54.4332 |
| 225 | 7.1760 | 37.5911 | 42.7026 | 6.9072 | 53.7449 | 56.6567 |
| 250 | 7.0998 | 38.8613 | 43.7551 | 6.8923 | 55.9301 | 58.8803 |
| 275 | 7.0621 | 40.2133 | 44.8726 | 6.8863 | 58.021 | 61.0707 |
| 300 | 7.0245 | 41.5653 | 45.9901 | 6.8804 | 60.1123 | 63.2612 |
| 325 | 7.0028 | 43.0392 | 47.2161 | 6.8779 | 62.271 | 65.2258 |
| 350 | 6.9811 | 44.5132 | 48.4421 | 6.8754 | 64.4297 | 67.1905 |
| 375 | 6.9595 | 46.1671 | 49.8244 | 6.8720 | 67.6065 | 70.9153 |

| | | | | | | |
|-----|---------------|----------------|----------------|---------------|----------------|----------------|
| 400 | 6.9379 | 47.8211 | 51.2067 | 6.8687 | 70.7834 | 74.6401 |
| 425 | 6.9306 | 49.2151 | 52.4031 | 6.8687 | 77.7668 | 83.8061 |
| 438 | 6.9234 | 50.6091 | 53.5996 | 6.8688 | 84.7503 | 92.9721 |

4.2.2 Analysis with Grayscale Image

In order to compare this performance, we also applied the new method to the gray scale image. After rank $K = 548$, we obtain:



Fig. 7 Image compressed results obtained on the: a. Python SVD function, b. Proposed method

Table 3 Image compression results for grayscale.jpg, 1024×960 , 480Kb, by using:
Python SVD function Proposed method

| K | Q_{comp} | MSE | PSNR | Q_{comp} | MSE | PSNR |
|-----|------------|---------|---------|------------|--------|---------|
| 25 | 4.9878 | 80.3421 | 27.6723 | 4.0621 | 9.5381 | 39.5372 |
| 50 | 4.9789 | 78.5091 | 29.2222 | 4.0589 | 9.4523 | 38.4098 |
| 75 | 4.6460 | 55.8911 | 31.08 | 4.0693 | 7.5163 | 39.5551 |
| 100 | 4.3132 | 33.2732 | 32.9378 | 4.0798 | 5.5803 | 40.7005 |
| 125 | 4.2067 | 25.1121 | 34.4039 | 4.1016 | 4.5246 | 41.7318 |
| 150 | 4.1002 | 16.9510 | 35.8701 | 4.1234 | 3.4689 | 42.7631 |
| 175 | 4.0779 | 13.2016 | 37.1421 | 4.1219 | 2.8566 | 43.7176 |
| 200 | 4.0556 | 9.4523 | 38.4142 | 4.1205 | 2.2443 | 44.6722 |
| 225 | 4.0699 | 7.5168 | 39.5574 | 4.1053 | 1.8652 | 45.5686 |
| 250 | 4.0843 | 5.5813 | 40.7006 | 4.0901 | 1.4861 | 46.4651 |
| 275 | 4.1037 | 4.5258 | 41.732 | 4.0756 | 1.2432 | 47.3227 |
| 300 | 4.1231 | 3.4704 | 42.7634 | 4.0611 | 1.0004 | 48.1803 |
| 325 | 4.1237 | 2.8574 | 43.7169 | 4.0531 | 0.8417 | 49.0217 |
| 350 | 4.1243 | 2.2444 | 44.6705 | 4.0452 | 0.6831 | 49.8631 |
| 375 | 4.1082 | 1.8626 | 45.5675 | 4.0346 | 0.5765 | 50.6617 |

| | | | | | | |
|-----|---------------|---------------|----------------|---------------|---------------|----------------|
| 400 | 4.0921 | 1.4808 | 46.4645 | 4.0241 | 0.4699 | 51.4603 |
| 425 | 4.0796 | 1.2405 | 47.3226 | 4.0198 | 0.3855 | 52.4072 |
| 450 | 4.0671 | 1.0003 | 48.1808 | 4.0156 | 0.3011 | 53.3541 |
| 475 | 4.0551 | 0.8422 | 49.0215 | 4.0139 | 0.2422 | 54.4873 |
| 500 | 4.0432 | 0.6842 | 49.8622 | 4.0123 | 0.1834 | 55.6206 |
| 525 | 4.0336 | 0.5770 | 50.6612 | 4.0112 | 0.1353 | 57.2296 |
| 548 | 4.0241 | 0.4699 | 51.4603 | 4.0101 | 0.0872 | 58.8387 |

4.2.3 Analysis with Other Methods

To evaluate the robustness of our scheme, we test it with other methods like: [10, 13, 14]. Added experiment results for two images are listed in Table 4.

Table 4 Image comparison with various algorithms
Color image (Fig. 4a) Grayscale image (Fig.4c)

| | Q_{comp} | MSE | PSNR | Q_{comp} | MSE | PSNR |
|-----------------|------------|---------|----------------|------------|---------|----------------|
| BTC method [13] | 9.2713 | 62.0951 | 30.2004 | 5.3912 | 16.1183 | 26.0905 |
| BTC method [10] | 7.3406 | 7.9635 | 39.1261 | 3.9808 | 19.0298 | 35.3689 |
| BTC method [14] | 6.7203 | 2.7451 | 43.7507 | 2.8441 | 3.4708 | 42.7644 |
| SVD method [14] | 7.3508 | 0.2900 | 53.4831 | 4.0261 | 0.4722 | 51.4612 |
| Proposed method | 7.3107 | 0.0013 | 76.9199 | 4.0110 | 0.0804 | 58.8387 |

In this paper, the proposed algorithm is compared with the Python SVD function [14] and the other state-of-the-art algorithms.

When applying the proposed method to image compression, Figs. 5, 6 and 7, it is shown that the compressed images by two approaches are similar to original images. But the human visual response to image quality is insufficient.

We compare the performances of the proposed method, several values were used in this study to measure the quality of the compressed image. We will discuss PSNR and MSE values, because, they are used to compare the squared error between the original image and the reconstructed image. There is an inverse relationship between PSNR and MSE. Therefore, a higher PSNR value indicates the quality of the image.

This analysis shows the comparison when SVD and proposed method are applied on the original images. In these experiments, we used the K rank for different images. We see in this case that the compression ratio and PSNR, and other values of images varied when changing the rank of image during the SVD process as showed in Tables 1, 2 and 3, and it is evident that the proposed technique gives better performance compared to the SVD. In addition, for the Python SVD function, the value of K which provides better PSNR value is the maximum value of $K = 438$, while for the proposed technique, a better, compression ratio, PSNR is provided from $K = 150$ for color images. We concluded that our proposed method result is 1/3 of K rank compare to other methods.

Concerning the grayscale image analysis, it seems that the value of K which gives better PSNR value is the maximum value of $K = 548$, while for the proposed method, a better, compression ratio, PSNR is provided from $K = 400$.

We compared the proposed algorithm with the other algorithms as shown in Table 4. Hence, show our proposed algorithm performs com-parable to other existing techniques. It is able to produce a compressed image with better visual quality, as indicated by its PSNR.

5 Conclusion

In this work a novel method for image compression, this technique is very simple, and it can be used to overcome limitations of existing algorithms, that used in the Python SVD function. The results shown that the proposed approach might be considered as a solution for the development of image compression. Our proposed method of image compression is provided faster due to the minimum number of iterations in the compression algorithm.

Future Scope

The future scope of this work is using the SVD for statistical applications to find relations between data, in the area of medical image denoising with different thresholding techniques associated with these multiwavelets, implements a compression technique using neural network.

References

- [1] Madhuri A.J.: "Digital Image Processing. An Algorithmic Approach", pp. 175–217. PHI, New Delhi, 2006.
- [2] Weinberger, M.J., Seroussi, G., Sapiro, G.: "The LOCO-I lossless image compression algorithm: principles and standardization into JPEG-LS", *IEEE Transactions Image Processing* **2**, pp. 1309–1324, 2000.
- [3] Alkhalayleh, M.A., Otair, A.M.: "A new lossless method of image compression by decomposing the tree of Huffman technique", *International journal of imaging & robotics* **15**(2), pp. 79–96, 2015.
- [4] Jianji, W., Nanning, Z., Yuehu, L., Gang, Z.: "Parameter analysis of fractal image compression and its applications in image sharpening and smoothing", *Signal Processing: Image Communication journal* **28**, pp. 681–687, 2013.
- [5] Bilgin, A., Michael, W., Marcellin, M., Altbach, I.: "Compression of electrocardiogram signal using JPEG2000", *IEEE Transactions on Communications Electronics (ICIP)* **49**(4), pp. 833–840, 2003.
- [6] Awwal, M.R., Anbarjafari, G., Demirel, H.: "Lossy image compression using singular value decomposition and wavelet difference reduction", *Digital Signal Process* **24**, pp. 117–123, 2014.
- [7] Adiwijaya, M., Dewi, B.K., Yulianto, F.A., Purnama, B.: "Digital image compression using graph coloring quantization based on wavelet SVD", *Journal of Physics Conference Series* **423**(1), pp. 012–019, 2013.
- [8] Ranade, A., Mahabalarao, S.S., Kale, S.: "A variation on SVD based image compression", *Image and Vision Computing journal* **25**(6), pp. 771–777, 2007.
- [9] Doaa, M., Chadi, A.F.: "Image compression using block truncation coding". *Cyber J. Multidiscip. J. Sci. Technol. J. Sel. Areas Telecommun. (JSAT)*, February, 2011.
- [10] Delp, E.J., Mitchell, O.R.: "Image compression using block compression", *IEEE Transactions on Communications* **27**(9), pp. 1335–1342, 1979.
- [11] Tsou, C.C., Wu, S.H., Hu, Y.C.: "Fast pixel grouping technique for block truncation coding", In: *Workshop on Consumer Electronics and Signal Processing (WCESp05)*, Yunlin, pp. 17–18 Nov, 2005.
- [12] El Abbadi, N.K., Al Rammahi, A., Redha, D.S., Abdul-Hameed, M.: "Image compression based on SVD and MPQ-BTC", *Journal Of Computer Science* **10**(10), pp. 2095–2104, 2014.
- [13] El Asnaoui, K., Chawki, Y.: "Two new methods for image compression", *International journal of imaging & robotics* **15**(4), pp. 1–11, 2015.
- [14] Bentbib, A.H., Kanber, A.: "Block power method for SVD decomposition", *Analele Stiintifice ale Universitatii Ovidius Constanta Seria Matematica* **23**(2), pp. 45–58, 2015.

Mathematical Analysis and Wavelength Transformation process for secure data-hiding in images

Dr.Perepi.Rajarajeswari

Associate professor,Department of Computer science and Engineering,
Kingston engineeringcollege,Vellore,Tamilnadu,India,Email:rajacse77@gmail.com

Dr.P.Rajasulochana

Professor,Department of bio information and Genetic engineering,Bharat institute of Higher education and research,Chennai,prsnellore@gmail.com

Abstract

Wavelet Transforms method can be used for image processing issues, medical image applications and their visual methods. The objective of this paper is to provide secure transmission in between sender and receiver. In this paper we provide data hiding techniques by using encryption and decryption transmission process for maintaining security issues. In this method we embedded the original image with secure information by using lossless data hiding method. We apply Discrete Wavelength Transform (DWT) for encrypting the input messages and at receiver side, when the message is arrived then we apply decryption technique using Inverse Discrete Wavelength Transform(IDWT) algorithm to get the original image and secret information.Reducing Noise ratio when to compare to existing system of various watermarking levels using DWT and IDWT algorithm.PSNR (Peak – Signal Noise Ratio) is high when compared to existing system, so noise ratio is very low.

Keywords: Data hiding, Wavelet transformation, Digital imaging process, Mathematical functions

1 Introduction

To maintain the data communication confidentiality is a major issue. Data hiding process is performed by using a non – conventional approach called steganography [1].Now a days Data communication and Secure the data is the major challenging task due to technological growth. Steganography is used to control the data hacking,unwanted actions of data from intruders .Robustness, lacking of security risks are the disadvantages of existing work [2].To overcome these problems,This research work focused on secure data hiding in image by using Wavelet transformation process. Various methods are clearly explained in different sections of this paper. Digital image processing techniques are to be used for the image manipulation by the computer devices.It is relatively developed recentlyby using man’s ancient fascination with visual stimuli. Image is a two-dimensional object which has photograph, screen display and as well as a three-dimensional statue. Images maybe captured by using optical components cameras, telescopes etc[3].

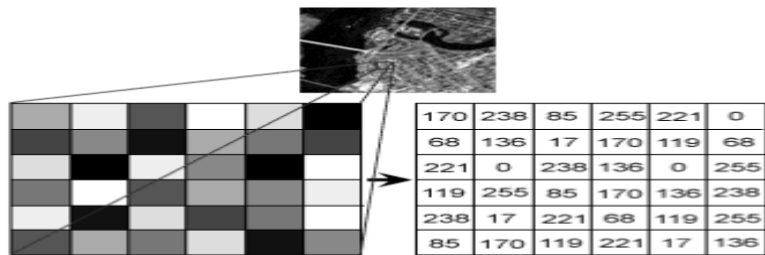


Figure 1. Representation of image in pixel

The word image can be expressed in the form of map, graphs, and piecharts. Image composition can be expressed in the form of pixels. Image resolution can be increased to increase the file size and compression can be done with the reduction of file size.

Image file formats: Images can be organized by using Image file formats.Compression of images is done in the form of pixel or vector data.

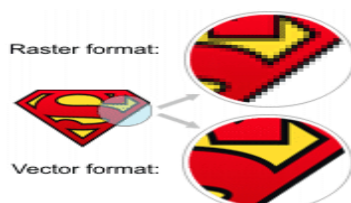
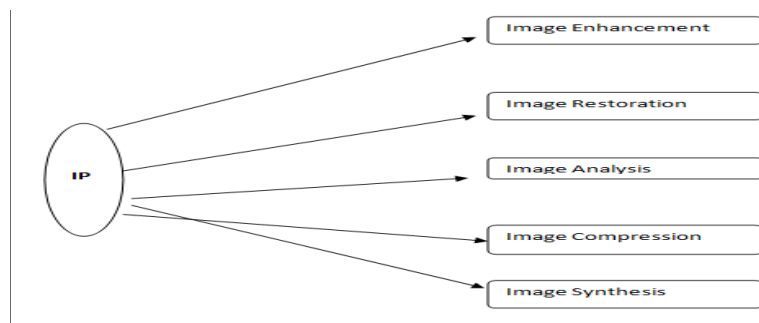


Figure2: Image files format types

Image processing techniques: Image processing techniques are image enhancement, image restoration, image analysis, image compression, image synthesis. These techniques are shown below. These type of operations are used to create images from other images or non-image data.

**Figure 3: Image processing techniques**

Mathematical functions are applied for Haar wavelet transformation methods. This method can be used for getting secured data with more accuracy. Haar wavelet transformation method

consists of standard decomposition method and nonstandard decomposition method.

Related works is presented in section 2. section 3 provides the wavelet transformation process. Section 4 gives system overview and methods and implementation is given in section 5. Results are given in section 6. Conclusion are presented in section 7.

2 Related works

Zhang et al described the reversible data hiding in encrypted images [4,5]. They have focused on survey of different methods for data reversible hiding of encrypted images. It provides security of embedded data. Encryption techniques are used for data hiding process. AES data encryption techniques for reversible data hiding in encrypted images. They proposed various algorithms for encrypted image. Qin et al describes the Reserving room before encryption based on reversible data hiding with encrypted images [4, 5]. They have focused on novel based analysis for retrieval of hidden data with digital color images and proposed the encrypted images for separable reversible data hiding process. This method proposed the encryption key methods for improving the embedding capacity. Hong et al [6] proposed the medical image process with watermarking techniques of encryption techniques. Rajeswari et al focused on Mathematical analysis [14]. Many researchers have been done work on the improvement of visual perceptibility performance. Based upon these analysis results, we can enumerate the disadvantages of the existing method.

3 Wavelet Transformation Process

We have proposed various methods which described secure data transmission for sending and receiving data with minimizing the noise when compared to existing system. Wavelet transformation process is described clearly.

3.1 Encoding process

In this process, we proposed a method for data hiding, steganography and watermarking techniques. First of all, Browse the Original image from library for embedding the secret message and transmit to the receiver end. And then edit the secret information or message in our text field and then push the button for embedding the original image and secret information or message. After that, to save the encoded image in folder and then select the encoded image for applying the various level of water marking techniques using DWT (Discrete Wavelet Transform) 1 to 5 levels of algorithm for reducing the noise ratio of the encoded image. Calculating the PSNR and MSE values of every stage of watermarking levels. Each and every level of watermarking will reduce the noise ratio of encoded image. In this process, finally we perform the IDWT (Inverse Discrete Wavelet Transform) using this algorithm Inverse extraction of watermarking process for decoding process to get the

watermarked final image with minimum noise ratio when compared to existing system[4]. Calculating the PSNR and MSE values of every stage of Inverse Discrete Wavelet Transform watermarking levels[5,6]. Each and every level of IDWT watermarking will be reducing the noise ratio for decoded image or IDWT Final watermarking image [7].

3.2 Decoding process

In this process, we have to select the final watermarked image or encoded image for decryption process from getting the image of Inverse Discrete Wavelet Transform and then select the decryption process .We get the Original image and secret information or secret message in receiver side. In this, few process of Watermarking reducing noise ratio when to compare to existing system.

4. System overview:

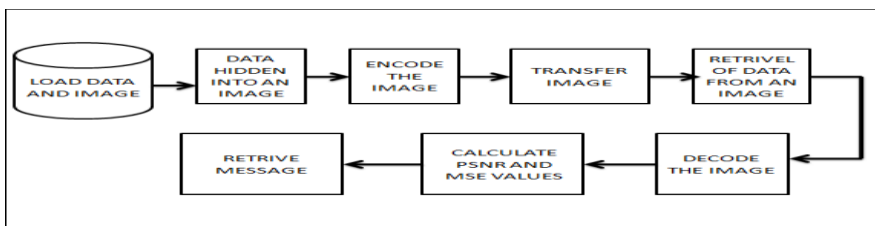


Figure 4. System architecture

The image and data is loaded from the system then the data is hidden into an image. The image is encoded and transfer to the receiver. By the calculation of PSNR and MSE values, the correct image and data is retrieved on the receiver side. Thus the secure data hiding is done using DWT and IDWT [8, 9,10].

4.1 Mathematical approach

In mathematics domain, the **Haar wavelet** transformation process needs a sequence of “square-shaped functions which are rescaled .These are combined to form a wavelet family Wavelet analysis follows just like to Fourier analysis which allowsa target function in an interval and represents the orthonormal basis function. This process follows an orthonormal system with in the space of interval [0,1].Haar wavelet is also known as **Db1**.It is simplest possible wavelet method and not continuous. Sudden transitions for signal analysis and monitoring of machine tool’s failures [11, 12,13].Description of the Haar wavelet's mother wavelet function can be formulated which are given below.

$$\psi(t) = \begin{cases} 1 & 0 \leq t < \frac{1}{2}, \\ -1 & \frac{1}{2} \leq t < 1, \\ 0 & \text{otherwise.} \end{cases} \quad \text{-----Eq (1)}$$

Its **scaling function** $\varphi(t)$ can be described as

$$\varphi(t) = \begin{cases} 1 & 0 \leq t < 1, \\ 0 & \text{otherwise.} \end{cases} \quad \text{-----Eq(2)}$$

5 Methods and Implementation

This Paper presents a secure transmission process of images with using various level of watermarking techniques. This present method that combine the secret message and image of data hiding technique, encryption and watermarking technique for denoised and secure image transmission purpose.Original image is embedded with secure information with the help of lossless data hiding method and do the encryption algorithm forthe secret images. Using DWT and IDWT algorithm, we get the watermarking images and reduced the noise ratio of final watermarking image when compared to an existing system[14]. We can apply inverse methods for getting the original image and secret information on receiver side, when the message is arrived thus the secret information and image is retrieved without any error in the receiver side[5].

5.1 Discrete wavelength transform techniques

Discrete Wavelet Transform techniques are used image pixels into wavelets, wavelet-based compression method and coding process. It reduces the noise ratio of final watermarking image [14].

5.1.1 DWT Procedure

The length of DWT is 16 bits. Low-pass sifted signal is in augmentations of two and the initial eight components of the vector are assembled in the subsequent coefficients. At Second phase of the DWT cycle: The first sign is considered as high-pass separated in the development of two and the coefficients are last eight components of vectors [8].

5.1.2 DWT Process

First of all one-dimensional DWT can be applied to all rows and also applied to all the columns of first-stage results which gives four band regions, such as LL, LH, HL and HH.

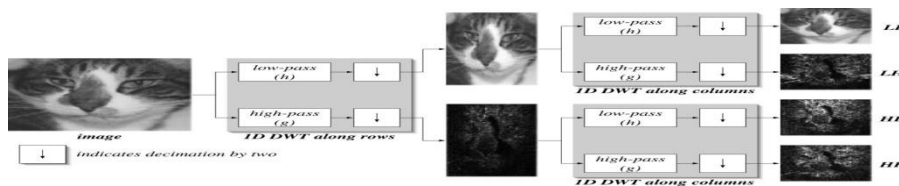


Figure 5.DWT Image Processing

5.2 Multilevel inverse discrete wavelength transforms Technique

In Inverse Discrete Wavelet Transform, we select the final encoded image for decryption process. And then by decrypting technique we get the original image and secret information or secret message in receiver side[15].

IDWT Procedure

First of all, interleave all the low-pass and high-pass components of the wave-let .The converse segment of low-pass channel can be applied two additions and the backwards converse of high-pass channel is applied in two augmentations. Procedure for registering the one-dimensional converse DWT, is to delineate the reverse DWT for a one-level DWT of length 16 (accepting channels of length four). Determine the High-pass channel is as per the following by utilizing low-pass channel

5.3 Multilevel ID Discrete Wavelet Transform of data

It provides the information about frequency components which are present and to increase the information about the signal for doing further processing. Particularly we will be able to get smooth images/signals at the subbands of the first level of decomposition. But we will recognize noise more hardly. Generally different levels of decomposition process to allow analyzing and processing the images or signal features of different scales, which are to be critical in some applications[16].

Proposed Algorithm:

Input: Input data-array

Wavelet: Object –Wavelet to use

Signal extension modes to use, **Level:** Decomposition level is greater than or equal to 0.

If level is none

Then it will be calculated by using the `dwt_max_level` function

Axis: Axis is over to compute DWT.

If not given, last axis is used.

Returns, Ordered list of coefficients arrays where `n` denotes the decomposition level.

For Direct reconstruction process,,take Coefficients type 'a', '&'d'

'ar' means approximations reconstruction, 'd' specifies the detailed reconstruction process.

arrays of coefficients are reconstructed.

wavelet : Wavelet object or name which is to use

it may be optional.

Multilevel reconstruction level.

Default is 1.

Take central part of length equal to 'take' from the result. Default is 0.

Returns: rec : ndarray

1-D array with reconstructed data from coefficients.

5.4 Applying a Digital wavelet transform to an image

Wavelet transformation techniques are using number of applications based on Fourier transformation process. Wavelet Transforms (WT) process can also be used Image compression methods, Feature extraction phases, image denosing and other medical image techniques, Speech recognition process, Computer vision method. Physics parameters have seen various operations such as dynamic operations, matrix allocation methods, optics, quantum mechanical properties.[18]. This method is implemented in Python environment. Mostly This method is more useful in health care applications(heart analysis rate, ECG-analysis etc.)[14].

6 Experimental Results and Discussion

Two matrices are used for the representation of Indexed images .A color map matrix and image matrix. Color map matrix representing all the image colors. Image matrix represents indexes which corresponds to the colormap.The size of color map matrix is $N \times 3$, Here N =different colors of images.The wavelet toolbox only supports indexed images that have linear, monotonic color maps. Often color images need to be pre-processed into a grey scale image before using wavelet decomposition and implementation in MATLAB environment [11,12,17]. A digital image is composed of pixels in the form of as small dots on the screen [13]. A typical size of an image is 512-by-512 pixels. Image format as 512-1024 pixels. Image contains information as 524288 pixels.



Figure 6. Restored

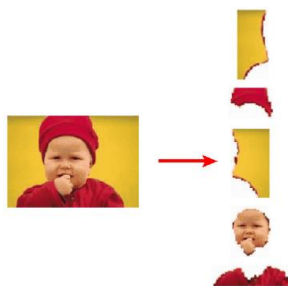


Image Figure 7.

Compression of image



Figure 8. Image enhancement

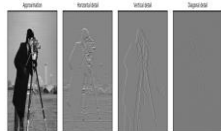


Figure 9. Embedded image



Figure 10. Digital wavelet transform image

7 CONCLUSION

Based upon these analysis results, we can enumerate the main advantages of the proposed method. Reducing Noise ratio when to compare to existing system of various watermarking levels using DWT and IDWT algorithm. PSNR (Peak – Signal Noise Ratio) is high when compared to existing system, so noise ratio is very low. Data hiding with DWT and IDWT techniques and no other techniques are used when compared to existing system. This paper provides the Multilevel ID wavelet transformation process and its implementation. Harr wavelet transformation process is also described by using mathematical functions. It provides accuracy and increases the resolution of images and easily get the digital wavelet transform to an image.

References

- [1] W. Zhang, K. Ma and N. Yu, "Reversibility improved data hiding in encrypted images," *Signal Processing*, vol. 94, pp. 118–127, 2014.
- [2] X. Zhang, "Separable reversible data hiding in encrypted image," *IEEE Trans. Inf. Forensics Security*, vol. 7, no. 2, pp. 826–832, Apr. 2012.
- [3] K. Ma, W. Zhang, et al. "Reversible Data Hiding in Encrypted Images by Reserving Room Before Encryption," *IEEE Trans. Inf. Forensics Security*, vol. 8, no. 3, 553-562, 2013.
- [4] Z. Qian, X. Han and X. Zhang, "Separable Reversible Data hiding in Encrypted Images by n-nary Histogram Modification," 3rd International Conference on Multimedia Technology (ICMT 2013), pp. 869-876, Guangzhou, China, 2013.
- [5] X. Zhang, "Reversible data hiding in encrypted images," *IEEE Signal Process. Letts.*, vol. 18, no. 4, pp. 255–258, Apr. 2011.
- [6] W. Hong, T. Chen, and H. Wu, "An improved reversible data hiding in encrypted images using side match," *IEEE Signal Process. Letts.*, vol. 19, no. 4, pp. 199–202, Apr. 2012.
- [7] J. Tian, "Reversible data embedding using a difference expansion," *IEEE Trans. Circuits Syst. Video Technol.*, vol. 13, no. 8, pp. 890–896, 2003.
- [8] M. U. Celik, G. Sharma, A. M. Tekalp, and E. Saber, "Lossless generalized-LSB data embedding," *IEEE Trans. Image Process.*, vol. 14, no. 2, pp. 253–266, 2005.
- [9] Z. Ni, Y. Q. Shi, N. Ansari, and W. Su, "Reversible data hiding," *IEEE Trans. Circuits Syst. Video Technol.*, vol. 16, no. 8, pp. 354–362, 2006.
- [10] D. M. Thodi and J. J. Rodriguez, "Expansion embedding techniques for reversible watermarking," *IEEE Trans. Image Process.*, vol. 16, no. 3, pp. 721–730, 2007.
- [11] Y. Meyer, *Wavelets: Algorithms and Applications*, Society for Industrial and Applied Mathematics, Philadelphia, 1993, pp. 13-31, 101-105.
- [12] James S. Walker. 1999. *A Primer on Wavelets and Scientific Applications*.
- [13] Applying the Haar Wavelet Transform to Time Series Information
- [14] P. Rajarajeswari, D. Vasumathi, A. Ramamohanreddy "Problem Solving Process Based on Conceptual Model with Mathematics Techniques," *International Journal of Computer & Mathematical Sciences IJCMS* ISSN, 2347-8527
- [15] X. Zhang, "Reversible data hiding in encrypted images," *IEEE Signal Process. Lett.*, vol. 18, no. 4, pp. 255–258, 2011.
- [16] X. Zhang, "Separable reversible data hiding in encrypted image," *IEEE Trans. Inf. Forensics Security*, 10.1109/TIFS.2011.2176120.
- [17] Image database [Online]. Available: <http://sipi.use.edu/database/>
- [18] R. C. Gonzalez, R. E. Woods, *Digital Image Processing*, 2nd edition, chapter 7, "Wavelets and Multiresolution Processing", Pages 372-386 Patrick J. Van Fleet, "Discrete Haar Wavelet Transforms", PREP - Wavelet Workshop, 2006.

An Automatic Attendance Monitoring System Using Python

J. Narmatha, V. Krithika, P. Ramana, V. Vidhya Assistant Professor
Salem College of Engineering and Technology, Salem, Tamilnadu

Abstract

Monitoring and recording attendance on a real-time basis in a technologically enhanced era seems to be a difficult task nowadays. There is a problem regarding analyzing the statistical attendance data as most of it is not accessible outside the educational campus. With an intention to keep students safe while fulfilling their basic rights to education, a design has been proposed that automatically updates the attendance of a student in the database and simultaneously sends information to the parent, class advisor and Head of the Department. This method has been designed to be implemented specifically in college, the approach of taking the attendance on daily and hourly basis is a reason for students to behave disciplined. Sometimes the traditional method was complicated and there are ways where a student can dodge and if taken physically it leads to more time consumption and can be prone to human errors. Hence several automated techniques were devised like fingerprint, Radio Frequency Identification (RFID), Iris recognition etc. these techniques have their own shortcomings, here a framework called Automated Attendance Tracker using Firebase Real-time Database is proposed. The attendance is taken by placing a web camera inside the classroom that endlessly captures the images of the student, identifies the faces in image and updates the attendance. The updated attendance is sent to the parent and class advisor through Short Message Service (SMS) and via Electronic-mail to the Head of the Department (HOD) and Administration wing. This highly improves the efficiency of system and is found to be less time consuming.

Keywords: -Automated Attendance Tracker, Firebase Real-time Database, Haar Cascade Algorithm, REST API

1 Introduction

Studies show that a significant amount of time is spent on taking attendance in the classroom, it is found that nearly 15% of the total time in one-hour lecture is consumed for taking attendance manually. To make the productive use of time inside the classroom, automated attendance tracking systems were proposed. These systems include Radio Frequency Identification (RFID) based Attendance Monitoring System, Fingerprint based Attendance System, Android Mobile Based Attendance System, Face Recognition based Attendance System etc. Initially the automated attendance tracking system had a hardware that has to be coded and a distant server that has to work together for acquiring data and processing it electronically. The standard way of taking attendance in school or college is by calling the names of the student by the teacher, students responding on their roll numbers and marking 'A' or 'P' on logbook subsequently. This technique looks better and cheaper. The biggest drawback in using the standard technique is, taking attendance is tedious, writing or marking the information and then calculating the percentage of attendance, sorting, transferring it onto a personal computer for additional backup etc. are complex and can be prone to errors. The system becomes ineffective when there are large number of students in a class. Hence moving to software based automated attendance system not only eliminates manual errors and makes the task simple, it ensures that the students uphold discipline by following the mandatory rules of the college and thereby uplift the quality of education in the institution

2 Literature Review

In this section some of the related work described for motivation to do the work to be carried out.

Hidayat, Muhammad Ayat, et al. [1] For students, attendance is a basic requirement. The participation of a student cannot be accessed by the faculty in the absence of the attendance process. Generally, manual attendance is taken using paper and later signed by the students. This process leads to various complications such as excessive usage of paper and challenging for the administration to summarize the results of the student attendance. Hence, attendance system is essential to gather data rapidly, precisely, and efficiently. In this paper, it is done by collecting data, analyzing, designing, and implementing the system. This system is formed by using Java Android programming languages, Ibeacon for identifying the classroom and PHP. The key purpose of this study is to schedule warnings based on IBEACON which makes the attendance process more efficient and can simply be examined by the faculty and the administration.

Othman, Mahfudzah, et al. [2] In academic institutions student's attendance record are one of the important documents which replicate on the reliability of institutions and student's performance. However, the managing process of these documents had been done using pen and papers by making it less efficient. This paper deliberates about the growth of new online attendance system and its architecture is based on the web. The

online attendance is made cost-effective by integrating various web-based technologies such as Apache Web Server, PHP, and MySQL. This system involves 4 key phases used in the construction of the framework. It is an automated process to generate warning reports and an online attendance report. Therefore, the system is well organized by the process of reporting and recording the attendance of a student.

Singh, Manjot, et al. [3] In today's era irrespective of the field of education or defining both qualitative and quantitative data, gathering of data is necessary for sustaining the reliability of research. The probabilities of error taking place can be reduced by data acquisition. In this paper, the proposed framework has small accessible hardware, a remote sensor, and software constituents for acquisition. It can be implemented in schools, colleges, industries, and hospitals. This system is used for taking attendance in colleges and schools making it modest and well-organized. The educational organizations are the main users where there is a prerequisite of user-friendly, energy-efficient, portable, and protected automated system. Therefore, the prototype delivers an integrated solution with an embedded attendance system. The advantages are small size and low power consumption.

Shah, Soumil Nitin, et al. [4] This paper presents a new model of observing student attendance using Radio Frequency Identification (RFID) with the Internet of Things (IoT). Many schools and colleges are almost worried about student unbalanced attendance. Student's overall performance can be exaggerated due to truancy. The outdated method of taking attendance by signing on paper or by calling names is very time overwhelming. The top solution to handle these difficulties is RFID based attendance system using the Internet of Things.

Sawhney, Shreya, et al. [5] For teachers, attendance management is a crucial task done manually. In order to overcome these complications smart attendance management system is implemented. Additionally, authentication is a significant issue in this system.

3 ProposedSystem

Haar Cascade Algorithm Haar Cascade algorithm is used for object detection and is a machine learning algorithm. With this algorithm one can identify objects in videos or images. This algorithm is operating in four stages as shown in Fig.1. Haar feature selection selects features in the face like eyes, eyebrows, nose, mouth etc. The feature selection is done based on Edge features, Line features, Four rectangle features. It differentiates the brighter part and darker part of our face as white color and black color. The output of this stage is given to the next part, creating integral images, this stage performs summation of intensities of pixels and shows certain specific regions (features) of the image.

Flowchart of algorithm



Fig(1). Flow chart of algorithm

Yet for more accurate manipulation, the output of the second stage is given to Adaboost training. This stage is a classification stage, wherein a group of poorly performing classifiers are used iteratively to bring about high and accurate results. Finally, the last stage is Cascade classifiers, which is already trained with the positive and negative pixels of the region of interest in an image that facilitates to take a decision if the image can be passed or rejected.

3.1 Introduction to REST API

Generally, a client requests a server for a required information and the server responds to the client. Normally the response sent by a server to a client is an HTML webpage. But in real-time receiving a HTML webpage for a request generated is annoying, as the required information is only data and that too data in a structured format. Structured data can be in the form of XML format or JASON format. In Representational State Transfer

(REST), a client will send a request to a server, at this juncture the RESTAPI creates an object for the data, searches for the data requested, on finding the data it responds to the client with the values (state) of that particular object. Since the state of the object is transferred to the client, it is called as Representational State Transfer. Hence REST API is an approach for communication between a client and a server, for web services application.

Features of REST API

- It is simpler than SOAP API
- It has proper documentation that is easy to understand for developing user defined applications
- It provides proper error messages that facilitates easy debugging Resources are the data a client is requesting for, to create a resource, read it, update it and delete it, HTTP methods can be used as shown in the Fig.2. REST API does communication via HTTP methods.

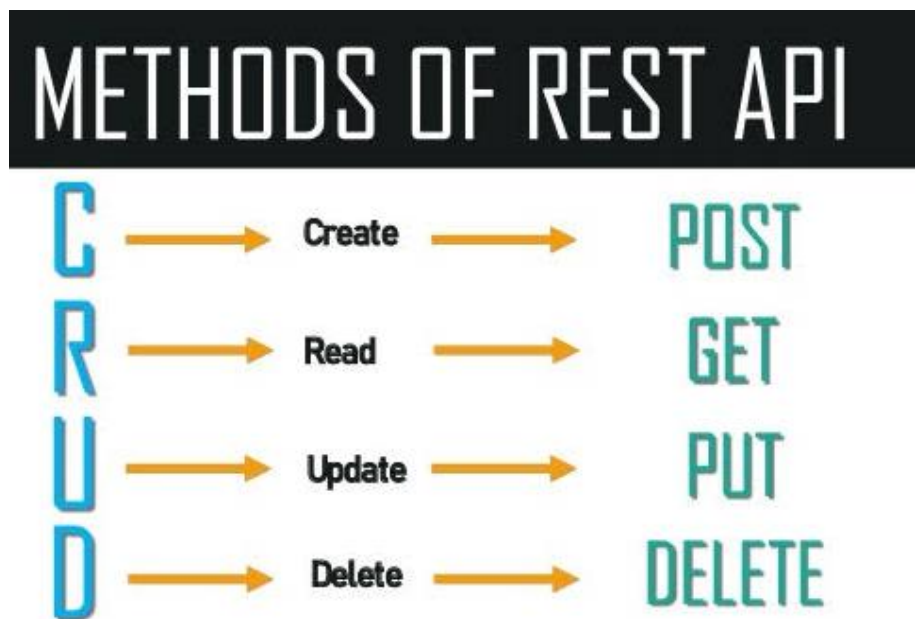
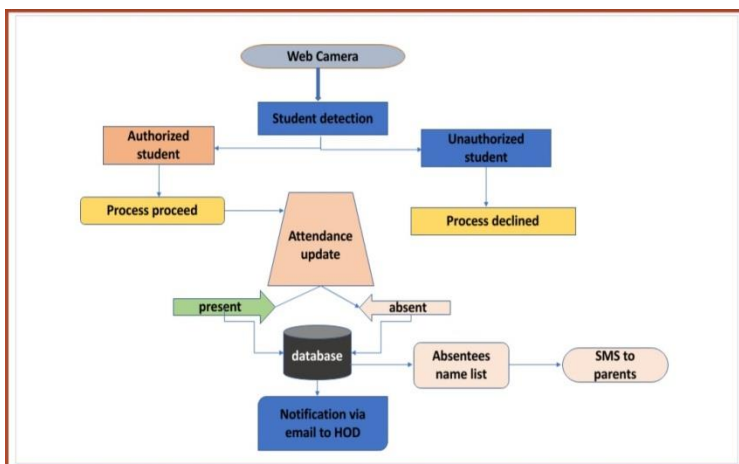


Fig.2

3.2.Introduction to Firebase Real-Time Database

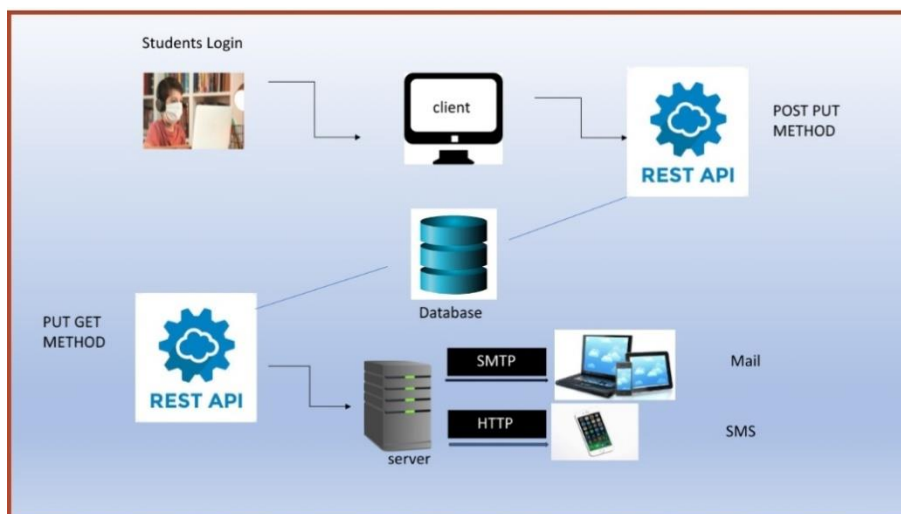
Firebase Real-time Database allows to store and synchronize data between users in real time. When data is put on a Firebase Real-time Database it stores the data on cloud and notifies all the connected devices simultaneously. This data base is optimized for offline use, when a user loses internet, the database uses a local cache on the device to serve and store changes, when the user next comes online the local data synchronizes automatically. In order to keep data secured in Firebase Real-time database, database security rules are used. Since the Firebase Real-time data base is hosted in cloud, there is no requirement for server maintenance or operations. D. Flow Diagram of the Proposed System A web camera is in ON condition and is placed inside the classroom. This will detect the face of the student and checks whether the student is authorized or not. If the student is authorized, further process is initiated, using facial recognition technique (Haar Cascade algorithm) the student present is sent to the Firebase Real- time database where manipulation is carried out and the absentees of the day are identified. The attendance status is updated and stored in the database. This list will be sent to the Head of the Department and Administration wing through e-mail. The absentees list is sent to the class advisor and the absentee's parents are notified via SMS. If the student is unauthorized further process is declined. The entire process is shown in Fig.3



Process Involved in Framework. The web camera captures the face of the student and the images are stored in the dataset. Previously, a set of photos are trained and stored in .jpg format by using Haar Cascade algorithm, the images in the dataset are compared with the trained photos. If it matches the student is present. The updated attendance is transferred to Firebase Real-time database through REST API by using POST or PUT method. The data stored in the database is in the form of Java Script Object Notation (JSON) tree format. Now, both present and absent list of the students are sent to server through REST API PUT method. The server reads it using PUT and GET method, the process continues by sending an email to the HOD and Administration wing via Simple Mail Transfer Protocol (SMTP), the absentee list is sent to the class advisor through SMS and further a notification is sent to the absentee’s parents through FAST2SMS via SMS

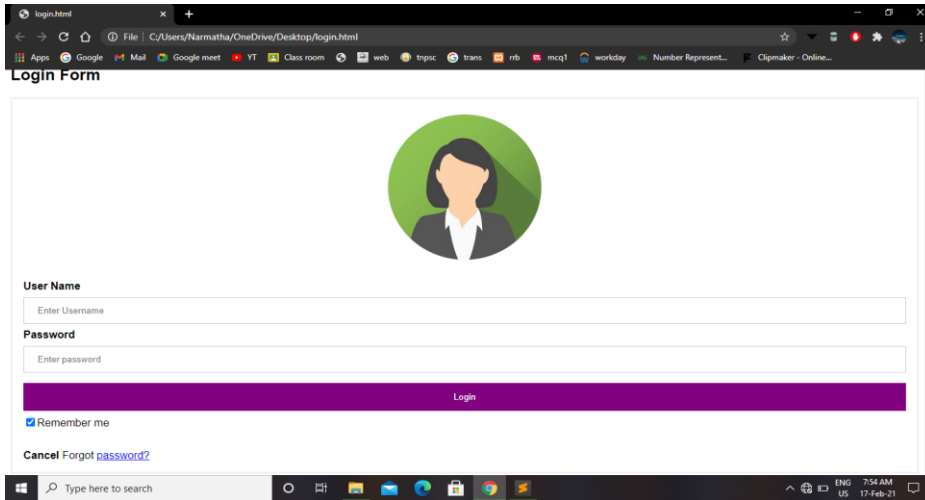
3.3. Process Involved in Framework

The web camera captures the face of the student and the images are stored in the dataset. Previously, a set of photos are trained and stored in .jpg format by using Haar Cascade algorithm, the images in the dataset are compared with the trained photos. If it matches the student is present. The updated attendance is transferred to Firebase Real-time database through REST API by using POST or PUT method. The data stored in the database is in the form of Java Script Object Notation (JSON) tree format. Now, both present and absent list of the students are sent to server through REST API PUT method. The server reads it using PUT and GET method, the process continues by sending an email to the HOD and Administration wing via Simple Mail Transfer Protocol (SMTP), the absentee list is sent to the class advisor through SMS and further a notification is sent to the absentee’s parents through FAST2SMS via SMS.



Fig(4).Working of proposed model

4 Sample Results



Fig(a). Student Login

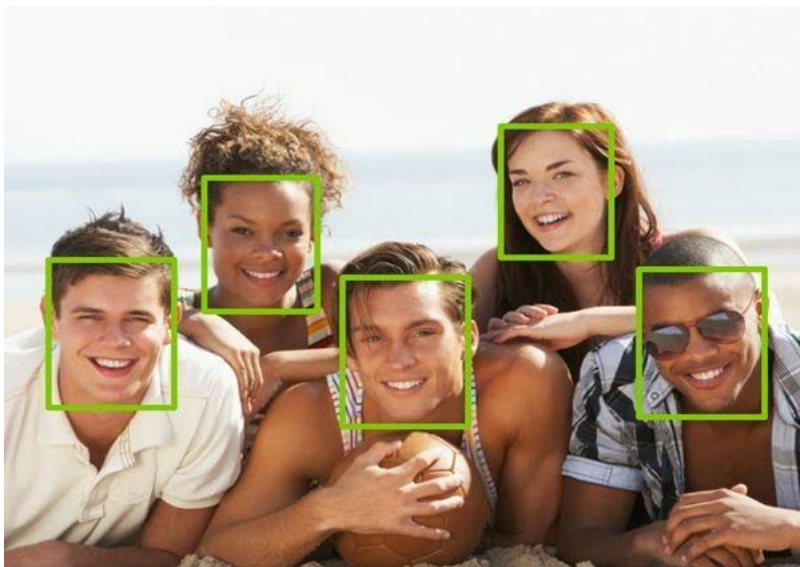


Fig (b). Show the face front of the webcam



Fig (c).Using haar cascade algorithm

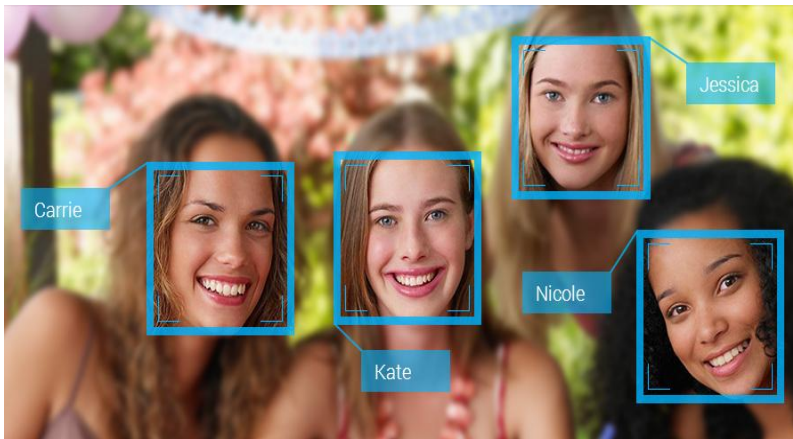
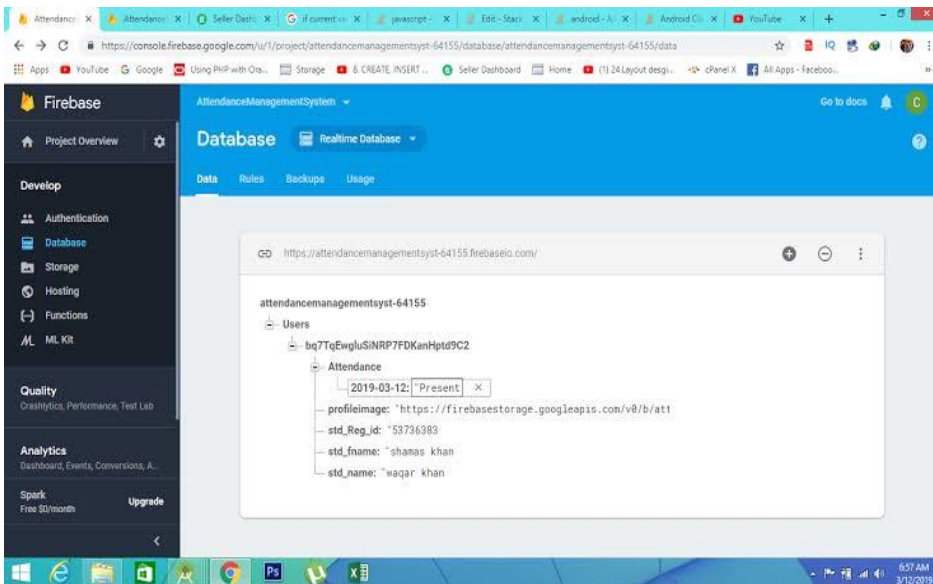
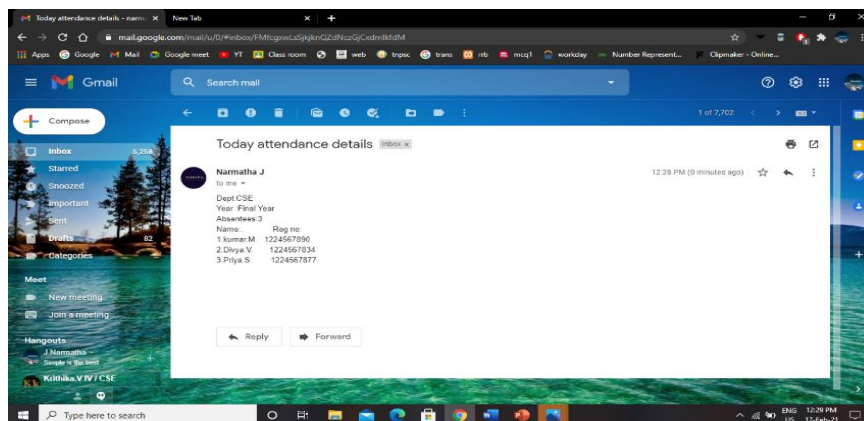


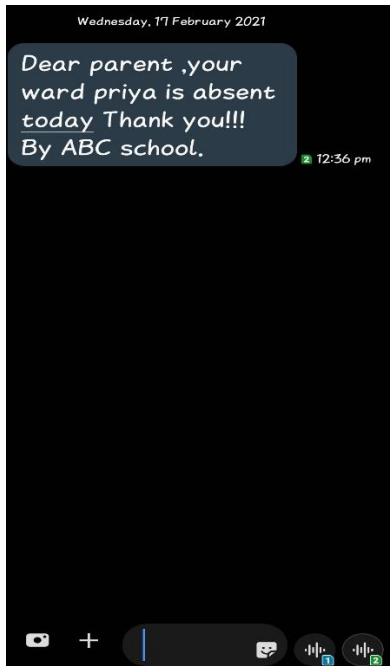
Fig (d). Detect the face



Fig(e).Store the data in Firebase database



Fig(f) E-mail sent to the HOD



Fig(g).SMS sent to parents

5 Conclusion and Future Works

The proposed attendance tracking system will serve as a useful approach to automate the attendance recording, it provides more accuracy and less prone to human error, works fast and is always synchronized to its connected devices. This seems to be an effective methodology when compared to conventional method and the other automated systems. As a future enhancement, live classes taken by the professor can be recorded and sent automatically to the absentees of the particular day.

Acknowledgement

I would like to express my special thanks of gratitude to my Professor Mrs. Saranya, who help me to do this wonderful project

References

- [1] M.Julie Therese, K. Reshma, R. Keerthana @ Rakshendra, K.Priyatharshiny, "Multilevel Secured Locker System Using IOT", International Journal of Advanced Research in Innovative Discoveries in Engineering and Applications (IJARIDEA), Vol. 5, Issue 1, pg.1-7, 2020.
- [2] Hidayat, Muhammad Ayat, and HolongMarisiSimalango. "Students Attendance System and Notification of College Subject Schedule Based on Classroom Using IBeacon." 2018 3rd International Conference on Information Technology, Information System and Electrical Engineering (ICITISEE).IEEE 2018.
- [3] Singh, M., Khan, M. A., Singh, V., Patil, A., &Wadar, S. (2015, February). *Attendance managementsystem*. In 2015 2nd International Conference on Electronics and Communication Systems (ICECS) (pp. 418-422). IEEE.
- [4] Shah, Soumil Nitin, and AbdelshakourAbuzneid. "IoT Based Smart Attendance System (SAS) UsingRFID." 2019 IEEE Long Island Systems, Applications and Technology Conference (LISAT). IEEE, 2019.
- [5] Sawhney, S., Kacker, K., Jain, S., Singh, S. N., & Garg, R. (2019, January). Real-Time Smart Attendance System using Face Recognition Techniques. In 2019 9th International Conference on Cloud Computing, Data Science & Engineering (Confluence) (pp. 522-525). IEEE.
- [6] Kamelia, L., Hamidi, E. A. D., Darmalaksana, W., &Nugraha, A. (2018, July). Real-Time Online Attendance System Based on Fingerprint andGPS in the Smartphone. In 2018 4th International Conference on Wireless and Telematics (ICWT) (pp. 1-4). IEEE.
- [7]] Akbar, M. S., Sarker, P., Mansoor, A. T., Al Ashray, A. M., & Uddin, J. (2018, August). *Face Recognition and RFID Verified Attendance System*. In 2018 International Conference on Computing, Electronics & Communications Engineering (iCCECE) (pp. 168-172). IEEE.

- [8] Noor, S. A. M., Zaini, N., Latip, M. F. A., & Hamzah, N. (2015, December). *Android-based attendance management system*. In 2015 IEEE Conference on Systems, Process and Control (ICSPC) (pp. 118-122). IEEE
- [9] Utomo, S. B., & Hendradjaya, B. (2018, October). *Multifactor Authentication on Mobile Secure Attendance System*. In 2018 International Conference on ICT for Smart Society (ICISS) (pp. 1-5). IEEE.
- [10] Johar, R., Qaisar, S. M., Subasi, A., & Kurdi, R. F. (2018, July). *A Raspberry Pi Based Event Driven Quasi Real Time Attendance Tracker*. In 2018 IEEE 3rd International Conference on Signal and Image Processing (ICSIP) (pp. 418-422). IEEE.
- [11] Raj, R., Das, A., & Gupta, S. C. (2019, January). *Proposal of an Efficient Approach to Attendance Monitoring System using Bluetooth*. In 2019 9th International Conference on Cloud Computing, Data Science & Engineering (Confluence) (pp. 611-614). IEEE.
- [12] Yadav, V., & Bhole, G. P. (2019, February). *Cloud Based Smart Attendance System for Educational Institutions*. In 2019 International Conference on Machine Learning, Big Data, Cloud and Parallel Computing (COMITCon) (pp. 97-102). IEEE
- [13] Shukla, V. K., & Bhandari, N. (2019, February). *Conceptual Framework for Enhancing Payroll Management and Attendance Monitoring System through RFID and Biometric*. In 2019 Amity International Conference on Artificial Intelligence (AICAI) (pp. 188-192). IEEE.
- [14] Matilda, S., & Shahin, K. (2019, March). *Student Attendance Monitoring System Using Image Processing*. In 2019 IEEE International Conference on System, Computation, Automation and Networking (ICSCAN) (pp. 1-4). IEEE.
- [15] Harikrishnan, J., Sudarsan, A., Sadashiv, A., & AS, R. A. (2019, March). *Vision-Face Recognition Attendance Monitoring System for Surveillance using Deep Learning Technology and Computer Vision*. In 2019 International Conference on Vision Towards Emerging Trends in Communication and Networking (ViTECoN) (pp. 1-5). IEEE.

A Novel Analysis on Outliers

S.Rajalakshmi¹, Research Scholar,
rajaylakshmiravi7@gmail.com

P.Madhubala², Research Supervisor,
 Department of computer science,
 Periyar University, Salem, Tamilnadu
madhubalasivaji@gmail.com

Abstract

This paper presents a novel analysis of outliers using *FCM (Fuzzy C-means Clustering method)* that aims to analyse the outliers using 4 datasets by z-curve graph. The effectiveness of the method is based on pre-processing, which removes noise and inconsistent data using techniques like aggregation and sampling. FCM is an iterative process where the data values result in *objective function (OF)* that is compared with the threshold value to identify as “*Outliers*”. Outlier detection, which are less sensitive to the presence of outliers provides an useful and interesting analysis information. This method enhances accuracy and improves the performance of detecting outliers assessed over four datasets. Thus the paper reveals an augmented study of modified fuzzy clustering approach to detect the unusual outliers. Experimental results and z-curve output shows the effectiveness of detecting perpetual outliers.

Keywords: *Outliers, fuzzy, Clustering, FCM, OF*

1 Introduction

Clustering is an important exploratory data analysis tool used to detect outliers. Cluster is a group of similar data items, which skews the representation of the inferred model. Clustering seems to be difficult in unsupervised learning where no prior knowledge is known. It is structured according to its similarity measure and used commonly in real world problems for various applications. Clustering technique is used to identify the outliers. Noise are taken as incorrect data entry, mechanical faults and natural disorders.

Outlier detection is also an important and complex task due to its uncertainty intolerance. Outlier known as anomaly identifies the extreme points from the dataset. It is also called a discordant object, an exception, a surprise, abnormality behaviour. There are three types of outliers namely-global, contextual and collective. Its applications are fraud detection, intrusion detection, image processing, health care informatics, surveillance, medical diagnosis, predictive maintenance and so on.

Why this Analysis is important?

During the quarantine, the psychology features of every human **differs from his/her behavior**. In Contemporary world, rare events happen due to technology advancement. Fuzzy clustering is the suitable method for handling the uncertainty. The degree of membership belongs from 0 to 1. In order to tolerate the uncertain and imprecise, it is a must to detect outliers.

1.1.1 Section 2 includes the literature survey, Section 3 describes fuzzy clustering, Section 4 includes the proposed fuzzy algorithm, Section 5 describes about the software packages used, Section 6 includes experimental results and Section 7 includes conclusion.

2 Literature Survey

Outlier analysis is studied from Charu.C.Aggarwal[2][4][7]. Outliers which may treated as error results in underestimation of uncertainty tolerance. Identification study of outlier is studied by Chapman, Hall and Hawkins [1]. A survey, various types of anomaly detection and characteristics of outliers is studied from Chandola, Banerjee and Kumar[3]. Clustering techniques are identified by Aggarwal, Chandan and Reddy[4]. The number of clusters indicate efficient generalization over learning of meta-cognitive factors by less computational effort. Two approaches were built, one for monitoring and other is controlling. It uses membershipship value, cardinality value, and cluster validation indices. Fuzzy introduction, Partitioning and its applications is studied from Bezdek and Harris[8]. The framework of Outlier detection is studied from Charu aggarwal[2]. A modified approach using feature based indexing for the labeled patterns with high membership function is considered for generalization [12]. How to detect the outliers in real time application using fuzzy clustering is studied from Rajalakshmi and Madhubala[5]. A generalized fuzzy index method and novel constraint function of membership is demonstrated by Lin Zhu et.al [13]. Fuzzy relations are studied by M.S.Yang[8]. Fuzzy c-means clustering algorithms studied in J.C.Bezdek, K.F.Yu, M.S.Yang[8]. R programming by Yanchang Zhao[24]. A detailed study of estimating ERR and EDR for z-score is demonstrated

in Bartos and Schimmack[14]. How the psych and z-curve package is evaluated in R-script is studied from [17][18][19][20][21]. Fuzzy set is studied from Bezdek[8] and klir yaun[25]. Fuzzy Cluster analysis is studied from Hoppner et.al[6]. A It defines the mental abilities to understand the dominant approach of various intelligence of human. The cognitive ability can be measured by the conceptualization of psychometric approach [10][20]. From the study, the non-adherence of protocol stemmed up by the mistakes of datapoints. Short term verbal memory, Reasoning, Vocabulary and verbal fluency parameters are based on some factors like social demographic, health behaviours and more.[9]. The Prediction model is used to calculate residuals of estimating various waves of cognitive decline.

3 Fuzzy Clustering

It is a soft clustering created by Jim Bezdek in 1981. It is the data object, which includes the member of all clusters with varying membership degrees from 0 to 1. It has high degree of membership which are closer and low degree of membership which are scattered. The matrix is generated by cluster prototype and membership degree. The distance will be carried out between the data point and cluster center. To detect it, first cluster the data, second calculate the centroid and distance using Euclidean distance method, third calculate OF(objective function) and if it is below threshold announce as outlier.

The borders have high degree of membership.

$$\sum_{i=1}^c u_{ij} = 1, \forall j = 1, \dots, n \quad (1)$$

$$\mu_{ij} = 1 / \sum_{k=1}^c (d_{ij} / d_{ik})^{(2/m-1)} \quad (2)$$

$$v_j = (\sum_{i=1}^n \mu_{ij}^m x_i) / (\sum_{i=1}^n (\mu_{ij}^m)), \forall j = 1, 2, \dots, c \quad (3)$$

where, 'n' indicates data points

'v_j' indicates jth center of the cluster

'm' indicates the fuzziness index, $m \in [1, \infty]$.

'c' indicates the cluster center

' μ_{ij} ' indicates the degree of membership

'd_{ij}' indicates the distance of Euclidean

Fuzzy clustering will be calculated by the given equation

$$J(U, V) = \sum_{i=1}^n \sum_{j=1}^c (\mu_{ij})^m \|x_i - v_j\|^2 \quad (4)$$

in which ' $\|x_i - v_j\|$ ' indicates the euclidean distance.

The objective function is,

$$J(U, c_1, \dots, c_c) = \sum_{i=1}^c J_i = \sum_j \sum_j^n u_{ij}^m d_{ij}^2 \quad (5)$$

Cluster center of fuzzy will be calculated by,

$$c_i = \sum_{j=1}^n u_{ij}^m x_j / \sum_{j=1}^n u_{ij}^m \quad (6)$$

Degree of membership for iteration matrix is given by ,

$$u_{ij} = 1 / \sum_{k=1}^c (d_{ij} / d_{kj})^{2/(m-1)} \quad (7)$$

Euclidean Distance of the Matrix is

$$d_{ij} = \|c_i - x_j\| \quad (8)$$

4 Fuzzy Proposed Algorithm

The fuzzy proposed algorithm includes the following steps such as

Step 1: Initialize membership matrix U

Step 2: Initialize no of clusters 'k'

Step 3: Estimate the centroid of each cluster center 'c'

Step 4: Calculate the minimum distance to each cluster using Euclidean distance

Step 5: If the object has no neighbor, define it is outlier

5 About the Software Packages

R tool (r 4.0.2 version) is used to analyse the outliers using fuzzy clustering. "psych" package is installed for factor analyzing the cognitive function of systems. William Revelle[18][19], clearly estimates ERR((Expected Replicability Rate), EDR(Expected Discovery Rate) and ODR(Observed Discovery Rate) using the packages psych and z-curve . Basic data analysis, regression model from mediation, moderation and set correlations are consent give brief explanation. Multiple level modeling is achieved by factor groups using statsBy. Classical test theory and reliability is estimation using confirmatory factor analysis. Comparing the factors and components using fuzzy clustering. *iclust()*, item cluster analysis used to partition space of the subject rather than space of the variable. It explains an implementation of z-curves – and method for estimating replicability rates (ERR) and expected discovery rates(EDR) on finding fitness, metrics etc.

By installing *zcurve* package, we used density method to find the increase number of iterations and decrease number of criterion for the dataset *stock_data*. Estimation of ERR(Expected Replicability Rate) and EDR(Expected Discovery Rate) is shown below.

Table 1: Analysis of outliers using clusters in datasets

| Dataset | No of clusters | Outliers detected |
|----------------|-----------------------|--------------------------|
| Iris | C=3 | FALSE |
| Stock_data | C=3 | TRUE |
| Wine | C=3 | FALSE |
| Advertising | C=3 | FALSE |

From the above table 1, we have estimated the density of outliers using z-curve package for iris and stock_data dataset. Stock_data dataset gives expected output for the proposed algorithm between 0 to 1(i.e., 0.05 to 0.999).

6 Experimental Results

RStudio 4.0.2 is used for analysis of outliers using fuzzy clustering to find the z-curve. The Packages used are "psych" and "zcurve", where zcurve developed by Frantisek Bartos on 27, September-2020 to detect the accuracy [14][17][18][19][20].

The proposed algorithm is treated with 4 datasets namely iris, advertising, wine and stock_data. From the dataset used, stock_data dataset works well in all aspects to identify the perpetual outliers. Iris dataset gives ideal output for the proposed algorithm whereas dataset wine and advertising gives negative/false values. Initially the proposed algorithm is detected using 't' test, 'z' test, and 'chi-square' test using 'ppclust' using R tool.

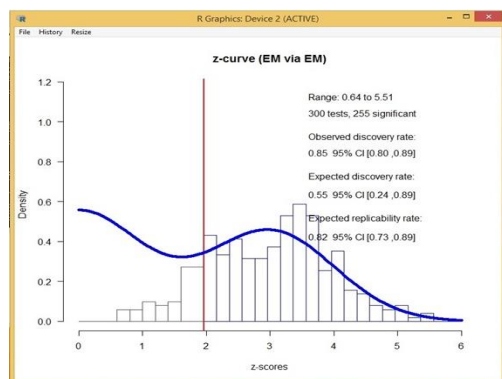


Fig.1 Analysis of outlier in z-curve

From the above figure 1, the number of iterations for estimating the replicability rate and discovery rate is shown. It also shows the error rate of perpetual outliers using Expectation Method (EM) by the range from 0.64 to 5.51, ODR(Observed Discovery Rate) of 0.85, EDR(Expected Discovery Rate) of 0.55, ERR(Expected Replicability Rate) of 0.82.

7 Conclusion

Towards the contemporary world of pandemic, researchers are making very close and accuracy to the human understandable efforts. Using utilization factor, the number of observation comes under the study is more efficient for the outcome of the outliers. Estimation is based on replicability rates and discovery rates of statistical testing such as t-test, F-test, chi-square test, Z-test, ERR and EDR. It simulates the robustness of outliers that undergoes uncertainty as significant to the margin. Thus concluding this paper, the proposed approach shows best result by analysing the outliers by 95% from the taken dataset stock_data. Thus perpetual outliers are identified in an effective manner using R and ppclust, z-curve, psych package. In future, this approach is implemented for complex dataset of various applications.

Acknowledgement

I would like to thank my research supervisor Dr.P.Madhubala, who really supported and encouraged for my research work.

References

- [1] D. Hawkins, "Identification of Outliers", 1980.
- [2] Charu C Aggarwal, "Outlier Analysis", Springer, 2013.
- [3] V. Chandola, A Banerjee, V Kumar, "Anomaly Detection: A survey", ACM.
- [4] Charu C Aggarwal, Chandan, K. Reddy, "Data clustering", CRC Press, 2014.
- [5] S. Rajalakshmi, P. Madhubala, "Outlier Detection: A research and Modified method using Fuzzy Clustering", IJITEE, ISSN:2278-3075, vol. 9, Issue 3s,2020.
- [6] F. Hoppner, F. Klawonn, R. Kruse, "Fuzzy cluster Analysis: Methods for classification", Data Analysis and Image.
- [7] Charu C Aggarwal, Manish Gupta, Jing Gao, "Outlier Detection for Temporal Data: A Survey", IEEE, 2014.
- [8] J. D. Harris, J. C. Bezdek, "Fuzzy Partition and relation - An axiomatic basis for clustering", Fuzzy sets and systems, Elsevier, 1978.
- [9] Gwenith G Fisher, S. Dorey, "Chaffee in work across the lifespan", 2019.
- [10] Aline Dugravot, Severine sabia, Archanna Singh, "Detection of Outliers Due to Participants Non-Adherence to protocol in a longitudinal study of cognitive decline", PLoS One, MNOUX, 2015.
- [11] S. V. Arunakumar, N. Sundararajan, "An Efficient Meta-Cognitive Fuzzy C- Means clustering approach", vol. 85, 105838, 2019.
- [12] Francesco Marcelloni, "Feature selection based on a modified fuzzy c-means algorithm with supervision", vol. 151, pages 201-226.
- [13] Lin Zhu et.al, "Generalized fuzzy c-means clustering algorithm with improved fuzzy partitions", IEEE, 2009.
- [14] F. Bartos, U. Schimmack, "Z-Curve.2.0: Estimating Replication Rates and Discovery Rates", <https://doi.org/10.31234/osf.io/urgtm>, 2020.
- [15] J. Brunner, U. Schimmack, "Estimating Population Mean Power Under Conditions of Heterogeneity and Selection for Significance", Meta Psychology in press, 2019.
- [16] Open Science Collaboration, "Estimating the reproducibility of psychological science", Science 349(6251) aac4716, 2015.
- [17] F. Bartos, U. Schimmack, "Z-Curve: An R package for fitting Z-Curves", R package version 1.0.6, 2020.
- [18] William Revelle, "How To: Install R and the psych package", 2020.
- [19] William Revelle, "An introduction to the psych package: Part I: Data entry and data description", 2020.
- [20] William Revelle, "An introduction to the psych package: Part II Scale construction and psychometrics", 2020.
- [21] zcurve Package. September 27, 2020.
- [22] George J Klir, Bo Yuan, "Fuzzy sets and Fuzzy Logic- Theory and Applications", PHI, 2005.

- [23] Irad Ben Gal, "Outlier Detection Data Mining and Knowledge discovery Handbook", kluwer Academic Publishers, 2005.
- [24] Yanchang zhao, "R and Data Mining: Examples and Case studies", 2012.
- [25] Klir Yuan, "Fuzzy set and fuzzy logic-Theory and Applications".

Modified Non-local Means Filtering Techniques to Remove Various Noise Types from MRI image

T. Anitha , Research Scholar,

T. Kalaiselvi, Assistant professor, Department of computer science and application,
The Gandhigram Rural Institute (Deemed to be University), Gandhigram.

Abstract

In this article, we proposed a modified non-local means (MNLM) technique to discard a rician noise from the magnetic resonance imaging (MRI) scans. MNLM method is also adaptable for generalized images to remove Gaussian noise salt and pepper noise. The implementation of the MNLM algorithm depends on the grayscale difference of images (GDI). Based on this GDI, we modified the traditional NLM algorithm in the Central processing unit(CPU) processor and also using a parallel processing technique with Compute Unified Device Architecture (CUDA) model. The main difference between traditional NLM and proposed MNLM algorithm is SWS, i.e, traditional NLM has fixed SWS like 3×3 or 7×7 and proposed MNLM has adaptive SWS (ASWS) like 3×3 and 7×7 and 9×9 . Hence, we have implemented the MNLM method by adaptively changing the SWS based on the GDI to remove noise effectively, and MNLM preserves the edge details in the image compared to existing methods. To prove the preservation of edge, we implement a new matrix-based edge detection algorithm. Brain web and IBSR datasets are used for experiments and evaluation. The results are compared with some existing denoising techniques using the performance evaluation metrics such as PSNR, SSIM. The experiments show that our proposed work yields the best results on the higher noise levels.

Keywords: Denoising, non-local means, parallel processing, GPU.

1 Introduction

Computational time is an essential aspect of the medical image processing field. Medical imaging has various types of imaging techniques that include X-ray, magnetic resonance imaging (MRI), etc. [1]. Sometimes MRI images occurred with noise due to the acquisition process. During the acquisition process, the machine or signals will introduce different noise types, i.e., Gaussian noise, salt and pepper noise and rician noise. The noise in the image removed by the denoising process. A massive amount of denoising techniques with unique characteristics are available in the image processing field. Most of the methods have computational issues. So we implemented our proposed method using Parallel processing algorithms with a Graphics processing unit (GPU) to avoid this computational issue. A parallel algorithm is executed for several instructions concurrently on different processing devices and produces final results by combines all separate outputs. A GPU can render images more quickly than a CPU because of its parallel processing architecture, allowing it to perform multiple calculations simultaneously [2]. The comparison of GPU and CPU architecture is shown in Figure 1.

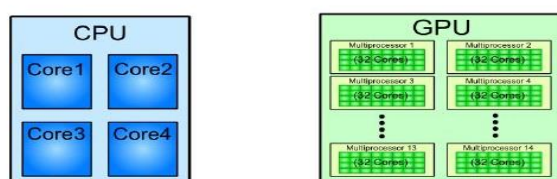


Fig.1: CPU and GPU architecture comparison

2 Related Works

Various types of NLM-based methods are developed in recent years. Buades et al. [3] developed an NLM algorithm to remove noise from the images using neighborhood similarity concepts. Joshi et al. [4] built an improved NLM technique (WENLM) to eliminate the Gaussian noise from the MRI images using a wavelet and median filter. Zhang et al. [5] proposed an NLM method (NAMF) to remove salt and pepper noise based on the image's gray level value. Experiments are done using standard images compared with state-of-the-art techniques and have a 41.3133 dB PSNR value for a 10 % noise level. Chen et al. [6] proposed an enhanced ANLM algorithm to discard the rician noise in MRI brain images by using the FCM algorithm in Brain web datasets and proved that their method gave better results than other state art methods. Kalaiselvi et al. [7] proposed a wavelet-based edge-preserving technique (WBDF) to remove MRI image noises. Experimental results are done

by using brainweb dataset. Zheng, Zhen, et al. [8] proposed a edge detection algorithm based on the grey prediction model. The experimental results are done by using general images.

This paper consists of the following sections: Section 3 contains a brief explanation of the traditional NLM algorithm. Section 4 contained the proposed method. Section 5 has the details of materials and metrics. Quantitative and qualitative results experimented by IBSR and Brainweb datasets are presented in section 6. Finally, Section 7 has a conclusion.

3 Traditional Non-Local Means Algorithm

Consider that $n(x)$ denotes the noisy images, $c(x)$ be the noise-free image. x represents the index of the picture element (pixel). By using equation (1), estimated picture element values are considered as the weighted average of all grayscale values within the predefined search region (sr_x) as

$$\widehat{c}_{nlm}(x) = \frac{\sum_{y \in sr_x} w(x,y)n(x)}{\sum_{y \in sr_x} w(x,y)} \quad (1)$$

Where the pixel x has a $\widehat{c}_{nlm}(x)$ as the restored pixel value. Weight $w(x,y)$ denotes the number of similarities that occurred between the centered local patches at pixel x and pixel y in the predefined search region (sr_x) obtained from equation(2)

$$w(x,y) = e^{-\frac{\|Np(x)-Np(y)\|_2^2, a}{sp}} \quad (2)$$

$Np(x)$ and $Np(y)$ denote the patch-centered $Pc \times Pc$ on the picture elements x and y . The smoothing parameter sp rules the extent of averaging. Choosing the minimum number of sp produces noisy images almost identical to input images. While determining the maximum amount of sp , create smooth images.

4 Proposed Method

This work is developed based on the grayscale difference (GDI) between images. The primary goal is to select the search window (SW) in an adaptive manner to discard the various noises from the images. The traditional NLM algorithm has a small and predefined SW size for denoising like 3×3 . But in our proposed work, the SW size is adaptively changed by the GDI of the MRI image. Due to this adaptive search window (ASWS), our proposed method eliminated the noise and preserve the edge details in the images better than state of the art methods. For the edge preservation we proposed a matrix based edge detection algorithm. The workflow of our proposed method is given in Fig.(2). we choose a noise-free image for manually add the Rician noise, Gaussian noise, salt and pepper noise with various level. First we done the experiments on MRI images by applying Rician noise based on the Coupe et al. algorithm [11].

Assume that I original image and \hat{I} be the noisy image with size $x2 \times y2$ is obtained by using rician distribution. Assume that picture element x in the image \hat{I} has an $s1 \times s1$ nearest window size know as Ω_k . From equation (3), the average of grayscale values is calculated,

$$\hat{I}_x = \frac{1}{s1 \times s1} \sum_{s=1}^{s1} \sum_{v=1}^{s1} \hat{I}(u,v) \quad (3)$$

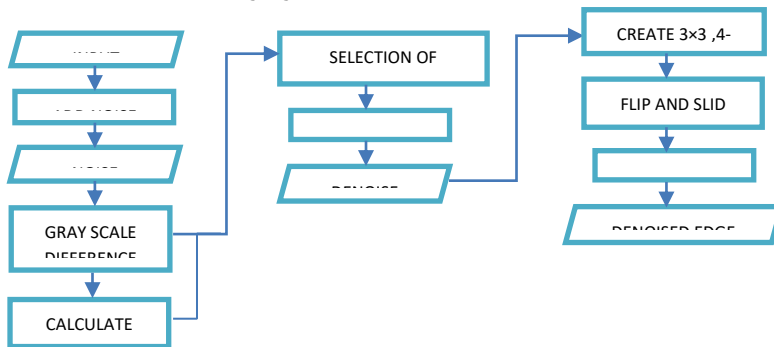


Fig.2. Flow chart of the Proposed method

u, v denotes the picture elements coordinates in the nearest Ω_k . Then calculate the similarity ($\Delta\hat{l}_x$) between l and \hat{l}_x is called the grayscale difference of picture element x , which as

$$\Delta\hat{l}_x = |l - \hat{l}_x| \quad (4)$$

Using equations (3) and (4), the grayscale difference is calculated for each picture element of the images. Then the thresholds value of T_1 and T_2 are defined as:

$$T_1 = \mu, T_2 = \mu + \alpha\sigma \quad (5)$$

In the equations (5) the α (alpha) denotes the control parameter. the **mean**(μ) and **standard deviation** (σ) of grayscale difference images are calculated from the equation (6) and (7).

$$\mu = \frac{1}{X_2 \times Y_2} \sum_{n \in \Delta l} \Delta\hat{l}_x \quad (6)$$

$$\sigma = \left[\frac{1}{X_2 \times Y_2} \sum_{x \in \Delta l} (\Delta\hat{l}_x - \mu)^2 \right]^{1/2} \quad (7)$$

The optimal search window $opsws_m$ for each picture element in the image is calculated by using the equation (8).

$$opsws_m = \begin{cases} \Delta\hat{l}_x < T_1, oswislarge \\ T_1 \leq \Delta\hat{l}_x \leq T_2, oswismedium \\ \Delta\hat{l}_x > T_2, opwissmall \end{cases} \quad (8)$$

The denoised ANLM image \hat{l}_{out} is obtained as given in equation (9)

$$\hat{l}_{out}^{(x)} = \frac{\sum_{y \in ops_w_x} w(x,y) J(x)}{\sum_{y \in ops_w_x} w(x,y)} \quad (9)$$

After the denoising process, the proposed edge detection algorithm is applied to the denoised image to find how much image details are preserved by our proposed MNLM method. For edge detection, we use convolution.

$$E = \hat{l}_{out}^{(x)} * m \quad (11)$$

Where $\hat{l}_{out}^{(x)}$ is the denoised image m is the mask "*" is convolution operator. First, take the 3×3 masking for the horizontal, vertical, principal, and secondary diagonal edges. Then the masks are flip horizontally and vertically to take the 180-degree rotation of an image. The masking process should be performed in each pixel of the image, for that mask slides onto the images. Finally, complete the convolution with the corresponding pixel value and add them for the edge image E .

5 Material And Performance Metrics

The evaluation is done by a IBSR normal brain image and Brain web dataset. The quantitative validation of the proposed work is tested by the PSNR and SSIM metrics.

PSNR (Peak-signal-to-noise-ratio) is used to calculate the noise ratio between original and noisy signals in the MRI images. PSNR is computed by using the mean squared error (MSE) and logarithmic decibel scale.

$$PSNR = 10 \log_{10} \left(\frac{MAX^2}{MSE} \right) \quad (10)$$

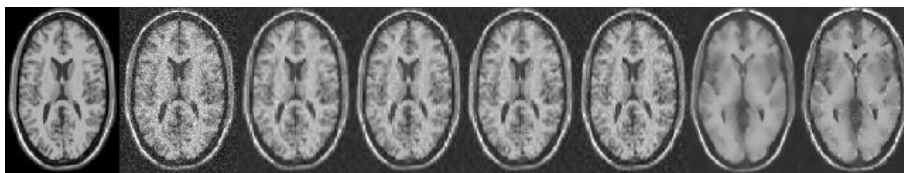
$$MSE = \frac{1}{m_2 n_2} \sum_{i=0}^{m_2-1} \sum_{j=0}^{n_2-1} [CI(i,j) - DI(i,j)]^2 \quad (11)$$

SSIM (Structure similarity index) measures the perceptual *difference* between two similar images. The mean of all the local SSIM values arrives at the **global** SSIM value by using equation (12).

$$MSSIM(X, Y) = \frac{1}{M} \sum_{j=1}^M SSIM(x_j, y_j) \quad (12)$$

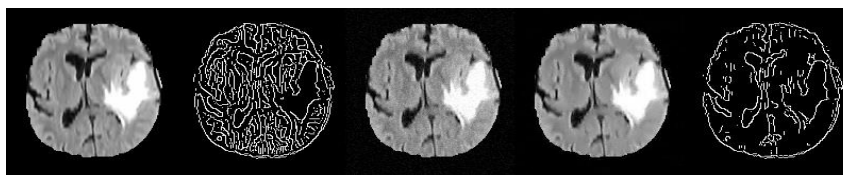
6 Result And Discussion

The MATLAB R2016a and Intel CORE i5 processor with 8GB RAM is used to implement our proposed work. The proposed MNLM results were compared with some of the existing methods such as traditional NLM algorithm, wavelet-based NLM filter (NLFMT), Bayeshrink, wavelet-based edge preservation techniques (WBDF) for its performance analysis and results are shown in Table 1. Figure (3) shows the qualitative comparison between existing methods and the proposed work for 15 % rician noise level. Our proposed MNLM method is adaptable for different noises. Figure (4) and Figure (5) show the result of 10% Gaussian noise and 0.05% of salt and pepper noise removal using the IBSR dataset. Table 2 shows the comparison of computational time and MSSIM values with existing edge detection method values for our MNLM denoising method in CPU and GPU processors. Table 2 shows that parallel processing with CUDA enabled GPU processor, reduce the time complexity, and provide faster result than CPU processor.



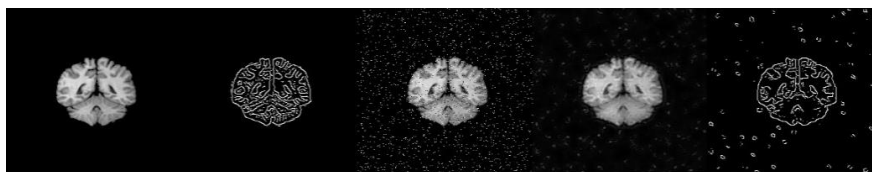
(a) (b) (c) (d) (e) (f) (g) (h)

Fig. 3. Comparison between the proposed method and existing method for 15 % of Rician noise level for Brainweb images (a) clear image (b) Noisy image (c) Bayes (d) INS (e) NLFMT (f) NWT (g) NLM (h) proposed method



a) (b) (c) (d) (e)

Fig.4. (a) Original Image (b) Proposed original ED Image (c) 10% Gaussian Noise Image (d) Denoised Image (e) Denoised ED Image



a) (b) (c) (d) (e)

Fig.5. Proposed denoising and edge detection (ED) method for 0.05% of Salt and Pepper noise IBSR Images (a) Original Image (b) Proposed original ED Image (c) Noisy Image (d) Denoised Image (e) Denoised ED Image

Table 1. PSNR of Proposed work compared with

| Rician noise (%) level | | 9 | 10 | 12 | 14 | | |
|---------------------------|----------|---------------|---------------|--------------|--------------|-----------------------------|----------|
| PSNR | NLFMT | 22.45 | 21.54 | 18.77 | 17.41 | | |
| | Bayes | 21.80 | 19.34 | 18.51 | 17.14 | | |
| | WBDF | 25.36 | 20.25 | 19.38 | 17.80 | | |
| | Proposed | 23.40 | 22.53 | 20.99 | 19.66 | | |
| Salt & pepper noise level | | 0.05 | 0.1 | 0.3 | 0.6 | | |
| PSNR | AEDA | 41.417 | 39.54 | 35.40 | 31.29 | | |
| | Proposed | 55.438 | 56.432 | 55.57 | 55.76 | | |
| Gaussian noise level | | 6 | 9 | 13 | 20 | | |
| PSNR | WENLM | 41.01 | 40.31 | 39.30 | 37.644 | | |
| Noise Level (%) | MSSIM | | | | | | |
| | Canny | Sobel | Prewitt | Roberts | Proposed | computational time for MNLM | |
| | | | | | | CPU | GPU |
| 10 | 0.99994 | 0.9999 | 0.99999 | 0.9999 | 0.9817 | 13.644276 | 0.000982 |
| 20 | 0.99988 | 0.99984 | 0.99984 | 0.99983 | 0.88288 | 12.871774 | 0.001173 |
| 30 | 0.9998 | 0.99976 | 0.99977 | 0.99973 | 0.79966 | 12.771390 | 0.001089 |
| 40 | 0.99970 | 0.99973 | 0.99973 | 0.99970 | 0.71581 | 12.933902 | 0.000857 |
| 50 | 0.99814 | 0.99966 | 0.99968 | 0.99964 | 0.86969 | 12.075330 | 0.001072 |

Table 2. MSSIM computational method for Types. time of the method

and the
the existing
Different Noise
proposed MNLM

7 Conclusion

We introduced a Modified NLM denoising filter with adaptive search windows named MNLM to suppress various noise from the MRI image. The results show that our proposed work has given better results than some of the existing methods for higher noise levels. The computational time of our proposed work is 20.003306 seconds for a single MRI image in the Brain web dataset and 3590 seconds to run the 181 images in the datasets. This time complexity will be handled by parallel processing techniques and provide 0.00982 seconds for a single MRI image in the Brain web dataset and 1044.1189 seconds to run the 181 images in the dataset.

References

- [1]. Kalaiselvi, T., P. Kumarashankar, and P. Sriramakrishnan. "Reliability of Segmenting Brain Tumor and Finding Optimal Volume Estimator for MR Images of Patients with Glioma's."
- [2]. Wiest-Daesslé, N., Prima, S., Coupé, P., Morrissey, S. P., & Barillot, C. (2008, September). Rician noise removal by non-local means filtering for low signal-to-noise ratio MRI: applications to DT-MRI. In International Conference on Medical Image Computing and Computer-assisted Intervention (pp. 171-179). Springer, Berlin, Heidelberg.

- [3]. Buades, A., Coll, B., & Morel, J. M. (2005, June). A non-local algorithm for image denoising. In 2005 IEEE Computer Society Conference on Computer Vision and Pattern Recognition (CVPR'05) (Vol. 2, pp. 60-65). IEEE.
- [4]. Joshi, Nikita, Sarika Jain, and Amit Agarwal. "An improved approach for denoising MRI using non local means filter." 2016 2nd International Conference on Next Generation Computing Technologies (NGCT). IEEE, 2016.
- [5]. Zhang, Houwang, Yuan Zhu, and Hanying Zheng. "NAMF: A Non-local Adaptive Mean Filter for Salt-and-Pepper Noise Removal." arXiv preprint arXiv:1910.07787 (2019).
- [6]. Chen, K., Lin, X., Hu, X., Wang, J., Zhong, H., & Jiang, L. (2020). An enhanced adaptive non-local means algorithm for Rician noise reduction in magnetic resonance brain images. *BMC Medical Imaging*, 20(1), 1-9.
- [7]. Kalaiselvi, T., N. Kalaichelvi, and V. NagaRajeshwari. "Edge Preserving Denoising Technique in Magnetic Resonance Images." *COMPUTATIONAL METHODS, COMMUNICATION TECHNIQUES AND INFORMATICS*: 170.
- [8]. Zheng, Zhen, et al. "Adaptive Edge Detection Algorithm Based on Improved Grey Prediction Model." *IEEE Access* 8 (2020): 102165-102176.
- [9]. Coupé, P., Manjón, J. V., Gedamu, E., Arnold, D., Robles, M., & Collins, D. L. (2010). Robust Rician noise estimation for MR images. *Medical image analysis*, 14(4), 483-49.

A Novelty Approach Of Exact String Matching

Armstrong Joseph¹ and C.R. Rene Robin²

Abstract

In this research we present three consecutive characters based exact string-matching algorithm. A new idea is introduced a shift by three consecutive characters in text. In pre-processing phase our algorithm creates a shift table by three consecutive characters in text. First two of three is right most character of text over pattern and the last one is the next character of these two characters is on text. The time and space complexity of pre-processing phase of our exact string matching is $O(m+\sum^3)$ and searching phase takes $O(mn)$ time complexity. The proposed algorithm is effective than the number of existing algorithms in many cases. In this paper we present experimental results for string matching algorithms which have exact string matching in a single cycle. Of these algorithms are the Boyer-Moore and its derivatives, they are famous for their speed in practice, We have evaluated the algorithms by counting the number of comparisons made and by timing taken to complete a given search. With these experimental results, we were able to introduce a new string-matching algorithm and compared it with the existing algorithms by experimentation. These experimental results clearly show that the new algorithm is more efficient than the existing algorithms from our chosen data sets. Using the chosen data sets over 500 separate tests were conducted to determine the most efficient algorithm.

Keywords: *string searching; string matching; text editing; algorithms on words.*

1 Introduction

String matching [4] is finding an occurrence of a pattern string in a larger string of text. This problem arises in many computer packages in the form of spell checkers, search engines on the internet, find utilities on various machines, matching of DNA strands and so on.

String matching is a basic tool in data compression, molecular biology and information retrieval all rely on efficient string-matching algorithms on challenging amounts of input data. For over 40 years string matching algorithms have been studied extensively. Speed, time and memory constraints are the crucial attributes of state-of-the-art matching algorithms. One of two classical approaches is used for checking the occurrence of the strings on all over the text. One is that entire text will be checked for string matching. Another is filtering that filter out portions of the text that cannot possibly contain a match, and, at the same time, find positions that can possibly match to search pattern. Character matching, automata and bit parallelism are applied in string matching algorithms. Automata helps to shift the pattern if suffix match with prefix of pattern. If pattern length is more than length of data word, pattern can be split in to several segments size of data word size. Each segment ordered by bit value so it is called bit parallelism. Parallelization is an essential part of algorithm design by Multithreading, heterogeneous computing and SIMD (single instruction streams multiple data stream).

Bit parallelism takes advantage of this fact by packing several variables into a single computer word. These variables can then be updated in a single instruction making use of the intrinsic parallelism of bit operations. For example, if we needed to keep track of $m \leq w$ Boolean variables, where w is the length of the computer word, we could store all these variables in a single computer word. Moreover, using SIMD [8] updates all the variables in one instruction instead of m instructions. As the length of the computer word in modern processors is 32 or 64 this technique can give us a significant speedup. Masking is used for filtering as encoding technique to separate a segment from existing data set.

Many promising data structures and algorithms discovered by the theoretical community are never implemented or tested at all. Moreover, theoretical analysis will show only how algorithms are likely to perform in practice, but they are not sufficiently accurate to predict actual performance.

In this paper we show that by considerable experimentation and fine-tuning of the algorithms we can get the most out of a theoretical idea. The string-matching problem has attracted a lot of interest throughout the history of computer science, and is crucial to the computing industry. Existing string matching algorithms which are known to be fast are described in the next section. Experimental results for these algorithms are given the following section. From the findings of the experimental results we identify two fast algorithms. We combine variations of Zhu-Takaoka and quick search algorithms and introduce a new algorithm. We compare the new algorithm with the existing algorithms by experimentation.

2 Problem Definition

We define the problem of string matching as the task of finding a pattern P of length $m = |P|$ in a text T of length $n = |T|$. Pattern and text are matched on an alphabet Σ . The results are the absolute positions of every occurrence of P in T . The input is dynamic, pre-processing of pattern or text has to take place at runtime. Only exact matches are returned.

3 Review of Literature

Brute force (BF) [3] or Naïve algorithm is, the pattern is aligned with the extreme left of the text characters and corresponding pairs of characters are compared from left to right. This process continues until either the pattern is exhausted or a mismatch is found. Then the pattern is shifted one place to the right and the pattern characters are again compared with the corresponding text characters from left to right until either the text is exhausted or a full match is obtained. This algorithm is very slow. It has no pre-processing phase and did not require extra space. Brute force algorithm time complexity in searching phase is $O(mn)$.

Knuth-Morris-Pratt (KMP) [11] algorithm is presented in 1977 to speed up the exact string matching by improving the lengths of the shifts. It compares the characters from left to right of the pattern. It uses the previous knowledge of comparisons to compute the next position of the pattern with the text when they match or mismatch. The time complexity of pre-processing phase is $O(m)$ and of searching phase is $O(nm)$.

Boyer-Moore (BM) [2] algorithm published in 1977 and at that time it considered as the most efficient string-matching algorithm. It performed character comparisons in reverse order from right to left of the pattern and did not require the whole pattern to be searched in case of a mismatch. Two shifting rules used to shift the pattern right. it uses two shift functions to shift the window to the right when they match or mismatch. These two functions are called the occurrence shift and the matching shift. The time and space complexity of pre-processing phase is $O(m+|\Sigma|)$ and the worst case running time of searching phase is $O(nm + |\Sigma|)$. The best case of Boyer-Moore algorithm is $O(n/m)$.

Boyer-Moore Horspool (BMH) [9] In 1980 Horspool proposed to use only the occurrence shift of the rightmost character of the window to compute the shifts in the Boyer-Moore algorithm. It used only the occurrence heuristic to maximize the length of the shifts for text characters corresponding to right most character of the pattern. It's pre-processing time complexity is $O(m+|\Sigma|)$ and searching time complexity is $O(mn)$.

Turbo Boyer Moore (TBM) [5] is variation of the Boyer-Moore algorithm, which remembers the substring of the text string which matched with suffix of pattern during preceding comparisons. It does not compare the matched substring again; it just compares the other characters of the pattern with text string.

Quick Search (QS)[13] In 1990 Sunday8 designed an algorithm perform comparisons from left to right order, it's shifting criteria is by looking at one-character right to the pattern and by applying bad character shifting rule. QS andHorspool algorithm worst case time complexity is same but it can take more steps in practice.

Zhu-Takaoka [14] is another variant of the BM algorithm. The comparisons are done in the same way as BM (i. e. from right to left) and it uses the good suffix function. If a mismatch occurs at $T[i]$, the last occurrence function determines the right most occurrence of $T[i-1 \dots i]$ in the pattern. If the substring is in the pattern, the pattern and text are aligned at these two characters for the next attempt. The shift is m , if the two-character substring is not in the pattern. The shift table is a two-dimensional array of size alphabet size by alphabet size.

Berry Ravindran (BR) [1] algorithm proposed by Berry and Ravindran in 1999, it performs shifts by using bad character shifting rule for two consecutive characters to the right of the partial text window of text string. The pre-processing time complexity is $O(m+(|\Sigma|)^2)$ and the searching time complexity is $O(mn)$.

Extended-Backward-Oracle-Matching (EBOM)[12] algorithm extends Backward-Oracle-Matching with a fast-loop. The fast-loop technique repeats a matching by trial and error method in a non-branching cycle. This is used to quickly locate the last character of the pattern in the currently observed text window. In each iteration two consecutive characters are handled.

Boyer-Moore Horspool with q-grams. The BMHq algorithm by Kalsietal. [10] is an efficient modification of the Horspool algorithm for the DNA alphabet. Filtering approach is used. Instead of inspecting a single character at each alignment of the pattern, their algorithm reads a q-gram and computes an integer called fingerprint from it. The idea is simple and consists in mapping the ASCII codes of characters in the DNA alphabet. At each alignment of the pattern the last q-gram of the pattern is compared with the corresponding q-gram in the current window of the text by testing the equality of their fingerprints. If the fingerprints match, a potential occurrence has been found, which has to be naively checked.

Exact-Packed-String-Matching was presented in 2013 by Faro and Kulekci [6][7]. It uses of bit-parallelism by packing several characters into a bit-word and Filtering the text T into chunks D_i . These Filtered bit-word sized chunks are compared. Filter implementation uses SSE registers as 128 bits. Example is SSEF algorithm.

4 The New Algorithm

We combined the calculations of a valid shift in Quick Shift and variations of Zhu-Takaoka algorithms to produce a more efficient algorithm, the new algorithm. If a mismatch occurs when the pattern $P[1 \dots m]$ is aligned with the text $T[j \dots j + m]$, the shift is calculated by the rightmost occurrence of the substring $T[j + m-l, j + m, j + m + 1]$ in the pattern. If the substring is in the pattern then the pattern and text are aligned at this

substring for the next attempt. This can be done shifting the pattern as shown in the table below. Let * be a wildcard character that is any character in the ASCII set. Note that if T[j + m - 1, j + m, j + m + 1] is not in the pattern, the pattern is shifted by m positions.

The pre-processing phase of our algorithm consists in computing for three characters (a, b, c) in the rightmost occurrence of 'abc' on the text factor y[j ..j+m+1]. In our algorithm, bad characters shift table is created by using three consecutive characters 'abc'. it is created by two bad character 'ab' table versus one character 'c' (occurrence of alphabet in pattern)

A two character 'ab' bad character table is a two-dimensional array of size two characters size by alphabet size. Note that three characters (a, b, c) are alphabets are in the pattern.

$$Bc(abc) = \begin{cases} k = Bc(ab) & \text{if, } x[i]x[i+1] = ab \text{ iff } k < m-2 \text{ and } x[m-k .. m-k+1] = ab \\ & \text{and } ab \text{ does not occur in } x[m-k+2 .. m-2] \\ m-1 & \text{or else if, } x[0] = b \\ \text{MIN}[Bc(ab), f(c)] & \text{or else if, } ab* \\ \text{MAX}[Bc(ab), f(c)] & \text{Otherwise} \end{cases} \dots (1)$$

Where m is the pattern length, k is an integer at position from right two characters of pattern. Create this bad characters shift table by three steps.

First step is, create a table by two character a, b they are in rightmost occurrence of ab on the text factor y [j ..j+m]. This table is a two-dimensional array of size alphabet size by alphabet size. It is the simulation of two consecutive character exhibits the filter of 2-gram filter or encoding base 2 or k=2 error as filter in approximate string matching.

$$Bc(ab) = \begin{cases} k & \text{if, } x[i]x[i+1] = ab \text{ iff } k < m-2 \text{ and } x[m-k .. m-k+1] = ab \text{ and} \\ & \text{ab does not occur in } x[m-k+2 .. m-2] \\ m-1 & \text{or else if, } x[0] = b \\ m & \text{Otherwise} \end{cases} \dots (2)$$

Second step is, create one-dimensional array f(c) of size of alphabet size. This array related to one variables vector. In the array, each alphabet has the values of position at pattern from right. It is the variation of quick search algorithm.

$$f(c) = \text{MIN} \begin{cases} i & \text{if 'c' occurs in pattern at position 'i' from right} \\ m & \text{Otherwise} \end{cases} \dots (3)$$

Third step is, create bad characters shift table by using Bc(ab) versus f(c). This table is two-dimensional array of size two-dimensional array size Bc(ab) by alphabet size. This shift table related to three variables vector. This shift table is used to shift right on the text factor y[j .. j+m+1] during mismatch occurred.

For example, the following shifts would be associated with the pattern, 'ONION'.

First step is, create Bad character table by two characters using occurred alphabet in pattern 'ONION'. In this pattern occurred alphabets from right are N,O,I and also unknown character *. According to equation 2, the following table is created.

| | | | | |
|---------------|---|----------|----------|----------|
| <i>Bc(ab)</i> | * | <i>N</i> | <i>O</i> | <i>I</i> |
| * | 5 | 5 | 4 | 5 |
| <i>N</i> | 5 | 5 | 4 | 2 |
| <i>O</i> | 5 | 3 | 4 | 5 |
| <i>I</i> | 5 | 5 | 1 | 5 |

Second step is creating one dimensional array by using one alphabet character in pattern 'ONION'. Since equation 3, we obtain as

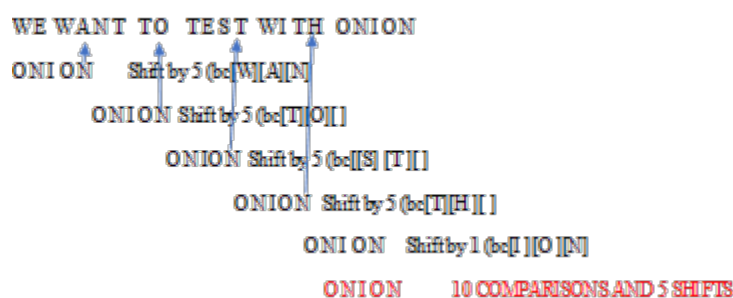
| | | | | |
|--|---|----------|----------|----------|
| <i>F(c)</i> | * | <i>N</i> | <i>O</i> | <i>I</i> |
| <i>Character Positions from right at Pattern</i> | 5 | 1 | 2 | 3 |

Third step is, to obtain our required bad character table using three consecutive characters, apply Bc(ab) and F(c) to equation 1 and get as follows.

| | | | | |
|----------------|---|----------|----------|----------|
| <i>Bc(abc)</i> | * | <i>N</i> | <i>O</i> | <i>I</i> |
| ** | 5 | 5 | 5 | 5 |
| * <i>N</i> | 5 | 5 | 5 | 5 |

| | | | | |
|-----------|---|---|---|---|
| <i>*O</i> | 4 | 4 | 4 | 4 |
| <i>*I</i> | 5 | 5 | 5 | 5 |
| <i>N*</i> | 5 | 5 | 5 | 5 |
| <i>NN</i> | 5 | 5 | 5 | 5 |
| <i>NO</i> | 4 | 4 | 4 | 4 |
| <i>NI</i> | 2 | 2 | 2 | 2 |
| <i>O*</i> | 5 | 5 | 5 | 5 |
| <i>ON</i> | 3 | 3 | 3 | 3 |
| <i>OO</i> | 4 | 4 | 4 | 4 |
| <i>OI</i> | 5 | 5 | 5 | 5 |
| <i>I*</i> | 5 | 5 | 5 | 5 |
| <i>IN</i> | 5 | 5 | 5 | 5 |
| <i>IO</i> | 1 | 1 | 1 | 1 |
| <i>II</i> | 5 | 5 | 5 | 5 |

Our new algorithm in action to find the pattern 'onion' over the text 'WE WANT TO TEST WITH ONION'.



In this example, our algorithm takes 10 comparisons and 5 shifts.

5 Experimental Results of Existing Algorithms

EBOM, BM, BR, BMHq, HOR, MS, QS, ZT and our algorithms were implemented in C language. The text T and pattern P are loaded into memory before computation and timing started. They executed using Intel Core i7 CPU, speed 300GHz, 8GB RAM and Linux kernel 5.0 generic operating system. All algorithms were compiled by GCC compiler.

A random text of 14,000 words (82205 characters) from the UNIX English dictionary was used for experiments. Then we used a pseudo random number generator to pick words from the UNIX dictionary and place them in the random text for the EBOM, BM, BR, BMHq, HOR, MS, QS, ZT, and our proposed algorithms. Bit-parallelism filtering algorithms such as Shift-or, BNDM and Encoding by masking filtering algorithms such as SSEF have not taken for comparing results. Because our algorithm supports character comparison under pattern length 'm' is less than computer word 'w'. it means that it does not support parallelism. All Filtering algorithm supports parallelism so they leads approximate string matching but our algorithm delivers exact string matching. To get an efficient comparison, we have taken exact string-matching algorithms such as EBOM, BM, BR, BMHq, HOR, MS, QS, ZT for comparisons.

For text of 14,000 words (82205 characters), the results were documented in Table 1 show that our algorithm is taking less or equal comparisons than the existing algorithms for when the pattern is large. Our algorithm is the fastest algorithm. This is due to the time for the pre-processing in our algorithm which is not as dominant in the BR algorithm. The main reason for the speed of our BR algorithm is the improved maximum shift of $m+2$ but our algorithm is improved maximum shift of m . Moreover, our algorithm has taken three consecutive characters to filter out easily. Figure 1 shows that graphical representation of number of comparisons vs pattern length between algorithms.

The entries in Table 2 are in percentage form and describe how many more comparisons existing algorithms did than our algorithm. For example, for a pattern length of 4 the BM algorithm takes on average 52.63% more comparisons than our algorithm. Note Percentage difference is the difference between two values divided by the average of the two values.

Table 1: The number of comparisons in 1000's for searching Text of 14,000 words (82205 characters)

| Pattern Length | EBOM | BM | HOR | BMHq | ms | QS | ZT | BR | Our Algorithm |
|----------------|------|----|-----|------|----|----|----|----|---------------|
| 2 | 3 | 3 | 3 | 3 | 2 | 2 | 3 | 2 | 2 |
| 3 | 7 | 7 | 7 | 7 | 6 | 6 | 7 | 4 | 4 |
| 4 | 12 | 12 | 12 | 12 | 10 | 10 | 11 | 7 | 7 |
| 5 | 13 | 13 | 13 | 13 | 12 | 12 | 12 | 9 | 8 |
| 6 | 13 | 13 | 13 | 13 | 12 | 12 | 11 | 9 | 8 |
| 7 | 12 | 12 | 12 | 12 | 11 | 11 | 10 | 8 | 7 |
| 8 | 11 | 11 | 11 | 11 | 10 | 10 | 9 | 7 | 6 |
| 9 | 10 | 10 | 10 | 10 | 9 | 9 | 8 | 7 | 6 |
| 10 | 9 | 9 | 9 | 9 | 9 | 9 | 8 | 6 | 6 |
| 11 | 9 | 9 | 9 | 9 | 8 | 8 | 7 | 6 | 5 |
| 12 | 8 | 8 | 8 | 8 | 8 | 8 | 6 | 5 | 5 |
| 13 | 8 | 8 | 8 | 8 | 8 | 7 | 6 | 5 | 4 |
| 14 | 7 | 7 | 7 | 7 | 7 | 7 | 6 | 5 | 4 |
| 15 | 6 | 6 | 6 | 6 | 6 | 6 | 5 | 4 | 4 |
| 16 | 7 | 7 | 7 | 7 | 7 | 7 | 5 | 4 | 4 |
| 17 | 6 | 6 | 6 | 6 | 5 | 6 | 4 | 4 | 3 |
| 18 | 7 | 7 | 7 | 7 | 7 | 7 | 5 | 5 | 4 |
| 20 | 3 | 3 | 3 | 3 | 3 | 3 | 2 | 2 | 2 |
| 21 | 5 | 5 | 6 | 5 | 5 | 5 | 4 | 3 | 3 |
| 22 | 6 | 6 | 6 | 6 | 6 | 6 | 4 | 4 | 3 |
| 32 | 5 | 5 | 5 | 5 | 5 | 5 | 4 | 4 | 3 |

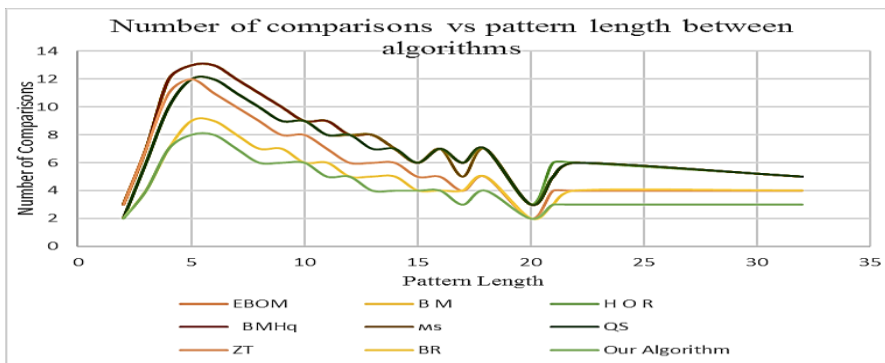


Figure 1: Graphical representation of number of comparisons vs Pattern length between algorithms.

Table 2: The average percentage difference in the number of comparisons between existing algorithms and our algorithm

| Pattern Length | EBOM | BM | HOR | BMHq | ms | QS | ZT | BR |
|----------------|--------|--------|--------|--------|--------|--------|--------|--------|
| 2 | 40.00% | 40.00% | 40.00% | 40.00% | 0.00% | 0.00% | 40.00% | 0.00% |
| 3 | 54.55% | 54.55% | 54.55% | 54.55% | 40.00% | 10.00% | 54.55% | 0.00% |
| 4 | 52.63% | 52.63% | 52.63% | 52.63% | 35.29% | 8.82% | 44.44% | 0.00% |
| 5 | 47.62% | 47.62% | 47.62% | 47.62% | 40.00% | 10.00% | 40.00% | 11.76% |
| 6 | 47.62% | 47.62% | 47.62% | 47.62% | 40.00% | 10.00% | 31.58% | 11.76% |
| 7 | 52.63% | 52.63% | 52.63% | 52.63% | 44.44% | 11.11% | 35.29% | 13.33% |
| 8 | 58.82% | 58.82% | 58.82% | 58.82% | 50.00% | 12.50% | 40.00% | 15.38% |
| 9 | 50.00% | 50.00% | 50.00% | 50.00% | 40.00% | 10.00% | 28.57% | 15.38% |
| 10 | 40.00% | 40.00% | 40.00% | 40.00% | 40.00% | 10.00% | 28.57% | 0.00% |
| 11 | 57.14% | 57.14% | 57.14% | 57.14% | 46.15% | 11.54% | 33.33% | 18.18% |
| 12 | 46.15% | 46.15% | 46.15% | 46.15% | 46.15% | 11.54% | 18.18% | 0.00% |
| 13 | 66.67% | 66.67% | 66.67% | 66.67% | 66.67% | 13.64% | 40.00% | 22.22% |
| 14 | 54.55% | 54.55% | 54.55% | 54.55% | 54.55% | 13.64% | 40.00% | 22.22% |
| 15 | 40.00% | 40.00% | 40.00% | 40.00% | 40.00% | 10.00% | 22.22% | 0.00% |
| 16 | 54.55% | 54.55% | 54.55% | 54.55% | 54.55% | 13.64% | 22.22% | 0.00% |
| 17 | 66.67% | 66.67% | 66.67% | 66.67% | 50.00% | 16.67% | 28.57% | 28.57% |
| 18 | 54.55% | 54.55% | 54.55% | 54.55% | 54.55% | 13.64% | 22.22% | 22.22% |
| 20 | 40.00% | 40.00% | 40.00% | 40.00% | 40.00% | 10.00% | 0.00% | 0.00% |
| 21 | 50.00% | 50.00% | 66.67% | 50.00% | 50.00% | 12.50% | 28.57% | 0.00% |
| 22 | 66.67% | 66.67% | 66.67% | 66.67% | 66.67% | 16.67% | 28.57% | 28.57% |
| 32 | 50.00% | 50.00% | 50.00% | 50.00% | 50.00% | 12.50% | 28.57% | 28.57% |

Figure 2 shows that graphical representation of percentage difference in terms of comparisons between existing algorithms and our algorithm.

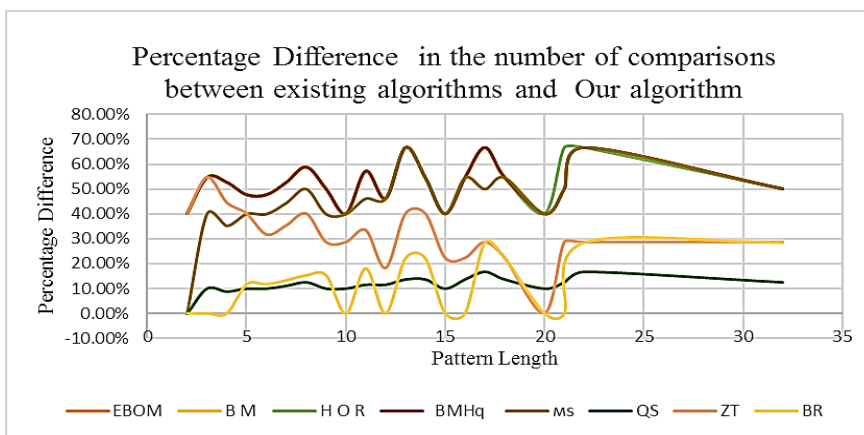
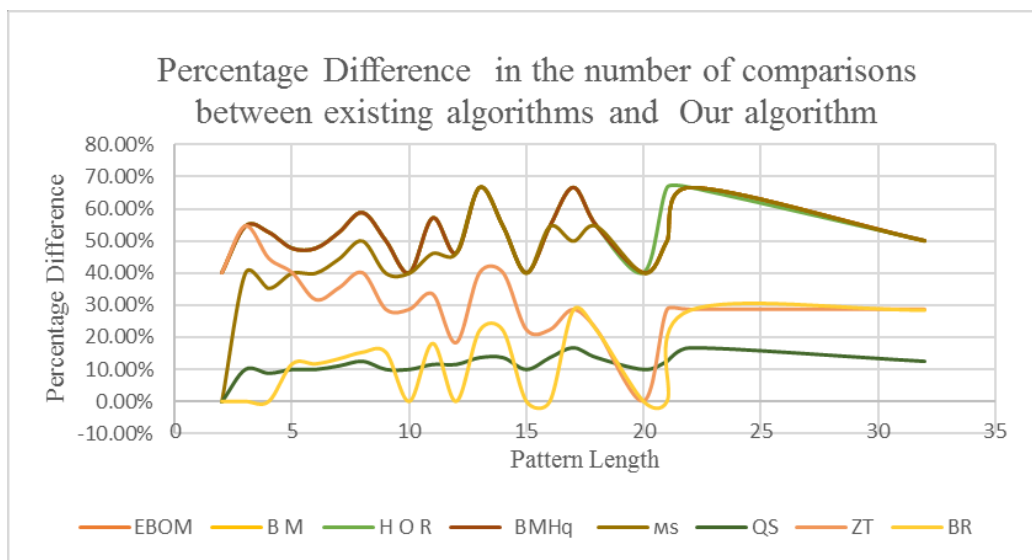


Figure 2: Percentage difference in terms of comparisons between existing algorithms and our algorithm



Each algorithm is evaluated more than five times for and the average time taken is given in Table 3. We have shown the average length of a shift performed by each algorithm in the second column. The timing was the last column shows the percentage difference of the user time between existing algorithms and our algorithm.

6 Conclusion

The experimental results show that our new algorithm is more efficient than the existing algorithms in practice for most of our chosen data sets. Over our random texts where the new algorithm is compared to the existing algorithms, our algorithm is more efficient for all but two of the texts. With the addition of special characters, it does not affect our algorithm. So, in the real world we would expect our savings to remain and make our algorithm competitive with the existing algorithms. It is also possible to apply some of our findings to what makes a fast algorithm to the existing algorithms. when large size of text used in string matching, our algorithm can be applied to set $k=2$ error level filter for approximate string matching, if pattern length m is greater than computer word w . our algorithm can be applied as 2-gram filter matching and encoding base2 used in approximate string matching. But B.R algorithm only can be applied for exact string matching.

Acknowledgement

We thank Prof. Mohan Babu is head of Sri Venkateswara college of engineering and Technology, Chittoor for allowing us to use experimental facilities.

References

- [1] Berry, T. Ravindran, S., "Tuning the Zhu-Takaoka string matching algorithm and experimental results", *Kybernetika*, Vol. 38, No. 1, pp.67-80,2002, Persistent URL: <http://dml.cz/dmlcz/135446>.
- [2] Boyer, R.S, Moore, J.S., "A fast string searching algorithm," *Communication of the ACM*, Vol. 20, No. 10, pp.762– 772, 1977.
- [3] Charras.C., Lecroq,T,*Handbook of exact string matching algorithms*, King’s Collage Publications, 2004.
- [4] Cormen, T.H., Leiserson, C.E., Rivest, R.L., *Introduction to Algorithms*, Chapter 34, MIT Press, pp 853-885, 1990.
- [5] Crochemore, M., Czumaj, A., Gasieniec, L., Jarominek, S., Lecroq, T., Plandowski. W., Rytter, W., "Speeding up two string matching algorithms," *Algorithmica*, Vol. 12, No. 4/5, pp.247-267, 1994.
- [6] Faro, S., Kulekci, M.O.: Fast and flexible packed string matching. *Journal of Discrete Algorithms* Vol. 28, 2014.
- [7] Faro, S., Lecroq, T.: The exact online string matching problem: A review of the most recent results. *ACM Computing Surveys*, Vol.45. No. 2, 2013.
- [8] Hassaballah,M,Omran.S, Mahdy.Y, A review of SIMD multimedia extensions and their usage in scientific and engineering applications. *The Computer Journal*, 51(6) November, pp. 630–649, 2008.
- [9] Horspool,R. N., "Practical fast searching in strings," *Software—Practice and Experience*, Vol. 10, No. 3, pp.501–506, 1980
- [10] Kalsi P, Peltola H, Tarhio J., Comparison of exact string matching algorithms for biological sequences. In: *Communications in computer and information science 13: proceedings of the second international conference on bioinformatics research and development, BIRD’08*. Springer-Verlag, Berlin, pp 417–426, 2008.
- [11] Knuth, D., Morris, J. H., Pratt, V., "Fast pattern matching in strings," *SIAM Journal on Computing*, Vol. 6, No. 2, doi: 10.1137/0206024, pp.323–350, 1977.
- [12] LecroqT., Fast exact string matching algorithms. *Information Processing Letters*, Vol. 102, No.6, pp. 229–235, 2007.
- [13] Sunday, D.M., A very fast substring search algorithm. *Communications of the ACM*, Vol. 33, No.8, 1990.
- [14] Zhu, R. F., Takaoka T.,“On improving the average case of the Boyer-Moore string matching algorithm”, *J. Inform. Process*,vol.10, 3, pp.173-177,1987.

Understanding Awareness Regarding Cyber Security And Preference For Advanced Protection Among Young Netizens

Shaswat Shetty
Assistant Professor
Mithibai College (Autonomous)
Vile Parle (West), Mumbai.

Abstract

Social engineering, which is also referred to as 'human hacking' is the activity of making people reveal their sensitive and private information for the purpose of obtaining illicit access to their accounts. People are lured with unbelievable offers and many people fall prey to the evil intentions of hackers. They end up clicking links and/or downloading malwares and thereby providing confidential information. The incidents of cyber-crimes are booming. This paper studies the awareness regarding cyber security. It also studies the preference for advanced protection i.e. paid antivirus software. In conclusion, measures are suggested so that people can combat the increasing number of incidents of cybercrimes and not fall prey to the cyber criminals.

Keywords: *illicit access, booming, awareness, malwares.*

1. Introduction

Today communication has become very easy and instant owing to smartphones and emails. It is imperative that this exchange of data takes place securely without compromising or leaking any data during transmission. Therefore, cyber security plays a pivotal role in our life. Modern means of communication have benefitted us due to easy and instant exchange of data. However, every coin has two sides. Safeguarding our privacy is becoming challenging and this paves the way for growing incidents of cybercrimes. Ensuring that the internet is safer, has therefore, become the focus for the development of new services. It is not very easy to combat and tackle the menace of cybercrime. Stringent laws on cybersecurity are essential to safeguard data of users. Every person must be trained on cybersecurity and measures to protect from cybercrimes.

2. Literature Review

G. Reddy and U.Reddy(2014) studied that cyber security plays a vital role in the domain of information technology. Several measures are being undertaken to minimize cybercrime. Despite several measures being undertaken, cyber security is still a very big concern. Cyber crime is a term that denotes illicit use of computer for the purpose of theft. In today's world, all information is stored in a digital manner. Millions of people are using social media websites. Hence, cyber criminals target such website users and endeavor to steal their data. Malware scanner is a software that scans all the files and documents in the system to detect harmful codes or virus. Antivirus softwares detect and remove virus and worm. Their research specified cyber ethics. Cyber ethics ensure that internet is used in a safe and proper manner.

N. Contech and P.Schmick(2016) analysed the risk, vulnerability and measures to prevent social engineering attacks. They studied five common types of social engineering attacks. Phishing attempts to procure information such as name, address, date of birth and other personal details. Pretexting attempts to steal information from an individual or business organisation. The attacker builds a credible history and hence individuals or organisations do not doubt the intentions of the attacker. Baiting is similar to phishing where cyber criminals promise goods and rewards upon

submission of confidential information. Under quid pro quo, attacker impersonates himself/herself as a technical expert and installs malware in the users computer. Under tailgating, the attacker tries to obtain access to restricted areas.

According to A. Tonge, S. Kasture and S. Chaudhari (2013), cyber security is a comprehensive term and is the process of safeguarding information and information system with the help of procedural and security measures. There is a dire need to incorporate Cyber ethics, Cyber safety and cyber security in the education. Approximately more than 3/4th of total commercial transactions are done online. There is growing reliance on cyber system. Threats to cyber security can be bifurcated into two categories – cyber attacks and cyber exploitation. Many measures have been undertaken by governments to combat specific types of cyber attacks or cyber exploitation. At an individual level, awareness of measures to tackle cyber attacks or exploitation must be made. Children should be explained terms like phishing, malware, trojan, spyware and adware.

I. Bandara, F. Ioras, K. Maher (2014) described that cyberspace is commonly referred to as the internet. Cyber security is the rules and regulations to be administered for protection of this cyberspace. There has been increasing use of E-Learning system, however limited attention is given to the issue of security of E-Learning system. E-learning is a method of learning which is dependent on the Internet. E-learning provides plethora of chances for students and teachers to develop and enhance their skills and knowledge. E-learning systems may be open, distributed and interconnected and this may pave the way for cyber-crime. University and college students are one of the largest users of social media platforms such as Facebook and Youtube. Hence, malwares and viruses can spread via these websites. While it may be difficult to block access to such sites, early identification of infected devices is important to avoid loss of crucial data. Measures such as installation of firewall, antivirus softwares, improvement of authentication and training of security professionals must be undertaken in order to mitigate risks and threats.

M. Abomhara and G. Koein (2015) explained that the number of threats and attacks against Internet of Things (IoT) devices are increasing rapidly. Attack is an action performed to damage a system that affects its normal operations. A physical attack tampers with hardware components. In case of denial of service attack, a machine or a network resource becomes non-operational and cannot be used by the intended user. In case of access attacks, third parties and unauthorized persons get access to networks or devices. Cyber espionage uses techniques and malicious programs to spy and/or obtain sensitive and private information of individuals, organizations and governments.

K. Valsalan (2020) described that cybercrimes are the fastest developing crimes in the world. The Information Technology Act helps us to deal with the issue of cybercrime. The research paper described various types of cybercrimes. Hacking in simple words refers to gaining access to one's computer device without permission. Phishing is generally executed with the help of email spoofing. Technology is a double-edged sword and therefore must be judiciously used.

3. Research Design

3.1 Objectives of Research

The objectives of the study are described as under:

- To understand the factors leading to neglect of cyber security among young netizens.
- To understand common features of phishing calls and emails
- To provide suggestions and recommendations to prevent the attacks of phishing and other cybercrimes.

3.2 Limitations of Research

- There are various kinds of cybercrimes. Today, communication is taking place mainly with the help of emails. Phishing is a technique where attackers send deceptive emails to obtain confidential data from people. Hence, the research paper focusses on phishing and primary features to identify phishing calls and emails are described. Measures to combat phishing and some general measures to offset the attacks of cybercrimes are suggested.

3.3 Data Collection and analysis

- Data required for the study is ascertained from both primary and secondary sources.
- Questionnaire was used to obtain data from the respondents. An online survey was created and was shared in social media platforms. The sample size is 100 respondents. Convenience sampling technique was administered in the study. Respondents are mainly the young users of cyberspace whose age is between 18 and 30 years. The respondents were made aware that data is used only for study and anonymity of their responses shall be maintained. To avoid multiple responses from the same user, only one response per user was permitted.
- The collected data was analyzed using percentage analysis and chi square test.

3.4 Hypothesis

- There is no relation between gender and preference for advance protection i.e. paid antivirus software. (Null hypothesis)
- There is significant relation between gender and preference for advance protection i.e. paid antivirus software. (Alternate hypothesis)

4. Data Analysis

4.1 Analyzing Demographic Profile of Respondents

Table 1: Demographic Profile

| Variable | Category / Choices offered to respondents. | Number of Responses | Percentage |
|--|--|---------------------|------------|
| Gender | Male | 65 | 43.33 |
| | Female | 85 | 56.67 |
| Age | Less than 20 Years | 40 | 26.67 |
| | 20 – 30 Years | 70 | 46.67 |
| | 30 – 40 Years | 22 | 14.67 |
| | Above 40 Years | 18 | 11.99 |
| Occupation | Business | 16 | 10.67 |
| | Profession | 14 | 9.33 |
| | Employed | 10 | 6.67 |
| | Student | 110 | 73.33 |
| Number of Internet Users in the family | Less than 5 | 70 | 46.67 |
| | 5 – 8 | 66 | 44.00 |
| | More than 8 | 14 | 9.33 |

Findings:

- Out of 150 respondents, nearly 43% respondents were male and the remaining 57% respondents were females.

- As the study wants to study awareness regarding cyber security among young netizens, questionnaires were mainly circulated to people below age of 40 years (nearly 88% respondents age was below 40 years).
- It was found that nearly 10% of respondents had more 8 active users of internet in the family.

4.2 Analyzing Factors Affecting Neglect of Cyber Security

Table 2: Causes of neglect in cyber security

| Question | Category / Choices offered to respondents. | Number of Responses | Percentage |
|--|---|---------------------|------------|
| I have a paid antivirus installed in my smartphone and/or computer. | Yes | 35 | 23.33 |
| | No | 115 | 76.67 |
| I am aware of cyber security and measures to prevent cybercrimes. | Yes | 90 | 60.00 |
| | No | 16 | 10.67 |
| | May be | 44 | 29.33 |
| I have been a victim of cyber-crime. | Yes | 27 | 18.00 |
| | No | 123 | 82.00 |
| My preference for annual subscription fee for antivirus software is | 1,000 to 2,000 | 62 | 41.33 |
| | 2,000 to 3,000 | 17 | 11.33 |
| | I prefer free software with limited protection. | 71 | 47.34 |
| I should share my debit card details with bank staff over the phone for verification purpose | Strongly Agree | 10 | 6.67 |
| | Agree | 24 | 16.00 |
| | Neutral | 16 | 10.67 |
| | Disagree | 66 | 44.00 |
| | Strongly Disagree | 34 | 22.66 |
| I use the same password for multiple websites as I often forget multiple passwords | Yes | 113 | 75.33 |
| | No | 37 | 24.67 |
| The last time I changed my primary email password was | Within 1 Year | 21 | 14.00 |
| | More than a year ago | 98 | 65.33 |
| | I have never changed password once created. | 31 | 20.67 |
| I check the website security before entering my personal details | Always | 69 | 46.00 |
| | Sometimes | 71 | 47.33 |
| | Rarely | 8 | 5.33 |
| | Never | 2 | 1.34 |
| I keep backup of my important data | Yes | 24 | 16.00 |
| | No | 126 | 84.00 |
| I click on links that provide attractive offers, promo codes and free gifts. | Always | 17 | 11.33 |
| | Sometimes | 73 | 48.67 |
| | Rarely | 46 | 30.67 |
| | Never | 14 | 9.33 |

Findings:

- It was observed that majority of respondents did not have a paid antivirus software in their smartphones and/or laptop. It implies that either these respondents do not use antivirus software or are currently relying on free antivirus software. Free antivirus software offers basic protection. Paid antivirus software provides comprehensive and advance protection.
- Nearly 30% of respondents were not certain regarding their knowledge on cyber security. This uncertainty implies that more awareness needs to be created regarding cyber security and measures to combat cyber-attacks.
- One positive fact observed was that majority of respondents were not victims of cyber-crimes.
- Around 47% of respondents do not prefer to pay a single penny towards subscription for antivirus software (i.e. for more advanced protection).
- It was alarming to note that around 7% of respondents would strongly agree to provide their confidential account details to bank staff. This indicates that such respondents can become easy targets for phishers who can impersonate as bank staff and ask for personal details.
- Human memory is limited and therefore many people prefer to use same passwords for multiple websites. This statement can be validated as nearly 75% of respondents use the same password for multiple websites.
- Around 20% of respondents have not changed their passwords since inception.
- 71 respondents mentioned that they sometimes check website security. It implies that such respondents may fall prey to websites that appear like authentic websites.
- It was disappointing to note that 84% of respondents do not keep backup of important data.
- Around 10% of respondents never click on links that offer attractive discounts or free gifts.

4.3 Testing of Hypothesis

Table 3: Chi Square Test – Observed Values

| Gender | Positive Preference for Paid Antivirus Software | Negative Preference for paid anti-virus software | Total |
|--------|---|--|-------|
| Male | 22 | 43 | 65 |
| Female | 13 | 72 | 85 |
| Total | 35 | 115 | 150 |

Table 5: Chi Square Test – Expected Values

| Gender | Positive Preference for Paid Antivirus Software | Negative Preference for paid anti-virus software | Total |
|--------|---|--|-------|
| Male | 15 | 50 | 65 |
| Female | 20 | 65 | 85 |
| Total | 35 | 115 | 150 |

Table 6: Chi Square Test – Workings

| Observed Value | Expected Value | $(\text{Observed} - \text{Expected Value})^2 / \text{Expected Value}$ |
|----------------|----------------|---|
| 22 | 15 | 3.27 |
| 13 | 20 | 2.45 |

| | | |
|----|-------|------|
| 43 | 50 | 0.98 |
| 72 | 65 | 0.75 |
| | Total | 7.45 |

As calculated Chi Square value exceeds critical value, we reject the null hypothesis and accept the alternate hypothesis. Hence, there is significant relation between gender and preference for paid antivirus software.

5. Suggestions and recommendations to prevent the attack of phishing and other cyber crimes

Phishing is illicit acquisition of personal data by deceiving the individual and making him believe that the attacker is trustworthy. It is normally done with the help of electronic mail. Such emails will usually contain some warning and ask the user to update personal data, address or password. Such emails often contain link to websites that are infected with malwares. Phishing is a big threat. Cybercriminals create fake websites that appear like the genuine ones so that they can know your username and password. There is a possibility that user may enter a phishing site by mistyping a website name. Due to phishing, billions of dollars have been lost by several companies and individuals. Below are sample phone call scripts to identify phishing:

Call Script 1: Am I Speaking to Mr. Shah? I am calling from ABC Bank. We need to verify your details as suspicious activities and purchases are made within last 7 days. Can you confirm your debit card number, expiry date and CVV for verification purpose?

Call Script 2: Hello Mr. Sharma. I represent LMN company and our records indicate that you owe us Rs. 50,000. Your address is 36 Model Apartments. Can you confirm your Adhar Card number and date of birth?

Below are few characteristics of phishing emails:

Phishing emails may contain IP address instead of website name. For example, please click on 'http://151.88.17.2/'.

Most phishing emails contain words like 'Click here', 'Login Immediately', 'Update the details', 'Suspend',

Prevention is regarded as better than cure. It is essential to take certain measures while making use of the cyberspace. A netizen should avoid revealing personal information to strangers. It is recommended that a user should not send his/her photographs to unknown people to avoid its misuse. Antivirus software should be installed and updated regularly. There are many anti-virus software that warn users regarding dubious websites. Browsers like Google Chrome also warn the user when they are accessing a website that is not secured by Secure Socket Layer. A backup of data should be created so that data can be retrieved easily, if the system is affected by cybercrime. One should enter details like credit /debit card number, expiry date and CVV only after verifying website security.

We normally set up passwords which are easy to remember. The same password is used for multiple websites. We should use different passwords and set up a strong password which is difficult to guess. Setting up different passwords for each website will help to minimize the damage if password used for accessing any website gets compromised. These measures shall be of great use to minimize instances of cybercrimes. We acknowledge that an individual's mind is unfathomable and his abilities are limitless. Hence, complete elimination of cybercrime appears to be herculean task. History has proved that no statute is capable of complete eradication of crime. Hence, it is in the interest of the people to become aware of cyber security and take the necessary measures.

References

- [1] Conteh, N. Y., & Schmick, P. J. (2016). Cybersecurity: risks, vulnerabilities and counter-measures to prevent social engineering attacks. *International Journal of Advanced Computer Research*, 6(23), 31.
- [2] Ayofe, A. N., & Irwin, B. (2010). Cyber security: Challenges and the way forward. *Computer Science & Telecommunications*, 29(6).
- [3] Gade, Nikhita Reddy & Reddy, Ugander. (2014). A Study Of Cyber Security Challenges And Its Emerging Trends On Latest Technologies.
- [4] Tonge, A. M., Kasture, S. S., & Chaudhari, S. R. (2013). Cyber security: challenges for society-literature review. *IOSR Journal of computer Engineering*, 12(2), 67-75.
- [5] Bandara, I., Ioras, F., & Maher, K. (2014). Cyber security concerns in e-learning education.
- [6] Abomhara, M., & Kjøien, G. M. (2015). Cyber security and the internet of things: vulnerabilities, threats, intruders and attacks. *Journal of Cyber Security and Mobility*, 65-88.
- [7] Valsalan, K. A CRITICAL ANALYSIS ON CYBER CRIMES AND SECURITY ISSUES IN INDIA.
- [8] Umarhathab, S., Rao, G. D. R., & Jaishankar, K. (2009). Cyber crimes in India: A study of emerging patterns of perpetration and victimization in Chennai City. *Pakistan Journal of Criminology*, 1(1), 51-66.
- [9] Dashora, K. (2011). Cyber crime in the society: Problems and preventions. *Journal of Alternative Perspectives in the social sciences*, 3(1), 240-259.
- [10] Gandhi, P., & Tripathi, O. A Smart Approach to Avoid Phishing.
- [11] Akinyelu, A. A., & Adewumi, A. O. (2014). Classification of phishing email using random forest machine learning technique. *Journal of Applied Mathematics*, 2014.
- [12] Chaudhry, J. A., Chaudhry, S. A., & Rittenhouse, R. G. (2016). Phishing attacks and defenses. *International Journal of Security and Its Applications*, 10(1), 247-256.

An Intelligent Algorithm With Feature Selection For Thyroid Disease Classification And Dignosis Using Data Mining Techniques

Parimala.S, Dr.P.SenthilVadivu

Abstract

Absurd potential for healthcare services is held by Data mining because of the aggressive proliferation in the massive amount of electronic health records. In the conventional time, health providers and physicians hold patient information manually. The data was very tedious to maintain. New techniques are introduced to reduce the human efforts by Modernizing and digitalizing the data and made available in an easy accessible way. The Main task is to detect disease diagnosis at the early stages with higher accuracy. In health care services, data mining plays a vital role in the part of Classification concept. Diagnosing the diseases and providing the necessary treatment for the patients becomes a primary challenge for the health care services. In this paper using enhanced data mining algorithms and classification system thyroid disease is being detected with higher accuracy which is more important in diagnose a chronic illness such as thyroid. This paper enlightens the issue of Dimensionality reduction for which Feature selection algorithms are used which considered one of the main task in feature is engineering. An algorithm is proposed which gives the solution to sort out the problems in the existing system of classification.

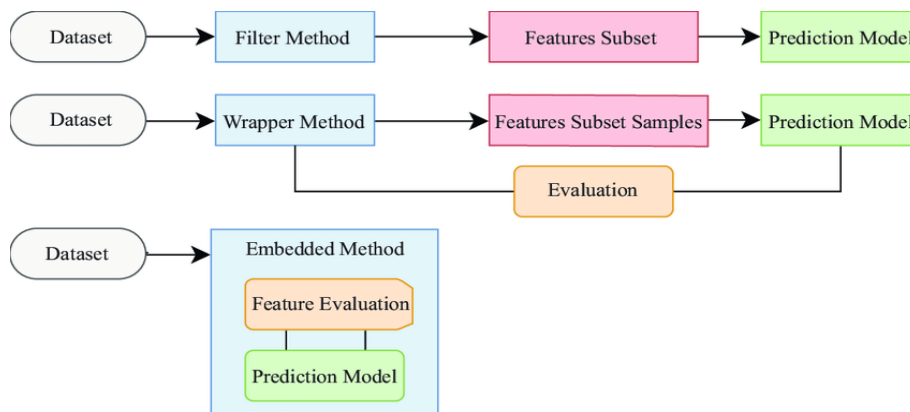
Keywords: Data mining, Thyroid, Dimensionality reduction, Feature selection algorithms.

1. Introduction

Diagnosis of health conditions is a very challenging task in field of medical science. Diagnoses of health conditions are based on the physician experience. Data mining technique plays role to diagnosis of diseases of patients. Classification is one of the important data mining applications for classification of data. In this work, our main purpose is to propose a robust classifier and compared with other existing classifier which is developed by various authors. We have developed classifications models and its ensemble model for classification of thyroid data. Feature selection is also applied to improve the classification accuracy and increases performance.

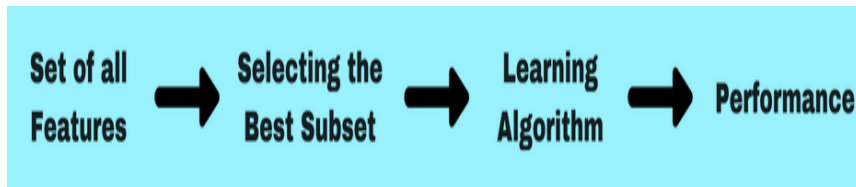
Feature selection is one of the frequently used and most important techniques in data preprocessing for data mining [1].The goal of feature selection for classification task is to maximize classification accuracy [2].The method of eliminating excessive or inappropriate features from the original data set is termed as Feature Selection.. So the carrying out time of the classifier that processes the data will decreases and also accuracy increases because irrelevant features can include noisy data affecting the classification accuracy negatively [3]. With feature selection the understandability can be improved and cost of data handling becomes smaller [4].

One contributing commitment, feature selection(FS), has already facilitated data mining for its good performance of seeking correlated features and deleting redundant or uncorrelated features from the original dataset [11], [6]. Feature selection is one of the most important data processing techniques, and is frequently exploited to seek correlated features and delete redundant or uncorrelated features from a feature set [7]. Random or noisy features often disturb a classifier learning correct correlations, and redundant or correlated features increase the complexity of a classifier without adding any useful information to the classifier [8]. A variety of feature selection methods, such as filter, wrapper, and embedded approaches [7] [9], have been developed.



One of the primary components of feature selection is producing the subset and subset evaluation. You must determine the search strategy and evaluation criteria you must indicate the approach for search and also the criteria for evaluation. There is always an association between Feature selection algorithms and data mining.

1.1 Filter Methods



As a pre-processing step, Filter based approach are used. For any data mining algorithms, the selection of features is independent. Instead, features are chosen on the basis of their scores in various statistical tests for their correlation with the outcome variable. For their correlation different statistical tests are performed based on their scores. We cannot able to predict for which algorithm which filter based approach can be used. In this research work ,we have used only the filter based approach for feature selection algorithm . Because when compared to wrapper method, Filter based approach are much faster as they do not involve in training the model and also they depend only on the features in the data set.

1.2 Benefits from Feature Selection

The basic idea of using feature selection is to obtain a new dataset with neither redundant features nor irrelevant features, as well as containing the original data pattern, and not losing any useful information in the original dataset. Nowadays, Feature selection methods are widely employed with their capability of dimension reduction, for instance, in the field of written text and DNA microarray analysis, and show their advantages when the number of features is large while the number of samples is small.

The main objective of the Feature selection is to identify the features which are based on the original dataset. It should be noted that some related features may be redundant since there might be another features which are strongly correlated [12]–[14]. The three privileges of conducting Feature selection on dataset are (1) the selected features can be used to construct a brief model for describing original data and thus are beneficial for improving the performance of criteria; (2) the selected features can reflect the core characters of original data and thus are helpful for tracing concept drifts of data expression with good robustness; and (3) the chosen features can help the decision-maker pick valuable information from a large number of noisy data [14], [15]

1.3 Systemizations and Interrelations

Commonly, feature selection techniques can be classified into filter, wrapper, and embedded according to the means of combining a classifier and a machine learning approach when selecting a feature subset [10], [13]–[15], regardless of supervised or unsupervised methods [13], [16], [17]. The difference between the supervised and unsupervised learning methods lies in whether the class labels are available or not. To evaluate the implication of features and offer rankings of these features, in the domain of feature selection, available label information is employed with the first-mentioned condition. . The latter seeks hidden structures in unlabelled data and constructs a feature selector by means of intrinsic properties of data [18].

For supervised feature selection algorithms, separability criteria, consistency criteria and error rate criteria are favourable for evaluating the performance of methods. In contrast, for those unsupervised feature selection methods, the clustering validity criteria, information theoretical criteria, and feature similarity criteria are now widely seen [20]–[22].

2 Issues during classification

Presence of irrelevant and noisy redundant features evokes two problems during classification includes i)Induce greater computational cost ii)May lead to over fitting .Thus, as a solution to solve the above issues, FS algorithms are used.FS algorithms work on the principal that not all features are important during data mining

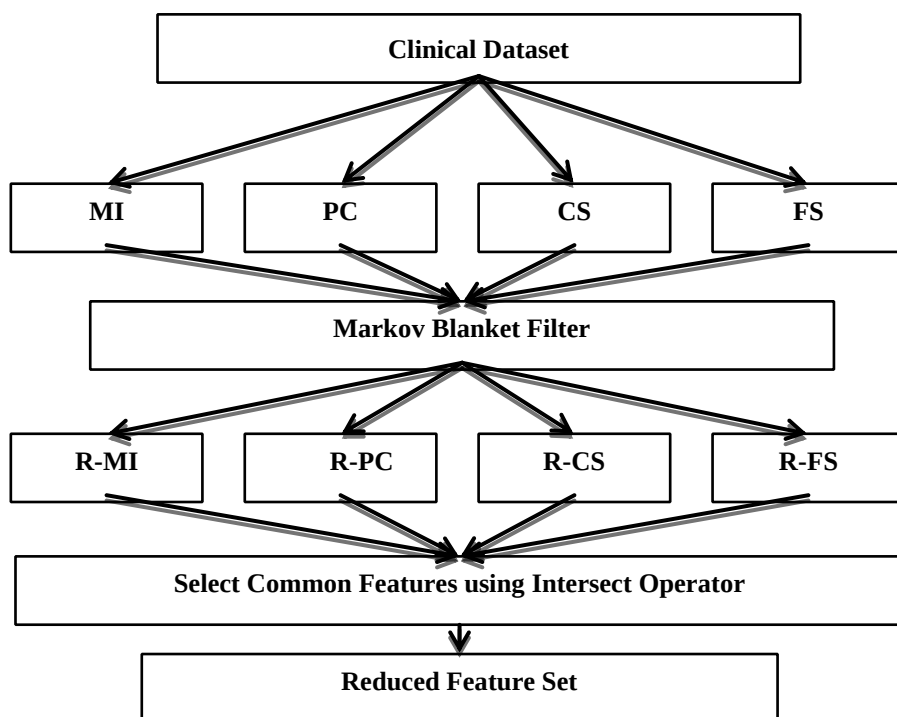
and these features can be removed without affecting the performance's is the task of selecting features that have the maximum impact on describing the results and to drop the features with little or no effect. It is a problem of universal interlacing amendment in data mining, which reduces the number of features, removes irrelevant, noisy and redundant data, and results in improving accuracy.

3 Proposed Algorithm

In general, a single feature selection algorithm is used to identify significant features. Several feature selection algorithms are being used for this purpose, with each having its own advantages and disadvantages.

In order to combine the advantages of various feature selection algorithms, this research work proposes the use of multiple feature selection algorithm to select optimal features.

In this research work, four important and frequently used algorithms are used. They are, Mutual Information, Information Gain, Fisher Score, Pearson Coefficient, Chi Square .This algorithm is termed as '**Multiple Feature Selection Algorithms (MFS)**'



The diagram shows the flow of proposed filter based approach. The proposed algorithm uses statistical tests to determine the subset of features with the highest predictive power.

The first step of M2FPS algorithm uses four feature selection filters such as Mutual information, Pearson Correlations, Chi-Square and Fisher Criterion Score to select optimal features. The resultant features are used as input to a more computationally intensive subset selection procedure known as Markov blanket filtering , which results with four sets of optimal reduced features, namely, R-MI, R-PC, R-CS and R-FS. These four sets are combined using intersection operation in order to select only common features that exist between the four subsets.

3.1 Data Sets

Dataset for this research work is taken from UCI Thyroid dataset (UTD)
 Taken from :<http://archive.ics.uci.edu/ml/datasets/Thyroid+Disease>

Number of Instances : 7200
 Number of Attributes : 21
 Number of Classes : Normal, hypo and hyper
 Performance Metrics : Accuracy
 The missing percentage was varied with values ranging from 0 to 60% in steps of 10.

4. Experimental Results

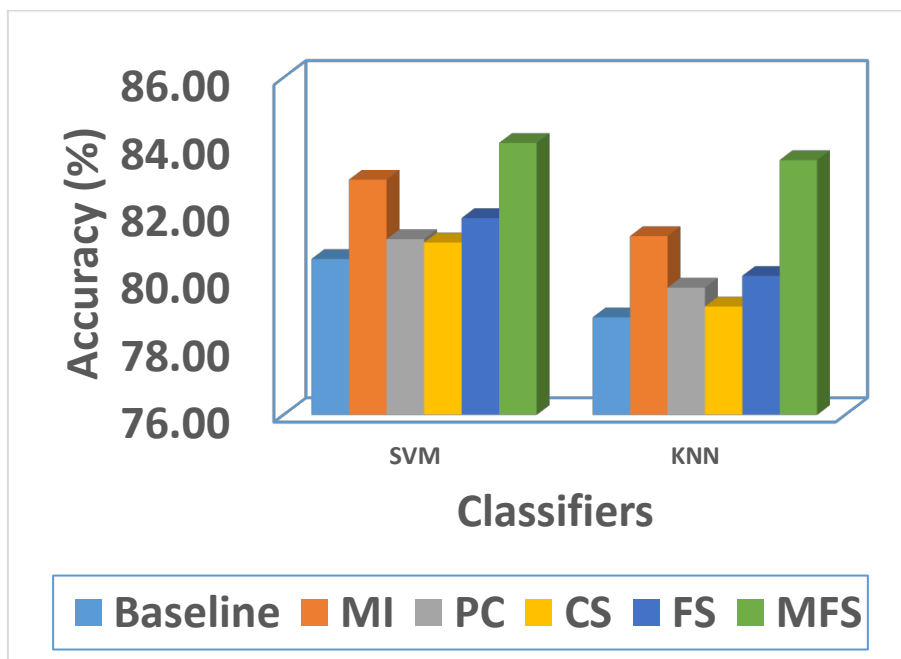


Figure: 2 Analysis of Feature Selection Algorithms Accuracy (%)

| Algorithms | Values (%) |
|----------------------------|------------|
| Baseline | 80.62 |
| Mutual Information | 82.97 |
| Person Coefficient | 81.21 |
| Chi-Square | 81.11 |
| Fisher Score | 81.83 |
| Multiple Feature Selection | 84.06 |

Table 1: Different types of Algorithms used and their results

4.1 Findings

While no feature engineering algorithms are used, the performance of the algorithm is very low. In fact, it degrades with increase in missing percentages. All the proposed algorithms detect thyroid disease in an improved fashion when compared with its existing counterparts. Comparison of the proposed unified models showed that with low missing percentage ($\leq 10\%$), the models that applied feature selection, followed by missing value followed by instance selection produces high accuracy. Table 1 clearly shows that only the proposed algorithm that is the Multiple Feature Algorithm gives high accuracy.

5. Conclusion and Future Work

We have four algorithms i.e., Mutual Information, Information Gain, Fisher Score, Pearson Coefficient, Chi Square .which is termed ‘Multiple Feature Selection Algorithms (MFS)’. In this work, we have solved the issue of Dimensionality reduction for which Feature selection algorithms are used which considered one of the main task in feature is engineering. Multiple Feature Selection Algorithms algorithm is proposed which gives the solution to sort out the problems in the existing system of classification. We have used svm and knn since widely used in thyroid disease. The analysis of Feature selection algorithm while using SVM and KNN classifier is clearly shown. Table 1 clearly shows that only the proposed algorithm that is the Multiple Feature Algorithm gives high accuracy. The proposed algorithm clearly improves the accuracy during thyroid disease classification. In future, few more issues and algorithms will be taken for research and will be enhance to improve the accuracy by implementing with datasets which can help to improve the accuracy of diagnosis.

References

- [1] Asha Gowda Karegowda, M.A.Jayaram and A.S. Manjunath, —Feature Subset Selection Problem using Wrapper Approach in Supervised Learning, International Journal of Computer Applications, Vol. 1, No. 7, pp. 0975–8887, 2010.
- [2] Ron Kohavi, George H. John, —Wrappers for feature subset Selection, Artificial Intelligence, Vol. 97, No. 1-2. pp. 273-324, 1997.
- [3] S. Doraisami, S. Golzari, A Study on Feature Selection and Classification Techniques for Automatic Genre Classification of Traditional Malay Music, Content-Based Retrieval, Categorization and Similarity, 2008
- [4] A. Arauzo-Azofra, J. L. Aznarte, and J. M. Benítez, Empirical study of feature selection methods based on individual feature evaluation for classification problems, Expert Systems with Applications, 38 (2011) 8170-8177.
- [5] Q. Tuo, H. Zhao, and Q. Hu, “Hierarchical feature selection with subtree based graph regularization,” Knowl.-Based Syst., vol. 163, pp. 996–1008, Jan. 2019. [Online]. Available: <http://www.sciencedirect.com/science/article/pii/S0950705118305094>
- [6] V. Bolón-Canedo, N. Sánchez-Marroño, and A. Alonso-Betanzos, “Recent advances and emerging challenges of feature selection in the context of big data,” Knowl.-Based Syst., vol. 86, pp. 33–45, Sep. 2015.
- [7] V. Bolón-Canedo, N. Sánchez-Marroño, and A. Alonso-Betanzos, “A review of feature selection methods on synthetic data,” Knowl. Inf.Syst., vol. 34, no. 3, pp. 483–519, 2013.
- [8] J. Wu and Z. Lu, “A novel hybrid genetic algorithm and simulated annealing for feature selection and kernel optimization in support vector regression,” in Proc. IEEE 5th Int. Conf. Adv. Comput. Intell. (ICACI), Oct. 2012, pp. 999–1003.
- [9] N. Abd-ElSabour, “A review on evolutionary feature selection,” in Proc. Eur. Modelling Symp., 2014, pp. 20–26.
- [10] H. Zhou, S. Han, and Y. Liu, “A novel feature selection approach based on document frequency of segmented term frequency,” IEEE Access, vol. 6, pp. 53811–53821, 2018.
- [11] W. Zhou, C. Wu, Y. Yi, and G. Luo, “Structure preserving non-negative feature self-representation for unsupervised feature selection,” IEEE Access, vol. 5, pp. 8792–8803, 2017.
- [10] I. Guyon and A. Elisseeff, “An introduction to variable and feature selection,” J. Mach. Learn. Res., vol. 3, no. 6, pp. 1157–1182, Jan. 2003.
- [12] J. R. Vergara and P. A. Estévez, “A review of feature selection methods based on mutual information,” Neural Comput. Appl., vol. 24, no. 1, pp. 175–186, 2014.

- [13] X.-Y. Liu, Y. Liang, S. Wang, Z.-Y. Yang, and H.-S. Ye, "A hybrid genetic algorithm with wrapper-embedded approaches for feature selection," *IEEE Access*, vol. 6, pp. 22863–22874, 2018.
- [14] F. Bagherzadeh-Khiabani, A. Ramezankhani, F. Azizi, F. Hadaegh, E. W. Steyerberg, and D. Khalili, "A tutorial on variable selection for clinical prediction models: Feature selection methods in data mining could improve the results," *J. Clin. Epidemiol.*, vol. 71, pp. 76–85, Mar. 2016.
- [15] M. Dash and H. Liu, "Feature selection for classification," *Intell. Data Anal.*, vol. 1, nos. 1–4, pp. 131–156, 1997.

Automatic Product Billing Through Camera Using Artificial Intelligence And Edge Computing

Harivyas S, Abishek M, Pavithran M M
UG Students

Department of Information Technology, Bannari Amman Institute of Technology
harivyas.it18@bitsathy.ac.in, abishek.it18@bitsathy.ac.in, pavithran.it18@bitsathy.ac.in

Abstract

Modern science and technology have increased the way of life for people. All of us incline toward quality in items we use in everyday lives. These results in the huge groups at the shopping center and malls which prompts long lines at the charging counters where the shop keeper needs to filter each item in the scanning machine and enter into the record to bill those products. The framework above is a bit tedious. There are much research works for the smart billing of products. The proposed work concentrates on designing a therapeutic electronic item to solve this issue. The object detection algorithm called the YOLO algorithm detects the items which allow the retrieval of information using Edge Computing stored in edge servers. The products placed in the conveyer belt are detected and stored in the cart and the information are shown in the screen. The information and the quantity of the products are calculated and the bill is generated automatically.

KEYWORDS- *object detection, YOLO algorithm, Edge computing.*

1. Introduction

The product in the billing counter is detected through camera considering various parameters like the size of the product, sort of product and generates the bill of those items. The dataset of the images are trained and reserved within the edge servers and data and attributes can be fetched by edge computing. The imutils library in the YOLO Algorithm which is a necessary picture handling functions like interpretation, rotation, resizing, skeletonization, showing Matplotlib pictures, arranging contours, detecting edges. The Scipy library helps the dimensions of the image that is captured using the `scipy.spatial.distance`. It computes the space matrix from a set of raw observation vectors stored during a rectangular array. The OpenCV Python is only a wrapper class for the first C++ library to be utilized with Python. Using this, OpenCV array structures changed over to Numpy arrays. This makes it easier to incorporate it with different libraries that utilize Numpy and Matplotlib. The Tkinter bundle ("Tk interface") is that the standard Python interface to the Tk GUI toolkit. The Tk class is started up without arguments. This makes a top-level widget of Tk which is the major window of an application. Each occasion has its own related Tcl interpreter. The OCR (Optical Character Recognition) is the way towards optical patterns contained during a digital image. The character recognition from an image is achieved through classification, feature extraction, and segmentation.

The Backend procedure includes an Edge server that might be a kind of edge gadget that gives an entry point into a system. An essential utilization of a CDN edge server is to store content as close as conceivable to a mentioning customer machine, which helps in diminishing latency and improving page load times. Edge gadgets are frequently set inside Internet trade focuses (IXPs) to allow various systems to append and share travel from the servers. A CDN supplier will put servers in numerous areas, yet some of the most significant are the association focuses on the edge between various systems. These edge servers will interface with various systems and license traffic to pass rapidly and effectively between systems.

The Jetson Nano might be a little, amazing PC for installing applications and AI IoT that conveys the capacity of ongoing AI. It begins quickly with the incomparable Jet Pack SDK with quickened libraries for deep learning, graphics, multimedia, Computer vision and, that's only the tip of the iceberg. Besides, it permits us to run different neural systems in equal for applications like object detection, processing the speeches, classification of images, and segmentation. It's a simple to-utilize stage that runs in as meager as 5 watts. So, product billing in **Jetson Nano** through camera gives more efficiency and compactable.

2. Literature Survey

Tanmay Singh et al. [1] proposed an Intelligent Self-Checkout System (ISCOS) comprises of a solitary camera to identify different items with no names continuously in real-time. The picture taken from the camera will be given as a contribution to the YOLO calculation. At the end of this algorithmic calculation will be a picture where all the things named with their name are available inside it and are inside the shaded limit indicating the specific area of the item inside the picture. Open-source datasets libraries such as Open CV or Image Net are used. MySQL Microsoft access or Oracle 9i database structure is used to store various qualities of the items that the client can buy in the store, for e.g., association name, amount, name, value, and so forth.

B Sudha et al. [2] used the Raspberry pi processor with a PI Camera and QR scanner. The images of the product/ object will have different values like 189, 170, 52, 0 and many more. When the customer moves in any direction with the help of a pi camera and gear motor, the image of the product in the trolley will be captured. The image captured by the camera will be forwarded and processed by the Raspberry pi. Raspberry processor will apply several image processing algorithms and detect the object.

N. Ragesh et al. [3] designed a system which has a camera that distinguishes the item utilizing Deep Learning strategies and a load cell that gauges the heaviness of the commodity appended to the shopping basket. This framework will produce the bill when the client scans the thing before the camera which is fixed in the Cart.

Ms. Vrinda, Niharika [4] proposed an idea of LCD used for offers, discounts, and the total bill. The technology which they proposed is the utilization of RFID innovation for programmed item charging acknowledgment inside the cart, subsequently nullifying client intercession in the procedure of the item in which the client is making payment.

3. Proposed Work

The grocery data set involves a huge number of attributes/information to predict the accurate product. Data mining can be implemented for extracting knowledge from the image data set taken. It also identifies the relationship between different attributes in the grocery data. With the help of size, shape, OCR, the camera recognizes the products and puts them in the cart. When every item is put before the camera, different data like item's price, products name are shown in the LCD screen set in the cart. This AI-based product billing will do an automatic billing process in various shopping malls. The above process is illustrated in Figure- 1.

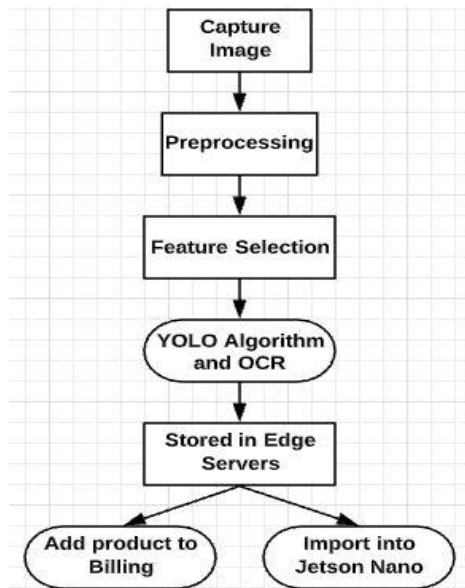


Figure 1: Flow chart of proposed work

The Billing items window in the Accounting Console is utilized to characterize item codes for items/services to be charged by the association. The billing items window characterizes product offering things, default estimating, association and Ledger account data. Just items with right item codes can be charged. One item code ought to be made for every potential levy or membership type item or administration that will be charged. Here, the item will be charged through Camera with the assistance of present-day innovations i.e., Jetson Nano which pursues the algorithm, for example, OCR(Optical Character Recognition), item's shape, item's size, Edge computing, and YOLO algorithm.

3.1 Data Preprocessing & Feature Selection:

A two-dimensional array numbers either pixels of an image between the scope of 0 and 255. It is characterized by the functions in the mathematics $f(x,y)$ where x and y are the coordinates of the vertical and horizontal plane. The estimation of $f(x,y)$ anytime is in the given picture will give return the pixel value. The algorithm is as follows,

3.1.1.YOLO Algorithm:

- 1) Load the input images and extract all its dimensions. Determine the output layers from the YOLO model. Perform a forward pass through YOLO network.
- 2) **Boxes:** The picture is surrounded by the boxes.
- 3) **Confidences:** The YOLO will assign a confidence value to the item. The lower certainty value the object won't be same the network thinks. The limit level ought to be kept up at 0.5.
- 4) Extract the **classID** and confidences to filter out weak detection.
- 5) The scale bouncing box directions will show them appropriately on original picture.
- 6) Extract coordinates and dimensions of the bounding box. YOLO returns bounding box coordinates in the form: **(centerX, centerY, width, height)**.
- 7) for keeping only the surest ones **Non-Maxima Suppression** (NMS) suppresses in a significant matter and the bounding boxes will be overlapped.
- 8) **NMS** additionally guarantees that there are no excess or incidental bouncing boxes.

- 9) NMS threshold and certainty limit, bounding boxes, confidences will be submitted by the NMS which is one of the in-built DNN module functionality of the Open CV.
- 10) Expecting a picture exists with a least in detection; the idxs will continue to loop determined by non-maxima suppression. At that point, basically draw the bounding box and content on the picture utilizing our colors in a random manner.
- 11) Finally, the picture will be shown until the client presses any key (guaranteeing the window opened by OpenCV is focused and selected).

3.1.2.OCR Algorithm:

The level of the noise in the picture ought to be improved and the zones outside the content are expelled. Preprocessing is particularly crucial for perceiving manually written reports that are progressively sensitive to noise. Preprocessing permits a character picture to yield better consequences of recognizing a picture.

3.2 Front End & Back End

One of the python's standard GUI library is Tkinter. Tk GUI toolkit is one of the object-oriented interfaces by the Tkinter. When python is combined with the Tkinter the work becomes simple and quicker to create a GUI(Graphical User Interface). The GUI and trained datasets are connected to Edge devices that produce data. These could be a sensor, industrial machines or other devices that produce or collects the data. The Edge Computing runs less number of processes in the clouds and moves those to the local places, such as the retail shop's computer, like an edge server. For building a pseudo-code Backend and GUI:

Input: Training data set (T); attributes(S).

Output: Generating Bill (B).

- 1) While true then the camera reads the given input.
- 2) If the value modulus 256 is equal to 27 the window is closed (esc=quit).
- 3) Else the image value is taken and given to training dataset (T) checks the value.
- 4) The OCR file is invoked so that it also gives the clear value of the product which is detected.
- 4) If the value is the same the defined attributes(S) are printed in the excel sheet.
- 5) The attributes are taken from the data in the Edge servers which is already stored using Edge Computing.
- 6) The bill (B) is generated by performing some mathematic functions.

4. Experimental Result

The User Interface of the proposed system is given in Figure 2. It comprises of Add to list button, Notification box, Quantity box which is should be entered physically, Capture button, View BILL button, Generate Bill button and QUIT button.

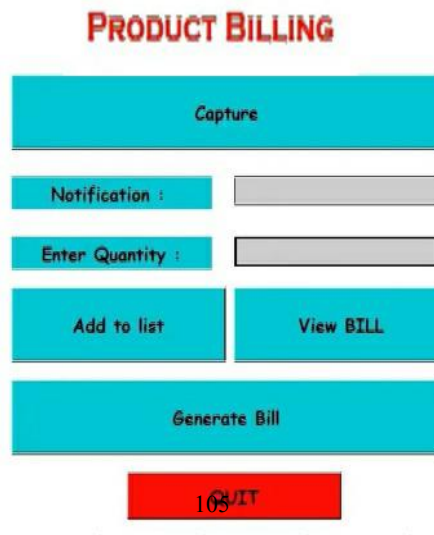


Figure 2: User Interface

The Figure 3 shows the process of capturing the product to be billed. Click the Capture button, the camera window is opened using OpenCV and the object needs to be placed in front of Camera.

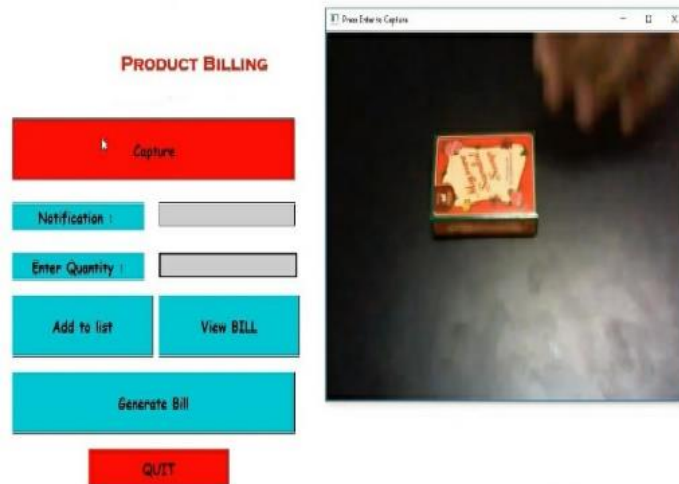


Figure 3: Capturing Product Image

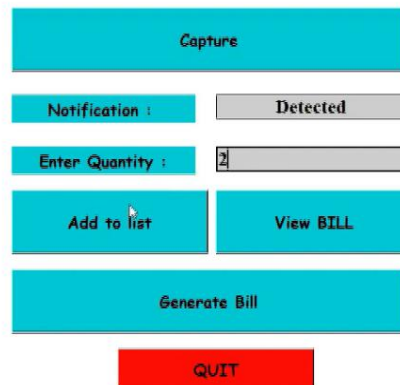


Figure 4: Adding Product to List

As soon as the item is placed in front of the camera, the camera recognizes the products with the help of size, shape and Optical Character Recognition, the notification shows “**Detected**” as shown in Figure 4. The next step is need to enter the Quantity manually and click Add to list i.e., the product which is to be billed will be added to the list.

| Name of Product | Quantity | Cost of Product | Final Cost of Product |
|-----------------|----------|-----------------|-----------------------|
|-----------------|----------|-----------------|-----------------------|

| | | | |
|--------------------|---|----|------------|
| SOAP Mysore Sandal | 2 | 10 | 20 |
| Gillette | 1 | 54 | 54 |
| Vovenac gel | 2 | 10 | 20 |
| Colgate Small | 2 | 10 | 20 |
| Colgate Large | 3 | 55 | 165 |
| FINAL COST | | | 349 |

Figure 5: Generated Bill

After billing all the products, click the View BILL button, the bill will be viewed with all the billed products with its **FINAL COST** and the bill will be generated if we click on Generate bill button as shown in Figure 5.

5. Conclusion

The task like provisioning of resources such as server, networking and hardware components which requires workers to take care of these billing systems are omitted with the use of this proposed work. There is a need to monitor and manage all those resources. All of the above tasks slow down the process of developing applications. These problems can be overcome by edge computing platforms which can be used to create a scalable, reliable, and secure and the environment with automation at every step. This helps shops to focus on creating and managing the applications rather than the provisioning and managing resource.

References

- [1] Tanmay Singh, Keshav Yadav, Ketan Kandalkar, Priya Porwal published Self-Checkout System Using Image Detection in IOSR Journal of Engineering (IOSRJEN) www.iosrjen.org ISSN (e): 2250-3021, ISSN (p): 2278-8719 Volume 14.
- [2] Appearance-based Image recognition-<https://classes.soe.ucsc.edu/cmpe264/Fall06/Lec20.pdf>.
- [3] Wu BF, Tseng WJ, Chen YS, Yao SJ, Chang PJ. An intelligent self-checkout system for smart retail. In System Science and Engineering (ICSSE), 2016 International Conference on 2016 Jul 7(pp. 1-4) IEEE.
- [3] Feature-based Image recognition-<http://www.massey.ac.nz/~rcflemme/feature-based%20object%20recognition.pdf>.
- [4] How to train YOLO-<https://timebutt.github.io/static/how-to-train-yolov2-to-detect-custom-objects>.
- [5] Redmon J, Divvala S, Girshick R, Farhadi A. You only look once: Unified, real-time object detection. In Proceedings of the IEEE conference on computer vision and pattern recognition 2016 (pp. 779-788).
- [6] Rossetti MD, Pham AT. Simulation modeling of customer checkout configurations. In Proceedings of the 2015 Winter Simulation Conference 2015 Dec 6 (pp. 1151-1162). IEEE Press.

- [7] Man KF, Tang KS, Kwong S. Genetic algorithms: concepts and applications [in engineering design]. IEEE transactions on Industrial Electronics. 1996 Oct;43(5):519-34.
- [8] Dr.Suryaprasad J, Praveen Kumar B O, Roopa D Arjun A K, “A Novel Low Cost Intelligent Shopping Cart”, Proceedings of the 2nd IEEE International Conference on Networked Embedded Systems for Enterprise Applications, NESEA 2011, Perth, Australia, December 8-9, 2011.
- [9] D.V.S Chandra Babu, “wireless intelligent billing trolley for supermarket”, International Journal of Advanced Research in Technology, vol.3, issue 1, Aug. 2012.
- [10] Raju Kumar, K. Gopalakrishna, K. Ramesha on “Intelligent Shopping Cart” in International Journal of Engineering Science and Innovative Technology (IJESIT) Volume 2, Issue 4, July 2013

Mitigation Scheme can Effectively Manage DDOS Attack in Cloud Computing / Prevention Technique of DDOS Attack in Cloud Computing

Manoj Kumar Dixit,
Assistant Professor, Department of Computer Science,
Kashi Institute of Technology
manojkumardixit@kashiit.ac.in

Abstract

Cloud computing is the modern technology within the field of data IT. It's speedily turning into a distinguished technique due to its growing and revolutionary nature in recent times. It assures to deliver a large number of resources like architecture, scalability, availability, fault tolerance, power of computation, huge storage and software application to consumers in the low cost. In other hand we have many issues with its security. This paper presents a stronger understanding of cloud computing and its security and threats, and identifies the mitigation scheme and their impact on its security.

Keywords: *Cloud Computing, Security, Mitigating Techniques, Concept Matrix*

1 Introduction

Cloud computing is the technique for delivering different resources through the internet which includes tools and applications like data storage, servers, databases, networking, and software to offer faster innovation, flexible resources at a cheap cost^[1]. In recent days the use of cloud-based computing has gained more popularity due to its application in on-line movies on demand, many social media platforms like Facebook, Twitter, Instagram, and others. Similarly, many types of threats and attacks have been obvious for cloud-based computing. Few attacks are like Distributed Denial of Service, Reflection Denial of Service, SQL Injection, and DNS amplification attack^[2].

The concept of cloud computing can be stated as demand-based services, which contribute a multitenant atmosphere towards clients. These services are used as various norms in the organization, to build competitive advantages among different organizations^[21]. Hence, this open network platform invites all types of users or clients, to be part of it to perform their tasks. Moreover, it has some dark sides which would be effect reverse on their platform. This paper would be focusing on various types of attacks, being happened on air. Furthermore, a discussion would also be focusing on important factors such as problem occurrence, and defense techniques comparison and prevention techniques as well^[22].

One of the major problems is the attack or theft of valuable information in the cloud. Among so many challenges, DDOS (Distributed Denial of service) attack is considered as high theft (manipulate) of information action. This is mainly due to the attack occupies the network bandwidth. In most of the situation, multiple nodes are used to send traffic to a site in DDOS^[20]. These types of attacks are mainly generated from the end-user system, and some available loopholes help an attacker to create an attack. On the other hand, this kind of problem can be defended and mitigate with few techniques as well.

1.1 DDOS Architecture

The DDoS attack is major trouble to the availability. The attacker can greatly degrade the quality or fully breakdown the victim's network connectivity. The attacker first compromises many agents or hosts and then uses these agents to launch the attack by depleting the target network^[33]. The main idea behind the DDoS attack is to make the victim suffer to use the resources. In most of the scenarios, targets could be web servers, CPU, Storage, and other Network resources.

The DDOS attack has become a major issue nowadays in cloud computing. The DDoS attack compromises host to send a lot of useless packets to the target in a short interval of time which can cause an outage of server operations^[11].

In the first, to compare prevention techniques of attack, we would have to focus on how attacks are originated. DDOS attack architecture shows the reasons behind the originated cause, followed the pattern, how to perform, and simulated into the network^[31]. There is main five components attacker computers, handler/ computer controller, agent/botnet, amplifying network, victim, or attached server.

Attacker/ master computer to initiates the attack and another one is the victim/Attacked server which is coming to attack by the master computer. These two components have created a denial-of-service attack. The three components in the middle one are Agent/Zombies/Botnet is to create a Denial of services of attacks are

carried out. The volunteers of computer or infected computer using internet browsing by the user, the user downloads malicious software, which is controlled by the attacker. There additional layer of handler/controlling computer which issuing command to an agent. And final components are reflecting layer which amplifies the number of requests to the attacker's server.

In this way, the attacker would generate a DDOS attack plan. There are several ways of DDOS attacks in cloud computing. For example, application later attacks, web attack, network layer attack, bandwidth depletion attack, amplification attack, protocol exploit attack (TCP SYN attack), Flood attack, and so on. On the contrary, this report will mainly focus on prevention techniques are Intrusion detection Mechanism for DDOS and Network Egress and Ingress filtering technique (NEIF)^[27]. This report will highly focus on these two techniques, its formula, effects, enhancement, and impact on architecture.

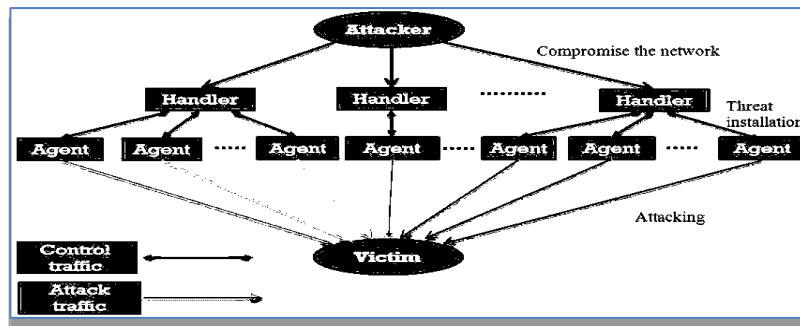


Figure 1: The architecture of a Distributed Denial of Service (DDoS) attack

2 DDOS Attack Scope

A DDoS attack is a malicious attempt to disturb an online service usually by disrupting the services of its hosting server.

The attack can be launched through many compromised devices referred to as “Botnet”. It is different from another DDoS attack where it uses a single internet-connected device to flood a target with some canny traffic.

2.1 Attack on Bandwidth

In this, a large packet of forged requests is sent to the computer using spoofing of the Internet protocol address. The reply to the request will send to the target victim such as the organization of servers. UDP/ICMP flooding attacks makes the network link congestion or overloading by sending a lot of UDP/ICMP and flooding packets [65].

2.2 Attack of Host Resource

These attacks are used to slow down the service available on the webserver. It keeps a number of connections to the victim server open and holds them for a long time and sending a large number of requests to the victims' website to disable it. By this HTTP gets the Flooding attack. In the HTTP Flooding attack, the attacker sends a large number of HTTP flood attack simultaneously from multiple computers [21].

2.3 Attack on System/Application Weakness

This ping of death can cripple network resources based on a flaw in the TCP/IP suite. If one sender has to send a packet larger than the size of bandwidth, the receiving computer would ultimately crash from confusion [16].

2.4 Attackers are primarily motivated by

Ideology – So-called “hacktivists” use DDoS attacks as a means of targeting websites they disagree with their ideologically. They can go to any extent to popularize their ideology.

Business rivalry – Businesses can use DDoS attacks to strategically take down their competitor websites.

Excitement – Cyber vandals use prewritten scripts to launch DDoS attacks. In their boredom, they attack a particular website to get some excitement.

Extortion – Attackers use DDoS attacks or the threat of DDoS attacks as a means of extorting money from victims.

Cyberwarfare – Government-backed DDoS attacks can be used to both cripple opposition websites and an enemy country's online infrastructure [67].

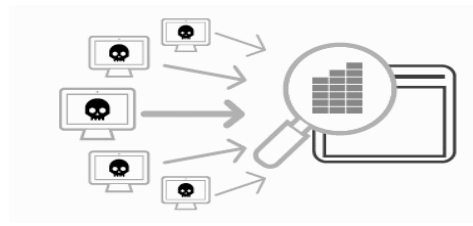


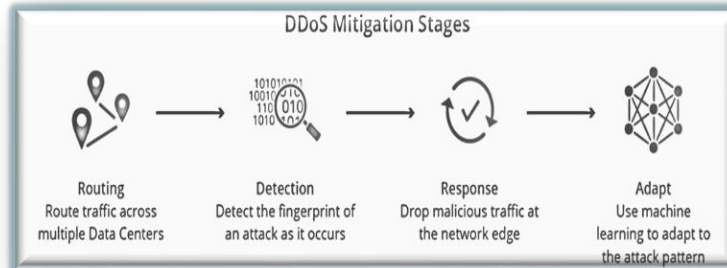
Figure 2: HTTP Flooding

| Article Authors | Challenges | | | | | | Prevention Techniques | | | | Methods | |
|--|-------------|-------------|-----------|--------------------|--------------|--------|-----------------------|----------|---------------|----------------------|-----------------|---------------|
| | HTT P Flood | IP spoofing | UDP flood | (IC MP) Ping flood | Syn Flooding | Botnet | Fir ew all | Capt cha | IP filt ering | Cook ies chall enges | Qu ant itat ive | qua litat ive |
| A Bhattacharya | ✓ | | | | | ✓ | ✓ | | | ✓ | ✓ | |
| U. Farooq ^[55] (2019) | | ✓ | ✓ | | | | | | | | | |
| D. Kirsch (2020) | | | | ✓ | ✓ | | | | | ✓ | ✓ | |
| A.Siris2007) | | | ✓ | | ✓ | | | | | ✓ | | |
| A.Abdul ^[60] (2014) | ✓ | | | | ✓ | | ✓ | ✓ | | | ✓ | |
| J. Chen (2014) | | ✓ | | ✓ | | ✓ | | | | | | |
| J. Guo(2013) | ✓ | | | | | | | | | | | |
| Christos(2018) | ✓ | ✓ | | | | | ✓ | | | | ✓ | |
| M. Villari(2014) | | | | | | ✓ | ✓ | ✓ | | | ✓ | |
| Y. Wang (2013) | ✓ | | | | ✓ | | | ✓ | | | | |
| Satyajit Yadav ^[2] (2016) | ✓ | ✓ | | | | ✓ | | | | | | ✓ |
| Nazrul ^[59] Hoque (2015) | | ✓ | | ✓ | | ✓ | | | ✓ | | | |
| Dr. P. ^[61] Varalakshm (2015) | ✓ | | ✓ | | | ✓ | | | ✓ | | | |
| Rashmi V. Deshmukha ^[65] (2015) | ✓ | | ✓ | | | | ✓ | | ✓ | | | ✓ |
| Wang Y, ^[61] Wang F (2013) | ✓ | | ✓ | | | | ✓ | | ✓ | | | ✓ |

Table 1: Concept Matrix

3 Mitigation Techniques

DDoS mitigation is the process of protecting a targeted network or server from a DDoS attack. By specially designed network equipment or cloud-based protection service, a targeted victim can mitigate the incoming attack [58].



There are 4 stages to reduce a DDoS attack.

Detection: To stop a distributed attack our server must be able to identify an attack from a high volume of normal traffic. IP Reputation, common attack patterns, and previously saved data can assist in proper detection [9].

Response: The DDoS protection network responds to an incoming identified warning by cleverly dropping malicious and absorbing the rest of the traffic. We can use the filtration process to handle low levels of warnings. By this, we can mitigate the attempt to disrupt the server.

Routing: By cleverly routing the traffic we can mitigate the DDoS attack to break the whole traffic into manageable chunks.

Adaption: The best network analyzes traffic for patterns such as repeating IP Blocks, a particular incoming attack can be avoided or we can divert an improper protocol. By adapting to attack patterns, a protection service can make it tough against attacks [11].

3.1 How Mitigation works

Bypassing, network traffic addressed to a potential target network through a high-capacity network with a different type of traffic scrubbing filters. DDoS mitigation can be effectively implemented via cloud-based solution providers. In which they can use hardware placed on-premise filtering with cloud-based filtering. It uses different tools for the purpose.

Scalability: we need an effective solution to handle DDoS attack at least 10X larger than the bandwidth.

Flexibility: We should create an ad hoc policy and pattern which allows our server to adapt to the incoming threats in real-time. We should keep the entire network online during the attack by implementing page rules and populate those changes.

Network size: We should identify the attack patterns that occur across the internet from a particular protocol over the change of time. If our network size is big enough for attack then we can respond to those attacks quickly in time and efficiently. Even we can stop such attacks before ever they occur [25].

4 Conclusion

Our dependency on cyber-physical systems and advancement in networking and cloud-based technologies have emerged with many threats that need the protection of network and computer infrastructure against DDoS attacks. Detection and mitigation of DDoS attacks have remained an unaccomplished task. Realizing this warning to our system, we have made several noticeable contributions [29].

In this regard, we have discussed major requirements and challenges in meeting this difficult task of prevention against DDoS attacks. The ease of management in the application of rules for detection and prevention against DDoS attacks is also required. Considering the emerging potential of mitigation schemes in meeting network-wide requirements of flexibility, management, scalability, and adaptability we assessed its capabilities against the prevention of DDoS attacks. We classified existing mitigation-based schemes according to various detection and prevention techniques and highlighted the pros and cons against each category. Our analysis revealed that existing solutions for DDoS detection and mitigation failed to meet application-specific requirements for DDoS detections. The existing solutions do not implement the same level of a threshold for each application. Existing solutions utilizing mitigation techniques incorporate a single controller. This not only creates a bottleneck

for the network traffic but also leads to a single point of failure for networks. Although, mitigation can incorporate a distributed platform existing solutions have realized it to its full potentials^[41].

We have addressed the problems by proposing an efficient system for DDoS attack detection through mitigation schemes. Our proposed framework incorporates application-specific criteria for network traffic threshold. This permits the implementation of customized criteria for the detection of DDoS attacks. Besides, we utilized a distributed controller platform that allows load balancing and reduces possibilities for device failure^[57].

The mitigation scheme is a major step in resolving the DDoS attacks. We anticipated that Mitigation techniques can potentially be utilized in a wide range of systems including cyber-physical systems, smart grid, and e-governance. All such applications exhibit varying degrees of tolerance for network attacks. Mitigations are required to implement consistency to the controllers to ensure the rapid implementation of rules of the network. This framework can be implemented in any cloud-based networks^[44].

As future steps of our research, we are planning to perform comprehensive experiments using mitigation schemes to study the effectiveness of our framework in protecting our applications. Lastly, Mitigation is not a silver bullet solution to all the network security problems. In this, we also highlighted open research issues, challenges, and recommendations related to mitigation schemes DDoS attack detection and prevention that require further research^[25].

References

- [1] Review clustering mechanisms of distributed denial of service attacks - Scientific Figure on ResearchGate. Available from: https://www.researchgate.net/figure/Architecture-of-Distributed-Denial-of-Service-DDoS-attack_fig1_265053091 [accessed 19 May 2020]
- [2] Geng, X.J.; Whinston, A.B.: Defeating distributed denial of service attacks. *IT Prof.* 2(4), 36–42 (2000)
- [3] Ottis, R.: Analysis of the 2007 cyber attacks against Estonia from the information warfare perspective. In: *Proceedings of the 7th European Conference on Information Warfare*, p. 163 (2008)
- [4] European renewable power grid rocked by cyber-attack. *EurActiv* (2012). <https://www.euractiv.com/section/energy/news/european-renewable-power-grid-rocked-by-cyber-attack/>
- [5] Gaffan, Marc (20 December 2012). "The 5 Essentials of DDoS Mitigation". *Wired.com*. Retrieved 25 March 2014
- [6] "Network Ingress Filtering: IP Source Address Spoofing". IETF. 2000
- [7] Leach, Sean (17 September 2013). "Four ways to defend against DDoS attacks". *Networkworld.com*. Retrieved 12 June 2018.
- [8] Musil, S.: Record-breaking DDoS attack in Europe hits 400 Gbps. *CNET* (2014). <http://www.cnet.com/news/recordbreaking-ddos-attack-in-europe-hits-400gbps/>
- [9] Saied, A.; Overill, R.E.; Radzik, T.: Detection of known and unknown DDoS attacks using artificial neural networks. *Commun. Comput. Inf. Sci.* 172, 385–393 (2016)
- [10] Hoque, N.; Bhattacharyya, D.; Kalita, J.: Botnet in DDoS attacks: trends and challenges. *IEEE Commun. Surv. Tutor.* 99, 1–1 (2015)
- [11] Arbor Networks Inc. <http://www.arbornetworks.com>
- [12] Arbor networks detects largest ever DDoS attack in Q1 2015 DDoS report. In: *Arbor Networks* (2015). <http://www.arbornetworks.com/arbor-networks-detects-largest-ever-ddosattack-in-q1-2015-ddos-report>
- [13] Jain, S.; et al.: B4: experience with a globally-deployed software defined WA. *ACM SIGCOMM Comput. Commun. Rev.* 43(4), 3–14 (2013)
- [14] Technol, I.: *Secure and Dependable SDNs*, Feb 2016 (2015)
- [15] Shalimov, A.; Zuikov, D.; Zimarina, D.; Pashkov, V.; Smeliansky, R.: Advanced study of SDN/openflow controllers. In: *Proceedings of the 9th Central & Eastern European Software Engineering Conference in Russia on - CEE-SECR '13 Oct pp.* 1–6 (2013)
- [16] Schehlmann, L.; Abt, S.; Baier, H.: Blessing or curse? Revisiting security aspects of software-defined networking. In: *Proceedings of the 10th International Conference on Network and Service Management, CNSM 2014, no. 1, pp.* 382–387 (2015)
- [17] Kreutz, D.; Ramos, F.M.V.; Verissimo, P.: Towards secure and dependable software-defined networks. In: *Proceedings of the second ACM SIGCOMM Workshop on Hot Topics in Software Defined Networking—HotSDN '13, p.* 55 (2013).
- [18] Wang, B.; Zheng, Y.; Lou, W.; Hou, Y.T.: DDoS attack protection in the era of cloud computing and software-defined networking. In: *2014 IEEE 22nd International Conference on Network Protocols, pp.* 624–629 (2014)

- [19] Thapngam, T.; Yu, S.; Zhou, W.; Beliakov, G.: Discriminating DDoS attack traffic from flash crowd through packet arrival patterns. In: 2011 IEEE Conference on Computer Communications Workshops, INFOCOM WKSHPs 2011, pp. 952–957 (2011)
- [20] Xia, W.; Wen, Y.; Member, S.; Heng Foh, C.; Niyato, D.; Xie, H.: A survey on software-defined networking. *IEEE Commun. Surv. Tutor.* 17(1), 27–51 (2015)
- [21] Liao, Q.; Li, H.; Kang, S.; Liu, C.: Application layer DDoS attack detection using cluster with label based on sparse vector decomposition and rhythm matching. *Secur. Commun. Netw.* 8(17), 3111–3120 (2015)
- [22] Stewart, J.M.: *Network Security, Firewalls and VPNs*. Jones & Bartlett Publishers (2013)
- [23] DDoS: website-crippling cyber-attacks to rise in 2016. BBC News. <http://www.bbc.com/news/technology-35376327>
- [24] Q1 2016 Global DDoS Threat Landscape Report. Incapsula. <https://www.incapsula.com/blog/q1-2016-global-ddos-threatlandscape-report.html>
- [25] Bawany, N.Z.; Shamsi, J.A.: Application layer DDoS attack defense framework for smart city using SDN. In: *Computer Science, Computer Engineering, and Social Media (CSCESM)* (2016)
- [26] Kreutz, D.; Ramos, F.M.V.; Verissimo, P.; Rothenberg, C.E.; Azodolmolky, S.; Uhlig, S.: Software-defined networking: a comprehensive survey. *Proc. IEEE* 103(1), 14–76 (2015)
- [27] Khondoker, R.; Zaalouk, A.; Marx, R.; Bayarou, K.: Featurebased comparison and selection of Software Defined Networking (SDN) controllers. In: *2014 World Congress on Computer Applications and Information Systems (WCCAIS)*, pp. 1–7. IEEE (2014)
- [28] Berde, P.; Gerola, M.; Hart, J.; Higuchi, Y.; Kobayashi, M.; Koide, T.; Lantz, B.; Snow, W.; Parulkar, G.; O’Connor, B.; Radoslavov, P.: ONOS. In: *Proceedings of the third workshop on Hot topics in software defined networking—HotSDN ’14*, pp. 1–6 (2014)
- [29] Linux Foundation. <http://www.opendaylight.org>
- [30] McKeown, N.; Anderson, T.; Balakrishnan, H.; Parulkar, G.; Peterson, L.; Rexford, J.; Shenker, S.; Turner, J.: OpenFlow: enabling innovation in campus networks. *ACM SIGCOMM Comput. Commun. Rev.* 38(2), 69–74 (2008)
- [31] Coughlin, M.: A survey of SDN security research. In: *Future Networks and Services (SDN4FNS)*, IEEE (2013)
- [32] Kim, J.; Firoozjahi, M.D.; Jeong, J.P.; Kim, H.; Park, J.-S.: SDN-based security services using interface to network security functions. In: *2015 International Conference on Information and Communication Technology Convergence (ICTC)*, pp. 526–529. IEEE (2015)
- [33] Yan, Q.; Yu, F.R.: Distributed denial of service attacks in softwaredefined networking with cloud computing. *IEEE Commun. Mag.* 53(4), 52–59 (2015)
- [34] Giotis, K.; Argyropoulos, C.; Androulidakis, G.; Kalogeras, D.; Maglaris, V.: Combining OpenFlow and sFlow for an effective and scalable anomaly detection and mitigation mechanism on SDN environments. *Comput. Netw.* 62, 122–136 (2014)
- [35] Lee, W.; Xiang, D.: Information-theoretic measures for anomaly detection. In: *Proceedings of the 2001 IEEE Symposium on Security and Privacy, S&P 2001*, pp. 130–143. IEEE (2001)
- [36] Gu, Y.; McCallum, A.; Towsley, D.: Detecting anomalies in network traffic using maximum entropy estimation. In: *Proceedings of the 5th ACM SIGCOMM conference on Internet Measurement*, p. 32. USENIX Association (2005)
- [37] Bereziński, P.; Szpyrka, M.; Jasiul, B.; Mazur, M.: Network anomaly detection using parameterized entropy. In: *Computer Information Systems and Industrial Management*. Springer, Berlin (2014)
- [38] Nychis, G.; Sekar, V.; Andersen, D.G.; Kim, H.; Zhang, H.: An empirical evaluation of entropy-based traffic anomaly detection. In: *Proceedings of the 8th ACM SIGCOMM Conference on Internet Measurement Conference-IMC ’08*, p. 151 (2008)
- [39] Brauckhoff, D.; Tellenbach, B.; Wagner, A.; May, M.; Lakhina, A.: Impact of packet sampling on anomaly detection metrics. In: *Proceedings of the 6th ACM SIGCOMM conference on Internet measurement*, pp. 159–164 (2006)
- [40] Androulidakis, G.; Chatzigiannakis, V.; Papavassiliou, S.: Network anomaly detection and classification via opportunistic sampling. *IEEE Netw.* 23(1), 6–12 (2009)
- [41] Wang, R.; Jia, Z.; Ju, L.: An entropy-based distributed DDoS detection mechanism in software-defined networking. In: *2015 IEEE Trustcom/BigDataSE/ISPA*, pp. 310–317 (2015)
- [42] Mehdi, S.,A.,S.; Khalid, J.; Khayam, S.,A.,S.: Revisiting traffic anomaly detection using software defined networking. In: *Proceedings of the 14th International Conference on Recent Advances in Intrusion Detection*, pp. 161–180 (2011)
- [43] Lakhina, A.; Crovella, M.; Diot, C.: Mining anomalies using traffic feature distributions. *ACM SIGCOMM Comput. Commun. Rev.* 35(4), 217 (2005)
- [44] sflow. <http://www.sflow.com>

- [45] Fiadino, P.; Alconzo, A.,D.; Schiavone, M.; Casas, P.: Challenging entropy-based anomaly detection and diagnosis in cellular networks. In: Proceedings of the 2015 ACM Conference on Special Interest Group on Data Communication (2015)

Short Text Sentiment Classification with Word Embeddings using LSTM Approach-A Survey

¹M.Rajalakshmi, ²Dr.A.SenthilKumar

¹Ph.D. Research Scholar, Department of Computer Science
Sankara College of Science and Commerce, Coimbatore
mail2rajiravi@gmail.com

²Associate Professor, Department of Computer Science
Sankara College of Science and Commerce, Coimbatore
senthask@gmail.com

Abstract

Slant order procedures have been broadly utilized for investigating client feelings. In traditional regulated learning strategies, hand-created highlights are required, which requires a careful comprehension of the area. Since online media posts are normally exceptionally short, there's an absence of highlights for compelling grouping. Accordingly, word installing models can be utilized to learn distinctive word uses in different settings. To recognize the conclusion extremity from short messages, we need to investigate further semantics of words utilizing profound learning strategies. In this paper, we explore the impacts of word inserting and long transient memory (LSTM) for assessment arrangement in web-based media. To start with, words in posts are changed over into vectors utilizing word inserting models. At that point, the word arrangement in sentences are contribution to LSTM to gain proficiency with the significant distance context oriented reliance among words. The exploratory outcomes indicated that profound learning techniques can successfully become familiar with the word use in setting of online media given enough preparing information. The amount and nature of preparing information significantly influences the exhibition. Further examination is expected to check the exhibition in various online media sources.

Keywords: *Sentiment Classification, Deep Learning, Long Short-Term Memory, Word2Vec Model.*

1 Introduction

Assumption grouping has been utilized in investigating client created substance for understanding clients' purpose and assessments in web-based media. Customary regulated learning techniques have been broadly researched, for example, sack of-words model utilizing TF-IDF, and probabilistic model utilizing Naïve Bayes, which for the most part need hand-made highlights. For web-based media content which are short and assorted in subject, it's hard to acquire valuable highlights for arrangement. In this manner, a more powerful strategy for short content assessment arrangement is required. Profound learning strategies have continuously demonstrated great execution in numerous applications, for example, discourse acknowledgment, design acknowledgment, and information grouping.

These techniques attempt to learn information portrayal utilizing a more profound chain of command of designs in neural organizations. Muddled ideas are conceivable to learn dependent on less difficult ones. Among profound feedforward networks, Convolutional Neural Networks (CNNs) have been appeared to take in neighborhood highlights from words or expressions [1], while Recurrent Neural Networks (RNNs) can learn transient conditions in successive information [2]. Given the short messages in online media, there's an absence of highlights. To get more helpful highlights, we further use circulated portrayal of words where each info is addressed by numerous highlights and each element is engaged with numerous potential information sources. In particular, we utilize the Word2Vec word inserting model [3] for circulated portrayal of Social posts.

In this paper, we need to research the adequacy of long transient memory (LSTM) [4] for assumption arrangement of short messages with disseminated portrayal in online media. Initial, a word inserting model dependent on Word2Vec is utilized to address words in short messages as vectors. Second, LSTM is utilized for learning significant distance reliance between word arrangement in short messages. The last yield from the last purpose of time is utilized as the expectation result. In our examinations of supposition grouping on a few social datasets, we contrasted the presentation of LSTM and Naïve Bayes (NB) and Extreme Learning Machine (ELM). As the exploratory outcomes show, our proposed strategy can accomplish preferable execution over customary probabilistic model and neural organizations with additionally preparing information. This shows the capability of utilizing profound learning strategies for notion investigation.

Further examination is expected to confirm the viability of the proposed approach in bigger scope. The rest of this paper is coordinated as follows: Sec. 2 records the connected works, and Sec. 3 portrays the proposed strategy. The exploratory outcomes are depicted in Sec. 4. Furthermore, a few conversations of the outcomes are summed up in Sec.5. At long last, Sec. 6 records the ends.

2 Related Work

Fake neural organization is an organization structure propelled by neurons in human minds. Hubs are coordinated into layers, and hubs in adjoining layers are associated by edges. Calculations are done in a feed-forward way, and blunders can be back-engendered to past layers to change the loads of comparing edges. Outrageous Learning Machines (ELMs) [5] are a unique kind of neural organizations where the loads are not changed by back spread. The concealed hubs are haphazardly doled out and never refreshed. In this manner, the loads are normally educated in one single step, which is generally a lot quicker.

For more intricate relations, profound learning strategies are received, which use various concealed layers. With more profound organization structures, it as a rule requires some investment. These strategies were made possible gratitude to the new advances of figuring powers in equipment, and the GPU handling in programming advances. Contingent upon the various methods of organizing different layers, a few sorts of profound neural organizations were proposed, where CNNs and RNNs are among the most well known ones. CNNs are normally utilized in PC vision since convolution activities can be normally applied in edge recognition and picture honing. They are likewise valuable in computing weighted moving midpoints, and figuring drive reaction from signals. RNNs are a sort of neural organizations where the contributions of shrouded layers in the current purpose of time rely upon the past yields of concealed layer. This makes them conceivable to manage a period grouping with fleeting relations, for example, discourse acknowledgment. As indicated by past relative investigation of RNN and CNN in characteristic language handling [6], RNNs are discovered to be more powerful in slant examination than CNNs.

Accordingly, we center around RNNs in this paper. As the time succession fills in RNNs, it's feasible for loads to develop out of hand or to evaporate. To manage the evaporating inclination issue [7] in preparing regular RNNs, Long Short-Term Memory (LSTM) [4] was proposed to learn long haul reliance among longer time span. Notwithstanding information and yield doors, fail to remember entryways are included LSTM. They are frequently utilized for time arrangement forecast, and hand-composing acknowledgment. In this paper, we use LSTM in learning opinion classifiers of short messages. For common language preparing, it's helpful to investigate the distributional relations of word events in archives. The least difficult path is to utilize one-hot encoding to address the event of each word in reports as a parallel vector. In distributional semantics, word implanting models are utilized to plan from the one-hot vector space to a constant vector space in a much lower measurement than regular sack of-words model. Among different word implanting models, the most famous ones are dispersed portrayal of words, for example, Word2Vec [3] and GloVe [8], where neural organizations are utilized to prepare the event relations among words and reports with regards to preparing information. In this paper, we embrace the Word2Vec word installing model to address words in short messages. At that point, LSTM classifiers are prepared to catch the drawn out reliance among words in short messages. The assessment of every content would then be able to be named positive or negative.

3 The Proposed Method

3.1 Preprocessing and Feature Extraction

In the first place, short messages are gathered with specially crafted crawlers for various web-based media. At that point, preprocessing errands are expected to cleanup post substance. For instance, URL joins, hashtags, and emojis are separated. Additionally, stopword expulsion is performed to zero in on substance words. For Chinese posts, we utilized Jieba for word division. At that point, we extricate metadata, for example, banner ID, posting time, and the quantity of retweets and preferences. These will be utilized as extra highlights for order.

3.2 Word Embedding

In sack of-words model, it's extremely high dimensional, and there's an absence of context oriented relations between words. To all the more likely address the restricted substance in short messages, we use Word2Vec word implanting model [3] to gain proficiency with the relevant relations among words in preparing information. Likewise, the fixed number of measurements in word implanting model can encourage more productive calculations. There are two general models in Word2Vec, Continuous Bag-of-Words (CBOW) and Skip-gram. Since much better execution for skip-gram model in semantic examination can be acquired

[3], we use word vectors prepared by means of Word2Vec Skip-gram model as the contributions to the accompanying phase of order.

4 Long Short-Term Memory (LSTM)

After representing each word by its corresponding vector trained by Word2Vec model, the sequence of words $\{T_1, \dots, T_n\}$ are input to LSTM one by one in a sequence, as shown in Fig.1

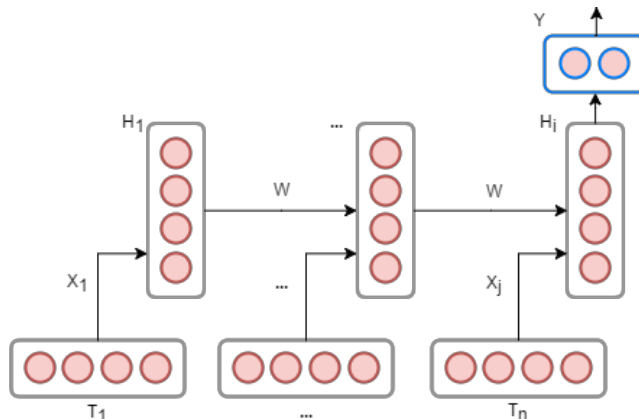


Figure 1: The idea of LSTM

In Fig.1, each term T_i is first converted to the corresponding input vector x_i using Word2Vec model and input into LSTM one by one. At each time j , the output W of the hidden layer H_j will be propagated back to the hidden layer together with the next input x_{j+1} at the next point of time $j+1$. Finally, the last output W_n are going to be fed to the output layer.

To suits the sequential input of LSTM, we first convert posts into three-dimensional matrix $M(X, Y, Z)$, where X is that the dimension of Word2Vec word embedding model, Y is the number of words within the post, and Z is that the number of posts. To avoid the very long training time, we adopt one hidden-layer neural network. The number of neurons in input layer is the same as the dimension of Word2Vec model, and the number of neurons in output layer is the number of classes, which is 2 in this case. By gradient-based back transmission from beginning to end time, we can adjust the weight of limits in out of sight layer at each position of time. After several epochs of coaching, we will obtain the sentiment classification model.

5 Sentiment Classification

5.1. Sentiment Classification Techniques

It's hard for machines to know human language, and more so when identifying complex human experiences like tone, attitudes, and emotion. Natural Language Processing (NLP) aims to unravel this problem by using linguistics and computing to rework text into something that computers can understand. By applying a spread of NLP techniques – like tokenization, lemmatization, dependency parsing, word meaning disambiguation, and bag-of-words to research the syntactic and semantic aspects of a text, classifiers are able on the way to method natural language data to realize emotions like annoy, anxiety, delight, and dissatisfaction. While some NLP models are more emotionally intelligent than others, sentiment classification systems generally use one among three algorithms:

- Rule-Based Systems
- Automated Systems (Based on Machine Learning)
- Hybrid Systems

5.2 Rule-Based Systems

This approach applies a series of hand-crafted rules to decide a pattern for every tag. For sentiment classification harms, rule-based systems rely on a glossary, which is a list of positive terms (like good quality, attractive, helpful, motivating, etc) and negative terms (such as bad, ugly, uncomfortable, frustrated, etc). When fed a bit of text, the model counts the quantity of positive and negative words that appear, and assigns the corresponding sentiment. If a turn of phrase contain more enriching than harmful words, it's tagged as

Positive. However, this approach has some limitations. It can't recognize words that don't appear surrounded by the lexicon, and separates words from their context units making it difficult to spot polysemy, sarcasm, and irony.

5.3 Automated Systems (Based on Machine Learning)

Automated system uses mechanism erudition algorithms that learn to calculate sentiment from past observations. For this AI approach, you would like an example dataset (similar to the info you'd wish to analyze) the length of side their corresponding tags. This is called training data. During the instruction process, the mock-up transforms text data into vectors (an collection of numbers with prearranged in sequence, principally, impressive that equipment can recognize) and identify a outline to associate each vector with one among the pre-defined tags ("Positive", "Negative", "Neutral"). After being fed an reasonably priced amount of relevant data, automated systems can start making their own predictions to classify unseen data. You can easily improve accuracy of folks models by providing more tagged examples.

5.4 Hybrid Systems

Hybrid systems merge together rule-based and machine learning-based approach. First, the form learns to notice sentiment from a series of tag example. Then, it compares the outcome with a lexicon to recover precision. The goal is on the way to get the simplest possible outcome, with none of the boundaries of each individual approach.

5.5 Applications of Sentiment Classification

Through sentiment classification, we resolve understand opinions on an huge scale. This can have many applications for businesses, similar to finding insights in customer feedback, keeping an gaze at fixed on brand reputation, and spotting marketing trends and opportunities.

5.6 Customer Feedback

Sentiment classification can help you insert up of customer feedback, and allow you to advise actionable insights from survey responses, product reviews, and customer support interactions. Analyzing sentiment in open-ended NPS responses can shed light on the explanation behind customers' quantitative scores, as well as on specific aspects of your business that require more attention. If the mainly complaint among your detractors is that customer support teams are slow to respond, for occurrence, you'll effort to automate a measurement of your customer service.

5.7 Social Media Monitoring

Companies use different metrics to watch user engagement and keep track of social media mentions. Sentiment classification allows you to travel beyond the numbers and find out how customers are talking about your brand, also as boost customer loyalty and brand value by replying swiftly and effectively to every customer.

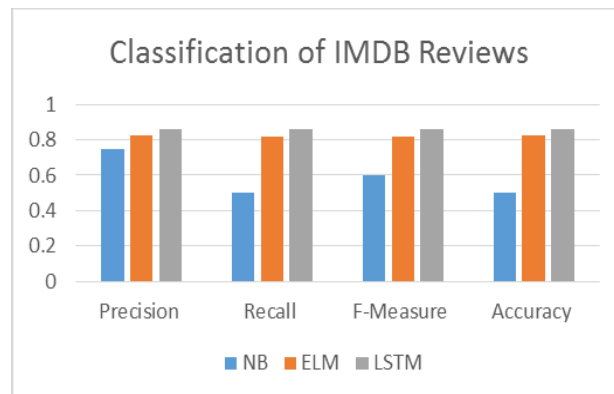
Analyze sentiment crossways social media platform can help you detect pessimistic and critical comments in immediate, so you can acquire achievement before they turn into a better problem. Imagine you received a bunch of responses during a similar vein to the present one, below. You'd want to detect them directly, and respond effectively and empathetically.

6 Experiments

In order to evaluate the performance of our proposed approach, we conducted three different experiments. First, we used English movie reviews from IMDB. Second, we experienced Chinese movie analysis annotations from Douban. Finally, we evaluated the performance for Chinese posts inside the PTT discussion forum.

In the primary dataset, there are 50,000 evaluation comments in IMDB Large Movie evaluation Dataset [9], where 25,000 were used as preparation and 25,000 as analysis data. To avoid influence from previous comments of the same movie, we collected no more than 30 reviews for each movie. The ranking of each movie was used as the position truth, where a rating above 7 as constructive, and a rating below 4 as pessimistic.

In the second dataset, we collected top 200 movies for each of the 10 categories in Douban Movies. The top 40 to 60 review comments were extracted from each movie according to their popularity. The ground truth of this dataset was set as follows: a rating of 1-2 as negative, and a rating of 4-5 as positive. The comments with a rating of 3 or no ratings are ignored. After removing these comments, there are 12,000 comments where 6,000 were used as training and 6,000 as test data. In the third dataset for the most popular social media platform PTT in Taiwan, we collected 3,500 posts during Aug. 31 and Sep. 1, 2015 and the corresponding 34,488 comments as the training data, and 1,000 posts during Sep. 2 and Sep. 3, 2015 and the



6,825 comments as the test data. The user ratings of like/dislike are used as the ground truth of this dataset. To evaluate the classification performance, standard evaluation metrics of precision, recall, F measure, and accuracy were used to compare three classifiers: Naïve Bayes (NB), Extreme Learning Machine (ELM), and Long Short-Term Memory (LSTM). Word2Vec model is applied for all three classifiers.

Figure 2: The performance comparison of three classifiers for IMDB reviews

For the first dataset of IMDB movie reviews, the performance comparison among three classifiers are shown in Fig.2. As shown in Fig.1, the best performance can be achieved for LSTM with a F-measure of 0.859. We can see the consistently better performance for LSTM than NB and ELM. Naïve Bayes is the worst due to its high false positive rates. This shows the better performance for neural network methods, especially for deep learning methods. Next, the performance for more casual comments in Douban Movies is shown in Fig.3

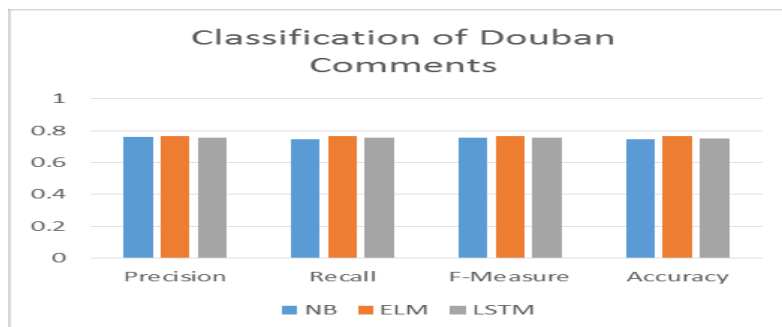


Figure 3: The performance comparison of classification for Douban comments

They are more difficult to classify than longer reviews in IMDB. To further evaluate the effects of training data size on the performance, we include more training data from 6,000 reviews to 10,000 and 20,000 in the next experiment. The test data size remains unchanged. The results are shown in Fig.3

As shown in Fig.2, the performance of all three classifiers are comparable with slight differences. The best performance can be achieved for ELM with a F-measure of 0.765, while LSTM obtained a comparable F-measure of 0.754. Since the comments are less formal and shorter in lengths, they are more difficult to classify than longer reviews in IMDB. To further evaluate the effects of training data size on the performance, we include more training data from 6,000 reviews to 10,000 and 20,000 in the next experiment. The test data size remains unchanged. The results are shown in Fig.3

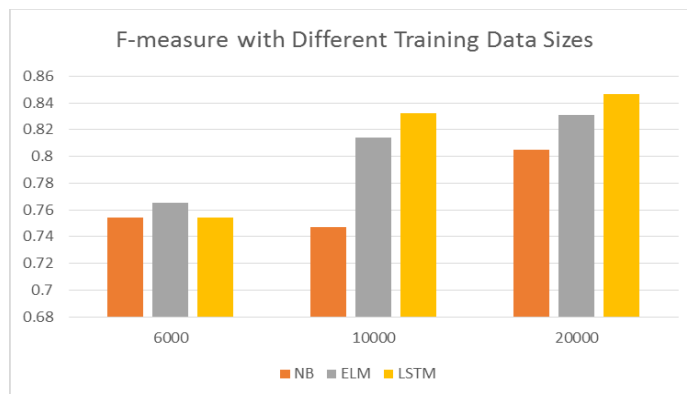


Figure 4: The effects of training data size on classification performance

As shown in Fig.4, as the training data size grows, the classification performance improves for all classifiers except for Naïve Bayes at 10,000. The best performance can be achieved for LSTM with a F-measure of 0.847 when training data size reaches 20,000. Next, the performance of three classifiers on PTT posts are shown in Fig.4.

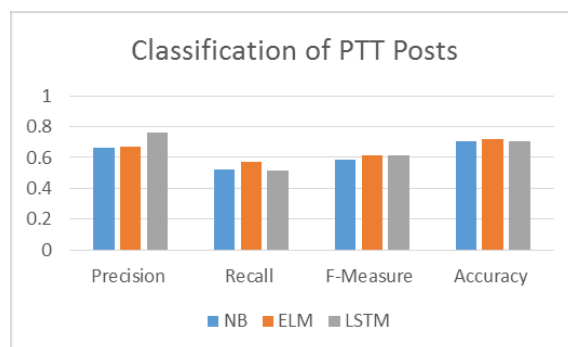


Figure 5: The performance comparison of classification for PTT posts

As shown in Fig.5, the best performance can be achieved for ELM with a F-measure of 0.615, and LSTM with a comparable F-measure of 0.613. LSTM got a higher precision but lower recall for negative posts. The reason is due to the mismatches between user ratings and the sentiment polarity of the corresponding user comments. Users often marks their ratings as “likes” for the posts they agree with, but express their strong negative opinions in their comments. This disagreement is more common in the online forum PTT due to the special characteristics in the community. The impact of this special behavior is larger for LSTM than the other two classifiers.

Discussions

From the exploratory outcomes, a few perceptions about the proposed approach are appeared as follows. To begin with, utilizing word installing models, the opinions of short messages can be viably grouped. Second, contingent upon various sorts of web-based media, the exhibition may shift. The arrangement execution is preferable for film audits over easygoing remarks and posts in online discussions. Yet, the presentation of LSTM is as yet tantamount to ELM and NB. This shows the possibility of a LSTM-based way to deal with short-text supposition arrangement. Third, information size can likewise influence the arrangement execution. All the more preparing information can prompt better execution. At long last, unique qualities in certain online discussions may prompt sub-par characterization execution. This conduct befuddle between client assessments in remarks and client appraisals mirrors the wry language utilized among the local area in PTT online discussion. To deal with this special characteristic, we need more training data to train "people group"- explicit estimation dictionary to mirror the online practices of web-based media local area

7 Conclusion

In this paper, we have proposed an opinion order approach dependent on LSTM for short messages in web-based media. Utilizing word embeddings, for example, Word2Vec model, it's doable to prepare the context oriented semantics of words in short messages. Likewise, profound learning strategies, for example, LSTM show better execution of notion arrangement when there are more measures of preparing information. For uncommon local area practices, further examinations utilizing "local area"- explicit conclusion vocabulary and bigger information sizes are required in future.

References

- [1] Y. Kim, "Convolutional Neural Networks for Sentence Classification," Proceedings of the 2014 Conference on Empirical Methods in Natural Language Processing (EMNLP 2014), pp. 1746–1751, 2014.
- [2] J. L. Elman, "Finding Structure in Time," *Cognitive Science*, Vol. 14, No.2, pp. 179-211, 1990.
- [3] T. Mikolov, K. Chen, G. Corrado, and J. Dean, "Efficient Estimation of Word Representations in Vector Space," Proceedings of the International Conference on Learning Representations 2013 Workshop.
- [4] S. Hochreiter and J. Schmidhuber, "Long Short-Term Memory," *Journal of Neural Computation*, Vol. 9 No. 8, pp. 1735-1780, 1997.
- [5] G. B. Huang, Q. Y. Zhu, and C. K. Siew, "Extreme Learning Machine: Theory and Applications," *Neurocomputing*, 70 (1): 489–501, 2006.
- [6] W. Yin, K. Kann, M. Yu, and H. Schütze, "Comparative Study of CNN and RNN for Natural Language Processing," *Computing Research Repository (CoRR)*, vol. abs/1702.01923, 2017.
- [7] S. Hochreiter, Y. Bengio, P. Frasconi, and J. Schmidhuber, "Gradient Flow in Recurrent Nets: the Difficulty of Learning Long-Term Dependencies," In S. C. Kremer and J. F. Kolen, editors, *A Field Guide to Dynamical Recurrent Neural Networks*. IEEE Press, 2001.
- [8] J. Pennington, R. Socher, and C. D. Manning, "GloVe: Global Vectors for Word Representation," Proceedings of the 2014 Conference on Empirical Methods in Natural Language Processing (EMNLP 2014), pp. 1532–1543, 2014.
- [9] L. Maas, R. E. Daly, P. T. Pham, D. Huang, A. Y. Ng, and C. Potts, "Learning Word Vectors for Sentiment Analysis," Proceedings of the 49th Annual Meeting of the Association for Computational Linguistics: Human Language Technologies (HLT 2011), pp. 142-150, 2011.

Adoption of WhatsApp and Telegram in India

Dr.S.Karunkaran¹, M.Santhiya², E.Harsiny³, B.Moviga⁴, T.M.Nivedhitha⁵
¹Associate Professor, ²Assistant Professor, ^{3,4,5}Third Year Information Systems
 Department of Computer Technology-UG
 Kongu Engineering College, Perundurai, India

Abstract

Social media has become a vital source of communication worldwide from human-to-human, human-to-machine, machine-to-machine and machine-to-human. Different forms of these communications have a variety of quality parameters and they are used in various application scenarios. Earlier started as a text exchange medium now has support for all forms of digital media. Race in computing speed and communication bandwidth leverage the growth of the social media. Particularly in India the revolution started when Orkut entered the market in 2007. Even though there was constraint in latest hardware technology and network bandwidth in India, the huge market place it has attracted developers to tune their applications for the available technological resources here. Today there are quite a good number of social media competitors in India. Features offered to customers by these social media vary in spite of their growth. People have different choices to use with. This article analyzes the penetration performance of WhatsApp and Telegram in India. The focus is to create technology awareness among the users of these two competitors.

Keywords: Social Media, MAU, Telegram, WhatsApp, Orkut, Digital Technologies Section Heading

1 Introduction

Growth of social media in India has a long history. It's not been easy task for the players to enter Indian market strongly and quickly. Difficult customer base, cultural values of the people, economical constraints and technological feasibility determine the entry nature in India. On entry business people make use of it to explore their customer base quickly and efficiently. Later, social media has become an undetectable part of life for everyone. Academic, science, researchers, industrialists, doctors, lawyers use social media for instant communication [1]. People use it for their personal and official communication. Nature of data exchange depends on the application scenario. In academic side, faculties communicate course details with their students. They can use it for assignments and testing course knowledge of students. In health sector, patients can check the availability of the medical prescription and even booking for consultation of doctors. Business people use social media as a important tool to find and maintain customer base. They can share with customer's product catalog, maintenance schedule and service solutions. Use it to convey their well wishers during personal and religious ceremonies. They also exchange multimedia content in the form of photos, videos and animation.

The entry of digital Technologies dramatically changed the pattern of Communication of common people. Different class of people expects varied convenience in communication. Connecting to your telephone exchange and making trunk phone call through landline phone was a revolutionary implementation one day. But soon technological advancements enable people to connect any phone number all over the world instantly without trunk booking. This gives much convenience for the customers. By today you can text, call and transmit images and videos all on a mobile handheld device. Communication now has become quicker, cheaper and smarter.

People's preference over communication is a matter of feel. Somebody likes to text any matter, somebody likes voice communication, while others go for instant chatting. Usually email and SMS are the preferred mode of text communication and social media way of communication was ideal for instant chatting. Landline devices and mobile phones are the tools for voice communication. Smart mobile devices enhance the communication by offering video calls.

Growth in network Technologies and fall in data rate among the service providers boost this provision. QoS requirement from communication sources also vary from domain to domain. Businessman like the information to be conveyed faster in both directions either B2C or C2B. Normal household people want the communication to be cheaper. Switching the service provider is not a big concern for people while this may reduce the reputation for business concern. People in gaming art movie and media may worry on quality of communication.

The worldwide competition for messaging superior looks like an uneven contest. WhatsApp with 1.6 billion Monthly Active Use [MAU] base seem to be unreachable for alternates like Telegram and signal.

2 Expansion of Telegram in India

Telegram with 200 billion global users with its encrypted service becomes patronized by journalist, government and public officials is now obtaining a big following in India. Because of the volume of the people that too mostly young generation, India was the top target for the service providers. Democracy, support for national-wide English

as a communication language, government policies, literacy rate, technology adoption, existing infrastructure are big support for the players to land here. Telegram seen 65 % improvement in user account in the year 2019.

| | December 2018 | March 2019 | June 2019 | September 2019 |
|---------------------------|---------------|------------|-----------|----------------|
| Monthly active users (cr) | 1.8 | 2.2 | 2.5 | 2.9 |
| Install penetration (%) | 6.9 | 8.8 | 10.3 | 11.5 |
| Monthly downloads (lakh) | 28.5 | 54.7 | 64.5 | 91.2 |

Figure 1: Telegram MAU Improvement

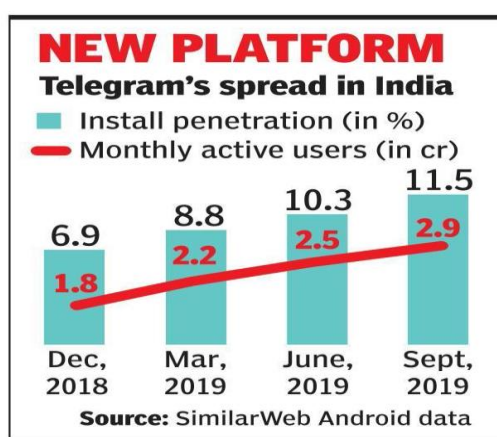


Figure 2: Telegram Spread in India

As a growth vision, Government of India promoting new startup companies in all the segments of business. These startups and other entry level small organizations use messaging app for effective marketing and customer engagement. Knowing the customer interests and predicting their purchase pattern are vital for the business growth.

Telegram unique program interface [API], inbuilt BOT future helps to engage with customers and analyze information. Business people prefer Telegram, because it carries pictures of WhatsApp in addition to security, privacy and accessibility. The ability to access among multiple devices without any added restriction on group size and file sizes are also a huge sales point [2].

For big organizations let it be industry or academic, connectivity to all its members with a single message group is preferable. Maintaining so many groups possess administrative challenges along with possibility of missing out certain important communications. Since, WhatsApp is restricting the number of group users to 500, professional organizations like Telegram as a better option in long term vision.

3 Telegram for Business Growth

'Halapay' a well-known sports platform, make Telegram services as a influencer board. The independence to have infinite members on the app's broadcasting functions boost the company's reach. To quote an example in the past couple of years, single influencer using Telegram brought in about 40000 people to the fantasy platform.

Candidates in India preparing for public and private competitive examinations needs scalability in group size, effective file sharing, privacy. This enables 'Edtech' education Technology sector in India as a big adaptor of telegram.

Engagement of young professionals between the age of 25 to 35 on Telegram was much focused and thus it directed traffic towards them. Especially for business startups, Telegram aids to create brand image and broadcast their offerings. With 7 Telegram groups 'Edurekas' channel provide recent updates on modern technologies.

‘Vedantu’ a Telegram based online mentoring platform interact with students lively by communicating session timings and solve problems raised by users nearly about 200 users online per hour with good level of involvement and interaction.

People in Tier- 1 towns can afford expensive technology platform. But in and around Tier-2 and Tier-3 towns, still competitive civil service examinations coaching for people was constrained by social and economical burden. **‘Oliveboard’** organization take this as an opportunity to keep UPSC toppers active in Telegram and make them away from Facebook and WhatsApp.

‘Pick Your Trail’ Chennai based travel technology feels the flexibility of Telegram open source application helps them to pull data analytics of customer and to enrich quality of engagement. Their customers like a separate platform instead of clubbing their social interaction using WhatsApp. Their Telegram group visualize engagement of 500 odd customers a month. This count rises during vacation period.

Telegram encrypted services boost crypto-currency and block chain community. **‘OKEx’** a crypto-currency exchange chooses Telegram, since it attains more Crypto specific community members, when compared to other messengers. Compared to Twitter and Facebook, Telegram was good in instant communication and group interactions [3].

Telegram Top ranks among users to worry about privacy and security. It uses MTProto encryption protocol to scramble and mask messages during transmission. Telegram channels can support countless members, allow up to 1GB data transfers, super groups with 1,00,000 users while mask their identity. **‘Patel wealth Advisors’** share stock market tips to its 1.7 lakh subscribers using single Telegram channel.

But at the other side of the coin raises few issues. Telegram’s channel facility offers seamless convenient to user. But this feature creates piracy issue especially with entertainment and education content. Entry of telegram posed a big threat to book publishers and other content companies. Data analytics confirm this by number of subscriber base in its Hollywood movies channel.

Telegram’s secret chat facility enable pure private chat, whereby deleting the messages immediately from devices and leaves no trails of it. This feature raises security concerns, since it may be tried for hateful propagations.

4 Telegram Vs. Whatsapp

The main concern about the usage of Whatsapp is its lower encryption quality when compared with Telegram [4]. There are many features between these two-messaging platforms. The elaborative feature comparison is shown in the following section.

4.1 Storage

In Telegram, the storage medium is based on the cloud. It allows unlimited amount of photos, videos and files to transfer. The file format may be docs, mp3 and zip. A total of 1.5 GB of data can be shared. It uses the cloud to store and does not use the phone storage. The infrastructure is multi-datacenter. In Telegram, 10,000 people can join a group and it offer support for Chatbots. Chatbot is referred to a computer program which is defined to simulate conversation with human users over the internet.

In Whatsapp, the storage medium used is phone storage and it has a limitation of phone memory. All file formats like zip, docs and mp3 can be shared. It allows only 256 people to join a group and it is yet to introduce Chabot. The maximum file size that can be shared in Android is 100 MB, IOS is 128 MB, Windows is 104.86 MB and for web it is 64 MB. Compression can be ignored in the latest updates.

4.2 File Sharing

Telegram allows sending all kinds of files in all formats with HD quality of compressed photos. HD movies can be shared using Telegram. Whatsapp limits us to send 160 MB of files and 17 MB of videos to others. All kinds of files cannot be shared in Whatsapp. Original quality of photos gets pixelated in Whatsapp [5].

4.3 Texting

According to comparison of Whatsapp and Telegram, texting has three features: draft, message editing, unsend your message. Telegram has a new feature called draft. This allows you to save the message. Telegram allows you to edit message which was sent whereas Whatsapp does not include these two features. Whatsapp allows you to unsend the message in limited time period but the receiver knows that the message was unsend, in Telegram, you can delete a message whenever you want and there is no limited time period, the receiver does not know about it [6].

4.4 Privacy

In Whatsapp, The chatting is done by using one’s phone number. It’s difficult for one to share his/her phone number to a newly met person. But in Telegram, there is no need of exchanging phone number, instead of phone

number one can share his/her Telegram username to chat. So that the phone number will not be shown. Telegram allows you to set different password apart from the phone [7].

4.5 Groups

In Telegram, one lakh people can join a group whereas Whatsapp allows only 256 people to join a group. Telegram has a key feature such as voting for a pole in a group. An unique feature offered by Telegram is channels, in which a set group of users can post and others can only read it. In Whatsapp, the group settings can be edited according to the admins choice.

| Feature | Whatsapp | Telegram |
|----------------------------------|--|---|
| Cloud sync | Yes~ Requires active internet on phone | Yes |
| End-to-End Encryption | Yes~ By default | Yes~ Via secret chats |
| File Sharing | Up to 100 MB | Up to 1.5 GB |
| In-App Browser | No | Yes |
| Live Location /Location Sending | Yes | Yes |
| Bots | No | Yes |
| Edit Sent Messages | No | Yes~ Up to 48 hours |
| Image Compression | Yes | Yes |
| GIFs | Yes | Yes |
| Image Editor | Yes | Yes |
| Internal Media Player | Yes | Yes |
| Open API | No | Yes |
| Secret Chats | Yes~ Encrypted by Default | Yes~ Optional |
| Public Groups | Up to 256 friends | Up to 75,000 friends |
| Public Channels | No | Yes |
| Simultaneous Multi-device access | No | Yes |
| Stickers | No | Yes |
| Two-step Verification | Yes | Yes |
| Status Message | Yes | Yes (Known as Bio) |
| Passcode Lock | No | Yes |
| Memory Usage Manager | Yes | Yes |
| Username | No | Yes |
| Themes/Customization | No | Yes~ Downloadable & Customizable themes |
| Sent Message Delete | Yes~ up to 7 minutes | Yes~ up to 48 hours |
| Voice/Audio Calls | Yes | Yes |
| In-built Proxy support | No | Yes |
| Video Calls | Yes | No |
| Web/Desktop Version | Yes~ Requires active internet on phone | Yes |
| Video Messages | Yes | Yes |

Table 1: Telegram vs. WhatsApp: Assessment of Technical Features

4.6 Multiple Accounts

In Whatsapp, you can create multiple accounts according the phone number but the disadvantage is that you have to remove the previous account or you should use dual app service. In Telegram, you can create more than one

account and the advantage is that you don't want to remove the previous account. It provides multiple account services.

4.7 Encryption

Telegram has a strong encryption. Telegram works on three layer encryption whereas Whatsapp works on two layer encryption. Telegram allows you and only the recipient to process the messages, media and files in the secret chat. In secret chats in Telegram, it allows you to set timer for chats to self-destruct after a specified time. Whatsapp allows end to end encryption to all the chats [8] whereas Telegram allows only for secret chats. In Telegram, notification will be displayed when the receiver takes screenshot and the messages can't be forwarded in secret chats [9][10].

5 Conclusion

Social media has become integral part of our daily life to connect with our loved ones and enjoy benefits from customer services offered by private and public organizations over the globe. Starting from Orkut, the penetration of social media in India had a long journey. This article in particular, has highlighted the escalation of Telegram in India. The review on success story of eight organizations from different sectors has supported the current analysis. WhatsApp and Telegram are the two major market share holders in Indian social media. The penetration performance of these two social media in India has been reviewed, and the technical differences of these two platforms has been compared and tabulated. The outcome of this work is to enable people, to have a detailed understanding of these two media and make better future decision for their personal relationship and to achieve business growth.

References

- [1] Waterloo, S.F., et al., Norms of online expressions of emotion: Comparing Facebook, Twitter, Instagram, and WhatsApp. *new media & society*, 2018. 20(5): p. 1813-1831.
- [2] Manna, R.A. and S. Ghosh, A Comparative Study Between Telegram and Whatsapp in Respect of Library Services. *International Journal of Library & Information Science (IJLIS)*, 2018. 7(2).
- [3] Dargahi Nobari, A., N. Reshadatmand, and M. Neshati. Analysis of Telegram, an instant messaging service. in *Proceedings of the 2017 ACM on Conference on Information and Knowledge Management*. 2017.
- [4] Sutikno, T., et al., WhatsApp, viber and telegram: Which is the best for instant messaging? *International Journal of Electrical & Computer Engineering (2088-8708)*, 2016. 6(3).
- [5] Pang, N. and Y.T. Woo, What about WhatsApp? A systematic review of WhatsApp and its role in civic and political engagement. *First Monday*, 2020. 25(12).
- [6] O'Hara, K.P., et al. Everyday dwelling with WhatsApp. in *Proceedings of the 17th ACM conference on Computer supported cooperative work & social computing*. 2014.
- [7] Saribekyan, H. and A. Margvelashvili, Security analysis of Telegram. 2017.
- [8] Cruz, E.G. and R. Harindranath, WhatsApp as 'technology of life': Reframing research agendas. *First Monday*, 2020.
- [9] Lee, J., et al. Security analysis of end-to-end encryption in Telegram. in *Simposio en Criptografía Seguridad Informática, Naha, Japón*. Disponible en <https://bit.ly/36aX3TK>. 2017.
- [10] J. Jakobsen, "A practical cryptanalysis of the Telegram messaging protocol," Master's thesis, Aarhus University, 2015

A New Discovery Of The Network Navigation Using Data mining

Dr. S.Selvam, Assistant Professor

N.M.S.S.Vellaichamy Nadar College, Nagamalai, Madurai-19.

E-mail: s.selvammscphil@gmail.com

Abstract

Due to increasing the act of Applied science College in Tamilnadu, the level of competition for admission price is also increased. By implementing some dynamic strategies only the academic introduction s can meet their own competition. One survey clearly commonwealth that more than 75% of the Engineering Colleges their forcefulness is less than thirty % of their actual intake. Hence the surveillance is the job for the insane asylum s. One more survey shows that every year 10% of the applied science college' windup their affiliation and blessing due to lack of admittance, and 5% of the engineering college have decided to sell due to lack of strength. With the strong effort and dynamic strategy framed by the institution, the nominee finds admission in an institution only when their own orientation matches exactly, otherwise the candidate continues to go by the next alternate in the list of preference [1]. This paper clearly emphasis some factors influenced to identify the pattern for getting the potency of the bookman to meet at least the breakeven point. In plus to the above, the Populace Wide Web in cyberspace plays an important role to store, part and distribute data about the academic innovation. A social survey states that more than 65% of the admissions gained by their effective network pages. The exponential ontogeny of the World Wide Web has provided an excessive prospect to study the potency student and their department by using WWW accession logs. If the institution's web sphere clearly contains the information required for the potential educate, surely they can attract the above by which they can get more number of admissions even beyond our jurisdiction.[2] Some of the attractions from the potential students while accessing the web site for getting the admission are: get the required information by clicking minimum act of hits from the vane Page, no network traffic occurred while accessing and navigating the college World Wide Web website. Search interrogation will be rectified within a short period of answer time by implementing the practice of search railway locomotive optimization, search engine spiders. Always use fastest and latest browsers and operating systems in their WWW and not to display much more web server erroneousness while navigating the college web site.

For attracting the counseling class and other state students, this network Thomas Nelson Page swordplay an important part. World Wide Web usage Mine lying is the practical application of data excavation techniques to very large data deposit to selection pattern radiation diagram. In general every World Wide Web server keeps a record book of all Synonyms/Hyponyms (Ordered by Estimated Frequency) of noun transaction needed for the potential students and act as a bridge between the potential students and introduction. The record contains full phase of the moon contingent about every user click to the entanglement documents of the entanglement site. The useful record 5 senses of detail needs to be scrutinized and inferred to gather knowledge about actual potential student and their parent preferences in accessing WWW pages. In recent years several method acting s have been proposed for mining web logarithm data. This theme its main intention is to use the statistical method of Poisson statistical distribution analysis to breakthrough out the higher probability session episode and also comparability the efficiency of our developed algorithm with Poisson value. The subject field of large volumes of click stream data demands the employment of data mining method . Conducting data mining on records of web host contains the determination of frequently occurring access sequences. A statistical method of toxicant distribution clearly shows the probability of oftenest of specific consequence when the norm probability of a single natural event is known. Here the probability of poison value is compared with the efficiency of our developed algorithm. For more bit of transactions, our developed algorithm its performance is better than poison value[3].Because our algorithms excerpt the authority tier as dependent rather independent. The Poisson distribution is used in this paper to find out the probability frequency of particular page is visited by the user as independent, but the result of the developed algorithm is dependent

Keyword: *Matrix-theoretic Approach, Sequence Alignment Algorithm, Appropriate Model, Statistical Methods, Data Mining Methods, Log Transactions.*

1 Introduction

The assessment of piloting al behavior in quantitative way is a fundamental task to understand the concurrent of network sailing s. The quantitative measures of potential drop bookman behavior will provide a better characterization of exploiter navigation and this will, in turn, suggest better ways of designing the anatomical structure of the college vane internet site s. The outcome of patterns used for vane access can be generated from record filing cabinet through which a Set of navigation academic term or lead are identified. The 11 senses of operation can be performed on session entropy which predicts important characterization of navigation behavior.[4]. The complete WWW site usage inside information can be availed by scrutinizing web site

potential student profile and their own access behavior. Several techniques have been proposed to analyze web traffic, search engine spiders, user browser and operating systems, web server errors and much more. Some authors adopt a ground substance -theoretic approach in modeling web log data and propose a set of algebraic operators, collectively called navigation operations, which can be employed to manipulate navigation matrices. The information of web usage can be generated from log files and a set of navigation sessions that represent the trail are formed during the navigation process. The trails are modeled as a weighted directed graphical record, called a transition graph, and then a corresponding navigation matrix is computed with deference to the underlying web topology. Regarding a minimal set of binary operations, includes sum, union, intersection and difference operations on the matrices.[5] These operations enable the user to analyze navigation from the capacity of two given navigation matrices. In descriptive statistical, network and graph psychoanalysis methods on user behavior data to derive user profiles. For graph analysis, the record file is first converted to an adj.

2 Simpleton Navigation Metrics

Statistical techniques are applied on preprocessed phonograph recording file to obtain descriptive sitting information. For each user session, figure of dealings required in the particular session to convert a particular inquiry in to accession and the number of clock time called for the above conversion .[6].The simple navigation metrics includes dwelling time or lodgment time of each dealings in a particular measurement of time. The analytic works begin with statistical method and calculates the frequency of the individual minutes and the time spent on each transaction. The time constituent is the most meaningful agent in the analysis and a positive degree correlation of time spent on a transaction and educate interest group has been identified. The work measures the dwell time between each transaction in a particular period of time and total time spent on each session.

3 Evaluation Of Record Files Using Poisson Distribution

A Poisson Process is a stochastic cognitive summons which consists of a solicitation of random percentage point in fourth dimension. An example of a Poisson process is the breaker point of clock time where the potential of educate arrive in a College. The construct of a Poisson process can be generalized to procedure with points in arbitrary sets instead of points in time. Poisson dispersion is a discrete probability distribution that expressage the probability of a bit of case occurring in a fixed period of time if these consequence s occur with a known average rate and independently of the time since the last event. It gives theoretical chance and theoretical frequency of a discrete variable [7] . This distribution can be applied when the happening of the event must be of two option such as success or failure. It is applicable when the number of lead 'n' is very large. Model of events as a Poisson distribution include: The number of phone telephone call made to convert an inquiry in to entree in any academic institution, the number of times the institution web internet site is accessed for admission purpose per arc minute and the number of times a student can be called for admission after a certain amount of time.

The Poisson distribution may be useful to exemplar consequence such as:

- The phone issue of scholars admitted in a particular academic year.
- The number of occurrences needed to convert the inquiry in to admission price.
- The number of bookman s admitting beyond 3fivesome km radius of the college.
- The number claim needed to convert the inquiry into admission.
- The dynamic strategy used to convert.
- Generalization of the procedure of admission by identifying the pattern.

The probability distribution of a random variable X representing the number of success occurring in a given time interval or a specified region of space is given in the following formula:

$$P(X) = \frac{(m^x e^{-m})}{x!} \quad [\text{Par 1}]$$

Where

e - floor of the natural logarithm (e = 2 .septet 1828).

x - actual no of successes that termination from the experiment (yield values 0,1,2...).

m - average no of successes per interval.

$$P(X - \text{got admission in 10 steps}) = \frac{m^x e^{-m}}{x!} = \frac{1^x e^{-1}}{x!}$$

$$P(X=0) = \frac{1^0 e^{-1}}{0!} = e^{-1} = 0.368 ; P(X=1) = \frac{1^1 e^{-1}}{1!} = 0.368$$

| X | P(X) |
|---|--------|
| 0 | 0.368 |
| 1 | 0.368 |
| 2 | 0.184 |
| 3 | 0.061 |
| 4 | 0.015 |
| 5 | 0.003 |
| 6 | 0.0005 |

The average number of transactions needed to convert the admission for this year is approximately 2.5 and the Poisson model is appropriate. Because the average event rate is 2.5 transactions per admission $m = 2.5$.

$$P(X=0; \text{student in a admission}) = \frac{2.5^0 e^{-2.5}}{0!} = e^{-2.5} = 0.082 ;$$

$$P(X=1; \text{student in a admission}) = \frac{2.5^1 e^{-2.5}}{1!} = 0.205$$

Table 1: Probability for 0 to 7 students in an admission

| X | P(X) |
|---|-------|
| 0 | 0.082 |
| 1 | 0.205 |
| 2 | 0.257 |
| 3 | 0.213 |
| 4 | 0.113 |
| 5 | 0.067 |
| 6 | 0.028 |
| 7 | 0.010 |

The poison distribution is applied for web criminal record data, since it contains large volume of web page hitting . The method is used to discover the probability measuring of each page visited against number of times in the web log[8].

The Poisson distribution is an appropriate model if the following assumptions are true.

- K is the number of clock sentence s an event occurs in an musical interval and K can take values 0, 1, deuce , ...
- The happening of one event does not affect the probability that a second event will occur. That is, outcome occur independently.
- The rate at which event occur is constant. The rate cannot be higher in some interval and lower in other intervals.
- Two events cannot occur at exactly the same instant.

- The probability of an event in an interval is proportional to the length of the interval.

If these shape are true, then K is a Poisson random variable star ,and the distribution of K is a Poisson distribution.

4 Experimental Results

The goal of the body of work is to break through the probability of happening of every dealings s using poison probability proficiency. The method finds the probability of number of dealing occurring in a fixed time measurements. Its performance is compared with our developed algorithm. The experiment is conducted on XL Clarence Day depository log transactions of an Engineering College, WWW server from 15-05-2019 to 24-06-2020 are collected and preprocessed with the information cleaning code. The cleaned monument records are converted in the sequence format which contains. The Board -1shows the session details of the repository log transactions and the probability of occurrence of all transactions of the above college . To find the Poisson probability, it requires in determination the frequency of 1,2,...n time occurrences of every transactions in each session in the given time period. Using Poisson distribution the expected frequency of 4 times occurring of each transaction is calculated. The Poisson probability result is show in Table-1.The frequency of 1-time, 2-time and 3-time occurrences of every transaction in the college is reported in the table. The result in the following table

Table 2: Poisson Probability for admission transaction

| S · N o | Trans action s | No. of Tr ans . | 1-time occurre nces | 2- time occurre nces | 3- time occurre nces | Poisso n value for x=4 |
|------------------|----------------------------|-----------------------------|---------------------------|----------------------------|----------------------------|------------------------------------|
| 1 | Moder ate fees | 4 | 2 | 1 | 1 | 0.9998 278 |
| 2 | State of the art lab | 6 | 3 | 2 | 1 | 0.9963 401 |
| 3 | Librar y | 5 | 2 | 2 | 1 | 0.9999 933 |
| 4 | Experi enced faculty | 6 | 3 | 2 | 1 | 0.9999 933 |
| 5 | Good result | 7 | 3 | 2 | 2 | 0.9998 278 |
| 6 | Placem ent | 8 | 3 | 3 | 2 | 0.9989 353 |
| 7 | Hostel facility | 3 | 2 | 1 | 0 | 0.9999 933 |
| 8 | Sports activit y | 3 | 2 | 1 | 0 | 0.9999 933 |
| 9 | Basic amenit ies | 4 | 2 | 1 | 1 | 0.9999 933 |
| 1 0 | Transp ort | 4 | 2 | 1 | 1 | 0.9999 |

| | | | | | |
|----------|--|--|--|--|-----|
| facility | | | | | 933 |
|----------|--|--|--|--|-----|

Table 3: confidence value derived from new algorithm

| S. No | Transaction | Confidence | S. No | Transaction | Confidence |
|-------|----------------------|------------|-------|--------------------|------------|
| 1 | Moderate fees | 100 | 6. | Placement | 127.5 |
| 2 | State of the art lab | 112.75 | 7 | Hostel facility | 86.6 |
| 3 | High volume Library | 88.5 | 8 | Sports activity | 84 |
| 4 | Experienced faculty | 99.5 | 9 | Basic amenities | 98.5 |
| 5 | Good result | 112.5 | 10 | Transport facility | 93.75 |

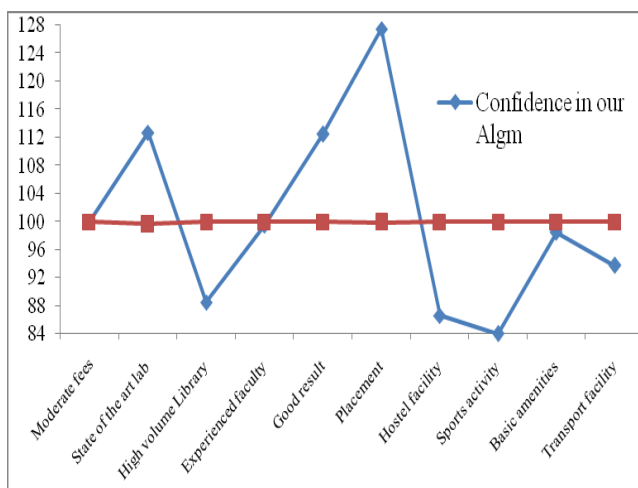


Figure 1: Admission related value derived from Poisson Probability and new algorithm

5 Conclusion

Appropriate 3 senses of metric can provide useful characterizations of potential student and their parent piloting demeanor and can diagnose a variety of problems. The ability to predict the opportunity of occurrences with precision would be extremely useful in practice. The workplace proposes a chance analysis of dealing file using Poisson distribution. The forty days logarithm 1 sense of dealing from 14-05-2015 to 23-06-2015 of Pannai College of Applied science and Technology monument has been collected for the Poisson probability analysis. The approach finds the probability and frequency of screening every transaction in the College. The Chassis -1 show that the transaction like Placement, Good result, experienced faculty, State of the art lab and Program library have more probability value. Hence the probability of occurrences of these transactions in the future is higher than the other transactions in the Engineering College.

References

- [1] Wilfred Ng, "Capturing the Semantics of Web Log data by navigation matrices", Proceedings of the IFIP TC2/WG2.6 Ninth Working Conference on Database Semantics, Pages: 155 – 169, 2001.
- [2] N. Zin and M. Levene, "Constructing web-views from automated navigation sessions", In Proceedings of the ACM Digital Library Workshop on Organizing Web Space, pp. 54-58, 1999.
- [3] Guandong Xu, Xiaofang Zhou and Yanchun Zhang, "A latent usage approach for clustering web transaction and building user profile, Advanced Data mining and Applications, volume 3584, pp: 31-42, 2005.
- [4] Jian Pei, Jiawei Han, BehzadMortazavi-asl and Hua Zhu, "Mining access patterns efficiently from web logs", In Pacific-Asia Conference on Knowledge Discovery and Data Mining, pages 396–407, 2000.
- [5] J. M. Kleinberg, R. Kumar, P. Raghavan, S. Rajagopalan and A. S. Tomkins, "The web as a graph: measurements, models and methods", Lecture Notes in Computer Science, Vol. 1627, pp: 1-18, 1999
- [6] Qiang Yang, Hui Wang and Wei Zhang, "Web-log mining for quantitative temporal event prediction", IEEE Computational Intelligence Bulletin, Vol.1, No.1, December 2002.
- [7] W. Wang and O. R. Zaïane, "Clustering Web Sessions by Sequence Alignment", Proceedings of DEXA Workshops, pp: 394-398. 2002.
- [8] R. Agrawal and R. Srikant. Fast algorithms for mining association rules in large databases. In Proceedings of the 20th International Conference on Very Large Data Bases, Santiago, Chile, August 29-September 1 1994.
- [9] M. Houtsma and A. Swami. Set-oriented mining of association rules. In Proceedings of the International Conference on Data Engineering, Taipei, Taiwan, March 1995.
- [10] Savasere, E. Omiecinski, and S. Navathe. An efficient algorithm for mining association rules in large databases. Technical Report GIT-CC-95- 04, Georgia. Institute of Technology, Atlanta. GA 30332, January 1995.
- [11] K.C.C Chan, A.K.C. Wong and D.K.Y. Chiu, "Learning sequential patterns for probabilistic inductive prediction," IEEE Trans. Systems, Man and Cybernetics, vol. 24, no. 10, pp. 1532-1547, 1994.
- [12] SudiptoGuha, Rajeev Rastogi, and Kyuseok Shim. CURE: An efficient clustering algorithm for large databases. In ACM SIGMOD International Conference on Management of Data, 1998.
- [13] Tian Zhang, Raghu Ramakrishnan, and MironLivny. BIRCH: An efficient data clustering method for very large databases. In ACM SIGMOD International Conference on Management of Data, 1996.
- [14] Haisun Wang, Wei Wang, Jiong Yang, and Philip S. Yu. Clustering by pattern similarity in large data sets. In ACM SIGMOD International Conference on Management of Data, 2002.

SIRD Model Simulation for Corona pandemic in Tamil Nadu

P.Ananthi¹ and Dr.S.Jabeen Begum²

PG scholar, Department of Computer Science and Engineering,
Velalar College of Engineering and Technology, Erode, Tamil Nadu, India

² Head and Professor, Department of Computer Science and Engineering,
Velalar College of Engineering and Technology, Erode, Tamil Nadu, India

Abstract

In this paper, Forecasting and spreading of Covid-19 in Tamil Nadu state is demonstrated by simulating an epidemiology model Susceptible-Infectious-Recovered-Demised (SIRD) model. Implicit analytical solution is applied for some parts of the model and for other parts finite difference methods are used. On the basis of SIRD model, values of coefficient of infection, coefficient of morality and coefficient of recovery can be found. In addition to the calibration of the model the ratio of the average rate of death to the average rate of recovery for the pandemic in Tamil Nadu is calculated. For this model, data is collected from Tamil Nadu Health and Family Welfare Department. The data has number of infected cases, death cases, recovered cases and hospitalized cases per day in Tamil Nadu State. The prediction results give good analysis and better understanding of the spread of the disease in the state. Based on the results, it is obvious that as the number of days increases that cumulative count of infected patients are also increased. But in the pandemic a fall would be expected after certain period of time. However this prediction model enables us to make quick response of the pandemic and get more insight about the data.

Keywords: Forecasting, Epidemic model, SIRD model, Analysis, Pandemic, Prediction

1 Introduction

In early November 2019, an outbreak of “Pneumonia of unknown etiology” was found in Wuhan, Hubei province, China and it was ravaging China and this disease becomes a threatening to reach a pandemic state. A new strain of beta corona virus is the causative agent and it is closely related to Severe Acute Respiratory Disease (SARS) and Middle East Respiratory Disease (MERS). The origin of the disease was determined based on the preliminary investigations are suggestive of bats. Similar to SARS and MERS, the novel virus also transmitted from one person to another person principally by respiratory droplets. According to Centers for Disease and Prevention (CDC), the symptoms of the disease may include fever, cough, shortness of breath and fatigue. Preliminary data suggest that older people and people with co-morbidities are likely to be infected severely while most of the infected patients experience mild symptoms some may develop to various organ failure and pneumonia which might result in death. In January World Health Organization named the virus “Covid-19” which refers to the meaning of “Corona Virus Disease 2019”. Covid-19 is a Public Health Emergency of International Concern and it was declared by the WHO Director-General. The virus has been continuous to spread in rapid rate all over the world. The rapid rise in the number of Covid-19 incidents worldwide has prompted the need for immediate counter measures to curb the catastrophic effects of the Covid-19 outbreak.

In India, the Covid-19 was reported on 30 January 2020. India has the largest number of confirmed cases in Asia and the second largest number of confirmed cases in the world. Tamil Nadu is one of the affected states of India. In March 7 2020, Tamil Nadu Government faced its first corona case. All the 38 districts are affected during the pandemic whereas Chennai the capital of state was affected the worst. Health Department reports that 88% of patients are asymptomatic while 84% of deaths were among those with co-morbidities. Tamil Nadu Government responded to the pandemic by following contact tracing, testing and surveillance model. Government has also imposed strict lockdown and restricted inter-state movement to control the pandemic.

As a contribution to the ongoing public health crisis, an epidemic model is built with the help of available data to get a small distance to bring the conclusion to the pandemic. The models and algorithm used here for simulating the forecasting and spreading of the virus are also used to find the other related coefficients of the pandemic such as reproduction number for a certain region.

2 SIRD Model Simulation

2.1 Methodology

This analysis is based on the concept of finding the relationship between the transportation that makes a vital role in spread of disease and the growth of patients count in a geographic location. In this model, certain population is considered for a particular geographic location i.e. Tamil Nadu state in this case. For this purpose Susceptible-

Infectious-Recovered-Demised model is proposed. This compartmental model is a mathematical model, where the disease can be moved people between categories such as healthy, infected or sick, recovered or developed immunity and fatal. This is a truly resulting way of modeling an infection that is spread from one human to other human. In Covid case, the infection is both contagious and deadly.

2.2 SIRD model

The SIRD model considers the total population that belongs to one of the four states and derives the relationship between the states. The four states are: the susceptible state $S(t)$, the infectious state $I(t)$, the recovered state $R(t)$ and the demised state $\delta(t)$. Various other models are also have been used for this purpose, some may have differential equations and some others may have fractional differential derivatives. This model also takes fatality into account. In this attempt the mean values of the main parameters like basic reproduction rate R_0 , case recovery rate γ and the case infection rate β .

Contact rate $U(N)$ is the number of individuals contracted to the disease by an infective in a unit time. The probability of infection to each contact is considered as β_0 then the adequate contact rate is traced as $\beta_0 U(N)$. The infection rate can be derived as the product of mean adequate contact rate of an infected individual to the susceptible $\beta_0 U(N) S/N$. The incidence of disease is the total number of newly infected patients by all the individual in the infected category per unit time ($\beta_0 U(N) S/N$) I .

The estimated parameters required for this model includes infection rate, recovery rate and demise rate of the disease in a population and it is gives as,

$$\beta = \frac{\text{the numbet daily confirmed cases at a time}}{\text{the number of accumulated confirmed cases at a time}} \quad (1)$$

$$\gamma = \frac{\text{the numbet daily recovered cases at a time}}{\text{the number of accumulated confirmed cases at a time}} \quad (2)$$

$$\delta = \frac{\text{the numbet daily death cases at a time}}{\text{the number of accumulated confirmed cases at a time}} \quad (3)$$

The SIRD model is described by four differential equations; the first equation represents the rate of susceptibility of cases in a certain population with respect to time period t . And it is represented by an equation,

$$\frac{dS}{dt} = \frac{-\beta S I}{N} \quad (4)$$

The rate of infected cases in a time are represented by the equation (5),

$$\frac{dI}{dt} = \frac{\beta S I}{N} - (\gamma + \delta)I \quad (5)$$

The recovery rate of the total population with respect to a time is given by,

$$\frac{dR}{dt} = I\gamma \quad (6)$$

The rate of demised cases with respect to a time is given the equation (7),

$$\frac{d\delta}{dt} = \delta I \quad (7)$$

Here, N is the total population of the geographic location and β , δ and γ are the rate of infection of patients, rate of demise and rate of recovery in that population. It is clear from all the four equations contain the infected cases I because it is the central aspect of the pandemic. The rate of population of susceptible, infection, recovery and demise are related to each other by the following equation,

$$\frac{dS}{dt} + \frac{d\delta}{dt} + \frac{dR}{dt} + \frac{dI}{dt} = 0 \quad (8)$$

The last equation represents the conservation of the total population in the system and it represents the critical condition of the system. It is very clear in the system that SIRD model considers a population and divides the population into four categories.

An individual belongs to one of the four categories but not more than one. So the sum of the entire four categories gives the total population as well,

$$S + I + R + D = N \quad (9)$$

The basic reproduction number is taken as R_0 . R_0 can be used to predict whether the infectious disease will spread into a population in near future or die out. R_0 represents the average number of victim's affected secondary cases that results after the introduction of a single infectious patient into a susceptible population during the infectious period. The basic reproduction number can be easily calculated from the parameters of SIRD model.

$$R_0 = \frac{\beta}{\gamma} \quad (10)$$

The values of the parameter in Covid 19 is defined as, the unit of days. The official time for incubation period followed worldwide is 14 day. The SIRD system is defined in a discrete time period $t=1,2,\dots,n$, with the corresponding initial state of the system with its four sub-population is given as $S(0)=N-1$, $I(0)=1$, $R(0)$, $D(0)=0$. The parameters β and γ are not corresponds to the actual per day count in aspects.

2.3 System design

The system flow architecture represents the flow of implementation of the system. The first step in building the model is collecting the raw data from the real world. The data which relevant to Covid-19 is taken into account in this case. Then the data is processed for finding the missing values and replacing the redundant with data that are appropriate for building the model. The cleaned dataset is taken as input to the system and SIRD model can be built by evaluating the parameters from the available dataset ad considering the population. The visualization of resultant model enables for better understanding of the data. Product knowledge and insight can be brought from the developed model as a data product. These model generation and results will the authorities for better decision making. In addition to the generation of the model, the cleaned data set can be used to get several exploratory data analysis results and models are made for assisting the generation of the model.

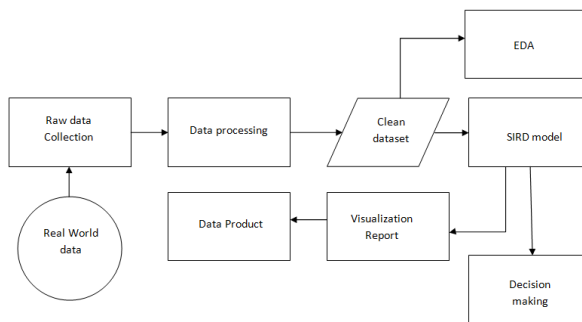


Figure 1: System flow architecture

2.4 Data set

The analysis is based on the publically available data that is being released by the Health and Family Welfare Department of Government of Tamil Nadu. The dataset is collected and compiled under circumstances from the daily official press release. Tamil Nadu government faced its first corona case on March 7 2020 and the dataset is continuously updated until September 21 2020. All the dataset is updated accurately as per the daily bulletin through state Government website www.stopcoronatn.com.

Table 1 has the summary details of corona case in Tamil Nadu. It has date in which the infection has occurred, how many patients has been confirmed to the infection, number of recoveries from the disease, how many patients are still in hospitalized state and number of death occurred due to disease.

Table 1: Case summary table of Tamil Nadu.

| DATE | Confirmed Cases | Recovered cases | Active cases | Death cases |
|-----------|-----------------|-----------------|--------------|-------------|
| 3/7/2020 | 1 | 0 | 1 | 0 |
| 3/8/2020 | 0 | 0 | 1 | 0 |
| | | | | |
| 9/20/2020 | 5516 | 5206 | 46703 | 60 |

Table 2 gives the data about the number of confirmed cases for all the 38 districts in Tamil Nadu. This dataset is also recorded from 7 March to 21 September. The datasets are checked for the completeness and detected for the presence of NaN values. But as the disease continuous to spread in our region, the dataset is continuously updated daily. The result of finding missing values results null in the dataset. The datasets are collected in the form of Comma Separated Values. The dataset are then transformed for developing the model.

Table 2: District wise confirmed cases in Tamil Nadu.

| DATE | Ariyalur | Chengalpattu | | Villupuram | Virudhunagar |
|---------|----------|--------------|-------|------------|--------------|
| 3/7/20 | 0 | 0 | | 0 | 0 |
| | | | | | |
| 9/21/20 | 3517 | 32799 | | 10525 | 14066 |

3 Results and Discussions

The available dataset is reported on a timeline. All the four parameters infected, recovered, active cases and deaths are reported for the available period of time. The vertical lines depict the dates of lockdown. The first two solid lines are for strict lockdown. The dashed lines are for extension of lockdown with some restriction. The rest dotted lines represent the extension of lockdown without border restriction and national level transportation.

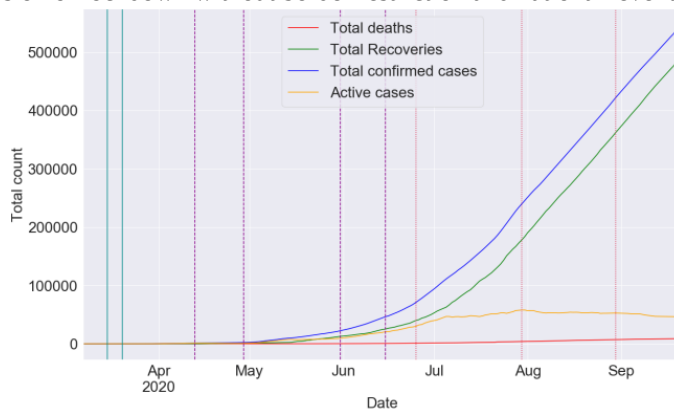


Figure 2: Timeline report of Covid-19 in Tamil Nadu

The parameters are compared with their moving average (MA) for analyzing the data points for multiple subsets of the entire dataset in a time series. The moving average is computed with the scale of 7 days. The comparison results help to find the outliers. Presence of outlier may cause poor results in performance. Outlier is the data point that does not fit with the rest of the data points.

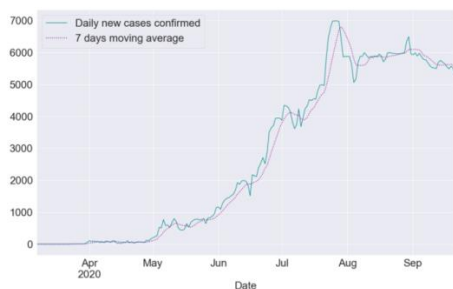


Figure 3: Confirmed cases vs. MA

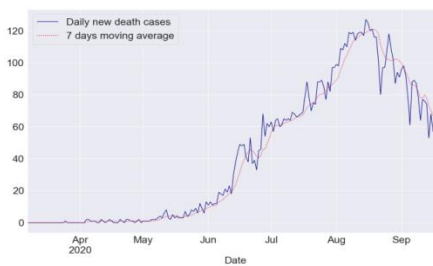


Figure 4: Death cases vs. MA

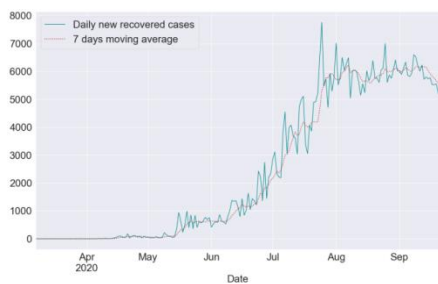


Figure 5: Recovered cases vs. MA



Figure 6: Active cases vs. MA

From Figure 3, 4, 5 and 6 it is clear that actual confirmed cases and its moving are similar from initial stage of disease. The comparison of recovered and death cases with its moving average shows that curve is not so smooth. The curves also have some fluctuation but there is no presence of outlier. The active case comparison with the moving average gives that main idea that both the curves are similar from initial stage to the end of available data period.

The SIRD model is built with four sub population: Susceptible fraction where people do not contract to the disease but vulnerable to get disease from an infected patient. In Covid situation, the disease is contagious and total population was considered in a susceptible state. The infected population is the number of people who are affected by the virus and remains in hospitalized state. The patient is potential of carrying the disease to an unaffected population and spread the disease. In the recovered set of population the patients develops immunity against the disease and hence recovered from the disease. But the recovered patient may or may not get the disease

for the second time. In death set, the disease is a fatal disease; the patients are unable to develop immunity which may lead to death. This category of people will never be recovered or transported to other category of population.

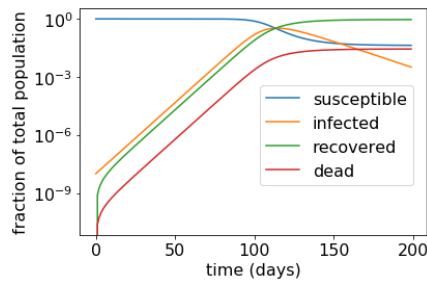
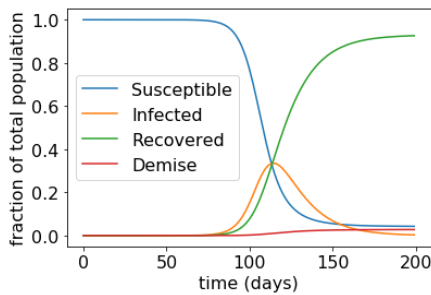


Figure 7: SIRD model without lockdown Figure 8: SIRD model with lockdown

Here the model is developed under lockdown scenario, where the total population for under the infected cases would be less when people have less contract rate to the disease. The rate of spreading the disease is very much less when compared to the worst scenario.

From the model, is observed that number of infected cases increases from a certain period of time and then eventually decreases. The susceptible fraction of population decreases as the virus is transmitted and then eventually drops to the absorbent state 0. For recovered cases where it starts from the state 0 it raises to a maximum value. But in the demised case, it starts from 0 and attain the difference value between the infected and recovered value.

Considering the worst case scenario, the population is considered in an open condition i.e. without lockdown. Large number of population will be in susceptible state and many people would get disease easily in this scenario. The number of infected cases will be large and recoveries would be less because of minimum available health facilities for a large affected population.

The parameters used to calculate the model is estimated by the using above differential equations. Tamil Nadu geographic location is considered in our case. The table below shows the parameters for the state.

Table 3: Parameters estimated.

| Parameters | Parameter Description | Parameter Value |
|------------|-----------------------|-------------------|
| N | Total population | 7.7×10^7 |
| β | Infection rate | 0.35 |
| δ | Death rate | 0.02 |
| γ | Recovery rate | 0.07 |
| R_0 | Reproduction number | 5 |

When trying to fit the Tamil Nadu dataset with the calculated model. It is observed that a drop would be expected in the bell curve after 170 days. But the results show that the drop was actually happened after 190 days.

The comparison is made for infected cases as well as recovered cases. The death case scenario, both Figure 2 and Figure 7 shows that number of death would be low. In Figure 9 and Figure 10 the blue solid lines are the actual data points and orange lines are for the smooth predicted curve of SIRD model.

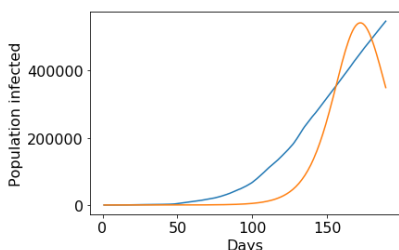


Figure 9: SIRD model fit with infected case in Tamil Nadu

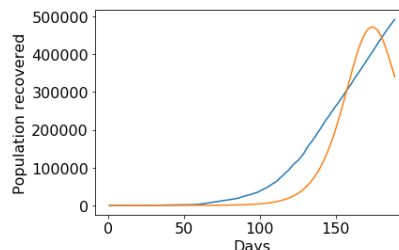


Figure 10: SIRD model fit with recovered case in Tamil Nadu

The goodness of fit of the curve is estimated by Mean square error (MSE), Root mean square error (RMSE) and R^2 . The accuracy gives the how much effectively the model was built against original data.

The table describes the error rate of Confirmed cases and recovered cases. From the calculate results the recovered cases prediction is way better than the infected cases. The error are taken in the way that smaller the estimated error value greater will be the accuracy of calculation.

Table 4: Error estimations.

| Attribute | MSE | RMSE | R ² |
|-----------------|----------|--------|----------------|
| Confirmed case | 21035.92 | 145.03 | 0.820 |
| Recovered cases | 193.13 | 13.89 | 0.63 |

4 Conclusion

The SIRD prediction system has been proposed for predicting the risk of Covid-19 in Tamil Nadu. The system analyses dataset containing the day-wise actual data and makes predictions for upcoming days using the compartmental model. The goodness of fit for the curves is also estimated. Observation makes a clear view that date and number of cumulative number of infection are positive correlated. The forecast model shows that the number of death cases will be very less when compared to the recovered cases in Tamil Nadu. Imposition of lockdown is the best move to control the pandemic and avoid the spread of disease for a large population geographic location. There are significant limitations to this model; the fact of how the disease is spread or does not spread throughout the space is neglected. In such case social distancing will be helpful. How different age group and with different health condition are susceptible to the disease. Health advisory reports that aged people with co-morbidities are likely to be affected more than other people.

Based on the results that the while large population is susceptible to the disease, the number of infected cases grows exponentially. A critical number of people are infected and begins to recover, the number of cases decays exponentially. There would be drop in susceptible and infected cases. The recovered and death cases will be zero at initial state and grows gradually to a maximum values.

As the infection rate is growing day by day the parameter that also growing similar to infected case is the recovered cases. When the number of infected cases the number of recoveries are also less. When the number is high out of the number of infection the number of deaths will be less.

Thus for a new virus pandemic situation SIRD model can be applied to get the vulnerability. In addition to this the same algorithm can be used to get reproduction rate. The primary need for this model is to get updated dataset with the number of observed case scenario for a certain population. The same algorithm can also be used to exact solution by using other epidemic model. At the time writing, vaccination was not taken into considered. In future vaccinated state can be included where susceptibility would be less in such case results in less number of infection in future which influence the number of recovered and death cases also.

References

- [1] Furqan Rustam , Aijaz Ahmad Reshi , Arif Mehmood ,Saleem Ullah , Byung-Won On, Waqar Aslam and Gyu Sang Choi “COVID-19 Future Forecasting Using Supervised Machine Learning Models”, IEEE ACCESS, pp.101489-101499 ,2020.
- [2] Romney B Duffey and Enrico Zio “Analysing Recovery From Pandemics by Learning Theory: The Case of CoVid-19” in IEEE Engineering in Medicine and Biology Society Section, vol.8, pp. 110789-110795,2020
- [3] Petar Radanliev, David De Roure and Rob Walton “Data mining and analysis of scientific research data records on Covid-19 mortality, immunity, and vaccine development - In the first wave of the Covid-19 pandemic”, Science direct, vol.3 ,pp. 1121-1132,2020.
- [4] Jooyeon Park, Jinhwa Jang and Insung Ahn “Epidemic Simulation of H1N1 Influenza Virus using GIS in South Korea”, in 2017 International Conference on Information and Communication Technology Convergence (ICTC), pp. 58-60, 2017.
- [5] Huadong Xia, Kalyani Nagaraj, Jiangzhuo Chen and Madhav Marathe “Evaluating strategies for pandemic response in Delhi using realistic social networks” in IEEE International Conference on Healthcare Informatics, pp. 121-130, 2013.
- [6] Vasilis Z. Marmarelis “Predictive modeling of Covid-19 data in the US: Adaptive phase-space approach” in IEEE Open Journal of Engineering in Medicine and Biology, pp. 207-211, 2020.
- [7] Fotios Petropoulos and Spyros Makridakis “Forecasting the novel coronavirus COVID-19” (ARGENTINA Lidia Adriana Braunstein, Universidad, Nacional de Mar delPlata), pp 1-8, 2020.
- [8] Hiba Asri, Hajar Mousannif, Hassan Al Moatassime and Thomas Noel “Using Machine Learning Algorithms for Breast Cancer Risk Prediction and Diagnosis” in The 6th International Symposium on Frontiers in Ambient and Mobile Systems, ScienceDirect, pp. 1064 – 1069, 2016/

- [9] Spyros Makridakis, Evangelos Spiliotis and Vassilios Assimakopoulos “Statistical and Machine Learning forecasting methods: Concerns and ways” forward Plos one (Alejandro Raul Hernandez Montoya, Universidad Veracruzana MEXICO), pp 1-26, 2018.
- [10] Shaobo He, Yuexi Peng and Kehui Sun “SEIR modeling of the COVID-19 and its dynamics” Springer Nature B.V, 2020.
- [11] Sharma and Milan “Coronavirus: Second ICMR report on random sampling test” results shows possible community transmission India Today, 2020.
- [12] Tamil Nadu State Health & Family Welfare Department daily Bulletin, www.stopcornatn.in , Tamil Nadu Government
- [13] Chen Y., Liu Q. and Guo, D. “Emerging coronaviruses: genome structure, replication, and pathogenesis”. *J. Med. Virol.* 92, pp 418–423, 2020.
- [14] Zhu N., Zhang D and Wang W., “A Novel Coronavirus from patients with pneumonia in China”, *New Engl. J Med*, pp 727-733, 2019.
- [15] Fanelli D., and Piazzia F “Analysis and forecast of Covid 19 spreading in China, Italy and France”, *Chaos Solitons Fractals*, pp 109761-109761, 2020.
- [16] Ceraolo C. and Giorgi, F.M “Genomic variance of the 2019-ncov Coronavirus”, *J. Med. Virol*, pp 522–528, 2020.
- [17] G. Bontempi, S. B. Taieb, and Y.-A. Le Borgne “Machine learning strategies for time series forecasting” *Proc. Eur. Bus Intell. Summer School. Berlin, Germany Springer*, pp 62-77, 2012.
- [18] Ji, W., Wang, W., and Zhao x. “Cross-species transmission of the newly identified coronavirus 2019-ncov”. *J. Med. Virol.* 92, pp 433–440, 2020.
- [19] J.C. Miller, “Mathematical models of SIR disease spread with combined non-sexual and sexual transmission routes *Infectious Disease Modelling*”, vol 2 pp 35-55, 2017.
- [20] J. M. Carcione , J. E. Santos, C. Bagaini and J. Ba. “A simulation of a COVID-19 epidemic based on a deterministic SEIR model”, *Front. Public Health*, 2020.
- [21] Hyndman R and Khandakar Y. “Automatic time series forecasting: the forecast package for R. *Journal of Statistical Software*”, pp 1-22, 2008.

Sentiment Analysis With Unsupervised Machine Learning And Natural Language Processing

Rahul Pandya, Suraj Moolya, Sujal Charak, Shivani Naik

Abstract

Sentiment Analysis has been a very important part of analytics for data scientists over the years. It has been a very detailed and an important area of research and development which enables the user to find the acknowledgement factor for the area of interest. Social media is always evolving and the most interactive media of individual communication and broadcasting. Sentimental analysis of is the best alternative for peer reviewing in terms of a certain criterion. This paper deals with an analytic study over a twitter based dataset which involves pulling of certain number of tweets using API linking and then performing the polarity check on the number of tweets pulled with respect to that particular keyword. An approach involving unsupervised machine learning algorithms along with natural language processing generates significant results in the task over the traditional lexicon method used.

Keywords: *Sentiment analysis, Twitter, Machine Learning, Social Networks, NLP*

1 Introduction

Sentimental Analysis has been a very in depth statistical studying topic in computer science and in developing fields. It has been a scope of study in data mining especially. In the earlier times, people relied upon the opinions of only the closer neighbours, that is, friends, family and relatives which used to form only a smaller group of people. The campaigners made it the larger part of audience through polls. The continuously evolving social media has now been the largest platform for opinion generation on topics in terms of relative review on personalised as well as mass areas of interest. This is a very developing opportunity as it involves organizing, classifying and detection of the relativeness between the particular opinions. Sentiment analysis is a very important aspect for organizations and big firms so as to achieve the review results for performance of their specific trademarks in terms of business queries.

Performing sentimental analysis is a challenging task. It is because of the pattern and nature of the text that has to be imported. Social media gives the researchers a very large data to access and perform analytics on as it is the biggest platform of interaction. So the amount of text and opinion extraction on such platforms is a demanding task. The linguistic barrier is one of them. However, by using natural language processing and machine learning algorithms these obstacles can be overcome. The opinion and emotion tracker is the most significant of all sections which involves the categorical word based classification of the texts and then assignment of the polarity to them accordingly.

The accuracy of prediction can then be calculated and improved significantly based on the model parameters. In this paper, the authors have performed a statistical polarity check of extracting a particular number of tweets from the social media platform Twitter. A definite keyword is used as a parameter to pull tweets related to that and then a check and measure is based on natural language processing along with classification is applied to generate a plot of distribution of favour and negative tweets.

The tweets can be categorised into three major sectors based on the criterion. Positive, strongly positive and weakly positive for tweets in support of the keyword. Negative, weakly negative and strongly negative for tweets not in favour of it and neutral for no such bias intended. The performed sentiment analysis can be performed on many platforms. For example, Movie suggestions or reviewer in Netflix and Hotstar, Restaurant suggestion and reviewer in applications like Zomato and Swiggy, Similar music suggestion based on genre and recent plays in Spotify, Gaana etc.

2 System Blueprint

Performing Sentiment analysis requires almost negligible costing. Our system involves using of a scripting language like Python or R along with the installation of an easy to use IDE. Here we have used Jupyter Notebook which comes built in with Anaconda Software [1]. Visual Studio and Pycharm could also be used. System processors having i3 intel processors and above versions with a basic graphic card is sufficient to run the libraries and ML algorithms. We suggest using Anaconda as it enables the user to download the whole bunch of libraries and software as a bundle and other required ones can be easily downloaded using a simple and efficient command pip.

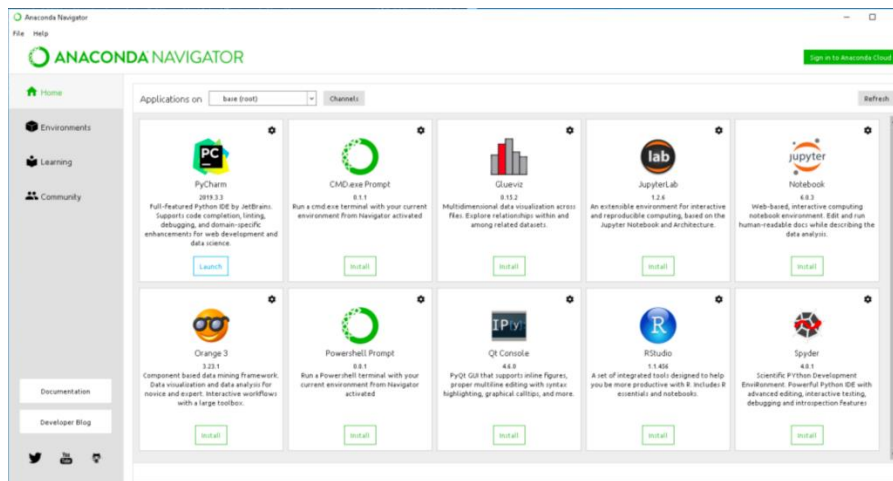


Figure 1: Anaconda Software

2.1 Specific Requirements

The following are the basic requirements to perform sentiment analysis:

- Tweepy, a basic python library for accessing the twitter API [2].
- Pandas – it is used to generate the CSV for the pulled and recorded tweets.
- Numpy package – it is used for numerical calculations in python library.
- Seaborn – it is a library used for statistical data visualisation [3].
- NLTK word tokenizer - A tokenizer that divides a string into substrings by splitting on the specified string (defined in subclasses) [4].

3 Methodology Adopted

There is a lot of information that needs to be imported from the social media platform. Twitter generates billions of tweets per year across approximately 187 million users. These tweets contain a diverse information on all sorts of topics across the globe and are multi lingual. Pulling data across such an active platform is a very exciting stuff to do. One can access almost all kinds of topics and generative study of them and get to know about the current affairs and get updated whilst putting his or her opinion on it. Regardless of these, sentiment analysis of social media platform like twitter gives a public opinion easily. Just mentioning that topic can generate thousands of results related to that topic. Here, we are going to perform a similar experiment. We shall be pulling a specific number of tweets related to a topic. The topic here shall be the keyword defined parameter.

3.1 API Authentication and Keyword Defining

Firstly, we need to import all the libraries required to perform the task. We import the libraries of numpy and pandas to generate the csv for maintaining the record of the pulled tweets and keep a count. We import 're' that is regular expression which specifies a set of strings that matches it; the functions in this module let you check if a particular string matches a given regular expression (or if a given regular expression matches a particular string, which comes down to the same thing) [5]. After the libraries are imported we create a csv file to save the tweets that we are about to pull.

Next is the API authentication via Tweepy. We need to connect or give access of our twitter account to the program we are building. This needs to be done through API authentication using an interface application. Twitter has an inbuilt developer application interface for API generation which can be used programmatically for analysing and retrieving data [6]. Once the authentication is done one can then start accessing twitter media via program. We take the user input to the program as a keyword to be searched on. The keyword is the topic or the area of interest on which the user intends to perform a research on. Also we need to specify the amount of tweets in text that we need to pull with respect to that keyword.

Here, in Fig. (2). we can see that we defined the keyword as 'Cricket' and the total number of tweets to be pulled related to that keyword as thousand. The tweets pulled shall only be in English as the language parameter defined here is English. This can be changed as per user requirement.

retrieved in the tweets and then plotting a visualising figure containing randomised number of words. Fig, (4). shows a word cloud for a hundred words in randomised tweets from the example used in this paper.

3.3 Testing Polarity and Results

The final stage involves the polarity testing of the tweets. This is the basic plotting of how the people are reacting on the searched term, that is, the defined keyword with respect to the number of searched terms, that is, the tweets. Polarities can be classified as mentioned earlier into three parts of negative and positive. Tweets with polarities in the range of 0 to 0.30 lie in weakly positive/weakly negative, tweets within the range of 0.31 to 0.60 in the positive/negative and tweets in the range greater than 0.61 to 1 are considered as strongly positive or strongly negative respectively. The polarity gets defined on the basis of the negation parameters like not, nor and such disregarding words present in the tweet's sentences. This is done natural language processing. One such experiment of finding the negative speech recognition within the tweets in the paper Deep Learning for Hate Speech Detection in Tweets [7].

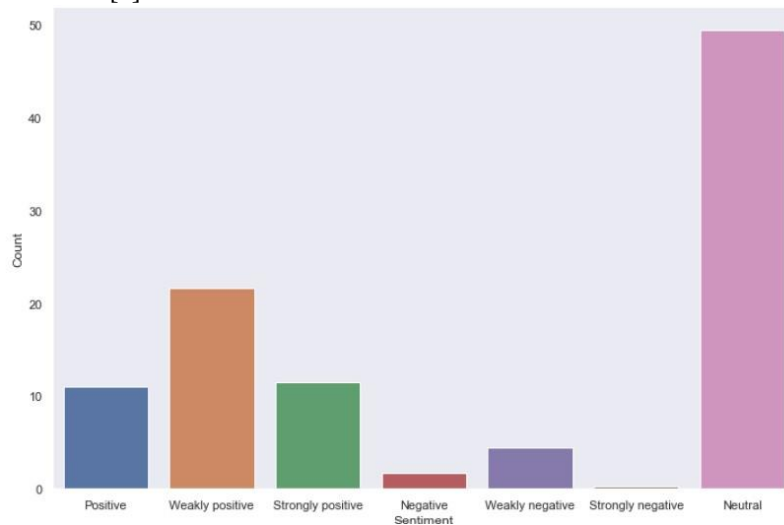


Figure 5: Plot of Sentiment Analysis

The Fig. (5) shows the polarity plot for the experiment performed. It can be observed from the bar plot that the neutral tweets with respect to the current Cricket norms are huge followed positive tweets.

The following was the count percentage of the sentiment analysis:

- Neutral: 49.46
- Strongly Positive: 11.52
- Positive: 11.07
- Weakly Positive: 21.57
- Strongly Negative: 0.22
- Negative: 1.66
- Strongly Negative: 4.43

4 Conclusions

This paper provides a basic evaluation on performing sentimental analysis in an easy approach. We achieved a bar plot for a thousand tweets for the keyword 'Cricket' and got a very positive response.

With respect to possible modifications, this method is expandable and flexible as the user can make multiple comparisons of multiple keywords using the similar approach and get a statistical plot for the same. Using of SVMs (Support Vector Machines) makes this a longer but more efficient analysis.

Applications of sentimental analysis is a very vital ingredient in business and for growing companies. They can keep a track on the user or customer indulgence of their products and how they are performing in the competitive market. Using of decision trees and regressions can improve the analysis features up to the prediction levels. Future scope involves using GANs (General Adversarial Networks) for sentiment analysis.

Acknowledgement

The authors are grateful to Prof. Abhishek Sawant for helping us with the experimental section and the study for the same.

References

- [1] Anaconda Software. <https://www.anaconda.com>
- [2] Tweepy python library. Available at: <https://docs.tweepy.org/en/latest/>
- [3] Seaborn library for statistical visuals. Available at: <https://seaborn.pydata.org>
- [4] NLTK word tokenizer. Available at: <https://www.nltk.org/api/nltk.tokenize.html>
- [5] Regular Expression python library. Available at: <https://docs.python.org/3/library/re.html>
- [6] Twitter Developer API formation. Available at: <https://developer.twitter.com/en/docs/twitter-api/getting-started/guide>
- [7] Deep Learning for Hate Speech Detection in Tweets, Pinkesh Badjatiya, Shashank Gupta, Manish Gupta, Vasudeva Varma. <https://arxiv.org/abs/1706.00188>

Authentication To Improve Atm Security By Using Internet Of Things

Kaviyalakshmi.T¹, Gopicka C², sandhiya G³, Anguraju.k⁴

¹kaviyarace@gmail.com, ²anguraju.k@gmail.com

¹Assistant Professor, Department of CSE, Kongunadu College of Engineering and Technology, Trichy, Tamil Nadu, India

²Professor, Department of ECE, Kongunadu College of Engineering and Technology, Trichy, Tamil Nadu, India

Abstract

Our venture proposes a made sure about ATM (Automated Teller Machine) framework utilizing a card filtering framework alongside LINK framework for improved security. Common ATM frameworks don't contain the LINK highlight for cash withdrawal. On the off chance that an aggressor figures out how to get hold of ATM card and the pin number, he may effectively utilize it to pull back cash deceitful. So our proposed framework bolsters the ATM card filtering framework alongside a LINK framework. This client may filter his card and login to the framework. In any case, after client is through with this confirmation he may see subtleties yet is approached to enter LINK when he clicks cash withdrawal alternative. At this stage the framework produces and sends a LINK to the enrolled portable number to that specific client. The secret phrase is produced advertisement sent to the client cell phone. He now needs to enter the LINK in the framework so as to pull back cash. In this way our framework gives an absolutely secure approach to perform ATM exchanges with two level security structure.

Keywords- *IOT,RFID tag and reader,ATM link*

1. Introduction

An implanted framework is a blend of PC equipment and programming, either fixed in capacity or programmable, that is intended for a particular capacity or for explicit capacities inside a bigger framework. Mechanical machines, agrarian and process industry gadgets, vehicles, clinical gear, cameras, family apparatuses, planes, candy machines and toys just as cell phones are largely potential areas for an implanted framework. Implanted frameworks are registering frameworks, yet can extend from having no (UI) - for instance, on gadgets in which the installed framework is intended to play out a solitary undertaking - to complex graphical UIs (GUI, for example, in cell phones. UIs can incorporate catches, LEDs, touchscreen detecting and that's just the beginning. A few frameworks utilize remote UIs too. Inserted frameworks can be chip or microcontroller based. In either case, there is a coordinated circuit (IC) at the core of the item that is commonly intended to complete calculation for continuous activities. Microchips are outwardly unclear from microcontrollers, however while the chip just actualizes a focal preparing unit (CPU) and in this way requires the expansion of different parts, for example, memory chips, microcontrollers are structured as independent frameworks. Installed frameworks can be microchip or microcontroller based. In either case, there is a coordinated circuit (IC) at the core of the item that is commonly intended to complete calculation for ongoing activities. Microchips are outwardly unclear from microcontrollers, however though the chip just actualizes a focal handling unit (CPU) and in this manner requires the expansion of different segments, for example, memory chips, microcontrollers are planned as independent frameworks.

With the advancement of PC organize innovation and internet business, oneself help banking framework has broad promotion with the trademark offering top notch 24 hours administration for client. These days, utilizing the ATM (Automatic Teller Machine) which furnishes clients with the helpful banknote exchanging is normal. Be that as it may, the monetary wrongdoing case rises over and again as of late; a ton of lawbreakers mess with the ATM terminal and take client's charge card and secret word by unlawful methods. When client's bank card is lost and the secret phrase is taken, the criminal will attract all money the most brief time, which will carry gigantic monetary misfortunes to client. The most effective method to carry on the substantial character to the client turns into the concentration in current money related circle. Conventional ATM frameworks confirm for the most part by utilizing the charge card and the secret key, the technique has some defects[4]. Utilizing charge card and secret phrase can't confirm the customer's personality precisely. Any individual who knows the PIN and have the ATM card can without much of a stretch access the client account. Figure1. ATM. This paper depicts another strategy consolidating with the customary technique. Here RFID and GSM is utilized to improve the security of the transaction[2][3]. To beat the detriments of embeddings the ATM card into the ATM machine, RFID card is utilized. It peruses the client data by detecting and it additionally oversees various banks accounts in a solitary RFID card. The GSM is utilized to improve the security by giving OTP and furthermore illuminates the client by a SMS on the off chance that the entered secret phrase isn't right.

The Internet of Things (IoT) is a game plan of interrelated handling contraptions, mechanical and automated machines, things, animals or people that are outfitted with exceptional identifiers and the ability to move data over a framework without anticipating that human-should human or human-to-PC affiliation. The IoT is a beast arrangement of related things and people – all of which assemble and offer data about the way in which they are used and about the earth around them. That consolidates a wonderful number of objects of each sort – from splendid microwaves, which normally cook your sustenance for the right timeframe, to self-driving vehicles, whose eccentric sensors separate fights in their way, to wearable wellbeing devices that measure your heartbeat and the amount of steps you've taken that day, by then use that information to prescribe practice plans custom fitted to you. There are even related footballs that can follow how far and brisk they are hurled and record those bits of knowledge by methods for an application for future getting ready purposes.

2. Literature Survey

2.1. N. K. Ratha, J. H. Connell, R. M. Bolle

Solid client verification is turning into an undeniably significant undertaking in the Web-empowered world. The results of an uncertain verification framework in a corporate or undertaking condition can be disastrous, and may incorporate loss of private data, forswearing of administration, and traded off information trustworthiness. The estimation of solid client verification isn't constrained to simply PC or system get to. Numerous different applications in regular day to day existence likewise require client verification, for example, banking, web based business, and physical access control to PC assets, and could profit by improved security. It is significant that such biometrics-based verification frameworks be intended to withstand assaults when utilized in security-basic applications, particularly in unattended remote applications, for example, web based business. Right now plot the intrinsic qualities of biometrics-based confirmation, distinguish the feeble connections in frameworks utilizing biometrics-based verification, and present new answers for dispensing with a portion of these powerless connections. Despite the fact that, for delineation purposes, unique finger impression confirmation is utilized all through, our investigation reaches out to different biometrics-based techniques.

2.2. Victor Fernandes, Ankita Karia

Persuasive Cued Click-Points (PCCP) is a coordinated assessment of the graphical secret key plan, including ease of use and security assessments, and execution contemplations. The methodical assessment gives an extensive and coordinated assessment of PCCP covering both convenience and security issues. A significant ease of use objective for information based confirmation frameworks is to help clients in choosing passwords of higher security, in the feeling of being from an extended viable security space. This exploration work investigates the chance of planning and building a module that is effectively pluggable into the current validation frameworks being utilized starting at now. The working model is an open source reenactment comprising of all the essential modules to fabricate the validation framework. This framework is constructed utilizing Java and Oracle 10g Express Edition as the database albeit most database frameworks can be utilized.

2.3. Yathiraj GR, Santosh VG, Sushma KR, Muthappa KU

Old style PIN passage component is extensively utilized for verifying a client. It is a well known plan since it appropriately balances the ease of use and wellbeing parts of a life form. In any case ,on the off chance that this plan is to be utilized in an open framework, at that point the structure may suffer since acknowledge surfing assault. Right now, unapproved client can totally or mostly watch the login session .Even the exercises of the login get-together can be recorded which the aggressor can utilize it not long after to get the real PIN. Right now ,propose a canny UI, known as Color Pass to restrict the acknowledge surfing assault so any real client can enter the session PIN without unveiling the legitimate PIN. The Color Pass depends on a somewhat perceptible aggressor model. The exploratory investigation shows that the Color Pass interface is secure and easy to utilize in any event, for beginner clients

3. Existing System

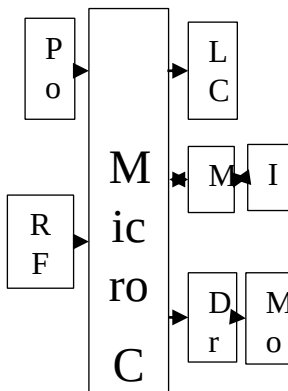
The current ATM Simulation System was worked for the first idea of provincial private banks. Little banks in towns and towns will support the necessities of the nearby network and will just expect records to record account subtleties. This framework is inclined to human blunder and makes undue dissatisfaction clients.

This framework was expanded with the presentation of exceed expectations sheets and messages. Banks could now record all data in an exceed expectations sheet and afterward set an update plan when they will mail all records to a focal center point where these records will again be prepared and merged to frame a brought together record of all record exchanges. These frameworks didn't empower simple access to cash and were extraordinarily inclined to unfortunate mistakes.

4. Proposed System

The proposed framework intends to understand this by steady refreshing of bank records. The Java based development of the framework will empower exchanges at any bank or ATM to be enlisted inside merely seconds. Security of these subtleties is additionally a top need right now. This focal center point will be gotten to by an ATM for secure client exchanges. In our venture we are going to put an additional catch in ATM machines. At the point when that catch gained squeezed the power window will be broadcasted to bookkeeper mobile phone. At that point the bookkeeper can enter the pin and sum physically in his mobiles broadcasted spring up window. By this control framework bookkeeper can keep his pin number with him and he can distribute the sum by his own control by the ideal individual

4.1 Block Diagram



MODULES

- Cloud ATM web UI
- Link generation
- SMS Alert
- Money loading

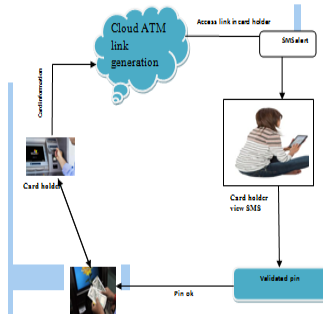
5. Modules Description

5.1 Cloud ATM web UI

Right now have the option to utilize an ATM a client should initially enlist a record number and a The ATM UI comprises of a keypad, a showcase window, a determination of Check Balance. Use cases depict the fundamental grouping situation and records. What's more, this module to utilized for card holder with optional individual

5.2 Link generation

Right now another module the ATM cloud Linker. This module is a simple access for cardholder and gives a total answer for creating the Link Element in a cloud site. It makes for a genuine option in contrast to constrained arrangements that either utilize the mentioned url (consequently not dispensing with copies) or that utilization a static html head incorporation (hence disposing of substance showed by means of question strings) this module access for card holder as it were.



5.3 SMS Alert

SMS alert module sends out alerts to industrial automation, building automation, cloud based link access in cardholder and similar applications, where the timely alert to cardholder are important. Based on the link, it sends pre-configured SMS text to pre-configured mobile numbers.

5.4 Money loading

In this module to provide for in an attempt to provide cash-handling solutions in the field of banking automation, a new ATM (automated teller machine) with cash currency can be customized by simply uploading validation software. In this module used in card holder secondary person

6. Conclusion

This entire execution guarantees us a made sure about and verified exchange through RFID and GSM procedure with most reduced expense and least upkeep. Humanity will use new and made sure about sort of cash exchanges. Interestingly, introductory expense of RFID change of the whole framework is the necessary one time venture. The worth included assistance that this framework gives builds the validity of the budgetary establishments, the banks improves the comfort to its client. Consequently as the world advances through the unavoidable and a dauntless journey for information, the part of security bound frameworks will undoubtedly yield with the developing advancements and clearly more vulnerabilities. Consequently our application may well comprehend the part of exchange security to an exact and extraordinary degree.

References

- [1] G.Udaya Sree, M.Vinusha “ Real Time SMS-Based Hashing Scheme for Securing Financial Transactions on ATM Terminal” ,*IJSETR*, ISSN 2319-8885 Vol.02,Issue.12, September-2013, Pages:1223-1227.
- [2] Khatmode Ranjit P, Kulkarni Ramchandra V, “ARM7 Based Smart ATM Access & Security System Using Fingerprint Recognition & GSM Technology”, ISSN 2250-2459, ISO 9001:2008 Certified Journal, Volume 4, Issue 2, February 2014.
- [3] M.R.Dineshkumar,M.S.Geethanjali,“Protected Cash Withdrawal in ATM Using Mobile Phone”, *International Journal Of Engineering And Computer Science* ISSN:2319-7242 Volume 2 Issue 4 April, 2013 Page No. 1346-1350.
- [4] Zaid Imran,Rafay Nizaami ,”Advance Secure Login”, *International Journal For Science and Research Publications*, Volume 1,Issue 1,December 2011.
- [5] M. Ajaykumar and N. Bharath Kumar,” Anti-Theft ATM Machine Using Vibration Detection Sensor”, *IJARCSSC* Volume 3, Issue 12, December 2013 ISSN: 2277 128X.
- [6] SURAJ B S and Dr. R GIRISHA, “ ARM7 based Smart ATM Access System”, *International Journal on Recent and Innovation Trends in Computing and Communication* ISSN: 2321-8169 Volume: 3 Issue: 5.
- [7] K.annan K, “Microcontroller Based Secure Pin Entry Method For ATM”, *International Journal of Scientific & Engineering Research*, Volume 4, Issue 8, August-2013 ISSN 2229-5518.
- [8] Hyung-Woo Lee,“Security in Wireless Sensor Networks: Issues and Challenges”, *ICACT*, ISBN 89-5519-129-4, Feb. 20-22, 2006.

Mango Image Feature Extraction for Quality Grading (A Pilot Study-1)

T.Kalaiselvi^{1*}, A.Thahira Banu², K.Somasundaram³, P.Veerakumar⁴

¹ Assistant Professor, ³ Professor (Rtd.), ⁴ MCA Student, Department of Computer Science & Applications

² Assistant Professor, Department of Home Science

The Gandhigram Rural Institute (Deemed to be University), Dindigul, Tamil Nadu, India

Abstract

The proposed work developed some feature extraction techniques for mango quality grading systems using image processing operations. The primary features such as size, color, and shape are extracted from the given mango images. The size of the mangoes is counted as the number of pixels within the mango surface. For the color feature, the mango skin color is analysed and used to separate into normal skin and defected skin areas. The shape features such as length and width are measured. They are used to define the mango pose and orientation for further processing. This proposed work supports to development of a machine vision-based learning models for grading the fruit qualities in food processing and agricultural applications.

Keywords: *Mango features, size, color, shape, image processing, quality grading*

1 Introduction

There are 1000 varieties in India; only 20 varieties are grown commercially. Tamil Nadu produces a significant amount of mango that belongs to the Anacardiaceae family. 152569 ha area in Tamil Nadu is under mango cultivation, and the significant districts growing mango are Krishnagiri, Dharmapuri, Dindigul, Vellore, and Tiruvallur [1]. Dindigul district has a horticultural crop area of 102284 Hectares, and mango cultivated in 15741 Ha of land areas [2]. Mango varieties grown in Tamil Nadu include Banganapalli, Bangaloura, Neelum, Rumani, Mulgoa, Alphonzo, Senthura, Kalapad, Imam, and Pasand [3]. The overall post-harvest loss of mango is estimated to be 34.49 percent (8.44 % at the field level, 4.93 % wholesale market, 5.46 % in retailing market, 5.65 % in the storage unit, 3.19 % in processing unit, and 6.82 % in consumers level)[4].

Fruits are sold based on quality for different use. In recent times, fruits have become very important from fruit processors, consumers, and exporters. The grading is the essential step towards a high standard of quality. In practice, manual grading is an expensive and time-consuming process, and labor shortage will affect the operation during peak seasons. It has become increasingly challenging to hire or train a person who is willing to handle the monotonous inspection task and often goes erroneous. These factors led to the search for quick and automated methods for quality grading. With the changing tastes and lifestyles of consumers, and the need to reduce the high levels of post-harvest losses, good post-harvest handling becomes a matter of concern.

Fruits' quality depends on outer parameters (size, color intensity, shape, surface appearances) and inner parameters (sugar contents, acid contents). Still, color and size are the most important factors for grading and sorting fruits [5]. Research on mango quality checking is limited [6].

The proposed work developed some feature extraction techniques for mango quality grading systems using image processing operations—the primary features such as size, color, and shape extracted from the given mango images. The number of pixels within the mango surface decides the size. For the color feature, the mango skin color is analyzed and separated into normal skin and defective skin areas. The shape features such as length and width are measured. They are used to define the mango pose and orientation for further processing. This proposed work supports developing machine vision-based learning models for grading the fruit qualities in food processing and agricultural applications.

2 Method

The proposed method consists of three phases. In phase 1 involves the mango image dataset preparation. The mango image features extracted using image processing operations in phase 2. The features will be analyzed and selected for the machine learning-based grading model aimed at phase 3.

The mango fruit skin features such as mango size, color, shape, and texture are primary features to grade mangos by vendors at markets. In this proposed work, we have used some image processing operations to find the mango surface's primary elements.

The number of pixels observed within the mango contour indicates the size. The color features analyzed using HSV model. The hue components related to yellow, orange and red are concentrated. The mango length and width are measured by finding the central axis and minor axis to shape features. With the mango axis's support, the mango orientation adjusted using geometric transformations such as rotation and translation.

The following procedures used to find the primary features from the mango. The methods given in bold and italic styles are developed by a set of image processing operations.

I. Procedure for Mango Size Detection

- 1) Color image is converted into gray scale
- 2) ***Contour detection technique*** is applied
- 3) The ***region inside the contour*** is counted
- 4) The total pixel is known as mango size

II. Procedure for Mango Color Detection

- 1) RGB is converted into HSV
- 2) The ***hue range related*** to mango colors are selected

III Procedure for Mango Shape Detection

- 1) ***Major axis*** is detected and known as mango length
- 2) ***Minor axis detection*** is done and known as mango width
- 3) Bounding box is drawn for ***mango pose fixation***

3 Results and Discussion

A small experimental study was done to extract the primary features from mangos. In Figure 1(a), a sample image with group of mangoes taken and processed to find the number of mangoes present in the image. The result of the count along with each mango contour is given in Figure 1(b). Gray level images are required for further processing such as edge and contour detection and size calculation. Figure 1(c) shows the converted gray scale image and the detected edges of mangoes are given in Figure 1(d).

The size calculation of each mango in terms of pixel count is done and shown in Figure 2. The colors detected for the mango images are given in Figure 3 and 4. The yellow color extraction is done perfectly as shown in Figure 3(b) and 4(b). Further the color extraction supports to find the defected surface areas as given in block holes in Figure 3(b) and 4(b). The shape of the mangoes measured in terms of length, width and bounding rectangle box are given in Figure 5.

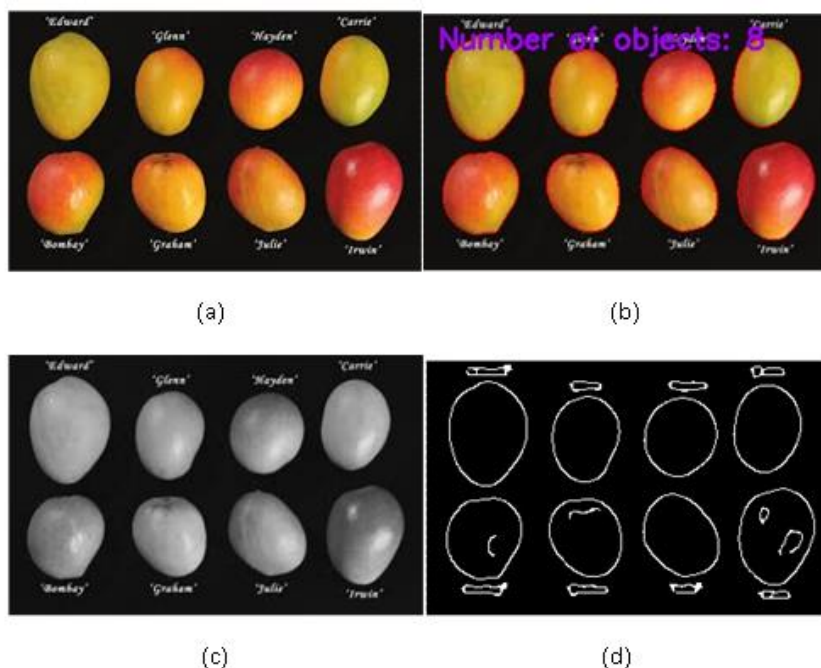


Figure 1: (a) An image with group of Mangoes (b) Detected mango contours (c) Gray image conversion (d) Edge detection

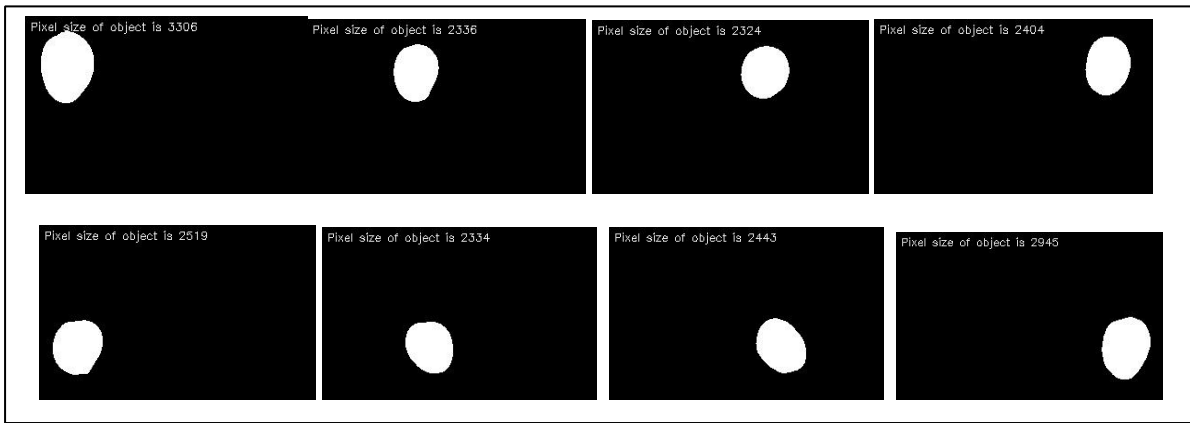


Figure 3: Mango color extraction (a) Original Image (b) Yellow color extraction

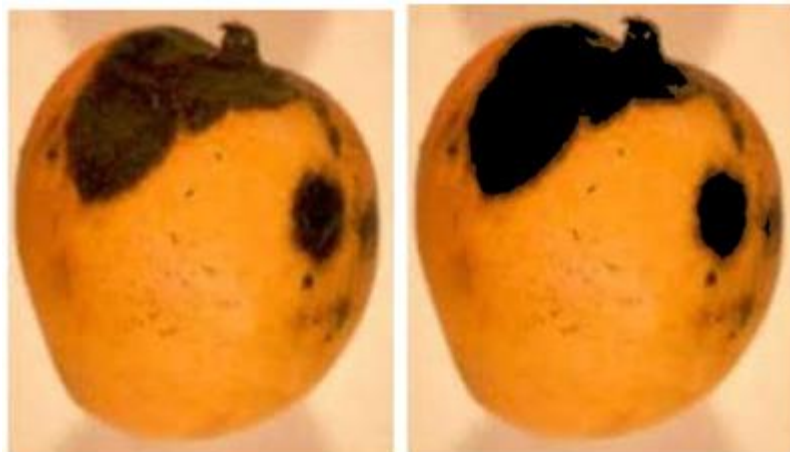


Figure 4: Mango color extraction (a) Original Image (b) Yellow color extraction

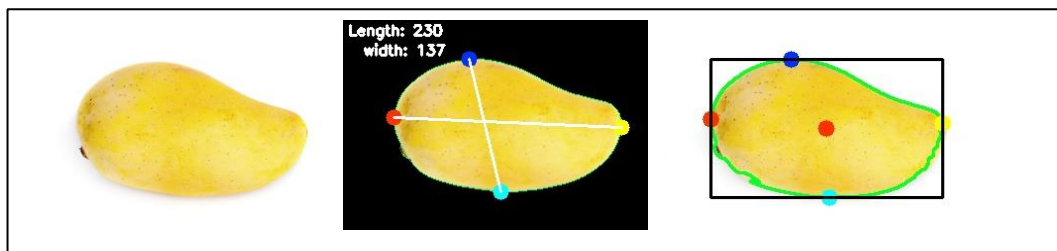


Figure 5: Mango length, width and bounding box

4 Conclusions

In the proposed pilot study, primary features of mango fruit images are extracted and verified with the field experts. The feature extraction is done with the image processing operations towards the quality estimation requirement. In future, machine learning based models will be developed with novel knowledge based image processing operations. This model supports to extract the optimal features based on field experts' requirements.

References

- [1] Department of Horticultural and Plantation Crops. (2020), Agriculture Department, Ministry of Agriculture, Government of Tamil Nadu.
- [2] Nanda, S. K., Vishwakarma, R. K., Bathla, H.V.L., Anil Rai, and Chandra, P. (2010). Harvest and Post Harvest Losses of major crops and livestock produce in India. All India Coordinated Research Project on Post Harvest Technology (ICAR), Ludhiana.
- [3] Retrieved on December 27th, 2020. <https://dindigul.nic.in/departments/horticulture-2/>.
- [4] Moula Sab., Ashok, M. B., and Sudhakara, S. N. (2017). Estimation of Post-Harvest Losses of Mangoes at Different Stages from Harvesting to Consumption. *Int.J.Curr.Microbiol.App.Sci*, 6(12), 310-318.
- [5] Mohammed A. H. Ali, and Kelvin Wong Thai. Automated Fruit Grading System. 2017 IEEE 3rd International Symposium on Robotics and Manufacturing Automation (ROMA).
- [6] Nandi, Chandra & Tudu, Bipan & Koley, Chiranjib. (2013). Machine Vision Based Techniques for Automatic Mango Fruit Sorting and Grading Based on Maturity Level and Size. *Sensing Technology: Current Status and Future Trends II*. 8. 27-46.

Healthcare Management Using Big Data

Vishnu Prakash S, Vibin Gowtham A

Abstract

The information in this document presented at “International Conference on Recent Developments in Science, Engineering and Technology (ICRDSET - 2021)”. The conference would be held at the St. Anne’s College of Engineering and Technology, Panruti during March 5th, 2021. ‘Bigdata’ can make wonders. In the healthcare industry, medical record of patients and hospital records are part of IOT. Research in biomedical industry derives a meaningful information which requires proper analysis and management. Using bigdata analysis with great computing knowledge we can solve a lot of challenges. This is the reason why hospitals are needed to be improved with good infrastructure in analysis for improving the health of public. This also can be a very good financial advantage for the healthcare industry. There can be a revolution in healthcare industry with this bigdata analysis in healthcare.

Keywords: *Biomedical research, bigdata analytics with IOT, healthcare, Quantum computing and Image analysing.*

1 Introduction

The information is the main key for all industries. The level of information we get is always decides the level of outcome. This is the most important reason for collecting data to understand the current trends and future needs. Now we are capable of generating a lot of data in every aspect such as hospitals, weather and development etc., Also we are available with more data which we cannot processed with our current technologies. Every new need should lead to the creation of new technology and this leads to the new term called “Big data”. These technologies must be useful to the society to overcome the present and future difficulties. Healthcare industries are producing tons of data where it can be use for our advantages and meanwhile there are also more challenges. Now in this paper we are going to see how big data need to be used in healthcare industry.

2 Big Data

By the term “**Big data**” we can understand it represents a large amount of data. It cannot be processed by traditional computing systems or internet-based software. Even though there are lot of definitions about big data, the definition was given by Douglas Laney is well accepted. According to him big data is growing in three dimensions such as velocity, volume and variety.

Big data has become popular in very recent years in every field like research and development, academics etc., for generating and analysing tons of data. There can be organised and unorganised data which cannot be processed by traditional software. For that we need to develop advanced technologies and high-end-computing tools for such tasks.

It is necessary to implement the algorithms of artificial intelligence and novel fusion to process that huge data. Along with this it would be great achievement to make automatic decisions by implementing machine learning techniques. With proper tools and data, the analysis must be very effective.

2.1. Big Data in Healthcare

Healthcare is an industry which must prevents, diagnosis and treat the diseases in human beings. The major components of healthcare industries are professionals (like doctors, nurses) and specialised hospitals. The healthcare professionals should provide accurate information about patient’s medical history and their medial data like imaging the laboratory examinations.

Using computers, the patient records are being digitalised nowadays. The term “**Electronic health records**” came from National academics of science, engineering and medicines in 2003. It is used to diagnose the patient’s health and relate the data from past and present. There are many advantages using EHR to handle the modern-day healthcare records of patients. The first advantage is that the entire medical history of patient like treatment, medicines and lab records can be accessed by the doctors. The faster accessing the medical data of patient leads to decrease the time. By reducing the time, we have observed a decrease in many vigorous diseases, also can have additional examinations and can decrease the error occurred due to illegible handwritings. With this EHR there can be a periodic examinations and greater interaction between professionals and patients by setting a periodic reminder. EHR also leads to increase

the quality of many healthcare insurance programs and costs of insurance benefits. EHR and internet provide valuable information for saving lot of critical patients.

2.2. Digitalisation of Data

EMR refers to Electronic Medical Data used to store the medical records in the computer systems. There are many components like EMR, EHR and MPM (Medical Practice Management) have the capability to improve the quality, services efficiency along with reduction in costs with reduces medical errors. The usage and management of this data must be dependant on IT.

The momentum has gained by the healthcare professionals by monitoring and using related software for analysing the medical records of patients. The tons of data provided by these devices need to be analysed to provide proper real-time medical care. This seems to be promising for improving the medical facilities and reducing cost.

2.3. Biomedical Using Big Data

A biological system is a very complex system which consists of human cell and that exhibits many events in that. In order to understand that components and events various research like biomedical or biological research are used. The research usually gathers data about the components and the events and it requires multiple experiments. This show the greater data we get, the greater we understand the biological process. This leads to modern technologies which achieved the integrating of quality technologies like NGS and GWAS that none can imagines the data generated to decode genetics.

Although the Next-Generation Sequencing provides data, it is not accessible previously. Now it is taken to a new dimension due to big data. From several experiments in “genomics” and “transcriptomics” they provide a lot of data with more information in their studies to acquire novel insights. Managing and analysing the such data can be very effective in healthcare industry.

3. IOT (Internet Of Things) And Its Advantages

When we compare with other industries, Healthcare related industries are not efficient in adapting to big data movement. Due to this reason, Healthcare sector can't utilize the benefits of big data. So, it still remains in its initial stage. Example such as unavailability of molecular pathology which is a by-product of combining big data and healthcare to improve service related to healthcare. The above-mentioned combination can be used to establish some different action mechanisms or aspects related to predictive biology. So, in order to examine an individual health status, maintaining clinical and bio molecular datasets is important.

Here IOT comes in the play for providing clinical data sets. Stating the fact that IOT becomes one of the big things which is implemented in various industries which also includes healthcare industries. The commonly used objects like wrist watches, cars, bikes, fridges and other devices which are used for health monitoring purposes are not able to create or process data and mainly they don't have internet connectivity.

Using IOT devices, the doctors have the extra advantage of measuring or monitoring his/her patients in their respective locations (either Home/Office) which reduces the travelling hurdle. Eventually, it reduces the burden of becoming hospitalized or it might even reduce healthcare expenses related to doctor visiting charges fitness bands, health tracking wearable's, bio sensor and so on come under this category. They can be able to produce large amount of data related to health care.

By integrating the gathered data into already existing data related to healthcare like EMRs or PHRs. It is easy to predict the status of patient and the progression from its early stage to pathological state. It states the most important fact that the data collected from IOT is most useful in various aspects and they provide better predictability and helps in various investigations. The Main advantage is that the data collected from these devices help us to monitor personal health of patients, to model the spread of a disease and controlling the spread of a contagious disease.

3.1. Analysing And Managing The Big Data

Big amount of various data which is produced at a rapid rate is called big data. The gathered data is mainly used for improving services to customers and restricting customer consumption. It also holds stable for big data gathered from biomedical research and healthcare. But it comes with a big challenge which is maintaining this huge capacity of information. The data has to be stored in a file format which has easy accessibility and readability for scientific community to analyse efficiently. In continuation with the above challenge, Health care data comes with another major problem which is the requirement of highly

powerful computing tools, protocols and high-end hardware in the prescribed setting. Professionals from different areas like it.

Professionals, doctors, statistics and maths are collaborated in order to reach this destined goal. The collected data from the sensors can be stored in a cloud storage along with some specific software tools created by analytic experts. Then AI experts develop some tools with specific data mining and machine learning algorithms which can transform the stored data information into specific knowledge. On implementing this we can improve the efficiency of gathering, storing, processing and displaying healthcare from big data.

The objective is to explain, combine and display very complex data in a respective way for understanding better. If it fails to do such operations, then the biomedical experts can't proceed further with the unorganized massive data. Then computer graphic designers develop specific tools for visualizing purposes (displaying) to showcase the newly produced data. It is not so useful for conventional aspects due to the difference in the type of data. The relatively large amount and different nature of healthcare related big data. To achieve machine learning and Artificial Intelligence in healthcare big data, Advanced Algorithms need to be implemented. Mostly Python or R programming languages are mostly used for big data in health care. People with good knowledge in IT and biology is needed for processing the big data. Such talent suits for bioinformatics. The common platforms used to process the big data are Apache spark and Hadoop.

4. Hadoop And Apache Spark

Loading huge amount of data in the hard disk of the is not efficient in performing big data. So, the best process is that distributing and processing the data in the multiple nodes. These data are large in size, so that many computer tools are required to process the big data with in given time. When working with these many amounts of system, it is difficult to handle the computations and failures. Hadoop is open source distributed application used for this purpose. Hadoop uses MapReduce algorithms for generating and processing large datasets. MapReduce is used to map the record in the input to a set of pairs and reduce the operation for all the same kind of records. It reduces the difficulty in handling the computation process and failures. Hadoop Distributed File System is used to provide the efficient, organised and replica-based storage data to form clusters. Many popular organisations like Yahoo, Facebook and Google use Hadoop to enhance the processing of data and storage system. Many large projects like correlation between quality of air and asthma admissions, drug development and many other healthcare industries are implementing Hadoop. Therefore, with these modern tools, healthcare analytics will not be held back.

Apache spark is an alternative to Hadoop. It is an incorporated engine for distributed data processing consists of higher-level libraries which can support SQL queries, machine learning algorithms and graph processing. These libraries increase developer productivity because it requires fewer coding efforts and can also create a multiple type of computations. By implementing RDD in memory processing, it can make spark 100 X than Hadoop in analytics. When memory size is more than the data size, it is very true. This indicates processing the more data requires a huge amount of memory. MapReduce is used to reduce the cost of memory for large datasets than the Apache spark. Apache storm was developed simultaneously, which can provide real-time framework for data processing. It supports many programming languages, also it is built-in-fault-tolerance capability and horizontal scalability for analysing the big data.

4.1. Extraction, Analysis And Predictions:

In hospitals, patient record consists of lab records, scan reports, health records and prescriptions. The EHR's records are digitalized into machine-readable format. Such datasets consist of more valuable information which can be processed by AI programs to take necessary steps for patient with critical health records. At first, AI is emerged as the application for big data in medicine. This system is very quick in decision making in diagnosis if diseases. For targeted abnormalities, healthcare professionals can use appropriate ML approaches to analyse the data. AL and ML techniques are used to refine the healthcare industries data processing potential.

We can extract valuable information in healthcare industry using Natural Language Processing. NLP is nothing but is an area in ML which can useful in speech recognition and identify the key syntactic in the text. Using ML system's image processing techniques, we can make automatic decision making in diagnostic system. Though healthcare professionals cannot be replaced by near future, it can assist them to make clear clinical decisions.

4.2. Accuracy And Image Processing:

Some recent studies have showed that reporting big data in EHR's or EMR's is not at full accuracy yet, because of complex workflows and misunderstanding of why big data need to be capture well. All these can be the draw backs in the big data analytics to sustain long. The EHR's quality need to be improved by good communication in the clinical workflows, though clinical reports show some discrepancies. The documentation quality needs to get improved by clearly understanding the patient's symptoms.

Image processing in healthcare is for CT, MRI, X-ray and ECG. The professional cannot find the observe and diagnose the condition which is still emerging. In these situations, image processing can make an impact on healthcare by diagnosing the disease from the biomedical images. These techniques use pattern recognition and ML for decision making and improve the diagnostic capability for decision making in medical imaging. Many software tools have been developed for image processing based on functionalities visualisation, reconstruction, segmentation and diffusion in order to find out the hidden information. Visualisation toolkit is usually available software which performs powerful processing and analysis the 3D medical images.

Also, Studies showed that various factors can alter the data quality and interpretation in data quality. Medical images can suffer from multiple types of artifacts and noises. Improper image handling leads to delineation of veins and arteries which is not relative with real time scenario.

5. Quantum Computing

Big data can be very huge in size. So, it is difficult for analysing even with the very powerful computing machines. For most of the analysis, it is based on the size of the memory and not in the processor. Super computers are increasingly developed with the requirements like latency in the memory, the capacity and the bandwidth. Quantum technique approach is an additional solution for the big data analysis. The common digital code for computer is binary digital code, but in quantum computation we use qubits or quantum bits. A qubit can represent a zero or one or any linear combination of states. So, qubits allow computer bits to operate in three states not like two states in classical computation. This is the reason why quantum computers are thousand times faster than the normal computers. For n points datasets conventional analysis need 2^n processing units, in quantum computing techniques it need only n processing units. Quantum computers need superposition and quantum entanglement to perform computational techniques.

Quantum processing can quick up the big data analytics process. Some problems seem to be unsolvable using conventional computers, but it can be possible using quantum computers. Some current encryption techniques such as Data Encryption Standard (DES) and Public Key look like impassable, but in future it would get through by quantum computers. Quantum computers require a very minimal number of datasets, when compared to conventional computers. Although there are open challenges and infancy in quantum computers, it is even implementing in big data.

5.1. Applications

Quantum computers look to be the greater solution for big data analytics. At Large Hardon Collider (LHC), production of Higgs Bosons will now be performed by using quantum computers. Collisions of huge data (1PB/s) will get filtered and analysed by quantum computers at LHC. Quantum annealing for ML (QAML) implements the combination of quantum computing and ML to help the human intervention and improve the assessing accuracy of particle-collision data. To classify data, quantum implements both training and classification stages. In many areas of science, such approach could get some applications. There are some applications of quantum approaches in healthcare like quantum sensors and quantum microscopes.

6 Conclusion

Now-a-days biomedical and healthcare industry generates huge amount of data which should be analysed and processed using big data. By the review of this paper patient specific medical speciality is under way. The companies who are working for healthcare industry and biomedical industry providing very effective and quality outcome. The ideology of these companies should be developing effective clinical

decisions, reducing the cost of analytics and will be platform for greater strategies. This is also helped to build a better personalised healthcare framework.

From super computers to quantum approach, they help to better understanding and reducing the time. Despite the infrastructure challenges, the healthcare industries are going to improve along with biomedical research industries using big data. There is leverage gap between structured and unstructured data which is well known hurdle to overcome in big data. It will show a significant impact in performance and decision making in healthcare industry. The tremendous growth of medical data has forced computational experts to design a technology to analyse and process such data.

The computational integration of research and healthcare industry will result in signified growth. The greatest feature present in big data is provides limitless possibilities. The advancement of birth and development of big data is ranging from health records management to drug development including neurodegenerative disease and cancer. We believe that big data will be will be an add-on, instead of replacing manpower. The structured information can lead to population health information in future health care. Therefore, we can understand big data will facilitate the healthcare industry with image processing, decision making, early warning of diseases and improve the strategies for quality of life.

References

- [1] Lanley D, Stamford Meta group;2001, controlling velocity, data volume and velocity, Application strategies.
- [2] Mauro AD, MA Grimaldi, Greco, A formal definitions of big data based on its essential futures.65(3): pg no.122-35
- [3] Reiser SJ, The clinical records learning from cases: 114(10):902-7.
- [4] Murphy G, Waters K, Hanken MA, Electronic Health Records: Changing the vision. Pg no. 627
- [5] Ezzati A, Saouabi M, A comparative between Hadoop Mapreduce and Apache spark on HDFS ACM:2017, pg.1-10.
- [6] Martin K, Schroeder W, Lorenson B; The visualisation toolkit 2006.
- [7] Chaung IL, Nielsen MA, Quantum computation and quantum information; 2011, pg. 708.
- [8] Woodward A, Buchanan W, Will quantum computing be end of the public key encryption? Cyber technol. 2007, 1(1); 1-22.

Speech Recognition Using Python

¹K.Shobikaa, ²K.Santhiya, ³R.Suguna
^{1,2}B.E. Computer Science and Engineering, ³Assistant Professor
 Department of Computer Science and Engineering
 Bannari Amman Institute of Technology, Sathyamangalam – 638 401,
 Erode, Tamilnadu, India

Abstract

Nowadays, Speech Recognition has become an increasing concept and popular in recent years. If the document to be written is too long, it is difficult to type within the given time and it makes the user bored to type. And also reading text is difficult for the people who have Dyslexia and other inabilities. Speech recognition helps the computer to translate the speech signal into text or commands through the detection and comprehension process. By the help of Speech Recognition, it makes the user time flexible and allows them to create the documents by recognizing the voice as an input and the document will be created faster as soon as possible when compared to a person typing the document. Speech Recognition involved in many fields like psychology, signal processing and even body language of humans. The main objective of speech recognition is to attain normal communication between human and the machines. In this paper we explain how the voice has been recognized and how it will be translated into text by the requirement of the end user and also the problems faced at the time of implementation. Using a microphone, we can get the user's input and PyAudio converts speech to string

Keywords: *Speech, Recognition, Communication*

1 Introduction

Speech is the most common means of communication around the world. Most of the population in the world relies on speech to communicate with each other. Suppose we are building a model and instead of a written approach we want our system to respond to speech, it becomes fairly difficult and requires a lot of data to be processed [3]. A speech recognition system overcomes this barrier by translating speech to text. Language is the medium of communication. Speech is the important tool for communicating between humans to each other [1]. Communication has been practically complete up to now by the use of display screens and keyboards, but for easy and efficient communication, speech is preferred. Speech recognition is a machine module which is done with the process of identifying, understanding and describing the input voice by the attributes of physiology, psychology and way of speech. It automatically understands the human spoken language by pattern recognition and signal processing [1][2]. It is also related with acoustic models, linguistics theory and pattern recognition theory. Speech Recognition is also known as automatic speech recognition. Speech Recognition mainly helps the people with disabilities by leaving them to speak and converting the speech into text. Speech Recognition is one of the emerging technologies in information technology. Unlike images, speech has some constraints that it should be either created by the vocal track of human beings or pre-processed by the machines [2]. PyAudio module is used to get the speech from the user through microphone and converts speech into a string (text). Speech recognition system basically translates the spoken utterances to text. There are various real life examples of speech recognition system. For example- siri, which takes the speech as input and translates it into text [5]. The advantage of using a speech recognition system is that it overcomes the barrier of literacy [5]. A speech recognition model can serve both literate and illiterate audience as well, since it focuses on spoken utterances. We can also make an inventory of all the endangered languages around the world using a speech recognition system. While it looks pretty intriguing and not complex at all, a speech recognition system faces a lot of challenges in the making. Every individual person has a varied style of speaking, including accents as well. As we all know, we have different accents for speaking English too. There is American English, British English and so many other accents when it comes to speaking the most common language in the world [5]. Pronunciation also makes it difficult for a speech recognition system to translate the speech altogether. Environment adds a lot of background noise to the system as well. An isolated room compared to an auditorium will have a lot a variability in background noises. Even echo can add a lot of noise in the system as well. An old person's voice may not be the same as that of an infant. The characteristics of a person's speech depends on many factors including the harshness and clarity as well. Some spoken utterances may not have a viable meaning when it comes to translation [6]. After overcoming these challenges, it is fairly achievable for any speech recognition system to translate speech to text. Now that we know how speech recognition works, let's take a look at different packages that are available for speech recognition in python. Using Speech Recognition and the PyAudio module in python, speech can be easily converted into text. Speech recognition technology is one from the fast growing engineering technologies. It has a number of applications in different areas and provides potential benefits. Nearly 20% people of the world are suffering from various disabilities; many of them are blind or unable to use their hands effectively [3]. The speech recognition systems in those particular cases

provide a significant help to them, so they can share information with people by operating computer through voice input [4].

2 Literature Survey

2.1 Robust Speech Recognition

Mazin G. Rahim et.al [1] created a signal bias removal (SBR) method based on the calculation for reducing undesirable effects in speech recognition systems such as distortion of channels, ambient noise. To diminish the acoustic mismatch, Maximum Likelihood (ML) stochastic matching approach is used. This approach is used between a set of speech models and was projected in [2] to reduce the recognition performance degradation. Wolfgang Reichl [3] has characterized strategies for moving forward acoustic modeling vigor and precision utilizing choice tree-based authoritative state. Xiong Xiao [4] has a novel strategy that normalizes the balance spectra of discourse signals. Giuluva Garauet.al [5] has explored the expansive lexicon of persistent discourse acknowledgement.

2.2 Noisy Speech Recognition

Mark D.Skowronski [6], introduced a resound state organized classifier by combining ESN with a state machine system for boisterous discourse recognition. Xiaodong [7] proposed a novel approach which is used to make strides in the acknowledgment execution in boisterous situations by using multi condition preparation. Jianping Dingebal [8] have given a new approach for discourse highlight upgrade within the expansive ghasly space for NSR.

2.3 Data Driven Approach

Jen Tzung Chein [8] has done a sequence of model selection approaches and gives Predictive Information Criterion (PIC) for hidden Markov model (HMM) selection. They have suggested top-down approaches of structural hyper-parameters for calculation. PIC builds a compact tree structure. Pornchai Chanyagorn[9], proposed the information driven flag decay strategy based on the Experimental Mode Deterioration (EMD) technique. The output can be used to analyze the nonstationary signals

2.4 Tamil Speech Recognition

A.P.Henry and Charles [10] construct upgraded discourse acknowledgement in Tamil with speaker independent, device free framework with persistent acknowledgement. Here the talked sentence is spoken to as grouping of autonomous acoustic phonetic units. The framework recognizes the talked questions within the setting of numerous applications as web browsing. R. Thangarajan, A.M. Natarajan and M. Selvam [11] proposed a medium lexicon triphone based nonstop discourse recognizer for Tamil dialect.

3 Proposed System

In this paper, we use Speech Recognition module to recognize the voice and to get the input from the user PyAudio is needed. To install Speech Recognition package is python, run the following command in the terminal and it will be installed on your system. Another approach to this, can be adding the package from the project interpreter if you are using pycharm. The package has a Recognizer class which is basically where the magic happens. It is basically a class which is used to recognize the speech.

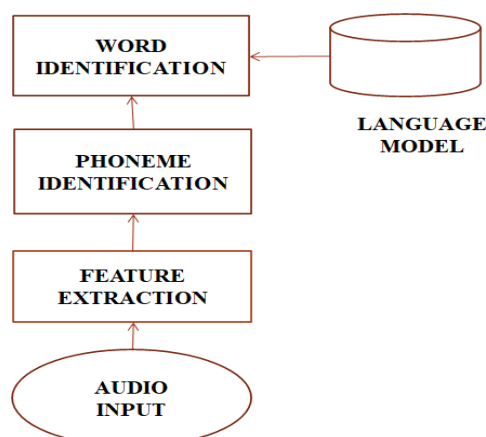


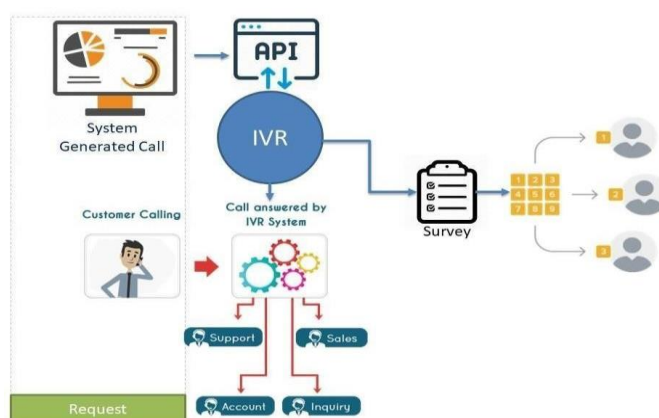
Fig 3.1 System Flow Diagram

From the above flow-diagram (Fig 3.1), it is to define how the process is going to execute. Speech voice has been received through microphone and it will be analysed by the attributes like language model and acoustic model. The next step is word identification whether the expressed word is valid or it is present in the provided dictionary or dataset. After that we check the phoneme identification. In phoneme identification, we check the sounds and sets of similar sounds are grouped together and finally extracts the output based on human voice characteristics and by understanding the context. Here, we have used 2 instances of Recognizer (). One for getting audio input from the user. Another for specifying web pages. Exception is implemented along with the code to avoid error and request-response failure.

4 Applications

4.1 Automated Call Distributor

IVR technology is ready and waiting to introduce automation that will help your business route incoming calls more quickly and efficiently. In the below figure (Fig. 4.2), we explain Interactive voice response systems by implementing this module.

**Fig 4.1 Interactive Voice Response System**

From the above figure (Fig 4.1), the system generates the call and the call will be responded to by IVR systems and customer calls to IVR. This system is handled by separate assistance and all this response has been taken as a survey and it will be distributed

4.2 Medical Documentation

In the health field Speech Recognition is more useful to write and retrieve the patient's record in an easy manner and it also makes communication between different departments in a hospital. For example after ECG has done, the records and values are conveyed to the attending doctor by Speech.

4.3 Banking

In the banking sector it will reduce employee stress and it boosts customer satisfaction. Request bank status without turning on the cell phone and receive information about transaction history and so on.

5 Implementation and Result

5.1 Implementation

5.1.1 Speech Recognition

Speech recognition mainly consists of pattern matching or processing. The voice which is through the microphone will be unknown, it will be converted into electrical signals for the identification of language models and establish a voice model based on voice characteristics of humans and extracts the required output on the basis.

Packages for Speech Recognition are,

- Speech Recognition
- Google_speech_cloud
- Pocket sphinx

Speech Recognition has separate Recognizer classes. Those consist of several methods which can read various audio sources.

(i) recognize_bing()

Uses Microsoft Bing Speech API to perform a conversion of audio file to audio data object.

(ii) recognize_google()

Perform speech recognition on audio data using Google Speech Recognition API and it also generates a specific API key.

(iii) recognize_google_cloud()

Powerful Speech Recognition which recognizes more than 120 languages and variants to support. It can also process the real-time streaming.

(iv) recognize_houndify()

It performs both recognition and understanding the language. Various operations can perform by using the option "Speech to Text Only".

(v) recognize_ibm()

It is the same as recognize_google() but it has the support of IBM Speech.

(vi) recognize_wit()

It performs speech recognition using Wit.ai API. These are not available without signup for an account.

(vii) recognize_sphinx()

Performs speech recognition using CMU Sphinx.

5.1.2 Pyaudio

Python provides this binding module to play and record audio on a variety of platforms. It is binding for PortAudio v18 API. It gets the input speech from the user and converts it into text (string).

5.1.3 Web Browser Module

This module is used to allow documents to display to the end user. This will work only when the open() function is included and the default browser starts and searches the URL given by the user. It provides high level interface.

5.1.4 Microphone

Microphone is also called a sound sensor, which is used for audio input. This module is to detect and record sound by analogue input from the microphone.

5.2 Result

1. The below figure (Fig 5.2) is the python program in which Speech Recognitions implemented. The code is implemented for directing web pages

```

1 import speech_recognition as sr
2
3 import webbrowser as wb
4
5 r = sr.Recognizer()
6
7
8 with sr.Microphone() as source:
9     print("Speak now!")
10    print("Search youtube")
11    audio = r.listen(source)
12
13 if "youtube" in r.recognize_google(audio):
14     url = "https://www.youtube.com/"
15     with sr.Microphone() as source:
16         print("Search your query")
17         audio = r.listen(source)
18
19     url = r.recognize_google(audio)
20     print(url)
21     wb.open(url)
22     wb.open(url)
23     print("Success")
24     except sr.UnknownError as e:
25         print("Failed", format(e))
26
27 if "python" in r.recognize_google(audio):
28     url = "https://www.youtube.com/watch?v=pythonhouseofsecrets"
29     with sr.Microphone() as source:
30         print("Search your query")

```

Fig 5.2 Python Implementation

2. After running the code, by displaying the command ‘speak now’, it asks us to speak i.e., we have to say either we need a web page or YouTube page (Fig 5.3).

```

Run: scratch_2 x
C:\Users\Admin\PycharmProjects\text_recognize\venv\Scripts\python.exe C:/Users/Admin/.PyCharmCE2019.1/config/scratches/scratch_2.py
[search edureka : search youtube]
speak now

```

Fig 5.3 Python Implementation

3. Next, it asks for a query by displaying the command ‘search your query’. One should give hint words related to the particular page (Fig 5.4).

```

Run: scratch_2 x
C:\Users\Admin\PycharmProjects\text_recognize\venv\Scripts\python.exe C:/Users/Admin/.PyCharmCE2019.1/config/scratches/scratch_2.py
[search edureka : search youtube]
speak now
search your query
python

```

Fig 5.4 Python Implementation

4. Finally, it redirects to the particular web page. The URL of the page is given in the code (Fig 5.5).

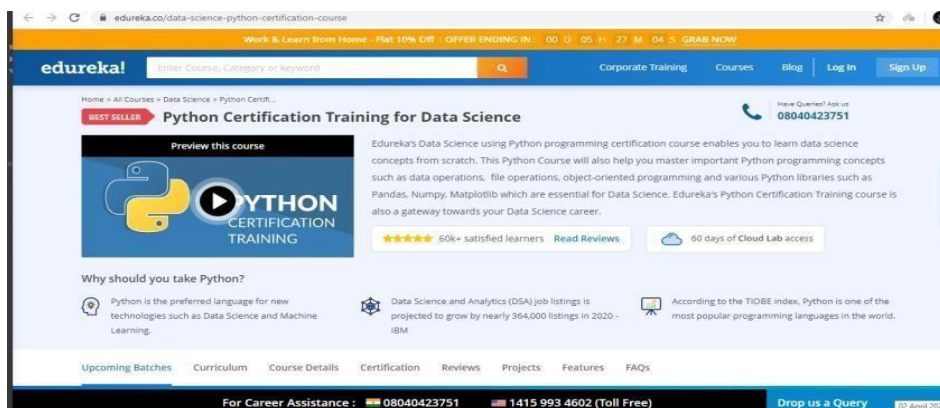


Fig 5.5 Implementation Result

5 Conclusion and Future Work

Speech is the foremost unmistakable and essential mode of communication between people. Speech Recognition helps to improve the efficiency and higher accuracy of feature extraction. It also plays a major role in physically challenged people's life and makes their life easier. Speech Recognition is useful for everyone because it saves time in typing the content. As it created a technological impact on the environment, it is expected to further flourish in the field of human machine interaction. We can further enhance Speech Recognition concept by using Artificial Intelligence. Artificial Intelligence would give better accuracy without any disruption.

References

- [1] Sanjivani S. Bhabad Gajanan K. Kharate International Journal of Advanced Research in Computer Science and Software Engineering , An Overview of Technical Progress in Speech Recognition Volume 3, Issue 3, March 2013.
- [2] B.Lowrre, 1990, The HARPY speech understanding system ,Trends in Speech Recognition, W.Lea,Ed., Speech Science Pub., pp.576-586.
- [3] Anusuya, M. A., & Katti, S. K., Front end analysis of speech recognition: A review. International Journal of Speech Technology, Springer, vol.14, pp. 99–145, 2011
- [4] Melanie Pinola (2011-11-02). "Speech Recognition Through the Decades: How We Ended Up With Siri".
- [5] J.W.Forgie and C.D.Forgie, 1959, Results obtained from a vowel recognition computer program , J.Acoust.Soc.Am., 31(11),pp.1480-1489.
- [6] L A Liporace.Maximum Likelihood for Multivariate Observation of MarkovSources, IEEE.Trans. IT, 1982, 28(5): 729-734.
- [7] Michael Nielsen,"Introduction to Statistical Machine Translation", Tata McGraw Hill Publication, 2017.
- [8] David M. Beazley, Python Essential Reference, 4th edition, Addison-Wesley Professional, Jun 29, 2009
- [9] Radio-Electronics website [Online]. Available: <http://www.radio-electronics.com/info/wireless/bluetooth/radio-interface-modulation.php>
- [10] Paul Ferrill, Pro Android Python with SL4A, Apress, Jun 26, 2011
- [11] Rabiner, Lawrence R, and Biing-Hwang Juang. 1993. Fundamentals of Speech Recognition.Vol. 14. PTR Prentice Hall Englewood Cliffs

Guarded Electronic Voting System Using Blockchain Technology

Parameshwari.V, Sajitha banu. M, Ramya. A
Department of Computer Science and Engineering,
Annai Teresa College of Engineering, Thirunavalur.

Abstract

The voting process takes the significant part of every countries and their citizens. Digital recording electronic systems are implemented replacing the paper ballots. Now a day, the election commission uses Electronic voting machines which need more power, time-consuming and also they are less trusted. The most issues which is faced by the Election Commission is No proper confirmation regarding the acknowledgement of casting the ballots, illegal casting and missing of outside people vote who belong to native constituency. The Electronic voting system caters for integrity of the polling process in terms of the requirements. This paper focuses the embedded in the design of process in well-secured authentication processes for the electors information such as fingerprint are will be match with database through the use of biometrics. Of utmost importance are the requirements for correctness, robustness, coherence, consistency, and security. In this paper, to develop the online voting is more ease way to poll the ballot for the outside people from their location. A new polling process which makes use of block chain technology which has improved trustworthy and transparency over currently used systems.

Keywords: *Biometric, Blockchain, Electronic voting system, Fingerprint*

1 Introduction

Voting system plays a vital role in countries “vote” means to choose a better candidate who is participating in the election. The process of choosing a leader in all the candidates from a list by casting their votes is called voting. Election allows the populace to choose their representative and express their preferences for how they are governed. Voting is very effective way to reveal opinion about a issue or subjects from a group of people based on the promise of greater efficiency, better scalability, faster, speed, lower cost and more convenience. In all earlier elections of India such as state or central election a voter his/her vote my making with stamp against their chosen candidate and then folding the ballot paper as per a prescribed method, before dropping it in the ballot box. This is a time consuming and very much prone to errors. In today’s world due to advance technology and rapid growth of mobile technology the old voting methods can be changed to the advanced technology. The online voting system provide a convenient, easy and efficient way to vote.

2 Background Research

This paper [1] deals with the homomorphic encryption method is able to perform operations of encrypted data without decrypting them. In this work we focus on the application of homomorphic encryption method on the cloud computing security, particularly the possibility to execute the calculations of confidential data encrypted without decrypting them. This paper [2] deals with the voting is a fundamental part of democratic system, it gives individuals in a community the faculty to voice their opinion. In recent years, voter turnout has dimensioned while concerns regarding integrity, security, and accessibility of current voting systems have escalated. E-voting was introduced to address those concerns. The block chain is an emerging, decentralized, and distributed technology that promoted to enhance different aspects of many industries. This paper [3] discusses about the secure verifiable ranked choice online voting system based on homomorphic Encryption. It requires each voter to sign their ballot using digital signature Algorithm (DSA). In this system the main concern is given to the confidentiality and security to the votes. here the security and performance analysis not only confirming the feasibility, but also here demonstrating the improvements achieved in the voting system. This paper [4] discusses the biometric based voting system. They are using the biometric verification to enhance the security and safety of voting process to avoid the electoral frauds. After successful voting, server will be updated and GSM module will get activated and using the phone number which is stored in voter’s database, it will send a message of successful voting to the voter’s phone. When last voter cast his vote. This paper [5] describes, The Arduino based fingerprint Voting System. We know Arduino is the open source electronic prototyping platform enabling users to create interactive electronic objects. Here Arduino of ATmega328 is used. In this system also we have create database for all the citizens. Here one database for the one district. There will be central database where it can control the database. It is offline version of electronic based fingerprint voting system using Arduino. The paper [6], describes the RFID based voting system. Where the system deals with the use of RFID, Microcontroller and GSM technology for the improvement

of election process by avoiding the electoral fraud and to ensuring the reliability, security, safety, transparency and guarantee for the smooth conduction of election. The GSM module that is used in this system is SIM900A. It has a built in RS-232 which is an added advantage and also provides the user to insert SIM. This paper [7], describes the mobile bases facial recognition using OTP verification for the voting process. It is verified by user identity in the software. Id is valid on that day only and password is encrypted using MD5 algorithm, then application will capture the face of the voter using mobile camera and compares it with already stored face of the voter. In this methodology is used by OTP based technique. For security sake his session id is destroyed and password is encrypted using MD5 algorithm. All the votes casted by voters are stored in the server, just by seeing it election officer can easily announce the election result. This system provides the high security in voting process.

3 Proposed System

In this paper focuses the online voting using Biometric technology and Blockchain technology. In this proposed system they are develop biometric verification to enhance the safety and secure of voting process using Mobile Application and the votes are secured by the Blockchain technology. The Election Commission has own records of each citizen like fingerprint, Address of the elector, Age and their contact number. This paper implemented by electors has split into the two categories like,

1. Android users (voting through online)
2. Polling station users (voting through polling booth)

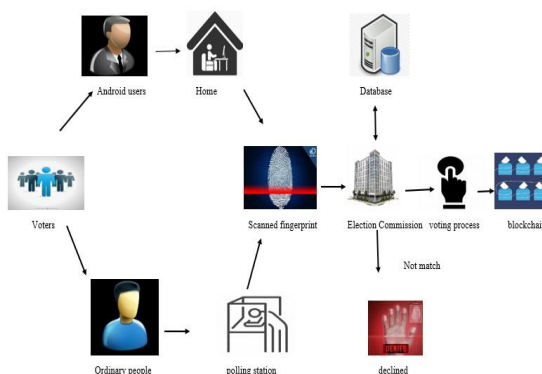


Fig 1. Block diagram

3.1 Authentication

On the day of election, elector has to login the Mobile Application through online, firstly voter has input their fingerprint, it will compare with fingerprint which is stored in database for the verification. After the successful fingerprint verification, then allow to forward procedures. The detail of the candidate that shows on the GUI (Graphical User Interface) candidate names and their party symbol is displayed. Otherwise the we choose the favorable candidate by casting the ballot. The ballots will be updated on the consist database. The voters to ensure their ballots are secure and authentication, by receive the Short Message Service (SMS) to their own contact number. In the election day, without the using mobile application, they are casting their votes through polling station. While using the polling station they enter the verification section, the proofs like Aadhar number, fingerprint and contact number are correct or true. To allow the casting votes by using the Electronic Voting Machine (EVM) in other side it will connected by the web source of application. By casting the ballots, the votes are stored in respective database. The usage of application-based method it will reduce the time-consuming, and cumulate the votes to avoid the electoral frauds.

3.2 Confidentially

The paper implemented by the blockchain technology for confidentially and stealthy purpose. The anonymity fear of electors is cleaned by the Blockchain technology will make ensure the security with high confidential. In this technology ability to engage and manage a constituency is crucial to the future of society, not just to produce a transparent outcome but to encourage all people to participate in their communities.

3.3 Blockchain Technology

Blockchain is one of the emerging technologies with strong cryptographic foundations enabling applications to leverage these abilities to achieve resilient security solutions. It is primarily a distributed decentralized database that maintains a complete list of constantly growing data records secured from unauthorized manipulating, tampering and revision. Blockchain allows every user to connect to the network, send new transactions to it, verify transactions and create new blocks. Each block is assigned a cryptographic hash (which may also be treated as a Fingerprint of the block) that remains valid as long as the data in the block is not altered. If any changes are made in the block, the cryptographic hash would change immediately indicating the change in the data which may be due to a malicious activity. Therefore, due to its strong foundations in cryptography, Blockchain has been increasingly used to militate against unauthorized transactions across various domains.

Block is the primary component of the blockchain. A block consists of the header and the body, the body of the block contains the transactions being written to the system. The header of the block contains the information about the block that includes previous hash, nonce value and difficulty, and the time stamp of the block and the transactions. The length of the block is variable and deemed to have been among 1 to 8 MB of size. The header of the block uniquely identifies the block to be placed.

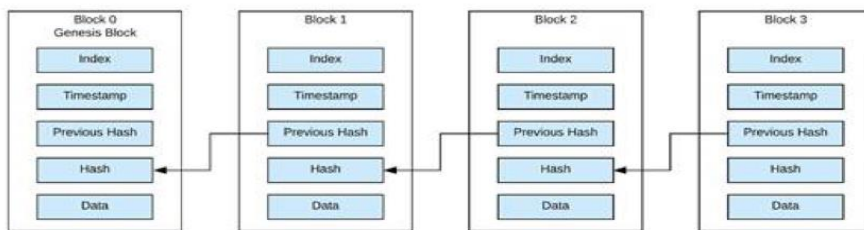


Fig 2. Block chain diagram

Blockchain has three different types, public blockchain, private blockchain, and consortium blockchain. Bitcoin and Ethereum are the examples of public blockchain. This is proofed by the complex mathematical functions. The private blockchain is the internal-public ledger of the company and the joining on that blockchain is granted by the company owning that blockchain. The block construction and mining speed is far better in the private blockchain as compared to public blockchain due to the limited nodes. The consortium blockchain however exists among the companies or group of companies and instead of the consensus the principles of memberships are designated to govern the blockchain transactions more effectively. In blockchain technology, implemented by hashing process.

3.4 Hashing Process

A hashing process is the technique which is used to convert the information into particular code as a output. In the process is done by the many types of algorithms which one is consist method for input and output rounds. Hashing is the process of changing the arbitrary and variable size input to a fixed size output. There are different functions that perform hashing of different level.

4 Secure Hashing Algorithm

SHA (Secure Hashing Algorithm) is another cryptographic hash function that yields 160 bit hash value consisting of 40 hexadecimal characters. The algorithm could not resist the collusion attacks against it and its usage has declined after 2005. In this time several new algorithms have also been proposed, including SHA 3, and SHA 256. The SHA 2 set of algorithms is designed by the US's Nation Security Agency. SHA 256 and SHA 512 are new hash functions that do not have collusion problems and deemed secure otherwise, at least as yet. Keccak is a family of algorithms designed by designed by Guido Bertoni, Joan Daemen, MichaelPeeters . The flexibility of the algorithm, in contrast to its other counterparts, is that it accepts any length of input and yields an arbitrary length of output, while all other algorithms produce a fixed length output.

| | VI | H | ME | BL | W | RO |
|----|----|---|-------|----|---|----|
| SH | | | 2^64 | 5 | | 8 |
| SH | | | 2^64 | 5 | | 8 |
| SH | | | 2^64 | 5 | | 6 |
| SH | | | 2^112 | 1 | | 6 |
| SH | | | 2^112 | 1 | | 8 |

Table 1 SHA Algorithm

4.1 SHA 256 ALGORITHM

In this paper implemented by the algorithmic section as SHA 256(Secure Hash Algorithms). It is member of SHA-2 cryptographic hash functions designed by the NSA. Cryptographic hash functions are mathematical operations run on digital data by comparing the computed "hash" (the output from the execution of the algorithm) to known and expected hash value. It generates an almost unique 32 byte signature for a particular text. The algorithm is a one way encryption technique which means once the text is encrypted it cannot be decrypted again and it also has a fixed size. Here, the SHA-256 algorithm will be implemented by the several steps, Step 1 : Padding bits First step of our hashing function begins with appending bits to our original message, so that its length will be same to the standard length required for the hash function. To do so we proceed by adding few bits to the message that we have in hand. The number of bits we add is calculated as such so that after addition of these bits the length of the message should be exactly 64 bits less than a multiple of 512. Let me depict it to you in mathematical terms for better understanding.

$$M + P + 64 = n * 512$$

$$M = \text{length of original message}$$

$$P = \text{Padded bits}$$

The bits that we append to the message, should begin with '1' and the following bits must be '0' till we are exactly 64 bits less than the multiple of 512.

Step 2 : Length bits Now that we have appended our padding bits to the original message we can further go ahead append our length bits which is equivalent to 64 bits s by calculating the modulo of the original message i.e. the one without the padding, with 2^{32} . the message we obtain we append we append those length to the padded bits and we get the entire message block on which must be a multiple of 512

Step 3 : Initialize the buffers We have our message block on which we will begin to carry out our computations to figure out the final hash. Before we begin with that I should tell you that we need certain default values to be initialized for the steps that we are going to perform

$$a = 0x6a09e66$$

$$b = 0xbb67ae85$$

$$c = 0x3c6ef372$$

$$d = 0xa54ff53a$$

$$e = 0x5510e527f$$

$$g = 0x1f83d9ab$$

$$h = 0x5be0cd19$$

keep these values in the back of your mind for a while, in the next step everything will be clearly understandable to you. There are more 64 values that need to be kept in mind which will act as keys and are denoted by the word 'k'.

Step 4 : Compression Function so the main part of the hashing algorithm lies in this step. the entire message block that we have 'n x 512' bits long is divided into 'n' chunks of 512 bits, are then put through 64 rounds of operation and output obtained is fed as input for the next round of operation.

We can clearly see the 64 rounds of operation that is performed on a 512 bit message. We can observe that two inputs that we send in are $W(i)$ & $K(i)$, for the first 16 rounds we further break down 512 bit message into 16 parts of each of 32 bit b :t after that we need to calculate the value for

$$W(i) \text{ at each step}$$

$$W(i) = W_{i-16} + \sigma_0 + w^{i-7} + \sigma_1$$

where,

$$\sigma_0$$

$$= (W_{i-15} \text{ ROTR } 7(X)) \text{ XOR } (W_{i-15} \text{ ROTR } 18(X)) \text{ XOR } (W_{i-15} \text{ SHR } 3(X))$$

$$\sigma_1$$

$$= (W_{i-2} \text{ ROTR } 17(X)) \text{ XOR } (W_{i-2} \text{ ROTR } 18(X)) \text{ XOR } (W_{i-2} \text{ SHR } 10(X))$$

$$\text{ROTR } n(X)$$

$$= \text{Circular right rotation of 'x' by 'n' bits}$$

$$\text{SHR } n(x) = \text{Circular right shift of 'x' by 'n' bits}$$

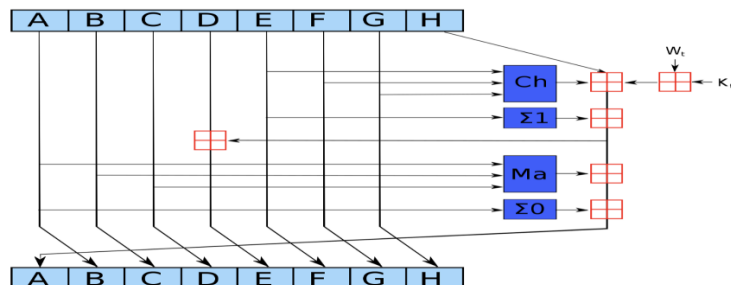


Fig 3, Hashing process

In the image above we can see exactly what happens in each of the functions carried out we can perform the entire hashing process.

$$\begin{aligned}
 Ch(E, F, G) &= (E \text{ AND } F) \text{ XOR } ((\text{NOT } E) \text{ AND } G) \\
 Ma(A, B, C) &= (A \text{ AND } B) \text{ XOR } (A \text{ AND } C) \text{ XOR } (B \text{ AND } C) \\
 \Sigma(A) &= (A \ggg 2) \text{ XOR } (A \ggg 13) \text{ XOR } (A \ggg 22) \\
 \Sigma(E) &= (E \ggg 6) \text{ XOR } (E \ggg 11) \text{ XOR } (E \ggg 25) \\
 + &= \text{addition modulo } 232
 \end{aligned}$$

These are the function that are performed in each of the 64 round that are performed over and over for 'n' number of times

Step 5: OUTPUT

The output from every round acts as an input for the next round and this process keeps on continuing till the last bits of the message remains and the result of the last round for the n^{th} part of the message block will give us the result. i.e. the hash for the entire message.

In the prototype of algorithm in this there is some data called IV which is of 256 bits. now the input we get will be in the very large .so be break it in size of 512 bits ,so some part of input will be left.

To this left input we do a padding - concatenate the input with 10^* bits before it. now our input is perfect multiple ,so we can proceed further. Now 512- bit input is added with 256-bit IV to get a total of 768 bit. this 768 bit is passed through a compression function 'c' to get an output of 256 bits only

This output 256 bit is again merged with 512 bit input from block B2. Again the total is passed through the compression function to yield a 256-bit output. This loop goes on till the 1st block(block n). Again a compression function and gives final 256 bits output, what we call it as hash of input data the important concept here is that if function c is SHA-256 is collision free.

5 Conclusion

It is dream of every country to hold a fair election where a common person can register their votes to decide the future of the country. This paper discusses the Electronic voting system is much secure and expeditious than the existing system. To build a biometric technology, that is free from unauthorized access throughout casting votes by elector. The result of simulations of mobile voting will increase the reliability and security using blockchain technology. This system enables us to secure the electronic voting system in a very fair and unbiased manner.

Acknowledgement

We thank our The Head of the Department Mrs. A. Ramya for this paper make it with permission and guideness.

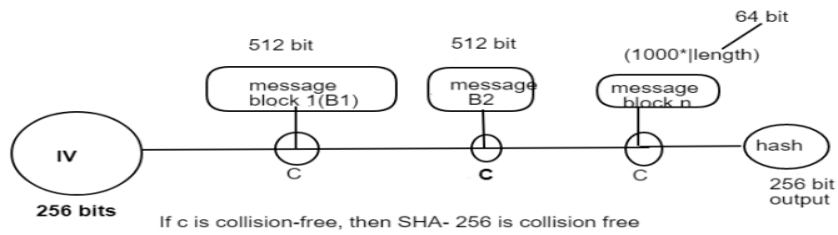
References

- [1] Aravind P. Gokul Raj S. Mohan raj S. And Dr.W. Gracy Theresa "Blockchain and finger print enabled E-voting, Feb2019"
- [2] Gaby G. Dagger, Matlo Milinkovic and Jordan Mahler, "Smart E-Voting System using block chain technology, 2018"
- [3] Xxecuchao Yang, Xun, Yi, Surya Nepal, Andrei Kelarev, and Fengling Han, "A secure verifiable Ranked choice online Voting System based on homomorphic encryption" 10.1109/access. 2018 2817518 IEEE access.
- [4] J. Deepika, S. Kalaiselvi, S. Mahalashi, S. Agnes Shifani, "Smart Electronic Voting System based on biometric identification Survey" 2017 Third international conference on Science technology Engineering & Management (ICOVSTEM).

- [5] A. Piratheepan, S.Sasikaran, P.Thanushkanth, S.Tharsika, M.Nathiya, C.Sivakaran, N.Thiruchchelvan, K.Thiruthamigesan, "Fingerprint voting System using Arduino" Middle-east Journal of scientific research 25(8): 1793-1802, 2017.
- [6] Shaik Mazhar Hussain, Chandrashekar Ramaiah, Rolito Asunuion, Shaik Azeemuddin, Nizamuddin, Rakesh Veerabhadrapa, "An RFID based smart EV system for reducing electoral frauds"2016 5th International conference on reliability , Infocom technologies and optimization (ICRITO) Sep.7-9,2016, AIIT, Amity Univesity, Uttar Pradesh Noida , India.
- [7] Ms. Ashwini Ashok, Mandavkar, prof. Rohini Vijay Agawane, "Mobile based facial recognition using OTP verification for Voting System" 2015 IEEE International Advance computing conference (IACC)

Appendix

SHA 256 Algorithm – collision tree



Diabetic Retinopathy Retinal Vessels Classification Using Deep Learning Techniques

Sis.Punitha Jilt¹, M.Aruna², R.Ashwini², M.R.Varsha²
 HOD¹,UG Student², Department of Computer Science & Engineering,
 ST.Anne's college of Engineering and Technology, Panruti

ABSTRACT

Diabetic retinopathy (DR) is an important causes of blindness worldwide[2]. However, DR is hard to detect in early stages and the diagnostic procedure can be time-consuming even for experienced experts[3]. Therefore, a computer-aided diagnosis method based on deep learning algorithms is proposed to automated diagnose the referable diabetic retinopathy (RDR) by classifying color retinal fundus photographs into two grades. In this work, A novel Convolutional neural network model with Siamese like architecture is trained with transfer learning technique.

KEYWORDS: *Diabetic Retinopathy, Deep Learning, Fundus Images, Training data, Test data*

1 Introduction

Diabetic retinopathy (DR) is a common complication of diabetes associated with retinal vascular damage caused by long-standing diabetes mellitus[2]. According to the research, DR has become one of the important causes of blindness and vision impairment worldwide, since 0.4 million cases of blindness and 2.6 million cases of severe vision impairment globally can be attributed to it in 2015[1]. In fact, the impairment of DR to vision can be controlled or averted if it is detected and treated in time[1]. However, many patients miss the best time for treatment since there are few signs or symptoms at the early stage of DR. Furthermore, the diagnosis of DR mostly depends on the observation and evaluation to fundus photographs (see Fig. 1) of which procedure can be time-consuming even for experienced experts.[4] Therefore, computer-aided automated diagnosis approaches have great potential in clinical to accurately detect DR in a short time, which can further help to improve the screening rate of DR and reduce the number of blindness.[5]

2 Tables and Figures

The distribution of testing data

| Label | Class | Test Data |
|-------|------------------|-----------|
| 0 | No DR | 495 |
| 1 | Mild | 264 |
| 2 | Moderate | 551 |
| 3 | Severe | 551 |
| 4 | Proliferative DR | 91 |

The distribution of training data

| Label | Class | Train Data |
|-------|------------------|------------|
| 0 | No DR | 1980 |
| 1 | Mild | 1051 |
| 2 | Moderate | 2204 |
| 3 | Severe | 360 |
| 4 | Proliferative DR | 308 |

Data View

| Variable | Label | Position |
|----------|--------------------|----------|
| 2 | Display Width: 12" | 1 |
| 3 | Display Width: 1" | 2 |
| 4 | Display Width: 5" | 3 |
| 5 | Display Width: 7" | 4 |
| 6 | Display Width: 7" | 5 |
| 7 | Display Width: 2" | 6 |
| 8 | Display Width: 3" | 7 |
| 9 | Display Width: 6" | 8 |
| 10 | Display Width: 5" | 9 |
| 11 | Display Width: 10" | 10 |
| 12 | Display Width: 8" | 11 |
| 13 | Display Width: 8" | 12 |
| 14 | Display Width: 8" | 13 |
| 15 | Display Width: 8" | 14 |
| 16 | 5 | U" |

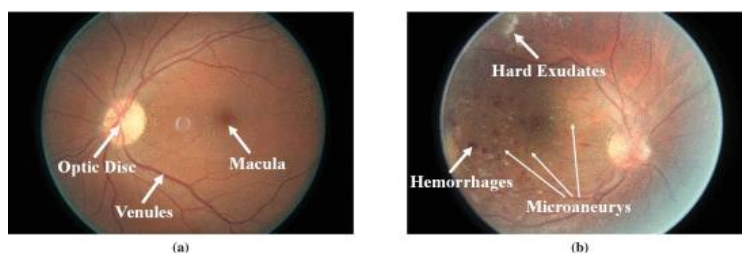


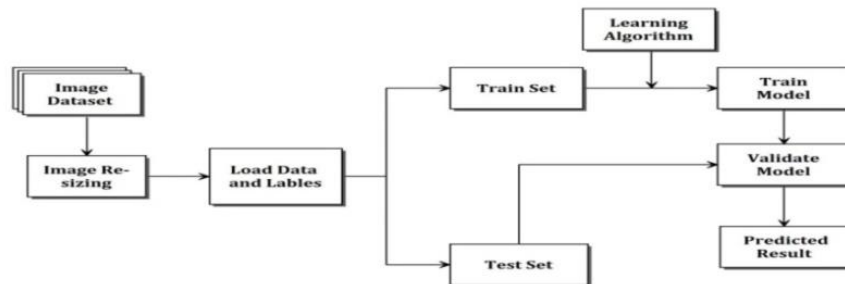
FIGURE 1: Typical fundus photographs. (a) Photograph of healthy fundus, showing the normal optic disk, venules and macula. (b) Photograph of fundus with severe DR, in which three common lesions (hemorrhages, microaneurysms and hard exudates) are pointed out.

3 Existing System

Nonetheless, there are some researches that report the development of automated systems for detecting DR by classifying DR into general detection categories, such as normal (no apparent retinopathy) or abnormal (retinopathy presence).[6] Also, there are other classification systems that provide more details about the retinopathy stages, which include normal, non-proliferative diabetic retinopathy (NPDR) and proliferative diabetic retinopathy (PDR). The researchers investigated and proposed a computer-based system for identifying normal, NPDR and PDR classes.[7] The Existing system uses colour fundus images[8,9], where the features are extracted from the raw image with image processing techniques and fed to a Support Vector Machine (SVM) for classification. The system has been later enhanced by using two types of classifiers, a Probabilistic Neural Network (PNN) and a Support Vector Machine. [9]

4 Proposed System

Different from previous works, the proposed model accepts binocular fundus images[9,10] as inputs and learns their correlation to help making prediction. For a deep learning model, the most important parts that should be focused on are data set, network architecture and training method. Before being used to train our model, fundus images data set obtained from public resources is preprocessed and augmented.[10] We proposed a system to detect referable DR by using a deep Convolutional neural network (CNN).[11]



2.1 Model Description

Gathering data

- Collect the raw X-ray image

Preparing that data

- Normalization
- Convert image to numeric matrix
- Split Train and Test

Choosing a model

- Select the algorithm
- Build the model
- Train the model

Evaluation

- Evaluate the model using Test Data

Prediction

- Predict the answer using new record

5 Algorithm

5.1 Deep Learning

Deep learning is a subset of machine learning in artificial intelligence (AI) that has networks capable of learning unsupervised from data that is unstructured or unlabeled. Also known as deep neural learning or deep neural network.[13]

5.2 CNN

In neural networks, Convolutional neural network (ConvNets or CNNs) is one of the main categories to do images recognition, images classifications. Objects detections, recognition faces etc., are some of the areas where CNNs are widely used.. Based on the image resolution, it will see $h \times w \times d$ (h = Height, w = Width, d = Dimension). Eg., An image of $6 \times 6 \times 3$ array of matrix of RGB (3 refers to RGB values) and an image of $4 \times 4 \times 1$ array of matrix of grayscale image.

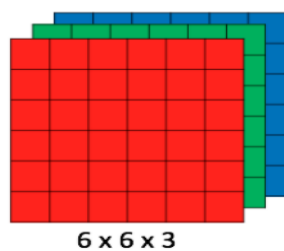
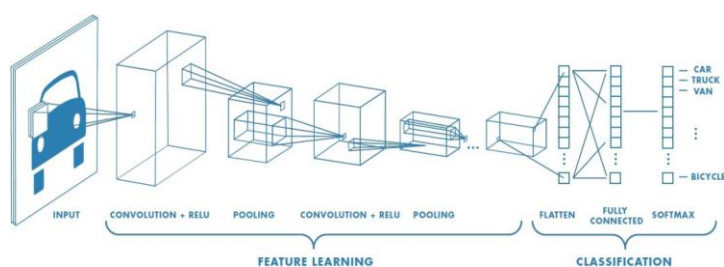


Figure 1 : Array of RGB Matrix

The below figure is a complete flow of CNN to process an input image and classifies the objects based on values.



5.3 Convolution Layer

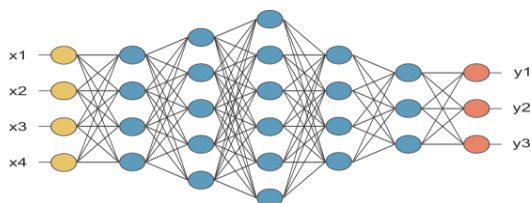
Convolution is the first layer to extract features from an input image. Convolution preserves the relationship between pixels by learning image features using small squares of input data[10]. It is a mathematical operation that takes two inputs such as image matrix and a filter or kernel.

5.4 Pooling Layer

Pooling layers section would reduce the number of parameters when the images are too large. Spatial pooling also called subsampling or downsampling which reduces the dimensionality of each map but retains the important information.

5.5 Fully Connected Layer

The layer we call as FC layer, we flattened our matrix into vector and feed it into a fully connected layer like neural network.



6 Functional Requirements

A function of software system is defined in functional requirement and the behavior of the system is evaluated when presented with specific inputs or conditions which may include calculations, data manipulation and processing and other specific functionality

6.1 Non-Functional Requirements:

Nonfunctional requirements describe how a system must behave and establish constraints of its functionality. This type of requirements is also known as the system's *quality attributes*. Attributes such as performance, security, usability, compatibility are not the feature of the system, they are a required characteristic.

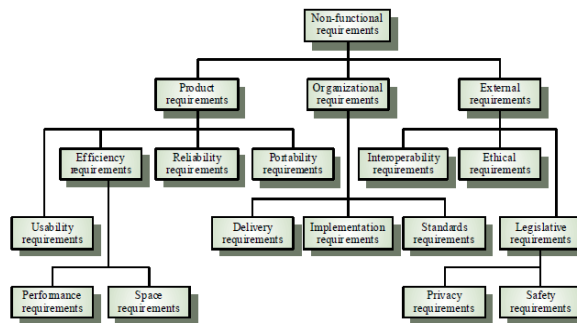


Figure 2: Proposed Image Classification

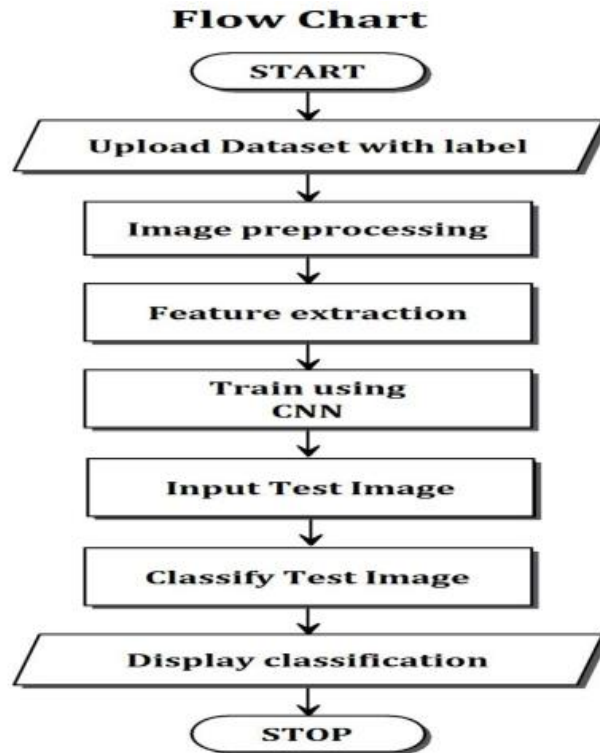
6.2 Algorithm : Proposed Algorithm

```

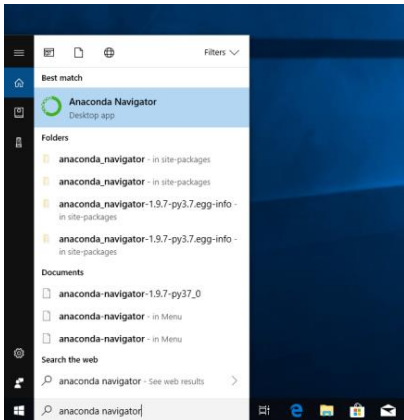
import cv2 #opencv its used for image processing
import numpy as np # used for array matrix
train_data_dir = 'input/train'
test_data_dir = 'input/test'
class_labels = os.listdir(train_data_dir)
print(class_labels)
['Mild', 'Moderate', 'No_DR', 'Proliferative_DR', 'Severe']
for wdir in os.listdir('input'):
print(wdir)
wdir_total = 0
for label in class_labels:
total = len(os.listdir(os.path.join('input', wdir, label)))
print(label, total)
wdir_total +=total
print(wdir,'-----',wdir_total)
def load_training_data():
#Load training images
labels = os.listdir(train_data_dir)
print(labels)
total = len(labels)
X_train = np.ndarray((nb_train_samples, img_rows, img_cols, 3), dtype = np.uint8)
Y_train = np.zeros((nb_train_samples,), dtype = np.uint8)

```

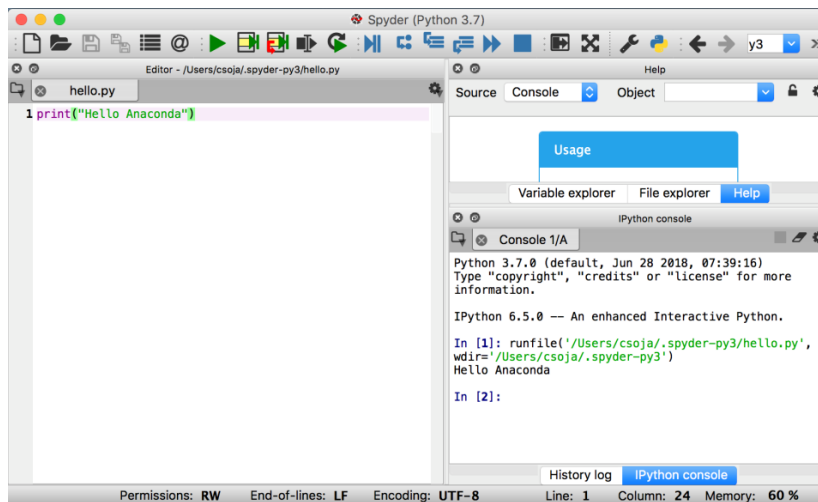
6.3 Flow Chart



6.4 Technology Tools



SPYDER IDE(Integrated Development Environment) to run python



7 Conclusion

Different from previous works, the proposed model accepts binocular fundus images as inputs and learns their correlation to help making prediction. In the case with a training set of only 5903 images and a test set of 1479 images, an area under the receiver operating curve (AUC) of 0.951 is obtained by the proposed deep learning model, which is 0.011 higher than that obtained by CNN model. To further verify the effectiveness of the binocular design, a binocular model for five-class DR detection is also trained and evaluated on a 10% validation set. The result shows that it achieves a normalized score of 127.8 which is higher than that of existing non-ensemble model.

Reference

- [1] V.Sujatha ,PrassanaDevi,VinuKiran,"Bigdata Analytics on Diabetic Retinopathy Study(DRS) on Real-Data Set Identifying Survival Time And Length of Stay,"vol.87,pp.227-232,2016.
- [2] SimoServant,Hernandez,"Diabetic Retinopathy in the context of patients with diabetes,"*Ophthalmic Res* 2019;62:211–217
- [3] Maya GeorgievaPandova-"Diabetic Retinopathy and Blindness :An Epidemiological Overview," no.3 32-542
- [4] HaiquanChen,Yuan Leon-"Automated Diabetic Retinopathy Detection based on binocular Siamese-like convolutional neural network."IEEE,2019,pp.2169-3536
- [5] U.RajendraAacharya,Kuang Chua Chua,Choo Min Lim-"Computer Aided diagnosis of diabetic retinopathy:A review,"vol.43,2013, 2136-2155
- [6] KetkiS.Argade,SandeepJore-"Automatic detection of diabetic retinopathy using image processing and data mining techniques,"*International Conference on Green Computing and Internet of things*,Vol.11,2015.
- [7] "Photocoagulation Treatment of Proliferative Diabetic Retinopathy: Clinical Application of Diabetic Retinopathy Study (DRS) Findings, DRS Report Number 8,"*The diabetic retinopathy study research group*,Vol.88, 583-600
- [8] W.M.Gondal,J.M.Kohler,R.Grzeszick,G.A.Fink,andM.Hirsch,:"Weakly-supervised localization of diabetic retinopathy lesions in retinal fundus images," in 2017 IEEE International Conference on Image Processing(ICIP).IEEE,2017,PP.2069-2073.
- [9] K.Ganesan,R.J.Martis,U.K.Archarya"Computer-aided diabetic retinopathy detection using trace transforms on digital fundus images,"*Medical and Biological Engineering And Computing*,vol.52,pp.663–672,2014.
- [10] AdarshPradhan,Rahul Kumar Nath,Ajay Das,"Diabetic Retinopathy Detection on Retinal Fundus Images Using Convolutional Neural Network,"vol.15,pp.978-981,2020.
- [11] A.Dalyac,M.Shanahan,andJ.Kelly,"Tackling class imbalance with deep convolutional neural networks,"*Imperial College*,pp.30-35,2014.
- [12] R.Ghosh,K.Ghosh,and S.Maitra,"Automatic detection and classification of diabetic retinopathy stages using cnn," in 2017 4th International Conference on Signal Processing and Integrated Networks(SPIN).IEEE,2017,PP.550-554.
- [13] S.Dutta,B.C.Manideep,S.M.Basha and N.Iyengar,"Classification of diabetic retinopathy images by using deep learning models,"vol.11,pp.89-106,2018.

A Multi Tasking Agriculture Robot Using Internet Of Things And Raspberry Pi

Brittadevi.V

Assistant Professor, Department of Computer Science & Engineering
St.Anne's College of Engineering and Technology, Panruti.

Abstract

Agriculture is the backbone of our country. Robots are playing an important role in field of agriculture for farming process autonomously. The proposed system aims at making the agriculture smart by using automation and IoT technologies. Agri-robot is a robot designed for agricultural purposes to minimize labour and energy consumption. The highlighting features of this project includes Raspberry Pi based remote controlled robot to perform tasks like Seed Sowing and Automatic Irrigation. The efficient mechanism of the disperse seeds are led to fall into the soil through the seed dispenser and it includes smart irrigation with pump automation and intelligent decision making based on accurate real time field data. The farmers can able to control the robotic actions by switching onto the desired modes through dashboard from the mobile connected to Internet. These operations will be performed by interfacing sensors, motor, smart phone Wi-Fi and actuators with Raspberry Pi. It is designed to minimize the labour wages in addition to increasing the speed and accuracy of the work. Thus the multitasking robot keeping the ideology that multiple small autonomous machines could be more efficient than traditional large tractors and human effort.

Keywords:Internet of Things, Raspberry Pi, Robot, smart phone.

1 Introduction

In the real world the farmers are progressively under pressure to feedstuff more people .This emergent inhabitants has about the food they eat. Yonder organic food, there is an global impulsion to variety farming greener through using less water and pesticides. These influences mean farmers prerequisite to produce more, at a higher quality, and in a ecological manner. Consequently arrive the robots set to improve production yield, while reducing resources required and making farming and exciting high-tech profession. Over the past few years technology and agriculture have come together in an unprecedented way, as advances in the Internet of Things. IoT is a part of a smart farming. The smart farming is an umbrella term that describe the adoption of digital technology allowing farm decisions to be augmented by information that comes from sensors, farm software and outside sources. It also refer to the automation of farm decision, where machines and system such as robots, autonomous vehicles and smart irrigation system, act in accordance to data coming in from the environment. The internet of things is now a household term and the world where anything can connect to anything via connectivity infrastructure that is significantly cheaper and far more granular than existing mobile networks, and devices can be added to the network at any place and time. Devices and application talk to each other across the network. Data is open and shared widely, with huge amounts of data being combined, analysed and fed into cloud-based software which automates and manages almost every aspect of life.The sensing devices measure changes in their environment and send data to a central computer to be gathered, analysed and turned into information that feeds into decision-support systems. Data from sensors trigger actuators, components of a system that move or control mechanisms. Sensors and actuators together in the IoT can automate processes that may have been previously carried out by humans.

2 Related Work

[1] The Arduino ATMEGA328at first, the vehicle will sow the seed by moving around the field. After some days, the vehicle covers all over distance of that agricultures field. After finishing the seed sowing process, the vehicle will return back, it provides the water pumping when the soil is seems to be dry. they use a soil sensor to monitor the humidity and temperature of the soil. Side by side it provides the good quality pesticide spraying and fertilizer spraying. The over usage of fertilizers are also leads to the plants death. To prevent the plants from over fertilizers, the time delays are set using the relays. It also provides the special function, which pick out the unwanted grass from the soil. [2] The automated system, depending on the crop considering particular rows & specific columns. The spacing between two seeds in a column has to be entered manually. Proximity sensor is used to measure the rotation of wheels. To detect the obstacle in the path of the vehicle IR LED with TSOP receiver is used and turning position is also depend on this sensor. To check whether seed container is empty or

not LDR sensor is used. All the operations are monitored and control by PIC microcontroller using sensors.[3]It plan a smart irrigation system innovation in ease which is usable by agriculturists. A mechanized water system framework was created to advance water use for rural harvests by utilizing raspberry pi. Mechanization enables us to control machines autom-atically. It control the water engine naturally, screen the plant development utilizing webcam and we can likewise observe live spilling of ranch on android mobiles by utilizing wifi.[4] It consist of PIC microcontroller system. The users presses the start button the robot starts moving in the forward direction. When the robot starts moving in the forward motion after few distance it stops and then it starts drilling with the help of a drilling mechanism. After this process, there's a Solenoid valve arrangement through which the seeds are being dispensed in the soil. This same procedure continues until the user does not switches off the circuit. Drilling process is done with DC motor and seed dropping in land is done with the help of a two port solenoid valve. All these process are displayed on LCD.

3 Proposed System

There are various machine used for agricultural purposes out of which some are cost effective but required more man power. In multitasking agricultural robot, we are trying to reduce the cost as well as human dependency by making it fully automated. The main processing unit is Raspberry pi 3 and it easy-to-use hardware and software It is used as an input and output device to get continues readings from sensors and based on these readings generate corresponding control signals to ensure the accurate working of the robot. All the modules like seed sowing, soil moisture sensors, directly communicate with raspberry pi using I/O ports. This paper consist of two fragments and using smart phone to control system. In the present system, every fragment is integration with different sensors and devices and they are interconnected to one central server via wireless communication modules. The server sends and receives information from farmer end using internet connectivity. This system allow the farmer to control multitasking robot appliances sensors and motors from mobile phone through an internet connections.

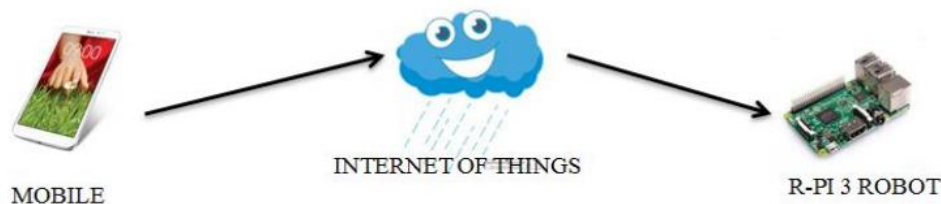


Figure 1 : System Overview

3.1 Seed Dispensing

For the process of seed dispensing, farmers from the mobile wireless connection they can operate the robot by switching the move bot mode and dispenser seed modes through dashboard. These mode signals are send to the raspberry pi 3. That the R-Pi controller wheel motors and devices. The move bot mode are assistance to travel the robot in forward direction. After the dispenser seed mode are doing the seed sowing process. The seed dispensing process is to provide a light and compact robot adapted to be pushed over the ground to be seeded and capable of distributing seeds evenly in uniform quantities. A seed distribution system constructed in an upright main hopper for containing a mass of seeds. Then the seeds which are allowed to pass through a valve to the seed dispenser. From where the seeds are led to fall into the soil through the dispenser whose movement is aided by a servo motor. This nothing but a simple electrical motor, controlled with help of servo mechanism. The way a servo motor reads the information it's being sent is by using an electrical signal called PWM. It sending ON electrical signals for a certain amount of time, followed by an OFF period, repeated hundreds of time a second. The amount of time the signal is on sets the angle the servo motor will rotate. So for 90 degrees, divided by 18, which is 5, then add 2, and we get 7. So on this servo 7% duty is 90 degrees.

3.2 Moisture Sensing and Automation

Soil moisture is basically the content of water present in the soil. This can be measured using a soil moisture sensor which consists of two conducting probes that act as a probe. It can measure the moisture content in the

soil based on the change in resistance between the two conducting plates. The resistance between the two conducting plates varies in an inverse manner with the amount of moisture present in the soil. This paper uses Python scripts run on a raspberry pi microcontroller to send GPIO PWN output to a servo motor to set its angle. GPIO stands for General Purpose Input/Output which mean these pins can either send electrical signals to drive hardware or receive them and read sensor data. We're using them as output, to send signals to a servo motor. That the servo motor act the soil moisture sensor. A typical soil moisture sensor consist of two components. A two legged lead, that goes into soil or anywhere else where water content has to be measured. This has two header pins which connect to an amplifier/ A-D circuit which is in turn connected to the arduino nano. The amplifier has a Vin, Gnd, Analog and Digital data pins. This mean that we can get the values in both analog and digital forms. The soil moisture sensor gives a resistance variation at the output. Its ends analog data which can be converted with an integrated analog to digital converted in the arduino nano. The arduino nano are connected to the raspberry pi with USB cables. It sends the current soil moisture sensor data in digital form to arduinonano. That digital signal is given to the raspberry pi 3 board. Then relay is switched ON/OFF to turn the water motor. If the soil moisture value is high then the water motor will be on, otherwise if the moisture level is low the motor will be off through the relay. Every moisture action indicated by the LCD display.

4 Experiment and Results

Test results shows that the robot can be controlled remotely using wireless transmission of mobile commands to R-Pi.R-Pi forwards the commands to arduino nano and gives signals to the relay in order to run the water motor.

4.1 Mobile Wi-Fi Controlled Robot Using Raspberry Pi

In this paper agriculture robot controlled by Raspberry Pi 3.As hardware, the robot body is build mechanically and electronic components. The robotic control is made wireless that is; it controlled by the WI-FI. The smart phone and Raspberry Pi 3 board is connected through WI-FI.The desired mode are generated from smart phone are sent to the raspberry pi and raspberry pi receives these signals according to a program written in the python programming language. At this point, it is possible to talk about one and only communication channel. From the farmer mobile they would able to see the dashboard to run the robot. Disperse seed mode used for seed sowing operation. Move bot mode using for robot running. Plant servo mode used for soil moisture sensing. The agriculture robot are controlled through the smart phone and raspberry pi 3. It consist of Raspberry Pi 3, the heart of the project. Small single computer like credit card size. It works on 5V supply. It has in build wireless LAN and Bluetooth connectivity. The multitasking robot is capable of performing multiple operations like seed sowing and smart irrigation. The mechanism of the robot is guided by the signals being sent out from the Raspberry Pi controller. The robot is composed of 6 motors out of which two is a servo motor and the remaining are RPM motors. The one servo mechanism is used for seed dispensing and another servo is used for smart irrigation. A 12V battery supply is feeded for the operation of wheels and other process. Four RPM motors are attached to the wheels on either side such that each side is driven by two motors each. From the mobile wireless connection farmer can operate the robot by switching onto the desired modes through dashboard. Shown in fig(2,3,4,5)



Figure 2 : Smart phone Wi-Fi Controlled the Robot

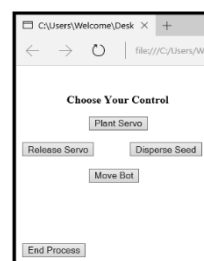


Figure 3 : Dashboard For Robot Running

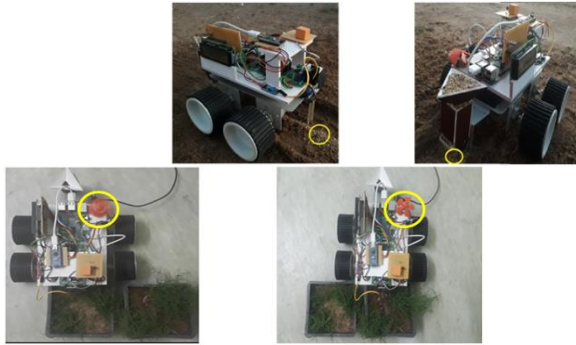


Figure 4 : Seed Dispenser System



Figure 5: Smart Irrigation System

5 Conclusion

In this paper, we have introduced a systematic vision of IoT technologies for the advancement of agriculture. It increase the agriculture field, make tranquil work to the farmers and save the water and energy conservation. The raspberry pi 3 is an incredible little machine with endless automatic process. This smart irrigation system proves to be a useful system as it automates and regulates the watering without any manual intervention. Another system has been developed for the sowing of seeds in an automatic way. Here with the help of a robot the seeds are been dispensed in the soil in a proper sequence hereby reducing the wastage of seeds.

References

- [1] Angel Nimisha Lorain F, Ramamalini.P,Udhayanithi.N, Veeralakshmi.R: “Smart Automated Agriculture Monitoring And Controlling System Using Arduino” *IOSR Journal of Electronics and Communication Engineering (IOSR-JECE)* e-ISSN: 2278-2834,(2017).
- [2] Prashant G. Salunkhe1, Sahil Y. Shaikh, Mayur S. Dhable, Danis I. Sayyad, Azeem S. Tamboli: “Automatic Seed Plantation Robot” *International Journal of Engineering Science and Computing*, volume no:6,Issue:4 April(2016).
- [3] BhagyashreeK.Chate, Prof.J.G.Rana: “Smart Irrigation System Using Raspberry Pi” *International Research Journal of Engineering and Technology (IRJET)* e-ISSN: 2395 -0056 Volume: 03 Issue: 05 May(2016).
- [4] Abdulrahman, MangeshKoli, UmeshKori, Ahmadakbar: “Seed Sowing Robot” *International Journal of Computer Science Trends and Technology (IJCTST)* – Volume 5 Issue 2, Mar – Apr(2017).
- [5] Mahendheran, Arun, Manickavasagam, Lawrence Justin and Parthasarathi : “Multifunctional Robotic Vehicle for Agriculture Application” (2017).
- [6] NikeshGondchawar, Prof. Dr. R. S. Kawitkar : “IoT based Smart Agriculture”(2016).
- [7] P.Hemalatha, Development of IOT Enabled Robotic Guide Dog for visually impaired people to enhance the guiding and interacting experience, *JARDCS , Scopus(Elsevier),02-Special Issue,pp 262-272(2017)*.
- [8] P.Hemalatha ,A Smart Healing Mechanism for Diabetic Neuropathy using IoMT,*IJARSE,Volume No.06, Issue No. 09,pp 77-83(2017)*.
- [9] P.Hemalatha,Cardiac Monitoring using Internet of Medical Things, *IJARSE, Volume No.06, Issue No. 09,pp 197-204(2017)*.
- [10] ArindamGiri, SubrataDutta, SarmisthaNeogy: “Enabling Agricultural Automation to Optimize Utilization of Water, Fertilizer and Insecticides by implementing Internet of Things(IoT) International conference of information technology (2016).

Attribute-Based Access Control With Data In Cloud Storage

S Rajarajan¹ Assistant Professor, K Monisha² Student,
D.Hemalatha³Student,, AThenaruvi⁴ Student
Department of computer science and engineering,
St.Anne's college of engineering and technology,
monishakaral@gmail.com

Abstract

Attribute Based Access Control (ABAC) uses attributes as building blocks in a structured language that defines access control rules and describes access requests. Attributes are sets of labels or properties that can be used to describe all the entities that must be considered for authorization purposes. ABAC is a “next-generation” authorization model that provides dynamic, context-aware, and risk-intelligent access control. It helps achieve efficient regulatory compliance, effective cloud services, reduced time-to-market for new applications, and a top-down approach to governance through transparency in policy enforcement. Attribute Based Access Control (ABAC) models are designed with the intention to overcome the shortcomings of classical access control models (DAC, MAC and RBAC) and unifying their advantages. ... OWL can be used to formally define and process security policies that can be captured using ABAC models. In this paper we proposed for an attribute based access control with data in cloud storage, here we give a data confidentially for the particular persons based on attributes of data/person.

Keywords: Access control, Authorized search, Cloud storage, Data sharing, Key-policy attribute based encryption

1 Introduction

Cloud storage as one of the most popular cloud-based application supplies users with scalable and elastic storage resources for remote data sharing, which dramatically reduces the local cost on data management and maintenance [1]–[3]. However, once the data is outsourced to the cloud, the security and privacy threats become huge concerns for data owners as they lose the physical control over their data [4], [5]. Moreover, the frequently happened data leakage incidents undermine the trust on the cloud service provider, which significantly impedes the wide adoption of outsourced cloud storage. Traditional one-to-one encryption is able to protect data confidentiality, but it is quite incompetent for data owners sharing their data with authorized users efficiently and flexibly. As well known, attribute-based encryption (ABE) can be used to achieve fine-grained access control and protect data confidentiality simultaneously, and key-policy attribute-based encryption (KP-ABE) enables the data owner to label each ciphertext with a set of descriptive attributes, and generate the private key that is related to an access policy to specify which type of ciphertext can be decrypted.

2 Related Work

2.1 Attribute-Based Encryption (ABE)

ABE mainly includes two forms: ciphertext-policy ABE (CP-ABE) and KP-ABE. In CP-ABE, the data is encrypted under a specified access policy, and only the users possessing attributes that satisfy the access policy are able to decrypt the ciphertext. While in KP-ABE, the data is encrypted under several attributes, and the user is assigned with an access policy. With the above properties, ABE soon became popular in the outsourced data access control systems. However, most of the existing schemes expose attribute information in the ciphertext, which may incur data or user privacy leakage, thus the research on anonymity of ABE is also necessary.

2.2 Public-Key Encryption With Keyword Search (PEKS)

The concept of PEKS was introduced by Boneh et al., and two constructions were given in their scheme to support equality queries. Later, many other PEKS schemes with better security or new functionalities are proposed to make it more practical, in which the following two directions are mainly included: (1) how to support more expressive and flexible search policy on keywords; and (2) how to resist the offline guessing attack. With regard to the first one, Park et al. presented a PEKS construction to support searching with conjunctive keywords.

2.3 Authorized Keyword Search (AKS)

Sun et al. first considered fine-grained search authorization in their attribute-based keyword search scheme, but only single keyword is supported. Shi et al. [5] put forward an authorized keyword search (AKS) scheme supporting expressive authorization policies and query predicates, but too much cost is incurred due to the composite-order groups and the data owner need generate trapdoor for each search policy.

3 Preliminaries

3.1 Access Structure

An access structure on an attribute universe U is a collection C , which includes non-empty sets of attributes. The sets in C are defined as the authorized sets.

3.2 Access Tree

Let, k_x , $\text{num } x$ denote the threshold value and the number of its children respectively, where $k_x = 1$. For the root node r , $\text{pr}(0) = \alpha$. For each non-root node, $\text{px}(0) = \text{ppar}(x)(\text{id}(x))$. For an attribute (leaf) node i , $\text{pi}(0) = \text{ppar}(i)(\text{id}(i))$ can be seen as the secret share assigned to it.

4 Key-Policy Attribute-Based Encryption

Four algorithms are included in the KP-ABE primitive.

- $\text{Setup}(\xi) \rightarrow (\text{PK}, \text{MSK})$. This algorithm takes as input a security parameter ξ , and generates the master secret key MSK as well as the public key PK.
- $\text{Encrypt}(\text{PK}, M, S) \rightarrow \text{CT}$. This algorithm takes as input PK, a message M , and an attribute set S . It generates the ciphertext CT.
- $\text{KeyGen}(\text{PK}, \text{MSK}, \text{AP}) \rightarrow \text{SK}$. This algorithm takes as input PK, MSK, and the access policy AP. It generates the secret key SK associated with AP.
- $\text{Decrypt}(\text{CT}, \text{SK}) \rightarrow M / \perp$. This algorithm takes as input CT and SK. It outputs the message M only if the attribute set S of CT satisfies the access policy related to SK, otherwise it outputs \perp .

5 Anonymous KP-ABE With Partially Hidden Attributes

$(T, \{[n_x : t_x] | n_x \in \text{atts}(T)\})$, if there exists an attribute name set N_1 in N such that

$$N_1 \subset N_S, \text{ and } \forall n_x \in N_1, s_x = t_x,$$

5.1 AKP-ABE Scheme

Setup(ξ) \rightarrow (**PK**, **MSK**) With the input of a security parameter ξ , the algorithm first generates a bilinear map $e : G \times G \rightarrow G_T$, where G and G_T are multiplicative cyclic groups of prime order p , and g is a generator of G . It computes $g_1 = g^{\tau_1}$, $g_2 = g^{\tau_2}$, $g_3 = g^{\tau_3}$, $g_4 = g^{\tau_4}$, where $\alpha, \tau_1, \tau_2, \tau_3, \tau_4 \in \mathbb{Z}_p^*$ are random values. Then, it randomly picks three group elements u, h, w from G . The public key PK is produced as

$$\text{PK} = \{hg, u, h, w, e(g, g)^\alpha, g_1, g_2, g_3, g_4\}.$$

Encrypt(**PK**, M , S) \rightarrow **CT** This algorithm takes as input the message M , the public key PK, and the attribute set S . As noted, each attribute in S is represented as $[n_x : s_x]$, where n_x means the generic attribute name, and $s_x \in \mathbb{Z}_p^*$ is the corresponding attribute value. It first randomly picks $s \in \mathbb{Z}_p^*$,

$$E_e = M \cdot e(g, g)^\alpha s, E = g^s.$$

$$S_{x,1}, s_{x,2}, z_x \in \mathbb{Z}_p^*$$

$$E_{x,0} = w^{-s} (u^{s_x} h)^{z_x}, E_{x,1} = g_1^{z_x - s_{x,1}}, E_{x,2} = g_2^{s_{x,1}}, E_{x,3} = g_3^{z_x - s_{x,2}}$$

$$E_{x,4} = g_4^{s_{x,2}}.$$

KeyGen(PK, MSK, AP) → SK

$$D_x = g^{px(0)} w^{\tau_1 \tau_2 t_{x,1} + \tau_3 \tau_4 t_{x,2}}$$

$$D_{x,0} = g^{\tau_1 \tau_2 t_{x,1} + \tau_3 \tau_4 t_{x,2}}$$

$$D_{x,1} = (u^{t_x} h)^{-\tau_2 t_{x,1}}, D_{x,2} = (u^{t_x} h)^{-\tau_1 t_{x,1}}$$

$$D_{x,3} = (u^{t_x} h)^{-\tau_4 t_{x,2}}, D_{x,4} = (u^{t_x} h)^{-\tau_3 t_{x,2}}$$

Decrypt(CT, SK) → M / ⊥

$$P_x = e(E, D_x) e(E_{x,0}, D_{x,0}) e(E_{x,1}, D_{x,1})$$

$$e(e_{x,2}, D_{x,2}) e(E_{x,3}, D_{x,3}) e(e_{x,4}, D_{x,4})$$

$$= e(g, g)^{px(0)s} e(u, g)^{zx(sx-tx)(\tau_1 \tau_2 t_{x,1} + \tau_3 \tau_4 t_{x,2})}$$

6 Attribute-Based Access Control With Data

In this section, we define the system model and design goals, give an overview of ABAC, and describe ABAC in detail. Note that, since ABAC is primarily based on AKP-ABE proposed in Section IV, we denote the algorithms in AKP-ABE as $ABE = \{ABE.Setup, ABE.Encrypt, ABE.KeyGen, ABE.Decrypt\}$.

Data owner (DO) DO encrypts the data based on its attributes before uploading it to the cloud, and assigns access policies over the data attributes to the data user. s based on their system roles or credentials.

Data user (DU). DU is allowed to decrypt the ciphertext whose attributes satisfy his access policy.

Cloud server (CS). CS is assumed with abundant storage and computing resources and is always online to render service. CS includes two parts: cloud storage server (CSS) and designated search server (DSS), where CSS helps DO store their data, and DSS performs data search on behalf of DU, and returns the matching data to DU.

ABAC is able to achieve fine-grained access control with authorized search on the data outsourced to cloud, simultaneously the data confidentiality and attribute privacy are protected effectively.

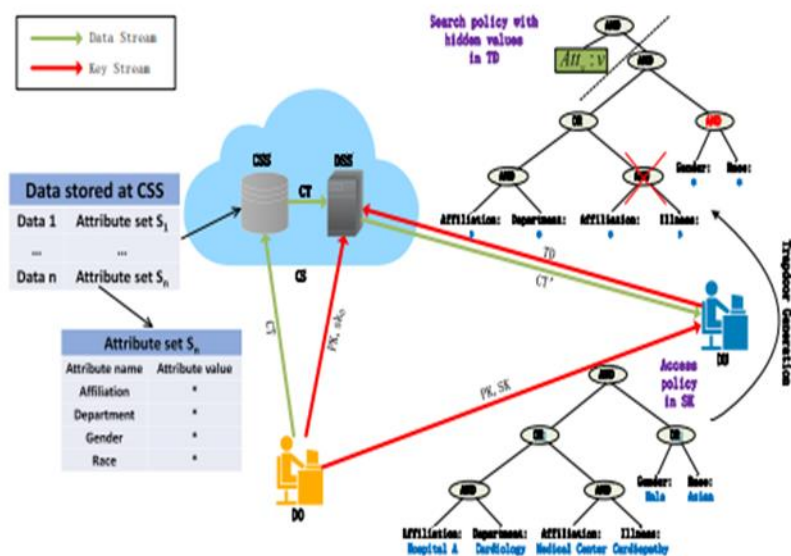


FIGURE 1: System model

$PK = hg, u, h, w, e(g, g)^a, g_1, g_2, g_3, g_4, [Att^v : v], pko^{-1}i$

Data Encryption

$$E_{x,0} = w^{-s} (u^{sx} h)^{zx}, E_{x,0}^1 = w^{-s} (u^{sx} h)^{zx},$$

$$E_{x,1} = g^{1zx-sx,1}, E_{x,2} = g_2^{sx,1},$$

$$E_{x,3} = g_3^{zx-sx,2}, E_{x,4} = g_4^{sx,2}.$$

Data Decryption

$$P_x = e(E, D_x) e(E_{x,0}, D_{x,0}) \cdot (Q_x)^{1/\delta y} = e(g, g)^{px(0)s}$$

We collect the running time of the Encrypt, KeyGen, TrapGen, Search and Decrypt algorithms with a simple access policy in AND gates, and the number of attributes are from 5 to 50.

To enable a visible comparison, we illustrate the results of KeyGen and TrapGen, Search and Decrypt. The running time of the algorithms increases linearly with the number of attributes.

It demonstrates that the encryption time in ABAC is almost the same as that in AKP-ABE and EKS. It shows that the total execution time of KeyGen and TrapGen algorithms in ABAC is less than the cumulative time of TrapGen in EKS and KeyGen in AKP-ABE.

7 CONCLUSIONS

In this paper, we have proposed an attribute-based access control with data (ABAC), which can meet the requirements for data sharing in cloud storage and protect the data confidentiality and attribute privacy effectively. In ABAC, the data users are able to specify the search policy based on their access policies granted by the data owner, and generate the corresponding trapdoor without the help of the data owner. Meanwhile, the cloud server is allowed to search the ciphertext on behalf of data users without knowing the attribute information and underlying plaintext. We have discussed the property, security and performance of ABAC, and implemented it to demonstrate that ABAC is efficient and effective for practical applications. In the future work, we will introduce anonymous KP-ABE with flexible data sharing and efficient data storage for e-health cloud.

References

- [1] "Cloud storage." [Online]. Available: <https://en.wikipedia.org/wiki/Cloudstorage>.
- [2] "Cloud storage service." [Online]. Available: <https://searchstorage.techtarget.com/definition/cloud-storage-service>.
- [2] "The best cloud storage services." [Online]. Available: <https://www.digitaltrends.com/computing/best-cloud-storage-servicescompared/>.
- [3] G. Wang, R. Lu, and Y. Guan, "Enabling efficient and privacy-preserving health query over outsourced cloud," *IEEE Access*, vol. 6, pp. 70831–70842, 2018.
- [4] J. Ni, X. Lin, and X. S. Shen, "Efficient and secure service-oriented authentication supporting network slicing for 5g-enabled iot," *IEEE J. SEL. AREA COMM.*, vol. 36, no. 3, pp. 644–657, 2018.
- [5] W. Guo, J. Shao, R. Lu, Y. Liu, and A. A. Ghorbani, "A privacy-preserving online medicalprediagnosis scheme for cloud environment," *IEEE Access*, vol. 6, pp. 48946–48957, 2018.
- [6] C. Huang, R. Lu, H. Zhu, J. Shao, and X. Lin, "Fssr: fine-grained ehrs sharing via similarity-based recommendation in cloud-assisted ehealthcare system," in *Proc. of ASIACCS'13*, pp. 95–106, ACM, 2016.

Preserving Sensitive Health Care Data in Distributed Cloud Using Block-Chain Concept

S.Meena¹, Dr.V.Gayathri²,

Research Scholar, Department of Computer Science, Periyar University, Salem

Assistant Professor, Department of Computer Science, Pee Gee College of Arts and Science, Dharmapuri

smeenamphil@gmail.com, gayhar11@gmail.com

Abstract

In the modern era, Cloud computing is a boon for computing and technology development. Government and private sectors, education and research, banking, healthcare and other fields generating the huge amount of data every day. Data is sensitive and playing a key role in each sector's growth. Data compromise cannot be acceptable due to natural disaster, stealing, tampering, human error, viruses, malware, power failure, physical damage or automatic failure. Data may be financial or technical or something else, if data is lost, the organization is lost. So, data back-up and security is the major concern. To conquer this issue, moving data towards the cloud will be the appropriate way to preserve data of the specific organization. The advantage of cloud solutions is substantial. Even though Cloud has the vulnerability for data integrity from external and sometimes internal breaches. So, putting raw data into the cloud is the highest risk. In this context, it is important to have latest and reliable systems in place to secure essential sensitive information. This paper proposes an approach for secure data storage is blockchain technique, which can offer global authenticity and security for data and transaction of any kind, diminish the cost and complication by eliminating centralized trust systems and creating data tamper-proof. The experiment is done by using healthcare data and sharing it via blockchain technique. Thus, the results and analysis proving the efficiency of this approach.

Keywords: *Cloud Computing, Data back-up, Data Security, Integrity, Healthcare, Blockchain*

1 Introduction

Global progress is connected to educational institutions, research centers, healthcare industries, banking sectors, and government offices, defense and more. Each of these fields creates a huge amount of data every day [1], which consists of customer information, employee information, and administrative strategies, Accounts or financial information, transactions etc. this information are backbone of all fields requiring rigid security and integrity [2] as it is an essential aspects of the firm's security stance. For the security purpose, the cloud provides the security as a service [3] which includes the several security procedures, policies, controls, and technologies. The created security parameter successfully monitors and protect the cloud system, infrastructure and data effectively. In addition to this, the security parameters continuously analyze the cloud system to regulate the customer authentication, user privacy by establishing the effective authentication rules. The authentication process [4] filters the unwanted users, intermediate access and traffic issues related activities successfully which helps to improve the overall business transactions. This discussed cloud data security process is implemented based on the service requester and service provider join responsibility. This created cloud security [5] provides several benefits such as centralized security, minimum cost for data access, reduces the administration burden, reliability, scalability, confidentiality, and integrity.

Even though the cloud provides the security [6] as a service, still the data privacy, authentication [7] is challenging issue. The cloud needs to provide the security in different levels such as database deposit, internet deposit, server deposit, program deposit and data level security. These different levels of securities are difficult to establish when it comes to the large amount of data. In addition to this, the cloud environment [8] should create the privacy right protection format for providing the safety, privacy related solutions while the user trying to access the data in cloud. For overcoming this security issues, many cryptography techniques [9] such as attributed based encryption, RSA algorithm, key based encryption algorithm, hybridized techniques and block chain approaches are used ensure the authentication between the user and service provider. Among the several methods, this work concentrated on the block chain based security establishment process because the block chain has several benefits compared to other methods. The block chain process [10] is one of the decentralized system. it is easy to access, more secure, easy to implement, cost effective, no down time and maintain several volumes of old and current data in one place successfully. Due to this reason, in this work block chain techniques are used to maintain the data security. Then, the rest of the manuscript is organized as follows, section 2 deals about the various authors' opinion regarding the cloud data security, section 3

discusses about the block chain based medical data security and efficiency of introduced system is evaluated in section 4. Conclusion discussed in section 5.

2 Related Works

This section discusses the various author's opinion about the security while storing data in cloud environment. (R. Josephius Arunkumar et al., 2017)[11] introducing security to health care sector's information such as ECG, temperature, heart rate, blood level, sugar level because it has to be stored in the cloud. During the health care data storing process, it may be accessed by the intermediate person. So, medical data security is handled by applying the dividing and storing concept. The medical data is split into different sub data and it is stored in different databases by performing the encryption process which is done by applying the advance encryption standards (AES) method. Then, the efficiency of the system is evaluated with the help of experimental results. (Vishwanath S Mahalle et al., 2014) [12] Proposed a securing the shared medical data by applying the hybrid RSA and advance encryption standard algorithm in cloud environment. During the data storage process, security algorithm maintains, the secret key, private key, public key and sharing data as well as encrypted information because it may be accessed by intermediate user. In addition to this, security algorithm successfully eliminates the redundant key while sharing the data. At last the efficiency of the system is evaluated using the experimental results.

(Nasrin Khanezaei et al., 2014) [13] Examining the data security in cloud by applying the advance encryption standard algorithm and RSA method. The method examines the cloud storage privacy, security while sharing data in cloud because most of the hackers are trying to access the medical data in cloud. To overcome this drawbacks building secure cloud storage service so it is projected integration of RSA and AES encryption methods to data store multiple users and secure cloud system. Then, the efficiency of the system is evaluated using experimental result in which security has been established with minimum time while sharing data in cloud data storage. (Majid Bakhtiari et al., 2013) [14] analyzed the Cloud Computing stored information to secure search over encryption. The cloud provides the enormous number of services to the cloud requester at the time security is one of the main issues. For overcoming this issues, data encryption standard algorithm is applied for restricting the cipher text searching process. In addition to this, the security is further improved by applying the secure searchable based asymmetric encryption algorithm that effectively manages the entire data security in cloud. Improved searchable encryption algorithm is indeed proven secure and it has the ability to perform a search within encrypted data without decrypting the sources.

(Cong Wang et al., 2012)[15] Uses the third party auditing and homomorphic linear authenticator to manage the privacy in the cloud data storage. This privacy based auditing process help to manage the cloud security as well as it reduces the burden of the user which is done with multiple sessions auditing process. Thus, the proposed system analyzes the cloud security, privacy with efficient and highly secure manner. (Sanchez-Artigas, 2013) [16] Proposed Oblivious RAM based privacy system for managing the cloud data storage. Initially the cloud data are stored by doing the encryption process and then the oblivious RAM process is used to provide the additional privacy for cloud data. Thus, the proposed system optimizes the data privacy in the cloud. (Nupoor et al., 2013)[17] Implements the encryption based cloud security and integrity system. This paper uses the third party auditing process to analyze the privacy of the particular user details. The user details are monitored and encrypted by applying the RC5 encryption algorithm which is stored in the cloud storage devices. During the authentication process the encryption algorithm achieves the secure communication between the cloud and the customers. According to the above descriptions, the cloud security is maintained by applying different encryption and decryption algorithm while sharing medical data in cloud storage. Even though the security algorithms are establishes the security, most of the algorithm is difficult to maintain the privacy, security while sharing sensitivity data also consumes more time while sharing data in cloud. For overcoming the security issues, this paper introduces the block chain based secure medical data storage technique for ensuring the privacy in cloud environment. Then, the detail explanation of the block chain-based security technique is explained as follows.

3 Block chain based Secure Medical Data Storage in Cloud

This section analyzes the block chain [18] based secure medical data storage in cloud environment. The healthcare data is stored in decentralized cloud; the stored data can be affected by several external factors such as physical damage, malware,

human error, viruses, natural disaster, tampering, stealing, power failure and automatic failure. Due to these external factors, data becomes completely loss; it will create severe damage to medical data. For overcoming this issue, effective secure technologies are created for maintaining the health care records, and related data need to be recovered after affecting natural disaster. So, in this paper the method maintains the medical records by utilizing the cryptography methodologies and effective hash function. In cloud health care records are stored by user as well as doctor because user may be access their health records in some other location due to the decentralized cloud storage. During this process, intermediate attacks need to be eliminated for maintaining the quality of the medical records as well as eliminating the malware issues. For managing the security and privacy, block chain methodology is introduced in is cloud and the related architecture shown in Figure 1. Then, the detail explanation of medical data storage process is explained as follows.

3.1 Hospital Side Data Storage in Cloud

This section analyzes the medical data storage process in the hospital side which is performed with the help of block chain methodology. The block chain technique [19] consists of series of records that are linked each other for ensuring the security while sharing or storing information in cloud environment. In addition to this, the block chain process has specific hash function, particular time stamp and transmitted or stored information. Once, the data has been changed in one record it will affect entire information stored in cloud. So, this block chain process based data storage process is difficult to access by intermediate user or unauthorized user. The block data has collection of records in which one record is linked with other record that helps to avoid the data loss in the future. Further, the data has self-backup that completely used to recover the data after data loss. At the time of data storing process, it utilizes particular hash function for maintaining the security of the data. Initially, the transmitted or stored data has been collected from the hospital side, after collecting information, related public and private key is chosen randomly. The selected key is concatenated with the message or information for hiding information from the unauthorized access. In addition to this, the concatenated message has been further encrypted by using cryptographic hash function. In this paper, hash based encryption algorithm is utilized for performing the encryption process. The defined hash encryption is one of effective symmetric algorithm that utilizes the various lengths of keys such as 128, 192 and 256 bits. With the help of the generated key, poly message is generated which is transmitted between parties such as user and cloud storage provider.

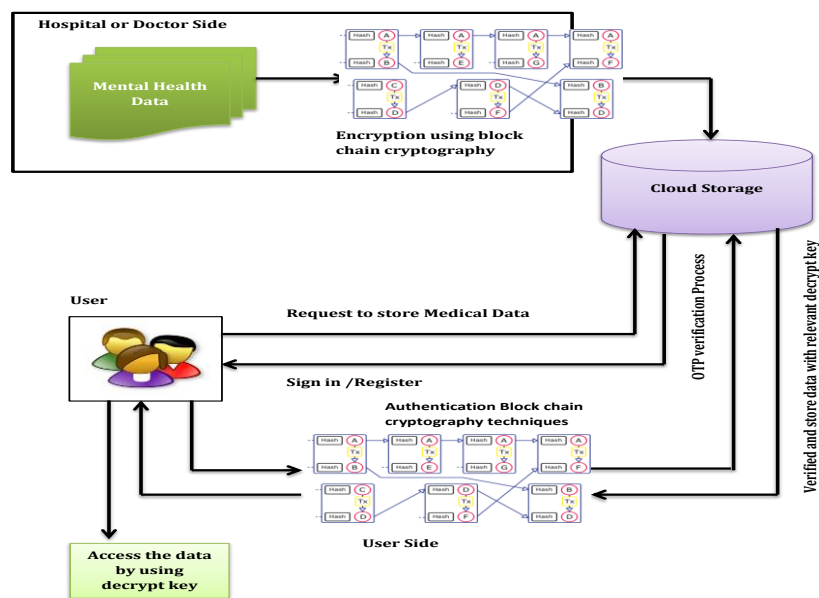


Figure 1: Architecture of Block chain based Secure Medical Data Storage in Cloud

The transmitted poly message helps to maintain the authentication and authorization while storing data into cloud. The defined authentication [20] is ensuring by different ways such as substitution bytes, shift rows, mix column and add rounded keys. These steps are performed in parallel because it helps to speed up the encryption process. First substitute byte step is applied to the information which used to exchange each byte that is done by using S-box operation. This substitution operation is used to replace the original plain text value by other value. The shifting row process is applied to information that changing one row value by other value that ensures the security based cryptographic operations. During the shifting process the 0th will never change due to the security issues. After performing shifting process, mix columns process is performed in which the one column input byte is mixed with the one output column. The mixing operation also makes confuse which two bytes are combined during the phishing attacks. Finally, Add Round Key step is applied, it is one of the simple X-OR operation should be performed between the current block and the expanded block key. The key has been derived from the main block. This process is performed continuously for converting the information in cipher text format. In addition to this cipher text based message, time stamp and link between next block is mentioned for maintaining the record list. The next block also contains the same information and encrypted format. This process is repeated continuously until getting the encrypted information and secure block chain list. Then, the algorithm of the block chain based encryption algorithm is discussed as follows.

Table 1: Block Chain based Cloud Data Encryption Algorithm

This section discusses the detailed processing steps of cloud data encryption process.

| |
|--|
| <p>Step 1: Initially, collect the information which wants to save in cloud storage.</p> <p>Step 2: Initialize the public and private key randomly, for concatenate the information with this generated key.</p> <p>Step 3: Chose the 128 bit plain text from the above step and variable keys, divided into two halves for doing the encryption process.</p> <p>Step 4: Select the look up table to performing the substitution bytes</p> <p>Step 5: Shift the rows expect the 0th row.</p> <p>Step 6: Mix the plain text and the outcome of the columns to get the expanded key.</p> <p>Step 7: Add rounded key operation is performed up to 9 rounds to achieve the better encryption data.</p> <p>Step 8: Apply the encryption up to 16 rounds using the following equation</p> $H = s^{k-1}(h(C_1)) \oplus s^{k-2}(h(C_2)) \dots \oplus s(h(C_{k-1})) \oplus h(C_k) \quad (1)$ <p>Step 9: Along with the encrypted message, time stamp and link between the next block for making the further encryption process.</p> <p>Step 10: Transmit to encrypt data to the user and the cloud storage provider to ensure the authentication and authorization in the cloud environment.</p> <p>Step 11: Repeat the process to get the security while sharing data in the cloud with effective manner.</p> |
|--|

According to the above algorithm procedure, the medical and other data is stored in the cloud with secure manner also the stored data is accessed by anytime while disaster happens. Likewise, the client or user side the data has been stored in same process also the data is accessed according to the user demands successfully, even after, the data becomes loss which is explained as follows.

3.2 User side Data Storage in Cloud

This section deals that the user side data storage in cloud also accessing the medical or other data in the cloud. Initially, the user request cloud storage provider for storing data into the cloud. The cloud storage provider wants user to register or sign in the respective website for making the secure information transaction in cloud. During this process, same block chain process is utilized for making the authentication process which works according to the Table 1 algorithm steps. After performing the encryption or user has to be authenticated by applying the one Time Pad (OTP) verification process [21]. The OTP pad has been displayed on the user screen with the help of the phone number because they register their phone number while performing sign-up process. The defined OTP is displayed on the user screen with particular time that establishes the authentication between user and cloud storage provider. After verifying the user, the data has been stored in the cloud storage provider, and the provider generates the particular key which helps to perform the decryption process. Based on the key, decryption process is performed

and the respective data has been accessed by user with effective manner. Then, user side secure data access process related algorithm step is explained as follows.

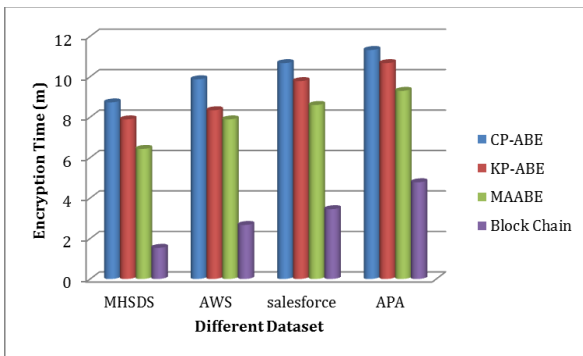
Table 2: Algorithm for Medical Data' Storing in User Side

| |
|---|
| <p>Step 1: User first send request to the cloud storage provider via sign up or sign in process.</p> <p>Step 2: Encrypt the user information by using the block chain process which is mentioned in Table 1.</p> <p>Step 3: Authenticate the user using the secret key (OTP) which is received from phone.</p> <p>Step 3: Enter the secret key using the OTP pad which is provided by the cloud storage provider</p> <p>Step 4: After authentication, exchange their key with cloud storage provider</p> <p>Step 5: Then, the decryption key values are exchange for accessing the data with related decryption key.</p> <p>Step 6: With the help of the key decryption process is performed and the data has been accessed.</p> |
|---|

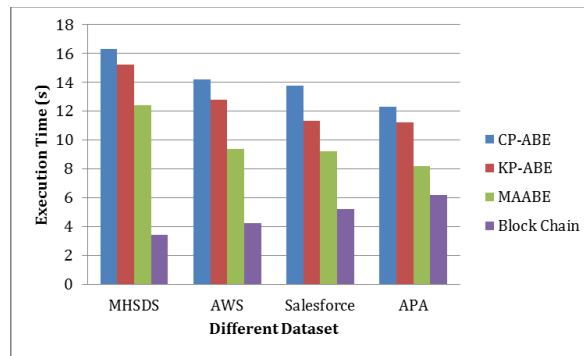
Thus, the above user side block chain encryption process and one time pad method helps to authenticate the user as well as store the data with secure manner. This process eliminates the intermediate attacks and unauthorized access, maintains the trust between user and cloud storage provider with effective manner. Then, the efficiency of block chain based encryption process based secure medical and other data transaction is evaluated using following experimental results that is explained as follows.

4 Experimental Results

This section analyzes the efficiency of the proposed block chain based secure data storage system in cloud environment. In this work different kinds of data such as health care data, education information, banking information and other details are stored in the cloud for making the research applications. So, different data set such as Mental Health Services Data Set (MHSDS) (<http://content.digital.nhs.uk/mhsds>), American Psychological Association (APA) (<http://www.apa.org/research/responsible/data-links.aspx>), Amazon Web Service (AWS) (<https://aws.amazon.com/public-data-sets/>) and Salesforce.com (<http://www.salesforce.com/in/>) are used to analyze the efficiency of the block chain based secure data storage process in cloud. The database has collection of several information such as login details, banking information, credit card information, health information, study details, personal information and so on. This information's are collected from various people such as children, working people, adults and so on. The stored information may consist of much sensitive information which may be affected by several intermediate attacks. For overcoming this security issue, block-chain method has been applied because it effectively utilizes the hash function that link one block to another block which is create more difficulties while accessing sensitive information, as well as key by third parties. The introduced block chain methodology successfully maintains the security, authentication, confidentiality, integrity and privacy also manages the trust between user and cloud storage provider. The managed block chain based secure cloud storage system efficiency is analyzed in terms of security and authentication based performance metrics. Then, the utilized efficient metrics [22] are listed as follows. **Security** : The important metric is securities because when the user trying to store the information in cloud, the stored data, key and other personal OTP messages are need to be hide from the third party access. **Data Sharing or Uploading** : The data sharing or storage is other important process which encrypts the stored data with relevant public, private key and hash function because it used to detect the unwanted access and data change. **Authentication** :The next important metric is authentication in which authenticate user only access and store the data in cloud environment. The generated hash function based block chain process successfully maintains the user authentication with minimum encryption time, execution time, cost and maximum amount of security. Then, the obtained encryption time is shown in Figure 2.



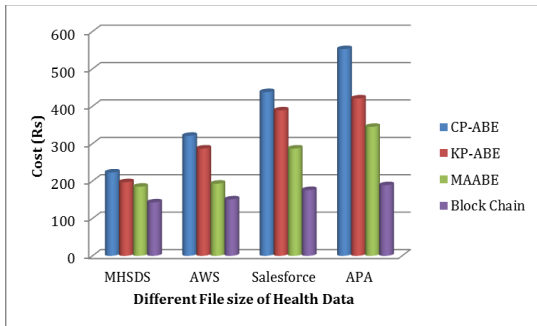
2(a) Encryption time



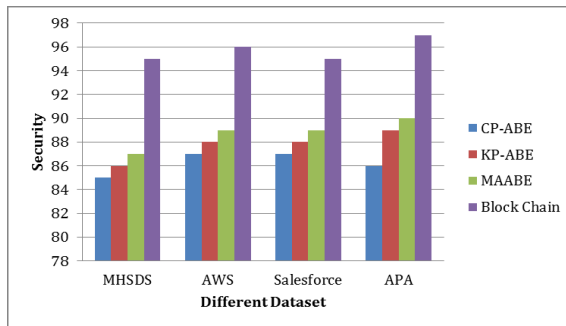
2 (b) Execution time

Figure 2 (a) & (b) : Encryption time and execution time for different encryption methods of different Cloud dataset

The Figure 2 (a) & (b) indicates that block chain based encryption method with minimum encryption and execution time. The algorithm successfully maintains the link between one hash function to another function that helps to maintains the shared key also encrypts the data with minimum encrypt time while storing different data in cloud. The stored dataset information may be different in file size but the introduce block chain method maintains the security, authentication and authorization with minimum encryption time. The minimum encryption time improves the overall execution time while sharing data and also establishing security in different dataset.



2(a) Cost



3 (b) Security

Figure 3 (a) & (b): Cost and Security for Different Encryption Method on Different Dataset

The Figure 3 (a) & (b) shows that introduced block chain methodology consumes minimum cost for storing different data in cloud when compared to other methods. Due to the minimum encryption and execution time, the block chain method maintains the high security while storing data in cloud. Then, the obtained security measure is shown in Figure 3(b) successfully manages the user sensitive information while storing data in both doctor and user side. Not only the medical data, it also manages the security in other data sets such as amazon web service and sales force data set. Thus the proposed system ensures the security with minimum time in the cloud environment when compared to the existing methods. So, the user details are managed successfully in the third party server.

5 Conclusion

This paper analyzes the secure data storage process in cloud by applying the block chain based encryption algorithm with one time pad authentication process. Initially the method maintains the security in both hospital and user side because both people are trying to store their data in cloud due to the upcoming research purpose. At the time of authentication process particular hash function is utilized for performing the encryption process in hospital side. The same hash based block chain process is utilized in the user side along with the OTP verification process for maintaining the authentication while storing data in the cloud. According to the OTP verification process, the key is provided to the authenticated client to access the data in

future use. Then, the efficiency of the system is evaluated with the help of java language in terms of the encryption time, execution time and cost. Thus, the introduced block chain based authentication process attains the maximum security (96%) while storing data in the cloud environment. Introduced secured block chain methodology helps to access the data in any time when external factors happens in cloud environment.

Reference

- [1] Jeon, B.S., Na, J.C.: A study of cyber security policy in industrial control system using data diodes. In: 2016 18th International Conference on Advanced Communication Technology (ICACT), pp. 314–317, January 2016. <https://doi.org/10.1109/ICACT.2016.7423374>
- [2] S. Pearson, “Taking account of privacy when designing cloud computing services,” in Proceedings of the ICSE Workshop on Software Engineering Challenges of Cloud Computing (CLOUD ’09), pp.44–52, Vancouver, Canada, May 2009.
- [3] M. Jensen, J. Schwenk, N. Gruschka, and L. L. Iacono, “On technical security issues in cloud computing,” in Proceedings of the IEEE International Conference on Cloud Computing (CLOUD’09), pp.109–116, September 2009.
- [4] M. Mowbray and S. Pearson, “A client-based privacy manager for cloud computing,” in Proceedings of the 4th International ICST Conference on Communication System Software and Middleware (COMSWARE’09), Dublin, Ireland, June 2009
- [5] Rong, C., Nguyen, S.T., Jaatun, M.G.: Beyond lightning: a survey on security challenges in cloud computing. *Comput. Electr. Eng.* 39(1), 47–54 (2013). <https://doi.org/10.1016/j.compeleceng.2012.04.015>, <http://www.sciencedirect.com/science/article/pii/S0045790612000870>. Special issue on Recent Advanced Technologies and Theories for Grid and Cloud Computing and Bio-engineering
- [6] Hashizume, K., Rosado, D.G., Fernández-Medina, E. et al. An analysis of security issues for cloud computing. *J Internet Serv Appl* 4, 5 (2013). <https://doi.org/10.1186/1869-0238-4-5>
- [7] Wang C., Wang D., Wang H., Xu G., Sun J., Wang H. (2019) Cloud-Aided Privacy Preserving User Authentication and Key Agreement Protocol for Internet of Things. In: Meng W., Furnell S. (eds) Security and Privacy in Social Networks and Big Data. SocialSec 2019. Communications in Computer and Information Science, vol 1095. Springer, Singapor
- [8] Shen, J., Gui, Z., Ji, S., Shen, J., Tan, H., Tang, Y.: Cloud-aided lightweight certificateless authentication protocol with anonymity for wireless body area networks. *J. Netw. Comput. Appl.* 106, 117–123 (2018)
- [9] Kumar S., Shekhar J., Singh J.P. (2018) Data Security and Encryption Technique for Cloud Storage. In: Bokhari M., Agrawal N., Saini D. (eds) Cyber Security. Advances in Intelligent Systems and Computing, vol 729. Springer, Singapore
- [10] Wei P., Yuan Q., Zheng Y. (2018) Security of the Blockchain Against Long Delay Attack. In: Peyrin T., Galbraith S. (eds) Advances in Cryptology – ASIACRYPT 2018. ASIACRYPT 2018. Lecture Notes in Computer Science, vol 11274. Springer, Cham
- [11] R. Josephius Arunkumar, R. Anbuselvi, 2017, “Enhancement Of Cloud Computing Security In Health Care Sector” *International Journal of Computer Science and Mobile Computing*, volume 6, issue 8.
- [12] Vishwanath S Mahalle ; Aniket K Shahade, 2014, “Enhancing the data security in Cloud by implementing hybrid (Rsa & Aes) encryption algorithm”, 2014 International Conference on Power, Automation and Communication (INPAC).
- [13] N Khanezaei, ZM Hanapi, “A framework based on RSA and AES encryption algorithms for cloud computing services”, *Systems, Process and Control (ICSPC)*, 2014 IEEE Conference on, 58-62
- [14] M Bakhtiari, M Nateghizad, A Zainal, “Secure Search Over Encrypted Data in Cloud Computing”, *Advanced Computer Science Applications and Technologies (ACSAT)*, 2013
- [15] Cong Wang, Sherman S.-M. Chow, Qian Wang, Kui Ren and Wenjing Lou, 2012, “Privacy-Preserving Public Auditing for Secure Cloud Storage” *IEEE Transaction on Computers*, Volume:62 , Issue: 2, pp. 362 – 375
- [16] Sanchez-Artigas, 2013, “Toward efficient data access privacy in the cloud”, *International Journal of Communications Magazine in IEEE* , Volume:51, Issue: 11, pp. 39 – 45.
- [17] Nupoor M. Yawale, Gadichha, 2013, “Third Party Auditing (TPA) for Data Storage Security in Cloud with RC5 Algorithm”, *International Journal of Advanced Research in Computer Science and Software Engineering*, Volume 3, Issue 11, pp. 1032-038
- [18] Pass, R., Shi, E.: Thunderella: blockchains with optimistic instant confirmation. In: Nielsen, J.B., Rijmen, V. (eds.) EUROCRYPT 2018. LNCS, vol. 10821, pp. 3–33. Springer, Cham (2018). https://doi.org/10.1007/978-3-319-78375-8_1
- [19] Natoli, C., Gramoli, V.: The balance attack against proof-of-work blockchains: the R3 testbed as an example. *Computing Research Repository* (2016). arXiv:1612.09426
- [20] Masala G.L., Ruiu P., Grosso E. (2018) Biometric Authentication and Data Security in Cloud Computing. In: Daimi K. (eds) *Computer and Network Security Essentials*. Springer, Cham
- [21] Ben Halima R., Kallel S., Klai K., Gaaloul W., Jmaiel M. (2016) Formal Verification of Time-Aware Cloud Resource Allocation in Business Process. In: Debruyne C. et al. (eds) *On the Move to Meaningful Internet Systems: OTM 2016 Conferences*. OTM 2016. Lecture Notes in Computer Science, vol 10033. Springer, Cham
- [22] S. Meena, Dr. V. Gayathri, “ An Approach To Secure Mental Health Data In The Cloud Using End-To-End Encryption Technique”, *International Journal of Computer Engineering & Technology (IJCET)* Volume 8, Issue 5, Sep-Oct 2017, pp. 87–98,

Iot Based Automated Safety Industrial System

N.Kumar¹, K. Kamali¹, K. Sivasankari¹, E.Sowmiya¹

sankari.k1999@gmail.com

Abstract

This project illustrates a precarious industrial environment monitoring and control for this monitoring information concerning safety and security. The proposed system uses a combination sensor network node with a system architecture and concept implementation, which are described mainly for an industrial safety monitoring scenario. The information is gathered by the deployed sensor network with focus on four main conditions: temperature, fire, gas leakage and Air pollution. This Project also enables an easy to use user interface and the accessibility of data through standards-based web server technologies. It is the most effective and most economical means of equipment safety monitoring.

Keywords: *Wireless sensor network (WSN),internet of things(IOT),gas,fire,air pollution,temperature.*

1.Introduction:

The environmental care has become one of the prime concerns for almost every country in the last decades. Even though the number of industrial accident has been increasing in the last few decades, the current scenarios in the industry have not improved. They tend to be more a dangerous environment rather than a safe one even with a wide range of modern technologies. Recently the current industries have been demanding sophisticated instrumentation for monitoring and control of environmental risk parameters in the danger-prone areas. Human safety and property losses are the essential to maintain a balance between industry and industrial environments. Five main components are the reasons for an accident to occur: the fire, gas leakage, radiation, over voltage and high temperature. An industrial accident usually occurs individually to the above mentioned factors or as the result of their combined effects. In this paper propose, combining the virtual monitoring technology with hazardous risk management together, a wireless multi-sensory monitoring system of hazardous site environment. Wireless sensor network architecture is adopted and based on virtual instrument technology, Virtual instrumentation environment. In this project we propose a combination of the real time monitoring technology with the sensors to keep a time to time track of the various factors which are ~~recognised~~ ~~recoognised~~ to cause an accident on site. In addition to this, internet of things wireless sensor network architecture are adopted. The function of real-time monitoring is to provide remote-distance hazardous parameters information, display the data, analyze, identify when the parameters cross threshold, provide warning in case of an accident. A wide range of industrial IOT applications have been developed and deployed in recent years. In an effort to understand the development of IOT in Industries.

2.Existing System:

The gas leakage has caused several damages in our homes, Laboratories among others. Installation of a gas leakage detection device was globally inspired to eliminate accidents related to gas leakage. We present an alternative approach to developing a device that can automatically detect and control gas leakages and also monitor temperature. The system detects the leakage of the LPG (Liquefied Petroleum Gas) using a gas sensor, then triggered the control system response which employs ventilator system, Mobile phone alert.

Disadvantages:

- Very low range of connectivity
- Require more time and space to operate.
- Data can't be accessed on time if there are any internet issues

3. Proposed System:

The proposed system uses a combination sensor network with a system architecture and concept implementation, which are described mainly for an industrial safety monitoring scenario. The information is gathered by the deployed sensor network with focus on five main conditions: temperature, fire, gas leakage and Air pollution. This paper also enables an easy to use user interface and the accessibility of data through standards-based web server technologies.

4 .Working Model:

The system comprises of a base station and a Wireless sensor node. A microcontroller acts as a base station. Temperature, Fire, Air Pollution and gas leakage sensors with associated signal conditioners attached to ATMEL 32 bit controller. Fig. 1 shows the block diagram of the system. In this project we are measuring the vital parameters. Any leakage of poisonous gases can be detected and if temperature is increased beyond certain limit it will intimate the concerned person. Similarly, if fire accidents occur then it will intimate to the owner through GSM which commonly called IOT protocol along with a message through Cloud server. If Gas leakage occurs we can on the power to the Exhaust fan .In addition to this we use a buzzer and a display for intimating the other workers about the accidents.

5. Hardware Description:

5.1 ATMel 328 Microcontroller:

The Atmel AVR® core combines a rich instruction set with 32 general purpose working registers. All the 32 registers are directly connected to the Arithmetic Logic Unit (ALU), allowing two independent registers to be accessed in a single instruction executed in one clock cycle. The resulting architecture is more code efficient while achieving throughputs up to ten times faster than conventional CISC microcontrollers. The ATmega328/P provides the following features: 32Kbytes of In-System Programmable Flash with Read-While-Write capabilities, 1Kbytes EEPROM, 2Kbytes SRAM, 23 general purpose I/O lines, 32 general purpose working registers, Real Time Counter (RTC), three flexible Timer/Counters with compare modes and PWM, 1 serial programmable USARTs , 1 byte-oriented 2-wire Serial Interface (I2C), a 6- channel 10- bit ADC (8 channels in TQFP and QFN/MLF packages) , a programmable Watchdog Timer with internal Oscillator, an SPI serial port, and six software selectable power saving modes.

5.2 16x 2 LCD Modules:

Liquid crystal displays (LCDs) have materials which combine the properties of both liquids and crystals. Rather than having a melting point, they have a temperature range within which the molecules are almost as mobile as they would be in a liquid, but are grouped together in an ordered form similar to a crystal.

The LCDs used exclusively in watches, calculators and measuring instruments are the simple seven-segment displays, having a limited amount of numeric data. The recent advances in technology have resulted in better legibility, more information displaying capability and a wider temperature range. These have resulted in the LCDs being extensively used in telecommunications and entertainment electronics.

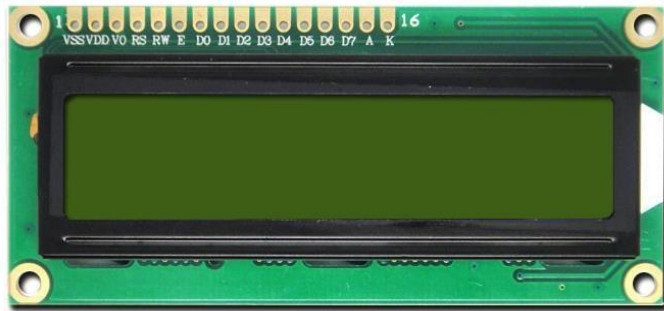


Figure2: 16x 2 LCD Modules

5.3GAS Sensor

The analog Smoke/LPG/CO Gas Sensor (MQ2) module utilizes an MQ-2 as the sensitive component and has a protection resistor and an adjustable resistor on board. The MQ-2 gas sensor is sensitive to LPG, i-butane, propane, methane, alcohol, Hydrogen and smoke. It could be used in gas leakage detecting equipment in family and industry. The resistance of the sensitive component changes as the concentration of the target gas changes.



Figure3: Gas Sensor

5.4FIRE Sensor:

A fire detector is a sensor intended to distinguish and react to the nearness of a fire or fire, permitting fire detection. Reactions to a recognized fire rely upon the establishment, however, can incorporate sounding an alert, deactivating a fuel line, (for example, propane or a gaseous petrol line), and enacting a fire concealment system.



Figure4:Fire Sensor

5.5 Buzzer:

A buzzer is a mechanical, electromechanical, magnetic, electromagnetic, piezoelectric audio signaling device. A piezo electric buzzer can be driven by an oscillating electronic circuit or with other audio signal source. A click or beep can indicate that a button has been pressed. There are several different kinds of buzzers which are based on their sound levels. The common sizes for Sound Level are 80 dB, 85 dB etc.



Figure5: Buzzer

5.6 Relay:

Relays are components which allow a low-power circuit to switch a relatively high current on and off, or to control signals that must be electrically isolated from the controlling circuit itself. Here is a quick rundown. To make a relay operate, you have to pass a 'pull-in' and 'holding' current (DC) through its energizing coil. And relay



Figure6: Relay

5.7 BLUETOOTH MODULE HC-05

HC-05 module is an easy to use Bluetooth SPP (Serial Port Protocol) module, designed for transparent wireless serial connection setup. The HC-05 Bluetooth Module can be used in a Master or Slave configuration, making it a great solution for wireless communication. This serial port Bluetooth module is fully qualified Bluetooth V2.0+EDR (Enhanced Data Rate) 3Mbps Modulation.



Figure7:Bluetooth Module Hc-05

5.8 IOT Platform:

A web page is used to provide a suitable interface between the user and the Industrial Safety Automation System. A particular IP address is provided for the particular industry and this IP does not change as it is hosted on Amazon Web Server. The screenshot in Figure 4.8 depicts the connecting page as seen on the user’s mobile phone. Only after authentication is an individual allowed access to check the condition of the industry. The screenshot shown in Figure 4.9 is the home screen that is displayed once login is successful. This contains the different columns representing different data. This is continuously updated every second and keeps track of previous data tooserver..

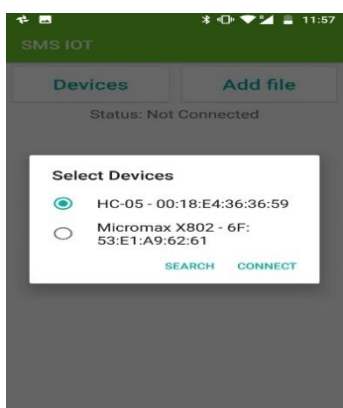


Figure8: Connect Page The IOT

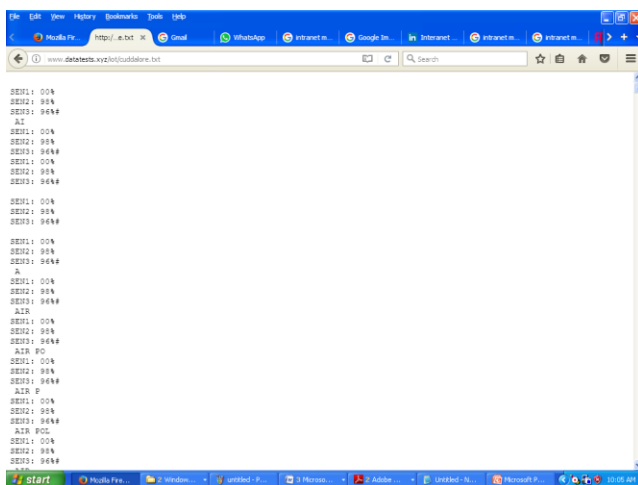


Figure9: Real time IOT based industry monitoring

6. Results:

The implemented system was tested efficiently and tested for proper working. The initialization of the IOT and working of the sensors were verified. Messages were obtained after each alert and corresponding data uploaded on to the cloud storage. The buzzer and sprinkler also worked efficiently.

7. Conclusion:

Our project was to provide a safe environment for the workers several industrial accident like fire and gas, Temperature etc. The incidents of unauthorized access can be resolved using our system A simple system to improve the standards is developed. It is a real time monitor able system developed with simple hardware which simplifies the possibility of error free security system. This IOT system can be easily implemented with maximum reliability and high security with low cost, It is a special enhancement.

REFERENCES:

- [1] Aparajita Das, ManashPratimSarma, Kandarpa Kumar Sarma, Nikos Mastorakis, 'Design of an I oT based Real Time Environment Monitoring System using Legacy Sensors ',22nd International Conference on Circuits,Systems, Communications and Computers (CSCC 2018)Volume 210, 2018.
- [2] Zumyla Shanaz F, Prem Kumar S R, Rahul R, Rajesh Kumar M, Santhosh Kumar C, 'IoT based Industrial Pollution Monitoring System ',International Research Journal of Engineering and Technology (IRJET), Volume:06 Issu, 03, Mar 2019.
- [3] Daudi S. Simbeye, 'Industrial Air Pollution Monitoring System Based on Wireless Sensor Networks', Journal of Information Sciences and Computing Technologies, November 21, 2017.
- [4] KashmiraThul, PritiDhote, AshwiniChokole, Samir Raipurkar. "GSM based industrial security system". International Journal of Innovations in Engineering and Science, e-ISSN:2456-3463 Vol.2 No.4, 2017.
- [5] Sureshkumar A , S Muruganand , Study on a Hazardous Environment Monitoring and Control Using Virtual Instrumentation , Journal of Instrumentation Technology , pp 1-10 ,2013.
- [6] Chung, P.W.H., Yang, S.H. and Edwards, D.W. (1999) 'Hazard identification in batch and continuous computercontrolledplants', Industrial & Eng. Chem. Research, Vol. 38, pp.4359–4371,2013.
- [7] A. Lay-Ekuakille,P.Vergallo, and N.I.Guannoccaro "Prediction and validation of outcomes from air monitoring sensors and network of sensors," in Proceedings of the 5th International Conference on Sensing Technology, pp. 73-78,2011.
- [8] Pravin J, Deepak Sankar A, Angeline Vijula D, 'industrial pollution monitoring system using labview and gsm ',International Journal of Advanced Research in Electrical,Electronics and Instrumentation Engineering, Vol. 2, Issue 6, June 2013.
- [9] T. Murugan, AzhaPeriasamy, S. Murugananad. "Embedded based industrial temperature monitoring system using GSM". International Journal of Computer Applications (0975-8887) volume 58-No. 19, November 2012.
- [10] Onengiye M. Georgewill, Chukwunazo J. Ezeofor. "Design and implementation of SMS-based industrial/homes gas leakage monitoring and detection alarm System". International Journal of Engineering Trends and Technology (IJETT)-Volume 35 Number 9-May 2016.

Deep Learning Based Identification Of Novel Corona Virus Using Lung (Lus)

J.Madhavan¹, G.Thirumalvalav²,P.Praveen Kumar³,P.JustinRaj⁴
MrN.Kumar⁵

Assistance Professor⁵

Department of Computer Science Engineering^{1, 2,3,4,5}
St.Anne's College Of Engineering And Technology^{1, 2,3,4,5}

Abstract

Theoretical—Deep learning (DL) has demonstrated effective in clinical imaging and, in the wake of the new COVID19 pandemic, a few works have begun to examine DLbased answers for the helped conclusion of lung infections. While existing works center around CT filters, this paper contemplates the use of DL methods for the investigation of lung ultrasonography (LUS) pictures. Specifically, we present a novel completely commented on dataset of LUS pictures gathered from a few Italian medical clinics, with names demonstrating the level of infection seriousness at a casing level, video level, also, pixel-level (division covers). Utilizing these information, we present a few profound models that address applicable assignments for the programmed examination of LUS pictures. Specifically, we present a novel profound organization, inferred from Spatial Transformer Networks, which at the same time predicts the infection seriousness score related to an info outline and gives limitation of neurotic ancient rarities in a feebly administered way. Besides, we present a new strategy dependent on uninorms for viable casing score conglomeration at a video-level. At last, we benchmark state of the craftsmanship profound models for assessing pixel-level divisions of COVID-19 imaging biomarkers. Trials on the proposed dataset show acceptable outcomes on all the thought about errands, making ready to future examination on DL for the helped conclusion of COVID-19 from LUS information.

Inroduction:

The quick worldwide SARS-CoV-2 flare-up brought about a shortage of clinical hardware. Notwithstanding an around the world lack of mouth covers and mechanical ventilators, testing limit has been seriously restricted. Need of testing was along these lines given to suspected patients and clinic staff. Nonetheless, broad testing and diagnostics are critical to successfully contain the pandemic. In reality, nations that have had the option to accomplish enormous scope testing of perhaps contaminated individuals joined with monstrous resident reconnaissance, reached significant control of the SARSCoV-2 infection. The insufficient testing limit in most nations has along these lines prodded the need and quest for elective strategies that empower conclusion of COVID-19. Likewise, the precision of the current lab test, turn around record polymerase chain response (RT-PCR) clusters, remains profoundly subject to clean method and area. Coronavirus pneumonia can quickly advance into a very basic condition. Assessment of radiological pictures of over 1,000 COVID-19 patients showed numerous intense respiratory misery condition (ARDS)- like attributes, like reciprocal, furthermore, multi-lobar glass ground opacifications (predominantly posteriorly and additionally incidentally circulated). All things considered, chest figured tomography (CT) has been begat as a potential elective for diagnosing COVID-19 patients. While RTPCR may require as long as 24 hours and requires various tests for definitive outcomes, finding utilizing CT can be a lot speedier. In any case, utilization of chest CT accompanies significant downsides: it is expensive, opens patients to radiation, requires broad cleaning after outputs, and depends on radiologist interpretability. Recently, ultrasound imaging, an all the more broadly accessible, costeffective, protected and continuous imaging method, is acquiring consideration. Specifically, lung ultrasound (LUS) is progressively utilized in purpose-of-care settings for location and the executives of intense respiratory problems. At times, it exhibited preferred affectability over chest X-beam in recognizing pneumonia. Clinicians have as of late depicted utilization of LUS imaging in the trauma center for determination of COVID-1. Discoveries propose specific LUS qualities and imaging biomarkers for COVID-19 patients which might be used to both recognize these patients and deal with the respiratory efficacy of mechanical ventilation. The expansive scope of pertinence and moderately low costs make ultrasound imaging an extremely useful technique in situations when patient inflow exceeds the regular hospital imaging infrastructure capabilities. Thanks to its low costs, it is also accessible for low- and middle-income countries. However, interpreting ultrasound images can be a challenging task and is prone to errors due to a steep learning curve. Recently, automatic image analysis by machine and deep learning (DL) methods have already shown promise for reconstruction, classification, regression and segmentation of tissues using ultrasound images. In this paper we describe the use of DL to assist clinicians in detecting COVID-19 associated imaging patterns on point-of-care LUS. In particular, we tackle three different tasks on LUS frame-based classification, video-level grading and pathological artifact segmentation. The first task consists of classifying each

single frame of a LUS image sequence into one of the four levels of disease severity, defined by the scoring system. Video-level grading aims to predict a score for the entire frame sequence based on the same scoring scale. Segmentation instead comprises pixel-level classification of the pathological artifacts within each frame. This paper advances the state of the art in the automatic analysis of LUS images for supporting medical personnel in the diagnosis of COVID-19 related pathologies in many directions. (1) We propose an extended and fully-annotated version of the ICLUS-DB database. The dataset contains labels on the 4-level scale proposed, both at frame and video-level. Furthermore, it includes a subset of pixel-level annotated LUS images useful for developing and assessing semantic segmentation methods. (2) We introduce a novel deep architecture which permits to predict the score associated to a single LUS image, as well as to identify regions containing pathological artifacts in a weakly supervised manner. Our network leverages Spatial Transformers Network (STN) and consistency losses to achieve disease pattern localization and from a soft ordinal regression loss for robust score estimation. (3) We introduce a simple and lightweight approach based on uninformative to aggregate frame-level predictions and estimate the score associated to a video sequence. (4) We address the problem of automatic localization of pathological artifacts evaluating the performance of state-of-the-art semantic segmentation methods derived from

Related Work

DL has demonstrated to be fruitful in a huge number of PC vision assignments going from object acknowledgment and identification to semantic division. Persuaded by these triumphs, more as of late, DL has been progressively utilized in clinical applications, for example for biomedical picture division or pneumonia identification from chest X-beam. These original works demonstrate that, with the accessibility of information, DL can prompt the help and robotization of starter analyze which are of gigantic significance in the clinical local area. In the wake of the current pandemic, late works have centered on the identification of COVID-19 from chest CT. , a U-Net sort network is utilized to relapse a bouncing box for each dubious COVID-19 pneumonia area on continuous CT checks, and a quadrant-based filtering is misused to lessen conceivable bogus positive identifications. In an unexpected way, limit based locale proposition is first used to recover the area of interests (RoIs) in the information examine and the Inception network is misused to order each proposed RoI. Likewise, , a VNET-IR-RPN model pre-prepared for pneumonic tuberculosis identification is utilized to propose RoIs in the info CT furthermore, a 3D adaptation of Resnet-18 is utilized to arrange each return on initial capital investment. In any case, not very many works utilizing DL on LUS pictures can be found in the writing A classification and weakly supervised limitation strategy for lung pathology is portrayed . In light of a similar thought, in a casing based classification and pitifully managed division technique is applied on LUS pictures for COVID-19 related example location. Here, Efficientnet is prepared to perceive COVID-19 in LUS pictures, after which class enactment maps (CAMs) are misused to deliver a pitifully managed division guide of the info picture. Our work has a few contrasts contrasted with all the past works. To start with, while CAMs are utilized for restriction, in this work we misuse STN to get familiar with a pitifully regulated limitation strategy from the information (for example not abusing express marked areas however surmising it from basic edge based classification names). Second, a classification problem is solved, we focus on ordinal regression, predicting not only the presence of COVID-19 related artifacts, but also a score connected to the disease severity. Third, we move a step forward compared to all previous methods by proposing a video-level prediction model built on top of the frame-based method. Finally, we propose a simple yet effective method to predict segmentation masks using an ensemble of multiple state-of-the-art convolutional network architectures for image segmentation. Additionally, the model's predictions are accompanied with uncertainty estimates to facilitate interpretation of the results.

Limitations Of The Dataset

Our division model can portion and segregate between zones in B-mode LUS pictures that contain foundation, solid markers and (various phases of) COVID-19 biomarkers at a pixel-level, arriving at a pixel-wise precision of 96% and a twofold Dice score of 0.75. Close by these divisions, we give spatial vulnerability gauges that might be utilized to decipher model expectations. Strangely, and significantly, none of the most noteworthy (and generally extreme) score list explanations in the test set were missed by our model, decided by visual appraisal of the coming about divisions, and by breaking down the relative imagelevel crossing points among the relating anticipated and commented on areas. Additionally, we noticed model expectations of COVID-19-positive locales, that had anyway not been explained accordingly. Fig. 6B shows a delegate model of such a case. After reexamining some of such models from the test set, along with the annotators, we discovered that the annotators were once in a while uncertain whether to clarify a district as for example score 2 or 3, and in this manner concluded that the marker was not satisfactory enough to clarify the area by any stretch of the imagination, prompting the previously mentioned inconsistency. Division execution and extraction of semantics could be

additionally supported by utilizing transient construction among outlines in a successive model. Such models could gain from explanations across full recordings, or through incomplete explanations and powerless management. We leave these augmentations of the current technique to future work.

Proposed System:

This paper propels the best in class in the programmed investigation of LUS pictures for supporting clinical faculty in the analysis of COVID-19 related pathologies in numerous headings. (1) We propose an all-encompassing and completely clarified rendition of the ICLUS-DB information base. The dataset contains marks on the 4-level scale proposed in [12], both at outline and video-level. Besides, it incorporates a subset of pixel-level explained LUS pictures valuable for creating and evaluating semantic division strategies. (2) We present a novel profound design which licenses to foresee the score related to a solitary LUS picture, just as to distinguish locales containing neurotic curios in a pitifully directed way. Our network use Spatial Transformers Network (STN) furthermore, consistency misfortunes to accomplish illness design restriction what's more, from a delicate ordinal relapse misfortune for strong score assessment. (3) We present a basic and lightweight approach dependent on uninformal to total edge level expectations and gauge the score related to a video succession. (4) We address the issue of programmed confinement of neurotic ancient rarities assessing the exhibition of best in class semantic division techniques got from fully convolutional architectures. (5) Finally, we conduct an extensive evaluation of our methods on all the tasks, showing that accurate prediction and localization of COVID-19 imaging biomarkers can be achieved with the proposed solutions.

Frame-Based Score Prediction Evaluation:

The substitution of the customary cross-entropy (CE) with the SORD misfortune for ordinal relapse unmistakably improves the exhibition. On the other hand, we found that the expansion of STN prompts a drop in the F1-score due to the extra teachable boundaries (as numerous as the CNN) presented by the STN and the shortfall of a regularization. Nonetheless, STN accompanies two positive results: (i) it gives pitifully directed restrictions without utilizing fine-grained management; and (ii) empowers the utilization of consistency-based regularization, which is very beneficial regarding execution. Our full model, which installs the STN module, the SORD misfortune and the proposed consistency misfortune accomplishes a F1-score of 65.1, beating all the baselines by a huge edge. To additionally examine if the support happens due to the consistency term or the STN, we directed a trial utilizing two sufficiently covering

Video-Based Score Prediction Evaluation

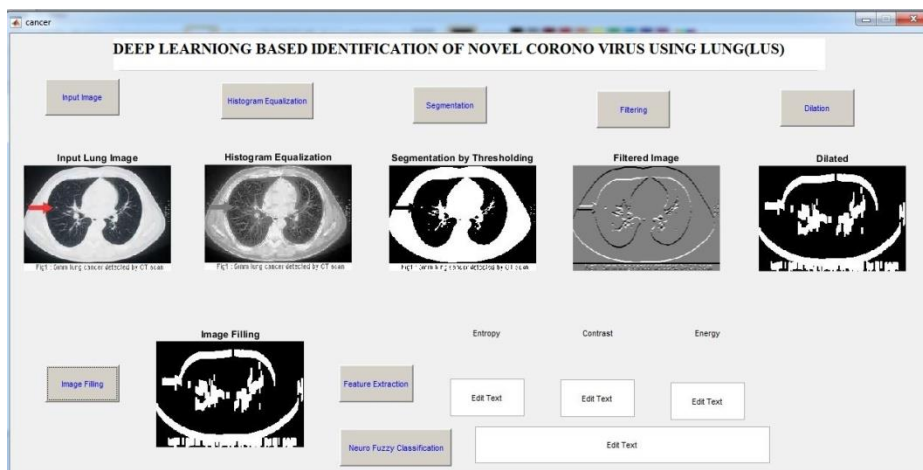
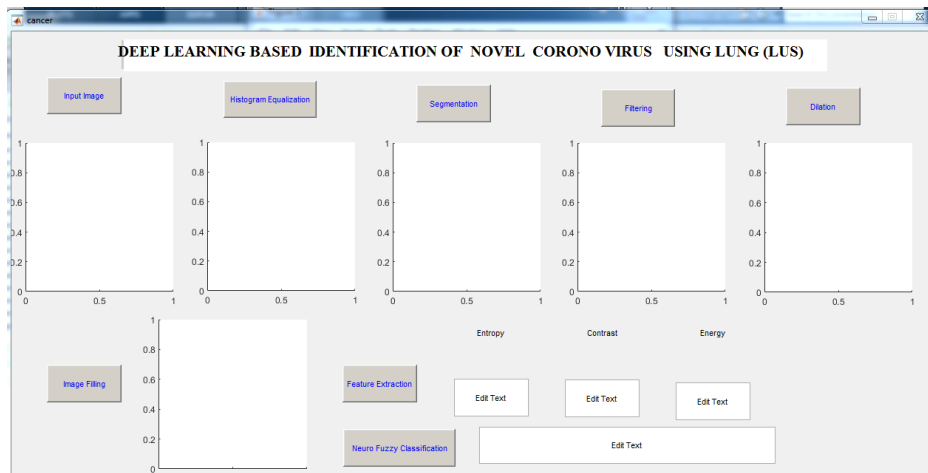
At the point when prepared on the comments by the most master clinician, video-based classification accomplishes a F1-score of 61%, an exactness of 70% and a review of 60%. It is observable that these qualities are in accordance with the low between annotator understanding detailed in Section III, which together to the little number of tests with video-level comments can clarify the high difference of the scores across folds. We anticipate that expanding our generally little arrangement of video-level comments will help balancing the marking commotion, increment the model execution and decrease its change.

Segmentation Evaluation

Our division model can portion and segregate between zones in B-mode LUS pictures that contain foundation, solid markers and (various phases of) COVID-19 biomarkers at a pixel-level, arriving at a pixel-wise precision of 96% and a twofold Dice score of 0.75. Close by these divisions, we give spatial vulnerability gauges that might be utilized to decipher model expectations. Strangely, and significantly, none of the most noteworthy (and generally extreme) score list explanations in the test set were missed by our model, decided by visual appraisal of the coming about divisions, and by breaking down the relative imagelevel crossing points among the relating anticipated and commented on areas. Additionally, we noticed model expectations of COVID-19-positive locales, that had anyway not been explained accordingly. Fig. 6B shows a delegate model of such a case. After reexamining some of such models from the test set, along with the annotators, we discovered that the annotators were once in a while uncertain whether to clarify a district as for example score 2 or 3, and in this manner concluded that the marker was not satisfactory enough to clarify the area by any stretch of the imagination, prompting the previously mentioned inconsistency. Division execution and extraction of semantics could be additionally supported by utilizing transient construction among outlines in a successive model. Such models could

gain from explanations across full recordings, or through incomplete explanations and powerless management. We leave these augmentations of the current technique to future work.

RESULTS AND DISCUSSION:



Conclouion:

A benefit of utilizing ultrasound is the generally safe of crossinfection when utilizing a plastic dispensable cover and separately bundled ultrasound gel on a versatile handheld machine [45]. This is conversely with utilization of CT, for which rooms and situation should be thoroughly cleaned to forestall pollution (and ideally saved for patients with a high COVID-19 doubt). LUS can be performed inside the patient's room without need of transportation, making it a predominant technique for purpose of-care evaluation of patients. Besides, ultrasound delivers continuous pictures and, joined with our DL strategies, gives results in a flash. It might additionally straightforwardly aid emergency of patients; first-look assessment of the infection's seriousness and the criticalness at which a patient should be tended to. Likewise, low and center pay nations, where conclusion through RT-PCR or CT may not continuously be accessible, can especially benefit from ease ultrasound imaging too. Anyway absence of preparing on the understanding of these LUS pictures could in any case restrict its utilization practically speaking. Our proposed DL technique may in this way encourage ultrasound imaging in these nations.

REFERENCES

- [1] WHO, "Laboratory testing strategy recommendations for COVID19: Interim guidance," Tech. Rep., 2020. [Online]. Available: <https://apps.who.int/iris/bitstream/handle/10665/331509/WHO-COVID-19-lab-testing-2020.1-eng.pdf>

- [2] R. Niehus, P. M. D. Salazar, A. Taylor, and M. Lipsitch, “Quantifying bias of COVID-19 prevalence and severity estimates in Wuhan, China that depend on reported cases in international travelers,” medRxiv, p. 2020.02.13.20022707, feb 2020.
- [3] Y. Yang et al., “Evaluating the accuracy of different respiratory specimens in the laboratory diagnosis and monitoring the viral shedding of 2019-nCoV infections,” medRxiv, p. 2020.02.11.20021493, feb 2020.
- [4] S. Salehi, A. Abedi, S. Balakrishnan, and A. Gholamrezanezhad, “Coronavirus Disease 2019 (COVID-19): A Systematic Review of Imaging Findings in 919 Patients,” Am J Roentgenol, pp. 1–7, mar 2020.
- [5] A. Bernheim et al., “Chest CT Findings in Coronavirus Disease-19 (COVID-19): Relationship to Duration of Infection,” Radiology, p. 200463, feb 2020. [Online]. Available: <http://pubs.rsna.org/doi/10.1148/radiol.2020200463>.
- [6] F. Mojoli, B. Bouhemad, S. Mongodi, and D. Lichtenstein, “Lung ultrasound for critically ill patients,” pp. 701–714, mar 2019.
- [7] R. Raheja, M. Brahmavar, D. Joshi, and D. Raman, “Application of Lung Ultrasound in Critical Care Setting: A Review,” Cureus, vol. 11, no. 7, jul 2019.
- [8] Y. Amatya, J. Rupp, F. M. Russell, J. Saunders, B. Bales, and D. R. House, “Diagnostic use of lung ultrasound compared to chest radiograph for suspected pneumonia in a resource-limited setting,” International Journal of Emergency Medicine, vol. 11, no. 1, dec 2018.
- [9] E. Poggiali et al., “Can Lung US Help Critical Care Clinicians in the Early Diagnosis of Novel Coronavirus (COVID-19) Pneumonia?” Radiology, p. 200847, mar 2020.
- [10] Q. Y. Peng et al., “Findings of lung ultrasonography of novel corona virus pneumonia during the 2019 – 2020 epidemic,” Intensive Care Medicine, no. 87, pp. 6–7, mar 2020.
- [11] G. Soldati et al., “Is there a role for lung ultrasound during the covid-19 pandemic?” J Ultrasound Med, 2020.
- [12], “Proposal for international standardization of the use of lung ultrasound for COVID-19 patients; a simple, quantitative, reproducible method,” J. Ultrasound Med., 2020.
- [13] K. Stefanidis et al., “Lung sonography and recruitment in patients with early acute respiratory distress
- [14] L. Tutino, G. Cianchi, F. Barbani, S. Batacchi, R. Cammelli, and A. Peris, “Time needed to achieve completeness and accuracy in bedside lung ultrasound reporting in Intensive Care Unit,” SJTREM, vol. 18, no. 1, p. 44, aug 2010.

AI In Agriculture

Kapil yaswanth S B, Karthick R, Mohanakrishnan V, Nagaraj K

Abstract

By 2050 the world population will reach more than 9 billion which requires a substantial amount of increase in agricultural production. The conventional methodology of agriculture has a reduced production rate due to issues like environmental changes, soil health, weeds, lack of proper irrigation system, weather conditions, etc. But these issues can be solved by applying several AI techniques like increasing crop productivity by the assistance of a planting application controlled by AI which will give a higher yield of 30%. [1] Using thermal cameras with AI models to monitor soil health and optimizing water usage on agricultural lands [3] using smart irrigation systems and pests, weeds can be controlled by using the 'see and spray' technique implemented by using AI models and using drones for spraying in an irrigation system powered by AI. The above techniques are briefly explained in this paper and also give an idea of how AI helps in Agriculture to increase food production.

Keywords: *Agriculture, Methodology, Environmental changes, and AI models.*

1 Introduction

The inadequacy & increasing labour prices, raising the price of cultivation and crop failures due to diseases, failure in precipitation, climatical variations and loss of soil fertility, unsteady market value in agriculture commodities, etc., has created an important negative impact. So, the use of the latest technological solutions to create farming a lot of economical remains one in all the best ways to accentuate agricultural production needs high energy inputs and market demands top quality food. By 2050, the United Nations comes that a common fraction of the world's population can sleep in urban areas, reducing the agricultural men. New technologies are required to ease the employment on farmers. Operations are done remotely, processes are done by machines, risks are known, and problems are solved. In the future, a farmer's skills could be a mixture of technology and biological skills instead of pure agriculture. Today's technology advancement in computer science, Big Data, IoT, Artificial Intelligence are getting the main in the field of agriculture which would be more useful for the farmers. This paper aims at giving an overall review of how artificial intelligence is transforming agriculture nowadays.

1.1 Improving Crop Productivity

Environmental change might be beneficial for certain plants by stretching the developing season. Anyway, unique effect of a hotter world, for example, more irritations, dry seasons, and flooding will diminish crop efficiency, particularly for anticipating climate designs that decide to cultivate rehearses for the season. The use of prescient investigation with the assistance of AI could be very useful. It could help decide suitable yields to develop in an ideal climate on a beneficial region and the planting strategy to upgrade efficiency and decrease cost. With the assistance of a planting application controlled by AI, a 30% higher normal in yield per hectare can be accomplished.

1.2 Soil Health Monitoring

Along with ideal atmosphere conditions, soil wellbeing containing a satisfactory degree of dampness and supplement holds the best approach to getting the best yield. Coursed soil checking performed through picture acknowledgment and profound learning models can be utilized to take remedial measures to re-establish soil wellbeing. Verifiable data about rainstorm, nearby previews of the ranch, crop-yield information, history of soil wellbeing, more fill in as contributions for the making of AI models. These models give essential information about the farmland, helping ranchers in arranging exercises identified with soil reclamation, crop advancement, ranch watering, etc. Field pictures can be broke down through PC vision, giving nitty-gritty reports for the current wellbeing of the dirt, state of leaves, or status of yields against moulds and microscopic organisms. This causes ranchers to control the sicknesses ideal utilizing irritation control techniques.

1.3 Crop Health Monitoring

On an average There has been three obstacles in monitoring crop and soil health. the first obstacle is improper use of pesticides, which is not only waste of money on lands but potentially harmful to human health and agricultural land. As

many farmers don't have the in-depth knowledge of what affects their crops and the shop owner haven't able to see what impacts their crops, which in turn leads to usage of wrong pesticide. The second thing is availability, quality and quantity. The farmers have little option to choose from their local, which led them to buy products at seller's price. The last but not least one is lack of data and information around the farmer's land. There is a tech start up called PEAT, developed PLANTIX application used deep learning algorithm which identifies the potential defects and nutritive deficiencies in a plant like plant disease, pests. This application uses image recognition technology by which user can take the image of the plant then the app will recommend suitable refurbishing technique and tips to overcome the defect. The benefit of better understanding our soil and improving its health yields tremendous human, environmental, and economic gains. Healthy soil is the foundation of a prosperous and thriving planet. TRACE genomics is another company which focuses on implementing machine learning into agriculture. they provide soil analysis services to the clients by harnessing ML they conduct cost efficient data analysis to compare against the large and growing set of soil data, which describes the strength and weakness of the soil.

2 Optimization of Pest and Weed Management

AI can be utilized for foreseeing the conduct of vermin which can be gainful for arrangement ahead of time of bug control. Productive irritation the board prompts lower crop and natural harm. A blend of distantly detected information, effective picture characterization instruments, climate information, and other applicable information focuses can be utilized to recognize the weed from the harvest. This will bind the utilization of weedicide just to the regions that require treatment. Far off satellites can screen crop wellbeing and caution against bother assaults. An AI-upheld innovation called 'See and Spray' created by a US organization is a weed controlling innovation that can lessen consumption on weedicides by 90%.

2.1 Water Management

Efficient water the board in farming can hugely affect the approaching issue of water shortage. Water utilization in rural land can be streamlined by utilizing warm imaging cameras that ceaselessly screen if crops are getting adequate measures of water. Usage of thermal image cameras could optimize the water usage on agricultural lands .That monitor continuously whether the crops are getting sufficient amount of water or not .Drones are used as substance sprayers by farmers and it is considered as effective and great importance on situations like cloudy climate and also solved problem of inaccessibility to a field of tall crops .Man-made intelligence, combined with proper picture order models, when utilized in farming can bring about improving yield creation, diminishing manual intercession, and diminishing occasions of harvest ailments

3 AI Based Autonomous Electric Tractors

Kubota Corporation which is a Japanese firm has developed an AI-based autonomous vehicle to prevent the issues that the Japanese farmers are facing like labour shortage. This vehicle is completely an unmanned autonomous vehicle that will do all the appropriate operations on its own at the correct time based on the data like weather, growth rate of the crops, etc. This tractor is a completely an electric vehicle which is powered with Lithium-ion batteries.

4 Automation Technique in Irrigation

Farmers are required to put a rigorous amount of labour during the process of irrigation. [1] Machines when trained with data of historical weather pattern, quality of soil and crops which have growth potential, can automate the process of irrigation and thus increase productivity. [2] When automation is implemented, almost 70% of the world's fresh water is being used for irrigation, out of which a huge portion can be conserved and farmers will manage their water resources in a better and efficient manner.

5 Implementation of Drones

Drone-based technology is emerging to be a promising technology, which has the solutions to solve the major problems being faced by agriculture. Drone technology gives a new feel and texture to one of the oldest occupations of the world.

[3] A recent study conducted by Price Water House Coopers (PWC) revealed that the global market for AI-powered drone-based technology solutions happen to be a whopping \$127.3 billion, out of which agriculture takes a share of about \$32.4 billion. This drone-based technology has the potential to deal with untimely weather patterns, enhanced productivity, satellite farming, agricultural yields.



Fig.1 Disease detection

Fig.1 shows the process involved in the detection of disease. It starts from image sensing and analysis, and those images of plants are categorized into the diseased area and non-diseased areas. Then the affected area is cropped and sent to the laboratory for further analysis. Then the disease and nutrient deficiency are identified and further processes are being made.

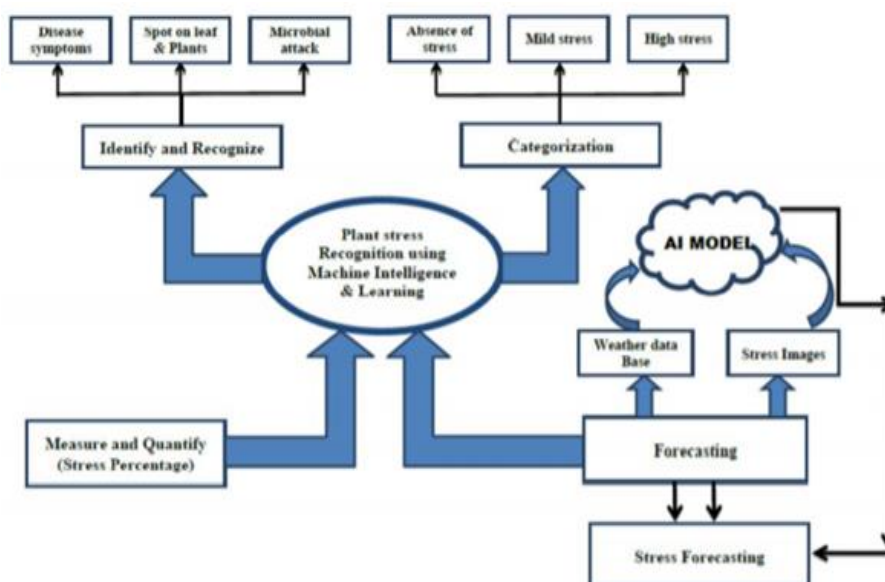


Fig.2 Plant Stress recognition using ML & AI techniques

Fig.2 describes the various cases of managing precision farming. With the help of high-resolution images, the stress levels in plants can be monitored through artificial intelligence techniques. A large amount of data is collected from these sources and fed as input to the machine learning models. The result collected from these sources will help in identifying the causes of plant stress recognition. This way of resulting in better and advanced decision making is possible through the continuous processes of recognition, categorization, quantification, and forecasting.

The software giant Microsoft in collaboration with United Phosphorous Limited has been in the process of developing a Pest Risk Prediction API which uses AI and ML techniques which can predict potential pest attacks [Fig 3]. Based upon the climatic changes and the growth of the crops the prediction will be in the range of high, medium, or low.

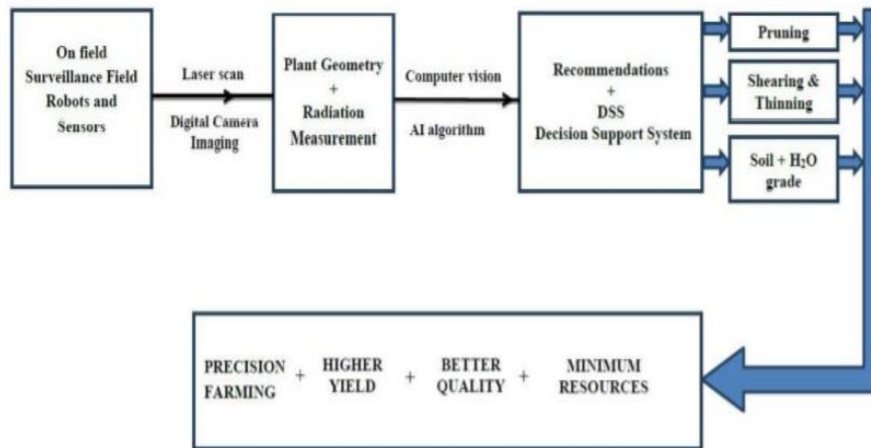


Fig.3 Robotics in digital farming

5.1 Here are six ways drones can be used for the entire crop cycle

- Ground data analysis: By creating 3-D maps of the fields, landscapes we maintain a beforehand ground analysis which plays a major role in the advanced planning of planting seeds and convocation of data for managing nitrogen and irrigation levels.
- Planting of seeds: The start-ups have created drone-planting systems that have cut the planting costs up to 85%. The drone systems shoot the pods consisting of seeds along with necessary nutrients for the healthy growth of plants into the ground.
- Crop spraying: Drones can scan the ground and spray the required amount of substances for the crops. It can even fetch the details of spraying in concurring time for the coverage.
- Monitoring of crops: The usage of outdated incapable methods is a huge blunder being made. Such inefficiencies can be corrected by the help of drones, by using time series animations which displays the growth of a crop and identifies the production defects, which leads to better management.
- Irrigation of crops: [1] Drones with the help of sensors can be used to identify the locations of the field which are dry and in need of advancements.
- Health assessment: Through the scanning of crops, with the help of visible and near-infrared light drone-carried devices identify the differences in plants, and send the plant's health record to the farmer of any disease. In the future UAVs loaded with drones that gather data and implement the tasks are possible. But, in reality, when hurdles like sensors having the capability of gathering high-quality data and related software are developed this distant dream is possible.

6 Conclusion

AI techniques like remote sensors for soil moisture content detection and automated irrigation system with GPS also helps the farmers. With the introduction of drones backed by AI farmers will be able to reduce their costs and improve their yields and minimizing the overall use of fertilizers, insecticides and other chemicals will improve the overall health of a plant. Thus, the benefits being provided by AI will create a digitalized farming culture resulting in a healthy global economy. The farming industry when leverage the power of Artificial Intelligence shows promising signs of a substantial amount of increase in the production of crops and reduced consumption of intensive labour-work in the fields. When the farmers can analyse the health of their crops through AI, immediate actions can be taken and appropriate nutrients can be given to the crops, thus reducing the wastage of crops affected by pest. The forecast

of weather conditions for the next year is also given, thus helping the farmers analyse their shortcomings and manage their finances in a better and efficient manner.

References

- [1] Implementation of artificial intelligence in agriculture for optimisation of irrigation and application of pesticides and herbicides available at <https://doi.org/10.1016/j.aiaa.2020.04.002>
- [2] A comprehensive review on automation in agriculture using artificial intelligence available at <https://doi.org/10.1016/j.aiaa.2019.05.004>
- [3] Artificial cognition for applications in smart agriculture: A comprehensive review available at <https://doi.org/10.1016/j.aiaa.2020.04.001>

Performance Analysis of Nature Inspired Optimization Algorithms for Virtual Machine Migration Problem in Cloud Environment

Deepak Kumar¹, Deepti Mehrotra², Vijay Anant Athavale³, Suresh Chand Gupta⁴

Panipat Institute of Engineering and Technology, Panipat Haryana India^{1,3,4}

Amity University Noida, Uttar Pradesh, India²

wadhwa123deepak@gmail.com dmehrotra@amity.edu vijay.athavale@gmail.com sureshguptaji@yahoo.com

Abstract

The virtualized framework among the terminal user and the computer platform was generated by the software called virtual machine (VM). End users are managed and for the fundamental bare hardware an identical interface was obtained by the virtual machine software. For the cloud infrastructure and cloud computing services, simulation and modeling are given by an extensible simulation tool called CloudSim. During migration of virtual machine the following challenges occurs; Transfer rate, Page resend, Missing pages, migration over WAN network, large applications, Resource availability, Address wrapping and migration in high speed LAN. Scheduling in cloud computing is required to reduce task completion time and to boost the effective use of the resources. It allocates the particular work to the particular resource at particular time. The resource allocation cloud computing is required for assigning the available resources to the required cloud application over the internet. It allows the service provider to control every individual module resources. To get quasi-optimal solutions several meta-heuristic procedures are implemented with Cloud simulator.

Keywords: *Virtual machine, Resource Allocation, Modified grey wolf algorithm, meta-heuristic, service level agreement, Virtual machine migration, Virtual Machine Scheduler, Service level Agreement Violation, Energy Consumption.*

1 Introduction

The cloud optimization optimizes the cloud resources usage. It provides integrated capabilities with other systems and gives strength in its security. The cloud optimization service consists of inventory visibility, usage statics; spend optimization, security and compliance. The cloud optimization in VM migration has the following issues or challenges; Network link issue, seamless connectivity, application performance, security concerns, Big VM data size and Inter VM migration. In this research focus is based on various factors VM migration, VM placements, energy consumption, Degradation SLA Performance because of Migration, SLA violation to be evaluated.

2 Related Work Findings

| Ref. | Aim | Method | Merits | Demerits |
|----------------------------------|---|---|--|--|
| [2] (Chen <i>et al.</i> , 2016) | To solve particle tracking problems in crowd sourcing | Novel application domain for human computation | Effective human and computation analysis, scalable | Enhancing the method leads to improve in modality and pace of the task |
| [3] (Chang <i>et al.</i> , 2014) | To develop crowd sourcing approach for creating innovative product concepts | Prototype crowdsourcing system with Neuro-fuzzy approach | Enhance the reliability and accuracy | Needs to improve its mathematical methods |
| [4] Zhuang <i>et al.</i> , 2015) | To estimate and localize the WiFi processing points (APs), (PPs) | Trusted Portable Navigator (T-PN) – novel crowd sourcing method | Accurate, user friendly and robust | Small degradation in positioning performance |
| [5] (Schempp | To analyze the real | Conceptual disaster | More effective | Screening the critical |

| Ref. | Aim | Method | Merits | Demerits |
|--|--|---|---|---|
| T <i>et al.</i> , 2018) | time relief during disaster | relief system | during real time analyzing during disaster | and heterogeneous information |
| [6] (Fan. J <i>et al.</i> , 2019) | To solve the issue of circulation mindful publicly supported substance gathering | Adaptive worker selection approach | Finds the exact solution with less estimation error | Has to be enhanced to get low estimation error during the issue in circulation mindful publicly supported substance gathering |
| [7] (Massalas. M <i>et al.</i> , 2018) | To support both the offline and real-time data aggregation | CrODA-gator | Efficient and scalable | Enhanced for real time crowd sensed data |
| [8] (Liu, Gao & Chen, 2014) | To analyze the digital disaster reduction | VDMS | Effective and availability | Enhanced to integrate VGI data into PGI data |
| [9] (Lin. X <i>et al.</i> , 2017) | To reduce the uncertainty of Probabilistic top-k ranking in crowd sourcing | pair wise crowd sourcing model | Efficient and effective | Enhanced for other Probabilistic queries and explore the correlation of the objects in crowd sourcing |
| [10] (Zhao. D <i>et al.</i> , 2017) | To develop and keep up enormous scale picture database in a visual based area acknowledgment framework | Crowd OLR | High validation and response time | Efficiency reduction, accuracy and response delay |
| [11] (Li. L &Ulaganathan, 2017) | To analyze disaster response | crowd sourcing mobile app | Accuracy, reliability and timeliness | Has to improved for supporting multiple languages |
| [12] (O'Leary. D, 2014) | To embedded the AI based crowd sourcing approach in big data lake | AI based crowd sourcing approach | Potential in privacy issues | Has to be improved in sensible interference of aligning databases and appropriate metadata |
| [13] (Zhang. Y <i>et al.</i> , 2017) | To positioning the wifi fingerprint in mobile crowd sourcing | WFP-C | High accuracy and less computational complexity | High processing time for large graphical area |
| [14] (Tiwari & Kaushik, 2014) | To enrich the information for tourist spot recommender system | location aware crowd sourcing approach | Highly feasible | Has to reduce the user time |
| [15] (Katagiri, Sato &Fujii, 2017) | To estimate radio propagation fluctuation in V2V communication system | Crowdsourcing-assisted Radio Environment Maps | High accuracy | Communication efficiency |
| [16] (Sai Wu <i>et al.</i> , 2014) | To evaluate the upper and lower bound exactness for a K- | probability-based matrix model | Efficient and privacy | Need to maintain high accuracy |

| Ref. | Aim | Method | Merits | Demerits |
|------|--------------------|--------|--------|----------|
| | Anonymity approach | | | |

3 Purposed frame Work

Varieties of metaheuristic procedures are implemented with Cloud Simulator to get quasi-optimal solutions. This optimization policy is employed to get as tuned as promising conformation parameters of the VM selections. Modified Gray Wolf Optimization (MGWO) technique is used to evaluate VM migration process. This technique used to enhance the migration by reducing the standard deviation of VM placement and migration, consumption of energy, migration depravity the performance of SLA and total SLA violation.

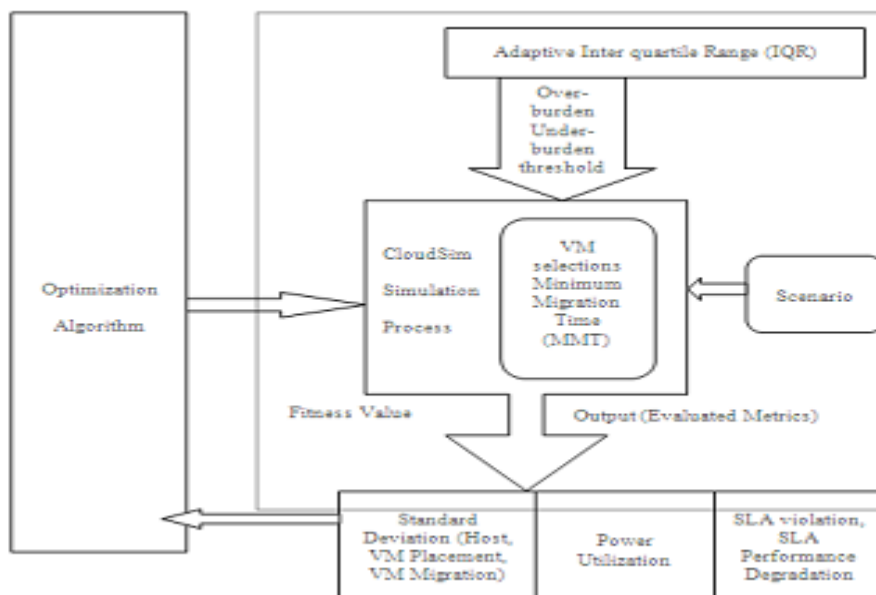


Figure 1.1: Proposed Framework

An excellence of the Information as a Service layer (IaaS) in cloud computing can be assessed by keeping in attention together quality of service (QoS) and power utilization. To identify both under loaded and overloaded hosts by using Adaptive Inter quartile Range (IQR): Over-burden threshold is planned with dynamism by Inter Quartile Range method and further more for VM selections Minimum Migration Time (MMT) is used [1].The investigational examination was done using the CloudSim toolkit. It is an open foundation package used by many researchers to simulate the Cloud background. In order to settle on the time to begin the migration of VMs from a number, a heuristic for setting associate higher and lower utilization threshold is required. IQR overload detection technique is utilized in planned work [17].Inter Quartile Range (IQR): This might be methodology for setting associate reconciling higher threshold.After the detection of a loaded host, the next footstep is to pick out the precise VMs to transfer from some host to the opposite. Minimum Migration Time (MMT): This strategy chooses a VM to migrate that require slowest capacity of your time to surface migrating, associated to other VMs prearranged to the host [18].

4 Results and Analysis

The above suggested evolutionary algorithm is applied on the cloud computing datasets. Further to justify the results two different public datasets are taken in consideration. These datasets are Dataset 1: Planet Lab, Dataset 2: NEC Personal

Cloud Trace. The working of the proposed algorithm on various factors VM migration, VM placements, energy consumption, Degradation SLA Performance because of Migration, and SLA violation is produced. For virtual machine selection, Minimum Migration Time procedure is evaluated. Total SLA violation, SLA performance degradation due to relocation, standard deviation of virtual machine migration, standard deviation of VM placement, standard deviation of host and power utilization are the six parameters that are used. The result for six parameters such as utilization of power, Host standard deviation, standard deviation of VM placement, virtual machine migration standard deviation, Degradation SLA Performance because of Migration, Total SLA violation formed by algorithm is given in tables 1.1 to 1.2.

4.1 Results Analysis on Two Datasets

The study is conducted on two data sets namely

Dataset 1: Planet Lab(<https://github.com/beloglazov/planetlab-workload-traces>),

Dataset 2: NEC Personal Cloud Trace <http://cloudspaces.eu/results/datasets> link <https://sites.cs.ucsb.edu/~rich/workload/>.

Standard deviation of Host, VM placement and VM migration, Energy consumption, degradation in SLA violation and Total SLA violation is evaluated for two datasets. The comparative analysis in given table:

4.1.1 Comparative Analysis Optimization Algorithms

For improving live VM migration process, algorithms like Ant Colony Optimization (ACO), Particle Swarm Optimization (PSO), Cuckoo search, Ant Lion Optimization (ALO) [22], social Spider and Firefly techniques are implemented to compare with Modified Gray Wolf Optimization (MGWO) [21], R. These optimization policies are used for the confirmation parameters of the VM selection. To reduce the standard deviation of VM placement and migration, energy consumption, SLA (service level agreement) appearance down due to relocation and total SLA violation these techniques are used to enhance the migration. By combining the quality of service (QoS) and power utilization, the excellence of the information as a service layer (IaaS) in cloud computing can be determined. Adaptive Inter Quartile Range (IQR) identifies both the under loaded and overloaded host. For VM selection, Minimum Migration Time (MMT) is used. A CloudSim toolkit is used to analyse the experimental result.

The working of each algorithm in all is compared on various factors VM migration, VM placements, energy consumption, Degradation SLA Performance because of Migration, SLA violation. For virtual machine selection, Minimum Migration Time procedure is evaluated. Total SLA violation, SLA performance degradation due to relocation, standard deviation of virtual machine migration, standard deviation of VM placement, standard deviation of host and power utilization are the six parameters that is used for comparing the performance of the planned optimization algorithms. The result for six parameters such as utilization of power, Host standard deviation, standard deviation of VM placement, virtual machine migration standard deviation, Degradation SLA Performance because of Migration, Total SLA violation formed by algorithms is given in tables below.

Table 1.1 *StandardDeviation of Host, VM Placement, VM Migration and Energy Consumption (For Dataset 1)*

| Optimizati on Algorithm | Host | | VM Placement | | VM Migration | | Energy Consumption | Degrada tion SLA Perfor mance becau se of Migra tion (%) | Total SLA Violation (%) |
|--|---------|---------|--------------|---------|--------------|-------|-----------------------|---|----------------------------|
| | SD | Mean | SD | Mean | SD | Mean | | | |
| IQR/MMT (without optimization) | 0.00363 | 0.00123 | 0.00484 | 0.00221 | 8.09 | 20.09 | 36.25 | 0.19 | 1.01 |

| | | | | | | | | | |
|---------------------------------|---------|---------|---------|---------|------|-------|-------|------|------|
| Modified Grey Wolf Optimization | 0.00358 | 0.00122 | 0.00473 | 0.00213 | 8.03 | 20.06 | 34.13 | 0.14 | 0.98 |
| Ant Colony Optimization | 0.00357 | 0.00151 | 0.0065 | 0.00596 | 7.89 | 17.62 | 47.85 | 0.23 | 1.05 |
| Particle Swarm Optimization | 0.00406 | 0.00179 | 0.00908 | 0.00613 | 7.93 | 20.33 | 46.86 | 0.26 | 1.13 |
| Cuckoo Search | 0.00389 | 0.00185 | 0.00746 | 0.0059 | 7.44 | 20.39 | 46.73 | 0.25 | 1.16 |
| Ant Lion Optimization | 0.00472 | 0.00188 | 0.00429 | 0.00181 | 7.95 | 20.35 | 34.35 | 0.14 | 3.17 |
| Social Spider | 0.00305 | 0.00144 | 0.00485 | 0.00254 | 7.28 | 18.01 | 35.55 | 0.15 | 1.2 |
| Firefly | 0.0035 | 0.0015 | 0.0047 | 0.0029 | 7.35 | 18.05 | 36.2 | 0.13 | 1.01 |

Table 1.2 *Standard Deviation of Host, VM Placement, VM Migration and Energy Consumption (For Dataset 2)*

| Optimization Algorithm | Host | | VM Placement | | VM Migration | | Energy Consumption | Degradation SLA Performance because of Migration (%) | Total SLA Violation (%) |
|---------------------------------|---------|---------|--------------|---------|--------------|-------|--------------------|--|-------------------------|
| | SD | Mean | SD | Mean | SD | Mean | | | |
| IQR/MMT (without optimization) | 0.00337 | 0.00091 | 0.00265 | 0.00076 | 8.2 | 21.56 | 36.30 | 0.16 | 1.1 |
| Modified Grey Wolf Optimization | 0.00328 | 0.00087 | 0.00243 | 0.00063 | 7.95 | 20.35 | 34.35 | 0.14 | 1.07 |
| Ant Colony Optimization | 0.00223 | 0.00052 | 0.00392 | 0.00188 | 7.93 | 20.33 | 46.86 | 0.26 | 1.13 |

| | | | | | | | | | |
|-----------------------------|---------|---------|---------|---------|------|-------|-------|------|------|
| Particle Swarm Optimization | 0.00406 | 0.00179 | 0.00908 | 0.00613 | 7.89 | 17.62 | 47.85 | 0.23 | 1.05 |
| Cuckoo Search | 0.00272 | 0.0008 | 0.00421 | 0.00192 | 8.02 | 20.38 | 49.32 | 0.26 | 0.98 |
| Ant Lion Optimization | 0.00249 | 0.00066 | 0.00392 | 0.00178 | 8 | 20.3 | 47.37 | 0.25 | 1.11 |
| Social Spider | 0.00325 | 0.00085 | 0.00435 | 0.00195 | 8.01 | 19.34 | 35.45 | 0.15 | 1.15 |
| Firefly | 0.00221 | 0.00025 | 0.00955 | 0.00715 | 7.99 | 20.15 | 36.05 | 0.23 | 1.12 |

Table 1.3: Ranking among different Algorithms

| Data Sets | Algorithms | VM Placement | VM Migration | Energy Consumption | SLA Performance | SLA Violation |
|-----------|---------------------------------|--------------|--------------|--------------------|-----------------|---------------|
| d1 | Ant Colony Optimization | 4 | 3 | 4 | 6 | 1 |
| d1 | Firefly | 5 | 5 | 3 | 4 | 2 |
| d1 | Ant Lion Optimization | 3 | 2 | 5 | 7 | 3 |
| d1 | Modified Grey Wolf Optimization | 1 | 1 | 1 | 1 | 4 |
| d1 | Particle Swarm Optimization | 6 | 6 | 6 | 3 | 5 |
| d1 | Social Spider | 2 | 7 | 2 | 2 | 6 |
| d1 | Cuckoo Search | 7 | 4 | 7 | 5 | 7 |
| d2 | Modified Grey Wolf Optimization | 2 | 4 | 1 | 2 | 1 |
| d2 | Ant Lion Optimization | 1 | 2 | 2 | 3 | 2 |
| d2 | Social Spider | 3 | 6 | 3 | 4 | 3 |
| d2 | Cuckoo Search | 5 | 1 | 5 | 6 | 4 |
| d2 | Particle Swarm Optimization | 7 | 3 | 6 | 7 | 5 |
| d2 | Ant Colony Optimization | 6 | 7 | 7 | 5 | 6 |
| d2 | Firefly | 4 | 5 | 4 | 1 | 7 |

5 Conclusion

Extra resources are required during the VM relocation process. Applications running on migrant VMs are harshly affected till VM migration finishes. VM migration procedure must be effectively accomplished within minimal migration time so that system resources can be made free as early as possible. Optimal server and network resources utilization is necessary to enhance application performance and migration transparency. Finally, by operating every simulations, it is shown that the outcomes of the delivered agreeable policy was found out and also shown the power usage of Ant Lion and modified Grey Wolf optimizations gives great result, compared with rest of the optimizations; for standard deviation of VM placement and SLA performance degradation due to migration Ant Lion and Grey Wolf produced good outcome. From our outcome we additionally discover that for standard deviation of VM migration Cuckoo search significantly outperforms other optimization algorithms. Particle Swarm optimization and Ant Colony optimization gives minimum overall SLA violation. The host overloaded figure out in the initial step and to migrate from one host to another by précising the VMs are figured out in the next step through optimizing the VM migration.

6 Future Scope

To improve the process of VM migration, the process known as VM consolidation is considered, where all PCs and servers are combined together to improve overall performance. Portraying the real time environment is complex task. In a real time system has many objectives so the study can be extended from the multi-objective problem to many objective optimization solutions. With advent of Internet of things (IoT) the cloud computing environment has also extended and FOG computing solutions are used for the handling the solutions where IoT based applications are designed. The optimization issues discussed for VM migration can be explored for the FOG computing environment and optimized solution of Fog environment can be proposed the process known as VM consolidation will be combined together.

References

- [1] Cho, D., Taheri, J., Zomaya, A. and Bouvry, P. Real-Time Virtual Network Function (VNF) Migration toward Low Network Latency in Cloud Environments. *IEEE 10th International Conference on Cloud Computing (CLOUD)*. 2017; pp. 798-801. ISBN 978-1-5386-1993-3. Available from: <https://ieeexplore.ieee.org/document/8030676>.
- [2] Chen, Chen, Paweł W. Woźniak, Andrzej Romanowski, Mohammad Obaid, Tomasz Jaworski, Jacek Kucharski, Krzysztof Grudzień, Shengdong Zhao, and Morten Fjeld. Using crowdsourcing for scientific analysis of industrial tomographic images. *ACM Transactions on Intelligent Systems and Technology (TIST)* 2016; 7 (4), pp. 52. Available from: <https://dl.acm.org/doi/10.1145/2897370>.
- [3] Chang, Danni, Chun-Hsien Chen, and Ka Man Lee. A crowdsourcing development approach based on a neuro-fuzzy network for creating innovative product concepts. *Neuro omputing*. 2014; Vol. 142, pp. 60-72. Available from : <https://www.sciencedirect.com/science/article/abs/pii/S0925231214005323>.
- [4] Zhuang, Yuan, Zainab Syed, Jacques Georgy, and Naser El-Sheimy. Autonomous smartphone-based WiFi positioning system by using access points localization and crowdsourcing. *Pervasive and Mobile Computing*, 2015; Vol. 18, pp. 118-136. Available from: <https://www.sciencedirect.com/science/article/abs/pii/S1574119215000358>.
- [5] Schempp, T., Hong, M., Zhang, H., Akerkar, R. and Schmidt, A. An Integrated Crowdsourced Framework for Disaster Relief Distribution. *5th International Conference on Information and Communication Technologies for Disaster Management (ICT-DM)*. 2018; Available from: DOI:10.1109/ICT-DM.2018.8636372.

- [6] Fan, J., Wei, Z., Zhang, D., Yang, J. and Du, X. Distribution-Aware Crowdsourced Entity Collection. *IEEE Transactions on Knowledge and Data Engineering*, 2016; 31(7), pp.1312-1326. Available from: DOI 10.1109/TKDE.2016.2611509.
- [7] Massalas, M., Konstantinidis, A., Achilleos, A., Markides, C. and Papadopoulos, a. CrODA-gator: An Open Access CrowdSourcing Platform as a Service. *IEEE International Conference on Pervasive Computing and Communications Workshops (PerCom Workshops)*.2018; pp. 585-590 Available from: DOI: 10.1109/PERCOMW.2018.8480231.
- [8] Liu, Q., Gao, Y. and Chen, Y. Study on disaster information management system compatible with VGI and crowdsourcing. *IEEE Workshop on Advanced Research and Technology in Industry Applications (WARTIA)*. 2014; pp. 464-468. Available from: DOI: 10.1109/WARTIA.2014.6976296.
- [9] Lin, X., Xu, J., Hu, H. and Fan, Z. Reducing Uncertainty of Probabilistic Top- k Ranking via Pairwise Crowdsourcing. *IEEE Transactions on Knowledge and Data Engineering*. 2017; 29(10), pp.2290-2303. Available from: doi: 10.1109/TKDE.2017.2717830.
- [10] Zhao, D., Wang, H., Ma, H., Xu, H., Liu, L. and Zhang, P. CrowdOLR: Toward Object Location Recognition With Crowdsourced Fingerprints Using Smartphones. *IEEE Transactions on Human-Machine Systems*. 2017; 47(6), pp.1005-1016. Available from: DOI: 10.1109/THMS.2017.2700443.
- [11] Li, L. and Ulaganathan, M. Design and development of a crowdsourcing mobile app for disaster response. *25th International Conference on Geoinformatics*. 2017; pp. 1-4. Available from: doi: 10.1109/GEOINFORMATICS.2017.8090943.
- [12] O'Leary, D. Embedding AI and Crowdsourcing in the Big Data Lake. *IEEE Intelligent Systems*. 2014; 29(5), pp.70-73. Available from: doi: 10.1109/MIS.2014.82.
- [13] Zhang, Y., Zhang, S., Li, R., Guo, D., Wei, Y. and Sun, Y. WiFi fingerprint positioning based on clustering in mobile crowdsourcing system. *12th International Conference on Computer Science and Education (ICCSE)*. 2017; pp. 252-256, Available from doi: 10.1109/ICCSE.2017.8085498.
- [14] Tiwari, S. and Kaushik, S. Information Enrichment for Tourist Spot Recommender System Using Location Aware Crowdsourcing. *IEEE 15th International Conference on Mobile Data Management*. 2014; pp. 11-14. Available from: doi: 10.1109/MDM.2014.59.
- [15] Katagiri, K., Sato, K. and Fujii, T. Crowdsourcing-Assisted Radio Environment Maps for V2V Communication Systems. *IEEE 86th Vehicular Technology Conference (VTC-Fall)*. 2017; pp. 1-5, Available from: doi: 10.1109/VTCFall.2017.8287980.
- [16] Sai Wu, Xiaoli Wang, Sheng Wang, Zhenjie Zhang and Tung, A. K-Anonymity for Crowdsourcing Database. *IEEE Transactions on Knowledge and Data Engineering*. 2014; 26(9), pp.2207-2221. Available from: doi: 10.1109/TKDE.2013.93.
- [17] Liyanage, S., Khaddaj, S. and Francik, J. Virtual Machine Migration Strategy in Cloud Computing. *14th International Symposium on Distributed Computing and Applications for Business Engineering and Science (DCABES)*. 2014; 44 pp. 147-150 Available from: DOI 10.1109/DCABES.
- [18] Kumar, N. and Agarwal, S. Self regulatory graph based model for managing VM migration in cloud data centers. *IEEE International Advance Computing Conference (IACC)*.2014; pp. 731-734 Available from: DOI 10.1109/IAdCC.2014.6779414.

- [19] Heidari, Ali Asghar, and Parham Pahlavani. An efficient modified grey wolf optimizer with Lévy flight for optimization tasks. *Applied Soft Computing*. 2017; Vol. 60, pp. 115-134. Available from: <https://www.sciencedirect.com/science/article/abs/pii/S1568494617303873>.
- [20] Kamboj, Vikram Kumar, S. K. Bath, and J. S. Dhillon. Solution of non-convex economic load dispatch problem using Grey Wolf Optimizer. *Neural Computing and Applications*. 2016; Vol. 27, No. 5, pp. 1301-1316. Available from: <https://link.springer.com/article/10.1007/s00521-015-1934-8>.
- [21] Kumar, D., Kumar, S., & Bansal, R. An integrated approach towards query based learning on multi-objective ant lion optimization. *Journal of Advanced Research in Dynamical & Control Systems*, 2018 10(4), 800-809. Available from: <https://www.jardcs.org/backissues/abstract.php?archiveid=3320>.
- [22] Kumar, D., Kumar, S., & Bansal, R. A Survey to Nature Inspired Soft Computing. *International Journal of Information System Modeling and Design*. 2017; 8(2), 112-133. Available from: <https://www.igi-global.com/article/a-survey-to-nature-inspired-soft-computing/199006>.
DOI: 10.4018/IJISMD.2017040107.

Automated Software Testing Using Genetic Algorithm

Hanusha R¹, Manisha Koyarala M¹, Vanitha B¹, Indhuma E²

¹UG Student , ²Assistant Professor , Department of Computer Science & Engineering,
St.Anne's college of engineering and Technology, Panruti.
anurjhs1406@gmail.com

Abstract

Software Testers waste a lot of their time in the process of software testing. It also has been seen in the industries that a lot of money is depleting on the software process. In software testing process we apply test cases as input and check for final output. So our first concern is to choose the appropriate test cases for the software testing process. To give the correct output, it is very difficult to choose test cases. So generation of the test cases is a NP problem. To generate automatic test cases many nature inspired optimization algorithms have been used. These nature inspired optimization algorithms help to generate appropriate test cases. In this paper for generating automatic test cases genetic algorithm and mutation analysis had been used.

Keywords: *Genetic Algorithms (GA), Software Testing, Automatic Test Case Generation*

1. Introduction

Developers want to produce high quality software now days. Maintain the quality of software is a most important task. Developing these types of software, the software testing plays its own role. With the use of the software testing one can develop quality software. How much these software are reliable it is dependent on their nature of producing outputs. If output is correct it means the software is correct but before delivering the software to a customer it is most important to test it properly.

In our paper we are discussing how to generate appropriate test cases for software. For generation of appropriate test cases we are combining mutation testing with genetic algorithm. First we will generate test cases randomly and after that we will apply genetic algorithm to find optimal test case.

1.1 Software Testing

Software testing is process of producing correct and reliable software for the customer. It is one of the phase of the Software Development Life Cycle. (SDLC). There are many different types of software testing.

- a) *Acceptance Testing:* For checking its own specific requirements, customer uses this type of testing.
- b) *Black Box Testing:* This type of the testing is done by the developer to check the customer requirements. Developer does this testing without knowing the internal structure of the software. He just checks require outputs.
- c) *White Box Testing:* White box testing is based on knowledge of internal logic of an application code.
- d) *Compatibility Testing:* This type of the testing is done by the developer to check the compatibility of the software with different operating systems, web application and hardware etc.
- e) *Functional Testing:* This type of the testing is also done by the developer. He checks all validation of behavior using different inputs.
- f) *Integration Testing:* In integration testing, all the coding modules are combined together for testing.
- g) *Unit Testing:* To check the correct behavior of component, developers use unit testing.

2. Genetic Algorithm

The genetic algorithm for optimization problem. Holland proposed a theory, now this theory becomes the most powerful technique for the researchers to solve optimization problems. The principle of genetic algorithm is based on evolution and genetics. Genetic algorithm is based on "Survival of fittest". In genetic algorithm, we represent the input set by the chromosomes. These chromosomes are represented in different numbers in computer. The maximum usable representation of chromosomes is binary representation. The solution of any optimization problem using genetic algorithm is represented by the following iterative steps.

1. Initialize the population by chromosomes
2. Apply the fitness function

3. If satisfied the fitness function than stop otherwise go to step 4.
4. Select the parent for crossover or mutation
5. Generate the next generation go to step 2

There is some operation in Genetic Algorithm. These are Selection, Reproduction, and Evaluation.

Selection: In selection we have different approaches to select the parent to generate the new population. We will use any one of the following Roulette wheel or Tournament selection.

Reproduction: In reproduction crossover and mutation operations are used.

Evaluation: Evaluation is a process in which we have used our fitness function.

3. Unit Testing

Unit testing is a type of testing in which we have different testing method. These testing are Boundary Value Testing, Equivalence Class Testing, Decision Table Based Testing, Path Testing and Control Flow Testing.

3.1 Boundary Value Analysis.

This type of the testing is mainly focused on the input domain. Here the concern is about the valid input or invalid input. Basically the consideration of boundary value analysis are of different type given below.

- Normal Boundary Value Testing.
- Robust Boundary Value Testing.
- Worst Case Boundary Value Analysis and
- Robust Worst Case Boundary Value Testing.

In normal boundary value testing only valid variable value can be taken. But in robust boundary value testing we can take both valid and invalid variable values.

The tester should devise test cases to check that error messages are generated when they are appropriate, and are not falsely generated. Boundary value analysis can also be used for internal variables, such as loop control variables, indices, and pointers. Strictly speaking, these are not input variables, such as loop control variables are quite common. Robustness testing is a good choice for testing internal variables.

3.2 Equivalence Class Testing

In equivalence partitions, the partitions refers to a collection of mutually disjoint subsets, the union of which is the entire set. The idea of equivalence class testing is to identify test cases by using one element from each equivalence class. If the equivalence classes are chosen wisely, this greatly reduces the potential redundancy among test cases.

3.3 Decision Table Based Testing

A decision table has four portions: the part to the left of the bold vertical line is the stub portion; to the right is the entry portion. The part above the bold horizontal line is the condition portion, and below is the action portion.

| Stub | Rule 1 | Rule 2 | Rule 3 | Rule 4,5 |
|-------------|---------------|---------------|---------------|-----------------|
| C1 | T | T | T | T |
| C2 | T | F | F | T |
| C3 | F | --- | T | F |
| A1 | X | X | | X |
| A2 | | X | X | |
| A3 | X | | X | X |

Fig.1 A Decision Table

3.4 Path Testing

In path testing, first we have to design a graph for program. With the given set of test cases for a program if all the nodes are traversed in the graph then it is called G node. If all the edges traversed then it called G edge. In a given graph for the given input test cases if we traverse G node and G edge then it is 100% coverage. In path testing we test Decision to Decision Path (DD-path) testing, simple loop coverage, predicate outcome testing,

independent pairs of DD-Paths, complex loop coverage, multiple condition coverage, statistically significant coverage and all possible paths coverage.

3.5 Control Flow Testing

Control flow testing is also the type of path testing. In control flow testing we used Define/Use testing, also called All-DU path testing. In All-DU path testing first we have to define the variable and then used these variables. There are two type of the use of the variable is available first is c-use (used in calculation) and second is p-use (used in predicate).

4. Related Work

Test case generation and its automation is a key problem in software testing life cycle. If we generate automatic test cases then it can improve the efficiency of software testing and also reduce the cost of software testing. As we know that simple random method is not sufficient to generate ample congeries of test data and automatic test case generation is also an optimization problem that's why we will use search based optimization techniques such as nature inspired Meta heuristics. In these search based algorithms genetic algorithm is more efficient among all the other techniques. Selection of suitable test data for a program using data flow information is similar to compiler optimization. Variable definition and use of variable is combine with compiler optimization.

An approach for inter-procedural test data generation of interactive programs has been already presented. In their paper authors first find the appropriate path and then covered maximum path. They also use inter procedural control flow graph (ICFG). Different clusters for the most critical path have been identified to assign weight. This weigh is distributed among the all paths according to their critically. Initially this is taken as 100 for large programs/software and 10 for small programs/software. The weight has been divided in 80:20 ratio. The 80% weight-age is given to predicate statements and 20% to the simple path. Test data generation is not a simple task; it is a superabundant, error prone and time consuming task. So there is need of automation of test generation process.

Test cases have been developed for large system and on these test cases black box and white box testing applied [6]. A novel algorithm is proposed to support test case generation of combination design. A combination-index table (CIT) is defined, based on which the adaptive genetic algorithm (AGA) is proposed to generate test cases. Process such as coding, the selection of fitness function and the improvement of hereditary operator, etc. and also generate test cases solved by genetic algorithm. Genetic algorithm has been applied to search suitable solutions for that a similarity between the target path and execution path with sub path overlapped is taken as the fitness function to evaluate the fitness for individuals. Some improved genetic algorithms have been applied for generating test cases automatically.

5. Proposed Method

In our proposed method first we generate random test cases, applied mutation testing to check it. If satisfied then stop.

5.1 Proposed algorithm :

1. Inject the mutant in the program.
2. Generate random test cases.
3. Find the mutation score with the formula, $\text{mutation score} = \frac{\text{number of mutants found}}{\text{total number of mutants}}$.
4. If the mutant score is satisfactory (Maximum) stop, otherwise go to step 5.
5. Refine the test case using mutation score. Test case having mutation score 20% or less drop them.
6. Apply Genetic Algorithm Operations on remaining test cases to generate new test cases. Go to step 3.

5.2 Genetic algorithm operations

1. *Selection*: Select the test cases using tournament process.
2. *Mutation*: Apply the mutation operation if mutation score is less than 50 %.
3. *Crossover*: Apply crossover operation if mutation score is more than or equal to 50%.

6. Pseudocode

```

START
Generate the initial population
Compute fitness
REPEAT
    Selection
    Crossover
    Mutation
    Compute fitness
UNTIL population has converged
STOP

```

7. Conclusion

This paper presented a new technique that uses genetic algorithm to generate better automatic test cases. These new test cases are generated using GA operations Selection, Mutation and Crossover.

We still have the same problems today such as testing need a more time and human resource and economy.

Proposed System is very useful for the organization/programmer to testing our deployed application without need of human resource for the testing purpose.

References

- [1] L. M. Surhone, M. T. Tennoe, and S. F. Henssonow, "Software Quality Assurance." Whitefish, MT, USA: Betascript Publishing, Sep. 2010.
- [2] A. Salahirad, H. Almulla, and G. Gay, "Choosing the fitness function for the job: Automated generation of test suites that detect real faults," *Softw.Test., Verification Rel.*, vol. 29, nos. 4–5, pp. 4–5, Jun. 2019.
- [3] M.-Z. Zhang, Y.-Z. Gong, Y.-W. Wang, and D.-H. Jin, "Unit test data generation for c using rule-directed symbolic execution," *J. Comput. Sci. Technol.*, vol. 34, no. 3, pp. 670–689, May 2019.
- [4] Wang Xibo, Su Na, "Automatic Test Data Generation for Path Testing Using Genetic Algorithms", 2011 Third International Conference on Measuring Technology and Mechatronics Automation, 978-0-7695-4296-6/11 \$26.00 © 2011 IEEE.
- [5] M. Alshraideh, B. A. Mahafzah, and S. Al-Sharaeh, "A multiple population genetic algorithm for branch coverage test data generation," *Software Quality Journal*, vol. 19, no. 3, pp. 489–513, 2011.
- [6] R. Khan, Mohd Amjad, "Automated Test Case Generation using Nature Inspired Meta Heuristics-Genetic Algorithm: A Review Paper", *International Journal of Application or Innovation in Engineering & Management (IJAIEM) Volume 3, Issue 11, November 2014 ISSN 2319 – 4847.*
- [7] SIGSOFT Software Engineering Notes May 2013 Volume 38 Number 3.
- [8] Haga, Hisashi, and Akihisa Suehiro. "Automatic test case generation based on genetic algorithm and mutation analysis." *Control System, Computing and Engineering (ICCSCE)*, 2012 IEEE International Conference on. IEEE, 2012.
- [9] Ali, B. M. Y. and Benmaiza, F., 2012. Generating Test Case for Object-Oriented Software Using Genetic Algorithm and Mutation Testing Method. *International Journal of Applied Metaheuristic Computing*, 3: 15–23.
- [10] Xiangjuan Yao, Dunwei Gong, "Testing Method for Software with Randomness Using Genetic Algorithm", 2020 IEEE International Conference on. IEEE, Volume 8, March 2020.

A Machine Learning Approach To Predict Air Quality In India

M. Raj Kumar¹, P.Sharchandar¹, P.Julian Kennady¹, Indhuma E²
¹UG Student , ²Assistant Professor , Department of Computer Science & Engineering,
 St. Anne's College of Engineering and Technology, Panruti.

Abstract

The foreseeing air quality is a mind-boggling task because of the unique nature, instability, and high changeability in reality of toxins what's more, particulates. Simultaneously, having the option to demonstrate, foresee, and screen air quality is getting increasingly important, particularly in metropolitan zones, because of the noticed basic effect of air contamination on residents' wellbeing and the climate. In this paper, we utilize a mainstream AI strategy, Support Vector Regression (SVR), to estimate toxin and particulate levels and to foresee the Air Quality Index (AQI). Among the different tried other options, outspread premise work (RBF) was the kind of piece that permitted SVR to get the most exact expectations. Utilizing the entire arrangement of accessible factors uncovered a more effective system than choosing highlights utilizing head segment examination. &e introduced results exhibit that SVR with RBF portion permits us to precisely anticipate hourly toxin focuses, similar to carbon monoxide, sulfur dioxide, nitrogen dioxide, ground-level ozone, also, particulate matter 2.5, just as the hourly AQI for the province of California. Classification into six AQI classes defined by the US Environmental Protection Agency was performed with a precision of 94.1% on inconspicuous approval information.

Keywords: *Air Quality Index(AQI)*, , *Support Vector Regression (SVR)*

1 Introduction

With the monetary and innovative advancement of urban communities ecological contamination issues are emerging, like water, commotion, and air contamination. Specifically, air contamination has a direct effect on human wellbeing through the openness of toxins and particulates, which has expanded the interest n air contamination and its effects among the scientific local area [1–3]. &e fundamental driver related with air contamination are the consuming of nonrenewable energy sources, horticulture, exhaust from manufacturing plants and enterprises, private warming, and normal catastrophes. Air quality has been read throughout the previous thirty years in the United States (US) since the making of the Clean Air Act program. Albeit this program has involved an improvement in air quality throughout the long term, air contamination is as yet a issue [4].

Complete ignition discharges in the US are responsible for around 200,000 unexpected losses each year because of the convergence of toxins like particulate matter 2.5 (PM2.5) and 10,000 passings each year because of ozone fixation changes. &e American Lung Association assessed that air contamination related ailments cost roughly 37 billion dollars every year in the US, with California alone hitting \$15 billion [5]. Notwithstanding progressively genuine natural contamination issues, researchers have directed a significant amount of related examination, and in those investigations, the guaging of air contamination has been of central significance. &us, in full information on the expanding contamination determined issues, the significance of precisely anticipating the degrees of air toxins has expanded, playing a significant part in air quality administration and populace anticipation against contamination hexes. &e study means to construct models for hourly air quality determining for the territory of California, utilizing quite possibly the most amazing existing AI (ML) approaches, to be specific, a variation of help Support vector machines (SVMs), called Support Vector Regression (SVR). &e proposition is to fabricate an SVR model for the expectation of every poison and particulate estimation on an hourly premise and a SVR model to anticipate the hourly air quality list (AQI) for the condition of California. &e paper is coordinated as follows. Segment 2 edges and inspires the work, giving a thought of the significant commitment addressed by an effective foreseeing model for air quality. Area 3 contains a basic correction of the writing, talking about past and related work. In Section 4, we present SVM, with a specific spotlight on the working of SVR. Area 5 contains a portrayal of the information utilized in this work. In Section 6, we examine the information preprocessing stage that we performed to acquire a more reduced and educational dataset to be utilized by SVR. Segment 7 presents our test study; it is apportioned into a depiction of the utilized test settings and a conversation of the acquired outcomes. At long last, Section 8 finishes up the paper and examines thoughts for future examination.

2. Proposed Prediction Model

The proposed air quality prediction model consists of three parts. In the first part, a deep learning model consisting of LSTM neural networks is realized. Numerous experiments have been conducted with varying hyper parameters to build best LSTM structure. After the experiments, the network structure that gives the best result is constructed. This network structure has an input layer, a hidden layer with 24 LSTM units, and an output layer. Other hyper parameters of the network are denoted in Table I.

| Hyperparameters | Values |
|-----------------|--------|
| Input Sequence | 8 |
| Hidden Layer | 1 |
| LSTM Units | 24 |
| Output Layer | 1 |
| Batch Size | 50 |
| Number of Epoch | 100 |

Another prediction method SVR is trained in model for evaluating the LSTM success. In the second part, a labeling unit is created that labels data according to the daily AQI values. In the last part, a decision unit is developed which maps according to the observed and predicted alarm situations. In the proposed model, a certain number of past sequential values are taken into account and predictions are made for the next step, denoted by Eq. (7).

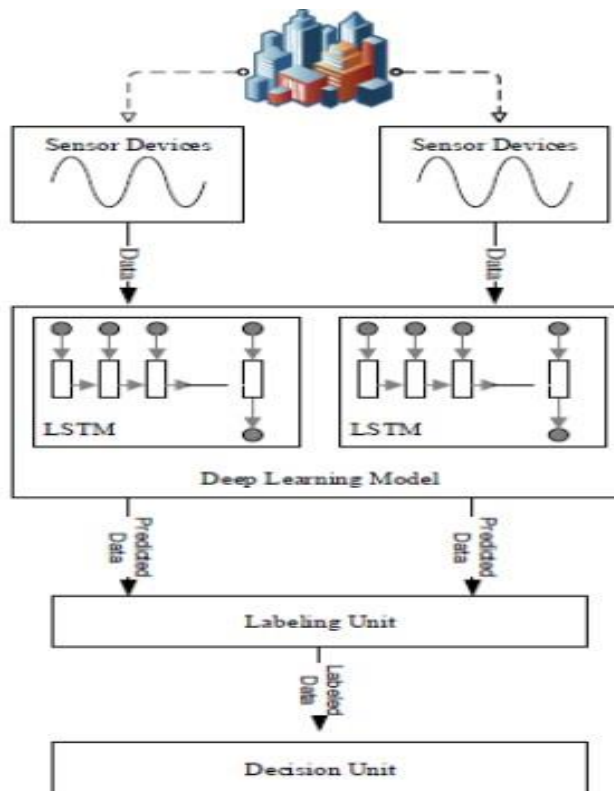


Figure 3. Proposed Prediction Model

3. Proposed System

Air contamination is considered to happen at whatever point hurtful or over the top amounts of defined substances like gases, particulates, and organic particles are brought into the climate & extreme emanations have self-evident results, causing sicknesses and demise of populaces and other living creatures and debilitating yields. Air contaminations can either be strong particles, fluid drops, or gases, which are classified into the accompanying: Essential toxins, which are discharged from the source straightforwardly to the environment. &e sources can be all things considered characteristic cycles, for example, dust storms or human-related, like industry and vehicle emanations. &e most regular essential poisons are sulfur dioxide (SO₂), particulate matter (PM), nitrogen dioxide (NO_x), and carbon monoxide (CO). Auxiliary poisons, which are air toxins shaped in the environment, coming about because of the substance or actual associations between essential contaminations. Photochemical oxidants and auxiliary particulate matter are the significant instances of auxiliary toxins. &e most regular air toxins are known as the models toxins, which compare to the most broad wellbeing dangers, e.g., CO, SO₂, lead, ground-level ozone (O₃), NO₂, and PM. &e levels of these toxins are estimated by the US Environmental Protection Agency (EPA), which controls by and large air quality. Scientific research has exhibited a relationship between's transient openness to this sort of toxins and numerous medical issues, like restricted capacity to react to expanded oxygen requests when working out (particularly for individuals with heart conditions), aviation route inflammation in sound individuals and expanded respiratory manifestations for individuals with asthma, respiratory crises especially for kids and the older, etc [6]. EPA, EU, and numerous other public natural organizations have set norms and air quality rules in regards to passable levels for these toxins. &e air quality record (AQI) is a pointer made to report air quality, estimating how perfect or unfortunate the air is and what related wellbeing effects may be a worry, particularly for hazard gatherings. It centers around wellbeing effects that can be capable inside a couple of hours or days in the wake of being presented to dirtied air. It is determined dependent on the most extreme individual AQI enlisted for the models poisons referenced previously. Building a determining framework, in view of the degrees of convergence of individual contaminations, that can foresee air quality hourly, will make the AQI more flexible and helpful for the populace's wellbeing. Frameworks that can produce alerts dependent on air quality are subsequently required and significant for the populaces. &ey may play a significant part in wellbeing alarms when air contamination levels may surpass the specified levels; likewise, they may coordinate existing discharge control programs, for example, by permitting natural controllers the alternative of "on-request" outflow decreases, operational arranging, or even crisis reaction.

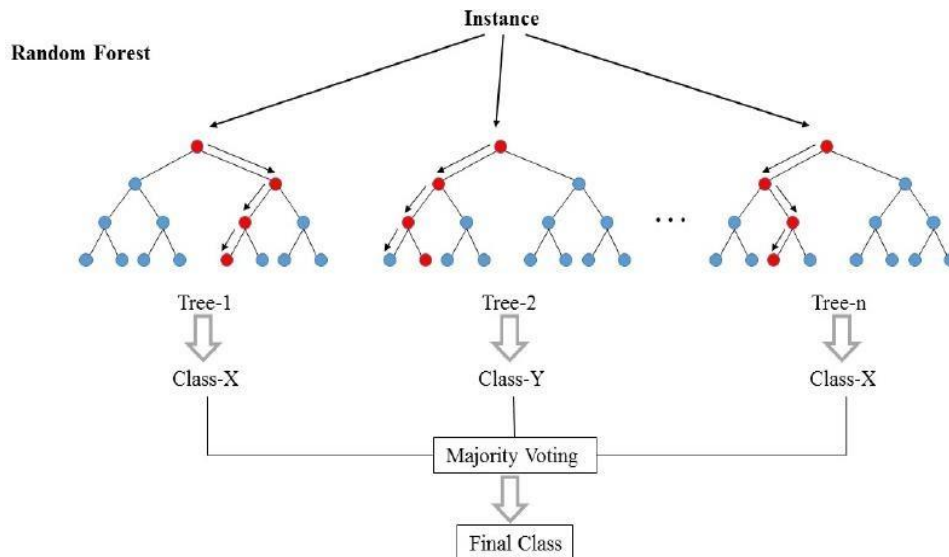
4. Problem Definition

To measure the air quality, several monitoring methods have been proposed and utilized. In Zheng et al.'s research they use public and private web services as well as a list of public websites to provide real-time meteorological, weather forecasts and air quality data for their forecasting. Small unmanned aerial vehicles are used in the work of Alvarado et al. as a methodology to monitor PM₁₀ dust particles, where they can calculate the emission rate of a source. With the development of smart city technologies, IoT devices have been shown to be an effective option to collect real time weather, road traffic, pollution and traffic information. Thus, IoT devices are also considered to enable air quality analysis. In addition to the fixed sensors, public transportation infrastructure such as buses has been used to collect air quality data. Also, there is one project engaged the entire community members in collecting data and developed an online air quality monitoring system based on it, which is also called crowdsourcing.

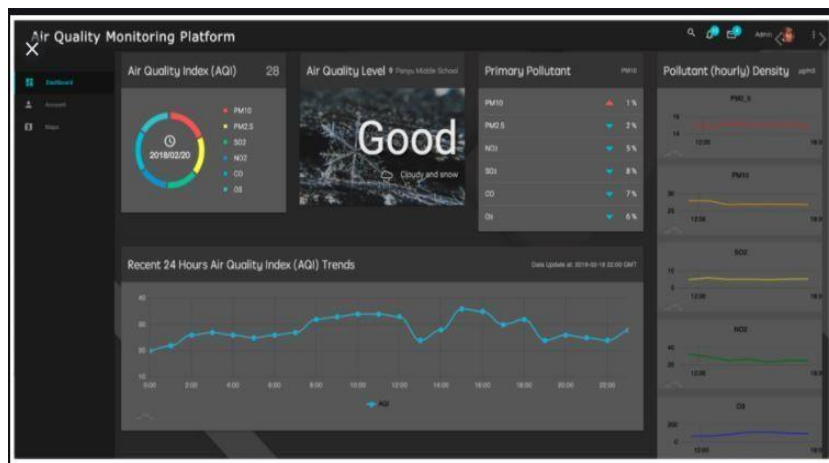
Hasenfratz et al. utilized sensor nodes to build a thousand models targeting at different time periods. All these aforementioned methods are either costly or time consuming. In our work, we explore the use of fixed and mobile IoT sensors together to improve the prediction performance, which has not been researched much yet. To meet the increasing query frequency of air quality in real time and also to enable citizens to react instantly to the pollution, there has been a large body of work on building connected monitoring sensor networks to share the current air quality information with them. Garzon et al. presented an air quality alert service. Their service continuously determines the areas, where the level of certain matter concentration exceeds the preset threshold, and notify users if they entered them. Maag et al. proposed a multi-pollutant monitoring platform using wearable low-cost sensors. Compared with above methods, our system can serve the similar functions to end users practically with either fewer sensors or less demand for computation.

5. Random Forest Alogrithm

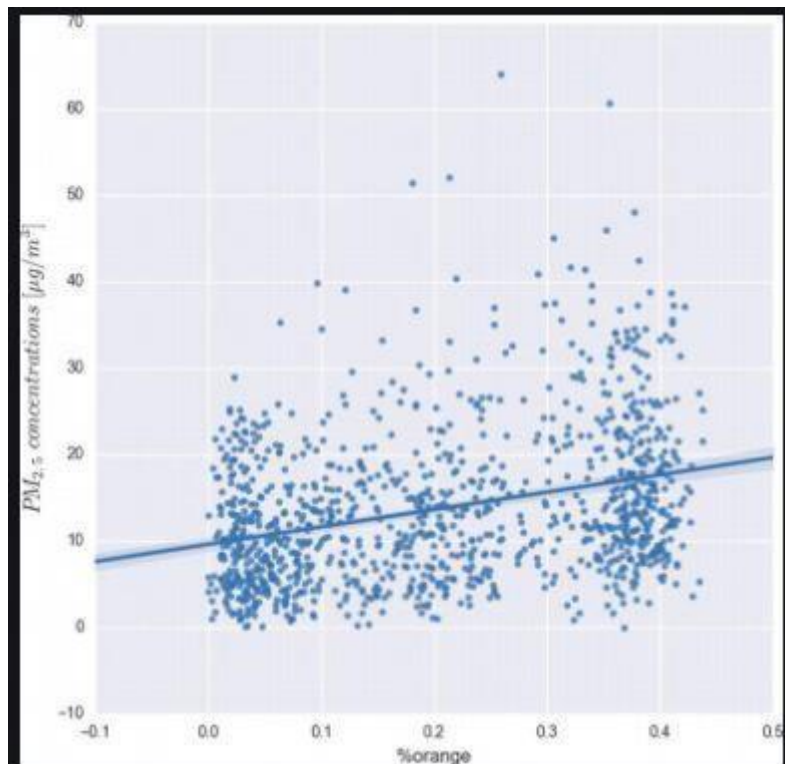
Random forests (RF) are basically a bag containing n Decision Trees (DT) having a different set of hyper-parameters and trained on different subsets of data. Let's say I have 100 decision trees in my Random forest bag!! As I just said, these decision trees have a different set of hyper-parameters and a different subset of training data, so the decision or the prediction given by these trees can vary a lot. Let's consider that I have somehow trained all these 100 trees with their respective subset of data. Now I will ask all the hundred trees in my bag that what their prediction on my test data is. Now we need to take only one decision on one example or one test data, we do it by taking a simple vote. We go with what the majority of the trees have predicted for that example.



In the above picture, we can see how an example is classified using n trees where the final prediction is done by taking a vote from all n trees. In machine learning language, RFs are also called an ensemble or bagging method.



6. Result



7. Conclusion

Anticipating the air quality is an unpredictable errand because of the dynamic nature, instability, and high inconstancy in space and season of toxins and particulates. Simultaneously, being ready to show, anticipate, and screen air quality is turning out to be an ever increasing number of significant, particularly in metropolitan zones, due to the noticed basic effects of air contamination for populaces also, the climate. This work introduced an investigation of support vector relapse (SVR) to conjecture toxins and particulates' levels and to accurately recognize the AQI. The examined technique created an appropriate model of the hourly barometrical contamination, permitting us to get, by and large, great precision in displaying contamination focuses like O₃, CO, and SO₂, just as the hourly AQI for the territory of California. As future work, we mean to improve and research the use of SVR to estimate air quality through the accompanying subjects:

Dataset and variable determination—thinking about an enormous dataset with more boundaries and estimations, which can uphold more exact prescient models for air contaminations and particulates, specifically, NO₂ and PM_{2.5}. SVR boundary enhancement—as SVR model execution is enormously influenced by the part work determination and the punishment boundary C, it would be fascinating to investigate different techniques, different from arbitrary pursuit, for hyperparameter streamlining such as hereditary calculations or molecule swarm streamlining. To wrap things up, we mean to look at the outcomes gotten by SVR to the ones accomplished by other machine learning calculations of a different nature, as artificial neural networks, Bayesian organizations, choice trees, irregular backwoods, what's more, hereditary programming.

References

- [1] U. A. Hvidtfeldt, M. Ketzel, M. Sørensen et al., “Evaluation of the Danish AirGIS air pollution modeling system against measured concentrations of PM_{2.5}, PM₁₀, and black carbon,” *Environmental Epidemiology*, vol. 2, no. 2, 2018.
- [2] Y. Gonzalez, C. Carranza, M. Iniguez et al., “Inhaled air pollution particulate matter in alveolar macrophages alters local pro-inflammatory cytokine and peripheral IFN production in response to mycobacterium tuberculosis,” *American Journal of Respiratory and Critical Care Medicine*, vol. 195, p. S29, 2017.
- [3] L. Pimpin, L. Retat, D. Fecht et al., “Estimating the costs of air pollution to the National Health Service and social care: an assessment and forecast up to 2035,” *PLoS Medicine*, vol. 15, no. 7, Article ID e1002602, pp. 1–16, 2018.
- [4] F. Caiazzo, A. Ashok, I. A. Waitz, S. H. L. Yim, and S. R. H. Barrett, “Air pollution and early deaths in the United States. Part I: quantifying the impact of major sectors in 2005,” *Atmospheric Environment*, vol. 79, pp. 198–208, 2013.
- [5] B. Holmes-gen and W. Barrett, *Clean Air Future, Health and Climate Benefits of Zero Emission Vehicles*, American Lung Association, Chicago, IL, USA, 2016.
- [6] US Environmental Protection Agency (US EPA), “Criteria air pollutants,” *America’s Children and the Environment*, US EPA, Washington, DC, USA, 2015.
- [7] CERN, *Air Quality Forecasting*, CERN, Geneva, Switzerland, 2001.
- [8] G. E. Box and D. A. Pierce, “Distribution of residual autocorrelations in autoregressive-integrated moving average time series models,” *Journal of the American statistical Association*, vol. 65, no. 332, pp. 1509–1526, 1970.
- [9] C. L. Hor, S. J. Watson, and S. Majithia, “Daily load forecasting and maximum demand estimation using ARIMA and GARCH,” in *Proceedings of the 2006 International Conference on Probabilistic Methods Applied to Power Systems*, pp. 1–6, IEEE, Stockholm, Sweden, June 2006.
- [10] L. Y. Siew, L. Y. Chin, P. Mah, and J. Wee, “Arima and integrated arfima models for forecasting air pollution index in shah alam, selangor,” *He Malaysian Journal of Analytical Science*, vol. 12, no. 1, pp. 257–263, 2008.
- [11] J. Zhu, “Comparison of ARIMA model and exponential smoothing model on 2014 air quality index in yanqing county, Beijing, China,” *Applied and Computational Mathematics*, vol. 4, no. 6, p. 456, 2015.
- [12] T. M. Mitchell, “Machine learning,” in *Proceedings of the IJCAI International Joint Conference on Artificial Intelligence*, Pasadena, CA, USA, July 2009.
- [13] U. Brunelli, V. Piazza, L. Pignato, F. Sorbello, and S. Vitabile, “Free hours ahead prevision of SO₂ pollutant concentration using an Elman neural based forecaster,” *Building and Environment*, vol. 43, no. 3, pp. 304–314, 2008.
- [14] G. Bontempi, S. Taieb, Y. Le Borgne, and D. Loshin, “Machine learning strategies for time series forecasting,” in *Business Intelligence*, pp. 59–73, Springer, Berlin, Germany, 2013.

Execution Of Cloud Computing Education In Current Scenario In The World Countries

S.Dharmaraj^{#1} and Dr.P,Kavitha ^{#2}

Department of Computer Applications Loyola College,Vettavalam
Department of Computer Science Paavendhar College of Arts & Science, Attur

Abstract

Education helps in the money related improvement of a country. Instruction has the ability to kill the destitution in a country. The undeniably perplexing foundation climate the board, improvement objectives and quickly changing innovation present new sorts of difficulties to instruction area. In this advanced time, the higher instructive organizations focus on most recent advances and devices to investigate learning. At mean time, the instructive assets dissemination may be lopsided across the nations. Cloud computing carries different advantages to coordinate into the scholastic field. There are hazard issues for receiving cloud in putting away and executing restricted information. This paper studies to dissect utilizes, issues in following cloud computing for the personnel, staff and students in college area. It likewise centers on security issues, hazard divisions. The survey perceived the zones in which cloud computing can have an impact in schooling and College field. Besides, this paper plans to examine about security the executives and the difficulties looked by the education area in non-industrial nations subsequently encouraging specialists to locate the significant issues, in which they can center their endeavors.

Keywords:-cloud computing, cloud computing architecture, cloudcomputing education, challenges.

Introducion

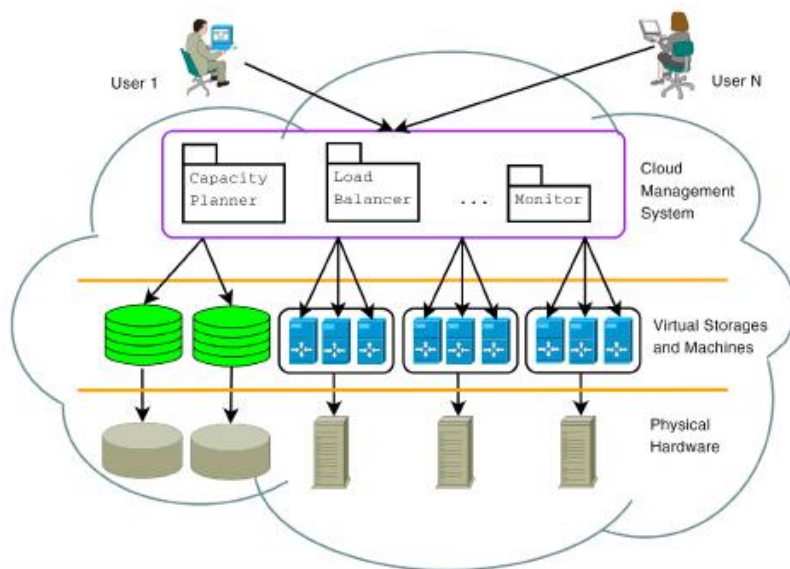
The National Institute of Standards and Technology NIST Definition of Cloud Computing: Cloud registering is a model for empowering omnipresent, helpful, on-request network admittance to a common pool of configurable registering assets (e.g., networks, workers, stockpiling, applications, and administrations) that can be quickly provisioned and delivered with negligible administration exertion or service provider association. This cloud model is made out of five fundamental attributes, three help models, and four organization models. In Cloud Computing the word cloud (likewise expressed as "the cloud") is utilized as an illustration for "the Web," so the expression cloud computing signifies "a kind of Internet-based processing," where various administrations — like Servers, stockpiling and applications — are conveyed to an association's PCs and gadgets through the Internet [20] Cloud computing: The actual meaning of distributed computing stays disputable. Counseling firm Accenture has made a valuable, compact definition: the dynamic provisioning of IT capacities (equipment, programming, or administrations) from outsiders over an organization. [8] Cloud computing developed as a fruitful utility registering worldview for Information and Correspondence Technology (ICT) assets conveyance as an assistance over the Internet. The appropriation of Cloud computing ranges across industry, government, and the scholarly community the same. [12] The enormous expansion of moderate PCs, Internet broadband availability and rich education content has made a worldwide marvel in which data and correspondence innovation (ICT) is being utilized to change instruction. Cloud computing is starting to play a key job in this change. [24] Instruction changes can rise above monetary and social obstructions, giving equivalent points of interest and freedoms to each and every individual who approaches ICT. In Portugal, for instance, it required only two years for a cross country exertion to change schooling and college accomplish critical monetary advantages. PCs are presently accessible to each elementary school understudy in the country — moving Portugal to the bleeding edge of computerized instruction while additionally making almost 1,500 new openings furthermore, adding Rs 2.26 billion to the nation's economy.[24]

2. Cloud Computing Overview

2.1 Ideas of Cloud Computing

The administrations that are made through equipment and programming associated with workers convey their information in a virtual cloud, guarantee it identifies with for all time without interference, with various gadgets (PC, tablet gadget, cell phones, and so on) in the wake of setting an uncommon code to open and bolt the

network, and along these lines are available from anyplace, whenever. It is the exchange of the treatment interaction from the client's PC to the house cleaner gadgets by means of the Internet, what's more, save client records to have the option to get to them from anyplace and any gadget, and to turn into programming administrations, and a computerized UI, and permits workers to numerous clients utilizing the equivalent administration. Cloud isn't just the most recent term for the Internet, however the Internet is an essential establishment for the cloud, the cloud is a more thing than the Internet. The cloud is the place where you go to utilize innovation when you need it, however long you need it. You don't introduce anything on your work area, and you don't pay for the innovation when you are not utilizing it the cloud can be both programming and foundation. It very well may be an application you access through the Web or a worker like Gmail and it very well may be likewise an IT foundation that can be utilized according to client's request.[1] The principle empowering innovation for cloud computing is virtualization. Virtualization programming isolates an actual processing gadget into at least one "virtual" gadgets, every one of which can be handily utilized and figured out how to perform registering errands. With working framework level virtualization basically making an adaptable arrangement of various autonomous registering gadgets, inactive processing assets can be designated and utilized all the more effectively. Virtualization gives the deftness needed to accelerate IT activities, and lessens cost by expanding framework utilization.

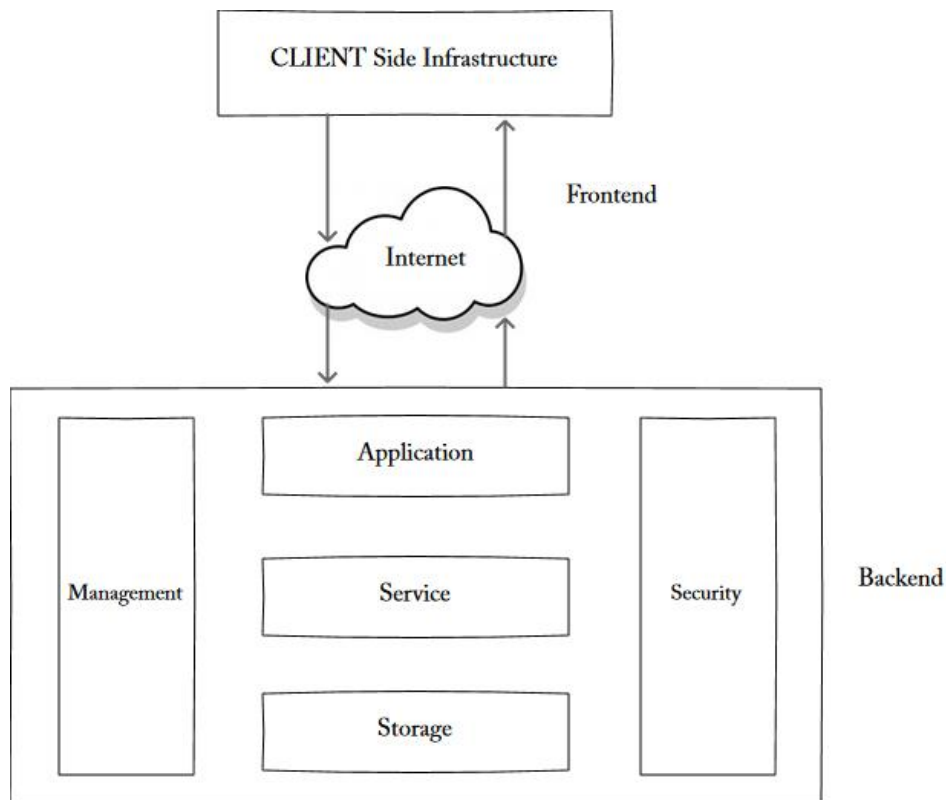


2.2 Prerequisites for the utilization of Cloud computing

- I. Personal PCs permitted associating with the Internet.
- ii. Working framework permits associating with the Internet.
- iii. A rapid association with the Internet is a connection between the client and the information and all the Programming it employments.
- iv. Web program permits the utilization of cloud administrations

2.3 Cloud computing Architecture

Cloud computing engineering alludes to the segments and subcomponents needed for cloud processing. This part depicts a layered model of cloud computing where a cloud computing climate can be isolated into four layers: the equipment/datacenter layer, the foundation layer, the stage layer and the application layer [25]. Cloud computing engineering alludes to the segments and subcomponents needed for cloud processing. These segments regularly comprise of a front end stage (fat customer, meager customer, cell phone), back end stages (workers, stockpiling), a cloud based conveyance, and an organization (Web, Intranet, Intercloud). Joined, these segments make up distributed computing engineering [22] appeared in Figure



2.4 Cloud computing service model

2.4.1 Software-as-a-service (SaaS)

SaaS is known as 'On-Demand Software'. It is a software distribution model. In this model, the applications are hosted by a cloud service provider and publicized to the customers over internet. In SaaS, associated data and software are hosted centrally on the cloud server. User can access SaaS by using a thin client through a web browser. CRM, Office Suite, Email, games, etc. are the software applications which are provided as a service through Internet. The companies like Google, Microsoft provide their applications as a service to the end users.

2.4.2 Platform-as-a-service (PaaS)

PaaS is a programming stage for designers. This stage is produced for the software engineers to make, test, run and deal with the applications. An engineer can undoubtedly compose the application and send it straightforwardly into PaaS layer. PaaS gives the runtime climate for application improvement and arrangement devices. Google Apps Engine (GAE), Windows Azure, SalesForce.com are the instances of PaaS.

2.4.3 Infrastructure-as-a-service (IaaS)

IaaS is an approach to convey a distributed computing foundation like worker, stockpiling, organization and working framework. The clients can get to these assets over distributed computing stage i.e Internet as an on-request administration. In IaaS, you purchase total assets as opposed to buying worker, programming, and datacenter space or organization hardware. IaaS was before called as Hardware as a Service (HaaS). It is a Cloud processing stage based model. HaaS contrasts from IaaS in the manner that clients have the uncovered equipment on which they can send their own foundation utilizing most suitable programming.

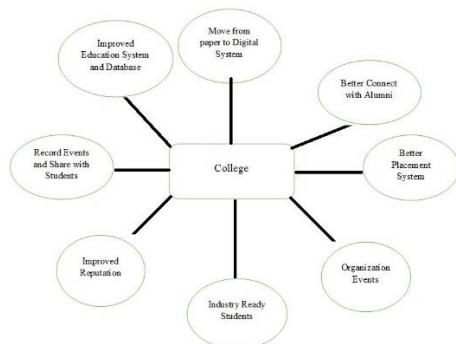
3. Cloud Computing In Education

registering administrations is one of the types of present day virtualization programming utilized on an enormous scale in the business areas and taxpayer supported organizations and electronic exchanges in the dominant part of nations on the planet, yet they as of late set forward a plan to be utilized in the zones of distance education and e-learning, with the multiplication of cloud computing is not, at this point a matter simply a hypothetical idea however transformed into solid application we are finding in various administrations in the Web, particularly in the field of e-learning, for instance, it moved to construct trial of programming that can be downloaded to the gadget to the administrations on the Internet doesn't need any uncommon programming to exploit them measure, The area (classmarker.com) and administration (quizschool), for instance, profited by the abilities of cloud computing to give facilitating Testing Service and assessed consequently free of charge or for an ostensible expense, where two locales offer the chance of crafted by trial of different sorts, like total vacuum, various decision, valid and mistake, and others, with the arrangement of the capacity to show the inquiries haphazardly or as indicated by a specific request, and the spread of the test through email or Web pages.

The schooling business currently faces another arrangement of difficulties that is driving a principal change across the training. Their client socioeconomics, practices and assumptions have changed. They face income pressures alongside expanding sensitivities from their clients on the profit from speculation for dollars spent on advanced education. [11] Simultaneously, training organizations are feeling the squeeze to convey more for less, what's more, they need to discover approaches to offer rich, reasonable administrations and devices. Those teachers who can convey these modern interchanges conditions, including the work area applications that managers use today, will help their understudies secure better positions and more prominent freedoms in the future.[2] In spite of all of focal points of cloud, processing it still not completely received in scholastic establishments area. It is just 4% of distributed computing utilized in instruction and the other 96% is identified with mechanical areas and administrations [6].

The instructive distributed computing industry is still in the first place. By the by, cloud processing can possibly assume a wide and critical part in instruction innovation in the close future. It is on the grounds that presently cloud computing spreads quick on the whole ventures. cloud computing administration offers numerous preferences for students, for example, testing straightforwardly (online),easy to send activities and tasks for students, simple admittance to the tests, works out, projects put together by understudies, criticism among understudies and instructors, simple of correspondence between understudies, help understudies and educators to utilize applications without stacked on their PCs and assist them with getting to put away records from any PC by utilizing the Internet and the understudy can get to all projects whenever, from anyplace.

Along these lines, it was conceivable to bridle cloud computing administration in the instructive targets administration in a few zones, including the arrangement of talks or courses quantity from a good ways, so they are available on the virtual cloud (which might be as a site or application on keen tablets or portable), and can be gotten to her away from the obstructions of time or spot.



4. Data Analysis and Presentation

The investigator has administered 439 Proforma, from which 335 Proforma was distributed among students and 104 among teachers. The students and teachers belong to selected schools of Rural and Urban area of Tiruvannamalai Tamil Nadu. After scrutinizing, investigator received 292 valid responses from students and 74 valid responses from teachers. After collection of samples researcher has analyzed and interpreted the results which are presented in table and fig. below:

Table I. Distribution of Sample

| Category | Responses (Faculties) | Responses (Students) |
|------------------------------|-----------------------|----------------------|
| Proforma Administered | 104(100%) | 335(100%) |
| Proforma Received | 74(71.15%) | 292(87.16%) |

Table I depicts that total 439 Proforma were administered, i.e. 335 among students and 104 among teachers. After scrutinizing, investigator received 292 valid responses from students and 74 valid responses from teachers.

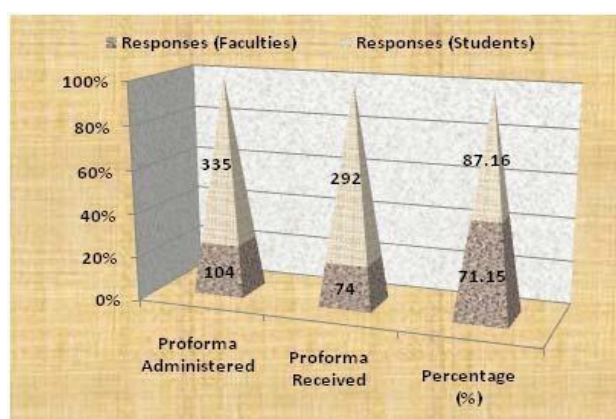


Fig.4: Distribution of Sample

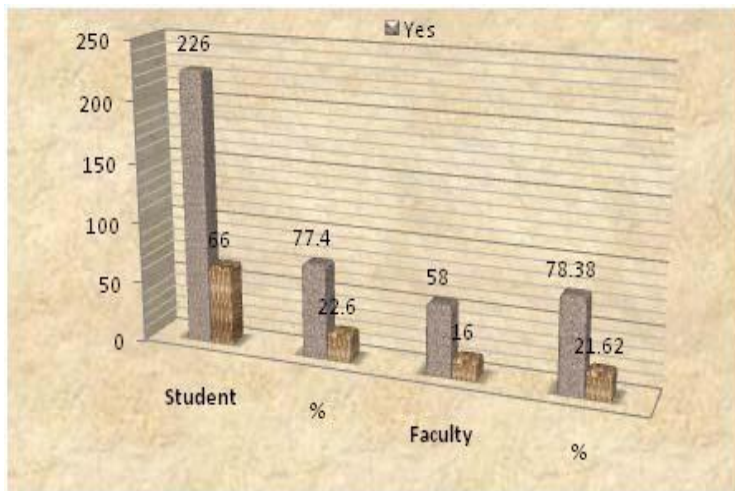
The above fig.5 depicts total sample size which was administered among students and teachers. In student responses, after scrutinizing, investigator found 292(87.16%) valid responses and 43(12.84%) responses were rejected due to incomplete information. 104 questionnaires were distributed among teachers, Investigator finally received 74(71.15%) as valid responses and 30(28.85%) responses were rejected due to incompetence.

Table II. Knowledge about Cloud Computing Technology

| Knowledge | Responses (Student) | Per(%) | Responses (Faculty) | Per(%) |
|--------------|---------------------|---------------|---------------------|---------------|
| Yes | 226 | 77.40 | 58 | 78.38 |
| No | 66 | 22.60 | 16 | 21.62 |
| Total | 292 | 100.00 | 74 | 100.00 |

Table II depicts the responses of students regarding their belief on Cloud Technology which is used to improve learning. Some students believe and some may not. According to table total 226 students, 58 teachers are interested in using Cloud Technology in education, 66 students and 16 teachers were not interested. So we can get maximum response of students and teachers in favor of Cloud Technology used in education.

Fig.5: Knowledge about Cloud Computing Technology



The above fig. 6 reveals that out of 292 maximum 226(77.40%) of students and 58(78.38%) teachers were responded positively, that they do believe in using Cloud technologies to improve learning, whereas 66(22.60%) students and 16(21.62%) teacher were disagreed of Cloud Technology to improve learning in education.

Table III. Performance in education can be increased by Cloud Computing Technologies

| Performance | Responses | | Responses | |
|--------------|-----------|---------------|------------|---------------|
| | (Faculty) | Per (%) | (Student) | Per (%) |
| Yes | 71 | 95.95 | 231 | 79.11 |
| No | 3 | 4.05 | 61 | 20.89 |
| Total | 74 | 100.00 | 292 | 100.00 |

Table III briefed that 231 students out of 292 and 71 teachers out of 74 responded very positively towards cloud computing technologies and of course our old traditional education system.

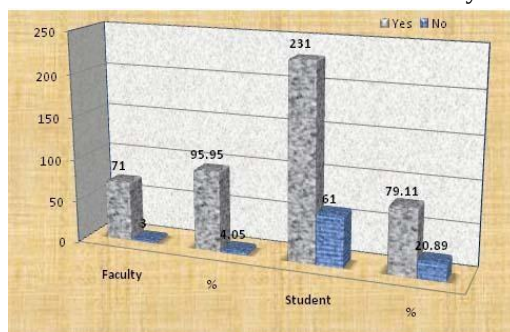


Fig.6: Performance in education can be increased by Cloud Computing Technologies

Fig.7 states out of 292, a very high positive response from students i.e. 79.11% and 95.95% from teachers out of 74 samples. It shows how the positive response received that cloud education system has better impact in teaching and learning than traditional education system.

Table IV. Given a chance to study in cloud environment, like to study by cloud technology

| Cloud Environment | Responses (Student) | Per (%) | Responses (Faculty) | Per (%) |
|-------------------------|---------------------|---------------|---------------------|---------------|
| 0- 25% | 18 | 6.16 | 2 | 2.70 |
| 26 - 50% | 62 | 21.23 | 23 | 31.08 |
| 51 - 75% | 107 | 36.64 | 35 | 47.30 |
| >75% | 68 | 23.29 | 7 | 9.46 |
| Can't Say / No Comments | 37 | 12.67 | 7 | 9.46 |
| Total | 292 | 100.00 | 74 | 100.00 |

Table IV very clearly indicating maximum 237 students from three category and 58 teachers from two categories were agreed learning using cloud environment being used at initial level education system. 37 students and 7 teachers were not interested at all from 292 students and 74 teachers. Therefore, we can say high number of students and teachers need cloud environment in education and very less students and teachers were not interested.

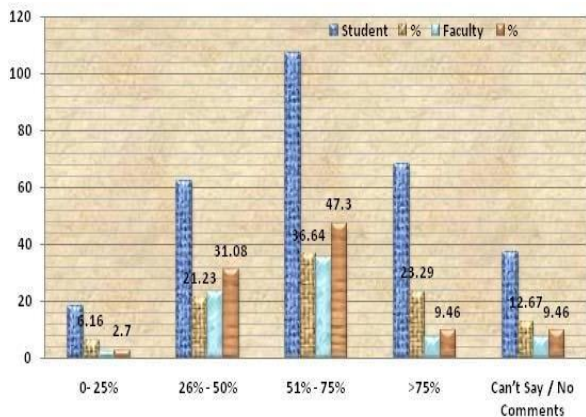


Fig.7: Given a chance to study in cloud environment, like to study by cloud technology

The fig.8 depicts that out of 292, 36.64% students from 51%-75% category and out of 74 teachers from same category, 47.30% positively agreed. Only 12.67% of students and little 9.46% students acted as that no such type of cloud environment in education system

5. Service Available To the Education Institution

Driving cloud suppliers have perceived the significance of changing their figuring administrations explicitly to the necessities of instructive establishments. The absolute most generally utilized instructive stages are recorded beneath:

1-Microsoft for Education: Microsoft instructive devices is a bunch of projects and sites equipped fundamentally to understudies to assist them with acquiring time and learning in a creative manner, as it is moreover planned for instructors to build up their exhibition and make proficient practices more appealing, through the ideal abuse of what can be allowed by the innovation in the field of Education.

2-Google Apps for Education: A bunch of apparatuses and participatory and cooperative arrangements given by Google, and that can be utilized by laborers to the field of training. Google's applications described by a few properties once in a while meet in helpful answers for other organizations, causing a large number of instructive foundations to decide to helpful answers for Google on its way towards the universe of innovation.

3-Amazon Web Services for Education (AWS): Is a simple scope of administrations, which gives powerful arrangements regarding cost, in colleges, junior colleges and professional schools. AWS can add to the production of foundation for data innovation adaptability in these establishments.

6. Execution Of Cloud Computing Education In Current Scenario In The World Countries:-

In most agricultural nations, barely any youngsters move on from auxiliary school and college many don't indeed, even completion elementary school. In Ghana, for instance, just 50% of kid's total evaluation 5, what's more, of those, not exactly half can appreciate a basic section. [17]

The greatest danger to all-inclusive training is just an absence of subsidizing. Large numbers of the educators in underdeveloped nations are volunteers. Positively, they are extraordinary resources and a tremendous need in third world nations. Nonetheless, to acquire school instructed educators would require reserves that they essentially don't have. There are some school and college taught instructors in underdeveloped nations yet frequently they work for almost no cash by any means. There is an enormous requirement for school and college instructed educators and for satisfactory classrooms. A large number of the homerooms have not many books and not close enough supplies. Supplies that huge nations underestimate are indeed hard to find in these different nations. Things like journals, papers, pens, and organizers are hard to come by in third world nations. [13]

Over the previous decade, training industry has filled fundamentally in the India.

This advancement in training and confronted difficulties, for example, absence of government spending on schooling and the deficiency of teachers authorities due to relocations and there is lack of qualified instructors in the country.

Representing a significant test for establishments Sudanese Higher Education to keep on tackling their work, the most significant of these arrangements is to slice spending and to give an appropriate climate to training is the haze of the best answers for these issues.

There are a scope of instructive and specialized issues at all created nations, particularly in Sudan that happened in earlier years, to explain and feature:

1. Shortcoming of government subsidizing for the training area
2. The absence of framework and structures appropriate for advanced education

3. Movements instructing staff
4. Absence of instructive materials (books - References - Software - Tools colleague)

Through distributed computing to give a few arrangements, for example,

1. Virtualization of registering climate
2. Flexible Cloud stockpiling.
3. Online course conveyance.
4. Online tasks and tests.
5. Merged email administrations with Cloud
6. Task joint effort
7. More prominent class investment.
8. Security.

7. Conclusion:

Soon of cloud computing in the field of schooling and college administration will turn into a fundamental wellspring of e-learning to give the chance for understudies and instructors to snappy admittance to different applications, frameworks and assets through the Internet, and offer records and reports, also, the trading of obligations and activities among understudies, a test that should defeat the extensive inclusion of the assistance and quick Internet access , to empower the understudy to take bit of leeway of this innovation applications.

Cloud computing is the answer for an enormous contributor to the issues of instruction at all created nations, however the test stays in the political and managerial choice to receive cloud computing in schooling and college

Through the arrangement of framework, programming as a help there are a ton of advantages of the instructive establishment in the less evolved nations, for example, empowers college, schooling organizations to zero in on the nature of training and the improvement of the human component and the utilization of assets in accomplishing instructive objectives without the need to put resources into the buy and support of specialized foundation. What's more, help in various study hall the board through a little gathering of instructors and will help to defeat the issue of deficiency of gifted instructors. Cloud administrations can be a less expensive alternative for instructive establishments confronting cuts in financing, yet at the same time need to put resources into innovation to improve learning levels. Just like the case at all created nations.

References

- [1] Ahmed. Gamaleldin .2013An Introduction to Cloud Computing Concepts: Practical Steps for Using Amazon EC2 IaaS Technology.
- [2] A Microsoft U.S. Education white paper "Cloud computing in education Savings, flexibility, and choice for IT"2010.
- [3] Amazon. 2012. AWS in Education Customer Experiences.

Mobile Camera-Based Assistive Text And ProductLabel Reading Using Android For Blind Persons

,S. Manavalan¹ Associate Professor,

S.Periya Nayaga Mary² Student

A.Babeyola³ Student, K.Bhuvaneshwari⁴ Student

Department of computer science and engineering,

St.Anne's College of Engineering and Technology

mano5500@gmail.com

Abstract

The number of visually impaired persons is increasing due to uncontrolled diabetes, age related causes, eye diseases, traffic accidents, and other causes. Cataract is leading cause of blindness and visual impairment. Mobile applications that provide the support to visually challenged person have become an essential device in visually challenged person's life. Recent advances in mobile technology, digital camera, computer vision and camera based application make it possible to support visually challenged persons by developing camera based application that combine computer vision with other existing technology such as optical character recognition (OCR) system. The main focus of our research is that the visually challenged person can get information about printed text, text boards, scene text, hoardings, and instructions on traffic sign boards in audio form. With this point of view, the system design for a camera based reading system that extract text from textual board and identify the text characters from the captured image and finally, textual information will be converted into speech.

Keywords: *Visual impact,Blindness,Optical character recognition(OCR),Text reading,Text to speech(TTS),Audio output,Android*

1 Introduction

The number of visually impaired persons are increasing in today's world due to many reasons.Recent development in computer technology,computer vision,digital camera that makes it feasible to assist these technology by developing such a new system like portable camera based product which combines the computer technology with existing product such as optical character recognition(OCR).Reading is one of the important factor in today's society. The printed text is anywhere in the form of reports, bank document, receipts, hotel menus, classroom boards, product label, bottle label, etc. And using such system like video magnifiers, screen readers help blind person and those with low vision to access the documents and text. The ability of people who are blind or have low visual impairments to read printed labels and documents will enhance independent living and social self-sufficiency.

The number of visually impaired persons is increasing due to uncontrolled diabetes, age related causes, eye diseases, traffic accidents, and other causes. Cataract is leading cause of blindness and visual impairment. Mobile applications that provide the support to visually challenged person have become an essential device in visually challenged person's life. Recent advances in mobile technology, digital camera, computer vision and camera based application make it possible to support visually challenged persons by developing camera based application that combine computer vision with other existing technology such as optical character recognition (OCR) system. With the rapid development of camera-based applications on smart phones and handy devices, understanding the pictures taken by these devices has gained growing attention from the computer vision community in recent years which will be helpful for these individuals. The main focus of our research is that the visually challenged person can get information about printed text, text boards, scene text, hoardings, and instructions on traffic sign boards in audio form. With this point of view, the system design for a camera based reading system that extract text from textual board and identify the text characters from the captured image and finally, textual information will be converted into speech.

2 Existing System

In Existing system researchers have attempted to ease the burden on blind people by proposing various techniques that converts text to audible sounds. Tyflos is a couple of glasses that have cameras attached to the side, earphones and a microphone. Voice mandates can be used to command the user and direct the platform. Some commands include “move paper closer,” “move paper up,” “move paper up, right” from the device to the user, and “rewind paragraph,” “forward paragraph,” and “volume up” from the user to the device. Nonetheless, the speech user integration might not work perfectly in a noisy environment, rendering it limited to indoor use. Finger Reader is one such device, a wearable ring with a camera which is present on the front. The voice user interface might not function perfectly in a chaos surrounding; rendering is restricted to indoor need.

2.1 Disadvantages of Existing System

1. Microcontrollers are used which costs more.
2. The voice user interface might not function perfectly in a noisy environment,
3. rendering it limited to indoor use.
4. More expensive because they use hardware.
5. They are less accurate.
6. They are not portable.

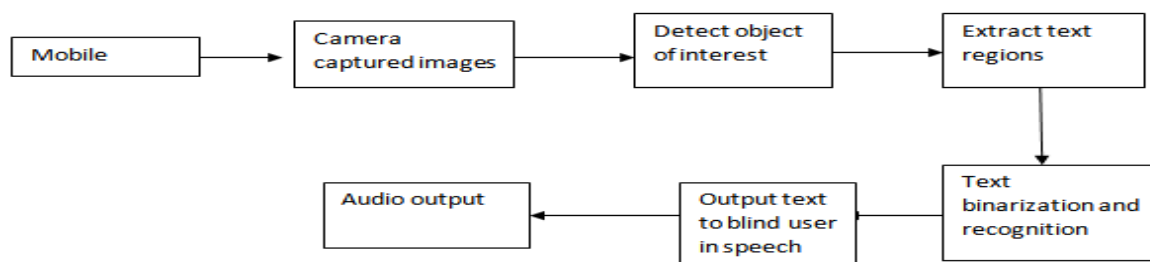
3 Proposed System

The concept of proposed system is the idea of developing Android app reader based text reading system for visually impaired persons. This illustrates the text reading system for visually impaired users for their self-independent. The problem stresses the high importance of visually impaired system is that self-dependency of visually impaired users. This extends the work towards the development of ease of collecting information, self-dependent. To achieve the desired result, framework combines a set of different modules, such as App reading device, TTS module and optical character recognition module. Android is an open source and Linux-based operating system targeted for mobile devices such as smart-phones and tablet computers. Applications are generally developed in Java programming language using the Android software development kit (SDK). If used correctly, the SDK, together with Eclipse (the officially supported IDE) and JDK (Java Development Kit) is capable to deliver modern software for Android devices.

3.1 Advantages of Proposed System

1. To evaluate accuracy of text to speech conversion.
2. Blind persons to recognize the hand held objects or products easy
3. We are using phone camera to cut down the expensive camera cost.

4 System Architecture



5 Implementation

5.1 Modules

- Optical Character Recognition
- TTS Module
- Audio module

5.2 Module Description

5.2.1 Optical Character Recognition

OCR is the mechanical or electronic conversion of images of typed, handwritten or printed text into machine-encoded text. It is a common method of digitizing printed text so that it can be used in machine process such as text-to-speech. OCR is optical character recognition module is the mechanical or electronic conversion of images of typed, handwritten or printed text into machine-encoded text. The input is given as text, using a finger device mounted camera which captures text and sends the input text to the OCR process where the extraction of text to speech is been done. From the captured input text is segmented as word by word detection thereby to read it as separate word. Boundary detection is done by detecting words which are fit inside the boundary, if not it eliminates the text which is unfit to read. The process of text extraction is carried out by matching with templates one by one and then forming a whole word. The mentioned line or a word will be read from the captured input text with a suitable coding. After matching with the templates and displays it as a text and reads it aurally. In this method a USB camera which captures the input given in text format and it is sent to OCR process which processes it as text and converts it into a speech form.

5.2.2 TTS Module

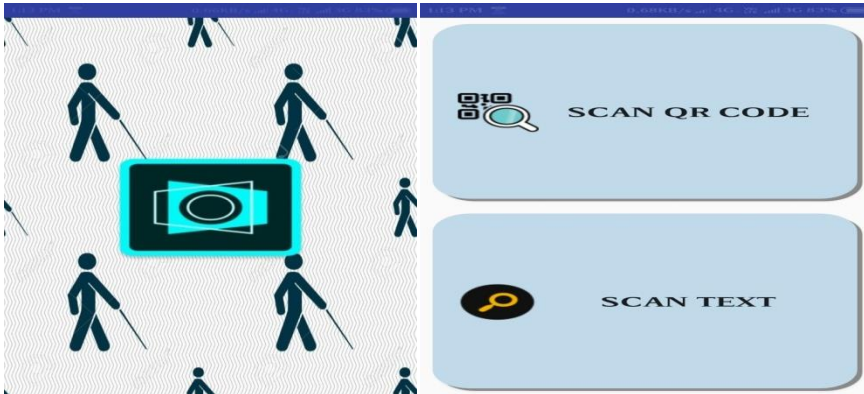
A text-to-speech (TTS) system converts normal text into speech other systems render symbolic linguistic representations like phonetic transcription into speech. A text-to-speech system is used to read each word as the user's finger passes over it, and distinctive audio and/or haptic cues can be used to signal other events, such as end of line, start of line etc. It is composed of two parts: a front-end and a back-end. The front-end has two major tasks. First, it converts raw text containing symbols like numbers and abbreviation into the equivalent of written-out words. This process is often called text normalization, pre-processing, or tokenization the front-end then assigns phonetic transcriptions to each word, and divides and marks the text into prosodic units, like phrases, clauses and sentences. The process of assigning phonetic transcription to words is called text-to phoneme or grapheme-to-phoneme conversion.

5.2.3 Audio Module

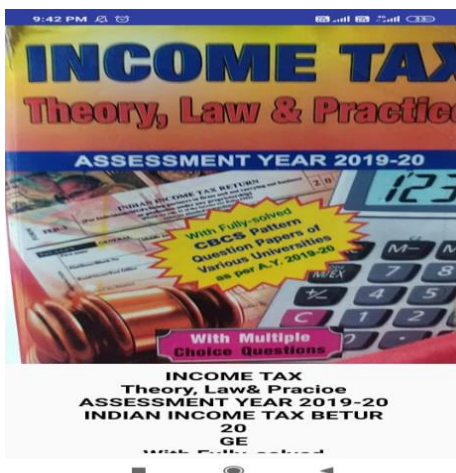
This module will get the extracted text as an input and it will read out the text using Text to Speech available in the mobile. If no text is recognized, then default audio output will be given. This will be done using SAPI libraries.

6 Output

The first left image is the next screen which is going to open after tapping on the application and the next right side image is the another screen which will asked to choose whether to scan a text or to scan a QR code.



Below are given some output where the application converted the text in speech which can be heard through headphone .



7 Conclusion

A text detection and recognition with speech output system was successfully demonstrated on Android platform. This system is very handy and useful for the visually challenged persons. Compared with a PC platform, the mobile platform is portable and more convenient to use. This system will be helpful for visually challenged persons to access information in written form and in the surrounding. It is useful to understand the written text messages direction in voice form by converting it from Text to voice. It is found that this system is capable of converting the sign boards and other text into speech.

References

- [1] 10 facts about blindness and visual impairment”, World Health Organization: Blindness and visual impairment,2009.
- [2] Advance Data Reports from the National Health Interview Survey, 2008. http://www.cdc.gov/nchs/nhis/nhis_ad.htm.
- [3] International Workshop on Camera-Based Document Analysis and Recognition (CBDAR 2005, 2007, 2009, 2011). <http://www.m.cs.osakafu-u.ac.jp/cbdar2011/>

- [4] X. Chen and A. L. Yuille, "Detecting and reading text in natural scenes," In CVPR, Vol. 2, pp. II-366 – II-373, 2004.
- [5] X. Chen, J. Yang, J. Zhang and A. Waibel, "Automatic detection and recognition of signs from natural scenes," In IEEE Transactions on image processing, Vol. 13, No. 1, pp. 87-99, 2004.
- [6] D. Dakopoulos and N. G. Bourbakis, "Wearable obstacle avoidance electronic travel aids for blind: a survey," In IEEE Transactions on systems, man, and cybernetics, Vol. 40, No. 1, pp. 25-35, 2010. [7] B. Epshtein, E. Ofek and Y. Wexler, "Detecting text in natural scenes with stroke width transform," In CVPR, pp. 2963-2970, 2010. [8] Y. Freund and R. Schapire, "Experiments with a new boosting algorithm," In Int. Conf. on Machine Learning, pp.148–156, 1996.
- [7] N. Giudice and G. Legge, Blind navigation and the role of technology, in The engineering handbook of smart technology for aging, disability, and independence, A.A. Helal, M. Mokhtari, and B. Abdulrazak, Editors. 2008, Wiley: Hoboken, N.J.

Farmer Trade Using Android Application

S. Manavalan¹ Associate Professor, M. Tech.,
J. Santhosh Kumar² Student, M. Srinivasan³ Student,
V. Tamil Selvan⁴ Student
Department of Computer Science Engineering
St. Anne's College Of Engineering And Technology

Abstract

Farmer Trade Application is an android application developed for farmers/seller's and retailers. This application gives support to the village farmers who want to use this facility and who want to learn how it is possible and how they can use - e-farming to sell their products. Which will help farmers from to sell their products to different cities through online. Farmers can use this facility and can learn how it is possible and how they can use e-farming to sell their products. They can know how they can open this site, register with it, and sell their products online etc.,

Keywords- Trade, Market Rates, e - Farming

1 Introduction

India is an agricultural country. About seventy percent of our population depends on agriculture. One-third of our National income comes from agriculture. The development of agriculture has much to do with the economic welfare of our country. Now our country is self-sufficient in food grains. In the upcoming years agriculture will see major changes. The vast majority of Indian farmers, which des small-scale producers are often unable to access the information and technological resources that could increase the yield and lead to better prices for their crops and products. This Android application for farmers who are using smartphones where they can get the real time updates about the seeds, fruit rates of every market in India and they will be able to sell their products at the proper rates. Our application will providing the feature where all the farming related notices from the government will be added and farmers will get a proper information about different schemes. Also adding feature of weather information which will help farmers to plan for next 2-3 days.

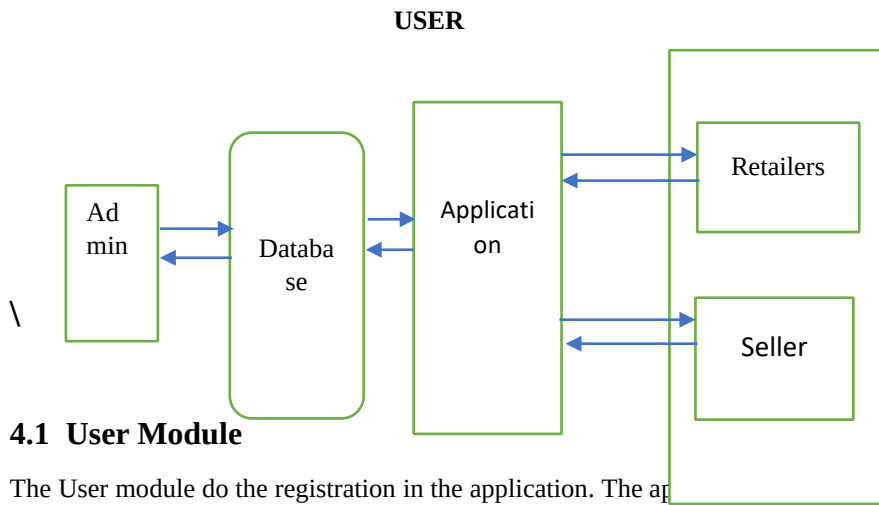
2 Existing system

Information and Communication Technology (ICT) in agriculture is an emerging field focusing on the enhancement of agricultural and rural development in India. It involves innovative applications using ICT in the rural domain. The advancement of can be utilized for providing accurate and timely relevant information and services to the farmers, thereby facilitating an environment for remunerative agriculture.

3 Proposed system

The farmers will derive greater benefit when they can make better decisions about where to sell their output after getting market prices for a variety of local and distant markets. One Stop Solution to all agricultural information needs. Location specific information delivery . Highly authentic and reliable database on agriculture.

4 Architecture



4.1 User Module

The User module do the registration in the application. The application provides details to the user that he wants to access. All the details of user will be stored into the database and it can be secured. Home Screen is the main page of this Application. this module shows some category options the user choice. By clicking someone option user get main page of that particular category which is easy to use by the user. Depending on the certain market conditions of current week and previous one or two week, our system will predict future rates. So it would be beneficial for farmers to sell their commodities at a particular time in a market.

5 Result

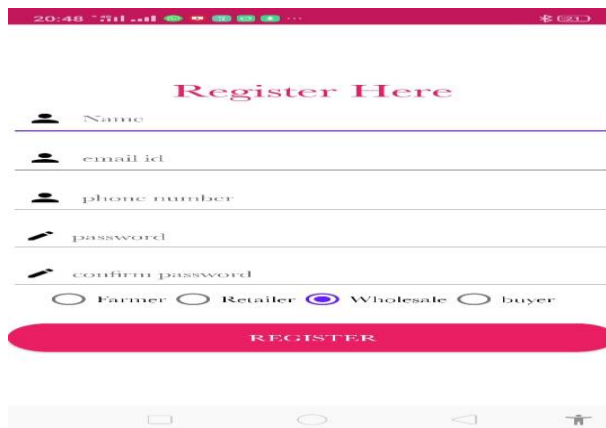


Figure 1: Register details



Figure 2: Login

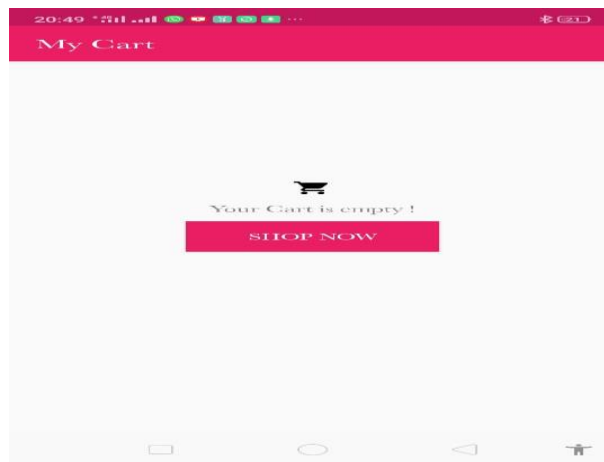


Figure 3: Cart details

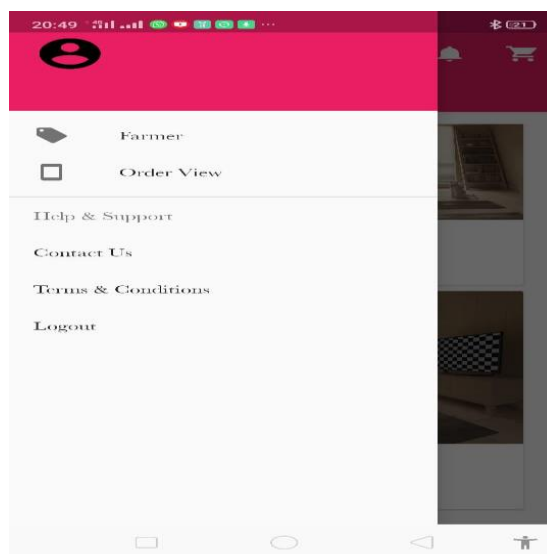


Figure 4: View Order details

Home screen

Home Screen is the main page of this Application. this module shows some category options to the user to their choice. By clicking someone option user get main page of that particular category which is easy to use by the user. It shows three type option.

Market rates

Market price is important module of this application. it shows the entire Vegetables and fruits price list that are available in the market. The vegetable price is updated by APMC. The price of vegetable is periodically updated by the admin or head of local market members.

Government schemes

Government of India will launch different Programs which are beneficial to Farmers but drawback of poor performance of this program are they are not able to reach every person and not able to give proper information so here we provide detailed information and Process of different programs.

Prediction

Depending on the certain market conditions of current week and previous one or two week, our system will predict future rates. So it would be beneficial for farmers to sell their commodities at a particular time in a market.

7 Conclusion

We have exhibited E-Business in Agriculture for effective communication between Merchants and Farmers for providing more help to all farmers and to stop black marketing. This project will be helpful for farmers to know more about market information. The site will guide the farmers in all the aspects, the current market rate of different products and the earned profit for the sold products, access to the new farming techniques through E-learning and centralized approach to view different government's agriculture schemes including the compensation schemes for farming. The main approach of this project is to prohibit the black marketing of the granary products. The government authorize person has easy see the whole transactions between the farmer and the merchant.

References

- [1] Krishi Ville-Android based solution for Indian agriculture. Authors-Manav Singhal Kshitij Verma, Anupam Shukla. ABV-Indian Inst. of Inf. Technol. & Manage., Gwalior, India. Advanced Networks and Telecommunication Systems (ANTS), 2011. IEEE fifth International Conference on Digital Object symbol ten.1109/ANTS.2011.636865. Publication Year: 2011.
- [2] Shakeel-Ul-Rehman, M. Selvaraj and M. Syed Ibrahim "Indian Agricultural Marketing- A Review", Asian Journal of Agriculture and Rural Development, 2012 Vol. 2, No.1, pp.no. 69-75
- [3] 3. Xiaolan Fu and Shaheen Akter, 'Impact of Mobile Telephone on the Quality and Speed of Agricultural Extension Services Delivery: Evidence from the Rural e-services Project in India' International Conference on Agriculture social scientist, 2012, issue no 2, pp.no. 1-32
- [4] Saurabha A, Ghogare, Priyanka M Monga 2015 'E Agriculture Introduction and Figuration of its Application' International Journal of Advanced Research in Computer Science and Software Engineering, 2006, vol 5, issue no 1, pp.no. 44-47. 2012
- [5] A Modern Farming Techniques using Android Application (International Journal of Innovative Research in Science, Engineering and Technology oct 2015) Santosh G. Karkhile, Sudarshan G. Ghuge B.E. Information Technology, M.I.T. Academy of Engineering, Alandi, Maharashtra.
- [6] Mahafarm (International Journal of Research in Advent Technology, E-ISSN: 2321-9637 april 2014) Aniket Bhavne, Rahul Joshi, Ryan Fernandes KJ Somaiya Institute of Engineering & Information Technology, Mumbai, India

The Impact of Big Data Analytics in Information Technology Sector

M. K. Ganeshan, Ph.D Research Scholar,

Alagappa Institute of Management, School of Management, Alagappa University, Karaikudi – 630 003, Sivagangai District, Tamil Nadu, India. Mobile: +919679523438, E-mail: mkganeshanmba@gmail.com

Abstract

Big Data is the present day, the newest buzzword around, and with the quantity of data being generated every minute by clients, and businesses universal, there is enormous value to be found in Big Data analytics. Companies are starting to realize the importance of data accessibility in bulky amounts in order to make the right decisions and sustain their strategies. With the enlargement of new technologies, the Internet and social networks, the making of digital data is continuously growing. The word "Big Data" refers to the assorted mass of digital data formed by companies and individuals whose characteristics as large volumes, unusual forms, speed of dispensation requiring particular and increasingly complicated computer storage and analysis tools. Internet data requirement per day 1 PB Facebook data per day, 500 M tweets per day (200 B tweets/ year), and Google processes 24 PB day. In this studies collected as secondary data only. This article intends to describe the concept of big data analytics; tools, information technology, futures, applications, as well as the importance of big data analytics. Visual data information innovation tools will be growing 2.5 times faster than take it easy of the Business Intelligence marketplace. This investing in this enabler of end user identity service will turn into a necessity for all organization and industry. The useful of latest digital technologies of big data like social media, smart city, transportation, the hospital for checkup patient, live road mapping for autonomous vehicle, discovering consumer shopping habit, and space researcher.

Keywords: *Information, Internet, Security, Storage and Software*

1 Introduction

The word "big data" was first used to pass on to increasing data volumes in the mid-1990s. In 2001, Doug Laney, then an analyst at consultancy Meta Group Incorporation stretched the meaning of big data. This extension described the increasing volume of data being stored and used by organizations, the variety of data being generated by organizations, and velocity, or speed, in which that data was being formed and modernized. Those three factors became recognized as the 3 Vs of big data. Gartner popularized this model after acquiring Meta Group and hiring Laney in 2005. Additional major development in the past of big data was the initiate of the Hadoop distributed processing framework. Hadoop was introduced and presented as an Apache open source project in 2006. This planted the seeds for a clustered proposal built on top of product hardware and that could run big data applications. The Hadoop framework of software tools is commonly used for organization big data. By 2011, big data analytics began to take a rigid hold in organizations and the public eye, subsequently with Hadoop and various related big data technologies. Initially, as the Hadoop network took form and in progress to established, big data applications were generally used by large internet and e-commerce companies like Yahoo, Google, and Facebook, as well as for analytics and marketing services providers. Newly, a broader diversity of users has embraced big data analytics as a key technology driving digital transformation. Most utility consumers are retailers, financial services firms, insurers, healthcare organizations, manufacturers, energy companies, and other enterprises.

The digital data produced is partly the result of the use of devices connected to the Internet. Therefore, smartphones, tablets, and computers transmit data about their users. Connected smart objects convey information about consumers' use of everyday objects. Apart from the connected devices, data come from a wide range of sources: demographic data, climate data, scientific and medical data, energy consumption data, etc. All these data consist of information about the place of users and their devices, their journey, their benefit, their utilization habits, their spare time activities, and their projects, etc. But also information on how the infrastructure, machinery, and apparatus are used. In the company of the rising digit of Internet and mobile phone utilize persons; the size of digital data is increasing quickly.

2 Objective of the Study

To study recent technology and work areas of big data analytics.

The importance of big data analytics in human and information.

The main role of big data in information technology.

To study the future of big data analytics in information technology.

3 Big Data Analytics

Big data analytics is the regularly complicated process of investigative big data. It also uncovers information such as hidden patterns, correlations, market trends, and customer preferences. It can help the industry make knowledgeable business decisions and supports. On a large scale, data analytics technologies and techniques give industries a way to analyze data sets and collect new information. Business intelligence queries answer fundamental questions about business operations and performance. Big data analytics is an outline of advanced technology analytics, which involves complex applications with elements such as predictive models, statistical algorithms, and analysis powered by analytics systems or information.

Table 1 TYPE OF BIG DATA

| Different Types of Data | |
|---|----------------------------|
| Structured data (Relational, Tables) | Typical Operations: |
| Semi Structured Data (XML, JSON, Log files) | Aggregation & Statistics |
| Unstructured Data (Free Text, WebPages) | Data warehouse, OLAP |
| Graph Data (Social Network, Semantic Web) | Index, Searching, Querying |
| Streaming Data Typical Operations | Keyword bases search |
| Graph Data (Social Network, Semantic Web) | Pattern matching |
| Streaming Data | Knowledge discovery |
| Data Mining | Statistical Modeling |

Big Data normally refers to data that exceeds the distinctive storage, processing, and computing capability of predictable databases and data analysis techniques. As a store, Big Data requires tools and methods that can be practical to investigate and take out patterns from large-scale data. The study of structured data participated due to the diversity and velocity of the data handle or control. Therefore, it is no longer sufficient to analyze data and create reports, the extensive variety of data way that the systems in place must be capable of supporting in the analysis of data. The analysis consists of automatically determining, within a variety of rapidly changing data, the correlations between the data in order to help in the exploitation. Big Data is definite as data that is enormous and massive in size. Big data is a word used to explain a collection of data that is vast in size and yet growing exponentially with occasion or time. Big Data analytics examples contain stock exchanges, social media sites, jet engines, etc.

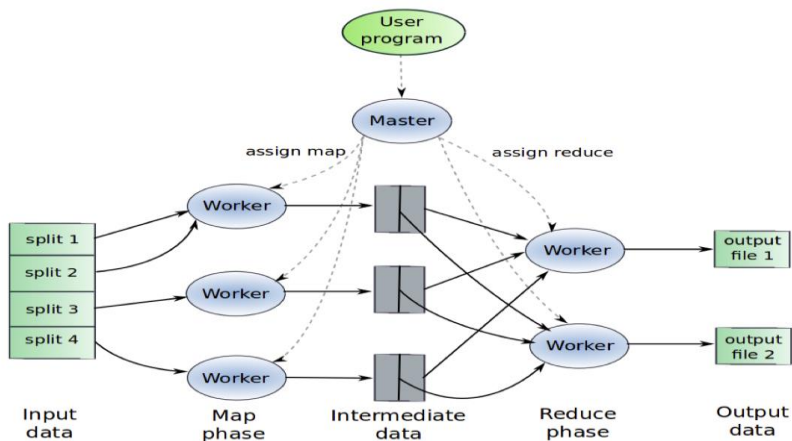


Figure 1 Big data work

3.1 Information Technology

One of the largest users of Big Data, information technology companies around the world are using Big Data to optimize their performance, improve employee output, and reduce risks in business activity, and operations. In the combination of Big Data technologies with machine learning and artificial intelligence, the information technology sector is frequently powering innovation to discover solutions still for the most difficult of problems.

3.2 Future of Big Data

Data volumes will continue to increase and transfer to cloud technology. Most of big data experts have the same opinion that the amount of generated or created data will be growing regularly and exponentially in the future aspect. In Data Age 2025 information for Seagate, IDC prediction the global datasphere will get to 175 zettabytes by 2025.

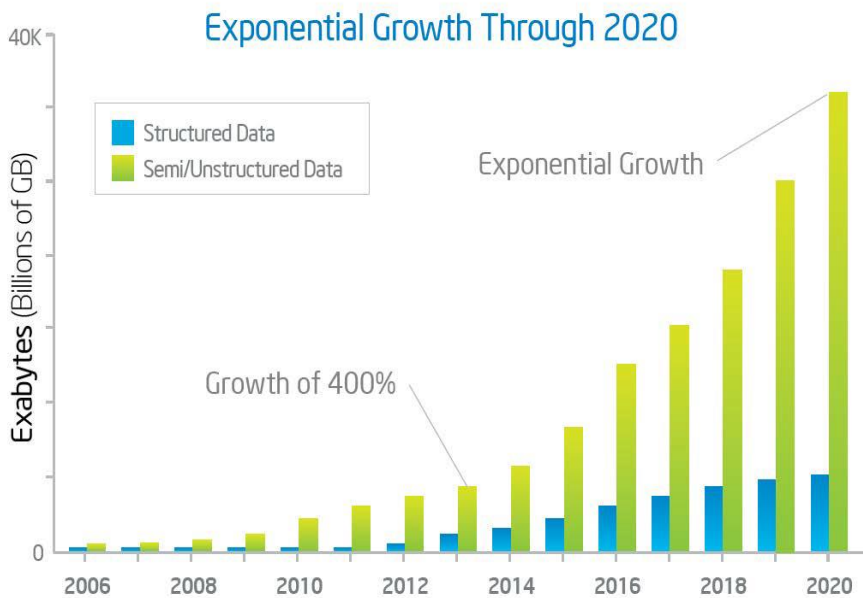


Figure 2 Growth of big data

Every minute of every day big data we used some of points given below

- ❖ More than 204 million email messages.
- ❖ Over 2 million Google search queries.
- ❖ 48 hours of new YouTube videos.
- ❖ 6, 84,000 bits of content shared on Facebook.
- ❖ More than 100,000 tweets.
- ❖ \$ 272, 000 spend on e-commerce

3.3 Importance of Big Data Analytics

The information technology industry can use big data analytics systems and software to make data-driven decisions that can better business-related output and solutions. The advantage may include a more successful promotion, innovative revenue opportunities, client personalization, and better operational competence. In the company of a valuable tactic, these benefits can provide spirited advantages over rivals.

Table 2 Business Intelligence and Advanced Analytics

| Business Intelligence VS Advanced Analytics | | |
|---|--|--|
| Business Intelligence | | Advanced Analytics |
| Answers the questions | <ul style="list-style-type: none"> ▪ What happened? ▪ When? ▪ Who? ▪ How many? | <ul style="list-style-type: none"> ▪ Why did it happen? ▪ Will it happen again? ▪ What will happen if we change? ▪ What else does the data tell us that we never thought to ask? |

| | | |
|----------|--|--|
| Includes | <ul style="list-style-type: none"> ▪ Reporting (KPIs, Metrics) ▪ Automated Monitoring and Alerting(thresholds) ▪ Dashboards ▪ Scorecards ▪ OLAP(cubes, slice, and dice, drilling) ▪ Ad hoc query ▪ Operational and Real time business Intelligence | <ul style="list-style-type: none"> ▪ Statistical or Quantitative Analysis ▪ Data Mining ▪ Predictive Modeling ▪ Multivariate Testing ▪ Big Data Analytics ▪ Text analytics |
|----------|--|--|

3.4 Big Data Analytics Applications

Big data analytics applications frequently incorporate information from both inside frameworks and outer sources, for example, climate data information or segment information on shoppers gathered by outsider data administrations suppliers. Also, streaming examination applications are getting normal in large information conditions as clients hope to perform an ongoing investigation on information taken care of into Hadoop frameworks through stream preparing engine, like Spark, Flink, and Storm.

Early big data practices were generally sent on-premises, especially in huge associations that gathered coordinated and examined gigantic measures of information. Yet, cloud stage suppliers like Amazon Web Services (AWS) and Microsoft, have made it simpler to set up and oversee Hadoop groups in the cloud. The equivalent goes for Hadoop providers like Cloudera-Hortonworks, which underpins the dispersion of the huge information structure on the AWS and Microsoft Azure mists. Clients would now be able to turn up bunches in the cloud, run them however long they need and afterward take them disconnected with use-based evaluating that does not need continuous programming licenses. Big data has gotten progressively useful in the store network. Big supply chain analytics uses large information and quantitative techniques to upgrade dynamic cycles across the production network. In particular, big supply chain analytics extends informational collections for the expanded investigation that goes past the customary interior information found on big Enterprise Resource Planning (ERP) and Supply Chain Management (SCM) frameworks. Additionally, large production network investigation actualizes profoundly successful factual techniques on new and existing data information sources.

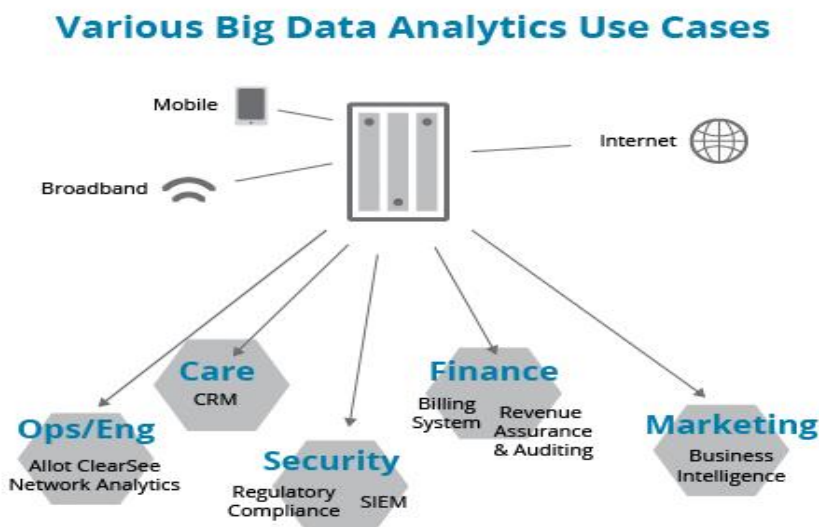


Figure 3 Big Data Analytics use

4 Conclusion

Big data refers to the set of statistical data created by the use of new technologies for personal or professional purposes. Big Data analytics is the process of examining these data in order to uncover hidden patterns, market trends, customer preferences, and other useful information in order to make the right decisions. Big Data Analytics is a fast-growing technology. It has been received by the most unforeseen ventures and turned into an industry all alone. But analysis of these data in the framework of Big Data is a process that seems sometimes quite intrusive. Analytics is data science. Business Intelligence takes care of the decision-making part while Data Analytics is the process of asking questions. Analytics tools are used when a company needs to do forecasting and wants to know what will happen in the future, while Business Intelligence tools help to transform those forecasts into common language. More often, Big Data is considered the successor to Business Intelligence. This comparison will be discussed in future work.

Acknowledgement

The Author M. K. Ganeshan, Ph.D Research Scholar, Alagappa Institute of Management, School of Management, Alagappa University, Karaikudi has greatly acknowledged under RUSA Phase 2.0 Scheme.

References

- [1] Acharjya D P, Kauset Ahmed P (2016), A Survey on Big Data Analytics: Challenges, Open Research Issues and Tools, International Journal of Advanced Computer Science Applications, Vol. 7, No. 2, PP.511-518.
- [2] Kevin Taylor (2016), Big Data: Understanding Big Data.
https://www.researchgate.net/publication/291229189Big_Data_Understanding_Big_Data
- [3] Yousra Riahi, Sara Riahi (2018), Big Data and Big Data Analytics: Concepts, Types and Technologies International Journal of Research and Engineering ISSN: 2348-7860 (O), 2348-7852 (P), Vol. 5 No. 9, September-October 2018, PP. 524-528
- [4] https://www.sas.com/en_us/insights/analytics/big-data-analytics.html
- [5] <https://www.simplilearn.com/what-is-big-data-analytics-article>
- [6] <https://www.guru99.com/big-data-analytics-tools.html>
- [7] www.webopedia.com/definitions/big-data-analytics
- [8] <https://www.slideshare.net/technakama/big-data-analytics-in-information-technology-132476532>
- [9] <https://www.datamation.com/big-data/what-is-big-data-analytics/>

Performance of a Knight Tour Parallel algorithm on Multi-core system Using OpenMP

Dr. Vidyaathulasiraman¹, S. Vijayakumar²

¹ Department of Computer Science, Government Arts & Science College (W), Bargur.

² PhD Scholar, MCA Department, Priyadarshini Engineering College, Vaniyambadi.

Abstract

Today's computers, desktops and laptops were build with multi-core architecture. Developing and running serial programs in this multi-core architecture fritters away the resources and time. Parallel programming is the only solution for proper utilization of resources available in the modern computers. The major challenge in the multi-core environment is the designing of parallel algorithm and performance analysis. This paper describes the design and performance analysis of parallel algorithm by taking the Knight Tour problem as an example using OpenMP interface. Comparison has been made with performance of serial and parallel algorithm. The comparison shows that the proposed parallel algorithm achieves good performance compared to serial algorithm.

Keywords: *Knight-Tour problem, Parallel algorithms, Multi-core Architecture, OpenMP, Performance analysis.*

1 Introduction

In a Multi-core architecture, there is more than one processor inside a single chip. This technology opens a way for parallel programming where several parts of a program are being executed in parallel [2], [3]. Multithreading is the technique used for achieving this parallelism. OpenMP is an Application Programming Interface (API) which impements multithreading where master thread forks a specified number of slave threads, each thread executes a parallelized section of code independently[7]. According to the Flynn's Taxonomy computer architecture can Classified into two categories: instruction level and data level. Sequential Computing is inefficient in multi-core environment[4].

2 Related Work

In the multi-core technology, parallel algorithms improves the performance of the applications [7]. To show the performance improvement in the multi-core architecture, parallel processing is implemented in a Knight Tour problem. To show the high performance in the application, first the sequential program has been developed with the partitions without backtracking and the same program has been implemented in a parallel program environment [1], [7]. This unique approach is to find the performance of Knight Tour problem on Multi-core system using OpenMP programming technique.

3 Overview of Proposed Work

3.1 Knight Tour Problem

In the chess game, the knight can jump in a special manner. Knight canmove eithertwo squares horizontally and one square vertically or two squares vertically and one square horizontallyineachdirection,SothecompletemovementlooklikeEnglishletter'L'asshowninis figure 3.1

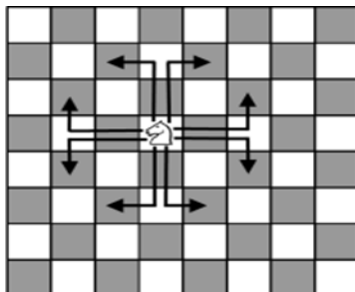


Figure 3.1 8X8 Chessboard shows the possible moves

In this problem, there is an empty chessboard, and the knight starts from any location in the board and it has to reach the given goal state [1], [6]. For our convenience the 8X8 chessboard is numbered as shown in the figure 3.2

| | | | | | | | |
|----|----|----|----|----|----|----|----|
| 0 | 1 | 2 | 3 | 4 | 5 | 6 | 7 |
| 8 | 9 | 10 | 11 | 12 | 13 | 14 | 15 |
| 16 | 17 | 18 | 19 | 20 | 21 | 22 | 23 |
| 24 | 25 | 26 | 27 | 28 | 29 | 30 | 31 |
| 32 | 33 | 34 | 35 | 36 | 37 | 38 | 39 |
| 40 | 41 | 42 | 43 | 44 | 45 | 46 | 47 |
| 48 | 49 | 50 | 51 | 52 | 53 | 54 | 55 |
| 56 | 57 | 58 | 59 | 60 | 61 | 62 | 63 |

Figure 3.2 8X8 Chessboard each square numbered from 0 to 63.

Given a start state S and a goal state G, the knight has to start from S and reaches G with legal moves [1]. Many algorithms were developed using graph approach with backtracking. In this paper a sequential and Parallel algorithm has been developed and the comparison is made to show the minimization of time in the parallel approach.

3.2 Eight Possible Moves of a Knight

From the figure 3.1 eight possible moves are shown

Move1: row=row-1 column=column+2

Move2: row=row-2 column =column+1

Move3: row=row-1 column =column-2

Move4: row=row-2 column =column-1

Move5: row=row+1 column =column+2

Move6: row=row+2 column =column+1

Move7: row=row+1 column =column-2

Move8: row=row+2 column =column-1

In the above 8 possible moves from the start state S some of the moves may be possible and the some of the moves may be not possible. For example, from the square 1 only 4 moves are possible. ie move1, move5, move6 and move8 are possible moves from square 1 as shown in the figure 3.3

| | | | | | | | |
|----|----|----|----|----|----|----|----|
| 0 | 1 | 2 | 3 | 4 | 5 | 6 | 7 |
| 8 | 9 | 10 | 11 | 12 | 13 | 14 | 15 |
| 16 | 17 | 18 | 19 | 20 | 21 | 22 | 23 |
| 24 | 25 | 26 | 27 | 28 | 29 | 30 | 31 |
| 32 | 33 | 34 | 35 | 36 | 37 | 38 | 39 |
| 40 | 41 | 42 | 43 | 44 | 45 | 46 | 47 |
| 48 | 49 | 50 | 51 | 52 | 53 | 54 | 55 |
| 56 | 57 | 58 | 59 | 60 | 61 | 62 | 63 |

Figure 3.3 All possible moves of square 1.

4 Proposed Parallel Approach Algorithm

The parallel portion of this algorithm is implemented in the eight function calls from any state with eight possible legal moves.

Algorithm Parallel_Knighttour()

Step 1. Initialize nxn dimension array as shown in Figure 1.2, n, s, g and visited[]

//s startstate & g goal state. Visited[] is an array to store the visited state

Step 2. Store S in visited[]

Step 2. Find the (r,c) value for S

Step 3. Call move(int r, int c)

Step 4. **move(r,c) calls the 8 possible moves from which gives p1, p2, p3, p4, p5, p6, p7, p8 in parallel**

For a valid move, $p_i >= 0$ otherwise $p_i = -1$, $1 <= i <= 8$

Step 5. If $g == p1$ or $g == p2$ or $g == p3$ or $g == p4$ or $g == p5$ or $g == p6$ or $g == p7$ or $g == p8$ then

Print("Goal Reached")

Print the elements in visited[]. Step 6. Goto step 16.

Step 7. Else

Step 8. If $p1 >= 0$ //valid move Store p1 in visited[] s=p1

goto step 2

Step 9. else

If $p2 >= 0$ //valid move Store p2 in visited[] s=p2

goto step 2

Step 10. else

If $p3 >= 0$ //valid move Store p3 in visited[] s=p3

goto step 2

Step 11. else

If $p4 >= 0$ //valid move Store p4 in visited[] s=p4

goto step 2

Step 12. else

If $p5 >= 0$ //valid move Store p5 in visited[] s=p5

goto step 2

Step 13. else

If $p6 >= 0$ //valid move Store p6 in visited[] s=p6

goto step 2

Step 14. else

If $p7 >= 0$ //valid move

Store p7 in visited[]

s=p7

goto step 2

Step 15. else

If $p8 >= 0$ //valid move

Store p8 in visited[] s=p8

goto step 2

step 16. End Parallel_Knighttour()

5 Experimental Results

The same start state and goal state were tested in sequential and parallel programs. The programs were executed on Intel® Core(TM) i3-5005U CPU @2.00GHz (4 CPUs) machine using Code block software and gcc compiler with windows10 operating system. Table 5.1 shows that time taken for serial and parallel algorithms with a given Start state and Goal State. It also shows the Number of intermediate state and the speedup. The chart shows the time taken for each algorithm

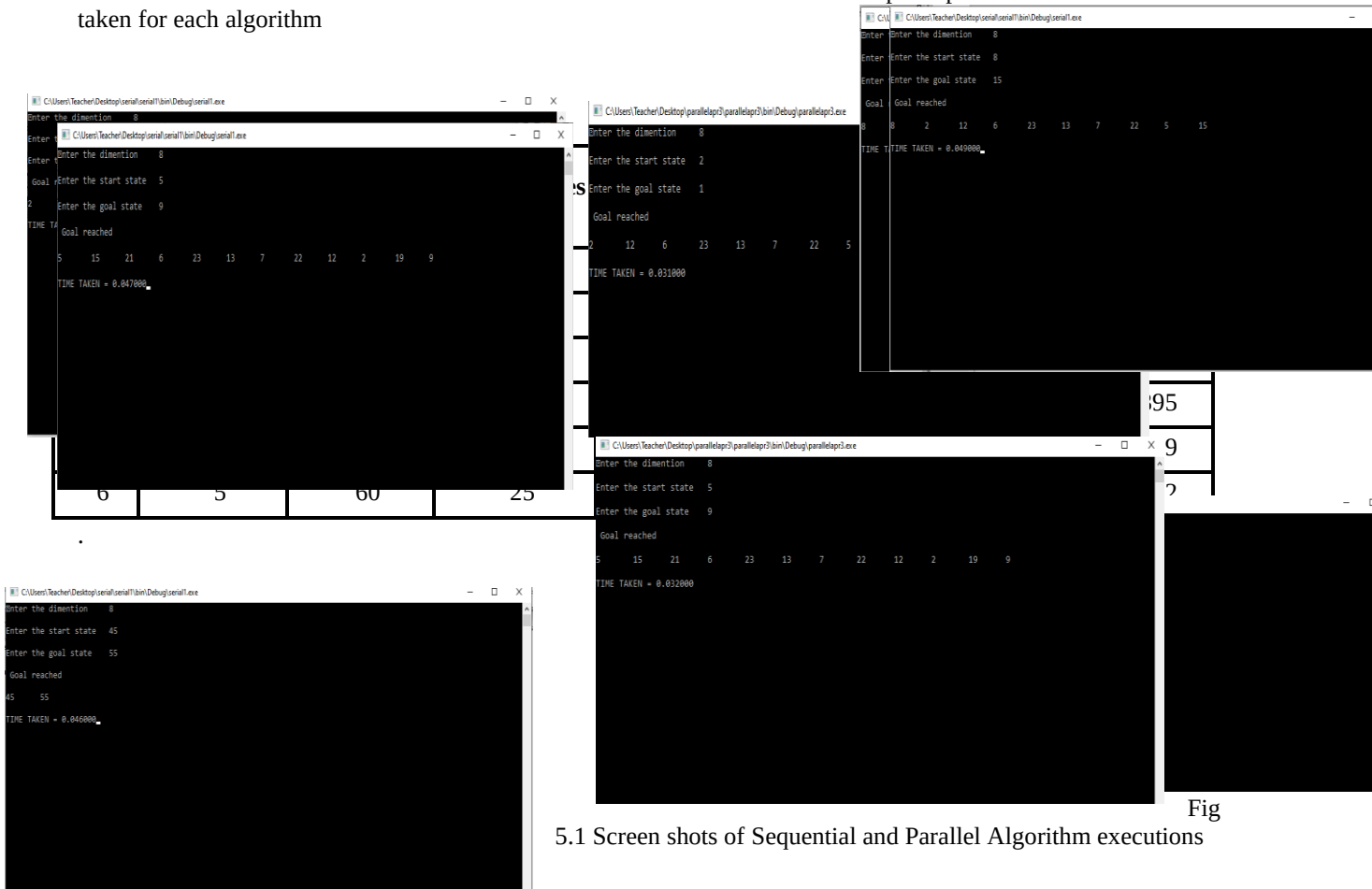


Fig 5.1 Screen shots of Sequential and Parallel Algorithm executions

Table 5.1 Serial & Parallel execution time and their speedup

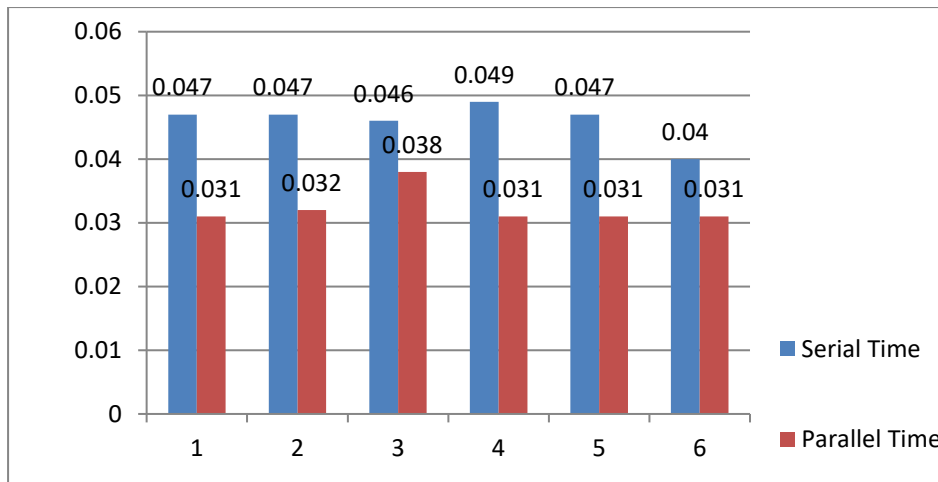


Fig 5.2 Execution time of serial and Parallel Algorithm of Knight Tour

The result shows that the parallel algorithm is efficient than the Sequential algorithm.

6 Conclusion and Future enhancement.

In the multi-core PC or Laptop developing serial program does not utilize the resources' available. Parallel programming platform like OpenMP will utilize the recourses' in Multi-core systems, so that we can increase the performance. The results of Knight tour problem proves this concept. In future if we use parallel programming platforms in multi-core system like Real-time computing, data Analytics, games, we can increase the performance of the program.

References

- [1] George F, Artificial intelligence structures and strategies for complex problems solving, IV Edition, Pearson Education 2007.
- [2] Najem N. Sirhan , Sami I. Serhan "MULTI-CORE PROCESSORS: CONCEPTS AND IMPLEMENTATIONS" International Journal of Computer Science & Information Technology (IJCSIT) Vol 10, No 1, February 2018.
- [3] Musaev Muhammadjon Mahmudovich and Berdanov Ulug'bek Abdumurodovich "The Technology of Parallel Processing on Multicore Processors" International Journal of Signal Processing Systems Vol. 4, No. 3, June 2016.
- [4] Balaji Venu "Multi-core processors - An overview" https://www.researchgate.net/publication/51945986_Multi-core_processors October 2011
- [5] Norma Alias and Md. Rajibul Islam, "A Review of the Parallel Algorithms for Solving Multi dimensional PDE Problems", Journal of Applied Sciences 10(19) pp2187-2197, 2010.
- [6] Mohd Muzafar Ismail, Ezreen Farina Shair "A Preliminary Study on Solving Knight's Tour Problem Using Binary Magnetic Optimization Algorithm", Science & Engineering Technology National Conference 2013
- [7] Sanjay Kumar Sharma, Dr. Kusum Gupta "Performance Analysis of Parallel Algorithms on Multi-core System using OpenMP" International Journal of Computer Science, Engineering and Information Technology (IJCEIT), Vol.2, No.5, October 2012.

A Blockchain-enabled Paradigm to Share Electronic Health Records using IPFS

Sagar Lachure, Dr. Ashish Tiwari

Abstract

The next important asset for patients is precise, complete, & up to date medical data. In medical services, the protection of privacy and the firm storage of medical data remain critical issues. For the general population, safe-storage and the extensive use of individual medicinal reports have always been an issue. The resurgence of blockchain-technology created a great opinion to tackle this issue. Blockchain-technology can be applied to securely accumulate individual therapeutic data as a hash-chain including the features of decentralization, verification, and permanent. In this paper, a blockchain-enabled EHR(Electronic Health Records) system was developed to ensure reliable, practical, and interoperable access by all the actor's patients, doctors, and third-party to therapeutic documents while conserving the secrecy of the data of the sensible sufferer. To store records that have the advantage of being distributed, we ought to use IPFS(interplanetary file system) to achieve record immutability. The suggested model also preserves the disease statistics without breaching any patient's privacy.

Keywords: *Blockchain, EHR, IPFS, security.*

1 Introduction

More than 75 percent of hospitals in the USA implemented basic electronic health record systems in 2014[6]. While many hospitals in developed countries yet lack the amenities needed to switch to an Electronic Health Record system, EHR enactment becomes spreading globally. However, while it reaches anonymity, assurance, and ease-of-use, conventional EHR practices hold several issues. The records are fully managed by the record-making hospitals. If some hospital doesn't have appropriate safety standards in-place, these documents can be misused. There remains a significant need for accord within the documents that are produced plus processed. The reports held at one hospital may not be available to the doctors of another hospital or maybe incomprehensible. This happens mainly because various hospitals use various vendors to develop their EHR software systems. Numerous ransomware initiatives within which hackers place malware on the computers of medical-associations have recently occurred.

They render the information unavailable and only release it after their conditions have been fulfilled. Incidents [7] at Howard-University-Hospital in Washington have shown that within the area of e-Health documents, appropriate data protection measures are needed. One of the hospital medical practitioners was replenished with infringing the HIPAA (Health Insurance Portability & Transparency Act) on May 14, 2013, as she sold details about private patients. In a separate event in the corresponding case, a contractor stored almost 34000 medical records on his laptop at the hospital. National eHealth Authority(NeHA)[8] is a recommended institution in India that seeks to create certain rules inside the domain of e-Health care. That is given to assure uniformity of e-Health records that, while ensuring privacy, will enable safe access to these records. For this very reason, the model suggested in this paper may be used. We have placed the principles of cryptography, blockchain, and IPFS to use to provide perfect secrecy and protection. Blockchain is a perpetual arrangement of records that remain deposited in blocks that are connected to the previous block for each block. All transactions waged among the accounts, including within a user & a smart-contract account, are collected inside a block in Blockchain. After they have been processed into a block, those transactions imply public and perpetual. That everybody can see who the smart contract has accessed. The Ethereum blockchain is used by us because that helps us to utilize smart-contracts. We practice a permitted variant where miners comprise the chosen participant's node. The entire record data is kept to the network-nodes that are components of IPFS (InterPlanetary File System) and on the blockchain.

2 Literature Survey

There have been many attempts to use blockchain as a technology for remotely storing health reports. The author [3] adopts the Ethereum-blockchain platform to provide patients, clinicians, and other third parties with safe, interoperable, & effective access to medicinal reports, protecting the privacy of confidential patient information. A decentralized report administration system for managing EHR's is Medrec[5]. On a blockchain, it stores a record signature and appraises the sufferer, which is essentially in-charge of where the report will go. That mark ensures that the record is obtained from an unaltered copy. This platform shifts constrain of the provider to the sufferer, and as consequence, both difficulties and prompts the patient to catch over authority. In the healthcare industry, Pokitdok[2] continues its blockchain called dok-chain, which contains both monetary as

well as clinical data. In a case-study of distributed decision-making for foreign treatment, Quick Healthcare Interoperability Tools Chain [4] illustrates a decentralized app employing digital health-identities to validate individuals. This illustrates the facts of patients attending the office of several different care providers over their lifetime. By consolidating blockchain and smart contract technology, a shared automated health reports searchable scheme was suggested via [1].

3 System Architecture

We define the system structure of our system quickly in this segment. The framework primarily involves five individuals, as shown in Figure 1, patient, doctor, Third party (data-requester), blockchain, & IPFS network. Potential synergies among various individuals are shown in Figure 1. The duties of each person in the system and their relationships are discussed below.

3.1 Functions of various object

Patient: The patient is also an owner of data or data-user, assuming that the hospital registers a patient to see a doctor. The hospital's server produces a patient certificate furthermore reverts it to the patient. At that time, toward the doctor's service registration list, the server stores. He would send the doctor a document to produce his personal medical history and see his historical health account when a patient goes to the doctor.

Doctor: After receiving the patient's permission, the doctor is accountable for producing a therapeutic report for the patient & extracting a list of keywords for the patient's medical information. A doctor is believed to be trustworthy in the scheme and not to cooperate with the third party (data-requester) to access the medical reports of patients for illicit gain. Besides, the patient & doctor negotiate an access-policy to encrypt the therapeutic report and the keyword to produce the ciphertext, to securely store interoperable data. The ciphertext consists of, one being the ciphertext of the therapeutic history of patients placed on the IPFS, and the other part being the keyword ciphertext stored on the smart contract.

Third-party: The data-requester is the owner, like a clinical research Institute, a medical insurance company, a family member of patients, etc., who is able to obtain suitable information since their characteristics comply with an appropriate access-policy.

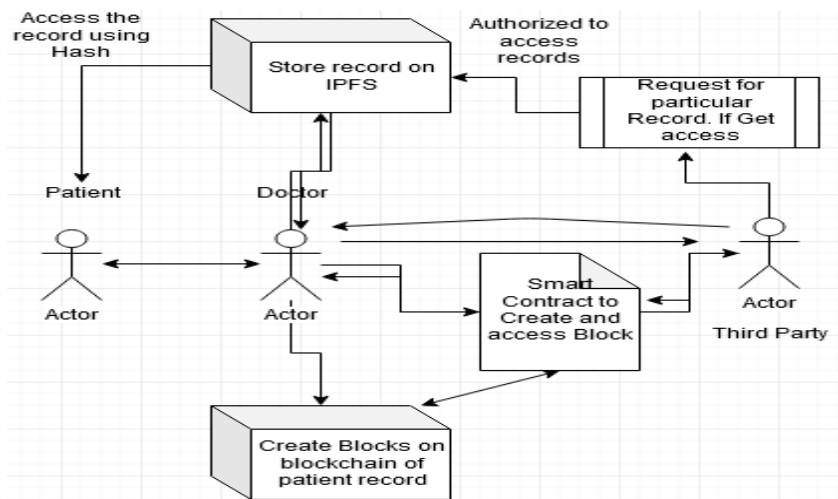


Figure 1: System model of proposed system.

Blockchain: Blockchain system is the cornerstone of this article, and without relying on central authorities, it executes smart-contracts in a shared manner, which remains crucial to ensure the secured storage and exchange of electronic health records. We adopt the Ethereum-blockchain to enhance device performance.

IPFS: The IPFS holds the doctor's encrypted ciphertext of the patient's therapeutic details furthermore delivers the corresponding hash-value to the doctor, where the hash value refers to the file address. If the address is obtained, the ciphertext according to the address can be downloaded by the approved data requester.

3.2 Working of proposed system model

Figure.1 shows overall working of our system model. Below we briefly analyze and divide the whole work into three phases.

Phase-1 (Contact Creation and Health reports generation)

- 1.The patient get an appointment of a doctor and visit to a hospital where his medical data generated by doctor.
- 2.The doctor employ smart-contract on a blockchain, medical report ,and blockchain saves message verified data.
3. With some pre define policy to available the record to patient, doctor encrypt the health record and upload it to IPFS.
4. IPFS in turn provide the location of health records to the doctor.

Phase-2 (Health reports storage)

1. Then doctor encrypt this reports location, load that ciphertext along with trx (transactions) and wait for validation of a block in blockchain.
2. Once validated, doctor captures the trx address.
3. Again doctor saves the trx address in to the smart-contract.
- 4.the third party request for a particular record to the doctor, after that doctor verify and add to the list of authorised users corresponding to smart-contract.
- 5.In the whole process doctor is the key generator who then share this key with third party though safe gateway.

Phase-3 (Sharing File)

1. Third party goes through a smart contact which through the attribute as a token.
2. The smart-contract verify the third party, and if it's there in user then smart-contract return the particular results to third party.
- 3.Third-party reads the transaction from the blockchain and got the file location.
4. Thus third party got the file location and then download the medical records from ipfs which are encrypted.
5. Finally if third party understand that his attributes, satisfy the access method of ciphertext , and if it satisfies then decrypt and get the health reports.

4 Results and Discussion

This structure makes therapeutic reports and management more operational and ensures that the requirements and benefits of patients are centered. There holds an agreement of efficient remedial reports with the use of our framework that can be easily imparted to the system through the instrument of the cipher key. Thusly, patient's medicinal reports may endure in diverse frameworks like hospital-EHRs, persistent-applications, drug-stores, etc. Blockchain could provide those distinct applications to gives and take the restorative data of a patient and, consequently, reflect a sole origin of truth. Information security is another benefit. To approve transactions, Blockchain uses current cryptographic tools, and that could combine a crucial dimension of trust in the distribution of information that blockchain commissions. The principal obligation of the current paradigm unites issues of interoperability and availability that have been used effectively via the blockchain. To conclude, the paradigm toward decentralization in an electronic medicinal report was gone and this was accomplished by the ethereum blockchain guide, recognizable accomplishment was security, that is very correspondent with the blockchain, and finally sharing of data is easy with the introduction of IPFS and partly division of the ciphertext into two parts which made the system more reliable.

5 Conclusions

To resolve the issue of protected storage and distribution of contemporary EHRs, we stated a model using blockchain and smart-contract technology. This system requires doctors to first encrypt electronic medical records and then upload the cipher-text to IPFS with acceptable access policies. The combination of IPFS and blockchain enables physicians, through IPFS, to treat massive amounts of electronic therapeutic data, to remove the necessity to place the details upon the chain itself, to conserve the blockchain's network-bandwidth. In future work, we will address a keyword index for searching encrypted medical records and also performed the keyword-based search in a decentralized paradigm.

References

- [1] Jin Sun, Lili Ren , Shangping Wang, Xiaomin Yao (2020),A blockchain-based framework for electronic medical records sharing with fine-grained access control, <https://doi.org/10.1371/journal.pone.0239946>
- [2] CB Insights Research, 5 Blockchain Startups Working to Transform Healthcare. <https://www.cbinsights.com/research/healthcare-blockchain-startups-medicine/>. [Feb 18 2021]
- [3] Dagher GG, Mohler J, Milojkovic M and Marella PB (2018), Ancile: Privacy-preserving framework for access control and interoperability of electronic health records using blockchain technology. *Sustainable Cities and Society*, **39**: 283-297.
- [4] Zhang P, White J, Schmidt DC, Lenz G and Rosenbloom (2018), FHIR Chain: Applying Blockchain to Securely and Scalably Share, *Computational and Structural Biotechnology Journal*, **16**: 267-278.
- [5] Ekblaw A, Azaria A, Halamka JD and Lippman A (2016), A Case Study for Blockchain in Healthcare: “MedRec” prototype for electronic health records and medical research data. MIT Media Lab.
- [6] S. Srivastava, ”Adoption of Electronic Health Records: A Roadmap for India.” *Healthcare Informatics Research* 22.4 (2016): 261269. PMC. Web., Sept 2018.
- [7] F. Ozair et al., ”Ethical Issues in Electronic Health Records: A General Overview.”, *Perspectives in Clinical Research* 6.2 : 73-76, 2015.
- [8] Concept Note-National eHealth Authority (NeHA), Government of India. https://www.nhp.gov.in/national_eHealth_authority_neha_mtl [Feb 18 2021]

Face Mask Detection and Person Identification

Sr. A. Punitha Jilt¹, N. Karthikeyan², S. Arunpandiyan², S. Santhosh², G. P. Vadalarasan²
HOD¹,UG Student² , , Department of Computer Science & Engineering.
ST.Anne's college of engineering and technology, Panruti

Abstract

Face veil recognition had seen critical improvement in the areas of Image handling and Computer vision, since the ascent of the Covid-19 pandemic. Many face location models have been made utilizing a few calculations and methods. The proposed approach in this paper utilizes profound learning, TensorFlow, Keras, and OpenCV to identify face veils. This model can be utilized for well being purpose since it is very asset effective to convey. The SSDMN2 approach utilizes Single Shot Multibox Detector as a face finder and MobilenetV2 engineering as a structure for the classifier, which is extremely lightweight and can even be utilized in installed gadgets (like NVIDIA Jetson Nano, Raspberry pi) to perform continuous cover location. The strategy sent in this paper gives us an exactness score of 0.9264 and a F1 score of 0.93. The datasets gave in this paper, was gathered from different sources, can be utilized by different analysts for additional high level models like those of face acknowledgment, facial tourist spots, and facial part recognition measure.

1 Introduction

COVID-19 pandemic had a lasting impact in many countries worldwide since December 2019. It originated in Wuhan, China. The World Health Organization (WHO) as on March 11, 2020, declared it as a deadly disease that gained its roots across the globe and severely affected 114 countries. Every medical professional, healthcare organizations, medical practitioners and researchers are in search for a proper vaccines (**Megahed & Ghoneim, 2020**) and medicines to overcome this deadly disease, however no breakthrough has been reported till date. The virus spreads through air channel when an infected person sneezes or communicate with the other person, the water droplets from their nose or mouth disseminate through the air and affect other peoples in the vicinity (**Kumar et al., 2020**). Face Mask detection has become a trending application due to the Covid-19 pandemic, which demands a person to wear face masks, keep social distancing, and use hand sanitizers to wash their hands. While other problems of social distancing and sanitization have been addressed until now, the issue of face mask detection has not yet been adequately addressed. Wearing a mask during this pandemic is a critical preventive measure (**Rahmani & Mirmahaleh, 2020**) and is most vital step in times when social distancing is hard to maintain. Wearing a mask is essential, particularly for those people who are at a greater risk of severe illness from COVID-19 diseases. It is found that the spread of COVID-19 is mainly among people who are in immediate contact with one another (nearly about 6 feet), it can be spread by people who do not have symptoms and are unaware of the fact that they are infected (Ge et al., 2020). So Centers for Disease Control and Prevention (CDC) recommended all people 2 years of age and older to wear a mask in public areas especially when other social distancing (**Sun & Zhai, 2020**) measures are difficult to maintain. Hence by reducing the risk of transmission of this deadly virus from an infected person to a healthy, the virus' spread and disease severity can be reduced to a great extent. Face Mask detection has turned up to be an astonishing problem in the domain of image processing and computer vision. Face detection has various use cases ranging from face recognition to capturing facial motions, where the latter calls for the face to be revealed with very high precision.

2 Existing methodologies

This technology is more relevant today because it is used to detect faces not only in static images and videos but also in real-time inspection and supervision. With the advancements of convolution neural networks (**Lawrence, Giles, Tsoi, & Back, 1997**) and deep learning (**Ahmed, Ahmad, Rodrigues, Jeon, & Din, 2020**), very high accuracy in image classification and object detection can be achieved. Hanvon Technology (**Wang et al. (2020)**) reported that the accuracy of masked face recognition is about 85 %. An accuracy of over 90 % was obtained from Mini-vision Technology (**Wang et al., 2020**). The face-eye-based multi-granularity model (**Wang et al., 2020**) achieves 95 % recognition accuracy. In (**Li, Wang, Li, and Fei (2020)**), the authors used the YOLOv3 algorithm for face Mask detection. This method achieved 93.9 % accuracy. The accuracies achieved were on artificial dataset which was not the case in this paper which uses both real and artificial images. A model named as SSDMNV2 has been proposed in this paper for face mask detection using OpenCV Deep Neural Network (DNN) (**Velasco-Montero et al, 2018**), TensorFlow (**Abadi et al., 2016**), Keras, and MobileNetV2 architecture (**Nguyen, 2020**) which is used as an image classifier. SSDMNV2 performs competently in differentiating images having frontal faces with masks from images having frontal faces without masks.

To impede the COVID-19 transmission the proposed model can be integrated with surveillance cameras so that it can be used for the detection of people who are not wearing face masks. Detection of face masks is an extremely challenging task for the present proposed models of face detection. This is because faces with masks have varied accommodations, various degrees of obstructions, and diversified mask types. They are used to facilitate self-focusing (**Huang, Ai, Li, & Lao, 2007**), the interaction between humans and computers (**Jun, Choi, & Kim, 2012**), and managing image database (**Ge, Li, Ye, & Luo, 2017**). Several reasons were found for the poor achievement of existing face mask detection model as compared to the normal ones. The first reason is lack of suitable datasets with properly masked faces and facial recognition. Secondly, the presence of masks on the face brings a certain kind of noise, which further deteriorates the detection process. These issues have been studied in some existing research papers such as (**Ghiasi & Fowlkes, 2014; Opitz et al, 2016; Yang et al, 2015**) still, there is an excellent challenge for a vast datasets so that an efficient face mask detection model can be easily developed.

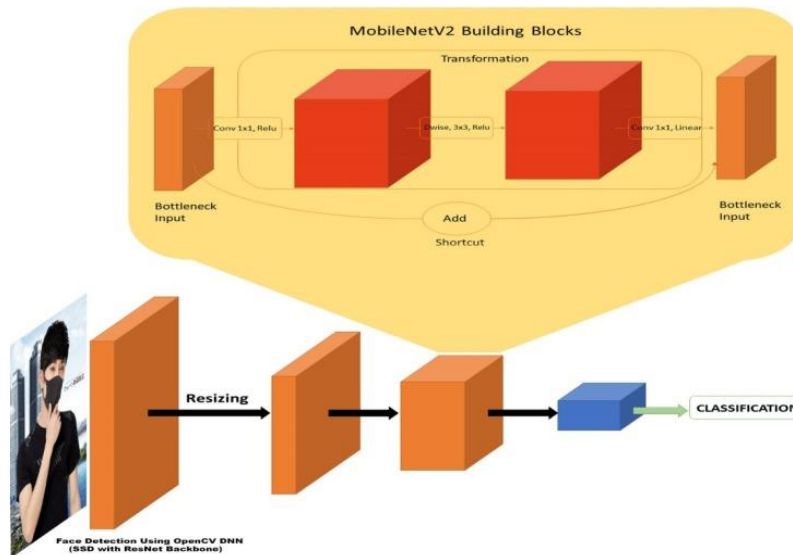
i.) A GitHub repository is made available, which contains a self-made Datasets of masked faces, including datasets taken from online resources. This dataset could be used for developing new face mask detectors and performing several applications.

ii.) OpenCV DNNs have been used for face mask detection, which allows for real-time detection without much resource usage. It can also detect faces in different orientations and can also detect occluded faces with good accuracy. The proposed SSDMNV2 model outperforms various previous models. Several provocations that were faced during the development of this model have been considered in this paper; this may help to develop more improved face mask detectors.

3 Proposed Methodology

To foresee whether an individual has worn a cover effectively, the underlying stage is trained the model utilizing a legitimate dataset. Insights concerning the Dataset have been examined, subsequent to prepare the classifier, an exact face identification model is needed to identify faces, so the SSDMNV2 model can order, if the individual is wearing a veil. The assignment is to raise the precision of veil recognition without being too asset weighty. For doing this undertaking, the DNN module was utilized

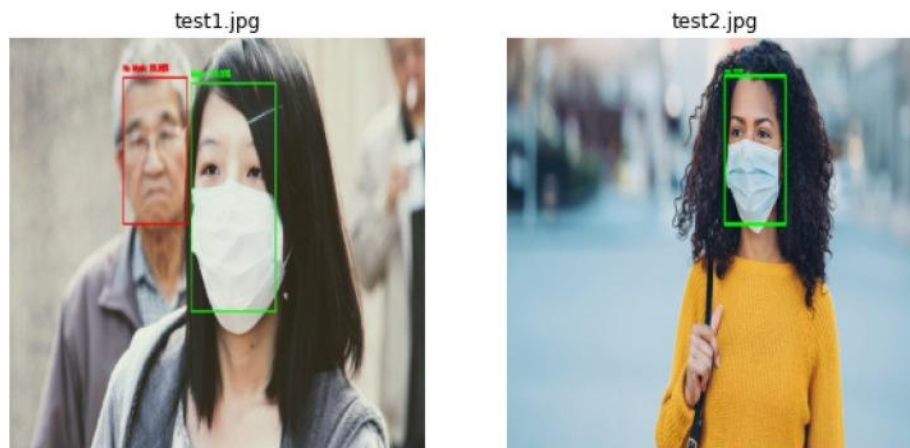
from OpenCV, which contains a 'Solitary Shot Multibox Detector' (SSD) (Liu et al., 2016) object location model with ResNet-10 (Anisimov and Khanova, 2017) as its spine engineering. This methodology helps in recognizing faces progressively, even on implanted gadgets like Raspberry Pi. The accompanying classifier utilizes a prepared model MobileNetV2 (Sandler, Howard, Zhu, Zhmoginov, and Chen, 2018) to foresee if the individual is wearing a cover.



This layer is the key square of the Convolutional Neural Network. The term convolution infers a numerical blend of two capacities to get the third capacity. It chips away at a sliding window component, which helps in extricating highlights from a picture. This aides in age highlight maps.

4 Results And Discussion





5 Conclusion

This paper introduced an examination on constant facemask acknowledgment with an alert framework through profound learning procedures via Convolutional Neural Organizations. This interaction gives an exact and quickly results for face mask discovery. The test outcomes show a recognized precision rate in recognizing people wearing a face mask and not wearing a facemask. The prepared model had the option to perform its endeavor utilizing the VGG-16 CNN model accomplishing a 96% outcome for execution exactness. Also, the examination presents a valuable instrument in battling the spread of the COVID-19 infection by distinguishing an individual who wears a face mask or not and sets an alert if the individual isn't wearing a face mask. Future works incorporate the reconciliation of physical separating, wherein the camera recognizes the individual wearing a facemask or not and simultaneously quantifies the distance between every individual and makes a caution if the physical separating doesn't notice appropriately. The reconciliation of a few models of CNNs and contrast each model and the best exactness during preparing to build the execution in identifying and perceiving individuals wearing face masks is proposed. Likewise, the analysts suggest a diverse streamlining agent, upgraded boundary settings, fine-tuning, and utilizing versatile exchange learning models.

References

- [1] Yu, P., Zhu, J., Zhang, Z., & Han, Y. (2020). A Familial Cluster oInfection Associated With the 2019 Novel Coronavirus Indicating Possible Person-to-Person Transmission During the Incubation PeriodThe Journal of infectious diseases, 221(11), 1757–1761<https://doi.org/10.1093/infdis/jiaa077>
- [2] Chavez, S., Long, B., Koyfman, A. & Liang, S. Y. Coronavirus Disease(COVID-19): A primer for emergency physicians. Am J Emerg Med, <https://doi:10.1016/j.ajem.2020.03.036> (2020).
- [3] World Health Organization. Coronavirus disease 2019 (COVID-19Situation Report– 142, 2020, [cited 10 June 2020]https://www.who.int/docs/default-source/coronaviruse/situationreports/20200610-covid-19-sitrep-142.pdf?sfvrsn=180898cd_6

- [4] Bai, Y., Yao, L., Wei, T., Tian, F., Jin, D. Y., Chen, L., & Wang, M. (2020). Presumed Asymptomatic Carrier Transmission of COVID-19. *JAMA*, 323(14), 1406–1407. Advance online publication <https://doi.org/10.1001/jama.2020.2565>
- [5] Centers for Disease Control and Prevention. Interim Infection Prevention and Control Recommendations for Patients with Suspected or Confirmed Coronavirus Disease 2019 (COVID-19) in Healthcare Settings. 2020 [cited 5 June 2020]<https://www.cdc.gov/coronavirus/2019-ncov/hcp/infection-controlrecommendations.html>
- [6] Korea Centers for Disease Control and Prevention. Infection Prevention and Control Recommendations for Patients with Suspected or Confirmed Coronavirus Disease 2019 (COVID-19) in Healthcare Settings [in Korean]. 2020 [cited 5 June 2020]<http://ncov.mohw.go.kr/duBoardList.do?brdId=2&brdGubun=28>
- [7] Sim, S. W., Moey, K. S. & Tan, N. C. The use of facemasks to prevent respiratory infection: a literature review in the context of the Health Belief Model. *Singapore Med J* 55, 160-167 <https://doi:10.11622/smedj.2014037> (2014).
- [8] Cowling, B. J. et al. Facemasks and hand hygiene to prevent influenza transmission in households: a cluster randomized trial. *Ann Intern Med* 151, 437-446, <https://doi:10.7326/0003-4819-151-7-20091006000142> (2009).
- [9] Tracht, S. M., Del Valle, S. Y. & Hyman, J. M. Mathematical modeling of the effectiveness of facemasks in reducing the spread of novel influenza A (H1N1). *PLoS One* 5, e9018 <https://doi:10.1371/journal.pone.0009018> (2010).
- [10] Jefferson, T. et al. Physical interventions to interrupt or reduce the spread of respiratory viruses. *Cochrane Database Syst Rev*, CD006207 <https://doi:10.1002/14651858.CD006207.pub4> (2011).
- [11] Feng, S., Shen, C., Xia, N., Song, W., Fan, M., & Cowling, B. J. (2020) Rational use of face masks in the COVID-19 pandemic. *The Lancet Respiratory medicine*, 8(5), 434–436. [https://doi.org/10.1016/S22132600\(20\)30134-X](https://doi.org/10.1016/S22132600(20)30134-X)
- [12] LeCun, Y., Kavukcuoglu, K., Farabet, C. & Ieee. in 2010 Ieee International Symposium on Circuits and Systems IEEE International Symposium on Circuits and Systems 253-256 (2010).
- [13] Zhang, K. P., Zhang, Z. P., Li, Z. F. & Qiao, Y. Joint Face Detection and Alignment Using Multi-task Cascaded Convolutional Networks Ieee Signal Proc Let 23, 1499-1503, <https://doi:10.1109/Lsp.2016.2603342> (2016).

Whale Optimized tively Regularized Kernel based Fuzzy C-Means for Multi-Objective Images Segmentation

N. Parvin,

Research Scholar, Periyar University, Salem.

P. Kavitha,

Department of Computer Science, Paavendhar College of Arts and Science, Salem.

D. Arul Pon Daniel,

Department of Computer Science & Applications, Loyola College, Namakkal,

Abstract

Most important key technologies of image processing are segmentation. The literature surveys have been proposed many clustering methods based on optimization technique to overcome the sensitivity to noise and initial values, very high in local optima entrapment. The effectiveness and simplicity of Fuzzy C-Means clustering procedures are widely used for image segmentation. The Whale optimization is to find the position of the search agent that is the selection of centroid. The proposed Whale Optimized Adaptively Regularized Kernel based Fuzzy C-Means for Multi-Objective Images Segmentation method to improve the performance of image segmentation of multi-objective images which was measured by the parameters such as Peak Signal to Noise Ratio (PSNR), Mean Square Error (MSE) and Root Mean Square Error (RMSE) for the WANG dataset. The outcome of the method was compared with the existing segmentation methods and reflects the best segmentation result.

Keywords: Image, Segmentation, Fuzzy C-Means, Clustering, WANG

1 Introduction

In computer vision and digital image processing the segmentation of images means the digital images are partitioning into multiple segments. So, the applications which supports decision oriented have been used image segmentation algorithm to classify the pixels of an appropriate images. Therefore, the image segmentation aims to change or simplify image representation into the form of most meaningful. Hence, the further analysis processes are also very easier. Image segmentation divides an image into multiple regions and each region can have high similarity pixels, but the properties are high contrast between the regions. Many applications in many field as medical image processing, health care, pattern recognition, etc., used the image segmentation in one of the valuable tool. Image segmentation has been used different approaches and techniques such as Region based segmentation, Edge or Boundary based segmentation etc. [1-5]. One of the powerful techniques in image segmentation is clustering. According to the attributes values the objects have been clustered which can have homogeneous. Clustering involves many algorithm such as K-Mean, FCM, KFCM etc. integrated with meta-heuristic algorithms such as ABC, PSO, Genetic algorithms for improving the accuracy, low computational complexity, easy do to further analysis of image segmentation. The edge detection is adopted in two stages; first one to enhance the image edges used by guided image filtering and followed optimization to produce the better results [6].

Image Normalization, Adaptive k-means segmentation, Morphological treatment have been proposed for Reduce the number of pixels and speed up image segmentation [7]. A regularized kernel-based fuzzy-clustering novel method proposed brain tissues are separate from magnetic resonance images as well as remove non-nuclei from Histopathological ROI image [8]. Pre-processing, segmentation and analysis of the segmentation performance have been proposed in three stages also based on AUC the statistical results are compared the technique FCM and K-Mean [9].

According to the humpback whales social behaviour implement the meta-heuristic optimization algorithm also compared with conventional methods [10]. Whale Optimization Algorithm adopted with chaos theory for tuning the WOA parameter and proves that the chaotic maps to improve the WOA performance [11]. An improved Whale Optimization Algorithm fused exploration of DE and exploitation of WOA proved better solutions [12]. Kernel Fuzzy Local Information C-Means (KFLICM) algorithm combined with level set propose new image segmentation method which is based Particle swarm optimization, wavelets proved that increased the effectiveness of MR image segmentation [13]. segmentation for brain magnetic resonance images based an adaptively regularized kernel based fuzzy c-means clustering techniques proposed the image details are preserved, maintain computational complexity and improve the accuracy in[14].Otsu's and multilevel thresholding are proposed four kinds of digital images and compared with the PSO search algorithm, it given better efficiency [15].

In this research work, a new clustering method WOA-ARK-FCM has been proposed. The hum back whales swam foraging behaviour is the base of Whale Optimization Algorithm. The main objective of the proposed

work is to enhance the performance image segmentation of multi-objective images. The performance have been compared with the well know existing algorithm such as thresholding, K-FCM and ARK-FCM by using the parameters PSNR, MSE, RMSE.

2 Proposed WOA-ARK-FCM method

The proposed framework adaptively regularized kernel-based FCM integrated with whale optimization involves adaptive regularization parameter, devise a weighted image devise and the function Gaussian radial basis and whale optimization are also adopted for better performance.

2.1 Adaptive regularization parameter

The contextual information has been control the desirable amount usually set the parameter in advance. Indeed, due to the variation of noise level of the window we may not fixed for every pixel. The prior knowledge about the presence of noise should need to set these parameter because noises always not available in reality. Hence, according to the process of pixel needs the adaptive calculation. In order to calculate the adaptive parameter for the processing of pixel first we calculate the coefficient of local variation (LVC). The local average greyscale have normalized to estimate the local window discrepancy of greyscales. Between the central pixel and its neighbours have high heterogeneity then, the result gives noise presence and local variation also increased.

$$LVC_j = \frac{\sum_{p \in M_j} (r_p - \bar{r}_j)^2}{M_X * (\bar{r}_j)^2} \quad (1)$$

Here, M_j is the local window and any pixels grayscale falling in it represents r_p which around the pixel (j), the cardinality of M_j as represents M_X and its grayscale mean defined as \bar{r}_j .

Next, the exponential function has been applied in LVC. The local window derive the weights is defined by following equation.

$$\zeta_j = \exp\left(\sum_{p \in M_j, j \neq p} LVC_p\right), \quad \rho_j = \frac{\zeta_j}{\sum_{p \in M_j} \zeta_p} \quad (2)$$

The local window average grayscale is associated with every pixel which the weights are assigned as following equation.

$$\varphi_j = \begin{cases} 2 + \rho_j, & \bar{r}_j < r_j \\ 2 - \rho_j, & \bar{r}_j > r_j \\ 0, & \bar{r}_j = r_j \end{cases} \quad (3)$$

The higher values are assigns the φ_j parameter for high LVC pixels. The grayscale average of its neighbors is not brighter than the pixel (j), φ_j assign $2 + \rho_j$, and in the case of the neighbourhood and LVC sum is large then ρ_j assigned as large otherwise it will be lower values. The central pixel grayscale is equal to the grayscale average of the local window then the vale zero will be assigned for and the algorithm as FCM standard algorithm. In the case of the value are two then to balance between the capability and convergence rate. It will be setting by the experiments for the details are preserved. The parameter φ_j is replaced by embedded the objective function of FCM which it is enhanced by using average filter and median filter with the adaptive parameter φ_j . This consists only greyscales which is relevant in a specified neighbourhood and it could be calculated before start the clustering process. So ultimately the computational cost can reduced greatly. According to the distribution of local grayscale the parameter φ_j yield a homogeneous clustering to provide the contextual information.

2.2 Weighted Image Devise

The grey level of median or average filter of the original image or weighted image $\bar{\xi}$ replace instead of the mean grayscale \bar{r} . The weighted image $\bar{\xi}$ as defined by following equation.

$$\bar{\xi}_j = \frac{1}{2 + \max(\varphi_j)} \left(r_j + \frac{1 + \max(\varphi_j)}{M_X - 1} \sum_{x \in M_j} r_x \right) \quad (4)$$

Here, the grayscale represents as r_x and M_j defined as the neighborhood of pixel j and the cardinality of M_j is M_X . weighted image is explicitly utilizes the parameter φ_j to make free which are not easy to adjust.

2.3 Gaussian Radial Basis Functions

If the data could be separated easily then the data projected their dimensional space is higher by using kernel functions for support vector machine. Using dot product to transform linear to non linear adopted by kernel

function. Replace the Euclidean distance function term $\|r_j - u_i\|^2$ into $\|\phi(r_j) - \phi(u_i)\|^2$ that is calculated using equation (5).

$$\|\phi(r_j) - \phi(u_i)\|^2 = P(r_j, r_j) + P(u_i, u_i) - 2P(r_j, u_i) \quad (5)$$

Here, the kernel function defined in P and u defines the cluster center.

In this proposed algorithm used GRBF kernel function is defined by using the equation (6).

$$P(r_j, u_i) = \exp\left(-\frac{\|r_j - u_i\|^2}{2\gamma^2}\right) \quad (6)$$

Here, the kernel function represents by γ .

The kernel function will be in equation (5) using GRBF as equation (7).

$$\|\phi(r_j) - \phi(u_i)\|^2 = 2(1 - P(r_j, u_i)) \quad (7)$$

In this function the kernel width expose large then the effect of exponential will be linear else the outliers can have sensitive cluster boundaries. In the case the kernel width is estimated by sample variance then the width will be fixed.

According to the distance variance the γ will be calculated among all pixels as equation (8)

$$\gamma = \left[\frac{\sum_{j=1}^M (t_j - \bar{t})^2}{M-1}\right]^{\frac{1}{2}} \quad (8)$$

Here, distance between the greyscale of pixel j and average greyscale of entire pixels represents $t_j = \|r_j - \bar{r}\|$ and \bar{t} represents all the distance (t_j) average.

2.4 The proposed WOA-ARK-FCM for multiple objective frame work

The frame work of proposed new adaptively regularized kernel-based FCM algorithm integrated with WOA is denoted as WOA-ARK-FCM. The contextual information has been control by the adaptive regularization parameter ϕ_j is calculated by using equation (3) which is associated with every pixel. The objective function is defined in the following equation (9).

$$J_{ARK_FCM} = 2 \left[\sum_{j=1}^M \sum_{i=1}^{c1} v_{ji}^{m1} (1 - P(r_j, u_i)) + \sum_{j=1}^M \sum_{i=1}^{c1} \phi_j v_{ji}^{m1} (1 - P(\bar{r}_j, u_i)) \right] \quad (9)$$

Here, the degree of fuzziness weighting exponent indicate as $m1$, cluster centers $u = \{u_1, u_2, \dots, u_{c1}\}$, $c1$ is a positive integer. The v_{ji} can be defined under the condition in equation (10).

$$\forall_j \in [1, M], i \in [1, c1] : \sum_{i=1}^{c1} v_{ji} = 1, v_{ji} \in [0, 1], 0 \leq \sum_{j=1}^M v_{ji} \leq M \quad (10)$$

The minimization of $J_{WOA_ARK_FCM}$ can be calculated using following equation.

$$J_{WOA_ARK_FCM} = 2 \left[\sum_{j=1}^M \sum_{i=1}^{c1} v_{ji}^{m1} (1 - P(r_j, u_i)) + \sum_{j=1}^M \sum_{i=1}^{c1} \phi_j v_{ji}^{m1} (1 - P(\bar{r}_j, u_i)) \right] \quad (11)$$

The algorithm WOA_ARK_FCM1/WOA_ARK_FCM2/WOA_ARK_FCMg is used to replace \bar{r} with average greyscale filter or median filter or weighted image $\bar{\xi}$ using equation (4). The cluster center u function and member function v of $J_{WOA_ARK_FCM}$ calculated by using equation (12) and equation (13).

$$v_{ji} = \frac{\left((1 - P(r_j, u_i)) + \phi_j (1 - P(\bar{r}_j, u_i)) \right)^{-1/(m-1)}}{\sum_{p=1}^{c1} \left((1 - P(r_j, u_p)) + \phi_j (1 - P(\bar{r}_j, u_p)) \right)^{-1/(m-1)}} \quad (12)$$

$$u_i = \frac{\sum_{j=1}^M v_{ji}^{m_1} (P(r_{j,u_i})r_j + \phi_j P(\bar{r}_j, u_i)\bar{r}_j)}{\sum_{j=1}^M v_{ji}^{m_1} (P(r_{j,u_i}) + \phi_j P(\bar{r}_j, u_i))} \quad (13)$$

2.4.1 Work Flow of proposed WOA_ARK_FCM algorithm

Step1: Initialize the threshold, loop counter, weighting exponent, membership.

Step2: Compute the parameter of adaptive regularization.

Step3: Compute \bar{r}_j using option average, median and weighted image.

Step4: Initialize and Compute cluster centre using WOA algorithm

S1: Initialize the population of whale

S2: Computer each search agent fitness

S3: Under the iteration associated each search agent update the Current search agent position under the condition

S4: Compute the search agent fitness

S5: Update best search agent

S6: Finally terminate the iteration in condition criteria

Step5: Compute the GRBF, Objective and membership function

Step6: If the condition criteria are satisfied then stop otherwise update the iteration and repeat to go to step 4.

3. Implementation results and discussion

The image segmentation performance was evaluated with three metrics such as Peak Signal to Noise Ratio (PSNR), Mean Square Error (MSE), and Root of Mean Square Error. PSNR is an expression for the ratio between the maximum possible value and the power of distorting noise. Here, Ex represents the experimental value and Mp denotes the model predictions. In this research work, WOA_ARK_FCM technique tested with 22 different multi-objective images from benchmark WANG dataset than can available publically shown in Fig. (4).

In this implementation involves multilevel thresholding with Ostu function, Fuzzy C-mean, K-FCM, ADRK-FCM and compared the metrics of this algorithm along with the proposed WOA_ARK_FCM for multi-objective images, Fig. (1) shows the MSE, Fig. (2) shows the PSNR, Fig. (3) shows the RMSE evaluation plots for the samples taken for this work.

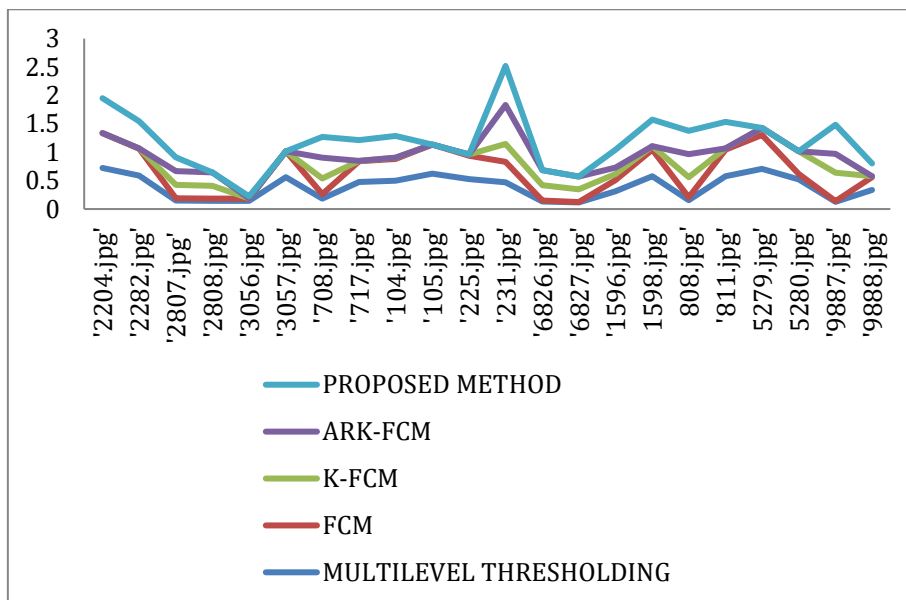


Figure 1: MSE values of our dataset images

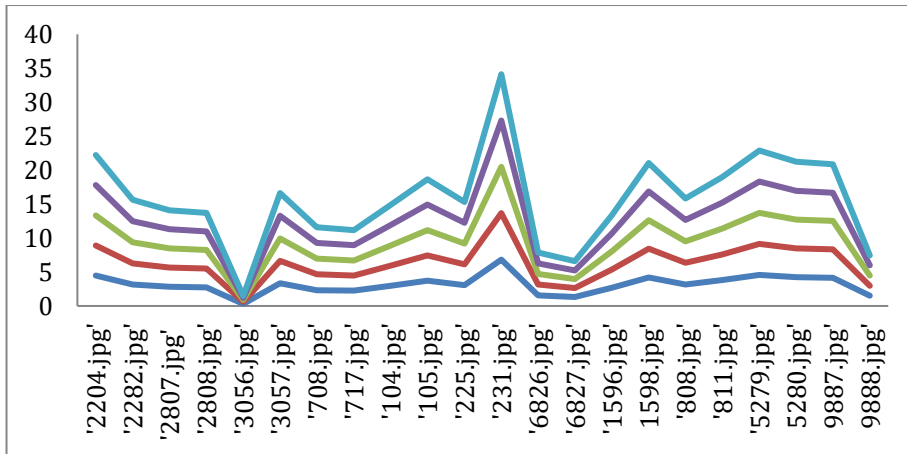


Figure 2: PSNR values of our dataset images

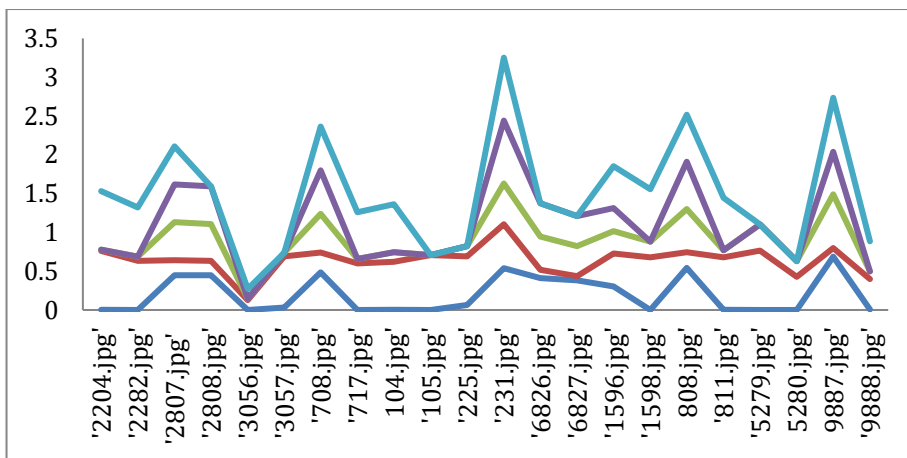


Figure 3: RMSE values of our dataset images

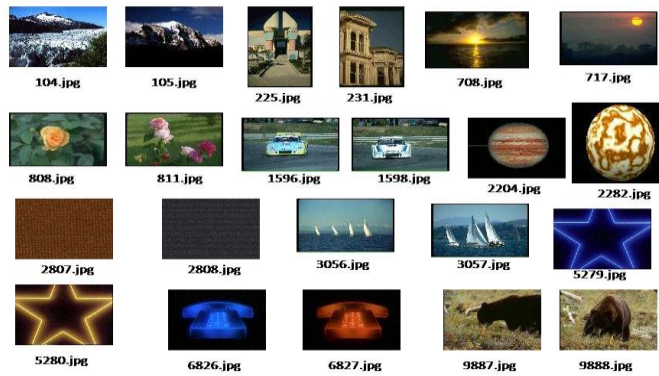


Figure 4: Random images from WANG Dataset for Experiment

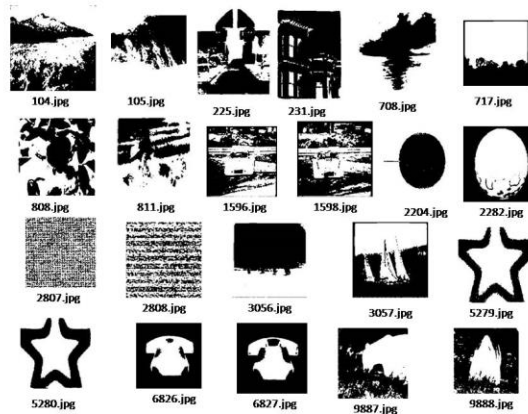


Figure 5: Ground Truth Images of Experimental Dataset

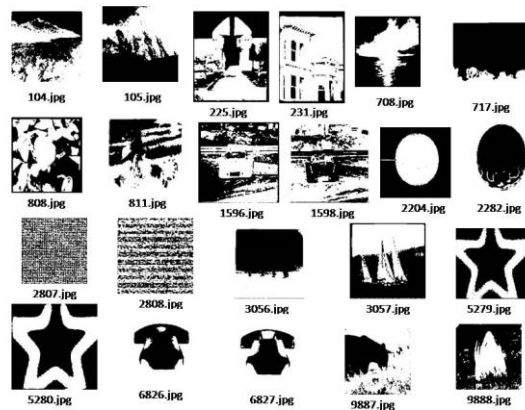


Figure 6: Results of our proposed WOA_ARK_FCM algorithm

The result of the implementation prove that the proposed method outperforms from the other in terms of the error rate are minimized and the performance of the segmentation improved..

4 Conclusions

The proposed images segmentation algorithm WOA-ARK-FCM for multi-objective segmentation was fused algorithm combines the pros of two algorithms such as ARK-FCM and WOA. The proposed method performance has been proved by its results while it was compared with the existing algorithm by using the metrics as PSNR, MSE, RMSE associated with manual ground truth image dataset given the better performance than the conventional algorithms. The proposed method will be use for further analysis of image processing in future.

References

- [1] P. Shashi and S. R, "Review Study on Digital Image Processing and Segmentation," Am. J. Comput. Sci. Technol., vol. 2, no. 4, p. 68, 2019, doi: 10.11648/j.ajcst.20190204.14.
- [2] N. M. Zaitoun and M. J. Aqel, "Survey on Image Segmentation Techniques," Procedia Comput. Sci., vol. 65, no. Iccmit, pp. 797–806, 2015, doi: 10.1016/j.procs.2015.09.027.
- [3] N. Dhanachandra and Y. J. Chanu, "A Survey on Image Segmentation Methods using Clustering Techniques," Eur. J. Eng. Res. Sci., vol. 2, no. 1, p. 15, 2017, doi: 10.24018/ejers.2017.2.1.237.
- [4] M. Waseem Khan, "A Survey: Image Segmentation Techniques," Int. J. Futur. Comput. Commun., no. July, pp. 89–93, 2014, doi: 10.7763/ijfcc.2014.v3.274.
- [5] Sharma and N. Tiwari PROF, "A Survey on Brief Study for Image Segmentation Approaches," Int. J. Res. Anal. Rev. www.ijrar.org, vol. 6, no. 04, pp. 6–10, 2018, [Online]. Available: www.ijrar.org.
- [6] G. Phonsa and K. Manu, "A survey: Image segmentation techniques," Adv. Intell. Syst. Comput., vol. 741, pp. 1123–1140, 2019, doi: 10.1007/978-981-13-0761-4_105.

- [7] M. H. Hesamian, W. Jia, X. He, and P. Kennedy, "Deep Learning Techniques for Medical Image Segmentation: Achievements and Challenges," *J. Digit. Imaging*, vol. 32, no. 4, pp. 582–596, 2019, doi: 10.1007/s10278-019-00227-x.
- [8] X. Zheng, Q. Lei, R. Yao, Y. Gong, and Q. Yin, "Image segmentation based on adaptive K-means algorithm," *Eurasip J. Image Video Process.*, vol. 2018, no. 1, 2018, doi: 10.1186/s13640-018-0309-3.
- [9] W. Wiharto and E. Suryani, "The Comparison of Clustering Algorithms K-Means and Fuzzy C-Means for Segmentation Retinal Blood Vessels," *Acta Inform. Medica*, vol. 28, no. 1, p. 42, 2020, doi: 10.5455/aim.2020.28.42-47.
- [10] S. Mirjalili and A. Lewis, "The Whale Optimization Algorithm," *Adv. Eng. Softw.*, vol. 95, pp. 51–67, 2016, doi: 10.1016/j.advengsoft.2016.01.008.
- [11] G. Kaur and S. Arora, "Chaotic whale optimization algorithm," *J. Comput. Des. Eng.*, vol. 5, no. 3, pp. 275–284, 2018, doi: 10.1016/j.jcde.2017.12.006.
- [12] S. Mostafa Bozorgi and S. Yazdani, "IWOA: An improved whale optimization algorithm for optimization problems," *J. Comput. Des. Eng.*, vol. 6, no. 3, pp. 243–259, 2019, doi: 10.1016/j.jcde.2019.02.002.
- [13] Mekhmoukh and K. Mokrani, "MR brain image segmentation using an improved Kernel Fuzzy Local Information C-Means based wavelet, particle swarm optimization (PSO) initialization and outlier rejection with level set methods," *Int. Arab J. Inf. Technol.*, vol. 15, no. 4, pp. 683–692, 2018.
- [14] Elazab, C. Wang, F. Jia, J. Wu, G. Li, and Q. Hu, "Segmentation of brain tissues from magnetic resonance images using adaptively regularized kernel-based fuzzy C -means clustering," *Comput. Math. Methods Med.*, vol. 2015, 2015, doi: 10.1155/2015/485495.
- [15] J. Qin, C. T. Wang, and G. H. Qin, "A Multilevel Image Thresholding Method Based on Subspace Elimination Optimization," *Math. Probl. Eng.*, vol. 2019, 2019, doi: 10.1155/2019/6706590.

Fake User Identification On Social Networks

Abinaya.K¹,Abirami.A¹,Anushiya.L¹,Brittadevi.V²

¹UG Student,¹Assistant Professor,Department of Computer Scincence and Engineering,
St.Anne`s College of Engineering and Technology ,Panruti.

Abstract

Social networking websites engage millions of users around the world. The users' interactions with Twitter and Facebook have a tremendous impact and occasionally undesirable repercussions for daily life. Twitter is an Online Social Network (OSN) where users can share anything and everything, such as news, opinions, and even their moods. Several arguments can be held over different topics, such as politics, Particular affairs, and important events. When a user tweets something, it is instantly conveyed to her followers, allowing them to outspread the received information at a much broader level. With the evolution of OSNs, the need to study and analyze users' behaviors in online social platforms has intensity Spammers can be identified based on: fake content, URL based spam detection, spam in trending topics, and fake user identification. And with the help of machine learning algorithms we are going to identify the fake user and spammer in twitter.

KEYWORDS: *spammer's identication ,fake user detection ,Classication, machine learning, online social platform.*

1 Introduction

It has become quite unpretentious to obtain any kind of information from any source across the world by using the Internet. The increased demand of social sites permits users to collect abundant amount of information and data about users. Huge volumes of data available on these sites also draw the attention of fake users .Twitter has rapidly become an online source for acquiring real-time information about users. Twitter is an Online Social Network (OSN) where users can share anything and everything, such as news, opinions, and even their moods. Several arguments can be held over different topics, such as politics, current affairs, and important events. When a user tweets something, it is instantly conveyed to his/her followers, allowing them to outspread the received information at a much broader level. With the evolution of OSNs, the need to study and analyze users' behaviors in online social platforms has intensive. Many people who do not have much information regarding the OSNs can easily be tricked by the fraudsters. There is also a demand to combat and place a control on the people who use OSNs only for advertisements and thus spam other people's accounts. Nowadays most of the people are using the twitter. In twitter also we have the fake users so in this survey we are find fake user identification from Twitter. In this paper we are going to identify the fake users based on : (i) fake content, (ii) URL based spam detection, (iii) spam in trending topics, and (iv) fake user identification. After identify the fake user. The fake user going to waste the times of others, they are going to post the post frequently and which is not related to the other user.

2 Related Work

C. Buntain and J. Golbeck. A feature analysis then identifies features that are most predictive for crowd sourced and journalistic accuracy assessments, results of which are consistent with prior work. We close with a discussion contrasting accuracy and credibility and why models of non-experts outperform models of journalists for fake news detection in Twitter[3]. C. Meda, E. Ragusa, C. Gianoglio, R. Zunino, A. Ottaviano. the analysis of open data and need effective techniques to filter troublesome information. In a real scenario, Law Enforcement Agencies analyze Social Networks, i.e. Twitter, monitoring events and profiling accounts. Unfortunately, between the huge amount of internet users, there are people that use microblogs for harassing other people or spreading malicious contents. Users' classification and spammers' identification is a useful technique for relieve Twitter traffic from uninformative content. This work proposes a framework that exploits a non-uniform feature sampling inside a gray box Machine Learning System, using a variant of the Random Forests Algorithm to identify spammers inside Twitter traffic. Experiments are made on a popular Twitter dataset and on a new dataset of Twitter users[4]. C. Chen, Y. Wang, J. Zhang, Y. Xiang, W. Zhou. In our labeled tweets data set, however, we observe that the statistical properties of spam tweets vary over time, and thus, the performance of existing machine learning-based classifiers decreases. This issue is referred to as "Twitter Spam Drift". In order to tackle this problem, we first carry out a deep analysis on the statistical features of one million spam tweets and one million non-spam tweets, and then propose a novel Lfun scheme.

The proposed scheme can discover “changed” spam tweets from unlabeled tweets and incorporate them into classifier's training process. A number of experiments are performed to evaluate the proposed scheme. The results show that our proposed Lfun scheme can significantly improve the spam detection accuracy in real-world scenarios.

3 Existing System

A survey on different behaviors exhibited by spammers on Twitter social network. The study also provides a literature review that recognizes the existence of spammers on Twitter social network.

4 Proposed System

This paper is to identify different approaches of spam detection on Twitter and to present a taxonomy by classifying these approaches into several categories. For classification, we have identified four means of reporting spammers that can be helpful in identifying fake identities of users. Spammers can be identified based on: (i) fake content, (ii) URL based spam detection, (iii) detecting spam in trending topics, and (iv) fake user identify. With the help of Machine learning algorithms like Random forest, Minimum weight and K-means we using these algorithms in different stages to identify the fake user sand spammer on twitter.

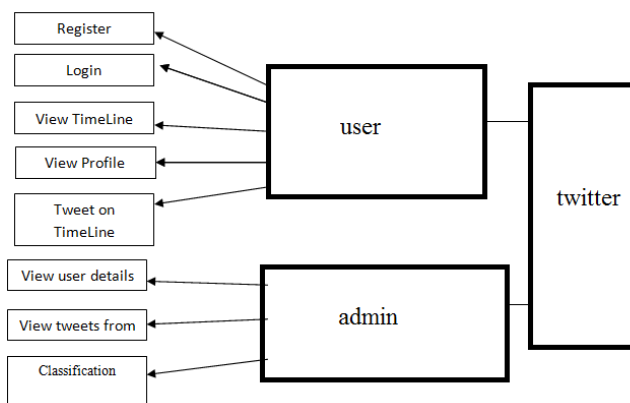


Figure 1 : architecture of the sysytem

4.1 Random Forest Algorithm

In this paper we are using random forest which is comes under supervised learning in machine learning. Random forest algorithm which is used to classification, in this paper we are going to identify the spammer and firstly we have to categorized the spammer after that we are going to identify the spammer. Steps for Random Forest algorithm Gather the different training data from the training dataset. In each data which we are gathered we have to take the particular information. Finally we have to predict the data

4.2 K-Means Algorithm

K-Means algorithm comes under the unsupervised learning which is used in cluster. This algorithm is used to identify the fake users in twitter. Steps of K-Means Algorithm: we need to identify the number of clusters, K is num of cluster, need to be generated by this algorithm.randomly select K value points and assign each value point to a cluster. That means, classify the data based on the number of value points. In this step it will compute the cluster data.keep follow the following steps until we get optimal centroid which is the assignment of data points to the clusters that are not changing any more.These are all the algorithms which we are used to done this survey.

5 Experimental Results

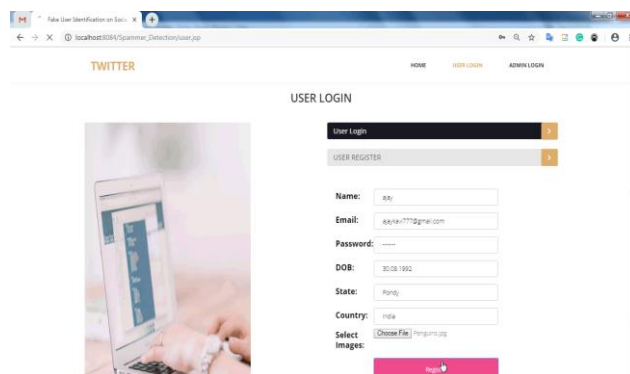


Figure 2 : User Profile

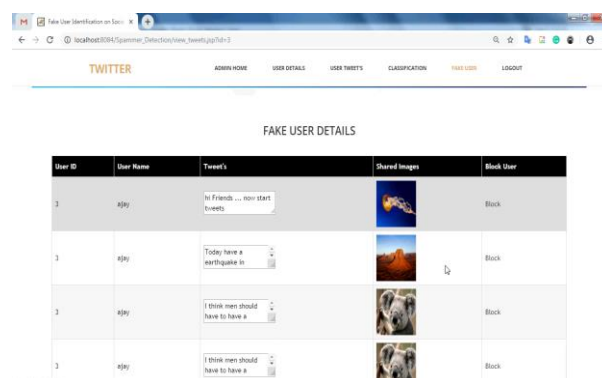


Figure 3 : Fake user Identification

6 Conclusion

we performed a review of techniques used for detecting spammers on Twitter. In addition, we also presented a taxonomy of Twitter spam detection approaches and categorized them as fake content detection, URL based spam detection, spam detection in trending topics, and fake user detection techniques. We also compared the presented techniques based on several features, such as user features, content features, graph features, structure features, and time features. Moreover, the techniques were also compared in terms of their specified goals and datasets used. It is anticipated that the presented review will help researchers and the information on state-of-the-art Twitter spam detection techniques in a consolidated form.

References

- [1] S. Ghosh, G. Korlam, and N. Ganguly, "Spammers' networks within online social networks: A case-study on Twitter," in Proc. 20th Int. Conf. Companion World Wide Web, Mar. 2011, pp. 41–42.
- [2] S. J. Soman, "A survey on behaviors exhibited by spammers in popular social media networks," in Proc. Int. Conf. Circuit, Power Comput. Tech-nol. (ICCPCT), Mar. 2016, pp. 1–6.
- [3] C. Chen, Y. Wang, J. Zhang, Y. Xiang, W. Zhou, and G. Min, "Statistical features-based real-time detection of drifted Twitter spam," IEEE Trans. Inf. Forensics Security, vol. 12, no. 4, pp. 914–925, Apr. 2017.
- [4] C. Buntain and J. Golbeck, "Automatically identifying fake news in popular Twitter threads," in Proc. IEEE Int. Conf. Smart Cloud (SmartCloud), Nov. 2017, pp. 208–215.

- [5] C. Chen, J. Zhang, Y. Xie, Y. Xiang, W. Zhou, M. M. Hassan, A. AlElaiwi, and M. Alrubaian, "A performance evaluation of machine learning-based streaming spam tweets detection," *IEEE Trans. Comput. Social Syst.*, vol. 2, no. 3, pp. 65_76, Sep. 2015
- [6] B. Erçahin, Ö. Akta³, D. Kiliç, and C. Akyol, "Twitter fake account detection," in *Proc. Int. Conf. Comput. Sci. Eng. (UBMK)*, Oct. 2017, pp. 388_392.
- [7] T. Wu, S. Wen, Y. Xiang, and W. Zhou, "Twitter spam detection: Survey of new approaches and comparative study," *Comput. Secur.*, vol. 76, pp. 265_284, Jul. 2018.
- [8] S. Sadiq, Y. Yan, A. Taylor, M.-L. Shyu, S.-C. Chen, and D. Feaster, "AAFA: Associative affinity factor analysis for bot detection and stance classification in Twitter," in *Proc. IEEE Int. Conf. Inf. Reuse Integr. (IRI)*, Aug. 2017, pp. 356_365.
- [9] G. Jain, M. Sharma, and B. Agarwal, "Spam detection in social media using convolutional and long short term memory neural network," *Ann. Math. Artif. Intell.*, vol. 85, no. 1, pp. 21_44, Jan. 2019.
- [10] F. Concone, A. De Paola, G. Lo Re, and M. Morana, "Twitter analysis for real-time malware discovery," in *Proc. AEIT Int. Annu. Conf.*, Sep. 2017, pp. 1_6.

Opinion classification for tourists reviews using support vector machine

G.Bharathi. Dr. G. Anandharaj

Abstract

The sentiment analysis has increased its significance in modern days. People had enhanced their approach of exposing their suggestions about any places of interest or any tourist paces of suggestions in Social media networks or travel platforms. Users express their experiences or feelings by reviews or by using some specific symbols like emoji, stickers etc. Social media networks or World's largest travel platform make available of a peoples' feelings or experiences on topics like most visited places. The World's largest travel platform like Booking.com, TripAdvisor, Airbnb etc., help to choose most visited places and share their experiences and feelings about visiting places. This paper proposed a framework to find the scores of the feelings or experiences and then using the scores derive final conclusions. The classification of feelings or experiences is called opinion mining, whereas generating the scores for those feelings or experiences are called sentiment analysis. In this paper Support Vector Machine is used as Classification techniques for opinion mining, finally concluded with the polarity detection and then by creating word cloud images. This system uses machine learning techniques which scrutinize the score result and then by classifying sentiment analysis of most visited places to travel and tourism.

Keywords: *Sentiment Analysis, Social media network, WebPages, Text mining, Opinion mining, Score, Word cloud.*

1 Introduction

Sentiment analysis is broadly applied to the appropriate places of interest in tourism reviews. Sentiment analysis or opinion mining is to conclude the characteristic of places of interest in tourism in terms of scores or positive words present in each reviews, searching out their places of interest, discovering the places of interest of reviews and the places of interest of each aspect of separate areas of tourist places reviews. If the users give their suggestions about their tourist experiences in the form of special characters or by using the positive words or negative words or by using comments such as likes or dislikes, actually there is no problem if the reviews are lies in the text format. As the tourist reviews dataset is as streaming data, the tourist review must be recapitulate or should be confirmed whether it's good reviews or bad reviews. For investigating, knowledge mining and decision making, machine learning techniques should be used to construct the model to recognize. The online Social media networks facility has its positive reviews and negative reviews. The excellent thing is that wherever the tourists could express their feelings as review messages, In addition the other side some tourists who write their feelings as unnecessary comments or by using special emoji on the social media networks which were absolutely meaningless and irrelevant. The next problem with the online review data's is that occasionally the authentic feelings may not be shared at all. They won't express their perfect feelings instead of sometimes they express unnecessary irrelevant data to the about a topic. The main thing that must be keep in mind that the sentiment or the opinion can be done not only on the whole review or the document, can also find the opinion based on a sentence and score it.

Most of the mainly used Natural Language Processing (NLP) method in differentiating the reviews is Text Classification. The main aim of text classification is to automatically classify the reviews into one or more categories such as positive or negative scores. The classification concern with one of the text classification method such as sentiment classification from Social media networks data such as Twitter, Face book, LinkedIn etc.,. This system scrutinizes real time reviews data to categorize scores or sentiments on places of interest of tourism such as Food, Road, and Hotel and finally about the most visited areas. The system will begin from crawling Social media networks reviews about most visited places of interest to travel and tourism. The pre-processing of the review text data is an necessary step as it put together the raw review text ready for text classification mining, i.e., it becomes more easier to take out valid information from the text and then by applying machine learning techniques to it. The main purpose of this step is to clean noisy data or by removing the less relevant words or reviews to find the sentiment of reviews such as different special symbols, emoji, punctuation, and special stickers in terms which don't bring much scoring words reviews in situation to the text. The most important highlight of the system is to find out the feature terms of Social media networks reviews.

In this paper, the system uses Machine learning techniques to calculate sentiment scores. Conclusion of the classification result is to classify sentiments on places of interest of tourism such as Food, Road, and Hotel and finally about the most visited areas of interest and then to determine the sentiment scores. Sentiment analysis requests to make use of the tourist review dataset for its best scoring performance, the importance of the places of interest about tourism also depends on the exact estimation of the scoring result.

2 Literature review

Hussein, D concluded that the challenges observed in the sentiment analysis were explained and the techniques available for the analysis were tabulated for easier observation. The latest updates of sentiment analysis was observed and the techniques which were recorded. A survey was done such that it was proved that the machine learning approaches are best when compared with the lexical approaches. There has been a significant investigation on the sentiment analysis of online reviews dataset. On the other hand, the majority of the investigations have focused on English comments. English words are obviously separate, whereas the words in other language sentences required to be segmented earlier than performing sentiment analysis. [1]

Pradhan et al. concluded that the different levels of opinion mining and supervised learning classifiers techniques and individuals results were evaluated with the other preceding or earlier researcher's results. Finally he accomplished that the supervised technique is the best method than the other ones. [2]

Michaels, M concluded that the most important steps of sentiment analysis are text classification, summarization and tracking. From the beginning the input corpus had removed the redundant review data and then main features are pulling out by using term-frequency matrix. Ranking was allocated at the ending step. The study selects three best cities to travel in U.S. based on TripAdvisor reviews, including New York, Los Angeles and Las Vegas. [3]

Li, R. et al., explained that the web data mining is also an important step in the analysis as the data collection and processing must be done from web. The web data mining architecture was clearly explained. The survey was on web usage mining to know which is the best one to refer or to collect data. The verbal communication of online reviews is unusual from official language, which means it not only includes domain-particular words but also a lot of Internet catchphrase, making it very hard to generate complicate words and correct domain dictionary. [4]

Vijayarani S et al., concluded that the development of text extraction and its dissimilar applications like information extraction, information retrieval, and categorization. The different approaches preprocessing techniques obtainable in text mining were give details along with the method that can be put into operation as stemming algorithms. This is most excellent reference paper for text mining researchers. [5]

Allahyari, M et al., concluded that how a review sentence sentiment classification and review word sentiment classification can be obtained, but the only disadvantage of this approach is not allowing for the neutral suggestions in the review dataset. Text mining classification, which label unstructured data with applicable grouping from a predefined set essential text-mining task. [6] Shaikh T concluded that realistic research was done by taking the tourists reviews which are scrutinize, analyzed and well thought-out to make a decision. The different machine learning algorithms like Naive Bayes, SVM, maximum likelihood and decision tree were used in the phase of sentiment classification. [7]

Khan et al. concluded that a semi supervised method based on domain lexicons and incorporate information achieved and cosine comparison to increase the performance of sentiment analysis and conquer issues such as data sacristy and domain independence. [8] Rafi et al. made a survey on machine learning algorithms to find which algorithms was majorly used compare SVM and NB classifiers for text categorization with originated that NB performed better. [9]

Kaushik A, et al., concluded that the group of survey has been completed on text mining and its approaches like summarizing the data, information extraction, categorizing, clustering, and tracking the topics, sentiment classification and finally the visualization of results. Their architectures were also giving explanation in a straightforward manner. Not only that the tools obtainable for the text mining and the common applications of text mining were give details briefly. [10]

Maheshwari A et al., concluded that the information sources accessible were make clear along with different techniques available for investigation. The unusual research challenges these days, the main purpose that can be completed and the tools accessible for doing this mining were give explanation briefly. [11] Nitin Pise had concluded that the architecture explained about the sentiment analysis i.e., how it begin and ends. Every technique for the analysis, both the lexicon approaches and the machine learning approaches were explained. Afterwards the functions of sentiment analysis, the tools accessible for it and the most important disputes of the analysis these days were also discussed. [12]

Sri RJ concluded that review of product reviews has been made using sentiment classification. The method called semantic orientation is projected which would assist in finding the common terms easily. A assessment of correctness and time complexity was calculated between the proposed and accessible ranking system and proved that semantic orientation is most excellent. The greatest thing is that the flow chart of the method was comprehensible. [13] Akhtar et al. concluded that methods for characteristics selection that is based on single-objective and sentiment analysis with other dissimilar classifiers. Their techniques choose the major features based on the possessions of the classifiers and domains and confirmed good quality results for a selection of different domains. [14]

3 Proposed Model

Flow analysis systems sentiment for travel and tourism domain using a hybrid approach consists of two main parts: the categorization reviews from Social media networks tourist reviews and reviews about transport route, food and lodging finally it helps to classify the reviews to find or calculate performance analysis scoring which analyzes the sentiment analysis in the domain of travel and tourism with the help of Social media networks and travel platform.

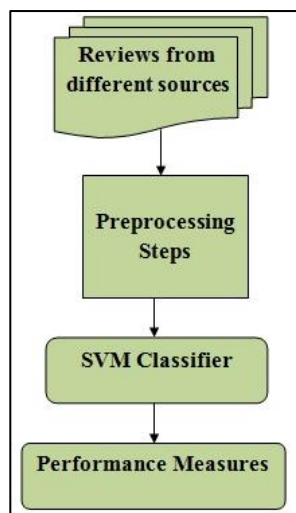


Figure 1: Architecture of Sentiment analysis.

3.1 Data

Data collected from Social media networks and WebPages. Users can create a Face book or Twitter account, by using twitter API by the developer. Users can request the data that tweets from the API by using keywords such as name of the most visited tourist places, about transport and Hotels then restore the review dataset from Social media networks and WebPages entered by the user. The number of reviews dataset extracted in each network or WebPages has to collect and then by using the machine learning technique. In addition to textual feedback of travelers, other relevant information, such as the type of routes and star rating of individual reviewers for the most visited places were also collected.

3.2 Preprocessing

The preprocessing of reviews dataset follows the procedural steps personalized from previous studies including eliminating special characters and symbol words, tokenization of word text, removing general negative words, removing irregular words and word stemming. After removing the non-textual contents and irrelevant data's from the review dataset then transformed the reviews into proper tokens. Tokenization technique breaks the text into smaller components. Screening is the method of finding information on which the document is selected from a dynamic text flow and relatively stable to meet specific information needs. Filtration method eliminates stop words of text preprocessing.

3.3 Polarity detection

In the polarity detection, the initial raw dataset reviews for the travel and tourism extracted can be used in machine learning models. This phase also includes the process of creating new features from actual existing data. And then the raw text data is converted to vector features and new features will be created using an existing dataset. The resulting feature of room's reviews, about food reviews and route or transportation review trained to use machine learning models such as Support Vector Machine.

3.4 Recognition of words

The next step is to detecting tourists' sentiment classification of different reviews dataset aspect entrenched in their reviews. Initially, each of the reviews is break into sentences by Sentiment Strength, and

every sentence is then assigned with scores of negative and positive value, since in actuality, one sentence may contain either positive or negative sentiments simultaneously. Sentiment Strength also intently scores the dictionary tokens that include regular emoticons. For instances, “like” is scored as +5 and for the “hate” is scored as -5. Note that simply when a word there within the dictionary, it is differentiate by a particular score. In addition, supplementary marks or attributive expressions may lead to score change, particularly the positive score word looks like “like” “!!!liked” as an alternative of “likes” same as negative word looks like “hate”, “hates!!!” as an alternative of “hate”, and they almost certainly increase the dictionary.

3.5 Measurements

The performance of the support vector classification is evaluated by important methods as noted in previous studies [15] with the precision, recall and accuracy being calculated by means of the Equations as suggested below. Precision is the fraction of correctly predicted positive comments to the total predicted positive observations. The recall indicates which part of the classified data has been correctly identified. *F* Measure is used to measure accuracy of a test that leads to merge both Precision and Recall values. The performance evaluation of most visited tourist places reviews based on datasets is as follows:

$$\text{Prec} = \frac{\text{true positive words}}{\text{true poistive} + \text{false positive}} \dots\dots\dots (1)$$

$$\text{Rec} = \frac{\text{true positive words}}{\text{true poistive} + \text{false negative}} \dots\dots\dots (2)$$

$$\text{F-Measure} = 2 \frac{\text{Prec} * \text{Rec}}{\text{Prec} + \text{Rec}} \dots\dots\dots (3)$$

4 Test Results

The dataset used is tourists review data collected social media networks and WebPages. It contains about positive and negative reviews dataset, as well as it includes the unnecessary spam reviews too. In the text mining process, remove all the symbols and stop words and then in polarity detection, finding word frequency and stemming. The lots of sentences are found by removing the repeated feelings and experiences. Now the opinion mining was done by adopting the Support Vector classifier and the classification of scores was done. After that to find the score of those feelings and experiences of positive and negative words is saved. Because the analysis selected is sentence sentiment classification. Finally the positive and negative scores were found and scored. Usually, the score recognition was done on positive and negative reviews dataset. With the help of lexicon dictionary, it might be able to compute the score for neutral or non-negative sentences. The scores were given from - 5 to +5 as denoted in the structural design.

This system is implemented using the R Programming language Word cloud, a generative probabilistic model for determining hidden semantic topics from a large text corpus, is developed to extract and make the dimensions of all tourists customer generated reviews for tours and travels. The word cloud is identified with the most visited tourist places in India aspects and the high frequency words are shown in Figure 2. The word font size is linearly proportional to the high frequency of words. Few aspects were considered such as Food, Road, and Hotel and finally about the most visited areas of interest. Feelings and experiences were defined as tourists responses as reviews straight away from the social media network and WebPages. Accordingly, In terms of consequence order of the above said aspects, most visited tourist places and their related words are exposed to be most commonly referred in the social media network and webpage reviews that are most regularly revealed in the online reviews.

- [10] Kaushik A, Naithani S (2016) A comprehensive study of text mining approach. International Journal of Computer Science and Network Security (IJCSNS) 16:2
- [11] Maheshwari A, Dadhich A, Mathur P (2015) Opinion mining: A survey. International Journal Advance Research Computer Communication Engineering 4(1).
- [12] Pise N (2016) A case study on sentiment analysis from social big data. International Journal Innovation Research Computer Communication Engineering 4(7)
- [13] Sri RJ, Ajitha P (2016) Survey of product reviews using sentiment analysis. Indian J Sci Technol 9:21
- [14] Akhtar, M. S., Gupta, D., Ekbal, A., & Bhattacharyya, P. (2017). Feature selection and ensemble construction: A two-step method for aspect based sentiment analysis. *Knowledge-Based Systems*, 125, 116–135.
- [15] Ali, F.; Kwak, K.S.; Kim, Y.G. Opinion mining based on fuzzy domain ontology and Support Vector Machine: A proposal to automate online review classification. *Appl. Soft Comput.* **2016**, 47, 235–250.

A Measurement Analysis of Website Attackers Using Onionbots

R. Ranjith kumar¹, A. Pradeep², S. Ajith Kumar³
 Mrs. D. Pauline Freeda⁴, Associate Professor/CSE
 St. Anne's College of Engineering and Technology^{1, 2, 3, 4}

Abstract

The Onion Router (Tor) is one of the significant organization frameworks that give mysterious correspondence and restriction circumvention. Peak empowers its clients to ride the Internet, talk, and send messages namelessly; be that as it may, digital assailants additionally misuse the framework for dodging crime identification. As of late, different methodologies that forestall or moderate maltreatment of Tor have been proposed in the writing. This paper, which presents one of the methodologies, addresses an IP traceback issue. In our model, onion switches that deliberately take an interest in assailant following recognize assault bundles recorded in the log les by offering essential data to an assaulted worker over an Ethereum blockchain network. The discovery calculation in this paper utilizes the insights of parcel travel furthermore, transfer times and yields assault parcel competitors. The proposed strategy appends a dependability degree to every competitor, which depends on the upper limits of its Type I and II blunder rates. A savvy contract running on the blockchain network positions the discovery results from onion switches as per the unwavering quality degrees.

Keywords: *Tor, Onion bots, Ip traceback, blockchain*

1 Introduction

Tor Network is free and open-source software for enabling anonymous communication by directing Internet, worldwide. The Tor Browser automatically starts Tor background processes and routes traffic through the Tor network. Upon termination of a session the browser deletes privacy-sensitive data such as HTTP cookies and the browsing history. Onion routing is a technique for anonymous communication over a computer network. In an onion network, messages are encapsulated in layers of encryption, analogous to layers of an onion. The Onion Router (Tor) is a broadly utilized overlay organization that gives low-inertness mysterious correspondence for transmission control convention applications and bypasses different restriction measures. As per Pinnacle Metrics, the Tor network right now comprises of something else than 6,000 onion switches, has a huge number of straightforwardly interfacing clients, and conveys many Gbit/s. Pinnacle, be that as it may, has been man handled by illicit administrations, for example, the notorious Silk Road and the Crypto Locker ransomware order also, control workers. It was accounted for in that some onion switches are malevolent and perform man-in-the middle, organized inquiry language (SQL) infusion, furthermore, cross-site scripting (XSS) assaults. As of late, different ways to deal with keep up the wellbeing of the Tor network have been talked about in the writing. Past investigations were centered around impeding traffic, switches, or concealed workers that are viewed as noxious. This paper, interestingly, thinks about an Internet convention (IP) traceback issue over the Tor organization to look for the law breakers who set off an assault.

In our model, volunteer onion switches research the IP address of the aggressor's machine related to the assaulted workers. We anticipate that effective examinations empowered by our plan will be a solid impediment to assaults regardless of whether it is just some what sent in the Tor organization. IP traceback issues have been seriously considered, specifically for countering denial of-administration and conveyed forswearing of-administration assaults. As indicated by, most of Tor research has been given to deanonymization, the plan of a breaking procedure. Deanonymization dependent on traffic examination is fairly like our methodology. From the point of view of assailants, the objective of deanonymization is to boost the achievement rate of connecting a source and an objective of any correspondence. In light of the viewpoint of a criminal examination, our approach coherently limits the possibility for assault bundles, parcels conveying the assailant's code or information, based on the proof leftover on the casualty worker. Subsequently, our approach may not recognize a solitary competitor however it does significantly decline the recognition blunder rates.

The reason of our methodology is not the same as that of traffic examination based deanonymization in that:

- 1) The methodology is centered around a specified correspondence, where an accomplice of the correspondence is a casualty worker, though foes all in all assault interchanges unpredictably.
- 2) To limit the impact on the Tor framework and clients, the approach modifies neither the Tor programming nor the Tor convention, though foes may do as such.
- 3) The methodology can get uphold from the person in question worker, while enemies could never get this uphold.
- 4) The methodology thinks about the security of Tor clients, though foes don't.

In our model, assaulted workers and switches structure an Ethereum blockchain network, in which a savvy contract, called assailant following (AT), goes about as an aggressor following supervisor that gets episode reports

from assaulted workers furthermore, identification reports from switches. Every discovery result incorporates an unwavering quality degree, which depends on the upper limits of Type I and II blunder rates. We utilize blockchain innovations, which check for log information phony and keep up the following cycles completely to guarantee no spillage of Tor clients' private data happens. The way toward following assailants comprises of two stages: learning and identification. Switches gather tests of parcel travel and hand-off occasions in the learning stage. The examples are then utilized in the recognition stage to distinguish assault parcels in the switch's log file.

2 Related Work

Since the initiation of the Tor framework, numerous deanonymization approaches dependent on traffic examination have been created. Traffic-examination assault strategies can be classified into two gatherings: inactive and dynamic. In the dynamic (detached) technique, aggressors (don't) adjust traffic designs. There exist two well known detached traffic-investigation assaults. To begin with, the Website fingerprinting assaults [17], [18] construe which Webpage a customer is visiting by distinguishing traffic designs that are special to the Website page. This strategy is viewed as successful when onion locales are recognized from standard destinations [17]. In this paper, it was not expected that the assaulted workers create trademark traffic. The methodology introduced in this paper distinguishes two bundles, a solicitation and a reaction, that are specific, not a row of unspecified numerous bundles. An extra assault exists called profound parcel review, which investigates in detail the information being shipped off describe the traffic, convention, also, application. Our methodology likewise investigates parcel fields, for example, the TCP push flag and time-stamps (TS) alternative, to limit the assault bundle applicants. In the interim, approaches exist that forestall or alleviate misuse of Tor. In [8], the creator talked about the countermeasures that forestall endeavors to arrive at the onion locations of C&C workers, for example, that of evade running as a Tor onion administration. The creators of [9] proposed a framework called Tor Ward, which was intended to find and group vindictive traffic over Tor utilizing an interruption recognition framework (IDS). In [7], the viability of nectar onions (H Onions) workers, which recognize and distinguish getting out of hand and sneaking around shrouded administration registries, was accounted for. Torpolice, a protection safeguarding access control system, empowers specialist organizations to deny access strategies against demands coming from Tor [10]. Compliant is a pluggable vehicle that permits Tor traffic to be covered up in the foundation traffic. To upgrade the chance of checking criminal operations over Tor, a docile based traffic identification strategy was proposed in [11]. This anticipation or on the other hand moderation approaches are centred around identifying noxious traffic or Tor segments, while this paper considers the issue of following back assault parcels to their birthplaces. The IP traceback issue is denied as distinguishing the real wellspring of any parcel sent across the Internet. Different methodologies have been proposed also, late examinations were centred particularly around DDoS assaults utilizing Internet of Things (IoT) gadgets [12]. Presently, there are six primary classes of IP traceback techniques: connect testing, informing, stamping, logging, overlay, and design examination. None of these can be applied to the model in this paper for three reasons. In the first place, since messages in the Tor network are encoded with different layers of encryption, it is difficult to relate parcel substance saw at onion switches with those noticed at the objective host. As needs be, checking, informing, and logging approaches that utilization bundle substance for identification is pointless. Second, Tor isn't an organization overseen by one association, and subsequently moves toward that accept participation between numerous switches, for example, interface testing and overlay, can't be utilized. Third, approaches requiring many assault parcels, for example, connect testing and example examination, are definitely not accessible. Our model accepts aggressors send one message and get one reaction.

3 Proposed Work

Pinnacle is a low-inactivity namelessness network dependent on an idea called onion directing, which works as follows. A customer who introduces an onion intermediary, an interface between a customer and the Tor organization, downloads onion switch data from a registry worker and picks three switches to build up a circuit. The first, second, and third switches are known as the passage, center, and leave switches, individually. Parcels from the customer to a worker go through the circuit. The customer sends bundles that are scrambled with numerous layers of encryption utilizing keys haggled between the customer and every switch. As bundles travel along the circuit, every switch takes off one layer of encryption. This layered encryption guarantees that every switch knows the personalities as it were of switches that are straightforwardly associated in the circuit. Concurring to [15], to counter traffic connection assaults, no two switches are browsed a similar family gathering to make a circuit. Now and again, a scaffold is presented as a shrouded section switch to oppose control further. Ethereum is the second-biggest cryptographic money stage on which clients broadcast exchanges (information parcels endorsed with their private keys). Ethereum and Bitcoin [16] are comparative in that distributed (P2P) innovation keeps a blockchain, a developing rundown of exchange records that are connected utilizing cryptography, through the opposition of tackling computationally escalated issues. While Bitcoin blockchains

are concerned distinctly with exchanges between client wallets, Ethereum blockchains present decentralized figuring conditions called Ethereum Virtual Machines (EVMs), on which shrewd agreements (stateful decentralized applications) can run. Two kinds of records exist in Ethereum: client accounts constrained by clients and agreement accounts controlled by shrewd agreements. Brilliant agreements act in a similar way as self-ruling specialists.

In Tor network, criminals can trigger the various attacks in smart contract block. We proposed a method to trace the website attacker and overcome the IP traceback problem using onion router's log file. The client i communicate with Server i via a bridge. Bridge is a private entry router and is used for controlling the volume of traffic passing through an entry router. The bridge, Client i and Server i execute the network time protocol for clock synchronization and TCP dump for recording the timestamps and contents of packets. In the past few years, Tor and hidden services have become increasing popular among privacy-concerned users. Specially, after revelations about large scale surveillance and data collection efforts by governments and corporations, more people are taking steps to protect their privacy online. Additionally, some users rely on Tor to evade censorship by ISPs and authorities to have free access to information. The privacy and security protections that Tor provides, have attracted a large variety of users. For example, many legitimate users such as journalists, activists, and ordinary people use Tor to practice their right of privacy. Many mainstream services such as DuckDuckGo search engine, the New York Times, and Facebook, already have a presence on Tor. At the same time, Tor's protections have also attracted illegal and malicious actors. For instance, ransomwares are a trivial subversion of basic cryptography primitives and cryptocurrencies such as Bit-coin. Botnets or online marketplaces for illegal drugs and contraband are other examples of abuse and subversion of privacy infrastructures.

3.1 System Architecture

We study the lifespan of hidden services in a privacy- preserving manner to gain more insight into the dynamics of hidden services, without compromising the Tor's safety and privacy standards. In the following we introduced these in three aspects. The Tor relays' bandwidth capability is at around 200 Gb/s, yet only 60% of this capacity is utilized. As the number of relays that participate in Tor network increases, the bandwidth capability of the Tor network also increases. The underutilized capacity of the Tor network at- tracts abuse from malicious actors. Specially, considering the privacy and security protection capabilities of the Tor network, combined with its bandwidth capacity, we are content that the next generation of botnets, which we call Onion Bots, will subvert and abuse Tor. Current detection and mitigation of botnets, heavily rely on IP-based network properties and DNS trace. However, Tor is an overlay network that operates independently from most Internet protocols. Therefore, these approaches do not work in the Tor network, and are not effective against Onion Bots. Besides using Tor and hidden services to protect communication channels, Onion Bots can achieve a low diameter and a low degree and be robust to partitioning under node.

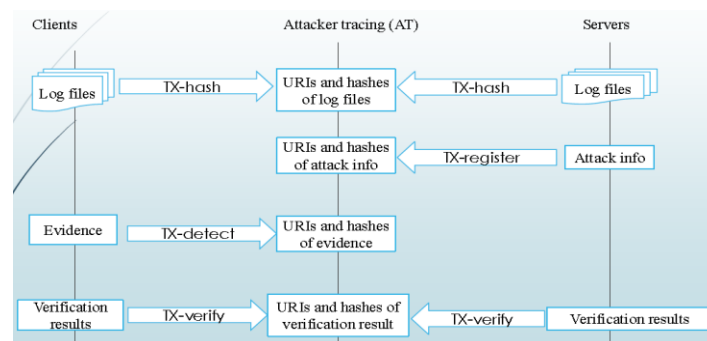


Figure 1: System Architecture Diagram

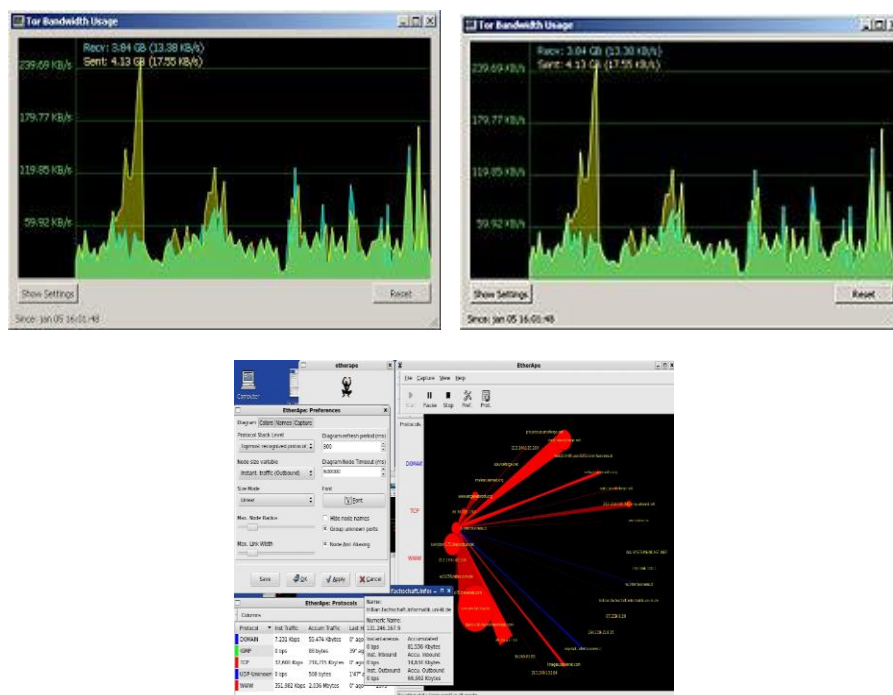
The victim server publishes a TX-register that contains the URI and the hash cost of the assault facts log files, which includes T2, T3, and a TCP port quantity of the server for sampling. Each co-operator then selects a patron that generates HTTP packets to the TCP port to pattern journey instances etc. To prevent log files forgery, the patron should ship TX-hash transactions during the sampling period. After calculating attack-packet candidates, every co-operator publishes a TX-detect that consists of the URI and the hash cost of the evidence, which consists of 4 times tamps T_r (pkt1), T_s (pkt2), T_r (pkt3), and T_s (pkt4) (which represent an attack-packet candidate) and reliability ranges of all candidates. The attacked server and co-operators can verify the proof and ship TX-verify transactions, including the URIs and the hash values of their very cation results. The most dependable candidates need to be veried. In the very cation process, the usage of log statistics that every co-operator or the server regionally possesses, it is checked that the proof is not logically in consistent. To keep away

from false superb and false negative errors, the proof ought to be cautiously varied from many distinct view points. The following explicates why the Ethereum technologies are used.

1. They routinely confirm and preserve the integrity of share information (the log files, assault information, evidence, and very cation results). When AT receives atranes action, it usually verifies the hash values in the transaction.
2. They assist forestall a server from forging a cyberattack incident. Contract AT tests two signatures in a TX-register: the digital signature of the server and the signature of a 1/3 birthday celebration who ensures the correctness of the assault information.
3. They enable all co-operators to examine at any time the tracing techniques of all previous incidents in their entirety. Cooperators can usually take a look at whether or not private ness violations occurred.

4 Results

In this paper, we proposed a packet detection approach, in which an entry router's onion bots is analysed to determine the packets that correspond to a request and response pair found on the server. The software scope of his method may additionally be enlarged and its detection accuracy improved by way of adding, deleting, or altering the conditions given in Problems 1 and two If the detection of solely an HTTP request message is required, the strategy can be adapted to this requirement with the aid of deleting all the stipulations associated to packets pkt3 and pkt4 in the problems. If the HTTP response consists of more than one IP packets, the method is superb after conditions that pick out one packet, e.g., the is packet, from the packet team are added. This is rendered feasible by checking the TCP sequence numbers. Furthermore, according to the Type I error price may additionally be similarly decreased by adding greater prerequisites to Problem 2. Ours strategy may also no longer require many onion routers to be co-operators. This is due to the fact the listing servers can provide information to consumers such that the consumers pick co-operators as their entry routers with a excessive likelihood.



5 Conclusion

We have up to this point examined methods for recognizing assailants parcels that might be recorded in an onion switch's log file with sufficiently low mistake rates and without trading off Tor clients' security. Our methodology was to limit the identification blunder rates as opposed to boost the recognition achievement rate. Subsequently, our methodology may not yield a solitary up-and-comer. We analysed and concluded the following points: (1) Attacked workers and co-operators, i.e., switches that intentionally consent to follow assailants, structure an Ethereum organization, wherein open furthermore, sealed blockchain advances forestall the duplicating of proofless and permit Ethereum members to screen the following cycles of all episodes completely. (2) Before performing assault parcel identification, co-operators gather travel and transfer time tests with the help of the

assaulted worker. (3) Each discovery result incorporates an unwavering quality degree that depends on its mistake rates, and accordingly, savvy contract AT can rank the location results announced by co-operators.

References

- [1] R. Dingledine, N. Mathewson, S. Murdoch, and P. Syverson, "Tor: The Second generation onion router (2014 DRAFT v1)," Cl. Cam. Ac. Uk, 2014.
- [2] M. Casenove and A. Miraglia, "Botnet over tor: The illusion of hiding," in Proc. 6th Int. Conf. Cyber Conict, Jun. 2014, pp. 273282.
- [3] A. Sanatinia and G. Noubir, "OnionBots: Subverting privacy infrastructure for cyber attacks," in Proc. 45th Annu. IEEE/IFIP Int. Conf. Dependable Syst. Netw., Jun. 2015, pp. 6980.
- [4] N. Christin, "Traveling the silk road: A measurement analysis of a large anonymous online marketplace," in Proc. 22nd Int. Conf. World Wide Web, 2013, pp. 213224.
- [5] D. Gonzalez and T. Hayajneh, "Detection and prevention of crypto ransomware," in Proc. IEEE 8th Annu. Ubiquitous Comput., Electron. Mobile Commun. Conf. (UEMCON), Oct. 2017, pp. 472478.
- [6] A. Sanatinia and G. Noubir, "H onions: Towards detection and identification of misbehaving tor hsdirs," in Proc. Workshop Hot Topics Privacy Enhancing Technol. (HotPETs), 2016, pp. 12.
- [7] N. Hopper, "Protecting Tor from Botnet abuse in the long term," The Tor Project, Seattle, WA, USA, Tech. Rep. 201311-001, 2013.
- [8] Z. Ling, J. Luo, K. Wu, W. Yu, and X. Fu, "Torward: Discovery, blocking, and traceback of malicious traffic over tor," IEEE Trans. Inf. Forensics Security, vol. 10, no. 12, pp. 25152530, 2015.
- [9] Z. Liu, Y. Liu, P. Winter, P. Mittal, and Y.-C. Hu, "TorPolice: Towards enforcing service-denied access policies for anonymous communication in the tor network," in Proc. IEEE 25th Int. Conf. Netw. Protocols (ICNP), Oct. 2017, pp. 110.
- [10] Z. Yao, J. Ge, Y. Wu, X. Zhang, Q. Li, L. Zhang, and Z. Zou, "Meek-based tor traffic identification with hidden Markov model," in Proc. IEEE 20th Int. Conf. High Perform. Comput. Commun., Jun. 2018, pp. 335340.
- [11] B. Cusack, Z. Tian, and A. K. Kyaw, "Identifying dos and ddos attack origin: Ip traceback methods comparison and evaluation for iot," in Interoperability, Safety and Security in IoT. Cham, Switzerland: Springer, 2016, pp. 127138.
- [12] S. Saleh, J. Qadir, and M. U. Ilyas, "Shedding light on the dark corners of the Internet: A survey of tor research," J. Netw. Comput. Appl., vol. 114, pp. 128, Jul. 2018.
- [13] V. Buterin, "Ethereum: A next-generation cryptocurrency and decentralized application platform," Bitcoin. Mag., vol. 23, p. 252, Oct. 2014.
- [14] A. Sanatinia, "Abusing privacy infrastructures: Case study of tor," Ph.D. dissertation, College Comput. Inf. Sci., Northeastern Univ., Boston, MA, USA, 2018.
- [15] S. Nakamoto, "Bitcoin: A peer-to-peer electronic cash system," Manubot, Tech. Rep., 2019. <https://git.dhimmel.com/bitcoinwhitepaper/>
- [16] A. Kwon, M. AlSabah, D. Lazar, M. Dacier, and S. Devadas, "Circuit finger printing attacks: Passive deanonymization of tor hidden services," in Proc. 24th Secur. Symp., 2015, pp. 287302.
- [17] G. Cherubin, J. Hayes, and M. Juarez, "Website fingerprinting defenses at the application layer," Proc. Privacy Enhancing Technol., vol. 2017, no. 2, pp. 186203, Apr. 2017.

Secure Scheme for Medical Image Storage in Cloud

R. Sangeetha¹, K. Aswini², E. Kanniyammal³
Mrs. D. Pauline Freeda⁴, Associate Professor/CSE
St. Anne's College of Engineering and Technology^{1, 2, 3, 4}

Abstract

Nowadays, medical care establishments depend on clinical imaging in the analysis of clinical cases, where there are colossal measures of clinical imaging information that are produced every day. A portion of these cases are needed to be divided between numerous specialists for teleconsultation or tele-conclusion purposes. The dependence on the nearby stockpiling frameworks doesn't ensure the accessibility of adequate stockpiling zones. Hence, the distributed storage innovation is presented that gives versatile capacity online access office. Nonetheless, far about that, information putting away in the cloud brings numerous security issues. Thus, in this paper, the cloud based framework is proposed for putting away and sharing the clinical pictures in secure way. The proposed framework dependent on number of cryptography methods to make better security for the clinical pictures over the transmission connect and on the cloud. Elliptic Curve Cryptography (ECC), Advanced Encryption Standard (AES), and Secure Hash (SHA-3) calculations are utilized here. For limiting the calculation over-burden on the customers' gadgets, the outsider examiner is utilized for checking clinical pictures respectability and legitimacy prior to putting away it in cloud.

Keywords: *Cloud, medical image, ECC, AES, SHA*

1 Introduction

Nowadays, with the enormous utilization of new advances in medical care frameworks, the customary techniques for managing wellbeing related data become more effective. The imaging devices are the foundation of clinical diagnosing and the premise in the accompanying up of the improvement of infection cases. The Massive number of clinical pictures created every day in the medical services establishments needed to be put away and chronicled. Consequently, medical services organizations search for answers for abrogate the expanded requests for giving colossal stockpiling frameworks. This discloses the need to give enormous scope stockpiling frameworks. Likewise, the sharing of clinical pictures among the specialists in other medical services establishments has become a fundamental piece of teleconsultation measures. This prompts another difficult that is a requirement for specialized and reasonable help for sharing the clinical information safely. To defeat these issues, as of late, distributed computing is created in medical services associations. Public Institute of Standards and Technology (NIST) needs to characterize distributed computing as another method for actualizing and creating IT administrations.

Presently, numerous clinical applications are constructed utilizing this worldview. Right now, distributed storage addresses the best obvious help offered by distributed computing. It very well may be considered as a help model that can give distant information putting away, overseeing, . In like manner, the fundamental preferences offered by distributed storage in putting away the information on available dispersed workers and limiting the capacity necessities on the association's frameworks are driven medical services associations to receive the distributed storage in the improvement of their frameworks. Regardless of utilizing distributed storage in medical care frameworks prompts increment profitability and productivity, however it experiences the issues of information security and protection that are the principle challenges that are confronting the embracing of distributed storage in medical services frameworks. Medical services establishments stress that information is unprotected while putting away it distantly. There's continually the chance that the information are revelation or alter. So the goal is to assemble a security component for putting away and sharing the clinical information in the cloud framework.

Numerous security boundaries like privacy, information possession, respectability, validation, and access control ought to be considered in the plan of medical services frameworks over the cloud. Different specialists proposed various answers for use distributed storage in medical care frameworks. A significant number of them attempted to lessen the security chances in the information stockpiling while at the same time overlooking them in the transmission. A few investigations have shown the significance of utilizing distributed storage in medical care frameworks. By creating cloud frameworks, a minor pace of capacity, handling, and refreshing could be given. However, information security and transmission transfer speed in cloud climate stay an open issue. Proposed a cloud-based framework to permit collaboration among specialists. In this plan, the two specialists and patients can store and share clinical pictures over the distributed storage. This is finished by copying and rehashing information across a few workers. Secret key and login ID are needed for individuals' validating. Security and protection necessities are restricted to this system. Along these lines, it is vital for the information to be moved in the protected channel, as recommended by the, they proposed a cloud-based structure to store clinical pictures

safely. TLS is utilized to make a safe connection between the cloud supplier and customers. Private and public certificates are utilized for both cloud supplier and clients. The public encryption calculation is utilized for information encryption. recommended the utilizing of lossless pressure and symmetric encryption to give a safe technique to medical image capacity to build participation among specialists. The symmetric calculation is accustomed to scrambling the packed picture for ensuring patients' information. The utilizing of numerous cryptography calculations in the clinical pictures getting was additionally investigated as in the where the analysts recommended cloud-based secure system for clinical information sharing utilizing a hybrid methodology depends on cryptography and factual examination advancements. Patients' clinical information are divided and encoded to improve security and protection. Another arrangement was for information dividing between medical services experts. This recommendation depends on Attribute Based Encryption (ABE) to characterize the customers that can have access to recorded ascribes. DSA and SHA-1 calculations are utilized for clinical records getting. SHA-1 is utilized to perceive a particular advanced record in the multi-cloud circumstance. assessed security targets for clinical information. They dependent on reversible watermarking to guarantee both respectability and authentication. Access control and detectability are fulfilled by the Central Authority (CA) and Organization Based Access Control (OrBAC). To protect information privacy, the AES calculation was utilized. In [20], the creators proposed cloud-based authentication framework utilizing biometric unique finger impression and digital signature to guarantee the security of clinical information. Symmetric and lopsided encryption and advanced mark are utilized. They guarantee information security, respectability, and privacy over the cloud.

2 Existing Work

In existing framework, the creators proposed a calculation for scrambling and recovering the clinical picture dependent on DWT and DCT. It utilizes recurrence encryption with calculated tumult encryption. On the opposite side, the specialists planned a system to store the clinical picture safely. Information division and watermarking are utilized to ensure information security. A trusted third party called CloudSec is utilized as a protected interface among clients and cloud suppliers. In a particularly model, clinical information is shipped off the CloudSec through SSL for keeping security during information move. CloudSec worker keeps patients' recognizing information in a neighborhood data set, and afterward, sends these advanced records to the cloud stockpiles. At last, the proposed a getting strategy for clinical records admittance to be utilized for serving crisis cases adequately. Patient's cell phone and believed outsider are utilized for clinical information retrieval measure. The patient's cell phone sends the suitable cryptographic keys to enacting the re-encryption measure in the cloud.

Security and protection necessities are restricted to this system. Along these lines, it is vital for the information to be moved in the protected channel, as recommended by the, they proposed a cloud-based structure to store clinical pictures safely. TLS is utilized to make a safe connection between the cloud supplier and customers. Private and public certificates are utilized for both cloud supplier and clients. The public encryption calculation is utilized for information encryption. recommended the utilizing of lossless pressure and symmetric encryption to give a safe technique to medical image capacity to build participation among specialists. The symmetric calculation is accustomed to scrambling the packed picture for ensuring patients' information. The utilizing of numerous cryptography calculations in the clinical pictures getting was additionally investigated as in the where the analysts recommended cloud-based secure system for clinical information sharing utilizing a hybrid methodology depends on cryptography and factual examination advancements. Patients' clinical information are divided and encoded to improve security and protection. Another arrangement was for information dividing between medical services experts. This recommendation depends on Attribute Based Encryption (ABE) to characterize the customers that can have access to recorded ascribes. DSA and SHA-1 calculations are utilized for clinical records getting. SHA-1 is utilized to perceive a particular advanced record in the multi-cloud circumstance. assessed security targets for clinical information. They dependent on reversible watermarking to guarantee both respectability and authentication. Access control and detectability are fulfilled by the Central Authority (CA) and Organization Based Access Control (OrBAC). To protect information privacy, the AES calculation was utilized. In [20], the creators proposed cloud-based authentication framework utilizing biometric unique finger impression and digital signature to guarantee the security of clinical information. Symmetric and lopsided encryption and advanced mark are utilized. They guarantee information security, respectability, and privacy over the cloud.

3 Proposed Work

Our commitment depends on guaranteeing the security of the clinical picture not in the cloud just but rather besides on the transmission moreover. In this paper, the cloud-based framework is proposed for getting clinical pictures in the distributed storage and over the transmission channel. The proposed plot dependent on symmetric and lopsided encryption strategies (Advanced Encryption System (AES), Elliptic bend cryptography (ECC)) and

cryptographic hash work (SHA-3) to ensures security administrations for the clinical pictures during its transmission and capacity. The recommended framework utilizes Third Party Auditor (TPA) that goes about as a moderate between the customers and distributed storage for checking information security prior to putting away it in the cloud. This is for decreasing the computational burden on the customers' machine. Here, the computerized mark is utilized to demonstrate information verification regarding validness and uprightness. Additionally, the framework grants specialists to impart clinical cases to validated specialists. Here the public key of the proposed specialist is utilized for information encryption to ensure the common picture will be seen by the planned specialist simply because there is none possesses the private key of the expected specialist aside from him.

Making the clinical pictures accessible online on the cloud workers as they are caught. With no component for guaranteeing clinical information, protection, and trustworthiness will make a ton of stress to both the specialist and the patient. The proposed framework gives secure component to clinical pictures putting away and sharing through relying upon the different encryption methods to guarantee the security of clinical pictures in the transmission and over the cloud. Be that as it may, the total framework comprises of seven phases. Individuals Authentication: In request to control the admittance to the framework benefits, the clients first need to enroll and give the necessary data to be legitimate for the framework. For every part, part's endorsement will make that contains part's broad data and access information (login ID/secret word). The steps followed in the proposed system is given in Figure 1.

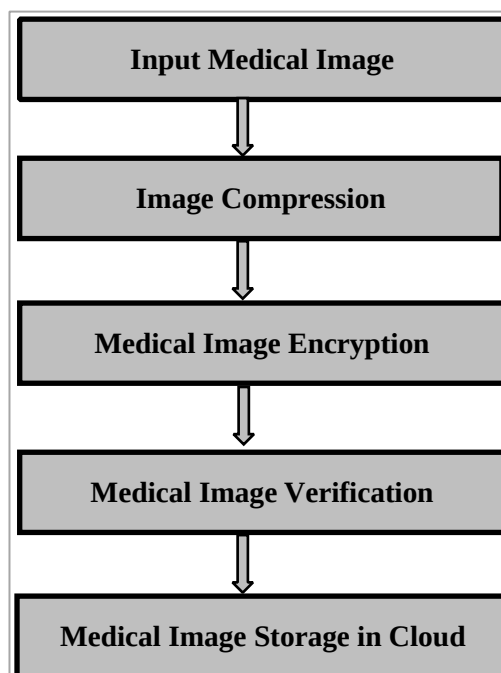


Figure 1 : System Architecture Diagram

Encryption Keys Generation: ECC will be utilized for producing of blend of public and private keys. customer has two encryption keys: the private key and the public key that is available with others. TTPA has three keys that are: the private key, public key, and symmetric key that is utilized in AES encryption.

Keys Distribution: Public keys are divided between customers and TTPA over a safe connection. In shared mode, the beneficiary public key is needed for information encryption.

Clinical Images Encryption: in the recommended plot, the clinical picture is scrambled twice: first in picture proprietor side and afterward in TTPA prior to putting away it in CSP. Thus, number of strategies are utilized for giving security that are ECC, AES, and SHA-3.

Clinical Images Verification: In this stage, clinical pictures honesty, privacy and genuineness ought to be checked to confirm if the information was hacked in the transmission or the distributed storage.

Clinical Images Storage: In the CSP, every part will give two segments that are private and shared area. Clinical pictures are put away in these segments.

Clinical Images Retrieval: Images documents put away in the CSP workers were scrambled, with the goal that it ought to be unscrambled prior to conveying it.

4 Results

The brain image is taken as input and process the image. Then the keys are generated and applied AES and ECC algorithm to encrypt the image. At the receiver end, the encrypted image is decrypted. The input and output images are given below.

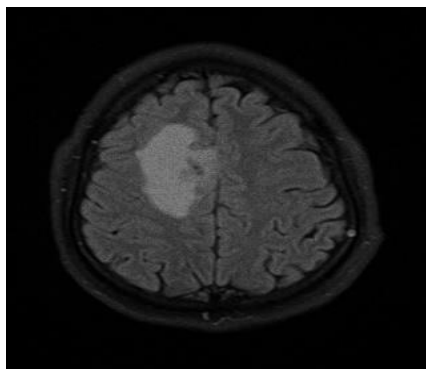


Figure 2 : CT Brain Image

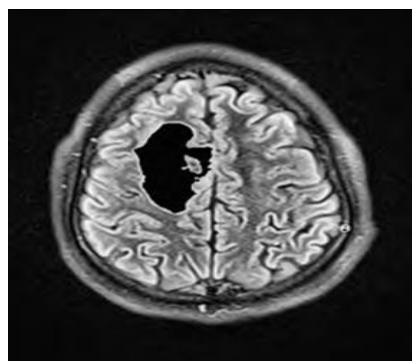


Figure 3: Enhanced Input Image

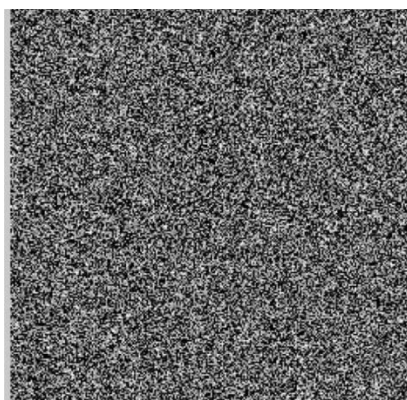


Figure 4 : Encrypted Image

5 Conclusion

The immense benefits of distributed storage frameworks like expense decrease, versatility, accessibility, energy utilization, and a greater amount of that make it alluring in the advancement of medical care frameworks. The dependability and effectiveness of the cloud-based frameworks have been influenced by different difficulties. Information security and protection concerns are the major testing issues in distributed storage frameworks that should be addressed. The proposed framework gives a security component to clinical pictures putting away and sharing over the cloud with the assistance of ECC, AES, and SHA-3 calculations. The proposed instrument confirms the privacy and honesty of the clinical information in the transmission and the capacity just as the confirmation of both the information and its source. The clinical information is communicated uniquely as encoded information over the transmission connect, which handles the issues of information secrecy and trustworthiness. Information is scrambled twice utilizing proprietor and TTPA keys. Along these lines, even TTPA and CSP can't revelation the information. The investigation and assessments showed that the framework could protect the security of clinical information with least calculation and capacity overhead. Information check measures are accomplished in TTPA will die down the calculation over-burden needed in the customers. Also, ECC is utilized here on the grounds that it diminishes the calculation cost as contrasted and RSA and can give a similar security more modest keys and more limited calculation time.

References

- [1] P. Mell and T. Grance, "The NIST definition of cloud computing" Tech. Rep. National Institute of Standards and Technology, 2009.
- [2] Shini.S.G, Dr. Tony Thomos, Chithraranjan .K, "Cloud Based Medical Image Exchange-Security Challenges", Elsevier, *Procedia Engineering* 38,2012, pp. 3454-3461
- [3] Y. Huo, H. Wang, L. Hu, and H. Yang, "A cloud storage architecture model for data-intensive applications", *IEEE International Conference on Computer and Management (CAMAN)*, 2011, pp. 1–4.
- [4] J. Vincent, W. Pan, and G. Coatrieux, "Privacy Protection and Security in eHealth Cloud Platform for Medical Image Sharing", *2nd International Conference on Advanced Technologies for Signal and Image Processing-ATSIP'2016*, March 2016, Monastir, Tunisia.
- [5] M. Marwan, H. Ouahmane, and A. Kartit, "Design a Secure Framework for Cloud-Based Medical Image Storage", *ACM, Proceedings of the 2nd international Conference on Big Data, Cloud and Applications*, Tetouan, Morocco — March 2017.
- [6] A. K. Pandey, P. Singh, N. Agarwal, and B. Raman, "SecMed: A secure approach for proving rightful ownership of medical images in encrypted domain over cloud", *IEEE Conference on Multimedia Information Processing and Retrieval*, 2018.
- [7] M. Ali, S. U. Khan, and A. Vasilakos, "Security in cloud computing: Opportunities and challenges," *Info. sciences*, vol. 305, 2015.
- [8] A. Tchernykh, U. Schwiegelsohn, E. Talbi, and M. Babenko, "Towards understanding uncertainty in cloud computing with risks of confidentiality, integrity, and availability," *Journal of Computational Science*, 2016.
- [9] D. S. Chauhan, A. Adarsh, B. Kumar, R. Gupta and J. P. Saini, "Double Secret Key Based Medical Image Watermarking for Secure Telemedicine in Cloud Environment", *IEEE 40th International Conference on Telecommunications and Signal Processing*, 2017.
- [10] A. Abbas, "E-Health cloud privacy concerns and mitigation strategies", *Medical Data Privacy Handbook*, Springer, pp. 389-421, 2015.
- [11] B. Fabian, T. Ermakova and P. Junghanns, "Collaborative and secure sharing of healthcare data in multi-clouds", *Information Sciences*, Elsevier, 2014.
- [12] Chia-Chi Teng and et.al., "A medical image archive solution in the cloud," *Proceedings of IEEE International Conference on Software Engineering and Service Sciences (ICSESS)*, Beijing, China, 2010.
- [13] C. Viana-Ferreira and C. Costa, "A cloud based architecture for medical imaging services" *IEEE 15th International Conference on e-Health Networking, Applications and Services (Healthcom)*, 2013.
- [14] A. Bahga and V. K. Madiseti, "A Cloud-based Approach for Interoperable Electronic Health Records" *IEEE Journal of Biomedical and Health Informatics*, VOL. 17, NO. 5. 2013.
- [15] C. Yang, L. Chen, W. Chou, and K. Wang, "Implementation of a medical image file accessing system on cloud computing", In *Proceeding of the 13th IEEE International Conference on Computational Science and Engineering (CSE)*, 2010,321-326.
- [16] T. Rostrom and Ch. Teng, "Secure communications for PACS in a cloud environment". In *Proceeding of the 33rd IEEE International Conference of the IEEE EMBS Boston, USA*, 2011, 8219-8222.
- [17] I. Hossain and K. Chellappan, "Collaborative compressed i-cloud medical image storage with decompress viewer", In *Proceeding of the International Conference on Robot PRIDE, Procedia Computer Science* 42, Elsevier, 2014, 114–121.
- [18] J. Yang, J. Li and Y. Niu, "A hybrid solution for privacy preserving medical data sharing in the cloud environment." *Future Generation Computer Systems*, Elsevier, 2014.
- [19] W. PAN, G. Coatrieux, D. Bouslimi and N. Prigent, "Secure public cloud platform for medical images sharing." *Studies in Health Technology and Informatics*, Vol. 210, 2015, 251-255.
- [20] C. Chen, J. Hu, C. Fan, and K. Wang, "Design of a secure medical data sharing system via an authorized mechanism", *IEEE International Conference on Systems, Man, and Cybernetics' SMC 2016'* Budapest.
- [21] C. Zhang, S. Wang, J. Li, and Z. Wang, "An Encrypted Medical Image Retrieval Algorithm Based on DWT-DCT Frequency Domain", *IEEE 15th International Conference on Software Engineering Research, Management and Applications (SERA)*, 2017.
- [22] K. Rabieh, K. Akkaya, U. Karabiyik, and J. Qamruddin, "A Secure and Cloud-based Medical Records Access Scheme for on-Road Emergencies", *15th IEEE Annual Consumer Communications & Networking Conference (CCNC)*, 2018.

A Subsystem for Network Traffic Analysis using Deep Learning

Bhuvaneswari G,
Department of Computer Science and Engineering
Sona College of Technology, Salem

Abstract

The application of classical machine learning (CML) and deep learning (DL) architectures are employed for network traffic data analysis and proposed scalable deep learning based framework. The Internet and its applications mainly peer-2-peer (P2P), voice over Internet protocol (VOIP), multi-media are following constant transformation. Thus, the patterns of traffic are very dynamic. This indicates that the traffic of present day protocols or applications is entirely different than the traffic of 2 years ago. The present day traffic may require either an additional feature sets or entirely new feature sets for machine learning based system to accurately identify the nature of the network traffic. The methods are widely growing applications and it can be future work for the Cyber Security researches

Keywords: *Deep Learning, peer-2-peer, voice over Internet protocol (VOIP), multi-media*

1 Deep Learning Framework for Network Traffic Analysis

1.1 Introduction

The network traffic is increasing exponentially. Identifying and monitoring network traffic is a significant task towards identifying the malicious activities. Most of the existing systems for network traffic identification are based on handcrafted features and they are inaccurate and easily evadable Fadlullah et al. (2017). Extracting optimal handcrafted features in feature engineering requires extensive domain knowledge and it is time-consuming approach. These methods are completely invalid for unknown protocol and applications. Thus, this work proposes DeepTrafficNet, a scalable framework based on DL which replaces the manual feature engineering with machine learned ones and these are harder to be fooled. The performance of various DL architectures are evaluated for 3 different network traffic use cases such as application network traffic classification, and malicious traffic detection with the public and privately collected data set. The performances obtained by various DL architectures are closer and moreover, the combination of convolutional neural network (CNN) and long short-term memory (LSTM) pipeline performed well in all the 3 network traffic use cases. This is due to the fact that CNN-LSTM has the capability to capture both spatial and temporal features.

The main aim of this work is as follows:

- Application of DL techniques is leveraged for traffic identification tasks such as application traffic classification, malicious traffic classification, and malicious traffic detection.
- To efficiently handle network traffic data in real-time, a highly scalable framework is constructed which has the capability to collect a very large amount of data and the capability can be increased by adding additional resources to the existing system architecture.

1.1.1 Description of the Data set

There are two types of data sets are used, one is privately collected data set named as Data set 1 and second one is UNSW-NB15¹. This is composed of 1 million bi-directional flows of application and malicious traffic. A network flow is a communication between two endpoints on a network. These endpoints exchange packets during the conversation. Packets are composed of two sections. One is the header section which provides information about the packet and the second one is payload which contains the exact message. A flow can be unidirectional or bi-directional. The data set was provided in packet capture (pcap) format from 22nd of January 2015 and 17th of February 2015. The samples of train and test data sets are disjoint. The most commonly used 5 applications are considered and remaining flows are labeled as unknown. Three different types of data sets are formed, one is for application network traffic classification, second one is for malicious traffic classification and

third one is for Malicious traffic identification. The data samples from 22 Jan 2015 are used for training and data samples from 17 Feb 2015 are used for testing and validation.

1.1.2 Proposed Architecture, Results and Observations

An overview of the proposed architecture, DeepTrafficNet for application traffic classification, malicious traffic classification, and malicious traffic detection is shown in Figure 8.1. This research work has developed a scalable framework to handle large amount of network traffic data and used distributed preprocessing, distributed database, and DL architectures for analysis. The framework composed of data set collection, preprocessing, classification section. This research work has used publically available data sets but the proposed framework has the capability to collect data inside an Ethernet LAN. Each flow contains information of length 1,000. This is passed into classification section. Classification composed of Autoencoder (AE) and DL architectures. AE facilitates to capture the important features. Finally, these features are passed into DL architectures for classification.

2 Network Traffic Prediction

2.1 Introduction

In modern society, the Internet and its applications have become a primary communication tool for all types of users to carry out daily activities. This can create a large volume of network traffic. Understanding the traffic matrix is essential for individual network service providers mainly due to the reason that their inferences are enormous. Traffic matrix provides the abstract representation of the volume of traffic flows from all possible sets of origin to a destination point in a network for definite time interval. The source and destination point can be routers, points-of-presence, Internet protocol (IP) prefixes, and links. Traffic matrix facilitates network service providers to make various network management decisions such as network maintenance, network optimization, routing policy design, load balancing, protocol design, anomaly detection, and prediction of future traffic trends (Fadlullah et al., 2017). A network service provider has to know the future trends of network parameters, routers, and other devices information in order to proceed with the traffic variability. To deal with the problem of predicting the future trends of network parameters, routers, and other devices information in real-time network traffic prediction approaches have been employed.

2.1.1 Description of the Data set

To evaluate the effectiveness of various RNN networks, FFN, and other classical methods, this research work uses the publically available and most well-known data set, GEANT backbone networks². The GEANT network includes 23 peer nodes and 120 undirected links. 2004-timeslot traffic data is sampled from the GEANT networks by 15 minute time interval. From the 10,772 traffic matrices, this research work chose arbitrarily 1,200 traffic matrices. Each traffic matrix TM is transformed to vector of size $23 \times 23 = 529$. These vectors are concatenated and formed a new traffic matrix TM of size 1200×529 TMV. The traffic matrix TM is randomly divided into two matrices such as training TMtrain 900×529 and TMtest 300×529 . There are various ways exist for predicting the future traffic. One way is to feed the vectors TMV in TM to prediction algorithms and predict one value of TMV at a time. This method was not correct due to the fact that the OD traffic is dependent on other ODs. Thus capturing the patterns exist in previous traffic can enhance the performance of prediction of traffic matrix. This research work uses the sliding window SW to create a training data set. This research work obtains $T S - SW + 1$ training records by sliding the window for the OD pair with T S time slots.

2.1.2 Proposed Architecture, Results and Observations

As LSTM network is a parameterized function, finding an optimal parameter have a direct impact on minimizing the mean squared error. Based on the hyperparameter approach, this research work selects the 5 layers with 500 units and learning rate 0.1 for all networks such as IRNN/GRU/LSTM/RNN to evaluate the performance on the

| Architecture | MSE |
|--------------|-------|
| FFN | 0.091 |
| RNN | 0.067 |
| LSTM | 0.042 |
| GRU | 0.051 |
| IRNN | 0.059 |

testing data set. This research work trains 3 models for each FFN/RNN/LSTM/GRU and IRNN using the training data of size 900*529. The performance of the trained model is evaluated on the test data of size 300*529. The detailed result is reported in Table. The deep learning architectures such as RNN, LSTM, GRU, and IRNN performed better than the classical neural network, FFN.

3 Secure Shell (SSH) Traffic Analysis with Flow Based Features using Shallow and Deep Networks

3.1 Introduction

Secure Shell (SSH) is a cryptographic network protocol which is primarily used for secure login to a remote computer. Additionally, it facilitates file transfers using SSH File Transfer Protocol (SFTP), Secure copy (SCP), tunneling, port forwarding, and so on. SSH traffic analysis is a challenging task mainly due to the reason that the underlying traffic is encrypted. Each SSH session allows users to run multiple services. These factors have made SSH traffic analysis more significant. It is very much required for many of the network management activities. In comparison to other applications, SSH reports a very less traffic. As a result, SSH produces a very imbalanced data set. Due to the encrypted nature in SSH traffic, protocol based mechanism cannot be employed. Port based method in SSH traffic produces higher error rates. To overcome this, in this work, flow based features with the classical ML and DL algorithms based system is developed for SSH traffic analysis.

3.1.1 Description of the Data set

Network monitoring solutions have largely relied on the idea of network flows. A flow is a sequence of network packets captured between two hosts. In this work, public traffic traces such as Defense Advanced Research Projects Agency (DARPA) 1999 Week1, DARPA 1999 Week3, Measurement and Analysis on the WIDE Internet (MAWI), National Laboratory for Applied Network Research (NLANR AMP) and private traffic trace such as Network Information Management and Security Group (NIMS) are used. Both public and private traces are obtained from³.

3.1.2 Proposed Architecture, Results and Observations

Hyper parameter tuning method is followed to find out optimal network parameters and network structure and proposed 8 layers RNN/LSTM network with 64 memory blocks architecture. RNN/LSTM 8 layers with 64 RNN units / 64 memory blocks, each memory block contains a single memory cell and learning rate as 0.1 was used and trained using the private data set such as NIMS. The trained model was evaluated on the public data sets such as AMP, MAWI, DARPA WEEK 1, and DARPA WEEK 3. The detailed empirical results of them are displayed in Table 8.4. Additionally, LSTM network was trained using the randomly selected samples of public data sets and the trained models are evaluated on the private data set. The results are consolidated in Table 8.3. Additionally, in all experiment configurations classical ML algorithms are evaluated and empirical results of them are displayed in Table 8.4. In all the experiments the deep learning based methods outperformed the classical methods based on ML.

4 Conclusions

In this work, the data preprocessing and feeding techniques of network traffic data to non-linear algorithms are discussed in detail. The performances of various non-linear algorithms are studied using GEANT backbone networks. The LSTM has performed well in comparison to the other RNN, IRNN, GRU, and FFN. However, the performance of both GRU and IRNN techniques is comparable to LSTM. Moreover, the GRU network has taken less computational cost in comparison to the LSTM networks. Overall, the proposed method has achieved the best performance by accurately predicting the traffic matrix. The discussed methods in the current work can be employed on these widely growing applications and it can be future work for the Cyber Security researches. The code and detailed results are made publicly available⁴ for further research.

5 References

- [1] Dave Larson. Distributed denial of service attacks—holding back the flood. *Network Security*, 2016(3):5–7, 2016.
- [2] Yann LeCun, Yoshua Bengio, and Geoffrey Hinton. Deep learning. *nature*, 521(7553): 436, 2015.

Integrated Level Aggregation Method for the Identification of Apps in Top Charts

R. Jeeva, N. Muthukumar

Abstract

Each platform of mobile devices has its own app store which is the source for apps, games, movies, books etc. The apps are categorized under predefined labels based on the rules formulated in app store. The apps have been ranked based on the ratings, reviews, downloads and no. of installs. It helps the user to download the top ranked app in a specific category. That ranking of an app makes them think that it will work better than others in an effective way. The evidence aggregation of the above attributes have less variation that doesn't reflect the current status of an app which influences the ranking. For that, the attributes that have been frequently changed due to developer and user actions to be collected for a specific category in top charts. The attributes includes version, last updated date, features of an app and keywords will undergo an independent process that produce the following levels: 1. Version change level, 2. Keyword matching level and 3. Feature matching level. Each value of a level have to be consolidated and aggregated to produce the final ranking of apps in a specified category. The actual ranking has been compared with the obtained ranking to find the deviation value and the false ranked app in the app store.

Keywords: *Evidence aggregation, Version change level, Keyword matching level, Feature matching level*

1 Introduction

Multihoming, a technique where a designer is distributing items for various platforms. Information assortment is in two stages. In the first stage, the scripts gather the novel identifiers of the applications which are generally well known in every category of the application store. In the second stage, the scripts gather the varied properties from the application's open sites at the application store. The assessment of multihoming application types was finished by breaking down their classifications in the application store. The level of accessible applications in every classification was determined and afterward contrasted with other application stores to spot the favored category alongside the mindful mobile application [1].

An integrated various leveled displaying approach has been utilized to quantify deals execution and affirm the outcomes with the utilization of the peril model and regression model. Application-level properties, for example, free application offers, high introductory positions, interest in less well-known categories, consistent quality updates, and high user survey scores impacts affect application manageability. Application-level investigation and vendor level examination has been performed with autonomous traits of an application which recognize the execution of the general deal of application sellers. It presumes that business execution was significantly higher for dealers while taking an interest in numerous classifications than something else. It didn't explicitly look at application explicit highlights or vender explicit attributes that may influence the positioning of an application [2].

Mobile application rating scale (MARS) is another tool utilized for evaluating the application regarding its predefined highlights communicated in a particular range. The application has been characterized by category dependent on the gathered unmistakable data, specialized viewpoints, target age gathering, and category explicit characteristics. The application quality conditions were grouped inside the commitment, usefulness style, data quality, and abstract quality classifications. The mean scores of above individual traits and generally speaking mean application quality complete score was resolved as the MARS scale. It has been widely grown distinctly for the wellbeing category to give a multidimensional proportion of an application [3].

Messaging applications are one of the most well-known applications for mobiles with a great many dynamic users. The specification gave by generally well known and business messaging applications has examined. After recognizing the significant applications, light and old renditions have been sifted through. The essential highlights of an application have been recognized by displaying activities like send a message to an individual contact, read and reply for the message, include a contact, erase contact, and discussion. The optional highlights of an application must be distinguished like user profile, sending pictures, sound, and video. Keystroke level displaying has been tried by tallying the no of communications to accomplish the above essential and optional highlights. Utilizing the heuristic assessment of the above-inferred values, ease of use issues has been raised of texting applications [5].

China is one of the biggest android markets where the users can't get to play store to purchase or introduce applications. For that, pre-introduced merchant explicit application markets and the number of autonomous application stores have developed. A review of an application incorporates gathering apk, different applications discharged by a similar designer, prescribed applications that are identified with it. At that point category, no. of downloads, min API level, outsider libraries included generally famous and publicizing categories with

application ratings are gathered. In the wake of sifting through the cloned applications, hash estimation of apk has been checked and named single-store or multistore dependent on its accessibility [4].

The rest of this paper is organized as follows. In Section 2, the evolution of app store optimization techniques has been discussed. Section 3 presents the architecture of the evidence aggregation system with different levels and its collection methods. Experiment results and analysis are shown in Section 4. The conclusions and further enhanced are given in Section 5.

2 Rank Evidence System

From the app store like Google Play, appland, amazon apps, the information about every top 10 applications in all the categories is collected using appbot. The information includes rating, review and ranking and each parameter will undergoes independent evaluation which will be consolidated later. In rating, monthly data has been collected and calculate successive difference them. The result will be checked against the threshold value which should be less than 1 set by the appbot. Those apps which have increase in ratings more than threshold value will be considered as negative. In review, the collected data will undergoes sentiment analysis using Word2Vec model which predicts the target word based on the weight assigned to them. It evaluates the review by splitting into tokens and undergoes stemming and stop word elimination processing. Then each word will be compared with the keyword base for retrieving its weight. The weights of matched words with a keyword base are summed to form a weight for a review. In ranking, categorize the data into rising phase, maintenance phase and recession phase to be passed for next stage. In evidence aggregation, all the results of three parameters are consolidated which determines the app's trustfulness in a store.

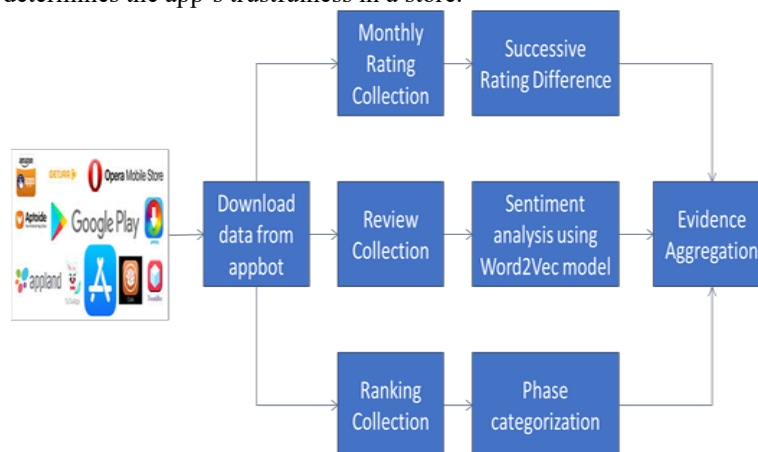


Fig 1. Aggregation of Ranking Evidence system

2.1 Data collection

The rating, review and ranking of an app will be collected from app store. Each app has its own id which can be used to refer in app store to retrieve the details like name, version etc. The rating and ranking is a definite value that indicates the status of the app in the store. But the reviews can't be processed directly. The reviews of an app pass through the preprocessing stage which remove the stop words and perform data segmentation based on the collected words that are treated as labels.

2.2 Sentiment analysis

The sentiment analysis will be performed to determine the nature of the review which is positive or negative using Word2Vec model. For that, the preprocessed data will undergo the extraction process which assigns weight for the words matched with the keybase. The words in the keybase are updated after every successful completion process of sentiment analysis. The weight can be both positive and negative depend on the emotion of the word. The collective weight of a review will be checked against the average threshold. If it met the value, it will be considered as a positive otherwise it is a negative.

2.3 Phase categorization & Rating filtration

The collected rank value will be different based on a category like top paid, top grossing, trending etc. The rank value of each category will be collected and the average of it will be considered as a final rank of an

app. The difference between the rankings of successive categories are noted and compared with the breaking limit. If it exceeds, the ranking will be marked for evidence evaluation. The same method has been followed for the monthly collected rating values to find out the large deviation with the breaking limit.

2.4 Evidence aggregation

The total number of positives and negatives in the preprocessed reviews using sentiment analysis has been collected. The rating and ranking has been checked whether it has been marked. If the majority of the above three results in positive, then the app may consider as a genuine app. If not, the app will be marked as fraudulent app that will be notified to the user and the app store.

3 Integrated Level Aggregation

App store has been playing the role of repository for various mobile apps with different categories at different levels based on specific parameters. There are 32 categories in the app store and each one have its own ranking in ordering the apps based on rating, reviews, downloads etc that can be collected. The Fig 2 shows that the character level matching of apps has to be collected and matched against the categorized ranked apps to identify the keyword matching level.

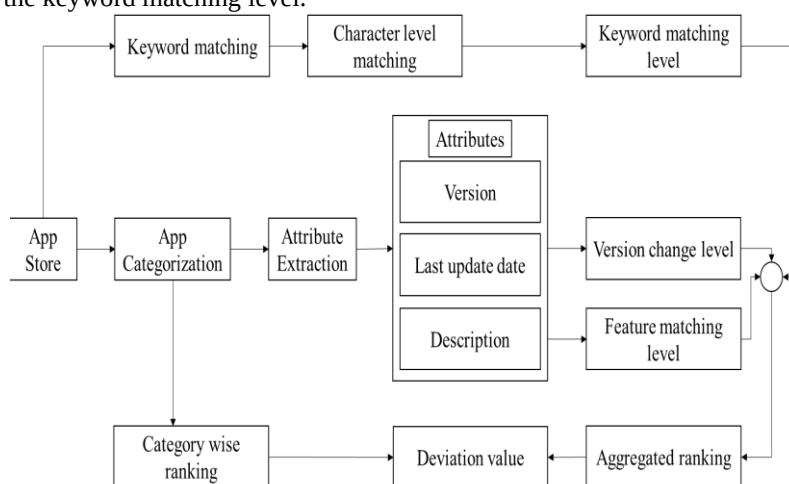


Figure 2: Architecture of Level Aggregation

The specific attributes like version, last updated are collected to identify how many the app has been revised after it has been launched which determines the version change level. The description of the app has been used to extract what are the primary features to be satisfied for the category has been matched that determines the feature matching level. The levels are aggregated and compared with the category ranking to identify the deviation value. This value reveals how far or ahead the apps have been ranked in the app store.

4.1 Keyword matching level

The keyword matching for the top ranked apps in each category can be verified by exploring the characters from a to z. For each result, it shows 5 results which may be the listed in top categories. If a single character doesn't give the required results, increase the search text with next character of the app name. It can be repeated with the remaining characters of the app name till a match occurs. If it matched, retrieve the no of characters and app name to determine the app search efficiency (ASV).

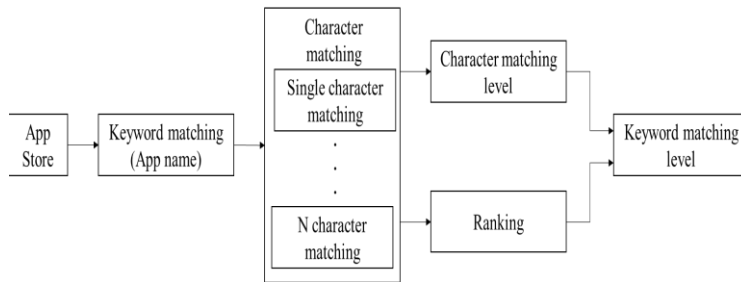


Figure 3: Keyword matching level

As shown in Fig 3, Search Impact Value (SIV) will be assigned with the varied ranges of ASV from 0 to 1. Placeholder Value (PV) will be calculated with product of the app’s place in the results and SIV. The average of ASV and PV can be expressed in percentile to determine the Keyword Matching Level (KML). If there is no match, the KML will be initialized to 0.

$$ASV = \frac{\text{No of chars required}}{\text{Length of app name}} \tag{1}$$

$$SIV = \begin{cases} 1, & ASV \geq 0.4 \\ 0.2, & 0.39 \leq ASV \leq 0.3 \\ 0.6, & 0.29 \leq ASV \leq 0.1 \dots 3 \\ 0.8, & ASV < 0.1 \end{cases} \tag{2}$$

$$PV = \frac{5 - \text{App place}}{5} * SIV \dots 4 \tag{3}$$

$$KML = \frac{ASV + PV}{2} \dots 5 \tag{4}$$

4.2 Version change level

A version of the app determines how many revisions and changes has made that can be split into major and minor versions. Based on that, calculate the how many versions has been released on every year from app launch that determines the average release of versions per year (ARVY). The difference of the last updated and its prequel will be calculated as elapsed cycle (EC). The update frequency (UF) will be assigned to 1 if the value of EC is less than 12. If not, UF will be assigned as 0.

$$UF = \begin{cases} 1, & EC < 12 \\ 0, & EC \geq 12 \end{cases} \tag{5}$$

$$VCL = \frac{ARVY * UF}{EC} \tag{6}$$

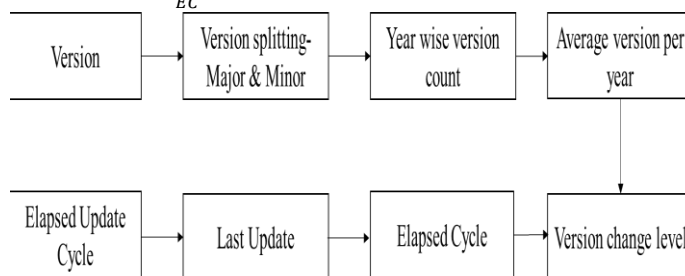


Figure 4. Version change level

4.3 Feature matching level

Each category have its own primary features to be satisfied irrespective of its additional features. After extracting description of an app, identify the features F in the text using scrapping and store in a repository. As the feature has not possess common name for all apps in the category, views V has been created for different set of features with unique weights. Each feature fi in F has been assigned a weight w that will be aggregated into a single view and match with the stored views to identify the optimal view for the app. The identified view weight has been averaged to the category feature score to determine the feature matching level (FML). Then identify how many SEO backlinks and Google tags has been used in the description excluding the duplicates to increase the app search optimization. Based on the matching occurrence in the repository of backlinks and tags, app optimization level (AOL) can be determined.

$$F = \{f_1, f_2, \dots, f_n\}$$

$$W = \sum_{i=0}^n f_i(w)$$

$$FML = \frac{\text{Weight of the identified view}}{\text{No of primary features of category}} \dots(7)$$

$$AOL = \frac{\text{No of identified backlinks and tags}}{\text{No of backlinks and tags in repository}} \dots(8)$$

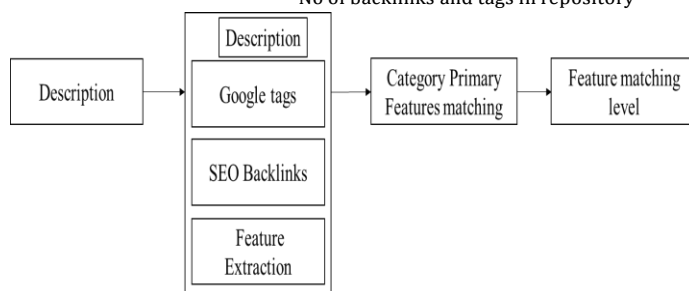


Figure 5. Feature matching level

4.4 Aggregated ranking

The identified levels are mapped to the scale of 1 to 5 with a range of values except VCL as the convention is not same. The product of computed scale that has been averaged with a consolidated value and VCL is termed as aggregated rank value. It will be compared with the collected category wise ranking for the apps from the store to pinpoint the deviation of the rank.

5 Experimental Analysis

The app store data has been collected that holds 33 categories of 10,843 apps information like rating, installs, version, category, genre, last updated, android versions, etc. From that, the following attributes are chosen to identify the deviation levels. The table 1 shows the top ranked apps rated by the concerned app store.

Table 1. Extracted parameters of top apps

| Rating | Size | Installs | Last Updated | Current Ver |
|--------|------|-------------|--------------------|-------------|
| 4.1 | 19M | 10,000+ | January 7, 2018 | 1.0.0 |
| 3.9 | 14M | 500,000+ | January 15, 2018 | 2.0.0 |
| 4.7 | 8.7M | 5,000,000+ | August 1, 2018 | 1.2.4 |
| 4.5 | 25M | 50,000,000+ | June 8, 2018 | Vary |
| 4.3 | 2.8M | 100,000+ | June 20, 2018 | 1.1 |
| 4.4 | 5.6M | 50,000+ | March 26, 2017 | 1 |
| 3.8 | 19M | 50,000+ | April 26, 2018 | 1.1 |
| 4.1 | 29M | 1,000,000+ | June 14, 2018 | 6.1.61.1 |
| 4.4 | 33M | 1,000,000+ | September 20, 2017 | 2.9.2 |
| 4.7 | 3.1M | 10,000+ | July 3, 2018 | 2.8 |
| 4.4 | 28M | 1,000,000+ | October 27, 2017 | 1.0.4 |

From that, the length of the app name and no. of chars required to search that app has to be calculated. The ratio of these two parameters gives the ASV. Using the equation, SIV value has been calculated based on the four ranges of values.

Table 2. Derivation of App search Efficiency and Search Impact Value

| app length | No. of chars Required | ASV | SIV |
|------------|-----------------------|-------------|-----|
| 46 | 5 | 0.108695652 | 0.6 |
| 19 | 1 | 0.052631579 | 0.8 |
| 52 | 23 | 0.442307692 | 1 |
| 37 | 3 | 0.081081081 | 0.8 |
| 26 | 11 | 0.423076923 | 1 |
| 39 | 9 | 0.230769231 | 0.6 |
| 16 | 2 | 0.125 | 0.6 |

| | | | |
|----|----|-------------|-----|
| 20 | 10 | 0.5 | 1 |
| 29 | 9 | 0.310344828 | 0.2 |
| 23 | 8 | 0.347826087 | 0.2 |

Table 3. Keyword matching level for app places

| app place | pv | KML |
|-----------|------|----------|
| 3 | 0.24 | 0.228696 |
| 3 | 0.24 | 0.330526 |
| 3 | 0.24 | 0.293077 |
| 1 | 0.8 | 0.859459 |
| 3 | 0.24 | 0.235385 |
| 4 | 0.04 | 0.404615 |
| 3 | 0.24 | 0.37 |
| 4 | 0.04 | 0.37 |
| 4 | 0.16 | 0.114483 |
| 4 | 0.16 | 0.123478 |

App place can be calculated with obtained SIV values that ranges between 1- 4. PV calculated using equation and the average of SIV and PV determines KML through equation.

The revision attribute reveals the number of major and minor versions of the app. The average version of app (ARVY) is obtained with the multiplicative factors 0.5, 0.25, 0.125 and so on. The setting of UF can be obtained through last updated date that has been compared with the current date fixed before the analysis. The VCL value calculated with equation with the obtained value of UF and ARVY.

Table 4. Version change level with Elapsed Cycle.

| ARVY | UF | EC | VCL |
|--------|----|-----|----------|
| 1 | 1 | 358 | 0.002793 |
| 2 | 1 | 350 | 0.005714 |
| 3 | 1 | 152 | 0.019737 |
| 1.5 | 1 | 206 | 0.007282 |
| 1 | 0 | 194 | 0.005155 |
| 1.5 | 1 | 645 | 0.002326 |
| 21.875 | 1 | 249 | 0.087851 |
| 7 | 1 | 200 | 0.035 |
| 6 | 1 | 467 | 0.012848 |
| 2 | 0 | 181 | 0.01105 |

Based on the category, the primary features required to be in the app is different. The primary features F for each category has been identified that matches with the available features in the app to determine feature weight FW. The ratio of FW and F determines the FML as specified in equation. Then the ratio of the available backlinks for each app has been collected from app store data to the required determines AOL as specified in equation.

Table 5. App Optimization level with backlinks.

| AF | FW | FML | BL NO | AOL |
|----|----|-------------|-------|-------------|
| 6 | 12 | 0.857142857 | 19 | 0.633333333 |
| 4 | 8 | 0.571428571 | 23 | 0.766666667 |
| 6 | 12 | 0.857142857 | 14 | 0.466666667 |
| 4 | 8 | 0.571428571 | 12 | 0.4 |
| 5 | 10 | 0.714285714 | 22 | 0.733333333 |
| 6 | 12 | 0.857142857 | 9 | 0.3 |
| 5 | 10 | 0.714285714 | 9 | 0.3 |
| 5 | 10 | 0.714285714 | 4 | 0.133333333 |
| 4 | 8 | 0.571428571 | 6 | 0.2 |

| | | | | |
|---|----|---|----|-------------|
| 7 | 14 | 1 | 16 | 0.533333333 |
|---|----|---|----|-------------|

The obtained KML, VCL, FML and AOL are aggregated to determine the new ranking efficiency (ORE) that has been compared with the actual (ARE) for identifying the deviation value.

Table 6. Obtained and Actual App Efficiency based on Level aggregation

| KML | VCL | FML | AOL | Agg | ORE | ARE |
|------|--------|------|------|------|-----|-----|
| 0.63 | 0.0028 | 0.57 | 0.47 | 0.42 | 40 | 75 |
| 0.38 | 0.0057 | 0.71 | 0.27 | 0.34 | 65 | 85 |
| 0.14 | 0.0197 | 0.57 | 0.3 | 0.26 | 95 | 5 |
| 0.25 | 0.0073 | 0.86 | 0.83 | 0.49 | 50 | 25 |
| 0.46 | 0.0052 | 0.57 | 0.27 | 0.33 | 20 | 60 |
| 0.16 | 0 | 0.57 | 0.47 | 0.3 | 45 | 35 |
| 0.4 | 0.0879 | 0.71 | 0.43 | 0.41 | 5 | 90 |
| 0.14 | 0.035 | 0.71 | 0.37 | 0.31 | 30 | 75 |
| 0.16 | 0 | 0.86 | 0.77 | 0.45 | 70 | 35 |
| 0.65 | 0.0111 | 0.86 | 0.5 | 0.5 | 80 | 5 |

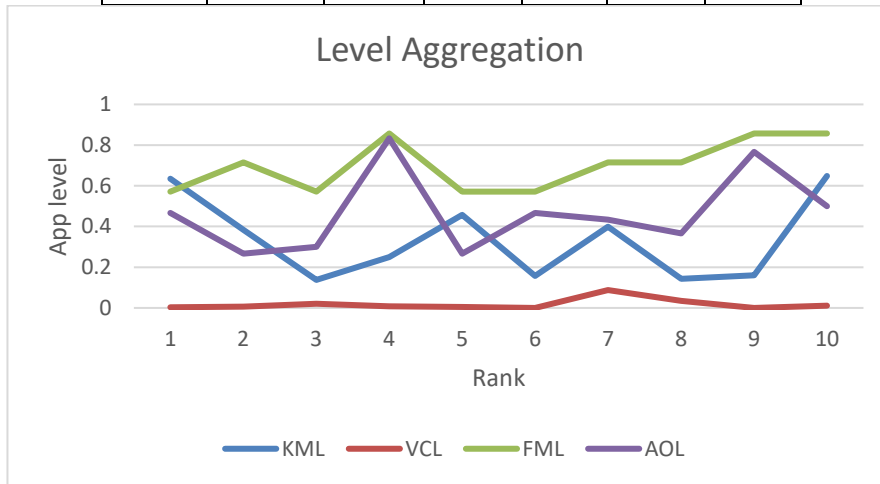


Figure 6. Mapping of KML, VCL, FML and AOL

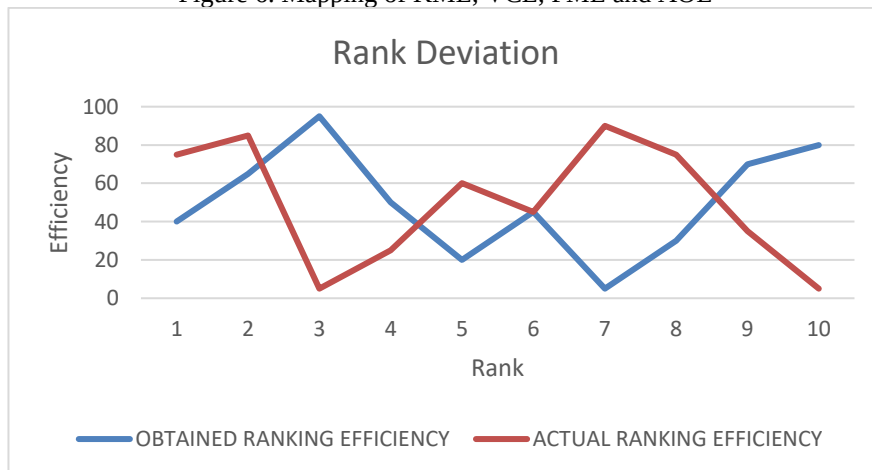


Figure 7. Rank deviation based on level aggregation

The figures and tables should be centred. The figure caption should be placed below the figure as shown in Fig. (1). Figures should be cited in the text as done in the previous sentence. Care should be taken to make the figure captions as clear as possible. Multiple sentences are encouraged in the figure caption, as shown in Fig. (1).

Tables are to be formatted as shown in Table 1. Table captions should be placed at the top. Tables should be cited in the text as shown in the first sentence of this paragraph.

6 Conclusion

This paper discussed the problem of ranking deviations that has not been reflected with the reputed parameters like rating and reviews. The app's ranking is not only based on the user side. From the developer's view parameters, the app ranking can be influenced.

Acknowledgement

This work was supported in part by Anna University Recognized Research Centre Lab at Francis Xavier Engineering College, Tirunelveli, Tamilnadu, India. Also, we would like to thank the anonymous reviewers for their valuable comments and suggestions.

References

- [1] Sami Hyrynsalmi, Tuomas Makil, Antero Jarvi, Arho Suominen, Marko Seppanen and Timo Knuutila.: App Store, Marketplace, Play! An Analysis of Multi-Homing in Mobile Software Ecosystems. Proceedings of IWSECO 2012,59-72.
- [2] Gunwoong Lee and T. S. Raghu, Determinants of Mobile Apps Success: Evidence from App Store Market, Journal of Management Information Systems, Volume 31, 2014 - Issue 2, 1-46.
- [3] Caro-Alvaro, Sergio & García, Eva & García-Cabot, Antonio & de-Marcos, Luis & Gutiérrez-Martinez, Jose-Maria. (2017). A Systematic Evaluation of Mobile Applications for Instant Messaging on iOS Devices. Mobile Information Systems. 2017. 1-17. 10.1155/2017/1294193.
- [4] Wang, Haoyu & Liu, Zhe & Liang, Jingyue & Vallina-Rodriguez, Narseo & Guo, Yao & Li, Li & Tapiador, Juan & Cao, Jingcun & Xu, Guoai. (2018). Beyond Google Play: A Large-Scale Comparative Study of Chinese Android App Markets.
- [5] Jeeva. R, Muthukumar. N, 'Identification of Fictitious Messages in Social Network using E-Hits and Newsapi', International Journal of Innovative Technology and Exploring Engineering, Vol. 9, Issue. 10, pp. 7- 11, August 2020.
- [6] Karthika. A, Muthukumar. N, Joshua Samuel Raj. R, 'An Ads-Csab Approach for Economic Denial of Sustainability Attacks in Cloud Storage', International Journal of Scientific & Technology Research, Vol. 9, Issue. 04, pp. 2575-2578, April 2020.
- [7] Zahra, Fatima & Hussain, Azham & Haslina, Haslina. (2017). Usability evaluation of mobile applications; where do we stand?. AIP Conference Proceedings. 1891. 020056. 10.1063/1.5005389.
- [8] J. Rebekah, D. C. J. W. Wise, D. Bhavani, P. Agatha Regina and N. Muthukumar, "Dress code Surveillance Using Deep learning," 2020 International Conference on Electronics and Sustainable Communication Systems (ICESC), Coimbatore, India, 2020, pp. 394-397, doi: 10.1109/ICESC48915.2020.9155668.
- [9] Chen, Ying & Xu, Heng & Zhou, Yilu & Zhu, Sencun. (2013). Is this app safe for children?: a comparison study of maturity ratings on Android and iOS applications. 201-212. 10.1145/2488388.2488407.
- [10] Zhu, Hengshu & Xiong, Hui & Ge, Yong & Chen, Enhong. (2015). Discovery of Ranking Fraud for Mobile Apps. IEEE Transactions on Knowledge and Data Engineering. 27. 74-87. 10.1109/TKDE.2014.2320733.
- [11] Hu, Bing & Liu, Bin & Gong, Neil & Kong, Deguang & Jin, Hongxia. (2015). Protecting Your Children from Inappropriate Content in Mobile Apps. 1111-1120. 10.1145/2806416.2806579.
- [12] Ali, Mohamed & Erfani, Mona & Mesbah, Ali. (2017). Same App, Different App Stores: A Comparative Study. 79-90. 10.1109/MOBILESoft.2017.3.
- [13] Martin, William & Sarro, Federica & Jia, Yue & Zhang, Yuanyuan & Harman, Mark. (2016). A Survey of App Store Analysis for Software Engineering. IEEE Transactions on Software Engineering. PP. 1-1. 10.1109/TSE.2016.2630689.

An Enhanced Hybrid Algorithm Using Levy Flight, Simulated Annealing and K-means Algorithm for clustering high dimensional datasets

R.Jensi,
Department of Computer Science and Engineering,
Dr.Sivanthi Aditanar College of Engineering, Tiruchendur

Abstract

Simulated annealing is a simple hill climbing technique which is guaranteed to escape from local optima. Data clustering is done using simulated annealing algorithm in the literature. In this paper, we propose an enhanced version of simulated annealing algorithm to solve data clustering problem. The proposed work is the combination of simulated annealing, Levy flight and K-means algorithms, called LSA-K, which can discover better cluster centroids. Levy flight is a random walk in which the steps are made in terms of the step-lengths, which have a certain probability distribution, with the directions of the steps being isotropic and random directions. The algorithm was initially tested and compared with other approaches using two synthetic and seven real life data sets. The experimental results show that the proposed algorithm is robust and efficient for data clustering.

Keywords: *simulated annealing, clustering, global search, convergence*

1 Introduction

Data clustering [5] is the method in which a group of data objects are divided into groups or clusters in such a way that the objects within the clusters are having high similarity while the data objects in different clusters are dissimilar. Data clustering is an unsupervised technique due to the unknown class labels. The similarity between data objects is measured by some distance metric. There are several distance measurements [1] such as Euclidean distance, Minkowski metric, Manhattan distance, Cosine similarity, Jaccard coefficient, Pearson correlation coefficient, and so on. Clustering is widely used in many fields of science and engineering and it must often be solved as part of complicated tasks in pattern recognition, data mining, and image analysis. The clustering algorithms are mainly classified into two [1]: hierarchical and partitional. A hierarchical clustering method is further classified into two types, agglomerative and divisive, based on how the hierarchical decomposition is formed. Agglomerative approach, also known as bottom-up approach, initially considers each object as a separate group and successively merges the objects based on some optimization criterions, until all of the objects are grouped into one. On the other hand, divisive approach, also known as top-down approach, starts with all of the objects in one cluster and successively divides the objects into clusters based on some optimization criterions, until each object is in one cluster or a termination criterion holds. The aim of partitional clustering algorithm is grouping the data objects into a predefined number of clusters based on some optimization criterions. The most well known partitional clustering algorithm is K-means which is the center-based clustering algorithm. The advantage of K-means algorithm is simple and efficient. But K-means suffers from initial cluster seed selection since it is easily trapped in local minimum. To overcome the shortcomings of K-means, several heuristic algorithms have been introduced.

Many nature-inspired algorithms, also known as Swarm Intelligence (SI) [4], have recently attracted the researchers to solve numerical optimization and engineering optimization problems. In the last few decades, many SI algorithms have been introduced inspired by the clever behaviors of animal or insect groups, such as ant colonies, bird flocks or fish schools, bacterial swarms, bee colonies, cuckoos, fireflies and flower pollination. Swarm Intelligence is based on heuristic approach, so SI algorithms were used to solve the clustering problems. Recent SI studies for data clustering include particle swarm optimization (PSO) [3], Ant Colony Optimization (ACO) [9], a hybrid technique K-NM-PSO combination of PSO, Nelder–Mead simplex searching and K-means algorithm [17], artificial bee colonies [18], novel artificial bee colony [10], hybrid artificial bee colony [11], improved particle swarm optimization (PSO) [19] [32], firefly [18], Bacterial Foraging [12].

In addition with SI algorithms, several evolutionary based algorithms were also employed for data clustering. These include tabu searching [16], genetic algorithms [14], and simulated annealing [7]. Hybrids of evolutionary and nature-inspired algorithms were developed for solving data clustering problem. These include PSO and SA [24], PSO, SA and K-means [25], ACO and SA [26], [26], PSO, ACO, K-means [33], modified imperialist competitive algorithm and K-means [30], and modified imperialist competitive algorithm and K-means [31].

Selim and Al-Sultan (1991) [7] presented a simulated annealing approach to the data clustering problem and they proved that the algorithm obtained global optimum solution. Maulik and Bandyopadhyay (2000) [14]

proposed a genetic algorithm approach to clustering. The superiority of the GA-clustering algorithm over the K-means is demonstrated for synthetic and real-life datasets. Krishna and Murty (1999) [38] presented another hybrid genetic algorithm approach called the genetic K-means (GKA) algorithm. In his paper, GA is hybridized with a classical K-means algorithm. K-means operator was used as a search operator in GA instead of crossover and also they defined a basic mutation operator for clustering. The results from GKA proved that the algorithm converged to the global optimum.

Y. Liu, Z. Yi, H. Wu, M. Ye, K. Chen, (2008) [16] proposed a tabu search-based heuristic to clustering. Shelokar et al. (2004) [9] presented an ant colony optimization (ACO) method for clustering. Their algorithm employs distributed agents that mimic the way real-life ants find the shortest path from their nest to a food source and back. The results obtained by ACO can be considered as a viable and an efficient heuristic to find or near-optimal cluster representation for a clustering problem.

Kao et al. (2008) [17] proposed a hybridized approach that combines PSO technique, Nelder–Mead simplex search and the K-means algorithm. The K-NM-PSO algorithm is tested on four data sets, and its performance is compared with those of PSO, NM-PSO, K-PSO and K-means clustering and it is proved that K-NM-PSO is both robust and suitable for handling data clustering.

D.Karaboga, C.Ozturk. (2011) [10] presented a novel clustering approach using Artificial Bee Colony (ABC) algorithm which simulates the foraging behaviour of a honey bee swarm. The performance is compared with PSO and other nine classification techniques on thirteen datasets from UCI machine laboratory and the simulation results show that the ABC algorithm can be efficiently used for data clustering.

Zhang et al. (2010) [18] presented the artificial bee colony (ABC) as a state-of-the-art approach to clustering. Deb's rules are used to tackle infeasible solutions instead of the greedy selection process usually used in the ABC algorithm. When they tested their algorithm, they found very encouraging results in terms of effectiveness and efficiency. X. Yan et al. (2012) [11] presented a Hybrid artificial bee colony (HABC) algorithm for data clustering. The genetic algorithm crossover operator was introduced to ABC to enhance the information exchange between bees. The HABC algorithm achieved better results.

Tunchan Cura. (2012) [19] presented a new PSO approach to data clustering and the algorithm was tested using two synthetic datasets and five real datasets and the results show that the algorithm can be applied to clustering problem with known and unknown number of clusters. Senthilnath, J., Omkar, S.N. and Mani, V. (2011)[8] presented data clustering using firefly algorithm. They measured the performance of FA with respect to supervised clustering problem and the results show that algorithm is robust and efficient.

Miao Wan ,Lixiang Li ,Jinghua Xiao ,Cong Wang , Yixian Yang. (2012) [12] presented data clustering using Bacterial Foraging Optimization (BFO). The algorithm proposed by these researchers was tested on several well-known benchmark data sets and Compared three clustering technique. The experimental results show that the algorithm is an effective and can be used to handle data sets with various cluster sizes, densities and multiple dimensions.

Abdolreza Hatamlou (2013) [15] presented a new heuristic algorithm for data clustering using black hole phenomenon. The black hole algorithm is similar to other population-based algorithms, initially populations of candidate solutions are randomly generated and at each iteration, the best candidate is selected to be the black hole which pulls other candidates around it, called stars. A new candidate solution is generated randomly when the star gets too close to the black hole. The algorithm was tested and the results showed that the algorithm outperforms the other traditional clustering algorithms such as K-means, PSO, GSA and BB–BC. Data clustering using a binary search algorithm was done in [29].

Taher Niknam [24] presented a hybrid data clustering technique using PSO and SA and the simulation results showed that the PSO-SA clustering algorithm has a better response and also converges more quickly than the K-means, PSO, and SA algorithms. Taher Niknam [26] proposed a hybrid evolutionary clustering algorithm based on ACO and SA and the simulation results showed that ACO-SA is suitable for data clustering.

In [25], three authors Bahamn Nahmanifirouzi, lokhtar sha sadeghi and taher niknam have proposed a new hybrid technique using PSO, SA and K-means. The hybrid algorithm outperformed well than PSO, SA, PSO-SA, ACO, K-PSO, NM-PSO, K-NM-PSO, GA, TS, HBMO and k-means.

Taher Niknam [33] proposed an efficient hybrid data clustering algorithm based on PSO, ACO, K-means called FAPSO-ACO-K. FAPSO-ACO-K reached global optimal solution in a minimum number of function evaluations and obtained high F-measure values in compared to those of other previously proposed algorithms. In [30] Taher Niknam presented a data clustering technique using modified imperialist competitive algorithm and K-means and in [31] Ganesh Krishnasamy presented a data clustering technique based on modified imperialist competitive algorithm and K-means. These hybrid algorithms proved better performance than those of PSO, ACO, SA, TS, GA, HBMO, K-means.

In this paper we present an enhanced version of simulated annealing algorithm which utilizes the random walk phenomenon of levy Flight method. LSA-K, hybrid data clustering algorithm, is simple and easy to implement. The results show that it is better than K-means, SA and other heuristic algorithms such as ACO, TS, GA, PSO, ACO-SA, HBMO, PSO-ACO and PSO-SA.

The remaining sections are arranged as follows. Section 2 provides the clustering problem statement. Section 3 briefly explains the K-means algorithm and SA algorithm. Section 4 describes Levy Flight method. Section 5 presents the proposed LSA-K approach. The experimental results are provided in Section 6, and followed by conclusion in section 7.

2 The problem statement

Clustering is the process of partitioning the set of N data objects into K clusters or groups based on some distance (or similarity) metric. Let $D = \{d_1, d_2, \dots, d_N\}$ be a set of N data objects to be partitioned and each data object $d_i, i=1, 2, \dots, N$ is represented as $d_i = \{d_{i1}, d_{i2}, \dots, d_{im}\}$ where d_{im} represents m^{th} dimension value of data object i .

The aim of clustering algorithm is to find a set of K partitions $C = \{C_1, C_2, \dots, C_k \mid \forall k : C_k \neq \emptyset \text{ and } \forall l \neq k : C_k \cap C_l = \emptyset\}$ in such a way that objects within the clusters are more similar and dissimilar to objects in different clusters. These similarities are measured by some optimization criteria, especially squared error function [30] and it has been calculated as follows:

$$\sum_{j=1}^k \sum_{i=1}^N \min(E(d_i, c_j)) \quad (1)$$

where c_j represents a j^{th} cluster center ; E is a distance measure between a data object d_i and a cluster center c_j . This optimization criterion is used as the objective function value in our study. There are many distance metric used in literature. In our study Euclidean distance is used as distance metric which is defined as follows:

$$E(d_i, c_j) = \sqrt{\sum_{m=1}^M (d_{im} - c_{jm})^2} \quad (2)$$

where, c_j is cluster center for a cluster j and is calculated as follows:

$$c_j = \frac{1}{n_j} \sum_{d_i \in c_j} d_i \quad (3)$$

where n_j is the total number of objects in cluster j .

3 K-means and SA Algorithms

3.1 K-means algorithm

K-means [1], [27] is the simplest partitional clustering algorithm and it is widely used due its simplicity and efficiency. Given a set of N data objects and the number of clusters k , the K-means algorithm proceeds as follows:

- Step 1: Randomly select ' k ' cluster centers.
- Step 2: Calculate the Euclidean distance between each data point and cluster centers.
- Step 3: Assign the data point to the cluster center whose distance from the cluster center is minimum of all the cluster centers.
- Step 4: Update cluster center using Eq. (3).
- Step 5: If no data point was reassigned then stop, otherwise repeat from

3.2 Simulated Annealing (SA) algorithm

Simulated annealing is a simple hill climbing (without the gradient) algorithm in which solution is improved at each iteration. Simulated annealing algorithm is originated from the concept of liquids freeze or metals recrystallize in the process of annealing [22]. During the annealing process, high temperature T is set and melt is disordered and is slowly cooled so that the system is in thermodynamic equilibrium at any time. When T is high, we call this the exploratory phase as simulated annealing is exploring the overall state space. When T is low, we call this the exploitation phase as simulated annealing climbs up the current hill, optimizing the value. If T is decreased slowly enough, simulated annealing is guaranteed to reach the best solution.

The pseudocode of SA algorithm [22] is given below:

```

algorithm : SA (dataset, k)
begin
  repeat
    Choose an initial solution  $S$  and an initial temperature  $T_{init}$ .
    for  $l=1$  to  $nsteps$ 
      Find a new solution, namely  $S_{new}$ , by modifying the last answer  $S$ 
      Calculate the energy differential  $\Delta E = f(S_{new})-f(S)$ 
      If  $\Delta E < 0$ 
        Accept the new solution  $S_{new}$ .
      else if  $\text{rand}(0,1) < \exp\left(-\frac{\Delta E}{T}\right)$ 
        Accept the new solution  $S_{new}$ 
      endif
      Decrease the Temperature  $T$ .
    end for
    Set  $T$  to a higher value.
  Until no more further improvement
end

```

4 Levy Flight method

Levy flight follows [21], [24], [25-27]; the generation of random numbers with levy flight consists of two steps: the choice of a random direction and the generation of steps which obey the chosen levy distribution. Random walks are drawn from Levy stable distribution. This distribution is a simple power-law formula $L(s) \sim |s|^{-1-\beta}$ where $0 < \beta < 2$ is an index.

Definition 5.1 Mathematically, a simple version of Levy distribution can be defined as:

$$L(s, \gamma, \mu) = \begin{cases} \frac{1}{\sqrt{2\pi}} \exp\left[-\frac{\gamma}{2(s-\mu)}\right] \frac{1}{(s-\mu)^{\frac{3}{2}}}, & \text{if } 0 < \mu < s < \infty \\ 0, & \text{if } s \leq 0 \end{cases}$$

where μ parameter is location or shift parameter, $\gamma > 0$ parameter is scale (controls the scale of distribution) parameter.

Definition 5.2 In general, Levy distribution should be defined in terms of Fourier transform.

$$F(k) = \exp[-\alpha|k|^\beta], 0 < \beta \leq 2$$

where α is a parameter within $[-1, 1]$ interval and known as skewness or scale factor. An index of stability $\beta \in (0, 2)$ is also referred to as Levy index. The analytic form of the integral is not known for general β except for a few special cases.

For random walk, the step length S can be calculated by Mantegna's algorithm as

$$S = \frac{u}{|v|^{\frac{1}{\beta}}} \quad (4)$$

where u and v are drawn from normal distributions. That is

$$u \sim N(0, \sigma_u^2), \quad v \sim N(0, \sigma_v^2), \quad (5)$$

where

$$\sigma_u = \left\{ \frac{\Gamma(1+\beta) \sin(\frac{\pi\beta}{2})}{\Gamma[\frac{1+\beta}{2}] \beta 2^{(\beta-1)/2}} \right\}^{1/\beta} \quad (6)$$

Then the step size is calculated by

$$stepsize = 0.01 \times S \quad (7)$$

5 The proposed Hybrid LSA-K Algorithm

Simulated annealing algorithm performs very efficient local search but its convergence depends on the selection initial starting solution. To perform global search or to escape from local optima, random walk is performed on the current solution using the levy flight method with the random probability. The current solution is improved in a given number of steps at a temperature. If the current solution is not improved then counter value is incremented. The counter is kept to keep track of whether the solution is accepted or not. If the solution is not improved in a pre-specified number of limit values, then K-means algorithm is executed. If K-means algorithm finds the improved solution, then counter is set to zero. The temperature is decreased and the above steps are repeated until the temperature is reached the minimum level. The solution is represented as shown in Fig.1. The size of the solution is $k \times m$ where k is the number of clusters and m is the dimension of the dataset.

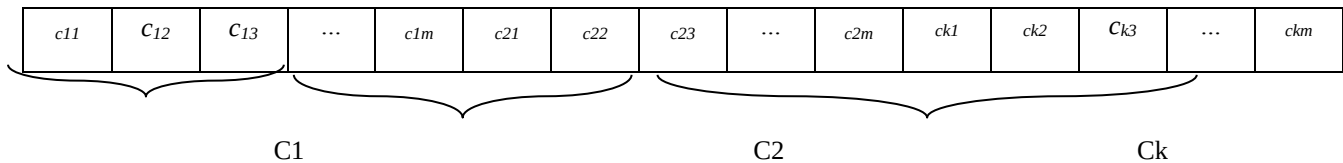


Fig 1. Representation of solution

The generation of the new solution depends on the probability R . If R is less than or equal to 0.5, then the new solution is generated as follows:

$$S_{new} = S_{curr} - 0.01 * (ub - lb) / 2 * \text{randn}(\text{size}(S_{curr})); \quad (8)$$

where

- Scurr- current solution
- ub – Maximum values in each attribute of the dataset
- lb – Minimum values in each attribute of the dataset
- .* - Element-wise multiplication

If R is greater than 0.5, then the new solution is generated using the levy flight method. That is,

$$S_{new} = S_{curr} + \text{stepsize} * \text{randn}(\text{size}(S_{curr})); \quad (9)$$

where stepsize is calculated using levy flight method and follows Eq. (7).

At a given temperature the solution is highly explored randomly in a number of steps. This execution phase is called the global search. When the global search is completed, a local search is done using K-means algorithm if the solution is not improved in a pre-specified number of times in global search phase. Then the temperature is decreased slowly and the above steps are repeated until the minimum temperature is reached.

The pseudocode of LSA-K algorithm is given below:

```

algorithm : LSA-K (dataset, k)
begin
counter=0;
repeat
Choose an initial solution  $S$  and an initial temperature  $T_{init}$ .
for  $l=1$  to  $nsteps$ 
if  $\text{rand}(0,1) \leq 0.5$ 
Generate a new solution  $S_{new}$  by Eq. (8)
else
Generate a new solution  $S_{new}$  by Eq. (9)
end if
Calculate the energy differential  $\Delta E = f(S_{new}) - f(S)$ 
if  $\Delta E < 0$ 
Accept the new solution  $S_{new}$ .
else if  $\text{rand}(0,1) < \exp\left(-\frac{\Delta E}{T}\right)$ 
Accept the new solution  $S_{new}$ 
else
counter=counter+1
endif
end for
if counter  $\geq$  limit
Run K-means algorithm and accept the solution if improved
counter=0;

```

```

end if
Decrease the Temperature T.
Until minimum temperature is reached
end

```

6 Experimental results

6.1 Datasets and parameter setting

The Simulated Annealing (SA) [22], K-means and proposed algorithm (LSA-K) are written in Matlab 8.3 and executed in a Windows 7 Professional OS environment using Intel i3, 2.30 GHz, 2 GB RAM. SA, LSA-K are executed with the parameters as shown in Table 1.

Table 1. Control Parameters and its values

| SA | | LSA-K | |
|------------------------|-------|------------------------|-------|
| Parameter | Value | Parameter | Value |
| Probability threshold | 0.98 | Probability threshold | 0.98 |
| Initial temperature | 5 | Initial temperature | 1 |
| Temperature multiplier | 0.98 | Temperature multiplier | 0.95 |
| Final temperature | 0.01 | Final temperature | 1e-15 |
| Number of iterations | 100 | Max. run | 25 |
| # iterations | 300 | Limit | 99 |

To evaluate the performance of proposed algorithm, nine datasets have been used. Two is artificial dataset drawn from Kao et al. (2008). The remaining seven datasets, namely, iris, wine, glass, Wisconsin Breast Cancer (WBC), Contraceptive Method Choice (CMC), crude oil and vowel, are collected from Machine Learning Laboratory [6] [20].

Table.2. Test dataset descriptions

| Dataset Name | # of | # of | # of instances(size of each class) |
|--------------|------|------|------------------------------------|
| Artset1 | 2 | 4 | 600(150,150,150,150) |
| Artset2 | 3 | 5 | 250(50,50,50,50,50) |
| Iris | 4 | 3 | 150(50,50,50) |
| Wine | 13 | 3 | 178(59,71,48) |
| Cancer | 9 | 2 | 683(444,239) |
| CMC | 10 | 3 | 1473(629,333,511) |
| Glass | 9 | 6 | 214(70,17,76,13,9,29) |
| Crude oil | 5 | 3 | 56(7,11,38) |
| Vowel | 3 | 6 | 871 (72, 89, 172, 151, 207, 180) |

6.2 Results and discussion

In this paper, to compare the performance of proposed algorithm, each algorithm was run 10 times. Table 3 presents the results obtained by K-means, SA [22] and proposed LSA-K algorithms and the average and standard deviation processing time taken to find the solution in 10 distinct runs of each algorithm. The performances of the algorithms are compared by the two criteria:

- (i) Total squared error function as defined in Eq. (1). The low value of the sum is, the higher the quality of the clustering is.
- (ii) The F-measure [23] which uses the ideas of precision and recall from information retrieval. The *precision* $P(i,j)$ and *recall* $R(i,j)$ for each class i of each cluster j are calculated as

$$P(i,j) = \frac{r_{ij}}{r_{ij} + p_{ij}} \quad (10)$$

$$R(i,j) = \frac{\gamma_{ij}}{\gamma_i} \quad (11)$$

where,

γ_i : is the number of members of class i

γ_j : is the number of members of cluster j

γ_{ij} : is the number of members of class i in cluster j

The corresponding F -measure $F(i,j)$ is given in Eq. (12):

$$F(i,j) = \frac{2 * P(i,j) * R(i,j)}{P(i,j) + R(i,j)} \quad (12)$$

Then the definition of F -measure of a class i is given as

$$F_{tot} = \sum_i \frac{\gamma_i}{n} \max_j (F(i,j)) \quad (13)$$

where, n is the total number of data objects in the collection. In general, the larger the F -measure gives the better clustering result.

Table 3 lists the best, worst, and average, standard deviation (in brackets) of objective function values obtained by K-means, SA and proposed LSA-K algorithms. Also Table 3 provides the average, standard deviation (in brackets) of F -measure of each algorithm. When examining the results in Table 3, the proposed LSA-K algorithm provides the global optimum value and very small standard deviation in compare to those of obtained by Simulated Annealing and K-means algorithms. For example, the best objective function value obtained by LSA-K algorithm is 16292.187 which is far better than the best objective function value obtained by K-means, SA algorithms, which are 16555.6794, 16304.485 respectively. LSA-K algorithm obtains optimum value for all data sets than those of obtained by K-means and Simulated Annealing algorithms. The time taken by the proposed algorithm is much smaller than of the time taken by the simulated annealing algorithm but larger than K-means algorithm. The smaller processing time of the proposed algorithm implies that quick convergence and thus reaching optimum value.

Table 3. Results obtained by K-means, SA, LSA-K for test datasets

| Dataset | | K-means | SA | LSA-K |
|---------|------------|----------------------|------------------|-------------------------|
| Artset1 | Avg.(Std.) | 531.5287(0.0000) | 531.699(0.297) | 530.875(0.000) |
| | Best | 531.5287 | 531.139 | 530.874 |
| | Worst | 531.5287 | 532.210 | 530.875 |
| | F-measure | 0.997(0.000) | 0.997(0.000) | 0.997(0.000) |
| | Time(s) | 0.005(0.005) | 14.49(0.29) | 8.01(0.17) |
| Artset2 | Avg.(Std.) | 2234.7522(354.0112) | 1734.832(0.972) | 1727.153(0.000) |
| | Best | 1728.7984 | 1734.040 | 1727.153 |
| | Worst | 2510.4159 | 1737.186 | 1727.153 |
| | F-measure | 0.855(0.102) | 1.000(0.000) | 1.000(0.000) |
| | Time(s) | 0.006(0.006) | 11.62(0.26) | 7.32(0.24) |
| Iris | Avg.(Std.) | 105.0109(12.3749) | 97.058(0.112) | 96.659(0.001) |
| | Best | 97.3259 | 96.853 | 96.657 |
| | Worst | 123.8497 | 97.199 | 96.660 |
| | F-measure | 0.827(0.104) | 0.896(0.004) | 0.899(0.000) |
| | Time(s) | 0.004(0.002) | 22.27(0.33) | 7.40(0.43) |
| Wine | Avg.(Std.) | 16712.4148(495.6408) | 16311.374(5.087) | 16292.332(0.233) |
| | Best | 16555.6794 | 16304.485 | 16292.187 |
| | Worst | 18123.0331 | 16320.052 | 16292.669 |
| | F-measure | 0.708(0.021) | 0.724(0.004) | 0.728(0.002) |
| | Time(s) | 0.004(0.001) | 10.98(0.50) | 8.05(0.27) |
| Glass | Avg.(Std.) | 223.3009(11.0845) | 245.522(11.267) | 211.342(1.327) |
| | Best | 215.6775 | 236.176 | 210.162 |
| | Worst | 253.6168 | 263.471 | 213.273 |
| | F-measure | 0.533(0.022) | 0.550(0.008) | 0.559(0.006) |
| | Time(s) | 0.009(0.005) | 21.50(1.35) | 8.16(0.25) |

| | | | | |
|------------------|------------|---------------------|-----------------|------------------------|
| Cancer | Avg.(Std.) | 2987.5479(0.7573) | 2969.718(0.615) | 2964.403(0.005) |
| | Best | 2986.9613 | 2968.952 | 2964.394 |
| | Worst | 2988.4278 | 2970.913 | 2964.408 |
| | F-measure | 0.961(0.001) | 0.964(0.001) | 0.965(0.000) |
| | Time(s) | 0.003(0.000) | 15.86(0.84) | 7.89(0.65) |
| CMC | Avg.(Std.) | 5703.9652(0.9067) | 5711.079(1.712) | 5693.841(0.031) |
| | Best | 5703.2002 | 5708.430 | 5693.796 |
| | Worst | 5705.2747 | 5713.238 | 5693.901 |
| | F-measure | 0.403(0.002) | 0.402(0.002) | 0.401(0.000) |
| | Time(s) | 0.011(0.004) | 18.91(0.63) | 11.69(0.33) |
| Crude oil | Avg.(Std.) | 279.5757(0.2249) | 278.190(0.243) | 277.228(0.037) |
| | Best | 279.2710 | 277.696 | 277.211 |
| | Worst | 279.7432 | 278.576 | 277.298 |
| | F-measure | 0.679(0.030) | 0.704(0.016) | 0.708(0.007) |
| | Time(s) | 0.008(0.004) | 20.56(0.38) | 6.98(0.08) |
| Vowel | Avg.(Std.) | 152993.7337 | 156229.728 | 149038.956 |
| | Best | 149433.7205 | 149175.531 | 148967.241 |
| | Worst | 161006.6053 | 160844.077 | 149093.860 |
| | F-measure | 0.562(0.031) | 0.571(0.023) | 0.534(0.005) |
| | Time(s) | 0.019(0.008) | 12.91(0.62) | 9.88(0.28) |

When examining the results given in Table 3, the proposed LSA-K algorithm achieves optimum value for the datasets wine, cancer and cmc datasets in compare to those of obtained by the other methods in the table. For iris dataset, LSA-K algorithm performs well compared to the other methods except PSO-ACO. PSO-ACO, PSO-SA and ACO-SA algorithms got better optimum values for glass dataset. For vowel dataset, LSA-K algorithm obtains better optimum values than other methods except one algorithm PSO-ACO. But LSA-K reached the best and worst values of 148967.241, 149093.860 respectively than PSO-ACO's the best and worst values of 148,995.2032, 149,101.6800 respectively. This means that LSA-K algorithm reaches near optimum in all runs. The running time of our proposed LSA-K algorithm is significantly smaller than SA algorithm while it is larger than K-means execution time. As a conclusion, the proposed LSA-K algorithm achieves optimum values in compared to other methods.

7 Conclusion

Simulated annealing algorithm is simple and easy to implement algorithm, but it fails to find the global optimum. In this paper, an enhanced version of simulated annealing algorithm called LSA-K is developed and explained in detail. LSA-K is a combination of Levy Flight method, Simulated Annealing and K-means algorithm. Levy flight method is used for its random walk behaviour so that the high exploration is done. The use of K-means in this paper is to produce local solution when the simulated annealing algorithm does not improve solution for a pre-specified number of times. The experimental results show that the proposed algorithm is much better than those of compared algorithms. The small standard deviation of proposed algorithm shows that our algorithm attains optimal solutions in all runs.

References

- [1] Jiawei han, Michelin Kamber , Data mining concepts and techniques, Elsevier, 2010.
- [2] R. Eberhart, J. Kennedy, Particle swarm optimization, Proceedings of the IEEE Int. Conf. on Neural Networks, Piscataway, NJ, (1995) 1942–1948.
- [3] D.M.Van, Engelbrecht A.P., Data clustering using particle swarm optimization, Proceedings IEEE Congress on Evolutionary Computation, Canbella, Australia, (2003) 215-220.
- [4] J.Kennedy, R.C. Eberhart, Swarm Intelligence, Morgan Kaufmann 1-55860-595-9, 2001.

- [5] A.K.Jain, M.N.Murty, P.J.Flynn, Data clustering: A review, *ACM Computing Survey* 31 (1999) 264-323.
- [6] C.L.Blake, C.J.Merz, University of California at Irvine Repository of Machine Learning Databases. <http://www.ics.uci.edu/mllearn/MLRepository.html>. 1998.
- [7] S.Z. Selim , K.S. Al-Sultan, A simulated annealing algorithm for the clustering problem, *Pattern Recognition* 24(10) (1991) 1003–1008.
- [8] J.Senthilnath,, S.N.Omkar, V.Mani, Clustering using firefly algorithm: performance study, *Swarm and Evolutionary Computation*. 1(3) (2011) 164–171.
- [9] P.S.Shelokar, V.K.Jayaraman, B.D.Kulkarni, An ant colony approach for clustering, *Analytica Chimica Acta* 509(2), (2004) 187–195.
- [10] Dervis Karaboga, Celal Ozturk., A novel clustering approach: Artificial Bee Colony (ABC) algorithm, *Applied Soft Computing* 11 (2011) 652–657.
- [11] Xiaohui Yan, Yunlong Zhu , Wenping Zou, Liang Wang, A new approach for data clustering using hybrid artificial bee colony algorithm, *Neurocomputing* 97 (2012) 241–250.
- [12] Miao Wan ,Lixiang Li ,Jinghua Xiao ,Cong Wang , Yixian Yang., Data clustering using bacterial foraging optimization, *Journal of Intelligent Information Systems* 38(2) (2012) 321-341.
- [13] K.Krishna, M.Narasimha Murty, Genetic K-means algorithm, *IEEE transactions on systems, man, and cybernetics—part b: cybernetics* 29(3) (1999) 433-439.
- [14] Ujjwal Maulik, Sanghamitra Bandyopadhyay, Genetic algorithm-based clustering technique, *Pattern Recognition* 33 (2000) 1455-1465.
- [15] Abdolreza Hatamlou, Black hole: A new heuristic optimization approach for data clustering, *Information Sciences* 222 (2013) 175-184.
- [16] Y.Liu, Z.Yi, H.Wu, M.Ye, K.Chen, A tabu search approach for the minimum sum-of-squares clustering problem, *Information Sciences* 178 (2008) 2680–2704 .
- [17] [Changsheng Zhang](#) , [Dantong Ouyang](#) , Jiaxu Ning, An artificial bee colony approach for clustering, [Expert Systems with Applications](#) 37(7) (2010) 4761–4767.
- [18] [Tunchan Cura](#), A particle swarm optimization approach to clustering, [Expert Systems with Applications](#) 39(1) (2012) 1582–1588.
- [19] <ftp://ftp.ics.uci.edu/pub/machine-learning-databases/>
- [20] P.Barthelemy, J.Bertolotti, D.S.Wiersma, A Levy flight for light, *Nature* 453 (2008) 495-498.
- [21] Taher Niknam, Bahman Bahmani Firouzi and Majid Nayeripour, An Efficient Hybrid Evolutionary Algorithm for Cluster Analysis, *World Applied Sciences Journal* 4 (2) (2008) 300-307.
- [22] Seyed Mohammad Razavi Zadegan, Mehdi Mirzaie, Farahnaz Sadoughi, Ranked k-medoids: A fast and accurate rank-based partitioning algorithm for clustering large datasets, *Knowledge-Based Systems* 39 (2013) 133–143.
- [23] Taher NIKNAM, Babak AMIRI, Javad OLAMAEI, Ali AREFI, An efficient hybrid evolutionary optimization algorithm based on PSO and SA for clustering, *Journal of Zhejiang University SCIENCE A* 10(4) (2009) 512-519.
- [24] Bahamn Nahmanifirouzi, lokhtar sha sadeghi and taher niknam, A new hybrid algorithm based on PSO,SA and K-means for cluster analysis, *International journal of innovative computing, information and control* 6(7) (2010) 3177-3192.
- [25] T. Niknam, J.Olamaei, B.Amiri, A Hybrid Evolutionary Algorithm Based on ACO and SA for Cluster Analysis, *Journal of Applied sciences* 8(15) (2008) 2675-2702.
- [26] A.K.Jain, Data clustering: 50 years beyond K-means, *Pattern Recognition Letters* 31(8) (2010) 651–666.
- [27] C.Ching-Yi, Y.Fun, Particle swarm optimization algorithm and its application to clustering analysis, in *Proceedings of the IEEE International Conference on Networking, sensing and control* (2004) 789–794.
- [28] Abdolreza Hatamlou , In search of optimal centroids on data clustering using a binary search algorithm, *Pattern Recognition Letters* 33 (2012) 1756–1760.
- [29] Taher Niknam , Elahe Taherian Fard , Narges Pourjafarian , Alireza Rousta, An efficient hybrid algorithm based on modified imperialist competitive algorithm and K-means for data clustering, *Engineering Applications of Artificial Intelligence* 24 (2) (2011) 306–317.
- [30] Taher Niknam , ElaheTaherianFard , NargesPourjafarian , AlirezaRousta , An efficient hybrid algorithm based on modified imperialist competitive algorithm and K-means for data clustering *Engineering, Applications of Artificial Intelligence* 24 (2011) 306–317.
- [31] Chi-Yang Tsai, I-Wei Kao, Particle swarm optimization with selective particle regeneration for data clustering, *Expert Systems with Applications* 38 (2011) 6565–6576.
- [32] Taher Niknam, Babak Amiri, An efficient hybrid approach based on PSO, ACO and K-means for cluster analysis, *Applied Soft Computing* 10 (2010) 183–197.

Integrity and privacy preserving of data for secure cloud storage using Third Party Auditor

Lizy Pravarthana. J¹, Roja.S², Kaviya.G³, Z. Asmathunnisa⁴,
Assistant Professor/CSE
St. Anne's College of Engineering and Technology^{1, 2, 3, 4}
Panruti

Abstract

Cloud is a common place for storing data as well as sharing of the data. However, preserving the privacy and maintaining integrity of data during public auditing remains to be an open challenge. The cloud must have to ensure data integrity and security of data of the user. Using cloud services, anyone can remotely store their data and can have the on-demand high quality applications and services from a shared pool of computing resources, without the burden of local data storage and maintenance. To overcome this issue, we are giving public auditing process for cloud storage that users can make use of a third-party auditor (TPA) to check the integrity of data. Not only verification of data integrity, the proposed system also supports data dynamics. In this paper, we introduce a third party auditor (TPA), which will keep track of all the files along with their integrity. Task of TPA is to verify the data, so that the user will be worry free. Verification of data is done on the aggregate authenticators sent by the user and cloud service provider (CSP). For this, we propose a secure cloud storage system which supports privacy-preserving public auditing and Blockless data verification over the cloud

Keywords: *Blockless data verification, data integrity, cloud storage, third party auditor(TPA), privacy preserving, public auditing.*

1 Introduction

Cloud service providers manage the data over the cloud. From users perspective, storing data remotely to the cloud is beneficial, because it can be accessed on-demand and in a flexible way. High level infrastructure that provides a scalable, secure and reliable environment for us. It brings relief of the burdens at a lower cost. Making use of the cloud saves both users time and money. In Cloud computing, the term cloud is a metaphor for the Internet, so the phrase Cloud computing is defined as a type of Internet-based computing, where different services are delivered to an organization's computers and devices through the Internet. Cloud computing is very promising for the Information Technology (IT) applications; however, there are still some issues to be solved for personal users and enterprises to store data and deploy applications in the Cloud computing environment. Data security is one of the most significant barriers to its adoption and it is followed by issues including compliance, privacy, trust, and legal matters. Therefore, one of the important goals is to maintain security and integrity of data stored in the cloud because of the critical nature of Cloud computing and large amounts of complex data it carries. The users concerns for security should be rectified first to make cloud environment trustworthy, so that it helps the users and enterprise to adopt it on large scale.

Third Party Auditor (TPA) offers its auditing service with more powerful computation and communication abilities. Cloud computing is a model for enabling ubiquitous, convenient, on-demand network access to a shared pool of configurable computing resources (e.g. networks, servers, storage, applications, and services) that can be rapidly provisioned and released with minimal management effort or service provider interaction".

Most of the cloud storage likes GoogleDrive and Dropbox offering space to the users which has become a routine for users to share for storage management, new and challenging security threats toward users' data. As the data is stored in an untrusted cloud, it can be easily be lost or it can also get corrupted due to disasters or failures or human errors. To verify the integrity of the data over the cloud, we introduce a thirdparty auditor (TPA) for public auditing. TPA offers its auditing service with more powerful computation and communication abilities. Data auditing is introduced in Cloud computing to deal with secure data storage. Auditing is a process of verification of user data which can be carried out either by the user himself (data owner) or by a TPA. It helps to maintain the integrity of data stored on the cloud. The verifier's role are categorized into two: first one is private auditability, in which only user or data owner is allowed to check the integrity of the stored data. No other person has the authority to question the server regarding the data. But it tends to increases verification overhead of the user. Second is public auditability, which allows anyone, not just the client, to challenge the server and performs data verification check with the help of TPA. The TPA is an entity which is used so that it can act on behalf of the client. It has all the necessary expertise, capabilities, knowledge and professional skills which are required to handle the work of integrity verification and it also reduces the overhead of the client. It is necessary that TPA

should efficiently audit the cloud data storage without requesting for the local copy of data. It should have zero knowledge about the data stored in the cloud server. It should not introduce any additional on-line burden to the cloud user .

1.1 Merits of the Methods

- a. Public Auditability** – it allows TPA to check integrity of data without retrieving it. TPA or external auditor should not have any knowledge about data i.e. blockless data verification.
- b. Storage correctness** – user’s data should correctly store on cloud.
- c. Privacy preserving** – this ensures that TPA cannot derive any data content.
- d. Lightweight** – auditing should be performed with minimum overhead

Specifically, the contribution can be summarized as the following three aspects.

- a. Our scheme achieves batch auditing where multiple delegated auditing tasks from different users can be performed simultaneously by the TPA.
- b. Our scheme provides a privacy-preserving auditing protocol.
- c. Our scheme provides the better security and justifies the performance of our proposed schemes through concrete experiments.

2 Literature survey

Cloud computing faces many problems on integrity and privacy of user’s data stored in the cloud. Hence it requires some secure and efficient methods which can ensure the integrity and privacy of data stored in the cloud. There are many techniques that are used to provide security to the user’s data over cloud. These techniques are also used for data correctness, data integrity and its security over the cloud. But there earlier techniques are not efficient to work on dynamic cloud and there are some disadvantages with these existing systems.

Following are some systems, with their pros and cons-

Ateniese et al. [2] is the one who took the public auditing into consideration, that is, they used “provable data possession” (PDP) model for possession of data over the untrusted cloud storage. They used homomorphic linear authenticator (HLA) scheme for public auditing. But there are some problems in this system related security. This system achieves the public auditability but exposes the data to the external auditors. So the privacy of the data is compromised in this system.

Juels et al. [3] has described a model called “proof of retrievability”(PoR). In this model, for “possession” and “retrievability” of data error correcting codes and spot checking is used. This model does not support public auditability. This is the disadvantage of this model. Also, this model does not support external auditor.

Wang et al. [9] has proposed a privacy preserving/ public auditing protocol which makes use of an independent TPA sst/o audit the data. It utilizes the public key based homomorphic linear authenticator (HLA) with random masking techniques. But this protocol is vulnerable to existential forgeries known as message attack from a malicious cloud server and an outside attacker.

To overcome this problem, Wang et al. [6] proposed a new improved scheme which is more secure than the protocol proposed in [9]. It is a public auditing scheme with TPA, which performs data auditing on behalf of users. uses HLA which is constructed from Boneh-Lynn- Shacham short signature referred as BLS signatures. It also uses random masking for data hiding. For the sake of data binding, this new scheme involves computationally intensive pairing operation thus making it inefficient to use.

Tejaswani et al. [5] has achieved integrity of data using a Merkle hash tree by TPA and the confidentiality of data is achieved using RSA based cryptography algorithm whereas Jadhav et al. [3] have introduced an attacking module which continuously keeps track on data alteration in the cloud. The attacking module is a small code which resides on cloud server. Confidentiality of stored data is achieved by encrypting the data using AES algorithm.

Arasu et al. [1] has proposed a method that uses the keyed Hash Message Authentication Code (HMAC) with homomorphic tokens to enhance the security of TPA. It is a technique for verifying the integrity of a data transmitted between two parties that agree on a shared secret key. HMAC’s are based on a key that is shared between the two parties, if either party’s key is compromised, it will be possible for an attacker to create fraud messages. Table 1. shows the Comparison of Existing Privacy Preserving Public Auditing Scheme..

Meenakshi et al. [2] has proposed a protocol which uses TPA to audit the data of the users using Merkle Hash Tree algorithm. It supports data dynamics but fails to provide confidentiality to the data stored in the cloud.

3 Methodology

Message Authentication Code (MAC) based scheme is also not useful for dynamic data. It has some disadvantages such as user has to recalculate new MAC. In HLA based scheme [6], cloud provider reveals user's data to the TPA which is the disadvantage of this scheme. This scheme is same as MAC based scheme but the only difference between MAC and HLA is that HLA can be aggregated.

By observing different existing system, there is need of such a system which provides public auditing services that will fulfill almost all the threats to the data over the cloud. To do this, we suggested certain requirements for public auditing services-

A. Accountability:

Auditing should be done in proper manner. That is it should identify the problems as well as the particular entity responsible for that problem if any unreliability occurs. Therefore there is need of system's accountability.

B. Performance:

The major aspect of any system is performance. In cloud computing also security of data storage and its integrity is important task.

C. Dynamic Support:

Cloud provides dynamic support for runtime system to access and share the data. The challenge is the legacy users. User has access to data and user can modify the data in the cloud. So, dynamic support in runtime system is the major challenge for public auditing system. In this paper, we proposed a secure and efficient system for public auditing which covers all the requirements mentioned above. In this system we use external auditor which is used for checking the integrity of the user's data.

At the same time external auditor should be unaware of the data so that the privacy will be preserved and the communication overhead will be less.

NOMENCLATURE

F - Data file is divided into blocks m_i ;

$i \in \{1,2,\dots,n\}$

F_i - Set of files

m_i - i th block of data file

h_i - Hash on block

Σ Signature

3.1 System Overview

The cloud data storage service involving three different parts, as shown in Fig. 1: the cloud user who stores has large amount of data in the cloud; the Cloud Server provides data storage service and has computation resources and storage space, the third-party auditor which has the responsibility to notify the user about the integrity of the data files stored in the cloud server by performing the important auditing task[5][6]. Cloud users depend on the Cloud Server for cloud data storage and data maintenance. They may also dynamically interact with the CS to access and update their stored data for various application purposes. Users no longer have their data locally. So it is very important for the users to ensure that the integrity of their data is properly maintained. Users cannot perform the correctness verification of data because it causes additional online burden and storage overhead.

3.2 Architecture of Public Auditing in Cloud Server

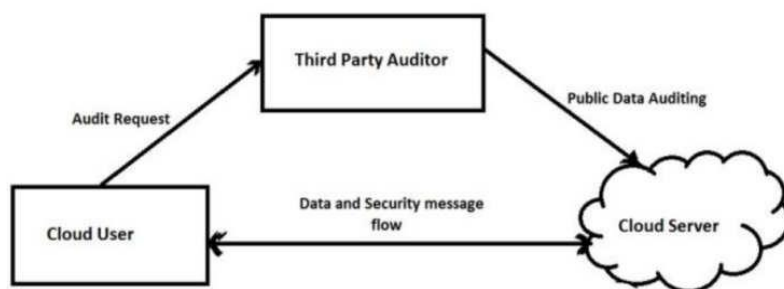


Fig 1. Architecture of Public Auditing in Cloud Server

To fully ensure the data correctness and for avoiding additional online burden, it is very important to enable public auditing for cloud data storage. Here users may resort to an independent third party auditor (TPA) to audit the outsourced data whenever needed. The TPA who has the capabilities that can check the integrity of all the data stored in the cloud server which provides an efficient method for the users to ensure their storage integrity in the cloud. Auditing will help users to assess the risk of their cloud data services.

In our work, we proposed a secure and efficient system for public auditing which covers all the requirements. In this system we use external auditor which is used for checking the integrity of the user's data. At the same time external auditor should be unaware of the data so that the privacy will be preserved and the communication overhead will be less. Also we use the **blockless** data verification scheme, which verifies the correctness of the data without having its knowledge.

4 Proposed System

There are three algorithms for integrity verification:

- a. **Key generation:** It is a process of generating keys Secret and public keys
- b. **Signing:** Signing means generation of proof for verification.
- c. **Verification:** The proof generated by the cloud service provider will be verified by the TPA.

For implementing this blockless verification we use **Boneh–Lynn–Shacham (BLS)** signature. The main purpose of using this scheme is it creates less overhead over the network which automatically decreases the communication cost. User, Cloud Service Provider (CSP) and Third Party Auditor (TPA). User is responsible for storing the data over the cloud. CSP has the large space to store the user's data and has the resources to manage the user's data, whereas TPA which is an external auditor is responsible for auditing.

This proposed scheme has been implemented practically on Amazon EC2 instance which demonstrates the fast performance of the design on both the cloud and the auditor side. But the full-fledged implementation of this mechanism on commercial public cloud is not been tested. So it is difficult to expect it to robustly cope with very large scale data.

4.1 Entities

Our system has 3 entities;

1. User
2. Cloud Service Provider(CSP)
3. Third party Auditor(TPA)

5 Definitions and framework of public auditing system

Our public auditing system can be constructed from the above auditing scheme in two phases, *Setup* and *Audit*:

- **Setup:** The user initializes the public and secret parameters of the system by executing **KeyGen**, and preprocesses the data file F by using **SigGen** to generate the verification metadata. The user then stores the data file F at the cloud server, deletes its local copy, and publishes the verification meta data to TPA for later audit. As part of pre-processing, the user may alter the data file F by expanding it or including additional metadata to be store data server.
- **Audit:** The TPA issues an audit message or challenge to the cloud server to make sure that the cloud server has retained the data file F properly at the time of the audit. The cloud server will derive a response message from a function of the stored data file F by executing **GenProof**. Using the verification metadata, the TPA verifies the response via **Verify Proof**.

5.1 Design Goals

To enable privacy-preserving public auditing for cloud data storage under the aforementioned model, our protocol design should achieve the following security and performance guarantee

- 1) **Public auditability:** to allow TPA to verify the correctness of the cloud data on demand without retrieving a copy of the whole data or introducing additional on-line burden to the cloud users;

- 2) **Storage correctness:** to ensure that there exists no cheating cloud server that can pass the audit from TPA without indeed storing users' data intact;
- 3) **Privacy-preserving:** to ensure that there exists no way for TPA to derive users' data content from the information collected during the auditing process;
- 4) **Batch auditing:** to enable TPA with secure and efficient auditing capability to cope with multiple auditing delegations from possibly large number of different users simultaneously;
- 5) **Lightweight:** to allow TPA to perform auditing with minimum communication and computation overhead.

6 Responsibilities of Entities

A. User:

- a. User first divides the file into blocks, i.e.

$$F = (m_1, m_2, m_3 \dots m_n).$$

- b. Once the file is divided into blocks hash value is calculated on each block, i.e.

$$\text{Hash}(m_i) \longrightarrow h_i$$

- c. After that digital signature is calculated, i.e.

$$\text{SignGen}(m_i) \longrightarrow \sigma_i, \text{ here 'i' denotes the } i^{\text{th}} \text{ block.}$$

- d. Finally the aggregate authenticator is calculated, i.e.

$$\text{Aggregate_auth}(\sigma_i) \longrightarrow \sigma$$

This aggregate authenticator is sent to the third party auditor (TPA) for checking the correctness of the data.

B. Cloud Service Provider (CSP):

- a. Calculate digital signature, i.e.

$$\text{SignGen}(m_i) \longrightarrow \sigma_i'$$

- b. Calculate aggregate authenticator, i.e.

$$\text{Aggregate_auth}(\sigma_i) \longrightarrow \sigma'$$

CSP sends the calculated aggregate authenticator to the TPA for verification of data.

7 Conclusion

Cloud storage is increasing day by day. Public auditing over the cloud is of critical importance. In this paper, a privacy-preserving public auditing system for data storage integrity in cloud computing is described. This method guarantees the cloud user that during the efficient auditing process the Third Party Auditor would not learn any details about the content of the file stored on the cloud server. Considering TPA concurrently handle multiple audit sessions from different users for their outsourced data files. Also proposed system achieves the privacy preserving public auditing and blockless data verification. We use multiple TPA for the auditing process which handles multiple users through batch auditing. Batch auditing improves the efficiency of the TPA as multiple requests are handled at the same time, which reduces the burden of TPA. Using different schemes the performance and security of this system can be improved.

References

- [1] Cong Wang, Student Member, IEEE, Sherman S.-M. Chow, Qian Wang, Student Member, IEEE, Kui Ren, Member, IEEE, and Wenjing Lou, Member, IEEE, "Privacy-Preserving Public Auditing for Secure Cloud Storage", 2018.
- [2] Michael Backes, Dario Fiore and Raphael M. Reischuk Max Planck, "Institute for Software Systems (MPI-SWS) Verifiable Delegation of Computation on Outsourced Data", 2017
- [3] Giuseppe Ateniese Sapienza, University of Rome ateniese@di.uniroma1.it, "Leakage-Resilient Identification Schemes from Zero-Knowledge Proofs of Storage", 2016
- [4] Qian Wang, Student Member, IEEE, Cong Wang, Student Member, IEEE, Kui Ren, Member, IEEE, Wenjing Lou, Senior Member, IEEE, and Jin Li, "Enabling Public Auditability and Data Dynamics for Storage Security in Cloud Computing", 2017.
- [5] Cong Wang, qian wang, kui ren, wenjing lou, "Privacy – Preserving Public Auditability for Secure Cloud Storage", IEEE transaction on Cloud Computing, 2013.

- [6] K. Yang and X. Jia, "An efficient and secure dynamic auditing protocol for data storage in cloud computing," *IEEE Trans. Parallel Distrib. Syst.*, vol. 24, no. 9, pp. 1717–1726, Sep. 2013.
- [7] Barsoum, A.F. and Hasan, M.A. "Provable multicopy dynamic data possession in cloud computing system", *IEEE Transactions Information Forensics and Security*, 10(3), pp.485-497,2015
- [8] Zhu, Y., Ahn, G.J., Hu, H., Yau, S.S., An, H.G. and Hu, C.J., "Dynamic audit services for outsourced storages in clouds", *IEEE Transactions on Services Computing*, 6(2), pp.227-238. 2013
- [9] Liu, J., Huang, K., Rong, H., Wang, H. and Xian, M., "Privacy-preserving public auditing for regenerating-code-based cloud storage", *IEEE transactions on information forensics and security*, 10(7), pp.1513-1528, 2015.

DISDet: DODAG Information Solicitation Attack Detection in IPv6 based Low Power Lossy Networks

Arul Anitha¹, Research Scholar, Dr. L. Arockiam², Professor
^{1,2}Department of Computer Science,
 St. Joseph's College (Autonomous), Tiruchirappalli
 arulanita@gmail.com

Abstract

Internet of Things (IoT) is an innovative trend which promotes technological and industrial developments. The special resource constrained characteristics of IoT and its voluminous inclusion technology tend to be more challengeable. RPL is the protocol used in Low power Lossy Networks which is prone to cause several security challenges and attacks. RPL constructs a Destination Oriented Directed Acyclic Graph (DODAG) to transmit the packets. Control Messages are the basic building blocks for constructing the DODAG. By altering the control message information, many attacks can be created by the internal and external attackers. DODAG Information Solicitation is a control message used by a new node to join the DODAG. The DIS attacker continuously feeds with a lot of DIS messages to its neighbours. It consumes more network resources and also leads to Denial of Service (DoS). To address this issue, in this paper, the negative impacts of the DIS attack are analysed in terms of the control overhead and energy consumption. This paper also proposes a technique called DISDet which alerts the administrator whenever it encounters any attack and also it mitigates the DIS attack to safeguard the network resources. DISDet detects almost all DIS flooding attacks with less false alarm rate.

Keywords: *IoT, RPL, Control Message, DODAG, DIS Attack, DISDet*

1 Introduction

Internet of Things (IoT) is a promising technology which is a heterogeneous network that consists of the conventional Internet and networks of constrained devices connected together using IP protocol [1]. RPL is the routing protocol used in the Low power Lossy Networks (LLNs) which was proposed by the Internet Engineering Task Force (IETF) working Group [2]. The resource constrained nodes in LLNs and their voluminous inclusion increase the security challenges in IoT [3]. This makes RPL prone to several security threats and attacks. An attacker may modify, insert, rerun, and generate data or control messages which will affect the normal operations of the RPL [4]. According to the authors in [5] and [6], the RPL attacks are classified into three categories such as attacks consuming network resources, attacks affecting topology and attacks increasing the network traffic.

The routing in RPL is performed by constructing a routing path towards a single destination called root node. It is called as Destination Oriented Directed Acyclic Graph (DODAG). The DODAG is constructed by using set of control messages. DODAG Information Solicitation (DIS) is a control message, which is sent by a node when it wants to join the existing DODAG topology. Whenever a node in the DODAG receives a DIS message, it has to send the DODAG Information Object (DIO) message and invite the sender to join the network. In DIS attack, the attacker node unicasts or multicasts a large volume of DODAG Information Solicitation (DIS) messages to its neighbour nodes which are in its transmission range. This tends the legitimate nodes to restart the Trickle algorithm [7] and broadcast a large number of DODAG Information Object (DIO) messages and consumes much energy and other resources of the legitimate nodes. Hence, the legitimate nodes due to unavailability will lead to Denial of Service (DoS) attacks in the IoT network [8].

To overcome the negative impacts of the DIS flooding attack, in this paper a novel detection and mitigation method DISDet is proposed. The proposed technique avoids the overwhelming DIS request from the malicious node and discards the duplicate messages sent by the same node again and again. Hence, the DISDet mechanism reduces the Packet loss, energy consumption issue and control overhead. The attacker node is also identified and quarantined from the DODAG. The proposed DISDet technique is implemented in the Cooja simulator and it performs well in terms of detection accuracy and false alarm rate.

The rest of this paper is organized as follows: Section 2 elaborates the literatures related to this research. Section 3 describes the Control messages for DODAG construction and the DIS attacks in detail. Section 4 explains the proposed DISDet technique. Section 5 explicates the experimental setup and the results obtained by the proposed model. Finally, Section 6 gives the conclusion of the research and suggests some directions for future work.

2 Related Works

The DIS flooding attack consumes more network resources and lead to severe problems in the network topology. In this section some of the important works related to the DIS attack and its impacts are highlighted.

Ruan et al. [9] designed a self-protecting architecture based on MAPE-K (Monitor, Analyse, Plan, Execute and Knowledge) control loop. The authors analysed the impacts of Sinkhole, Selective Forward, Black hole and flooding attacks in IoT. According to the user defined security policies, the nodes react to the attacks and protect themselves from such attacks.

S. Evmorfos et al. [10] proposed a Neural Network Architecture for detecting the SYN flooding attacks in IoT. Random Neural Network with Deep Learning and Long-Short-Term-Memory (LSTM) neural network were trained with normal and attack network traffic. The TCP SYN Flood attacks were simulated and the captured packets were used for the training and testing neural networks. According to their findings, the Random Neural Network performed well in terms of detection accuracy and false alarm rate.

Another study was performed by N.K.Thanigaivelan et al. [11] in which the authors presented a hybrid anomaly based Intrusion Detection System for detecting the internal attacks. A novel RPL Control message called Distress Propagation Object (DPO) was created in this work to report the anomalous activities of the neighbour nodes to its parent node. This system detected packet flooding attacks, selective forwarding attacks and clone attacks with less false positive rate. For large scale implementation it requires more computational cost.

T. Nguyen et al. [12] conducted a case study on the flooding attacks in low power lossy networks. The damages caused by this attack were analysed in terms of Packet Delivery Ratio, end-to-end delay and energy consumption. Using the overhearing mechanism proposed in this research, the attacks are detected and eliminated.

Cong Pu [13] investigated the DIS spam attack which sent large amount of DIS message with different identifiers and lead to DoS attack in RPL based environment. The research was implemented in OMNet++ simulator. The researcher also evaluated the negative impacts of the DIS flooding attack in the lossy networks in terms of energy consumption and node lifetime. The attack detection phase was not considered in this work.

A. Verma et al. [14] conducted an experiment on DIS flooding attack. The memory and energy consumption of such attack were denoted and they proposed a lightweight technique called Secure-RPL for mitigating such attacks in order to improve the performance of the lossy networks. The attack detection rate of the proposed technique and the impacts of network performance after implementing the technique were not given in their work.

Qureshi et al. [15] proposed a framework to detect flooding attack, version number attack, sinkhole attack and black hole attack in IIoT environment. The authors introduced some threshold values based on characteristics and functionalities of the control messages in order to identify the attacks. Detection accuracy, throughput, packet delivery rate and end-to-delay are the important evaluation metrics in this research.

3 RPL Control Messages and DIS Attack

3.1. Control Messages in RPL

RPL is a distance vector routing protocol that provides a specific routing solution for the resource constrained lossy networks. To maintain the network status, RPL constructs DODAGs. Each DODAG is identified by RPL Instance ID, DODAG ID, and DODAG Version Number. The DODAG consists of a root node and number of child nodes in a tree like structure [16]. The code field of the ICMPv6 protocol is used to identify the four types of control messages which are the basic elements for constructing the DODAG. The control messages of the ICMPv6 are listed in Table 1.

Table 1. Control messages of ICMPv6 [17]

| Code | Message |
|------|--|
| 0x00 | DODAG Information Solicitation (DIS) |
| 0x01 | DODAG Information Object (DIO) |
| 0x02 | Destination Advertisement Object (DAO) |
| 0x03 | DODAG Destination Advertisement Object Acknowledgement (DAO-ACK) |

DODAG root issues the DIO message to its neighbours and initiates the DODAG construction process. The DIO message consists of the routing metrics and constraints like root node's ID, the rank, and an Objective Function. When a node receives the DIO message, it adds the sender of DIO message to its parent list, computes

its own rank according to the Objective Function, and passes on the DIO message with the updated rank information. When the DIO message reaches the leaf node, the route towards the root node is built through its parent list. To form end-to-end communication from root to other nodes, the leaf node issues a DODAG Destination Advertisement Object (DAO) control message to broadcast reverse route information and record the nodes visited along the upward routes. After receiving DAO message, the DODAG root replies a DODAG Destination Advertisement Object ACK (DAO-ACK) message to the source of DAO message [18]. Hence, by sending the DIO, DAO, DAO-ACK and DIS messages the DODAG is constructed and it is directed towards the root node from other nodes.

3.2. DODAG Information Solicitation (DIS) Attack

When a new node wants to join the DODAG, it requests the routing details to its neighbour nodes by sending the DIS message. While receiving the new node’s request, the neighbours have to respond using the DIO message. The new node transmits the DIS message again and again until it receives a DIO message [19]. In order to send the routing information periodically, the Trickle Algorithm is set for each node. As per the network stability of the DODAG, the duration for initiating the Trickle Algorithm will vary. When a node gets a DIS message from its adjacent nodes, it ends the current DIO transmission and reruns the Trickle Algorithm and the time is set as minimum [20]. The DIS_DELAY is the delay to initiate the first DIS message by the new node and the DIS_INTERVAL is the waiting time for the new node to send the second and so on. When a new node does not receive any DIO messages from its neighbours during that interval, it has to wait for the DIS_INTERVAL time to send next DIS message. The default value defined in RPL for DIS_DELAY is 5 seconds and DIS_INTERVAL is 60 seconds.

Let $X = \{x_1, x_2, x_3, \dots, x_n\}$ is a set of new nodes wish to join the DODAG where $|X|=n$. The neighbours of each new nodes are represented by using $Y = \{y_1, y_2, y_3, \dots, y_m\}$ where $|Y|=m$. Here, X and Y are distinct sets. Hence, $X \cap Y = \Phi$. The sets X and Y form n x m matrix.

After a small interval Δt (DIS_DELAY), the new nodes send DIS messages to their neighbours to get back DIO message. The DIS flooding attack will occur during the time t (DIS_INTERVAL). The DIS attacks to be occurred in the new nodes take I different values, x_i ($i = 1, 2, \dots, I$), and the probability of the value x_i being taken is $P(x_i)$, the set of numbers $P(x_i)$ is said to be a probability mass function. The variable takes one of the values as it is given in Eq. 1.

$$\sum_{i=1}^I P(X_i) = 1 \tag{1}$$

It will take any value in this $0 \leq P_X(x_i) \leq 1$ range for all x_i . The probability mass function can be defined in Eq.2.

$$P(x_i) = m_i / Z \tag{2}$$

where, Z is the total number of DIS attacks and m_i is the node from which the DIS attack is initiated. To represent the number of attacks, whenever the new nodes enter into the network n x m matrix M is constructed. The row elements are the new nodes and the column elements are their neighbours. Whenever there is a DIS message sent from a node to its neighbours after the DIS_DELAY and before the completion of the DIS_INTERVAL, the corresponding M_{ij} value is incremented. The DIS flooding attack concept is depicted in the Fig.1.

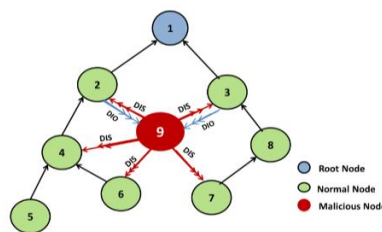


Fig.1. DIS Flooding Attack

As it is given in the Fig.1, the node ‘9’ is the malicious node which sends multiple DIS messages to its nearby nodes. The multiple arrows from the node ‘9’ indicate the multi-requests initiated by the attacker node. On receiving this requests, the adjacent nodes ‘2’, ‘3’, ‘4’, ‘6’ and node ‘7’ restart the Trickle Timer Algorithm to send the DIO message to the node ‘9’. This malicious act of the node ‘9’ will consume the resources of its neighbouring nodes like memory, processing and energy and also jams the routing process. This unnecessary resetting of the Trickle timer increases the control traffic and makes the network and communication links to be unavailable for the resource constrained IoT devices.

4 Proposed DISDet Technique

The DISDet technique has been proposed in this section as a countermeasure to address the DIS flooding attacks in RPL based IoT networks. Keeping in mind with the characteristics of the DIS message and the DIS flooding attacker, the DISDet technique has been deployed. The unnecessary reset of trickle timer and the overwhelming DIS message generation are circumvented using this DISDet. The steps involved for detecting the DIS flooding attack is explained in the Fig.2.

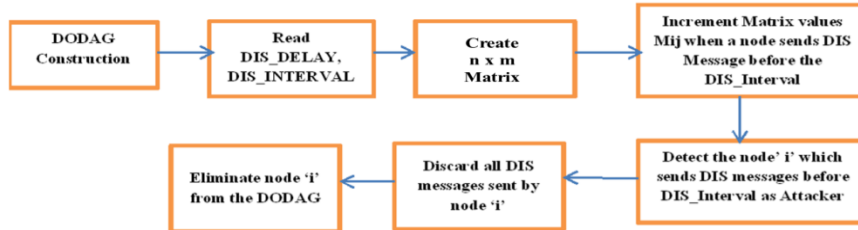


Fig 2. DISDet steps to Detect and Mitigate DIS attacks

As it is given in Fig.2, the DODAG is constructed using the normal procedure. When a new node enters, it has to wait until DIS_DELAY. After this waiting time it sends the first DIS message. Meanwhile, an n x m is constructed, where ‘n’ is number of new nodes and ‘m’ is corresponding neighbours. If there is a single node, then the matrix will be like a list or array. The matrix is given in the Fig. 3.

| | | | | | |
|------------|-----------------|-----------------|-----------------|-----------|-----------------|
| | 1 | 2 | 3 | .. | m |
| 1 | M ₁₁ | M ₁₂ | M ₁₃ | .. | M _{1m} |
| 2 | M ₂₁ | M ₂₂ | M ₂₃ | .. | M _{2m} |
| 3 | M ₃₁ | M ₃₂ | M ₃₃ | .. | M _{3m} |
| ... | .. | .. | .. | .. | .. |
| n | M _{n1} | M _{n2} | M _{n3} | .. | M _{nm} |

Fig.3. m x n Matrix to address DIS attack

In Fig.3, the row is denoted by using ‘i’ and column is represented using the variable ‘j’. At first, the matrix is initialized with zero. The matrix will record number of DIS messages sent from node ‘i’ to the node ‘j’ during the DIS_INTERVAL (60 seconds) time. Whenever a DIS message is sent from a node ‘i’ to the node ‘j’, the corresponding value of M_{ij} will be incremented. After the DIS_INTERVAL, the values in the matrix ‘M’ will be analysed and the attacker will be detected using the M_{ij} values as it is given in the Eq.3.

$$M_{ij} = \begin{cases} = 0 & \text{if 'i' is a normal node} \\ > 0 & \text{if 'i' is anttacker node} \end{cases} \quad (3)$$

Hence, if any cell M_{ij} has greater than zero value then the particular ‘i’ node is treated as the attacker node. All the messages generated during the DIS_INTERVAL by the node ‘i’ is discarded and the node ‘i’ is declared as an attacker and removed from the DODAG. Then the DODAG with the remaining nodes are reconstructed. The timer and the matrix values are reset after the DIS_INTERVAL and the process will be continued. The symbols used in DISDet algorithm are given in the Table 2.

Table 2. Symbol and Descriptions used in DISDet

| Symbol | Description |
|-----------------|------------------------------|
| D _D | DIS_DELAY; 5 Seconds |
| D _I | DIS_INTERVAL; 60 Seconds |
| t | Counter clock (60 to 0) |
| M | n x m matrix |
| (Row in M) i | A new node i |
| (Column in M) j | Neighbours of the new node i |

The Algorithm used for implementing the DISDet technique used in this research work is explained in Fig. 4.

Algorithm DISDet

1. Start
2. Read DIS_DELAY, DIS_INTERVAL // 5, 60 seconds respectively
3. Assign D_D=DIS_DELAY and D_I=DIS_INTERVAL

```

4. Construct the DODAG
5. if (n new nodes join the DODAG) then
6. { // wait for  $D_D$  time
7.   construct  $n \times m$  matrix  $M$ 
8.   Initialize the  $M_{ij}$  values as zero
9.   Set the counter clock  $t$  as  $D_I$ 
10.  if ( $t \neq 0$  and node_  $i$  sends DIS message) then // Check new node send DIS within  $D_I$ 
11.  {
12.    for( $i=1$  to  $n$ ) do
13.      for( $j=1$  to  $m$ ) do
14.        Increment  $M_{ij}$  value
15.      end for
16.    end for
17.  }
18.  for ( $i=1$  to  $n$ ) do // Detect Attacker
19.    for ( $j=1$  to  $n$ ) do
20.      if ( $M_{ij} > 0$ ) then
21.        {
22.          declare node_  $i$  as an attacker
23.          discard all DIS messages from node_  $i$ 
24.          isolate the node_  $i$  from DODAG
25.        }
26.      end for
27.    end for
28.    Reconstruct DODAG excluding node_  $i$ 
29.  }
30. End DISDet

```

Fig.4. Algorithm for Detecting the DIS flooding attack

The output of the algorithm is to make a decision on whether there is a DIS flooding attack in the IoT network or not and to disconnect the attacker. If all M_{ij} values of the matrix M contains zero then there is no attack present there. Otherwise, there is DIS attack and the corresponding i^{th} node is detected as the source of the attack. By implementing this algorithm, the DIS flooding attacks in the RPL based lossy networks can be detected.

5 Results and Discussion

5.1 Experimental Setup

In this experiment, maximum 50 nodes with unique identifier are included to form a 6LoWPAN network using random topology. The border router (6BR) acts as the root node. There are 50 normal nodes in this scenario and one node is a malicious node which sends DIS messages very often. The sample snapshot taken from the simulation experiment is shown in Fig.5.

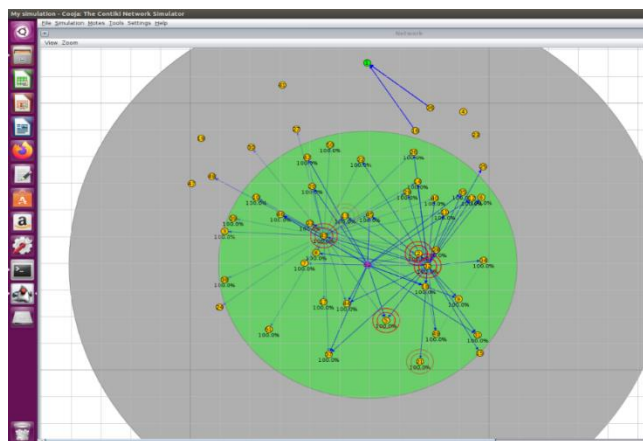


Fig.5. Screenshot with Attacker Scenario

The nodes represented using the green colour is the root node. The yellow colour nodes are the normal nodes and the purple colour node is the attacker node. The lines between the nodes represent the communication among the nodes. The transmission range (50 meters) is given as the green colour region and the interference range (100 meters) is shown using the grey colour region. The simulation grid of size 200 m x 200 m is used in this experiment. The simulation parameters are listed in the Table 3.

Table 3 Simulation Parameters

| | |
|-------------------------|---------------------------------------|
| No. of legitimate nodes | 51 (including root node) |
| No. of attacker nodes | 1 |
| Mote Type | Tmote Sky |
| Operating System | Contiki 3.0. |
| Simulator | Cooja Simulator |
| Topology | Random |
| Radio Medium | Unit Disk Graph Medium: Distance Loss |
| Topology Dimension | 200 m x 200 m |
| Transmission Range | 50 m |
| Interference Range | 100 m |
| Tx Ratio | 100% |
| Rx Ratio | 100% |
| Simulation Time | 30 minutes per Simulation |

5.2 Comparing Normal and Attacker Simulation

5.2.1 Network Graph

First, the normal scenario with 50 nodes and a root node was implemented in the Cooja Simulator and the simulation was performed for 30 minutes. Then a DIS attacker is included in the normal scenario and simulated for 30 minutes. The network graph captured from the normal and attacker scenarios are given in Fig.6.

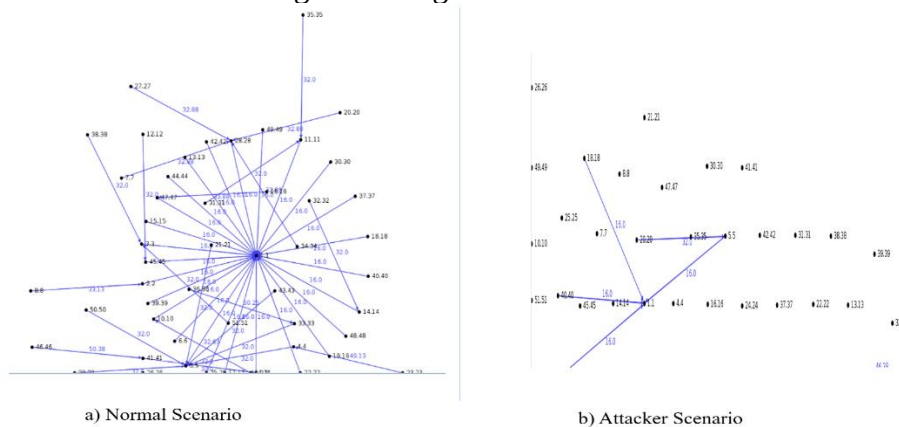


Fig. 6. Network Graph Captured in Normal and Attack Scenarios

As the normal scenario in Fig.6 denotes, the root node is connected to all child nodes without any loop in the DODAG. All nodes are able to communicate one another and there is no inconsistency. In the attacker simulation, because of the presence of the attacker node, there is a difficulty in constructing the DODAG and the nodes are unable to communicate.

5.2.2 Control Overhead

To construct the DODAG, number of control messages such as DIO, DAO, DAO-ACK and DIS are generated. The increase of the control messages in LLNs will reduce the performance. The number of control messages obtained in the normal and attacker environment after 5 minutes, 15 minutes and 30 minutes simulation are shown in Fig.7.

| Simulation Time | No. of Control Messages | |
|-----------------|-------------------------|----------|
| | Normal | Attacker |
| 5 minutes | 5875 | 9218 |
| 15 minutes | 13998 | 25678 |
| 30 minutes | 28889 | 52314 |

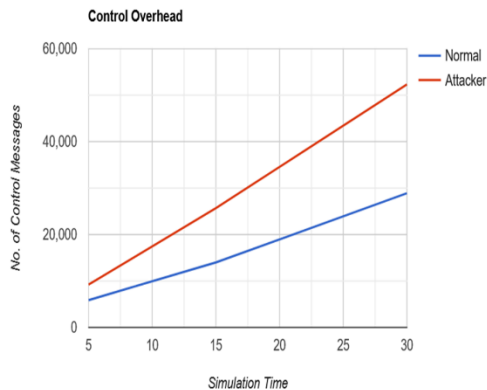


Fig. 7 Control overhead in Normal and Attacker Scenario

As it is depicted in Fig.7, the control overhead is higher in the attacker scenario. Because the attacker continuously sent DIS messages without considering the DIS_INTERVAL and for each DIS message, the Trickle Timer is restarted and the DIO messages are regulated. This increased the control overhead in this scenario.

5.2.3 Energy Consumption

Next, the energy consumption of each node in normal and attacker scenario are monitored using the collect view. The average power consumption details of each node in both scenarios are shown Fig. 8.

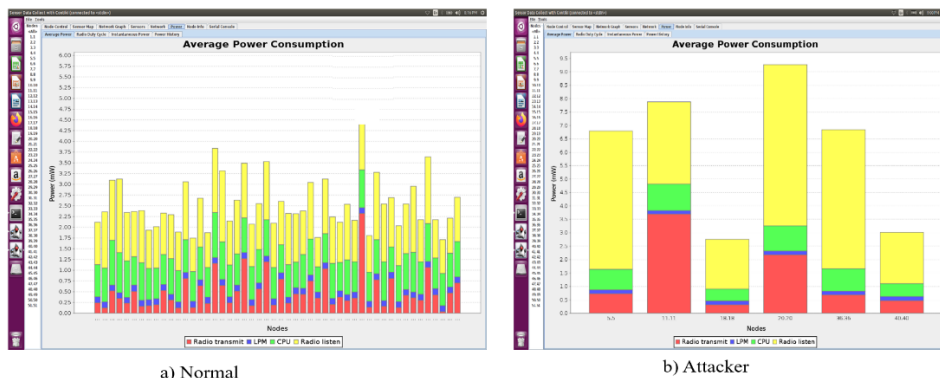


Fig.8 Energy Consumption in Normal and Attacker Simulation

According to the two graphs in Fig.8, the nodes in the attacker scenario consumed more energy than the normal scenario. The average energy consumed by all nodes in the normal scenario is 2.5 mV, whereas the attacker simulation nodes consumed 6 mV. Hence, the nodes in the attacker environment dropped their energy very soon than the normal environment. The lifetime of the nodes are also decreased due to this issue.

5.3 Implementing DISDet Technique

The proposed DISDet technique detects all DIS flooding attacks in RPL based IoT network. It has two phases such as Detection and Mitigation phase.

5.3.1. Detection Phase

In the Detection Phase, the number of DIS attacks and the source of DIS attack are identified. The proposed DISDet technique was installed in the border router in order to safeguard the IoT networks from DIS flooding attacks. The sample screenshot after implementing the DISDet is given in Fig.9.

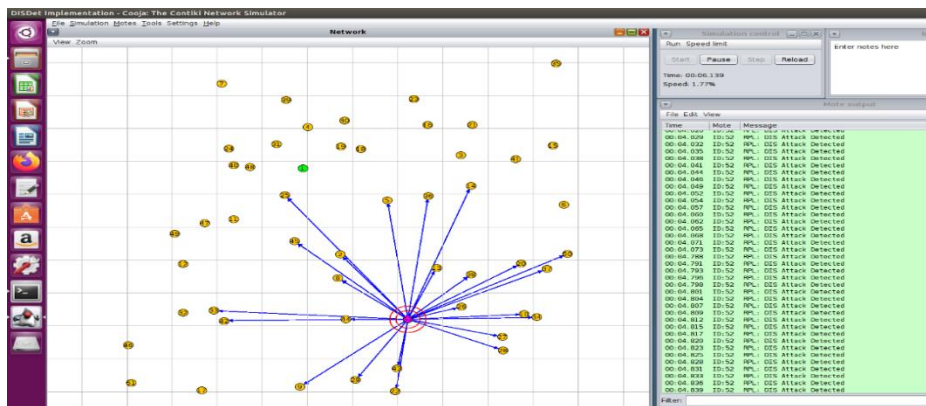


Fig.9. Screenshot after implementing the DISDet

The DISDet approach almost detects all initiated attacks by the DIS flooding attackers. The $n \times m$ created by the DISDet easily identifies the attacker and the number of attacks that enter into the networks from a particular node. The DISDet detection system detected 98.9% attacks during the simulation period.

5.3.2. Mitigation Phase

In Mitigation Phase, the identified attacker details are broadcasted and the attacker node is isolated from the DODAG and the root node is left to initiate the global repairing process in which the attacker will be excluded from the new DODAG. Sample DODAGs to illustrate the effect of the DISDet before and after the deployment of the mitigation phase are given in Fig.10.

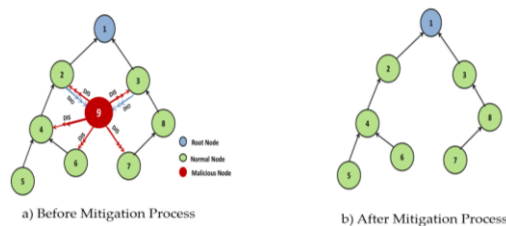


Fig.10. Mitigation Phase in DISDet

As the Fig.10 depicts, the attacker node '9' is removed from the DODAG after the implementation of the DISDet. The DIS messages initiated by the node '9' are also discarded. This saves the resources of the legitimate nodes and makes them available for their normal routing related responsibilities. Thus, the negative impacts of the DIS flooding attacks are minimized.

6 Conclusion

In this paper, the Characteristics and the negative impacts such as control overhead and energy consumption of the DIS flooding attacks were analysed. The proposed DISDet technique detects and mitigates the DIS flooding attacks effectively. After the implementation of the DISDet technique in the attacker scenario, the network performance is improved. The proposed technique detected almost all DIS flooding attacks with less false alarm rate. In future, other RPL attacks will be considered and AI based solutions will be provided to improve the attack detection rate of the system.

References

- [1] L. Wallgren, S. Raza and T. Voigt, "Routing Attacks and Countermeasures in the RPL-Based Internet of Things", International Journal of Distributed Sensor Networks, Hindawi Publishing Corporation, vol.2013, Article ID 794326, 11 pages, 2013, DOI:10.1155/2013/794326.
- [2] T. Winter and P. Thubert, "RPL: IPv6 Routing Protocol for Low-Power and Lossy Networks", RFC Standard 6550, March 2012.
- [3] S. Mangelkar, S. N. Dhage and A. V. Nimkar, "A comparative study on RPL attacks and security solutions", International Conference on Intelligent Computing and Control (I2C2-2017), 2017, pp. 1-6, DOI: 10.1109/I2C2.2017.8321851.

- [4] A.-S. Baghani, S. Rahimpour, and M. Khabbazia, "The DAO Induction Attack Against the RPL-based Internet of Things", arXiv: 2003.11061v1 [cs.CR], 2020.
- [5] A. Mayzaud, R. Badonnel, I. Chrisment, "A Taxonomy of Attacks in RPL-based Internet of Things," *International Journal of Network Security*, vol. 18, no. 3, pp. 459–473, 2016.
- [6] A.T. Le, J. Loo, K.K. Chai, M. Aiash, "A Specification-based IDS for Detecting Attacks on RPL-based Network Topology," *Information*, vol. 7, no. 2, pp. 25, 2016.
- [7] P. Levis, T. Clausen, J. Hui, O. Gnawali and J. Ko, "Trickle Algorithm", RFC 6206, Internet Engineering Task Force, ISSN:2070-1721, March 2011.
- [8] Cong Pu, "Sybil Attack in RPL-Based Internet of Things: Analysis and Defenses", *IEEE Internet of Things Journal*, Volume: 7, Issue: 6, pp. 4937 – 4949, 2020, DOI: 10.1109/JIOT.2020.2971463.
- [9] Ruan de A. C. Mello, Admilson de R. L. Ribeiro, Fernando M. de Almeida and Edward D. Moreno, "Mitigating Attacks in the Internet of Things with a Self-protecting Architecture", *The Thirteenth Advanced International Conference on Telecommunication- IARIA 2017*, ISBN: 978-1-61208-562.
- [10] S. Evmorfos, G. Vlachodimitropoulos, N. Bakalos and E. Gelenbe, "Neural Network Architectures for the detection of SYN flood attacks in IoT systems", *PETRA '20: The 13th Pervasive Technologies Related to Assistive Environments Conference*, June 2020, DOI:10.1145/3389189.3398000.
- [11] N. K. Thanigaivelan, E. Nigussie, S. Virtanen and J. Isoaho, "Hybrid Internal Anomaly Detection System for IoT: Reactive Nodes with Cross-Layer Operation", *Security and Communication Networks*, Vol.2018, Article ID. 3672698, 15 pages <https://doi.org/10.1155/2018/3672698>.
- [12] T. Nguyen, T. Ngo, T. Nguyen, D. Tran, H. A. Tran and T. Bui, "The Flooding Attack in Low Power and Lossy Networks: A Case Study", *International Conference on Smart Communications in Network Technologies (SaCoNeT)*, 2018, DOI:10.1109/saconet.2018.8585451
- [13] Cong Pu, "Spam DIS Attack Against Routing Protocol in the Internet of Things", *International Conference on Computing, Networking and Communications (ICNC)*, IEEE, 2019, DOI:10.1109/icnc.2019.8685628.
- [14] A. Verma and V. Ranga, "Mitigation of DIS flooding attacks in RPL-based 6LoWPAN networks", *Trans Emerging Tel Tech.*, 2019; Wiley, DOI: 10.1002/ett.3802.
- [15] K.N. Qureshi, S.S Rana, A. Ahmed and G. Jeon, "A Novel and Secure Attacks Detection Framework for Smart Cities Industrial Internet of Things", *Sustainable Cities and Society* (2020), DOI: 10.1016/j.scs.2020.102343
- [16] H. Tian, Z. Qian, X. Wang and X. Liang, "QoI-Aware DODAG Construction in RPL-Based Event Detection Wireless Sensor Networks", *Journal of Sensors*, Vol. 2017, Article ID 1603713, 9 pages <https://doi.org/10.1155/2017/1603713>.
- [17] A. Badach, "RPL messages and their Structure", *Internet of Things- Technologies, Protocols and Applications*, August 2018, https://www.researchgate.net/publication/326960497_RPL_messages_and_their_structure.
- [18] José V. V. Sobral, Joel J. P. C. Rodrigues, Ricardo A. L. Rabêlo, Jalal Al-Muhtadi and Valery Korotaev, "Routing Protocols for Low Power and Lossy Networks in Internet of Things Applications", *Sensors* 2019, 19, 2144; doi:10.3390/s19092144.
- [19] D. Sourailidis, R. Koutsiamanis, G. Papadopoulos, D. Barthel, N. Montavont. RFC 6550: On Minimizing the Control Plane Traffic of RPL-based Industrial Networks. 2020 IEEE 21st International Symposium on "A World of Wireless, Mobile and Multimedia Networks" (WoWMoM), Aug 2020, Cork, Ireland. pp. 439-444, [ff10.1109/WoWMoM49955.2020.00080ff](https://doi.org/10.1109/WoWMoM49955.2020.00080ff). [ffhal-02749045f](https://doi.org/10.1109/WoWMoM49955.2020.00080ff)
- [20] B. Farzaneh, M.A. Montazeri, and S. Jamali, "An Anomaly-Based IDS for Detecting Attacks in RPL-Based Internet of Things", *5th International Conference on Web Research (ICWR)*, 2019, DOI:10.1109/icwr.2019.8765272

Integration of A Chatbot With Education For The Smart Learning

Kavitha.K¹, Monisha.M¹, Vishnupriya.R¹, Brittadevi.V²

UG Student¹, Assistant Professor², Department of Computer Science & Engineering,
ST.Anne's college of engineering and technology, Panruti

Abstract

Chatbots are software agents used to interact between a computer and a human communication. Chat bots use natural language to communication with human users. Chatbots are used a lot in customer interaction, marketing on social networks sites and instantly messaging the client. Many conversational agents (Bot) are developed to answer users questions in a specialized domain. In everyday use of Bot user experience may extend beyond satisfying information needs to the enjoyment of conversations with Bot, some of which represent playful interactions. Intelligent bot systems interact with users in natural language. There is a growing excitement around conversational agents (CAs) or "chatbots". From tech giants' core products such as Apple Siri, Amazon Alexa, IBM Watson.

Keywords: chatbot, knowledge base, AIML

1 Introduction

A computer program that can talk to humans in natural languages! Uses Artificial Intelligence Markup Language (AIML) to represent knowledge. For a chatbot to perfectly emulate a human dialogue, it must analyze the input given by a user correctly and formulate a relevant and appropriate response. Chatbots are currently gaining a lot of popularity especially in business sector as they have the potential to provide customer service and reduce human efforts. All possible answers are then outputted as the answer. Although, the bot cannot generate new answers if trained Dialogue systems can be divided into goal-driven systems on a lot of question and answer dataset, and if the data set is pre-processed smartly, the bot can handle queries fairly such as technical support services, and non-goal-driven systems, such as language learning tools or computer games. The creation of these bots are relatively straightforward using some rule-based approach, but they can be used for realistic settings. All the components of the bot are not efficient in answering questions, whose pattern end-to-end systems are trained on past dialogs, so it does not match with the rules on which the bot is trained. Domain specific, thus it can be automatically scaled to new domains. Those bots can be created by using languages like Artificial domains.

2 Related Work

This section starts with an introduction of the primary elements of MemN2N used for Question answering. Then, we review another area relevant to this work, namely memory dynamics in such models. Also, the implementation of goal-oriented dialog systems.

2.1 End-to-End Memory Networks

The MemN2N architecture, introduced by Sukhbaatar[4], consists of two main components: supporting memories and final answer prediction. Supporting memories are in turn comprised of a set of input and output memory representations with memory cells. The input and output memory cells, denoted by m_i and c_i , are obtained by transforming the input context x_1, \dots, x_n (or stories) using two embedding matrices A and C (both of size $d \times |V|$ where d is the embedding size and $|V|$ the vocabulary size) such that $m_i = A f^3(x_i)$ and $c_i = C f^3(x_i)$ where $f^3(\cdot)$ is a function that maps the input into a bag of dimension $|V|$. Similarly, the question q is encoded using another embedding matrix B of size $d \times |V|$, resulting in a question embedding $u = B f^3(q)$. The input memories $\{m_i\}$, together with the embedding of the question u , are utilized to determine the relevance of each of the stories in the context, yielding a vector of attention weights.

2.2 Memory Dynamics

The necessity of dynamically regulating the interaction between the so-called controller and the memory blocks of a Memory Network model has been studied in [2]. In these works, the number of exchanges between the controller stack and the memory module of the network is either monitored in a hard supervised manner in the former or fixed a priori in the latter. In this paper, we propose an end-to-end supervised model, with an automatically learned gating mechanism, to perform dynamic regulation of memory interaction.

2.3 Goal Driven Dialog System

Goal driven dialog system is a system based on a specific goal. Perhaps the most successful approach to goal-driven systems has been to view the dialogue problem as a partially observable Markov decision process (POMDP)[14]. Most deployed dialogue systems use hand-crafted features for the state and action space representations, and require either a large annotated task-specific corpus or a horde of human subjects willing to interact with the unfinished system, hence limits its usage to a narrow domain. Our aim is to generate random conversations for goal oriented scenarios. This is equivalent of user simulators that are used to train POMDP [14].

3 Existing System

In this Existing System Hospital appointment ,Where the goal is to get the doctor appointment .model is trained with training data that contains input user utterances with expected output. The creation of these bots are relatively straightforward using some rule-based approach, but the bot is not efficient in answering questions, whose pattern does not match with the rules on which the bot is trained. Those bots can be created by using language like Artificial Intelligence Markup Language(AIML), a language based on XML that allow developer's write rules for the bot to follow.

4 Proposed System

Our proposed system is Education Bot, very useful for Students. Students as well as Faculty not require to take all books for College Just He/She go to College with the single Education Bot by these Innovative Technology. My Education bot is used for educational purposes. These bot contain all Engineering Book. For eg: If Student Text to bot :1st year. Then Bot reply to student : SEM 1/SEM 2?Then Student replay to Bot: SEM1 . Then Bot replay to Student : ENGLISH, or PYTHON or MATHS or PHYSICS or ENGINEERING GRAPHICS?Then Student replay to Bot: PYTHON. Then Bot giving PYTHON BOOK DOCUMENT to the Student.

Model is trained with training data that contain input user utterances with expected output. In an interactive environment user can chat with the bot in his own language, since we are using memory network rather than rule based, dialogues are context specific and bot give appropriate responses. Proposed system uses gated end-to-end memory networks model. This is an end-to-end supervised model with an automatically learned gating mechanism to perform dynamic regulation of memory interaction [11]. This will replace hard attention mechanism in Memory networks where attention values are obtained by softmax function. Gated End-to-End Memory network uses the idea of adaptive gating mechanism of Highway Networks and integrate it into MemN2N. Highway Networks, first Highway Networks, first introduced by Srivastava [3], include a transform gate T and a carry gate C, allowing the network to learn how much information it should transform or carry to form the input to the next layer.

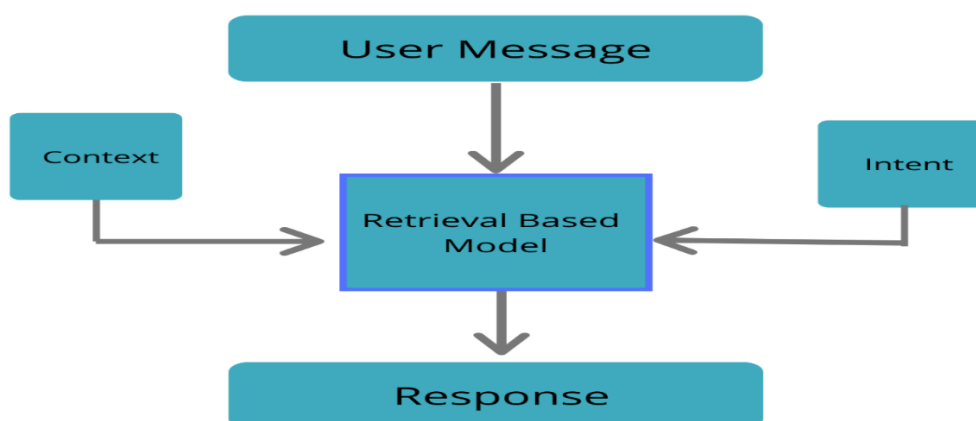


Figure 1: Architecture of the chatbot

5 Experiments & Result

In this section, we first describe the natural language reasoning dataset we use in our experiments. Then, the experimental setup is detailed. Lastly, we present the results and analyses.

5.1 Restaurant Reservation Simulation

If Student Text to bot :1st year. Then Bot reply to student : SEM 1/SEM 2?Then Student replay to Bot: SEM1 . Then Bot replay to Student : ENGLISH, or PYTHON or MATHS or PHYSICS or ENGINEERING GRAPHICS?Then Student replay to Bot: PYTHON. Then Bot giving PYTHON BOOK DOCUMENT to the Student.

5.2 Datasets

Datasets for training, validation and testing are generated by randomly running scripts. These three are mutually exclusive datasets. Validation dataset is used to minimize overfitting as training dataset actually produces an increase in accuracy. A user request implicitly forms a query that contains the required fields for API call. The bot must ask questions for filling the missing fields and eventually generate the correct corresponding API call. The bot asks questions in a deterministic order bot utterance and API calls.

5.3 Training

Learning rate η is initially assigned a value of 0.001 with 500 epochs. Linear start is used in all our experiments as proposed by [4]. With linear start, the softmax in each memory layer is removed and re-inserted after 10 epochs. Batch size is set to 32 and gradients with a 2 norm larger than 40 are divided by a scalar to have norm 40. All weights are initialized randomly from a Gaussian distribution with zero mean and $\sigma = 0.1$ except for the transform gate bias b which we empirically set the mean to 0.5. Only the most recent 50 sentences are fed into the model as the memory and the number of memory hops is 3. In all our experiments, we use the embedding size $d = 20$. Optimizer used is Adam Optimizer. We also constrain ourselves to the hop-specific weight tying scheme in all our experiments since GmemN2N benefits more from it than global weight tying.

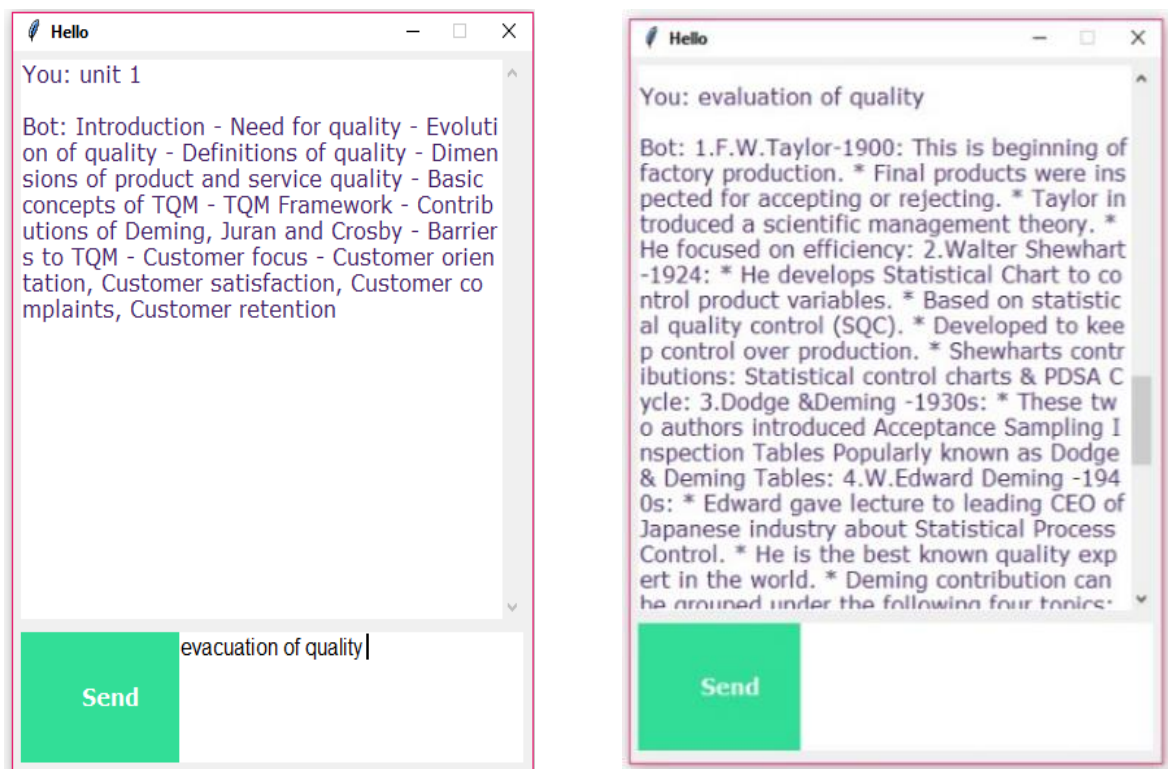


Figure 2: Conversation between student and bot

6 Conclusion And Future Work

In this paper we have proposed an attempt of incorporating an iterative memory access control to an end-to-end trainable memory enhanced neural network architecture. We showed the advantage of dynamic regulation of memory interaction, but it is still lack in some areas. In future work, we will investigate our model in language modeling and predictive learning so

that the machine is more intelligent in goalbased applications even though we are using synonyms or out of vocabulary words during conversation.

References

- [1] Bordes and J. Weston. Learning end-to-end goal- oriented dialog. In Proceedings of ICLR.March 2017
- [2] A. Kumar, O. Irsoy, P. Ondruska, M. Iyyer, J. Bradbury, I. Gulrajani, and R. Socher, Ask Me Anything: Dynamic Memory Networks for Natural Language Processing. In Proceedings of the 33rd International Conference on Machine Learning (ICML 2016), New York, U
- [3] R. Srivastava, K. Greff, and J. Schmidhuber. Highway networks. In ICML 2015 Deep Learning workshop
- [4] S. Sukhbaatar, A. Szlam, J. Weston, and R. Fergus. 2015. End-to-end memory networks. In Proceedings of Advances in Neural Information Processing Systems (NIPS 2015), pages 2440–2448, Montreal, Canada.
- [5] J. Weston, S. Chopra, and A. Bordes. 2015. Memory networks. In Proceedings of the 3rd International Conference on Learning Representations (ICLR 2015), San Diego, USA.
- [6] J. Weston, A. Bordes, S. Chopra, A. Rush, B. Merriënboer, A. Joulin and T. Mikolov. 2016. Towards AI-complete question answering: A set of prerequisite toy tasks. In Proceedings of the 4th International Conference on Learning Representations (ICLR 2016), San Juan, Puerto Rico.
- [7] C. Xiong, S. Merity, and R. Socher. 2016. Dynamic memory networks for visual and textual question answering. In Proceedings of the 33rd International Conference on Machine Learning (ICML 2016), pages 2397–2406, New York, USA.
- [8] R. Srivastava, K. Greff, and J. Schmidhuber. 2015b. Training very deep networks. In Proceedings of Advances in Neural Information Processing Systems (NIPS 2015), pages 2377–2385, Montreal, Canada
- [9] A. Miller, A. Fisch, J. Dodge, A. Karimi, A. Bordes, and J. Weston. 2016. Key-value memory networks for directly reading documents. In Proceedings of the 2016 Conference on Empirical Methods in Natural Language Processing (EMNLP 2016), Austin, USA.
- [10] Y. Chen, D. Hakkani-Tür, G. Tur, J. Gao, and L. Deng, (2016). End-to-end memory networks with knowledge carryover for multi-turn spoken language understanding. In Proceedings of Interspeech.
- [11] F. Liu, J. Perez (2017). Gated End-to-End Memory Networks. In Proceedings of the 15th Conference of the European Chapter of the Association for Computational Linguistics (ACL 2017), Spain
- [12] H. Wang, Z. Lu, H. Li, and E. Chen, (2013). A dataset for research on short-text conversations. In EMNLP.
- [13] Z. Wang, and O. Lemon, (2013). A simple and generic belief tracking mechanism for the dialog state tracking challenge: On the believability of observed information. In Proceedings of the SIGDIAL 2013 Conference.

Computer-Aided Detection System for Mammogram Screening – A Review Using Image Processing and Machine Learning Techniques

K. Poornambigai^{#1}, K. Balasubramanian^{#2}, and K. Karthikeyan^{#3}

^{#1}*District organization commissioner, Hindhustan Scout & Guide, Cuddalore – 607302, Tamil Nadu, India.*

^{#2}*Research Scholar, Department of Mechanical Engineering, Annamalai University, Annamalai Nagar – 608002, Tamil Nadu, India.*

^{#3}*Research Scholar, Department of Electrical Engineering, Annamalai University, Annamalai Nagar – 608002, Tamil Nadu, India.*

Abstract

This paper aims to review the previously developed Computer-aided detection (CAD) systems for mammogram screening because increasing death rate in women due to breast cancer is a global medical issue and it can be controlled only by early detection with regular screening. Till now mammography is the widely used breast imaging modality. CAD systems have been adopted by the radiologists to increase the accuracy of the breast cancer diagnosis by avoiding human errors and experience related issues. This study reveals that in spite of the higher accuracy obtained by the earlier proposed CAD systems for breast cancer diagnosis, they are not fully automated. Moreover, the false-positive mammogram screening cases are high in number and over-diagnosis of breast cancer exposes a patient towards harmful overtreatment for which a huge amount of money is being wasted. In addition, it is also reported that the mammogram screening result with and without CAD systems does not have noticeable difference, whereas the undetected cancer cases by CAD system are increasing. Thus, future research is required to improve the performance of CAD system for mammogram screening and make it completely automated.

Keywords: *Breast cancer screening CAD system Classification Medical imaging systems Segmentation*

1. Introduction

Breast cancer counts 1 in 4 among all cancer cases in women [1] and this itself expresses the severity of the disease. This disease not only raises concern for women, but it can happen to men also, although the number is limited [2]. Since the death rate is high due to breast cancer and early symptoms are rarely found, hence, regular screening is the only option to save a life. There are two ways of breast cancer detection, namely via imaging and clinical laboratory evaluation. Imaging diagnosis is hypothetical and it includes interpretation of different medical images by either radiologists or using computer-aided detection (CAD) systems. Whereas, laboratory tests involve nipple aspirate fluid (NAF) analysis, breast biopsy and genetic test. These biological tests are costly, invasive, risky, and can contribute to patients' discomfort during the procedure and hence, image screening is performed to find out the presence of carcinoma in breast tissues before an individual is referred for invasive means of biological diagnosis.

Detection of abnormal tissues in medical images is the signs on which non-invasive imaging diagnosis is based. There are several available methods for imaging of the breast, such as mammography, ultrasound, magnetic resonance imaging (MRI), computed tomography (CT), positron-emission tomography (PET) and microwave imaging as illustrated in Figure 1. A CAD system first reads a medical image before it sequentially performs pre-processing, segmentation, feature extraction, and classification activities [3] on that malignant tumors from abnormal cases. The working procedure of mammogram screening through a CAD system is depicted in Figure 2.

CAD systems are of high preference for automatic image analysis to avoid misdiagnosis due to the involved radiologist's lack of experience. In addition, it was also expected to save money by avoiding double reading by radiologists while considering single reading by CAD system. Several researches were already done on different CAD system for breast cancer diagnosis. But report says [4] that the false-positive rate of mammographic screening has been increased substantially than past years which in turn raises the over-diagnosis rate for breast cancer. Moreover, it was also revealed

[5] that the results obtained after screening the mammogram with and without CAD systems for both sensitivity and specificity are nearly similar and the non-accurate breast cancer diagnosis by a CAD system increases the false-negative cases [5]. Altogether, a huge amount of money is being wasted per year although the recent CAD systems are more sensitive towards breast cancer diagnosis. Therefore, further research is required to propose an improved CAD system for mammogram screening. The objective of this study is to review the past researches on proposed CAD system for mammogram screening to find the area of improvements for future research. This paper is divided in few sections to provide an introduction on the terminologies of breast cancer and then an extensive review was done on different types of breast imaging systems and stages of CAD system followed by a discussion. In the last section, this paper is concluded.

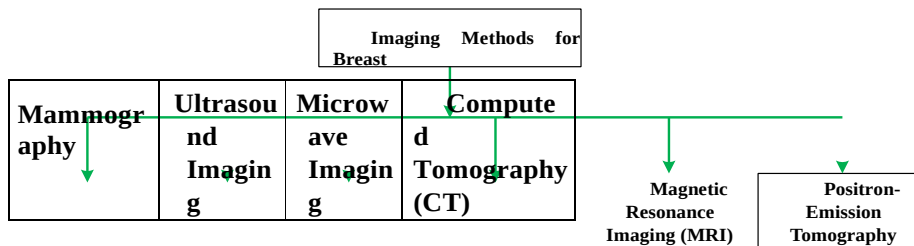


Figure 1. Different imaging methods for breast

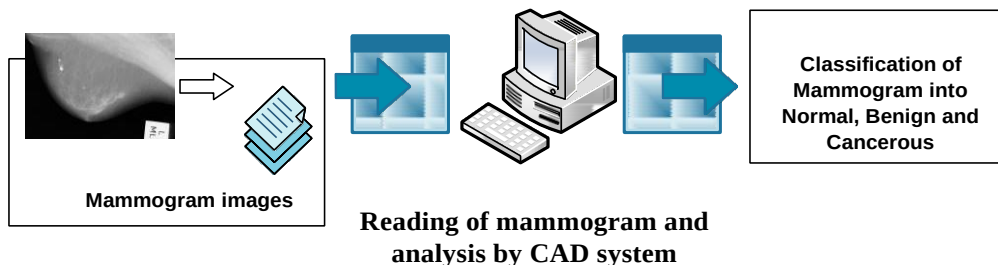


Figure 2. Working procedure of a CAD system

1. Construction Elements Of Breast And Different Tumors

Lobules, ducts and connecting tissues are the main constructing elements of the breast. Milk is produced in lobules, which are generally known as milk glands, and it is carried up to the nipple through ducts which are actually tiny tubes. Different fibrous and fatty tissues are responsible for the size and shape of the breast and keep other tissues in place. In most cases, cancer initiates either in ductal or lobular tissues of women’s breast due to the uncontrollable growth of breast cells, which ultimately generates tumors or lumps [6]. Two types of breast tissues can be identified during diagnosis namely normal, and abnormal. Benign and malignant are two types of tumors among abnormal tissues. While the normal tissues do not possess any tumor, the presence of malignant cells differentiates benign from cancerous tumors [7]. Lump at any point of the breast is the main indication of breast cancer. Other symptoms such as swelling at any part of the breast, discharge from the nipple, redness of nipple and pain in the breast or nipple may also be accounted for breast cancer. The risk factors associated with

breast cancer are breast density, age, personal history, family history, first menstrual cycle, pregnancy history, being overweight, and the habit of alcohol consumption. In addition, the use of combined hormone therapy, oral contraceptives and previous chest radiation exposure would also increase the chance of having breast cancer. However, the mechanism of these factors in the development of breast cancer remains unknown [6].

Figures 3 (a) and (b). A mass is a space-occupying lesion with features such as location, density, and margin. Benign masses are generally round shaped with smoother and well-defined margins having low-density. The high-density masses of stellate or speculated shape with improper margins is usually found as malignant. Architectural distortion and bilateral asymmetry are other aspects of cancerous masses.

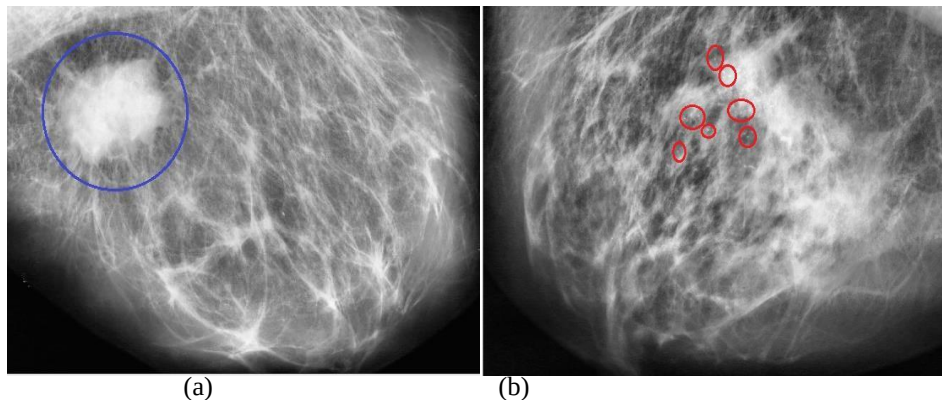


Figure 3. (a) Spiculated mass, (b) Microcalcifications as referred from MIAS dataset

Minute calcium depositions in the breast can be seen as tiny bright spots in mammogram and they are known as Calcifications. Depending on size, it is classified as macro and microcalcifications. The main concern is with the latter one as the probability of malignancy is high. Around 0.3 mm is the size of microcalcifications in general and its possession of mass is not necessary. Benign calcifications are usually identical, large in size (diameter around 1–4 mm), coarse, round or oval-shaped, and dispersed or diffused. Microscopic, stellate-shaped, clustered in branches, innumerable (more than 5 in numbers) microcalcifications of different size and shape are found to be as malignant [3].

2. Medical Images Used For Breast Cancer

All Medical images contain information of the human body and their composition or characteristics. They are formed by the signals due to their different penetration level through the tissues or by the re-emission of energy from the tissues, wherein these signals may not be of the same type. The information depicted by an image varies due to the changing contrast between different types of tissues. The target location of these images may be inside the body, even several centimeters below the accessible surface. Electromagnetic signals of frequency ranging between few hertz to exahertz have the capabilities of penetration and accordingly, they are used in medical imaging systems. Two key objectives are mainly considered in the previous studies in developing these imaging modalities; they are location specificity and lesion detection. Different techniques for breast imaging are discussed below.

Mammogram is a special type of X-ray for breast tissues. Lower dose X-ray of frequencies ranging from 30 petahertz to 30 exahertz is utilized to obtain two or three dimensional (2D or 3D) mammography images [9]. Film and digital are two types of mammograms. Film mammography was considered as a powerful tool for breast cancer screening from a longer time [10]. But it has drawbacks, such as lower sensitivity towards the dense breast, limited contrast characteristics, longer processing time and grain effect. The contrast can be manipulated in digital

mammography and thus, presence of the lesion can be visible. Moreover, the processing time is less and better sensitivity can be obtained for dense breasts in digital mammography. Another limitation of mammography is that the patients are exposed to X-ray ionizing radiation.

Sound waves ranging from 2-20 MHz [9] are used in ultrasound imaging to produce the images of a single plane. This technique provides a better result for lesion detection in dense breast and can be used in real time. On top of that, tissue elasticity can also be determined as was elaborated in [10] for classification purposes. Nevertheless, it mostly depends on the expertise of the operator since real-time tuning of gain, pressure, focal zones, patient positioning, dynamic range are required along with the recognition of peculiarity of the lesion.

Magnetic Resonance Imaging (MRI) system is built with RF coils along with a big size magnet (3-5 Tesla). An intravenous injection of gadolinium is given to the patients before capturing 3D images through MRI. It can detect minute abnormalities of breast tissues and also the ductal carcinoma in situ in the dense breast along with its spread to the chest wall [10], this is largely because it has better temporal and spatial resolution [9]. Nonetheless, MRI cannot be used for those with a medical history of kidney disease as the injection can cause nephrogenic systemic fibrosis [9]. Moreover, the patients with a pacemaker and any metal implant are also not suitable for MRI due to its magnetic effect. Additionally, it is time-consuming and generates blur images [9]. Therefore, incorrect reading of MRI image may require a patient to go through the same process for several times.

Computed Tomography (CT) uses high dose x-ray radiation to generate the detailed scans or images of inside body. In most of the cases, CT machines generate continuous pictures in a helical (or spiral) fashion rather than producing a series of pictures of individual slices of the body. Helical CT has several advantages such as it is fast, it produces better 3-D images and it has better sensitivity in the detection of small abnormalities [11]. The newest CT scanners, called multislice CT or multidetector CT scanners, allow more slices to be imaged in a shorter period of time. Sometimes, contrast agent like iodine and barium are injected into the blood or given by mouth or enema as a way to do the CT scan. However, its high exposure to relatively large amounts of ionizing radiation than standard x-ray procedure makes it least favorable as a regular screening method.

In Positron Emission Tomography (PET) imaging system, a radioactive substance is injected into the blood to identify the most active body cells, especially the cancerous tissues. PET scan can be added with computed tomography (CT) so that both anatomical and functional views of the suspected cells can be observed. PET is not restricted to breast density and is useful in identifying axillary nodes and distant metastases [10]. However, it has poor sensitivity in detecting small tumors because of their small size.

The wavelengths ranging from a millimeter to a meter can penetrate many optically opaque mediums like living tissues based on the presence of ionized molecules due to a variety of dissolved substances, such as sugar, and the permittivity of any tissue is strongly dependent on its water content [12]. This theory is utilized in microwave imaging either by using a contrast agent or by utilizing radar [13] and this technique is quite new to biomedical engineering. Microwave signals scatter significantly from malignant breast tissues due to their water content and these scattered signals are captured in microwave imaging system [14]. Time requirement is considerably less in microwave imaging, but the heavy computational load is the main drawback of this system [13].

Ultrasound imaging and MRI are used along with mammography to increase the screening specificity [9]. Other than the mammography, ultrasound, and microwave imaging, the rest of the imaging systems discussed above are costly for regular screening. It is also observed that the use of microwave imaging as a regular screening tool is still subjected to further study and also under trial. Whereas, the accuracy of ultrasound imaging is fully dependent on the expertise of the operator. Moreover, despite all its limitations, to date mammography is the widely accepted imaging method. Radiation issue can be controlled by increasing the gap between two consecutive screenings. Therefore, the following subsections are devoted only to digital mammogram mainly due to its easy availability, ease of image manipulation, and fast screening time.

3. Stages Of Cad Systems

Each stage of a CAD system has some objective to finally achieve the obtained result and those

can be obtained by applying different techniques, such as cropping, noise removal, and enhancement are done during the pre-processing stage. Likewise, image segmentation is significant in segregating the image background along with identification and partitioning of the area of interest (AOI) because different breast tissues have different resolutions. Different stages and various methods to perform the activity of that stage are shown in Figure 4.

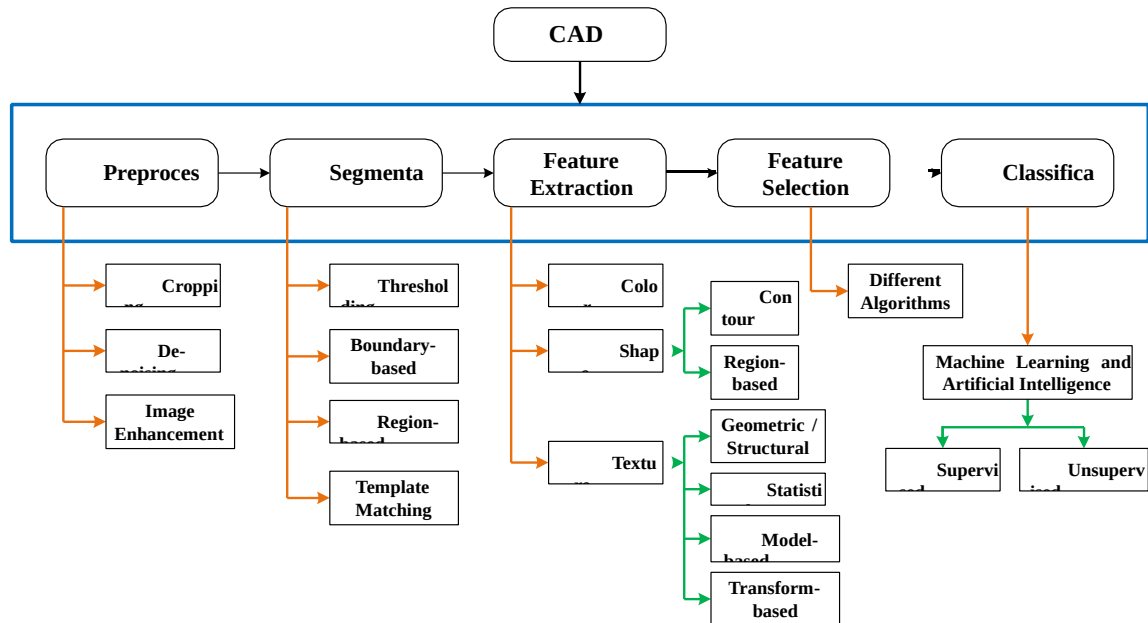


Figure 4. Stages of a CAD system and different methods of each stage

3.1. Pre-processing

Noise, uneven illumination and low contrast are the main drawbacks of the mammogram and thus, AOI identification and feature extraction are tough in this case. To negate the effects of these defects, cropping, de-noising, and enhancement of images are performed at the pre-processing stage before performing segmentation and feature extraction. The unwanted labels, artifacts and the image portion without information can be removed by cropping. During the acquisition of a digital image, noises which include readout and shot noise may be present. Several types of noises and all possible de-noising methods were discussed in earlier work [15]. De-noising of an image not only removes the noise but also smoothen the signals. Based on the histogram of an image, the enhancement procedure improves the contrast level of an image and hence, the features are more identifiable.

Detection of masses is far complicated than that for microcalcifications as the traits of masses are hard to perceive and sometimes they appear like normal breast tissues [16]. Since the microcalcifications have higher contrast than the rest of the region, and they are corresponded to high-frequency components, they may be easily detected through image enhancement and de-noising as it was done in [17] by using dyadic wavelet processing. Meanwhile, masses have low contrast, varying densities, spiculated structures, and have low-frequency components. The implementation of Contrast Limited Adaptive Histogram equalization (CLAHE) along with Median filtering provided the sensitivity and specificity of 96.2% and 94.4%, respectively, for the detection of masses [18].

3.2. Segmentation

The removal of image background and the selection of AOI are the vital tasks in image processing, as is required in the segmentation stage. The common procedures used in image segmentation include thresholding, boundary-based segmentation, region-based segmentation, and

template matching as illustrated in Figure 5.

3.2.1. Thresholding

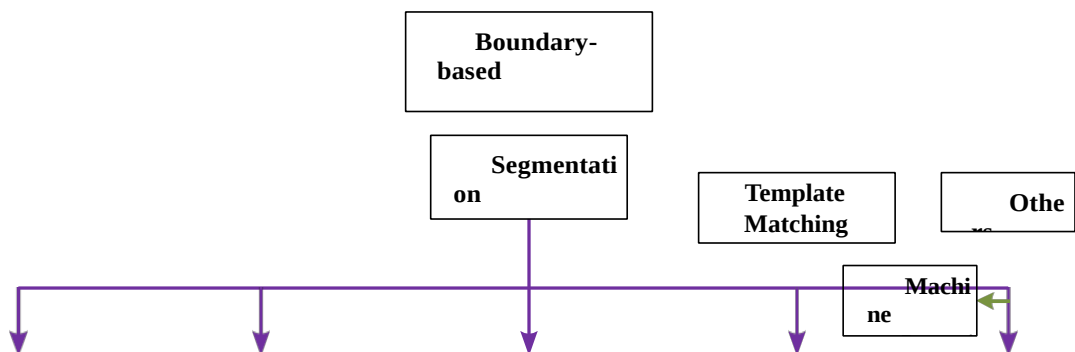
This is a very common method to partition an image where the image background that does not carry any essential information, is removed. Based on the gray level histogram, the threshold value is selected and the difference between the useful and background image pixel intensities segments the image [19]. It is a fast and simple method to implement but does not guarantee object coherency for which post-processing may be required by some other operators. When only one threshold, T , is set on the basis of the entire image $x(i, j)$ then, it is called global. If an image is segmented in sub-regions and T is selected for each sub-region depending on both and some local image property $L(i, j)$, then it is known as a local threshold. Thresholding is classified as bi-level and multilevel thresholding; it can be expressed as $T = [T_1, T_2, \dots T_N]$ so that all pixels,

$$(i,j) \in [T_k, T_{k+1}]$$

(1)

where $k = 0, 1, \dots N$. Therefore, $(N + 1)$ sub-regions will be generated. An image is divided into two parts, namely the useful region, which is denoted by white, and the background is reflected by black in bi-level thresholding. Multilevel thresholding is required for images with different surface characteristics [20]. The maximum entropy method, the minimum error method, and Otsu's method are among the classic thresholding techniques [21]. Otsu's thresholding is sensitive towards salt and pepper noise and hence, before its application, de-noising is required to smooth the image. Researchers in [22] used thresholding to segment a mammogram at multiple levels and a set of features was computed from each of the segmented regions. Their study achieved 80% sensitivity with an average rate of 0.32 false-positives per image. Another study [23] proposed a probabilistic adaptive thresholding technique based on texture information and its probability to obtain the most feasible threshold values for specific parts of the mammogram. In this adaptive thresholding method, the threshold values were neither calculated using histogram nor by the shape of the region. This was done to eradicate the issues related to non-uniform intensities in the background region of a mammogram for which global threshold-based methods may fail. In [24], three classes threshold method along with edge detection algorithm was implemented for segmentation. Hybrid image segmentation along with Otsu's thresholding was used in [25] for accurate detection of a breast tumor, and its size.

Thresholding is simple to implement even in real-time applications. It is fast and computationally inexpensive. Moreover, no prior information about the image is required. Nonetheless, its performance is poor for noisy image and also for images having no peak or broad, or flat valleys. The main drawback of thresholding is that it ignores spatial data of an image and thus, it fails to inform about the contiguousness of the segmented areas. Furthermore, only correct threshold selection can avoid the under or over segmentation. Thresholding along with other method can provide a better output as can be found from the works in [22–25].



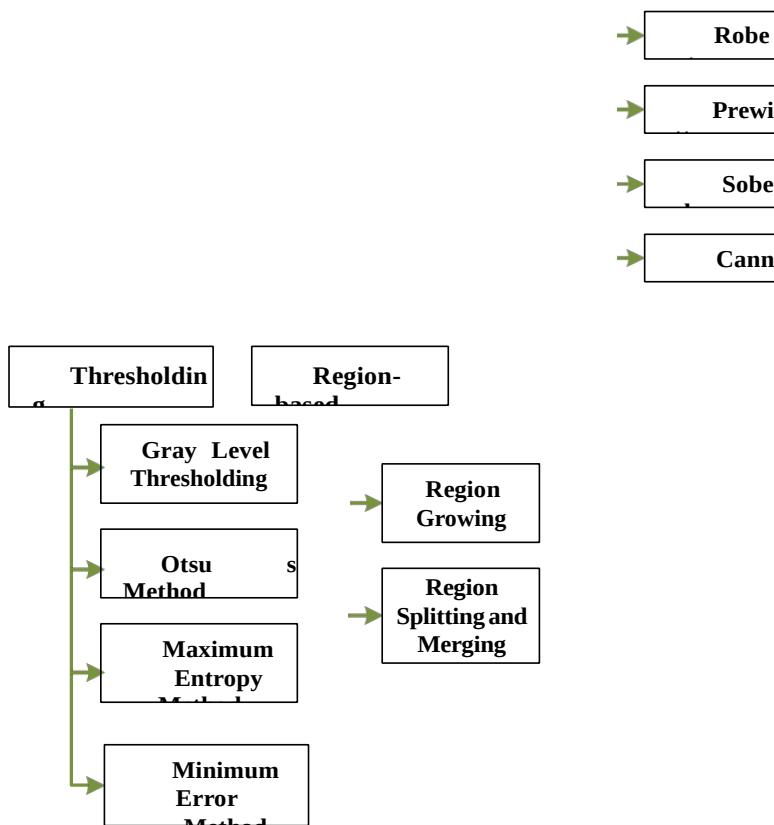


Figure 5. Different techniques of segmentation

3.2.2. Boundary-based segmentation

In this method, boundary or contour or edge of AOI is outlined to identify discontinuities or abrupt changes in a gray level image. There is no golden rule to determine the edge. It solely depends on the choice of the application. High pass filter and gradient filters such as Roberts, Prewitt, Sobel, and Canny are the basic techniques of edge detection. Nevertheless, edge detection based on the first order derivatives is not robust. They are highly sensitive to noise and a threshold is required. Meanwhile, detection based on the second order derivatives is able to locate the edge at zero-crossing; it is also more robust, less sensitive to noise and does not require the use of threshold in post-processing. The operator’s size and computational complexity are proportional to each other in this method and it also ignores the spatial information of an image. An algorithm was proposed in [26] to enhance the mammogram before passed it onto Radial Speculation Filter for detection of the spiculated lesion. Butterworth high-pass filter along with Sobel edge detection operator was used in [27] and the experimental result was considerably effective. In [28] Sobel edge detection was implemented for initial contour estimation. Non-linear Polynomial Filtering was employed in [29] to enhance the edges and sharpen the lesions in mammograms so that the dependencies on pre-selected thresholds may be minimized.

3.2.3. Region-based segmentation

Different regions of similar features like gray level, color, texture, are identified in an image by region based segmentation. This is known as Region Growing or Splitting mechanism. In this process, AOI is selected through a predefined condition based on the previously obtained result by the intensity or edge details of the image so that tumor regions can be identified. However, this method needs additional operations such as uniform blocking, merge and split etc. [30] that shall be performed before the

application of this method. In addition, its requirement for the manual depiction of an initial point makes it disadvantageous [19]. A study in [31] used this method for segmenting out the pectoral tissues from the mammogram and it was further used for classification. Mean Based Region Growing Segmentation (MRGS) was implemented in [32]. Researchers applied an automated region growing segmentation technique in [33] where the threshold was obtained from a trained Artificial Neural Network (ANN). In both [34, 35] works, automatic seed selection was done before the use of region growing method.

Region-based segmentation is flexible in choosing between interactive and automatic method. An identifiable object boundary is generated due to the flow from an inner point to the outer region. The output of this method is better than any other segmentation procedure when an appropriate seed is selected. Conversely, noisy seed selection may lead to faulty segmented area. By nature, it is sequential and does not have significant effect on minute regions. The main limitations of this method are stopping criteria, higher computation time and memory.

3.2.4. Template matching

Detection of an object's presence in an image is an important task. This problem can be resolved with a priori knowledge of the detected object or template, which may be used to identify its location in a given scene. Therefore, if there is no prior knowledge of any tumor, it is difficult to utilize this technique and this is the main drawback of this technique. Researchers in [36] used Sech template to identify the suspicious areas and optimize them with thresholding. Template-matching technique was also used in [37] along with a local cost function and dynamic programming to optimize the contour.

3.3. Feature extraction and selection

An image feature may include color, shape, and texture. The contour-based and region-based representations are two types of techniques to provide shape features. The first method depends on the boundary information to provide the shape feature, but despite this limitation, it is more popular among researchers than the latter method that provides the shape features based on the complete region [38]. The texture features are geometric or structural, statistical, model-based, and transform-based and they were widely used in several earlier researches. Structural features are dependent on a set of primitives or patterns such as blobs, and edges and also on their spatial arrangement in hierarchy. But in most of the cases, this method provided unacceptable results for biological images due to their homogeneous spatial arrangements [39]. Statistical features are the spatial distribution of intensity values of the pixels and they can be of first order (e.g. mean, variance, standard deviation, skewness, kurtosis, and entropy) and second order. When first order provides information about particular pixel and its associated intensity, the second order such as Gray Level Co-occurrence Matrix (GLCM) reveals the relation in terms of contrast, correlation, energy, and homogeneity between particular pair of pixels having specified distance and angle. The first order statistical features are simple and of low computational cost. Second order statistical features provide better result despite the fact that the increasing statistical order raises the computational cost exponentially. Nonetheless, the efficiency and accuracy of the results are dependent on the selected distance and angles between pixels in case of GLCM and in [40], researchers efficiently calculated the geometric and texture related measures using GLCM. Local Binary Pattern (LBP) is a technique combining structural and statistical texture analysis methods. It reveals the intensity relations between a pixel and its neighbor through binary pattern. Although it is robust, its computational cost is expensive especially when the number of features considered is high. A fusion method was implemented in [41] combining the Completed LBP (CLBP) and Curvelet sub-band features and an accuracy of 96.68% was achieved with a reduced number of false positive in comparison with the experiment based on only CLBP features. Autoregressive models, Random Fields (e.g. Markov Random Fields) and Fractals are the Model-based methods for texture analysis in which a priori model is considered as a texture descriptor. While Random Fields methods suffer huge computational

burden, Fractal procedures gain attraction due to their ability to find spatial complexity at different scales making it easier to find out the architectural distortion. In [42], fractal dimension was used to identify different textural patterns in the breast region, and the obtained classification result was satisfactory using the non-automated procedure. Transform-based texture analysis through spatial

domain filters, Frequency domain filters, Gabor and Wavelet transform methods divides an image into different spaces to extract the features. Spatial domain filters (e.g., Robert and Sobel) are extensively used in detecting the edges, but their output in case of irregular texture is poor. Discrete Cosine Transform (DCT) and Discrete Fourier Transform (DFT) are able to analyze the spatial frequency of an image but both approach lack the spatial localization. Therefore, Gabor or Wavelet transform is advantageous for its ability to identify the spatial location. Even though wavelet is not translation invariant, this can be overcome with curvelet analysis [3].

Besides all these conventional procedures, researchers proposed a new feature extraction method namely Square Centroid Lines Gray Level Distribution method (SCLGM) and Run Difference Method (RDM) in [43]. Discrete Wavelet Transform (DWT) and Spherical Wavelet Transform (SWT) were used to extract texture features from the images in [44]. According to the researchers [45], statistical properties of curvelet coefficients can be used in future works to improve the classification accuracy. The use of different feature extraction methods may be better than using the curvelet coefficients. In recent years, researchers are concentrating on the study of complete breast parenchyma for extracting the texture features incorporating lattice-based strategy to identify the heterogeneity of breast tissues as was done in [46] and the huge pool of features were reduced using Convolutional Neural Network (CNN).

It must be mentioned that the presence of redundant and irrelevant features may significantly degrade the precision. If the features are not properly selected, it may also reduce the learning speed of the appointed algorithm [47]. Therefore, the accuracy of classification depends largely on feature selection from a large set of data, especially in the case of artificial intelligence. Several algorithms found their uses in earlier researches on CAD system for mammogram analysis; among which Genetic Algorithm (GA) appeared promising because it works in a vast solution space with high dimensional features. This technique can minimize the redundancy and achieve better accuracy. It is a population-based metaheuristic search or optimization technique inspired by Darwin's evolution theory [48] and its performance extensively depends on its control parameters such as population size, crossover rate, and mutation probability. Therefore, these parameters must be selected properly to avoid any unsatisfactory result. The researchers in [49] proposed a computational technique for detection and segregation of AOI in mammogram using GA and multi-resolution technique that offered relatively high accuracy result. They proposed transform functions for specified advantages like phase information, high directionality, and shift insensibility [49].

3.4. Classification

Classification is the last stage of image analysis to distinguish firstly, the normal and abnormal tissues and secondly, to segregate the benign and malignant tumors from abnormal cases. This is viable with pattern recognition [19]. Selected features can be classified either by supervised or by unsupervised method. In the supervised method, it is required to train the system first and then the rest of the data can be tested by the trained system. However, an unsupervised method is dependent on machine learning to describe the hidden structure of unlabeled data.

A feature space is the whole range of a defined function of an image. The classifier is a supervised method to divide a feature space that is done by using labeled data [50] for training purposes to segment new set of data automatically. The functions, which are already defined in feature space, are responsible to divide this feature space further into several regions [19]. Classifiers are computationally fast and can be implemented in multichannel images [50]. There are several methods to train a classifier namely Parzen window, nearest neighbor, k-nearest-neighbor, maximum likelihood/Bayes classifier, and decision tree. Parzen window and k-nearest-neighbor (KNN) classifiers provide no underlying assumption about the statistical structure of the data for which they are considered as the non-parametric classifiers. The maximum-likelihood/Bayes classifier is, however, a parametric classifier that considers pixel intensities as independent samples from a mixture of probability distributions. The computational burden of these methods is quite high, particularly with large data set.

Clustering is an unsupervised method to classify an image; this technique can be described as a classifier without using training data, but it needs initial parameters or segmentation process [50]. The self-training is done by iteratively dividing an image through segmentation and train itself with the existing data. K-means, expectation maximization (EM) and Fuzzy c-means are considered as clustering methods. Since it does not require initial spatial modeling, it may be sensitive to intensity in

homogeneities and noise. Clustering is mainly applied in segmenting MRI and in the cases where pixel intensity distributions are detached [19].

ANN is an information processing technique that is inspired by the way human brains process information. It is through a set of inter-connecting nodes, usually known as neurons, which deliver the output through a computer model. Each node is associated with gain or weight that can be adjusted to get the required output from the given input. Learning, and recall is the two working phases [3]. Weight adaptation of the nodes is done to train the ANN about the task during the learning phase either through supervised or unsupervised methods [19, 50]. The recall is for validation and resolving an issue. Feed forward and back propagation are two ways of learning procedure. ANN can also select features for which the weights or gains of the nodes should be adjusted and trained accordingly. Feed forward Neural Network (FNN) was used as a classifier that was trained through Jaya algorithm in [51] and the obtained sensitivity and specificity were of $92.26\% \pm 3.44\%$ and $92.28\% \pm 3.58\%$ respectively. The main advantage of ANN is that it has parallel processing capability and can predict the output even with insufficient training data although the accuracy is dependent on large data set. Its computational cost highly depends on the hidden layers and connected neurons.

Several other classification techniques were tried on mammograms. The breast abnormalities of the mammogram were classified in [52] by incorporating a new pattern classifier approach through the Particle Swarm Optimized Wavelet Neural Network (PSOWNN) that was based on extracting Laws Texture Energy Measures. In an experiment [33], the researchers tried both the region growing method along with ANN and cellular neural network (CNN) for segmentation. Then GA was applied for feature selection and the classifications in both cases were done using various classifiers such as KNN, support vector machine (SVM), naïve Bayes, random forest, and multi-layer neural network (MLP). It was observed that MLP performed best in both cases. An evaluation was done in [53] on three unsupervised classifiers namely Optimum-Path Forest (OPF), Gaussian Mixture Model (GMM) and k-Means, and it was found that OPF outperformed the others.

A different approach was tried in [54] for automatic evaluation of different breast tissues. Here the researchers engaged with radiologists and clinical practitioners for their expert opinions on the previous predicted reports to segregate the qualitative mammographic features. The optimal decision threshold was calculated based on statistical analysis for benign and malignant cases and taking into account the shape and size of the tumors. These features were used as datasets for real training of different classifier architectures such as linear classifiers, neural networks (NN) and SVM and for optimal feature sets, in which up to 95% accuracy was obtained. It was concluded that specialized image processing algorithms along with powerful pattern recognition models of non-linear and highly adaptive architecture may provide a better result.

4. Discussion

Different medical imaging systems for breast were studied in the beginning of this paper and they are summarized in Table 1 based on several criteria. It is found that the sensitivity of finding small tumors even in dense breast is high for MRI, Ultrasound and CT scan. However, CT scan cannot be considered for regular screening method as it increases the chances of cancer and the outcome of Ultrasound imaging depends on the expertise of the operator. On the other hand, MRI is costly and it has restricted use due to gadolinium and strong magnetic effect. So, although the sensitivity of digital mammography is moderate to detect tumors in dense breast, it is widely accepted throughout the world as regular screening method due to its low cost and minimum processing time.

An extensive study has been done in this paper on recent CAD system for mammogram screening and a brief summary is tabulated in Table 2 to highlight different technologies that were used in each stage. There are several researches on a particular stage of a CAD system, such as segmentation or feature extraction where either one technique was evaluated or different methods were compared and hence, they are not included in Table 2. The analysis of Table 2 reveals that the obtained accuracy in most of the researches is at higher side irrespective of the technologies used in each stage. However, none of the developed CAD system are fully automatic, except the work done in [33] and this is mostly because of the semi-automatic or manual segmentation techniques. Even, the work [45] that attained highest accuracy 98.59% during classification, also used manual cropping for segmentation. It can also be

observed that at classification stage, machine learning and neural networks were implemented in all the works, but with different algorithms and classifiers. Therefore, the future research can implement unsupervised machine learning methods to segment the AOI automatically along with supervised algorithms to classify the image for improved performance of the CAD system.

Table 1. A Brief Summary of Medical Images used for Breast Cancer Diagnosis

| Imaging Method | Frequency Range | Ionizing Effect | Sensitivity in Detecting Small Tumors | Processing Time | Cost | Injected Agent |
|----------------------------------|--|-----------------|---------------------------------------|-----------------|---------------------------------|---|
| Digital Mammography | 30 petahertz - 30 exahertz | Low | Moderate | Low | Low | No |
| Magnetic Resonance Imaging (MRI) | 1-100 MHz | None | High | High | High | Gadolinium |
| Ultrasound Imaging | 2-20 MHz | None | High | Moderate | Moderate | No |
| Computed Tomography | Much higher dose than conventional x-ray | Very high | High | High | High | Contrast agent like Iodine and Barium Radioactive substance |
| Positron-Emission Tomography | Done with CT | Very high | Low | High | High | |
| Microwave | 1 millimeter - 1 meter | None | Low | Low | Unknown since it is under trial | Contrast agent |

Table 2. A Brief Summary of Recently Developed CAD Systems for Breast Cancer Diagnosis

| Author Names | Pre-processing | Segmentation | Used Techniques Feature Extraction | Feature Selection | Classification | Accuracy |
|-----------------------------------|---|---|---|-------------------------------------|---|----------------|
| S. Wang <i>et al.</i> , 2017 | Median filtering, Homomorphic filtering and Logarithmic enhancement | Region growing followed by thresholding | Weighted-type fractional Fourier transform (Texture) | Principal component analysis (PCA) | Feed-forward Neural Network Trained by Jaya Algorithm | 92.27 ± 3.49 % |
| R. Rouhi <i>et al.</i> , 2015 | Manual cropping, Histogram equalization and Median filtering | Cellular neural network with parameters determined by genetic algorithm | Intensity, textural, and shape features | Genetic algorithm | MLP | 96.47% |
| SJS. Gardezi <i>et al.</i> , 2015 | Manual cropping | Manual cropping | Texture features from completed local binary pattern (CLBP) and curvlet | Fusion of CLBP and curvlet features | Nearest neighbor classifier | 96.68% |
| K. Ganesan <i>et al.</i> , 2014 | Manual cropping & Normalization | - | Spherical Wavelet | | SVM | 88.8% |

| | | | | | | | |
|-------------------------------------|-----------------|---|------------------------------|-----------------|--|--|--------|
| N. Azizi <i>et al.</i> , 2014 | - | Co-occurrence matrix, H U moments and Central moments | Texture and Shape | Transform (SWT) | Genetic Algorithm | SVM classifier using Gaussian kernel function | 89% |
| X. Liu <i>et al.</i> , 2014 | Manual cropping | Level-Set-Based with Fuzzy c-means Initialization | Geometry (shape) and Texture | | SVM-based recursive feature elimination procedure with a normalized mutual information feature selection | SVM classifier with a leave-one-out (LOO) scheme | 94% |
| J. Dheeba <i>et al.</i> , 2014 | - | Global thresholding | Laws Texture Energy Measures | | - | Particle Swarm Optimized Wavelet Neural Network Euclidean distance | 96.85% |
| M. M. Eltoukhy <i>et al.</i> , 2010 | Manual cropping | Manual cropping | Curvlet transform | | Ratios (10-90%) of the biggest coefficients from each scale decomposition level | | 98.59% |

5. Conclusion

The main purpose of this study is to review the past researches on proposed CAD systems for breast cancer diagnosis and it has been noticed that along with classic image processing methods, more importance is given on machine learning and artificial neural network based systems to make the system automated. The above discussion reveals that till date the acceptability and use of mammogram is high for regular screening considering all its limitations and all the stages of a CAD system are equally important in identifying several factors like image content, intensity and texture that contributes to achieve higher accuracy during classification. Each stage can be performed following several methods that are discussed elaborately in this study highlighting their pros and cons. However, neither a single technique is applicable to all types of images nor all the techniques perform well for one particular image. Furthermore, none of the segmentation procedure is fully automatic. So, machine learning based intelligent systems can help to make the complete procedure automated. Unsupervised method can be implemented during segmentation to identify the AOI and supervised method can improve the classification performance through the appropriate training of the system. Although the CAD system is adopted by radiologists to avoid their experience related errors, as well to reduce the double reading cost, however, report reveals that in reality there is not much identifiable difference in terms of sensitivity and specificity for mammography screening with and without CAD systems. Moreover, missed breast cancer cases by a CAD system put a threat to a life. Therefore, it can be interpreted that still there are rooms for improvement in developing a new CAD system for mammogram screening.

REFERENCES

- [1] F. Bray, J. Ferlay, I. Soerjomataram *et al.*, “Global Cancer Statistics 2018: GLOBOCAN Estimates of Incidence and Mortality Worldwide for 36 Cancers in 185 Countries,” *CA Cancer J Clin*, vol. 68, no. 6, pp. 394–424, 2018.
- [2] M. Hung, C. Liu, C. Teng, Y. Hu, and C. Yeh, “Risk of Second Non-Breast Primary Cancer in Male and Female Breast Cancer Patients: A Population-Based Cohort Study,” *PLoS One*, vol. 11, no. 2, pp. 1–12, 2016.
- [3] S. Bagchi and A. Huong, “Signal Processing Techniques and Computer-Aided Detection Systems for Diagnosis of Breast Cancer – A Review Paper,” *Indian Journal of Science & Technology*, vol. 10, pp. 1–6, 2017.
- [4] M. S. Ong and K. D. Mandl, “National Expenditure for False-Positive Mammograms and Breast Cancer Overdiagnoses Estimated at \$ 4 Billion a Year,” *Health Aff.*, vol. 34, no. 4, pp. 576–583, 2015.
- [5] C. D. Lehman, R. D. Wellman, D. S. M. Buist, K. Kerlikowske, A. N. A. Tosteson, and D. L. Miglioretti, “Diagnostic Accuracy of Digital Screening Mammography with and without Computer-Aided Detection,” *JAMA Intern. Med.*, vol. 175, no. 11, pp. 1828–1837, 2015.
- [6] H. Lee and Y. P. P. Chen, “Image based Computer Aided Diagnosis System for Cancer Detection,” *Expert Syst. Appl.*, vol. 42, no. 12, pp. 5356–5365, 2015.
- [7] R. Mousa, Q. Munib, and A. Moussa, “Breast cancer Diagnosis System Based on Wavelet Analysis and Fuzzy- Neural,” *Expert Syst. Appl.*, vol. 28, no. 4, pp. 713–723, 2005.
- [8] J. Suckling *et al.*, “The Mammographic Image Analysis Society Digital Mammogram Database,” *Expert. Medica, Int. Congr. Ser.*, vol. 1069, pp. 375–378, 1994.
- [9] M. S. Islam, N. Kaabouch, and W. C. Hu, “A Survey of Medical Imaging Techniques used for Breast Cancer Detection,” *IEEE Int. Conf. Electro Inf. Technol.*, pp. 10–14, 2013.
- [10] G. I. Andreea *et al.*, “The Role of Imaging Techniques in Diagnosis of Breast Cancer,” *Expert. Medica, Int. Congr. Ser.*, vol. 1069, no. 12, pp. 5356–5365, 2013.
- [11] T. Uematsu, M. Sano, K. Homma, M. Shiina, and S. Kobayashi, “Three-Dimensional Helical CT of the Breast: Accuracy for Measuring Extent of Breast Cancer Candidates for Breast Conserving Surgery,” *Breast Cancer Res. Treat.*, vol. 65, no. 3, pp. 249–257, 2001.
- [12] D. O’Loughlin, M. O’Halloran, B. M. Moloney, M. Glavin, E. Jones, and M. A. Elahi, “Microwave Breast Imaging: Clinical Advances and Remaining Challenges,” *IEEE Trans. Biomed. Eng.*, vol. 65, no. 11, pp. 2580–2590, 2018.
- [13] L. Wang, “Early Diagnosis of Breast Cancer,” *Sensors (Switzerland)*, vol. 17, no. 7, 2017.
- [14] Y. Medina, M. Augusto, and A. V. Paz, “Microwave Imaging for Breast Cancer Detection: Experimental Comparison of Confocal and Holography Algorithms,” *Proc. 2016 IEEE ANDESCON, ANDESCON 2016*, pp. 0–3, 2017.
- [15] S. Bagchi, A. Huong, and K. G. Tay, “Investigation of Different Spatial Filters Performance Toward Mammogram De-Noising,” *Int. J. Integr. Eng.*, vol. 9, no. 3, pp. 49–53, 2017.
- [16] J. Tang, R. M. Rangayyan, J. Xu, I. E. El Naqa, and Y. Yang, “Computer-Aided Detection and Diagnosis of Breast Cancer with Mammography: Recent Advances,” *IEEE Trans. Inf. Technol. Biomed.*, vol. 13, no. 2, pp. 236–251, 2009.
- [17] A. Mencattini, M. Salmeri, R. Lojacono, M. Frigerio, and F. Caselli, “Mammographic Images Enhancement and Denoising for Breast Cancer Detection using Dyadic Wavelet Processing,” *IEEE Trans. Instrum. Meas.*, vol. 57, no. 7, pp. 1422–1430, 2008.
- [18] N. Al-Najdawi, M. Biltawi, and S. Tedmori, “Mammogram Image Visual Enhancement, Mass Segmentation and Classification,” *Appl. Soft Comput. J.*, vol. 35, pp. 175–185, 2015.
- [19] M. A.-M. Salem, A. Atef, A. Salah, and M. Shams, “Recent Survey on Medical Image Segmentation,” *Comput. Vis.*, no. 1, pp. 129–169, 2018.
- [20] V. S. Manjula, “Image Edge Detection and Segmentation by using Histogram Thresholding method,” *Int. Journal of Engineering Research and Application*, vol. 7, no. 8, pp. 10–16, 2017.
- [21] C. Sha, J. Hou, and H. Cui, “A Robust 2D Otsu’s Thresholding Method in Image Segmentation,” *J. Vis. Commun. Image Represent.*, vol. 41, pp. 339–351, 2016.

- [22] A. Rojas Domínguez and A. K. Nandi, "Detection of Masses in Mammograms Via Statistically Based Enhancement, Multilevel-Thresholding Segmentation, and Region Selection," *Comput. Med. Imaging Graph.*, vol. 32, no. 4, pp. 304–315, 2008.
- [23] H. H. Aghdam, D. Puig, and A. Solanas, "Adaptive Probabilistic Thresholding Method for Accurate Breast Region Segmentation in Mammograms," *Proc.-Int. Conf. Pattern Recognit.*, pp. 3357–3362, 2014.
- [24] H. Al-Shamlan and A. El-Zaart, "Feature Extraction Values for Breast Cancer Mammography Images," *ICBBT 2010 - 2010 Int. Conf. Bioinforma. Biomed. Technol.*, pp. 335–340, 2010.
- [25] T. L. V. N. Swetha and C. H. H. Bindu, "Detection of Breast Cancer with Hybrid Image Segmentation and Otsu's Thresholding," *2015 Int. Conf. Comput. Netw. Commun. CoCoNet 2015*, pp. 565–570, 2016.
- [26] M. P. Sampat and A. C. Bovik, "Detection of Spiculated Lesions in Mammograms," *Annual International Confermce of the IEEE Engineering in Medicine and Biology*, pp. 810–813, 2004.
- [27] Z. Zhang and G. Zhao, "Butterworth Filter and Sobel Edge Detection to Image," *2011 Int. Conf. Multimed. Technol. ICMT 2011*, pp. 254–256, 2011.
- [28] S. Chakraborty, M. K. Bhowmik, A. K. Ghosh, and T. Pal, "Automated Edge Detection of Breast Masses on Mammograms," *IEEE Reg. 10 Annu. Int. Conf. Proceedings/TENCON*, pp. 1241–1245, 2017.
- [29] V. Bhateja, M. Misra, and S. Urooj, "Non-linear Polynomial Filters for Edge Enhancement of Mammogram Lesions," *Comput. Methods Programs Biomed.*, vol. 129, pp. 125–134, 2016.
- [30] S. Kamdi and R. K. Krishna, "Image Segmentation and Region Growing Algorithm," *Int. J. Comput. Technol. Electron. Eng.*, vol. 2, no. 1, pp. 2249–6343, 2012.
- [31] I. K. Maitra, S. Nag, and S. K. Bandyopadhyay, "Technique for Preprocessing of Digital Mammogram," *Comput. Methods Programs Biomed.*, vol. 107, no. 2, pp. 175–188, 2012.
- [32] Zaheeruddin Z. A. Jaffery, and Laxman Singh, "Detection and Shape Feature Extraction of Breast Tumor in Mammograms," *Lect. Notes Eng. Comput. Sci.*, vol. 2198, no. 1, pp. 719–724, 2012.
- [33] R. Rouhi, M. Jafari, S. Kasaei, and P. Keshavarzian, "Benign and Malignant Breast Tumors Classification Based on Region Growing and CNN Segmentation," *Expert Syst. Appl.*, vol. 42, no. 3, pp. 990–1002, 2015.
- [34] R. G. R. KK, "Automated Mammogram Segmentation using Seed Point Identification and Modified Region Growing Algorithm," *Br. J. Appl. Sci. Technol.*, vol. 6, no. 4, pp. 378–385, 2015.
- [35] K. Yuvaraj and Ragupathy, U. S., "Automatic Mammographic Mass Segmentation Based on Region Growing Technique," *3rd Int. Conf. Electron. Biomed. Eng. its Appl.*, pp. 29–30, 2013.
- [36] Shen-Chuan Tai, Zih-Siou Chen, and Wei-Ting Tsai, "An Automatic Mass Detection System in Mammograms Based on Complex Texture Features," *IEEE J. Biomed. Heal. Informatics*, vol. 18, no. 2, pp. 618–627, 2013.
- [37] E. Song *et al.*, "Hybrid Segmentation of Mass in Mammograms using Template Matching and Dynamic Programming," *Acad. Radiol.*, vol. 17, no. 11, pp. 1414–1424, 2010.
- [38] D. Zhang and G. Lu, "Review of Shape Representation and Description Techniques," *Pattern Recognit.*, vol. 37, no. 1, pp. 1–19, 2004.
- [39] S. Di Cataldo and E. Ficarra, "Mining Textural Knowledge in Biological Images: Applications, Methods and Trends," *Comput. Struct. Biotechnol. J.*, vol. 15, pp. 56–67, 2017.
- [40] X. Liu and J. Tang, "Mass Classification in Mammograms using Selected Geometry and Texture Features, and a New SVM-Based Feature Selection Method," *IEEE Syst. J.*, vol. 8, no. 3, pp. 910–920, Sep. 2014.
- [41] S. J. S. Gardezi and I. Faye, "Fusion of Completed Local Binary Pattern Features with Curvelet Features for Mammogram Classification," *Appl. Math. Inf. Sci.*, vol. 9, no. 6, pp. 3037–3048, 2015.
- [42] I. Zyout and R. Togneri, "A Computer-Aided Detection of the Architectural Distortion in Digital Mammograms using the Fractal Dimension Measurements of BEMD," *Comput. Med. Imaging Graph.*, vol. 70, pp. 173–184, 2018.

Crop yield prediction based on phenotype applying time series analysis

*S.Iniyan¹, R.Jebakumar²

¹SRM Institute of Science and Technology, Kattankuathur, Chennai 603203.

¹iniyans@srmist.edu.in

²SRM Institute of Science and Technology, Kattankuathur, Chennai 603203.

²jebakumr@srmist.edu.in

* S.Iniyan

Abstract

Agriculture has vital role in growth of nation's GDP. Indian economy is widely influenced by crop production. Our civilization is due to agriculture. All trading and businesses have agriculture as its key support. Crop selection plays a vital role in agricultural planning system. It depends on certain parameters like MSP, rate of production and certain government policy so based on above facts it can be concluded that several changes are required in agriculture/farming for increase in Indian Economy. It can be achieved by implementing various machine learning strategies in agricultural sector. Along with a great advancement in agricultural equipment and various modern cropping strategies used in farming, correct and precise knowledge about certain factors like seasonal variations, amount of rainfall, humidity, soil conditions, land variations and several other factor plays a vital role in crop selection and getting maximum yield from a minimum expenditure and wise planning of harvesting.

Keywords: *Machine Learning Algorithms, Crop Harvesting, modern crop selection strategies.*

1. Introduction

Using less amounts of resources either money, land or fertilizers if we are successful in producing maximum yield then goal of agricultural planning is reached which can be done with the help of various Machine Learning and Artificial Intelligence techniques. During unfavorable conditions there is a great need to wisely select a particular type of crop to increase crop yield rate. It can be achieved using various strategies which can be either manual or AI based but the major drawback of manual method is labour cost and more time. Also due to certain failures backtracking is not possible.

We will be taking into consideration various parameters like amount of rainfall, humidity, quality of seed, land quality, terrain/grassland and apply univariate and bivariate analysis on the features and get the clear idea of how features are interdependent and affects yield rate.

The crop selection mainly depends on favourable and unfavourable conditions. Till now various researches have been carried out in this field to improve agricultural planning with the ultimate goal of getting maximum yield.

The crop production is largely influenced by various climatic as well as geographic conditions like river, terrain, grassland, humidity, temperature, amount of rain. Type of soil can be sandy, clayey, saline etc. Composition of elements like Cu, K, P, N, Mn, Fe, Ca and pH value of carbon. Based on all of these parameters and certain new parameters like need of hour and farmer's own willingness to promote a particular crop in a region plays an important role. So all these can be broadly divided into two categories – Traditional and Machine Learning Algorithm.

2. Literature Survey

[1] Ramesh Medar et la (2019.March) have done research on crop prediction with machine/artificial learning technique and concluded that it helps in getting better crop selection technique based on various parameters/available features and data analysis.

All these will prosper the GDP of our nation and solve issues of farmers.

The models they have used were Naïve Bayes Algorithm and KNN. A java based API was used for this purpose having three parts which includes management of huge dataset using embedded SQL, testing phase supported by an interactive front end and Machine Learning as backend and lastly analysis of results.

Testing phase takes input of hidden dataset which has been segregated for validation/ testing and analysis is done using ensemble models and the best out of the given algorithm is taken into account.

Drawback of KNN is its more complexity in terms of time and space. Naïve Bayes has inaccuracy. For any two binary predictors, X and Y, and predicted variable Z, it is possible that $P(Z|X, Y)$ doesn't equal $P(Z|X, \sim Y)$, contrary to the assumptions of naive Bayes classification. Naïve Bayes Classifier has a major drawback that any extra category in testing dataset presently not in training dataset is assigned 0 probability and hence prediction fails.

[2] PotnuruSaiNishant et la.(June,2020) have concluded that when stacked regression is applied it improves the final result rather than using separate models for prediction. The output was displayed on a local web server but they are willing to build a model based on simple application in regional language to be easily accessed and familiarized with the farmers. The methodology they followed was Stacked Regression which included Lasso, Ridge and ENET Regression with Lasso Regression at the top of stack. A meta model was added which was trained using predictions of other models.

Whole process was a 4-stage process. Training set was divided into training and hold-out validation set. First the model has to be trained on training dataset then validation set validates the accuracy of model and finally the output of testing phase acts as an input to the meta model.

Root Mean Squared Error metric was used. The error for ENET was 4% and for Lasso it was 2% and Kernel around 1%. After stacking the error was less than 1%.

The drawbacks of this model are since stack is used for validation and training purpose so the best model if present at bottom of stack will suffer from waiting and also it leads to complexity.

The work [3] utilized Regression algorithm for the investigation of crop. Choice tree calculation and Classification are utilized in examining of more than 362 datasets and give arrangement. The preparation informational index here is redirected into natural, inorganic and land for anticipating the sort of soil. Arrangements registered by this framework are exact just as dependable.

The examination in [4] took care of data to access the test informational collection. Back Propagation Network utilize shrouded layer that is used in the better execution in anticipating soil properties. This gives about high precision and performance superiority in the days of yore utilized strategies nonetheless, now and again the framework gets unhurried and irregularity is found in the yield.

In the paper [5] two relapse managed AI strategies are utilized from work: SVM and RVM displays viability in soil quality expectations. A shrewd remote innovation detects soil dampness and meteorological information are utilized. The remote gadget shows a mistake pace of 15% and 95% precision. Be that as it may, it has not been tried in the ongoing information.

The examination [6] includes in the checking of Soil Fertility and Plant Nutrients by utilizing back engendering calculation. The yields are exact and empowers upgrading of soil properties. This gives better when contrasted with conventional strategies. Be that as it may, framework is moderate wasteful and not consistent. Fundamentally centers are utilizing the dirt parameters for a better crop production. Innocent Bayes calculation is utilized right now to group the soil and a 77% exactness is accomplished. Apriori

calculation is additionally used to connect the dirt with harvests that can give a huge yield.

A correlation of precision is accomplished in grouping, utilizing JRIP, Naïve Bayes, and J48 [7]. Rub et al gives a similar report on relapse models that are utilized for anticipating crop production. The calculations utilized right now are recognition Model, Regtree (Regression tree), and SVM. They are outlined in such a way that SVM fills in as a superior model most definitely.

[8]. Sujatha et al delineates the motivation behind different arrangement thoughts that could be utilized for crop yield expectation. A little information mining strategies, for example, J48. Naïve Bayes, arbitrary timberlands, bolster vector machines, counterfeit neural systems were introduced. A framework utilizing the atmosphere information and yield features used to gauge crop development is put forward.

[9]. Kushwaha gives the appropriateness about yield for a specific climatic properties and conceivable outcomes in increasing the harvests quality by utilizing climate and illness related informational indexes.

In [10] they have proposed an investigation, order and forecast calculation that is useful in building a choice emotionally supportive network for accuracy cultivating. It is mostly founded on the Hadoop document framework.

3. Existing System

An agro-based nation has agriculture as its backbone. Due to increased population the involvement of people in agricultural sector is influenced a lot which in turn increases the GDP of nation. Various traditional approaches like measurement of seed quality, hybridization, fertilizers and pesticides are done. Apart from the above-mentioned approaches certain researchers and biologists propose crop sequencing technique. One of such method is crop selection method (CSM). We have taken example of CSM to demonstrate how it helps farmers in achieving more yield.

4. Proposed System

In our system we are making use of a classification algorithms to improvised the crop yields.

The algorithms may vary depending on the accuracy we will get. The algorithms mostly includes Naive Bayes, Decision Tree, Random Forest Classifier, Ensemble Models and advanced ML algo like Artificial Neural Networks and Backpropagation Algorithm.

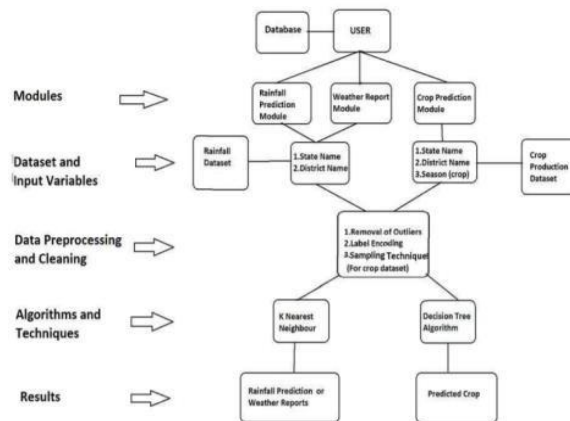
The various stages of Predictive Modelling will include:

1. Problem Definition.
2. Hypothesis Generation
3. Data Extraction/Collection
4. Data Exploration & Transformation
5. Predictive Modelling
6. Model Deployment/Implementation

The metrics we will be using are accuracy, TPR, TNR, FPR, FNR, Precision & Recall, AUC-ROC Metric and Log Loss.

The python libraries like Keras, Scikit learn, Matplotlib, Numpy, Tensorflow and pandas will be used.

5. Uml Diagram



6. Module

Data Manipulation Model:

Exploratory Data Analysis: Throughout this progression we played out some distinct investigation and decided the objective variable. We additionally found what number of classes were in the objective and a determination of other conceivably tricky (high cardinality) factors. I likewise Visualized the objective variable in a histogram which is a superior system for understanding the circulation of the information to aid parameter tuning.

Data Cleaning : We dropped those high cardinality factors during this procedure as an antecedent to the pre handling step.

Pre-processing & Transformation: We erased the objective variable from the whole informational collection and changed the straight out factor into a model framework with one-hot encoding. This is once in a while the interest for specific calculations to process the information in a scanty framework group. Other measurable programming, for example, R, mechanizes this procedure when creating models. I ascribed the missing qualities inside the information to 0. I scaled the persistent factors by utilizing the min-max standardization which changes esteems onto a scale from 0 to 1 to square factors on various scales vigorously affecting the coefficients.

Data Training Model:

Data Partition: We apportioned the pre handled information into the preparation and test informational index. Data partitioning is a classification in supervised machine learning which is used to separate pre-defined classes of data. This is typically used in splitting the data into multiple chunks. Data partition can be used in obtaining both training and testing datasets.

Demonstrating: We additionally manufactured a k-NN classifier model, utilizing 10 neighbour classes and the Euclidean separation.

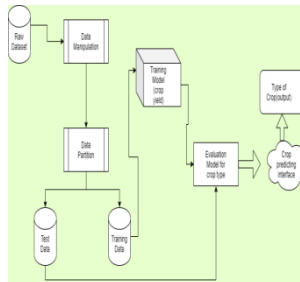
Testing And Evaluation Model:

Evaluation: We scored the classifier on inconspicuous test information and determined the R squared data for both the preparation and test information regarding the output would be obtained.

Output Model:

The output will be displayed on the interface that can be an android application or a windows based application.

7. Architecture Diagram



REFERENCES

- [1] "data.gov.in." [Online]. Available: <https://data.gov.in/>
- [2] Ananthara, M. G., Arunkumar, T., & Hemavathy, R. (2013, February). CRY—an improved crop yield prediction model using bee hive clustering approach for agricultural data sets. In 2013 International Conference on Pattern Recognition, Informatics and Mobile Engineering (pp. 473-478). IEEE
- [3] Awan, A. M., & Sap, M. N. M. (2006, April). An intelligent system based on kernel methods for crop yield prediction. In Pacific-Asia Conference on Knowledge Discovery and Data Mining (pp. 841-846). Springer, Berlin, Heidelberg.
- [4] Bang, S., Bishnoi, R., Chauhan, A. S., Dixit, A. K., & Chawla, I. (2019, August). Fuzzy Logic based Crop Yield Prediction using Temperature and Rainfall parameters predicted through ARMA, SARIMA, and ARMAX models. In 2019 Twelfth International Conference on Contemporary Computing (IC3) (pp. 1-6). IEEE.
- [5] P. Vinciya, Dr. A. Valarmathi, "Agriculture Analysis for Next Generation High Tech Farming in Data Mining" IJARCSSE, Issue 5, 2016.
- [6] Shivnath Ghosh, Santanu Koley, "Machine Learning for Soil Fertility and Plant Nutrient Management using Back Propagation Neural Networks" IJRITCC, Issue 2, 292-297, 2014.
- [7] Zhihao Hong, Z. Kalbarczyk, R. K. Iyer, "A Data Driven Approach to Soil Moisture Collection and Prediction" IEEE-Xplore, Issue 2, 292-297, 2016
- [8] Sabri Arik, Tingwen Huang, Weng Kin Lai, Qingshan Liu, "Soil Property Prediction: An Extreme Learning Machine Approach" Springer, Issue 4, 666-680, 2015. Hemageetha, N., "A survey on application of data mining techniques to analyze the soil for agricultural purpose", in 3rd International Conference on Computing for Sustainable Global Development (INDIACom), pp. 3112-3117, 2016.
- [9] Rub, G., "Data Mining of Agricultural Yield Data: A Comparison of Regression Models", 9th Industrial Conference, Volume 5633, pp. 24-37, 2009.
- [10] Sujatha, R., Isakki, P., "A study on crop yield forecasting using classification techniques", International Conference on the Computing Technologies and Intelligent Data Engineering ICCTIDE, pp. 1-4, 2016.
- [11] Kushwaha, A. K., Sweta Bhattacharya, "Crop yield prediction using Agro Algorithm in Hadoop", International Journal of Computer Science and Information Technology & Security (IJCSITS), Vol. 5, pp. 271-274, 2015.

Design of Low Power Capable Logic Circuit Using Adiabatic Performance

G. Ramachandran¹, T. Sheela², G. Sureshkumar³

¹Assistant Professor, Department of ECE, Vinayaka Mission's Kirupananda Variyar Engineering College, Vinayaka Mission's Research Foundation, Salem, Tamil Nadu, India

²Associate Professor, Department of ECE, Vinayaka Mission's Kirupananda Variyar Engineering College, Vinayaka Mission's Research Foundation, Salem, Tamil Nadu, India

³Assistant Professor Department of ECE, Vinayaka Mission's Kirupananda Variyar Engineering College, Vinayaka Mission's Research Foundation, Salem, Tamil Nadu, India

Abstract

The heat produced by the circuit itself can burn the whole integrated circuit. The power dissipation of the conventional static CMOS logic is bounded by the charging and discharging processes of the gate capacitance. The Power dissipation in traditional CMOS circuits can be minimized through adiabatic method. The adiabatic technique is highly dependent on parameter variation. The energy consumption is analyzed by variation of parameter with the help of MICROWIND tool. In analysis, two logic families, ECRL (Efficient Charge Recovery Logic) and PFAL (Positive Feedback Adiabatic Logic) are compared with conventional CMOS logic inverter and Multiplexer. Power consumption plays a major role in present day VLSI design technology. The demand for low power consuming devices is increasing rapidly and the adiabatic logic style is said to be an attractive solution. Power dissipation in circuits and systems is the critical factor for most of the researchers and industries. Many power dissipation techniques have been proposed but most of these techniques have some trade-offs. This logic makes use of charge recovery technique to achieve comparatively low power consumption to the CMOS logic. The new technology can be used to drive and be driven by conventional static CMOS logic directly. As the size of the integrated circuit grows and more devices are fabricated per unit die area with the technology progress, the power dissipation of the integrated circuit becomes a very important concern.

Keywords : CMO, ECRL, Integrated Circuit Power Consumption, PCFAL.

1 Introduction

The project aim will be indicated in this chapter. The distinction between static CMOS and dynamic CMOS logic and the origin of power dissipation in an integrated static and dynamic CMOS circuit will be implemented to promote the understanding of adiabatic technology and its low power properties.

1.1 Adiabatic Logic

Reducing the electronic devices' power consumption is becoming a very hot subject of research. The industry demanding low-power electronic devices has two key factors. Nowadays, portable electronic products like mobile phones, notebook computers, and so on are very popular. As most of these items are powered by batteries, reducing the power consumption means increasing the running time until batteries are replaced or recharged. Since the increase in power consumption due to increased operating frequency is not reducible by the traditional static CMOS technology mentioned in chapter 1.3.1, scientists have found different ways to minimize digital circuit power consumption, such as reducing static CMOS operating voltage. Nevertheless, the process voltage reduction seems to have a maximum of 0.9V which will be reached early. At this moment we have another adiabatic approach principle that uses adiabatic charging and charging recovery technique.

1.2 History of adiabatic logic

The biggest advance in adiabatic logic is to recover the charge stored in a digital circuit's node capacitance that shows logic levels and use adiabatic charging technique to reduce the on-resistance loss. Unlike traditional static CMOS, adiabatic logic re-distributes the charges in the condensers rather than discharges them to the table. In theory, adiabatic logic should employ zero energy after the circuit is initiated. This is why the technology is called "Adiabatic Logic".

Younis and Knight [1] and Merkle [2] first proposed adiabatic logic in 1993, with dissipation almost zero power.

In 1995, adiabatic dynamic logic (ADL) was introduced by Dickinson and Denker [3], and Wang and Lau [4] introduced adiabatic pseudo-domino logic (APDL). All the suggested enhancements mentioned are not compatible with the static CMOS logic design, however. This means the conversion of the static CMOS architecture into adiabatic logic is difficult. For example, adiabatic dynamic logic will use a four-phase clock precharge, input, evaluate and hold phases. Compared to the CMOS domino logic, adiabatic pseudo-domino logic uses a clock to control the charging and evaluation phases. It is proposed in the thesis to preserve consistency with the traditional static CMOS, which uses quasi-static architecture. The key difference between CMOS from ADL and APDL is that the CMOS can drive and be powered directly via a standard static CMOS logic system. The basic principle of the CMOS is to use a fairly high frequency adiabatic clock, rather than multi-stage operation. This makes it possible to convert the concept to CMOS, based on traditional static CMOS. Information on CMOS technology will be addressed and discussed in chapter 3.

2 Literature survey

The existing VLSI systems organize erratic reasoning, large modules and memories. Thus, the performance of adiabatic circuits will depend on the economic implementation of not only random logic, but the opposite elements of a VLSI network in tandem. Yibin Ye and. In their 1996 paper entitled "On the Design of Adiabatic SRAMs," Al. described the design of low-power circuits as adiabatic low-power circuits, adiabatic logic shows nice promise. Research has, however, targeted adiabatic circuits / family logic to date. They furnish a system of adiabatic Static RAM, which could be applied although the area of simple logic gate efficiency could not be greatly increased. The design notes the very high complexity of constructing ultra-low power memory circuits inside a VLSI. Their estimated result for a 4Kb memory core block indicates energy savings of approximately seventy-fifth for each search, and writes operations. Higher square measure of power savings achieved within the address decoder and I/O drivers [30].

Yong Moon, and, etc. The Efficient Charging Recovery Logic (ECRL) is planned in 1996 as a candidate for low-energy adiabatic logic circuits. The power analysis is performed on an electrical converter chain with entirely different logic circuits and a bring look ahead adder (CLA). As a pipeline system, ECRL CLA is expected to obtain equivalent output as a traditional static CMOS CLA [12]. Vojin G. Oklobdzija et.al in research entitled "Pass-Transistor Adiabatic Logic Using Single Power-Clock Supply." Presented new adiabatic pass-transistor logic

(PAL) that operates from one power-clock supply and beats the aforementioned adiabatic logical methods as far as their vitality is used. PAL can be dual-rail logic with fairly low gate complexity: a PAL gate is made up of true and true and complementary NMOS practical blocks, and a try of cross-coupled PMOS devices [24].

Lolas, Z.C. ET.A. In 1999 a low-power array architecture solution was introduced based on energy recovery techniques. Reversible pipeline main concepts have been adopted [14]. In 1999 K later. W. NG et K. T. Lau engineered a low-power 4:2 compressor, which shows a major power reduction [16].

Hamid Meimand Mahmoodi et. al. Introduced a low-power, low-noise adder design with pass-transistor adiabatic logic in 2000. Because of their theoretical zero power dissipation, classical CMOS circuits, whose power consumption is usually a huge problem, consider reversible solutions plausible. Alternatively, growing technologies usually introduce inherent quantum effects that are inherently reversible. So prospect circuits are generated from reversible logic gates at some reason. The adiabatic adder shows energy savings of seventy-six to eighty seven percent and eighty seven to ninth percent, with the help of the post-layout simulation tests. Similar to its static CMOS counterparts [11], it also displays a significant reduction in switching noise.

H. H. Wong, K. In 2002, T. Lau lowered power utilization in multipliers and acquired enormous power decrease in the general computerized system. (7, 3) one of those counters However, segments used as part of parallel multipliers are not as prevalent as the compressor (4:2). Some (7, 3) counters have been accounted for and the majority of them are usually executed in traditional CMOS style [10]. J. Y. Park, with S. J. Hong developed the Latched Pass-Transistor Adiabatic Logic (LPAL) in 2002 and proposed a low-power design scheme that energy-efficiently replaces traditional CMOS circuits. Simulation using 0.35um CMOS technology has contrasted the energy dissipation between Pass-transistor Adiabatic Logic (PAL) and LPAL. The LPAL demonstrates 44 per cent energy savings relative to the PAL[15].

Ettore Admirante, and. In a 1.2V, 0.13um CMOS system, Developed an adiabatic 8-bit Ripple Carry Adder to demonstrate the ability of adiabatic logic for low power applications. The adiabatic block architecture was consistent with standard cells that had static CMOS. This allows massive adiabatic circuit blocks to be implemented with manageable complexity of design. At $f = 20$ megacycle the energy was in static CMOS by an

aspect of seven below, and energy savings on the far side $f = 100\text{MHz}$ were possible. For the conversion between adiabatic and static CMOS signals interface circuits are shown. The test comes to validate the utility of the adiabatic adder inserted into a static state of CMOS. An evaluation of the vitality performance of a complete adiabatic system including a four-stage trapezoidal power clock generator, obtaining an energy saving by a factor of 6 at $f = 20\text{MHz}$ [8].

Natarajan Aiyappan et. Al. 2003, introduced Addressable Memory (CAM) hybrid adiabatic material. The CAM uses an adiabatic change method to reduce the use of vitality within the match line while preserving the read / compose operation execution. For ultra-low-power, low-performance applications such as sensible cards and transportable devices, the adiabatic CAM was suitable. For the match line, CAM uses a clocked power supply while the rest of the circuit was constant due to the simple CAM [6].

W.J. Yang et. al. 2003 gave a novel low power programmable logic array (PLA) structure based on adiabatic switching is presented. Simulation results urged that the power consumption is comparable to it of the adiabatic pseudo-domino logic (APDL) PLA, however whereas common place semiconductor transistor size for the isolation transistor are often applied, in APDL PLA this semiconductor device was designed with a bigger breadth [29].

3 Proposed Work

In 1988, Bennett [5] proved there must be energy dissipation not less than $kT\ln 2$ (where k is the constant of Boltzmann and T is the temperature) for any activity of an irreversible system. Consider Merkle's example regarding an irreversible device's energy dissipation[2]. When a "AND", power supply gate IV allows 100 electrons to flow from the ground to the supply during switching. The dissipated energy will be $100eV$. This value is roughly $4000kT$, since T is 300 K, which is still comparatively much greater than the theoretical maximum. Nonetheless, by following the modem electronics phenomenon, we will be hitting the $4000kT$ value before the year 2000 and the physical limit by 2015. Reversible devices must be built to overcome the barrier $kT\ln 2$ which limits the operating frequencies of electronic devices as described in chapter 1.5.1 above.

3.1 Reversible Electronics

Consider the operation of a CMOS inverter in Figure 3-1.

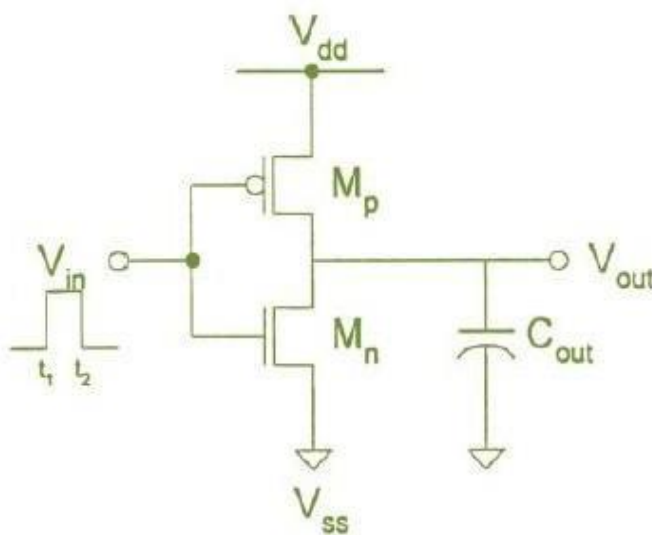


Figure1: Inverter for reversible devices description

At time t_1 , M_n can discharge the charge deposited in C_{out} to V_{ss} . When time = t_2 , M_p charges the C_{out} to V_{dd} , these two operations completely delete the original status of the system for the new details. Through Maxwell's historical paradox, the Demon in Knowledge System Thermodynamics [6], Through such erasing operation is

equal to an increase of at least $k \ln 2$ of entropy in the universe as a whole. Therefore no less $kT \ln 2$ energy dissipation is inevitable. The charging phase typically dissipates $1/2 CV^2$ of energy, and the discharging process also dissipates $1/2 CV^2$ of energy.

Nevertheless, if we can, by any way, deposit the charge originally stored in C_{out} (information) instead of discharging (erasing) it to V_{ss} at t_1 , and remove the charge stored at t_2 and recover it to C_{out} we can prevent the irreducible thermodynamic cost since the information is never erased. Examples of reversible operations are this charging recycling and non-erasing process. All devices that do reversible operations are often called reversible devices. Theoretically, we can build circuits which consume zero power by using reversible devices.

3.2 Adiabatic Switch

When the input of a CMOS inverter goes from high to low, the circuit can be modelled as shown in Figure 3.2.

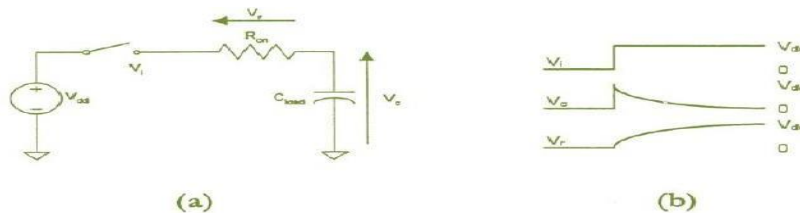


Figure 2: Conventional charging model

When the switch is closed, the full supply potential appears across the R_{on} on-resistance, causing charging to start with the load capacitance C_{load} . R_{on} voltage decreases as the capacitance is charged to V_{dd} . Once the charging capacitor is fully charged, a charge $q = C_{load} V_{dd}$ flows from the source to the capacitance of the charging. The $E_r = qV_{dd} = C_{load} V_{dd}^2$ is transferred from the supply by calculating the energy consumption. Only 50 percent of the energy consumption goes to capacitance while only $1/2 C_{load} V_{dd}^2$ is the energy stored in the capacitance. The other $1/2 C_{load} V_{dd}^2$ is mainly in the on-resistance as heat dissipated. Any reversible devices will never recover the energy that is dissipated as heat. The same condition happens when the capacitance to load is discharged. Once the inverter input goes high, the load condenser is discharged to V_{ss} and the energy stored is completely dissipated as heat by the n channel transistor's on-resistance.

4 Results and discussion

The energy consumption in adiabatic circuits is heavily dependent on variations in the parameters [29-31]. For the two logic families, the effect of parameter variations on energy consumption is investigated with respect to the CMOS logic circuit, using TSPICE simulations. Simulations are performed at a node of 250 nm technology. The W/L ratio of PMOS and NMOS are taken as $9\lambda/2\lambda$ and $3\lambda/2\lambda$ respectively, Where $\lambda = 125\text{nm}$.

4.1 Layout and Simulation Results

Figure.5.1 indicates the energy dissipation of the two adiabatic logic families per cycle versus the switching frequency and the CMOS for the inverter logic. Figure.5.2 indicates the energy dissipation of the two adiabatic logic families per cycle against the switching frequency and the CMOS for the 2:1multiplexer.

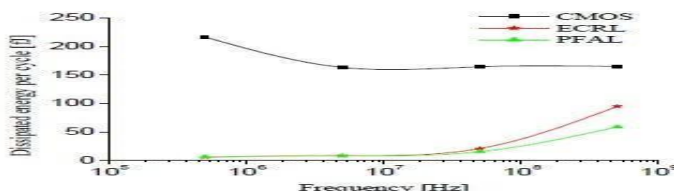


Figure 3: Energy consumption per cycle versus frequency for an inverter at $V_{DD} = 2.5\text{V}$ and load capacitance = 20fF .

It is shown that the action is no longer adiabatic for high frequency, and hence the energy dissipation increases. At low frequencies the dissipation energy will increase due to the leakage currents of the transistors for both CMOS and adiabatic logic. Thus the simulations are conducted only at reasonable frequency range to provide better results with respect to CMOS.

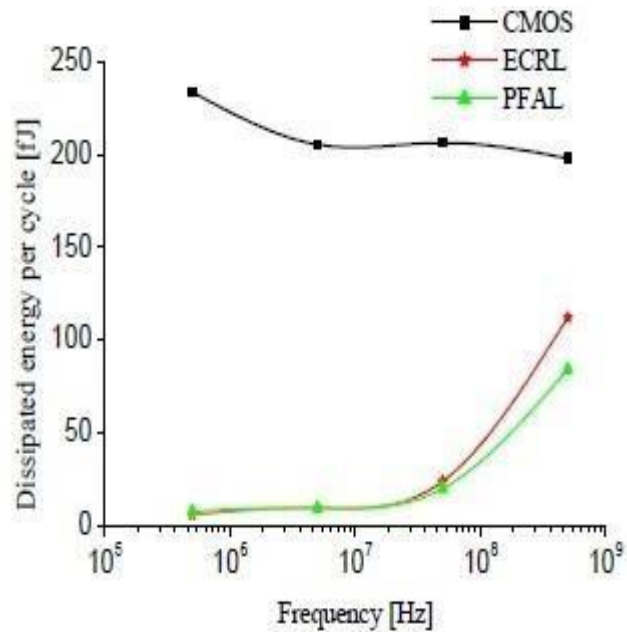


Figure 4: Energy consumption per cycle versus frequency for a 2:1 multiplexer at VDD = 2.5V and load capacitance = 20fF

Load capacitance variation

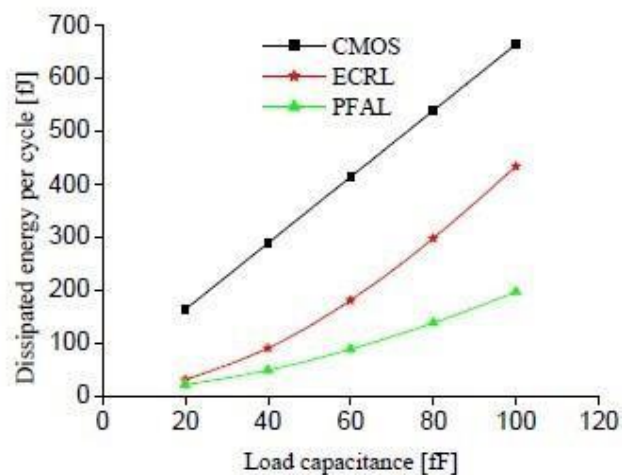


Figure 5: Energy consumption per cycle versus load capacitance for an inverter at VDD = 2.5V and frequency = 100 MHz.

Figure.5.3 demonstrates the energy dissipation of the two adiabatic logic families and CMOS for the inverter logic by cycle versus load capacitance. Figure.5.4 indicates the energy dissipation per cycle versus load capacitance for the 2:1 multiplexer of the two adiabatic logic families and the CMOS. The Figures show that adiabatic logic families have greater energy efficiency over a large range of load capacitances than CMOS logic. At high load range PFAL displays better energy shavings than ECRL.

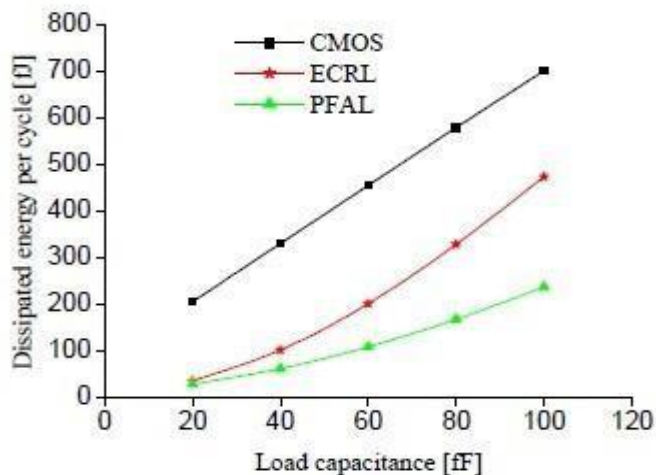


Figure 6: Energy consumption per cycle versus load capacitance for a 2:1 multiplexer at $V_{DD} = 2.5V$ and frequency = 100 MHz.

4.2 Supply Voltage Variation

Figure.5.5 shows the energy dissipation of the two adiabatic logic families per cycle versus the supply voltage and CMOS for the inverter logic. Figure.5.6 indicates the energy dissipation per cycle against the two adiabatic logic families' supply voltage, and the 2:1 multiplexer CMOS. Supply voltage is seen to decrease, the gap between CMOS and the logic families is reduced. But ECRL and PFAL still display significant energy savings over a wide range of supply voltage.

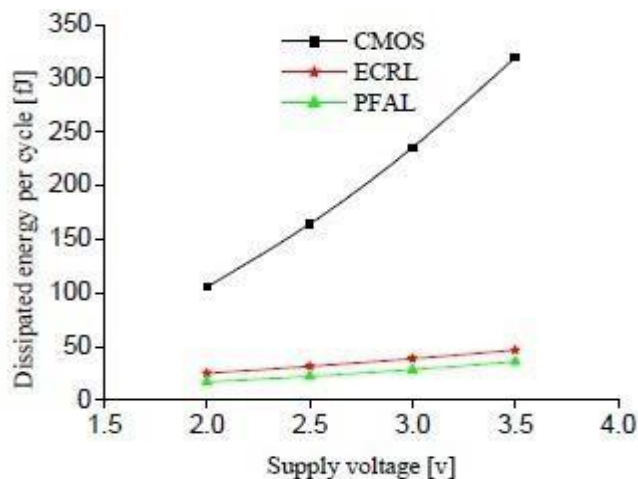


Figure 7: Energy consumption per cycle versus supply voltage for an inverter at load capacitance = 20fF and frequency = 100 MHz.

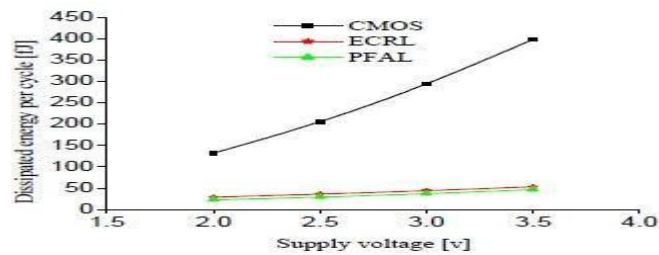


Figure 8: Energy consumption per cycle versus supply voltage for a 2:1 multiplexer at load capacitance = 20fF and frequency = 100 MHz.

5 Conclusion

The Power dissipation in traditional CMOS circuits can be analysed through adiabatic method. The diabetic technique is highly dependent on parameter variation. The energy consumption is analyzed by variation of parameter with the help of MICROWIND tool. In analysis, two logic families, ECRL (Efficient Charge Recovery Logic) and PFAL (Positive Feedback Adiabatic Logic) are compared with conventional CMOS logic inverter and Multiplexer. The different variations of parameters are investigated against adiabatic logic families, which show that adiabatic logic families are highly dependent upon it. Yet less energy consumption can still be done in adiabatic logic families across the broad spectrum of parameter variations than the CMOS logic. At high frequency and high load efficiency PFAL displays better energy shavings than ECRL. Thus adiabatic logic families can be used across the broad range of variations in parameters for low power applications. Further adiabatic logic is to be implemented in the future which will help to address the drawbacks of recent adiabatic logic circuits. For instance- DFAL (Free Adiabatic Logic Circuit diode). Future work also involves the design of the proposed buffer / inverter's larger adiabatic gates and circuits, and higher frequency dissipated energy analysis and comparison with other adiabatic families.

References

- [1] E. Amirante, A. B. Stoffi, J. Fischer, G. Iannaccone, and D.S. Landsiedel, "Variations of the power dissipation in adiabatic logic gates," in Proc. 11th Int. Workshop PATMOS, Yverdon-Les-Bain.
- [2] A. Voss and M. Glesner, "A low power sinusoidal clock," In Proc. Of the International A. Kramer, J. S. Denker, S. C. Avery, A. G. Dickinson, and T. R. Wik, "Adiabatic computing with the 2N-2N2D logic family," in IEEE Symp. on VLSI Circuits Dig. of Tech. Papers, pp. 25-26, Jun.2016.
- [3] A. Blotti, S. D. Pascoli, R. Saletti, "Sample Model for positive feedback adiabatic logic power consumption estimation," Electronics Letters, Vol. 36, No. 2, pp. 116-118, Jan.2000.
- [4] A. K. Lo and P. C. H. Chan, "An adiabatic differential logic for low power digital systems," IEEE Trans. Circuits Syst. II, vol. 46, pp.1245– 1250, Sept.2017.
- [5] A. Kramer, J. Denker, B. Flower and J. Moroney, "Second Order Adiabatic Computation with 2N-2P and 2N-2N2P Logic Circuits", Proceedings of international symposium on low power design, pp. 191- 196, 2017.
- [6] A. Vetuli, S. Di Pascoli, and L. M. Reyneri, "Positive feedback in adiabatic logic," Electron. Lett., vol. 32, pp. 1867–1869, Sept.2014.
- [7] Aiyappan Natarajan, David Jasinski, Wayne Bursleson, Russell Tessier, "A Hybrid Adiabatic Content Addressable Memory for Ultra Low-Power Applications", Great Lakes Symposium on VLSI (GLSVLSI), April 28-29,2003.

An Effective Optimization Technique of Extracted Watermark Image Using Particle Swarm Optimisation

. M. Selvaganapathy¹, R. Kayalvizhi²

¹Ph.D. Scholar, Annamalai University, Annamalai Nagar, Chidambaram, Tamil Nadu, India

²Professor and Head, Annamalai University, Annamalai Nagar, Chidambaram, Tamil Nadu, India

Abstract

Nowadays the presence of noises in the extracted image is a major constrain in the Image Processing environment. An ultimate goal of this paper is to optimize the watermark image using particle swarm optimization. Earlier, the research focused on the video watermarking process where the watermark image is embedded into the video as invisible and can be sent to the receiver side for an extraction. While at the extraction stage, the image what embedded was not been retrieved at the receiver side due to the presence of various noises and occurrence of errors in the medium. Hence while comparing the extracted image with the original image, the accuracy was poor and non re constructable. So this paper serves solution for the above said problem using Particle Swarm Optimization Technique. As the end, the extracted image can be reconstructed to the maximum extent as equal to the input image. This scheme can be widely used in the Medical Imaging application, Defence, etc.

Keywords: Video Watermarking, Particle Swarm, Embedding, Extraction, Image reconstruction, Optimization.

1 Introduction

Particle Swarm Optimization (PSO) is a sturdy technique based on the drive and intelligence of swarms. This Optimization technique applies the concept of social interaction to problem solving techniques. This Optimization Technique was developed by James Kennedy and Russell Eberhart in the year 1995.

PSO is considered to be an efficient optimization algorithm by searching an entire high – dimensional problem space. It uses number of agents considered as particles; that constitute a swarm moving around in the search space looking for the best solution. Each particle is considered as a point in an N – dimensional space which adjusts as a flying experience of other particles. In particle swarm optimization, if a member finds a desirable path, the rest will be followed by the swarms. Each member learns not only from its own experience but from others especially from the best performer. As of the Particle Swarm Optimization, there are two variants which are Basic Variant Particle Swarm Optimization and Modification variant Particle Swarm Optimization. The basics of Particle Swarm Optimization include:

The standard version of the PSO algorithm is essentially described by the following two simple velocity and position update equations, shown in 1 and 2 respectively.

$$V_{id}(t + 1) = W V_{id}(t) + C_1 R_1 (P_{id}(t) - X_{id}(t)) + C_2 R_2 (G_{bid}(t) - X_{id}(t)) \quad (1)$$

and

$$X_{id}(t + 1) = X_{id}(t) + V_{id}(t + 1) \quad (2)$$

Where,

$$W = \frac{W_{max} - (W_{max} - W_{min})}{T} \times t \quad (3)$$

W → Inertia weight.

W_{max} → Initial Weight.

W_{min} → Final Weight.

T → Maximum Iteration.

t → Current Iteration.

V_{id} → Rate of position change (velocity).

X_{id} → Position of the i^{th} particle in the d^{th} dimension.

P_{id} → Historically best position of the i^{th} particle in the d^{th} dimension.

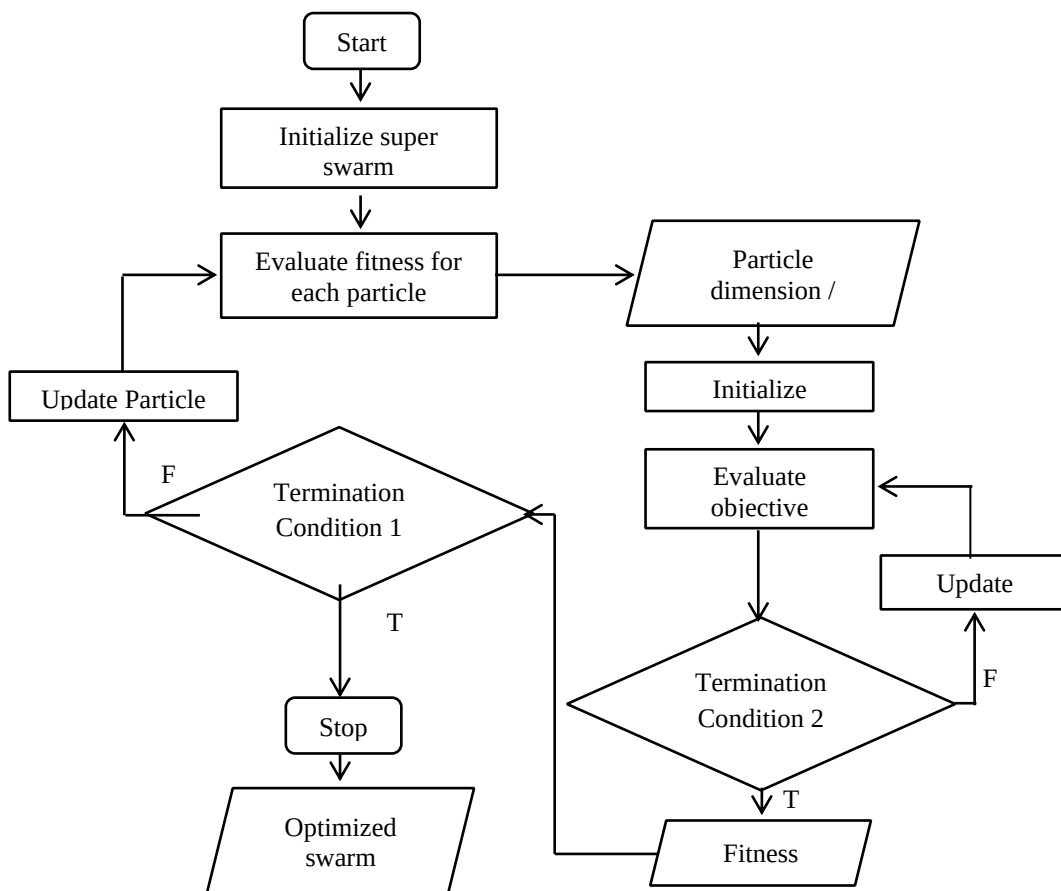
R_1 and R_2 → n – dimensional vectors.

c_1 and c_2 → Cognitive and Social parameters.

2 Work Flow of the Project

- Step 1: Initialize the particles.
- Step 2: Calculate the fitness value for each particles.
- Step 3: If fitness value is better than the particles best fitness value (Pbest) in the history set current value as the new Pbest.
- Step 4: Repeat step 2 and 3 for all the particles.
- Step 5: Choose the particle with best fitness value compared to all the particles and label as the global best (gbest).
- Step 6: Calculate and update each particles velocity and position for all the particles.
- Step 7: Calculate the fitness value for each particles.
- Step 8: If a minimum error criterion ((i.e.) desired fitness value of 90% of all the particles) is not achieved, goto step 3.
- Step 9: Display the particles.

The above diagram represents the research flow graph where the particle swarm optimization undergoes various level of updation in order to get the optimized swarm output. Initially, the process initializes the super sparm where the image consists of multi swarm in which the Super swam are identified. Those super swarms are considered to be the super sized swarm. Then the process is continued to evaluate the fitness of each particles of the swarms. This in turn measures the dimension of the particle or swarm parameters. The next process is to initialize all the sub swarms following to the super swarms and then the object functions are



3 Objective of the Research

General Objective

The general objective of the research is to enhance the quality of an image using Particle Swarm Optimization.

Specific Objective

The specific objective of the research includes:

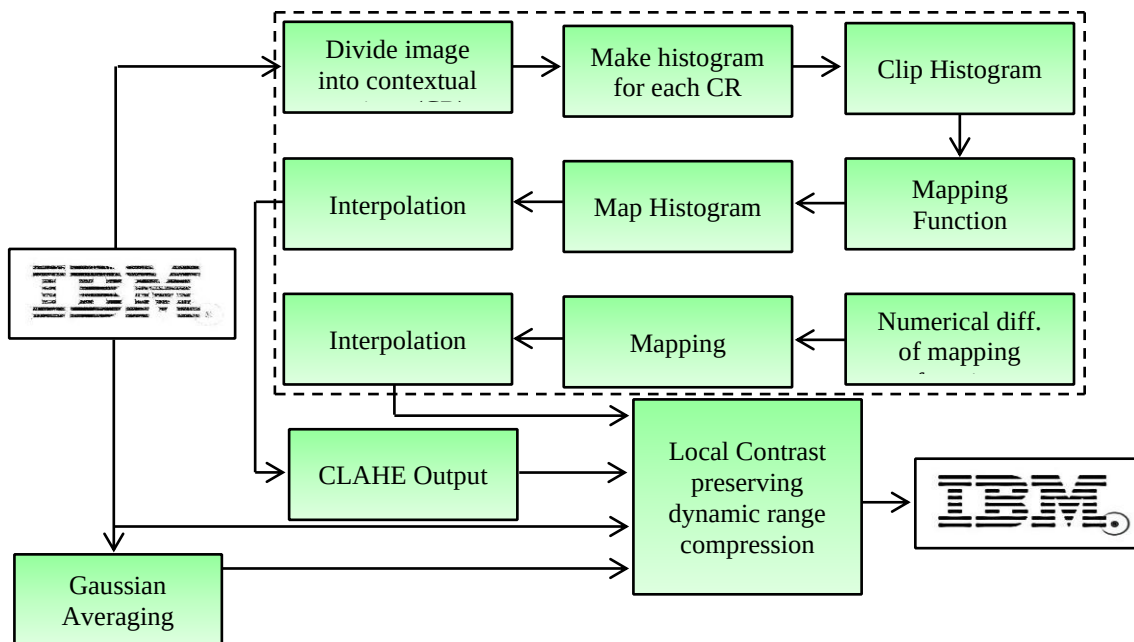
1. To improve the interpretability of an image.
2. To improve image perception.
3. To reduce the noise occurrence.
4. To improve the better output.

4 Block Diagram

In this method, the local gain parameters were used. Along with the above said parameters, the problems with other image enhancement techniques were overcome. The following diagram is the block diagram for the proposed research where the extracted image can be enhanced using Contrast Limited Adaptive Histogram Enhancement (CLAHE) method.

$$r(f(x, y), f_{avg}(x, y)) = \left(\frac{f(x, y)}{f_{avg}(x, y)} \right)^{\alpha \left(1 - \frac{f(x, y)}{p(f(x, y))} \frac{dp(f(x, y))}{d(f(x, y))} \right)} \quad \text{--- (4)}$$

Where, $\alpha \rightarrow$ Local contrast enhancement gain factor.



In the above proposed algorithm, approximated logo of IBM which is extracted from the water make process has been taken for consideration. This IBM logo is used as mapping functions. The mapping function used directly affects the enhancement result of an image. For different purpose the fundamental tone – mapping curve $p(f(x,y))$ can be determined randomly.

Therefore, the proposed system uses the numerical differentiation of CLAHE mapping function. The gain parameter plays vital role in contrast enhancement. The range of gain parameter differs from image to image. The larger and smaller values of gain parameter are used for the region with higher pixel edge density and lower pixel edge density respectively. Because of the variation in gain parameter, we can say that the value of gain

parameter for each pixel depends on the image local region of that pixel and vary linearly in the proposed method.

5 Simulation Result

The proposed algorithm has been tested with various numbers of Logos, medical images and images downloaded from the internet databases. Based on the various images, the following result has been obtained. In this section, the various performance of the image enhancement method is discussed over. The parameters taken into the considerations are Peak Signal to Noise Ratio (PSNR) and Bit Correction Rate (BCR). And the Simulation Result for the proposed algorithm stands the following table which is prescribed in the Table 1.

| Attacks | Parameters | PSNR | | BCR | |
|------------------|---------------|---------|----------|---------|----------|
| | | W/O PSO | With PSO | W/O PSO | With PSO |
| Without Attack | ---- | 43.6064 | 63.6599 | 0.9914 | 0.9917 |
| JPEG Compression | QF = 20 | 43.6064 | 63.6599 | 0.9914 | 0.9917 |
| Gaussian Noise | Noise = 3% | 42.7871 | 63.8049 | 0.9937 | 0.9939 |
| Uniform Noise | Noise = 5% | 42.0378 | 54.1498 | 0.9902 | 0.9905 |
| Salt & Pepper | Noise = 10% | 36.1234 | 40.1291 | 0.7513 | 0.7732 |
| Low Pass Filter | STD Devi = 10 | 40.3923 | 49.5222 | 0.9688 | 0.9697 |
| Median Filter | =5 | 43.3176 | 61.7385 | 0.9817 | 0.9854 |
| Sharpening | --- | 40.9541 | 50.1475 | 0.9914 | 0.9943 |
| Gamma Correction | Value = 5 | 32.2006 | 34.0687 | 0.9997 | 0.9999 |

References

- [1] Q. Liping, M. Yan, L. Dongheng and X. Hai-Bo, "A Quantum Particle Swarm Optimization Algorithm with Available Transfer Capability," 2020 19th International Symposium on Distributed Computing and Applications for Business Engineering and Science (DCABES), Xuzhou, China, 2020, pp. 267-270, doi: 10.1109/DCABES50732.2020.00076.
- [2] S. Mahapatra, M. Badi and S. Raj, "Implementation of PSO, it's variants and Hybrid GWO-PSO for improving Reactive Power Planning," 2019 Global Conference for Advancement in Technology (GCAT), BANGALURU, India, 2019, pp. 1-6, doi: 10.1109/GCAT47503.2019.8978348.
- [3] Y. Shen et al., "Research on Swarm Size of Multi-swarm Particle Swarm Optimization Algorithm," 2018 IEEE 4th International Conference on Computer and Communications (ICCC), Chengdu, China, 2018, pp. 2243-2247, doi: 10.1109/CompComm.2018.8781013.
- [4] D. Pal, P. Verma, D. Gautam and P. Indait, "Improved optimization technique using hybrid ACO-PSO," 2016 2nd International Conference on Next Generation Computing Technologies (NGCT), Dehradun, 2016, pp. 277-282, doi: 10.1109/NGCT.2016.7877428.
- [5] J. H. Lee, J. Kim, J. Song, Y. Kim and S. Jung, "A Novel Memetic Algorithm Using Modified Particle Swarm Optimization and Mesh Adaptive Direct Search for PMSM Design," in IEEE Transactions on Magnetics, vol. 52, no. 3, pp. 1-4, March 2016, Art no. 7001604, doi: 10.1109/TMAG.2015.2482975.
- [6] U. Khusanov and C. H. Lee, "Image Enhancement based on local histogram specification", Journal of Korean Institute of Intelligent System, Vol. 23, No. 1, pp. 18 – 23, 2013.
- [7] D. Ghimire and J. Lee, "Non linear transfer function based image detail preserving dynamic range compression for color image enhancement", Advance Image and Video Technology, pp. 1 – 12, 2012.
- [8] C. C. Sun, S. J. Ruan, M. C. Shie and T. W. Pai, "Dynamic contrast enhancement based on histogram specifications", IEEE Transactions on Consumer Electronics, Vol. 51, No. 4, pp. 1300 – 1305, 2005.

- [9] N. J. Kim and Y. S. Kim, "Image contrast enhancement Technique using clustering algorithm", Journal of Korean Institute of Intelligent Systems, Vol. 14, No. 3, pp. 310 – 315, 2004.
- [10] G. B. Lee, Y. S. Kim, "An image contrast enhancement technique using improved integrated adaptive fuzzy clustering model", Journal of Korean Institute of Intelligent Science, Vol. 11, No. 9, pp. 777 – 781, 2003.
- [11] D. J. Jobson, Z. U. Rahman and G.A. Woodbell, "Statistics of visual perception", Proceedings of SPIE, Vol. 4736, 2002.
- [12] G. Ramponi, N. K. Strobel, S. K. Mitra and T. H. Yu, "Non – linear un sharp masking methods for image contrast enhancement", Journal of Electronics Imaging, Vol. 5, No. 3, pp. 353 – 366, 1996.

Tumble Gear Based Smart Vehicle for Physically Challenged People

N. Nishavithri¹, M. Selvaganapathy²

¹Assistant Professor, Dept. of ECE, Mailam Engineering College, Mailam, Tamil Nadu, India

²Assistant Professor, CK College of Engineering and Technology, Cuddalore, Tamil Nadu, India

Abstract

In this paper we design and implement the motor bike with reverse gear system which helpful for physically challenged person to take reverse their bike from parking without another person help. Here we used "tumbler gear" mechanism for our prototype model the gear usually used to change the direction of gear consist of two gear which place n parallel by changing their position with motor direction of rotation can be changed but n real time application we need to use deal gear system with gear box also the bike consist of ultrasonic sensor which work based on echo signals to give alert on taking reverse to avoid collision between other object consist of "GPS" which help their family to locate their position easily n case of any emergency and no boards used to control all these electronic modules which pre-programmed to do this operation of ultrasonic and GPS module and relay driver circuits used to drive the motor n our prototype.

Keywords: Reverse Gear System, Smart Vehicle, Tumble Gear, Ultrasonic sensor, Motor, GPS, etc.

1 Introduction

In our day to day life we are crossing many physically challenged persons they driving their two wheeler but they are really struggling to take reverse their vehicle they need the help of other people we partially proposed a solution for them to operate the vehicle reverse direction which n prototype consist of "Tumbler Gear" mechanism but when we got on or mal motorbike we need to fit an gearbox with deal gear, lets we see

1.1 Tumbler Gear

The mechanisms are the apart of the machines and wont to transfer one sort of motion to other types there are many sort so mechanisms there we see about Tumbler gear. The tumbler gear typically w'ont to change the direction of feed rod and lead screw.

The mechanisms often described as an appointment of drugs wheels which employed to reverse the direction of rotation of any machine.

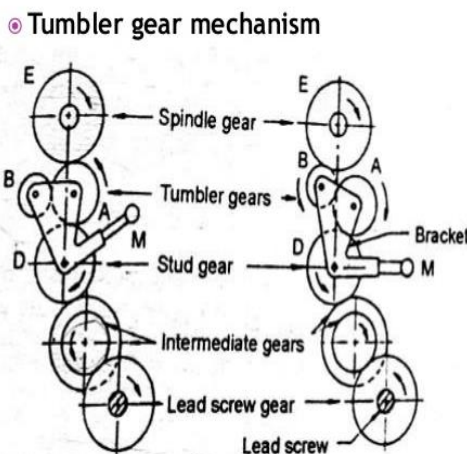


Figure 1:Tumble Gear Mechanism

2 Components of Vehicle

- a. Wheel Assembly(Supporting Wheels)
 - For grip n the road areas/surfaces.
 - Flexibility for shocks.
 - For perfect dynamic balance.

- b. Tyre Assembly
 - For Load support.
 - For providing shocks cushion.
- c. Suspension System
 - For these parathion of axle and wheels.
 - For the isolation of vehicle from shocks and vibrations.

3 Hardware Components

3.1 Ultrasonic sensor

Item it's a ultra sound at 40000Hz which travels through the air and there's an object or obstacle on to the module. Considering the time period and therefore the speed of the sound you 'calculate the space. The HC-SR04 Ultrasonic Module has 4pins, Ground, VCC, Trig and Echo. The bottom and therefore the VCC pins of the module must be connected to the bottom and the 5 volt spins on the Arduino Board respectively and the trig and echo pins to any Digital/Opinion the Arduino Board. So as to get the ultrasound you would like to line the Trig on a High State for $10\mu\text{s}$. which 8 cycles on IC burst which will travel at the speed sound and will be received within the Echo pin. The Echo pin will output the time microseconds the acoustic wave travelled. An ultrasonic. By recording the time period between the acoustic waves are being generated and there fore the acoustic wave bouncing back. Here we connected to the Arduino and place of the vehicle which measures the space between the thing behind the vehicle and provide signal to the Arduino board to which connected to buzzer to supply sound when certain distance reached to avoid accidents. The sensor module contains four pins ground, VCC, trigger, Echo which the bottom and VCC are connected to respective supply pins with Arduino and trigger and echo connected to any digital/O pins of Arduino board.

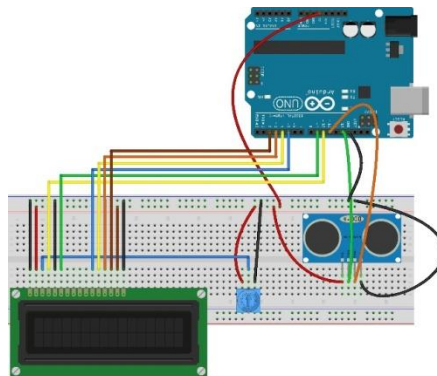


Figure 2:PinConfiguration

3.2 Arduino

The Arduino Uno one quite microcontroller supported ATmega328, and Uno. Arduino Uno known as for marking the upcoming release of microcontroller board namely Arduino Uno Board 1.0. This board includes digital/Opins-14, an influence jack, analog /ps-6, cera micresonator A16MHz, a USB connection, an RST button, and an CSP header of these can support the microcontroller for further operation by connecting this board to the pc the facility supply of this board are often through with the assistance of an AC to DC adapter, a USB cable, otherwise A battery this text discusses what's an Arduino Uno microcontroller, pin configuration, Arduino Uno specifications or features, and applications. The ATmega 328 one quite single-chip microcontroller formed with Atmel with in the mega AVR family. The architecture of this Arduino Uno may be a customized Harvard architecture with 8 bit RISC processor core. Other boards of Arduino Uno include Arduino Pro Mini, Arduino Nano, Arduino Due, Arduino Mega, and Arduino Leonardo. It is an open source computer hardware we used Arduino UNO board the boards pre programmed with help of embedded Arduino compiler. The boards used to control the ultrasonic, buzzer, GPS module, and display to given and get the proper output which easily programmable and cheap totally tact as brain for those operation which need low power and high efficiency.



Figure 3: ARDUINO UNO Board

3.3 GPS Module

The GPS module employed to locate the position of the vehicle case of any emergency like loss of auto or any accidents happen to the one that drives which their relations can find the place easily. Needs 12v here we used a GPS transmitter (HC12) which transmit the knowledge from GPS with no additional programming which transmits GPS coordinate store mote location with a small GPS receiver which received by another HC12 transceiver which processed by Arduino board. The GPS module for Arduino may be a small electronic circuit that permits to attach to your Arduino board to urge position and altitude, also as speed, date and time on UTC (Universal Time Coordinated).

3.4 Buzzer

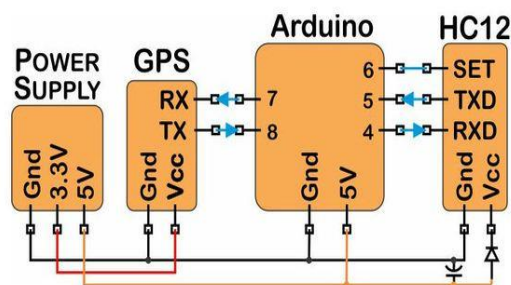


Figure 4: Buzzer.

3.5 Motor

Here we used 60 RPM motor for our prototype which makes the small gear to run



Figure 5: Motor

4 Advantages of the Proposed System

- Highly comfortable.
- Easy reverse gear operation.
- Independent of others.
- Improved guidance level.
- Reduced time.

5 Conclusion

The disabilities of the physically challenged people are taken as a main constraint this system. Here we proposed a small solution for driving two wheelers in reverse direction. But in large scale, we need to improve this system further.



Figure 6: Prototype

References

- [1] elims.awad "Voice technology in the instrumentation of the automobile", member IEEE transactions on instrumentation and measurement, VOL. 37, NO. 4, DECEMBER 1988
- [2] Margaret Ducusinha "Modeling of a Series Hybrid Electric High-Mobility Multipurpose Wheeled Vehicle in the journal IEEE TRANSACTIONS ON VEHICULAR TECHNOLOGY, VOL. 56, NO. 2, MARCH 2007.
- [3] Ananda ManiPaudel and Philipp Kreutzmann "Design and performance analysis of a hybrid solar tricycle for a sustainable local commute", volume 41, pp.473-482, 2014
- [4] Selvaganapathy Manoharan, Nishavithri Natarajan, "Brain controlled wheelchair for the physically challenged people using Neuro – Sky Sensor", International Journal of Innovative Research in Science, Engineering & Technology, Volume 4, Issue 12, December 2015, P. No.11985 – 11992.
- [5] Ravikumar Kandasamy, Sachin Raut, Deep Varma, Ganesh There, "Design of Solar Tricycle for Handicapped Person", volume 5, issue 2, pp.11-24, 2013.
- [6] Lucas H.V. van der Woude, Sonja de Groot and Thomas W.J. Janssen, "Manual wheelchairs: Research and innovation in rehabilitation, sports, daily life and health", Medical Engineering & Physics, volume 28, pp. 905–915, December 2005.
- [7] M. Selvaganapathy, N. Nishavithri, T. Manochandar, G. Manikannan, "Modern vehicle for the physically challenged people using blue eye technology", International Journal of Mechanical Engineering and Technology, 8 (1), 2017, pp. 208 – 212.
- [8] Po Er Hsu, Yeh Liang Hsu, Kai Wei Chang and Claudius Geiser "Mobility assistance design of the Intelligent Robotic Wheelchair", International Journal of Advanced Robotic Systems, volume 9, pp. 1-10, 2012.
- [9] Giuseppe Quaglia, Walter Franco and Riccardo Oderio "Wheel chair.q, a motorized wheelchair with stair climbing ability", Mechanism and Machine Theory, volume 46, pp.1601-1608, 2011.
- [10] Mohd Razali Md Tomaria, Yoshinori Kobayashia, Yoshinori Kunoa, "Development of Smart wheel chair system for a user with severe motor impairment", International Symposium on Robotics and Intelligent Sensors, volume 41, pp. 538-546, 2012.
- [11] P.K. Nag, J.T. Panikar, M.G. Malvankar, C.K. Pradhan and S.K. Chatterjee, "Performance evaluation of lower extremity disabled people with reference to hand cranked tricycle propulsion", Applied Ergonomics, volume 13.3, pp. 171-176, 1982.
- [12] Madarasz R.L., Heiny LC., Crompt R.F. and Mazur N.M. (1986). "The design of an Autonomous Vehicle for the Disabled." IEEE Journal of Robotics and Automation, vol. RA2.

A Circular Shaped DGS for Coplanar Waveguide Transmission

Pavithra L¹, Baranidharan V², Ragavi B³

^{1,2,3} PG Scholar, Department of Electronics and Communication Engineering,
Bannari Amman Institute of Technology, Sathyamangalam, India.

Abstract

In this paper, we designed and manufactured the circular-shaped DGS for coplanar waveguides. The CPW DGS technology is mainly used because of its band performance which does not require holes in the shunt and series connections and they provide the attenuation to poles at both higher and lower band ends in-order to improve the bandwidth. The purpose of designing the CPW is they are widely used in the WiMAX applications and selection of the DGS is depending upon the bandwidth requirements. Therefore, to reduce the loss in the bandwidth performance of the circular shaped DGS for a coplanar waveguide with the one column, hence we introduced a two-three column circular-shaped DGS which improves the transmission coefficient by 0.8066 that is (-1.10 dB). This simulated and fabricated results shows that this structure outperforms than the existing designs

Keywords: Coplanar waveguides, DGS, Wi-max, Transmission coefficient, Bandwidth.

1 Introduction

The growth of wireless communication has been increasing rapidly due to the effect of easily transferable transmitter and the receiver. Because it uses the filter which has the design specifications such as low loss, cost-effective and less weight. This radar and measuring equipment's are used to choose the required band of signals minimized losses are done by using the filter which is used in the front end of the microwave system. The methods like high temperature superconducting, bulk acoustic waves are used to design the microwave filter. In such case, one of these methods is to manufacture by utilizing the miniaturized small strip line innovation. In earlier, most of the methods used microstrip line techniques to fabricate the system by considering all the known planar transmission methods we found that coplanar waveguide transmission is considered to better because of its greater frequency and mounding ability in the parallel and series components of the single plane. The most important component of the microwave and the cellular communication system is the band pass filter. Therefore, the microwave system must need a better filter structure.

Coplanar waveguide transmission offers a better results for reduced and ease structure of microwave circuits for current remote applications system because of their numerous central as lightweight and low volume. Therefore, coplanar waveguide transmission with defected ground structure uses the stop band rejection filter to achieve losses in the system. A periodic structure like photonic band gap and defected ground structure for the coplanar waveguide has a good interest because of their higher potential capability. The periodic structure combined with a transmission line has accurate band pass and rejection bands like low pass filters. The main purpose of using coplanar waveguide transmission over standard transmission is that they are used only for the simple transmission over the broadband. Coplanar shaped DGS for coplanar waveguide structure is utilized to improve the reaction execution of channel, without including periodical structures, and consequently holds a reduced size.

2 Literature Survey

Currently, in microwave technologies DGS is mainly used, among filter is the main devices used with the DGS especially for the coplanar waveguide transmission, because there presents planar geometry which offer ground with the sufficient surface to be etched by any defects.

Mahajan.C, "Design and implementation of DGS for coplanar waveguide", [1] they study with the coplanar waveguides which have been used with a defected ground structure to reduce the losses in the reflection coefficient. It shows that, there is a reduction in the loss of the reflection coefficient, it does not satisfies much because this system uses the one column DGS for coplanar waveguides.

Mukesh Kumar, "Fundamental analysis of the defected ground structure in the wireless applications", [2] they proposed the history of the DGS system and the various forms of the forms DGS other than the EBG and PBG. The PBG and EBG are the methods which are used in the earlier periods and they doesn't matches with coplanar waveguide transmission. In order to overcome the disadvantages in that DGS method which is well suited for the coplanar waveguide transmission is described in this paper.

Anushiya, "Implementation of U-shaped DGS with the open stub in CPW", [3] proposed a method was focused on the defected ground structure of the U-shaped structure, which is used to increase the frequency response of the band pass filter. However, this method is not suitable for all kinds of the filter it is specifically designed better only for the band stop filter.

Jong Sik Lim, "Spiral shaped DGS for coplanar waveguides", [4] discussed the defects in the spiral-shaped DGs and the slow-wave characteristics of the spiral-shaped DGS in to order to increase the coplanar waveguide transmission lines. Therefore, this technique is better suitable for the band rejection filters.

Abbas, "2D DGS for coplanar waveguide transmission", [5] this paper deals about the two-column and three-column DGS waves in which the shape of the DGS depends on the number of the DGS unit cell is required to improve the bandwidth. This techniques has the advantage that the capacitance remains constant when the inductance varies by increasing the number of cells, thus making the circuit design easy.

3 Coplanar Waveguide Transmission line with DGS

3.1 Coplanar Waveguide Transmission

Coplanar waveguide transmission was most commonly used in the circuit design of microwave system. The coplanar waveguide transmission has been widely used because it overcomes the several disadvantages in the microstrip based planar transmission line. Figure 1- shows the structure of coplanar waveguide transmission. The coplanar has the basic configuration which consists of the conductor strip placed at the center of the top dielectric substrate which has two ground conductors by the distance S on both sides of the transmission and the substrate material thickness is given as ' h '. In an implementation, the substrate back of the coplanar waveguide transmission is often in contact with the set off the metal layer. Therefore, the signal line of the ground is present at the same planes, the inductance that is in contact with the ground plane got reduced. Hence, the width of the substrate material and the thickness of the substrate material depends on the characteristics impedance of the transmission. Thereby, it is known that the particular characteristics impedance can be determined by the different ways the coplanar waveguide. Therefore, to minimize the losses in the conductor channel width can be increased in order fed them into the small transistor which has minimal impedance.

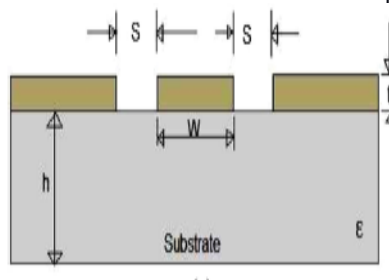


Figure 1: Structure of coplanar waveguide transmission

The main purpose of using coplanar waveguide transmission is that the low cost-effective and the fabrication process is done easily. There are no radiation losses because they eliminate the coplanar layer through the holes.

3.2 Defected Ground Structure

The defected ground structure is made of the unit cell or the number of periodic and aperiodic defected. The defected ground structure is known by the compact embedded slots on the ground plane of the microwave circuits. The main purpose of using the DGS with the coplanar waveguide transmission is that the previously introduced methods like electromagnetic band gap and photonic band gap methods do not have the uni planar structure whereas the coplanar waveguide transmission with DGS has the accurate results with the simulation because it has the uni planar structure. The periodic DGS is mainly used with the coplanar waveguide transmission. Because the defects that made on the ground plane interrupt the current distribution to the ground plane. Thereby, it changes the transmission line characteristics. Hence, any defects that engraved in the ground plane below the strip line thereby it changes the effective capacitance and inductance. Therefore, DGS acts as an equivalent RLC circuit. The designation of the DGS is easier when compared to the EBG and PBG because they have high accuracy in the regular planar structures. Figure 2- shows the RLC equivalent circuit of the DGS unit cell.

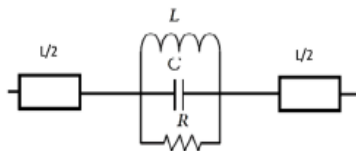


Figure 2: RLC Equivalent circuit

4 Experimental analysis of CPW for Defected Ground Structure

This section explains the coplanar waveguide in the selection DGS in cells determined by analysis and staging methods. The changes that are done through the periodic DGS to determine the particular characteristics of the coplanar waveguide are known by the reflection and transmission loss of the S-parameter values (S_{11} and S_{21}). These analyses are carried to get low reflection loss and high transmission efficiency.

4.1 Designation of the Simple Coplanar waveguide transmission

The design of the simple coplanar waveguide transmission has some limitations are the center strip of the conductor is separated by the shape edge gap from the two ground planes on both sides and it requires zero cuts off frequency because the wideband requires the zero cut off frequency. After all, it is based on the quasi TEM modes. The simple coplanar waveguide transmission line which has 50 ohms has the design specifications as (110mm)x(55mm)x(1.8mm) has been prepared for the designation. The relative permittivity of the FR-4 substrate is 4.8. The designation is carried out and simulated by using HFSS and it is considered for all the values of 1 to 10 GHz frequency ranges. The S-parameter which indicates S_{11} and S_{21} are obtained from the HFSS ports of the transmission lines. Therefore, the region around the entire simulation design of the radiated airbox has been applied.

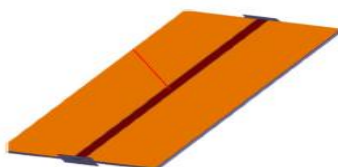


Figure 3: Simple CPW transmission line

Figure 3- shows the demonstration of the S-parameter that present on both sides of the coplanar waveguide transmission. Figure 4- gives the components of the coplanar waveguide transmission line, where their width is given by 'W' and the gap between the coplanar waveguide transmission is given by 'g' and the coplanar ground plane. To obtain the impedance of 50 ohms, the strip width and the strip gap of the coplanar waveguide transmission is considered to be as 4.4 mm and 0.6mm. the S-parameter of the S_{11} which is known as the reflection coefficient is given by -44.87dB at 8.81 GHz frequency is obtained by the simulation result. Therefore with the assistance of the microstrip line which is used by the coplanar waveguide transmission is 551MHz from the values of 6.981 to 8.405GHz which are the values of the return loss and impedance matching.

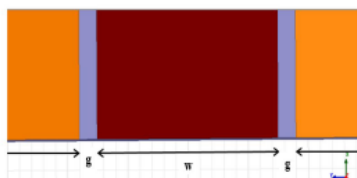


Figure 4: Dimension components of CPW line

In order, to get the perfect standard coplanar waveguide transmission line, we must improve the bandwidth of the impedance and the reflection coefficient and transmission gain of the system. In the proposed system, we

introduce a different state of shapes in coplanar waveguide transmission of the ground plane which is engraved on both sides of the coplanar waveguide transmission which acts as a defected ground structure.

4.2 Designation Circular shaped DGS for Coplanar waveguide transmission

The DGS circuit of the proposed circular shaped unit cell, which is placed on the metallic ground plane. By utilizing the determined circular defected ground structure the micro strip line by increasing the parallel inductance. The successful arrangement of the inductance presents the specific frequency at the cut off trademark. The arrangement of the inductance offers growth to the smaller cutoff frequency is done by expanding the engraved area of the circular DGS. In the engraved circular DGS their present attenuation poles. Therefore the parallel capacitance with series inductance can be clarified by using these attenuation poles. The resonant frequency is equal to the LC circuits, due to the series inductance has been increased. Therefore, the cut off frequency and attenuation poles become smaller.

The CPW line with the physical measurements is as the easy structure of CPW for DGS are thought and circular shapes are engraved. The circular-shaped DGS unit cell is structured making the perfect shapes and at last they are combined into the single structure. The circular-shaped DGS unit cell consists of the 25 numbers of periodic cells which are arranged periodically to balance the plots of the coplanar waveguide transmission.

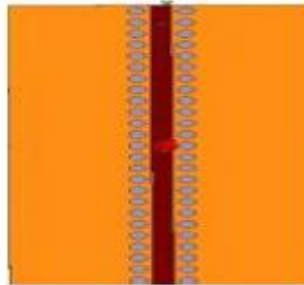


Figure 5: CPW line for circular DGS

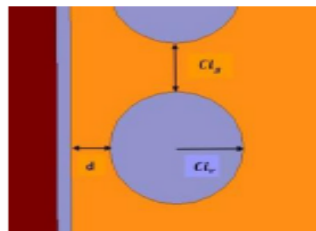


Figure 6: Measuring elements of CPW line for circular DGS

Table 1: Components measurements of the DGS cell

| Parameters | Units(mm) |
|------------|-----------|
| C_{IR} | 1.4 |
| C_{IG} | 1.8 |
| D | 1 |

Figure 5- determines the coplanar line for circular shaped DGS with a single section. Therefore, the DGS of the circular shape has been explored and the segments are expanded. Figure 6- determines the elements of the circular shaped DGS of the coplanar waveguide transmission where the C_{IR} is the circle radius, C_{IG} is the separation between the two-unit cell of DGS. Table 1- determines the components used in the DGS unit cell of the coplanar waveguide transmission. Figure 7- determines the frequency at -31.30dB at 9.43GHz as the return loss and transmission gain at 6.48dB. Hence, the single section of the circular shape DGS does not support for all bandwidth. In such case, the number of segments needed to be increased.

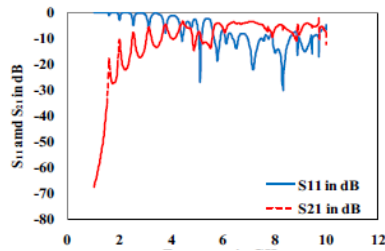


Figure 7: S-parameter analysis for single section circular shaped DGS

So we introduced two and three sections for the coplanar waveguide with the circular-shaped DGS. Therefore, figure 8 and 9 determines the CPW line for the two and three sections of DGS based on the circular shaped. Figure 10- determines the distance between the two-unit cells of DGS which is measured as 0.8mm.

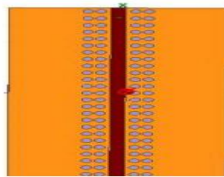


Figure 8: Two section of CPW for DGS

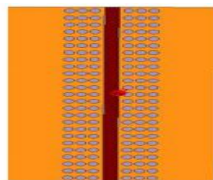


Figure 9: Three section of CPW for DGS

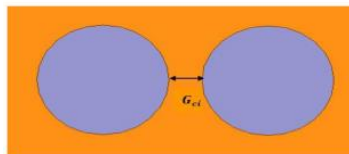


Figure 10: Separation between the two cells of CPW for DGS

Figure 11-determines the return loss of the two-section of circular-shaped DGs at -31.69dB at 9.35GHz and obtained gain value is 1.10dB to know the graph difference between return loss and the transmission gain. Therefore, by comparing the obtained results with a single section of the DGS cell, it has been noticed that the return loss and the transmission gain are upgraded and the obtained bandwidth value is 1.67GHz which is obtained due to the return loss is below -10dB which ranges from 7.91 to 9.48GHz.

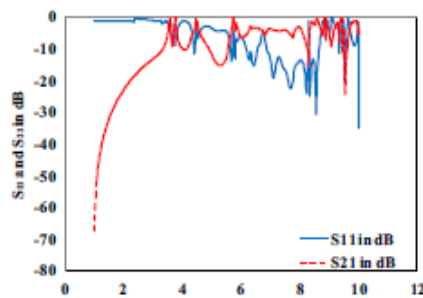


Figure 11: S-parameter for Two section circular shaped DGS

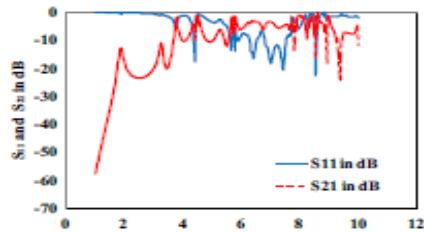


Figure 12: S-parameter for Three section circular shaped DGS

Table 2: Comparison between the number of section in the circular shaped DGS

| Design | S ₁₁ (dB) | F (GHz) | S ₂₁ (dB) | Impedance range |
|----------------|----------------------|---------|----------------------|-----------------|
| Single section | -31.30 | 9.34 | -5.48 | 0.82 |
| Two section | -31.69 | 9.35 | -1.10 | 1.81 |
| Three section | -21.57 | 8.34 | -5.91 | 1.95 |

Figure 12-determines the returns of the three-section circular-shaped DGS that has 21.57dB at 8.34GHz and the obtained gain value is -5.91dB to know the graph difference between the return loss and transmission gain. Table 2- determines the comparison between the number of sections in the circular shaped DGS cell. Therefore, by comparing the obtained results with the single section of the DGS cell, it has been noticed that the return loss and the transmission gain are upgraded and the obtained bandwidth value is 1.87dB which is obtained from the return loss below -10dB which ranges from 7.91 to 9.48GHz.

5 Manufacturing and Testing of the Circular Shaped DGS

The CPW line with a periodic DGS is examined and then its execution is tried for circular shaped and the number of sections of DGS cells. The S₁₁ (return loss) and S₂₁ (transmission gain) are acquired as the created consequences of each analysis. From the perceptions, it is discovered that structure with two segments of the circular DGS gives both these qualities at an ideal range. The structure which has the uniform DGS coupling and the shapings at occurs naturally is obtained by the circular shaped DGS. It is noticed that there is a decrease in the diffraction losses in the circular shaped DGS because there is an absence of sharp edges. Along these lines, the transmission gain is higher contrasted with different shapes. Besides, the arch of the circular shaped DGS presented to the transmission is bigger contrasted with different shapes. These outcomes into an impressive decrease in bordering fields which improves the transmission gain. Subsequently, this structure is manufactured to test and approval utilizing the measurements are clarified. Figure 13 shows a snapshot of the designed CPW line with two sections of the circular shaped DGS.

The manufactured CPW transmission line is tried utilizing R and S ZNB Vector Network Analyzer (VNA) for approving the S₁₁ diagram. The losses in the material utilized for CPW line creation and welding of the connectors are considered for the adjustment of the interfacing links. Figure 14 shows a plot of a return loss estimated utilizing VNA and the simulated outcome. Table 3-determines an examination of both the measured and simulated results and it is discovered that the return loss is found in the deliberate outcome is - 31.08 dB though, in the recreation result, it is - 32.28 dB. The measured outcome is acquired as 7.91 GHz resonant frequency and for the reproduced outcome it is 7.85 GHz. The transmission capacity acquired from the simulated outcome is 1.63 GHz (6.97–8.50 GHz) though in the measured outcome it is 1.20 (+) GHz. Here, (+) implies that it is more prominent than the tried supplier to convey the web associations utilizing channels to the clients relying upon the speed of the web-dependent on the data transmission of the channel required by a client.

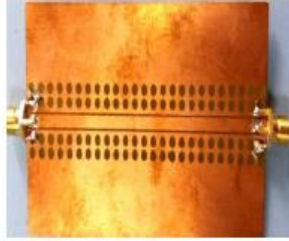


Figure 13: Snapshot of the manufactured circular shaped DGS

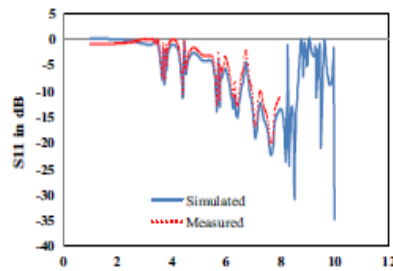


Figure 14: Analysis between simulated and measured S-parameter for two section circular DGS

Table 3: Analysis between the simulated and measured parameters

| Units | Simulation | Measured |
|--------------------------------------|------------|----------|
| Return loss s_{11} (dB) | -31.28 | -30.58 |
| Resonant frequency f_r (GHz) | 7.85 | 7.81 |
| Impedance range (dB) | 1.53 | 1.10(+) |

6 Conclusions

The paper is associated with the survey of a CPW transmission line with PDGS having ordinary unit cells along the two sides of the line. The unit cells are de-metalized from the outside of the co-planar ground surface. The choice of the states of the opened unit cells was done with different reproductions just as the elements of the shape were enhanced for the 50-ohm quality impedance of the CPW line. The quantity of the unit cell additionally changes as indicated by their shapes for the better impedance coordinate. From the simulated results, it is noticed that roundabout formed DGS gives better outcomes to s_{11} and s_{21} . Although, there is constantly an exchange off between the parameter choice and its exhibition. Consequently, the transmission loss is the main consideration for the unit cell choice and along these lines the circular-shaped PDGS configuration was created and tried. In this way the circular-shaped PDGS gives great outcomes in both the creation and tested process.

References

- [1] Rajshri C.Mahajan, "Design and implementation of Defected Ground Structure modified CPW", SN applied science (2019).
- [2] Madhuri Sahal, "Wideband CPW fed antenna using planar transmission line DGS", International Conference on signal processing and integrated networks, February-2020.
- [3] D.Ahn, "A spiral shaped defected ground structure for Coplanar Waveguide", IEEE microwave and wireless components-October 2002.
- [4] Ehab.K.I, "2D periodic defected ground structure for Coplanar Waveguide", Gemic(2005).

- [5] Young Ki Hong, "Spiral defected ground structure in grounded Coplanar Waveguide", IEEE Radio and Wireless Symposium, January-2011.
- [6] Heba, "Novel Reconfigurable Defected Ground Structure Resonator on Coplanar Waveguide", IEEE Transactions on Antenna and Propagation, November-2010.
- [7] Mukesh Kumar, "Defected structure ground –fundamentals, analysis and applications in modern wireless trends", International Journal of Antenna and Propagation, volume-2017.
- [8] AhmedErrki, "A novel compact CPW band-stop filter using O-DGS configuration" international journal of electrical and computer engineering, volume-9.
- [9] Chen-Cheng-wang, "Novel uniplanar synthesized coplanar waveguide and the application to miniaturized rat race coupler", IEEE-2010.
- [10] Anushiya, "Design and fabrication of an U-shaped DGS", International Journal of Engineering and Technology, RTICCT-2017, special issue-2017.
- [11] Bomson Lee, "Analysis and synthesis of Defected Ground structure using Transmission Line Theory", European Microwave Conference, October-2009.
- [12] Annaram, "Harmonic suppressed miniaturized koch hybrid coupler using circular DGS", International Journal of Microwave and Optical Technology, volume-4, no-4, july-2009.
- [13] Omar, Nadim.G, "control of band stop response of cascaded microstrip low-pass band stop filter using arrowheads slots in backside metallic ground shape, IEEE antenna and Propagation.
- [14] Shi XW, Chen XQ, "An overview on defected ground structure", Propagation Electromagnetic* Res B 7:173–189 (2008).
- [15] MortezaRezaee, "2D displacement sensor based on CPW Line by DGS with two separate zones", IEEE Sensors Journal, February-2017.

Resource Allocation Scheme Based on NOMA in OFDM

Pavithra L¹, Ragavi B², Nandhini V D³

^{1,2,3} PG Scholar, Department of Electronics and Communication Engineering,

Bannari Amman Institute of Technology, Sathyamangalam, India.

Abstract

This paper describes a model to deduce the usage of power by the user in the demand condition to the power allocation to the system. It is required source since the effect of frequency of the selective channel is ignorable which are by using the NOMA it enhances the future network capability. This paper proposes the technique, which is used to provide the resources techniques. The purposes of the allocation scheme made its allocated the power as per the users in the system to give the equal amount of the power to the users resources allocation scheme. The calculation of the resource allocation is done by number of users, sum rate and the power allocated during the transmission. Therefore, here the MATLAB software is used to give the simulation results and the NOMA proves better when compared the OFDM. From the proposed system, the total co-efficient increases by 50% in terms of power and the 20% in the indicator in terms of the users.

Keywords: OFDM, NOMA, 5G, Matlab

1 Introduction

In recent technology, by using mobile applications such as internet and internet of are widely used under wireless networks and communication. In mobile communication, these technologies act as smart and also gives a system capability to expand a work with recent technologies. Due to lack of frequency resources these frequency struggled with greater demand under conventional multiple systems. There are various types 5G modes used under non-orthogonal multiple access. The spectral efficiency is increased by using this technology and also suits with large scale user access. In recent days, it is main thing used 5G technology. For each user the radio resources are allocated under conventional orthogonal multiple access techniques. The NOMA technology uses overlay coding on the transmit side and uses power division multiplexing technology to provide the better channel condition for user at less power and more power to users even in poor channel conditions. Therefore, a channel that allows better justice for users. Compared to OMA, the NOMA receiver adds more complexity, but its greatest advantage is its spectral efficiency is higher. This is equivalent to increasing receiver complexity at the expense of spectral efficiency. As processor performance improves, more sophisticated receivers can be used with the device, and real world system uses the NOMA technology where the receiver receives successive Interference Cancellation (SIC) and uses multiuser isolation. Implementation is also possible. In the NOMA system, due to long decoding delay and serious error propagation, it is not practical to overlay all users in the same resource block

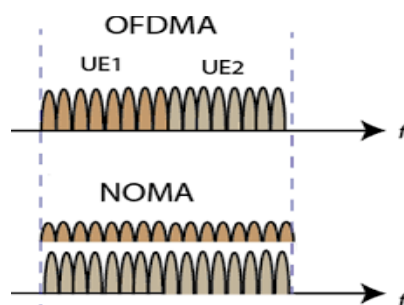


Figure 1: Non-Orthogonal Multiple access

Anyway, after a late improvement in processor performance, progress is proceeding with a desire to be postponed as a 5G innovation. NOMA can be ordered in three different customer multiplexing zones: NOMA with SIC (Progressive Obstruction Canceller / SOMA (Semi-Orthogonal Multiple Entrance), SCMA and IDMA. Frequencies And despite traditional time spaces, these plans strengthen the limits for NOMA with SCM / SOMA by multiplexing the customer in force fields, in force and code areas for SCMA, and multiplying by area.

2 Wireless Communication under MIMO in OFDM

The improvement of MIMO has recently started and has become a further perspective under enormous amount of high data rate under transmission of sender to receiver. Traditional MIMO is a remote cell design that allows you to use multiple send and receive lines that allows fast data transmission and achieves less time consumption. M transmissions and N receive wires between the remote association are carried out by using MIMO direct. The address MIMO channel coefficients contains $M \times N$ segments. The energy room is used for NOMA for processing of multiple access. However, in the past centuries, universal structures have relied on the time, frequency, code domain. Take, for example, the conventional orthogonal frequency division multiplex multiple input used by 3GPP- LTE. A major problem with this orthogonal multiple input (OMA) system is that its unearthly efficiency is low when some transmission restriction resources, such as

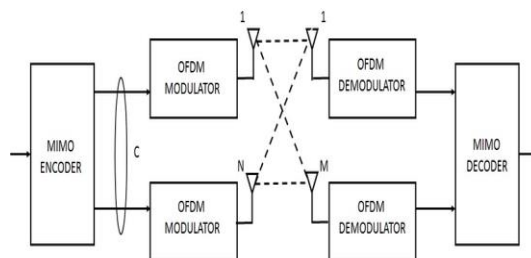


Figure 2: OFDM-MIMO wireless communication

On the other hand, the use of NOMA engages each user to move to the remaining channels of lessons, and therefore the information tricks allocated to users with weak CSIs can be achieved by users with strong CSIs, regardless of limited resources. Will, which is very strong. Basic levels improve vague productivity. The proposed delay for the Non-Orthogonal Multiple 3GPP Long term evolution (LTE) is starting and the fifth phase (5G) is considered a key part of the portable framework. The primary purpose of NOMA is to serve multiple users at the same time, frequency, code, albeit with different power levels, which increases the effectiveness of basic hunting compared to standard orthogonal mothers. This article aims to incorporate NOMA, as well as trade between NOMA and Abstract Radio.

3 NOMA in 5G communication

Non-Orthogonal multiple access has been currently acknowledged as the promising multiple access method in order to improve the spectral efficiency of the mobile communication networks. In past days, the TDMA, FDMA and CDMA has been used for 1G,2G and 3G networks. The OFDM is used for the LTE and the advanced method of the LTE systems which are known as the 4G networks. Hence, to meet the high demand of the radio access systems in future which is known as the 5G networks. Therefore, this increasing demands in the mobile internet and the internet of things has been challenged for the 5G wireless communication networks.

In NOMA downlink, the signal transmitted from the base station and the signal received at the UE receiver are made of the superposition of the transmitted signal at the UE's. whereas, in order to introduce the UE side the multi user signal separation is required so that the signal can be retained by the each UE's and their own data can be decoded. This process is achieved through the non-linear receivers mainly maximum likelihood detection or SIC(successive interference cancellation).

In case of using SIC, the decoding of the optimal order will decrease the channel gain normalized by noise and the power of ICI. By considering this order, we assume that any user can decode signals of the other users correctly. Hence, to separate the signals from each other NOMA the power domain. Because, the NOMA gives a prefect dimensions to separate the signals and give access to the base station.

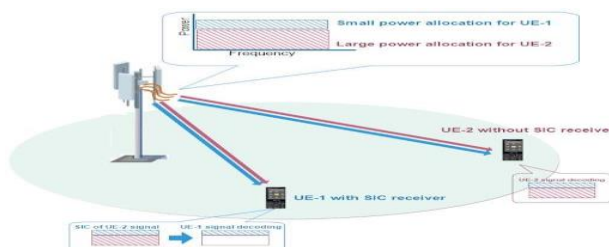


Figure 3: Downlink NOMA in 5G communication

4 Resource allocation in OFDM and NOMA

Resource allocation for user information carried in the frequency and time domains of OFDM technology. For example, in LTE systems, the smallest unit in the frequency domain is a subcarrier with a bandwidth of 15 kHz. The smallest unit in the time domain is 1/14ms OFDM symbols. Each resource unit has valid symbols and OFDM symbols. The LTE system adopts multi-antenna and uses the degree of freedom introduced in the spatial domain to transmit user information. In particular, each antenna uses the same frequency spectrum and time domain resources as the other antennas. In the power domain, the LTE system's OFDM technology does not adopt the power domain for transmitting user information because the frequency domain and the time domain have the same user information power. This is a two-dimensional plane of equipment transport system, the transmission capacity of wireless channel is relatively poor.

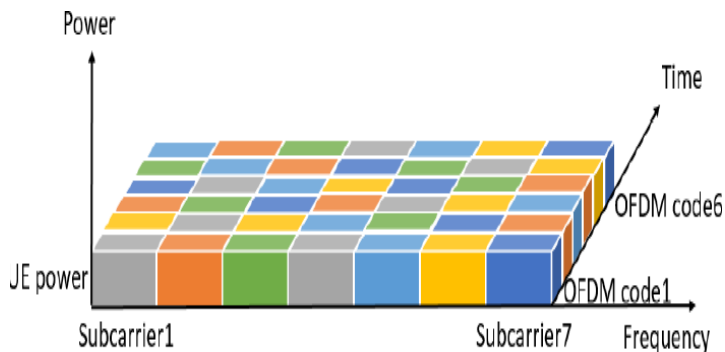


Figure 4: Resource allocation on OFDM base systems

Figure 5 shows the frequency, timing and allocation of resources in the electrical domain in the NOMA system. Frequency domain and time domain FIG in NOMA system. Is the same as in 2. However, the difference between them is that in terms of time domain and frequency domain each resource unit can transfer power to multiple users. Various hints. Clearly, NOMA technology is a system for three-dimensional resource allocation. As a result, NOMA offers greater flexibility in resource allocation than traditional OMA system. However, it is expected that there will be significant multi-user interventions and more sophisticated intervention management techniques.

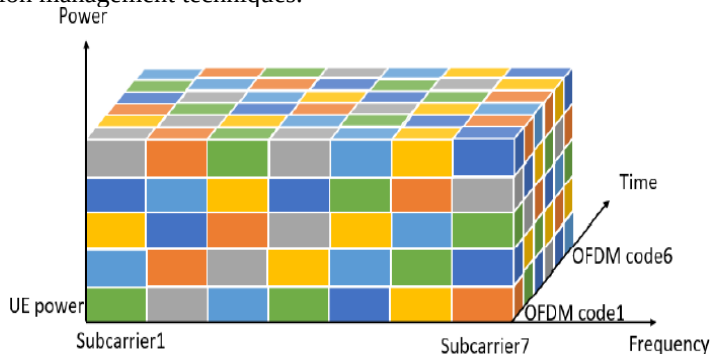


Figure 5: Resource allocation in NOMA base system

5 Proposed system

The operation of NOMA is mainly guided by the selection of users established in a specific sub band and the allocation of power to multiplexed users in a sub band.

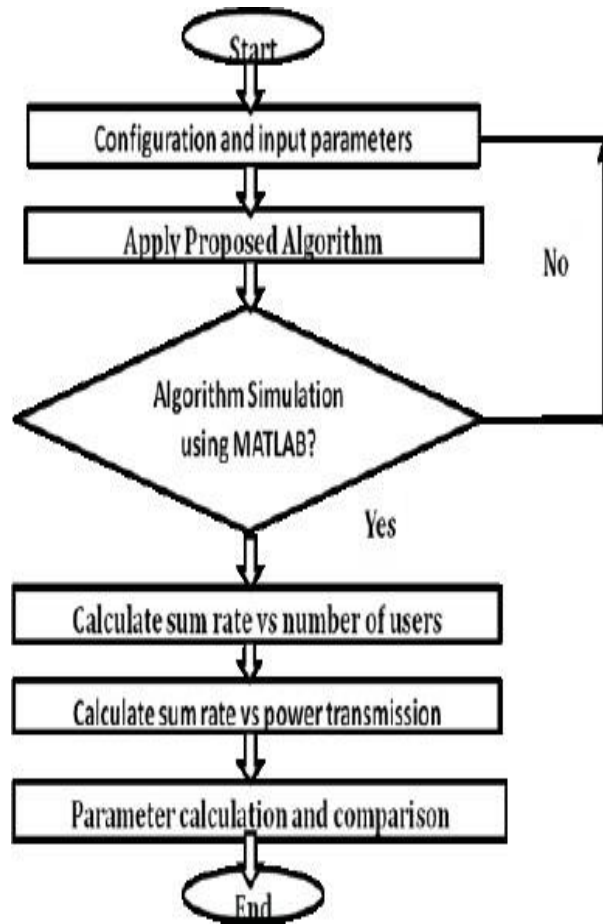


Figure 6: Flow chart of the steps involved in the proposed system

Steps:

Input parameters are assigned.

Create a model for the D FDMA and Noma system.

The matlab software is used for the simulation process.

The amount of sum rate is calculated with respect to the power transmission.

By considering the number of users the sum rate is calculated.

As the results all the products are calculated and compared with existing work.

6 Simulation results

The MATLAB software is used to simulate the proposed work. The input source which are given to the system are given in the table 1,

Table 1: Input source

| Parameter | Value |
|------------------------------|-------|
| Cell diameter | 350 |
| Path loss(V) | 4 |
| Noise power density(N_0) | -176 |
| Total bandwidth(WT) | 6 |
| No. of. RBs(S) | 28 |
| Bandwidth per RB(B_s) | 300 |

Figure 7- represents the performance of the transmission power and the sum rate using the NOMA technique and found to be better than the OFDM and the table 2 shows the numerical improvement in the proposed system.

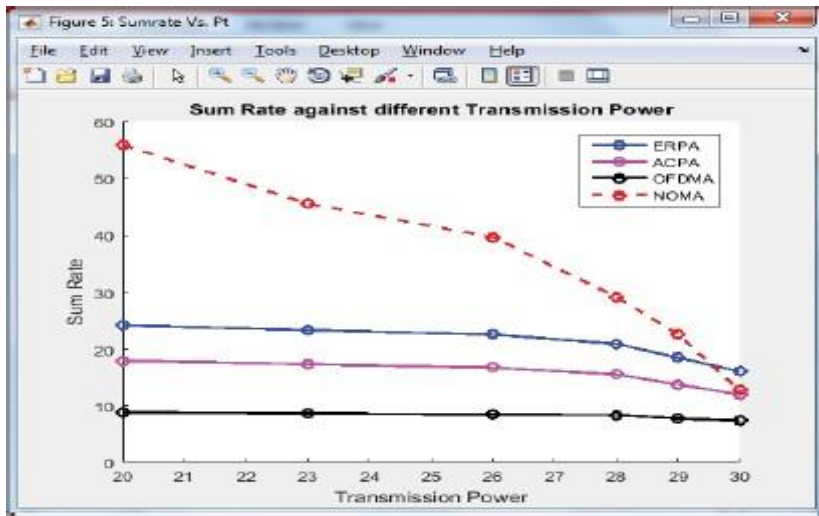


Figure 7: Transmission power versus sum rate

Table 2: Simulation results between transmission power versus sum rate

| Method | Transmission power | Sum rate |
|--------|--------------------|----------|
| ERPA | 35 | 12 |
| ACPA | 35 | 20 |
| OFDMA | 35 | 27 |
| NOMA | 35 | 60 |

Figure 8- represents the performance analysis between the number of users and the sum rate to is achieved by Using the NOMA and find to better the OFDM technique and the table 3 shows the numerical improvement in the proposed system.

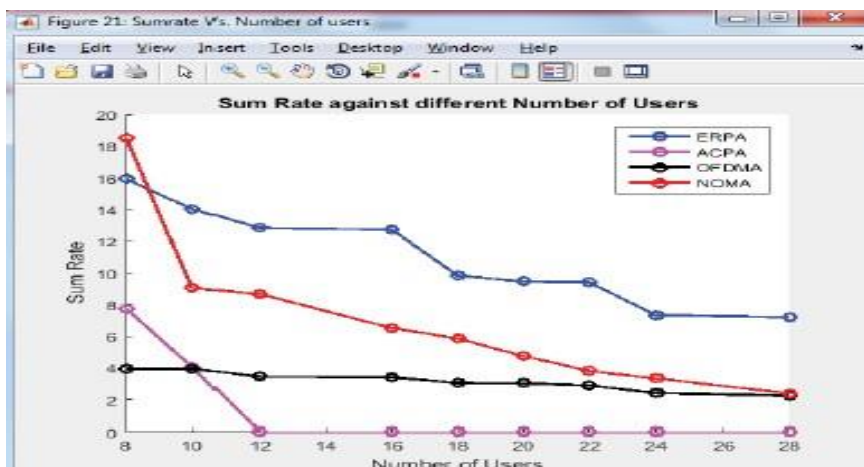


Figure 8: No. of users versus sum rate

Table 3: Simulation result of No. of. Users versus sum rate

| Method | No. of. Users | Sum rate |
|--------|---------------|----------|
| ERPA | 30 | 5 |
| ACPA | 30 | 9 |
| OFDMA | d30 | 17 |
| NOMA | 30 | 19 |

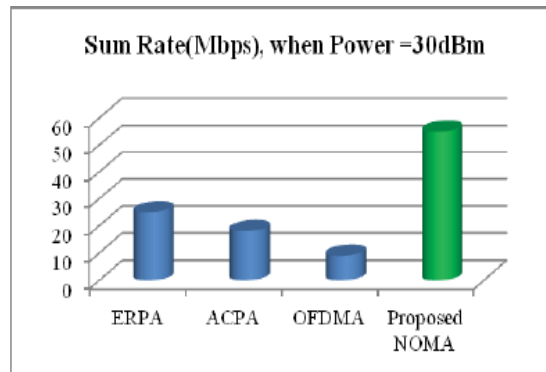


Figure 9: Sum rate versus power

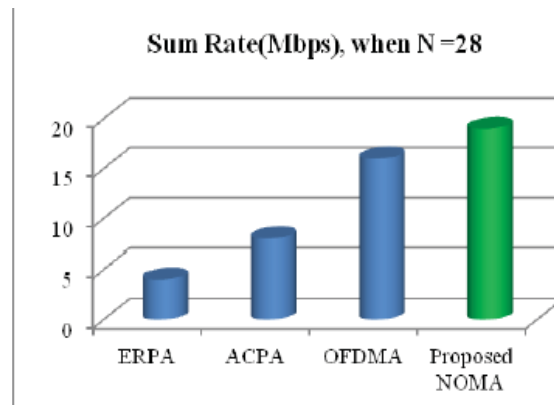


Figure 10: Sum rate versus no. of. Users

Therefore, figure 9 represents the sum rate when the given power is 30dBm and it gives the better power transmission compared to the other methods and figure 10- represents the sum rate when numbers of users is 28.

7 Conclusion

In this proposed system the resource allocation is the main subject under an radio resource allocation. Under an RBs allotment and characterisation calculation the square was distributed under an NOMA calculation. It will increase an data transmission rate for every client or sender to receiver for countless clients. The NOMA system which improves the total rate of data transmission. By comparing all OFDMA, CDMA, TDMA , the high data transmission has been achieved by using the NOMA. In future, the resource allocation will used under NOMA and also reduce the power consumption effectively. Hence, NOMA is preferred in order to improve the high transmission data rate.

References

- [1] L.Dai, B.Wang ,”Non-orthogonal Multiple Access for 5G:Solutions, Challenges, Opportunities, “IEEE Conference, Vol 53.Sept 2015.
- [2] Z.Ding, “Application of Non-Orthogonal Multiple Access in LTE and 5G networks: IEEE Conference Vol:55,Feb 2017.
- [3] B.Wang, Z.Wang, “Spectrum and efficient beam space MIMO-NOMA and mm Wave Communication,”IEEE Communication Conference, Vol 35, Oct 2017.
- [4] S.Chen, Q.Geo,” Pattern Division Multiple Access A Novel Non-Orthogonal Multiple Access for 5th Generation Radio Network”, IEEE Transaction , Vol 66, April 2017.
- [5] Z.Yang, Z. Ding. “ A general Power Allocation Scheme to generate Quality of service in NOMA System”, IEEE Wireless Communication , Vol 15, Nov 2016.
- [6] H.Zang, Downlink Energy Efficiency of Power Allocation and Wireless Back Haul Bandwidth Allocation in Heterogenous.”IEEE Wireless Communication , Vol14, June 2017.
- [7] C.Frang, “Resource Allocation for Cognitive Small Cell Network:Cooperative Bargaining Game theoretic Approach,”IEEE Wireless Communication , Vol 14, June 2015.
- [8] A.Fehske, G.Buzok.”The Novel Footprint of mobile communication Ergodical and Economic Perspective,” IEEE Communication Conference, Vol 47, August 2011.
- [9] Y.Chen, S.Zhang,”Fundamental table offer on green wireless network: IEEE Communication Conference,”Vol 49.June 2011.
- [10] G.Aver,C.Dessert,”How much Energy is needed to run a wireless Network,”IEEE Wireless Communication Conference, Vol 18, Oct 2011.
- [11] W.Hao, “Energy-efficient power allocation in millimetre wave massive MIMO with non-orthogonal multiple access”, IEEE wireless communication conference, vol- 6, Dec-2017.

Design of Dielectric Coupled Line Resonator with Defected Ground Structure in Linear Wave Filter

B.Ragavi¹, V. Baranidharan², L.Pavithra³

^{1,2,3} PG Scholar, Department of Electronics and Communication Engineering,
Bannari Amman Institute of Technology, Sathyamangalam, India.

Abstract

In microwave communication, Microwave Integrated, circuits (MIC), there are various methods and techniques, which are used for designing a Defected Ground Structure (DGS). In recent years, Microwave and mm-Wave frequency transmission plays a major role in wireless communications. so we are using a Microwave Band pass filter to reduce noise and a circuit is smaller. In this paper, we designed a dielectric coupled line resonator based on Defected Ground Structure (DGS). The hole is created in a defective structure, which improves a current dispersion. The level of frequency response, which is high with a uniform level and to protect a signal which is, received under an electric and magnetic field (E&H) variation over the desired band. The design of a Dielectric coupled line resonator (DGS) is widely used to improve a Signal to Noise Ratio (SNR) and reduces another signal distortion in the circuit. The simulated results show the proposed designs outperform the existing DGS designs.

Keywords: *Dielectric, coupled line resonator, microwave frequencies, Band pass filter, Magnetic and electric field.*

1 Introduction

In communication systems, microwave band pass filters are widely used which is the characteristic of smaller in size, Early integration among a different substrate, and different generating frequency. DGS has been adopted as a new technique to improves the various parameters in microwave circuits such as narrow pass band, cross-polarization, low gain, etc. In telecommunication technology, various market requirements and government regulations, used under the invention and development of new applications in wireless communication. Compact geometric slots are embedded in the ground plane of microwave circuits. This is called defective ground structures (DGS). DGS can have a single defect (unit cell) or multiple cell configuration defects. Thus, the intermittent and periodic defects are engraved in the basal plane of flat microwave chains are called DGS.

These new technologies provide several features in telecommunication networks, which in turn provide three essential elements to customers. The first is coverage, which means that each client needs to maintain a minimum level of electromagnetic Wave signal the second is bandwidth, which means that the client must have a sufficient data rate. The quality of service (QOS) guarantees the quality of data transmission from the transmitter to the receiver without errors in downlink and uplink the data transmission. To provide additional bandwidth, the strategy should be to open certain frequency areas for new applications or systems.

In microwave engineering, the microwave filters are divided into various types such as Low pass filter, high pass filter, band pass filter, Band stop filter. A Band pass filter, which supports all kinds of modern communication devices because it supports both the band selection in digital image processing and spurious rejection capability. Because of low insertion loss, it also supports flexibility under modern communication devices. When compared to normal wave the microwave, which is effectively given under a high accuracy and high performance. The band pass filter may allow the propagation of a signal under a particular frequency, attenuation of signal that falls under a range. The filter used in multimode gives a certain parameter such as Insertion loss (IL), Frequency selection (Q), Return loss (RL), Group Delay(GD).

A Band pass filter is categorized under and wideband frequency and narrowband frequency. The figure of Merit is ten times greater than frequency selection, named as a wideband and less than ($Q > 10$) which is called a narrow band. A selectivity, is directly proportional to Quality Factor and inversely proportional to Bandwidth. Generally, the Band pass filter contains active and passive filters. A Passive filter that contains an (RLC) and an active contains op-amps and transistors, which are used under radio frequency applications. A multimode resonator, which satisfies both the coupled line waveguides and Micro strip line filter. In the microwave communication system a band, pass filter, which offers more flexibility. A UWB (3.1-10.6 GHz) is used in the multimode resonator, which achieves a low cost, and size.

2 Literature Survey

Design of Bandpass filter with sharp transition based Microstrip Multilayer technique and defected ground structure under a Bandpass filter which can be used with DGS to make better optimization in the frequency the main purpose is to reduce the loss, and size[1]. The Xiao-Mingo Zhuang proposed a new "Design a low pass filter based on a defected ground structure proposed the defected ground structure for a Microstrip line in well designed to confirm the validity of the dumbbell-shaped DGS however is not suitable to all the microstrip lines [2]. Prayoot, proposed a Bandpass filter using the asymmetrical coplanar open-end structure for size reduction. The design is used to reduce the insertion loss on the low pass filter. The result shows that it is only for the conventional method [3]. Hussum proposed a "Bandpass filter with a wideband pass for a wireless communication system, they proposed the designation of the filter by two-column of the coupled lines which is used to increase the efficiency of the filter design [4]. The author Min-Hang proposed the design of UWB pass filter by using a coupled true line microstrip structure they design the filter prototype that is used to reduce the size and cutoff frequency [5]. An ultra-wide Bandpass filter with a stop band describes by using a lumped coupling capacitor, which is lumped by external coupling to speed impedance, and a capacitor, which converts a cutoff frequency [6]. These materials are usually suffer from large increase losses due to weak pairing between feed lines and ring, as well as due to ring rotation, so using linear and conical microstrip lines. The main advantage of this technique is that the reduction in enrollment is more than 7db compared to the normal. A new Bandpass filter uses two turning plugs based on a Bandpass filter. The design of the Bandpass filter uses an orthogonal feed line directly connected to the ring resonator. This method allows the use of compact, highly efficient, and low-cost filters designed duplex satellite communication systems. The conventional Ring resonators are adjusted to form a double half-ring to ensure compactness in size and to suppress multiple harmonics. Besides, the passband tonality is achieved by the use of ring resonators with many open plugs. For service, a WLAN frequency band dielectric ring resonator is also recommended.

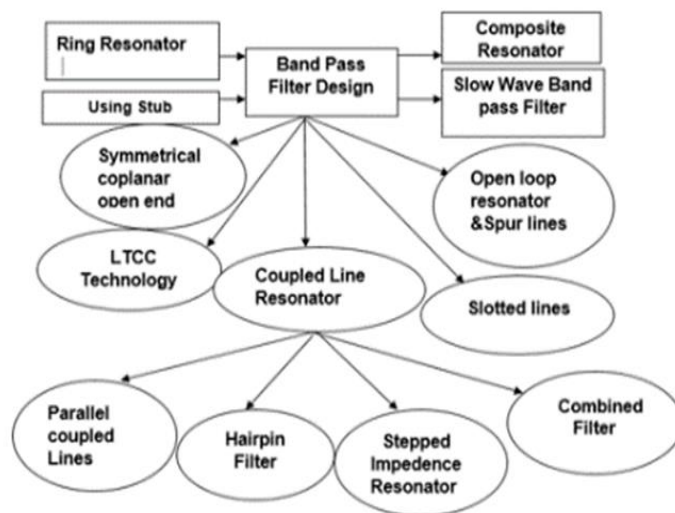


Figure 1: Design of Band pass filter Resonator

3 Design and implementation

This section explains the design OF DGS (Dielectric Coupled Line) microwave filters. This step work reduces the size of a circuit and gives a harmonic nature form too. In DGS, some portions are etched on the top of the Rogers 4350 microstrip line in the Z-shaped form. The microstrip dielectric constant is 3.66. Two dielectric resonators are mounted above the strip line portion of the DGS. The resonator dielectric constant used in this filter is 60, the dielectric resonator radius and height is 7mm, respectively, and height is 3.4mm.

A double bandpass filter is introduced here, due to turning, and optimization is achieved by connecting the line between the micro strips and the two resonator. Two dielectric resonators are located 14.5mm apart on a microstrip sheet. For the high Q, value is the main responsible for the Dielectric resonator, while the Defected

Ground Structure (DGS) and Deviated Microstrip Structure are used for both inductive and additional capacitive coupling as well as size reduction. The "W" strip on the microstrip lines helps optimize the resonator capacitive.

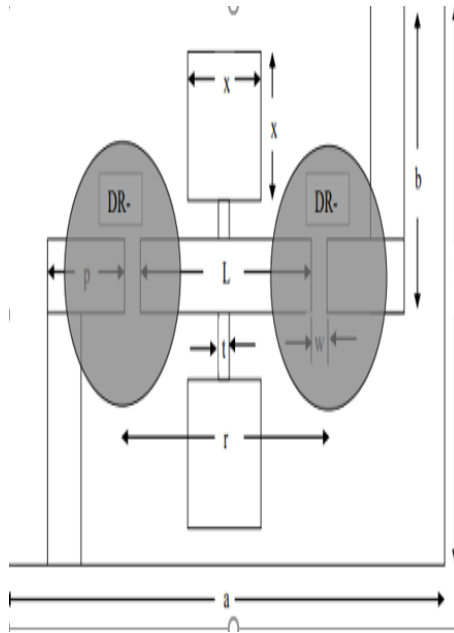


Figure 2: Geometric view of Band-pass filter with $a= 30.0$ mm, $h=20.0$ mm, $L=13.78$ mm, $b=10.854$ mm, $p=4.051$ mm, $x=5.50$ mm, $w=0.81$ mm, $t=0.31$ mm, $r=14.15$ mm.

The concept behind the Z-shaped structure is to get full discontinuity in the line of microstrip. In this paper, we use a cylindrical shape resonator used in the filter with a 3.75mm or 3.5mm radius and height, and a dielectric constant, to maintain the discontinuity of the microstrip line. For optimization, a bandpass filter is created and realized.

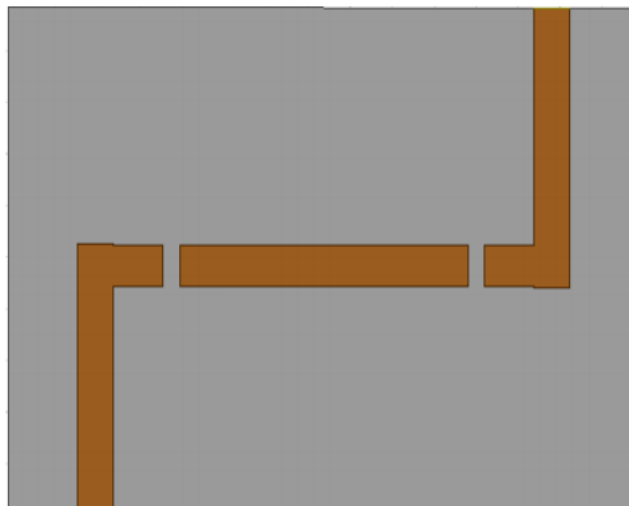


Figure 3 :Top view of the filter by using an FHSS (without DRS)

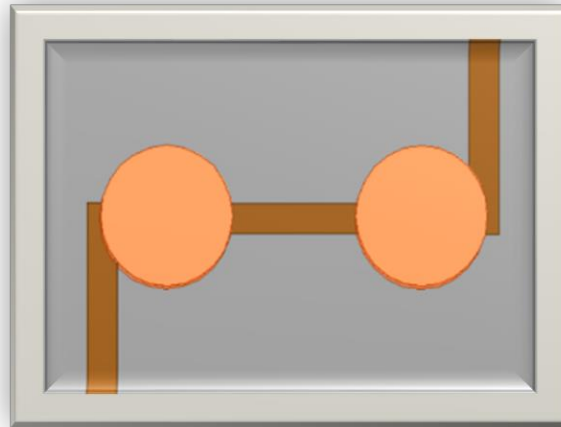


Figure 4: Top view of the filter by using an FHSS (with DRS)

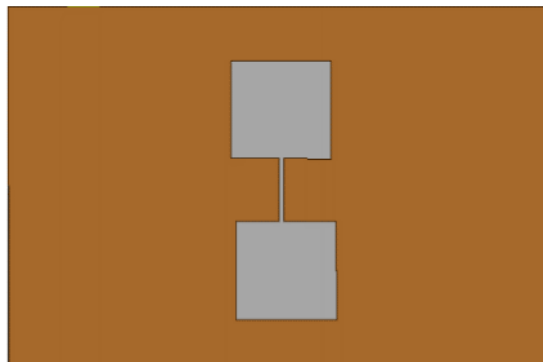


Figure 5: Bandpass Filter Bottom View (With DGS).

This filter is structured, developed, and modelled by using the FHSS simulator (high-Frequency Simulator). Return Loss and low pass filter estimated backflow loss. This filter has a resonance at 875 GHz frequency. The Filter bandwidth is between 1.0489 GHz to 2.935 GHz. Field Management (Field E and Field H) which suppressing an undesired signal.

DGS has unique and essential features, which are particularly useful for improvement under microwave components and performance, which are given, in the printed form. The most important features are to incorporate the frequency response of microstrip-line and coplanar waveguide components in transmission zersin.

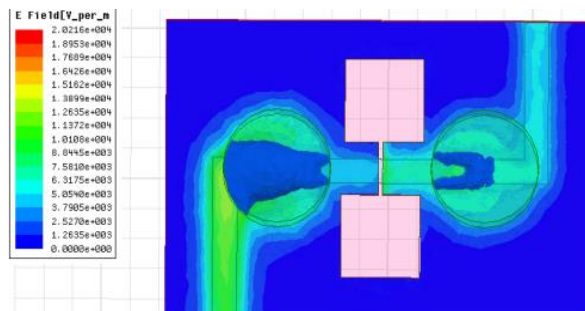


Figure 6: Bandpass filter which shows an E-field variation

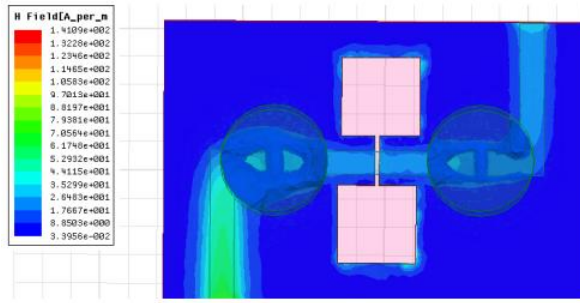


Figure 7: Bandpass filter which shows an H-field variation

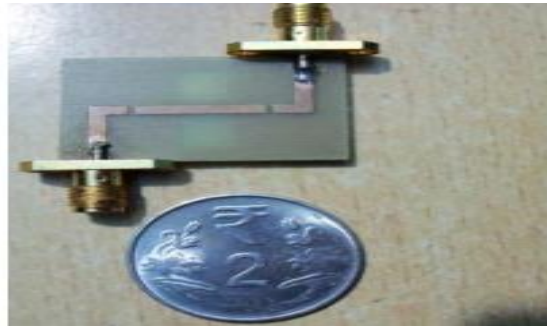


Figure.8: Top view after fabrication in MSL



Figure 9: Bottom view after fabrication in MSL

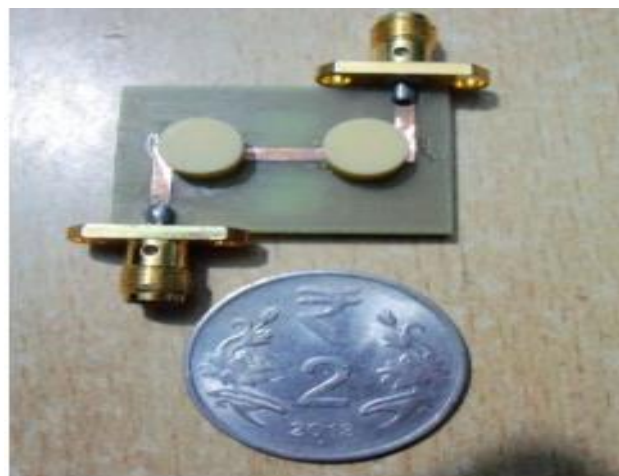


Figure 10: Fabricated model with DR band-pass filter

4 Result

Frequency response in band pass filters plays a major role to transmit a limit. The transmission line is allocated over bandwidth in an output signal. It will prevent a transmitter from interference and other stations and simulating over an S11 and S21.

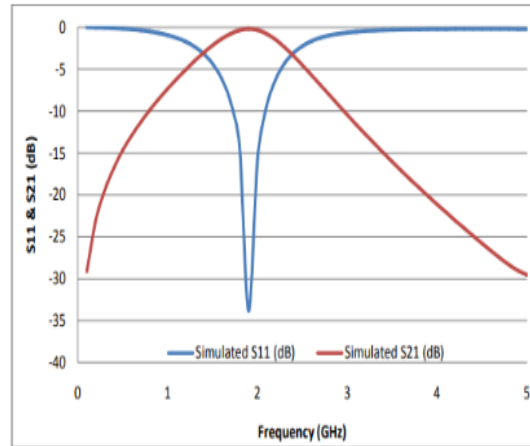


Figure 11: Frequency response in dB

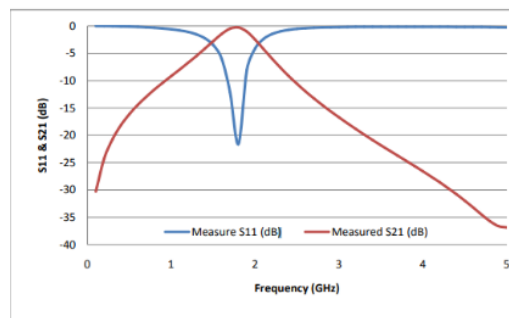


Figure 12: Simulated result of the frequency response in S11 and S21 (dB)

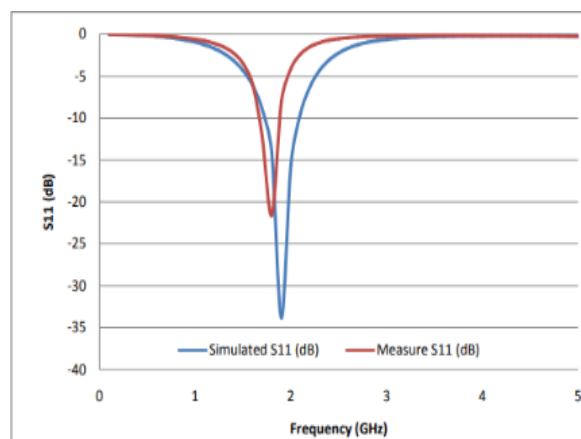


Figure 13: Simulated result of the frequency response in S11 (dB)

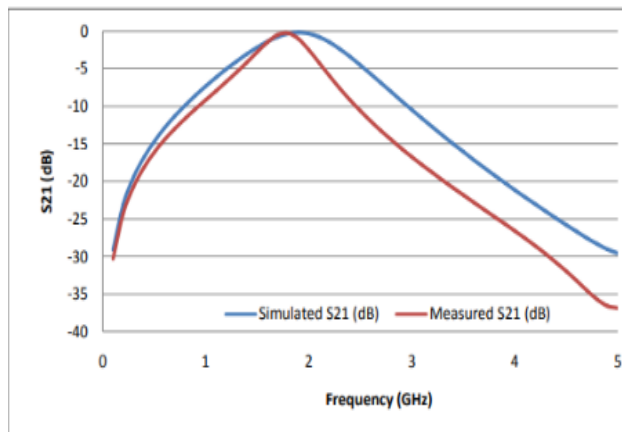


Figure 14: Simulated result of the frequency response in S21 (dB)

Table 1: Analysis between the simulated and measured parameters

| Parameters/Filter | Simulated Result | Measured |
|--------------------------------------|------------------|----------------|
| Lower Cut-off Frequency(-3dB) | 1.03GHz | 1.50GHz |
| Uppercut-off Frequency(-3dB) | 2.020GHz | 2.05GHz |
| Resonant Frequency(fo) | 1.880GHz | 1.70GHz |
| Bandwidth(-3dB) | 946GHz | 510MHz |
| Fractional Bandwidth | 52.98% | 31.23% |

Thus, the modified design of dielectric line completed DGS has been modeled using HFSS. The simulator and VNA measure the simulated result and the measured Frequency response curve (Insertion loss and return loss). Simulation and measurement results are compared and there is little difference between measured and simulated outcomes. This may be because the FR4 epoxy substrate provided as the dielectric of the microstrip line and the damage in FR4 Epoxy Resin is greater than that of the RT Dioroid. A comparison of the loss of return and the loss of the inclusion of simulated and measured effects gives the value of various parameters simulated and measured. The simulated result is approximately based around 1.880 GHz, while the measured result resonant frequency of 1.70 GHz. The calculated results and simulated results are at the bandwidths of both 946 MHz and 510 MHz respectively.

5 Conclusion

In the microwave circuit, the filter plays a large and primary part in this communication system. In our paper, a dielectric coupled line resonator DGS is based on frequency response, it gives a simulated result under a 1.880GHz, and measured results are 1.76 GHz that improves a current dispersion. The Resonant

Frequency, which gives under a value of 946MHz and 510 MHz, which protects a signal received over the desired band. The frequency response is usually for the design of microstrip components and circuits properly configured by choosing the form and height of the conductor lines. Defective Ground Structure (DGS) provides an alternative way to improve a sequence success.

References

- [1] Archana R. Tiwari and Snehal V. Laddha, "Rectangular Microstrip Patch Antenna for WLAN application International Journal of Electronics and Computational System", *IJECS ISSN 2348117X*, vol. 6, no. 8, August 2017
- [2] C-W., Tang, "Design of a microstrip filter using multiple capacitive-loaded coupled lines." no. 3 (2007), *IET Micro., Ant. & Prop.* 1651-656.
- [3] Naheed Anjum Khan and Bharati A. Singh, "Microstrip Antenna Design with Defected Ground Structure", *IOSR Journal of Electronics and Communication Engineering (IOSR-JECE)*, vol. 9, no. 2, pp. 4650, Mar-Apr. 014, ISSN 2278-2834.
- [4] Preach Patil ,Shweta Goilkar, Lokmanya "MICROSTRIP ANTENNA USING THE DEFECTED GROUND STRUCTURE FOR BANDWIDTH ENHANCEMENT" 4th International Conference on Recent Trends on Electronics, Information, Communication & Technology (RTEICT-2019), MAY 17th & 18th 2019 978-1-7281-0630-4/19/\$31.00 ©2019 IEEE 1384 .
- [5] Kai Chang, Chan Ho, Kim, "Ring resonator bandpass filter with switchable bandwidth using stepped-impedance stubs." *IEEE Trans. -58, Micr. Theory and Techn.*, no. 12 (2010): 3936- 3944.
- [6] Archana R. Tiwari and Snehal V. Laddha, Rectangular Microstrip Patch Antenna for WLAN application International Journal of Electronics and Computational System, *IJECS*, ISSN 2348117X, Volume 6, Issue 8, August 2017.
- [7] Konkyana, F. A. L. B., & Sudhakar, B. A. A Review on Microstrip Antennas with Defected Ground Structure Techniques for Ultra-Wideband Applications. 2019 International Conference on Communication and Signal Processing (ICCSP). doi:10.1109/iccsp.2019.8697941
- [8] Abdul Fatah Awang Mat, Ambak, Zulkifli, Muhammad RedzuanSaad, Rosidah Alias, Sabrina MohdShapee, Azmi Ibrahim, MohdZulfadli, Mohammed Yusoff, Mohamed RazmanYahya, "The microstrip coupled line Bandpass filter using LTCC technology for 5GHz wireless LAN application." *IEEE International*, 2008, pp. 496-499. In *RF and Micr. Con., RFM*.
- [9] Abdurrahim Toktas, Mehmet Yerlikaya, Enes Yigit," Microstrip-fed Triangular UWB Microstrip Antenna Based on DGS" *International Journal of Applied Mathematics, Electronics and Computers*, vol 4 pp 43-47, 2016.
- [10] N. Benabdallah, Seghier, F. T. Bendimerad, Nasreddine Benahmed, Salima, "Design of parallel-coupled microstrip bandpass filter for FM Wireless applications." *IEEE*, 2012. pp. 207-211, 6th International Conference, In *Sci. of Electro., Technologies of Information and Telecommunications (SETIT)*.
- [11] Hussein Nasser, Shaman. "New S-band bandpass filter (BPF) with wideband passband for wireless communication systems." *IEEE* 22,2012. no. 5: 242-244, *Microw. and Wireless Components Lett.*
- [12] Stosic, A. S. Atanaskovic., B. P., N. S. Doncov, "Response calculation of parallel-coupled resonator filters by use of synthesized wave digital network." *IEEE*, 2013., vol. 1, pp. 253-256, 11th International Con., In *Telecommunication in Modern Satellite, Cable and Broadcasting Services (TELSIKS)*.

Advanced Handwritten Signature Identification System with Use of HU's Moment Invariants

¹ Jayesh Rane

¹Assistant Professor, Pillai HOC College of Engineering and Technology, Rasayani, Maharashtra

Abstract

This paper introduces a system of Fuzzy Min-Max Neural Networks signature recognition and evaluate the impact of moment invariants on the identification of signatures by analysing the precision of the identification. In addition, the database is also being evaluated for signature recognition by fuzzy min-max neural networks, resulting in more accurate measurements. In the person recognition method developed through MATLAB, image processing and fuzzy neural network toolboxes have been used. For the recognition of signatures, the database is generated with thirty iterations for five individuals. By scanning the photographs and then transforming them to regular binary images, these signatures are pre-processed. The characteristics are picked and collected, presenting details about the signature structure. The efficiency of the model by implementation of fuzzy min max neural networks classifier is also investigated in this paper.

Keywords: CNN, Fuzzy min max neural networks, handwriting signatures, artificial neural network, HU's seven moment invariants.

1 Introduction

In the field of handwritten signature identification, the recognition of signatures is a significant research area. In terms of enhancing the interaction between human beings and machines, understanding of human handwriting is important. It would have a more appealing and economical human-machine interface if the computer device is wise enough to comprehend person handwriting. Signature is a special case in this sector that offers safe means of authentication, permission of attestation in many high security environments.[1] The purpose of the method of acknowledgement of signatures is to distinguish between two categories: the initial and the forgery, which are connected to intra- and interpersonal heterogeneity. Intra Personal Variation is called the variance between the signatures of the same individual. Inter Personal Varia is considered the variation between originals and the morphed or forgeries.

For the identification of characters, signature authentication is so different, since signature is always unreadable, because it seems like it is only a picture of certain unique curves that reflect the individual's writing style. The person signature is only a specific handwriting event which is mostly just a mark. It is also wisdom and it is only important to deal with a signature as a full picture with a special pixel distribution and reflecting a certain type of writing and not as a set of letters and terms. Two groups may be separated into a signature authentication scheme and the methods used to address this problem: online and off-line.[2] Signature details may be accessed from an electronic tablet through an online environment and, in this situation, dynamic knowledge regarding writing operation is available, such as writing speed, pressure applied and number of strokes.

This paper deals with offline signature authentication in this paper, which is based on the geometric core and helps to distinguish qualified forgeries from the originals. Compared to the earlier algorithms based on the geometric centre, the algorithms used have provided better performance.

1.1 Types of Forgeries

The difference between the identification of a signature and the authentication of a signature is that verification determines if an assertion that a certain signature belongs to a certain class (writer) is valid or false, while recognition determines which of that all number of objects (writers) belongs to a specific signature.[3] Two groups are categorized into automated handwritten signature recognition systems: Signature recognition in online mode and on offline mode. A specific pen, called a stylus and digitizing device, is recorded in the online machine signature and interpretation is focused on complex characteristics such as friction, velocity, acceleration and capture period at each stage on the course of the signature.

1.1.1 Random or simple forgeries

The forger may not have the form of the person's signature, but ends up with a lettering of his own. He may originate this from the name of the writer. This forgery accounts for most instances of forgery, while naked eyes are simple to identify. This type of forgery shown in figure 1.(b)

1.1.2 Unskilled /casual forgeries

The falsifier acknowledges the signature style of the authors and attempts without any experience to mimic it. This type of forgery shown in figure 1. (a) and (c)

1.1.3 Skilled forgeries

This is when the forger has free access to and ends up with a forged example of the actual signature form. This type of forgery shown in figure 1.(d)

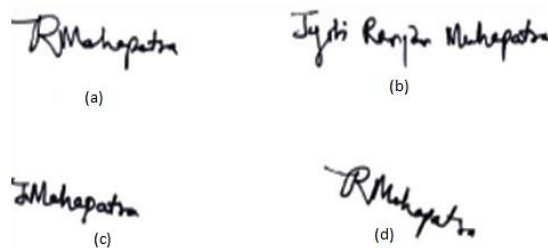


Figure 1:(a) Original Signature (b) Random Forgery(c) Simple Forgery (d) Skilled Forgery

2 Preprocessing of Signatures

2.1 Database Formation

To develop an automated individual recognition system centered on handwritten signatures, a handwritten signature database is needed. An in-house handwritten archive of signatures, including photographs of 5 individuals, is collected. IDs 001 through 005 identify the entities in this handwritten signature recognition index. Each person was required to sign 30 times on a white sheet comprising a table of 20 cells. It is necessary to highlight that a black coloured pen was used by all participants to sign on the white board. The cumulative number of handwritten signature photos is then calculated as follows in this handwritten signature database:

$$\begin{aligned} \text{Total Signature Images} &= 30 \text{ Signatures images} * 5 \text{ Persons} \\ &= 150 \text{ Signatures images} \end{aligned}$$

These 150 signatures span the training and research data sets, so 20 replications per person are used in the training data set. Different pre-processing measures should be considered, such as generating a digital copy of the signature form by hand, cropping the signature image by hand, and converting the input image to create a ready-to-use handwritten signature image database. Write a normal binary image and the image scale will be standardized and changed.

The signatures are screened using the printer after both people have completed signing on the white paper in order to create a digitized representation of the hand signatures. In order to crop and cell and save it into a separate (.png) format, the Microsoft paint method is then used. For one of the individuals, the following figure demonstrates an illustration of a cropped handwritten signature images.



Figure 2: The Cropped Handwritten Signature Picture Illustration

The pre-processing steps are performed individually on any cropped database picture using MATLAB commands. The pre-processing phase provides the picture to derive its characteristics from it in the state.

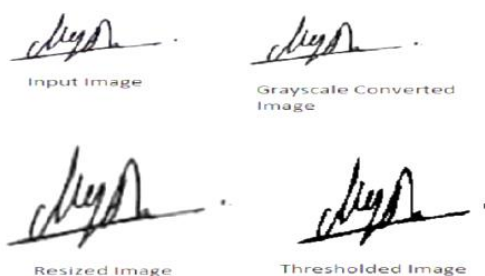


Figure 3:Pre-processing Steps performed on input signature Image

2.2 Feature Extraction

This section explains the range of prevailing features that are used for the identification of signatures. For the automated individual recognition system based on handwritten signatures, the feature extraction process is important since it is essential to find an efficient range of features in order to create high-performance systems. It is chosen and extracted to be capable of representing knowledge about the configuration of the hand signature picture features to be used in training and evaluating the established method. The chosen characteristics include the density and angle of energy that are explained below:

2.2.1 Energy Density

Energy density of an Image is calculated by segmenting the image into four parts and calculating energy at every section by the formula:

$$\text{Energy} = \sum X(n)^2 \quad (1)$$

The value of $X(n)^2$ may be 0 or 1 therefore will be 0 or 1. Taking the mean of all the values in the matrix, the energy of the cropped image is calculated.

2.2.2 Angle

To find the characteristic of the angle, the image is divided into three parts. Each part is divided into sixteen parts. The value of angle is calculated by

$$\text{Value} = \frac{a_{max} - a_{min}}{a_{max} + a_{min}} \quad (2)$$

$$\text{Angle} = \text{atan}(\text{value}) * \frac{180}{\pi} \quad (3)$$

By using these formulas, only one angle can be calculated from each line segment. Take the average of all the angles to get the total rounding angle.

3 Classification of Signatures

The implementation of the fuzzy min-max classifier as a neural classifier. It is possible to automatically control the parallel network, the essence of the classifier and the process for gradual and rapid implementation effectively. [5] The neural network that performs it is seen in the blurry min-max classifier. The topology of this method is neural network is rising to satisfy the requirements of the crisis. Everyone in this three-layer neural network, the FC node is a super neural network. Fuzzy box set where the min-max is the FA to FB link. The FB points and. The hyper box transferring role is Equation-defined membership feature. The points in min are stored in the V matrix, the max points are stored in the V matrix. W matrix. [8] The relation is updated using the learning method. The next segment explains the algorithm. The draws between links Two-fold evaluation and storing of the FB and FC points in the U-matrix.

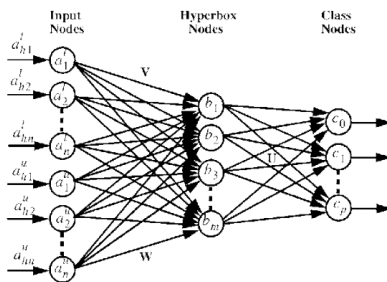


Figure 4:Architecture of fuzzy min-max neural network

4 Results and Discussions

Table 1: Comparison of Performance between Fuzzymin-max Neural networks without and with HU’ssmoments

| Accuracy (%) | Number of Occurrences By FMMN (Without Moment) | Number of Occurrences By FMMN (Using HU Moment) |
|--------------|--|---|
| 0 | 0 | 0 |
| 10 | 0 | 0 |
| 20 | 0 | 0 |
| 30 | 10 | 1 |
| 40 | 15 | 5 |
| 50 | 20 | 5 |
| 60 | 22 | 11 |
| 70 | 20 | 25 |
| 80 | 08 | 29 |
| 90 | 04 | 29 |
| 100 | 01 | 12 |

As can be seen from the table above, the accuracy of using a simple FMMN architecture to recognize handwritten signatures is approximately 60% to 70%, while the number of accurate signatures recognized using FMMN with HUs Moment is included. between 85 and 90%. That is, when we use the blurry maximal minimal neural network it can correctly identify multiple characteristic HU moments. The graphical representation below shows a comparison of there cognition accuracy.

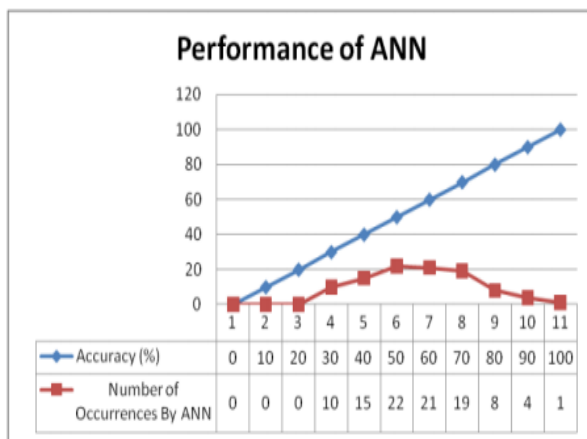


Figure 5:Performance of FMMN without HU’s Moments

As shown in the figure above, signature recognition performance is indicated by a red line. The number of recognized firms is in the range of approximately 60-70%.

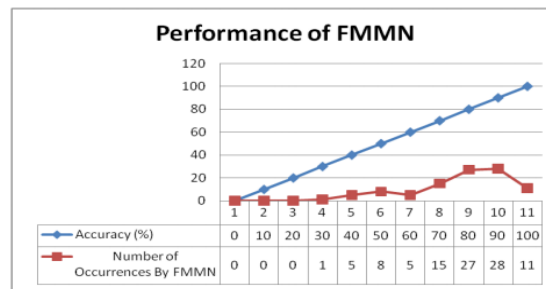


Figure 6: Performance of FMMN with HU's Moments

Figure: 6 shows the performance of using a fuzzy maximum minimum neural network classifier for signature recognition. The red line indicates that the recognition rate is between 85-90%, which is better than the artificial neural network classifier.

5 Conclusions

This paper offers a comparative features of the efficiency of signature recognition using various approaches focused on biometric signature authentication and identification. In this paper, a thorough steps, configuration, and implementation of the automated individual recognition method centered on a handwritten signature is provided. An efficient collection of features is chosen for the accuracy measurement. The presented method is checked with the massive database to get more detailed findings such that the amount of signature repetitions improves. Thus, for broad datasets, this approach should be tested. By using classifier, i.e.fuzzy min max classifier, the contrast indicates the stronger detailed results. The accuracy of the present method can be increased by integrating local features and global features.

References

- [1] Khuat, T.T. and Gabrys, B., Accelerated learning algorithms of general fuzzy min-max neural network using a novel hyperbox selection rule. *Information Sciences*, 547, pp.887-909 January 2021.
- [2] Al Sayaydeh, Osama Nayel, Mohammed Falah Mohammed, and Chee Peng Lim. "Survey of fuzzy min-max neural network for pattern classification variants and applications." *IEEE transactions on fuzzy systems* 27, no. 4 (2018): 635-645.
- [3] Grelewicz P, Khuat TT, Czczot J, Klopot T, Gabrys B. Application of Machine Learning to Performance Assessment for a class of PID-based Control Systems. *arXiv preprint arXiv:2101.02939*. 2021 Jan.
- [4] Hanifa RM, Isa K, Mohamad S. A review on speaker recognition: Technology and challenges. *Computers & Electrical Engineering*. 2021 Mar 1;90:107005
- [5] Ahmed, A.A. and Mohammed, M.F., 2018. SAIRF: A similarity approach for attack intention recognition using fuzzy min-max neural network. *Journal of Computational Science*, 25, pp.467-473.
- [6] Chandrashekhar, A. and Kumar, J.V., 2017. Fuzzy min-max neural network-based intrusion detection system. In *Proceedings of the International Conference on Nano-electronics, Circuits & Communication Systems* (pp. 191-202). Springer, Singapore.
- [7] Xi, X., Tang, M., Miran, S.M. and Luo, Z., 2017. Evaluation of feature extraction and recognition for activity monitoring and fall detection based on wearable sEMG sensors. *Sensors*, 17(6), p.1229.
- [8] Julita, A., Fauziyah, S., Azlina, O., Mardiana, B., Hazura, H. and Zahariah, A.M., 2009, March. Online signature verification system. In *2009 5th International Colloquium on Signal Processing & Its Applications* (pp. 8-12). IEEE.
- [9] Fauziyah, S., Azlina, O., Mardiana, B., Zahariah, A.M. and Haroon, H., 2009, March. Signature verification system using support vector machine. In *2009 6th International Symposium on Mechatronics and its Applications* (pp. 1-4). IEEE.
- [10] Zdobnov, E.M. and Apweiler, R., 2001. InterProScan—an integration platform for the signature-recognition methods in InterPro. *Bioinformatics*, 17(9), pp.847-848.
- [11] Faundez-Zanuy, M., 2005. Signature recognition state-of-the-art. *IEEE aerospace and electronic systems magazine*, 20(7), pp.28-32.

Energy-Efficient Adaptive Encoding for Off-Chip Communication

V.Venkatesan¹, S.DuraiRaj², B.Arunkumar³

^{1,2,3} Assistant Professor, Department of Electronics and Communication Engineering , St. Anne's College of Engineering and Technology, Panruti

Abstract

The data transfer has an increasing effect on the total system energy as technology scales, often overtaking computation energy. To reduce the power of interchip interconnects, an adaptive encoding scheme called adaptive word reordering (AWR) is proposed, which effectively decreases the number of signal transitions, leading to a significant power reduction. A novel circuit is implemented, which exploits the time domain to represent complex bit transition computations as delays and thus, limits the power overhead due to encoding. The effectiveness of AWR is validated in terms of decrease in both bit transitions and power consumption. AWR is shown to yield higher power savings compared with three state-of-the-art techniques reaching 25% and 65% during the transfer of multiplexed address-data and image files, respectively, at just 1-mm wire length.

Keywords: *Encoding scheme, Energy efficiency, Interconnects, Low power, Off-chip communication, Switching activity.*

1 Introduction

An effective solution to decrease the dynamic power consumption is to reduce signal transitions through data coding. The benefits of using an encoding scheme are investigated in [6]. When BI is applied to double-data-rate fourth-generation (DDR4) memory, the I/O power as well as the power-supply noise are decreased. The energy cost of transferring data across the memory hierarchy is estimated between 18% and 40% of the total system energy for scientific applications and is expected to further increase in upcoming systems. In addition, the energy of transferring data does not scale as fast as the energy for computation. For instance, the energy consumed for off-chip communication is estimated 115 higher than that of an ADD operation in smart phone devices [4]. Thus, the power reduction of interchip communication is a key challenge for modern integrated systems. Encoding schemes can achieve significant energy savings, particularly when the switching behavior of the data stream is known in advance. However, this may not be feasible or the characteristics of the data stream may vary over time. Therefore, this work extends our recent work, where an adaptive encoding scheme, namely adaptive word reordering (AWR), is proposed for wide off-chip buses. AWR decreases the switching activity without affecting the communication bandwidth where the statistics of the data stream are not known a priori. The core idea of this technique is the reordering of the words of the data stream such that signal transitions are minimum. Optimal reordering requires a formidable amount of computations; therefore, a heuristic algorithm, namely nearest neighbor (NN), is preferred. The proposed scheme is envisioned for block data transfers, such as direct memory access (DMA) where the data are transmitted only after a block is fully available and thus, the latency introduced by encoding does not affect the performance of the communication. In this work, AWR is compared with state-of-the-art techniques in terms of total power savings, including the power overhead of the encoder and decoder logic.

Although reordering data have been attempted in, the related algorithm does not fully exploit the potential of this approach in reducing switching activity as only the two most recent words are considered in the reordering operation. Consequently, the provided reduction in switching activity is comparable to BI, which is shown to typically be inferior to AWR. Furthermore, However, as shown in [9], the effectiveness of encoding in reducing power consumption is often restricted by the high implementation overhead, thereby diminishing and often eliminating the benefits offered theoretically by data encoding techniques. Hence, the efficiency of the encoding technique cannot be evaluated properly. In addition, a novel circuit that implements NN is proposed, which exploits the time domain for complex computations of Hamming distances, to decrease the power overhead of encoding. Encoding schemes for interconnect buses have been proposed aiming either latency [10] or power, where the majority of these methods target primarily to decrease power. Encoding schemes can be classified as either static or adaptive. Static schemes exploit the statistical properties of data streams, considered known at design time, and are discussed.

1.1 Static Schemes

Signals in address buses belong to the static category. Gray code, for example, ensures a single-bit transition when the data words are consecutive. T0 code prevents transitions in case of sequential addresses using one extra bit line. Modified versions of this technique, T0-BI, Dual-T0, and Dual-T0-BI, are proposed to further reduce the switching activity of address buses. In the case of data buses, the data words are not sequential, and therefore, the previous techniques are rather most effective. The words with high probability of occurrence are

mapped to codewords with lower Hamming weight to decrease the overall transitions. This idea is implemented using reversible circuits where only part of the statistics is given. Algorithms that automatically generate low activity codes based on statistical information are presented in [17]. In the partial bus invert (PBI) method is proposed, where a sub group of bus lines is composed according to the transition probabilities and the transition correlations among the bus lines. These lines are inverted to reduce transitions.

1.2 Adaptive Schemes

The efficiency of static techniques depends strongly on the behavior of the application. Therefore, the benefits of static schemes diminish if the statistical properties of data vary temporally. To cope with this situation, several encoding techniques do not rely on a priori information of data statistics. BI is one of the early encoding schemes for decreasing transitions. The data word is inverted if more than half of the bits switch. One extra bus line is used to inform the receiver whether the data word is inverted or not. This technique remains popular because of its effectiveness and simple circuit implementation. However, BI provides limited savings in switching activity compared to more elaborate techniques, especially in cases where the data are highly correlated.

The adaptive partial bus invert (APBI) is an extension of PBI, according to which the data stream is observed over time and the subgroup of encoded lines is changed periodically. The effectiveness of this technique is restricted to highly correlated data streams, such as image files. Bus shifting (BS) rotates the word to be transmitted by a number of bits to minimize transitions and uses spatial redundancy to send this number to the decoder. However, the calculation of Hamming distance for all possible rotations of each data word increases significantly the hardware complexity. The working zone encoding is well-suited to address buses and assumes that applications use specific subgroups of the address space. Frequent value is an adaptive technique that encodes the frequently transmitted words and leaves the rest of the words un encoded. Adaptive dictionary encoding uses a dictionary to store recurring patterns to reduce the number of bits required to represent large patterns. The effectiveness of this technique is restricted to data with high correlation of adjacent bits. Sequence-switch coding is based on the reordering of words to reduce transition activity. The heuristic proposed in considers only the two most recent words in the reordering operation and therefore, the resulting decrease in switching is comparable to BI. This scheme, however, requires a more complex implementation than BI. Consequently, the overall performance of this technique is inferior to BI. Data exchange using synchronized counters (DESC) is a time-based technique where the data values are represented by delays between the consecutive clock pulses. The limitation of this scheme is that the bandwidth is decreased by 3.15 on average. Adaptive time-based encoding (ATE)

Several encoding techniques focus only on the decrease in relative switching between adjacent bus lines, whereas the self-transitions of individual lines are not considered. Therefore, the applicability of these methods is restricted to those interconnects, where the coupling capacitance

1.3 Adaptive Word Reordering

The proposed encoding scheme (AWR) is based on the observation of the data stream over a fixed window of N words and the dynamic reordering of these words in order to decrease the total number of transitions on the encoded bus. The proposed scheme can be applied to memory interfaces that do not use asymmetric termination such as LPDDR3 where power can be saved by reducing the number of bit transitions. Furthermore, access to LPDDR3 is burst oriented. Therefore, a block of read or write data is fully available at the beginning of the transmission, which is required by the encoder of AWR in order to not introduce additional latency. The process of identifying the order of the words that yields the minimum switching activity, as well as the NN algorithm on which the proposed approach is based, is discussed in Section III-A. In Section III-B, an evaluation of the proposed technique is provided, where AWR is compared with state-of-the-art encoding schemes in terms of decrease in switching activity. The problem of the optimal word reordering can be described by considering each word as a vertex of a complete, undirected, weighted graph $G(V, E)$. The weight of each

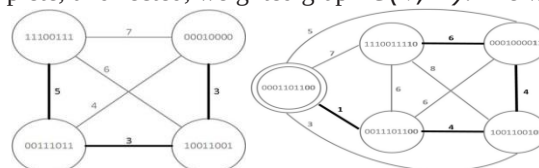


Figure 1: Examples of routes that reduce bit transitions. (a) Minimum weight route that visits all vertices exactly once. (b) Route followed by the NN algorithm. The search is assumed to start at the vertex 00011011.

edge w is the Hamming distance of each pair of words. The problem can be reformulated as the identification of the minimum weight route that visits all the vertices of the graph exactly once. This is very similar to the traveling salesman problem (TSP) classified as NP-hard. The difference between the two problems is that the route in TSP is cyclic and has to end to the starting vertex. The most straightforward solution to the TSP is an exhaustive search, for which the calculation of the cost of all possible rearrangements (N) is required. However, the computational cost remains high and the hardware complexity of these algorithms is prohibitive if any savings in power are to be harvested. There is a plethora of heuristic algorithms that determine near-optimal solutions to the TSP problem. In this work, the NN search is implemented as a less complex approach. The NN algorithm is properly adapted for the specific problem. In each clock cycle, the search starts with the previously transmitted word and the weights with all the unvisited vertices are calculated.

```

while Queue with words not empty do
  Update the  $N$  words to be reordered
  Assign a unique code of  $K$  bits to all  $N$  words
  for  $i \leftarrow 0$  to  $N - 1$  do
    for  $j \leftarrow 0$  to  $N - 1$  do
      if word[ $j$ ] not transmitted then
        Calculate the Hamming distance between
        word[ $j$ ] and previously transmitted word
        including the unique code of  $K$  bits
      end if
    end for
  end for

```

Figure 2: Pseudo code of the NN algorithm amended to the requirements of AWR.

These K bits are included in the calculation of the Hamming distance to ensure that these bits do not notably increase the switching activity. In the example of Fig. 1(b), the previous word is assumed to be 00011011, and thus, the search starts from this vertex. The last two bits of each word are the order bits. The route followed by the NN algorithm to reduce transitions is highlighted. The pseudo code of the algorithm is shown in Fig. 2. N transmissions are required to transfer the N words over the interconnect. Therefore, index i is used to count the transmissions, whereas index j is used to iterate between all the words to find the one with the minimum Hamming distance for each transmission. If a word has been transmitted, then the Hamming distance is not calculated and the word is not considered for retransmission.

1.3.1 Performance Evaluation

The theoretical performance of the proposed reordering technique is determined by the switching activity, which is compared with three other encoding schemes. *Compared Techniques*: Three state-of-the-art encoding techniques are selected that do not require *a priori* knowledge of data statistics and a circuit implementation is provided. BI is a low-power adaptive scheme that calculates the Hamming distance of consecutive data words and inverts the transmitted data word if the Hamming distance is higher than half of the word length. To indicate whether a word is inverted or not, one extra bus line is used. APBI observes the data stream for a window of a fixed number of N word and forms a mask with the bus lines with a higher probability of switching. BI is then applied to these bus lines and one extra bit is used to inform the decoder about inversion. ABE selectively encodes a cluster of highly correlated bus lines. First, observe the data characteristics over a window of N words. Based on these characteristics, a cluster is formed and the line with the maximum correlated transitions with the lines of the cluster is selected as the basis line. The lines in the cluster are finally XORed with the basis. The parameters of the compared techniques APBI and ABE are specifically selected such that the techniques yield the highest reduction in switching activity according. In this way, a fair comparison is conducted that provides the highest savings for each technique. For all of the simulations, the bus width is considered to be M 64 bits, whereas the observation window is N 32 words or APBI and N 16 words for ABE. The mask computation of the APBI technique can be executed in each window of N words (APBI₁), but intervals of 16 windows (APBI₁₆) are also explored to further reduce the power consumption of encoding and decoding and provide a fairer comparison. Therefore, both of these scenarios are included. Furthermore, two cases for ABE are considered. In the first case, ABE is applied to the entire bus (ABE₁), whereas in the second case, the bus is split into four groups of $M/4$ bits and ABE is applied individually to each group (ABE₄) to best exploit this technique. The decrease in switching activity of AWR is reported using both N 32 (AWR₃₂) and N 64 (AWR₆₄) re ordered words. Therefore, 32 and 64 reordered words are selected as high savings in switching activity are provided, while the power overhead is restrained.

2 Proposed Circuit Architecture

2.1 Encoder

The encoding of data is implemented as follows. In each clock cycle, the Hamming distances between the previous word and the words that have not yet been transmitted are evaluated. The word with the lowest Hamming distance is then transmitted through the bus. This method requires N register at the transmitter and the receiver to store the reordered words. Conventionally, the computation of the Hamming distance is implemented using adder trees. This approach is highly inefficient in terms of power, especially for wide buses, counteracting any energy savings produced from encoding. Therefore, a different approach is followed, where the Hamming distance is determined as a delay in the time domain, drastically reducing the overhead in power due to encoding.

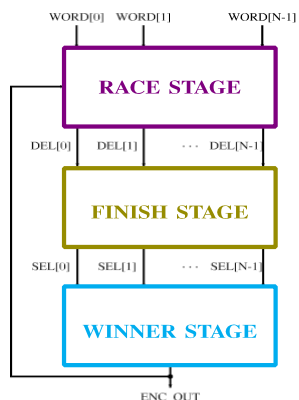


Figure 3: Encoder circuit

The proposed encoder circuit comprises three stages, as shown in Fig. 3. The first stage is the race stage, where a variable delay line is assigned to each word. In each delay line, a clock pulse is propagated and delayed according to the number of bits that switch. The delay is shorter for a lower number of transitions and, thus, the fastest signal

The DEL signal that arrives first at the finish line of the race stage prevents the others from propagating. This condition is implemented in the finish stage. Before any signal arrives, a “0” is stored in all of the latches (LA) and the PER signal is set to 1 using a weak pull-up resistor. The signal that arrives first sets the respective latch and resets PER. After all the DEL signals are reset, PER switches slowly back to 1 due to the weak pull-up resistor. The winner stage is composed of the selection block and two registers. The selection block is a digital circuit that decides which word wins the race according to the received SEL [0..N] signals. In case two or more signals arrive at the same time (i.e., these words yield the same number of switching bits), such that more than one of the SEL signals is equal to 1, the word with the lowest index is chosen.

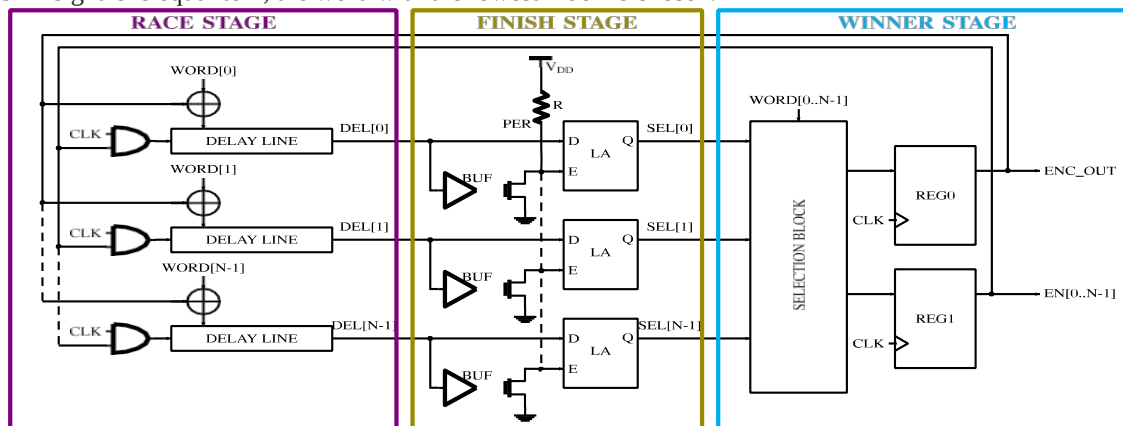


Figure 4: Encoder circuit

Transmitting the word with the lowest index can potentially decrease the delay of decoding. For example, if WORD [0] and WORD [7] arrive at the same time, there is no benefit in transmitting WORD [7] since the receiver cannot utilize WORD [7] if all the previous words have not been read. The winning word is stored in

the register REG0. To keep track of the transmitted words, a second register (REG1) is used, where the enable signals $EN [0 \dots N - 1]$ are stored. Once the word to be transmitted is selected, the respective EN signal is switched to 0 and remains low until all N words are transmitted. All EN signals switch to high whenever a new block of N words is to be transmitted. EN signals enable or disable the respective delay lines allowing the propagation of the clock only for the words that have not been transmitted.

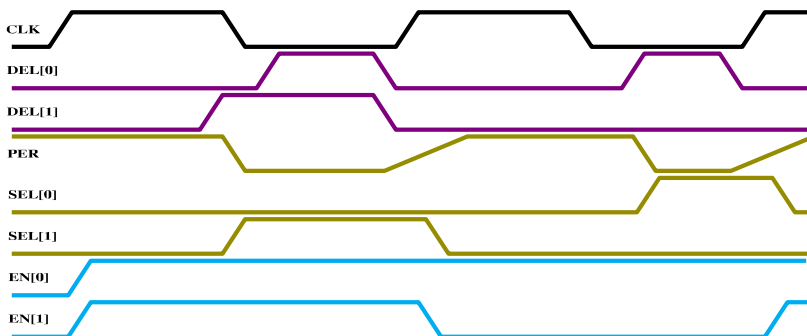


Figure 5: Signal propagation of the encoder circuit

An example of signal propagation with $N=2$ is shown in Fig. 4. It is assumed that in the first clock cycle, the Hamming distance of Word [1] is the lowest; therefore, DEL [1] is set to 1 faster than DEL [0]. DEL [1] causes both SEL [1] and PER signals to transition. Thus, SEL [1] is set to 1 and the latches are disabled before DEL [0] transitions to 1. PER switches slowly back to 1 after both DEL [1] and DEL [0] are reset. In the second clock cycle, the state of EN [1] changes to 0 as Word [1] was selected, whereas the clock pulse does not propagate through the delay line of Word [1]; therefore, DEL [1] remains 0. Word [0] is selected in this cycle since DEL [0] is the only signal that transitions to 1, causing SEL [0] and PER to flip. In the third clock cycle, both EN [0] and EN [1] are equal to 1 in order to enable the reordering of the next two words.

The delay line consists of a modified inverter chain as shown in Fig. 5, where W is the minimum width and the length is the minimum for all devices as determined by the utilized technology library. Each inverter is connected either to the ground or the supply voltage through a pair of devices. A detailed description of this delay line can be found in [45]. Briefly, when the i th bit switches, $T(i)$ switches to 1 and the i th inverter is connected to ground (i is odd) or V_{DD} (i is even) through only one device. In case no transition takes place, the inverter is connected to either V_{DD} or ground through two devices connected in parallel. Hence, in the former case, the delay is larger than in the latter case. The delay of only the first edge of each inverter (falling for even and rising for odd) is affected by the Hamming distance since the pair of devices is only added to either the pull-down (even inverters) or pull-up (odd inverters). The delay of the second edge of each inverter is constant. This implementation ensures that the delay of the falling edges of the DEL signals is constant. Therefore, the PER signal switches to 1 at a specific time in every clock cycle as this happens exactly when DEL signals switch to 0. Hence, the risk of a DEL signal switching to 1 while PER is still low is eliminated.

2.2 Decoder

The role of the decoder at the receiver side is to place the words back in the initial order. To achieve that, the decoder

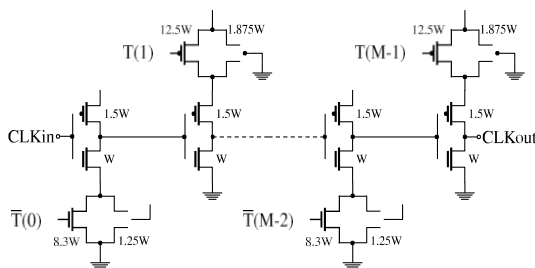


Figure 6: Delay line circuit

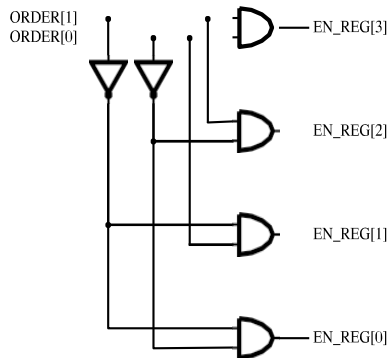


Figure 7: Decoder circuit.

uses N registers to store the words in the right order as they arrive. The order of each word is transmitted by using low spatial redundancy. K more bits are added to each word that indicates the order. Thus, for N words, $K \log_2 N$ additional bus lines are required. The decoder reads the K bits and enables the corresponding register to store the word, whereas the rest of the registers remain disabled. The circuit that implements this function is a basic K -to- N decoder with each output connected to the enable input of the appropriate register. A two-to-four decoder circuit is shown in Fig. 6. The K bits are also considered in the encoding process, and thus, they are included in the calculation of the Hamming distance. Consequently, it is ensured that they do not considerably increase the power overhead.

3 Simulation results

The power efficiency of the proposed AWR scheme is evaluated in this section. The simulation setup is described. The overheads of AWR and the state-of-the-art encoding techniques are discussed. Furthermore, the reduction in power of AWR is quantified in Section V-C and is compared with the state-of-the-art techniques in Section V-D. Finally, the robustness of AWR under process variations is investigated in Section V-E.

3.1 Adaptive word reordering method

The effectiveness of the proposed AWR method is explored for an interchip link for 2.5-D integration as interposers support a high wire density. However, note that the method is equally applicable to other state-of-the-art or emerging packaging approaches, such as embedded multi die interconnect bridge (EMIB) and more broadly to applications that require wide and slow links. The link is assumed to connect two dies that are bump bonded on top of a silicon-based.

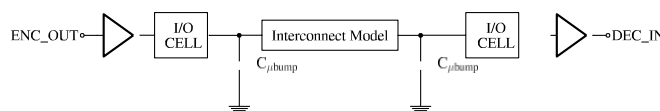


Figure 8: Electrical model for an interposer-based interconnect

Table 1:

Electrical Characteristics Of Wires

| $R(\Omega/mm)$ | $L(nH/mm)$ | $C_{GND}(fF/mm)$ | $C_c(fF/mm)$ |
|----------------|------------|------------------|--------------|
| 40.74 | 1.52 | 222.55 | 52.45 |

Interposer. The circuit of the interconnect is shown in Fig. 7 and consists of the distributed wire model, I/O cells, and the parasitic capacitance of μ bumps, $C_{\mu bump}$ 30 fF [47]. For the sake of simplicity, the mutual inductances are not considered. The global wire dimensions for a 65-nm technology. The electrical characteristics of the wires for minimum pitch are listed in Table I.

3.2 Circuit Implementation and Overheads

The encoder and decoder circuits of AWR as well as the other three techniques are implemented with a 65-nm technology. The overheads in power and delay are measured using Spectre, Cadence at nominal conditions (typical device corners, 27°C), and Design Compiler, Synopsys where the bus is assumed to be 64 bits wide and the operating frequency is 400 MHz. A high overhead in power can diminish the efficiency of encoding and even increase power consumption. BI exhibits the lowest overhead in power since the least amount of computations is required with this technique.

4 Conclusion

In this work, an adaptive encoding scheme (AWR) was proposed for parallel off-chip interconnects. AWR decreased the interconnect power by changing the order of the transmitted words to effectively reduce switching activity. AWR outperformed state-of-the-art techniques in terms of both decrease in switching activity and overall power savings for real data streams for several applications relating to high-performance computing where energy reduction is a primary objective. AWR yielded up to 25% and 70% savings in power for multiplexed address-data and image benchmarks, respectively, at just 1-mm interconnect length. Finally, the robustness of AWR investigated under process variations.

References

- [1] S. Borkar, "Role of interconnects in the future of computing," *J. Lightw. Technol.*, vol. 31, no. 24, pp. 3927–3933, Dec. 15, 2013.
- [2] G. Kestor, R. Gioiosa, D. J. Kerbyson, and A. Hoisie, "Quantifying the energy cost of data movement in scientific applications," in *Proc. IEEE Int. Symp. Workload Characterization (IISWC)*, Sep. 2013, pp. 56–65.
- [3] P. Kogge and J. Shalf, "Exascale computing trends: Adjusting to the 'new normal' for computer architecture," *Comput. Sci. Eng.*, vol. 15, no. 6, pp. 16–26, Nov. 2013.
- [4] D. Pandiyan and C.-J. Wu, "Quantifying the energy cost of data movement for merging smart phone workload on mobile platforms," in *Proc. IEEE Int. Symp. Workload Characterization (IISWC)*, Oct. 2014, pp. 171–180.
- [5] M. R. Stan and W.P. Burlison, "Bus-invert coding for low-power I/O," *IEEE Trans. Very Large Scale Integr. (VLSI) Syst.*, vol. 3, no. 1, pp. 49–58, Mar. 1995.
- [6] H. Y. To, "An analysis of data bus inversion: Examining its impact on supply voltage and single-ended signals," *IEEE Solid State Circuits Mag.*, vol. 11, no. 2, pp. 31–41, Jun. 2019.
- [7] E. Maragkoudaki, P. Mroszczyk, and V. F. Pavlidis, "Adaptive word reordering for low-power inter-chip communication," in *Proc. Design, Automat. Test Eur. Conf. Exhib. (DATE)*, Mar. 2019, pp. 980–983.
- [8] M. Yoon, "Sequence-switch coding for low-power data transmission," *IEEE Trans. Very Large Scale Integr. (VLSI) Syst.*, vol. 12, no. 12, pp. 1381–1385, Dec. 2004.
- [9] C. Kretzschmar, A. K. Nieuwland, and D. Müller, "Why transition coding for power minimization of on-chip buses does not work," in *Proc. Design, Automat. Test Eur. Conf. Exhib.*, 2004, pp. 512–517.
- [10] P. P. Sotiriadis and A. Chandrakasan, "Reducing bus delay in submicron technology using coding," in *Proc. Conf. Asia South Pacific Design Automat. (ASP-DAC)*, 2001, pp. 109–114.
- [11] C.-L. Su, C.-Y. Tsui, and A. M. Despain, "Saving power in the control path of embedded processors," *IEEE Des. Test. Comput.*, vol. 11, no. 4, pp. 24–30, Oct. 1994.
- [12] L. Benini, G. De Micheli, E. Macii, D. Sciuto, and C. Silvano, "Asymptotic zero-transition activity encoding for address buses in low-power microprocessor-based systems," in *Proc. Great Lakes Symp. VLSI*, Mar. 1997, pp. 77–82.
- [13] L. Benini, G. De Micheli, E. Macii, D. Sciuto, and C. Silvano, "Address bus encoding techniques for system-level power optimization," in *Proc. Conf. Design, Automat. Test Eur.*, 1998, pp. 861–866.

Optimization and Simulation of Capacitive Pressure Sensor with Improved Parameters

G.Mohammed Althaf¹, Kaustubh Kumar Shukla²

¹Assistant Professor, Department of Electronics and Communication Engineering, Sree Vidyanikethan Engineering College, Tirupati.

²M Tech Scholar, Department of Electronics and Communication Engineering, Sree Vidyanikethan Engineering College, Tirupati.

Abstract

Asset of this paper is to style and simulate the pressure sensing element victimisation using COMSOL Multi physics and analyse the performance of the pressure sensing element. There are different kinds of pressure sensors like piezo resistive and capacitive pressure sensors; this paper is targeted on the capacitive pressure sensor. Generally, the MEMS capacitive pressure sensor sensing elements have gained benefits over the piezo resistive pressure sensor because of high sensitivity, low power consumption and un changing of temperature. MEMS sensors have the advantage of terribly tiny size, this implies they answer tiny changes in pressure. This paper shows the characteristics of the capacitive pressure sensor sensing element. the current work demonstrates the planning of MEMS primarily based capacitive pressure Sensor victimisation Multi physics. It permits elaborate image of varied structures and indicates the distribution of stress and displacements and provides big selection of simulation choices. In this work strain of the capacitive pressure Sensor is also computed. The capacitance measuring value has been computed through simulation for a capacitive pressure sensor. The new capacitance value is $1.88659e-13F$. This increased capacitance provides more sensitivity which may use in medical applications.

Keywords: *Capacitance, COMSOL, Pressure Sensor, Displacement, Poisson's Ratio, Young's Modulus*

1 Introduction

A Sensor is a device which measures the physical quantity and translate it to a signal. The quantities are usually Pressure, Temperature, Flow level, displacement etc. Pressure sensor is an instrument consisting of pressure sensitive elements to determine the actual pressure sensor applied to the sensor and convert into the output signal. Pressure is also known as forces per unit area.

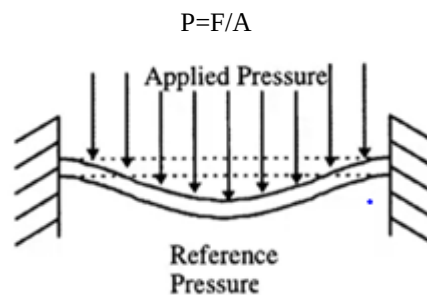


Figure 1: Cross section of a typical pressure sensor diaphragm. Dotted lines represent undeflected diaphragm.

When the pressure is applied on the diaphragm the diaphragm gets a deflection. The measure of the diaphragm is the measure of the pressure. When the pressure is measured with respect to vacuum it is known as the absolute pressure, if the pressure is measured with respect to the atmospheric pressure then it is known as gauge pressure, and if the pressure is measured with respect to the reference pressure then it is known as differential pressure. There are many different types of sensing principles for the pressure sensor they are piezo resistive pressure sensing, capacitive pressure sensing and piezo electric pressure sensing.

In Piezo resistive sensor the Piezo resistors bonded with diaphragm changes their piezo resistance once they are strained by the applied pressure using wheat stone bridge this alteration are often detected successively applied pressure are often found.

The capacitive pressure sensor uses two parallel plates which form a capacitor, the upper plate is act as the movable plate and it is fixed from the all sides, and the bottom plate is grounded. When the pressure is applied to the upper plate it deforms and changes the distance between the two plates of the capacitor, the change in capacitance can be observed to sense the pressure.

MEMS sensor are designed for the perception of external mechanical, thermal, chemical and other influences, but not only for conversion, processing and transmission of electrical signals. Capacitive pressure sensors are getting more popular than the piezo sensor because the capacitive pressure sensors consume less energy, high sensitivity, and invariance of temperature. MEMS sensors have the major advantage of very small size, this means the sensors can easily respond to small changes in the pressure. The capacitive pressure sensors are used to measure the pressure in the human bodies at different places and it can also measure gases or liquids pressures in the jet engines and car tyres and these sensors are used as the tactile sensors in the wearable devices or to measure the pressure applied to the switch's or the keyboards etc. whatever the capacitive pressure sensors are highly intended while compare to other sensing mechanisms because of it have the enhanced sensitivity and stability and repeatable responses of pressure sensing ranging frame low to high reign. A capacitive mechanism is most important mechanism in sensing pressure and strain and it reports to high sensitive, while comparing with other mechanism typically. A dielectric material is placed between the two conductors as a sandwich, when the pressure is applied, the capacitance is increase with respect to the pressure sensitivity of the pressure sensor.

Model geometry is shown in fig 3. Pressure sensor is a part of a silicon crystal that has been fused with a metal plate 70c. since the geometry is symmetric only one quadrant must be included in model, and one can use the symmetry boundary condition

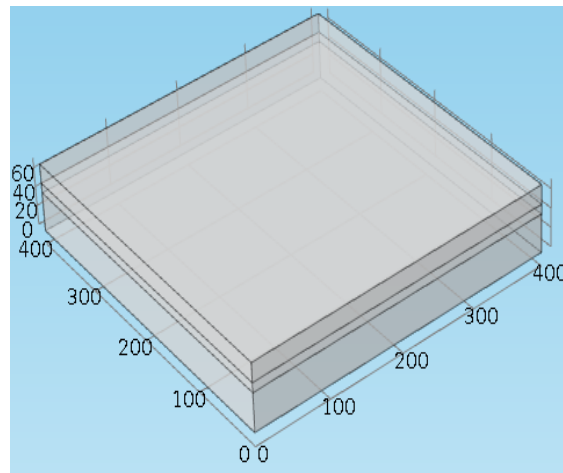


Figure 2 : Model geometry of capacitive pressure sensor Diaphragm

The upper thin membrane plate is kept at a fixed potential of 1v and separated bottom membrane is ground plane in the vacuum as shown in the fig.3.the Chambers sides are insulated to prevent the connection between the membrane and plate grounding. The designs of the MEMS sensor devices are depends upon the multiple parameters like materials, structures and shapes etc. here the substrate is silicon is preferred because it has the high melting point and low thermal expansion coefficient and the les mechanical hysteresis[4] etc. Based on all of these properties the shape of the diaphragm is developed in square shape, here the square shape is chosen because of easy an isotropic etching of silicon in bulk. All these parameters are required for the design of the capacitive pressure sensor are

upgraded with the square shape. The optimized dimensions of the silicon diaphragm is $400\mu\text{m} * 400\mu\text{m} * 60\mu\text{m}$ stress and displacement is improved using these dimensions of the square diaphragm

Table 1: Silicon Material Properties

| Silicon<100>Diaphragm | |
|-------------------------------|--------------------------|
| Young's modulus | 169e9[Pa] |
| Poisson ratio | 0.28 |
| Density | 2329[kg/m ³] |
| Thermal Expansion coefficient | 2.6e.6[K ⁻¹] |
| Thermal Conductivity | 130[W/M*K] |
| Relative permittivity | 11.7 |

1.1 Mathematical Background

The applied pressure is directly proportional to the capacitance between the diaphragms. The capacitive value is calculated using the below equation.

$$C_0 = \frac{\epsilon_0 \epsilon_r A}{d_0}$$

Where,

C_0 =Capacitance value

ϵ_0 = Relative permittivity of free space = $8.854 * (10^{-12})$ F/m,

ϵ_r = Relative permittivity of free dielectric medium, A = effective surface area.

d_0 = separation distance between the membrane.

The theory of the parallel plates and their small deflections are used for the design compensation of the diaphragm, the parallel plates refers the condition of $h_1 \cong \frac{a}{10}$ were the small deflections refers to $W_{\max} \cong \frac{h}{4}$ [6].

The deflection $W(x, y)$ is caused by applying pressure to the parallel plate surface can be settle through the solution of equation.

$$\frac{\partial^4 w(x,y)}{\partial x^4} + 2 \alpha \frac{\partial^4 w(x,y)}{\partial x^2 \partial y^2} + \frac{\partial^4 w(x,y)}{\partial y^4} = \frac{P(x,y)}{Dh^3} \quad (1)$$

Where ,,

$P(x, y)$ is applied pressure

D is flexural rigidity of the plates

h is thickness of diaphragm

W_{\max} is maximum center displacement of the diaphragm

$$W_{\max} = 0.01512(1 - \nu^2) \frac{P_i a^4}{Eh^3} \quad (2)$$

D is flexural rigidity of the plates which is defined as

$$D = \frac{Eh^3}{12(1-\nu^2)} \quad (3)$$

Where E is the young's modulus, h is the thickness of the membrane and ν is poisson's ratio

Capacitance is calculated by using this equation

$$C = \iint \frac{\epsilon dx dy}{d-w(x,y)} \quad (4)$$

Here,

d is the initial gap between the electrodes,

$$C1 = C_0 \left(1 + \frac{12.5Pa^4}{2025dD} \right) \quad (5)$$

Here,

C1- new capacitance, C0-initial capacitance, P-Pressure applied, a-half the length of diaphragm, d-gap between the electrodes, D-flexural density.

Sensitivity: Sensitivity of the diaphragm is defined as the change in the capacitance to the change in the applied pressure. The equation used to find the sensitivity of the designed models is given in equation (6) [8].

$$S = \frac{49\epsilon a^6}{2025d^2D} \quad (6)$$

Where, a=half the length of diaphragm, D= Flexural density, d= gap between the electrodes

1.2 Simulation Setup Of Pressure Sensor

The model of the capacitive pressure sensor is designed and the simulation of the sensor is done through the COMSOL/MULTIPHYSICS. The model design is in square shape with silicon as diaphragm and SiO_2 as a dielectric material. The distance between the two electrodes such that the diaphragm and substrate is $20\mu\text{m}$. the model of the square diaphragm with dimensions of $400\mu\text{m} \times 400\mu\text{m}$ and thickness is $60\mu\text{m}$ the model subject is determine's the electro mechanical analysis with the application of load varying from 1Kpa to 25Kpa

There are some of the parameters which are used for the analysis of the model.

Total Displacement: there will be a deflection of the diaphragm when pressure is applied.

Total Capacitance: when the pressure is applied capacitance will be in contact with the designed model.

Sensitivity: the definition for the sensitivity is the ratio of change in the capacitance with respect to unit change in applied pressure.

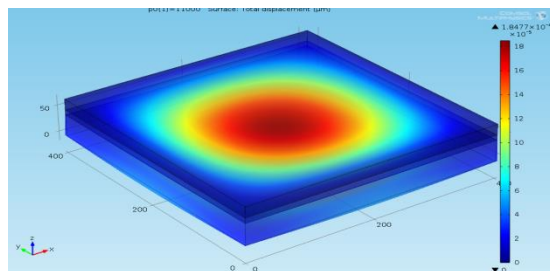


Figure 3: The total Displacement of the diaphragm

In the above fig.4 represents the total Displacement of a diaphragm with respect to the Deflection of the diaphragm against the pressure applied.

The next we can observe the electric potential of the capacitive pressure sensor with the 1v is applied to the sensor in the Fig.5

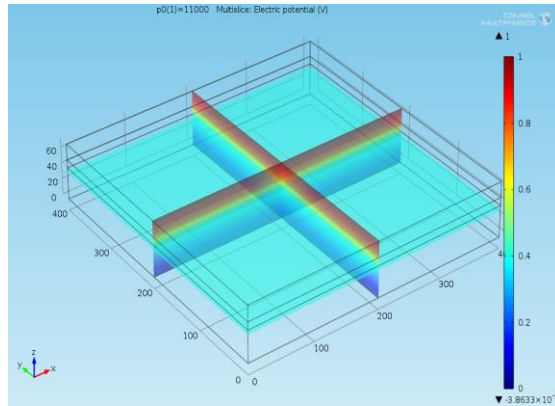


Figure 4 :Electric potential with 1v.

The total capacitance of the model against to the pressure applied is 1.88659×10^{-13} as shown the below Fig6. Here the capacitance is measured when the pressure is applied to the diaphragm.

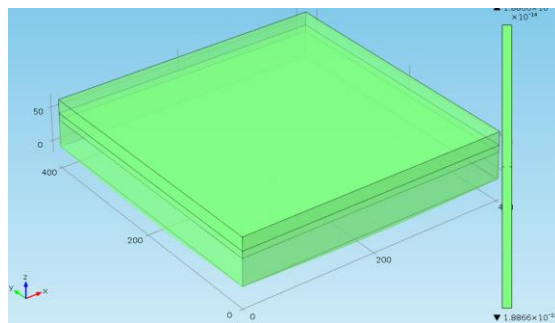


Figure 5: The total Capacitance vs Applied Pressure

And also Fig 7. Shows the stress behavior of diaphragm with respect to variable Boundary load

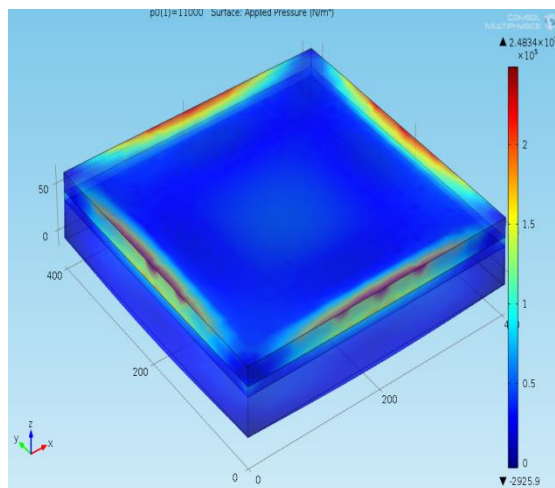


Figure 6: Stress vs Applied pressure diaphragm.

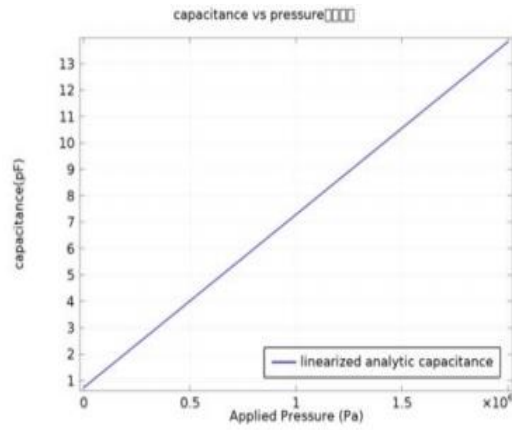


Figure 7:Plot of capacitance variation as function of applied voltage.

Capacitive sensors are consonant with most mechanical structures, and they have high sensitivity and low temperature changes. Fig.4 shows capacitive pressure sensors.

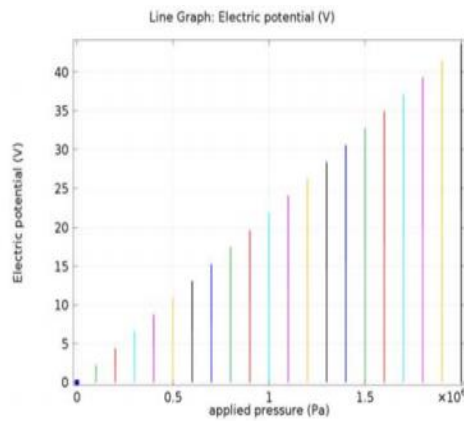


Figure 8:Graph of Applied pressure (Pa)Vvs Electric potential(V).

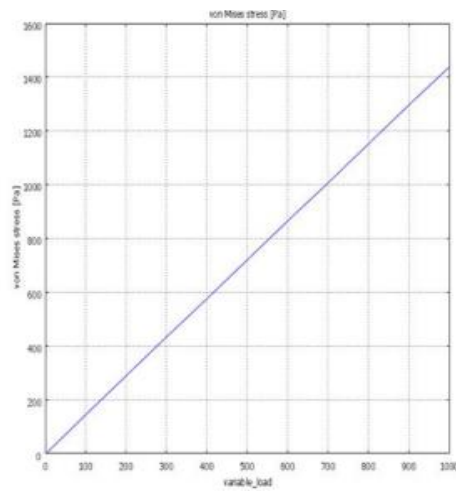


Figure 9:Stress measurement on diaphragm with variable load

2 Conclusion

This paper presents the modeling, simulation and analysis of the capacitive pressure sensor. COMSOL/Multi physics has been used to model the structure. This paper demonstrates the Displacement and Stress Analysis of a capacitive Pressure sensor. The design parameters for the capacitive pressure sensor are optimized and capacitance is about 1.88659×10^{-13} farad.

References

- [1] Kirankumar B. Balavalad, B. G. Sheeparamatti, "A Critical Review on MEMS Capacitive Pressure Sensors", Sensors & Transducers journal, IFSA publication, ISSN: 2306-8515, e-ISSN 1726-5479 Volume 187, Issue 4, pp120-128, April 2015.
- [2] Simulation Of Mems Based Capacitive Pressure Sensor Using Comsol Multiphysics Gitesh Mishra, Neha Paras, Arti Arora, P.J.George Kurukshetra Institute of Technology & Management, Kurukshetra giteshmishra001@gmail.com, neharao1993@gmail.com.
- [3] Priya Singha Roy, Madhurima Chattopadhyay, "Simulation of MEMS Based Capacitive Pressure Sensor Using Comsol Multiphysics", Kurukshetra Institute of Technology & Management, Kurukshetra.
- [4] Satu Kärki and Jukka Leikkala Tampere University of Technology, Institute of Measurement and Information Technology, Tampere, "Pressure Mapping System For Physiological Measurements", XVIII IMEKO WORLD CONGRESS, Metrology for a Sustainable Development, September, 17 – 22, 2006, Rio de Janeiro, Brazil. J. Clerk Maxwell, A Treatise on Electricity and Magnetism, 3rd ed., vol. 2. Oxford: Clarendon, 1892, pp.68–73.
- [5] Shivam Kohli, Anish Saini, "MEMS Based Pressure Sensor Simulation For HealthCare and Biomedical Applications", International Journal of Engineering Sciences & Emerging Technologies, Dec. 2013, ISSN:2231-6604, Vol. 6, Issue 3, PP: 308-315.
- [6] S. Timoshenko, S Woinowsky-Krieger, "Theory of Plates and Shells" Mc. Graw-Hill Book Company, Inc., Kogakusha Company Ltd., Tokyo, 1959, pp. 13, 105, 202
- [7] Madhurima Chattopadhyay and Deborshi Chakraborty, "A New Scheme for Determination of Respiration Rate in Human Beings using MEMS Based Capacitive Pressure Sensor: Simulation Study", Proc. Of the 8th International Conference on Sensing Technology, Sep. 2-4, 2014, Liverpool, UK.
- [8] Bulk Micromachined Pressure Sensor.
- [9] "Capacitance Based Pressure Transducer Handbook", Understanding, specifying and applying Capacitive Pressure Transducers.
- [10] Y. Zhang, R. Howver, B. Gogoi and N. Yazdi, "A High Ultra-Thin MEMS Capacitive Pressure Sensor", IEEE Transducers'11, Beijing, China, June 5-9, 2011, 978-1-4577-0156-6/11.
- [11] Toshihiko Omi, Syo Saskai, Fumihiko Sato and Mikio Matsumoto, Central R&D Laboratory Corporate Research and Development Headquarters, Omron Corporation, "Capacitive Pressure Sensor Technology and Applications for Semiconductor Manufacturing Equipment".
- [12] Sensitivity Analysis of MEMS Capacitive Pressure Sensor with Different Diaphragm Geometries for High Pressure Applications
- [13] Bulk Micromachined Pressure Sensor Lynn F. Fuller, Fellow, IEEE, Steven Sudirgo, Student Member, IEEE
- [14] Capacitive sensors: when and how to use them* Robert Puers Katholieke Universiteit Leuven, Departement Elektrotechniek, ESAT-MICAS, Kardinaal Mercierlaan 94, B-3001 Heverlee (Belgium).
- [15] UNDERSTANDING AND SPECIFYING SENSATA TECHNOLOGIES' CAPACITIVE PRESSURE TRANSDUCERS
- [16] PRESSURE MAPPING SYSTEM FOR PHYSIOLOGICAL MEASUREMENTS Satu Kärki and Jukka Leikkala Tampere University of Technology, Institute of Measurement and Information Technology, Tampere, Finland satu.karki@tut.fi, jukka.leikkala@tut.fi.
- [17] College Physics, Volume 1, By Nicholas Giordano.
- [18] Ko, W.H.; Wang, Q. "Touch mode capacitive pressure sensors for industrial applications", IEEE International Conference
- [19] Chapter 6, Experimental Methods for Engineers, 6th edition, J.P. Holman, 1994, PRESSURE MEASUREMENTS, www.mech.uq.edu.au/courses/metr3100/ST5_Press_M eas.pdf

- [20] Robert Puers, Katholieke Universiteit Leuven, Department Elektrotechniek, ES A T -M I C A S, Kardmaal Mercierlaan 94, B-3001 Heverlee (Belgium), "Capacitive sensors: when and how to use them", *Sensors and Actuators, A* 37-38 (1993) 93-105
- [21] Y. Hezarjaribi, Golestan University, Gorgan, Iran, M. N. Hamidon, A. R. Bahadorimehr University Putra Malaysia, 43400 UPM Serdang, Selangor, Malaysia, S. H. Keshmiri, University of Ferdowsi, Mashhad, Iran "Capacitive pressure sensor technology and applications", *ICSE 2008 Proceedings*. 2008, Johor Bahru

Early Diagnosis of Parkinson's Disease using Convolutional Neural Network

S. Jothi¹, S. Anita², S. Sivakumar³

¹Assistant Professor, Jayaraj Annapackiam College for Women (Autonomous), Tamilnadu India

²Associative Professor, St. Anne's College of Engineering and Technology, Tamilnadu, India

³Professor, Cardamom Planters' Association College, Tamilnadu, India

Abstract

Early-stage diagnosis of Parkinson's Disease (PD) is still a challenging task to the neurologists. An effective system is used for volume-based slices of Single Photon Emission Computed Tomography (SPECT) image to diagnose early PD. 16 slices which has significant region of interest are taken out from the SPECT images which is called as two-dimensional volume-based slices (2Dvs) for the analysis. The normalization technique called bilateral filter is used to enhance the Striatum of 2Dvs which make the architecture simpler. A deep learning technique called modified VGG16 architecture is used as a neural network to learn significant features from 2Dvs which could be able to discriminate Early PD from healthy control (HC). The architecture offers highest accuracy for discriminating Early PD from HC based on 10 cross fold validation. These techniques are practiced to develop a promising diagnostic model for early diagnosis of PD.

Keywords: SPECT, Early PD, VGG 16, Deep Learning

1 Introduction

PD is a movement disorder, causes due to deterioration of dopamine content in the striatum region of the Substantia Nigra (SN). The PD is clinically recognized by the cardinal symptoms like resting tremor, rigidity, postural instability, and bradykinesia, cognitive and psychiatric disturbances and it has an effective response to the drug levodopa (medication used to treat PD) in the advanced stage. However, these symptoms are unknown and ineffective response to levodopa at an early stage of the disorder [1, 2].

The SPECT images are used for the proper identification of PD. The procedure to take SPECT images are: The radiopharmaceutical drug is injected into the human body and it binds to the dopamine transporters in the striatum. The distribution of the drug in the brain locates the dopamine content in it [3]. Hence the quantification of dopamine content in the human brain found to be an appropriate biomarker for diagnosing PD. The GE health care report [4] states that the normal SPECT scan has high striatal uptake (dopamine), which forms symmetric shape or two comma shaped focal regions. Where as an abnormal scan has reduced striatal uptake or circular region in one of the striatum, forming asymmetric shape. Changes in the shape of striatum is clearly identified by the image processing techniques [5,6].

The significant image processing technique is an intensity normalization approaches which is to rectify the errors that arise due to physiological reasons and baseline calibration of a gamma camera. The integral and Cube based intensity normalization [7, 8, 9] approaches compute the mean integral value and cumulative intensity values of the image pixels by setting reference region outside the striatum. In another method, the normalization is done based on the maximum intensity value of the voxels, which may lead to wrong normalization because of peak intensity values due to noise. The bilateral filter calculates the weighted sum of nearby pixel values. The weight of the pixels basically depends on both the spatial and the intensity distance of the pixels. The noise of the nearby pixels is averaged to preserve the edges of the images well [10].

The analysis of 2D image and averaging image slices are the initial stage of early PD diagnostic process and it must be improved [11]. In addition to that, voxel (3D view of pixels) based analysis [12, 13] was also carried out, where the voxels are treated as features. The voxels are ranked based on its significance and top most features are taken for the analysis to diagnose Parkinson's disease. Voxel based analyses are found to be very tough for clinical practices [14]. Hence, the CAD system is involved to quantify the features of volume-based image slices [15], which may comprehend the specific uptake pattern during the normal and diseased state.

The machine learning techniques play a major role in medical image analysis to diagnose the disease. In particular, deep learning algorithm is a significant tool in learning the features directly for image classification.

It is highly accurate system than machine learning because it learns the features directly than extracting features from hand designed manner. Recently, Convolutional Neural Networks (CNNs) is a powerful tool for analyzing medical images especially SPECT image to diagnose PD [16].

Bounding box technique was implemented on regions of interest (ROI) by calculating the intensity threshold. The rest of the regions are removed. The performance metric of the network is evaluated by 10-fold cross-validation. Another deep learning network called PDNet is designed for PD classification. [17]. In their study, the system was trained on SPECT images obtained from PPMI and it shows a high accuracy. Though the system is more accurate, it is complex to implement and time consuming. The practical implementation of such network solutions is not feasible, as time is of crucial importance in the diagnosis of PD. To overcome this issue an efficient CNN is developed to classify Early PD from HC which offers a high-performance metric in terms of accuracy.

This paper organizes as follows. Section 2 contains the methods used like bilateral filter, The proposed network structure (modified VGG16). Section 3 describes the results and related discussions. Finally, conclusions are drawn.

2 Methods and Materials

2.1 The Dataset Used

The SPECT images are taken from the international PPMI database for the analysis. The hybrid ordered subset expectation maximization (HOSEM) algorithm, Iterative reconstruction, Attenuation correction has applied for processing the raw SPECT images. The details of the dataset used for the analysis are given in Table.1. The mentioned SPECT images are enhanced by bilateral filter and the images are trained by the proposed network. Fig. 1 illustrate the 2Dvs for early PD and HC.

Table 1: Details of input dataset

| Categories | Features |
|------------------------|-------------|
| Total number of images | 700 |
| No. of classes | 2 |
| Data type | Image |
| Size of the image | 224, 224, 3 |

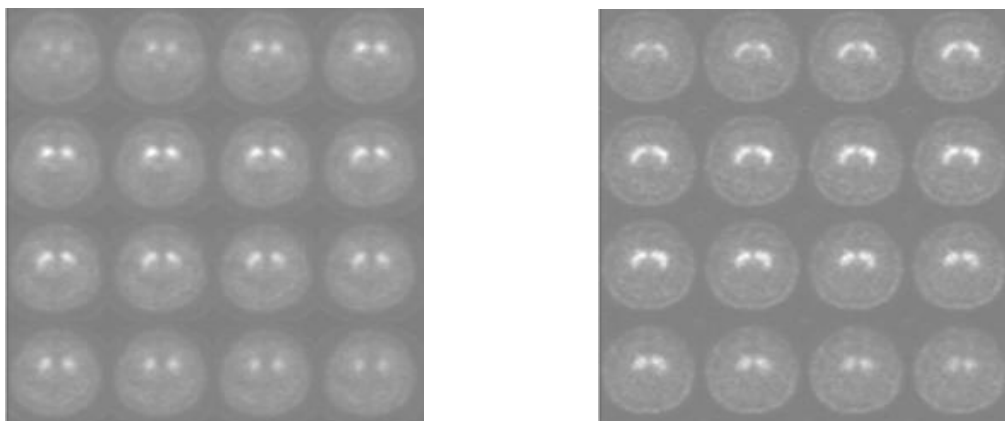


Figure 1: Two-dimensional volume-based image slices chosen from the SPECT (a) early PD (b) HC

2.2 The Modified VGG 16 Network Architecture

The overall flow of the proposed work is clearly explained in Fig.2. The 2Dvs are preprocessed using bilateral filter. The preprocessed image slices are given to the CNN architecture in order to make the network much simpler. The proposed network is a modified version of VGG 16. The network consists of four convolution layers and two dense layers for discriminating early PD from HC.

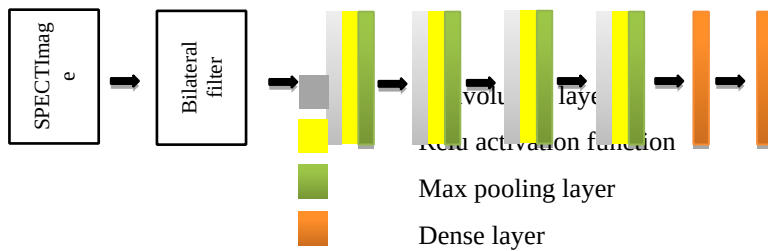


Figure 2: Overall workflow of the proposed work

VGG 16 is one of the best deep neural networks that has been employed for image classification tasks. The network consists of 13 convolutional layers, five max pooling layer and three dense layers with the uniform kernel sizes like 3x3 as shown in Fig. 3. However, one of the main drawbacks of the network is overlapping pixel blocks, which leads to an increase of memory consumption for learning the features of image.

On contrary, the proposed modified VGG 16 networks have only four convolutional layers and three dense layers, each with a kernel size of 3 × 3. The uniform kernel size is taken for the network which leads to much better feature learning with least number of training parameters. These smaller sized kernel gives lower costs due to less number layers than larger sized kernel. Though the multiple number of larger sized kernels provide more in-depth network architecture which is time-consuming and not feasible for medical applications. Therefore, by reducing the kernel size, the proposed network gains the advantage of learning the features from the image faster. Furthermore, the proposed network is more robust and performs better than VGG 16 with admirable accuracy, sensitivity, and specificity (Fig.5). The ReLU (Rectified Linear Unit) activation function allows faster training of CNN, since the calculation of its derivative has a lower computational cost, without losing any of its generalization ability [18].

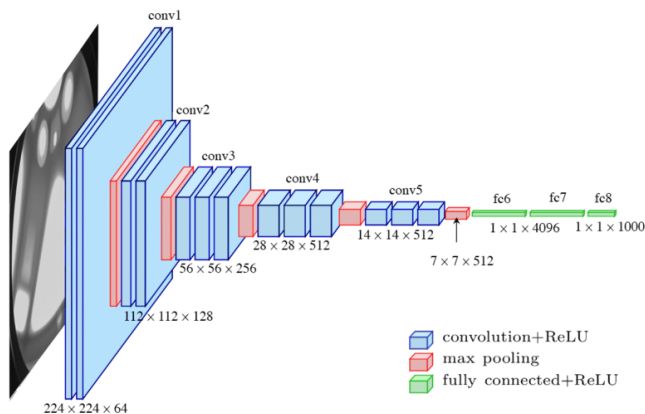


Figure 3: Pretrained network of VGG16 [19]

The ReLU itself is a non-saturating activation function and is defined by

$$f(x) = x^+ = \max(0, x) \tag{1}$$

where x is the input to a neuron. The image normalization process is done by bilateral filter which described below. In addition, our network only utilizes the ReLU activation function in all three layers. The proposed network model is optimized using the stochastic gradient descent with momentum optimizer (sgdm) with the learning rate of 0.01. These standard parameters of sgdm have been proven for neural networks to be computationally efficient, little memory usage and well suited for problems with big data. Hence these parameters are utilized in the proposed network. The input images utilized to train the network are resized from the original size of 522 × 529 × 3 to 224 × 224 × 3. Since this paper is focused on the classification between early PD patients and HC, i.e., a binary classification problem. In the architecture 112 nodes are used in each of our layers. Dropouts are used in the proposed work to avoid overfitting of data which will also improves the performance of the network.

2.3 Image Preprocessing

The preprocessing technique is used to highlight the region of interest (ROI) in an image. The bilateral filter is implemented for SPECT images in order to enhance the edges of the striatum region to get the original shape of the striatum, hence it plays a major role in diagnosing early PD. It calculates the weighted sum of nearby pixel values. The weight of the pixels basically depends on both the spatial and the intensity distance of the pixels. The noise of the nearby pixels is averaged to preserve the edges of the images well. The basic mathematical equation of the bilateral filter is given in following equation.

$$I(\tilde{x}) = \frac{1}{c} \sum_{y \in N(x)} e^{\left(\frac{(x^2 - y^2)}{2 * \sigma_d^2}\right)} e^{\left(\frac{-I(x^2 - y^2)}{2 * \sigma_r^2}\right)} \quad (2)$$

Where, σ_d & σ_r – Parameter that controls weights of spatial and intensity domain. The pre processed 2Dvs image slices are shown in Fig. 4. It shows the deviation between PD and HC.

2.4 Training and Testing the Network

A modified VGG 16 is trained and tested using the 500 SPECT images for both early PD and HC. The augmentation process is not done for identification of the PD in the early stage. The 10-fold cross validation is accomplished to evaluate the performance of the modified VGG 16. It consists of 10 subset of data which includes PD and HC. The dataset is divided equally for the subset. One subset is used for testing and the remaining subset is used for training the network. The evaluation metrics of the network is calculated from the confusion matrix and it is given as

3 Results and Discussion

3.1 Preprocessing using Bilateral Filter

The extracted sixteen slices are normalized using bilateral filter to enhance the edges of the striatum region alone for the subsequent analysis. Fig. 4 shows the normalized image slices of early PD and HC. It is evident from the Fig. 4 that PD has reduced comma shaped striatum and the HC has comma shaped striatum. The preprocessing technique increase the focus on the striatum which also increases the diagnostic accuracy and reduces the computational cost. Hence the classification takes the important role to discriminate early PD and HC. These enhanced images are given to the network for learning the features of the images.



Figure 4: Enhanced image for (a) early PD, and (b) HC

3.2 Network Performance

The enhanced 2Dvs are given to the modified VGG 16 networks. The network has designed in such a way that it provides highest performance and less computational cost. The network parameters are given in the Table.2. These parameters are selected by design calculation of the network. Using the given parameter, the network is trained by the 2Dvs SPECT image slices to diagnose early PD.

Table 2: The parameters of the proposed network

| S. No. | Network Parameters | Numeric value |
|---------------------|--------------------|---------------|
| 1 | Image size | 224,224,3 |
| Convolution | | |
| 2 | No. of filters | 32 |
| 3 | Kernel size | 3x3 |
| 4 | Stride | 1,1 |
| 5 | Padding | same |
| Max. Pooling | | |
| 6 | Kernel size | 3x3 |
| 7 | Stride | 2,2 |
| 8 | Padding | 0 |
| 9 | Output size | 2 |
| 10 | Dropout | 50% |

The enhanced images are given to the network for training it appropriately. The ten-fold cross validation method is executed to evaluate the performance of the network to overcome the variability in the classification. 50% dropouts also minimize the overfitting of data which in turn improves the classification accuracy. Table 3. Illustrates that the classification task converged quickly and achieved appreciated diagnostic accuracy of 95.90%, sensitivity of 94.39%, specificity of 91.37%. The performance metrics confirm that the proposed network offers high probability of diagnosing early PD when compared with the pretrained neural network (VGG 16). It elucidates clearly that the modified VGG 16 network offers appreciated output in discriminating early PD from HC.

Table 3: performance metrics of the proposed neural network

| Folds | Training Accuracy (%) | Testing Accuracy (%) | Sensitivity (%) | Specificity (%) | Pretrained Network (%) |
|-------|-----------------------|----------------------|-----------------|-----------------|------------------------|
| 1 | 92.35 | 94.87 | 97.87 | 93.87 | 92.01 |
| 2 | 90.15 | 98.78 | 94.17 | 94.94 | 90.32 |
| 3 | 95.45 | 97.77 | 91.26 | 80.00 | 93.56 |
| 4 | 96.70 | 96.00 | 94.00 | 91.18 | 91.78 |
| 5 | 93.55 | 96.87 | 95.73 | 92.38 | 95.54 |
| 6 | 94.54 | 94.99 | 97.00 | 86.49 | 94.25 |
| 7 | 96.25 | 95.99 | 94.75 | 100.00 | 90.21 |
| 8 | 91.98 | 95.98 | 92.26 | 95.00 | 93.45 |
| 9 | 95.25 | 91.88 | 93.21 | 89.47 | 91.02 |
| 10 | 92.74 | 95.89 | 93.65 | 90.32 | 90.25 |
| | 93.90 | 95.90 | 94.39 | 91.37 | 92.23 |

4 Conclusion

An early diagnosis of Parkinson's Disease (PD) is made easy using a recent technology called Convolutional Neural Network. The two-dimensional volume-based slices (2Dvs) are extracted from the SPECT images based on the high striatal uptake region. The edges of the 2Dvs are enhanced using bilateral filter. The enhanced 2Dvs is subjected to the modified VGG 16 to enrich the diagnostic accuracy to reduce the rate of misclassification between PD and HC. The network uses reduced number of layers and optimal parameter to reduce the computational cost and to use minimum memory. The network offers high diagnostic accuracy of 95.90%, sensitivity of 94.39%, Specificity of 91.37%. Hence the proposed system aids the clinicians to diagnose PD in earlier stage.

References

- [1] L. M. De Lau, M. Breteler, "Epidemiology of Parkinson's disease", *The Lancet Neurology*, vol. 5, pp. 525-535, 2006.
- [2] D. J. Moore, A. B West, V. L Dawson, T. M Dawson, "Molecular pathophysiology of Parkinson's disease" *Annual Review Neuroscience* 28, 57-87, 2005.
- [3] I. A Illan, J. M Gorrz, J. Ramirez, F. Segovia, J. M. Jimenez-Hoyuela, S. J. Ortega Lozano. "Automatic assistance to Parkinson's disease diagnosis in DaTSCAN SPECT imaging", *Medical Physics*, 39:5971–5980, 2012.
- [4] S. Fahn, D. Oakes, I. Shoulson et al., "Levodopa and the progression of Parkinson's disease," *N Engl. J Med.*, vol. 351, no. 24, pp. 2498-508, Dec 9, 2004.
- [5] J. Seibyl, D. Jennings, R. Tabamo et al., "The role of neuroimaging in the early diagnosis and evaluation of Parkinson's disease," *Minerva Med.*, vol. 96, no. 5, pp. 353-64, 2005.
- [6] K. Marek, D. Jennings, and J. Seibyl, "Long-term follow-up of patients with scans without evidence of dopaminergic deficit (SWEDD) in the ELLDOPA study," *Neurology*, vol. 64 (Suppl. 1), pp. A274, 2005.
- [7] Karl J. Friston, John T. Ashburner, Stefan J. Kiebel, Thomas E. Nichols, William D. Penny, *Statistical Parametric Mapping: The Analysis of Functional Brain Images. chapter Statistical Models and Experimental Design*, Academic Press, Massachusetts, United States, 2011.
- [8] S. J. Ortega Lozano, M. D. Martinez del Valle Torres, J. M. Jimenez-Hoyuela Garcia, A. L. Gutierrez Cardo, V. Campos Arillo, "Diagnostic accuracy of FP-CIT SPECT in patients with parkinsonism", *Rev. Espanola Med. Nucl. (English Edition)* 26 (5), 277–285, 2007.
- [9] S.J. Ortega Lozano, M.D. Martinez del Valle Torres, E. Ramos Moreno, S. Sanz Viedma, T. Amrani Raissouni, J.M. Jimenez-Hoyuela, "Quantitative evaluation of SPECT with FP-CIT", importance of the reference area, *Rev. Espanola Med. Nucl. (English Edition)* 29 (5) (2010) 246–250.
- [10] Zhang, Ming, (2009), "Bilateral filter in image processing," Master's Thesis, Louisiana State University.
- [11] Prashanth R, Dutta Roy S, Ghosh S, Pravat Mandal K, "Shape features as biomarkers in early Parkinson's disease", 6th International IEEE/EMBS conference on neural engineering (NER); 2014.
- [12] Francisco P M Oliveira, and Miguel Castelo-Branco, "Computer-aided diagnosis of Parkinson's disease based on [123I] FP-CIT SPECT binding potential images, using the voxels-as-features approach and support vector", *J. Neural Eng.* 2015; 12:10pp.
- [13] F. J. Martinez–Murcia, J. M. Gorrz, J. Ramirez, I. A. Illan, A. Ortiz, "Automatic detection of Parkinsonism using significance measures and component analysis in DaTSCAN imaging", *Neurocomputing*, 126:58-70, 2014.
- [14] D. S. Djang, M. J. Janssen, N. Bohnen, J. Booij, T. A. Henderson, K. Herholz, et al "SNM practice guideline for dopamine transporter imaging with 123I-ioflupane SPECT 1.0", *J Nucl. Med.*, 53:154-163,2012.
- [15] S. Anita and P. Aruna Priya, Three-Dimensional Analysis of SPECT Images for Diagnosing Early Parkinson's Disease Using Radial Basis Function Kernel- Extreme Learning Machine", *Current Medical Imaging Reviews*, vol. 15, no.5, pp.461 – 470, 2019.
- [16] Farhan Mohammed, Xiangjian He, Yiguang Lin, "An easy-to-use deep-learning model for highly accurate diagnosis of Parkinson's disease using SPECT images", *Computerized Medical Imaging and Graphics* 87 (2021) 101810
- [17] Choi, H., Ha, S., Im, H.J., Paek, S.H., Lee, D.S., "Refining diagnosis of Parkinson's disease with deep learning-based interpretation of dopamine transporter imaging", *Neuroimage Clin*, 2017, Vol. 16, pp. 586-594.
- [18] Krizhevsky, A., Sutskever, I., Hinton, G.E., 2012. ImageNet classification with deep convolutional neural networks. *Advances in Neural Information Processing Systems* 1097-1105.
- [19] <https://medium.com/towards-artificial-intelligence/the-architecture-and-implementation-of-vgg-16050e5a5920b>.

Investigation of ZnO as Substitute Explicit Materials in Sensor Innovation

Kaustubh Kumar Shukla¹, Dr.T.Muthumanickam², Dr.T.Sheela³

¹Research Scholar, Dept.of ECE, Vinayaka Mission's Research Foundation(Deemed to be University), Salem,Tamilnadu,India.

²Professor and Head, Dept.of ECE, Vinayaka Mission's Kirupananda Variyar Engineering College- VMRF(DU), Salem, Tamilnadu, India.

³Associate Professor, Dept. of ECE, Vinayaka Mission's Kirupananda Variyar Engineering College-VMRF(DU), Salem, Tamilnadu, India.

Abstract

Essential focal point of this paper is to show the significant social difficulties and their answers through MEMS innovation. Here the purpose for picking the MEMS innovation is interminable on the grounds that it has parcel numerous applications with special highlights. In this paper certain investigation has been finished utilizing diverse detecting materials. Perhaps the main material utilized here is ZnO. Different mechanical boundaries has been tried in multiphysics climate. As a yield as far as uprooting through this examination report it has been acquired as $6.98 \times 106 \mu\text{m}$ and $4.28 \times 106 \mu\text{m}$ while profundity and tallness is variable respectively. This sort of exploration is extremely helpful for organic applications like early discovery of daises. Microcantilever is taken as a design here on the grounds that it is quite possibly the most basic and delicate gadget at miniature level. Utilizing this design some stunner focuses has been examined in this paper about how it tends to be valuable for gas finding and related work.

Keywords: MEMS, Micro cantilever, Sensor, Toxic Gas, Zinc Oxide (ZnO).

1 Introduction

Present situation of ebb and flow research is multidisciplinary patterns to help the whole world and first needful individuals. To accomplish this objective most extreme analysts are discovering arrangements as multipurpose in nature. So in this circumstances extraordinary compared to other innovation which is prevalently known as MEMS(Micro-Electro-Mechanical-Systems)[1-12]. It is a crossover innovation which is able to deliver a constant gadget commonly it could be decreased in size, improved precision, less force utilization, primary change and economical[13-21]. In this paper one MEMS based design has been chosen named as miniature cantilever. Figure-1 showing the 3D perspective on a miniature cantilever structure [8-9]. From the figure-1 it is unmistakably justifiable that at whatever point miniature cantilever term is coming, one needs to comprehend it will be fixed from one side and free from inverse side just as power or pressing factor will be applied on free end in light of the fact that on account of fixed end applied power impact will be zero due to no redirection and fixed end [10-12]. For understanding its avoidance impact let us consider another figure-2 as given underneath.

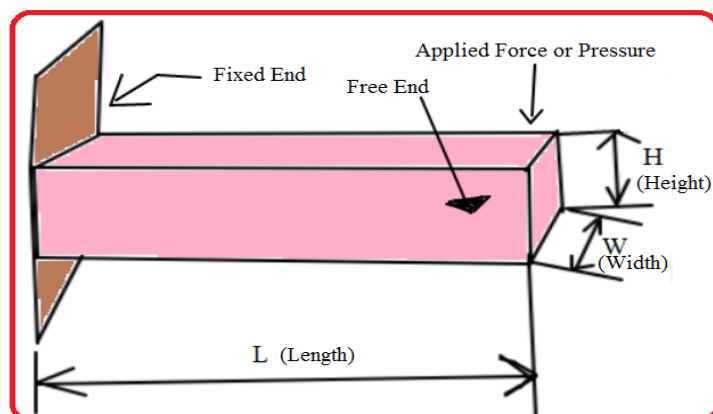


Figure 1: 3D Concept of micro cantilever

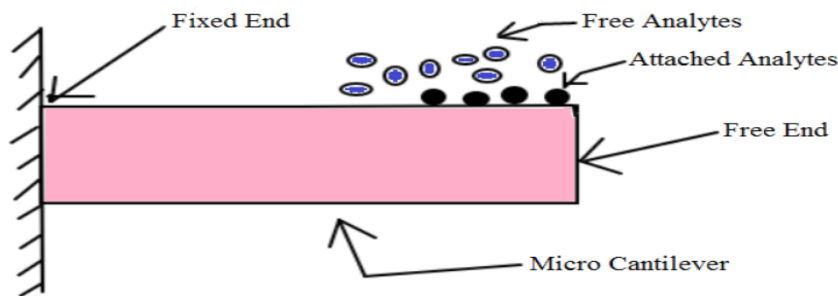


Figure 2: Analyse detection using micro cantilever

From the above figure-2 model one can undoubtedly comprehend the impacts of target analyse on free end. The idea driving it is at whatever point any analyse will get connected with miniature cantilever it will be get diverted so dependent on its redirection effectively we can discover its belongings in multi physics climate [3-5]. This is the primary explanation individuals need to upgrade the affectability of miniature cantilever since, supposing that it will be more delicate than just it will give more exactness, selectivity and redirection. So for improving the affectability need to check and dissect a few boundaries of various materials [6]. In short we can say that determination of materials assumes an imperative part in the field of MEMS for any sort of construction planning and demonstrating [1-2].

2 Design And Analysis

In this examination work following measurements has been utilized to investigate the ZnO based impact with reaction to CO₂ gas.

Table 1: Dimensions of Designed Structure

| Parameters | Value | Unit | Comments |
|------------|-------|------|---|
| Width(W) | 5 | µm | Basic construction has been made using these parameters in multiphysics environment tool. |
| Depth(D) | 25 | | |
| Height(H) | 15 | | |

Case-1: For this situation under multiphysics as a matter of first importance without Co₂ gas, miniature cantilever has been saved with ZnO and under straight versatile material investigation examination density(ρ) chose from material.

Table 2: Density (ρ) selected from material

| Eigen frequency(Hz) | Stress(N/m ²) | | Strain(1) | | Displacement (µm) |
|---------------------|---------------------------|-----------------------|-----------------------|----------------------|---------------------|
| | Minimum | Maximum | Minimum | Maximum | Maximum |
| 7.85E6 | 1.59X10 ¹³ | 9.38X10 ¹⁵ | -4.21X10 ⁴ | 4.28X10 ⁴ | 3.3X10 ⁶ |
| 1.92E7 | 2.63X10 ¹³ | 2.55X10 ¹⁶ | -1.06X10 ⁵ | 1.05X10 ⁵ | 3.2X10 ⁶ |
| 2.34E7 | 1.27X10 ¹⁴ | 2.43X10 ¹⁶ | -1.14X10 ⁵ | 1.11X10 ⁵ | 4.4X10 ⁶ |
| 4.19E7 | 4.3X10 ¹⁴ | 4.65X10 ¹⁶ | -2.02X10 ⁵ | 2.04X10 ⁵ | 3.4X10 ⁶ |

| | | | | | |
|---------|-----------------------|-----------------------|-----------------------|----------------------|---------------------|
| 6.15E7 | 2.96X10 ¹² | 4.45X10 ¹⁶ | -7.37 | 1.79X10 ⁵ | 2.4X10 ⁶ |
| 6.635E7 | 3.08X10 ¹⁴ | 5.43X10 ¹⁶ | -2.31X10 ⁵ | 2.32X10 ⁵ | 3.4X10 ⁶ |

Case-2: Here Co₂ gas has been kept on microcantilever on which as of now ZnO was saved prior to presenting Co₂ gas, under straight versatile material examination investigation density(ρ) has been consider as chosen from material.

Table 3: Density (ρ) selected from material

| Eigen frequency(Hz) | Stress(N/m ²) | | Strain(1) | | Displacement(μ m) |
|---------------------|---------------------------|-----------------------|-----------------------|----------------------|------------------------|
| | Minimum | Maximum | Minimum | Maximum | Maximum |
| 7.69E8i | 2.23X10 ¹⁵ | 1.19X10 ¹⁷ | -5.89X10 ⁶ | 4.89X10 ⁶ | 6.82X10 ⁶ |
| 1.11E8 | 3.17X10 ¹⁴ | 1.69X10 ¹⁶ | -4.96X10 ⁵ | 6.13X10 ⁵ | 3.79X10 ⁶ |
| 2.668E8 | 3.38X10 ¹⁴ | 1.17X10 ¹⁶ | -6.81X10 ⁵ | 5.29X10 ⁵ | 3.53X10 ⁶ |
| 3.142E8 | 1.77X10 ¹⁴ | 1.77X10 ¹⁶ | -8.27X10 ⁵ | 1.02X10 ⁶ | 4.8X10 ⁶ |
| 5.664E8 | 1.89X10 ¹⁵ | 8.38X10 ¹⁶ | -3.86x10 ⁶ | 3.18X10 ⁶ | 5.93X10 ⁶ |
| 6.964E8 | 2.73X10 ¹⁵ | 1.16X10 ¹⁷ | -5.15X10 ⁶ | 4.95X10 ⁶ | 6.56X10 ⁶ |

Case-3: This progression has been consider as without Co₂ gas, miniature cantilever has been saved with ZnO and under straight versatile material examination investigation density(ρ) has been presented as client characterized which is 1.98kg/m³.

Table 4: Density (ρ) has been introduced as user defined which is 1.98kg/m³

| Eigen frequency (Hz) | Stress(N/m ²) | | Strain(1) | | Displacement (μ m) |
|----------------------|---------------------------|-----------------------|-----------------------|----------------------|-------------------------|
| | Minimum | Maximum | Minimum | Maximum | Maximum |
| 7.901E6 | 1.59X10 ¹³ | 9.38X10 ¹⁵ | -4.21X10 ⁴ | 4.28X10 ⁴ | 3.3X10 ⁶ |
| 1.938E7 | 2.63X10 ¹³ | 2.55X10 ¹⁶ | -1.06X10 ⁵ | 1.05X10 ⁵ | 3.2X10 ⁶ |
| 2.355E7 | 1.27X10 ¹⁴ | 2.43X10 ¹⁶ | -1.14X10 ⁵ | 1.11X10 ⁵ | 4.4X10 ⁶ |
| 4.219E7 | 4.3X10 ¹⁴ | 4.65X10 ¹⁶ | -2.02X10 ⁵ | 2.04X10 ⁵ | 3.4X10 ⁶ |
| 6.188E7 | 2.96X10 ¹² | 4.45X10 ¹⁶ | -7.37 | 1.79X10 ⁵ | 2.4X10 ⁶ |
| 6.673E7 | 3.08X10 ¹⁴ | 5.43X10 ¹⁶ | -2.31X10 ⁵ | 2.32X10 ⁵ | 3.4X10 ⁶ |

Case-4: Co₂ gas has been saved on microcantil ever on which as of now ZnO was kept prior to presenting Co₂ gas, under straight versatile material examination investigation density (ρ) has been presented as client characterized which is 1.98kg/m³.

Table 5: Density (ρ) has been introduced as user defined which is 1.98kg/m^3

| Eigen frequency(Hz) | Stress(N/m^2) | | Strain(1) | | Displacement (μm) |
|---------------------|--------------------------|-----------------------|---------------------|--------------------|--------------------------------|
| | Minimum | Maximum | Minimum | Maximum | Maximum |
| 7.394E8i | 2.23×10^{15} | 1.19×10^{17} | -5.89×10^6 | 4.89×10^6 | 6.82×10^6 |
| 1.074E8 | 3.17×10^{14} | 1.69×10^{16} | -4.96×10^5 | 6.13×10^5 | 3.79×10^6 |
| 2.564E8 | 3.38×10^{14} | 1.17×10^{16} | -6.81×10^5 | 5.29×10^5 | 3.53×10^6 |
| 3.021E8 | 1.77×10^{14} | 1.77×10^{16} | -8.27×10^5 | 1.02×10^6 | 4.8×10^6 |
| 5.444E8 | 1.89×10^{15} | 8.38×10^{16} | -3.86×10^6 | 3.18×10^6 | 5.93×10^6 |
| 6.694E8 | 2.73×10^{15} | 1.16×10^{17} | -5.15×10^6 | 4.95×10^6 | 6.56×10^6 |

On the whole four cases the reactions of miniature cantilever has been investigate altogether after that by considering Si as a substrate and no other material has been kept on it to examine the all out removal by shifting the elements of the gadget. Only for instance one of the examinations has been appeared with the assistance of table-6.

3 Result And Discussion

Fig.-3 to fig.-6 showing the simulation result based on dimensions variations of micro cantilever.

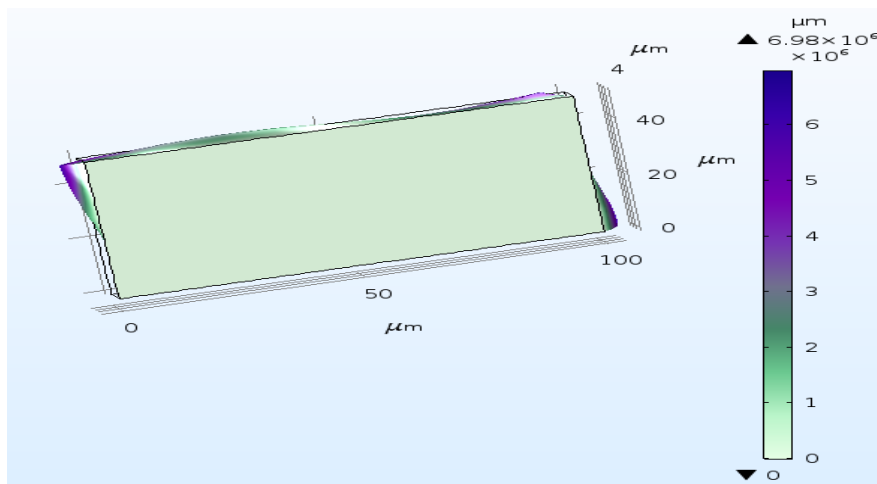


Figure 3: Simulation result based on dimensions variations of micro cantilever

4 Conclusion

Entirely through this work investigation has been done to appraise the most extreme removal in various circumstances like by adjusting the materials and primary alterations. At one specific point it has been seen that dislodging is greatest by shifting the dimensional boundaries in three distinct circumstances, so finally viewed as that specific measurements and mimicked the specific construction to consider the most extreme displacement. Finally, we may say that it very well may be helpful to get greatest reaction of miniature cantilever as a transducer or diversion of delicate layer can be distinguish effectively in various circumstances.

As a yield regarding dislodging through this examination report it has been acquired as $6.98 \times 106 \mu\text{m}$ and $4.28 \times 106 \mu\text{m}$ while profundity and tallness is variable individually.

References

- [1] Archana R. Tiwari and Snehal V. Laddha, "Rectangular Microstrip Patch Antenna for WLAN application International Journal of Electronics and Computational System", *IJECS ISSN 2348117X*, vol. 6, no. 8, August 2017
- [2] C-W., Tang, "Design of a microstrip filter using multiple capacitive-loaded coupled lines." no. 3 (2007), *IET Micro., Ant. & Prop.* 1651-656.
- [3] Naheed Anjum Khan and Bharati A. Singh, "Microstrip Antenna Design with Defected Ground Structure", *IOSR Journal of Electronics and Communication Engineering (IOSR-JECE)*, vol. 9, no. 2, pp. 4650, Mar-Apr. 014, ISSN 2278–2834.
- [4] Preach Patil ,Shweta Goilkar, Lokmanya "MICROSTRIP ANTENNA USING THE DEFECTED GROUND STRUCTURE FOR BANDWIDTH ENHANCEMENT" 4th International Conference on Recent Trends on Electronics, Information, Communication & Technology (RTEICT-2019), MAY 17th & 18th 2019 978-1-7281-0630-4/19/\$31.00 ©2019 IEEE 1384 .
- [5] Kai Chang, Chan Ho, Kim, "Ring resonator bandpass filter with switchable bandwidth using stepped-impedance stubs." *IEEE Trans. -58, Micr. Theory and Techn.*, no. 12 (2010): 3936- 3944.
- [6] Archana R. Tiwari and Snehal V. Laddha, Rectangular Microstrip Patch Antenna for WLAN application International Journal of Electronics and Computational System, *IJECS*, ISSN 2348117X, Volume 6, Issue 8, August 2017.
- [7] Konkyana, F. A. L. B., & Sudhakar, B. A. A Review on Microstrip Antennas with Defected Ground Structure Techniques for Ultra-Wideband Applications. 2019 International Conference on Communication and Signal Processing (ICCSP). doi:10.1109/iccsp.2019.8697941
- [8] Abdul Fatah Awang Mat, Ambak, Zulkifli, Muhammad RedzuanSaad, Rosidah Alias, Sabrina MohdShapee, Azmi Ibrahim, MohdZulfadli, Mohammed Yusoff, Mohamed RazmanYahya, "The microstrip coupled line Bandpass filter using LTCC technology for 5GHz wireless LAN application." *IEEE International*, 2008, pp. 496-499. In *RF and Micr. Con., RFM*.
- [9] Abdurrahim Toktas, Mehmet Yerlikaya, Enes Yigit, " Microstrip-fed Triangular UWB Microstrip Antenna Based on DGS" *International Journal of Applied Mathematics, Electronics and Computers*, vol 4 pp 43-47, 2016.
- [10] N. Benabdallah, Seghier, F. T. Bendimerad, Nasreddine Benahmed, Salima, "Design of parallel-coupled microstrip bandpass filter for FM Wireless applications." *IEEE*, 2012. pp. 207-211, 6th International Conference, In *Sci. of Electro., Technologies of Information and Telecommunications (SETIT)*.
- [11] Hussein Nasser, Shaman. "New S-band bandpass filter (BPF) with wideband passband for wireless communication systems." *IEEE* 22,2012. no. 5: 242-244, *Microw. and Wireless Components Lett.*
- [12] Stosic, A. S. Atanaskovic., B. P., N. S. Doncov, "Response calculation of parallel-coupled resonator filters by use of synthesized wave digital network." *IEEE*, 2013., vol. 1, pp. 253-256, 11th International Con., In *Telecommunication in Modern Satellite, Cable and Broadcasting Services (TELSIKS)*.

Approaches on Different Power Management Techniques for IoT enabled 5G Communication – A Survey

Manikannan Govindasamy¹, P.Prabakaran², B.Theeban Chakkaravarthy³

^{1,2,3}Assistant Professor, Department of Electronics and Communication Engineering, CK College of Engineering and Technology, Cuddalore, Tamil Nadu, India

Abstract

The Internet of Things (IoT) hassles new challenges in deploying the IoT ecosystem with diverse sensor platforms connecting billions of heterogeneous objects over the internet. Power Reduction is one of the major challenges in expanding the network of IoT connected devices. Mostly Low-energy sensors are used to transmit data sporadically or continuously. While considering billions/trillions of sensors connected together with various user applications, their energy efficiency becomes a major issue. This survey discusses the future IoT enabled 5G technology from a bird's eye view covering all its statistical/architectural trends, challenges, use cases and future enhancement. This study gives various approaches and design strategies that have to be developed for reducing Power consumption and power management techniques to increase the reliability in devices connected in IoT Networks. The major contribution of this study will significantly contribute to the Internet of Things (IoT) for Next-Generation (5G) Smart Systems.

Keywords: *Internet of Thing (IoT), Fifth-Generation, Power Management Techniques, Challenges in IoT, Power Consumption*

1 Introduction

Universe is moving towards a drastic change in connection between every things and processing will lead to a Forth industrial revolution named Industry 4.0. This revolution combines several sciences and technologies with one another, such as, Data Acquisition, Wireless Sensor Networks, Power Consumption, Data Analytic, Radio and Mobile Communications and Processing, Internet Technology. IoT finds wide spread application from wearable fitness trackers to consumer electronics, connected cars, transportation, healthcare and many others. The conventional use of the Internet has become scanty to meet the industrial and domestic requirements.

The IoT is the technology which always ready to adapt new technologies to internet technology by enabling communications with and among smart objects, thus leading to vision of “anywhere, anytime, any media, anything” communications. The real large growth IoT is predicted from all other types of connected small devices in areas like home automation, smart energy, elderly care at home, transportation, asset tracking and many others which will be a real candidate to be IoT devices. So, IoT is a system relies on billion smart sensors and actuators and to build such a system, new ideas about intelligent sensors and data computations and processing must be introduced. IoT creates a platform in which physical objects can mimic certain human sensory capabilities, such as perception, vision, hearing, smell and thinking. Sustained by these human sensory capabilities and the emerging tactile Internet, machines can communicate with each another, share relevant information and make real-time decisions with less human input, especially now that we are migrating to the 5G era, in which the expected wireless network delay is 1 ms [1-9].

Table 1: Summary comparison of the using wireless technologies for IoT.

| Parameters | LoRa | Bluetooth | LR-WPAN | Mobile Communication | WiMAX | WiFi |
|--------------------|--------------|----------------------------|------------------------|--------------------------------|-----------------------------------|-------------------------|
| Standard | LoRaWAN R1.0 | IEEE 802.15.1 | IEEE 802.15.4 (ZigBee) | 2G-GSM, CDMA 3G-UMTS, 4G-LTE-A | IEEE 802.16 | IEEE 802.11 a/c/b/d/g/n |
| Energy consumption | Very Low | Bluetooth: ; BLE: Very Low | Low | Medium | Medium | High |
| Frequency Band | 868/900 MHz | 2.4 GHz | 868/915 MHz, 2.4 GHz | 865 MHz–2. GHz | 2–66 GHz | 5–60 GHz |
| Data rate | 0.3–50 Kb/s | 1–24 Mb/s | 40–250 Kb/s | 200 kb/s–1 Gb/s | 1 Mb/s–1 Gb/s (Fixed) 50–100 Mb/s | 1 Mb/s–6.75 Gb/s |
| Transmission Range | <30 Km | 8–10 m | 10–20 m | Entire cellular area | <50Km | 20–100 m |
| Cost | High | Low | Low | Medium | High | High |

In general, when selecting a wireless technology for connected devices, a few considerations must be taken into account depending on the final application.

- Maximum throughput.
- Power consumption.
- Maximum distance range.

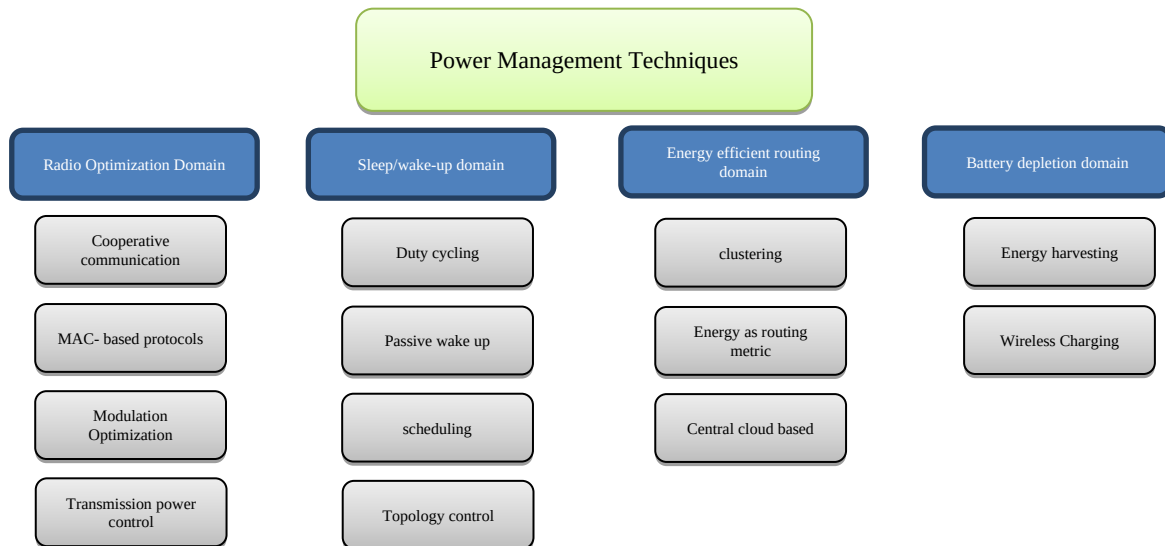


Figure 1: ISO model classification of energy saving techniques

Figure 1 provides various power management and power reduction techniques that can be incorporated to IoT enabled 5G communication. In this paper, a study uses a comparative analysis for different techniques/approaches which influence power management / power reduction of a wireless communication system for IoT-5G applications.

2 Radio Optimization Techniques

The radio unit is the most noticeable energy consumption unit in the WSN. The energy reduction by the radio unit is caused by two parts: (i) source powering of the circuit, and (ii) power utilized during transmission. Short distances communication utilize more energy in powering the devices [20], while powering the transmitted signal in long range communication require more power consumption. Several strategies have been investigated to enhance EE by adjusting transmission power level dynamically. In addition, the authors in [21] projected advance saving energy cooperative infrastructure, in which sensor nodes with higher remaining energy is at liberty to increase transmitting power leading to other nodes to decrease their own transmitting power. The proposed technique reduces interference and improves connectivity due to the decrease in transmission power. However, an increase in delay potentials is expected, because more hops will be required for packet forwarding. Nevertheless, the problem of delay can be overcome through cooperative communications among the neighbouring sensor nodes, which creates a virtual multiple-antenna environment (spatial diversity). Virtual multiple-antenna reduces data retransmission, effectively improving the quality of the received signal by overcoming multi-path fading and shadowing phenomenon. Jayaweera [24], compared the energy consumption of both Single Input Single Output and virtual multiple-antenna (Multiple Input and Multiple Output) systems and showed that virtual multiple-antenna systems can provide higher energy savings and minimize E-2-E delays over certain propagation range distances.

On the other hand, Cui et al. [25] examined the connection among the energy consumption, transmission time, and bit error rate. The results showed that optimising the transmission time could have minimised the energy consumption needed to attain a stated bit error rate as well as delay requirement. Moreover, the authors in [26] presented a relative study on the Energy Efficiency of three modulation techniques to select the ideal modulation scheme that yields the lowest energy utilization with various distances between nodes. To discourse the problem of joint transmission power and rate allocation in the uplink of a cellular wireless network, several

works have considered transmission power and rate allocation. The two basic methods that have been proposed in the recent literature are explained below.

Joint rate and power control are modelled as two distinct games (i.e., an uplink transmission rate allocation and an uplink transmission power allocation problem), which are based on the game theoretic perspective. Users determine first their uplink transmission rate and then given their uplink transmission rate, they apply power control to allocate their uplink transmission powers. The main disadvantage of this approach is that the optimisation problem is cracked asynchronously and discretely considering the two systems' resources. Thus, the combined outcome of the two distinct optimisation problems is less efficient than jointly solving the problem. The joint rate and power control problem is revised in a single-variable problem of the ratio of uplink transmission rate to the uplink transmission power. However, this approach is limited in realistic cases and can only be applied in specific studies where shortened forms of utility functions are assumed (i.e., where the ratio of uplink transmission rate to power appears).

As a result, the use of this approach strongly depends on problem formulation. The single variable problem is solved with respect to the substituted ratio. To determine users' optimal pair of uplink transmission rate and power, the maximum value of one resource is assumed and the other one is determined, so the ratio is equal to the optimal one. While users update their uplink transmission rate and power in the same step, the obtained answer remains inferior compared with the corresponding solution of the actual joint two-variable optimisation problem. Tsiropoulou et al. proposed a novel utility-based game theoretic framework to address the problem of joint transmission power and rate allocation in the uplink of a cellular wireless network.

Initially, each user is associated with a generic utility function that can properly express and represent mobile users' degree of contentment in relation to the allocated system's resources for heterogeneous services with various transmission rates. The results showed the dominance of the proposed framework over other various state-of-the-art approaches.

2.1 Sleep/Wake-up Technique

Switching off (sleep mode) the non-active transceivers have become the ultimate approach towards the realization of EE in Information and communications technology, due to the fact that it can save large amount of energy. The philosophy behind the proposed approach is to exploit dense and redundant deployment of sensor nodes, leading to a small coverage area. The sensor nodes' off/on switching method is more desirable for improving WSN Energy Efficient and prolonging the battery lifetime of the wireless sensors. However, the coverage issue should be considered, and it should be guaranteed by the remaining active nodes. Misra et al. proposed a subset solution in which nodes with minimum overlap areas are activated and must be capable of reducing network energy. Meanwhile, Karasabun et al. modelled the Energy Efficient issue as a subset selection problem of active connected sensors for correlated data payload gathering. Using three-dimensional correlation, the sensor information of non-active sensor nodes can be obtained from those of active nodes, which makes it a good strategy. Equation (1) gives the average power consumption as the sleep power multiplied by the percentage of duration the system is in sleep mode plus the active power multiplied by the percentage of duration the system is in active mode all divided by 100. In a situation in which the system is designed to have bigger sleep energy comparable to the active energy, it is then feasible to engage power reduction strategy by tuning the sensor node to its lowest power mode. There are two scenarios in which the active power term can be larger than the sleep power term either (i) the power ratio per event is large or (ii) active power events have higher frequency.

$$P_{avg} = \frac{(P_{sleep} \times \%time\ asleep) + (P_{active} \times \%time\ active)}{100}$$

On the other hand, one can exploit the duty cycling schemes to make a sensor node switched on/off based on network activity (traffic conditions). Duty cycling schemes can be broadly classified into three categories: on-demand, asynchronous, and scheduled rendezvous. In the interim, duty cycle-based protocols are certainly the most Energy Efficiency. Still, it should be taken into account that the low duty cycle has the capability to conserve a large big volume of energy but can lead to high communication delays. To decrease the delay, the protocol parameters can be tuned before deployment for ease, even though it may result in inflexibility, or dynamical settings can be deployed to reflect the sudden traffic conditions. Furthermore, the active period of nodes in order to optimise power consumption is a function of the traffic load, buffer runoffs, delay requirements or harvested energy.

2.2 Energy Efficient Routing Protocols

Commonly, designing of single-path routing protocol is stress-free than a multipath routing protocol. The drawback of a single-path protocol is that it swiftly drenches the energy when selected as the path. Moreover, in scenarios where a single-path protocol node is out of energy, a fresh route must be recomputed. In the interim, multipath routing creates a platform to equally re-distribute the energy among the sensor nodes by rotating the forwarding nodes. These have the capacity to increase network reliability by provisioning multiple routes, speeding up network recovering rate from a failure. For bibliophiles interested in the multipath routing protocols for WSN, a complete survey. In terms of the energy efficiency of the multipath routing protocols for WSN, the

Energy-Efficient Multipath Routing Protocol (EEMRP), emphasizes on discovering multiple node-disjointed paths based on a cost function driven by the energy levels and hop distances of the nodes, and consequently allocates the trac rate to each selected path. Furthermore, Energy-Efficient and Collision Aware (EECA), is proposed as a dual node disjointed and collision-free route considering source and sink. The results exposed that the efficiency of the multipath routing protocols in terms of the energy are better than single-path routing protocols. Furthermore, it is capable of additional improving both the Energy Efficient as well as lifetime of the WSN, if the routing algorithms are not only the function of the shortest paths, but consider the residual energy before selecting the next hop. Liu et al. proposed dual novel energy-aware cost functions to improve the energy-balancing performance of the routing protocol by considering nodes in hotspots consumes more energy:

Exponential and Sine Cost Function-based Route (ESCFR) function, maps a miniature variation in remaining nodal energy to a big variation in the cost function value. The idea of the ESCFR, operates by giving higher preference to sensor nodes having bigger remaining energy during route selection, thus creating energy equilibrium. The Double Cost Function-based Route (DCFR) protocol makes decisions by taking into deliberation the energy consumption rate of nodes, as well as the residual energy, which augments the energy-balancing enactment of the routing protocol, even in networks facing obstructions.

Regrettably, the location of the sensor nodes may deplete energy in a given region or create energy holes. However, optimal sensor node placement via uniform distribution or by including a few sensor relay nodes with enhanced capabilities can be deployed to address the issue. Commonly, this leads to energy balance improvement among the sensor nodes, avoiding hot-spots sensor nodes and assurance RF coverage and link connectivity. Plethora of research has directed on tracing the least number of sensor relay nodes or optimal sensor relay placement that will extend the network lifetime. For the time being, other studies have proposed a cluster architecture method, which organizes the sensor nodes into clusters. The motive of this approach is dependent on the cooperation among sensor nodes in the same cluster. In the interim, each cluster is managed by a selected node known as the cluster head, which is responsible for coordinating the members' activities and communicating with other cluster heads or the base station. Cluster architectures is one of the most necessary approaches to improving the Energy Efficiency of the WSN. Cluster architecture comes with many benefits, such as: improvement in WSN energy-efficiency and network scalability by sustaining a hierarchy in the network. To entirely derive these benefits, these strategies must be measured:

- i. Reduction in transmitting distance of cluster members will leads to lower transmission power.
- ii. Cluster heads prevents the transmissions frequency as a result of fusion.
- iii. Delegating the cluster head to perform all the energy-sapping functions.
- iv. Permit to power-off few cluster members even though the cluster head assumes the forwarding roles.
- v. Substitute the choice of cluster head among the nodes so as power consumption in the network.

2.3 Battery Depletion Domain

Key features of wireless sensors energy cradle such as sustainability and reliability, as well as reduction of greenhouse gas emissions can be met through advances in renewable energy technology. Furthermore, the renewable energy technology is one of the favourable ways to address the Energy Efficiency issue of WSN located in rural and remote areas. In this topographical profile, it is difficult to replace batteries due to terrestrial limitations, which makes access to these sites problematic. The solar cells have low preservation needs and high reliability, with an expected life span of 20–30 years.

Additionally, new sensor technologies have emerged that harness power from their immediate environments, such as wind and kinetic energy. The harvested energy is then converted to electrical signals, which are either consumed directly or stored for later usage. For example, using solar panels to charge a rechargeable battery during daytime. At night, nodes switch to conservative mode drawing energy from the stored power. During the conventional design stage, deliberation must be given to uneven residual energy distribution, which is the difference in the quantity of energy collected. In a case that there is no power to connect, battery life cycle capacity is formulated to calculate whether its total storing capability referenced to the magnitude of charge/discharge cycles, stated as depth-of discharge (DoD), is enough for the job.

The life cycle capacity is estimated as:

Life cycle capacity = Rated battery capacity x Rated charge discharge cycle life x DoD

For example, for the ML1220 rechargeable coin cell, the rated capacity is 17 mAh, charge discharge cycles is 1000 cycles, and DoD is 10%; thus life cycle capacity = 17 mAh x 1000 cycles x 10% per cycle = 1.7 Ah.

Renewable energy technology is related with energy estimation schemes for smart energy management. Therefore, there is the need to undertake inept energy-saving mechanisms in addition to renewable energy technology in order to achieve a high reliability status. The sensors may include dynamic behaviour tendencies in the face of the estimated energy not been able to sustain them in the next recharge cycle. Hereafter, they can optimise decisive parameters such as sampling rate, transmit power and duty cycling to adapt their power consumption according to the periodicity and magnitude of the harvestable source. On the other hand, it is admissible to allocate sensor nodes with large residual power with bigger sleep duration and shorter RF range, whereas, those with bigger residual power are selected as the desirable routing route. However, efforts have not been made to develop protocols assuming battery degradation over time (leakage, storage loss), which will impact WSN performance. The characteristics and operations of the renewable energy sources available in outdoor environmental conditions are very different from those found in indoor industrial and commercial environments.

Table 2: IoT devices/applications and their suitability for use with energy harvesting sources.

| IoT Applications | Energy Harvesting Source | | | |
|------------------|--------------------------------|----------------|-----------------|----------------|
| | Solar Panel | Wind Generator | Electromagnetic | Thermoelectric |
| Smart Home | <i>Outdoor sensor</i> | ✓ | ✓ | ✓ |
| | <i>Smart thermostat</i> | ✓ | ✓ | |
| | <i>Air quality monitor</i> | ✓ | ✓ | |
| | <i>Lighting</i> | ✓ | | ✓ |
| | <i>Security monitor</i> | ✓ | | |
| | <i>Smart door lock</i> | ✓ | | |
| Wearables | <i>Smartwatch</i> | ✓ | | |
| | <i>Monitoring and tracking</i> | ✓ | | |
| Health | <i>Medical patch</i> | ✓ | | ✓ |
| | <i>Fitness band/monitor</i> | ✓ | | |
| Industrial | <i>Factory automation</i> | ✓ | ✓ | |
| | <i>Machine monitor</i> | ✓ | | ✓ |
| Vehicles | <i>Wireless parking meter</i> | ✓ | ✓ | |

3 Conclusions

IoT has reached the attention in recent years, many researchers started to build the strong infrastructure of IOT technology. This study has provided an overview of recent research trends on energy-efficient IoT and 5G Communications, which are considered to be the two important parameters of IoT applications and cover recent industry requirements. Power Management and Power reduction techniques are vital for this infrastructure. This discussion gives some of the energy efficient techniques. Every technique has its own pros and cons over another, but the application and network which it is being used will decide which technique is the best to use on the demand of its requirements. By considering energy consumption and the required QoS, further research is required to select a proper power management mechanism that is directly related to efficiency and lifetime of the battery.

References

- [1] Arshad, R.; Zahoor, S.; Shah, M.A.; Wahid, A.; Yu, H. Green IoT: An investigation on energy saving practices for 2020 and beyond. *IEEE Access* 2017, 5, 15667–15681.
- [2] Al-Fuqaha, A.; Guizani, M.; Mohammadi, M.; Aledhari, M.; Ayyash, M. Internet of things: A survey on enabling technologies, protocols, and applications. *IEEE Commun. Surv. Tutor.* 2015, 17, 2347–2376.
- [3] Zanella, A.; Bui, N.; Castellani, A.; Vangelista, L.; Zorzi, M. Internet of things for smart cities. *IEEE Internet Things J.* 2014, 1, 22–32.
- [4] Almotiri, S.H.; Khan, M.A.; Alghamdi, M.A. Mobile Health (m-Health) System in the Context of IoT. In *Proceedings of the 4th IEEE International Conference on in Future Internet of Things and Cloud Workshops (FiCloud)*, Vienna, Austria, 22–24 August 2016; pp. 39–42.
- [5] Alsharif, M.H.; Nordin, R. Evolution towards fifth generation (5G) wireless networks: Current trends and challenges in the deployment of millimetre wave, massive MIMO, and small cells. *Telecommun. Syst.* 2017, 64, 617–637. [CrossRef]

- [6] Lee, C.-S.; Kim, D.-H.; Kim, J.-D. An energy efficient active RFID protocol to avoid overhearing problem. *IEEE Sens. J.* 2014, 14, 15–24. [CrossRef]
- [7] Tsai, C.-W.; Lai, C.-F.; Chiang, M.-C.; Yang, L.T. Data mining for Internet of Things: A survey. *IEEE Commun. Surv. Tutor.* 2014, 16, 77–97. [CrossRef]
- [8] Mukherjee, A.; Paul, H.S.; Dey, S.; Banerjee, A. Angels for Distributed Analytics in IoT. In *Proceedings of the IEEE World Forum on Internet of Things (WF-IoT)*, Seoul, Korea, 6–8 March 2014; pp. 565–570.
- [9] Gelenbe, E.; Caseau, Y. The impact of information technology on energy consumption and carbon emissions. *Ubiquity* 2015, 2015, 1. [CrossRef]
- [10] Shaikh, F.K.; Zeadally, S.; Exposito, E. Enabling technologies for green internet of things. *IEEE Syst. J.* 2017, 11, 983–994. [CrossRef]
- [11] Zhu, C.; Leung, V.C.; Shu, L.; Ngai, E.C.-H. Green internet of things for smart world. *IEEE Access* 2015, 3, 2151–2162. [CrossRef]
- [12] Miorandi, D.; Sicari, S.; de Pellegrini, F.; Chlamtac, I. Internet of things: Vision, applications and research challenges. *Ad Hoc Netw.* 2012, 10, 1497–1516.
- [13] Baliga, J.; Ayre, R.W.; Hinton, K.; Tucker, R.S. Green cloud computing: Balancing energy in processing, storage, and transport. *Proc. IEEE* 2011, 99, 149
- [14] Shaikh, F.K.; Zeadally, S. Energy harvesting in wireless sensor networks: A comprehensive review. *Renew. Sustain. Energy Rev.* 2016, 55, 1041–1054.
- [15] Akkaya, K.; Guvenc, I.; Aygun, R.; Pala, N.; Kadri, A. IoT-Based Occupancy Monitoring Techniques for Energy-Efficient Smart Buildings. In *Proceedings of the IEEE in Wireless Communications and Networking Conference Workshops (WCNCW)*, New Orleans, LA, USA, 9–12 March 2015; pp. 58–63.
- [16] Alsharif, M.H.; Nordin, R.; Abdullah, N.F.; Kelechi, A.H. How to make key 5G wireless technologies environmental friendly: A review. *Trans. Emerg. Telecommun. Technol.* 2018, 29, e3254
- [17] Rault, T.; Bouabdallah, A.; Challal, Y. Energy efficiency in wireless sensor networks: A top-down survey. *Comput. Netw.* 2014, 67, 104–122. [CrossRef]
- [18] Sinha, R.S.; Wei, Y.; Hwang, S.-H. A survey on LPWA technology: LoRa and NB-IoT. *ICT Express* 2017, 3, 14–21.
- [19] Ahmed, N.; Rahman, H.; Hussain, M.I. A comparison of 802.11 ah and 802.15.4 for IoT. *ICT Express* 2016, 2, 100–102. [Cross Ref]
- [20] Alsharif, M.H.; Nordin, R.; Ismail, M. Energy optimisation of hybrid o -grid system for remote telecommunication base station deployment in Malaysia. *EURASIP J. Wirel. Commun. Netw.* 2015, 2015, 1–15.
- [21] Chu, X.; Sethu, H. Cooperative topology control with adaptation for improved lifetime in wireless sensor networks. *Ad Hoc Netw.* 2015, 30, 99–114. [Cross Ref]
- [22] Lin, S.; Miao, F.; Zhang, J.; Zhou, G.; Gu, L.; He, T. ATPC: Adaptive transmission power control for wireless sensor networks. *ACM Trans. Sens. Netw.(TOSN)* 2016, 12, 6.
- [23] Cui, S.; Goldsmith, A.J.; Bahai, A. Energy-efficiency of MIMO and cooperative MIMO techniques in sensor networks. *IEEE J. Sel. Areas Commun.* 2004, 22, 108.
- [24] Jayaweera, S.K. Virtual MIMO-based cooperative communication for energy-constrained wireless sensor networks. *IEEE Trans. Wirel. Commun.* 2006, 5.
- [25] Cui, S.; Goldsmith, A.J.; Bahai, A. Energy-constrained modulation optimization. *IEEE Trans. Wirel. Commun.* 2005, 4, 2349–2360.

Design of Low Power Magnitude Comparator Using GDI Technique

M.Sahinipiriya¹, B. Mary Amala Jenni ², D. Umamaheswari ³

^{1,2} Assistant Professor, Department of Electronics and Communication Engineering, St.Anne’s College of Engineering And Technology, Panruti

³Associate Professor, Department of Electronics and Communication Engineering, St.Anne’s College of Engineering And Technology, Panruti

Abstract

In recent trends there is an increasing demand for portable devices which are battery operated and designing these devices with low power is very essential. Comparator is one of the most fundamental component that performs comparison operation in circuits. In this paper an efficient and low power Multiplexer based 2 bit Magnitude Comparator circuit is designed using GDI(Gate Diffusion Input) technique. This technique reduces power consumption, propagation delay, and area consumption of digital circuits at the same time maintaining low complexity of logic design when comparing with the traditional circuit. The performance analysis of proposed 2 bit magnitude comparator is compared with the existing technology. The simulations are performed in Tanner EDA tool.

Keywords: Magnitude Comparator, GDI (Gate Diffusion Input), GDI-Cmos Hybrid Design, Tanner EDA

1 Introduction

Nowadays the semiconductor industry has been exhibiting a rapid pace of performance improvements in its products by shrinking the device geometries. The electronic devices of such products need to dissipate low power in order to conserve battery life and meet packaging reliability constraints. Consequently power consumption is a dramatic problem for all integrated circuits designed today. Most of these devices are battery operated and thus power consumption has become a critical design constraint. Therefore, researchers set out to discover new methods for designing low-power electronics. Comparator is an integral part of many of the electronic circuits

Fig 1 depicts a 2 bit magnitude comparator with inputs A1, A0, B1, B0 and outputs A<B, A=B and A>B



Figure 1: 2 bit magnitude comparator

The outcome of 2-Bit magnitude comparator is shown in Table 1 for different combinations of input vectors. According to different condition of inputs, appropriate outputs are generated. The truth table for the 2 bit magnitude comparator is shown below

Table 1: Truth table of 2 bit magnitude comparator

| Inputs | | | | Outputs | | |
|----------------|----------------|----------------|----------------|---------|-------|-------|
| A ₁ | A ₀ | B ₁ | B ₀ | A < B | A = B | A > B |
| 0 | 0 | 0 | 0 | 0 | 1 | 0 |
| 0 | 0 | 0 | 1 | 1 | 0 | 0 |
| 0 | 0 | 1 | 0 | 1 | 0 | 0 |
| 0 | 0 | 1 | 1 | 1 | 0 | 0 |
| 0 | 1 | 0 | 0 | 0 | 0 | 1 |
| 0 | 1 | 0 | 1 | 0 | 1 | 0 |
| 0 | 1 | 1 | 0 | 1 | 0 | 0 |
| 0 | 1 | 1 | 1 | 1 | 0 | 0 |
| 1 | 0 | 0 | 0 | 0 | 0 | 1 |
| 1 | 0 | 0 | 1 | 0 | 0 | 1 |
| 1 | 0 | 1 | 0 | 0 | 1 | 0 |
| 1 | 0 | 1 | 1 | 1 | 0 | 0 |
| 1 | 1 | 0 | 0 | 0 | 0 | 1 |
| 1 | 1 | 0 | 1 | 0 | 0 | 1 |
| 1 | 1 | 1 | 0 | 0 | 0 | 1 |
| 1 | 1 | 1 | 1 | 0 | 1 | 0 |

A 2 bit magnitude comparator is a hardware electronic device that takes two numbers as input in binary form and determines whether one number is greater than, less than or equal to the other number by utilizing various logic gates. Truth table for 2- Bit magnitude comparator is given above, it compares two numbers A and B and gives output $A > B$ as 1, when A is having more magnitude than B and $A < B$ as 1, when B is having more magnitude than A and $A = B$ as 1, when B is having same magnitude of A

2 Literature Survey

Most of the digital circuits are generally designed using various logic styles. In existing work a 2bit Magnitude Comparator was designed using two or more trending low power techniques which are combined to form an effective circuit exhibiting low power, area and delay.

2.1 GDI-CMOS Hybrid Design

The 2 bit magnitude comparator is designed using hybrid combination of GDI and CMOS logic style. The design comprises of different logic gates designed with GDI and CMOS. Gate Diffusion Input (GDI) is a Technique in which lengthy expressions can be realized using less amount of hardware as PMOS and NMOS source/drain can be either Power rails or primary inputs or intermediate inputs or any constants with logic0 or logic1. "Basic Cell of GDI looks like a basic CMOS inverter as shown in figure 2.1^[8]

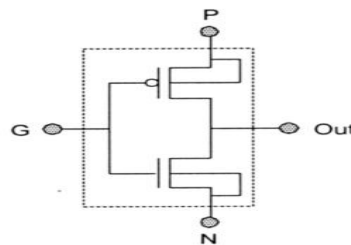


Figure 2: Basic GDI cell

G, P and N are considered as inputs to the GDI Cell

G activates at a time either PMOS or NMOS based upon the logical value applied.

N input is applied to source/Drain of NMOS

P input is applied to the source/drain of PMOS.

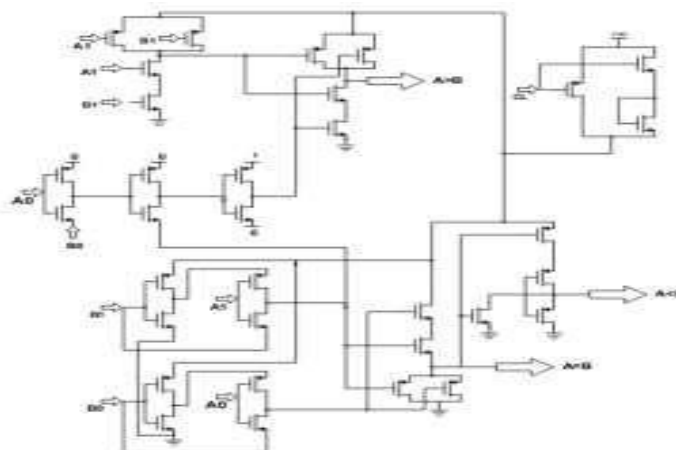


Figure 3: GDI-CMOS circuit

Despite having many advantages with GDI its performance declines when technology is scaled down and which we can expect voltage scaling and logic 0 and logic 1 regions get minimized such that noise margins become reduced. The existing design shows good performance and power reduction with the incorporation of low power technique called SVL in the design but the design consists of more number of transistors. Thus, the design occupies more area when compared to other techniques. Hence the circuit can be modified with the same operation in order to reduce the number of transistors and also reduce power and delay when compared to the existing design.

3 Proposed Methodology

3.1 Multiplexer based 2 bit comparator

Any combinational logic circuit can be designed using mux and choosing the size of mux is the concern and it will be based on the number of inputs of a circuit. Depending upon the mux size chosen the resultant hardware will vary.

3.1.1 Design for A>B

Two conditions will be there for A>B to become true so we can expect two number of product terms in which each product term represents one condition. We have chosen mux size of 4 to 1 because choosing mux size of 2 to 1 is leading to very lengthy expressions and mux size of 8 to 1 by default lead to more hardware .We have chosen inputs a1 and b1 as selection lines and it is leading to minimum hardware out of 12 possible cases. All possible cases were investigated and with choice of a1b1 has lead to minimum hardware

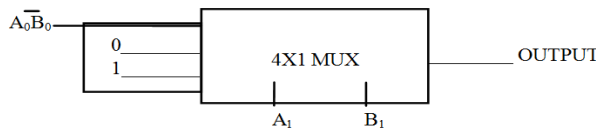


Figure 4: Design for A>B

Above figure has 4 possible cases

Case1:when A1B1=00 then substituting these values in expression 1 leaves us with A0B'0. So this evaluated expression should be passed on the top data input line.

Case2:when A1B1=01 then substituting these values in expression 1 leaves us with 0. So this value should be passed on the second data input line.

Case3:when A1B1=10 then substituting these values in expression 1 leaves us with 1. So this value should be passed on the third data input line.

Case4:when A1B1=11 then substituting these values in expression 1 leaves us with A0B'0. So this value should be passed on the bottom data input line.

3.1.2 Design for A<B

Two conditions will be there for a<b to become true so we can expect two number of product terms in which each product term represents one condition.

$$ALB = A'1 B1 + A'0 B0 (A'1 + B1) \dots \dots \dots (2)$$

We have chosen mux size of 4 to 1 because choosing mux size of 2 to 1 is leading to very lengthy expressions and mux size of 8 to 1 by default lead to more hardware. We have chosen inputs a1 and b1 as selection lines and it is leading to minimum hardware out of 12 possible cases

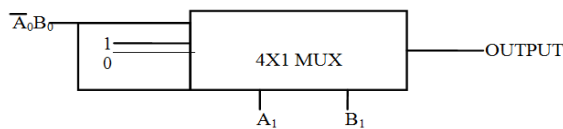


Figure 5: Design for A<B

3.1.3 Function required for the design

Total of 4 functions are required for the design which are $A > B$, $A < B$, MUX 2 TO 1 and NOR so in total 4 cells are required. Below Table shows the Total number of cells required and their Transistor count

Table 2: Transistor count of the Proposed work

| Function required | Number of cells | Total number of Transistors |
|-------------------|-----------------|-----------------------------|
| $A > B$ | 1 | 20 |
| $A < B$ | 1 | |
| MUX 2 TO 1 | 6 | |
| NOR | 1 | |

3.2 Proposed design

Total of 4 functions are required for our design which are $A > B$, $A < B$, MUX 2 TO 1 and NOR so in total 4 cells are required. Hence the logic for all the four cells are given below

3.2.1 Design for $A > B$

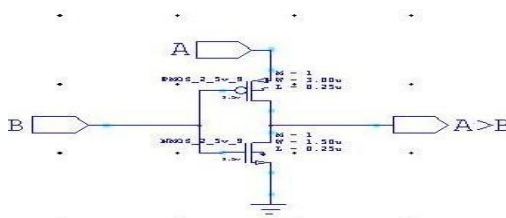


Figure 6: Design for $A > B$.

Above figure describes about $A > B$ function and it is the careful selection of where A and B has to be given.

3.2.2 Design for $A < B$

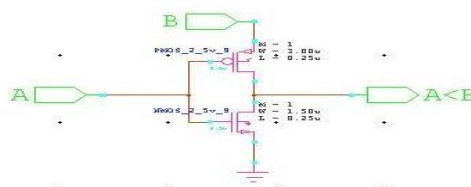


Figure 7: Design for $A < B$.

Above figure describes about $A < B$ function and it is the careful selection of where A and B has to be given.

3.2.3 Design for 2:1 Multiplexer

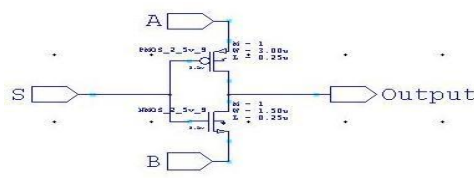


Figure 8: Design for Mux 2 to 1

Above figure describes about Mux 2 to 1 function and it is the careful selection of where A, B and S has to be given.

3.2.4 Proposed 2-bit magnitude comparator

A new Optimized Architecture for magnitude comparator is proposed with 20 transistors. Block Diagram of Proposed Modified GDI Magnitude Comparator is shown in Fig.3.6

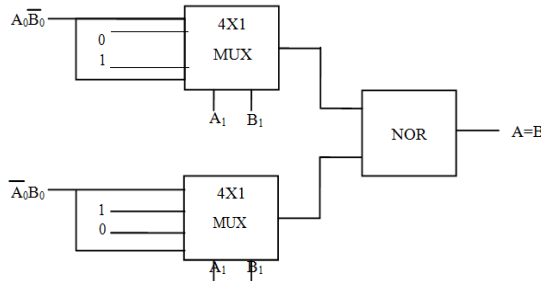


Figure 9: Block diagram of Proposed 2bit Magnitude Comparator

Above figure shows the Mux based implementation of 2-bit Comparator in which very less hardware is needed at the data inputs of the Mux. The approach was to first realize circuit in parallel for $A > B$ and $A < B$. Nor gate was needed to obtain $A = B$.

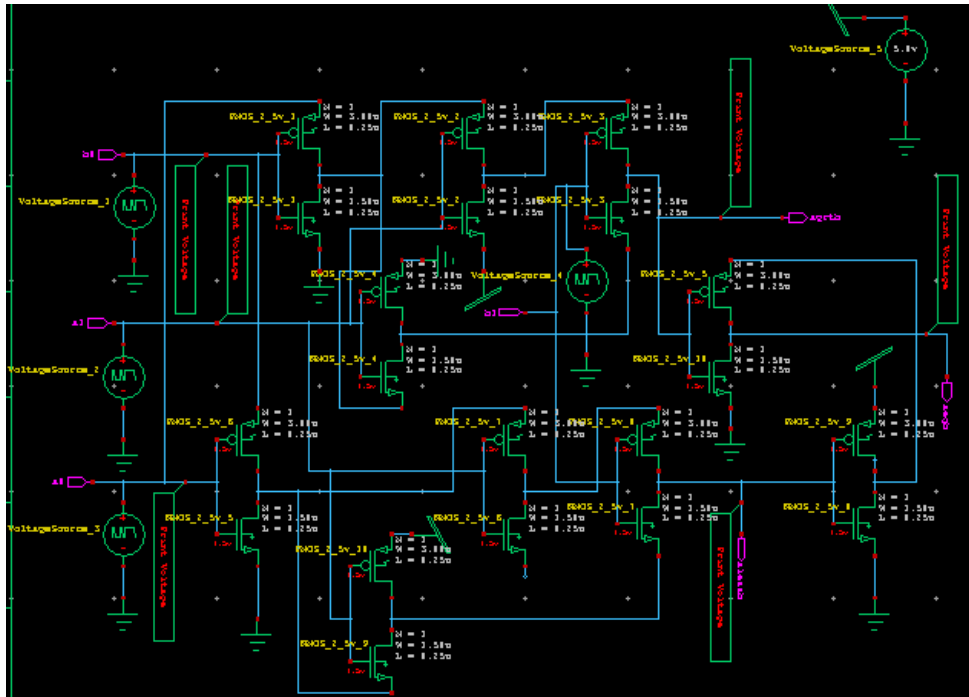


Figure 10: Design of proposed 2-Bit Magnitude Comparator

The Function ($A > B$) can be realized using Modified GDI with three Mux 2 to 1(6 transistors) and one $A > B$ cell(2 transistors) making it a total of 8 transistors. The Function ($A < B$) can be realized with three Mux 2 to 1(6 transistors) and one $A > B$ cell(2 transistors) making it a total of 8 transistors. The Function ($A = B$) can be realized using GDI with 4 transistors using NOR. The proposed 2-Bit Magnitude Comparator using modified GDI is implemented and simulated in TANNER S-EDIT in 250nm Technology. Schematic is shown in Fig. 3.7

4 Result

Simulation results for the proposed 2-Bit Magnitude Comparator using Mux based GDI is been given below.

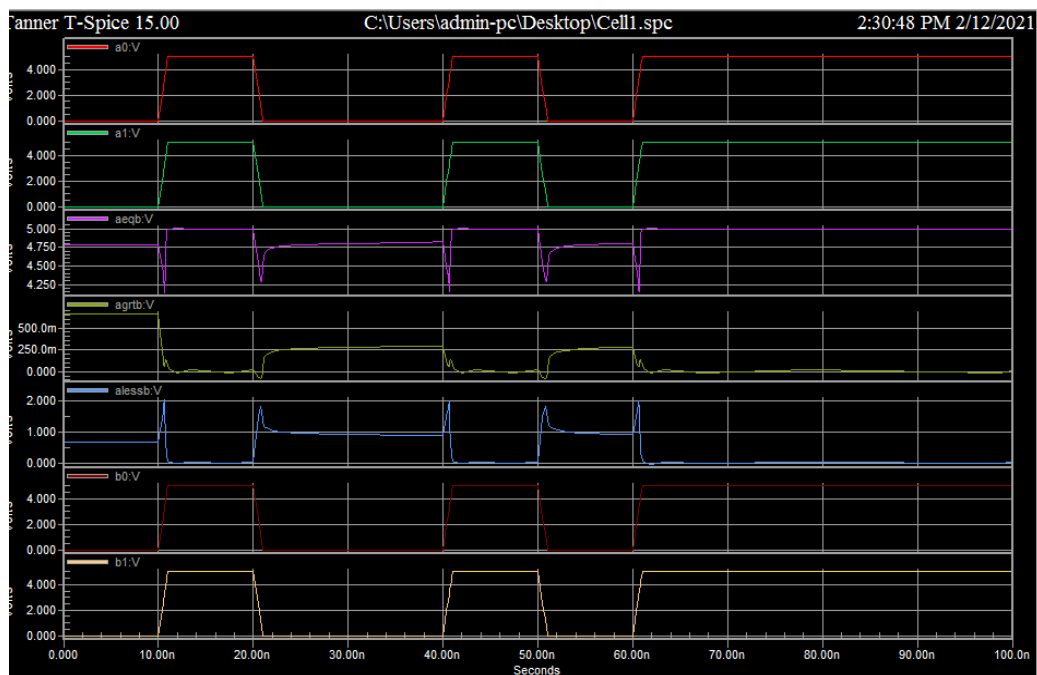


Figure 11 : Simulation results of proposed 2-Bit Magnitude Comparator

Thus the simulation result for proposed 2 bit Magnitude Comparator has been calculated and compared with the existing design. From the result transistor count, power and delay has been calculated for both the existing and proposed designs and compared. The proposed work has reduced the transistor count, power and delay when compared to the existing 2 bit Magnitude Comparator.

Table 3: Parameter comparison for existing and proposed design.

| S.No | Parameter | Existing Design | Proposed Design |
|------|-----------------------|-----------------|-----------------|
| 1 | Number of transistors | 33 | 20 |
| 2 | Average power(w) | $37.14e^{-006}$ | $19.68e^{-006}$ |
| 3 | Delay(s) | 1.54 | 1.29 |

Proposed Comparator requires only 20 number of transistors to design the circuit, thus it consumes less number of area, power and delay. Thus an optimized and efficient 2 bit magnitude comparator is being designed.

5 Conclusion and Future Work

Designing a maximum optimized VLSI circuit is never end research area. As a logic designer we need to go for many number of design iterations such that we might finally end up with a quality of design. Mux based approach is very powerful especially when designing circuits in GDI. Logic minimization has also been done and choosing the Mux size as well as selecting which inputs should be given for select lines is also a concern for maximum optimization. A innovative proposal is made for the design and implementation of 2-bit Magnitude comparator using an Enhanced GDI technique in terms of VLSI Design constraints. The proposed design using Modified GDI technique compared with Conventional design has reduction in transistor count in which equal probability of PMOS and NMOS transistors were minimized.

In future we can use other VLSI logic techniques and can design the 2bit Comparator. In this paper Mux based GDI technique is being used. The drawback of the GDI technique is that it has voltage swing at the time of operation. In future we can go for any other logic techniques which can overcome the voltage swing.

References

- [1] B. Keerthi Priya , R. Manoj Kumar “ A New Low Power Area Efficient 2Bit Magnitude Comparator using Modified GDI Technique in Cadence 45nm Technology” 2016
- [2] Conference on Advanced Communication Control and Computing Technologies (ICACCCT) 25-27 Ramanathapuram, India, May 2016.
- [3] Vijaya Shekhawat, Tripti Sharma and Krishna Gopal Sharma, “2-Bit Magnitude Comparator using GDI Technique” in IEEE International Conference on Recent Advances and Innovations in Engineering (ICRAIE-2014), Jaipur, India. pp.1-5, May 09-11, 2014.
- [4] Pankaj Verma, Ruchi Singh and Y. K. Mishra “Modified GDI Technique-A Power Efficient Method For Digital Circuit Design” International Journal of Electronics and Computer Science Engineering, 2014.
- [5] H.-M. Lam and C.-Y. Tsui “High-performance single clock cycle CMOS comparator” IEEE International Symposium on ISCAS 2006, Vol. 42 No. 2, pp.782, May 2006.
- [6] Hing-Mo Lam and Chi-Ying Tsui “A MUX-based High-Performance Single-Cycle CMOS Comparator ”IEEE Transactions On Circuits And Systems—II: Express Briefs, Vol. 54, No. 7, pp.591-595, July 2007.
- [7] Vandana Choudhary, Rajesh Mehra, “2-Bit CMOS Comparator by Hybridizing PTL and Pseudo Logic,” in International Journal of Recent Technology and Engineering (IJRTE) ISSN: 2277-3878, Volume-2, Issue-2, May 2013.
- [8] Anjuli, Satyajit Anand, “2-Bit Magnitude Comparator Design Using Different Logic Styles” International Journal of Engineering Science Invention ISSN (Online): 2319 – 6734, ISSN (Print): 2319 – 6726 www.ijesi.org Volume 2 Issue 1 PP.13-24, Jan 2013.
- [9] Arkadiy Morgenshtein', Alexander Fish2 and Israel A. Wagner, “ Gate-Diffusion Input (GDI) – A Technique For Low Power Design Of Digital Circuits: Analysis And Characterization” Proc. IEEE ISCAS ,pp. 1477 - 1480 vol. 2002

Real Time Fabric Flaw Detector Using Arduino

A. Selvarasi¹

¹Assistant Professor, Department of Electronics and Communication Science,
Alpha College of Engineering, Chennai, India

Abstract

Textile industries are one of the most growing and competitive markets worldwide and form a major part of manufacturing, employment and business operations in several developing countries. Among the numerous failures faced by textile industries, fabric flaws constitute more than 85%. So extra efforts are taken in manufacturing improved quality of fabrics. Defects in textile fabric are a major threat to textile industries. So, defect detection becomes an essential step in the manufacturing process of textiles. But the process of detection of fault in fabrics includes only manual inspection strategy. This traditional human visual inspection leaves the process to be inefficient and time consuming. These methods employed so far were time complex and less effective. So, automation in this process through image processing technique is introduced later. The image processing technique is used to spot the faults as simulation output and Arduino kit is used for fault detection. Here automated fabric inspection system has been proposed to enhance the accuracy of fabric defect detection. This system is made using MATLAB with image processing techniques and this idea is implemented on Arduino kit for real time applications. Neural Networks with Back Propagation algorithm is used as a finest classifier for classification of faults. Recently, Arduino has become a liable target for the execution of algorithms suited to Microcontroller based processing applications. Whenever the software notices a defect in the fabric it sends a signal to the microcontroller and it halts the system for a while to eradicate the flawed fabric part. And the buzzer is switched ON then the detected fault is displayed in the LCD. And the speaker will give the voice alert after noticed the fault.

Keywords: *Arduino, Fabric Fault classification, Image processing, MATLAB, Morphological operators.*

1 Introduction

Textile industries are one of the fastest growing and competitive markets worldwide and form a major part of production, manufacturing, employment in many developing countries. S. L. Bangare et al. (2017) [13] described that the textile industry internationally has experienced dramatic technological changes during the last few decades. The changes have increased both yield and quality of fabrics, apart from reducing expenses and labor cost. This paper work focuses on proposing real time flaw detector to detect defects from fabrics.

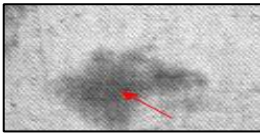
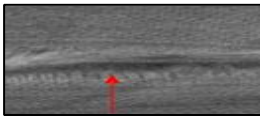
2 Objective




- The purpose of this paper is to improve the fabric quality level by detecting major defects during production with reduced computational cost and time.
- Elimination of human drawbacks such as errors and/or subjective judgment.
- Increasing the manufacturer's credibility
- Elimination of labor problem.

3 Fabric Defect and Its Types

Selvarasi A et al. (2015) [11] and Aqsa Rasheed et al. (2020) [15] defined some of the fabric defect types are listed in Table 1.

Table 1: Table for most common defects appear in more or less extended areas

| S. No | Defect Name | Defect Definition | Defect Image |
|-------|-------------|---|--|
| 1 | Oil Spot | A fabric area contains oil spots. It is caused by too much oiling on loom parts or from other external sources. It is shown in below Fig. 1 |  <p>Figure: 1 Oil Spot</p> |
| 2 | Scratch | Damaged fabric portions differ from holes in that it has a random uneven shape. It is shown in below Fig. 2 |  <p>Figure: 2 Scratch</p> |

| | | | |
|---|--|---|---|
| 3 | Irregular pick density or Broken picks | It is a mechanical fault caused by an irregular beating up force. It is shown in below Fig. 3 |  Figure: 3 Irregular Pick Density or Broken picks |
| 4 | Float | A portion of a yarn in a fabric that extends or floats, unbound, over two or more adjacent picks. It is shown in below Fig. 4 |  Figure: 4 Float |
| 5 | Hole | A fabric area free of both of warp and weft threads. It can be happen due to the sharp edge of machine parts. It is shown in below Fig. 5 |  Figure: 5 Hole |

4 Detection Algorithm

The proposed system for software design is shown in Fig.6. It consists of various stages.

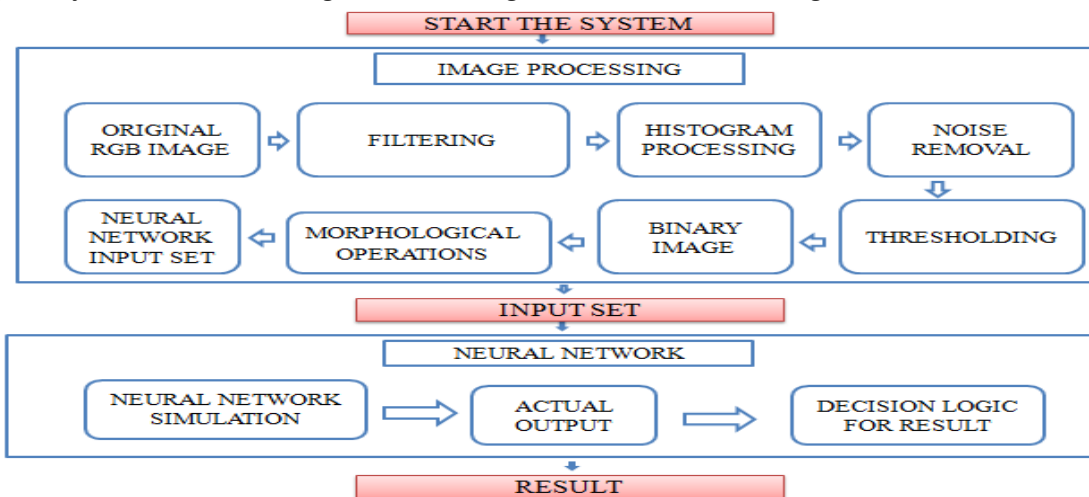


Figure 1: Block diagram

4.1 Image acquisition

Shalaka Subhash Patil et al. (2018) [14] described that the Textile/fabric image is acquired by using the CCD camera from top of the surface from a distance adjusted so as to get the finest probable view of the surface. Basically, the images are attained at RGB color scale.

4.2 Filtering

The impulse noise is the most commonly referred type of noise. This noise, generally known as salt & pepper noise, is produced by malfunctioning pixels in camera sensors. Median filtering is considered as popular method

4.3 Histogram processing

A histogram is a graphical representation of the distribution of data. A histogram output obtained from the overall processing is used for drawing the conclusions for fault classification.

4.4 Noise removal

Digital images consist of many types of noise. Noise is the outcome of faults in the image acquisition process. This phase basically deals with the removal of external noise and disturbances in the image.

4.5 Thresholding

As binary images are easy to operate, other storage format images. The purpose of thresholding is to abstract those pixels from some image which represent an object.

4.6 Binary image

Jagruti mahure et al. (2013) [7] described that it is a digital image that has only two possible for each pixel. Typically, two colors used for a binary image are black and white. Each pixel stored as a single bit i.e., 0 or 1.

4.7 Morphological operations

Morphological image processing is an assembly of non-linear operations associated to the shape or morphology of features in an image.

4.8 Training and classification

Dr.G.M.Nasira et al (2013) [8] described that Artificial neural network are inspired by the animal's central nervous systems, are presented as systems of interconnected neurons and used to approximate unknown functions.

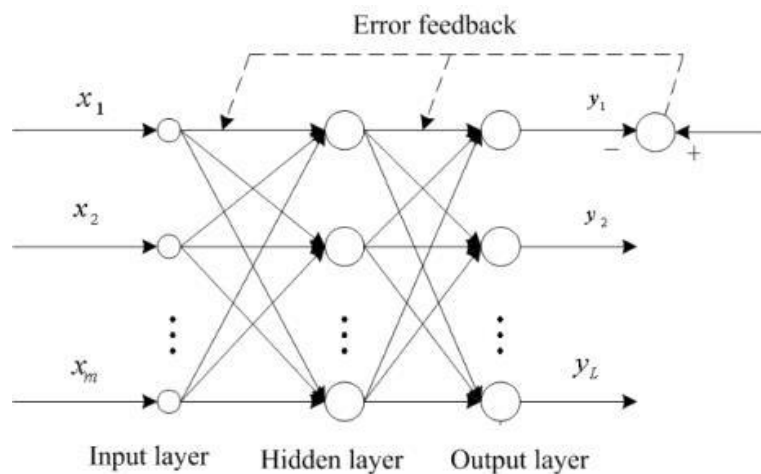


Figure 2: The BP neural network structure

The design of BP neural network is to determine the number of layers, the number of neurons in each layer and various parameters. The structure is illustrated in Fig.2

5 Simulation Result and Discussion

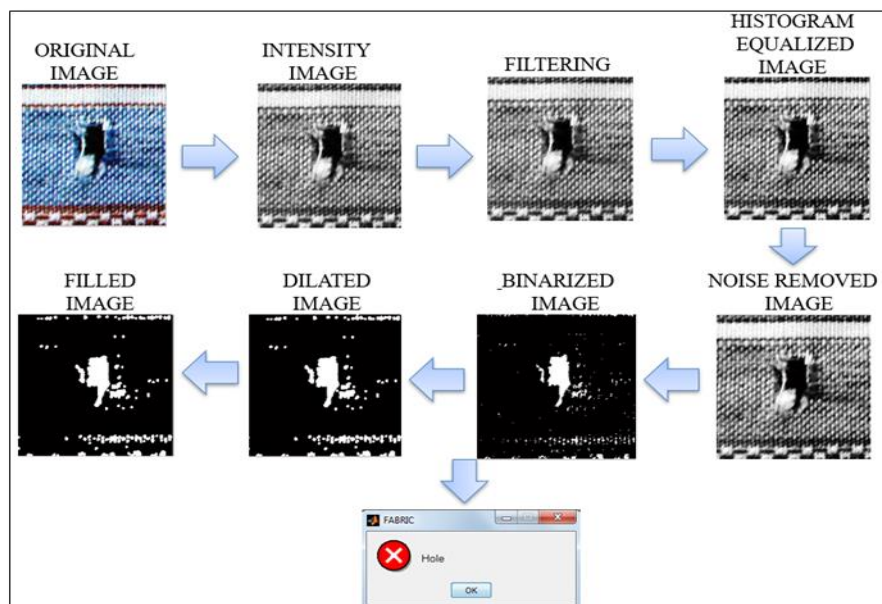


Figure 3: Various stages during processing an input image and Simulation Result.

The first step in the proposed work is to acquire the fabric using the digital camera from the textile industry (Maya garments, Tirupur) and the image is stored in computer as PNG format. The capture image of defect fabric is shown in Fig. 8.

In sample image of the defect fabric, the color of a pixel is made up of red, green, and blue (RGB). It can be explained based on its pixel intensity values. RGB color image require large space to store so it is converted to gray value. After gray scale conversion Fig. 8(Intensity Image) is obtained.

The preprocessing is used to remove the noise of an input image. H. Ibrahim et al. (2013) [10] says that Filtering in image processing is a process that cleans up appearances and allows for selective highlighting of specific information. The image obtained after the filter is shown in Fig. 8(Filtering).

Dr.R.S.Sabeenian et al. (2011) [9] suggested that Histogram equalization (Fig.8 –Histogram Equalized Image) is a method for stretching the contrast by uniformly distribution the gray values enhances the quality of an image. It enhances the contrast by transforming the values in an intensity image.

With the removal of external noise and disturbances in the image that is given in Fig. 8(Noise Removed image).

The noise of the image is being totally removed in the noise removal part of the system. The next step after the noise removal from the fabric image is the conversion of the noise removed image to the binary image (Fig. 7- Binary image) of the original image.

Then the morphological operations are done on the above binarized image to find the structure of the fault. Dilation (Fig.8 – Dilated Image) is the process of enlarging the boundaries of foreground image.

Then the output window is show in Fig 8.

6 Hardware Implementation

The block diagram of hardware module in Fig.9

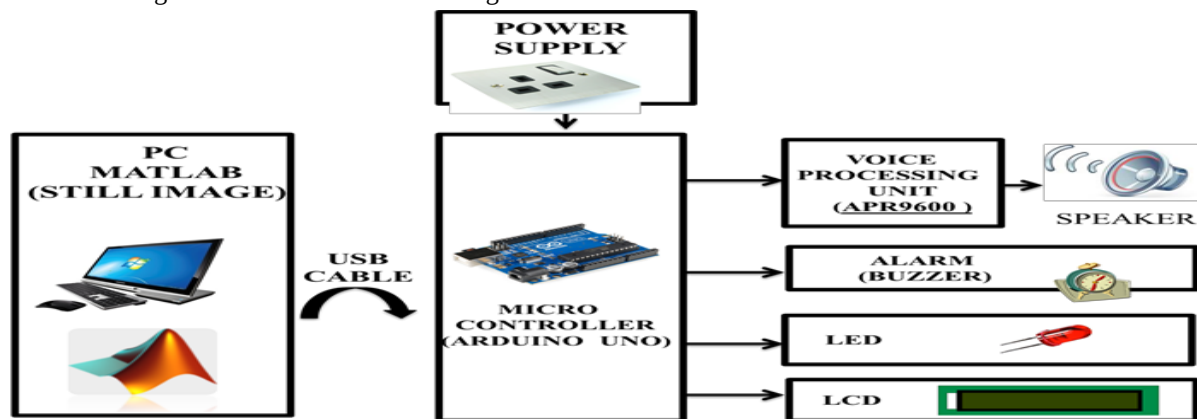


Figure 4: Block Diagram

6.1 Buzzer

Ms. A. Selvarasi (2016) [12] described that a buzzer or beeper (Fig.10) is a signaling device.

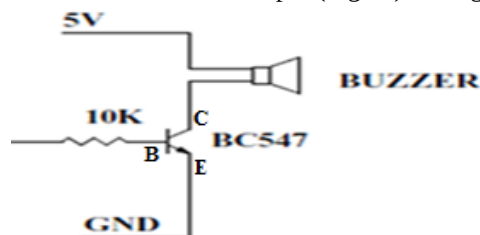


Figure 5: Buzzer Diagram

Above circuit is designed to regulate the buzzer. The buzzer ON and OFF is regulated by switching transistor (BC 547). When high pulse (5 Volt) signal is given to base of the transistor, the Buzzer will ON. When low pulse is given to base of transistor, it will turn OFF.

6.2 Arduino

The Arduino Uno is just a microcontroller based on the ATmega328. This Arduino software is flexible enough for advanced users.

6.3 LCD

LCD (Liquid Crystal Display) screen is an electronic display in that 16x2 LCD is used here. A 16x2 LCD means it can show 16 characters per line and there are 2 such lines.

6.4 Power Supply

The ac voltage(220V) is connected to a transformer, which steps that ac voltage down to the level of the desired dc output.

6.5 LED

An LED is a flat panel display which practices an array of light emitting diodes as pixels for a video display.

6.6 APR9600 Re-Recording Voice IC

It is a Single-chip, high-quality voice recording & have playback solution. This device supports both random and sequential access of multiple messages.

7 Arduino Kit Interfacing

The Arduino kit is interfaced with PC as shown in Fig. 11.

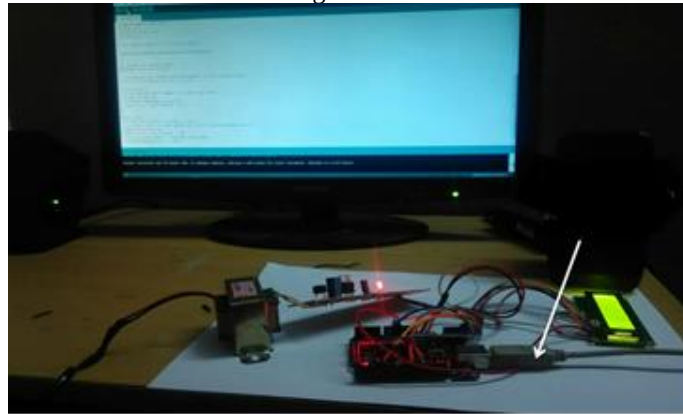


Figure 6 : Arduino kit is interfaced with PC using RS 232 Cable

7.1 Steps for upload file to Arduino

1. Load file -> Blink into IDE
2. Make sure you select the correct board
3. Tools -> Board -> Uno
4. Make sure you select the correct serial port
5. Click on the upload button

Once we upload the file, we get the buzzer sound, LED blinking, voice output of the detected fault and the detect fault will be displayed in the LCD. The screenshot of the outputs is shown in below Figures 12,13,14,15 and 16.

Oil Spot:

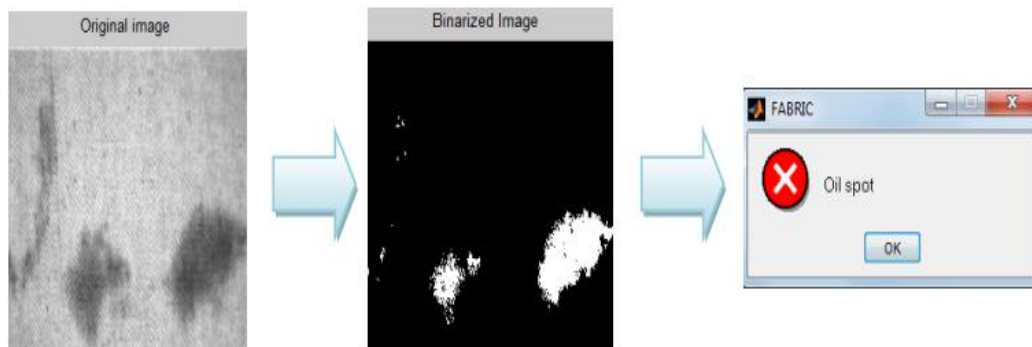


Figure 7: Input , Binarized image and Output window of oil spot

Scratch:

Figure 8 : Input , Binarized image and Output window of Scrath

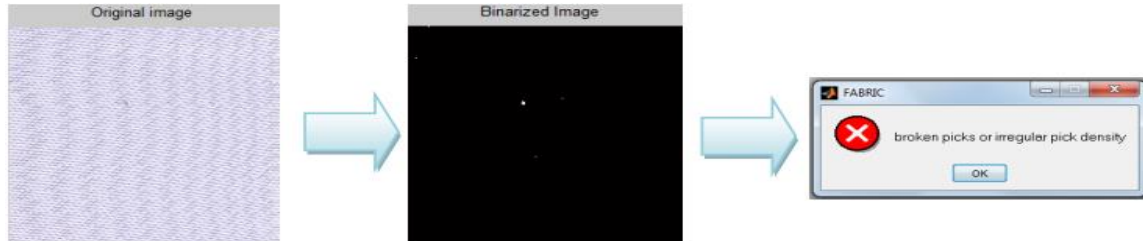
Irregular Pick density or Broken Picks:

Figure 9 : Input , Binarized image and Output window of Irregular Pick density or Broken Picks

Float:

Figure 10: Input , Binarized image and Output window of Float

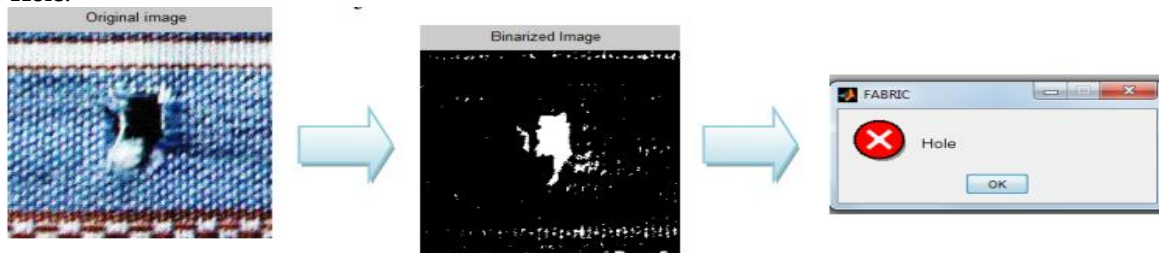
Hole:

Figure 11: Input, Binarized image and Output window of Hole

8 Conclusions

In this paper, a new intelligent fabric defect inspection model is presented. The recognizer acquires digital fabric images by image acquisition device and converts that image into binary image by morphological operators along with filtering & histogram equalization is used for fault detection. The proposed algorithm in this paper detects 5 different types of faults unlike the existing algorithm. Further the method is extended by using neural network as classifier for classification of defects based on the output. Thus, this method helps in both detection of faults as well as the classification of various types of faults. This method would serve as a boom for fabric industry for quality production. This is done as a simulation for a still image. Whenever the software notices a fault in the fabric it sends a signal to the microcontroller and it stops the system for a while to eliminate the defective part of the fabric. The buzzer is switched ON and the detected fault is displayed in the LCD. The speaker will give the voice alert of the detected fault.

References

- [1] Dorrity J., Vachtsevanos G. and Jasper W.: Real-time fabric defect detection and control in weaving processes, National Textile 1995, pp. 143-152.
- [2] Kumar A.: Computer vision-based fabric defect detection: a survey, IEEE, Transactions on Industrial Electronics, Vol. 55, Issue 1, 2008, pp. 348-363.
- [3] Mahajan P.M., Kolhe S.R. and Pati P.M.: A review of automatic fabric defect detection techniques, Advances in Computational Research, ISSN: 0975–3273, Volume 1, Issue 2, 2009, pp.18-29.
- [4] Mitropoulos P., Koulamas C., Stojanovic R., Koubias S., Papadopoulos G., and Karagiannis G.: A real-time vision system for defect detection and neural classification of web textile fabric, Electronic Imaging '99 International Conference, January 23-29, 1999.
- [5] Malamas E.N., Petrakis E.G.M., Zervakis M., Petit L. and Legat J.D.: A survey on industrial vision systems, applications and tools, Image and Vision Computing, Vol. 21, 2003, January pp.171
- [6] Priyanka Vyas, Manish Kakhani “Fabric Fault Processing Using Image Processing Techniques” International Journal of Multidisciplinary Research and Development 2015. 2(2): 29-31.
- [7] Jagruti mahure1 & Y.C. Kulkarni2 “Fabric Faults Processing: Perfections And Imperfections” International Journal of Computer Science and Technology (IJCST) ISSN: 0976-8491 (Online) | ISSN: 2229-4333 (Print) Vol.4, Issue 2, April-June 2013.
- [8] Dr.G.M.Nasira1, P.Banumathi2 “Plain Woven Fabric Defect Detection Based On Image Processing And Artificial Neural Networks” International Journal of Computer Trends and Technology(IJCTT) – volume 6 number 4–Dec 2013.
- [9] Dr.R.S.Sabeenian 1, M.E.Paramasivam 2 and P.M.Dinesh3 “Detection And Location of Defects In Handloom Cottage Silk Fabrics Using MRMRFM & MRCFSF” IJTE jan 2011 vol2 pp.1-21
- [10] H. Ibrahim, L. Canan, Mehmet. Developing An Algorithm For Defect Detection of Denim Fabric: Gabor Filter Method Tekstil Ve Konfeksiyon 23(2), 2013.
- [11] Mrs.J.Rajalakshmi and Miss.A.Selvarasi .An Hybridized Algorithm for Fabric Fault Detection International Journal of Research in Engineering, Science and Technologies(IJRESTs) Vol.: 1 No.:3.,2015
- [12] Ms.A. Selvarasi. An automated fabric fault detection using a microcontroller i-manager’s Journal on Pattern Recognition, Vol. 2 | No. 4 | Dec 2015 - Feb 2017
- [13] S. L. Bangare1 , N. B. Dhawas2 , V. S. Taware3 , S. K. Dighe4 , P. S. Bagmare5. Fabric Fault Detection using Image Processing Method IJARCCCE ISSN (Online) 2278-1021 ISSN (Print) 2319 5940 International Journal of Advanced Research in Computer and Communication Engineering ISO 3297:2007 Certified Vol. 6, Issue 4, April 2017
- [14] Shalaka Subhash Patil1 , Dr. V. T. Gaikwad2 .Defect Detection in Fabric using Image Processing Technique International Research Journal of Engineering and Technology (IRJET) e-ISSN: 2395-0056 Volume: 05 Issue: 12 | Dec 2018 www.irjet.net p-ISSN: 2395-0072

Smart Health Tracking Band – A Curator for Well Being

Mr. Pravin Savaridass M¹, Praveen C², Rakshith J³, Pavithra N⁴, Praveena N⁵, Kapil Yaswanth S B⁶

¹Electronics and Instrumentation Engineering, Bannari Amman Institute of Technology, Erode, India

^{2,3}Information Technology, Bannari Amman Institute of Technology, Erode, India

^{4,5}Electronics and Communication Engineering, Bannari Amman Institute of Technology, Erode, India

⁶Computer Science and Engineering, Bannari Amman Institute of Technology, Erode, India

Abstract

In the current world, discovering time to see the specialist to affirm your wellness is not really conceivable. Due to the increase of COVID-19 cases across the world day-by-day, it is difficult to treat a huge number of patients in hospitals. In order to wither the viral infection rate and to monitor patient's health who stay in hospitals; also to monitor the patients who are in need of home hospitalization, this integrated sensor network is quite helpful in various aspects. This paper proposes about the monitorization of bed-ridden patients or who can't approach a caretaker, with the smart health monitoring band which is embedded with the sensors that are helpful in tracking the health condition of the patient. This system plays a great evolutionary role in the healthcare sector to relax the mental health of patients as well as the doctor's stress level.

Keywords: *Hospitalization at homes and clinical centers, Smart wearable band, Integration of sensors, Ease of patient's health monitorization*

1 Introduction

Wearable innovation impacts the everyday life of its clients. The medical electronic sensors integrated within the band plays a significant role in monitoring the patient's health system. Implementation of this proposal is for the monitorization of patients or who can't move toward a guardian, so this band integrated with sensors provides a solution for the problem. Due to the continuous tracking of body temperature, oxygen level in the blood and heart rate, it is also possible to unmask silent hypoxia which is known to be the earliest symptoms of coronavirus entry into the human body. The sensors that are embedded within the band to track the patient's health status include ultrasonic sensor, temperature sensor, buzzer module, controller, LCD display. This band not only helps the patients affected with some health issues but also serves as a helping hand to any person who aren't able to seek help from a doctor at an immediate instance which means they themselves can come to know about their health status at any required situation. The important message to be noticed is that the authorized doctor who monitors the patient's health status in a digitalized mode can access the particular patient's medical data from anywhere at any needy situation. Also, these sensors work in a mannerism by sending intimation to the authorized person when the integrated parameter value exceeds the threshold range. The required data can be viewed in the display of the wearable band at any instance by the person who togs it. This band plays a major part during home hospitalization too. At the time of abnormal conditions in the parameter values that are set to a limited cut-off range, this band makes an alert intimating to the authorized person that the particular person is in need of immediate medical assistance.

2 Literature Survey

The utilization of sensor networks in medical care applications is expanding day by day because of the different sensors integrated in it, which is helpful in remote health monitoring and most probably in elderly care. For this purpose, a wearable medisuit is designed for measuring different physiological parameters which includes temperature, heart rate, pulse rate and tiltations, so that it gives the alert messages to the authorized person during variations in parametric values. This concept has been a main source to make a blend of these sensors into a source like band. Unlike other sensor networking technologies, the unique part which has been implemented into this paper is about the ultrasonic sensor's manipulation. Generally, the ultrasonic sensor measures distance of the object irrespective of its colour, shape and texture. But providing an alert to the respective person or the caretaker, during the detection of an object or person nearby to them, all the time is unnecessary and it creates an irritation and disturbance to the person too. In order to ignore this issue, an ultrasonic sensor with a combination of gyroscope and accelerometer is used to sense the bodily motions of the person who is tied with these wearable sensors and provide an alert only when the patient is in movemental progress and indicates the person to maintain social distance accordingly. The detection of every sensible movement and the fall of patients are monitored very keen. Implementation of this technology becomes the advantageous part of this paper. Aggregation of all these sensors together play an important role for monitoring

patient's health parameters and makes an forewarning during their abnormal condition and report their health status to the respective person or caretaker, so that necessary medical help could be made to the patient subsequently.

3 Methodology

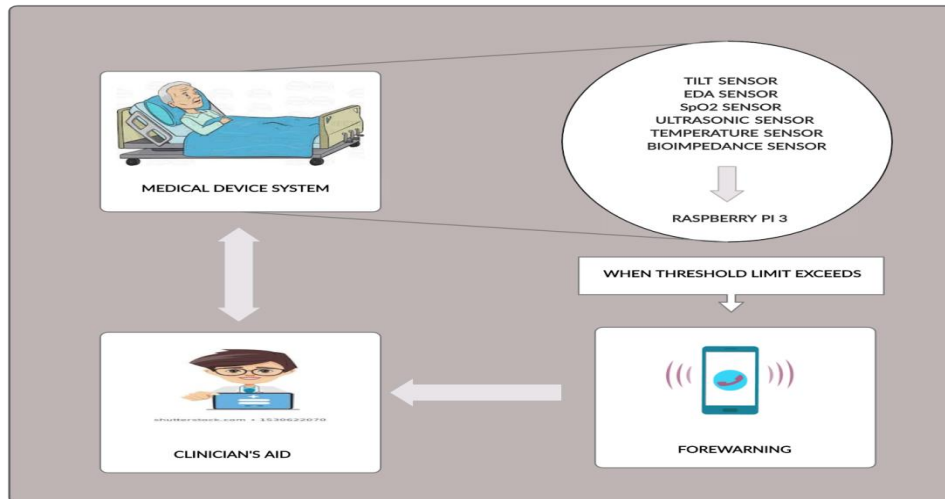


Figure 1: System architecture diagram

The proposed system is a band-based device in which a count of sensors are incorporated together to the raspberry pi centered to receive and transfer the data. The architectural scheme of the entire proposal will be justified here.

3.1 Pulse oximeter

Cardiac changes are the fundamentals that progress in our body. Heart is the important organ that is maintaining the circulation of nutritious enriched blood and oxygen. When an irregular routine of alteration occurs, there might be great risk. One of such an irregular unusual metric may result in COVID-19 existence.

3.2 Heart rate

The heart beat is the key factor of the human body that is essential for the circulating blood and other vital nutrients. The elderly people are the most concerned. As their body gets weaker, the oxygenation and deoxygenation would vary than the normal. Heart beat is the central process, because this process is directly connected to the count of heart beat rate and amount of blood pumped out. BPM (Beats Per Minute) is the count of heart beats in a minute. An usual heart beat rate is calculated of 60-100 in a minute. It is nothing but the sound of the heart valves that occur during the contraction and expansion during the blood flow. An anomalous variation with increased or decreased rate may bring forth several problems. An increased heart rate of counts above 100 offshoot as tachycardia (fast heart). And a decreased heart rate below 60 outgrowths as bradycardia (slow heart). An integration of pulse oximeter and heart rate monitoring sensor solution MAX30100 pulse oximeter is accustomed. Whenever a heart beat occurs the capillaries volumes up with a slight more amount of blood and volumes down a bit in between the heartbeats. Such a change in this flow influences the amount of light when passed through the tissue. The method of photoplethysmography is proposed that monitors the volume of the blood that flows when the finger is placed in between the device. The concept is that when the finger is illuminated with a light source it either transmits or reflects the light. Also some amount of light is absorbed by the blood, depending on the tissue volume in that region. The rest which have been unabsorbed are beholden by the receiving sensor diode. It possesses a slight variation which can be sensed by the pulse oximeter and the heart beat rate can be calculated.

3.3 SPO2 sensor

SpO₂ is the estimation of oxygen in the hemoglobin, primarily the arterial oxygen. A similar way in which heart rate is obtained can also be used for measuring oxygen saturation level. The oxygen content can be evaluated by placing the finger in centered between the light source like a LED that emits light and a receiving detector to measure how much light passes through. When a path of light is passed over the finger, the blood absorbs a amount of light. But there will occur a variation in the wavelength when passed through the oxygenated, which absorbs more IR light and allows more light to pass through and deoxygenated blood, which does not absorb more IR light and does not allow more light to pass through. The transmitted light which is left unabsorbed are measured. Its outcome is then inverted and the absorbed amount is calculated.

3.4 Ultrasonic sensor with MPU6050 and vibration sensor

The COVID_19 pandemic has ruined our regular routine. In these conditions all are advised to practice a distancing pattern to ensure safety. By bringing into play ultrasonic sensors in our ideology, we can provide additional support by a non-contactable methodology. The movement of a person cannot be monitored throughout in all conditions. Since the ultrasonic sensor is used to alert us we must also keep an eye over the positioning of the person. In such conditions it is necessary to track their physical movements. MPU6050 is spied here, which measures the velocity, acceleration and displacement of their movement, orientating angle and also other motion like activities. When any such activities occur MPU6050 transfers signals to pi. Then the pi makes the ultrasonic sensor to activate. The ultrasonic sensor works by emitting ultrasonic sound waves and converting the reflected sound into an electrical signal. It is used to measure the distance of a target object. These waves move faster than audible sound that humans can hear. HC SRO4 is used here. It is capable of measuring from a wide range of 0.02 m to 4 m. A DC Vibration Sensor is accustomed to warn with vibrations. Generally, the ultrasonic sensor measures distance of the object and provides an alert to the respective person by detecting the object or person nearby to them. In order to ignore the detection of objects unnecessarily, the ultrasonic sensor is combined with a gyroscope and accelerometer. They are used to sense the bodily motions of the person and indicates the person to maintain social distance accordingly. The distance can be calculated by measuring the time it takes between the emitted sound from the transmitter to its concerned object or person with the receiver.

3.5 Temperature sensor

For a well routine life, a proper concentration of our physical health is unavoidable. One of those is our body temperature. Maintaining our body in a normal condition is a must. Implementation of a temperature sensor will be necessary in order to monitor the temperature. An IR based temperature sensor is incorporated here. The normal body temperature ranges from 97°F (36.1°C) to 99°F (37.2°C) and temperature monitoring sensor used here. It is an advantage that it provides non-contactable sensing. It is capable of monitoring temperature ranging from -40 to 125°C for ambient temperature and from -70 to 382.2 °C for the object temperature.

3.6 Light sensor

The Ambient Light Sensor (ALS) is used to measure the ambient light intensity which resembles the human eye's response to light for various conditions. It is a photo detector device, measuring the ambient light required and alters the intensity of the display. This is the photometry used for measuring the intensity when light passes through the eye. These techniques are mostly used in smartphones to reduce the additional consumption of battery. Similarly by incorporating the ALS, the power consumption of LCD displays can be reduced.

3.7 Bio-impedance sensor

The bioimpedance sensor works by measuring the resistance on the skin by taking the electricity provided by it. By providing a small amount of current the electrodes measure the sleep, heart rate, respiration rate, water level, intracellular and extracellular water, lean mass, fat mass. Along with the usage of four electrodes, it drives a part of electrical energy and measures the result.

3.8 EDA sensor

EDA measures the electrical properties of the skin when changed. The alterations in sweat secretion and sweat gland activity results in changing of the sympathetic nervous system activity. Due to these changes, the autonomic nervous system is highly triggered, then sweat gland activity also increases, which causes an increased skin conductance. EDA (Electrodermal activity or galvanic skin response or GSR) measures the stress by detecting the electrical changes in the sweat level of the skin.

3.9 Raspberry pi controller

All the sensor data outputs are collected and compared together in this pi microcontroller unit. Whenever the monitored value is breakthrough the threshold limit alerts are accompanied. An SD card provided that acts as the hard drive. All the data is stored here, since it is like a mini-computerized device. By USB port we can transfer the data and store them for later uses, which would be also an advantage for the doctors to analyze their reports.

3.10 Forewarning

The LCD display of the values can be viewed, which are being currently updated. Whenever the threshold value of the sensors altered the pi alerts by blinking of LED.

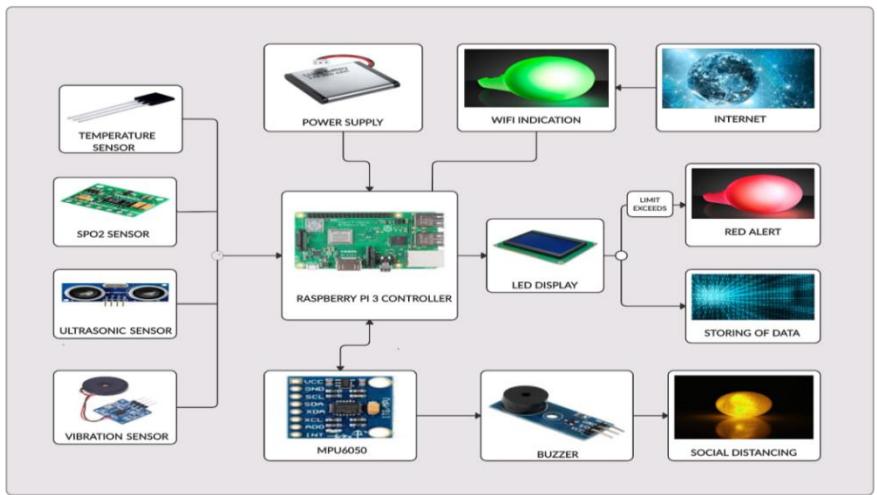


Figure 2: Components integrated in sensor network

4 Implementation

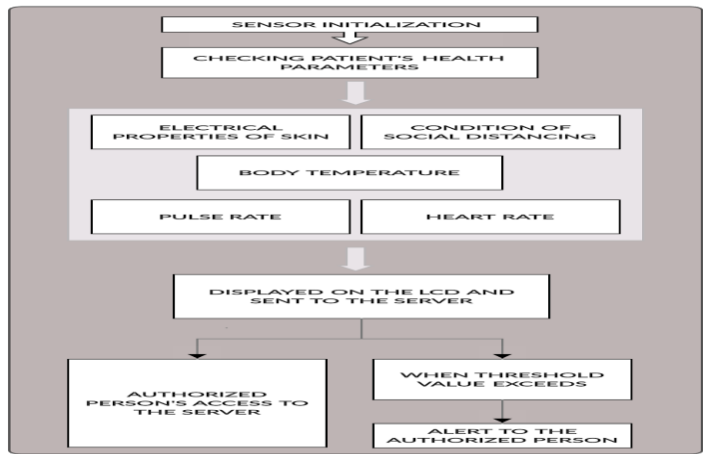


Figure 3: Algorithm proposed for healthcare system

Integrating sensors becomes a prominent solution. The sensors are integrated to form a band. Blood oxygen level, heart rate, pulse rate, social distance and body temperature are the foremost factors of the sensors that will continuously monitor the patients. In order to measure the electrical properties of the skin, EDA and bioimpedance sensors are incorporated into the sensor network. Ultrasonic sensor helps to maintain social distance which takes the guidance of the gyroscopic and accelerometric values, to ensure that the person is maintaining social distance. Active buzzer module is controlled programmatically by tweeting sound output to high-mid-low when threshold limit exceeds raspberry pi activates this buzzer. The bodily motions like acceleration, velocity, orientation and displacement of the patient are monitored and the values of these data are compared with the normal range. LCD displays the patient's dynamic data digitally. Raspberry pi 3 is the controller used to explore computing, which enhances speed in computing with built in Wi-Fi and bluetooth for wireless communications. When the threshold value gets limited the alerts raised by the pi controller rushes up the alerts by buzzing and blinking of LED. All the analysis observed by the sensors are collected and fed to the server, which stores the data. In case of medical checkups and later use, the data can be retrieved from the firebase (ie) database and used for future reference.

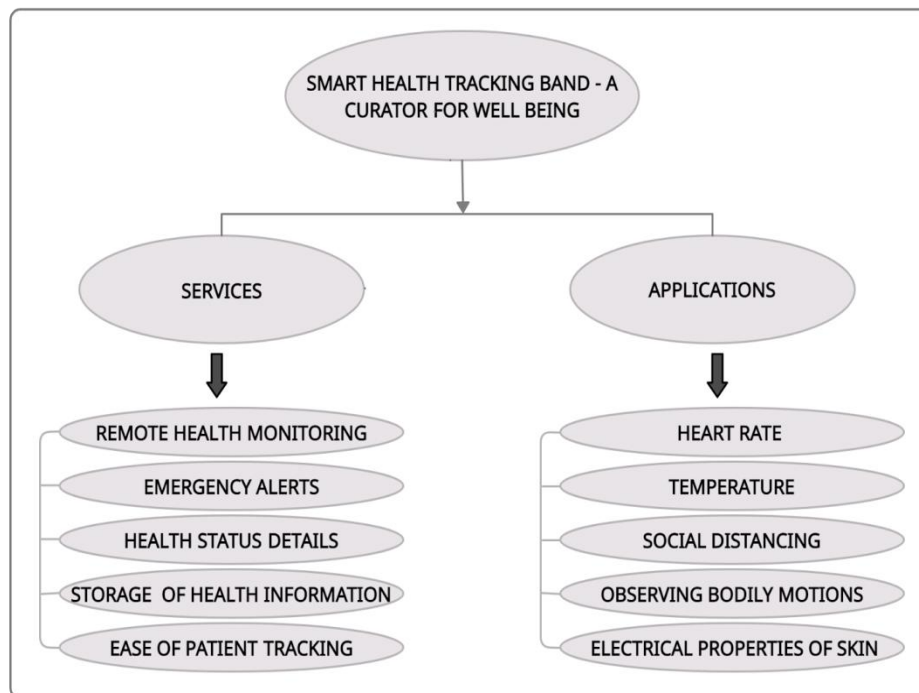


Figure 4: Services and applications of the wearable gadget

5 Results and discussion

Carrying out this technology to track a patient's physiological parameters improves the quality of care since at any time of deformity in parametric values, an alert will be sent to the caretaker and so the practitioner will provide the necessary help to the patient at the particular instance. This system is helpful in providing proper medical assistance in a quick manner with easy access and continuous monitoring of patients is not required all the time. The data stored in the medical database helps the doctors for the further reference to treat the patient.

6 Conclusion

The proposed health monitoring system using wearable sensors focuses on treating bedridden patients by providing quality and a proper health assistance at critical situations. Using this algorithm, a patient's health status can be monitored easily. Presence of caretaker every time nearby the patients can be reduced by implementing our system. With this health monitoring technique the changes in the physiological metrics of the patient's health status can be retrieved from the database at any time. So that the authorized persons can have the reference of these variations in the patient's health condition during treatment of the patient. Through this

springing up technology the clinical inmates can be benefited by having a retrenchment in their medical expenses.

References

- [1] A. Ghosal, *Robotics: Fundamental Concepts and Analysis*. New Delhi: OxfordUniversity Press, 2006.
- [2] Rajesh Kannan Megalingam, Goutham Pocklassery, Athul Ashokan Thulasi, Vivek Jayakrishnan Vazhoth Kanihiroth, MediSuit: Wearable health monitoring system for elders and bed-ridden patients, January 2016, DOI: 10.1109/ISCO.2016.7727091. Conference: 2016 10th International Conference on Intelligent Systems and Control (ISCO).
- [3] D.K.M Unnikrishnan, Vineeth Radhakrishnan, d.c Jacob, Published 2012. Wireless gadget for Homebound Patients (using IEEE Standard 1073 for Medical Device Communications) .
- [4] Roshan Kumbhar, Health Monitoring Using Fitness Band and IOT, IOSR Journal of Computer Engineering (IOSR-JCE).

Segmentation of Retinal Fundus Images for Global Eye Disease Diagnosis

Vijayan T¹, Sangeetha M²

¹Research scholar , Department of Electronics and Communication Engineering
BIST, Bharath Institute of Higher Education and Research, Chennai

² Professor , Department of Electronics and Communication Engineering
BIST, Bharath Institute of Higher Education and Research, Chennai

Abstract

Diabetic retinopathy is a common disease who having with long standing diabetic. Early detection of this disease protects patients from losing their vision. At first, diabetic retinopathy does not cause any kind of symptoms or solely delicate vision issues. Diabetic retinopathy symptoms may include Blurred vision, colour blindness, dark wool and Vision loss. Diabetic retinopathy usually affects both eyes. The condition can develop in anyone who has type 1 or type 2 diabetes. Type 1 is a chronic condition in which the pancreas produces little or no insulin and type 2 is a long term metabolic disorder that is characterized by high blood sugar and insulin resistance. It occurs mostly due to the less control over the diabetes and less care taken to control it. In this project is discussed about the methods of diagnosing of diabetic retinopathy using artificial intelligence. The retinal image samples are collected from hospitals or captured using fundus camera. The retinal image of the deceased is segmented to find the diabetic levels of the patient through which the stage of the disease is diagnosed. Initially the image of the deceased is segmented and pre-processed using image processing. The segmented image is classified and identified using Artificial Intelligence (AI).

Keywords: *Image processing, neural network, medical image processing, Fundus camera, Classification*

1 Introduction

Diabetic retinopathy (DR) is additionally constant eye infection is an ailment in which the diabetes mellitus adding to visual impairment makes harm the retina of the face. This wrecks the daylight delicate tissue's veins at the rear of the eye (retina).At first it doesn't show any indications or mellow vision issues. This condition generally occurs in sort 1 and type 2 diabetic patients. It occurs generally due to the less order over the diabetes and less consideration taken to control it. A bit of the typical appearances are clouded vision, fluctuating vision and debilitated concealing vision. In the earlier days the revelation of the disease takes extra time and logically complex method. So the treatment to the ailment is furthermore made inconvenient provoking the deficiency of vision to the patients. In light of the turn of events and progress in the advances the diagnosing of the infirmity is made dynamically less troublesome. In this paper the area of the diabetic retinopathy is done using the modernized thinking (AI) and picture planning to make measure progressively less intricate and less complex. Computerized picture preparing is that the usage of PC with MATLAB to do all estimations to perform picture investigation on cutting edge pictures. The field of computerized signal preparing is progressed picture measure has a couple of points of interest over straightforward picture measure since they have various subcategory. It empowers wide extent of estimations to be applied to the PC report to avoid issues like structure up of commotion and sign contortion all through cycle. Since the pictures are portrayed in two estimations the high level picture taking care of may be done as multidimensional structures. For example it will in general be used to channel a picture to underline certain features or remove various features. Picture measure assignments approved with isolating handle smoothing, sharpening, and edge improvement. The filtering methodology is done by applying count regards to the assessments of the pixel. Such isolating cycle are •Low pass channel (Smoothing) •High pass channel (Edge discovery, honing) Picture division is that the strategy for dividing an advanced picture into numerous fragments.

The objective of division is to choose the specific piece of picture for investigating and contrast the outcome and the typical picture division of picture is of a ton of incredible significance and helpful for research. Picture division is commonly utilized for changing over the given picture into the most significance ful part in the picture to fix our target ie examination of DR . All the more precisely, picture division is that the technique for task a mark to every segment in a picture such pixels with consistent name share sure qualities. The consequences of picture division might be a bunch of sections that set up cowl the total picture, or an assortment of shapes extricated from the picture. Every one of the pixels in a really area square measure comparable concerning some trademark or processed property, similar to shading, force, or surface. Neighboring districts square measure impressively totally unique concerning steady attributes. At the point when applied to a pile of

pictures, normal in clinical imaging, the following shapes once picture division is wont to create 3D recreations with the help of introduction calculations like Marching 3D squares.

In designing science, software engineering (AI), by and large alluded to as machine knowledge, is incontestible by machines, in qualification to the regular insight showed by people and various creatures. Software engineering characterizes AI investigation in light of the fact that the investigation of keen specialists that expresses that any gadget that sees its environmental factors and makes moves that expands its probability of with progress accomplishing its objectives. All the more explicitly, Kaplan and Heinlein diagram AI as a frameworks capacity to appropriately decipher outer data, to be told from such data, and to utilize those figuring out how's to achieve explicit objectives and errands through adaptable transformation. Likewise the term computerized reasoning is utilized to portray machines that mirror psychological capacities that people partner with other human personalities, for example, learning and critical thinking. The AI and the picture preparing strategies are utilized in the identification techniques for the diabetic retinopathy

2 Proposed Segmentation System

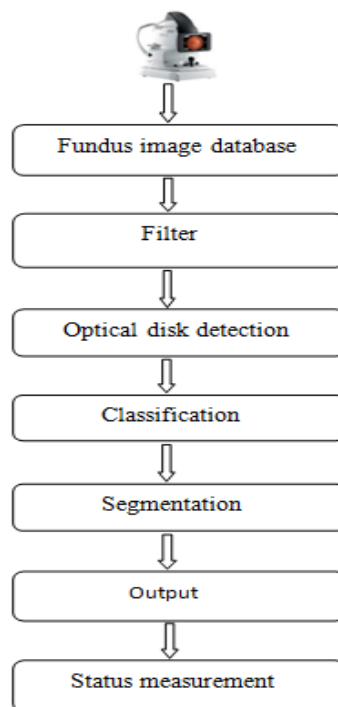


Figure 1: Flow chart of Fundus Image Segmentation

2.1 Database for Fundus image

Retinal image taken by Fundus camera this is called as Fundus retinal images. this images efficient way to analysis eye disease in global world. The image contains all the severity condition in the eye disease.

2.2 Filters

Image filter involved major task in image processing technique, such as image contract enhancing, smoothing, sharpening, edge detecting, compression, boundary detection and segmentation process. Image filter extract image to numerical values for analysis performance in the computer systems.

2.2.1 Optical disk detection

The optic disc is likewise the passage of many veins that supply the retinal district. Essentially, in an ordinary individual the optic circle contains around 1-1.2 million afferent nerve strands from eye to mind. The optic plate discovery is one of the most basic strides in the examination of advanced diabetic retinopathy frameworks. The exact recognition of optic plate is valuable in distinguishing diabetic retinopathy where the delicate vessels created in the retina which is the fundamental driver of diabetic retinopathy.

2.2.2 Segmentation

Segmentation is a very important pre-processing technique to diagnosis disease based medical image analysis. It is the method of partitioning a medical image into multiple segments. Diabetic retinopathy diagnosis based on condition on blood vessels in the retinal fundus images. Image segmentation process done by kernel-based vessel tracking algorithm. All retinal vessel segmentation methods segment common stages: pre-processing stage, processing stage and post-processing stage

2.2.3 Gray image

The gray image or gray scale image is the one in which the value of each pixel is the sample representation of amount of light that is it carries only intensity information about the image. This is achieved by using the command in Matlabie RGB to gray. These images consist of black and white or gray monochrome exclusively consists of shades of gray. The conversion of the colour to gray image is done by shooting black and white films with different coloured photographic filters on cameras of different weighting of the colour channels.

2.2.4 Erosion image

Erosion imaging mainly consist of two essentials in morphological image processing from which all the other morphological functions are carried out. In this process it removes the islands and small objects so that the substantive objects remain.

2.2.5 Dilated image

The dilated image also comes under the morphological operation. It is one of the basic operations of the mathematical morphology. It is first developed for the binary images then it later used for gray scale images and then used to complete the lattices. This process is also called morphological dilation which makes the objects more visible and fills the small holes in the object.

2.2.6 Edge detection

Edge detection is mainly used to find the boundaries of the object in the images. It mainly works by detecting the discontinuities in brightness of the image. The most commonly used algorithms are sobel, canny, prewitt, Roberts and fuzzy logic.

2.2.7 Adjusted image

The image adjusting is a non destructive image editing tools that adds colour and tonal adjustments to the image without permanently changing the pixel of the image.

2.2.8 Mask image

A mask picture is essentially a picture where a portion of the pixel force esteems are zero and others are non-zero. At the point when the pixel force esteem is zero in the cover picture then the pixel power of the subsequent veiled picture is set to the foundation estimation of the picture.

3 Methodology

The input image is given. Then the optic disk removal is done using the gray imaging, optimized imaging and erosion imaging. The obtained image is edge detected for the further processing of the image. Now the obtained

image is masked, adjusted and the disc image is obtained. Finally the blood vessel extracted image is obtained from which the output is obtained.

4 Result and Discussion

The segmentation results produced as shown in Figure 1 to. Fig11. This segmentation techniques clearly shown the Diabetic retinopathy severity based on blood vessel thickness.



Figure 2: original image and Gray image



Figure 3: Optimized image and Dilated image

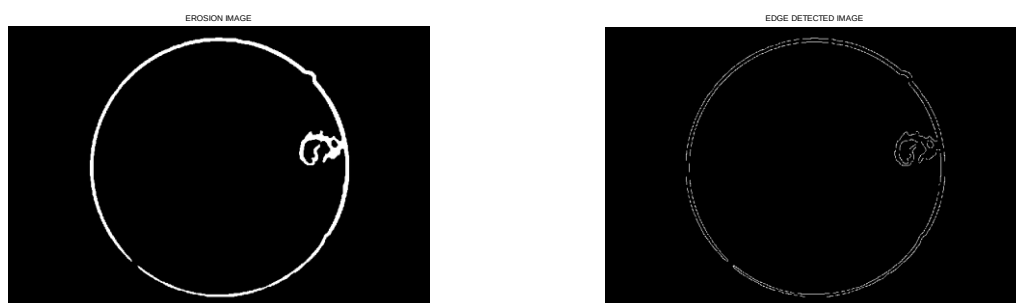


Figure 4: Erosion image and Adjusted images



Figure 5: Mask image and Disc image Removal



Figure 6: Disc image and Extracted blood vessel

5 Conclusion

The discussed segmentation method will identify the diabetic retinopathy identification signs such as thickness of blood vessels, micro aneurysms, haemorrhages and exudates more effectively if the classes are defined properly.

References

- [1] B. Wu, W. Zhu, F. Shi, S. Zhu, and X. Chen, "Automatic detection of microaneurysms in retinal fundus images," *Computerized Medical Imaging and Graphics*, vol. 55, pp. 106–112, 2017.
- [2] R. Maher, S. Kayte, and D. M. Dhopeswarkar, "Review of automated detection for diabetes retinopathy using fundus images," *International Journal of Advanced Research in Computer Science and Software Engineering*, vol. 5, no. 3, pp. 1129–1136, 2015.
- [3] D. J. Browning, *Diabetic retinopathy: evidence-based management*. Springer Science & Business Media, 2010.
- [4] R. Maher, S. Kayte, D. Panchal, P. Sathe, and S. Meldhe, "A decision support system for automatic screening of non-proliferative diabetic retinopathy," *International Journal of Emerging Research in Management and Technology*, vol. 4, no. 10, pp. 18–24, 2015.
- [5] R. S. Maher, S. N. Kayte, S. T. Meldhe, and M. Dhopeswarkar, "Automated diagnosis non-proliferative diabetic retinopathy in fundus images using support vector machine," *International Journal of Computer Applications*, vol. 125, no. 15, pp. 7–10, 2015.
- [6] B. Singh and K. Jayasree, "Implementation of diabetic retinopathy detection system for enhance digital fundus images," *International Journal of advanced technology and innovation research*, vol. 7, no. 6, pp. 874–876, 2015.

Monaural Speech Separation by Means of Video Stream Digital Image Processing

Kalaiselvi B ¹, Karthik B ², Vijayan T ³

^{1,3}Asst Professor, Department of Electronics and Communication Engineering Bharath Institute of Higher Education and Research

²Associate Professor, Department of Electronics and Communication Engineering Bharath Institute of Higher Education and Research

Abstract

In real life scenario, speech heard by the listener gets affected by the addition of more than one noise source. This addition affects the quality of speech and increases the listener's fatigue. The human auditory system successfully separates speech from the noisy sound sources. However the machine implementation of the same fails to perform as human beings. This has a lot of possible claims such as involuntary speech recognition, Voice identification, audio retrieval etc. The current speech separation systems uses acoustic features performs well under a controlled environment and failed to perform in a noisy environment. Recently researchers started to use visual features along with the acoustic features to separate the target speech from the noisy speech mixture. This of course increases the speech separation accuracy in terms of Voice quality and perspicuity. This project aims to develop a computational auditory scene analysis (CASA) based speech separation to separate the target speech from the noisy speech mixture using the visual cues. The visual cues will be extracted by the mouth detection using Viola Jones Algorithm and the lip movement tracking using Kanade Lucas Tomasi (KLT) algorithm. Finally, the extracted visual cues will be used to suppress the noisy speech and retain only the target speech with good quality and intelligibility.

Keywords: *CASA, KLT, BSS, IBM, ROI, AV*

1 Motivation

The presence of speech activity and the voice activity can be detected from both audio and video strength the SNR is high, speech is dominant compared to noise, thus it is more reliable to detect the presence of speech activity from audio stream itself. But when the SNR reduces, and as the noise dominates speech, it is not reliable to detect onsets and offsets from audio stream as it may treat some noisy parts as speech or vice-versa. In such cases it is advisable to detect onsets and offsets from video stream as it is independent of SNR of the signal. The onset and offset times of video stream can be detected by tracking the mouth of the target speaker. The detected onset and offset time of the video stream is then plotted and compared with the plot of audio stream, and checked for one-to-one correspondence. After it matches, the mask is passed on to the synthesis filter bank to produce an enhanced target speech.

2 Objective

Our project aims to develop a mathematical model for auditory scene analysis (CASA) based speech separation to separate the target speech from the noisy speech mixture using the visual cues. The main objectives of the project is to determine the voice activity of the audio stream and to determine the voice activity of the video stream and to match the target speech activity of the audio stream with the corresponding video streams and to finally separate the target speech by eliminating the other speakers speech. This helps to suppress the noisy speech and retain only the target speech with good quality and intelligibility.

3 Speech Onset And Offset Speech Detection [Audio]

Dissimilar to multi-channel discourse division, spatial data can't be used. Just those characteristic acoustic highlights, for example, pitch, symphonious structure, nearby time or recurrence nearness can be misused to isolate discourse. Pitch data has been generally viewed as a decent method to extricate symphonious structure.

Yet, it is exceptionally hard to assess precisely pitch shapes from target discourse while meddling discourse is available. The traditional model is the "mixed drink party issue", where individuals are talking at the same time in a room, and one is attempting to follow of the conversations. Single channel speech separation (SCSS) is shown in Figure. 1

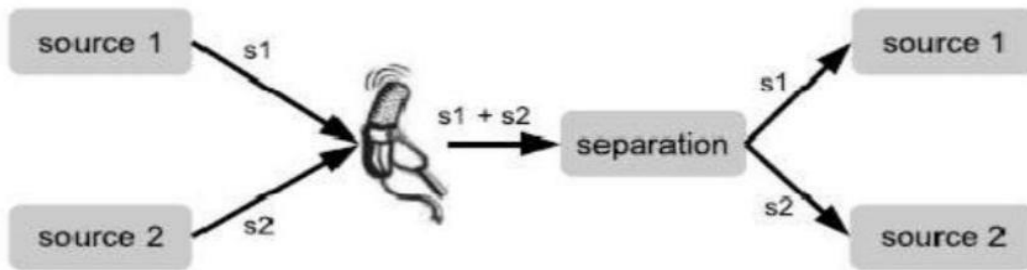


Figure1: Single Channel Speech Separation (SCSS)

The approaches proposed to solve the single channel speech separation (SCSS) problem are: Blind source separation (BSS), Model Based SCSS and Computational auditory scene analysis (CASA)[7][9]. In the above methods, both BSS and model based SCSS rely on prior knowledge of sources obtained during training phase. But CASA based seek discriminative features in the observation signal to separate the speech signals.

3.1 Speech Onset And Offset Speech Detection [Video]

Face recognition is the process of identifying a face a three dimensional object based on its two dimensional image. These systems can identify a target individual accurately provided the condition are favourable. Facial recognition systems are commonly used for security purposes but are increasingly being used in a variety of other applications. Among the technologies that are used to determine a person’s identity, face recognition is the least intrusive as it is a non- contact process.

The course object finder utilizes the Viola-Jones calculation to recognize individuals' faces, noses, eyes, mouth, or chest area. You can likewise utilize the Training Image Labeller to prepare a custom classifier to use with this System object. Prepared course characterization model, determined as a comma-isolated pair comprising of 'Classification Model' and a character vector. This worth sets the grouping model for the indicator. You may set this character vector to a XML document containing a custom grouping model, or to one of the substantial model character vectors recorded beneath. You can prepare a custom arrangement model utilizing the train Cascade Object Detector work. The capacity can prepare the model utilizing Haar-like highlights, histograms of situated inclinations (HOG), or neighborhood paired examples (LBP). Detection threshold, specified as a comma-separated pair consisting of the 'Merge Detections' and a scalar integer.



Figure2 :Merge threshold

Use locale of premium, indicated as a comma-isolated pair comprising of 'UseROI' and a legitimate scalar. Set this property to consistent with distinguish objects inside a rectangular area of interest inside the input image using the step method [14].

3.2 Samples to Frames Conversion

Features from audio and video streams are extracted separately and then analyzed together in order to check their synchrony. Initially, features from audio stream will be plotted as a function of samples per second whereas features from video stream will be a function of frames per second. So our next task is to plot audio features in terms of frames per second.

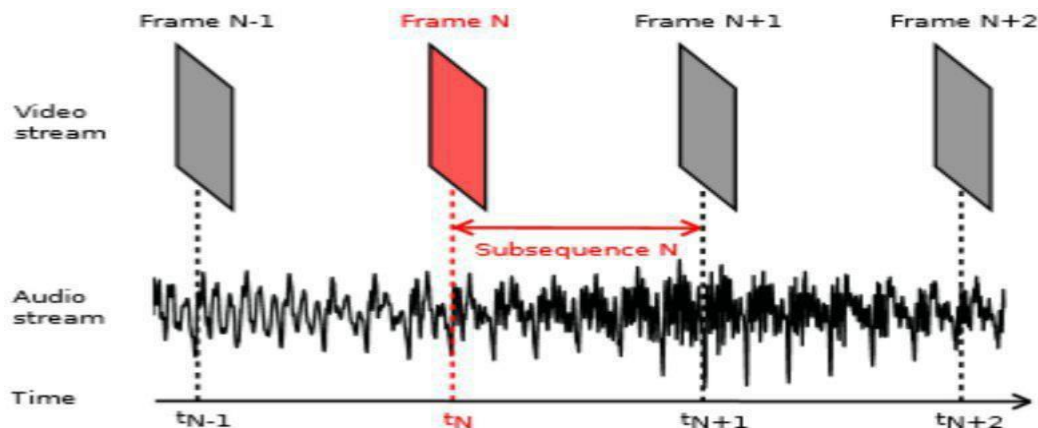


Figure 3: Audio subsequence corresponding to a frame

3.3 Windowing

An acoustic speech signal contains a variety of information. It contains a message content as well as information from which the speaker be identified. The first step involved in conversion is framing. A frame can be seen as the result of a speech waveform multiplied by a rectangular pulse whose width is equal to the frame length. As we want to compute one audio feature vector in respect to each video frame, the frame length will be equal to the time difference between two consecutive video frames (i.e. 40ms for frame rate 25fps). Windowing by a rectangular shape window would introduce a significant high frequency noise at the beginning and end points of each frame, because of the sudden changes from zero to signal and from signal to zero. To reduce this edge effect, the Hamming window is used instead. The general formula to determine the number of frames in a given audio stream is that,

$$\text{No. of audio frames} = \text{No. of audio samples} / (\text{Window length} * \text{Overlap})$$

However, the number of video frames is significantly smaller than the number of determined audio frames. But we have to analyze speech activity present in the audio and video frame by frame. Thus we can go for linear interpolation of video frames so that the plot of video onset detection versus video frames can be compared with that of plot of audio onset detection versus audio frames to check for one-to-one correspondence. Interpolated values between the two points μ ranges between 0 and 1. Values of μ outside this range result in extrapolation.

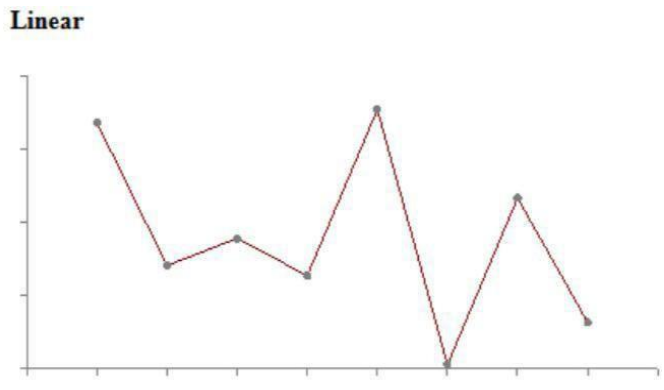


Figure 4 :Linear interpolation

After windowing followed by linear interpolation, the number of frames in the video frames will be the same as that of audio stream so that the onset presence can be compared frame by frame in each. Based on the variation in the output of each, two parameters can be used namely hit and miss.

4 Proposed System

The block diagram for onset and offset detection from the given Audio- Visual speech signal is shown in the following figure.5 Here the audio-visual input is processed in two different ways and are plotted with the same scale to compare each other. The first part consists of auditory segmentation in which the audio is separated from video and is then smoothed to remove any fluctuations and normalized to get peaks at appropriate regions.

The resulting onset and offset are then plotted. The second part consists of mouth detection followed by lip movement tracking and the resulting onset and offset are then plotted based on a certain threshold. The above two plots are compared to identify the hits and misses for speech separation.

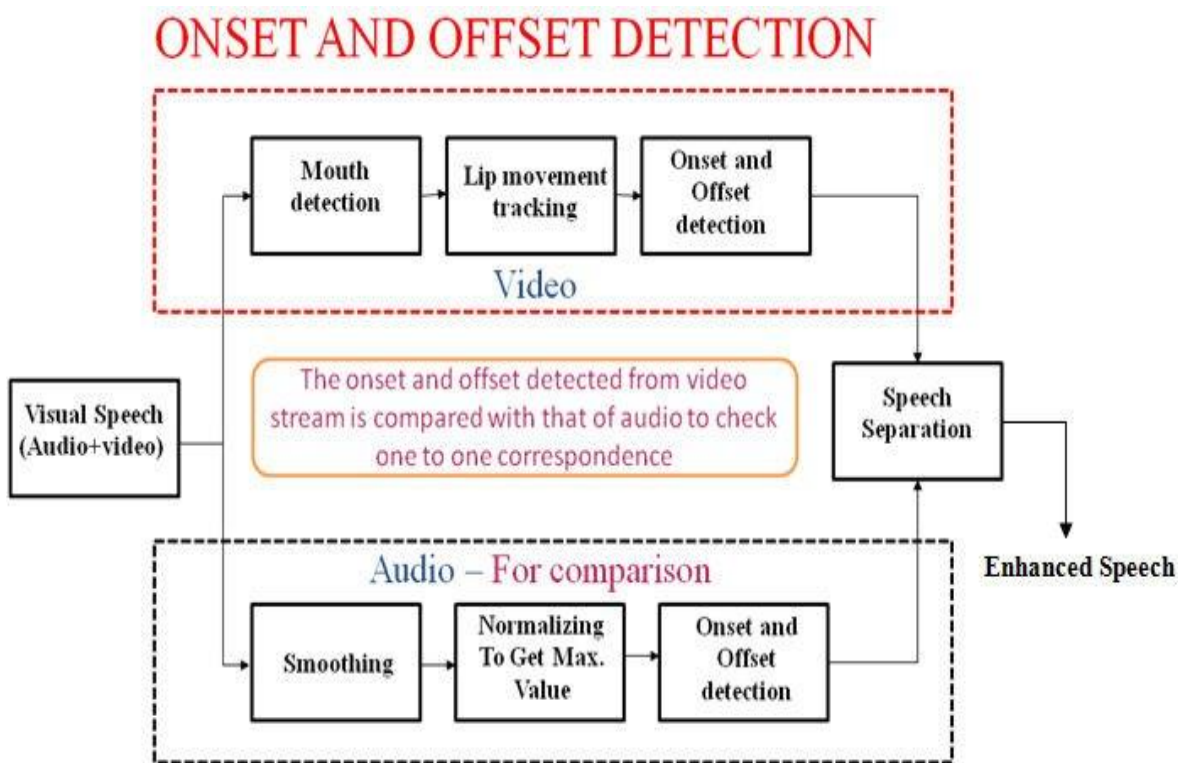


Figure 5: Block Diagram of the proposed system

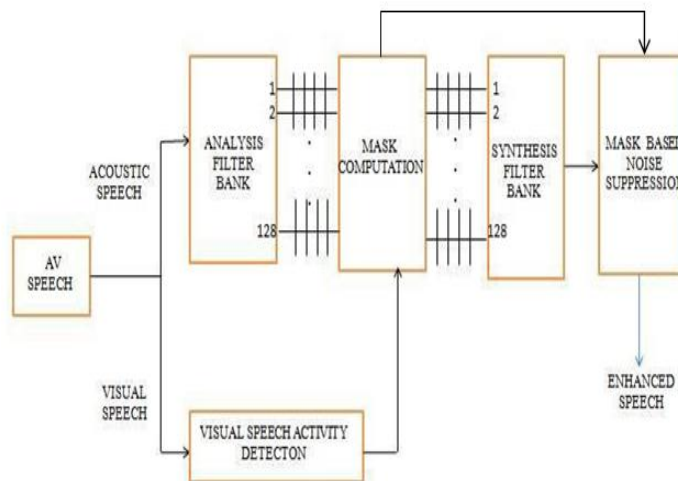


Figure 6: Block Diagram of speech separation using video stream

Single audio-visual speech is taken and separated into audio and video separately using mp3 video convertor and each taken into two different cases. In first case the visual speech of the speaker is recorded and the voice activity of the target speaker is found by lip movement tracking algorithm and this output is mapped with the input audio for one-to-one correspondence. If both seems to matching equally then the mask is given into synthesis filter bank for processing and thus produce an enhanced speech. This block diagram gives an overall perspective of the complete project.

5 Experimental Results and Discussion

By tracking the two arbitrary points in a video, the pixel distance between the two points against the frame number is plotted and threshold to a certain value to get the speech onset and offset in the video

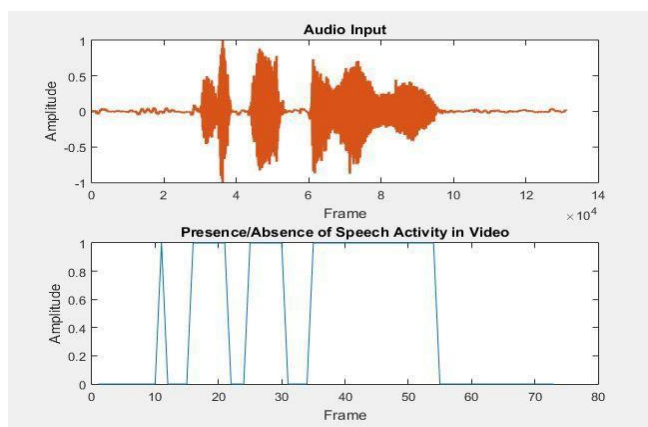


Figure 7: Plot of video onset and offset speech activity

The speech onset and offset obtained from the video as less frames when compared to that of audio. So we must interpolate the frames to match the audio.

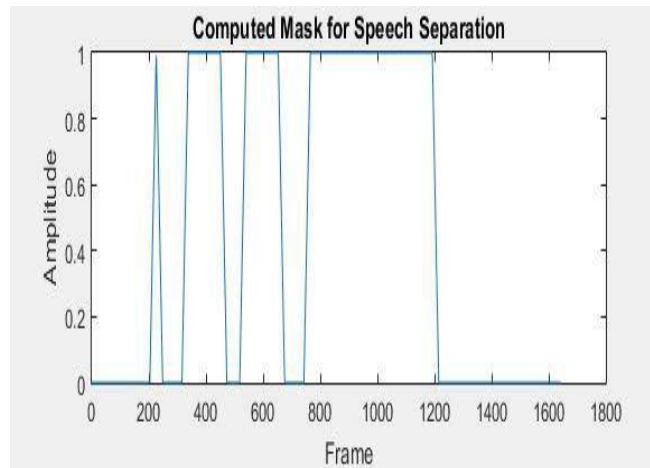


Figure 8: Plot of computed mask for speech separation

The computed mask and the noisy speech is given to CASA system, where the system successfully separates the speech from the noise when the speaker according to the mask .

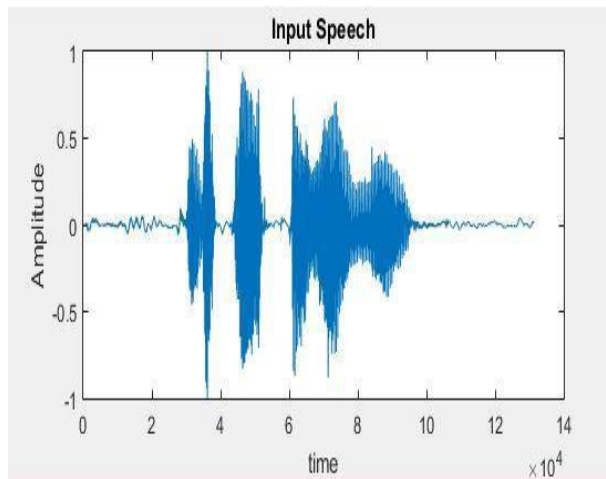


Figure 9: Plot of input speech for speech separation

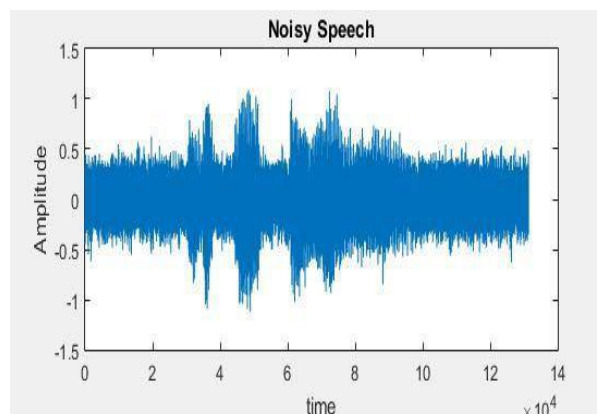


Figure 10: Plot of noisy speech for speech separation

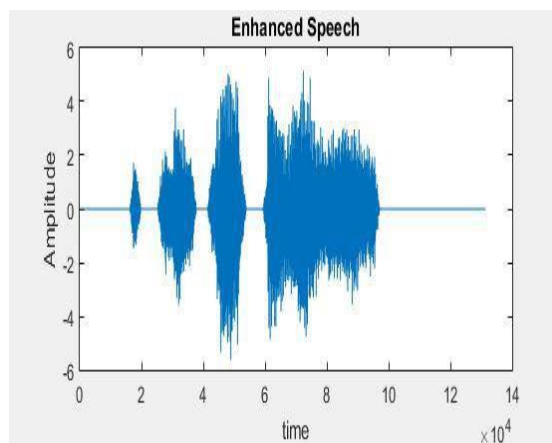


Figure 11: Plot of enhanced speech for speech separation

Table 1: Signal to Noise Ratio enhancement of the proposed system for the speech shaped noise at various i/p SNR's

| I/P SNR(dB) | O/P SNR(dB) | Enhancement(decibels) |
|----------------|-------------|-----------------------|
| 0 | 5.9010 | 5.9010 |
| 2 | 7.0512 | 5.0512 |
| 4 | 8.4022 | 4.4022 |
| 6 | 9.9231 | 3.9231 |
| 8 | 11.5650 | 3.5650 |
| Average | 8.5685 | 4.5685 |

We implemented our algorithm to a video and its corresponding audio of various SNR and computed the SNR of the enhanced speech and plotted in the above table. This article discusses about the results of video onset and offset activity detection obtained by Viola Jones algorithm and KLT algorithm from the sample video and the mask for speech separation is simulated by interpolating to match with the audio frames. Finally, CASA is implemented on noisy speech using the computed mask and the resulting enhanced speech is plotted.

6 Conclusion

The results that are obtained from the MATLAB. The onset and offset obtained from the video stream is found to be accurate at all SNRs. Thus, the enhanced speech signal obtained is found to be equivalent with the clean speech signal.

References

- [1] A. Ghosal, Robotics: Fundamental Concepts and Analysis. New Delhi: Oxford University Press, 2006.
- [2] Abrar Hussain, Kalaivani Chellappan, Siti Zamratol M, "Single Channel Speech Enhancement Using Ideal Binary Mask Technique Based On Computational Auditory Scene Analysis", Journal of Theoretical and Applied Information Technology, Vol.91. No.1, 15th Sept 2016.
- [3] Alireza Kazemi, Reza Boostani and Fariborz Sobhanmanesh, "Audio visual speech source separation via improved context dependent association model" EURASIP Journal on Advances in Signal Processing, 2014.
- [4] B. Rivet, W. Wang, S. M. Naqvi, J. A. Chambers, "Audiovisual speech source separation: An overview of key methodologies", IEEE Signal Process. Mag., vol. 31, no. 3, pp. 125-134, May 2014.
- [5] L. Wang, G.J. Brown, "Fundamentals of Computational Auditory Scene Analysis", in Computational Auditory Scene Analysis, D.L Wang and G.J Brown, Wiley-IEEE Press, pp. 1-38, 2006.
- [6] H. Talea, K. Yaghmaie, "Automatic visual speech segmentation", Proc. 3rd International Conference Communication Software Networking, pp. 184-188, May 2011.

- [7] Jihen Zeremadini, Mohamed Anouar Ben Messaoud and Aicha Bouzid, "A comparison of several computational auditory scene analysis (CASA) techniques for monaural speech segregation", *Brain Informatics*, Vol. 2, Issue 3, pp. 155 – 166, Sept2015.
- [8] N.Harish Kumar, R.Rajavel, "Monaural speech separation system based on optimum soft mask," *IEEE Int. Conf. on Computational Intelligence and Computing Research*, 18-20 Dec2014.
- [9] Q. Liu, W. Wang, "Blind source separation and visual voice activity detection for target speech extraction", *Proc. Int. Conf. Awareness Science and Technology (iCAST)*, pp. 457-460,2014.
- [10] R. Dansereau, "Co-channel audiovisual speech separation using spectral matching constraints", *Proc. IEEE Int. Conf. Acoustics Speech Signal Processing (ICASSP)*, vol. 5, pp. 645-648,2004.
- [11] S. Shoba, R. Rajavel, "Adaptive energy threshold for monaural speech separation" *International Conference on Communication and Signal Processing*, 6-8 April2017.
- [12] Shoba. S, Rajavel. R, "Image processing techniques for segments grouping in monaural speech separation" *Circuits, Systems, and Signal Processing (Springer)*, Published online - Dec 2017, "<https://doi.org/10.1007/s00034-017-0728-x>".
- [13] V.A. Mane, Prof. Dr. S. B. Patil, "Survey of Methods and challenges in Computational Auditory sense analysis", *International Journal of Innovative Research in Electrical, Electronics, Instrumentation and Control Engineering*, Vol. 4, Issue 9, Sept2016.
- [14] Vikram K, Dr.S. Padmavathi, "Facial parts detection using Viola Jones algorithm", *International Conference on Advanced Computing and Communication Systems (ICACCS)*, pp 1-4, 2017.

Hybrid System Design of FSO- Tech and RF Signals in Spatial Communication

B. Mary Amala Jenni ¹, D. Umamaheswari ², M.Sahinipiriya³

^{1,2} Assistant Professor, Department of Electronics and Communication Engineering, St.Anne's College of Engineering And Technology, Panruti

³Associate Professor, Department of Electronics and Communication Engineering, St.Anne's College of Engineering And Technology, Panruti

Abstract

Free-space optical communication (FSO) is an optical communication technology that uses light propagating in free space to wirelessly transmit data for telecommunications or computer networking. Li-Fi is a wireless communication system which makes use of Free Space Optics to transmit and receive data instead of traditional RF as in Wi-Fi. This paper gives a comparison between FSO and RF wireless communication signals in terms of efficiency, transmission rate and capacity in Space communication. It gives the introduction to Hybrid System which can be used in Spatial Communication.

Keywords: - FSO, Radio Frequency Signals, Hybrid System, Satellite Communication

1 Introduction

The wireless technology has bloomed to a greater extent. Various wireless communication schemes such as Wi-Fi make use of radio or micro wave frequencies of required bandwidth to transmit and receive data. Radio frequencies are finite due to constrained bandwidth. Data can be transmitted by making use of illumination; this technology is the Lifi technology Free Space Optics and Radio frequency waves both are used in communication. Free Space optics is not a new technology and is cheap in terms of installation, and are installed in places where no large antennas and other communication devices cannot be installed. Radio Frequency waves have lower band width but are used for long distance communication. Free Space Optics alone cannot control data rate so, they are used with Fiber Optic technology for controlling and optimization of data rate. Fiber Optic technologies are also incorporated by Radio frequency signals to improve data rate. Technology used for lower data communication. Now with the introduction Laser technology, it has improved the use of Free Space optics to a greater extent. FSO technology was developed by NASA and is used in military purposes with high speed communication link. This technology has many similarities with fiber optics technology but it acts differently depending on the field of use with respect to transmission in both the technologies.

Radio frequency technology is very old wireless technology used for communication of data and been used for more than 100 years. In the year 1901 Marconi achieved his first successful data transmission using Radio signals from one remote station to other. The bandwidth of Radio frequency waves varies from lower frequency of 1 KHz to maximum 1GHz. Initially the Radio signals are used for lower band frequency to transmit and receive data for purpose of radio and some military applications.

2 Laser Light In Spatial Communication

Various satellites are present around the Earth; these satellites are controlled and coordinated by ground station on Earth. The grounds stations communicate with the satellites and inter satellite communication make use of Radio waves. The data collected by the satellites are in range of terabytes. The Radio waves for space

communication whose frequency varies from 3 kHz to 300GHz, So transferring such huge data simultaneously is not possible and time lag takes place. This can be overcome by making use of Laser light as a medium to transmit data; the frequency of laser light varies from 400THz to 700THz so transmission of data takes place continuously with no time delay

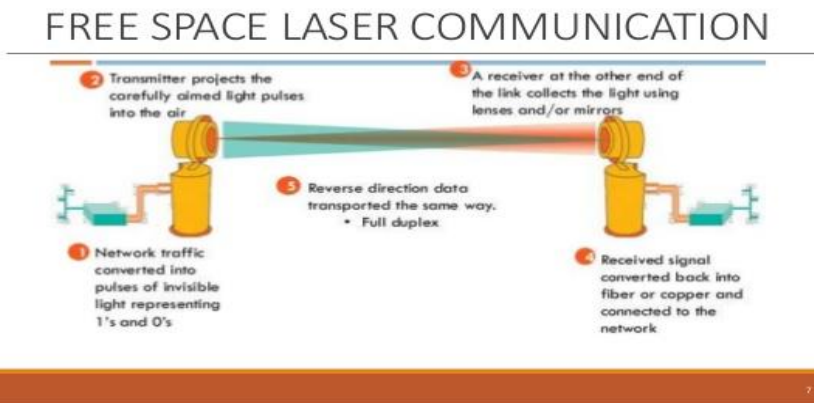


Figure 1: Two solar powered satellites communicating via laser light

3 FSO and Radio Frequency System

Free Space Optic system is a wireless connection between two units called Optic Receiver and Optic Transmitter for single line of communication, and for a two way connection that is flow of data in both the ways we make use of Optical Transceivers. An Optical light source is incorporated in transmitter used for producing a beam of light in a given direction to the required location in atmosphere or to the required satellite. The receiver also consists of lens to detect incoming light signal and is routed using optical cable fiber .A beam of conical shaped light is produced from the transmitter to transmit the data. The signal transmitted should be straight and should be in line with the receiver to ensure proper communication link between transmitter and receiver. The figure 2 shows the position of the transmitter, receiver and the beam of light between them, the line of sight is the first required condition for successful transmission of data. Although if there is slight modification in line of sight signal data can be sent, For Long distance high rate transmission with no minimum error the line of sight is very important and needs to be considered.

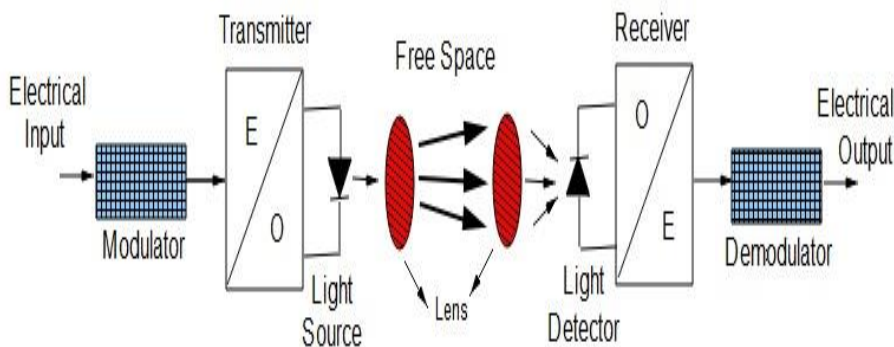


Figure 2: FSO and RF system

Radio frequency system is also wireless system consisting of transmitting and receiving devices. Initially huge radio transmitters are installed in required place and receivers are carried by persons .The transmitter

part has two sections Base station and Controller; if the base station is not together, then it acts as connector between the receiver and the base. Mobile technology has improved a lot due to which transceiver are used instead of transmitter and receiver connected by Radio frequency link.

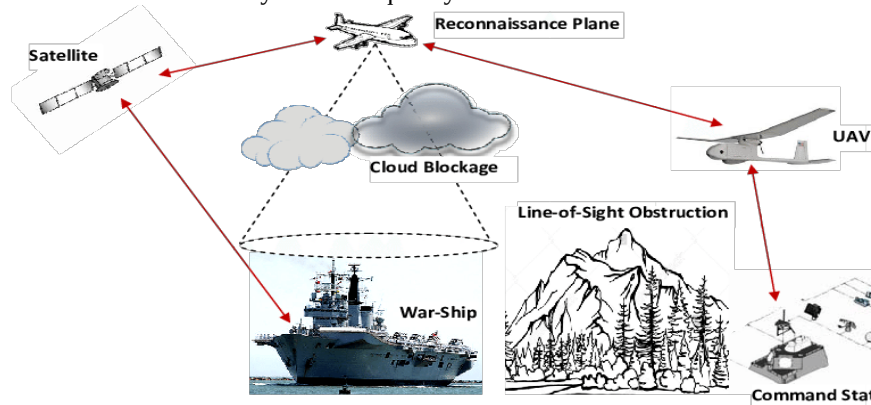


Figure 3: Atmospheric Laser Communication

4 System Configuration And Channel Model

In hybrid FSO/RF-FSO system, the FSO link works in parallel with a mixed RF-FSO .The source (S) contains an RF transmitter in addition to the regular FSO transmitter. The relay (R) is capable of receiving RF signal and subsequent RF-FSO conversion destination (D), there are two distinct optical receivers present; one for receiving data via S-D link and another for receiving the data through the relay, i.e. via S-R-D link. The channel state information (CSI) about the primary FSO link is sent from D to S via a feedback path. If the primary FSO link is obscured due to atmospheric turbulence, S switches from FSO to RF transmission and notifies D to switch to the receiver aligned with R. At regular intervals, S transmits a pilot signal through primary FSO link to gauge the turbulence condition. If the link quality meets the desired service level, D confirms it by sending a feedback, and the primary FSO link is re-activated

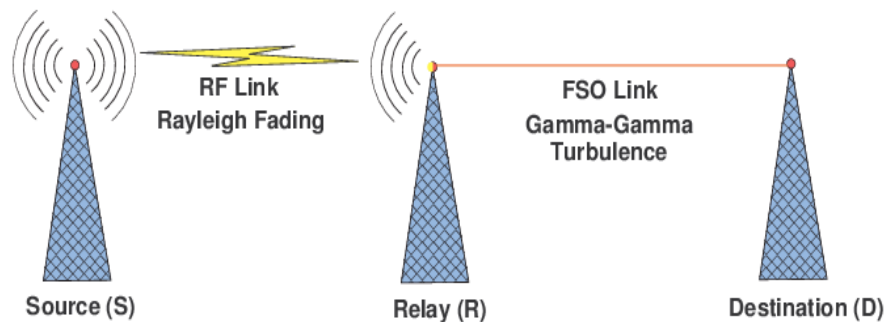


Figure 4: Dual-hop backup RF-FSO link with S-R RF hop and R-D FSO hop.

5 Performance of RF And FSO

Analyzing the performance of Free Space Optic communication various parameters has to be considered. These parameters are divided into two parts (I) External parameters and (II) Internal parameters. The specifications, rating of the components used which includes operating frequency, divergence, power consumed, and angle of transmission etc comes under Internal parameters. The capability of lens, error rate comes under Receiver end.

External parameters include environmental factors such as:

1. Alignment
2. Atmospheric attenuation
3. Weather condition
4. Scintillation

To make use laser light as a medium to communicate between satellite and ground stations depends on the amount of surface covered with clouds, area clear for continuous communication, amount of haze and Fog. So the performance of them depends on visibility condition. The visibility condition of Free Space optic laser system with respect to distance and weather condition.

Performance depends on the type of system used. There are various systems in the field of GPRS, Bluetooth, and GSM etc. Even in this case weather conditions play a major role in the performance, the distance between the receiver and transmitter and the number of users determines the performance of Radio Frequency signals. For example in Broadband access the channel bandwidth is shared with many users, in this the number of users are inversely proportional to the data rate that is if the total number of persons using the broadband channel increases the data rate decreases and at any time if the total number of persons using the broadband channel decreases the data rate increases as whole channel is shared among all the users. Other parameters involve site availability according to the configuration of cell. The Site for base station available for performance and installation of systems depends on the type of location. Performance of Radio signals are affected by electromagnetic signals and different noises.

Free Space technology is improving day by day to increase and maximize the bandwidth of the signal so that data at high speed can be transmitted. Free Space Optic technology is similar to fiber optic communication, only change is that is the path flow of signal i.e. wireless communication takes place between transmitter and receiver with no cable between them so reducing the cost and can higher efficiency. The efficiency of Free Space technology mainly depends on the external parameters or the medium between transmitter and receiver if the medium is clear then data transmission takes place with no loss and with high speed. Just by making use of LED data can be transmitted up to range of 100Mbps, various experiments are conducted to increase the data rate. In the satellite interconnection for space communication we are not using LED as medium instead we make use of Laser because of high speed communication, and the operation frequency of Laser light varies from 400 terra Hertz to 700 terra hertz. As a result for high speed communication we make use of laser light as medium to communicate between satellites. The efficiency also depends on the system used the transmitter and receiver should be high accurate, for continuous data transmission the line of sight is very important. Different technologies are used which transmits data at a particular data rate as shown in the below Figure 5

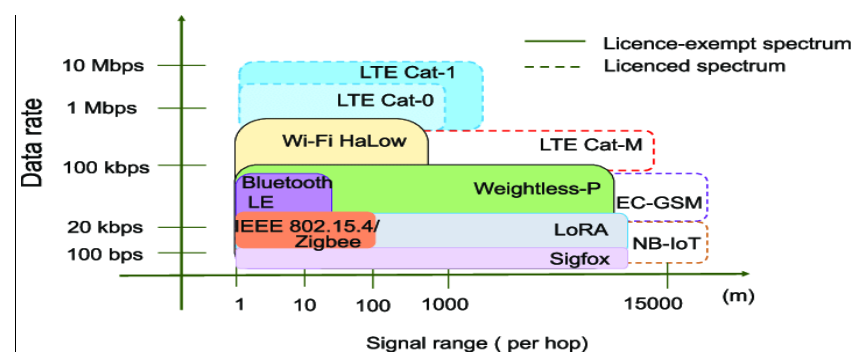


Figure 5: Different technologies with Data rates

Radio Frequency communication is an all time growing technology now growing in the fields of Mobile communication and Broadcasting. The data rate depends on the receiver capability. Lower data rate provides

optimum sensitivity in the receiver part and the signal can be detected for longer distance range. Radio frequency signals efficiency depends on the optimum distance between the transmitter and receiver and the bandwidth. To increase the efficiency the distance should be less with high bandwidth. The Radio signal frequency varies from 3 kHz to 300GHz. So the use of radio frequency signals for satellite communication is not preferable as the bandwidth of radio signals are less and the distance for inter-satellite communication are in the range of few hundred or thousands of kilometers.

Table 1: RF V/s FSO

| PARAMETERS | FSO | RF |
|----------------|-----------------|------------------|
| Power | 2.00E-03 (J/Mb) | 2.31E-02 (J/Mb) |
| Power Loss | 5-15db/km | 108db/km |
| Output Power | 5-500mWatt | 50mWatt |
| Range | 4km | 4km |
| Data Rate | 10Gbps | 100Mbps |
| Capacity | Not Allowed | Allowed |
| Advantage | Unlicensed Band | No line of Sight |
| Security | High | Low |
| Limitation | Environment | Spectrum |
| Spectrum Range | 0.8-1.2THz | 2-6GHZ |

6 Hybrid System

As we discussed the performance and limitations of both Free Space optic and Radio frequency systems, using both them helps in having a Hybrid system. The cost is also comparatively less. For inter-satellite Communication Free Space optics can be used as the operational frequency of them are higher than Radio Frequency signals, even transmission speed is high. For communication between satellite and ground station we cannot use Laser light as various environmental factors come into picture. The line of sight is not possible due to construction large tall buildings, for satellite to ground station communication we make use Radio frequency signal as a medium to transmit data as Radio signal does not require line of sight for it communication. This mutual requirement led to the development of hybrid system with both free space and Radio frequency systems.

- The Hybrid System mainly consists of:
- Laser Link
- RF link
- Switch

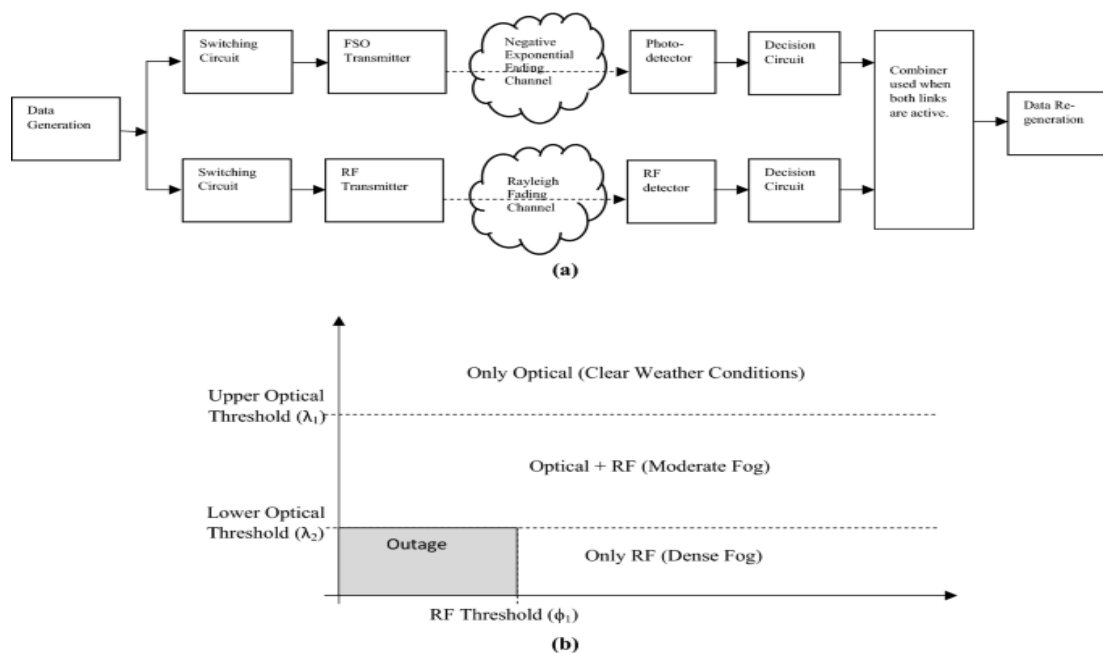


Figure 8: Basic Hybrid System

7 Conclusion

The use of Free Space technology and Radio Frequency signals are necessary in satellite communication. The two technologies can be used alone or can be used together. For high efficient and long distance transmission two technologies are combined and used together. Hybrid systems are used so as to compensate distance and weather condition and to achieve greater efficient transmission of data. FSO offers many advantages over existing techniques which can be either optical or radio or microwave. Less cost and time to setup are the main attraction of FSO system. Optical equipment can be used in FSO system with some modification. Merits of FSO communication system and its application area make it a hot technology but there are some problems arising due to the attenuation caused by medium. FSO system poses some problem like attenuation in medium that can affect the performance of transmission as power loss would be there.

Different models based on these studies are used to study the system performance before installing it at the location. This can lead to the improvement of the system. Different techniques like OFDM-FSO, WDM-FSO based system are new approach to improve the system performance with high speed and longer distance. So new techniques can be designed by combination of these and, by enhancing these techniques, system designing can be improved and the demerits of FSO system can be reduced to a minimum level.

References

- [1] LiFi: Conceptions, Misconceptions and Opportunities Harald Haas LiFi Research and Development Centre, The University of Edinburgh, Edinburgh EH9 3JL, UK, h.haas@ed.ac.uk.
- [2] Free Space Optics Vs Radio Frequency Wireless Communication, Rayan A. Also mme rai and Sheik Tahir Bakhsh, Hani Also mme rai.
- [3] Z. Zhao, et al., "Radio frequency interference mitigation in OFDM base passive bistatic radar" AEU - International Journal of Electronics and Communication, vol 70, pp. 70-76.2016

- [4] M.Usman, et al., "Performance Analysis of Switching Based Hybrid FSO/RF Transmission," in Vehicular Technology Conference (VTC Fall), 2014 IEEE 80th, 2014, p. 1-5.
- [5] "Performance Analysis of Hard-Switching Based Hybrid FSO/RF System over Turbulence Channels "Hira Khalid 1, S. Sheikh Muhammad , H.E. Nistazakis and G.S. Tombras Received: 30 April 2019; Accepted: 4 June 2019; Published: 6 June 2019
- [6] L. Hou, et al., "Radio frequency heating for postharvest control of pests in agricultural products: A review," Postharvest Biology and Technology, vol. 113, pp. 106- 118, 2016.
- [7] Z. Li, et al., "Combinational-deformable-mirror adaptive optics system for atmospheric compensation in free space communication," Optics Communications, vol. 320, pp. 162-168, 2014.
- [8] Banibrata bag, Akinchan "Performance analysis of hybrid FSO systems Using FSO/RF-FSO link adaptation" volume 10,number 3,june 2018

Raspberry Pi Based Automatic Vehicle Speed Detection Warning and Control System

B.Arunkumar¹, V.Venkatesan², S.Durai Raj³

^{1,2,3} Assistant Professors, Department of ECE, St. Anne's College Of Engineering And Technology, Panruti

Abstract

Now days, people used to drive vehicle very fast and thus there is occurrence of accidents in the critical zone such as school, college, hospital, residential area increases even though speed breakers, warning alerts are provided. Moreover many people do not have passion to follow the traffic rules, hence we need a system that automatically detect the pedestrian density/traffic density in critical zones and to measure the vehicle moving speed and to warn the driver, if the driver goes beyond the speed limit. The proposed system not only warns the driver but also provides real time automatic vehicle speed control if the speed limit breaches. The objective of this project is to develop a system to keep the vehicle secure and protect the human life. The main aim of this project is to design and develop a system automatic speed control of vehicle and accident avoidance using Raspberry Pi processor and IR sensor.

Keywords: *Signboard detection, Raspberry pi, Open CV, Image processing, Pedestrian density.*

1 Introduction

According to a survey many people lost their life in road accidents. Most of the traffic accidents are the result of carelessness, ignorance of the rules and neglecting traffic signboards, both at the individual level and by the drivers. When someone neglects to obey traffic signs, they are putting themselves at risk as well as life of other drivers, their passengers and pedestrians. Many existing systems are android based and needs third party software to work. This may cause extra cost to system and is not very practical to implement. Some of the system requires an android mobile phone to implement the work which is very difficult. Some systems used Arduino UNO board. Arduino board requires personal computer to process the image, output data can viewed in the receiver side. Even though the warning system and alert system are provided, Speed control system is not implemented in the existing systems along with sign board detection. Hence a system is needed for providing alertness to the driver about the presence of traffic signboard on the way as well as speed control system. The system provides the driver with real time information from road signs, which constitute the most important, and challenging, task. This warning then allows the driver to take appropriate corrective decisions in order to mitigate or completely avoid the event. Then alertness to the driver is given as audio output. If the driver doesn't follow the alert, the automatic speed control system gets activated and the speed of the vehicle is reduced step by step based on program done in Raspberry Pi processor. The objective of the system is to design and develop a warning system for drivers and to control the vehicle speed automatically in critical zones. Raspberry pi is simply a computer on a single board, so there is no need for a PC. Raspberry PI had dedicated port for connecting touch LCD display which is a feature that completely omits the need of monitor. Raspberry PI also has dedicated camera port so we can connect camera without any hassle to the PI board. Raspberry PI also has PWM outputs for application use. So in this system we have used Raspberry processor for Interfacing with pi camera to capture sign boards in critical zones, measuring real time vehicle speed using speed sensor and to provide warning through buzzer and LCD output, real time automatic vehicle speed controlled using DC motor through PWM output. Using Mask R-CNN we can automatically segment and construct pixel-wise masks for every object in an image. Using Mask R-CNN we can generate pixel-wise masks for each object in an image, thereby allowing us to *segment* the foreground object from the background Mask R-CNN architecture with OpenCV and Python enable us to segment complex objects and shapes from images which traditional computer vision algorithms would not enable us to do.

2 Literature survey

In the paper "Traffic Sign Board Detection and Voice Alert System Along with Speed Control" by Anju Manjooran, Anphy Varghese, Annmariya Serby and Krishnadas J [1], traffic sign board is detected and alertness is provided to driver by voice alert system. In the paper "Detection and Recognition of Alert Traffic Signs" by Chia-Hsiung Chen, Marcus Chen, and Tianshi Gao [2], deals with the automatic detection and recognition of traffic sign boards. But it is still a challenging problem with a number of important application areas, including advanced driver assistance systems, keeping track of rules followed and autonomous control of vehicle's speed. In the paper "Android Based Signboard Detection using Image and Voice Alert System" by Sanchita Bilgaiyan,

Sherin James, Sneha. S Bhonsle, Shruti Shahdeo, Keshavamurthy [4], an android mobile phone is required to detect the traffic sign board and to provide voice alert to driver.

In the paper “Traffic Sign Board Detection” by Annmariya Seby [5], the existing system needs third party software to work. This may cause extra cost to system and is not very practical. Some of the system requires GPS module to get real time information of vehicle location and it is practically difficult to detect critical zones specifically; again it becomes a hard part to program GPS server about all critical zones such as schools, colleges, Hospitals, residential areas. Speed control system is not implemented in the existing systems along with sign detection.

3 Proposed system

The basic idea of proposed system is to provide alertness to the driver about the presence of traffic/critical zone signboard at a particular distance apart. This system provides the driver with real time information from road signs. The system consists of Raspberry Pi processor which detects the pedestrian sign boards in critical zones such as schools, hospitals, residential areas using camera interfaced with it and simultaneously measures the vehicle moving speed using speed sensor. If the vehicle speed is within the prescribed limit then the system doesn't take any action. If the vehicle speed is above the prescribed limit then warning is given to driver through alert sound and warning message in LCD display. The warning allows the driver to take appropriate actions in order to avoid the accident. If the driver doesn't reduce the speed, then the system automatically reduces the speed step by step. Image processing technology is mostly used for the identification of the sign boards. The alertness to the driver is given as an audio output as well as on LCD display.

3.1 Block Diagram of proposed system

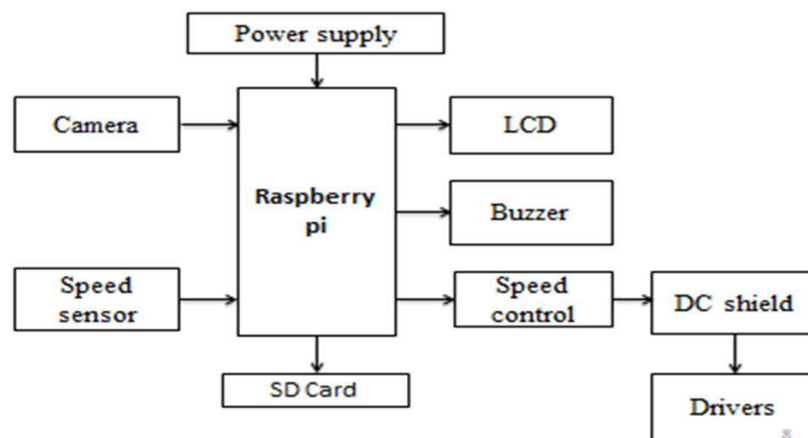


Figure 1: Block diagram of proposed system

Here Raspberry Pi system is used with the camera interface. The system will look onto the road, whenever it detects the critical zone sign boards such as school zone, hospital zone, high pedestrian density zone.. etc.

It will recognize the sign and confirms the road sign as in the box (trained image in the algorithm).The masked RCNN algorithm in the Raspberry pi processor process the image within few seconds.

Then according to the program, the Raspberry Pi provides warning through alert sound and warning message through LCD display, if the vehicle speed is not reduced by the driver, the processor gradually reduces the vehicle speed.

4 Hardware and Software

The following are the hardware used in this system.

- Raspberry Pi 3 processor
- PiCamera
- IR Sensor

- LCD/Buzzer
- Speed Control system
- Masked RCNN with open CV

4.1 Raspberry PI

Raspberry pi is simply a computer on a single board, so there is no need for a PC. Raspberry PI had dedicated port for connecting touch LCD display which is a feature that completely omits the need of monitor. Raspberry PI also has dedicated camera port so we can connect camera without any hassle to the PI board. This main processing chip connects a camera and display. The Raspberry Pi design does not include a built in hard disk or solid state drive, instead used an SD card for booting and long term storage. This board is intended to run Linux Debi based operating systems. The image processing is a form of signal processing where the input is an image, like a photograph or video frame, the output of an image processing may be either an image or a video frame or a set of characteristics or parameters related to the image.



Figure 2: Raspberry pi3 processor

Raspberry PI platform is most used after ARDUINO. Although overall applications of PI are less it is most preferred when developing advanced applications. The Raspberry PI is an open source platform where one can get a lot of related information so you can customize the system depending on the need.

4.2 Pi Camera module

When the camera shutter opens, the sensor capture the photons that is converted to an electrical signal that the processor in the camera read and interprets colours, this information is then stretched together to form an image.

4.3 IR Sensor

An infrared sensor is an electronic device that emits and/or detects infrared radiation in order to sense some aspect of its surroundings. Infrared sensors can measure the heat of an object, as well as detect motion.



Figure 3: Infrared sensor

Many of these types of sensors only measure infrared radiation, rather than emitting it. An infrared sensor is an electronic device that emits in order to sense some aspects of the surroundings. An IR sensor can measure the heat of an object as well as detects the motion. These types of sensors measure only infrared radiation, rather than emitting it that is called a passive IR sensor. When IR light falls on the photodiode, the resistances and the output voltages will change in proportion to the magnitude of the IR light received.

4.4 LCD display

A liquid-crystal display (LCD) is a flat panel visual display which shows over the vehicle speed limit of message to warn the drives. To perform the write operation on LCD the read/write pin is connected to ground.

4.5 DC motor

Very basic construction of a DC motor contains a carrying armature, connected to supply end through segment and brushes. Armature placed between North Pole and South Pole. We supply current direct connected armature.

4.6 Masked RCNN Algorithm

Masked R-CNN is an extension over Faster R-CNN. Faster R-CNN predicts bounding boxes and Mask R-CNN essentially adds one more branch for predicting an object mask in parallel. Using Mask R-CNN we can automatically segment and construct pixel-wise masks for every object in an image. We can use Mask R-CNNs to process both images and video streams. Masked R-CNN algorithm can automatically segment and construct pixel-wise masks for every object in an image.

4.6.1 Masked R-CNN with Open CV

OpenCV is the open-source library for computer vision, machine learning, and image processing and it plays a major role in real-time operation which is very important in our systems. By using OpenCV code written in python language in our system we will detect the sign boards in critical zones such as schools, hospitals. The algorithm first detects the critical zone sign board in the road side by taking the input image using pi camera and then it compares the image with the image in database. If the image is detected and recognized as the image in the database then the input is fed to raspberry pi processor. The real time vehicle speed is detected by IR sensor interfaced with the processor. Masked RCNN algorithm works faster and detects the sign board and process the image and produces within a few seconds.

The flowchart depicting the entire proposed system and the workflow are shown below.

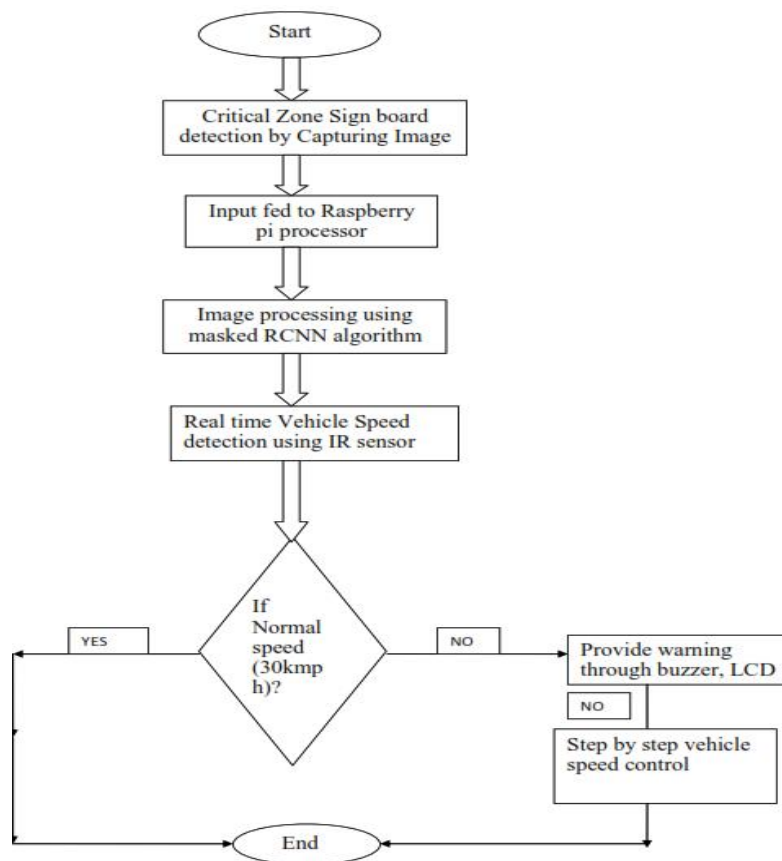





Figure 4: Flowchart showing entire work flow

As per the program, the Raspberry pi processor compares the vehicle speed with the prescribed speed limit in critical zone (30kmph in our system). If the vehicle speed is within the limit, the Raspberry pi does not take any action.

If the vehicle speed is beyond the limit then the system alerts the driver through buzzer sound and displays the message through LCD display. If the speed is not controlled by driver, the system takes the vehicle to automatic mode and reduces the vehicle speed gradually.

4.7 Example for sign board

Table 1: Sign board

| SYMBOL | MEANING |
|---|--|
|  | This sign designator the speed of traffic on road the limit specified must be invariably followed to avoid penal action and accidents on the road. |
|  | This sign indicates that there is hospital nearby the drivers should be careful while driving through this stretch and should no honk unnecessarily. |
|  | This sign indicates entry to a pedestrian underpass/subway. Pedestrian should invariably use this underpass/subway to cross the road. |

5 Results and Discussions

5.1 Critical Zone detection using Raspberry pi

When the vehicle enters the critical zones such as schools/colleges, high pedestrian density, residential areas, the pi camera module captures the sign boards in roadside and compares with the images in system database using masked RCNN algorithm and if the critical zone sign board is detected then the Raspberry pi processor automatically checks the vehicle speed using IR sensor. If the vehicle speed is within the prescribed limit (30kmph) then the system doesn't take any action and the output is displayed as "NORMAL SPEED" as shown in figure 5.1.

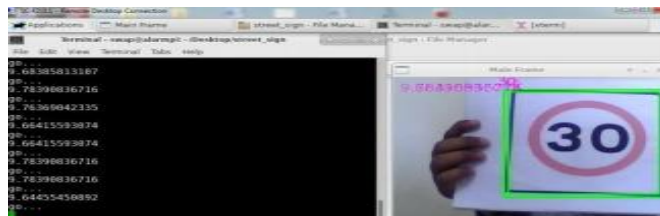


Figure 5: Critical Zone detection using Raspberry pi



Figure 6: Critical Zone detection using Raspberry pi

5.2 Warning system for drivers

If the vehicle speed is beyond the limit (more than 30 kmph), a warning is given to the driver as buzzer sound and emergency information will be displayed as “HIGH SPEED” shown in figure 5.2.

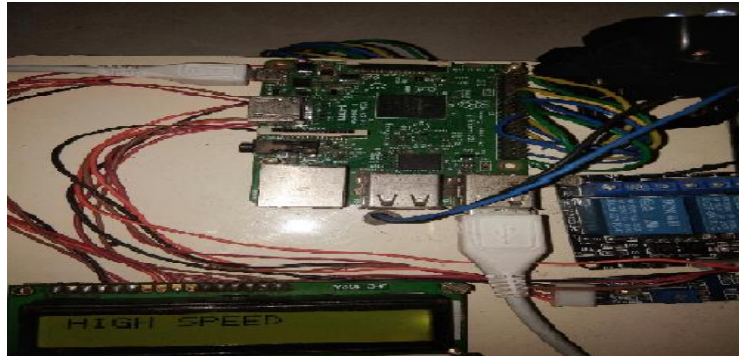


Figure 7: Real time Vehicle speed detection

5.3 Vehicle Speed Control

If the vehicle speed is not controlled by driver, even though the warning is issued, the proposed system controls the vehicle speed automatically. In the proposed model, DC motor can be used to reduce the vehicle speed gradually in steps for our demonstration purpose and the output will be displayed as “Speed control School Zone” as shown in figure 5.3.



Figure 8: Image showing Real time Vehicle speed control

6 Conclusion and Future Work

The Proposed system can be used to save human life by preventing accidents due to negligence of pedestrian sign boards in critical zones such as schools, hospitals, residential areas. The main idea of this project is to prevent road accidents that take place due to driver’s ignorance of traffic signs. The system monitors the real time vehicle speed using speed sensor and critical zones. If the vehicle speed is more than the prescribed limit then the system warns the drivers through alert message and buzzer sound.

If the driver doesn't reduce the speed, the system automatically reduces the vehicle speed. By our project we expect that we can able to reduce the accidents in critical zones such as schools, hospitals, Residential areas up to 40%.

The proposed masked R-CNN algorithm which is successfully able to recognize almost all type of signs at different day timing and weather conditions and it also works well as speed controller to vehicle. This project can be extended to detect the drowsiness of driver using sensors and we can provide alert to the driver and also cut-off fuel if required. In future, we can increase number of traffic speed control sign detection by using high pixel and resolution cameras. The project can be modified by improving system performance with high resolution cameras and also large number of traffic signs can be detected by training with the advanced neural network technique. The masked R-CNN algorithm is best algorithm for image compare processing technology. We can use advanced Raspberry pi, with 4GB RAM and advanced ARM processor, if we have high speed and high accuracy device we may get better results.

References

- [1] Anushree A. S1, Himanshu Kumar, Idah Iram, Kumar Divyam4, Rajeshwari. 'Automatic Sign board Detection System by the Vehicles', International Journal of Engineering Science and Computing, May 2019.
- [2] Anju Manjoran, Anphy Varghese, Anamariya Seby and Krishnadas J 'Traffic Sign Board Detection and Voice Alert System Along with Speed Control' Asian Journal of Applied Science and Technology (AJAST) Volume 2, Issue 1, Pages 28 1-286, 2018.
- [3] Sanchita Bilgaiyan, Herin James, Sneha. SBhonsle, Shruti Shahdeo, Keshavamurthy 'Android Based Signboard Detection using Image and Voice Alert System', IEEE International Conference on Recent Trends In Electronics Information Communication Technology, May 20-21, 2016, India.
- [4] Ankita Mishra , Jyoti Solanki , Harshala Bakshi , Priyanka Saxena , Pranav Paranjpe "Design of RF based speed control system for vehicles" International Journal of Advanced Research in Computer and Communication Engineering, Vol. 1, Issue 8, October 2012.
- [5] Anushree. A. Himanshu Kumar, Idah Iram, Kumar Divyam Rajeshwari. J 'Automatic Signboard Detection System by the Vehicles' International Journal of Engineering Science and Computing, May 2019.
- [6] Frank Lindner, Ulrich Kressel, and Stephan Kaelberer 'Real-time Vision for Intelligent Vehicles' IEEE Instrumentation & Measurement Magazine June 2001.
- [7] Greenhalgh and Majid Mirmehdi' Real-Time Detection and Recognition of Road Traffic Signs Jack, IEEE Transactions on Intelligent Transportation Systems, Vol. 13, No. 4, December 2012.
- [8] Rubel Biswas, Hasan Fleyeh, Moin Mostakim. 'Detection and Classification of Speed Limit Traffic Signs' IEEE 2014.
- [9] Ali and H. A. Hussein, 'Traffic lights system based on RFID for autonomous driving vehicle', in 2017 Annual Conference on New Trends in Information Communications Technology Applications (NTICT), pp. 122-127.
- [10] Kassem, N. Microsoft Corp., Redmond, WA, USA Kosba, A.E.; Youssef, M.; VRF-Based Vehicle Detection and Speed Estimation vehicular Technology Conference (VTC Spring), IEEE (2012).

Safety System for Automobiles Through Vehicle –to-Vehicle Communication Using Lifi

Pavithra.S¹, Abirami.S², Sharmila.R³,Thiyagarajan.V⁴

^{1,2,3} UG students, Department of Electronics & Communication Engineering, V.R.S College of Engineering &Technology, Villupuram, Tamil Nadu, India

⁴Associate Professor, Department of Electronics & Communication Engineering, V.R.S College of Engineering &Technology, Villupuram, Tamil Nadu, India

Abstract

The new vehicle execution has been persistently improved and the examination results identifyingwiththewellbeingofvehicledrivinghaveadditionallybeenconsistentlyannounced and illustrated, it is attempting to discover an equalization point between the advancement of vehicle speed limit and the assurance of driver's security. Li-Fi is a VLC, visible light communication innovation that manages move of information through enlightenment by removing fibre from optics by sending information through a LED light that fluctuates in the force quicker than a human eye can pursue. In this undertaking we attempt to build up a framework to give the before mishap data to the vehicle control unit with the goal that it. Vehicle to vehicle correspondence is the best arrangement that has been utilized so as to decrease vehicles' mishaps.Theproposed utilization of Li-Fi innovation in this task involves the light emitting diode (LED) bulbs as methods for network by sending information through light range as an optical remote vehicle for signal en gending. Truth be told, the use of LED dispenses with the need of complex remote systems and conventions.

Keywords: *LightEmittingDiode;Photodiode;VehicleteVehicleCommunication;VisibleLight Communication.*

1 Introduction

As per the statistics released by the Ministry of Road Transport and Highways of India,more than 1.5 lakh people lost their lives due to road-accident last year with 1 person dying every 4 minutes on the roads. Globally, more than 1 million people lose their lives due to road accidents every year. Ofthe1.5lakh, more than 60% of the death is of youth between the age of 15-34 years and every day, 20 children under the age of 14 die due to road-accidents.

Li-Fi is a significant and mainstream innovation in the correspondence framework. LiFi is known as Light loyalty correspondence frame works. It is the exceptionally quick and cheap remote correspondence frame works and is the optical form of the Wi-Fi. The innovation works by adjusting light transmitting diode (LED's) to send computerized kind of data, undetectable to the unaided eye. In this, we structure model which depends on Li-Fi innovation for vehicle to vehicle information transmission. Vehicle to vehicle correspondence is the best arrangement that has been utilized so as to diminish vehicles mishaps. In LI-Fi innovation information transmission through light for this reason wellspring of light is utilized as LED. Vehicle to vehicle interchanges, for example, is one of the past patterns, which is one of the best systems that will actualize in cars to give wellbeing and a convention of correspondence. Extra to existing remote innovations. To restores rapid association rapidly (if there should be an occurrence of calamity issue). Li-Fi is utilized in light of the fact that it is quick and optical form of Wi-Fi which is modest.

1.1 Literature Review

A Tutorial Survey on Vehicular Ad Hoc Networks [1] VANETs include vehicle-to-vehicle and vehicle-to-infrastructure interchanges dependent on remote neighborhood advancements. The unmistakable arrangement of competitor applications (e.g., impact cautioning and nearby traffic data for drivers), assets (authorized range, battery-powered power source), and nature (e.g., vehicular traffic stream designs, protection concerns) make the VANET an extraordinary region of remote correspondence.

Standard for Information Innovation Telecommunications and data trade between frameworks Local and metropolitan zone systems [2] to extend the utilization of Ethernet to incorporate endorser access organizes so as to give a critical increment in execution while limiting gear, activity, and support costs. Vehicular Channel Characterization and its Implications for Wireless System Design and Performance [3] assess and advance ITS applications arranged to vehicular security dependent on remote frameworks, the learning of the spread channel is imperative, specifically the way misfortune. Strong Channel Estimation in Wireless LANs for Mobile Environments [4] versatile remote channels, the relationship of the channel recurrence reaction at various occasions and frequencies canbeisolatedintotheincreaseofthetime-andrecurrenceareaconnectioncapacities.Henceforth, our MMSE channel estimator can be a recurrence area channel utilizing the quick Fourier change (FFT), trailed by time space channels.

Mid-saunter supported OFDM execution examination in high portability vehicular channel [5] Mid-wander helped channel estimation and its exhibition investigation of OFDM signal in high versatility vehicular radio channel.

2 Materials and Methods

The proposed framework requires a transmitter and a receiver in every vehicle in both back and front sides of the vehicle. Along these lines the situation will be examined in this paper.



Figure 1: Vehicle to vehicle communication using LiFi

2.1 System Diagram

The 12v transformer receives the power supply voltage and steps down the voltage. Then it is passed through the rectifier which converts the alternating current into direct current by allowing the current to flow through one direction only. Further the current is passed to the Arduino Uno board which is programmed according to the requirement.

It has digital and analog input/output pins used to convert the input into desired output. It delivers a 5v supply to ultrasonic sensor, LiFi transmitter module and Trimpot. The ultrasonic sensor uses the SONAR to determine the distance between the object. Its 'trigger' and 'echo' terminals are connected to the 6th and 7th pins of the Arduino board respectively. Trimpot is used to vary the speed. It works like a variable resistor. LiFi transmitter module is connected to a LED light source to emit light as the source of information. It is then received by a solar panel which is connected to the LiFi receiver module. The received information is sent to the arduino board. Then to L293D motor

driver which allows the DC motor to drive in either direction. Its IN1 and IN2 terminals are connected to the 8th and 9th pin of the Arduino board respectively which is used for direction regulation. EN1 is connected to the 10th pin of the Arduino which is used for speed regulation.

The motor driver can control a set of two DC motors simultaneously in any direction. Here, the motor driver is connected to a single motor which rotates by the change in voltage.

Sender Module:

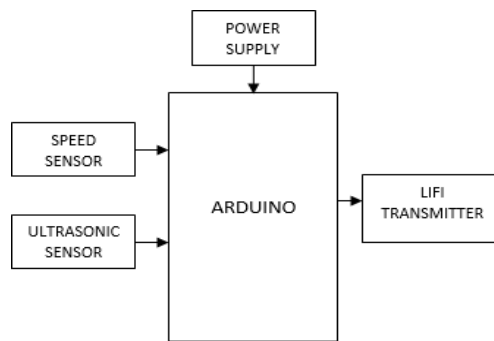


Figure 2: Block diagram of Sender Module

Separate power supply unit and Arduino board is used for the sender module. The sensors used are speed sensor and ultrasonic sensor. A LED is used as a LIFI transmitter.

Receiver Module

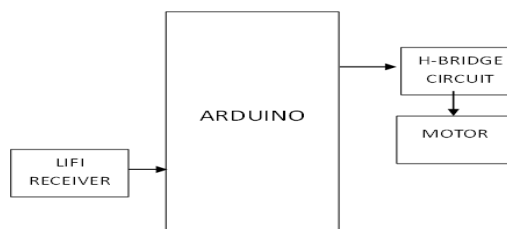


Figure 3: Block diagram of Receiver Module

Separate power supply unit and Arduino board is used for the receiver module. A solar panel is used as a LIFI receiver. A motor driver is used to drive the motor.

3 Results and Discussions

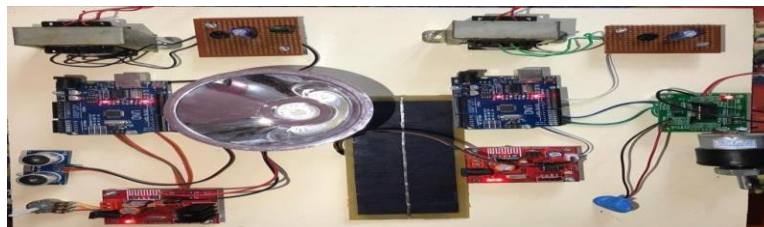


Figure 4: Project Model

- [6] S.I.Kim,H.S.Oh,andH.K.Choi,“Mid-ambleAidedOFDMPerformanceAnalysisin HighMobilityVehicularChannel,”Proc.IV’08,pp.751–754,Eindhoven,Netherlands,Jun.2008.
- [7] W. Cho, S. I. Kim, H. K. Choi, H. S. Oh, and D. Y. Kwak, “Performance Evaluation of V2V/V2I Communications: The Effect of Mid amble Insertion,” Proc. Wireless VITAE’09, pp. 793–797, Chennai, India, May2009.

Design and Implementation of Miniature U-slot Patch antenna for 5G Communication

S. Durai Raj¹, B. Arunkumar², V.Venkatesan³

^{1 2 3} Assistant Professor, Department of Electronics and Communication Engineering , St. Anne's College of Engineering and Technology, Panruti

Abstract

In this paper Compact size and high gain U-slot rectangular microstrip patch antenna for 5G wireless communication is proposed. The U slot antenna concept has been used in patch antenna designed to reduce antenna size. In fact 5G wireless communication system requires a compact size, low profile and simple design structure to make sure the reliability, mobility and high efficiency. The proposed antenna is designed on a compact Rogers Substrate RT duroid with relative permittivity ϵ_r of 2.2 and loss tangent δ value 0.0009. The proposed design provides a very high gain of 10 dBi at resonance frequency of 30 GHz which is one of the distinct features of the proposed antenna. The proposed antenna is designed and fabricated to meet the best possible result using a simulation software: An soft HFSS (High Frequency Structure Simulator) software version 15.0. Microstrip patch antennas are widely used because of their several advantages such as light weight, low volume, small size and low fabrication cost. The proposed antenna was measured and compared with the simulation results to prove the reliability of the design. The performance of the designed antenna was analyzed in term of gain, return loss, VSWR, and radiation pattern at frequency is 30 GHz.

Keywords: *compact size, High gain, High Efficiency, millimeter wave, Low profile, 5G, HFSS*

1 Introduction

In association with the trend of drastic advancement in wireless networks, the currently allocated frequency spectrum as reached its bottleneck. Millimeter waves (MMW) are anticipated as a promising solution for upcoming wireless systems. Incorporating MMW antennas will be highly instrumental which offers the advantages of miniaturization, wider bandwidth, narrow radiation beam and are well suited for enhancing the data rates with lesser delays.

International Telecommunication Union (ITU) has been prompted by the daily increasing number of users in mobile communication users to take an initiative for its Fifth Generation (5G) in near future [1]. Usage of much more social media applications and current demands for the multimedia contents with high quality needs to handle with high rates of data, throughputs. data rates considered high starts from 5 Gbps up to 50 Gbps are promised by 5G technology [2]. These enormous bandwidths and high data rates are visualize to make sure this by only stepping from range bellow 6 GHz of band to above the range of 6 GHz ,known as spectrum of millimeter waves. To make it sure and to verify that this spectrum is very excellent and aligned choice for the millimeter wave communication which can really provide the sufficient communication performance both the feasibility studies as well as the experimentations has been done in[2]. The working mechanism and architecture of the upcoming technology of 5G networks decree that the structure and the design imitate to a whole set of specification for better comparable Performance. These specific terms are listed as listed as the large impedance bandwidth, very high level of gain, narrow in beam width, and stable radiation energy Pattern, small size.

Different bands of frequencies have been assigned for different individual countries in the globe, but among all of these frequency bands the most prominent and mostly reported are one is 28 GHz band and the second one assigned is 38 GHz frequency band to the United States of America [3]. Besides the two licensed frequency bands, some unlicensed bands like 60 GHz, band has also been assigned for 5G mm wave. However, The 60 GHz band demands so many extra complex challenges as well as having the critical atmospheric absorption characteristics [4] various antenna designs have been proposed by different researchers [5]–[9]. 2.3 GHz wide bandwidth and have achieved a very high gain of 13.97 dBi but its structure composed of different layers make its design very complex.

It is derive that the resonant frequency is inversely proportional to the slot length and feed point and at the same time as it increases with increasing the coaxial probe feed radius and slot width. In recent years, some papers were reported for Dual/triple band operation by using single/double U slot in the microstrip antenna. It is

seen that the applications which require dual frequency operation with small frequency ratio were designed by using the U slot in a wideband micro strip antenna [9]. Micro strip antennas are suffer from low impedance bandwidth characteristics to increase 5G system applications. To avoid this suffering of antennas, there have been various bandwidth enhancement techniques like coplanar parasitic patches, stacked patches, or novel shapes patches such as the U and H -shaped patches. Here in this design one method is used, called as special feed networks or feeding techniques, to compensate for the natural impedance variation of the patch. To avoid the use of coplanar or stacked parasitic patches we can do the etching process on the patch with U -slot, which increases either the lateral size or the thickness of the antenna. So, sometimes with enhancing the impedance bandwidth, changing the current distribution on the micro strip patch more than one resonant frequency is obtained. In 1995, two scientists named as Huynh and Lee was presented a broad band single layer probe fed patch antenna with a U -shaped slot on the surface of the rectangular patch [10-13]. In this paper, we design a rectangular microstrip patch antenna in which U shaped slots are cut in microstrip patch to enhance its gain and radiation efficiency.

The Proposed design has overcome all these limitations and provide a very high Gain of 10dbi and efficiency of more than 98 % with a sharp notch depth at resonance frequency of 30 GHz. The working mechanism and architecture of the upcoming technology of 5G networks decree that the structure and the design imitate to a whole set of specification for better comparable Performance.

2 Antenna Designing Methodology

Microstrip antenna in rectangular shape is the easiest geometry for designing and implementation. The basic U - slot loaded rectangular micro strip patch antenna design is seen in below Figure. 1. Here, W is the patch length, L is the patch width, d is the feed point, U_{y1} is the vertical slot length, U_{x1} is the horizontal slot length, U_{a1} is a slot thickness. The proposed antenna is fabricated using Roger RT duroid substrate dielectric constant $\epsilon_r = 2.2$ and loss tangent of 0.0009 to print. Roger RT duroid is used as the substrate material as it is light in weight and also have good mechanical strength with high performance. These properties make Roger RT duroid very attractive to be used as substrate.

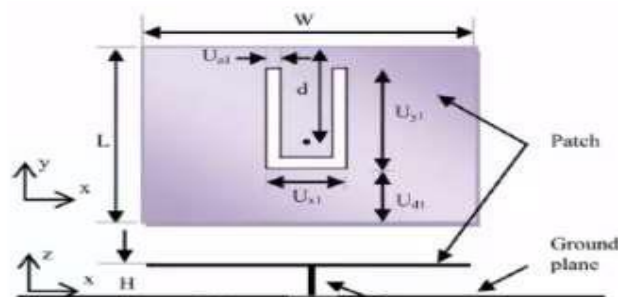


Figure 1: Basic U -slot loaded rectangular micro strip patch antenna design

Fig.2 is the proposed rectangular single-patch antenna with U-slot structure that is calculated and optimized using patch antenna equations [13].

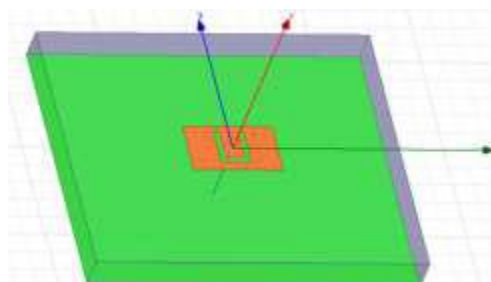


Figure 2: Proposed Rectangular single-patch antenna with U-slot structure

The geometry of the presented work is designed using ROGERS-5880 having dielectric constant (ϵ_r) of 2.2 and loss tangent of 0.0009 (δ), while the structure of the proposed antenna has been designed from the conventional simple Patch antenna, where the length of the patch(P_x) can be calculated using equation [21].

$$P_x = c/4fr(\epsilon_{eff})^{1/2} \tag{1}$$

where c is the speed of light which is $3 \times 10^8 \text{ ms}^{-1}$, f_r is the central resonating frequency which is given by

$$f_r = c/\lambda_g(\epsilon_{eff})^{1/2} \tag{2}$$

where λ_g is the guided wavelength and ϵ_{eff} is the effective dielectric constant which is given by

$$\epsilon_{r_{eff}} = (\epsilon_r + 1)/2 + (\epsilon_r - 1)/2 [(1 + 12 P_y)]^{-1/2} \tag{3}$$

where ϵ_r is dielectric constant of the substrate, P_y is the width of the Patch and h is the thickness of the substrate.

Table 1: .The Optimized Parameters of Proposed Antenna Design

| Parameters | W | L | W1 | W2 |
|-------------|-----|------|-------|-------|
| Values (mm) | 5 | 4.8 | 2.99 | 0.8 |
| Parameters | W3 | L1 | L2 | L3 |
| Values (mm) | 0.3 | 2.73 | 1.165 | 1.035 |

3 Simulation And Results

Figure 3. shows the S11 Parameter of the proposed design. The S11 Parameters basically present the resonance frequency and the bandwidth coverage of that Antenna for a stable radiation the s11 parameter value must be equal to or less than -10 dB which is the required standard criteria in our design the value of S11 parameter fulfil the basic criteria of $|S_{11}| \leq -10 \text{ dB}$ In the Proposed design a simple patch antenna which is modified with a rectangular slot introduced on the top centre of the patch which is optimized in such a way to improve the gain and efficiency of the Antenna and to achieve a sufficient bandwidth. A 50 ohm microstrip feed line is used as a feeding source to the modified rectangular patch of Antenna. Fig 2 shows. In Table I the optimized S parameters list is given in detail.

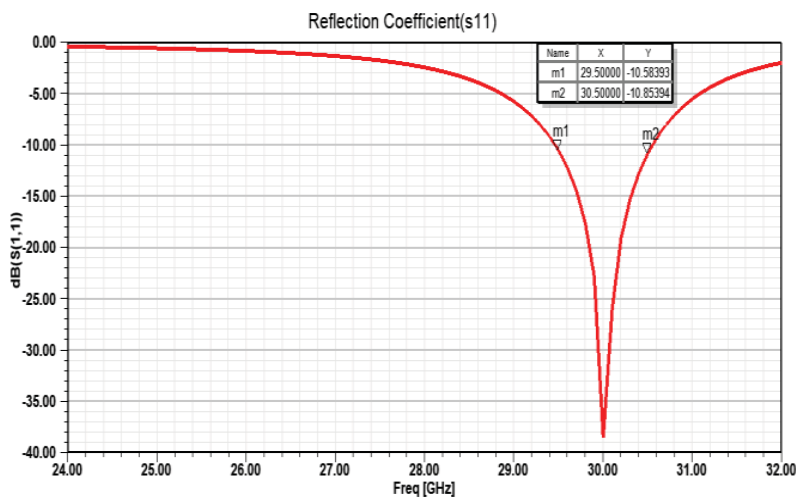


Figure 3: S11 Parameter

Fig.4. Shows the Voltage Standing Wave ratio of proposed design. VSWR value should be in between 1-2 for a standard reliable communication, the VSWR value in our designed case follows the standard criteria of value between 1-2. The simulation results shows that the proposed design has an accurate optimal VSWR value of 0.205 on resonance frequency of 30 GHz.

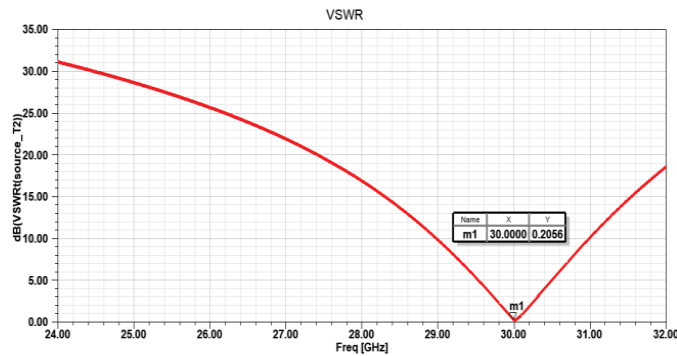


Figure 4: Voltage Standing Wave ratio (VSWR)

In Fig. 5 Gain of the proposed Antenna with stable directional radiation Pattern is shown. The Antenna provide a very High gain of 10 dbi on a single element such a high gain is a very Challenging task and needs very careful optimization. The stable uniform directional radiation pattern shows a very smooth radiation of the proposed design as shown in the Fig. which shows that all beams are equally on same wide directional position which indicates for increasing spectral efficiency and reliable services to the subscriber and leads to cover the maximum number of subscribers on same time with an efficient way due to its sufficient spectrum bandwidth of 1GHz.

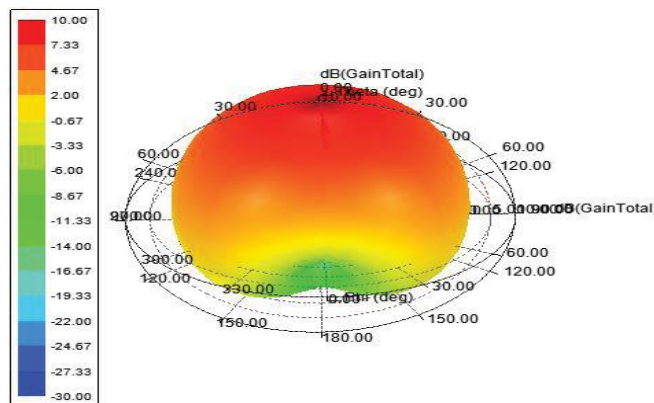


Figure 5: Gain of the proposed Antenna

Efficiency plots of the proposed Antenna design in 30 GHz frequency range is shown in Fig 6. It can be seen clearly from Fig. 6 as shown in both cases of Phi is 0 degree and Phi is 90 degree the Antenna exhibit stable radiation Pattern with no back and side lobes in the range of proposed targeted resonance frequency of 30 GHz.

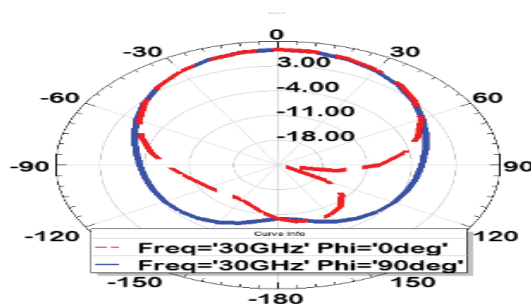


Figure 6: Radiation Efficiency of the proposed Antenna

The comparison of different Performance parameters of our proposed work with previous latest research is summarized in Table II.

Table 2: Summarized Performance Parametric Analysis

| References S.No | Antenna Size (mm) | Frequency (GHz) | Gain (dBi) | Efficiency (%) |
|----------------------|-------------------|-----------------|------------|----------------|
| [10] | 6*6 | 28 | 7.6 dBi | 85.6% |
| [11] | 130*70 | Array 30 | 12.3 dBi | - |
| [12] | 14*4 | 28 | 5.4 dBi | 93% |
| [13] | 22*19 | 11 | 6.3 dBi | - |
| [14] | 120*40 | 28 | 6.6dBi | 77% |
| [15] | 5*5 | 28 | 6.6 dBi | 73% |
| [16] | 3*7 | 28,38 | 3.7dBi | 69% |
| [17] | 21*21 | 10,28 | 7.5dBi | 62% |
| Proposed Work | 5*4.8 | 30 | 10dBi | 97% |

4 Conclusion

A compact size mm Wave U slot antenna high Gain and High efficiency Microstrip patch Antenna is presented. To achieve high gain and high efficiency a rectangular slot has been introduced on the top and centre of the Patch. The Proposed Antenna structure provides a very high gain of 10 dBi and High efficiency of more than 98%. The Proposed design performance is very attractive these attractive characteristics makes the proposed antenna as a suitable candidate for 5G mm wave wireless communication. Antenna the flexibility of reconfigurable also can be easily utilized for near future 5G wireless communication. The stable radiation pattern, high gain and high efficiency made the proposes work a potential candidate for 5G mm-wave communication.

References

- [1] Y. Wang, J. Li, L. Huang, Y. Jing, A. Georgakopoulos, and P. Demestichas, "5G mobile: spectrum broadening to higher frequency bands to support high data rates," *IEEE Vehicular Technology Magazine*, vol. 9, no. 3, pp. 39–46, 2014.
- [2] Iftikhar Ahmad, Houjun Sun, Yi Zhang, Abdul Samad "High Gain Rectangular Slot Microstrip Patch Antenna for 5G mm-Wave Wireless Communication", 2020 5th international conference on computer and communication system.
- [3] W. Roh, J.-Y. Seol, J. Park, B. Lee, J. Lee, Y. Kim, J. Cho, K. Cheun, and F. Aryanfar, "Millimeter-wave beam forming as an enabling technology for 5G cellular communications: theoretical feasibility and prototype results," *IEEE Communications Magazine*, vol. 52, no. 2, pp. 106–113, 2014.
- [4] Rappaport, Theodore S., James N. Murdock, and Felix Gutierrez. "State of the art in 60-GHz integrated circuits and systems for wireless communications." *Proceedings of the IEEE* 99.8 (2011): 1390-1436.
- [5] Park, Seong-Jin, Dong-Hun Shin, and Seong-Ook Park. "Low Side- Lobe Substrate- Integrated-Waveguide Antenna Array Using Broadband Unequal Feeding Network for Millimeter-Wave Handset Device." *IEEE Transactions on Antennas and Propagation*, vol. 64 no.3 pp. 923-932, 2016.
- [6] P. N. Choubey, W. Hong, Z. C. Hao, P. Chen, T. V. Duong and J. Mei, "A Wideband Dual-Mode SIW Cavity-Backed Triangular- Complimentary-Split-Ring-Slot (TCSRS) Antenna," *IEEE Transactions on Antennas and Propagation*, vol. 64, no. 6, pp. 2541- 2545, 2016.
- [7] + M. Khalily, R. Tafazolli, T. A. Rahman and M. R. Kamarudin, "Design of Phased Arrays of Series-Fed Patch Antennas With Reduced Number of the Controllers for 28-GHz mm-Wave Applications," *IEEE Antennas and Wireless Propagation Letters*, vol, pp. 1305-1308, 2016.
- [8] Dadgarpour, M. Sharifi Sorkherizi and A. A. Kishk, "Wideband Low- Loss Magnetolectric Dipole Antenna for 5G Wireless Network With Gain Enhancement Using Meta Lens and Gap Waveguide Technology Feeding," *IEEE Transactions on Antennas and Propagation*, vol. 64,no. 12, pp. 5094-5101, Dec. 2016.

- [9] A Rida, M Tentzeris, S Nikolaou, "Design of low cost microstrip antenna arrays for mm-wave applications", IEEE APS-URSI, 2011.
- [10] Muhammad Khattak, Ubaid Khan, Zakaullah and Gunawan witjaksono, Elliptical Slot circular Patch Antenna Array with Dual Band behaviour for future 5gmobile communication, "Progress in Electromagnetic ResearchC-January 2019.
- [11] Di Paola, C., Zhao, K., Zhang, S., & Pedersen, G. F. (2019). SIW Multibeam Antenna Array at 30 GHz for 5G Mobile Devices. *IEEE Access*, 1–1. doi:10.1109/access.2019.2919579
- [12] Rahman, A., M. Y. Ng, A. U. Ahmed, T. Alam, M. J. Singh, and M. T. Islam, "A compact 5G antenna printed on manganese zinc ferrite substrate material," *IEICE Electronics Express*, Vol. 13, No. 11, 2016037720160377, 2016.
- [13] Sam, C. M. and M. Mokayef, "A wide band slotted microstrip patch antenna for future 5G," *EPH International Journal of Science And Engineering (ISSN: 2454-2016)*, Vol. 2, No. 7, 1923, 2016.
- [14] Thomas, T., K. Veeraswamy, and G. Charishma, "MM wave MIMO antenna system for UE of 5G mobile communication: Design," 2015 Annual IEEE India Conference (INDICON), 15, IEEE, December 2015. Sam, C. M. and M. Mokayef, "A wide band slotted microstrip patch antenna for future 5G," *EPH—International Journal of Science And Engineering (ISSN: 2454-2016)*, Vol. 2, No. 7, 1923, 2016.
- [15] Ali, M. M. M. and A. R. Sebak, "Dual band (28/38 GHz) CPW slot directive antenna for future 5G cellular applications," 2016 IEEE International Symposium on Antennas and Propagation (APSURSI), 399400, IEEE, June 2016.
- [16] Ahmad, W. and W. T. Khan, "Small form factor dual band (28/38 GHz) PIFA antenna for 5G applications," 2017 IEEE MTT-S International Conference on Microwaves for Intelligent Mobility (ICMIM), 2124, IEEE, March 2017.
- [17] Jandi, Y., F. Gharnati, and A. O. Said, "Design of a compact dual bands patch antenna for 5G applications," 2017 International Conference on Wireless Technologies, Embedded and Intelligent Systems (WITS), 14, IEEE, April 2017.
- [18] A. H. Naqvi, and S. Lim. "Design of Polarization Reconfigurable Antenna using Liquid Metal." In 2018 International Symposium on Antennas and Propagation (ISAP), pp. 1-2. IEEE, 2018.
- [19] W. A. Awan, A. Zaidi, N. Hussain, S. Khalid, and A. Baghdad. "Characterization of dual band MIMO antenna for 25 GHz and 50 GHz applications." In 2018 International Conference on Computing, Electronic and Electrical Engineering (ICE Cube), pp. 1-4. IEEE, 2018.
- [20] A. H. Naqvi, and S. Lim. "Microfluidically polarization-switchable metasurfaced antenna." *IEEE Antennas and Wireless Propagation Letters* 17, no. 12 (2018): 2255-2259
- [21] Riyadh Khlf Ahmed and Israa H. Ali "SAR Level Reduction Based on Fractal Sausage Minkowski Square Patch Antenna." *Journal of Communications* Vol. 14, No. 1, January 2019.
- [22] Vu Van Yem and Nguyen Ngoc Lan. "Gain and Bandwidth Enhancement of Array Antenna Using a Novel Metamaterial Structure." *Journal of Communications* Vol. 13, No. 3, March 2018.

Smart Saline Monitoring Device Using LoRa Technology

Balabasker S¹, Umamaheswari D², Radhakrishnan B³

^{1,3}Associate Professor, St. Anne's College of Engineering and Technology

²Assistant Professor, St. Anne's College of Engineering and Technology

Abstract

In the Hospital during medication processes there is a common practice to treat patient with saline for dehydration and other medical illness to improve their health condition. In many hospitals, the nurses are responsible for monitoring the level of saline bottle but due to negligence and unusual condition, the exact timing of removing the needle from the patient's vein is ignored which causes serious problems and may lead to death also. Therefore, to prevent this type of issues due to the ignorance of nurses and to provide remote surveillance, we have proposed a Low cost smart saline level monitoring device which includes the combination of weight sensor and LoRa (Long Range) technology. LoRa wireless communication technology allows facilitating the development of data communication network over a large-area, improving sensing reliability, extending battery life as well as reducing total system costs. Our proposed system continuously monitors the weight of the saline bottle, if the level is low then it alerts the care taker in the room with the ISD1820 playback module and also nurse using our device remotely with the alarm sound. If no action is performed for a particular time then the system will close the saline flow using a solenoid valve connected to the bottle, thus help to monitor the safety of the patients.

Keywords: *Saline, Weight Sensor, Lora Technology, wireless sensor networks*

1 Introduction

Internet of things is one the innovative and smart technology of this era. It has enabled the ability of objects to connect and communicate via internet. There are many applications of IOT. However, in the rural areas where there is no internet, isn't communication important and necessary for people living there, And also considering the scenario where the receiver is at far end and there is a low internet signal quality in between the transmitting and receiving end in that case we can use LoRa technology. "LoRa" term can be abbreviated as Long Range, LoRa is a technology which is used to communicate over long distances without any internet. There are two main reasons for opting LoRa which are long range communication and has low power consumption rate [1]. Compared to various other technologies like internet, Wi-Fi, blue-tooth and Zigbee it is observed that LoRa consumes less power, uses low bandwidth, it has high transmission range approximately 30- 40 kms, uses license free sub-gigahertz radio frequency bands like 433 MHz, 868 MHz (Europe), 915 MHz (Australia and North America) and 923 MHz (Asia), it is also multipath resistant but the data rate is comparatively low [2]. The latest report of Global Health Observatory (GHO) data on the density of physicians per population states that globally the ratio of physicians is less than 1 per 1000 persons [3]. Building smart healthcare [4] including telehealth is a need so that the care must be reachable. In order to make the healthcare system smart, it is required to automate the function of diagnosis, treatment, management, and decision, so that the services are available both for rural and urban people. One of the important challenges related to the management of healthcare is to watch the saline level. Almost in all hospitals, a caretaker/nurse is responsible to keep an eye on the saline level and if they fail to monitor this, it is the patient who suffers. Saline bottle when emptied and if the needle is not removed from the patient's vein then due to the pressure difference, the blood flows outward into the bottle which may lead to serious casualty. So, it is the need to automate the surveillance in order to prevent such accident. Further, long distance monitoring by the clinician is also a requirement in telehealth [5] services. Many authors [6], [7], [8] have addressed the above discussed problem with the alert notification system. The authors [6] have used the buzzer sound to alert the nurse. Buzzer sound alert system creates noise which is not suitable for the hospital which requires a soundless environment. Moreover, this buzzer system is not expandable for telehealth. On the other side, the authors of [7], [8] have used SMS messaging system for sending an alert message to the nurses mobile number. This system has used GSM (Global System for Mobile Communications) technology [7], which is an open cellular technology, for transmitting data services. However, the authors [8] have discussed that accessing cellular data is more expensive than WiFi. WiFi is a local area network (LAN) run in a local environment or in a distributed setting. WiFi network protocol is one of the leading communication technology used in the IoT world which supports low transmit power along with low cost [9]. For providing the cost-effective solution, we have proposed IoT based saline level monitoring system using ultra-low power low-cost WiFi technology. The components, we have used to build this system includes a load sensor [10] and ESP32 WiFi chip [11]. The load sensor converts the current weight of the saline bottle into a specific voltage. The

ESP32 WiFi chip receives continuous voltage level from the load sensor and publishes notification message to the nurse station, doctor, nurse, caretaker etc., once the specified threshold saline level is reached.

1.1 LoRa

LoRa network topology is generally a star-of-stars where the gateway acts as a bridge to connect LoRa nodes to the central network. Gateway connects to the internet by using IP connections, while LoRa nodes communicate with each other by using single-hop wireless communication method. Generally, LoRa nodes communicate in two directions, but if necessary, LoRa node can also broadcast to all nodes around. Communication between LoRa nodes and the gateway can be configured according to the used frequency and used data rate. The value of the data rate determines the distance and the length of time of a packet data transaction. Communication using different data rates will not interfere with each other, so the gateway can receive packets of data from multiple LoRa nodes simultaneously [4]. The quality of a wireless communication technology is determined by 3 things, distance, and speed and power consumption. Only 2 of the 3 specifications can be applied at a same time. The comparison of some wireless communication technology is shown in Figure.

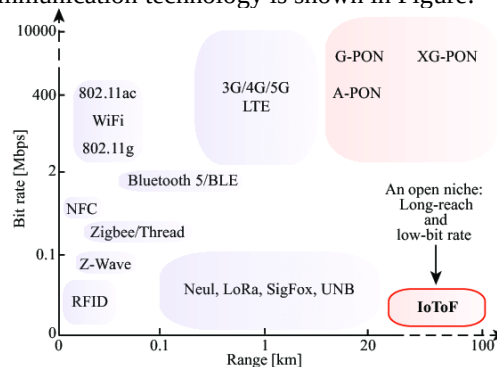


Figure 1: Bandwidth vs Range of wireless technology

1.2 Objective of the Project

The objective of the project is to develop a device that stimulate the data transmission between the transmitting and receiving end which are kept quite apart from each other by using LoRa as source of connection establishment and not by using the internet. This helps us in understanding how the long-range connectivity and communication can happen in rural areas where there is no internet available. However, as every coin has two phases this budding technology has also got pros and cons. Pros of this technology include long range communication, maximum utilization of the bandwidth, low power consumption, multipath resistance and high robustness and when it comes to disadvantages the data rate is low compared to other technologies therefore video cannot be transmitted and the noise is high as it operates just below the noise floor. LoRa can be used in the rural areas to enable the connectivity and communication over long distances with low power consumption. This was the main motive behind our project as we had thought that isn't communication necessary and vital for people who are living in rural areas where there is no internet facility? In our project we have developed a prototype which has transmitting and receiving end our ultimate aim is to transmit information successfully from transmitting end to receiving end without using any kind of internet so that it gives us an idea of how data can be communicated in rural areas without any internet. Through this project we would like to prove data can be transmitted over long range with low power consumption. Usually the range of LoRa is believed to be more than several Kms. However, as this a prototype we are testing for 1Km. The principle on which it operates is CSS where spreading factor plays a major role usually spreading factor between 7-12 are used. By using this method the overall cost of communication between IoT devices can be reduced.

1.3 Existing System

In the present health care systems nurses are responsible for taking care of patients. They are the one who monitors the saline level and uses roller clamp for controlling the flow of saline manually. When the clamp is rolled in upward direction it compresses the tube and stops or slows the saline rate [6][7]. If it is rolled in

downward direction it releases the tube and increases the fluid rate. In the present world there exists no system which will reduce the dependency of nurses in monitoring the saline levels. Thus there is a need for development of automatic saline level monitoring system [15].

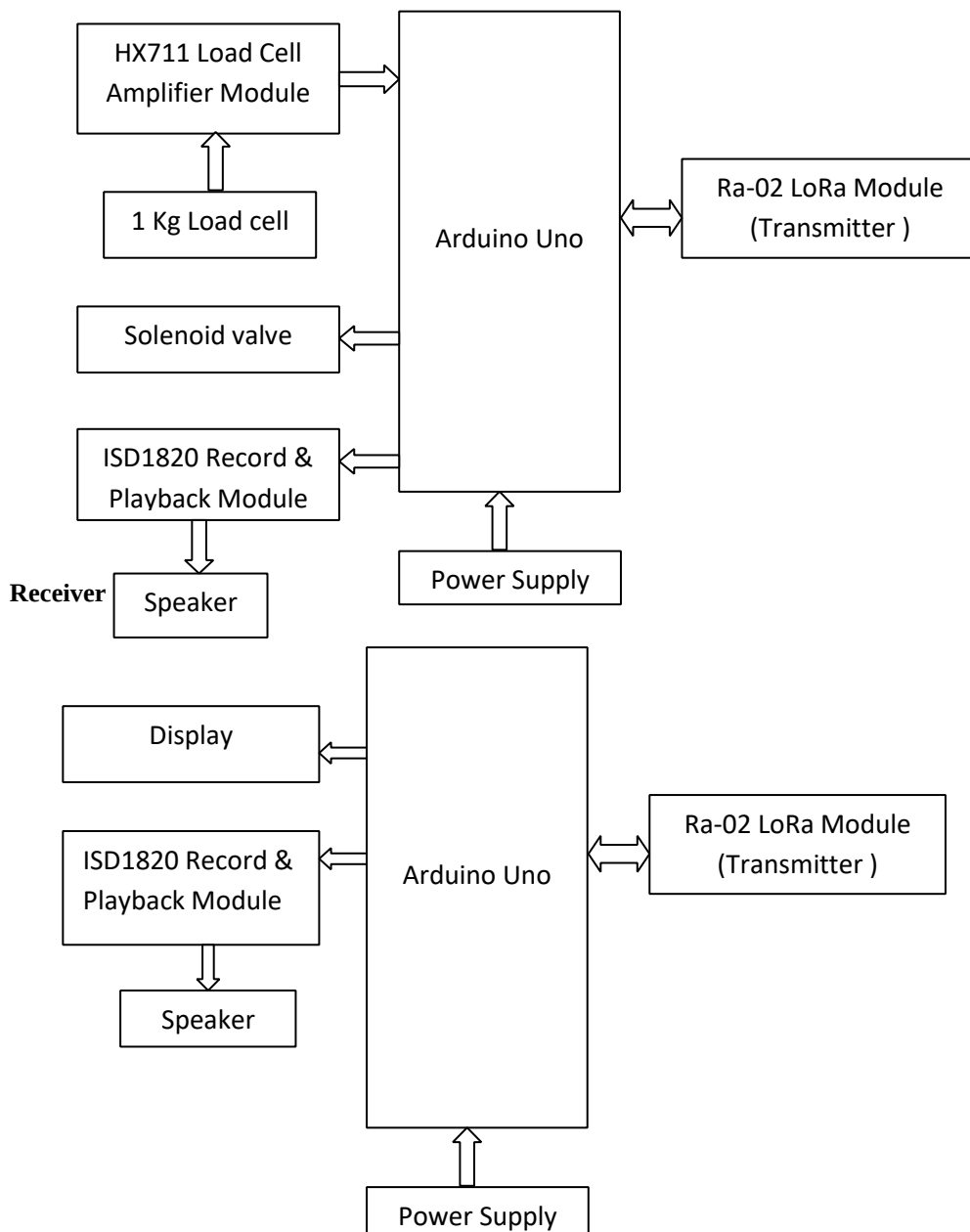
2 Proposed System

The system is composed of five components: Load Sensor, Solenoid valve, arduino uno, LoRa Module (Ra-02), ISD1820 Module. The load sensor is fixed on saline hanger and bottle is hung on it. This sensor converts the varying weight of the bottle into different voltages. So, each level of saline weight corresponds to some specific voltage. The output voltage from the load sensor is fed in the arduino uno. Out of the continuous input voltage received, when the specific voltage of interest is obtained, arduino uno checks under the following conditions.

- 1) Mode 1, when the saline bottle is full (1000ml).
- 2) Mode 2, when the liquid level is reduced to 15% (150ml).
- 3) Mode 3, when only 5% (50ml) of the liquid level is left in the bottle.

The general process of the proposed system is shown in figure 1. In the next section, we will describe each of the components in detail

Transmitter Side:



3 System Specification

In the proposed system, the weight of the saline bottle is monitored so that when the liquid reaches to its minimum level, Arduino uno with Ra-02 Lora module is used to send alerts to the nurse away from patient room. Below we describe the working of each module:

Load Sensor: It is comprised of a load cell and a HX711 chip. The load sensor works on the principle that on applying a mechanical load, the piezoelectric material of strain gauge in the load cell deforms that leads to change in resistance and thereby the output voltage will change. So, the load cell in a sensor acts as a transducer that converts load into measurable electrical output. This analog output is fed to the HX711 chip which amplifies and converts the analog voltage into a pulse width modulated (PWM) digital voltage. Further, the amplified output voltage from the HX711 chip is fed in one of the GPIO input pin of the ESP32 chip shown in figure 2.

Ra-02 LoRa: Ra-02 is used for ultra-long distance spread spectrum communication and compatible FSK remote modulation and demodulation rapidly. Ra-02 is widely used in a variety of networking processes, for meter reading, home automation, security, irrigation systems, is the best solution for networking applications. Ra-02 is available in packages called SMD packages and is used for efficient production using SMT equipment. It gives very high reliability connections based upon the respective modes reaching customers requirement. The essential features of LoRa may include high blocking resistance, provides preamble detection and half-duplex communication and many more [4].

Solenoid Valve: The Solenoid valve is an electro mechanical device in which the solenoid uses an electric current to generate a magnetic field and thereby operate a mechanism which regulates the opening of fluid flow in a valve.

Arduino Nano: Arduino Nano is a small, compatible, flexible and breadboard friendly Microcontroller board, developed by Arduino.cc in Italy, based on ATmega328p (Arduino Nano V3.x) / Atmega168 (Arduino Nano V3.x). It comes with exactly the same functionality as in Arduino UNO but quite in small size. It comes with an operating voltage of 5V, however, the input voltage can vary from 7 to 12V. Arduino Nano comes with a crystal oscillator of frequency 16 MHz. It is used to produce a clock of precise frequency using constant voltage. Arduino Nano Pinout contains 14 digital pins, 8 analog Pins, 2 Reset Pins & 6 Power Pins. Flash memory is 16KB or 32KB that all depends on the Atmega board i.e Atmega168 comes with 16KB of flash memory while Atmega328 comes with a flash memory of 32KB. Flash memory is used for storing code. The 2KB of memory out of total flash memory is used for a bootloader.

ISD1820: It is a small Voice Recorder and Playback module that can do the multi-segment recording. The user can achieve a high quality of recording (for 8 to 20secs) for each application with the adjustment of the on-board resistor. This Voice Recorder/Playback module is designed with embedded-Flash memory, which can hold data for up to 100 years and erase/record the life cycle up to 100,000.

4 Hardware setup

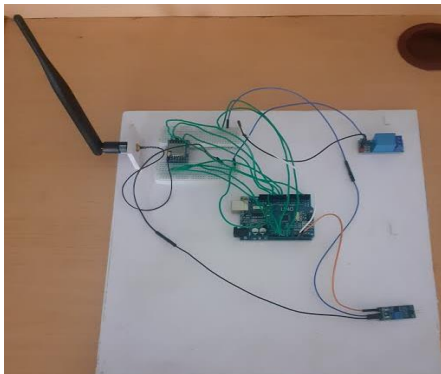


Figure 2: Transmitter side

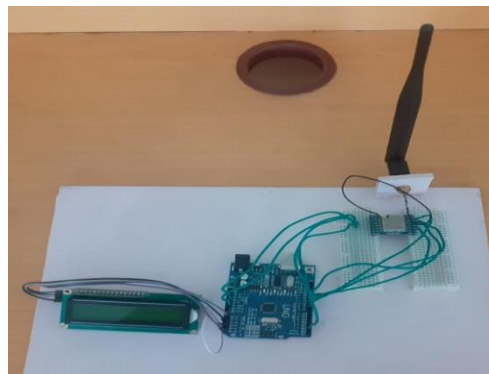


Figure 3: Receiver side


```

COM6
LoRa Sender
Sending packet: 0
Sending packet: 1
Sending packet: 2
Sending packet: 3
Sending packet: 4
Sending packet: 5
Sending packet: 6
Sending packet: 7
Sending packet: 8

COM5
LoRa Receiver
Received packet 'hello 2' with RSSI -65
Received packet 'hello 3' with RSSI -69
Received packet 'hello 4' with RSSI -68
Received packet 'hello 5' with RSSI -65
Received packet 'hello 6' with RSSI -69
Received packet 'hello 7' with RSSI -69
Received packet 'hello 8' with RSSI -68

```

Figure 4: Lora Module test output

5 Conclusions

In this paper, we have proposed a cost-effective smart saline level monitoring device by which the level of the saline bottle fed to the patient can be monitored remotely by the nurse, caretaker, hospital staff, doctor etc. We have adopted LoRa Technology as it is efficient for low cost and low power devices. Furthermore, we have believed that using this proposed monitoring system one can monitor the level of the saline bottle from a distant position which will aid in building smart healthcare system.

References

- [1] "LoRa Modulation Basics" (PDF). Semtech. Archived from the original (PDF) on 2019-07-18.
- [2] Ramon Sanchez-Iborra; Jesus Sanchez-Gomez; Juan Ballesta-Viñas; Maria-Dolores Cano; Antonio F. Skarmeta (2018). "Performance Evaluation of LoRa Considering Scenario Conditions". *Sensors*. 18 (3): 772. doi:10.3390/s18030772. PMC 5876541. PMID 2951 0524.
- [3] WHO: http://www.who.int/gho/health_workforce/physicians_density/en/
- [4] Lei Yu, Yang Lu & XiaoJuan Zhu, Smart Hospital Based on Internet of Things, *Journal Of Networks*, Vol 7, No. 10, 2012.
- [5] Priyadharshini.R, Mithuna.S, Vasanth Kumar.U, Kalpana Devi.S, SuthanthiraVanitha.N., Automatic Intravenous Fluid Level Indication System for Hospitals, *International Journal for Research in Applied Science & Engineering Technology*, Vol 3, Issue VIII, 2015.
- [6] S. Gayathri & C.S. Sundar Ganesh, Automatic Indication System Of Glucose Level In Glucose Trip Bottle, *International Journal of Multidisciplinary Research and Modern Education*, Vol 3, Issue 1, 2017.
- [7] Ram Kumar S, Saravana Kumar S, Sukumar M, Remote Monitoring The Glucose Bottle Level In Hospitals, *International Conference on Emerging Trends in Applications of Computing*, 2017. GSM: <https://www.gsma.com/aboutus/gsm-technology/gsm>.
- [8] Pallavi Sethi and Smruti R. Sarangi, Internet of Things: Architectures, Protocols, and Applications, *Journal of Electrical and Computer Engineering*, 2017
- [9] I. Muller and R. M. de Brito and C. E. Pereira and V. Brusamarello, Load cells in force sensing analysis – theory and a novel application, *IEEE Instrumentation Measurement Magazine*, 13, 1, 15-19, 2010.
- [10] ESP32: <https://www.espressif.com/> [12] Eugster, Patrick Th. and Felber, Pascal A. and Guerraoui, Rachid and Kermarrec, Anne-Marie, The Many Faces of Publish/Subscribe, *ACM Comput. Surv.*, vol 35, June 2003.
- [11] T. Petric, M. Goessens, L. Nuaymi, L. Toutain, A. Pelov. 2016, Measurements Performance and Analysis of LoRa FABIAN a real-world implementation of LPWAN, *Personal Indoor and Mobile Radio Communications (PIMRC) 2016 IEEE 27th Annual International Symposium on*. IEEE, pp.1-7.
- [12] Mikhaylov, K, Petäjälärvi, J, Hänninen, T. 2016 . Analysis of capacity and scalability of the LoRa low power wide area network technology. In: *European wireless conference 2016 (EW16)*, pp.1–6. Berlin: VDE-Verlag.
- [13] LoRa Alliance. <https://www.lora-alliance.org/> (accessed 22 June 2018).
- [14] Network, T. T. (2016). *Forum: The Things Network..* (accessed 22 June 2018).
- [15] Rodrigo Pantoni , Cleber Fonseca and Dennis Brandaõ 2012. Street Lighting System Based on Wireless Sensor Networks, *Energy Efficiency Moustafa Eissa, IntechOpen*, DOI: 10.5772/48718.
- [16] F. Adelantado, X. Vilajosana, P. Tuset, B. Martinez, J. MELIA-SEGUI, T. Watteyne. (2017) Understanding the limits of lorawan, *IEEE Communications Magazine*.

- [17] Augustin, A.; Yi, J.; Clausen, T.; Townsley, W.M. 2016) A Study of LoRa: Long Range & Low Power Networks for the Internet of Things. *Sensors* 2016, 16, 1466

A Survey On Gps Based Smart Speed Control For Electric Vehicle In Speed Restricted Zone

¹Dr.M. PheminaSelvi, ²R.Thenmozhi, ³M.Yuvarani, ⁴N.Helka, ⁵K.Priyanka

^{1,2,3,4,5} University College of Engineering Villupuram

Abstract

Electric vehicle (EV) is a thrust area of research in the recent trends due to the increase in the green house effect . Electric vehicle refers to the vehicles that runs only on electricity. It requires an electric motor to run instead of burning a mix of fuel and gases. It helps in reducing global warming , low maintenance, zero emission, greater convenience and low maintenance. EVs works on the principle of transducing effect. By 2030, the government aims to make India a 100% EV nation. It has proposed that two wheelers below engine capacity of 150cc sold in country after March 31, 2025 and three wheelers sold after March 31, 2023 should be EV. So, it is beneficial to use Electric vehicles.This papers gives a detailed survey on various types of electric vehicle available and the various types of speed control techniques that have been used for various applications.

1 Introduction

EVs have existed since nineteenth century. In 1996, the first commercial electric scooter was produced by Peugeot. In recent years, existing automobile manufacturers and new dedicated companies have put interesting effort in transforming conventional vehicle into an electrical vehicle. The electric scooter works on batteries . These are rechargeable batteries and are either of Lead or Lithium types. In order to limit the speed of the vehicle in speed restricted areas like ,schools, hospitals, malls and crowded areas ,a microcontroller needs to incorporate in the vehicle. In 1915, Autoped introduced the first stand-up scooter in which pulling back on the handlebar disengaged the clutch and applied the brake. Autoped continued production until 1921. Krupp belongs Germany built the Autoped under license from 1919 to 1922. In 1986, Go-ped introduced the first production stand-up scooters , “Roadster” and the “Sport”. In 2001, Go-ped introduced the first primary full suspension stand-up electric scooter, the “Hoverboard”.In 2004, Evo Power boards introduced the first primary scooter with a two-speed transmission, the “2x”.In 2009, Go-ped introduced its first completely propane-powered scooter and go-kart, the “GSR Pro-Ped” and therefore “GSR Pro-Quad”. In 2013-2014, Light electric folding scooters that are charged by lithium batteries and brushless hub motors become available. In 2018, Dockless scooter –sharing systems are rolled out in major cities , largely as expansions of bike-sharing systems.This evolution of electric vehicle has passed decades improvising its working performance on various aspects and the current trend of vehicles is marching toward fully electric eco friendly systems. Electric Vehicles are quite convenient to use. It doesn’t emit any harmful gases such as CO, CO₂, NO, S,SO₂ so it is eco-friendly to environment. It posses less noise pollution, charge at home Fast and smooth acceleration, Low cost operation. So it is better to use electric vehicle than internal combustion engine.

2 Types Of Electric Vehicles

There are three types in electric vehicle namely Battery Electric Vehicle(BEV), Plug-in Hybrid Electric Vehicle(PHEV) and Hybrid Electric Vehicle(HEV).

BATTERY ELECTRIC VEHICLE:

A BEV runs fully on a battery without an internal combustion engine. Electricity is stored in overboard batteries that are charged by plugging into electricity grid. The batteries in turn gives power to one or more electric motors.

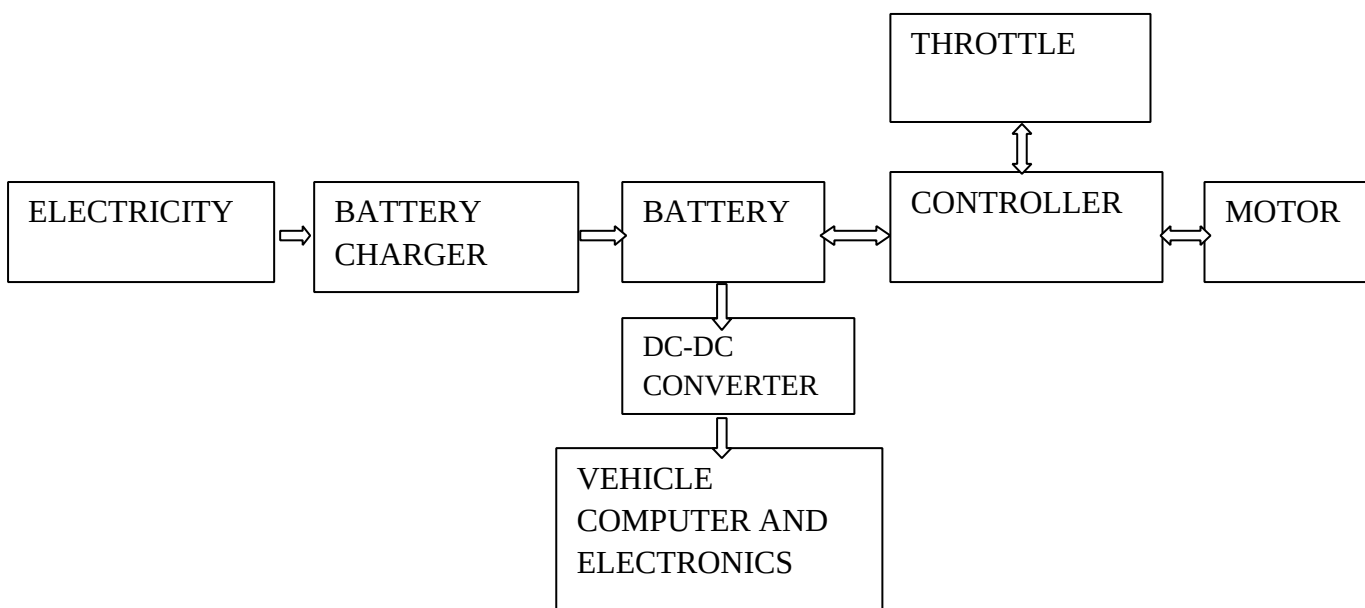
PLUG-IN HYBRID ELECTRIC VEHICLE:

A PHEV runs on battery and gasoline. PHEVs have rechargeable battery packs which handover 20-80km of all-electric driving before internal combustion engine or generator activates for extended trips.

HYBRID ELECTRIC VEHICLE:

A HEV has two complementary drive systems a internal combustion engine and fuel tank and an electrical motor and battery. The internal combustion engine and electric motor simultaneously turns the transmission, which powers the wheels. HEV can't be recharged from the facility grid. Their electric energy integrately comes from regenerative braking and most of their driving is spent using gasoline.

3 General Block Diagram Of Electric Vehicle



The battery is the main energy storage . It is used to convert the electricity from mains to charge the battery. The battery voltage DC and current (I) is inverted into switched-mode signal through power electronic controller to drive the motor. The characteristics of the charger depend on the components, switching strategies control algorithm. This algorithm can be implemented digitally using microcontroller. The motor controller is a device that serves to govern in some predetermined manner of performance of an electric motor. The motor controller controls all the functional capabilities and it is the central component of the system. Motor controller can be adjusted to synchronize with other brushless motor. To drive and control the BLDC motor, the use of motor controller is implemented. BLDC motor is a synchronous electric motor which is powered by direct current electricity and which has electrically controlled commutation system. DC-DC controller converts a source of direct current (DC) from one voltage level to another. When the throttle is engaged the motor provides power and the vehicle forward. Most Throttle Fine Tuned Like A Volume Dial Between Low And Full Power. When The Torque Increases, The Speed Of The vehicle decreases. Thus the speed is controlled in such a manner.

The following table give a complete survey of the various types and models of electric vehicle , its features with its merits and demerits available in india. The different types and models varies in their structure , shape and functional operation of providing the application intended.

4 Electric Scooter Companies In India

| Model | Founder | Motor used | Features | Advantages | Disadvantages |
|-----------------|---------------------------------------|------------------------------------|---|---|--|
| Ather 450 | Tarun Mehta Swapnil Jain (2013) | Brushless Dc motor | 7" dashboard touch screen, On-board navigation, LED lighting, Auto cancelling indicator, Cloud connectivity, IP67 for water & dust proof. | Best quality provide, High torque output, Maximum power rating. | Price tag is too high, Anti-theft mechanism is unavailable, Rear disc brake frequently locks up wheel under hard braking, Braking has been an issue. |
| Ather 450x | Tarun Mehta Swapnil Jain (2013) | Permanent Magnet Synchronous Motor | Combining Braking system, Digital speedometer, LED tail light. | The maximum power rating of the 450x's motor has now been bumped upto 6kW, 0.6kW more than old 450. | Limited availability, Rear disc brake frequently locks up wheel under hard braking. |
| Bajaj chetak | Jamnallal Bajaj (2019) | Brushless DC motor | Keyless start-stop system, Water resistant (IP67 rating), Glove box, Battery Warrently (3 years , 50,000 km), Reverse gear, Regenerative braking system, Touch sensitive switches. | Combining braking system, Digital odometer, Digital tripmeter, Top-notch build. | No ABS, Digital speedometer is difficult to read at the bright sunlight, Ride quality at speed feels a little harsh. |
| TVS iQube | Venu Srinivasan (2020) | Brushless Dc motor | TVS smart connect, Geofencing Remote battery charge status, Navigation assist, Last park location, Incoming call alert, SMS alert, Q-Park assist, Regenerative braking, Smart ride statistics, Range indication over speed alert. | High torque at wheels, Powerful hub motor, features Q-park, Well balanced suspension setup. | Annoying startup time, The raised floorboard, Doesn't support fast charging. |
| Okinawa praise | Jeetender Sharma (2018) | Brushless DC motor | Keyless entry, Find my Scooter function, Mobile charging USB port, Motor walk, LED rear winklers, Licence plate lamp, Aerodynamic design | Reverse mode, Digital odometer, central locking system, Anti-theft system, E-ABS. | No GPS Navigation, Geo fencing, Mobile app connectivity, Parking assist and Hill assist |
| Okinawa ipraise | Jeetender Sharma (2019) | Brushless DC motor | Tracking riding status, Geo fencing, Anti-theft alarm, Keyless entry, Mobile charging USB | Smooth electric motor, Good top speed. | Pricey tag, Limited service network. |

| | | | | | |
|--------------------|------------------------------|------------------------------|--|--|--|
| | | | port, Speed alert, Regenerative braking system | | |
| Okinawa praise pro | Jeetender Sharma (2019) | Brushless DC motor | Motor walk assist, Keyless entry, Mobile charging USB port, Speed alert, Regenerative braking system | Simple portable, Reverse mode. | Shorter battery replacement, Bulky, Low facilities for maintenance |
| Hero photon 48V | Brijmohan lall Munjal (2007) | Brushless DC motor Hub motor | Polycarbonate head lamp for clear night vision, front telescopic suspension a front brake disk and an anti-theft alarm, Reverse mode, Mobile app connectivity, GPS & Navigation, Touch Screen display, Central locking system. | Smooth ride, awesome pickup, high quality motor. | High charging time and low top speed. |
| Ampere Reo | Hemalatha annamalai (2008) | Brushless DC motor | Digital speedometer , charging point, coil spring rear suspension | Digital console, Anti-theft alarm, Keyless entry, High power acceleration. | No fuel gauge, Low speed. |

5 Survey On Automatic Vehicle Speed Control System

Sigeru Omatu(1993) worked on speed control of an electric vehicle system using PID type neurocontroller. He preferred PID Controller to control the speed of electric vehicle. In order to improve the performance of speed control, a neural network is applied to tuning parameters of PI controller. Neurocontrol is well known as an attractive approach which can overcome many difficulties by conventional control. Neural network(NN) which is the core of neurocontroller(NC), has properties of self organization through learning and generalization due to large number of simple non-linear processors. Self organization enables the NC to perform adaptive control and deals with a system with unknown structures. The auto tuning PID – type NC which is the PID controller using a neural network to obtain automatically PID gains is applied to speed control. He believed that PID controller to be effective for tuning control.

M. C. Tsai(2001) worked on control of variable – winding brushless motor in electric scooters. He presented the drive control of a variable-winding brushless DC motor for electric scooters. The approach is predicted on changing the winding connection on the motor's stator where the 2 sets of motor windings are controlled alternately to realize both high starting torque and high operating speeds. The series connection is employed at low speed operation for top torque and provides smooth acceleration from a standing start, and therefore the parallel connection is employed mainly for high-speed operation. A closed-loop torque control scheme is used such that the torque-speed characteristics of the drive output have a function almost like that of continuously variable transmissions (CVT). By combining the motor winding connection control and therefore the torque control, this 2-state-CVT is in a position to enhance the general efficiency and reduce the load of electric scooters.

Suk won cha(2009) worked on HEV Cruise control strategy on GPS information. He demonstrated the development of the hybrid vehicle control system with the GPS (Navigation) system of a vehicle travelling a pre-planned driving route. To verify the improvement in vehicle fuel economy, he developed the forward-facing simulator, which can be applied to the proposed HEVs control system. The proposed HEVs control system finds upcoming driving patterns because it has terrain(uphill, downhill) and speed information. The controller calculates the parameters related to pattern recognition during a sampling time to choose a comparable driving cycle and to classify into three driving modes(Urban/Extra-Urban/Highway mode). A dynamic programming approach is proposed to obtain the optimal fuel economy and the state of charge (SOC) trajectory. For this approach, he developed a rule-based controller to manage the battery SOC according to the target SOC range. The amount of the target SOC range depends on the driving pattern recognition during a selected period of time. The conventional HEV control system maintains the battery SOC within a limited range. Compared to the traditional controller, the proposed system, by using road slope and speed information, gives results that confirm improved fuel economy.

Chih-Hong Lin and (2011) worked on The Hybrid RFNN Control for a PMSM Drive Electric Scooter Using Rotor Flux Estimator. He demonstrated the hybrid recurrent fuzzy neural network (HRFNN) control for permanent magnet synchronous motor (PMSM) drive system using rotor flux estimator is developed to control electric scooter. First, the dynamic models of a PMSM drive system were derived in consistent with electric scooter. Owing to the load of electric scooter existed many uncertainties, for example, non linear friction force of the transmission belt, and so forth. The electric scooter with nonlinear uncertainties made the PI controller to disable speed tracking control. Moreover, so as to scale back interference of encoder and price down, an HRFNN system using rotor flux estimator was developed to regulate PMSM drive system so as to drive electric scooter. The rotor flux estimator consists of the estimation algorithm of rotor flux position and speed supported the rear electromagnetic force (EMF) so as to provide with HRFNN controller. The HRFNN controller consists of the supervisor control, RFNN, and compensated control with adaptive law is applied to PMSM drive system. The parameters of RFNN are trained consistent with different speeds in electric scooter. The electric scooter is operated to provide disturbance torque. To show the effectiveness of the proposed controller, comparative studies with PI controller are demonstrated by experimental results.

Vishnu Sidharthan(2015)worked on Brushless Dc Motor Driven Plug In Electric Vehicle. He deals with the electric scooter in which a Brushless DC(BLDC) motor is incorporated at the rear wheel of the scooter. The controlling of BLDC motor is completed by a Control Unit during which the motor rotates supported current commutation. With the hall sensor outputs at each position of rotor there'll be a switching scheme of six different states. Start stop and speed control of vehicle are controlled by the MCU. A 60V,1000W BLDC Motor is chosen to drive the vehicle. The mathematical modelling of BLDC motor is implemented in matlab simulink. Also the closed loop system speed control of BLDC motor is completed in matlab. Hardware control of motor is done using Arduino uno development board in which At mega 328 microcontroller is embedded. Corresponding pulses are obtained to drive each switch at different commutation states. Then he proposes the complete controlling of electric vehicle which is driven by brushless dc motor.

M. Sathyendra kumar(2015) works on Mathematical modeling of permanent magnet brushless dc motor for electric scooter. He mainly deals on simulation using Matlab / Simulink for mathematical model of the PMBLDC motor for electric scooter application. He used PMBLDC motor because this motors are successfully developed to find the wide application in low power automotives due to high efficiency, silent operation, compact size, lower maintenance and high reliability. Due to the advancement in power electronics ,PM Brushless dc motors have become potential drive for automotive applications. The steady state and transient models of PMBLDC motor for efficient performance of control. The transfer function of the motor springs to reach the steadiness of the motor.

Priyanka V.Mandavgade (2017)worked on Automatic Vehicle Speed System Using Zigbee Technology. She demonstrated to automatically control the speed of the vehicles at speed restricted areas such as school and hospital zone etc. She mainly developed to avoid accidents due to high speed vehicles and also to enable the public to cross

the road without any danger from high speed vehicles. Usually the drivers drive the vehicles at high speed without considering the general public in speed limited areas too. Even though the traffic police control them we cannot achieve full response from them. Also it's impossible to watch those areas in the least time to manage their speed. Thus she gives the way for controlling the speed of vehicles within certain limit in those restricted zones without the interruption of the drivers. Here she use Zigbee transceiver communication method for controlling purpose. In order to implement this in public then she want to attach the Zigbee receiver along with the vehicle and Zigbee Transmitter with these Zones. She developed to improve bad driving behavior of driver, Traffic Management, road safety, violation management.

Indra Sidharta (2018) worked on design of performance and parameter measurement system for brushless direct current (BLDC) Motor. The electric scooter needs a controller to drive and control a brushless direct current DC (BLDC) motor. To design a controller, the designer needs some motor parameters which will not tend by the manufacturer. She presented a design of performance and parameter measurement system for BLDC in electric scooter application. The investigated parameters were stator resistance, stator inductance, battery current, Back Electromotive Force (BEMF) constant, speed, torque constant, inertia moment, and friction. To obtain these parameters, a microcontroller was used to read some output signals from voltage, speed, current, resistance, and inductance sensor. Resistance and inductance were tested before the motor was run. The motor was then given a unit step. During 5 seconds of motor running, the microcontroller recorded speed and current data. After that, the motor was unpowered. Later, the microcontroller recorded speed and back EMF voltage on each motor phase. The results revealed that the proposed system could measure the most motor parameters, such as 0.078 ohm of stator resistance, 76.52 μH of stator inductance, 20.28 volt/krpm of back EMF constant, 0.1936 Nm/A of torque constant, 0.0174Nms of friction, and 0.0471 kgm².

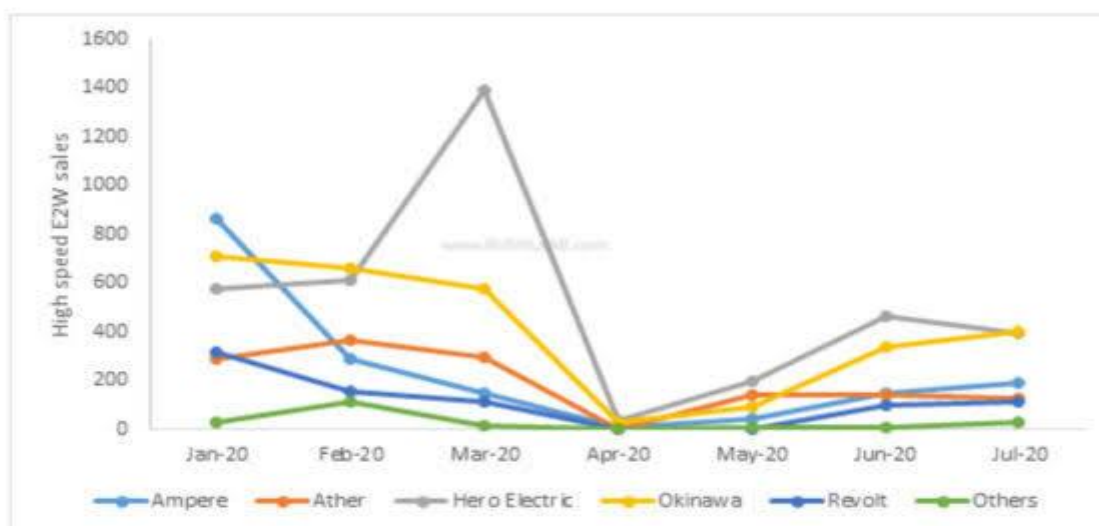
Alexandra-Iu Radu-Codrut (2019) works on Speed and Acceleration Control of BLDC Drives Using Different Types of Observers. He presents five design approaches for the speed and acceleration control of an electric drive system with time-varying inputs – speed reference and load torque – built around a brushless direct current motor. Five observers are developed and tested within the context of a cascade control structure with two control loops, which uses a variable structure controller within the inner loop (the current loop) and a classical PI controller in the outer loop (the speed loop). The observers supported predictive feedback have the advantage of faster convergence and a reduced sensitivity of estimation to parameter variation. A comparative analysis of the five proposed design approaches are in order to highlight how the specified control system performance is achieved. Then he leads to dynamically and permanently improved performance as oscillations in speed and acceleration control of BLDC.

S Sathishkumar (2020) worked on Automatic Vehicle Speed Control System in a Restricted Zone. His aim is to give a practical, compact and simple design to develop an automatic vehicle speed control system, which has to be quickly get implemented in school, college, hospital, sharp turning zones to reduce the number of accidents. This automated speed controlling system is made using the microcontroller-based platform of the Arduino Uno board. Here the Arduino is programmed in such how that, the prescribed regulation was incorporated within the transmitter unit which transmits the signals, and it had been received by the receiver in the vehicle using Zigbee wireless communication technology and the speed of the vehicle was automatically controlled by the input signals by the receiver, with help of speed encoder sensor. Once this technique was implemented the accidents will be reduced on a larger rate, and also reduce the nuisance by some drivers.

6 Electric Scooters Specification

| Parameter | ATHER 450 | BAJAJ CHETAK | TVS iQUBE | OKINAWA IPRAISE | HERO PHOTON 48V | AMPERE REO |
|------------------|---|---|---|--|---|---|
| Model |  |  |  |  |  |  |
| Max Range | 75 km | 95km | 75km | 160km | 100km | 55-65km |
| Top speed | 80km/h | 78km/h | 78km/h | 70km/h | 45km/h | 55km/h |
| Acceleration | 3.9 seconds | NA | 4.2 seconds | 9.43seconds | NA | 12 seconds |
| Charging time | 5 hours 15 min | 5 hours | 5 hours | 4 hours | 5 hours | 8-10hours |
| Battery capacity | 2.4 KWh | 3KWh | 4.5 KWh | 3.3KWh | 48V, 28Ah | 48V,28Ah |
| Peak torque | 20.5NM | 16NM | 16NM | NA | NA | 16NM |
| Motor power | 5.4kW | 3.8kW/4.08kW | 3kW/4.4kW | 1000W | 1200W | 250W |

Player-wise high-speed E2W sales trend



The Indian electric scooter and motorcycle market has experienced continuous growth since 2014. In 2019, about 152.0 thousand electric scooters and motorcycles were sold, a 20.6% rise on an annual basis from 2014. It is predicted that the yearly retail sales volume will reach 1,080.5 thousand units by end of 2025, with a CAGR of 57.9% during 2020–2025 (forecast period). Meanwhile, the retail sales value is predicted to rise to over \$1.0 billion by 2025, a CAGR of 63.9% during the 2020–2025 period.

India is the third-largest carbon emitting country in the world, accounting for around 6% of the global CO₂ emissions from fuel combustion. According to a report published by IQAir, in 2019, 21 of the world's 30 most polluted cities were in India. Also, consistent with the WHO's Global Pollution Database (2018), 14 out of the 20 most polluted cities within the world are in India. Two-wheelers are the largest vehicle class in India, accounting for 70% of the 200 million on the road currently and 80% of new vehicle sales every year. They represent an important source of pollutant emissions, responsible for 20% of the total CO₂ emissions and about 30% of the particulate matter (PM) emissions in urban areas.

To regulate the pollution by vehicles, the central, state, and native governments have taken several initiatives in recent years, including tax exemptions, purchase rebates, and financial incentives to the buyers of electric vehicles (EV). The rising government focus to curb pollution levels within the country promises a positive regulatory push for electric two-wheelers, thus helping the Indian electric scooter and motorcycle market grow. This graph represents the overall market sales of electric scooter companies in India. In Feb 2020 onwards Hero photon gradually increased and peaked at March 2020 then suddenly falls and now a days slightly increasing.

7 Conclusion

However, there are many advantages in electric vehicle like pollution free, low running cost, greater convenience, low maintenance, reduce global warming. In above surveys they controlled speed automatically in various ways. we are focusing to control the speed automatically in speed restricted zones by GPS module.

References

1. C.C. Chan, "Novel Wide Range Speed Control of Permanent Magnet Brushless Motor Drives," IEEE Trans. on Power Electronics, 1995.
2. R.-E. Precup, S. Preitl, M. Balas, and V. Balas, "Fuzzy controllers for tire slip control in anti-lock braking systems," in Proc. IEEE Intl. Conf. Fuzzy Syst., Budapest, Hungary, 2004.
3. S. Han and D. Divan, "Bi-directional DC/DC converters for plug-in hybrid electric vehicle (PHEV) applications," in Proc. 23rd Annu. IEEE Appl. Power Electron, 2008
4. Beomsoo kim, Talchol kim, Suk won cha , "HEV Cruise control strategy on GPS information", World Electric Vehicle Journal, 2009.
5. G. H.B. Foo and M. F. Rahman, "Direct Torque Control of an IPM-Synchronous Motor Drive at Very Low Speed Using a Sliding-Mode Stator Flux Observer," in IEEE Transactions on Power Electronics, 2010.
6. A.Kiruthika, A.AlbertRajan "Mathematical modelling and Speed control of a Sensored Brushless DC motor using Intelligentcontroller "2013 IEEE International Conference on Emerging Trends in Computing, Communication and Nanotechnology, 2013.
7. Amarnar Ayanan, Challa Saikumar, Chandramohan, "Automatic over speed controlling of vehicle", International Journal of Scientific and Technology Research , 2016.

8. Vaishal B Niranjane, Priyanka V Mandavgade, “Automatic vehicle speed control system using Zigbee technology”, International Journal of Scientific and Technology Research , 2017.
9. Amulya A M , Karuna C V, “Intelligent vehicle speed controller”, International Research Journal of Engineering and Technology(IRJET), 2018.
10. Alexandra-Iulia Szedlak-Stinean, Radu- Emil-Precup, “Speed and Acceleration Control of BLDC Drives Using Different Types of Observers”, IEEE International symposium , 2019.
11. Sathish kumar S , Hariprakash, “Automatic vehicle speed control system in restricted zone using Zigbee technology”, International Journal of Scientific and Technology Research , 2020.

Home Automation For Paralyzed People Using Eye Blink Sensor

S.D.Sindhuja¹, G.Umamageshwari², K.Sabarinathani³

^{1,2} Student, C.K. College of Engineering and Technology

Department of Electronics and Communication Engineering

³ Assistant Professor, C.K. College of Engineering and Technology

Department of Electronics and Communication Engineering

Abstract

The constant demand to improve daily living standards for paralysis patients or general people serves as a motivation to develop newer technology. The tasks once performed by big traditional computers are now solved with smaller smart devices. The study here talks about the development of a blink sensor device which used for automated home designs for disable people. This sensor is able to detect an intentional blink from a normal blink, which is useful for the paralysis patients especially Tetraplegic patients to regulate their home devices at ease without any help. This helps save a lot of electricity and can be installed into automated home devices easily.

Keywords: *Microcontroller, Tetraplegic, Average Flux, Home Automation*

1 Introduction

In the era of modern technology, automation is taking place everywhere. From Home to Industries, the blessing of automated system has improved the efficiency by a large magnitude. One of the great examples of the Automation System is the Home Automation. Some of the largest tech giants like, Google, Amazon etc. Already have flooded the market with the smartest home automation systems. Though, the automation is meant for simplifying our daily life however, a very targeted group of people have always been overlooked by all of these companies. Therefore, we mainly focused on this group of people who are physically challenged or paralyzed. As, this group of people are physically challenged, they mostly rely on other people's assistance. Even, they have to rely on someone else for day to day tasks. Therefore, any innovative and effective home automation technologies can be a great help for the senior citizen, disabled people and paralysis patients. As mostly these patients have limitations on physical movement, they even cannot move their hands or even talk. Furthermore, there has not been any significant medical improvement to remedy this type of disability. Though, in many cases, physical exercises and proper medication can benefit the patient, Consequences are lifelong physical disability. However, the only controls they have are their eyes. Therefore, we decided to work on an automation technology, which they can control easily using their eyes.

The existing home automation systems are mostly designed and developed for general a person who has the access to any device by physical movement. This is not useful for a paralysis patient. Hence, to develop a home automation system for patients which could be used with least or minimal effort to control the home appliances such as light, fan, air conditioner. In this paper we have worked on a Home Automation Project mainly aimed for paralyzed people to develop an IR based eye blink sensor which will be used to control electronic devices as mentioned earlier.

1.1 Motivation

The advancement of the technologies has always fascinated us. On the other hand, we also found that, there are not significant researches on automation devices for physically challenged or disabled people. Therefore, we started to look into the published papers and innovations around us. Now-a-day's medical science improving day by day. On this developing procedure human beings innovating greater strengthen scientific accessories such as smart belt which locate patient respiration as well as electro dermal activity (EDA) sensors to sequentially display for physiology symptoms of seizures at night time. Medical operations are now getting easier. Newly developed high-tech gadgets implemented in patient's body to restore normal activities. Especially paralysis patients, such as Tetraplegic Patients who suffering a lot for their physical disabilities. It's now highly important to develop a system which may help paralysis patients like Tetraplegic Patients. Moreover, people are highly interested to digitize their daily life with less physical movement. To fulfil both requirements it's high time to develop a system which may help Tetraplegic Patients as well as people who are

interested to use for efficient and comfortable life. After researching a lot in lab and over the internet, we found an Idea to develop such a system which may help a person to control any appliance which we use in our daily life by less physical effort. We found a concept to develop such a system which we can use by eye blink to automate our home electrical appliance. Though, there are many prototypes developing earlier but most of them are not user friendly or not innovative solutions. The Paper aims to develop a system eye blink based sensor for home automation which is compact hardware and simple to use for control home electricity appliance. This will also help to reduce electricity wastage and help a paralysis patient to control light and fan without any assistance of other person.

1.1.1 Overview

Our system is the solution for the paralysis patient to help them to operate various electric devices and peripheral using their eye blinks. Our system will detect patient's intentional blinks and understands the signal by predefined algorithm and operate the specified device as per instruction. To keep the cost low yet a scalable and efficient system, we used the open source Node MCU platform for the hardware using Arduino IDE.

1.2 Objective

▪ Develop user friendly sustainable appliance control system:

Developing a system that relies on minimum effort of learning curve but works efficiently. As our targeted groups of peoples are physically disabled, therefore we decided to work with eye blink. So, depending on a pattern and series of eye blinking, the system can be activated, take command and execute.

▪ Reduce Electricity Bills:

This device will also help to reduce electricity wastage as the patient has no need to call anyone to switch off or on any electronic device as this system will help them to do all these tasks instantly without any third person's assistance so, as the system works instantly, it reduces electricity wastage by saving the time between arrival of assistance and performing tasks.

▪ Design innovative solutions:

This system communicates over wireless technology so that wire hassle is reduced. Moreover, various sensors and modules shape up this as an innovative solution.

▪ Provide hands free control system:

This system helps a person or patient to operate almost everything with eye blinks so that there is no need of helping hands for physically disabled person or paralysis patients.

2 Background Study and Literature Review

Now-a-days, the rapid growth of technology has made our PC become outdated. The tasks that once we used to do with PC are now being handled by mobiles or other smart devices. Introduction of network enabled devices or IOT devices have led to advanced home automation systems. However, the usage is limited for people with physical disorders as remote control of an appliance becomes difficult. In this paper the work is about for those people who are suffering from Paralysis (As example, Tetraplegia Patients) and the difficulties which they face while controlling home appliances. Tetraplegia Paralysis is brought about by harm to the cerebrum or the spinal line this patient; client needs to control the appliance.

3 Working Methodology

The system consists of four major embedded electronics: TCRT 5000 as the Eye Blink sensor, Pair of Node MCU one at Transmitter end and other at Receiver end & Relay Modules. Additionally, a rechargeable lithium ION battery is attached with the both Transmitter Glass Frame Module and the Receiver Module. Both Transmitter Glass and Receiver Modules are connected wirelessly over Wi-Fi LINK. The TCRT 5000 sensor is a Reflective Optical Sensor which can measure the intensity of IR bounced back on the eye or eyelid. As of its cheap price and availability it suits best for our needs. When the eyes are closed the reflection value gets lower than when the eye lids are open. Therefore, we can easily identify whenever the person closes the eyes for

a specific interval. Additionally, we can also detect eye blinks. As eye blink is a natural process of human body, therefore, we specified a pattern to activate the system. Whenever the user closes the eyes for 4 seconds, the system identifies it as the start for taking action and gets ready. Otherwise it will take the eye blink as usual unintentional human behavior and the system will do nothing. Here the input will take after the system is ready to take the action after triggering the IR sensor and this system will work as per instructions.

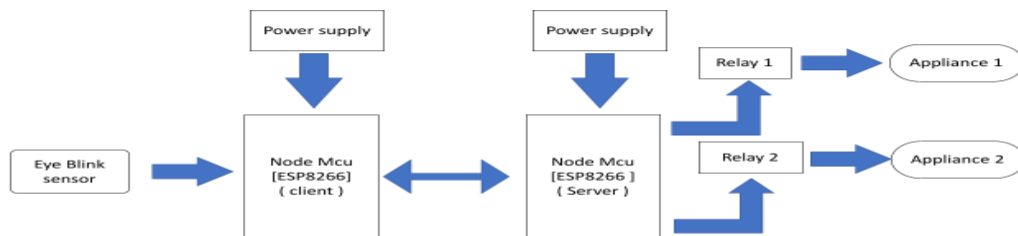


Figure 1: Home Automation Block Diagram

3.1 Work Flow

As the entire system is developed for physically disabled people, therefore we have prepared the system and the interaction easy enough that takes minimum to no effort to adopt and operate for a new person. As there are two major parts of the system, one is the wearable glass frame module, which also is actually a transmission device. And the second one is the electrical peripheral control unit, which is actually a receiver module. The glass frame is the unit that the user will be using to control the entire system. When powered on the embedded Infrared Reflection Sensor will calibrate itself by reading thousands of values for Five seconds. Then it determines the average value by doing a simple math

After it determines the average value, it then creates a Two seconds long beep to indicate that the system is on and running. From this phase, the system takes continuous reading of Infrared Reflection values from the sensors and checks if the value is less than the value of Average value. Therefore, whenever the user closes the eye lids, the reflection value usually drops by 60 (sixty) to 130 (one hundred and thirty) so, the system can identify this as “The Eyes Are Closed” or a ‘Blink’.

As the skin tone or the surrounding lighting condition may vary significantly time to time, therefore we have to introduce a Biased Value which in this case is the offset value. So that, in any condition we can identify the closing eyes or the blink more accurately. The system then also takes a record of last value of “System Time in Milliseconds”. We record it in order to trigger the Action Mode manually. As eye blinking or closing eyes is a very generic human behavior, therefore we have to trigger the Action Mode in a more specific way. Therefore, if the user keeps closes his eyes for more than 4 seconds but less than 5 seconds, the system determines it as an Action Code and starts the Action Mode.

By this time, the system makes a very tiny beep to so that the user can open his/her eyes. However, if the user keeps the eyes shut even longer by this time, the system identifies it as the user behavior of resting or sleeping. Otherwise, the system plays two 500 Milliseconds long beep to indicate that, it is ready to take “Blink Action”. By this time, user can blink his/her eyes for any number of times for the desired action. The system will then make a beep to indicate that the blink has been registered. The system takes any number of blink commands during the period Four seconds after starting action mode and registers all the blinks. When the counter finishes the four seconds mark then the system interprets the blink command. If then checks, how many times the user blinked. Depending on that, the system decides whether to send the command to the Wi-Fi module present at Node MCU of transmitting section

4 Result and Data Analysis

In this paper we will be discussing about our result

4.1 Result Analysis

To verify whether our IR sensor is working or not we check the Serial Monitor output value for Average Flux. As we will detect the intentional blink we need appropriate Light for flux value. IR takes some continues value of light counting the lux (intensity of light) then it sets an average value a scenario describe bellow:

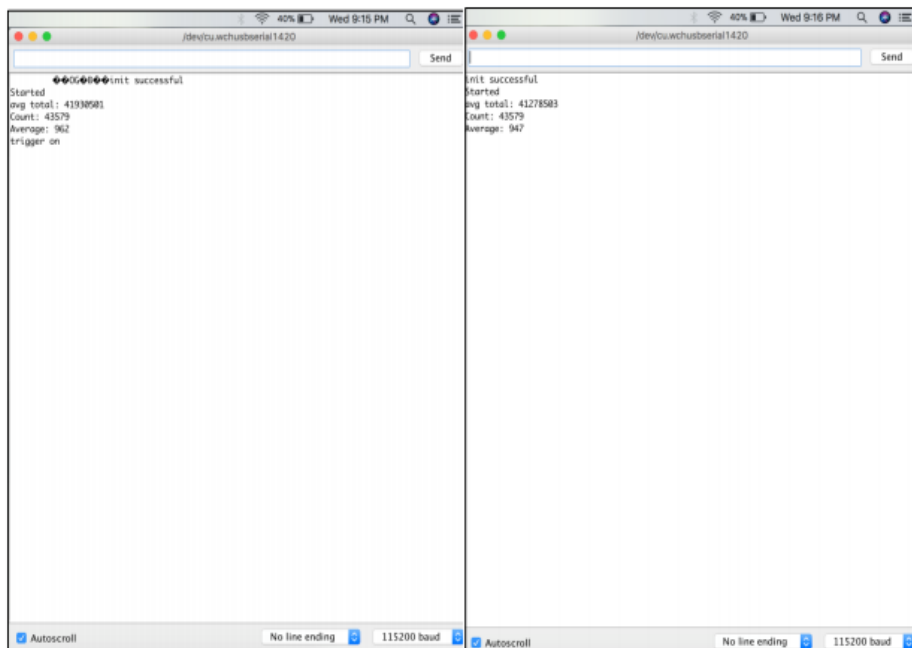


Figure 2: Flux Average Value and Trigger Status

Average Value (Flux): 805then, it works as following:

| STATE | CONDITION |
|-------------------------------|-------------|
| Average Value < Flux Received | Eyes Closed |
| Average Value > Flux Received | Eyes Open |

Figure 3: Flux Average Value and Trigger Condition

This system will take action for 5 seconds after action taken mode is ON. In this period of time, patients have to give instruction as they want to operate. Patients have to give valid eye blinks.

Table 1: Eye Blink Interactive Appliance\

| TIMES | BINARY VALUE | APPLIANCES NUMBER | BLINK LENGTH |
|-------|--------------|-----------------------------------|--------------|
| 1x | 0001 | #1 (Sending Message) | Short |
| 2x | 0011 | 2 nd Appliances ON/OFF | Short |
| 3x | 0111 | 3 rd Appliances ON/OFF | Short |
| 4x | 1111 | 4 th Appliances ON/OFF | Short |

4.2 Result Display

It takes around four seconds to get ready to take data, and then sensor sends data to Micro Controller. Output is perfect as its detecting eye blink. It shows the status. Finally, we get a confirmation by getting a message of data receiving.

| INPUT (LUX) | AVERAGE (LUX) | ACTION | NOTE | BINARY INPUT |
|--------------------------------------|---------------|--|--|--------------|
| 785 777 792 745 753 . | ≈ 805 | Trigger On | Eye Closed For 4-5 Sec | |
| 790 789 773 778 . | ≈ 805 | Action Taken Action Taken Action Taken Action Taken | Blink 01 Blink 02 Blink 03 Blink 04 | |
| 946 1021 1023 1021 . | ≈ 805 | | Eyes Open | |
| 1023 | ≈ 805 | Action Over | 4 No Relay Switch On | 1111 |
| 957 995 980 . | ≈ 962 | Trigger On | Eye Closed For 4-5 Sec | |
| 801 820 795 652 | 962 | Action Taken Action Taken Action Taken Action Taken | Blink 01 Blink 02 Blink 03 Blink 04 | |
| 1027 1102 . | | | Eyes Open | |
| 1021 | | Action Over "1111" | 4 No Relay Switch Off | |
| 805 890 950 . | ≈ 881 | Action Taken Action Taken | Blink 01 Blink 02 | 0011 |

Figure 4: Flux Value and Sensor Data

5 Conclusions

This venture is essentially for paralysis patients who endure a great deal. We are attempting a little bit through this venture so that at any rate they can control the home appliances. We have additionally plan to enhance this venture with better showing advantages an eye blink sensor is transducer which detects an eye blink, and gives a yield voltage at whatever point the eye is shut that can help the patient to control the home appliances and others, for example, switch on/off the light or control the fan speed. To sum up we want to say this is doing works using Node MCU and various sensors was a great experience as we got to know many valuable things. Our paper will be useful mainly for the paralysis patients and senior citizen.

One of the main motives of our project was to help patient to make their life easier and our system will be fulfilled when we can use the system in real life and people will be benefited

References

- [1] S. K. Subramaniam, S. H. Husin, S. A. Anas, A. H. Hamidon , —Multiple Method Switching System for Electrical Appliances using Programmable Logic Controller.
- [2] Joseph K George, Subhin K B, Arun Jose, Hima T —Eye Controlled Home-Automation For Disablel pp6-7 (ERTEEI'17)
- [3] T. S. (2016). Eye-Blink Detection Using Facial Landmarks. Eye-Blink Detection Using Facial Landmarks, 1-55.
- [4] Spinal Cord Injury: Paraplegic & Quadriplegic Tetraplegic Information", Apparelyzed.com: Spinal Cord Injury Peer Support. Retrieved, April 2013.
- [5] A. Juric& A. Weaver, —Remote Medical Monitoring, IEEE Computer, PP96-99 April 2008
- [6] K. Bilstrmp, —A Preliminary Study of Wireless Body Area Network, Tech. Report, IDE0854, University of Halmstad, Sweden, PP1-36, Aug. 2008

Automatic Detection for Diabetic Retinopathy Using Deep learning in Modified AlexNet CNN Architecture

D. Umamaheswari¹, Dr.N.Nachammai²

¹Research Scholar, Department of Electronics and Instrumentation Engineering, Annamalai University , Chidhambaram

²Associate Professor, Department of Electronics and Instrumentation Engineering, Annamalai University , Chidhambaram

Abstract

Diabetic retinopathy is a kind of vascular disorder where the fluid leaks from blood vessels into the retina which causes retinal damage .and the main cause of blindness is among working age population therefore the retinal images of the both gender patients with ages in the range of (18-35) years are taken from all over Tamil Nadu. For detection of diabetic 155 images from DR category and 35 images from normal category are used. The Exciting methodology for the detection of DR in retinal images has three techniques. Among that the image pre-processing, feature extraction, feature selection. The Proposed methodology directly raw images are taken in this project. The texture feature which is related to diabetic is extracted to differentiate between the normal and DR images using convolution neural network in Modified AlexNet architecture. we proposed a diabetic retinopathy Interpretable classifier which is capable of classifying retinal images in different levels of disease severity and of explaining its results by assigning a value for every point in the input and hidden space, calculating its contribution to the final classification in a smooth way

Keywords: *Diabetic Retinopathy, deep learning, Convolution Neural Network, Alex Net*

1 Introduction

Diabetic retinopathy is a common complication of diabetes that affects blood vessels in the light-sensitive tissue called the retina. It is the most common cause of vision loss among people with diabetes and the leading cause of vision impairment and blindness among working-age adults. Recent progress in the use of automated systems for diabetic retinopathy diagnostics has offered new challenges for the industry, namely the search for a less resource-intensive architecture. The classification of fundus images according to the severity of DR so that we can perform end-to-end classification in real-time from the fundus image to the state of patients. For this task, we use pixel normalization techniques to highlight various clinical features (blood vessels, exudates, microaneurysms, and others) and then classify the retinal image into the appropriate stage of the disease.

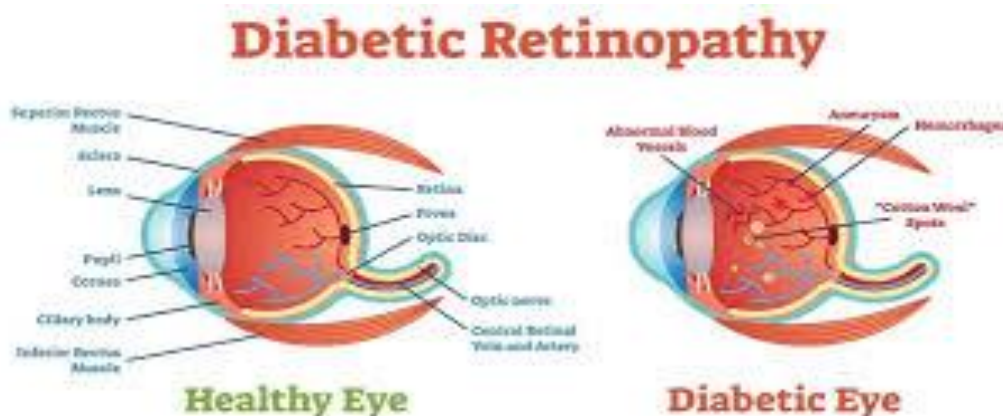


Figure1: Neovascularisation

This can be describe as abnormal growth of blood vessels in areas of the eye including the retina and is associated with vision loss. This occurs in response to ischemia, or diminished blood flow to ocular tissues. If these abnormal blood vessels grow around the pupil, glaucoma can result from the increasing pressure within the eye. These new blood vessels have weaker walls and may break and bleed, or cause scar tissue to grow that can pull the retina away from the back of the eye. When the retina is pulled away it is called a retinal detachment and if left untreated, a retinal detachment can cause severe vision loss, including blindness. Leaking blood can cloud the vitreous (the clear, jelly-like substance that fills the eye) and block the light passing through the pupil to the retina, causing blurred and distorted images. In more advanced proliferate retinopathy; diabetic fibrous or scar tissue can form on the retina.

We propose a CNN-based approach to precisely diagnose DR, utilizing an extensive database of SPECT images (100 images). Our approach outperforms the benchmark studies with improvements in accuracy, sensitivity, and specificity. • Our network analyzes entire images and learns features from the images, resulting in optimal performance. • The architecture of our proposed network is minimal, with three convolutional layers with a filter size of 3×3 and two dense layers. The minimal complexity of our network provides a clear advantage for implementation and applications. Given its excellent performance and lower complexity, the CNN-based model could revolutionize the diagnosis of DR.

1.1 Materials and methods

The aim of this research is to classify DR patients from the healthy controls utilizing SPECT imaging. The images are collected from PPMI. All the images are pre-processed and ready for experimentation. The study shows a methodological approach for obtaining fundus images with subsequent diagnosis by neurocomputing algorithms and comparing the results with the opinion of ophthalmologists. The mentioned above neurocomputing algorithms are

Convolutional Neural Networks. CNN have made remarkable achievements in a large number of computer vision and image classification, significantly exceeding all previous image analysis methodologies. Then, a Deep Learning Approach is applied in which the processed image is fed into a Convolutional Neural Network to predict whether the patient is diabetic or not. This methodology is applied on a dataset of 30 High Resolution Fundus Images of the retina.

1.2 Database for the study

The High-Resolution Fundus (HRF) Image Database (benchmark dataset) consists of 30 High Resolution Fundus Retinal Images out of which, 15 images are labeled as Healthy and 15 images are labeled as Diabetic. 1]. Sample Images are shown in Figure 2.

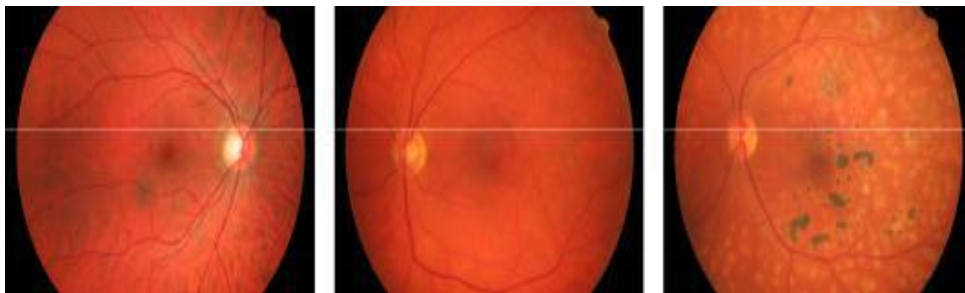


Figure 2: Dataset Sample

In the model training and subsequent primary validation, we used preprocessed versions of the original images. The preprocessing consisted of image cropping followed by resizing. Each image was cropped to a square shape which included the most tightly contained circular area of fundus. The procedure removed most of the black borders and all of the patient related annotations from the image data. Each of the cropped images were then resized to five different standard input image sizes of 256×256 , 299×299 , 512×512 , 1024×1024 , and 2095×2095 pixels. The largest image size was the smallest native resolution of the retinal cameras after the

preprocessing steps. Here the creation of multiple resolutions was done for the purposes of analyzing the effect of the input image resolution on the classification performance. The obtained processed datasets were divided into three sets: training, tuning, and primary validation set in the 70%, 10% and 20% proportions of the whole image dataset, respectively, separately for each of the grading systems used in the experiments. In the division per a particular grading system, the different sets were to have similar grade distributions, and that the dataset data per patient to not reside in multiple but only in one of the three sets in order to prevent the possibility of obtaining over-optimistic results due to data memorization., CNN have made remarkable achievements in a large number of computer vision and image classification, significantly exceeding all previous image analysis methodologies

- Conversion to Weighted grey scale: As all the images which were colour (RGB) initially, were converted to grey scale by taking a weighted average of the RGB pixels in which 0.299 of the Red (R) Component, 0.587 of the Green (G) Component and 0.114 of the Blue (B) Component are considered. where I is the Resultant Pixel
- Resizing: All the converted grey scale images are resized to a fixed size of 1000 x 1000 pixels.
- Pixel Rescaling: For every image, each and every pixel values are rescaled into a value between 0 and 1 by dividing by 255 for easy computation.

1.3 Network structure

Our network is a modified version of AlexNet in fig 4. AlexNet is one of the first deep neural networks that has been utilized for image classification tasks. The network consists of five convolutional layers and three dense layers with different kernel sizes. The first layer has a kernel size of 11×11 . The second layer has a kernel size of 5×5 and layers three to five each has a kernel size of 3×3 . However, one of the disadvantages of this approach is the duplication of data. This occurs because of the overlapping blocks of pixels, which leads to an increase of memory consumption for processing the image. In contrast, our network has only three convolutional layers and two dense layers, each with a kernel size of 3×3 . This is because smaller sized kernels of fewer layers lead to lower costs those larger-sized kernels with more layers. More layers and multiple larger-sized kernels lead to more in-depth network architecture which is time-consuming and not feasible for medical applications. Therefore, by reducing the kernel size, our network gains the advantage of learning the features from the image faster. Furthermore, our network is more robust and performs better than AlexNet with excellent scores in accuracy, sensitivity, and specificity

$$\text{Accuracy} = \frac{TP + TN}{TP + FP + TN + FN} \quad (1)$$

$$\text{Sensitivity} = \frac{TP}{TP + FN} \quad (2)$$

$$\text{Specificity} = \frac{TN}{FP + TN} \quad (3)$$

In AlexNet, Local Response Normalization (LRN) is added to the first two convolutional layers and then the activation layer, Rectified Linear Unit (ReLU), is added to the next three layers. The ReLU function enables faster training of CNN, since the calculation of its derivative has a lower computational cost, without losing any of its generalization ability (Krizhevsky et al., 2012). The function itself is a non-saturating activation function and is defined by

$$f(x) = x^+ = \max(0, x) \quad (4)$$

Where x is the input to a neuron.

In AlexNet, such processes are used to amplify the features in the image, such as enhancing the brightness of the image, for better classification of the image. However, in our network, overall image normalization is used

because LRN leads to increased memory consumption and computation time. The normalization process is carried out during the pre-processing stage, and the network is trained on the image that is generated. This process allows more distinguishable features to be visible during training. Our image normalization process is described below. In addition, our network only utilizes the ReLU activation function in all three layers.

Figs. 5(a) and (b) illustrate the architectures of AlexNet and our network. The input images utilized to train our network are resized from the original size of 512×512 to 96×96 . Since this research study in this paper is focused on the classification between DR patients and healthy controls, i.e., a binary classification problem, binary cross-entropy (BCE) is utilized as the loss function.

Binary cross-entropy is defined by:

$$\text{BCE} = - \sum_{i=1}^I \sum_{j=1}^J t_{i,j} \log(s_{i,j}), \quad (5)$$

Where $I=2$ represents the number of classes,

J is the number of training images,

$t_{i,j}$ is the binary indicator pf value of either 1 or 0 depending on whether or not the class label i is the correct label of sample j ,

$s_{i,j}$ is the predicted probability that sample j belongs to class i .

In order to tackle the issue of over fitting, a technique called dropout is used. Dropout works by “turning off” some neurons with a probability “ $1 - p$ ”, and using only the reduced network. After this step, the “off” neurons are turned on again with their last weight matrix. This procedure was repeated in every training iteration. At testing time, all neurons are active, so their outputs are weighted by a factor of “ p ”, as the approximation of results using all possible 2^n networks.

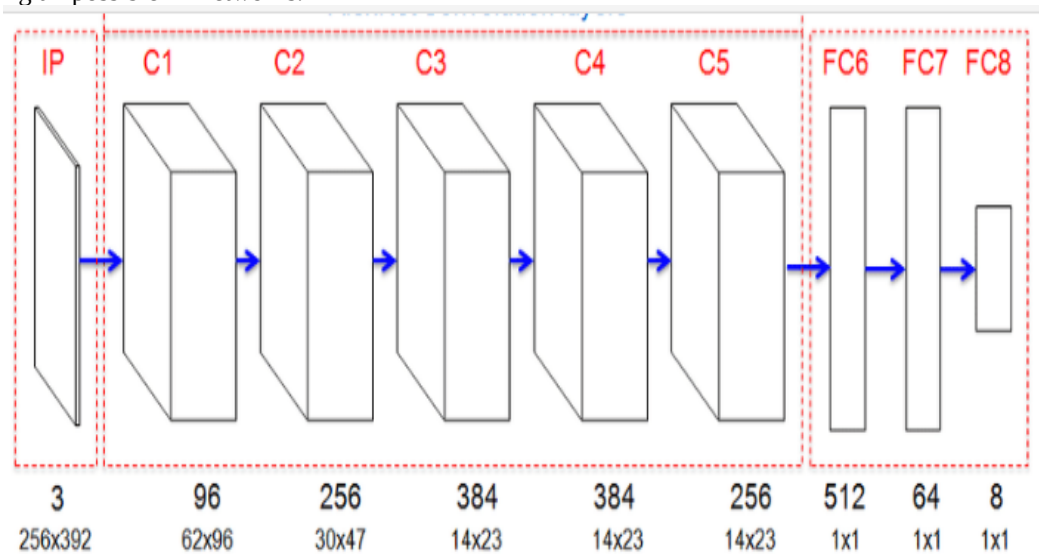


Figure 4: AlexNet Architecture

In this work, we used a dropout probability of 0.1 (i.e., $p = 0.9$) for every convolutional layer and 0.5 for the final dense layers. Finally, our layer structure also differs considerably from AlexNet. In AlexNet, there are different numbers of nodes in different layers. For example, each of layers one and two have 96 nodes, each of layers three and four has 256 nodes, each of layers five and six has 384 nodes, and each of the last two layers has 256 nodes. In our architecture, we have 128 nodes in each of our layers. To understand the impact of different network architectures on accuracy and provide a reason for why our network has three convolutional layers and two dense layers, and why we have 128 nodes in each layer, we test different combinations of layers in network architecture.

1.4 Modified AlexNet

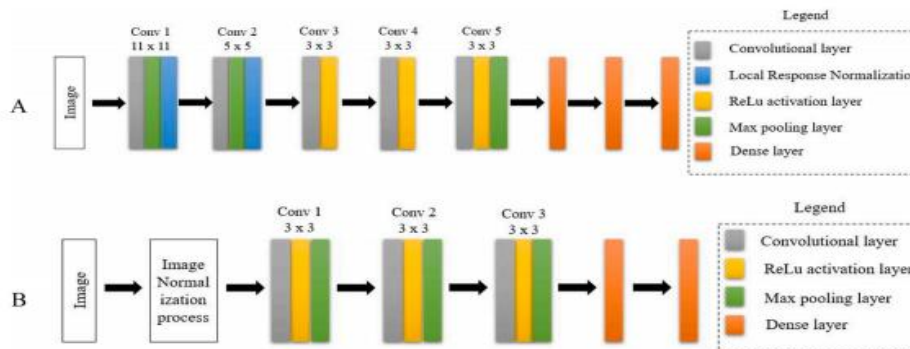


Figure 5: Network difference of (A) AlexNet and (B) of Modified network

2 Deep learning

Deep learning (DL) is a branch of machine learning techniques that involves hierarchical layers of non-linear processing stages for unsupervised features learning as well as for classifying patterns [11]. DL is one computer-aided medical diagnosis method [12]. DL applications to medical image analysis include the classification, segmentation, detection, retrieval, and registration of the images. Recently, DL has been widely used in DR detection and classification. It can successfully learn the features of input data even when many heterogeneous sources integrated [14]. There are many DL-based methods such as restricted Boltzmann Machines, convolutional neural networks (CNNs), auto encoder, and sparse coding [15]. The performance of these methods increases when the number of training data increase [16] due to the increase in the learned features unlike machine learning methods. Also, DL methods did not require hand-crafted feature extraction. CNNs are more widely used more than the other methods in medical image analysis [17], and it is highly effective [15]. There are three main layers in the CNN architecture, which are convolution layers (CONV), pooling layers, and fully connected layers (FC). The number of layers, size, and the number of filters of the CNN vary according to the author's vision. Each layer in CNN architecture plays a specific role. In the CONV layers, different filters convolve an image to extract the features. Typically, pooling layer follows the CONV layer to reduce the dimensions of feature maps. There are many strategies for pooling but average pooling and max pooling are adopted most [15]. A FC layers are a compact feature to describe the whole input image. SoftMax activation function is the most used classification function. There are different available pretrained CNN architectures on ImageNet dataset such as AlexNet [19], Inception-v3 [20] and ResNet [21]. Some studies like [22,23] transfer learning these pretrained architectures to speed up training while other studies build their own CNN from scratch for classification.

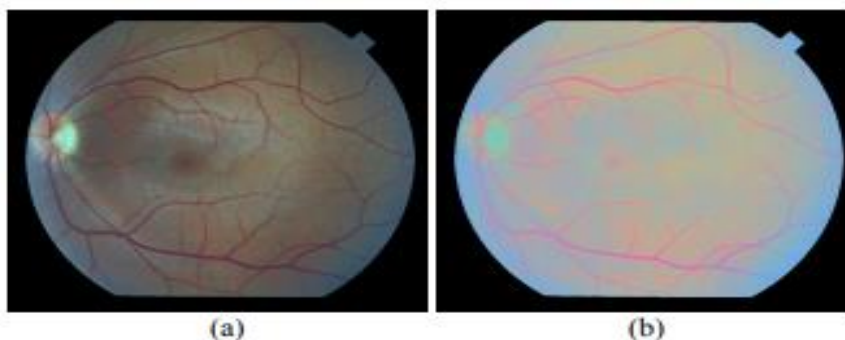


Figure 6. Colour Normalization of Fundus images (a) Gray world Normalization
(b) Comprehensive Normalization

2.1 Gray-World Normalization.

It aims to eliminate the effects due to illumination color [13, 19] (Fig5(a)). The new values ($r^{new}, g^{new}, b^{new}$) new new new r g b for any pixel (r, g, b) can be simply calculated using the following algebraic equation by Finlayson et al. [19]:

$$r^{new} = \frac{r}{R_{Avg}}, g^{new} = \frac{g}{G_{Avg}}, \text{ and } b^{new} = \frac{b}{B_{Avg}} \quad (3)$$

Comprehensive Normalization. Whereas gray-world normalization can successfully remove the effect of different illuminant colors, Chromaticity is a representation of digital images which is invariant to light geometry (i.e. light source direction and power) [13, 19]. Therefore, chromaticity values represent an image while discarding the intensity (brightness) information, and so can be thought of as hue and saturation taken together [20]. For any pixel (R, G, B), the chromaticity normalized values (r, g, b) are defined as:

$$r = \frac{R}{R + G + B}, g = \frac{G}{R + G + B}, \text{ and } b = \frac{B}{R + G + B} \quad (4)$$

Further, only two chromaticity values are needed to represent a color, since $r + g + b = 1$. Since practically, both variations (in lighting geometry and color) don't occur separately.

3 Result & Conclusion

The task of early detection of diabetic retinopathy is an actual problem of predictive medicine. Diabetic retinopathy is the most common cause of blindness among the old aged group of people. Due to the development of technologies the diagnostics methods become available for all segments of the population. The most advanced techniques that help detect the stage of diabetic retinopathy resides in a field of neuro computing.. In the paper, we show the possibility of the various pixel normalization techniques to highlight various clinical features (blood vessels, exudates, microaneurysms, and others) and then classify the retinal image into the appropriate stage of the disease.. The numerical experiments were conducted on the High-Resolution Fundus (HRF) dataset. Further work assumes the augmentation of the algorithm with preprocessing in order to reveal clinical-pathological features and performance upgrades.

Table 1: Performance Measures And Estimated Values Of Proposed System

| Performance Measures | Values (%) |
|----------------------|--------------|
| Accuracy | 73.32% |
| Sensitivity | 75.56% |
| Specificity | 74.99% |

Figure 7 shows. Color normalization chromaticity plots (a) Gray-world normalization (b) Comprehensive normalization. The red dash-dotted ellipse & the plus signs '+' represent the non-vessels cluster, while the blue solid ellipse & the points '.' represent the vessels cluster.

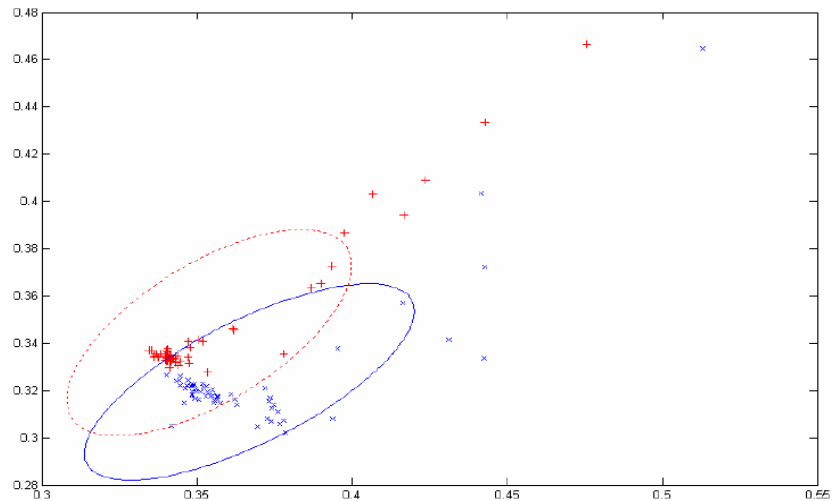


Figure 7: (a). Gray-world Normalization

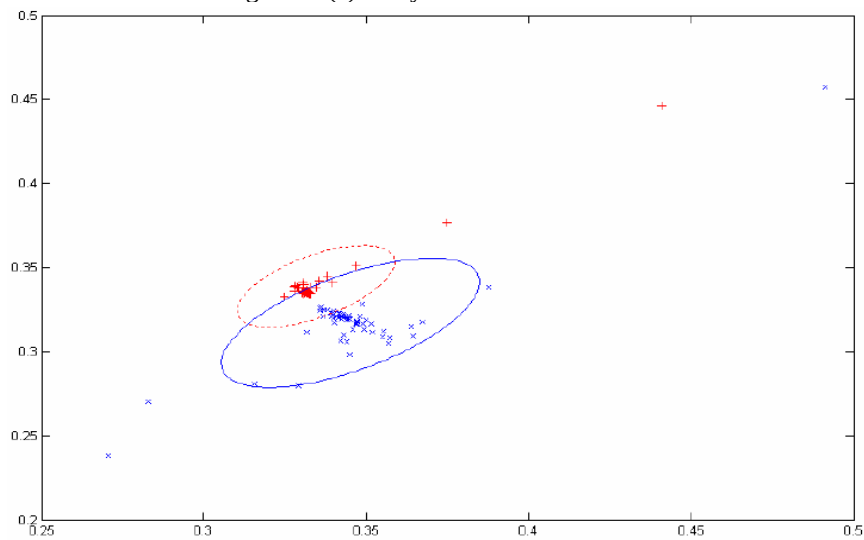


Figure 7: (b) Comprehensive Normalization

References

- [1] Wejdan L. Alyoubi *, Wafaa M. Shalash, Maysoon F. Abulkhair Diabetic retinopathy detection through deep learning techniques: A review (2020) <http://www.elsevier.com/locate/imu>
- [2] Wang, X., Lu, Y., Wang, Y., Chen, W.: Diabetic retinopathy stage classification using convolutional neural networks. In: IEEE International Conference on Information Reuse and Integration (IRI), pp. 465–471 (2018). <https://doi.org/10.1109/IRI.2018.00074>
- [3] Burewar, S., Gonde, A.B., Vipparthi, S.K.: Diabetic retinopathy detection by retinal segmentation with region merging using CNN. In: IEEE 13th International Conference on Industrial and Information Systems (ICIIS), pp. 136–142 (2018). <https://doi.org/10.1109/ICIINFS.2018.8721315> at <https://www.kaggle.com/c/aptos2019-blindness-detection/>.
- [4] Zeng, X., Chen, H., Luo, Y., Ye, W.: Automated diabetic retinopathy detection based on binocular siamese-like convolutional neural network. IEEE Access 7, 30744–30753 (2019). <https://doi.org/10.1109/ACCESS.2019.2903171>

- [5] Kanungo, Y.S., Srinivasan, B., Choudhary, S.: Detecting diabetic retinopathy using deep learning. In: 2nd IEEE International Conference on Recent Trends in Electronics, Information & Communication Technology (RTEICT), pp. 801–804 (2017). <https://doi.org/10.1109/RTEICT.2017.8256708>
- [6] Lin, G.-M., et al.: Transforming retinal photographs to entropy images in deep learning to improve automated detection for diabetic retinopathy. *J. Ophthalmol.* (2018). <https://doi.org/10.1155/2018/2159702>
- [7] Ma, J., Fan, X., Yang, S.X., Zhang, X., Zhu, X.: Contrast limited adaptive histogram equalization based fusion for underwater image enhancement. *Int. J. Pattern Recogn. Artif. Intell.* **32**(07) (2018). <https://doi.org/10.1142/S0218001418540186>
- [8] Chauhan, R., Ghanshala, K.K., Joshi, R.C.: Convolutional neural network (CNN) for image detection and recognition. In: First International Conference on Secure Cyber Computing and Communication (ICSCCC), pp. 278–282 (2018). <https://doi.org/10.1109/ICSCCC.2018.8703316>
- [9] Doshi, D., Shenoy, A., Sidhpura, D., Gharpure, P.: Diabetic retinopathy detection using deep convolutional neural networks. In: International Conference on Computing, Analytics and Security Trends (CAST), pp. 261–266 (2016). <https://doi.org/10.1109/CAST.2016.7914977>
- [10] Ghosh, R., Ghosh, K., Maitra, S.: Automatic detection and classification of diabetic retinopathy stages using CNN. In: 4th International Conference on Signal Processing and Integrated Networks (SPIN), pp. 550–554 (2017). <https://doi.org/10.1109/SPIN.2017.8050011>
- [11] Ruder, S.: An overview of gradient descent optimization algorithms. ArXiv, abs/1609.04747 (2016)[Google Scholar](https://scholar.google.com/citations?view_op=view_citation&hl=en&user=88888888888888888888&citation_for_view=88888888888888888888:1609.04747)
- [12] deng Li. A tutorial survey of architectures, algorithms, and applications for deep learning. *APSIPA Trans. Signal Inf Process* 2014;3(2):1–29.
- [13] V Vasilakos A, Tang Y, Yao Y. Neural networks for computer-aided diagnosis in medicine : a review. *Neurocomputing* 2016;216:700–8.
- [14] Wilkinson CP, et al. Proposed international clinical diabetic retinopathy and diabetic macular edema disease severity scales. *Am Acad Ophthalmol* 2003;110(9): 1677–82.
- [15] Chen XW, Lin X. Big data deep learning: challenges and perspectives. *IEEE Access* 2014;2:514–25.

Design and Analysis of a Lab IP Spy Camera and Alarm System using Raspberry Pi and ATMEGA328P

Shameera.S¹, Nivetha.K², Meera.S³, Sadiq Basha.G⁴, Abitha.B⁵

^{1,2,3,4,5} Department of Electronics and Communication Engineering, V.R.S College of Engineering & Technology, Arasur, Villupuram

Abstract

Security is a very important thing to be concerned in our day-to-day life. Everyone wants to be secured as much as possible. Knowing our home or office is secure provides us peace of mind. With the increasing concern over better protection of people and assets, security departments are required to provide a higher level of security than before: proactive prevention, better situational awareness, earlier detection, quicker identification and prompter action. Now many organizations are continually reevaluating and enhancing their video surveillance to provide optimal daily security and operational efficiency. As the technology is advancing day by day, there are various alternatives occurring for the already present or previous technologies. Internet of Things (IOT) is an upcoming technology that makes use of Internet to control/monitor physical devices connected to the Internet. The basic premise is to have smart sensors collaborate directly without human involvement to deliver a new class of applications. IOT gives user the ability to control more than one digital thing easily through a comfortable Graphical User Interface (GUI) over the Internet. This paper aim to design an Embedded Real-Time Security System Based on Raspberry Pi for intruder observation that reinforces surveillance technology to provide essential security to the Lab equipment and associated control. And also to design a low cost Alarm system based on Microcontroller and ultrasonic sensor that takes proper measure to prevent intrusion, unwanted and unauthorized user(s) into the Lab. Ultrasonic sensor sense the presence of an intruder & Controller reads the signal from sensor, if intruder is detected, it turns on the buzzer. At the same time the live stream vide of the intruder can be monitored, and also the IP spy camera control system will send an image of the intruder via Gmail to the user. The designed system has been proven to be a reasonable advancement in access control and security system technology.

Keywords: IOT, Raspberry Pi, IP Camera, Microcontroller, Ultrasonic sensor, Gmail notification, Security.

1 Introduction

The demands on video surveillance systems are rapidly increasing in the present day. One of the first things people will want to know about their surveillance system is whether or not they have the ability to connect to it over the internet for remote viewing. In the past, security systems had to be monitored by a guard who was locked away in a room all day watching the monitors to make sure that nothing would happen. The other option was to come back and review the footage but damage could have happened. Therefore, researchers and scientists had to come up with ways of overcoming that and thus improving security at large. In security risk areas, people often install alarms which are triggered by sensors. There are many types of sensors being used in the security systems. As the technologies expand rapidly through the time, security systems have moved forward from alarms to cameras and even computers. There are many kinds of sensors such as infrared sensor, PIR sensor, radio frequency and ultrasonic sensor. However, for ultrasonic sensor, it is only used to trigger alarm in case of an intruder because of its uniqueness and high sensitivity to movement. Lab IP spy camera and Alarm system is an essential mean of protecting Labs from illegal intrusion. A general Lab security system consists of Ultrasonic sensor, IP spy camera, and Buzzer alarm. IP camera captures image in 24 hours to identify what goes around the Lab and in the Lab around the door which holds evidences if there is any intrusion in the Lab and sends the image of the intruder to the Lab attendant via Gmail (SMTP server).

1.1 Objectives

The main objective of this research paper is to design and implement a low cost and power consumption friendly security system that includes features such as motion detection, image processing, alarm system and emailing notification system. The system is to be based on Raspberry Pi and Microcontroller.

To design a security system that ease problems of unauthorized entry in the Lab.

To design and implement a security system with an alarm system that alert the Lab attendant if an intruder entered in the restricted area.

1.2 System Description

The Raspberry Pi and Microcontrollers are capable of implementing a low power consumption, cost effective, and low maintenance security system for various applications. This new arising technology related to security provides a comfortable and safe environment for Labs. The various objectives of the system are to detect an intruder, take an image of the intruder and also convey an alert message to the Lab attendant. In doing so it thus allows remote monitoring of Labs from anywhere in the world via live stream video. In this system, raspberry pi and microcontroller are used to control all the attached devices across the external electronics equipment which are: ultrasonic sensor, IP camera, fan and buzzer. All these devices are combined to make a surrounding environment secure from unknown intruders. Security is an essential part for Lab, office and other insecure regions. Ultrasonic sensor sense the presence of an intruder & Controller reads the signal from sensor, if intruder is detected, it turns on the buzzer immediately. At the same time the live stream vide of the intruder can be monitored using smart phones or laptop computers via IP address of the system, and also the IP spy camera control system will send an image of the intruder via Gmail to the user. The power supply provides the voltage and current required for effective performance of the system. This supply is tapped from the 12V DC power source and then regulated before being fed to the system.

This system consists of two parts, Hardware and Software.

The Hardware parts include:

- IP spy Camera
- Ultrasonic sensor
- Raspberry Pi 3 B
- ATMEGA328P
- Fan
- WiFi Router
- 12V DC Transformer
- Buzzer
- 5V DC Regulator
- Resistors, Capacitors and Diodes.

Software parts include:

- Motion-eye-OS Raspberry Pi3
- Arduino IDE

2 Flow Chart

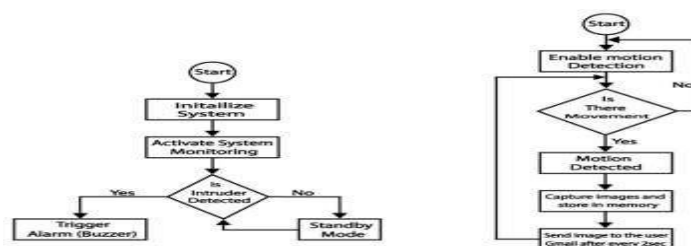


Figure 1: The flow chart of the system

2.1 Block Diagram

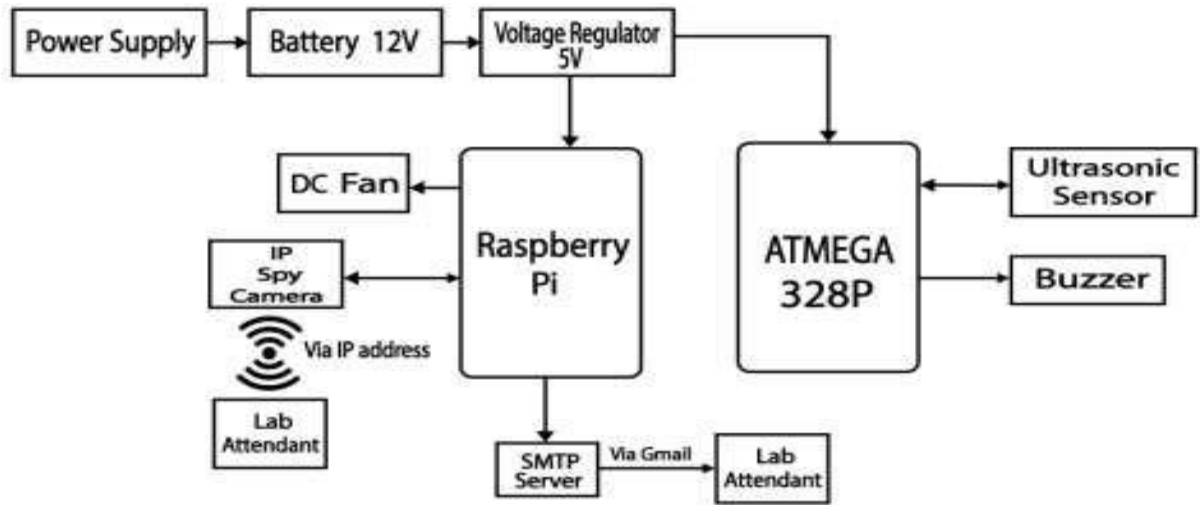


Figure 2: The block diagram of the system

2.2 Circuit Diagram

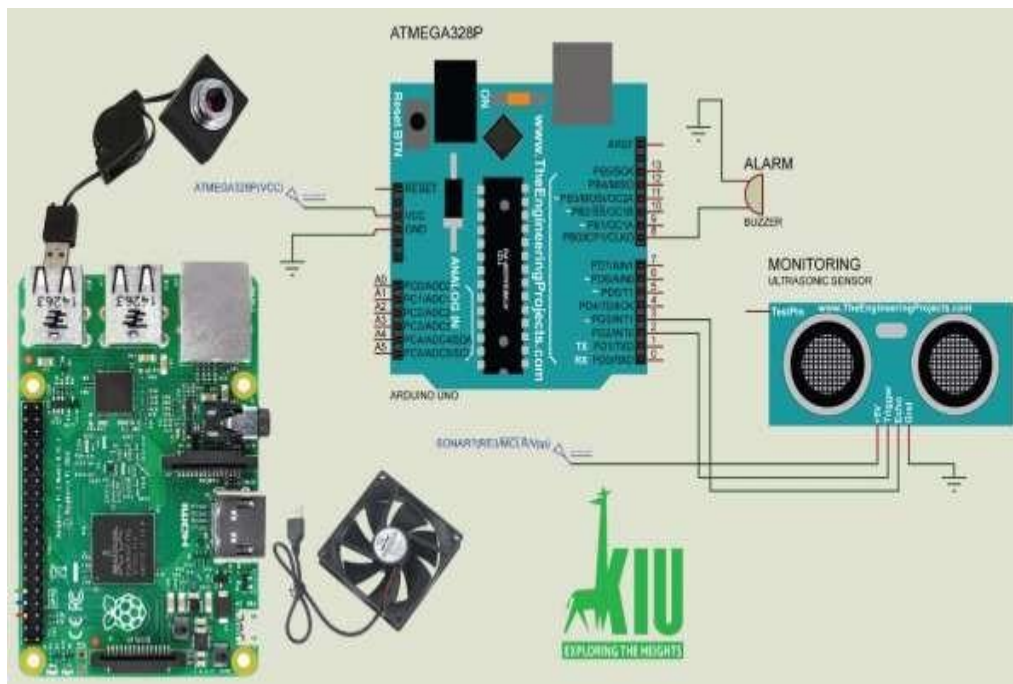


Figure 3: The circuit diagram of the system

2.2.1 System Overview

The following figure 4 shows the entire overview or the structure of the system.



Figure 4: The entire System Overview

2.2.2 Applications

- Currently, this system is applied at Kampala International University, School of Engineering and Applied Science, Telecommunication Lab under the department of Electrical, Telecommunication and Computer Engineering.
- It can also be applied in home, office, and big/small organizations.
- Server room, examination room, hospitals, etc.

3 Results

The following are the results achieved from this work:

The IP spy camera and ultrasonic sensor scan for intrusion movement around the access door of the Lab. On detection of motion, the ultrasonic sensor sends a signal to the Arduino which triggers the alarm (buzzer), and the camera captures the image of the intruder and sends a Gmail notification to the Lab attendant with that image attached to it.



Figure 5 :The IP Spy camera result pictures

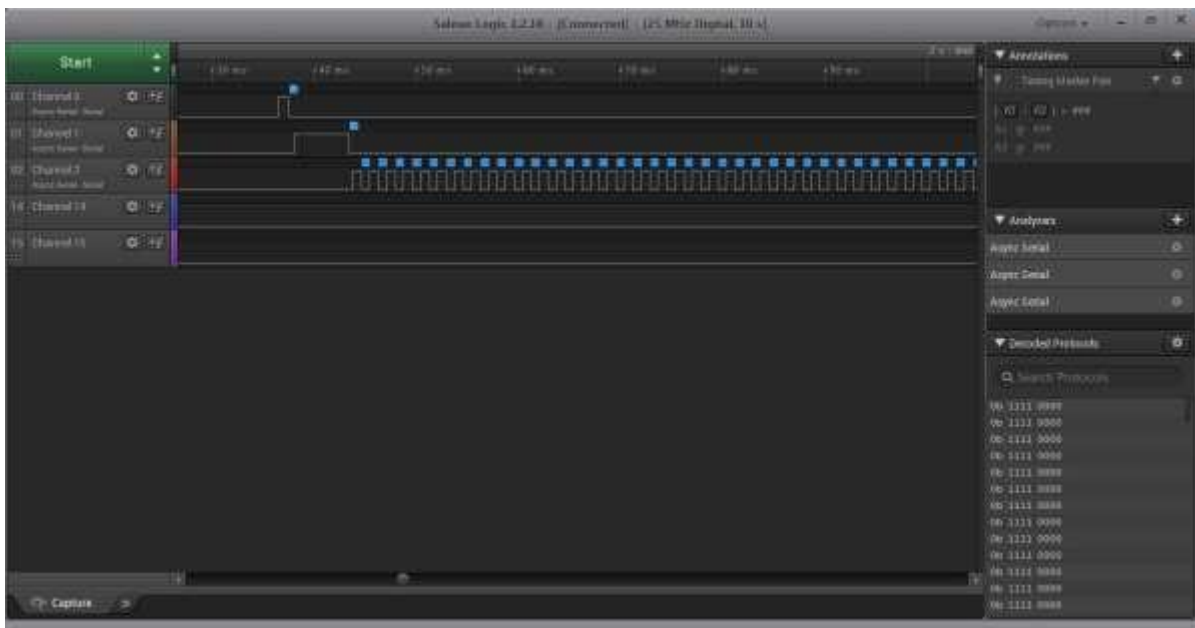


Figure 6: The ultrasonic result via Saleae Logic

4 Conclusion

The system informs the Lab attendant of any intrusion in the Lab via Gmail no matter where he/she is, except if he/she is in the region where there is no network coverage at the time of intrusion. This system is affordable and easily operated, so that anyone can make use of it. All the devices communicate well, especially, the Ultrasonic Sensor communicates well with the Arduino, the IP spy camera communicates well with the raspberry Pi, which communicates well with the SMTP server and Gmail notification sent successfully. It can be concluded here that the system has been successfully implemented and the aim is achieved without any deviations. The results achieved in this project are genuine and are a product of sincerity and hard work.

References

- [1] S. Sneha, "IP Camera Video Surveillance using Raspberry Pi.," Feb. 2015.
- [2] F. C. Mahima and A. Prof. Gharge, "Design and Develop Real Time Video Surveillance System Based on Embedded Web Server Raspberry PI B+ Board. International Journal of Advance Engineering and Research Development (Ijaerd), NCRRET.," pp. 1– 4, 2015.
- [3] V.Krishnaveni, A.Priyanga , V.Vidya ,G. GaneshKumar." An Advanced IOT based Antitheft Security System with Video Monitoring Facility" International Journal of computer science and engineering, (IJCSE). ISSN: 2348-8387, March 2019.
- [4] Saurabh Vinayak Lawate and M. S. Ali. "Electronic Eye for Security System" International Journal of Electronic and Electrical Engineering. ISSN 0974-2174 Volume 7, Number 9 (2014), pp. 961-970.
- [5] S. Tanwar, P. Patel, K. Patel, S. Tyagi, N. Kumar, M. S. Obaidat, „An Advanced Internet of Thing Based Security Alert System For Smart Home". India : May 2019

Integrated technique for data integrity and confidentiality

Shanmuga Priya.P¹, Helan Vidhya.T²

^{1,2} Assistant Professor, Rajalakshmi Engineering College, Thandalam, Chennai 602105

Abstract

In this world of digitization, security is considered to be one of an important parameter, as in case of any inadequacy in the system it gives the penetrator a well-constructed passage for them to exploit the data. The proposed goal is to achieve a secured transmission between the sender and the receiver as it's always said the channel isn't the problem but the main concern is from the source and the destination from where the data is forged. The idea is to create a well- defined environment applying the hybrids of encryption and steganography. To improve the efficiency on the transmitting side, randomizing pixels algorithm is used for better encryption followed by splitting this image into RGB plane of the cover image considering PSNR and efficiency as an important parameters whereas on the reception side only authorized person can access the image which is transmitted and this is done by confirming the person using Biometric fingerprint and RFID which the person is expected to provide.

Keywords: *Randomized, RGB plane, encryption, Steganography.*

1 Introduction

In this generation we are living Darwinism or the theory of Darwin is said to be completely true as only the person who can consistently bring changes in the system keeping the environment in mind can exist. We must keep our system updated in order to face any consequences by the penetrator. The suggestion here is to make the transmission as secured as possible and to do this we have used a hybrid of encryption and steganography at the sender's end and similarly multiple level of authentication is done on the receiver's end in order to decrypt the image only to the rightful person. In this encryption the area of cryptography is always said to be on the top as it is said to master the art of hiding information and steganography is again the ability of hiding the information.

Encryption process involves transforming the data into another form, known as cipher text, whereas original data to be encrypted is known as plain text. Plain text is an input to an algorithm, which create a cipher text. This cipher text can be decrypted with a valid key. The steganography used comprises of one of the efficient method, i.e., Least Significant Bit (LSB) exchange among the cover and the secret image and embedding them in RGB plane of cover image. On the other hand receiver confirmation is done by fingerprint of the authorized person who is expected to be sole person and not any unauthorized person who receives the image which is transmitted. A multilevel check is done in the presence of RFID of the authorized person to match a particular frequency and is expected to be a key to the lock of encryption.

2 Literature Survey

Achieving Data Integrity and Confidentiality Using Image Steganography and Hashing Techniques - Ahmed Hambouz, Yousef Shaheen, Abdelrahman Manna, Dr. Mustafa Al-Fayoumi, and Dr. Sara Tedmori - 2019 - In this paper the latest implemented technique for encryption is suggested which is embedding the text data into the digital image using hashing technique. This hashing is simple compression of one form of data into another compressed form which is done using a AES and a MD5 algorithm for compressing of text into simpler formats which is implemented in order to increase the robustness and quality of the encryption.

An Efficient Image Cryptography using Hash-LSB Steganography with RC4 and Pixel Shuffling Encryption Algorithms - May H.Abood- 2017: This study is the latest implementation of the proposed system of hybrid of steganography and encryption used. Here the encryption suggested is by using cryptography which is done by using RC4 algorithm where a new value is generated each time and the pixels of rows and columns gets interchanged similarly LSB substitution of the cover and the secret image is done using a proposed method of Hash Least

Significant Bit(HLSB) and then inserted in the RGB using the 2-2-3 principle and then extracted in the similar way
 An overview of steganography techniques applied to the protection of biometric data - Mandy Douglas & Karen Bailey & Mark Leeney & Kevin Curran - October 2017 :This study is a brief explanation of why is biometric ranked as the best possible of authentication and why is fingerprint the most opted way over other human body parts such as voice recognition , iris scanner and face recognition. Another couple of reasons are no two fingerprints are the same and they will not change through the course of a person's lifetime helping in authentication in an efficient manner. A hybrid of steganography is again used here for more efficiency.

3 Proposed Work

Encryption which is done on the transmitter side uses a non-repeatable integer generator to generate values till the maximum size of secret Image and these values are stored as array into one of the plane of Cover image as per users choice. Authentication is done on the reception side in order to only grant access to a authorized person and not anyone who is present on the receiver's side. Decryption is done by taking out important parameters from the RGB which is embedded in the cover image and then the process of decoding is done.

In the transmitter side, the encryption and steganography is completely processed by transmitter end where the secret image is first encrypted using the principle of pixel interchanging of row and column which is imposed into the cover image using LSB method which acts like an RGB pixel plane, in which the data is embedded in all the planes and according to which the pixels are replaced finally generating a Stegoimage. Receiver side function is the exact reverse of the transmitter where the image is decrypted after the authenticated user verifies his identity after placing his or her Fingerprint and RFID to confirm the presence

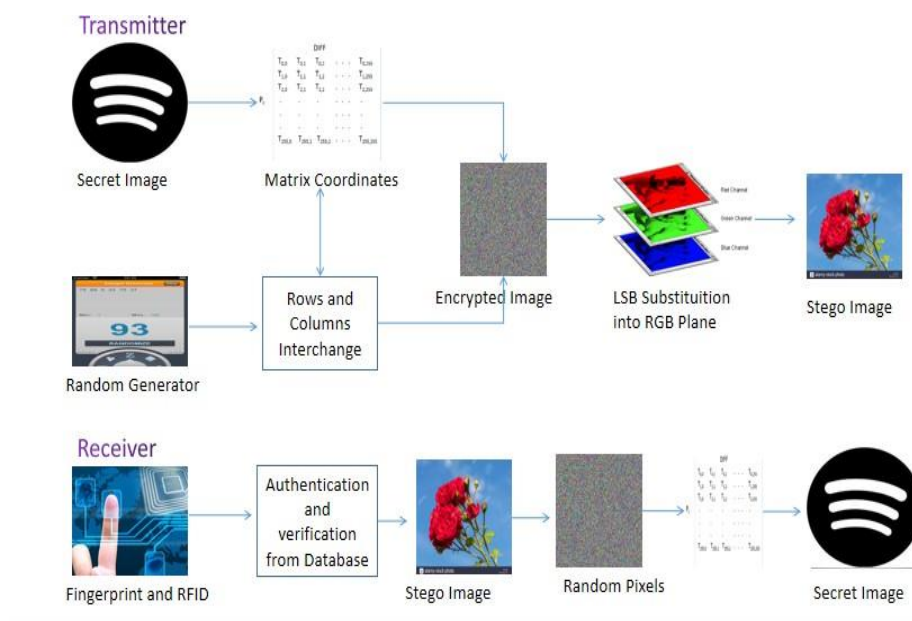


Figure 1: Schematic block diagram of proposed method.

4 Result Analysis

The output is executed in python and the parameters used to determine the quality are Peak signal-to-noise ratio (PSNR), Mean squared normalized error (MSE), Structural Similarity Index (SSIM). It is noticed that better the distribution of data, better is the encryption which makes the total quality of picture better. The idea is that there should be no difference in histogram of the cover image and the image which is

transmitted after embedding of secret image into cover image.

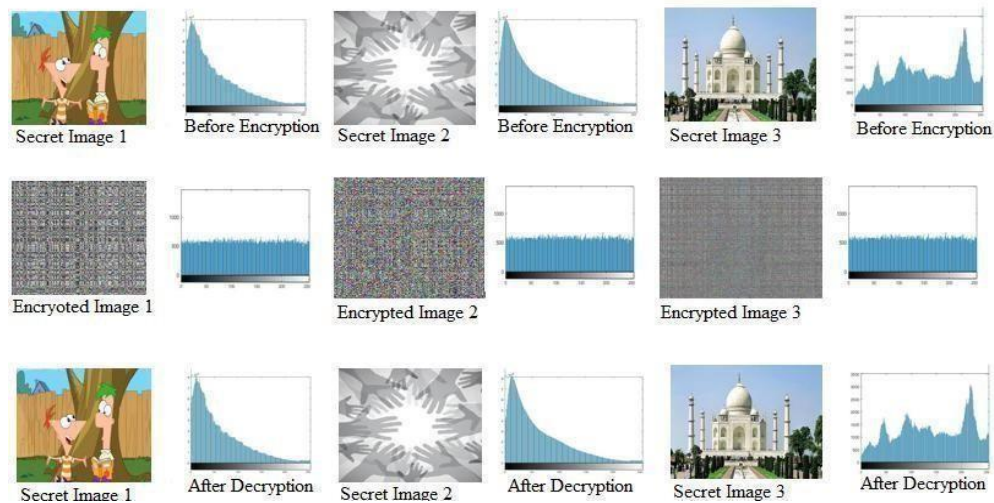


Figure 2: Schematic block diagram of proposed method.

The other parameters which are the key for determining the image quality are PSNR, MSE and SSIM which are again determined to make sure that no compromising is done regarding the image security which makes the intruder hard to determine the presence of the picture used.

$$SSIM(x, y) = \frac{(2\mu_x\mu_y + C_1)(2\sigma_{xy} + C_2)}{(\mu_x^2 + \mu_y^2 + C_1)(\sigma_x^2 + \sigma_y^2 + C_2)}$$

5 Conclusions

We can hereby conclude by registering the above system to be a better methods as an additional layer of security is provided, which will enhance the security of this system. One of the major requirements of steganography is to send the secret message inside the carrier image without creating much difference to the original image, in other words it is more robust. The above discussed steganographic method allows a high capacity of data to be hidden inside the color image. The entire idea of this work is to get the image received by the authentic user alone and this is done by confirming one's identity by fingerprint module and RFID which is to increase the security at the ends and makes intrusion in the channel a challenge.

References

- [1] Pooja Rani and Apoorva Arora – 2015, "Image Security System using Encryption and Steganography", International Journal of Innovative Research in Science, Engineering and Technology, Vol 4, Issue:6, June 2015
- [2] Ahmed Hambouz, Yousef Shaheen, Abdelrahman Manna, Dr. Mustafa Al- Fayoumi, and Dr. Sara Tedmori, 2019, "Achieving Data Integrity and Confidentiality Using Image Steganography and Hashing Techniques", 2nd International Conference on new Trends in Computing Sciences (ICTCS)
- [3] May H.Abood, 2017, "An Efficient Image Cryptography using Hash-LSB Steganography with RC4 and Pixel Shuffling Encryption Algorithms", 2017 Annual Conference on New Trends in Information &

Communications Technology Applications (NTICT).

- [4] Mandy Douglas, Karen Bailey, Mark Leeney and Kevin Curran, October 2017, “An overview of steganography techniques applied to the protection of biometric data”,Multimedia Tools and Applications, springer.
- [5] KonakantiBhargavi, Thota Sri Harish Reddy, ThotaBhaskara Reddy, 2016 , “Multilevel Crypting Approach for Ensuring Secured Transmission of Clandestine Images”,International Conference on Electrical, Electronics, Communication, Computer and Optimization Techniques (ICECCOT).
- [6] SevierdaRaniprima; BambangHidayat; NurAndini, 2016, “Digital Image Steganography with Encryption Based on Rubik’s Cube Principle”, International Conference on Control, Electronics, Renewable Energy and Communications (ICCEREC).
- [7] George Amalarethinam D.I, J.SaiGeetha – 2015, “Image Encryption and Decryption in Public Key Cryptography based on MR”International Conference on Computing and Communications Technologies (ICCCCT)

Jaspal Kaur Saini, Harsh K Verma, 2013, “A Hybrid Approach for Image Security by Combining Encryption and Steganography”, IEEE Second International Conference on Image Information Processing (ICIIP-2013).

Smart Irrigation Monitoring System Using Lora Technology

Radhakrishnan. R ¹, Balabasker. S ²

^{1,2}Assistant Professor, Department of Electronics and Communication Engineering
St. Anne's College of Engineering and Technology, Panruti, Tamilnadu

Abstract

This paper explains smart methods of agriculture using technology from the Internet of Things, which increases yield and ensures less human interference for agricultural work. High accuracy and Low- power are the prime factors to make any IoT arrange favorable and allowable to the Ranchers. In this project we have designed the controlling mechanism for the flow of water in to agriculture farm depends on the wetness of the soil which is required for the specific crops. The Humidity and Temperature value will be sensed for the specific action by the farmer. The long range data transmission of the sensed data is possible as projects adopt LoRa technology.

Keywords: *Smart Agriculture, Internet of Things, LoRa Technology, Ranchers*

1 Introduction

Agriculture is a crucial sector for many countries, and economic growth is also important. Agricultural yield production is entirely depends on the climatic situation. The climate conditions are currently uneven and very surprising, which can ruin development. Automatic and sudden responses to climate change are very important in this situation. Using sensor technology and the Internet of things, this issue can be solved. These technologies are used by modern agriculture to allow remote monitoring of the climatic condition of agricultural farms. This project mainly focuses on monitoring of the climatic condition in Agriculture Farms and required amount of watering the based on the threshold value of the soil moisture. This project focuses primarily on the monitoring of the environment at Agriculture Farms and the amount of water needed, based on the soil moisture threshold value. This project uses the Aurdino controller which accepts the sensor value and controls the operation of the water pump. This project focuses on upcoming IoT Networks-integrated communication technologies. That technology is LoRa. LoRa technology means Long Range Network can transmit the data up to 15km; usage of this communication module ensures the remote site data transfer operation. Using LoRa Technology, sensed environmental parameters are communicated to smart mobile farmers. This long range data transfer is essential at times so that remote observation and operations are possible.

2 Literature Survey

Now-a-days cultivating crops are becoming a very hectic task for the farmers because of the unpredictable climate and expense cost of the seeds. Due to the unpredictable and sudden change of the climate the damage ratio will be high and even the loss rate will be high. So in order to overcome this scenario we have to adopt a design procedure which should be effective. The solution for this problem is by following the techniques of precision agriculture also known as smart agriculture. This paper explains the automatic irrigation using communication Bluetooth module. They have used arduino as Boot loader and have simulated the complete system using Proteus design software. As they incorporated Bluetooth as communication module, the range of data transfer is limited. They have implemented the Wireless Sensor Network using LoRa Technology for smart agriculture. They have not integrated GSM module to the system. They have developed soil moisture monitoring system using Zigbee low range communication module. It requires additional routers to pass on the data.

3 Methodology

The proposed project is to develop a system that measures the soil moisture, temperature and humidity of the atmosphere in the field and transmits the information to the remote receiver on or off the farm. A laptop connected to the LoRa transceiver is a remote receiver (Fig.:2 Receiver). As shown in Fig.:1, the suggested device consists of Aurdino as the processing unit and the WSN base station.

A soil moisture and temperature humidity sensor is fetched to the WSN data collection node. The sensor node also consists of a LCD module, where the sensor output is shown in real time. The sensor node is building unit of the WSN. The duty of sensor node is to achieve the perception, collection, processing and wireless transmission. The WSN data collection node is fetched by a soil humidity and temperature humidity sensor. The sensor node also consists of an LCD module in which the output of the sensor is displayed in real time. The sensor node is the WSN building machine. The role of the sensor node is to achieve wireless transmission, aggregation, processing and perception.

The sensor node converts the physical quantity to the voltage signal and Arduino UNO board controls the

processing, and manages the We utilized different types of sensors for Automatic Smart irrigation system. Sensors like LDR, Soil moisture sensor, DHT Sensor, water pumping Motor and we are using Relay circuit model at transmitter LoRa device. Here Relay interacts with all sensors which are fabricated on LoRa device. In this paper we are mainly concentrated on controlling the flow of water by checking the temperature, Humidity, and Soil moisture. Thus, it helps to set the land parameters for specific crops. If the values from all sensors exceeds there Threshold voltage set in program its automatically Water pump turns Off. At the Receiver End (Fig.:2): User can get all desired sensed values through Lora WAN Gateway. In addition, we use the receiver side of the GSM module with 2G SIM allowed. Where the sensed value is analog in nature, the master controller will obtain the sensed value, which will be converted to digital by the slave controller. If the value is higher than the threshold value, the action taken will be initiated.

3.1 Block Diagram

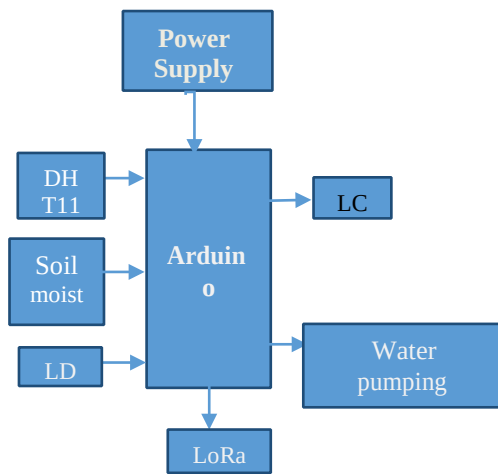


Figure 1: Transmitter Section

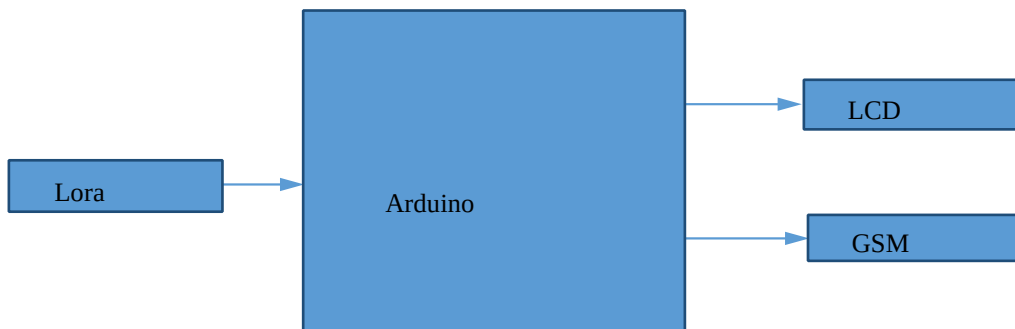


Figure 2: Transmitter Section

4 Components Used

The proposed work consists of following hardware components:

- Arduino- ATMEGA328P
- Humidity sensor-DHT11
- Temperature sensor-LM35
- Light dependent sensor-BH1750
- Relay circuit module
- Moisture sensor-FC28
- LoRa module
- GSM module-SIM900
- Cloud database and End device

4.1 Arduino Uno

Arduino Uno is a microcontroller board which has its design dependent on ATmega328P. It has 14 digital input/output pins. It has all that expected to help microcontroller. The regulator has 32KB memory with 0.5Kb for bootloader. Fig. 3 presents the image of Arduino Uno board. It has accompanied's 2 KB of static Slam and 1 KB of EEPROM. The Uno board is related to 6 simple pins from A0 to A5 each furnishes with 10bit of goal..

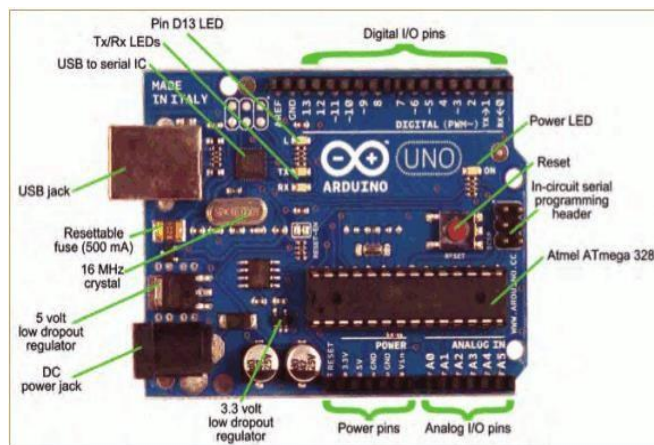


Figure 3: Arduino Uno

4.2 DHT11

The temperature and humidity sensor uses single bus communication with its controller. 40 bit data is transmitted in single line from sensor to the controller.

The format of data is represented as follows

8bit Integral Humidity + 8 bit decimal data + 8 bit Integral temperature + 8 bit decimal data + 8 bit parity.

8bit bit Parity
Integra l decim al



4.3 Moisture Sensor FC-28

Water is a vital asset and a main thrust in water system. Advanced utilization of water is a need of great importance. Effective water system helps in saving water, improving plant yields, reduce dependency on fertilizers and improve crop quality. For a successful irrigation, it is necessary to monitor soil moisture content continuously in the irrigation farms. The selection of soil moisture probes is an important criteria in measuring soil moisture as different soil moisture sensors have their own advantages and disadvantages. The soil moisture sensors is used intensively at present because it gives real time reading. For experimental purpose the sensor used is FC-28 as given in Fig. 5. The pin connections and specifications are listed below.

Pin connection with microcontroller FC-28

| | |
|------------|-----|
| VCC | 5V |
| GND | GND |
| A0 | A0 |



Figure 5: Soil Moisture Sensor

4.4 Light sensor

By utilizing BH1750 light sensor, the power can be straightforwardly estimated utilizing lux meter, without need of numerous counts. The information which is yield from the sensor is straightforwardly in lux. Table 10 records out the power esteems for various environmental conditions.



Fig. 6: Light Sensor

Table 1: Light Intensity values

| | Environment Conditions | Illuminance in LUX |
|-----------------|-------------------------------|---------------------------|
| | Night | 0.001-0.02 |
| Moonlight night | | 0.02-0.3 |
| Cloudy indoor | | 5-50 |
| Cloudy outdoor | | 50-500 |
| Sunny indoor | | 100-1000 |

4.5 Relay Circuit

A relay is an electrically operated switch. It consists of a set of input terminals for a single or multiple control signals, and set of man oeuvre contact terminals. The switch may have quite a few association in different contact structures, for example, make contacts, break contacts, or associations thereof. Hand-off is utilized where it is important to control a circuit by an independent low-power signal, or where a few circuits should be constrained by one sign.

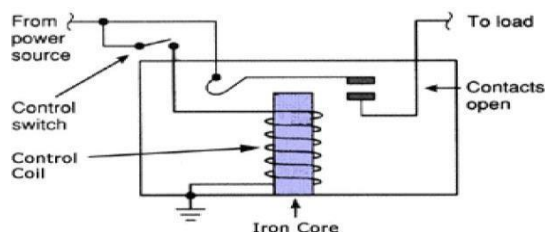


Figure 6: Relay circuit

4.6 Cloud database and End device

Cloud database is used to store the parameters in the internet enabling them to be accessed from anywhere and End device is used to monitor those parameters. Here the cloud database used is “Thinkspeak.com” and End device can be anything from a PC to mobile phone given it has internet connection.

4.7 LoRa device

- LoRa is a spread spectrum modulation technique derived from chirp spread spectrum (CSS) technology.
- It is mainly targeted for M2M and IoT networks, this technology will enable public or multi-tenant networks to connect a number of applications running on the same network.
- Each LoRa gateway has an ability to handles up to millions of node



Figure 7: LoRa Communication

4.8 Lora Features

- **Geo-Location:** It enables GPS-free, low power tracking system.
- **Low Cost:** Decreases the cost in three ways: infrastructure investment, operating expenses and end-node sensors, A LoRa base station cost a few hundred dollars and set themselves up with a network. It is easy to plug into the existing pedestal and offers a solution to serve battery-operated IoT application.
- **Standardization:** LoRa establishes global standards and improves global inter-operability speeds adoption and roll out of LoRa WAN-based networks and IoT applications.
- **Low connection cost:** LoRa Technology operates in the unlicensed ISM band, which means no or very low spectrum cost.

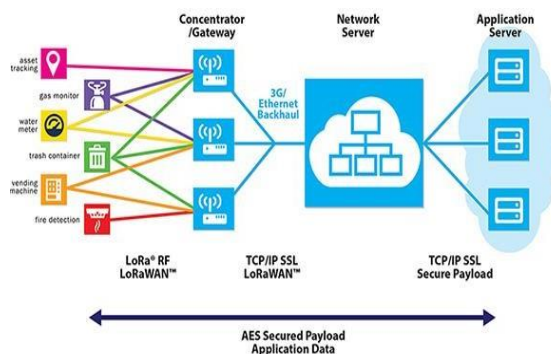


Figure 8: LoRa Gateway

5 Software Used

It is an open-source IoT application and an API used to store and retrieve information by utilizing HTTP protocol over the Web. The information captured from sensors is shown on the window of ThingSpeak demonstrating the status of the environment.

Blynk Application: The blynk application is created through the blynk platform by a new venture. The application will be updated routinely through the notifications sent over blynk cloud with a certain timestamp.

Thing Speak:

The primary element of Thing Speak activity is the *channel*, which contains data fields, location fields, and a status field. After you create a Thing Speak channel, you can write data to the channel, process and view the data with MATLAB code, and react to the data with tweets and other alerts. The channel window is presented in Fig.8.

The typical Thing Speak workflow lets you:

1. Create a Channel and collect data
2. Analyze and Visualize the data
3. Respond on the data using any of several Apps

The sensors connected to monitor the agriculture environment are temperature, humidity, light, moisture sensor. The values are analyzed for the period of time and sent to cloud. The deviations are controlled and brought back to normal by enhancing the controlling mechanism by the master controller. The actions executed can be opening of water pump to increase the moisture content, put on the lights to increase the intensity artificially. The data can be viewed anywhere in the world which makes the proposed method as successful and the cost effective using IOT.

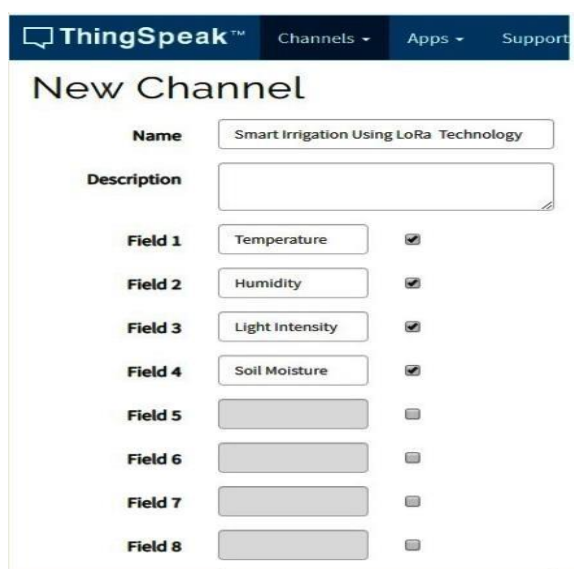


Fig.: 9: Channel Settings

6 Results

Parameters: Threshold Range Values of all Sensors

- **Temperature Threshold Value:** If temperature Reach above 30 degrees it shows High temperature
- **Soil Moisture Sensor:** If it reaches above 400 it will display Soil is wet motor is off. Else if it is below 400 it will display Soil is dry motor is turned on

- **LDR:** When Light is turned ON Led is OFF. When light is Turned Off. Led is On

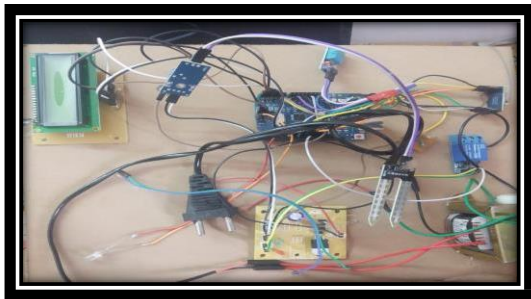


Figure 13: Receivers

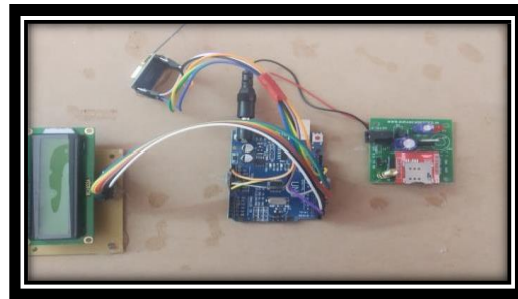


Figure 14: Transmitter

7 Conclusion

The project leads as the model and the successful arrangement over the issue of irrigation management. The Temperature, Humidity, Light Intensity, Soil Moisture values are obtained at the remote site using the LoRa technology. So this cost effective project ensures the great yield production and Less Human Intervention.

References

- [1] Miss Nikitha.S1, Miss Nandhini.T2, Miss Pavithra.K3, Mrs. Mary Joy Kinol.A4 International Research Journal of Engineering and Technology (IRJET) e-ISSN: 2395-0056 Volume: 05 Issue: 03 | Mar-2018
- [2] Prof. Amol V. Dhumane & MrAqsa Mahir "Soil Monitoring System using ZigBee for Smart Agriculture" IJSTE - International Journal of Science Technology & Engineering | Volume 4 | Issue 7 ISSN (online): 2349-784X January 2018.
- [3] Prof. G. Anitha & Nomitha Chawla "Wireless Sensor Network using LoRa for Smart Agriculture" International Journal for Research in Applied Science & Engineering Technology (IJRASET) ISSN: 2321-9653; Volume 7 Issue VI, June 2019.
- [4] Anushree M K and Krishna R "A Smart farming using Arduino based Technology", International Journal of Advance research –Block and ideas and Innovations In Technology,2018
- [5] Raul Aquinosanto, Apolinar Gonz, Arthur Edwards RauAlejandro Virgen "Developing a New Wireless Sensor Network Platform and Its Application in Precision Agriculture", Sensors ISSN 1424-8220, www.mdpi.com/journal/sensors
- [6] Jeyshree P, Meghana M and Sameera reddy B, "mart agriculture Using LoRa Technology", International journal of emerging technology and innovation engineering, Vol. 5 Issue 4 April 2019 [ISSN:2394-6598]
- [7] Juha Petajarvi- On the Coverage of LPWANs: Range Evaluation and Channel Attenuation Model LoRa Technology. Presented 2015 14th International Conference on ITS Telecommunications (ITST).
- [8] Coleman- "Radio Frequency Signal and Antenna Concepts" in Certified Wireless Network Administrator Official Study Guide(ebook), Wiley & Sons, Inc pp.564-522,2011.
- [9] LGhiro- "LoRa from the City to the Mountains: Exploration of Hardware and Environmental Factors", International Conference on Embedded Wireless Systems and Networks (EWSN), pp. 317- 322, 2017.

A Source-Location Privacy in Wireless Sensor Networks Using Multi-Sinks

V.Dhivyapriya¹, J.Sumitha Josphine²,
^{1,2}Assistant Professor, Idhaya Engineering College for Women
Chinnasalem

Abstract

Identification of source node is a major problem in WSN. Why because they are deployed in different places randomly. We know that the source node sends the valuable information about the targeted destination but due to traffic in the network targeted destination is affected easily. So in our paper CPSLP Scheme is proposed to address the issues in the source location privacy for each and every node transmission. Here Cloud shaped fake hotspot is introduced to add a fake packets more flexibly and it may confuse the adversary mode. Therefore for the hotspot locating adversary node finds difficult to route the information through the path. IN our paper the simulation results are illustrated by using the CPSLP scheme to prevent this adversarial capture and at the same time it maintain the high level of security protection.

Keyword : *Source identification, Node privacy, Wireless sensor network.*

1 Introduction

Wireless Sensor Networks (WSNs) can be defined as a self-configured and infrastructure less wireless networks to monitor physical or environmental conditions, such as temperature, sound, vibration, pressure, motion or pollutants and to cooperatively pass their data through the network to a main location or sink where the data can be observed and analysed.

Wireless sensor network (WSN) refers to a group of spatially dispersed and dedicated sensors for monitoring and recording the physical conditions of the environment and organizing the collected data at a central location.

WSNs are spatially distributed autonomous sensors to monitor physical or environmental conditions, such as temperature, sound, pressure, etc. and to cooperatively pass their data through the network to a main location. The more modern networks are bi-directional, also enabling control of sensor activity.

The WSN is built of "nodes" – from a few to several hundreds or even thousands, where each node is connected to one (or sometimes several) sensors. Each such sensor network node has typically several parts: a radio transceiver with an internal antenna or connection to an external antenna, a microcontroller, an electronic circuit for interfacing with the sensors.

The Internet of Things (IOT) is an emerging key technology for future industries, and environmental monitoring. The Internet of Things (IOTs) can be described as connecting everyday objects like smartphones, Internet TVs, sensors and actuators to the Internet where the devices are intelligently linked together enabling new forms of communication between things and people, and between things themselves.

2 Relevant Work

The proposed scheme was implemented in MATLAB to illustrate the effectiveness with a cloud-based scheme and ARR . The CPSLP scheme was evaluated based on previously mentioned metrics (security, network lifetime, energy consumption, capture ratio, etc.).

2.1 Simulation setting

The energy consumption model was outlined in Section IIIC. These experiments randomly deployed 2500 sensor nodes in an 800m*800m square area. The adversaries initially waited around four sinks deployed at four vertices. As previously mentioned in [6], the maximum length of a fake branch is 10 ($L \leq 10$); other simulation parameters are shown in Table 2. Initially, only one adversary exists in the network.

2.2 Total energy consumption

Energy consumption is a reasonable concern in WSNs, for it limits data transmission and network lifetime. Energy consumption also reveals the complexity of each algorithm loaded by the sensor nodes. For instance, nodes in the hotspot relay more packets per round than those around the periphery. The simulation in this study involved a complete transmission round, including delivering the real packet to the destination sink and generating fake branches and a fake hotspot. All packet transmissions were considered. A detailed comparison

of total energy consumption in 1000 rounds with three protocols is also presented. The ARR scheme transmitted fewer packets than the other two schemes; it only generated real packets to the sink. The cloud-based scheme flooded many fake packets into the network to hide the source location (but less than in the multi-sinks scheme). Although the CPSLP scheme consumed slightly more energy than the ARR and cloud-based scheme, it provided better privacy preservation by using fake hotspots and packets. As the number of transmission packets increased, the choice of the destination sink became more diversified. The CPSLP exhibited a slight incensement by balancing energy consumption.

2.3 Node utilization ratio

The node utilization ratios of the three schemes are depicted. The node utilization ratio is defined as the percentage of network nodes whose residual energy is smaller than 99%. The node utilization ratio increased in the three protocols. As the cloud-based scheme first created a fake hotspot, its node utilization ratio was initially quite high; however, the growth was small compared with other schemes. ARR randomly chose one sink to which to send a packet. Nodes in different corners participated in source privacy protection; its node utilization ratio was therefore higher than in the cloud-based scheme. To prevent a hotspot problem in the surrounding area of the source node, the CPSLP scheme constructed a cloud based routing structure. It used nodes with more remaining energy as much as possible, and the establishment of a cloud shaped hotspot balanced energy consumption. The CPSLP scheme involved nodes in other areas in packet transmissions and hence had the highest node utilization ratio. The cloud center adopted θ to restrict the size of the propagation area of fake packets. This process consumed node energy in regions with more residual energy; the CPSLP scheme was therefore energy-efficient. Although the cloud-based scheme built fake hot spots, increasing the node utilization rate at first, the scheme also demonstrated a hot-spot problem: it limited the participation of nodes in other regions. Node utilization was ultimately the lowest among the three schemes. Because ARR had the shortest transmission path, it also had less node utilization.

2.4 Transmission delay

The transmission delay is the hop count in the main path, related to the distance between the source node and sink node. The arrangement is reasonable as the network delay depends on the routing mode of the three schemes. With an increase in side length, the transmission delay increased in kind. The cloud-based scheme used greedy routing and thus exhibited the smallest delay. The CPSLP scheme attempted to compensate for the time delay in the search phase for the intermediate node, namely by adopting the shortest routing path in the second delivery phase. Thus, this metric was slightly larger than for the cloud-based scheme. The introduction of an agent node in ARR extended the routing path so the transmission delay was greater than in other schemes. Multiple sinks reduced network delay and routing redundancy and routed packets more randomly. Multiple sinks may also disturb the backtracking of adversaries.

2.5 Network security

In this section, network security is defined as the average number of hops in a complete packet transmission to evaluate privacy protection. The path length of fake packets should be taken into consideration. Security represents hop counts for adversaries traversing the routing path. The CPSLP scheme achieved the highest level of security. To ensure the safety of source location privacy, it generated fake branches in the entire real-packet transmission period. The hotspot created by the cloud center accumulated additional data transmission and led to inconsistent traffic in a small area. A cloud of fake data packets served as a hotspot per round, used to activate the hotspot-locating attacker. As a result, adversaries were forced to traverse many paths to locate the source node.

2.6 Node capture probability

In the simulation, the number of attackers is assumed to increase by four each time; thus, the whole network was divided into four parts to which multiple attackers were deployed. Assume that adversaries in each area appear at random locations in every round. If nodes in the adversaries hearing range participated in the transmission of real data packets, the round was considered a successful capture. The node capture probability is defined as the likelihood (percentage) of being captured in 300 rounds. As the number of adversaries increased, the node capture probability of the three schemes grew gradually. Because ARR only sent real packets in the network, it was easy for attackers to sense. ARR had a limited impact in hiding the main path as the number of adversaries increased. The CPSLP scheme gave the adversary an illusion that the target appeared in the location of the cloud

center. Source location was much better obscured in this scheme and hence difficult to determine. The CPSLP scheme therefore provided confidentiality of source location privacy and minimized the probability of the adversary locating the source node. The capture probability also increased at a slower rate than in other algorithms. The hearing range of an adversary is assumed to increase gradually, and the strength of an attacker grows accordingly. Simulation results of the capture probability. As the attacking radius expanded, so did the capture probabilities of all algorithms. The capture probability also depended on network security. The CPSLP scheme achieved a longer safety period against back-tracing eavesdroppers.

2.7 Network lifetime

This simulation assumes that source location will not be found when calculating network life. If the energy of one sensor node is depleted, the current number of successfully transmitted packets is defined as the network lifetime. The lifetime of ARR was the longest because each transmission cycle consumed little energy. The cloud based scheme exhibited a hotspot problem; excessive energy was consumed around the source node, leading to premature node death. Although the energy consumption of CPSLP was highest, the lifetime was not the lowest given an increase in the node utilization ratio; surplus energy was utilized outside the hotspot area.

3 System Model and Assumptions

The proposed system is based on the panda-hunter game model. To save energy and improve the strength of privacy protection, the authors assume there are multiple sink nodes in the network, unlike having only one sink in [19]. Four sinks are placed at four square vertices, expressed as $sink_i$ ($i = 1, 2, 3, 4$). The coordinate of $sink_i$ is denoted as (x_{sink_i}, y_{sink_i}) . The source node periodically generates event packets and sends them to one of the sinks. However, illegal hunters always try to trace network traffic and locate pandas. The proposed scheme aims to keep adversaries from analyzing real packet transmission by using fake traffic flow and thus preventing them from acquiring the locations of pandas. Fig. 1 illustrates the following assumptions about the proposed network model (1) Many homogenous sensor nodes are randomly and uniformly deployed in the 2-D WSN.

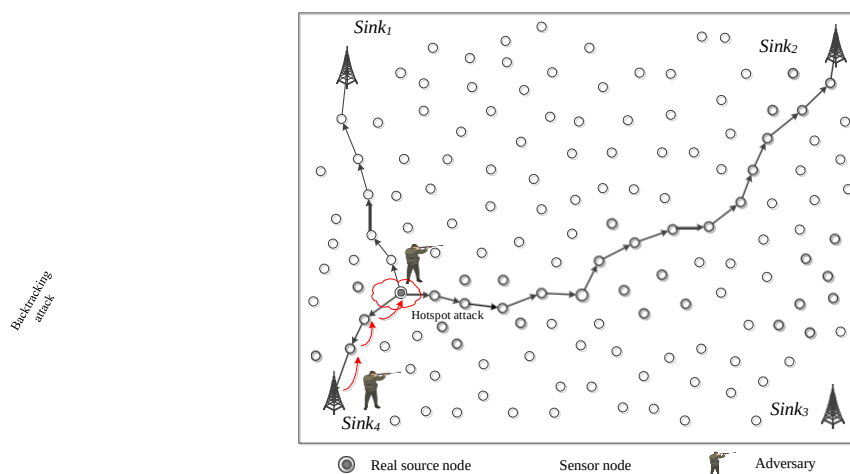


Figure 1: Backtracking attack and hotspot attack used by adversaries

Each sensor node has the same transmission range, defined as d_{min} . Multi-hop communication is used in the whole network. When a sensor node transmits data packets to neighbor nodes, a pair of secret keys is used to encrypt and decrypt data packets.

- (1) Each sensor node has limited energy, memory, and sensing radius and is equipped with identical computing and wireless communicating components. The absolute position of the node is known because of GPS. Nodes are aware of immediately adjacent neighbor nodes. Each sensor node maintains a routing table, including the distance from each sink node.
- (2) The network is a square area. Four sinks are deployed on the vertices of the square, respectively. After network initialization is completed, these sinks and sensor nodes remain stationary. The coordinates of the sinks are public. Each sink has sufficient energy and a powerful computing capacity to communicate directly with other sinks through wireless channels.
- (3) Key generation, distribution, and data privacy encryption are beyond the scope of this paper. CPSLP

emphasizes source location privacy protection; data privacy will be discussed in future work.

(4) PROPOSED CPSLP SCHEME

Our proposed CPSLP scheme consists of: (1) selecting sink node based on criteria, (2) selecting intermediate node, and (3) building a cloud (including packet transmission and cloud center selection).

After nodes are deployed, each sink broadcasts the initial beacon, including its location, the sink ID, and so on. Once the node realizes the sink coordinates, it is easy to calculate the distance to each sink. A neighbor list is Established According To Hop Count.

When a panda appears at a certain time somewhere, the source node begins to send event packets to the sink. The best approach for the source node is to change the final destination per round. The source node thus carries out a strategy to choose the final destination sink of the current round, called the destination sink. Taking energy consumption and privacy protection into consideration, the CPSLP scheme sets a value for $sink_i$ to decide which sink is selected as the destination sink, denoted as $T(s_i)$. Assume that the distance between the source node and $sink_i$ is d_{s_i} , and each sink calculates $T(s_i)$ of the current period.

Instead of the shortest routing algorithm, the routing of a real packet should be complex and random. The CPSLP scheme introduces a definition of the intermediate node. The intermediate node is supposed to be far from the actual source node without concealing important information about the source location. Then the source node routes the real packet to the intermediate node.

4 Performance Analysis

The proposed scheme was implemented in NS2 to illustrate the effectiveness with a cloud-based scheme [13] and ARR [7]. The CPSLP scheme was evaluated based on previously mentioned metrics (security, network lifetime, energy consumption, capture ratio, etc.).

The energy consumption model was outlined. These experiments randomly deployed 2500 sensor nodes in an 800m*800m square area. The adversaries initially waited around four sinks deployed at four vertices. Initially, only one adversary exists in the network.

Energy consumption is a reasonable concern in WSNs, for it limits data transmission and network lifetime. Energy consumption also reveals the complexity of each algorithm loaded by the sensor nodes. For instance, nodes in the hotspot relay more packets per round than those around the periphery. The simulation in this study involved a complete transmission round, including delivering the real packet to the destination sink and generating fake branches and a fake hotspot. All packet transmissions were considered. A detailed comparison of total energy consumption in 1000 rounds with three protocols is also presented. As depicted in the ARR scheme transmitted fewer packets than the other two schemes; it only generated real packets to the sink. The cloud-based scheme flooded many fake packets into the network to hide the source location (but less than in the multi-sinks scheme). Although the CPSLP scheme consumed slightly more energy than the ARR and cloud-based scheme, it provided better privacy preservation by using fake hotspots and packets. As the number of transmission packets increased, the choice of the destination sink became more diversified. The CPSLP exhibited a slight incensement) by balancing energy consumption

The node utilization ratios of the three schemes are depicted in Fig. 9. The node utilization ratio is defined as the percentage of network nodes whose residual energy is smaller than 99%. The node utilization ratio increased in the three protocols. As the cloud-based scheme first created a fake hotspot, its node utilization ratio was initially quite high; however, the growth was small compared with other schemes. ARR randomly chose one sink to which to send a packet. Nodes in different corners participated in source privacy protection; its node utilization ratio was therefore higher than in the cloud-based scheme. To prevent a hotspot problem in the surrounding area of the source node, the CPSLP scheme constructed a cloud-based routing structure. It used nodes with more remaining energy as much as possible, and the establishment of a cloud-shaped hotspot balanced energy consumption. The CPSLP scheme involved nodes in other areas in packet transmissions and hence had the highest node utilization ratio. The cloud center adopted θ to restrict the size of the propagation area of fake packets. This process consumed node energy in regions with more residual energy; the CPSLP scheme was therefore energy-efficient. Although the cloud-based scheme built fake hot spots, increasing the node utilization rate at first, the scheme also demonstrated a hot-spot problem: it limited the participation of nodes in other regions. Node utilization was ultimately the lowest among the three schemes. Because ARR had the shortest transmission path, it also had less node utilization.

The transmission delay is the hop count in the main path, related to the distance between the source node and sink node. The arrangement in Fig. 10 is reasonable as the network delay depends on the routing mode of the three schemes. With an increase in side length, the transmission delay increased in kind. The cloud-based scheme used greedy routing and thus exhibited the smallest delay. The CPSLP scheme attempted to compensate for the time delay in the search phase for the intermediate node, namely by adopting the shortest

routing path in the second delivery phase. Thus, this metric was slightly larger than for the cloud-based scheme. The introduction of an agent node in ARR extended the routing paths so the transmission delay was greater than in other schemes. Multiple sinks reduced network delay and routing redundancy and routed packets more randomly. Multiple sinks may also disturb the backtracking of adversaries.

In this section, network security is defined as the average number of hops in a complete packet transmission to evaluate privacy protection. The path length of fake packets should be taken into consideration. Security represents hop counts for adversaries traversing the routing path. As shown in Fig. 11, the CPSLP scheme achieved the highest level of security. To ensure the safety of source location privacy, it generated fake branches in the entire real-packet transmission period. The hotspot created by the cloud center accumulated additional data transmission and led to inconsistent traffic in a small area. A cloud of fake data packets served as a hotspot per round, used to activate the hotspot-locating attacker. As a result, adversaries were forced to traverse many paths to locate the source node.

This simulation assumes that source location will not be found when calculating network life. If the energy of one sensor node is depleted, the current number of successfully transmitted packets is defined as the network lifetime. The lifetime of ARR was the longest because each transmission cycle consumed little energy. The cloud-based scheme exhibited a hotspot problem; excessive energy was consumed around the source node, leading to premature node death. Although the energy consumption of CPSLP was highest, the lifetime was not the lowest given an increase in the node utilization ratio; surplus energy was utilized outside the hotspot area.

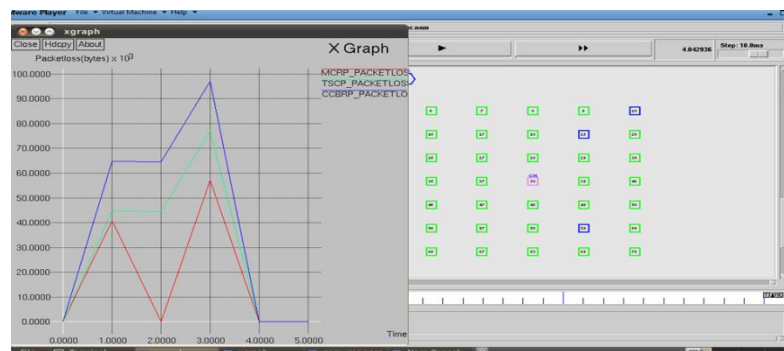


Figure 2: It illustrates the CPSLP scheme can prevent adversarial capture.



Figure 3: CPSLP scheme maintain a high level of privacy protection.

5 Conclusion and Future Work

In this paper, a CPLSP scheme is proposed to achieve high security performance. This multi-sink strategy makes it difficult for adversaries to trace back packets because the scheme ensures random and safe routing. The destination sink is generally changed per round to hide the source location and packet destination. The cloud center deployed in the network seeks to complicate detection for the hotspot-seeking adversary. In addition, the cloud shape is irregular; its location and arrangement change each time. The source node sends the real packet per period. The introduction of fake branches defends effectively against the back-tracing adversary. As adversaries are deployed around each sink initially, fake branches in the CPLSP scheme draw adversaries away from the main path and obscure the traffic flow of the real packet. In addition, the CPLSP scheme can protect source privacy under a back-tracing attack and hotspot-locating attack. The simulation results in NS2 show the CPLSP scheme utilizes network energy as much as possible.

References

- [1] Guangjie Han, Xuan Yang, Li Liu, Mohsen Guizani, Wenbo Zhang, A disaster management-oriented path planning for mobile anchor node-based localization in wireless sensor networks, *IEEE Transactions on Emerging Topics in Computing*, DOI: 10.1109/TETC.2017.2687319, Mar. 2017.
- [2] Guangjie Han, Li Liu, Sammy Chan, Ruiyu Yu, Yu Yang, HySense: A Hybrid Mobile CrowdSensing Framework for Sensing Opportunities Compensation under Dynamic Coverage Constraint, *IEEE Communications Magazine*, Vol. 55, No. 3, pp: 93-99, Aug. 2017.
- [3] Guangjie Han, Lina Zhou, Hao Wang, Wenbo Zhang, Sammy Chan, A Source Location Protection Protocol Based on Dynamic routing in WSNs for the Social Internet of Things, *Future Generation Computer Systems*, DOI: 10.1016/j.future.2017.08.044, Aug. 2017.
- [4] Jun Long, Anfeng Liu, Mianxiong Dong, Zhi Li, An energy-efficient and sink-location privacy enhanced scheme for WSNs through ring based routing, Vol. 81-82, Part C, pp: 47-65, Apr. 2015.
- [5] Pandurang Kamat, Yanyong Zhang, Wade Trappe, Celal Ozturk, Enhancing Source-Location Privacy in Sensor Network Routing, 25th IEEE International Conference on Distributed Computing Systems, Columbus, USA, pp: 599-608, Jun. 2005.
- [6] Honglong Chen, Wei Lou, On protecting end-to-end location privacy against local eavesdropper in wireless sensor networks, *Pervasive and Mobile Computing*, Vol. 16, Part A, pp: 36-50, Jan. 2015.
- [7] Na Wang, Jiwen Zeng, All-Direction Random Routing for Source- Location Privacy Protecting against Parasitic Sensor Networks, *Sensors*, Vol. 17, No. 3, pp: 614-632, Mar. 2017.
- [8] Jian Wang, Fengyu Wang, Zhenzhong Cao, Fengbo Lin, Jiayan Wu, Sink location privacy protection under direction attack in wireless sensor networks, *Wireless Networks*, Vol. 23, No. 2, pp: 579-591, Feb. 2017.
- [9] Wei Tan, Ke Xu, Dan Wang, An Anti-Tracking Source-Location Privacy Protection Protocol in WSNs Based on Path Extension, *Internet of Things Journal IEEE*, Vol. 1, No. 5, pp: 461-471, Oct. 2014.
- [10] JiaDong Zhang, ChiYin Chow, REAL: A Reciprocal Protocol for Location Privacy in Wireless Sensor Networks, *IEEE Transactions on Dependable and Secure Computing*, Vol. 12, No. 4, pp: 458-471, Jul. 2015.
- [11] Changqin Huang, Ming Ma, Yuxin Liu, Anfeng Liu, Preserving Source Location Privacy for Energy Harvesting WSNs, *Sensors*, Vol. 17, No. 4, pp: 724-756, Mar. 2017.
- [12] Yun Li, Jian Ren, Source-Location Privacy through Dynamic Routing in Wireless Sensor Networks, *INFOCOM, 2010 Proceedings IEEE*, San Diego, USA, pp: 1-9, Mar. 2010.
- [13] Mohamed M.E.A. Mahmoud, Xuemin Shen, A Cloud-Based Scheme for Protecting Source-Location Privacy against Hotspot-Locating Attack in Wireless Sensor Networks, *IEEE Transactions on Parallel and Distributed Systems*, Vol. 23, No. 10, pp: 1805-1818, Oct. 2012.
- [14] Jun Long, Mianxiong Dong, Kaoru Ota, Anfeng Liu, Achieving Source Location Privacy and Network Lifetime Maximization Through Tree- Based Diversionary Routing in Wireless Sensor Networks, *IEEE Access*, Vol. 2, No. 10, pp: 633-651, Jun. 2014.
- [15] Min Shao, Yi Yang, Sencun Zhu, Guohong Cao, Towards Statistically Strong Source Anonymity for Sensor Networks, *ACM Transactions on Sensor Networks*, Vol. 9, No. 3, pp: 466-474, May 2013.
- [16] Petros Spachos, Dimitris Toumpakaris, Dimitrios Hatzinakos, Angle- based Dynamic Routing Scheme for Source Location Privacy in Wireless Sensor Networks, *Vehicular Technology Conference (VTC Spring)*, 2014 IEEE 79th, Seoul, South Korea, pp: 1-5, May 2014.
- [17] Yun Li, Jian Ren, Jie Wu, Quantitative Measurement and Design of Source-Location Privacy Schemes for Wireless Sensor Networks, *IEEE Transactions on Parallel and Distributed Systems*, Vol. 23, No. 7, pp: 1302-1311, Jul. 2012.
- [18] Prabhat Kumar, J.P Singh, Prateek Vishnoi, M.P Singh, Source Location Privacy using Multiple-Phantom Nodes in WSN, *TENCON 2015 - 2015 IEEE Region 10 Conference*, Macao, China, pp: 1-6, Jan. 2016.
- [19] Hao Wang, Guangjie Han, Chunsheng Zhu, Wenbo Zhang, TCSLP: A trace cost based source location privacy protection scheme in WSNs for smart cities, *Future Generation Computer Systems*, DOI: 10.1016/j.future.2017.07.051, Jul. 2017.
- [20] Leron Lightfoot, Yun Li, Jian Ren, STaR: design and quantitative measurement of source-location privacy for wireless sensor networks, *Security and Communication Networks*, Vol. 9, No. 3, pp: 220-228, Feb. 2016.
- [21] Guo Cheng, Songtao Guo, Yuanyuan Yang, Fei Wang, Replication Attack Detection with Monitor Nodes in Clustered Wireless Sensor Networks, 2015 IEEE 34th International Performance Computing and Communications Conference (IPCCC), Nanjing, China, pp: 1-8, Dec. 2015.
- [22] Shuai Chang, Jialun Li, Xiaomei Fu, Liang Zhang, Energy Harvesting for Physical Layer Security in Cooperative Networks Based on Com- pressed Sensing, *Entropy*, Vol. 19, No. 9, pp: 462-473, Sep. 2017.
- [23] Fang Wei, Xinming Zhang, He Xiao, Aidong Men, A modified wireless token ring protocol for

- wireless sensor network, 2012 2nd International Conference on Consumer Electronics, Communications and Networks (CECNet), Yichang, China, pp: 795-799, Apr. 2012.
- [24] Jun Huang, Meisong Sun, Shitong Zhu, Yi Sun, Cong-cong Xing, Qiang Duan, A source-location privacy protection strategy via pseudo normal distribution-based phantom routing in WSNs, the 30th Annual ACM Symposium on Applied Computing, New York, USA, pp: 688-694, Apr. 2015.
- [25] Praveen Kumar Singh, Atul Kumar Prajapati, Arunesh Singh, R.K. Singh, Modified Geographical Energy-Aware Routing Protocol in Wire- less Sensor Networks, International Conference on Emerging Trends in Electrical Electronics & Sustainable Energy Systems, Sultanpur, India, pp: 208-212, Mar. 2016.

IoT Based Automatic Ration Product Dispensing System

Dr.A.Uma Maheswari¹, A.Pavithra²

¹Assistant Professor, Department of Electronics and Communication Engineering
University College of Engineering – Panruti

²UG Student Final year , Department of Electronics and Communication Engineering
University College of Engineering – Panruti

Abstract

This paper proposes automation in ration distribution using smart card based on RFID and IOT technology. Using this technology, we can achieve secure and interactive approach for automation of ration distribution. In automated system, we replace the conventional ration card by smart card (RFID based), which contains the family member details. The customer needs to show this tag to the RFID reader and enter the password. The Arduino microcontroller connected to the reader will check for the user authentication. If the user is found authentic then the quantity of ration to be given to the customer according to the total number of family members will be displayed on the display device. After customer purchases the material, amount gets deducted from the registered bank account. This smart ration card is free from theft as the information about the delivered ration will be sent directly to the customer using global system for mobile communication (GSM) and also updated in the government database without manual feeding using IOT technology. The database can be accessed by both consumers and by the government main stream invigilators for distribution centres from their head office. Therefore, this project ensures corruption free ration centre working system which will also enhance the direct communication of the consumers with the government and will definitely provide transparency.

Keywords: *RFID tag, IOT, Authentication, Automation, GSM, Cloud database*

1 Introduction

Ration card is one of the most important documents in India. The ration card is mainly used for purchasing subsidized foodstuffs and fuel. It is used in identification process while making passports, PAN card, Aadhar cards and acts as an address proof for citizens of India. It also provides connection with government database for over 75 crore beneficiaries under the PDS (Public Distribution System) scheme. The present ration card distribution system has many drawbacks such as inaccurate quantity of goods, manual work, low processing speed, large waiting time, and redundant data. Distribution of ration in a country like India is not an easy task. India is second largest populated country in the world. Public distribution system is a major public sector which manages and distributes the essential commodities to all the citizens of the India below the poverty line and some reserved categories such as police and military persons. People who are accessing the ration shop for food products will be given subsidy on the cost of food products based on their ration card type such as APL (above poverty line) or BPL (below poverty line) or AAY (antayodana anna yojana) no food materials will be provided free of cost. In ration shop, materials such as rice, wheat, sugar, dals, kerosene, oil are provided to the people. Many times shopkeepers also indulge in forgery by providing ration under false names, in the names of ineligible people, dead people, and duplicate names from other areas. Shopkeepers also tend to show fake quantities of goods available in shop to higher authority person. Total outflow due to corruption stands at ₹ 358 crore per annum. Over 50% of goods sold in the black market. While Ration cards are used as address proof there are 3 crores of duplicates reported. Hence there is a need to improve our current corrupt ration distribution system.

2 Literature Survey

Ration distribution system in India mainly helps BPL category people by supplying them with food grains, kerosene, LPG, sugar, etc. at relatively cheaper rate. This system works in different levels. Registered shopkeepers get ration from government dealers. At different levels quantity information and other transaction details are maintained separately. All this work is done manually. The smart card with the QR code which contains the details of family members distributed to the families. This smart card includes each family member's name, age, gender and relation with family head. The smart card is given to the ration distributor. He scans the QR code using the scanner. After successful verification the family member tells the required products he wants to buy. The ration distributor manually enters the products that the family member provided to the database. Ration distributor collects the money for the products from the family member manually. Then the family member is given a token which contains the products and the quantity to be distributed. The family member gives the token to the respective worker who measures and gives the product. The worker manually measures the

products and distribute it to the family member. The SMS sent to the registered mobile number. The ration card which is currently in use is as below.



Figure 1: Currently Used Ration Card

Having discussed about the problems in the existing system. We can understand that the process is very slow. There is no authentication in QR code, so that anyone can misuse these details. The measurements of products are not accurate. The human errors are high in this system. This system lacks in transparency. There is no record of previous transactions available to the consumers. There is a chance that the products may be distributed less than the allocated quantity. There is no proper price list available to the consumers so there may be fraud on the price of the products. Some people may get more quantity of products than the allocated quantity by using their influence.

3 Proposed System

In our proposed system, initially each user has to register at government database. He has to give all details about his family and also password. After verification by government, each user is provided with a RFID card as a Smart Ration Card. RFID card contains details of each user's family member and also their thumb impressions. User has to show the RFID card near the RFID reader which is present at each ration shop. RFID reader reads data from card verifies with government database and displays an appropriate message on LCD screen that the user is valid or invalid.

If the user is valid, it displays the family head name then it asks for the verification pin. If it is not valid the process is canceled. After successful authentication the system asks for the products to buy. If no product is entered then after 30 seconds the process is automatically canceled. After selecting the products payment is made using credit/debit card. After the payment the product is delivered automatically to the consumer with a beep sound. Then the details about the purchase products sent to the consumer via SMS and also updated in the cloud database with full transaction history with no manual work. The consumer can check transactions anytime by login into the cloud platform.

3.1 Block Diagram

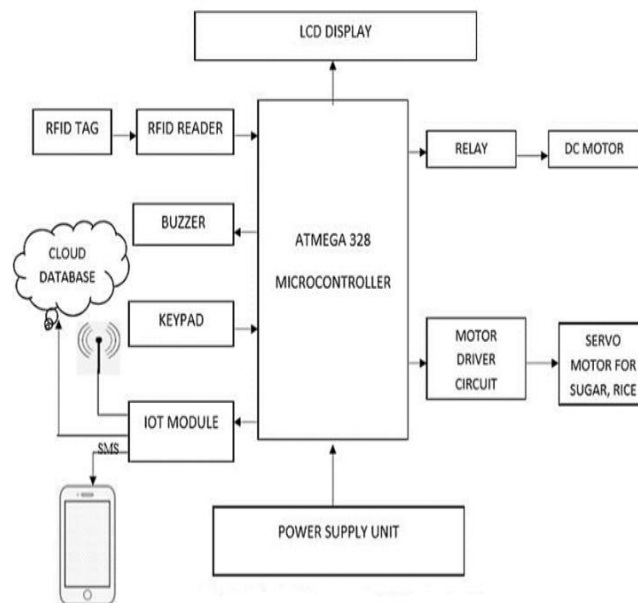


Figure 2: Block Diagram

When the Smart Ration Card in the form of RFID tag is shown over the RFID reader the reader transmits the unique 12bit hex code of the tag to the Atmega 328 microcontroller. The RFID reader generates electromagnetic waves and radiates them. When the tag comes in contact with these waves, some part of the waves containing unique hex code is reflected back to the reader. A 4x4 keypad is used for entering required data in the system. It is also used to enter password and selecting products. Atmega 328 microcontroller takes care of the all the Processes. It verifies the card by matching it with the database connected via internet. It updates the database and delivers the products. A 16x2 LCD display shows messages whether it is valid or invalid and also the details about transaction such as user name, product and quantity purchased by him/her. The IoT module updates the cloud database through internet and also takes care of sending sms to the customer's mobile through GSM gateway. Arduino embed language is used for interfacing all the hardware to the microcontroller by using the KEIL C compiler. Thing speak cloud platform is used as cloud database to store information.

4 Experimental Results

Figure 3 shows the overall implemented system which includes LCD display, keypad, power supply, RFID reader, IoT module, Atmega 328 microcontroller board and dc motor.

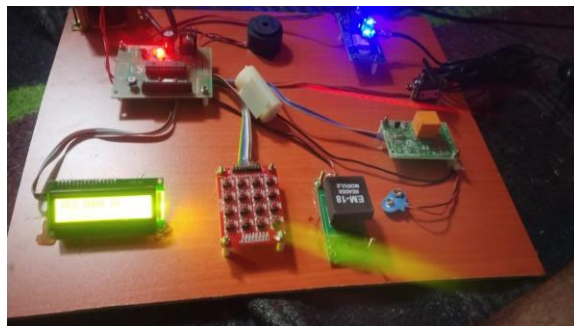


Figure 3:Overall Implemented System

The figure below shows the initial state of the system. The system is waiting for the RFID tag scan.



Figure 4: System Initial State

When the rfid tag shown near the rfid reader it checks if the use is valid or not. The figure below shows the name of the family head after successful verification.



Figure 5:Display Shows the Family Head Name



Figure 6: System Asking for Password

The figure above shows that after identification of family member it asks for password. After successful authentication it asks for products to select.



Figure 7:Waiting for Selection of Products

The fig 7 shows that the system waiting for the selection of products. If the products are not selected before the time out period indicated as T the process is automatically canceled.

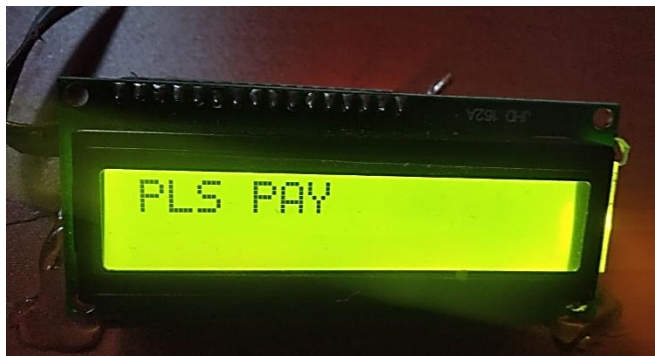


Figure 8: System Waiting for Payment

After product selection system will ask for payment. The payment is made via debit/credit card. After successful transaction products are delivered to the customer.

| | A | B | C | D | E | F | G | H | I | J | K | L |
|----|-------------------------|----------|--------|---------|--------|--------|--------|--------|----------|-----------|-----------|--------|
| 1 | created_at | entry_id | field1 | field2 | field3 | field4 | field5 | field6 | latitude | longitude | elevation | status |
| 2 | 2020-03-13 12:44:55 IST | 1 | PRIYA | 2 L | ISSUED | | | | | | | |
| 3 | 2020-03-13 12:55:04 IST | 2 | PRIYA | 4 kg | ISSUED | | | | | | | |
| 4 | 2020-03-13 12:57:46 IST | 3 | PRIYA | 2 L | ISSUED | | | | | | | |
| 5 | 2020-03-15 16:58:14 IST | 4 | PRIYA | oil 1 L | ISSUED | | | | | | | |
| 6 | 2020-03-15 16:59:30 IST | 5 | PRIYA | oil 1 L | ISSUED | | | | | | | |
| 7 | 2020-03-15 17:05:28 IST | 6 | PRIYA | oil 1 L | ISSUED | | | | | | | |
| 8 | 2020-03-15 17:08:28 IST | 7 | PRIYA | oil 1 L | ISSUED | | | | | | | |
| 9 | 2020-03-15 17:11:10 IST | 8 | PRIYA | oil 1 L | ISSUED | | | | | | | |
| 10 | 2020-03-15 17:12:01 IST | 9 | PRIYA | oil 1 L | ISSUED | | | | | | | |
| 11 | 2020-03-15 17:13:40 IST | 10 | PRIYA | oil 1 L | ISSUED | | | | | | | |

Figure 9 :Downloaded Data From The Database

The above figure shows the downloaded data from the cloud database (Thing speak). All transactions made by the family is available from the database. The customer and government can access the information at any time.

5 Conclusion

This proposed project is for the benefit of common people and the government. The device find's its application in the ration shop run by the government. Also, this project's electronic device can also be modified and made to be used in the glossary shops and markets as a vending machine in a smart and automated manner which saves workers and time employed for the process of measuring and delivery of goods. Also, when implemented in the Ration shops across Tamil Nadu, the government official can have a check on the on-going of each and every transaction done in the ration shops from their head office and this access of information privilege is given to every citizen of India as a Right to Information under the Act of Consumer Rights. To access the database and authentication of user requires internet connectivity which can be a problem in remote locations. It will be a contribution to the scheme "One Ration One Nation" and can also became a part of e-governance that India is under taking at present.

References

- [1] Alfandi, Omar; Hasan, Musaab; Balbahaith, Zayed (2019), "Assessment and Hardening of IoT Development Boards", Lecture Notes in Computer Science, Springer International Publishing, pp. 27–39, doi:10.1007/978-3-030-30523-9_3, ISBN 978-3-030-30522-2.
- [2] Balekar Swati D, Kulkarni Rituja R, "Online Ration Card System by using RFID and Biometrics", International Journal of Advanced Research in Computer Science and Software Engineering, 2015.
- [3] Eadline, Douglas. "Moving HPC to the Cloud". Admin Magazine. Admin Magazine. Retrieved 30 March 2019.
- [4] "Frequently Asked Questions - RFID Journal". www.rfidjournal.com. Retrieved 2019-04-22.

- [5] Hassan, Q.F. (2018). Internet of Things A to Z: Technologies and Applications. John Wiley & Sons. pp. 41–4. ISBN 9781119456759.
- [6] K.Balakarhik, “Closed – Based Ration Card System Using RFID and GSM Technology” vol.2, Issue 4, Apr 2013.
- [7] Michael, L. Mccathie, “The Pros and Cons of RFID in Supply Chain Management”, Proceedings of the IEEE International Conference on Information and Automation(ICIA), 2005.
- [8] Neha Sharma, Ayushi Gupta, Vinod Ghadge, Mayank Harwani, “IoT Based Ration Card System Using Bluetooth Technology”, International Journal of Engineering Science and Computing, Volume 7 Issue No.3 , March-2017.
- [9] Parvathy A, VenkattaRohit Raj, Venumadhav, Manikantha, “RFID Based Exam Hall Maintenance System”, IJCA Special Issue on “Artificial Intelligence Techniques – Novel Approaches & Practical Applications” AIT, 2011.
- [10] Swapnil.R.Kurkute, Chetan medhe, Ashlesha Revgade, Ashwini.Kshirsagar "Automatic ration distribution system" 3rd International Conference on Computing for Sustainable Global Development (INDIACom), 2016, IEEE.
- [11] Swapnil, Chetan, ashlesha, Ashwini “Automatic Ration Distribution System –A Review” IEEE 978-9-3805-4421-2/16.
- [12] S. Valarmathy, R. Ramani “Automatic Ration Material Distributions Based On GSM and RFID Technology” I.J intelligent systems and applications, 2013, 11, 47-54.
- [13] Y.A. Badamasi, “The working principle of an Arduino”, in Electronics, Computer and Computation (ICECCO), 11th International Conference on Information Communication Embedded Systems, pages 1–4, 2014.
- [14] Yerlan Berdaliyev, Alex Pappachen James, “ RFID-Cloud Smart Cart System”, IEEE Intl. Conference on Advances in Computing A Communications and Informatics (ICACCI), Sept. 21-24, 2016.

Driver Drowsiness Detection And Alert System

J. Nisha¹, C.Sugapriya², B.Arunkumar³

^{1,2} UGstudent's final year, Department of ECE, St. Anne's College Of Engineering And Technology, Panruti

³Assistant Professor, Department of ECE, St. Anne's College Of Engineering And Technology, Panruti

Abstract

In recent few years, there has been rapid increase in road accidents across worldwide and India as well. The most significant reasons for the accidents are driver drowsiness and fatigue. The conventional vehicle safety system and the sensor-based detection for drowsiness are often very late in detecting and preventing fatalities on road. To detect the driver drowsiness of driver, currently many systems are being developed; among them the computer vision- based detection system proved to be best in detecting driver drowsiness. In the existing system, only the drowsiness of the driver is detected, no method is suggested or used to wake him up from drowsy state. The proposed system uses Raspberry pi3 processor to detect the driver drowsiness through eye closure level using eye detection algorithm. The system not only detects the drowsiness but also provide alertness to the driver through buzzer. In addition, the system also tries to wake up the driver from drowsy state by providing mild vibration to driver and sprinkling water on driver's face.

Keywords: *Raspberry pi, Open CV, Image processing,*

1 Introduction

According to a survey many people lost their life in road accidents. Most of the traffic accidents are the result of drowsiness, the individual level by the drivers. Drowsiness is a sleepy feeling which is cannot be controlled by the person. It is identified as one of the reasons for road accidents especially on highways. Drowsiness is mainly caused when the person is not getting enough sleep or feeling tired on night drives or if the person is under medication. Since falling asleep is not in the driver's hand an external entity is required to help him stay awake. The system provides the driver with real time information from the raspberry pi 3processor. Among these factors, driver drowsiness is the major cause of mortality traffic accidents worldwide. Driver Drowsiness Detection is one of the car safety features that helps prevent accidents caused by the drowsydriver. Drivers drowsiness cause many accidents every day. According to the National Highway Traffic Safety Administration (NHTSA), more than 1,550 people are death and 71,000 are injured per year as a main reason of drowsy driving. Thus, main goal of driver drowsiness detection is very important to prevent accidents and save lives. This paper suggests a method to overcome this issue by using Raspberry Pi processor

2 Literature survey

In the paper "Driver Drowsiness Detection (IEEE journal Communication and Signal Processing 2020 by K.Satish, A.Lalitesh, K.Bhargavi, M.Sishir Prem and Anjali.T" [1], the system detects the drowsiness of driver effectively using facial feature extraction and eye blink threshold is set by calculating blink value but the blinking rate varies from person to person. In the paper "Driver Drowsiness Detection System Based on Binary Eyes Image Data (IEEE journal on image processing 2020) by Maninder Kahlon and Subramaniam Ganesan"[2], the system monitor whether the eyes are open or closed using eye detection algorithm. In the paper "Real-Time Driver Alert System Using Raspberry Pi. Jie Yi Wong¹ and Phooi Yee Lau²"[3], the driver head position is monitored and the drowsiness is detected by driver's head position. In the paper "Driver Drowsiness Detection with Audio-Visual Warning Nikita G. Prajapati Ms. Pooja M. Bhatt PG Student Assistant Professor Department of Computer Engineering Department of Computer Engineering IIET-Dharmaj IIET- Dharmaj"[4] the System monitor eye and mouth posters and these parameters are considered for drowsiness detection, the drowsiness detection by mouth poster may vary from person to person. In the paper "cc" [5], driver drowsiness is detected by using HAR algorithm. In the paper "Emotion Analytics for Advanced Driver Monitoring System. Nandyala, S. Gayathri, K.Bhushan, C. Gandhi, V. et al.,[6], in this Advanced Driver Monitoring System emotions are continuously analysed and separate pattern for sleepiness is

extracted, but this module needs node training with various emotions of human being such as happiness, sad, angry, neutral, and sleepy which is tedious task.

3 Proposed system

In the proposed system Raspberry pi processor is use. eye detection algorithm can be used. The algorithm monitors both eye point coordinates and eye ball movement using camera. Raspberry pi continuously captures the driver’s face and process it to detect the drowsiness of the person.

3.1 Block Diagram

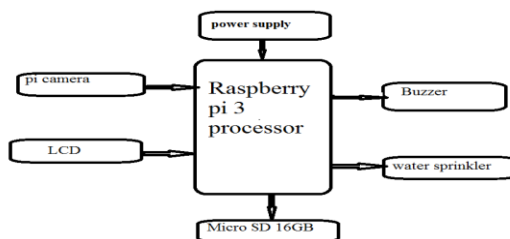
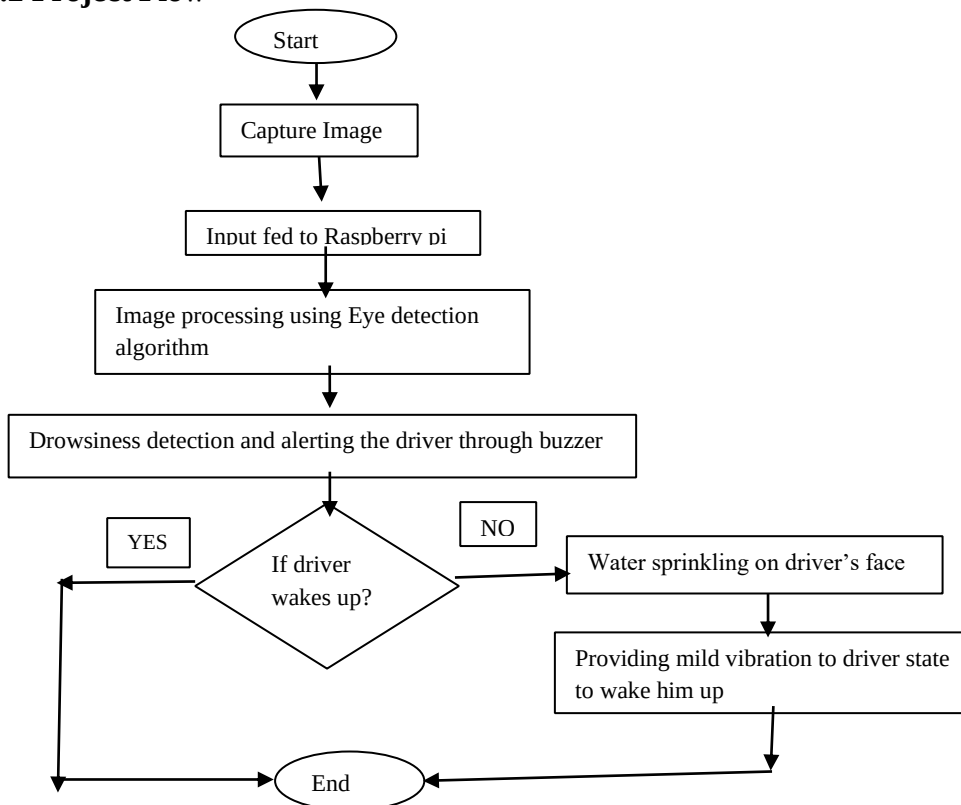


Figure 1: Block diagram of proposed system

3.2 Project Flow



4 Hardware And Software

Hardware:

- Raspberry pi 3 processor
- pi Camera

- Buzzer
- Water sprinkler
- LCD display

Software:

- Open cv

4.1 Raspberry PI 3 processor

This main processing chip connects a camera and display. The Raspberry Pi design does not include a built-in hard disk or solid-state drive, instead used an SD card for booting and long-term storage. This board is intended to run Linux Debi based operating systems. The image processing is a form of signal processing where the input is an image, like a photograph or video frame, the output of an image processing may be either an image or a video frame or a set of characteristics or parameters related to the image. RASPBERRY PI platform is most used after ARDUINO. Although overall applications of PI are less it is most preferred when developing advanced applications. The RASPBERRY PI is an open source platform where one can get a lot of related information so you can customize the system depending on the need.



Figure 2: Raspberry pi3 processor

4.2 Pi Camera module

When the camera shutter opens, the sensor captures the photons that is converted to an electrical signal that the processor in the camera read and interprets colours, this information is then stretched together to form an image.

4.3 LCD display

A liquid-crystal display (LCD) is a flat panel visual display which shows over the vehicle speed limit of message to warn the drives. To perform the write operation on LCD the read/write pin is connected to ground

4.4 Buzzer

The **buzzer** is **used** to alert the driver whenever the driver feels **drowsy**. Whenever the sensor values are not in the range of threshold value.

4.5 Water sprinkler

The warning system aims to wake up the **driver** from the **drowsy** state. The system consists of an alarm system and a **water sprinkler**. When the **driver** is found in a **drowsy** state by the processor an alarm sound will be produced, and **water** will be sprayed into the face.

5 Result

If driver's eyes are open the system does not take any action and continues to monitor. If eye lids are closed for a particular period of time the driver is drowsy, then the system tries to wake up the driver by giving buzzer sound and mild vibration through vibrator placed at the bottom of the driver's seat. If the driver does not respond and continues to drowsy the system wakes up the driver by sprinkling water over his face.



Figure 4: Image showing eyes closed



Figure 5: Typical image showing Real time driver's drowsiness detection

6 Conclusion and Future Work

In this project, driver drowsiness detection system is built to identify driver's drowsy state and make him conscious while driving in order to reduce accidents caused due to drowsiness. The Processor along with Raspbian camera is utilized to capture the driver continuously. Sleepiness is estimated by extracting Eye from face utilizing shape-indicator and calculating Eye Aspect Ratio (EAR). At the point when the system detects drowsiness, the driver will be frightened by a noisy notice that will awaken the driver from the rest state. The system also tries to wake up the driver through a mild vibration and by sprinkling water over his face if he doesn't respond to alert sound. The work can be extended to cut off the fuel to vehicle if the driver not responds to alert message for longer time.

References

- [1] Ueno H., Kanda, M. and Tsukino, M. "Development of Drowsiness Detection System", IEEE Vehicle Navigation and Information Systems Conference Proceedings, (1994), ppA1-3, 15-20
- [2] Sean Enright, Electronics Engineering Student, 506-650-3611, May 26-2011, Alcohol Gas Detector "Breathalyzer".
- [3] Weirwille, W.W. (1994). "Overview of Research on Driver Drowsiness Definition and Driver Drowsiness Detection," 14th International Technical Conference on Enhanced Safety of Vehicles, pp23-26.
- [4] Arpit Agarwal, "Driver Drowsiness Detection System", portfolio of projects on human computer interaction, December, 2010.

- [5] Paul Stephen Rau, National Highway Traffic Safety Administration, United States, Paper Number05-0192 Drowsy Driver Detection and Warning System for Commercial Vehicle Drivers: Field Operational Warning System for Commercial Vehicle Drivers: Field Operational Test Design, Data Analyses and progress.
- [6] Mallis, M.M., et al., Bio Behavioral Responses to Drowsy Driving Alarms and Alerting Stimuli, DOT HS 809 202,February 2000.
- [7] Rhody Chester, H. F. ‘‘Hough Circle Transform‘’, CarlsonCenter for ImagingScience Rochester Institute of Technology October 11, 2005.
- [8] Mario I Chacon-Murguia Claudia Prieto-Resendiz, ‘‘Detecting Driver Drowsiness-A survey of system designs and technology,’’ IEEE Consumer Electronics Magazine, pp.107-108,October 2015.
- [9] Mayank Chauhan, Mukesh Sakle ‘‘Study & Analysis of Different Face Detection Techniques’’ International Journal of Computer Science and Information Technologies, Vol. 5 (2) , pp 1615-1618,2014.
- [10] Paul Viola and Michael j. Jones, ‘‘Rapid Object Detection using a Boosted Cascade of Simple Features,’’ International Journal of Computer Vision 57(2), pp 137–154, 2001

Intravenous Flow Monitoring System Using Lora Technology

Malini¹, Divya², Radhakrishnan³

^{1,2} IV Year, Department of ECE, St. Anne's College Of Engineering and Technology, Panruti

³ Assistant Professor, Department of ECE, St. Anne's College Of Engineering and Technology, Panruti.

Abstract

The Automated Glucose Stream Control and Observation System is associated with monitoring the progression of glucose as a result. At any point, if patients have a lot of fatigue, the medical caretaker will put the glucose for patient recovery at any time. She just needs to monitor the progression of the amount of glucose while placing the glucose bottle. In the event that the glucose bottle is unfilled, the container should be replaced or evacuated by a medical caretaker. In case nurse is not there that time in invert bearing, body blood patients will flow into the container. We can screen the glucose stream by utilizing this observing framework. We'll consider the weight of glucose bottles in the Glucose Monitoring System. We use the Weighing Scale for the weight of the bottle. The flow will control the progression of glucose, as indicated by the weighing scale. The stopper will close the valve so that blood will not come back into the bottle on the off chance that the container has been unfilled.

Keywords: *Arduino microcontroller, Solenoid Valve, Load Sensor.*

1 Introduction

New data advancement are well-being observing frameworks integrated into a telemedicine system that would provide the option to assist in the early discovery of odd conditions and reverse the genuine effects. Many patients will benefit from continuous wandering examination, optimum maintenance of a chronic condition as a part of a demonstrative technique or during a particular recovery from an adverse accident or surgery. The electrocardiograph is a transthoracic interpretation of the heart's electrical activity over an undefined time period, characterized by electrodes connected to the skin surface and registered by an external instrument registered by a computer external to the body. Another type of electronic valve with quantitative control is designed to fulfill the role of quantitative control in a variety of stream frames. The valve receives stream flow signals from the Hall flow sensor of the impeller to measure the flow value and accumulate the absolute value, the micro controller chip is used. It is also used for hand-off control as well as for continuous solenoid valve control. The load sensor will sense the heaviness of the synthetic concoctions and show it on the LCD monitor in this paper we are interfacing a load sensor to the Arduino microcontroller. In the current system, patient monitoring is performed by manual procedure that may result in the switching of blood stream during the trickle phase. It could end up in the reverse blood stream at the point where the bottle becomes unfilled and if health care faculties do not know about it. Especially in trickles bottle, manual procedure can not achieve accuracy patients observing late night troublesome controller. This can be modified in the programmed glucose stream control in hospitals, in physical vapor deposition, in plant supply control of substances that grow in water (hydroponics). The weight of the drip bottle is measured using an electronic load cell and data about it will be sent to the hospital's LORA. Here, via the Wi-Fi module, we send the data to the simple Android mobile app for exhibition purposes. Lingerie to the Wi-Fi module at the point where the container gets a threshold amount and sends the details to the doctor and hospital staff. By sending commands from the mobile, specialists may monitor the stream rate.

2 Literature Survey

1. A usually closed solenoid valve and a relay are part of the electronic valve module . The measurement module uses the Hall flow sensor impeller, which connects to the control module counter to capture and process
2. On the salt hanger, the load sensor is set and the bottle is hanged on it. This sensor transforms the bottle's changing weight into various voltages. The output voltage is fed into the ESP32 WiFi chip from the load sensor.ulse signal.

3 Proposed Method

Especially in trickles bottle, manual procedure can not achieve accuracy. Patients observing late night is troublesome and communication among specialist and patient is less. The answer for the previously mentioned issue is consequently close the valve without human administrator. The load cell is utilized to persistently screen the weight age of the saline container and it will be shown on the LCD display, when it arrives at the critical level a programmed message will be sent to hospital staff's through Android application. It's lingerie for the hospital workers at the point where the container hits the threshold mark. Methodology

The Arduino controller, Load Cell, Solenoid Valve, Keypad, Relay, and ESP8266 are part of the glucose monitoring system. The weight of the Drip Bottle is calculated using an electronic load cells and data about them will be sent to the doctor. We are sending data to the simple Android Mobile App for exhibition purposes. It is lingerie for specialists and hospital staff at the stage where the bottle hits the threshold mark. By sending orders from mobile devices, specialists can monitor the stream rate. The stage at which the weight of the container becomes absolutely empty. The Arduino controller gives the order to the valve system with the final purpose of blocking it and not reversing the blood stream. The temperature sensor is used to monitor the internal heat level after the patient is injected with the drip. On the off chance that low values are recognized by the temperature, the valve will also be shut at that stage and it will be inferred to experts. Sensor Heartbeat Sensors and temperature sensors can be modified by sending orders from cell phones to doctors. When the container weight becomes absolutely vacant, the Arduino controller sends the order to the Valve instrument with the ultimate objective that it will be blocked and no converse bloodstream will occur.

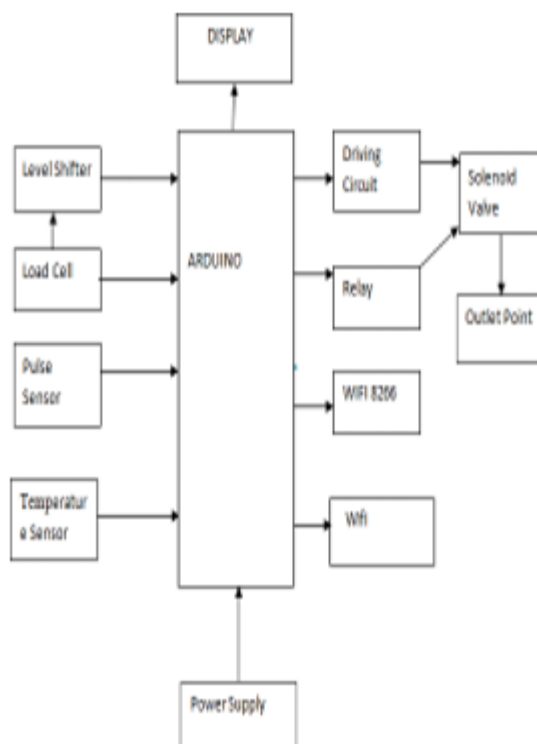


Fig1:Block diagram of intravenous flow monitoring system

Flex Sensor associated with patient hand will peruse hand signal of a patient using which we can atomize the switching of devices in the room. Centered on a 16-bit / 32-bit ARDUINO CPU with real-time emulation and embedded trace support, the LPC2141/42/44/46/48 arm microcontrollers combine microcontrollers with embedded highspeed flash memory ranging from 32 KB to 512 KB.



Fig2: model of intravenous flow monitoring system

LPC2141/42/44/46/48 is suitable for applications where miniaturization, access control and point of sale are a key requirement because of their small size and low power consumption. Serial communication interfaces ranging from a full-speed USB 2.0 device, many UARTs, SPI, SSP to I2C-bus and 8KB to 40KB SRAM chip, make these devices very suitable for communication gateways and Providing both large buffer size and high processing capacity, protocol converters, soft modems, speech recognition and low end imaging. High versatility in the use of LCD displays. Lora uses sub gigahertz radio frequency bands such as 169MHZ, 433MHZ, 868MHZ and 915MHZ that are license-free. Flex sensors that, depending on the amount of bending in the sensor, adjust resistance.

In the proposed method, the level of the liquid can be determined by the weight of the saline container, such that when the liquid hits its minimum level, the ESP 8266 WiFi communicator is used to submit warnings to end-users.

1) **LOAD SENSORS:** A load sensor is a system that calculates the weight of items such as cars. If a vehicle's weight reaches the threshold value (1.5 kg here), the gate is locked.



Fig 3: Load sensor

2) **SOLENOID VALVES:** The electronic valve is an electro-mechanical system in which the solenoid produces a magnetic field using electric current and thus operates a mechanism that controls the opening of the fluid flow in a valve.



Fig 4: Solenoid valve

3) LCD Monitor: A small, low-cost display is an LCD. The controller is common on many screens, which means that many micro-controllers have libraries that make it as simple as a single line of code to display messages. It offers users elevated versatility



Fig 5: LCD display

4) FLEX SENSORS: The Flex sensors which, depending on the amount of bending in the sensor, change the resistance. They are usually 1" -5" long in the shape of a thin strip. The more the bend, the greater the resistance value, the more they translate the change in bend to electrical resistance. In gaming gloves, auto controls, fitness products, measurement instruments and so on, Flex sensors are analog resistor.



Fig 6: Flex sensor

5) TEMPERATURE SENSORS: The LM35, which is an integrated circuit sensor that can be used for temperature measurement with a temperature-proportional electrical output. The temperature sensor LM35 calculates the temperature more precisely than using a thermistor.



Fig 7: Temperature sensor

6) ESP 8266 WIFI COMMUNICATOR: The ESP8266, which provides a full and self-contained Wi-Fi networking solution that enables the application to be either hosted or all Wi-Fi networking functionality to be unloaded from another application processor. In order to boost the device efficiency in such applications and to minimize microcontroller memory requirements, it has incorporated cache ,microcontroller-based architecture with easy UART interface or CPU AHB bridge interface connectivity. Alternatively, wireless Internet access can be applied to any microcontroller-based design with easy connectivity through the UART interface or the CPU AHB bridge interface, acting as a Wi-Fi adapter.



Fig8:ESP 8266 wifi communicator

7) EMBEDDED C: You can access individual bits. Data is taken from external devices. No need for standard input functions, therefore. To save memory, Char Data Form is used. Unlike C, it is platform-specific. Instead of is used, enabling the compiler to use the controller architecture. Computer software, written to monitor machines or devices that are not usually thought of as computers, generally referred to as embedded systems, is the embedded C language most commonly used to program the microcontroller embedded software.

4 Experimental Results

It is capable of measuring the drip bottle via this project. Weight monitoring using a load cell, and also we can set the Flow control using the electronic valve and hall flow sensor which is very much helpful in looking after

the patients in the hospitals for the observations particularly during the night time. And the reverse controls it even When the glucose level is zero, the patient's blood flow displays all the data on the LCD monitor and also tests the patient's body temperature through the temperature sensor placed on the patient's side, and if the patient needs a fan ON/OFF, then he or she can operate only bending the finger through the flex sensor placed on the patient's finger, the in-room fan. All these information will be displayed on the LCD monitor as shown in Fig.5 and all the data will be sent via the Android App of the Hospital Faculty's Wi-Fi module as shown in Fig.10



Fig 9: Android app



Fig 10:LCD display

5 Conclusion

This paper overcomes the effects of incompetence in tracking the IV flow. The level of the saline bottle can be tracked from a distant location using suggested monitoring, which will help to create a smart health care system. Electronic Quantitative control device valve, to grasp drip flow control as a small, compact and advanced medical technology. Here, 25 percent, 50 percent, 75 percent of the IV cannula pipe automatically regulates the continuous flow of medication via drip to the patient at three different flow rates. This can be accomplished by calculating the medication level through the drip and comparing it with the set point. When it hits the desired critical stage, the flow of medication is halted. Here, LORA replaces applications such as user-friendly mobile apps with manual switches so that doctors can monitor the flow rate by sitting on the spot. Doctors can sit in a different city, different floor of a building, or in their house and patient can be anywhere, monitoring and flow rate controlling can be done.

References

- [1] Fan Yang, Yu Wang "New Electronic Valve System Research with Quantitative Control" IEEE Third Global Intelligent Systems Congress, 2012.
- [2] Sneha Shetty, Dr. Vijayakumar, International Journal of Scientific Progress "Electronic Valve with Quantitative Control System for Medical Application" International Journal of Scientific Development and Research.
- [3] ESP32 and MQTT-S Smart Saline Level Monitoring System, Debjani ghosh, Ankit Agarwal, IEEE 20th International Health Networking Conference.
- [4] Instant Warning Smart Drip Infusion Control System-Ramisha Rani K, Shabana N, Tanmayee, Loganathan S, Dr. Velmathi G, 2017, IEEE, via nRF24L01.
- [5] Embedded Electro-hydraulic Proportional Valve Controller Study, Lu Quan Sen, Bao Hong and Electronic Valve with Quantitative Control System for Medical Application Research.

Reconfigurable H-Shaped Dielectric Resonator Antenna

Nandhini M¹, Abitha S², Durai Raj S³

^{1,2} UG Student, Department of ECE, St. Anne's College of Engineering and Technology, Panruti

³ Assistant Professor, Department of ECE, St. Anne's College of Engineering and Technology, Panruti

Abstract

A Reconfigurable Dielectric Resonator Antenna (DRA) using a H shaped Aperture Slot. The slot Aperture designed has been analysed over different slot dimensions with input impedance. This antenna can be used for wideband applications at 5G frequency band. The slot aperture feed used to neglect spurious radiation to resonator antenna and also RT duroid has low dielectric constant ($\epsilon_r=2.2$) compared to FR4 substrate. By using substrate and feed technique to achieved gain above 5 dB. The proposed antenna is designed to meet the best possible result using a simulation software: Ansoft HFSS (High Frequency Structure Simulator) software version 15.0. The proposed antenna was measured and compared with the simulation results to prove the reliability of the design. The performance of the designed antenna was analyzed in term of gain, return loss, VSWR, and radiation pattern.

Keywords: DRA, 5G, HFSS, VSWR, Gain

1 Introduction

The day by day the compact device is occupied entire spectrum of wireless applications. There are plenty of compact antenna is playing key role for transcription/reception of communication link. But the researchers are focusing on no metallic losses antenna structure at both low and high frequency applications. The DRA is satisfying the above required application and which is very compact nature and flexible to place the antenna in any places.

The DRAs have been popular over the years due to their attractive features like degree of freedom in terms of aspect ratio, minimal conductor losses, high radiation efficiency and ease of excitation. Bandwidth enhancement and compact size are the two major challenges to meet the requirements of modern communication systems, numerous designs have been proposed to meet these requirements. In, laterally radiating rectangular dielectric resonator antenna (RDRA) has been proposed with small ground plane, however design results in limited bandwidth of around 10:9% with a low gain of around 4:6 dB. Dielectric resonator antennas (DRAs) have gained widespread attention in wireless communication systems due to their attractive features such as high radiation efficiency (due to lack of surface wave and conductor losses), relatively wide bandwidth, and light weight. Moreover, its size and bandwidth can be controlled by the dielectric constant of the material used to design the DRA. Being a volumetric radiator (3D structure), it offer more design flexibility and versatility than the conventional planar antennas.

However, for the single-mode DRA the impedance bandwidth is typically 10%, which may not be sufficient for some broadband wireless communication systems. The bandwidth enhancement of DRA has been the vital topic of study over the years and different techniques have been proposed to widen the bandwidth of DRAs. By using a suitable excitation technique, any dielectric structure can become a radiator at defined frequencies. It is to be noticed that, for a given resonant frequency, the size of the dielectric resonator is inversely proportional to the relative permittivity of the constitutive material. The lowest dielectric constant material adopted in DRA design is reported in, where commodity plastics with relative dielectric constant smaller than 3 have been utilized for the realization of Super shaped DRAs.

2 Antenna Design Analysis

In order to achieve wideband characteristics many modified RDRA have been proposed like T- shaped [6], L- shaped [7], U- shaped [8], Z- shaped [9], embedded DR [10]. However these proposed structures have increased volume and fabrication complexities. In this work, first a RDRA is designed to resonate at 2.4 GHz with the fundamental TE_y111 mode. Material used for the design of RDRA is Rogers TMM10i with a relative permittivity, $\epsilon_r = 2.2$, loss tangent $\tan \delta = 0.0009$. The design is modified in the H-shaped DRA which improves bandwidth by reducing the effective dielectric constant and retains the fundamental TE_y111 mode which decides the radiation characteristics.

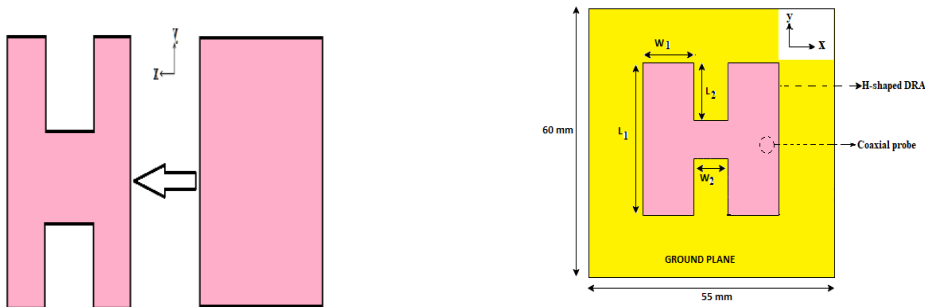


Figure 1: Stages involved in designing of proposed antenna (without ground plane) (a) Top view of RDRA (b) Top view of proposed (H-shaped) DRA.

Fig. 1: (a) Top view of the proposed antenna, (b) Cross sectional view of proposed Antenna. where, H is the height of the DRA and O_x is the offset along x-axis from centre and L is inner probe length. (2.28–2.36 GHz) at $f_c = 2.2$ GHz. The proposed H-shaped DRA is $20 \times 20 \times 12.7$ mm³ or $0.278\lambda_c \times 0.278\lambda_c \times 0.176\lambda_c$ at 4.18 GHz where λ_c is the wavelength at central operating frequency.

Fig. 1a shows the geometry of the proposed structure (top view) where substrate and ground plane are made up of 55 mm × 60 mm in dimension. Material used for substrate is Rogers RT6002 with a thickness of 0.762 mm, $\epsilon_r = 2.2$ and $\tan\delta = 0.0009$. Material used for DRA is Rogers TMM10i with, $\epsilon_r = 9.8$, $\tan\delta = 0.002$. First, the original RDRA is designed to resonate at 2.4 GHz using dielectric waveguide model (DWM)[1]

$$k_{y \tan}(k_y L_1 / 2) = ((\epsilon_r - 1)k_0^2 - k_y^2)^{1/2} \tag{1}$$

$$f_r = c / 2\pi(\epsilon_r)^{1/2} (k_x^2 + k_y^2 + k_z^2) \tag{2}$$

$$k_0 = 2\pi / \lambda_0 \tag{3}$$

$$k_x = \pi / L_1 \tag{4}$$

$$k_z = \pi / (2W_1 + W_2) \tag{5}$$

k_x, k_y, k_z are the wave numbers in the x, y, z directions

Where c is the speed of light in free space and f_r is the resonant frequency of RDRA.

The dimensions are calculated to be $L = W = 20$ mm, and height $H = 12.7$ mm for fundamental TE_{y111} mode with the value of offset (-10 mm, 0) for excitation of probe. It is modified in the form of H-shape by cutting two slots each of size (7.5 × 5 × 12.7 mm) with length as L_1 and width (2 $W_1 + W_2$) with $W_1 = 7.5$ mm, $W_2 = 5$ mm, $L_1 = 20$ mm, $L_2 = 7.5$ mm, as shown in the Fig 1a and 1b. It is excited using a coaxial probe of length $L = 8$ mm and placed at an offset of (8 mm, 0 mm) along x-axis from the center. Probe is placed inside the DRA in order to avoid impedance mismatch. The effective dielectric constant, ϵ_{eff} reduces after modifying original RDRA into H-shape. To achieve the optimum antenna performance, a parametric analysis was carried out on probe height and offset with the commercially available HFSS, which is based on the computational technique of finite integration method

Table 1: Parameters of Proposed Antenna Design

| Parameters | W,L | H | W1 | W2 |
|-------------|-----|------|-----|----|
| Values (mm) | 20 | 12.7 | 7.5 | 5 |
| Parameters | - | L1 | L2 | - |
| Values (mm) | - | 20 | 7.5 | - |

3 Result And Discussion

The simulations of the antenna structure were performed using HFSS (High Frequency Structure Simulator) software. The antenna’s performances are evaluated in terms of return loss, gain and VSWR and directivity. The

valid radiating frequency of antenna is described by two measuring parameters of antenna that are the “return loss” And the “VSWR”. If the return loss an antenna for specific frequency is more than -10 dB it indicates that whatever power fed to antenna out of maximum power is rejected. So, for a good radiating element, return loss should be less than -10 dB and VSWR is less than 2. Another useful measure describing the performance of an antenna is the gain. Although the gain of the antenna is closely related to the directivity, it is a measure that takes into account the efficiency of the antenna as well as its directional capabilities. However, directivity is a measure that describes only the directional properties of the antenna, and it is therefore controlled only by the pattern.

3.1 Return Loss

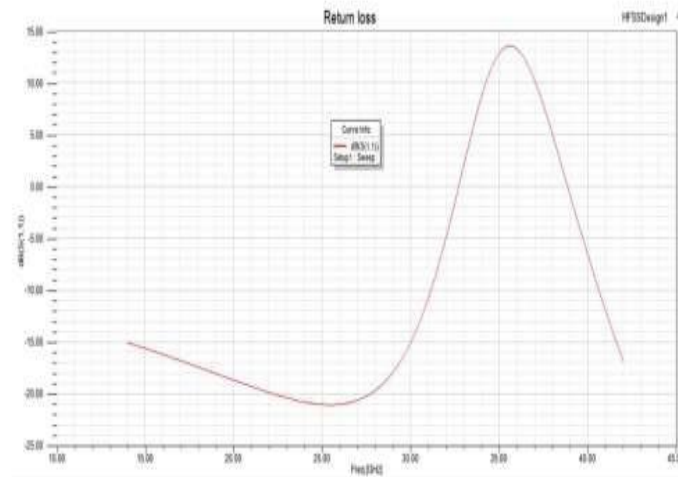


Figure 2: S11 Parameter

Return loss is used to indicate the amount of power that is lost to load, and the lost power does not return as reflection. Return loss is an aspect similar to VSWR to be a sign of how well the matching between transmitter and antenna has taken place. Ideal value of return loss is approximately -13dB which corresponds to VSWR of less than 2. As shown in figure: 3 the value of Return loss is -20dB.

3.2 VSWR

The Voltage Standing Wave Ratio or VSWR is defined as the relation between the maximum voltage and the minimum voltage all along the transmission line. Further definition of the VSWR can be derived from the level of forward and reflected waves, it is also a sign of how capably or intimately an antenna’s terminal input impedance is matched to the characteristic impedance of the transmission line.

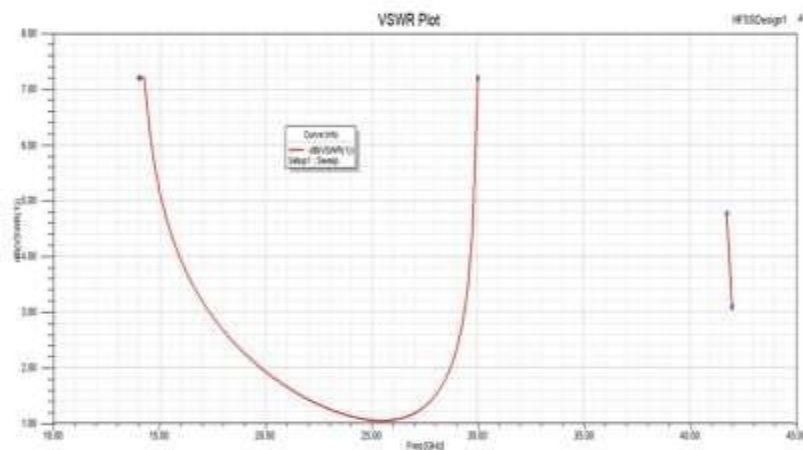


Figure 3: Voltage Standing Wave ratio (VSWR)

Also, VSWR and mismatch between the transmission line and antenna are directly proportional to each other that are when there is an increase in VSWR indicates an increase in the mismatch between the transmission line and antenna. As shown in figure: 4 the value of VSWR is 1.02.

3.3 Gain

Gain of an antenna (in a given direction) is defined as “the ratio of the intensity, in a given direction, to the radiation intensity that would be obtained if the power accepted by the antenna were radiated isotropically. As shown in figure: 5 the value of Gain is 5.42 dB

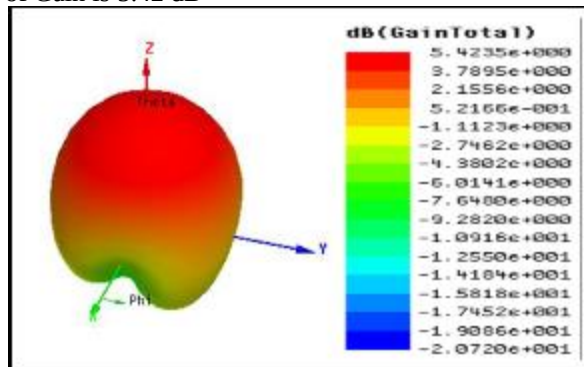


Figure 4: Gain of the proposed Antenna

3.4 Radiation pattern

In many cases, the protocol of an H -plane and E -plane pattern or sweep is used in the presentation of antenna pattern data. The H -plane is the plane that contains the antenna’s radiated magnetic field potential while the E -plane is the plane that contains the antenna’s radiated electric field potential. These planes are always orthogonal. These quantitative aspects generally include the 3 dB beam width (1/2 power level), directivity, side lobe level and front to back ratio. The 3 dB beam width of antenna is simply a measure of the angular width of the -3 dB points on the antenna pattern relative to the pattern maximum.

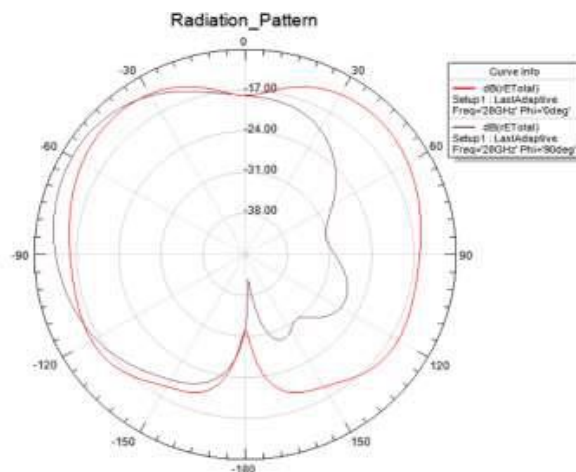


Figure 5: Radiation Pattern of the proposed Antenna

4 Conclusion

The proposed design achieves a 10 dB impedance bandwidth of 24% (3.7 – 4.5 GHz) with gain of 5.4 dB at resonant frequency of 4.1 GHz and radiation efficiency of more than 90% in the bandwidth of operation. The fundamental TE_y111 mode is retained in the proposed H-shaped DRA. The proposed Reconfigurable H-shaped DRA design is compared with the existing designs and improvement in the bandwidth from 9% to 24% is attained by modifying the geometry.

References

- [1] A. Petosa, Dielectric resonator antennas handbook. Boston, MA:Artech House, 2007.
- [2] A. Abdulmajid, Y. Khalil, and S. Khamas, "Higher-order-mode circularly polarized two-layer rectangular dielectric resonator antenna," *IEEE Antennas and Wireless Propagation Letters*, vol. 17, no. 6, pp. 1114–1117, Jun. 2018.
- [3] Y. M. Pan, K. W. Leung, and L. Guo, "Compact laterally radiating dielectric resonator antenna with small ground plane," *IEEE Transactions on Antennas and Propagation*, vol. 65, no. 8, pp. 4305–4310, Aug. 2017.
- [4] M. Abedian et al., "Compact wideband circularly polarised dielectric resonator antenna," *Electronics Letters*, vol. 53, no. 1, pp. 5–6, Jan. 2017.
- [5] S. Fakhte, H. Oraizi, and L. Matekovits, "Gain improvement of rectangular dielectric resonator antenna by engraving grooves on its side walls," *IEEE Antennas and Wireless Propagation Letters*, vol. 16, pp. 2167–2170, May 2017.
- [6] Y. Gao, Z. Feng, and L. Zhang, "Compact asymmetrical T-shaped dielectric resonator antenna for broadband applications," *IEEE Transactions on Antennas and Propagation*, vol. 60, no. 3, pp. 1611–1615, Mar. 2012.
- [7] T. A. Denidni, Qinjiang Rao, and A. R. Sebak, "Broadband L shaped dielectric resonator antenna," *IEEE Antennas and Wireless Propagation Letters*, vol. 4, pp. 453–454, Dec. 2005.
- [8] L. N. Zhang, S. S. Zhong, and X. L. Liang, "Wideband U-shaped dielectric resonator antenna fed by triangle patch," *Microwave and Optical Technology Letters*, vol. 52, issue 11, Nov. 2010.
- [9] T. A. Denidni, Z. Weng, and M. Niroo-Jazi, "Z-shaped dielectric resonator antenna for ultrawideband applications," *IEEE Transactions on Antennas and Propagation*, vol. 58, no. 12, pp. 4059–4062, Dec. 2010.
- [10] A. Petosa et al., "Design and analysis of multisegment dielectric resonator antennas," *IEEE Transactions on Antennas and Propagation*, vol. 48, no. 5, pp. 738–742, May 2000.
- [11] M. Abedian et al., "Wideband rectangular dielectric resonator antenna for low-profile applications," *IET Microwaves, Antennas & Propagation*, vol. 12, no. 1, pp. 115–119, Jan. 2018.
- [12] Jitendra Kumar, Biswajeet Mukherjee, and Navneet Gupta, "A novel tetraskelion dielectric resonator antenna for wideband applications," *Microwave and Optical Technology Letters*, pp. 2781-2786, May. 2015
- [13] Y. Wang, J. Li, L. Huang, Y. Jing, A. Georgakopoulos, and P. Demestichas, "5G mobile: spectrum broadening to higher frequency bands to support high data rates," *IEEE Vehicular Technology Magazine*, vol. 9, no. 3, pp. 39–46, 2014.
- [14] Iftikhar Ahmad, Houjun Sun, Yi Zhang, Abdul Samad "High Gain Rectangular Slot Microstrip Patch Antenna for 5G mm-Wave Wireless Communication", 2020 5th international conference on computer and communication system.
- [15] W. Roh, J.-Y. Seol, J. Park, B. Lee, J. Lee, Y. Kim, J. Cho, K. Cheun, and F. Aryanfar, "Millimeter-wave beam forming as an enabling technology for 5G cellular communications: theoretical feasibility and prototype results," *IEEE Communications Magazine*, vol. 52, no. 2, pp. 106–113, 2014.

Design of Low Power Hybrid Full Adder Using XOR/XNOR Circuit

Anandh .S¹, Punniyakodi .A², Venkatesan.V³

^{1,2}UG Student , Department of Electronics and Communication Engineering , St. Anne's College of Engineering And Technology, Panruti

³Assistant Professor, Department of Electronics and Communication Engineering, St. Anne' s College of Engineering And Technology, Panruti

Abstract

In now days, electronic devices usage was increased in our life days ,it can be designed with higher speed and more reliability. the full adder has consumes more power ,it can be rectified by design of new XOR-XNOR gates. Simulation results are performed in tanner tool. Four new XNOR, XOR gates are proposed in this paper. These new XOR/XNOR circuits are designed to have high speed and less power consumption compared to other XOR/XNOR gate circuits. This is possible due to less output capacitance. Each one of the proposed new hybrid full adder circuit has its own advantages of speed, power consumption and driving ability. From results, proposed circuits are found to be better than novel XOR/XNOR gate circuits. The novel structures of XOR - XNOR gate are 6 transistors .the design of hybrid full adders with low power, high speed and less PDP. The proposed new hybrid full adder has superior speed against other full adder circuits with less number of transistors.

Keywords: CMOS XOR-XNOR Gate, Hybrid Full Adder, Low Power, High Speed, Less Transistors.

1 Introduction

Now a days, the usage of electronic devices has been increased simultaneously. These devices require to have low power consumption and high speed. In previous work, Low power and high speed full adder using new XOR/XNOR Gates. The novel XOR - XNOR gate is composed of 6 transistors . In this circuit, Q1, Q2 are PMOS transistors and Q3, Q5 are NMOS transistors. XOR output is inverted by a static CMOS inverter that produces XNOR output. the novel hybrid full adder, consisting of 14 transistors . This full adder consists of two 2-1 MUX gates and the Novel XOR- XNOR gate. This is a full-swing XOR- XNOR gate with only six transistors and it is low- power XOR- XNOR gate. The XOR- XNOR signals are connected to the inputs of 2:1 MUX as select lines This XOR- XNOR gate is designed with an additional feedback structure. Here A, B, *Cin* are the inputs that add three input numbers and generate Sum and carry i.e. S and *Cout*. The output S is an EX- OR between the input A and the half adder SUM output B. The *Cout* will be high only if any of the 2 inputs out of 3 are high or at logic 1. Since there is a slow response problem in the Novel XOR-XNOR gate when input passes from 10 to 00, there is also a slow response problem in this proposed hybrid full adder when input passes from 100 to 000.The proposed full adder has compared to other full adders to achieved reduction in delay, low power, less PDP While designing a system, power consumption is a parameter which is to be optimized for better system performance. In many circuits, which perform arithmetic operations, full adder is a fundamental block. Many full adder circuits were designed using various logic styles, each of them has its own merits and demerits . The designs existing till now can be divided into 2 categories. They are static and dynamic styles. The advantage of static full adders is high reliability and they are simple having low power consumption .Dynamic full adders have less on chip arearequirement compared to static full adders. the power consumed by the full adder is reduced by optimum design of XOR/ XNOR gates. These can be used in a variety of multipliers, such as Vedic, Wallace, Array, etc. When more than one logic style, are used for their implementation, this is called as hybrid CMOS logic style. Examples of such design are hybrid pass logic with static CMOS (HPSC), Twelve number of transistors available in new hybrid full adder . Such designs take advantage of the features of various logic styles to enhance the efficiency of the designs using a single logic type. All hybrid designs use the best possible modules implemented using different logic types or improve the available modules in an attempt to create a low power full adder circuits. In this paper, several circuits for the XOR/ XNOR and simultaneous XOR-XNOR gates are evaluated and new circuits are offered. All the circuits have been simulated and power, delay and PDP values are calculated for the comparison. Among these, efficient XOR/ XNOR gate is further used to offer new low-power hybrid full adder. Proposed XOR/ XNOR gate is efficient in terms of high speed and less PDP. It is further used to design high speed and low PDP hybrid full adder.

2 Proposed New XOR/XNOR Circuits

Generally full adders are designed by using XNOR and XOR gates. The major power consumer in full adder is XOR or XNOR circuit. So the power consumption of the full adder can be reduced by minimizing the

power consumption of XOR or XNOR circuit. Also, XOR or XNOR gate is used in many other circuits such as parity checking circuits and comparators. High speed and low power XOR, XNOR and simultaneous XOR-XNOR circuits are proposed in this paper. Proposed XNOR, XOR circuits are shown in below. For all the input combinations these circuits give full swing output, because of using level restoring transistors. These circuits have less delay and low power consumption. Also, these circuits have good driving capability.

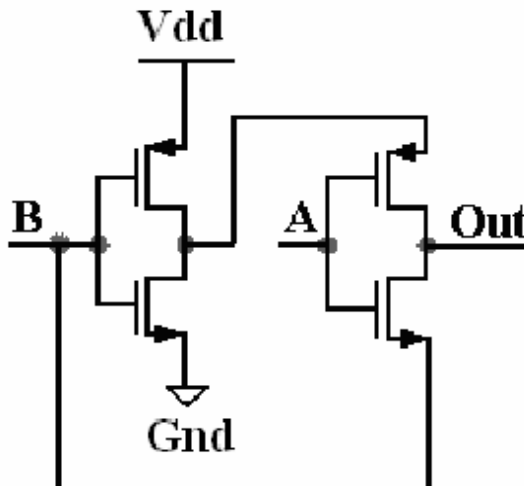


Figure 1: Proposed New XOR/XNOR Gate Circuit

The results show that the performance of this XOR- XNOR gate in terms of low power and low PDP is better than that of the compared to other XOR/XNOR gate circuits. This gate is also used for developing low power, high speed and low PDP hybrid full adder

2.1 Table I Truth Table of Proposed XOR- XNOR Gate

Table 1: Truth Table Of Proposed XOR- XNOR Gate

| A | B | Q1 | Q2 | Q3 | Q5 | XOR | XNOR |
|---|---|-----|-----|-----|--------|--------|------|
| 0 | 0 | ON | ON | OFF | OFF | Weak 0 | 1 |
| 0 | 1 | ON | ON | ON | OFF | 1 | 0 |
| 1 | 0 | OFF | OFF | OFF | High-Z | Weak 1 | 0 |
| 1 | 1 | OFF | OFF | ON | ON | 0 | 1 |

2.2 Proposed Hybrid Full Adder

Using the proposed XOR, XNOR circuits, new hybrid full adders are proposed. Fig 3 shows the proposed fulladders. These circuits use hybrid logic style. Each proposed full adder use the proposed XOR or XNOR or simultaneous XOR-XNOR circuit and 2to1 multiplexer structure Another possible hybrid full adder consists of 14 transistors and shown in Fig. 3. This HFA consists of novel XOR-XNOR gate and two 2:1 MUX gates. The new XOR- XNOR gate is made of 6 transistors. This XOR-XNOR gate decreases the voltage swing from 10 to 00, but it is a low- power XOR-XNOR gate. This voltage swing reduction also reduces the voltage swing when used in full adder from 100 to 000 inputs.

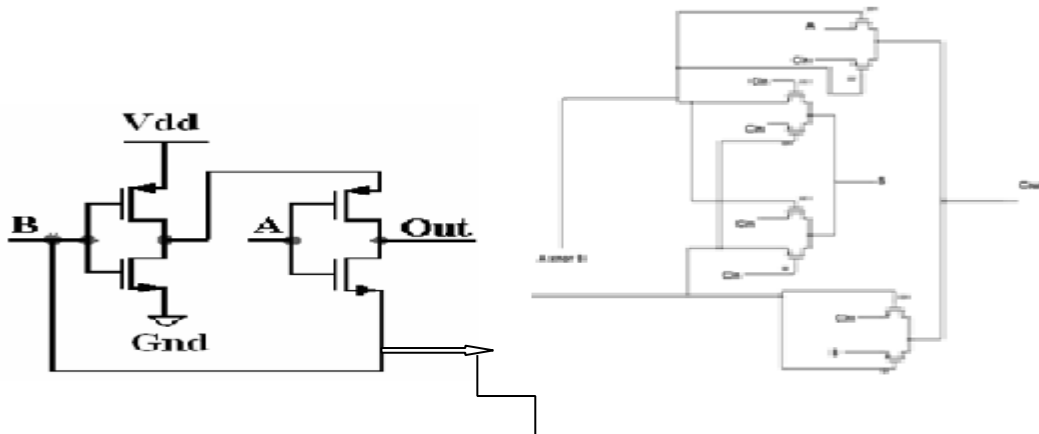


Figure 2: Proposed New Hybrid Full Adder Circuit

This is proposed hybrid full adder featuring hybrid logic designs. The inputs here are A, B, C_{in} which adds three input numbers to produce Sum and carry signals. This full adder has the advantages of low power, high speed and low PDP with less number of transistors. Therefore, XOR and XNOR node capacitance reduces and circuit delay improves. So Hybrid full adder circuit has less delay and power consumption compared to other full adders has less delay and power consumption compared to novel hybrid full adder. By using C_1 bar signal, proposed hybrid full adder has better driving capability compared to other full adder has better driving capability compared to novel hybrid full adder respectively.

3 Simulation Results

The simulation results are based on the standard CMOS technology, tanner tool with voltage power supply. The values of delay are considered at critical circuit paths. The PDP is determined by multiplying the power and the delay values at the circuit's critical paths. All simulations are done in Tanner tool. The power supply used for simulations is 1.2v. the simulation waveform of proposed XOR/XNOR gate circuits and simulation results of proposed hybrid full adders has been declared . HFA-22T has minimum delay and PDP.

3.1 Proposed New XOR/XNOR Gate Circuit Design



Figure 3: proposed new XOR/XNOR gate circuit design

3.2 Proposed XOR/XNOR Gate Output

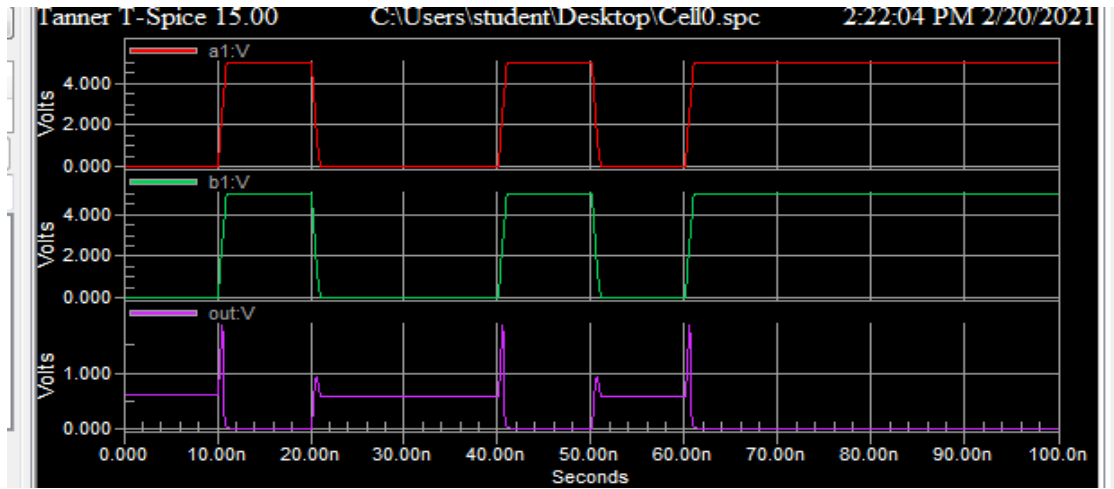


Figure 4: New XOR/XNOR Gate Output

3.3 Proposed new hybrid full adder circuit design

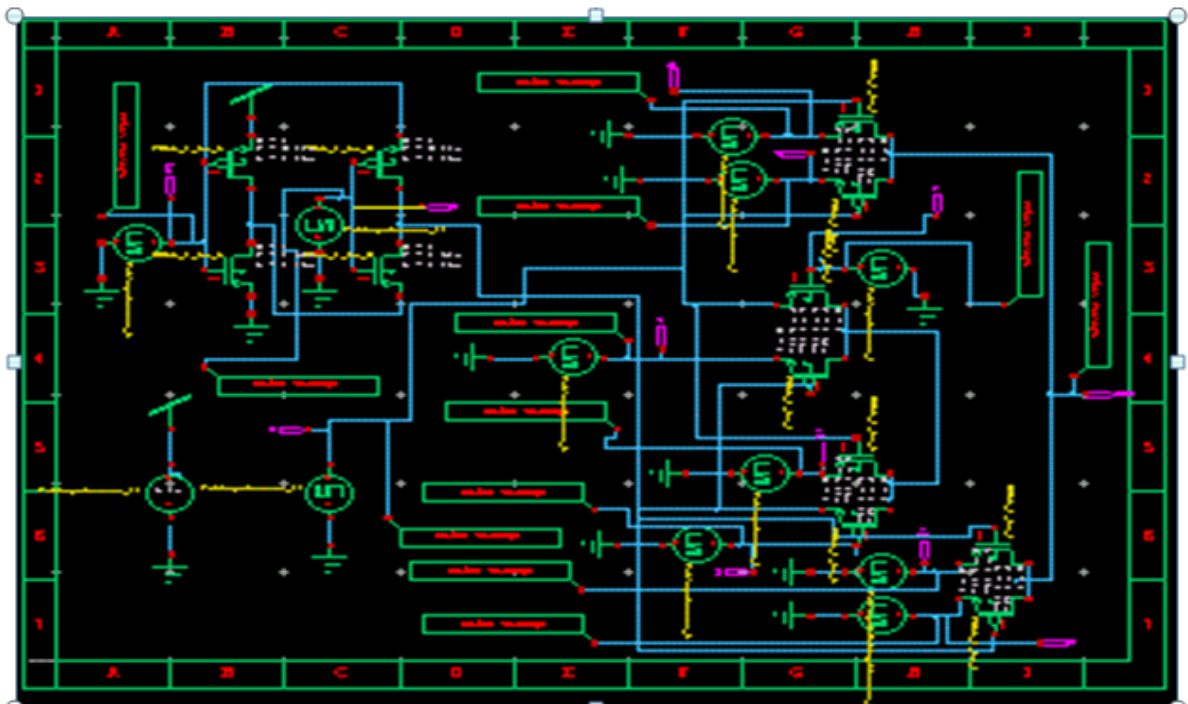


Figure 5: Proposed New XOR/XNOR Gate Circuit Output

3.4 Proposed Hybrid Full Adder Output

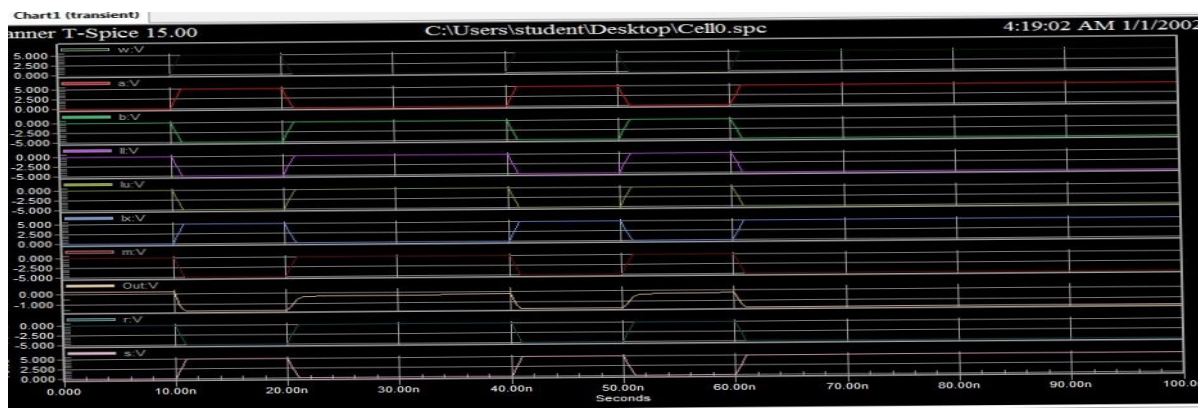


Figure 6: New Hybrid Full Adder Circuit Output

Simulation results show that, compared to its best equivalent, the proposed Hybrid full adder circuit c saves PDP up to 88.56%, respectively. This hybrid full adder also saves up to 70% delay and 50.2% power as compared to other full adders. The proposed novel hybrid full adder circuit also saves up to 58.4% power over its strongest counterpart, respectively. The proposed Hybrid full adder has superior speed compared to other full adder circuits with fewer transistor numbers. Also, as the number of transistors is reduced, the Area of the proposed hybrid full adders is also reduced.

3.5 Table II Comparison Of XOR/XNOR Gates

Table 2: Comparison Of XOR/XNOR Gates

| XOR/XNOR design | No. of transistors | Power (nW) | Delay (ns) | PDP (nJ) |
|----------------------|--------------------|------------|------------|----------|
| DPL | 12 | 0.128 | 2009 | 257.15 |
| PTL | 10 | 0.086 | 3008 | 258.6 |
| CPL | 10 | 0.108 | 3009 | 324.9 |
| Goel | 8 | 3.344 | 3145 | 10516 |
| Radhakrishnan | 6 | 0.070 | 3026 | 262.3 |
| Chang et al's | 10 | 0.088 | 3010 | 264.8 |
| M.A.valashani | 10 | 0.114 | 3010 | 343.1 |
| H. Naseri's | 12 | 0.080 | 3007 | 240.5 |
| H. Naseri's XOR-XNOR | 12 | 0.081 | 3007 | 243.5 |
| Novel XOR-XNOR | 6 | 0.062 | 3013 | 186.8 |
| New XOR/XNOR | 4 | 0.058 | 3007 | 183.2 |

Comparison of Existing XOR/ XNOR designs with novel XOR- XNOR design i.e., novel XOR- XNOR design and new XOR- XNOR design, with less transistor numbers, have less power than the other structures compared. The results indicate therefore that the efficiency of the proposed XOR- XNOR gate is better than that of the comparative structures. Those XOR- XNOR gates are also included in the proposed full adder.

3.6 Table III Comparison of Full Adder Designs

Table 3: Comparison Of Full Adder Designs

| Full adders | No. of transistors | Power (nW) | Delay (ns) | PDP (nJ) |
|-------------|--------------------|------------|------------|----------|
| HFA-20T | 20 | 0.134 | 3010 | 403.3 |
| HFA-17T | 17 | 0.129 | 1011 | 130.4 |
| HFA-B-26T | 26 | 0.283 | 3012 | 852.3 |
| HFA-NB-26T | 26 | 0.228 | 3010 | 686.2 |
| HFA-22T | 22 | 0.146 | 3000 | 438 |
| HFA-19T | 19 | 0.139 | 1010 | 140.3 |
| HFA-14T | 14 | 0.129 | 3087 | 398.2 |
| HFA-12T | 12 | 0.147 | 1011 | 148.6 |

Comparison of full adder designs with new Full adder i.e., HFA-14T and HFA-12T indicate less transistor counts than other Full adders compared. HFA-14T has less power and HFA-12T has less power, high speed and low PDP. Consequently, the results indicate that the performance of proposed Full adders is better than that of comparative structures.

4 Conclusion

In this paper, several XOR/ XNOR and XOR- XNOR circuits are evaluated. If the more of the transistor number, the more power and delay, the more of the dereliction So, XOR / XNOR gate with less transistor number ensuring less power, delay and PDP is proposed. These two hybrid full adders have fewer transistors than full adder structures compared. Consequently, the results indicate that the performance of proposed hybrid full adders is better than that of comparative structures. The proposed full adders have high speed and less power consumption because of using new proposed XNOR, XOR circuits. From simulation results, the proposed full adders have low power consumption, less delay and best power delay product compared to existing circuits.

5 References

- [1] N. E. H. Weste and D. M. Harris, CMOS VLSI Design: A Circuits and Systems Perspective, vol. 53, no. 9, 2013.
- [2] N. Zhuang and H. Wu, "A New Design of the CMOS Full Adder," IEEE J. Solid-State Circuits, vol. 27, no. 5, pp. 840–844, 1992, doi: 10.1109/4.133177.
- [3] P. Kumar and R. K. Sharma, "Low voltage high performance hybrid full adder," Eng. Sci. Technol. an Int. J., 2015, doi: 10.1016/j.jestch.2015.10.001.
- [4] H. T. Bui, Y. Wang, and Y. Jiang, "Design and analysis of low-power 10-transistor full adders using novel XOR- XNOR gates," IEEE Trans. Circuits Syst. II Analog Digit. Signal Process., vol. 49, no. 1, pp. 25–30, 2002, doi: 10.1109/82.996055.
- [5] A. Dubey, S. Akashe, and S. Dubey, "A novel high- performance CMOS 1 bit full-adder cell," 7th Int. Conf. Intell. Syst. Control. ISCO 2013, vol. 47, no. 5, pp. 312– 315, 2013, doi: 10.1109/ISCO.2013.6481169.
- [6] S. R. Chowdhury, A. Banerjee, A. Roy, and H. Saha, "A high speed 8 transistor full adder design using novel 3 transistor XOR gates," Int. J. Electron. Circuits Syst., vol. 2, no. 4, pp. 217–223, 2008.
- [7] M. Aguirre-herandez and M. Linares-aranda, "CMOS full-adders for energy efficient arithmetic applications," vol. 19, no. 4, pp. 718–721, 2011.

- [8] S. Goel, A. Kumar, and M. A. Bayoumi, "Design of robust, energy-efficient full adders for deep-submicrometer design using hybrid-CMOS logic style," *IEEE Trans. Very Large Scale Integr. Syst.*, vol. 14, no. 12, pp. 1309–1321, 2006, doi: 10.1109/TVLSI.2006.88780

Design and Analysis of RF LNA with Transistor Configurations

Priyadharshini.K¹, Nandhini.K², Maryamalajenni.B³.

^{1 2}UG students St. Anne's College of Engineering and Technology.

³ Assistant Professor, St. Anne's College of Engineering and Technology.

Abstract

In radio frequency (RF) the major role is played by low noise amplifiers (LNA). This paper elucidates the design of an LNA with optimizing its stability factor, gain and with different configurations of transistors in the frequency range of 5-6 GHz. Design-optimization of low noise amplifier has been performed with standard transistor (BJT and MOSFET) in circuit simulation software. For comparison we considered the following configurations of LNA: (i) a single stage BJT LNA, (ii) BJT and NMOS cascade LNA, and (iii) BJT and CMOS cascade LNA. Simulation results are compared to other configurations BJT-NMOS cascade LNA depicts the highest gain of 20.42 dB and the lowest noise figure of 0.25. On the other hand, BJT-CMOS cascade LNA demonstrates the highest stability factor of 1.07 followed by BJT LNA and BJT-NMOS cascade LNA configurations respectively. Further improvement in the LNA performance metrics is feasible by parametric optimization of transistor parameters and passive elements in the matching network.

Keywords: *Radio frequency (RF), Low Noise Amplifier (LNA), Noise Figure, Gain, Stability Factor*

1 Introduction

In recent years the advent of new wireless technologies much focus has been on the design of radiofrequency(RF) low noise amplifier(LNA) for various applications. In a transceiver module an LNA forms an important constituent of the front end of any receiver module. The LNA amplifies the signal without degrading the signal to noise ratio (SNR). The design of a LNA is a multi-variant problem with parameters to optimize that include gain, noise figure, stability factor, non-linearity to cite a few. A basic LNA constitutes the following three stages: (i) input impedance matching circuit, (ii) amplifier stage, (iii) output impedance matching circuit. As shown in Fig. 1. Literature encompasses various example so integrated circuit(IC)LNA designs with various device configurations. A novel LNA design with the combination of BJT-MOSFET along with BJT impedance matching has been reported. The design proposed in the reference results in a gain and noise figure of 16 dB and 1.6 dB respectively. Similarly, CMOS combination based LNA design has been implemented in references. On the other hand, variations of impedance matching circuits and MOSFET based LNA has been reported in references respectively.

2 Simulation Environment

In this present work, we compare the performance metrics of LNA implemented with different device configurations here for comparison. we have considered a single stage NPN-BJT LNA and cascade configurations of NPN BJT-NMOS LNA and NPN BJT-CMOS LNA. In this paper, we have considered same impedance matching circuit for investigating the performance of the three LNA configurations. Simulation is performed in a circuit simulation software. In this work, the three different LNA configurations have been investigated using a circuit simulation software. For comparison, the following performance metrics are compared: (i) gain, (ii) noise figure and (iii) stability factor. Further we have considered the same topology of input and output impedance matching networks. Parametric analysis of the afore mentioned metrics has been performed over the frequency spectrum. Gain function is dependent on the S parameter value is calculated by the simulation controller. Similarly, stability factor and noise figure of various LNA configurations is computed by simulation software.

3 Result And Discussion

This section details the variation in the performance metrics of the three configurations of LNA

In NPN BJT based LNA, the NPN BJT implemented in common emitter (CE) configuration as shown in Fig 2. In this design the transistor is used in CE configuration since the power amplification factor for CE amplifier is higher than common base (CB) and common collector amplifier configurations.

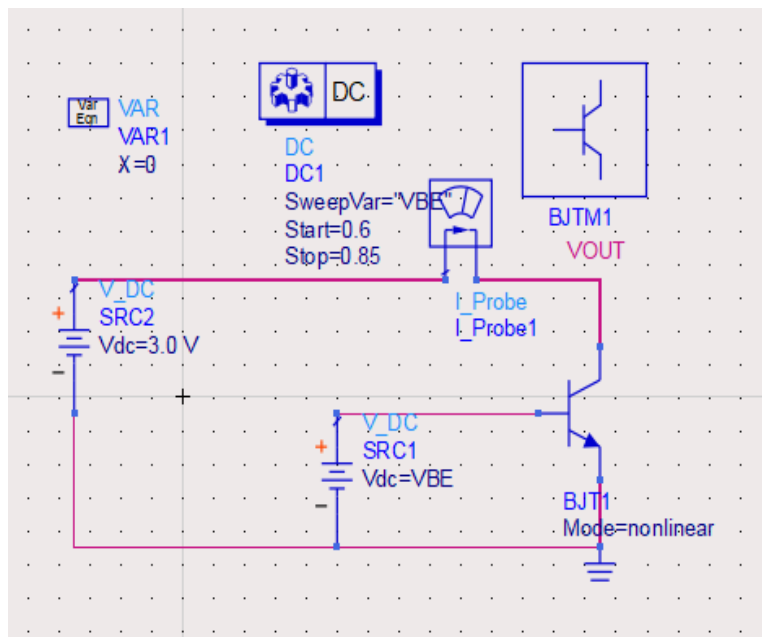
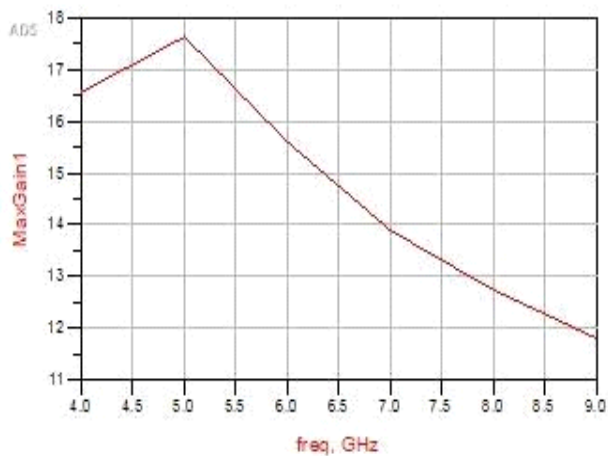
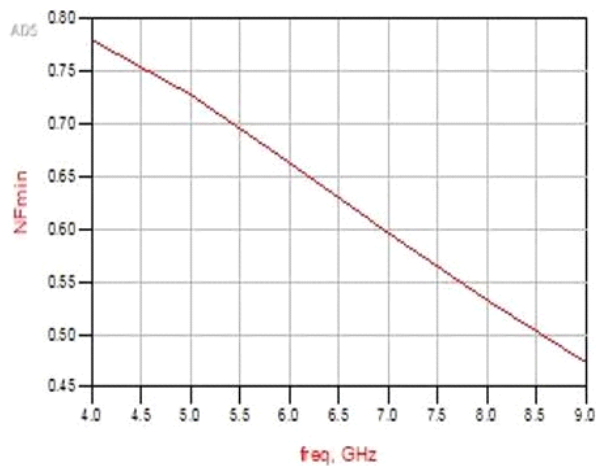


Figure.1:SchematicofBJTbased LNAconfiguration

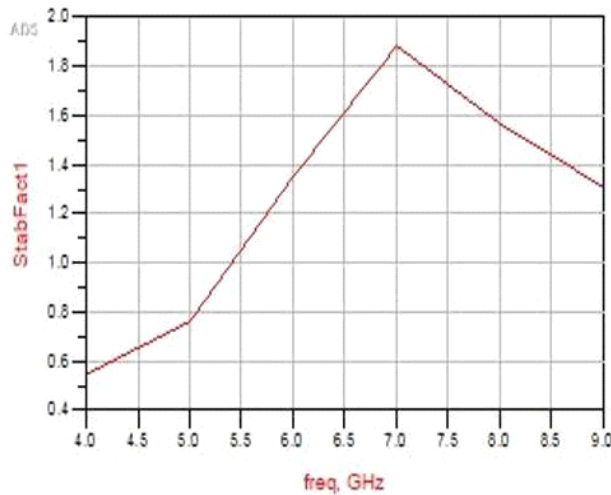
The simulation results of performance metrics of a single stage BJT LNA is shown in Fig 3.



(a)



(b)



(c)

Figure 2: (a)Frequency response,(b)noise figure as a function of frequency, (c)stability factor of a NPN BJT based LNA

The frequency response plot depicting the LNA gain at the desired frequency is plotted in Fig 3 (a). It is observed that at 5 GHz frequency the LNA has a gain of 17.64 dB. The higher and lower cut-off frequency is due to the device and external capacitances in the circuit respectively. Reduction in the gain in this type of LNA is due to the device junction capacitances (C_{BE} & C_{BC}) of BJT.

The variation in noise figure of the LNA as a function of frequency is depicted in Fig. 3 (b). A low value of noise figure is desirable to achieve high SNR. The noise figure of LNA is found to be 0.72 dB for the desired frequency. The stability factor of LNA for a range of frequency is depicted in Fig. 3(c). It is observed that at 5 GHz, the stability factor of the LNA is 0.763.

2. Analysis of a BJT and NMOS cascade based LNA

The schematic of a BJT and NMOS cascade LNA is shown in Fig.4. In the cascade circuit, BJT and NMOS are connected in common emitter (CE) and common gate(CG) configurations respectively.

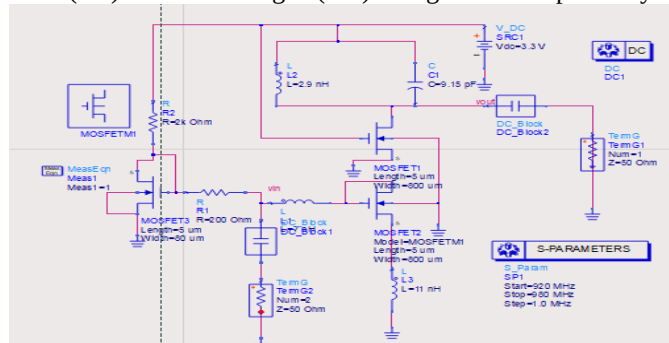
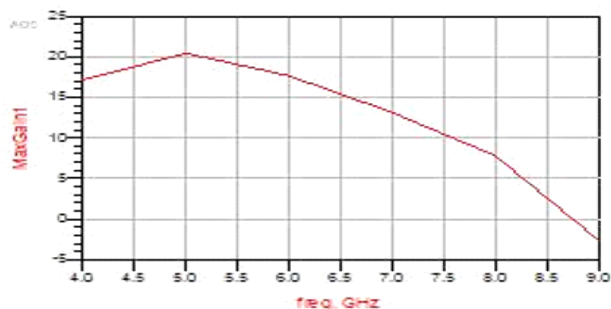


Figure 4.Schematic of a BJT and NMOS cascade LNA

Variation in the performance metric of the LNA is depicted in Fig5.



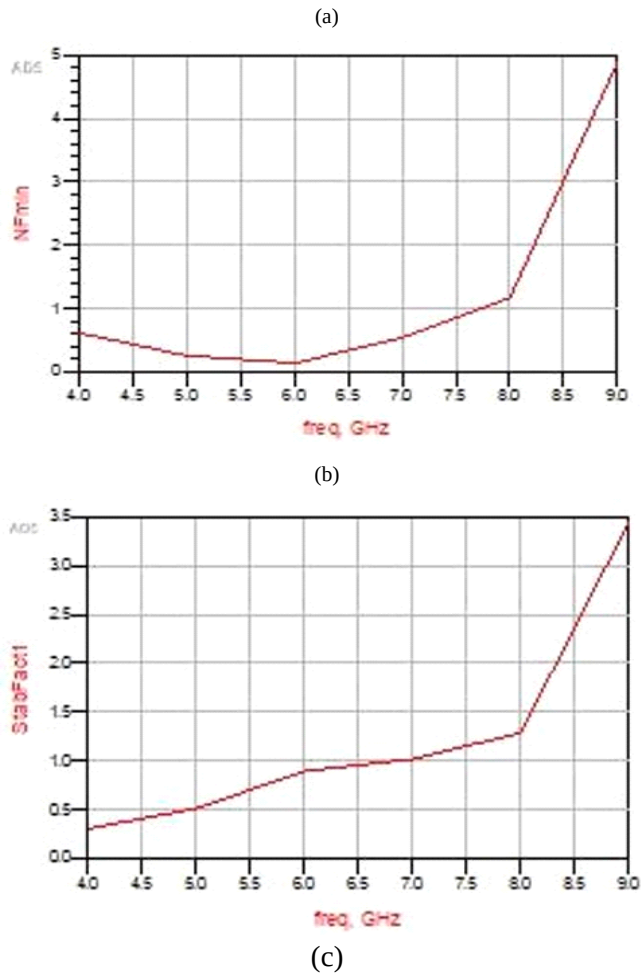


Figure5(a)Frequency response,(b)noise figure as a function of frequency, (c)stability factor of NPN BJT and NMOS cascade LNA

Gain of the NPN BJT and NMOS cascade LNA as a function of frequency is shown in Fig. 5(a). The plot depicts a similar trend of NPN BJT LNA shown in Fig. 3(a). It is observed that at 5 GHz, the gain of the amplifier is 20.424 dB. The gain obtained in this configuration is found to be higher than the previous configuration in Fig.3(a). It may be noted that the chosen configuration results in higher gain as compared to NPN BJT and PMOS cascade LNA due to the higher transconductance of NMOS. The variation in noise figure is depicted in Fig.5(b). It is found that at the desired frequency the noise figure is 0.25 dB which is relatively lower than the LNA with NPN BJT in CE configuration. The stability factor of LNA at the desired frequency is found to be around 0.51, which is lower than the value obtained in the previous amplifier configuration. A sudden increase in stability factor may be due to the leakage and input current in the NPN transistor.

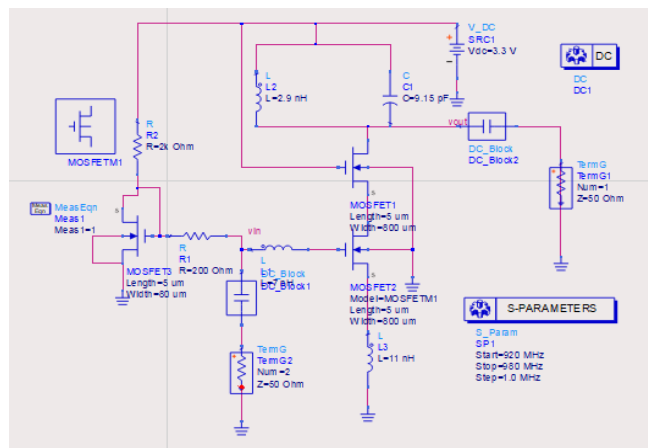
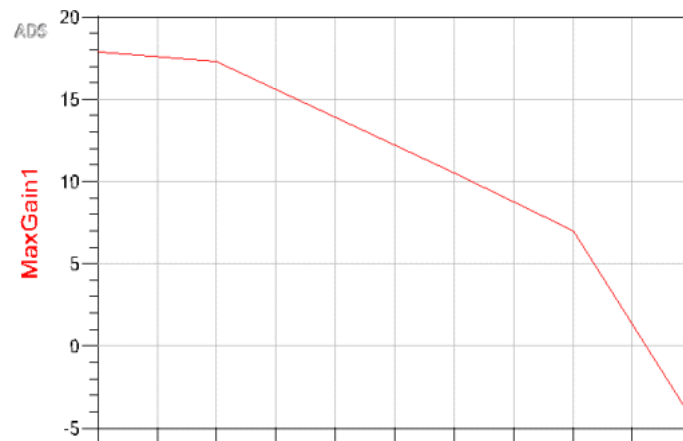
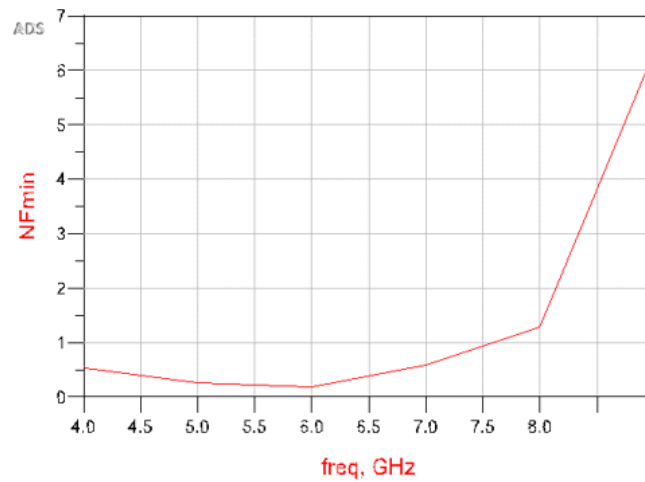


Figure6 Schematic of BJT-CMOS LNA configuration

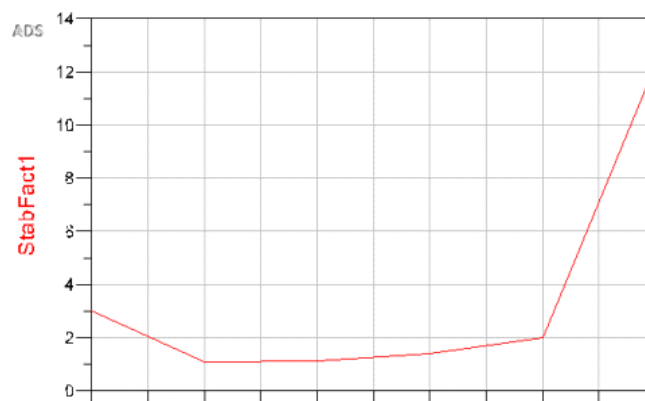
The variation in gain, noise figure and stability factor is shown in Fig.7.



(a)



(b)



(c)

Figure7(a)Frequency response,(b)noise figure as a function of frequency, (c) stability factor of a NPN BJT and CMOS cascade LNA configuration

The gain plot(Fig.7(a))depicts a typical frequency response of a LNA. It is found that at 5 GHz, the LNA demonstrates a gain of 17.31 dB. The gain is found to be the lowest among the three configurations. The noise figure as a function of frequency is shown in Fig. 7 (b). At the desired frequency, the noise figure for the particular circuit is found to be 0.25 dB which is comparable to the configuration of NPN BJT and NMOS LNA.

Stability Factor Of The LNA Is Plotted In Fig.7 (C). It Is Observed That At The Stability Factor Is 1.07 which Is The highest among the three configurations.

The comparison of the performance metrics of the three configurations of LNA is summarized in Table 1.

Table 1: Comparison of the three LNA configurations

| Sl.NO | CONFIGURATION | GAIN | NOISE | STABILITY FACTOR |
|-------|------------------|--------|-------|------------------|
| 1. | BJT CMOS LNA | 17.642 | 0.728 | 0.763 |
| 2. | BJT AND NMOS LNA | 20.424 | 0.258 | 0.516 |
| 3. | BJT AND CMOS LNA | 17.314 | 0.259 | 1.078 |

From Table 1, it is observed that among the three configurations, NPN BJT-NMOS LNA depicts the highest gain of 20.42 dB. In addition, it depicts a noise figure of 0.25 which is the lowest among the three configurations. Further, it is seen that compared to other configurations, NPN BJT-CMOS LNA depicts the highest stability factor of 1.07 followed by NPN BJT LNA (0.78) and NPN BJT-NMOS LNA (0.51) respectively.

It may be noted that further improvement in performance metrics can be obtained by parametric optimization of transistor parameters and passive components of the matching circuits. In addition, the stability of NPN BJT-NMOS LNA can be improved by using compensation techniques.

4 Conclusion

This paper elucidates the performance analysis of three configurations of LNA mainly (i) NPN BJT LNA (single stage), (ii) BJT and NMOS cascade LNA, and (iii) BJT and CMOS cascade LNA. Simulation results show that among the single stage and cascade LNA configurations, BJT-NMOS LNA has the highest gain and the lowest noise figure of 0.25. However, low stability factor of 0.51. In terms of stability, BJT-CMOS LNA depicts the highest stability factor of 1.07 followed by BJT LNA with 0.78 and BJT-NMOS LNA of 0.51 respectively. Future work includes, improving the stability of BJT-NMOS LNA.

References

- [1] I. Stefigraf, and S. Rajaram, "Design and analysis of low noise amplifier for satellite transponder", IEEE International Conference on Circuits and Systems (ICCS), December 2017
- [2] M. Challal, A. Azrar, H. Bentarzi, A. Recioui, M. Dehmas, and D. Vanhoenacker Janvier, "On Low Noise Amplifier Design for Wireless Communication Systems", Proceedings of International Conference on Information and Communication Technologies: From Theory to Applications, April 2008.
- [3] J.K. Basil, K.V. Sandeep, K. Shambavi, Z.C. Alex, "Design of a high gain low noise amplifier for wireless applications", IEEE Conference on Information & Communication Technologies, April 2013.
- [4] A. Zaid, J. Moheidat, Y. Hamada, "Design of high gain 2.4 GHz CMOS LNA amplifier for wireless sensor network applications", IEEE Jordanian International Electrical and Electronics Engineering Conference (JIEEE), May 2017.
- [5] P. Ma, M. Racanelli, J. Zheng, M. Knight, "A Novel Bipolar-MOSFET Low-Noise Amplifier (BiFET LNA), Circuit Configuration, Design Methodology & Chip Implementation", IEEE Transactions on Microwave Theory and Techniques, vol. 51, no. 11, November 2003.
- [6] Y. Liu and J.S. Yuan, "CMOS RF Low-Noise Amplifier Design for Variability and Reliability" in IEEE Transactions on Device and Materials Reliability, vol. 11, no. 3, September 2011.
- [7] H. Sahoolizadeh, A.K. Kordalivand, Z. Heidari, "Design and Simulation of LNA circuit for 5 GHz to 6 GHz", International Journal of Electronics and Communication Engineering, vol. 3, no. 3, 2009.
- [8] Priyansha, K.R. Samartha, S. Sivasundarapandian, "A Novel Input Output Impedance Matching Network for LNA", International Conference on Communication and Signal Processing, April 6-8, 2016, India.

Deep CNN Based Automated Diabetic Retinopathy Disease Identification System

M.Stephygrafi¹, R.Shalini², D.Umamaheswari³

^{1,2} IV Year, Department of ECE, St. Anne's College of Engineering and Technology, Panruti

³Assistant Professor, Department of ECE, St. Anne's College of Engineering and Technology, Panruti

Abstract

Diabetes is the most widely found chronic disease present in people of various age groups having insufficient insulin production, which produces high blood sugar. Diabetic Retinopathy (DR) is an eye disease caused by diabetes, which results in damaged retinal blood vessels and may lead to vision loss. Many computer-aided diagnostics systems have been developed in the past, which used traditional techniques where handcrafted features are used. With the advent of Deep Learning, especially in medical image analysis, more accurate and robust results are produced, as it performs feature extraction task automatically. Convolutional Neural Networks (CNNs) are the most commonly used deep learning method in medical image classification.

Keywords: *Diabetic Retinopathy, Deep Learning, convolutional Neural Network*

1 Introduction

Diabetic Retinopathy (DR) is a complication of diabetes that causes the blood vessels of the retina to swell and to leak fluids and blood. DR can lead to a loss of vision if it is in an advanced stage. Worldwide, DR causes 2.6% of blindness. The possibility of DR presence increases for diabetes patients who suffer from the disease for a long period. Retina regular screening is essential for diabetes patients to diagnose and to treat DR at an early stage to avoid the risk of blindness.

1.1 DR Classification

Based on the morphological changes in the fundus images, Diabetic Retinopathy has been classified into two types, Non-proliferative Diabetic Retinopathy (NPDR) and Proliferative Diabetic Retinopathy (PDR)

Non-proliferative Diabetic Retinopathy (NPDR)

Non-proliferative Diabetic Retinopathy (NPDR) occurs as an early-stage DR retinal disease which shows the following symptoms

Microaneurysms (MA) is the earliest sign of DR that appears as small red round dots on the retina due to the weakness of the vessel's walls. The size is less than 125 μm and there are sharp margins.

Haemorrhages (HM) appear as larger spots on the retina, where it size is greater than 125 μm with an irregular margin.

Hard exudates appear as bright-yellow spots on the retina caused by leakage of plasma. They have sharp margins and can be found in the retina's outer layers. Soft exudates (also called cotton wool) appear as white spots on the retina caused by the swelling of the nerve fiber. The shape is oval or round.

Cotton wool spots, also called Soft exudates, appear to have white spots on the retinal area due to the swollen nerve fibre.

MA and HM are the red lesions, whereas hard exudates and Soft exudates are the bright lesions found in the retinal area.

Proliferative Diabetic Retinopathy (PDR) occurs as an advanced stage DR retinal disease which shows the following symptoms,

Neovascularization mainly occurs in the PDR stage, where new abnormal blood vessels are formed at the optic disc or elsewhere in the retinal region.

Vitreous hemorrhage - The abnormal retinal blood vessels may proliferate or spread within or around the vitreous body

1.2 DR Risk levels

According to the Early Treatment Diabetic Retinopathy Study (ETDRS), the Diabetic Retinopathy (DR) risk levels are listed in Table

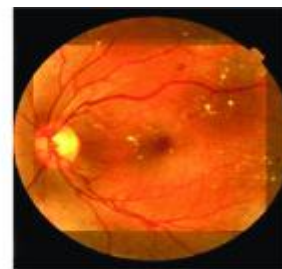
| DR Risk level | Lesions |
|---------------|--|
| No DR | No Lesions |
| Mild NPDR | Presence of MA |
| Moderate NPDR | Presence of MA and HM Presence of cotton wool spots and Exudates |
| Severe NPDR | Venous beading in 2 quadrants Presence of MA and extensive HM in 4 quadrants o Intra retinal micro vascular abnormalities in 1 quadrant |
| PDR | Neovascularization Presence of pre retinal & vitreous HM |



Without DR



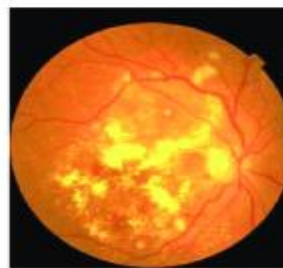
Early diabetic retinopathy



Mild NPDR



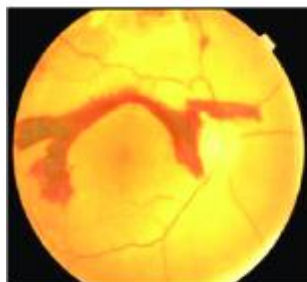
Moderate NPDR



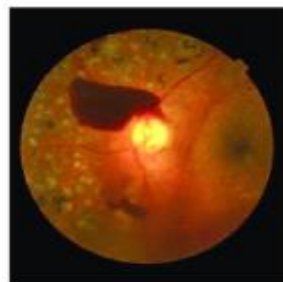
Severe NPDR



PDR and neovascularization



PDR with vitreous hemorrhage



PDR with vitreous hemorrhage and PLM



Vitreoretinal traction bands

1.3 Deep Learning

Deep learning (DL) is a branch of machine learning techniques that involves hierarchical layers of non-linear processing stages for unsupervised features learning as well as for classifying patterns. DL is one computer-aided medical diagnosis method. DL applications to medical image analysis include the classification, segmentation, detection, retrieval, and registration of the images.

Recently, DL has been widely used in DR detection and classification. It can successfully learn the features of input data even when many heterogeneous sources integrated. There are many DL-based methods such as restricted Boltzmann Machines, convolutional neural networks (CNNs), auto encoder, and sparse coding. The performance of these methods increases when the number of training data increases due to the increase in the learned features unlike machine learning methods. Also, DL methods did not require hand-crafted feature extraction.

CNNs are more widely used more than the other methods in medical image analysis and it is highly effective. There are three main layers in the CNN architecture, which are convolution layers (CONV), pooling layers, and fully connected layers (FC). The number of layers, size, and the number of filters of the CNN vary according to the author's vision. Each layer in CNN architecture plays a specific role. In the CONV layers, different filters convolve an image to extract the features. Typically, pooling layer follows the CONV layer to reduce the dimensions of feature maps. There are many strategies for pooling but average pooling and max pooling are adopted most. A FC layers are a compact feature to describe the whole input image. SoftMax activation function is the most used classification function. There are different available Pretrained CNN architectures on ImageNet dataset such as AlexNet, Inception-v3 and ResNet. Some studies like transfer learning these pretrained architectures to speed up training while other studies build their own CNN from scratch for classification. The transfer learning strategies of pretrained models include finetuning last FC layer or finetuning multiple layers or training all layers of pretrained model.

Generally, the process used to detect and to classify DR images using DL begins by collecting the dataset and by applying the needed preprocess to improve and enhance the images. Then, this is fed to the DL method to extract the features and to classify the images.

2 Literature Review

Diabetic retinopathy is one of the most prominent ailments among the diabetic patients and patients can be prevented from vision loss if the disease is diagnosed at an earlier stage. Once the disease is diagnosed the patient has to be evaluated for every six months to know the progress of the disease. An efficient algorithm to detect and classify the fundus images will be helpful for the ophthalmologist to a greater extent in eradicating the vision loss due to DR. Researchers have developed a number of algorithms for application in the study of images to facilitate precise diagnosis of diabetic retinopathy. The configuration of human eye includes optic disc and optic nerves. Detection and classification of DR can be carried out by segmenting the images of the portions of the parts from the fundus image or by examining the fundus image for the occurrence of hemorrhages, lesions, micro aneurysms, exudates, etc

Among various CNN architectures, AlexNet is one of the most efficient architectures that are widely employed to address problems in image classification and it has eight layers. In which the first five layers are convolutional and maximum pooling layers, followed by three layers fully connected to the neural network. In which the first five layers are convolutional and maximum pooling layers, followed by three layers fully connected to the neural network.

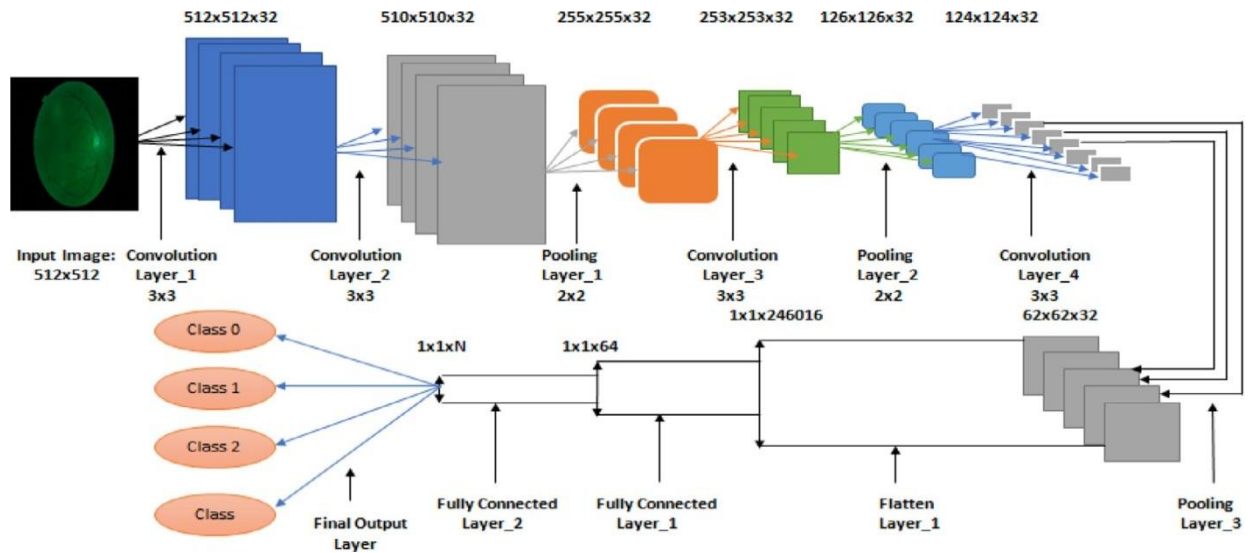
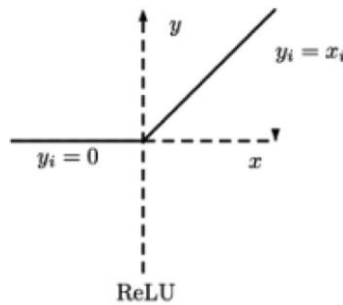


Fig 1: AlexNet architecture to detect diabetic retinopathy

The operations involved in the implementation of the proposed AlexNet architecture are described below:

- The first step is to resize the input fundus image to the size of 259×259 pixels corresponding to the breadth and height and the three color channels representing the depth of the input fundus image.
- The output of neurons is computed as a scalar product of a small portion of the image with their corresponding weights. This process is repeated along the length and breadth. This operation is performed in convolutional layer.
- In Rectifier Linear Unit (ReLU) layer, an element-wise activation function is employed. This layer replaces all the negative activations with 0 by introducing nonlinearity to the system and by applying the function $f(k) = \max(0, k)$.



Activation function

- In pooling layer, the samples are reduced along the spatial coordinates. This process is known as decimation.
- Fully Connected (FC) layer computes the Class scores for each image and gives the prediction.

3 Proposed System

Our network is a modified version of AlexNet. AlexNet is one of the first deep neural networks that has been utilized for image classification tasks. The network consists of five convolutional layers and three dense layers

with different kernel sizes. The first layer has a kernel size of 11×11 . The second layer has a kernel size of 5×5 and layers three to five each has a kernel size of 3×3 . However, one of the disadvantages of this approach is the duplication of data. This occurs because of the overlapping blocks of pixels, which leads to an increase of memory consumption for processing the image. In contrast, our network has only three convolutional layers and two dense layers, each with a kernel size of 3×3 . This is because smaller-sized kernels of fewer layers lead to lower costs than larger-sized kernel with more layers. More layers and multiple larger-sized kernels lead to more in-depth network architecture which is time-consuming and not feasible for medical applications. Therefore, by reducing the kernel size, our network gains the advantage of learning the features from the image faster. Furthermore, our network is more robust and performs better than Alex Net with excellent scores in accuracy, sensitivity, and specificity

In AlexNet, Local Response Normalization (LRN) is added to the first two convolutional layers and then the activation layer, Rectified Linear Unit (ReLU), is added to the next three layers. The ReLU function enables faster training of CNN, since the calculation of its derivative has a lower computational cost, without losing any of its generalization ability. The function itself is a non-saturating activation function and is defined by

$$f(x) = x^+ = \max(0, x) \quad (1)$$

Where x is the input to a neuron.

In AlexNet, such processes are used to amplify the features in the image, such as enhancing the brightness of the image, for better classification of the image. However, in our network, overall image normalization is used because LRN leads to increased memory consumption and computation time. The normalization process is carried out during the pre-processing stage, and the network is trained on the image that is generated. This process allows more distinguishable features to be visible during training. Our image normalization process is described below network

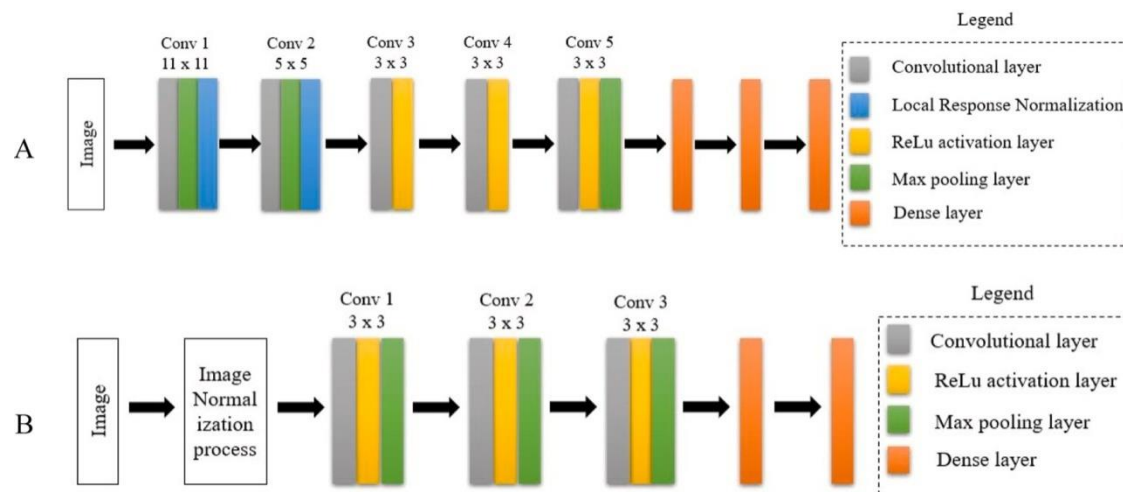


Fig 2: proposed method architecture

Our network model is optimized using the Adam optimizer with the default learning rate of 10^{-3} . The learning rate is decayed exponentially with a decay of 10^{-8} . These standard parameters of Adam have been proven for neural networks to be computationally efficient, of little memory usage and well suited for problems with big data. Hence these parameters are utilized in our network. The input images utilized to train our network are resized from the original size of 512×512 to 96×96 .

Finally, our Layer structure also differs considerably from AlexNet. In AlexNet, there is different number of nodes in different layers.

Discussion section

. All of the studies mentioned in the current work manipulated the diabetic retinopathy screening system using deep learning techniques. The need for reliable diabetic retinopathy screening systems became a critical issue

recently due to the increase in the number of diabetic patients. Using DL in DR detection and classification overcomes the problem of selecting reliable features for ML; on the other hand, it needs a huge data size for training. Most studies used data augmentation to increase the number of images and overcome overfitting on training stage.

4 Conclusion

Automated screening systems significantly reduce the time required to determine diagnoses, saving effort and costs for ophthalmologists and result in the timely treatment of patients. Automated systems for DR detection play an important role in detecting DR at an early stage. The DR stages are based on the type of lesions that appear on the retina. Most researchers have used the CNN for the classification and the detection of the DR images due to its efficiency.

References

- [1] T. Shanthi, R.S. Sabeenian Modified “AlexNet architecture for classification of diabetic retinopathy images” journal homepage: www.elsevier.com/locate/compeleceng
- [2] Valarmathi S, Dr. R. Vijayabhanu, “A Review on Diabetic Retinopathy Disease Detection and Classification Using image processing”, international research Journal of Engineering and Technology.
- [3] Muhammad Mateen, Junhao Wen, Song sun, Shaikat Hayat, “Exudate Detection for Diabetic Retinopathy Using Pretrained Convolutional Neural Network”, <https://doi.org/10.1155/2020/5801870>
- [4] Dutta, S., Manideep, B., Basha, S., Caytiles, R. and Iyengar, NCSN, “Classification of Diabetic retinopathy Image by Using Deep Learning models”, *Int J Grid Distr Comput*, 2018, 11(1):99-106
- [5] Dr. Chandrasekhar M, “An Approach for the Detection of Vascular Abnormalities in Diabetic Retinopathy”, *International Journal of Data mining Techniques and Application*, 2013, Vol. 02, pp. 246-250
- [6] Jaspreet Kaur and Dr. Sinha, H. P, “Automated localization of optic disc and macula from fundus images”, *International Journal of Advanced Research in Computer Science and Software Engineering*, 2012, vol. 2, Issue 4, pp. 242-249
- [7] Hussain F. Jaafar, Asoke K. Nandi and Waleed Al-Nuaimy, “Detection of Exudates from digital fundus images using a Region based segmentation Technique” in 19th European signal processing Conference, Barcelona, Spain, 2011
- [8] Jiang, X. and Mojon D, “Adaptive local thresholding by verification based multi-threshold probing with application to vessel detection in retinal images” in *IEEE Transactions on Pattern Analysis and Machine Intelligence*, 2003, Vol. 25 No. 1, pp. 131-137
- [9] Sanchez, C.I., Garcia, M., Mayo, A., Lopez, M. and Hornero R, “Retinal image analysis based on mixture models to detect hard exudates”, *Medical Image Analysis*, 2009, Vol. 13, pp. 650-658
- [10] Jonathan Goh, Lilian Tang, George Saleh, Lutfiah Al turk, Yu Fu and Antony Browne, “Filtering Normal Retinal Images for Diabetic Retinopathy Screening Using Multiple Classifiers” in *International Conference on Information Technology and Applications in Biomedicine*, 2009, pp. 1-4.
- [11] Gerald Liew, Tien y. Wong, Paul Mitchell and Jie Jin Wang, “Retinal vascular imaging –A New Tool in Micro vascular disease Research”, *Circulation: Cardiovascular Imaging*, 2008, pp. 156-161
- [12] Reza, A.W., Eswaran, C and Dimiyati K, “Diagnosis of Diabetic Retinopathy: Automatic Extraction of Optic Disc and Exudates from Retinal Images Using Marker-controlled Watershed Transformation”, *J Med Systems* 35,

2011, pp. 1491–1501

[13] Hoover, A and Goldbaum M, “Locating the optic nerve in a retinal image using the fuzzy convergence of the blood vessels” in IEEE Transactions on Medical Imaging, 2003, Vol. 22 No. 8, pp. 951–958

Design of 4:1 Multiplexer Based Adder Using Various Logic Techniques

P.Yuvarani¹, K.Raja²,M.Sahinipiriya³

^{1,2}IV year, Department of ECE, St.Anne's College Of Engineering And Technology, Panruti

³Assistant Professor, Department of ECE, St.Anne's College Of Engineering And Technology, Panruti

Abstract

In recent trends, low power consumption and high speed has become an important consideration while designing any computational devices. Thus designing a circuit with high speed and with less number of transistors are the real challenges in VLSI. This paper introduces varying techniques for designing high speed 4:1 Multiplexer (MUX) based adder. The multiplexer is designed with different logic styles such as Pass Transistor Logic, Transmission Gate Logic and GDI technique and finally, using the design 1 bit full adder is designed and the results are being compared with the existing technologies. This paper thus presents, speedy and efficient multiplexer for low power applications like telecommunication system, computer memory etc. Simulations were performed using Tanner Tool (S-edit, Tspice, and W-edit) 250nm technology.

Keywords: Pass transistor logic, Transmission gate logic, GDI technique, 4:1 Multiplexer, Tanner EDA.

1 Introduction

With the evolution of communication systems and the evolvement of shrinking technology, there search endeavour in low-power circuitry has been strengthened and low-power Very Large Scale Integration (VLSI) systems have appeared to be high in demand. Addition is one of the foundational arithmetic operations and is practice mostly in several VLSI systems. The main purpose of addition is adding two binary numbers ;It is the root of many other functional operations such as subtraction, multiplication, division, and ALU circuits. Binary Addition can be accomplished utilizing Adders in Logic Circuits. Two types of Adders can be used to conduct the addition namely, Half Adder (HA) and Full Adder (FA). Half Adder can take in two inputs (digits) out of the two Binary numbers under consideration, and generate a Sum and a Carry Out (Cout) .But if there is any initial Carry (Cin) from any previous step or previous addition, we need a Full Adder (FA) as it can take 3 inputs and produce the same outputs as the Half Adder (HA). In this project, a 4:1 Multiplexer is being designed with various technologies. A 4:1 Multiplexers takes two controlled inputs, which are in turn controlled by one selected input. It gives away one output just like every other type of MUX(s).

2 Literature Survey

In previous work, a 2:1 Multiplexer was used using various logic styles. 2:1 Multiplexers takes two controlled inputs, which are in turn controlled by one selected input. It gives away one output just like every other type of MUX(s).

2.1 2:1 Multiplexer

Mux is a data chooser that picks one of the analog or digital input data and redirects the picked data within a single output line. A multiplexer with two data inputs and one control line is referred as 2:1 multiplexer. A multiplexer having 2^n inputs has n selected lines and only 1 output.[1]

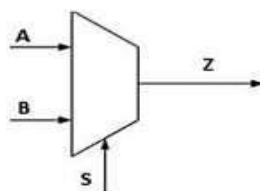


Fig 2.1 A 2:1 Multiplexer

The work on this project was initiated by pre-planning, initial drafting and designing the whole circuit before jumping into the implementation and simulation part. It not only made the job simpler, but also paced up the work as we moved through the steps following a pre-set goal.

2.2 1 Bit Full Adder

The work on this project was initiated by pre-planning, initial drafting and designing the whole circuit before jumping into the implementation and simulation part. It not only made the job simpler, but also paced up the work as we moved through the steps following a pre-set goal. The very first step of the project was to construct a Truth Table consisting of Two Variable inputs, Carry in (C_{in}), Sum, and finally a Carry out (C_{out}). The outputs for the Sum and C_{out} were derived out from the following Boolean Expressions for the Sum and C_{out} for an FA as provided by the instructor.[1]

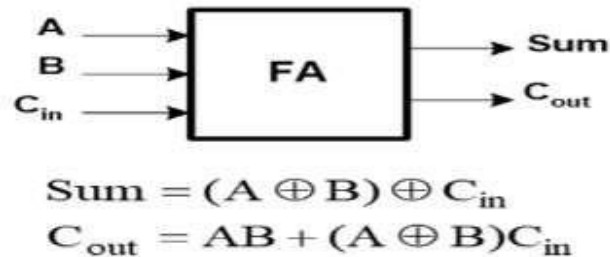


Fig 2.2 1 bit Full Adder

2.3 2:1 Mux using Complementary CMOS Logic style

Any task in complementary CMOS is obtained by NMOS pull-down and PMOS pull-up networks bridged between gate, output and power cables. Multiplexing, on the other hand, is more like switching functionality that we might implement using logic gates because they're readily available and they get the job done. They do indeed get the job done, but not very efficiently—the gate configuration shown below seems rather awkward for a task as simple as selecting between one of two input signals, especially when you consider that each inverter-based AND gate and OR gate requires six transistors.

2.4 2:1 Mux using Pass Transistor Logic

Pass-transistor multiplexers can be built using transmission gates or the “lone NMOS” type of switch. In terms of pure logic functionality, these are interchangeable—they both pass or block an input signal based on the state of a control signal. The pass-transistor logic minimizes the number of transistors needed, by granting the primary inputs to steer gate terminals in conjunction with source-drain terminals. The superiority is that one pass-transistor network (either NMOS or PMOS) is sufficient to perform the logic operation. Mostly we are selecting NMOS transistor for establishment.

2.5 2:1 Mux using Transmission Gate Logic

When the control signal C is high i.e. at “logic 1” then the uppermost transmission gate operates and it sweeps A over it so that output is A . When the control signal C is low i.e. at “logic 0” then the uppermost transmission gate shuts OFF and it will not let A to sweep over it, simultaneously the lower transmission gate operates and it allows B to sweep over it so the output is B . In stark contrast to the inverter-based CMOS implementation, a PTL 2-to-1 multiplexer requires only six transistors: two each for two transmission gates, and two for the inverter that provides the complement of the S (select) signal.

3 Proposed Methodology

To implement 1-bit Full adder; first of all 4:1 Mux using various logic styles is designed. Then we generate symbol for this 4:1 Mux and use this representation for the further implementation. The implementation is done in the following manner

3.1 4:1 Multiplexer

Multiplexer is a fundamental component in designing control systems and dynamic circuits [7]. To increase the quantity of data which is sent through system within a definite duration of time and bandwidth multiplexers are used. A Multiplexer can be called as data selector.[3]

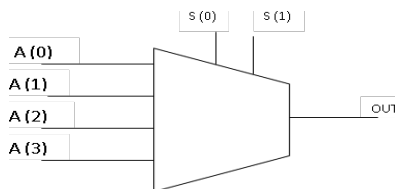


Fig 3.1A 4:1 Multiplexer

3.2 4:1 Mux using different Logic Styles

Logic styles can be defined as how transistors are used to realize logic function. Speed, size, power dissipation and wiring complication are the features which rely on which logic style is used.

3.2.2 4:1 Mux using GDI technique

Gate Diffusion Input (GDI) is a lowest power design technique which offers improved logic swing and less static power dissipation. Using this technique several logic functions can be implemented using less number of transistor counts. This method is suitable for design of fast, low-power circuits, using a reduced number of transistors (as compared to TG and CMOS).[4]

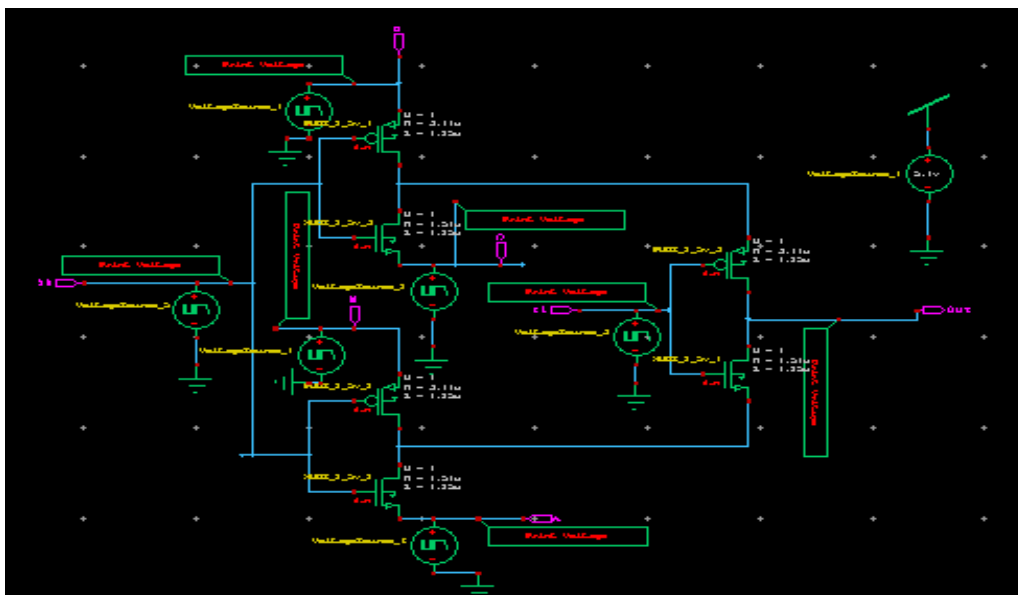


Fig 3.2 Design of 4:1 Mux using GDI Technique

3.2.3 4:1 Mux using Transmission Gate Logic

4:1 mux using Transmission gate type is formed when PMOS is connected in front of NMOS and it works as a switch. NMOS devices pass a strong zero but a weak 1, while PMOS pass a strong one on the other hand, a weak 0. In TGL neither transistor is connected to VDD or GND. The transmission gate takes the finest properties from both type of transistor by inserting NMOS in front of PMOS device. Four transmission gates square measure are used to create an MUX structure

Table3.1 Truth table of Transmission Gate

| X | IN | OUT |
|---|----|-----|
|---|----|-----|

| | | |
|---|---------------|-------------------|
| H | H | H |
| H | L | L |
| L | X(don't care) | Z(high impedance) |

Hence, the design of transmission gate based 4:1 MUX is shown below.

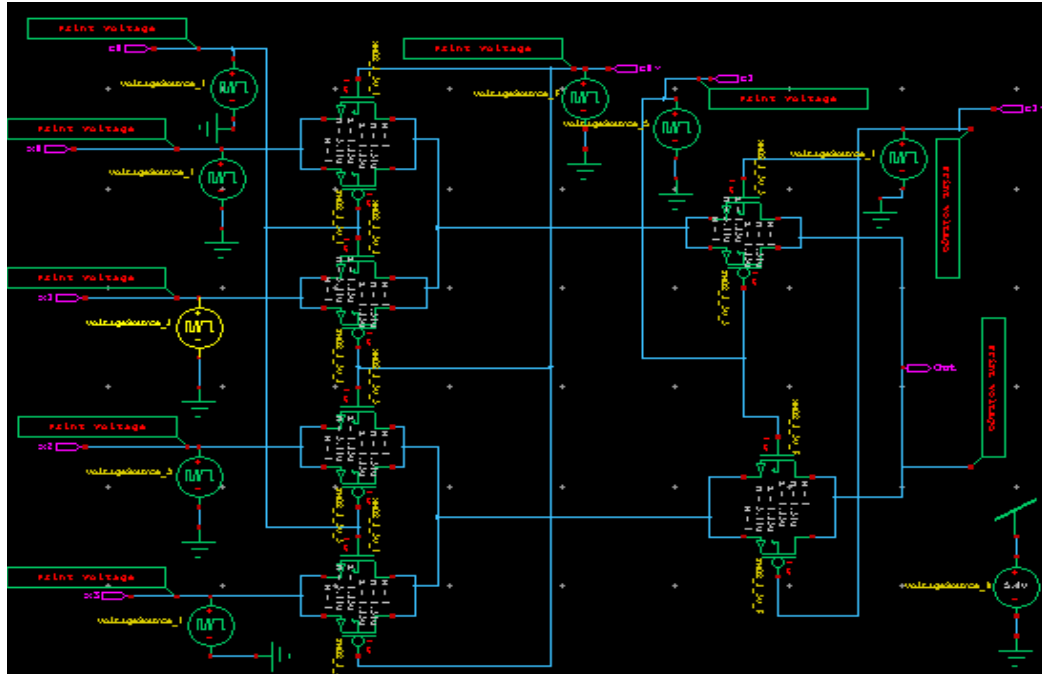


Fig 3.3 Design of 4:1 Mux using Transmission Gate logic

3.2.4 4:1 Mux using Pass Transistor Logic

The 4-to-1 multiplexer discussed in this section uses NMOS switches, mostly because the resulting diagram is more straightforward. Just remember that the NMOS transistor is more or less a placeholder for whatever type of pass/block element is used in the actual circuit. In many cases a transmission gate will be the preferred implementation, or if you want to experiment with these circuits in the lab you could even replace the FETs with a relay. Since there are four input signals, we need a two-bit select signal. These two bits provide four possible binary numbers, and each number corresponds to one of the input signals.[4]

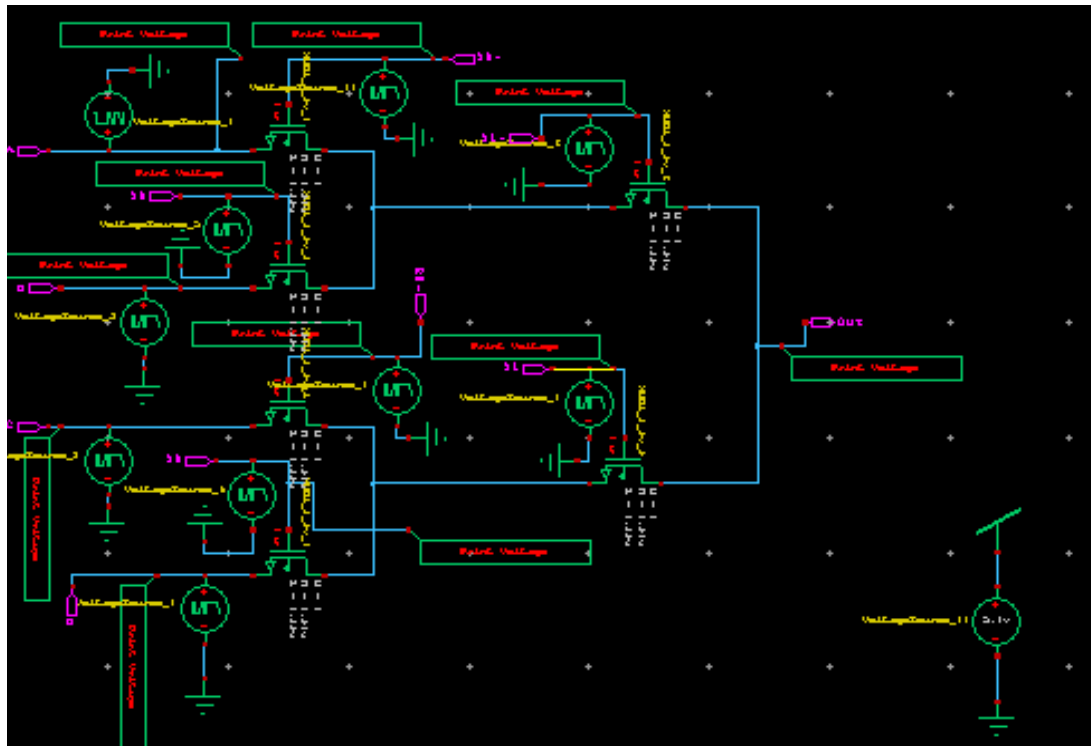


Fig 3.4 Design of 4:1 Mux using Pass Transistor logic

3.3 Proposed design of a Full adder

To implement 1-bit Full adder; first of all 4:1 Mux using GDI logic, PTL and transmission gate is designed. Then we generate symbol for this 4:1 Mux and use this representation for the further implementation. The implementation is done in the following manner

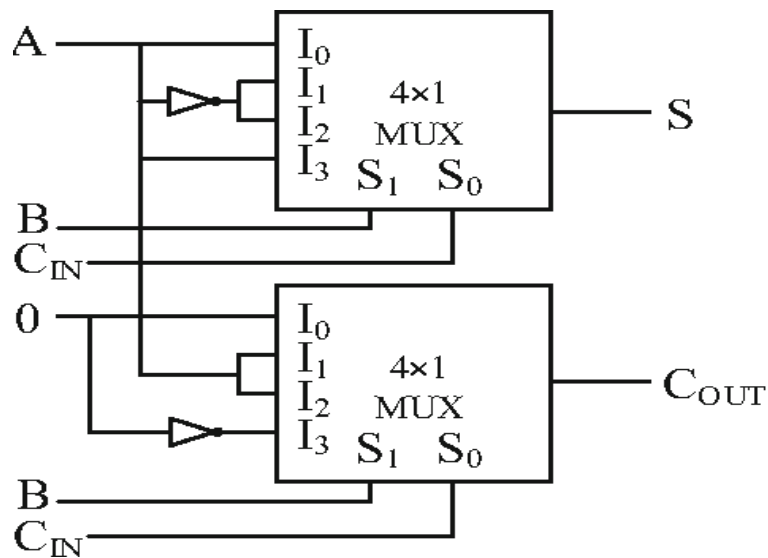


Fig 3.5 Design of 1 bit Full adder using 4:1 Multiplexer

4 Results

Simulations in this project are done using Tanner Tool. The schematic is prepared with S-Edit, the waveform is seen using W-Edit where as the power and delay is seen with T-spice. To check the waveforms first of all we have to go on setup simulation and change the settings and then go to run option. Based on power and

delay, analysis is done on 250nm technology and for supply voltage 5V

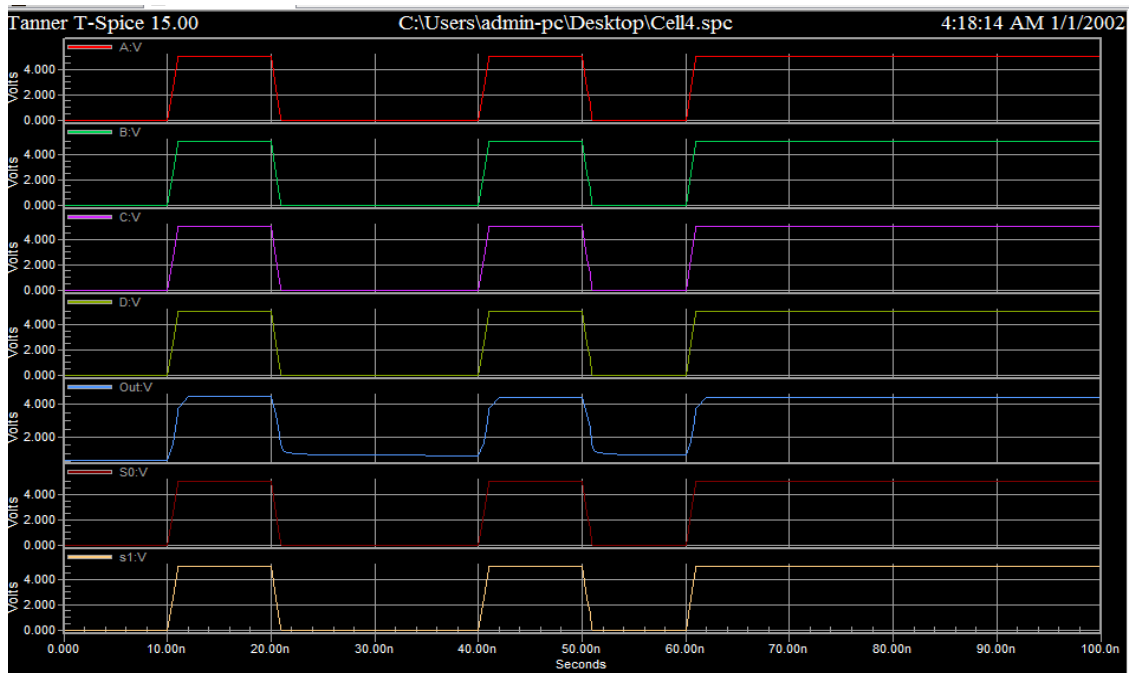


Fig 4.1 Simulation result of 4:1 Mux based on GDI

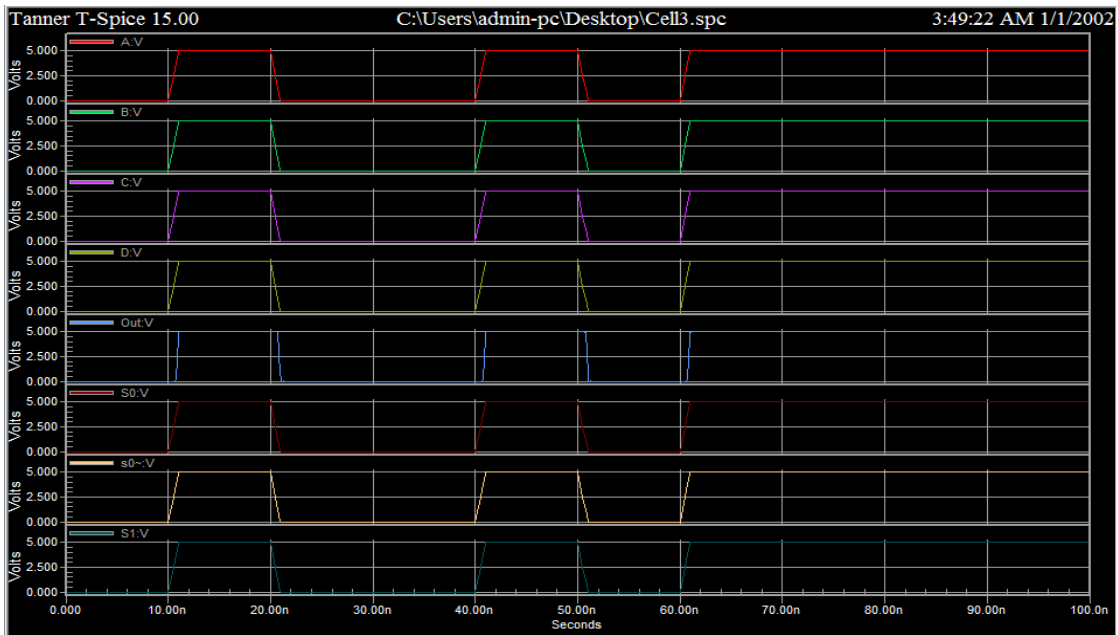


Fig 4.2 Simulation result of 4:1 Mux based on Pass Transistor logic

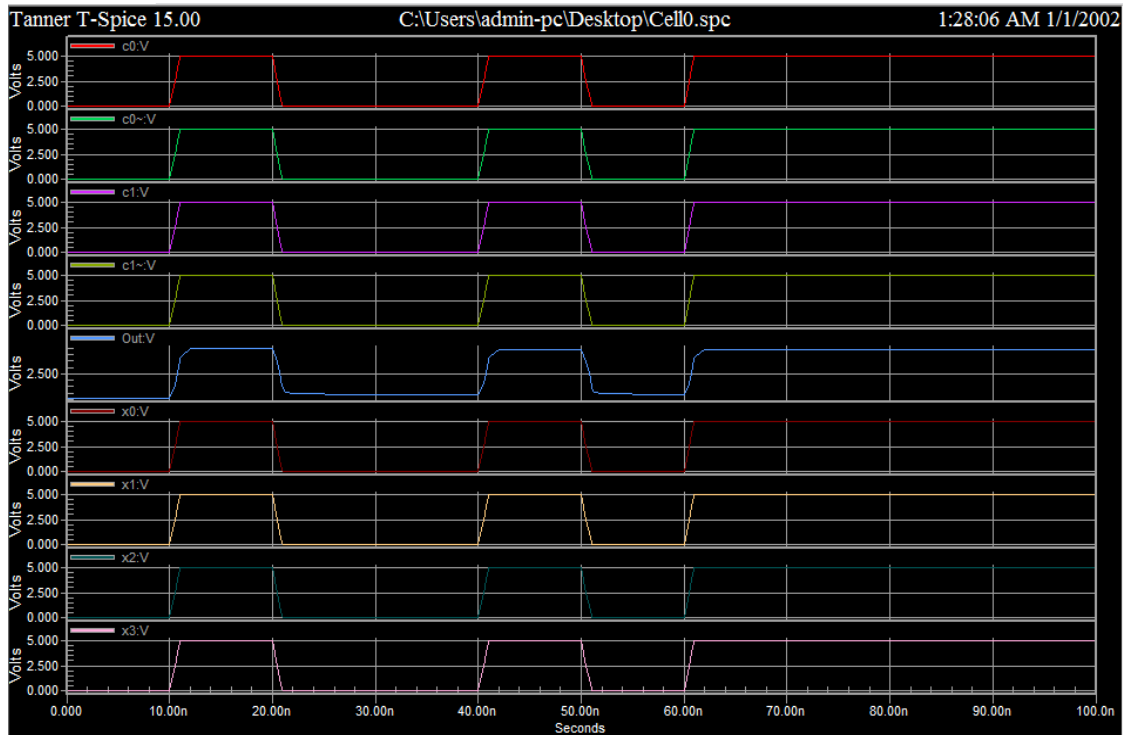


Fig 4.3 Simulation result of 4:1 Mux based on Transmission Gate logic

Table 4.1 Comparison between various methodologies for 4:1 Mux

| Logic Type | Power(w) | Delay(s) | Transistor count |
|-------------------|-------------------------|----------|------------------|
| Transmission Gate | 1.60 e^{-005} | 1.04 | 12 |
| Pass Transistor | 1.65 e^{-005} | 0.75 | 10 |
| GDI | 1.54 e^{-005} | 1.40 | 6 |

5 Conclusion and Future work

From the simulation outcomes it is examined that 1-bit Full Adder using GDI Technique 4:1 MUX is the most coherent adder as it has the most optimized power dissipation and reduced number of transistors. Therefore, it is the fastest adder among 4:1 multiplexer of GDI, Transmission Gate and Pass Transistor Logic. Reduction in power consumption delivers several benefits like minimal heat is generated, which minimizes the complications related with high temperature, as this required demand for the heat sinks. This delivers the user with a product that charges less. An additional benefit of the reduced power consumption is the enlarged life of the battery in battery-powered systems.

In future the 1 bit full adder can be designed using any other logic styles other than the styles we have used in this paper. We have designed 4:1 multiplexer, in future we can also go for 8:1 or 16:1 multiplexer to design a full adder.

Acknowledgement

We would like to express our gratitude and thanks to our respected secretary **Rev.Dr. Sr. Y. YESUTHANGAM, SAT., Dr. R. AROKIADASS M.E., Ph.D.,** Principal, **Dr.Sr. S. ANITA., M.TECH., Ph.D.,** Head of the Department of Electronics and Communication Engineering, St. Anne's College of Engineering & Technology, for proving us an excellent environment to prepare and submit the paper in International conference

References

- [1] P.D.Khandekar,S.Subbaraman,A.V.Chitre,“LowPower 2:1 MUX forBarrel Shifter, “Proceedings of International Conference on Emerging Trends in Engineering and Technology ICETET’08, pp.404-407, July2008.
- [2] H.E. Chang, J.D. Huang, C.I. Chen, “Input Selection Encoding for LowPower Multiplexer Tree,” Proceedings of International Symposium on VLSI Design, Automation and Test, pp.228-231,2005.
- [3] X.Sun,J.Feng,“A10Gb/sLow-power4:1Multiplexerin 0.18 μ m CMOS,”Proceedings of International Symposium on Signals, Systems and Electronics (ISSSE2010),2010.
- [4] YallaHareesh, YelithotiSravanaKumar, “Design of operation of 4X1 Low power multiplexer using different logics”. International Journal of Emerging Science and Engineering(IJESE), ISSN:2319-6378, Volume 4 Issue 8, Feb 2017
- [5] U.Narayanan,H.W.Leong,K.S.Chung,C.L.Liu,“Low power Multiplexer Decomposition,”Proceedings of International Symposium on Low Power Electronics and Design,pp.269-274,1997.
- [6] S.M. Kang and Y. Leblebici, “CMOS Digital IntegratedCircuits,”McGraw-HillCompanies2003.
- [7] K.Numata, M.Fujii, T.Maeda, M.Tokushima, “Ultra Low PowerConsumptionHeterojunction-FET8:1Mux/1:8 Demux for 2.4 Gbps Optical Fiber Communication Systems,” Proceedings ofGaAs IC Symposium Technical Digest,pp.39-42,Oct-Nov1995(17thAnnualIEEE).
- [8] K.Tanaka, “High Speed 8:1 Multiplexer and 1:8 DemultiplexerIC’susingGaAsDCFLCircuit,”GaAsIC SymposiumTechnicalDigest,pp.229-232,1991.
- [9] T.Seshita“ A20GHz8-bitMultiplexerICImplemented with0.5WNx/W-GateGaAsMOSFET’s,”IEEEJournalof Solid-State Circuits, vol. 29, no. 12, pp.1583-1588, 1994.

Design and Implementation of Internet Controlled Switch Box

M. Selva¹, N. Rajadurai², S.Balabasker³

^{1,2}UG Student , Department of ECE, St.Anne's College Of Engineering And Technology, Panruti

³Associate Professor, Department of ECE, St.Anne's College Of Engineering And Technology, Panruti

Abstract

Nowadays the smart home technology provides security, convenience and energy management by allowing them to control devices by using a smart home application on their Smartphone or other networked connected device. As energy management is becoming a bigger issue all around the world due lack of awareness in implementing the emerging techniques and technologies. Therefore designing a low cost Smart Switchboard is becoming an essential thing to efficiently manage the devices thereby reducing the unwanted energy consumption. Our proposed system consists of a touch sensor, Node MCU, Liquid crystal Display (LCD), Temperature Sensor, Humidity Sensor and relay drivers to control the switch box. The traditional switch box can be easily converted to a smart switch box, so that home users can control and monitor it both manual and by using the Internet. We also can control light and control, speed of the fan and other electrical appliances in a home or office in a smarter way. Our system is low cost, more flexible and easily usable by all kinds of people, especially elderly and the disabled persons who live alone. It is more desirable for conservation and efficient use of energy.

Keywords: Node Mcu, LCD, temperature sensor, touch sensor, low cost and flexible switch box

1 Introduction

The development of internet based smart devices improves the human's living standards and also helpful for the disabled and elder people. The development of intelligent electronics such as smart phones, smart wearable gadgets are now becoming our part of life. In order to implement mobile terminal control of household switchbox over the Internet of Things. The purpose of this paper is understanding the concepts of IoT and designing the internet based switchbox module which is converts the traditional switch box into smarter and without changing the function of the existing switch box it means controlling both manual and smartphones. The first section should provide the background to the subject matter of the paper. It should not occupy more than 25% of the whole paper.

1.1 Literature review

Siddharth karanchery[1] designed a smart switch box the Internet of Things. It's a simple power socket, designed with plug and play configuration using nodemcu esp8266 wi-fi enabled microcontroller. It can only operate by your handset. He didn't utilize the full function of the microcontroller and he designed single socket. Jiawei Zhang[2] The system provides the user a mobile interface for remote monitor and control home electrical devices. The system queries the real-time electrical parameters of current device and surrounding environmental data including voltage, current, power energy, temperature and humidity. At the same time, user can switch on and off the device by smartphone. Sharmila M[3] developed fully automated power socket with current and voltage monitoring devices. This system utilizes the wifi module to communicate home appliances with user interface. This system only has wi-fi to control the whole system, so it is not suitable for longer range. Musleh et. al [4] utilizes a master slave architecture smartplug. The plug used voltage and current sensing circuits for power measurement by the smart plug. The Master was connected to the internet through WiFi and communicated to slaves via the ZigBee protocol in mesh configuration. A limitation of their work is that for outlet boards, the entire circuit will have to repeat multiple times and will add to significant costs. Monzer M. Krishan[5] proposed a new type of system is designed with esp8266 wifi module and RFID module connected to identify the load are connected or not, then the power socket will be activated through the IR sensor. This system is controlled through the internet as a IoT application. Santhoshsivan N V[6] this system is similar to an Siddharth karanchery design it's also designed with node mcu microcontroller this system is accessed and controlled by smart home application

2 Proposed System

In our proposed system is designing and implementing a smart power socket module with nodemcu esp8266 microcontroller. This system is similar to the daughter board design so making connection is easier. The microcontroller relay module and other components are placed in single pcb board which is designed by our

self ,so it is compact is size and more flexible the result of this module is converts the existing switch box in to smart box as well as without changing the function of the existing Switch box, so it can operated in both manual and smart devices

2.1 Block Diagram Of Proposed System

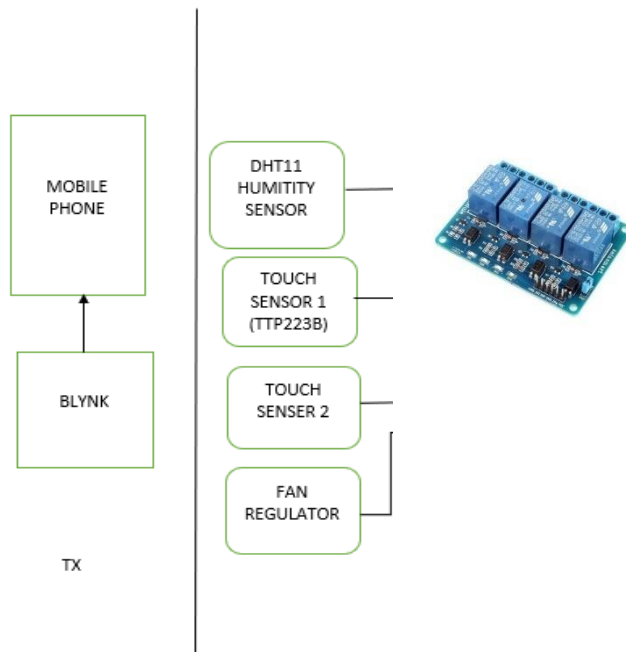


Fig. 1 Block diagram of proposed system

2.2 Hardware Requirements

NODE MCU:The NodeMCU ESP8266 development board comes with the ESP-12E module containing ESP8266 chip having Tensilica Xtensa 32-bit LX106 RISC microprocessor. This microprocessor supports RTOS and operates at 80MHz to 160 MHz adjustable clock frequency. NodeMCU has 128 KB RAM and 4MB of Flash memory to store data and programs. Its high processing power with in-built Wi-Fi / Bluetooth and Deep Sleep Operating features make it ideal for IoT projects.



Fig 2: node mcu esp8266 microcontroller

RELAY MODULE: The relay uses an electric current to open or close the contacts of a switch. This is usually done using the help of a coil that attracts the contacts of a switch and pulls them together when activated, and a spring pushes them apart when the coil is not energized

Fig3: Relay module

HUMIDITY SENSOR: The **DHT11** is a commonly used Temperature and humidity sensor. The sensor comes with a dedicated NTC to measure temperature and an 8-bit microcontroller to output the values of temperature and humidity as serial data. The sensor is also factory calibrated and hence easy to interface with other microcontrollers. The sensor can measure temperature from **0°C to 80°C** and humidity from **0% to 100%** with an accuracy of $\pm 1^\circ\text{C}$ and $\pm 1\%$.

Fig 4: DHT11 Humidity Sensor

TOUCH SENSOR: The module is based on a touch-sensing IC (TTP223B) capacitive touch switch module. In the normal state, the module output low, low power consumption. When a finger touches the corresponding position, the module output high, if not touched for 12 seconds, switch to low-power mode.



Fig 5: TTP223B Touch Sensor

3 Conclusions

As the result of this module is can control and monitoring your household appliances over the internet and manual mode. You can operate lights, controlling the speed of the fan and find your room temperature .the future work of this system is adding some additional features like voice assistance

References

- [1] Siddharth karancherry and International Conference on Inventive 2020)
- [2] Jiawei Zhang¹, Yuechuan Tao¹, Jing 4/19/\$31.00_c 2019 IEEE “ Design of a management systems”
- [3] Sharmila M.Yash K. GuptaHarshal “Designing and Development of Users” Proceedings of the Fifth International Conference on Inventive Computation Technologies (ICICT-2020) IEEE Xplore Part Number: CFP20F70-ART; ISBN: 978-1-7281-4685-0
- [4] A. S. Musleh, M. Debouza and M. Farook, "Design and implementation of smart plug: An Internet of Things (IoT) approach," 2017 International Conference on Electrical and Computing Technologies and Applications (ICECTA), Ras Al Khaimah, 2017, pp. 1-4.
- [5] Monzer M. Krishan, 2 Tariq M. Younes and 3 Farouq M. Al-Tawee”New Design of Socket Modules for Smart Home Applications” International Journal of Engineering Research and Technology 2019. ISSN 0974-3154
- N.Rakesh Proceedings of the Fifth Computation Technologies (ICICT- Qiu1, Xiao Han1:978-1-7281-0106-smart socket for smart home energy
- U. Akole Mayur V. Chavan Automated Smart Socket for Wi-Fi



- [6]Santhoshsivan N V 1, Senthilkumar S2, Arunkumar K3,Umasankar S4,Jagadeeshraja M” HOME AUTOMATION USING SMARTPLUG” International Research Journal of Engineering and Technology (IRJET) e-ISSN: 2395-0056
- [7]Lei Liu “A Multi Functional Smart Socket Design”2019 International Conference on Communications, Information System and Computer Engineering
- [8] K. Patil, J. Metan, T. S. Kumaran and M. Mathapatil, "IoT based powermanagement and controlled socket," 2017 International Conference onElectrical, Electronics, Communication, Computer, and OptimizationTechniques (ICEECCOT), Mysuru, 2017, pp. 243-247.

Supervisory control & data acquisition (SCADA) systems in power stations

Kamalesh Kumar S, Yogesh S, Gowtham R

Department of Electrical and Electronics Engineering,
Bannari Amman Institute of Technology,
Sathyamangalam, Erode.

Abstract

Supervisory Control and Data Acquisition (SCADA) Systems are controlling and monitoring critical plants of the nation's infrastructure such as power generation and distribution, oil, gas, water and waste management. SCADA is a system in which the message that are individuals are sends to the external world. In this presentation to understood SCADA concept in control operations and systems components and example of use. The application of SCADA are Supervisory computers, Remote terminal units, Programmable logic controllers, Communication infrastructure, human- machine interface alarm handling, PLC /RTC programming, PLC commercial integration, communication infrastructure and methods SCADA architecture development. SCADA systems can be relatively simple, such as one that monitors environmental conditions of a small office buildings or incredibly complex, such as a system that monitors all the activity in a nuclear power plant or the activity of a municipal water system. First SCADA was used in 1960s.

From the wireless SCADA system which is proposed in setup the temperature of around 30 degree of Centigrade could be sufficiently recorded from remote location. In the similar manner reading of electric energy meter could be read 225Kilowatt Hour (KWH) or 223 units.

The properly designed SCADA system saves time and money by eliminating the need of service personal to visit each site for inspection, data collection or make adjustments. To understand four types of SCADA functions such as Data acquisition, Networked data communication, Data presentation and Control.

At present, an evolution at SCADA systems is at a very high rate and it is also entering the market of plants with a huge number of input and output channels. UNIX, VMS and DOS are availed by the systems of SCADA.

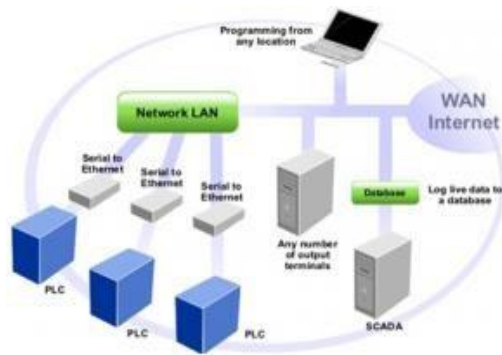
Scada System Architecture

Generally, the SCADA system is a centralized system that monitors and controls the entire area. It is a pure software package that is positioned on top of the hardware. A supervisory system gathers data on the process and sends the commands control to the process. The SCADA is a remote terminal unit which is also known as RTU. Most control actions are automatically performed by RTUs or PLCs. The RTUs consists of the programmable logic converter which can be set to specific requirement. For example, in the thermal power plant, the water flow can be set to a specific value or it can be changed according to the requirement.

The SCADA system allows operators to change the set point for the flow, and enable alarm conditions in case of loss of flow and high temperature, and the condition is displayed and recorded. The SCADA system monitors the overall performance of the loop. The SCADA system is a centralized system to communicate with both wired and wireless technology to Clint devices.

The SCADA system controls can run completely all kinds of the industrial process.

Hardware:

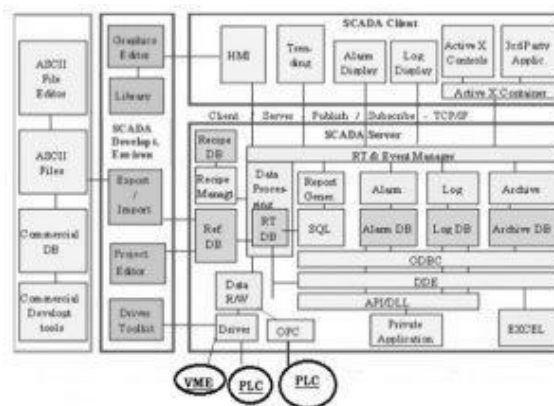


The data server layer handles most of the process of data activities.

The SCADA station refers to the servers and it is composed of a single PC. The data servers communicate with devices in the field through process controllers like PLCs or RTUs. The PLCs are connected to the data servers either directly or via networks or buses. The SCADA system utilizes a WAN and LAN networks, the WAN and LAN consist of internet protocols used for communication between the master station and devices.

The physical equipment like sensors connected to the PLCs or RTUs. The RTUs convert the sensor signals to digital data and sends digital data to the master. According to the master feedback received by the RTU, it applies the electrical signal to relays.

Most of the servers are used for multitasking and real-time database. The servers are responsible for data gathering and handling. The SCADA system consists of a software program to provide trending, diagnostic data, and manage information such as scheduled maintenance procedures, logistic information, detailed schematics for a particular sensor or machine, and expert-system troubleshooting guides. This means the operator can see a schematic representation of the plant being controlled.



Software Architecture of SCADA

Examples are alarm checking, calculations, logging, and archiving; polling controllers on a set of parameters, those are typically connected to the server.

SCADA System Working:

The SCADA system performs the following functions

- Data Acquisitions

- Data Communication
- Information/Data presentation
- Monitoring/Control

These functions are performed by sensors, RTUs, controllers, a communication network.

The sensors are used to collect the important information and RTUs are used to send this information to the controller and display the status of the system. According to the status of the system, the user can give the command to other system components. This operation is done by the communication network.

Data Acquisition:

The real-time system consists of thousands of components and sensors. It is very important to know the status of particular components and sensors. For example, some sensors measure the water flow from the reservoir to the water tank and some sensors measure the value pressure as the water is released from the reservoir.

Data Communication:

The SCADA system uses a wired network to communicate between users and devices. Real-time applications use a lot of sensors and components which should be controlled remotely. The SCADA system uses internet communications. All information is transmitted through the internet using specific protocols. Sensors and relays are not able to communicate with the network protocols so RTUs used to communicate sensors and network interfaces.

Data Presentation:

The normal circuit networks have some indicators which can be visible to control but in the realtime SCADA system, there are thousands of sensors and alarm which are impossible to be handled simultaneously. The SCADA system uses the Human Machine Interface provide all of the information gathered from the various sensors. The SCADA system uses different switches to operate each device and displays the status of the control area. Any part of the process can be turned ON/OFF from the control station using these switches.

SCADA system is implemented to work automatically without human intervention but in critical situations, it is handled by manpower.

Scada Component:

The SCADA system components include the following.

Supervisory System:

The supervisory system works like a communication server among the human-machine interface software within the control room of workstations as well as its apparatus such as RTUs, Sensors, PLCs, etc. Smaller SCADA systems include simply a single personal computer to serve like a master system otherwise supervisory whereas, large SCADA systems include numerous servers, sites for tragedy recovery as well as distributed software applications. The servers are connected like hot-standby formation otherwise dual-redundant to monitor server failure continuously.

Remote Terminal Unit:

The RTU or remote terminal unit is an electronic device and it is also known as remote telemetry units. This system comprises physical objects that are interfaced through RTUs. The controlling of these devices can be done through microprocessors. Here, microprocessors are utilized for controlling RTUs which are used to transmit the recorded data toward the supervisory system. The data can be received from the master system for controlling the connected objects.

Using Plc:

The term PLC stands for programmable logic controllers which are used in SCADA systems with the help of sensors. These controllers are connected to the sensors for converting the output signal of the sensor into digital data. As compared with RTUs, these are used due to their flexibility, configuration, versatility & affordability.

Communication Infrastructure:

In the SCADA system, a mix of radio & the direct-wired connection is used. But, SONET or SDH can also be utilized for superior systems such as power stations & railways. Few standardized 7 recognized protocols are used between the compact SCADA protocols to deliver information simply once the RTUs are polled through the supervisory station.

Scada Programming:

In HMI otherwise master station, SCADA programming is mainly used to make maps, diagrams to provide very important information throughout progression otherwise when event failure occurs. Most of the commercial SCADA systems utilize consistent interfaces in C programming language otherwise derived programming language can also be used.

Human Machine Interface:

The SCADA system uses the human-machine interface. The information is displayed and monitored to be processed by a human. HMI provides access to multiple control units which can be PLCs and RTUs. The HMI provides the graphical presentation of the system. For example, it provides a graphical picture of the pump connected to the tank. The user can see the flow of the water and the pressure of the water. The important part of the HMI is an alarm system that is activated according to the predefined values.

Types of SCADA System:

SCADA systems are classified into four types which include the following.

- ‡ Monolithic SCADA Systems
- ‡ Distributed SCADA Systems
- ‡ Networked SCADA Systems
- ‡ IoT SCADA Systems

SCADA Security:

At present, SCADA networks are used extensively in current industries to check & examine real-time data, industrial processes can be controlled, communicate with devices. So SCADA systems are essential for industrial organizations because these systems include hardware & software. So, SCADA security is also essential in industries.

The term SCADA security is used to protect the SCADA networks which are fabricated with computer hardware. SCADA networks used by some of the systems are electricity, natural gas, etc. The private and government organizations have taken the measures of these networks because of the valuable role to make sure the security of the SCADA systems. Examples of SCADA Security:

The threats that occur in SCADA systems include the following.

- † Hackers
- † Terrorists
- † Malware
- † Error Inside

The weakness of SCADA security mainly occurs because of the following reasons.

- † Poor Training
- † Loopholes Development of App
- † Issues while Monitoring
- † Less Maintenance

The SCADA system can be protected by mapping all present systems, monitoring, and detecting the institute, and create processes for the security of the network.

PV Panel Cooling Using Stack Effect

Rajkumar¹, Ujjwal K Menon¹, Shahrooq Shahjahan², Sundaramoorthi P¹

¹Department of Electrical and Electronics Engineering, Nehru College of Engineering and Research Centre, Kerala.

²Department of Mechatronics Engineering, Nehru College of Engineering and Research Centre, Kerala.

Abstract

Unsatisfactory performance of the solar panels is one in every of the foremost issues among the promotion of solar photo voltaic technology. A vital factor affecting cell performance is its operative temperature. The cell potential declines near linearly with a rise of the cell operative temperature. The temperature condition on the operating surface of a PV panel is usually 20-30 °C beyond the normal temperature conditions. On the premise of those issues, the potency of the solar panels will be refined by sustaining their operative temperatures as low as possible. This paper portrays a technique of Photo voltaic panel cooling using convection generated by the chimney effect. This paper considers the reduction of heat from the Photovoltaic panel for both active and inactive conditions.

Keywords: *air cooling, convection, solar cell cooling, solar photovoltaic.*

1 Introduction

Today, the world is dealing with some serious issues of energy deficiency, warming and degeneration of environment sources and energy power resources, renewable energy sources have gotten more attention. energy is one of the comparable candidates. Energy source is widely obtainable with no cost. Energy is transformed into electric power by PV effect. PV system is consistent, quiet and freed from moving parts which leads to reduction of operation cost and servicing cost of the system. Being pollution free and pure source of energy, PV method has earned far more importance. Output power of PV method depends mainly on solar irradiance, temperature of cell and operating voltage. However they still present an infinite area of competition comparing to straightforward energy resources due to their heavy cost and low efficiency during energy conversion.

The photovoltaic (PV) cells are ready to produce energy source from the abundant resource of sunlight. Since the PV components are exposed directly to the sunlight, it produce heat still as electricity. A PV module transforms solely 12-15% of the input solar power to electricity and also the undefined power is actually released as heat energy. The good and comfortable atmosphere affects this density/voltage (J/V) characteristics of the PV components wherever their electrical capabilities are adversely stricken with the numerous rise of cell operative temperature throughout absorption of radiation [10].

By applying a cooling methodologies to a PV component the worth of different energy is reduced in 3 ways. First, cooling improves the electrical output of PV components. Second, cooling method makes possible the utilization of concentrating PV method by protecting the PV cells from reaching the temperatures at which permanent loss occurs, even below the irradiation of several suns. As this drives it possible to alter PV cells with probably more cost-effective concentrators. Finally, the heat is removed by the PV cooling method is employed for constructing the heating system or cooling system, or in industrial applications. to the current outcome, hybrid photovoltaic/thermal (PV/T) solar systems are explored as a way of reducing the temperature of PV components and improve their electrical capabilities. This kind of a system is termed Solar Photovoltaic thermal (PV/T) collector. The PV/T collector produces thermal and current simultaneously.

The hybrid PV thermal systems are still under development. J.K. Tonui, Y. Tripanagnostopoulos [11] discussed about an enhanced PV/T solar collector with heat extortion by forced and natural circulation of air while R. Mazon-Hernandez et al [14] discussed about the heat reduction process from the PV panels located on the roof of greenhouse by using air because the thermal energy carriers. The steady state effect of vertical fins on a PV/T solar air heater was been studied by Marc A. Rosen, Rakesh Kumar [15] while experimental study of air based Photovoltaic Thermal (PV/T) collector with various styles of Heat exchangers was being carried by Mohd. Yusof H J [16].

This paper illustrates a cooling method for the PV panel. The passive cooling method is within the model of an oblong duct, which envelops the rear of the panel and expands above top of the panel. The cooling effect is induced here by stack effect. Both active and passive cooling is being studied using the identical system with an addition of fan connected at the very best section that's being powered using the device. during this technique, air is used because of the warmth carrier. Designing and Theoretical analysis of the technique is explained below.

2 System Description

The design comprises of an absorber section additionally to the planning proposed by Tonui and Tripanagnostopoulos [1]. the rate of air rising up within the chimney is directly proportional to the energy consumed by the air, so addition of an absorber section will help to reinforce the natural draft of air which might be utilized for cooling of PV panels. The passive cooling method will accommodate mainly two parts, top part and middle part as in Fig 1. Top part contains of the vertical extension to the center part. Top part will act sort of a chimney during this setup to reinforce the natural draft created by the nice and cozy rising air. The beam of radiated rays is incident on the absorber section that's product of glass. These incident solar rays are consumed by the air that's under the absorber section that eventually gets warm up and its density declines. The nice and cozy air will try to arise due to the buoyancy force and flee through the chimney. The tall chimney will deliver a pressure difference between the underside and also the top which can further assist within the draft of the surrounding air.

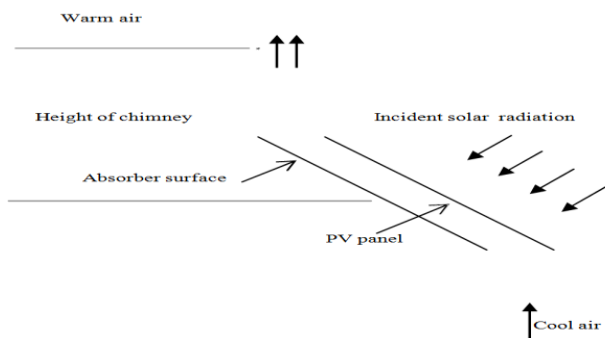


Fig.1. Layout of cooling system

The middle portion of Solar cooling chimney consists PV panel section and absorber section. The absorber section is meant such its length is larger than the PV panel length. As in Fig. 2. A transparent glass sheet is planted over the duct that's formed of low- carbon steel. PV panel is mounted on the lower 1/2 middle part while the transparent glass sheet at the upper 1/2 the center section acts because the absorber section. Middle part of solar cooling chimney is mounted at an inclination angle capable local latitude to create sure that the PV panel and absorber section receives maximum radiation over the year.

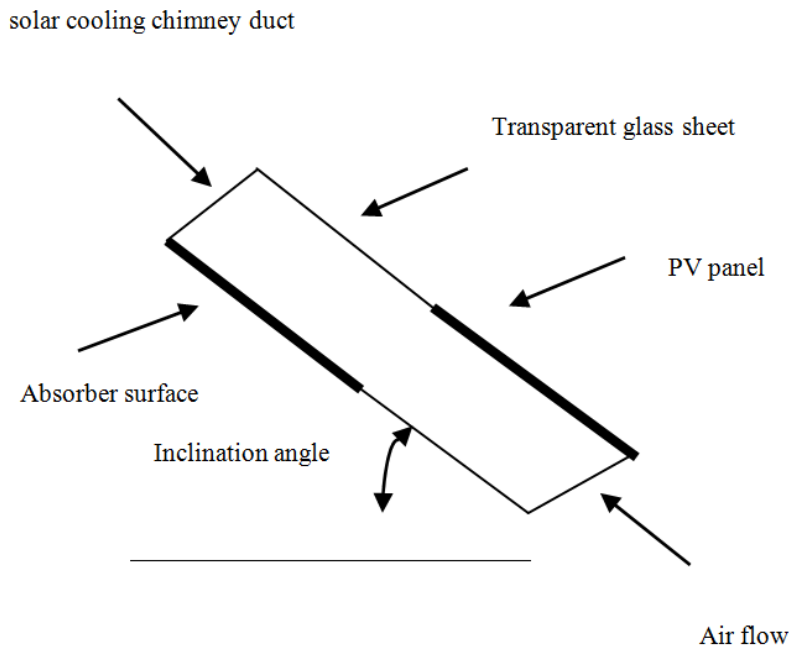


Fig.2.Middle section of cooling system

Most of the incident solar energy will undergo the transparent sheet reckoning on its emissivity and reflectivity and fall on absorber surface. Absorbing surface is coated black to maximise the portion of energy absorbed. As a result the temperature of the absorbing surface will increase. Warmth absorbing surface will transfer the heat to the surrounding air coming from the PV board panel section. Warm air with lesser density will rise upwards towards the best section. Elevation of the best part will assist the great and comfortable air to

rise toward the best due to the static head difference. Air flow velocity will increase if we increase the altitude of chimney. The natural air draft within the duct induced due to the density variation between the air within the center part and ambient air above the best part will create the suction to allow ambient air to infiltrate from bottom. Ambient cool air entering from the underside will engulf the heated PV panel surface and reduce its temperature.

3 Experimental Setup

The cooling method was built using mild steel for concept demonstration. The experimental model comprises of two key parts as described in the “Design” section of this paper. The top section was optimized for better natural draft. A PV panel of 10W, 12V Polycrystalline was utilised in the test setup. The panel is mounted on the inclined section just below the absorber and the same panel is placed on a standalone frame to have a comparison study. Plain glass of 5mm thickness was used to act as the transparent sheet that allow to pass solar radiation into the absorber section. The walls of the channel or duct made of mild steel is insulated with glass wool so that to avoid heat loss. Fig 3 portrays the isometric view of the air channel for the cooling system with dimensions in mm.

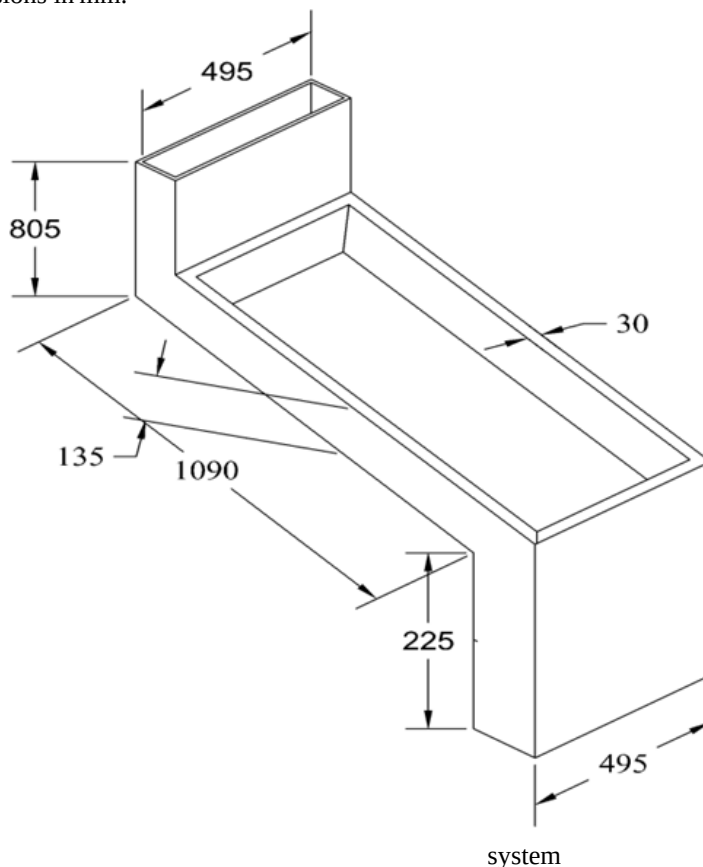


Fig.3.Isometric view of cooling

system

The system is mounted on a stand that is fabricated using mild steel L angle. During experiments the PV panel temperature T_{pv} , inlet T_{in} and outlet T_{out} air temperatures for different solar insulations are estimated using a Infrared thermometer and the readings are noted for further calculations. Passive cooling of the PV panel is being studied using this experimental setup.

The active cooling of PV panel using the same setup can be studied by making small changes in the design. In active cooling system exhaust fan driven by the PV panel is employed to provide the desired cooling effect as in Fig.4 .Here the cooling effect is expected to be more than that of passive cooling system. A 12V exhaust fan is connected at the top part of the cooling system. A 12V. 7AH battery is also used here.

4 Model Theoretical Analysis

An analytical model is formulated to simulate the energy balance. The incoming solar rays is incident on the absorber section and the PV panel in the model. The height of top section is optimised for the maximum natural draft and reduced shading effect. Depth of duct is considered to be 0.1m. Size of the absorber surface is larger than the size of the PV panel. The amount of heat that enters the system should be equal to the volume of energy

that leaves the system. The heat energy that enters the structure can be given as (Randall, Mitchell [2]; Frank P. Incropera; Brinkworth[3]; Akbarzadeh, Johnson et al. [4]).

$$Q_{in} = I \times A_{absorber} \times (1 - r) \times \tau \quad (1)$$

Fig. 4 illustrates the PV panel section where the PV panel is mounted on the inclined duct of the solar cooling chimney.

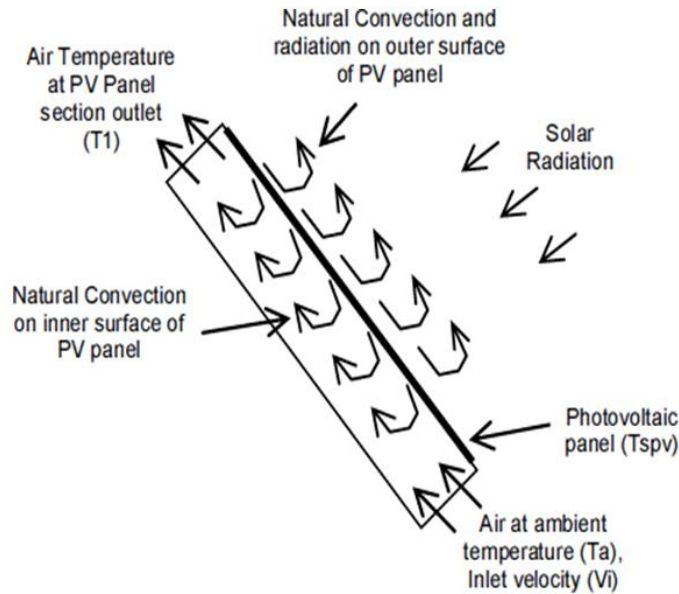


Fig.4. Heat transfer over the panel surface

Considering the model has all the walls adiabatic except the transparent sheet. The total heat amount that leaves the system can be given as

$$Q_{out} = Q_{air} + Q_{conv-cond} \quad (2)$$

Heat absorbed by the air inside the channel or duct can be given as

$$Q_{air} = V_i \times A_{duct} \times \rho_i \times C_{p\ air} \times (T_o - T_i) \quad (3)$$

Heat loss due to convection and conduction through the transparent sheet can be expressed as

$$Q_{conv-cond} = \frac{\frac{T_i + T_o}{2} - T_i}{R_{conv-inside} + R_{cond} + R_{conv-outside}} \quad (4)$$

Convective thermal resistance inside the chimney duct

$$R_{conv-inside} = \frac{1}{h_i \times A_{absorber}} \quad (5)$$

Conductive thermal resistance for transparent sheet

$$R_{cond} = \frac{\text{Thickness}}{K \times A_{absorber}} \quad (6)$$

Convective thermal resistance outside the chimney is given as follows

$$R_{conv-outside} = \frac{1}{h_o \times A_{absorber}} \quad (7)$$

The heat entering the system increases the air temperature inside the chimney duct. The total draft pressure created across the absorber section and the top end of the chimney can be formulated as (Brinkworth 2000[3]; Akbarzadeh, Johnson et al. 2009[4])

$$\Delta P = (\rho_i - \rho_o) \times g \times H \quad (8)$$

Pressure drop across the system possibly given by (Bazilian, Leenders et al.[7]; Cengel, Turner et al.[8]; Ong[9])

$$P_{drop} = f \times \frac{1}{D_h} \times \frac{1}{2} \times \rho_i \times V_i^2 \quad (9)$$

By equating the equations for heat entering the system and heat leaving the system an equation can be formulated with reference of the outlet velocity. Similarly the equations for total draft pressure and pressure drop across the system can be rearranged with reference of outlet velocity. By resolving these equations altogether the outlet velocity and temperature of the outlet air can be predicted

5 Conclusion

The natural air draft that is achieved by buoyancy effects in a chimney can be utilized as a passive cooling medium for PV panels. Simple modification in the plan of the system and including the additional absorber section can help to enhance the induced natural draft of air and also as a result, helps to improve the efficiency of the PV panel. Simple and preliminary analysis shows that by coupling an air passage channel and an absorber section with a PV panel we can achieve considerable cooling of the PV panel and improve the potency of the PV panel.

6 Reference

- [1] Tonui, J. K., & Tripanagnostopoulos, Y, "Performance improvement of PV/T solar collectors with natural air flow operation". *Solar Energy*, 82, pg.1-12, 2008
- [2] Randall, K. R., J. W. Mitchell, et al, "Natural Convection Heat Transfer Characteristics of Flat Plate Enclosures." *Journal of Heat Transfer*, pg. 120-125,1979.
- [3] Brinkworth, B. J. "Estimation of flow and heat transfer for the design of PV cooling ducts." *Solar Energy*,pg.413-420,2000
- [4] Akbarzadeh, A., P. Johnson, et al. "Examining potential benefits of combining a chimney with a salinity gradient solar pond for production of power in salt affected areas." *Solar Energy*,pg. 1345- 1359,2009
- [5] Sandberg, M. and B. Moshfegh "Investigation of fluid flow and heat transfer in a vertical channel heated from one side by PV elements, part II - Experimental study." *Renewable Energy* pg. 254-258.
- [6] Sandberg, M. and B. Moshfegh. "Buoyancy-induced air flow in photovoltaic facades: Effect of geometry of the air gap and location of solar cell modules." *Building and Environment* , pg.211-218,2002
- [7] Bazilian, M. D., F. Leenders, et al. "Photovoltaic cogeneration in the built environment." *Solar Energy*, pg. 57-69,2001
- [8] Cengel, Y., A. R. Turner, et al. "Fundamentals of Thermal- Fluid Sciences." *Applied Mechanics Reviews*, 2003
- [9] Ong, K. S, "A mathematical model of a solar chimney." *Renewable Energy* ,pg 1047-1060, 2003
- [10] K. Nishiokaa, T. Hatayamaa, Y. Uraokaa, T. Fuyukia, R. Hagiharab,M. Watanabec, "Field-test analysis of PV system output characteristics focusing on module temperature", *Solar Energy Materials & Solar Cells* ,Vol.75,pp. 665–671,2003
- [11] J.K. Tonui, Y. Tripanagnostopoulos, "Improved PV/T solar collectors with heat extraction by forced or natural air circulation", *Renewable Energy*,Vol.32, pp. 623–637,2006
- [12] Adnan Ibrahim, Goh Li Jin, Roonak Daghigh, Mohd Huzmin Mohamed Salleh, Mohd Yusof Othman, Mohd Hafidz Ruslan, Sohif Mat and Kamaruzzaman Sopian, "Hybrid Photovoltaic Thermal (PV/T) Air and Water Based Solar Collectors Suitable for Building Integrated Applications", *American Journal of Environmental Sciences*,Vol.5, pp. 618-624, 2009
- [13] Gur Mittelman, Aiman Alshare, Jane H. Davidson, "A model and heat transfer correlation for rooftop integrated photovoltaics with a passive air cooling channel", *Solar Energy* ,Vol. 83, pp. 1150– 1160, 2009
- [14] R. Mazon-Hernandez, JR Garcia-Cascales, F Vera-Garcia, A Sanchez-Kaiser, B Zamora-Parra, "Development of an installation to reduce the temperature of photovoltaic modules and improve their efficiency", International Conference on Renewable Energies and Power Quality (ICREPQ'10), 23th to 25th March, 2010
- [15] Marc A. Rosen, Rakesh Kumar, "Performance of a photovoltaic/thermal solar air heater:Effect of vertical fins on a double pass system", *International Journal of Energy and Environmental Engineering* ,Vol.2 / No.4 , pp.1-12, 2011
- [16] Mohd. Yusof H J. Othman , Faridah Hussain, Kamaruzzman Sopian, Baharuddin Yatim & Hafidz Ruslan, "Performance Study of Air-based Photovoltaic-thermal (PV/T) Collector with Different Designs of Heat Exchanger", *Sains Malaysiana* Vol. 42(9), pp. 1319–1325 ,2013

A Joint Optimal Algorithm Design for Envi-Economic Power Generation by Using Communicative Smart Grid

P.Madhumathi¹ Dr.K.Thenmalar² S.B.Kayalvizhi³ S.Mutharasu⁴

Abstract

Distribution of Energy from numerous Resources involving small grids is growing trend for the economical technique of power generation or distribution to a bigger extent. The increasing penetration of distributed generation resources demands higher economic performance of small grids. Therefore EDP i.e., Economic Dispatch drawback should be handled in a very right method. The most objective of the economic dispatch is delineated because the technique for looking the best answers for the minimization of the generation value taking into consideration of the required constraints. A comprehensive environmental-economic dispatch technique for good small grids area unit projected, with the target for minimizing the summation of generation and emission prices within the system however providing the facility generated as per the required demand. Energy management systems (EMSs) and improvement strategies area unit most needed to effectively and safely utilize energy storage as a versatile grid plus that may give multiple grid services. A changed organic process Multi-objective improvement formula has been outlined within which, the good Grid Management is taken into account such every of the generators communicate regarding their generation value and therefore the demand still because the deviations to their neighbors. Utilizing such knowledge the generators ought to severally amendment their force yield to asymptotically eradicate the heap balance a minimum of expense. The results of the system are simulated and verified victimization PROTEUS.

Keywords: EDP, EMS, MEMO, NS2 and PROTEUS

1 Introduction

In my research reference papers are reducing the fuel cost and solve multi & single-objective problems arises by CEED problems [1]. Overall economic and emission of system is reduced by using hybrid intelligence techniques like GWO, SCA, CSA and MGWO [2]. Renewable energy sources are freely available sources like solar and wind systems are consider and its CEED problems are minimized [3]. Grasshopper optimization algorithm (GOA) is implemented to reduce the cubic functions of the CEED. IOT is used to monitor the microgrid in the management of solar radiation for easy predictable of radiation & it gives better efficiency [5]. Water wave optimization algorithm is used for solving CEED problems in the lesser number of iterations & time [6]. Combined economic emission dispatch in power system of renewable sources is reduced by Evolutionary algorithm like TLBO, Pacet, Jaya OA. In this algorithm multi objective function is reduced to single objective function by price penalty factor [7-14]. In Artificial Bee Colony optimization Algorithm minimizes the cost & reduces the emission also [15]. Evolutionary algorithm like TLBO, HAS, MACO are used for solving the economic and emissions dispatch at the load side are implemented on renewable side for the reduction of CEED problems [16-23].

2 Proposed System

The main objective of economic dispatch and Emission dispatch is described has the method for searching the optimal solution for the minimization of the generation cost. A comprehensive Environmental-combined Economic and Emission Dispatch method for Micro Grids are proposed .In optimization method have modified evolutionary multiple-objective (MEMO) algorithm and combined Evolutionary and Meta-heuristic search Algorithm has been used in Micro grid management is considered such that each of the generators communicate about their generation cost and the demand as well as the deviations to their neighbors. Using such information the generators autonomously adjust their power output to asymptotically erase the load balance at a minimum cost. Two optimization algorithms are used to solve both the economic load dispatch and emission dispatch (EED) problems with transmission losses. The result of the system is simulated and verified using PROTEUS.

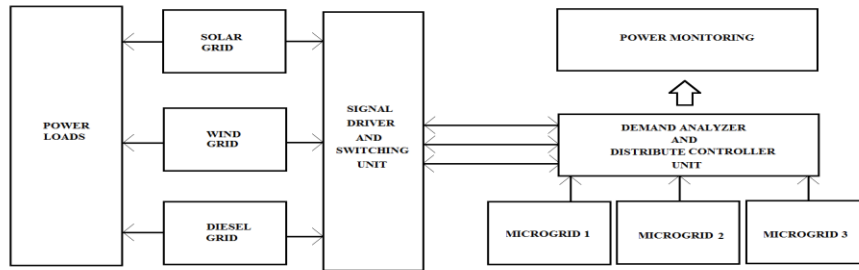


Figure: 1 Functional block diagram of the system

The framework comprises of various networks, for example, sun based, wind and diesel and sign driver with exchanging unit, request analyzer with convey regulator unit and force observing unit and numerous Microgrid specialists. Each inexhaustible and non-sustainable sources is associated with framework is producing the power when it gathers input source from regular or counterfeit boundaries. The scope of yield power level of the every network depends on their information source. The producing power station ceaselessly offers capacity to the relating loads through dispersed electrical organization from the energy stockpiling units. The sign driver is accustomed to recognizing the energy level just as burden conditions from each sustainable and non inexhaustible source associated with network. The force checking unit shows the status of the networks just as their boundaries.

3 MEMO Algorithm

We have proposed here a Modified Evolutionary Multi Objective Algorithm (MEMO) which uses interval analysis in three phases. In the first phase of MEMO, global minimum is roughly estimated with the application of interval arithmetic, which provides the upper and lower bounds of the objective function. In the second phase of MEMO we use an interval branch and bound algorithm, which we describe here along with, cut off test and monotonicity test. It produces boxes with relatively small widths and gives upper and lower bounds of the objective function. The global minimize exists with certainty in one of these boxes.

The above piece of information is used to initialize the population. In the third phase, MEMO algorithm modifies the new population, which is obtained after mutation, crossover and selection operations, by using a subset of new population. Then it constructs a shrinking box for this subset using interval arithmetic; and as the algorithm proceeds the width of shrinking box gets reduced. Finally the algorithm terminates with specified tolerance on the width of the shrinking box. As the formation of shrinking box depends on the number of individuals in the subset, it acts as a convergence check for the algorithm.

4 Experimental Results

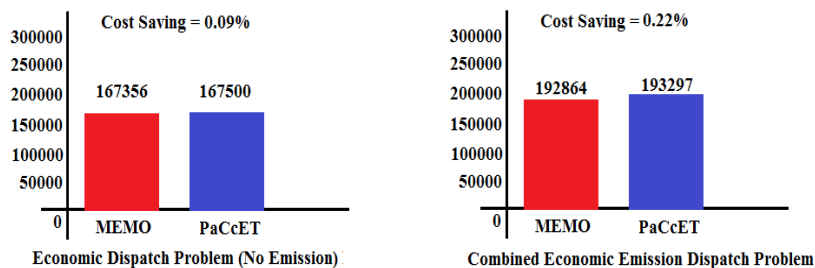


Table 1: Solar

Generation In terms of hours

Table 2: Wind Generation In terms of Hours

| Time(Hrs) | Solar generation(MW) | Time(Hrs) | Solar generation(MW) | Time(Hrs) | Solar generation(MW) |
|-----------|----------------------|-----------|----------------------|-----------|----------------------|
| 1 | 0 | 9 | 24.05 | 17 | 9.57 |
| 2 | 0 | 10 | 39.37 | 18 | 2.31 |
| 3 | 0 | 11 | 7.41 | 19 | 0 |
| 4 | 0 | 12 | 3.65 | 20 | 0 |
| 5 | 0 | 13 | 31.94 | 21 | 0 |
| 6 | 0.03 | 14 | 26.81 | 22 | 0 |
| 7 | 6.27 | 15 | 10.08 | 23 | 0 |
| 8 | 16.18 | 16 | 5.30 | 24 | 0 |

| Time (Hrs) | Wind generation (MW) | Time (Hrs) | Wind generation (MW) | Time (Hrs) | Wind generation (MW) |
|------------|----------------------|------------|----------------------|------------|----------------------|
| 1 | 1.7 | 9 | 20.58 | 17 | 3.44 |
| 2 | 8.5 | 10 | 17.85 | 18 | 1.87 |
| 3 | 9.27 | 11 | 12.80 | 19 | 0.75 |
| 4 | 16.66 | 12 | 18.65 | 20 | 0.17 |
| 5 | 7.22 | 13 | 14.35 | 21 | 0.15 |
| 6 | 4.91 | 14 | 10.35 | 22 | 0.31 |
| 7 | 14.66 | 15 | 8.26 | 23 | 1.07 |
| 8 | 26.56 | 16 | 13.71 | 24 | 0.58 |

5 Conclusion

In this framework, a use of a MEMO for EED issue in SMG is created. The proposed EED model for SMG considers the minimization of age and discharge costs as the goal while taking various imperatives, for example, energy balance, activity cutoff points of force sources, and organization qualities into account. To improve streamlining execution, without changing the looking through instrument presents the variable advance size enhancement which improves the development speed and empowers the streamlining resistant to the nearby optima. The adequacy of the proposed technique is affirmed by contrasting the outcomes and the most as of late announced writings, including QGA, EP, and GA. The comparing results show that the ideal planning plan acquired by the proposed EED model will create more prominent financial advantage and social advantages, especially for the huge scope applications. Besides, MEMO has prevalent union, vigor, and less computational intricacies when contrasted with different strategies.

References

- [1] Bishwajit Dey, Shyamal Krishna Roy, Biplab Bhattacharyya, “Solving Multi-Objective economic emission dispatch of a renewable integrated microgrid using latest bio-inspired algorithms”, Elsevier (2019).
- [2] Bishwajit Dey, Parama Das, “Dynamic economic dispatch of microgrid system using hybrid intelligence techniques”, IEEE (2019).
- [3] Dr.E.B.Elanchezian, “Combined Economic Emission Dispatch Considering Renewable Energy Sources”, IJSTR (2019).
- [4] Karthikeyan. R, Subramaniam.S, Elanchezian.E.B, “Grasshopper Optimization Algorithms on Combined Economic Emission Dispatch Problem Involving cubic Functions”, IJEAT (2019).
- [5] Manh Duong Phung, Michel De Villefromoy, Quang Ha, “Management of solar energy in Microgrids using IOT based Dependable Control”, IEEE (2017).
- [6] M.Siva, R.Balamurugan, L.Lakshminarasimman, “Water Wave Optimization Algorithm for Solving combined Economic and Emission dispatch Problem”, ARPN Journal (2017).
- [7] Dongara Ganesh Kumar, Dr.P.Umapathi Reddy, “ Combined Emission Dispatch and Economic Dispatch of Power System Including Renewable Sources”, IJAREEIE (2017).
- [8] Sudhir Phulambrikar, “Solving Combined Economic Emission Dispatch solution using Jaya Optimization Algorithm Approach”, IRJET (2016).
- [9] Wei gu, Zhi Wu, Rui Bo, Wei Liu, Gan Zhou, Wu Chen, Zaijun Wu, “Modeling, planning and optimal energy management of combined cooling, heating and power microgrid: A review”, Elsevier (2014).
- [10] Upasana Sapra, “Solving Combined Economic and Emission Dispatch using Cuckoo Search”, IJETT (2013).
- [11] Qiang Fu, Luis F.Montoya, Ashish Solanki, “Microgrid Generation Capacity Design with Renewables and Energy Storage Addressing Power Quality and Surety”, IEEE Transactions on Smart Grid (2012).
- [12] Vahidsarfi, Haniflivani, Loganyliniemi, “A new multi objective economic emission dispatch in microgridsPaCcet algorithm”, IEEE 2017.
- [13] Tapanprakash, V. P. Singhself, “Economic load dispatch problem: quasi-oppositional self-learning tlbo algorithm”, Springer Paper, July 2016.
- [14] Sneharanisubhajitroy, Kuntalbhattacharjee, “Teaching learning based optimization to solve economic and emission scheduling problems”, International Conference, December 2016.
- [15] S. Bhongade, Sourabharwal, “An optimal solution for combined economic and emission dispatch problem using artificial bee colony algorithm”, IEEE paper, October 2016.
- [16] N.Kherfane, R.L.Kherfane, M.Younes, F.Khodja, “Economic and emission dispatch with renewable energy using harmony search algorithm”, Elsevier paper, June 2014, pp. 970-979.
- [16] R. Arul, S.Velusami, G.Ravi, “Solving combined economic emission dispatch problems using self-adaptive differential harmony”, ICCPCT Conference, 2014.
- [17] Mojtabaghasemi, Sahandghavidel, Mohsengitizadeh, Ebrahimakbari, “An improved teaching-learning based optimization algorithm using lévy mutation strategy for non-smooth optimal power flow”, Elsevier paper, October 2014, pp. 375-384.
- [18] Naveedahmed Khan, Ahmedbilawan, Anzarmahmood, “Combined emission economic dispatch of power system including solar photo voltaic generation”, Elsevier Paper, December 2014, pp. 82-91.
- [19] R. Gopalakrishnan, A. Krishnan, “An efficient technique to solve combined economic and emission dispatch problem using modified ant colony optimization”, IEEE transaction power system. Vol. 38, part 4, August 2013, pp. 545-556.
- [20] A. Chatterjee, S.P. Ghoshal, V. Mukherjee, “Solution of combined economic and emission dispatch problems of power systems by an opposition-based harmony search algorithm”, Elsevier Paper, February 2012.
- [21] R. Venkatarao, R. Vivekpatel, “An improved teaching-learning-based optimization algorithm for solving unconstrained optimization problems”, Elsevier Paper, October 2012, Pp. 710-720.
- [23] R. Venkatarao, Vivekpatel, “Multi-objective optimization of heat exchangers using a modified teaching-learning-based optimization algorithm”, Elsevier Paper, March 2012, pp. 1147-1163.

Effect of DC Ripple and Commutation on the Line Harmonics of Current-Controlled AC-DC Converters

V. Balaji
Assistant Professor EEE Department

Abstract

Line harmonics are usually predetermined under the simplified assumption that the dc current is sufficiently smoothed. However, in practical operation of controlled converters, e.g., feeding medium-size dc drives, it frequently happens that the dc ripple cannot be neglected. For the predetermination of line harmonics, this means that the operating point is specified by the emf and the mean value of the dc current, i.e., the associated control and commutation angles, are unknown. The consideration of the basic effects of commutation and dc ripple leads to line current harmonics that are separated into positive and negative sequence systems. Selected results of systematic evaluations show the amplitude and phase as a function of dc reactance as well as of the emf and mean dc current in the range of usual low- and medium-voltage supply networks. In comparison with the conventional pre calculation assuming sufficient dc smoothing, significant deviations occur in the case of higher dc ripple.

Introduction

Since the share of converter loads in electrical power supplies is increasing, the disturbances they cause must also be increasingly taken into account. In the case of current-controlled ac/dc converters, these disturbances include not only the variable reactive power consumption but, in particular, the harmonics of the line current that generate corresponding voltage harmonics at the internal impedance of the supply network. In the interest of other loads, these voltage disturbances may not exceed certain limits (compare, e.g., [1] and [21]) and should therefore be known at the planning stage. The line current harmonics are usually predetermined under the assumption that the dc current is sufficiently smoothed. For Paper ICPSD 91-9, approved by the Power Systems Engineering Committee of the IEEE Industry Applications Society for presentation at the 1991 Industrial and Commercial Power Systems Conference, Memphis, TN, May 6-9. Manuscript released for publication September 11, 1992. M. Grotzbach is with the Department of Electrical Engineering, University of Federal Defence Munich, Neubiberg, Germany. Draxler is with the Municipal Utility, Munchen, Germany. IEEE Log Number 9210103.

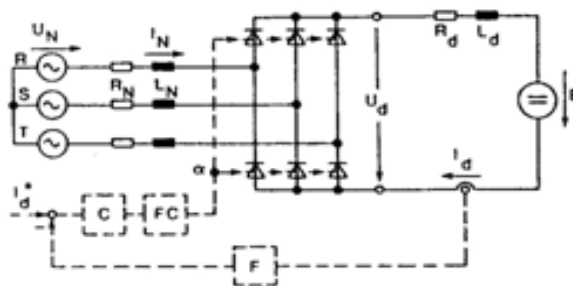


Fig.1. Basic circuit of a current-controlled six-pulse bridge converter:

the calculation, this means a decoupling between the three-phase and the dc side, and therefore, a correspondingly simple predetermination is feasible. However, in practical operation of controlled ac/dc converters, it frequently happens that the dc current shows a ripple that cannot be neglected. This appears in cases such as medium-size dc drives in which an additional dc inductance is omitted for cost reasons.

Starting from a simplified time behavior of the line current, [3] specifies the basic effect of the dc ripple on the harmonics, [4] takes the influence of commutation into account approximately, and calculations are carried out in [5] and [6] for given control angles. For controlled converters, however, the mean dc current determines the operating point, i.e., the associated control and overlap angles are unknown and must therefore be determined. This is usually performed by means of digital simulation in the time domain or directly with the aid of Newton's method [7], [8]. Starting from these preliminary

works, the influence of dc ripple and commutation will be investigated systematically. Fig. 1 shows the basic circuit of a controlled six-pulse bridge converter considered here, where

C: current controller, FC: firing control, F : filter, and I_d : current set point given by supervised control system, e.g., for dc drives usually by the speed controller.

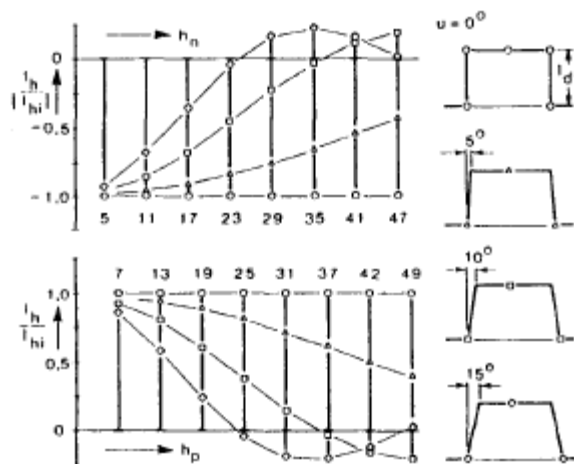
Basic effect of Commutation and Ripple

In this introduction, the basic effect of commutation and dc ripple on the harmonics of the line current will be derived from the literature and presented in line with our further objectives. For the *idealized* square-wave shape of the line current of a six-pulse bridge circuit, i.e., neglecting commutation and dc ripple, the well-known Fourier series applies if the zero-point $\omega t = 0$ is chosen at the midpoint of a positive square wave. From the ideally smoothed dc current I_d , the amplitude of the fundamental is $I_{h1} = 2\sqrt{3} I_d / \pi = 1.10 I_d$. The harmonics of order $h = 6k \pm 1$ are determined by $I_{hi} = I_{h1} / h$, where $h = 6k + 1 = 7, 13, 19, \dots$ represent positive and $h = 6k - 1 = 5, 11, 17, \dots$ negative sequence systems [9].

The effect of the *commutation* can be described approximately in the usual firing-angle range of controlled ac/dc converters by a trapezoidal line current waveform, and then applies for the harmonics, where U is the overlap angle [lo]. It should be noted that the curve $I_{hc} = f(h)$ for $hu/2 = R$ contains a zero crossover, $7r < hu/2 < 27r$ means a sign change with respect to the idealized value I_{hi} . Fig. 2 shows line current waveforms and the corresponding harmonics split into negative sequence systems $I_{hc}/I_{hi} (= f(h_n))$ and positive sequence systems $I_{hc}/I_{hi} = f(h_p)$. The special case $U = 0$ corresponds to the idealized square-wave shape according to (1), which is further used as the reference value for the harmonic amplitudes.

To explain the basic effect of the *dc ripple*, it is initially useful to consider the operation at the pulsation limit with $\text{emf } E = 0$. Neglecting the ohmic resistances, the mean value of the dc current is where U_N phase voltage of the network $X_d = \omega L_d$ dc reactance $X_N = \omega L_N$ network reactance $\omega = 2\pi f$ with f network frequency. In this boundary case, the amplitude of the fundamental of the line current $I_{h1} = 1.12 I_d$ is idealized value $I_{h1} = 1.10 I_d$, where $I_d = I_{d, \text{mean}} = I_d = \text{const}$ as shown in Fig. 1 with respect to the further treatment of current-controlled converters. For the harmonics of the positive and negative sequence systems applies [lo], and the reference to the idealized value $I_{hi} = I_{h1} / h$ according to (1) and (3) lead to the normalized harmonics of the line currents.

With this, the basic effect of dc ripple on the amplitudes of the line current harmonics is represented in Fig. 3, where it is separated into negative and positive sequence systems. Thereby, the symbol “o” indicates the idealized dc smoothing $I_d/I_{d, \text{mean}} = 1$, where $I_{d, \text{mean}}$ is the mean dc current. The other boundary case “0” characterizes the behavior at the pulsating limit, i.e., $I_d/I_{d, \text{mean}} = 0$. The parameter $I_d/I_{d, \text{mean}} = 0.75, 0.5,$ and 0.25 corresponds to the part of the idealized dc current,



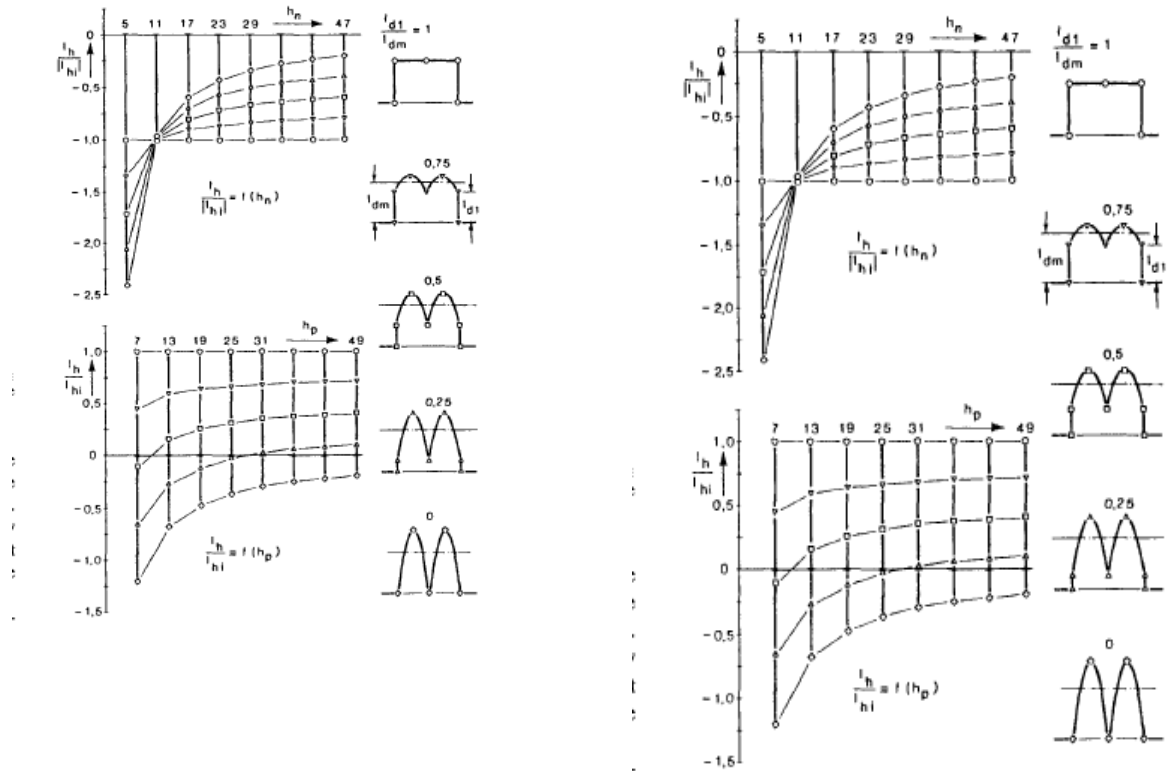


Fig. 3. Normalized amplitudes of the line current harmonics $I_h / |I_h|$ for the current ratios $= 1$ (o), 0.75 (v), 0.5 (U), 0.25 (A), and 0 (0).

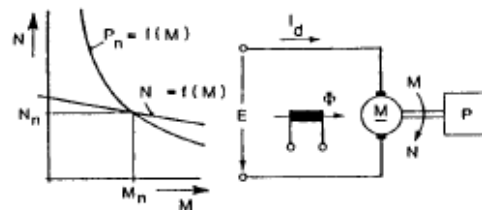


Fig. 4. Working point given by a dc drive (example): N versus M -Diagram and basic configuration.

and the mean dc current I_{dm} is kept constant. This presentation shows very clearly the distinct effect of the dc ripple; all positive sequence systems have the property of traversing a zero point at higher ripple ending in the opposite phase. The negative sequence systems retain their sign, and the strong increase of the fifth harmonic contrasts with correspondingly great reductions in the higher harmonics.

Determination of the Working Point

In practical operation, the mean value of the dc current and **not** the control angle is the characteristic value for the working point of the controlled converters. As an example, the torque of a dc shuntwound motor is produced proportionally to the mean dc current. The working point of the converter follows from the mechanical requirements

on the shaft (see Fig. 4), where N is the rotational speed, M is the torque, and P is the actual power. In the base speed range $N \leq N_b$, and in field-weakening range $N > N_b$, the mean dc current is given

By respectively. In both cases, the emf follows under consideration of the motor efficiency η at the working point as where $I, M, N,$ and P , are nominal motor values. In summary, the working point of the controlled converter is determined by the mean dc current I_{dm} and the emf E . This leads to the objective, for the case under consideration of a rippled dc current, of determining the associated control and overlap angles.

The calculations are based on a current-controlled six-pulse bridge as shown in Fig. 1, stationary-symmetrical conditions and simple commutation in continuous operation assumed; discontinuous operation was investigated in [11]. The parameters considered are, apart from the operating point (mean dc value $I_{dm} = I_d$; and emf E) the circuit data (network and dc reactance $X_N = 2r_f N L N$ and $X_d = 2T f N L d$, where $f N$ is the net frequency). Usually, the ohmic resistances R_N and R_d have less influence on the harmonic spectrum [12], [13]; if required, they can be taken into account approximately by an additional emf $A_E = I_{dm} (R_d + 2R_N)$. The complete calculation of the line current harmonics has already been treated in preliminary works; the most important points will now be summarized. Starting from a piecewise analytical description, the difference equation of the dc current can be set up; its stationary value at the beginning of commutation is which agrees with the result of the conventional converter model which is valid for good dc smoothing [9], [16]. It should be noted that the actual dc mean current I_{dm} is always greater than the approximated dc current $I_{d0} = I_d$; compare this with the corresponding time behavior in Fig. 5.

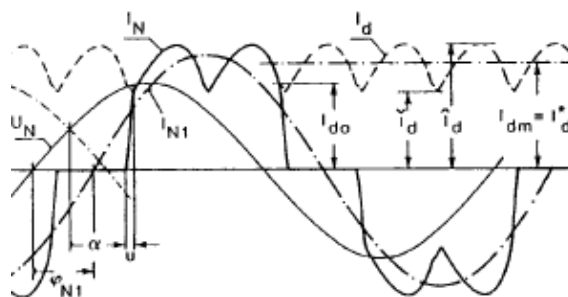


Fig. 5. Selected time curves for definitions.

Fig. 5. Selected time curves for definitions.

After the differential equations given in each time interval have been solved, the line current can be specified analytically as a function of the control and overlap angles. For these two unknown values α and U , two nonlinear conditions can be specified from the circuit function, $I_d = I_{dm}(\alpha, U)$ after integration of the dc current and $E = E(\alpha, U)$ from the end of commutation [15]. In this way, the operating point specified by I_{dm} and E determines the unknown angles α and U , which can be most conveniently calculated by Newton iteration. The spectrum of the line current can be simply determined with the aid of a standard FFT program since the line current is given in piecewise analytical form.

Representation of Selected Results

A. Normalization and Assumption

To simplify the presentation, the following normalization is used: Reference for the reactances is $R = U_N / \omega$, i.e., the normalized values $X_d = \omega R$, and $X_N = X_N / R$, are proportional to the mean dc current. The emf E is usually referred to the idealized dc voltage $u_{dio} = 2.34 \cdot U_N$, i.e., $e = E/u_{dio}$ and $A_e = I_{dm} (\omega R + 2R_N)$

/ **U d i o** . The phase Of the complex harmonics **I h** refers, corresponding to Fig. 5, to the zero transition of the supply voltage, i.e., $v_h = A(uN, I_h)$.

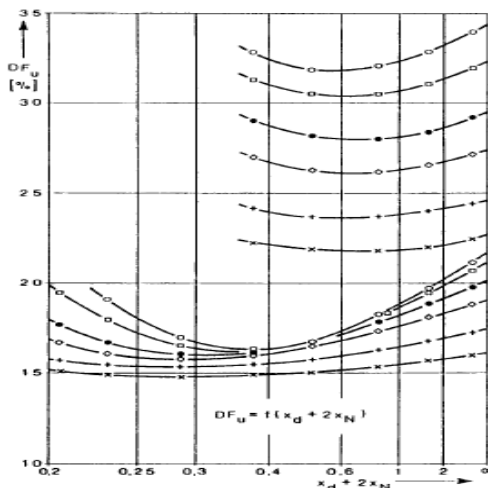


Fig. 6. Amplitude spectrum of the line current harmonics negative (left) and positive sequence systems (right); low-voltage supply ($z, y = 7.5\%$) and emf $e = 0$ assumed; parameter: reactance

In this section, the complex line harmonics will be investigated as a function of the dominant parameters, i.e., depending on the circuit data such as net and dc reactance as well as on the operating point given by emf and mean dc current. Using the proposed reference value $R_s = \frac{uN}{Idm}$, these parameters are reduced to XN , x_d , and e . Only two network reactances $xN = 7.5$ and 15% are considered for reasons of space, corresponding to a usual low- and medium-voltage supply network, respectively. In order to reduce parameters, the influence of ohmic resistances is not considered here, i.e., $Ae = 0$.

B. Amplitudes of the Line Current Harmonics

The behavior of the amplitude spectrum for various values of the reactance sum $X_d + 2X_N$ is investigated here, taking the sign into account at the operating point $e = 0$ but only the amplitude at $e = 0.8$. Figs. 6 and 7 represent the results for the exemplary low-voltage network. Table 1 explains the symbols used and additionally specifies the angles U and a as well as the dc current ripple with id and Id as in Fig. 5. Figs. 8 and 9 show the corresponding results for the selected medium-voltage network, and Table 11 lists the relevant explanations. It should be noted that in the case of emf $e = 0$, the simple relation $a + u/2 = 90^\circ - eZ$ is valid for any dc ripple [151].

TABLE I
SYMBOLS FOR THE REACTANCE SUM $x_d + 2x_N$ USED IN FIGS. 6 AND 7 AND CORRESPONDING SPECIFICATIONS

| symbol | (•) | (x) | (Δ) | (+) | (□) | (∇) | (○) |
|----------------|------|------|------|------|------|------|-------|
| $x_d + 2x_N$ | 16 | 1 | 0.6 | 0.4 | 0.3 | 0.25 | 0.218 |
| $u[^\circ e1]$ | 3.5 | 2.8 | 2.4 | 1.8 | 1.1 | 0.5 | 0 |
| $r[\%]$ | 1.8 | 29.8 | 50.5 | 77.4 | 106 | 129 | 151 |
| $u[^\circ e1]$ | 5.8 | 5.3 | 4.9 | 4.3 | 3.8 | 3.2 | 2.6 |
| $a[^\circ e1]$ | 33.9 | 34.1 | 34.3 | 34.6 | 34.9 | 35.2 | 35.5 |
| $r[\%]$ | 1.1 | 17.3 | 29.4 | 44.5 | 60.0 | 76.1 | 92.8 |

The representation of the line current harmonics separated into positive and negative sequence systems permits a direct comparison with the fundamental dependencies according to Figs. 2 and 3, i.e., a discussion of the effect of commutation and ripple. If the waveform for good smoothing is compared with the actual behavior of the spectrum, then the greatest differences occur at the low-frequency harmonics $h = 5$ and 7 . In addition, the deviations of the positive sequence systems

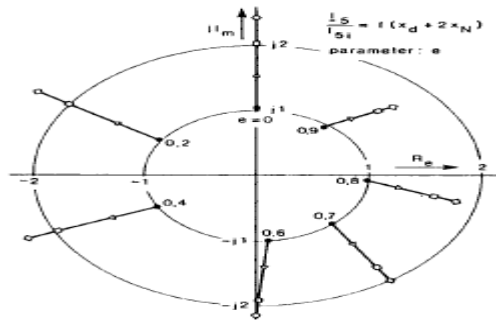


Fig. 7. Amplitude spectrum of the line current harmonics negative (above) and positive sequence systems (below); low-voltage supply ($X N = 7.5\%$) and emf $e = 0.8$ assumed; parameter: reactance sum $i d + 2 X N$.

TABLE II
SYMBOLS FOR THE REACTANCE SUM $x_d + 2x_N$ USED
IN FIGS. 8 AND 9 AND CORRESPONDING SPECIFICATIONS

| symbol | (*) | (v) | (x) | (+) | (Δ) | (O) | (Q) |
|----------------|------|------|------|------|------|------|------|
| $x_d + 2x_N$ | 16 | 2 | 1.2 | 0.8 | 0.6 | 0.45 | 0.35 |
| $u[\%e1]$ | 7.0 | 6.5 | 6.1 | 5.6 | 5.1 | 4.3 | 3.3 |
| $r[\%]$ | 1.6 | 13.1 | 22.2 | 33.9 | 46.0 | 63.1 | 88.3 |
| $u[\%e1]$ | 11.8 | 11.4 | 11.1 | 10.8 | 10.4 | 9.7 | 9.2 |
| $\alpha[\%e1]$ | 30.5 | 30.7 | 30.9 | 31.0 | 31.2 | 31.5 | 31.7 |
| $r[\%]$ | 0.9 | 7.4 | 12.5 | 18.8 | 25.7 | 37.6 | 45.5 |

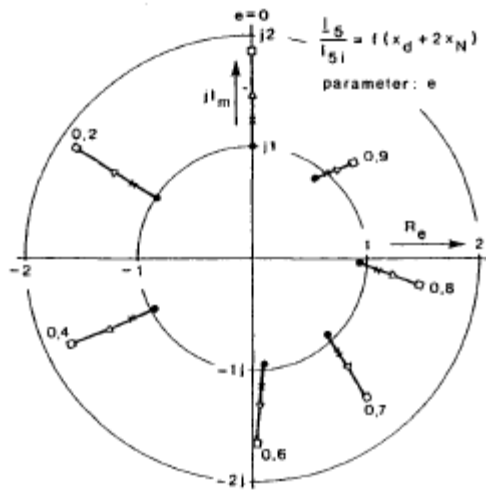


Fig. 8. Amplitude spectrum of the line current harmonics negative (above) and positive sequence systems (below); medium-voltage supply ($Z N = 15\%$) and emf $e = 0$ assumed parameter: reactance sum $X d + 2 X N$.

h , are generally greater than those of the negative sequence systems h , which can be explained by the negative sign in(6). As a result of the dc ripple, higher harmonics can also reach greater values than those described by the conventional model assuming good dc smoothing.

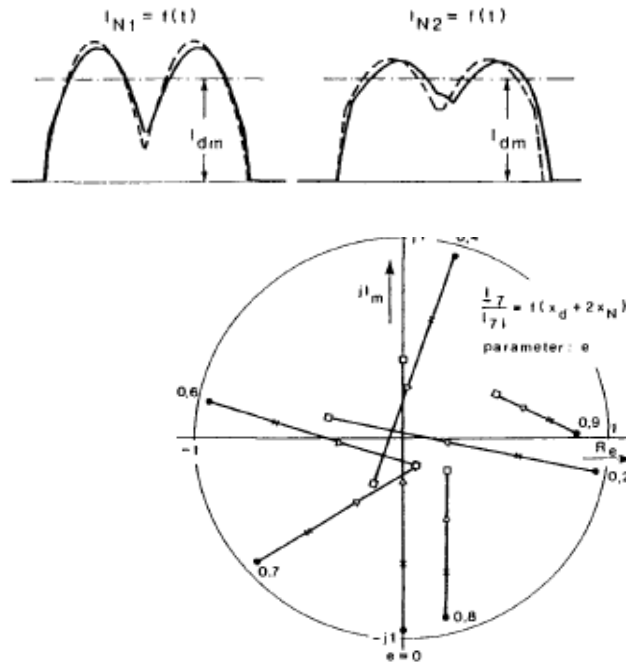


Fig. 9. Amplitude spectrum of the line current harmonics negative (above) and positive sequence systems (below); medium-voltage supply ($x \approx 15\%$) and emf $e = 0.8$ assumed; parameter: reactance sum $X d + 2x_N$.

This means in relation to the value for ideal current harmonics $D_{i,} = 30\%$, an increased distortion by 77%. Note that the errors caused by using the smoothed dc current assumption are even higher; compare also simulations and laboratory experiments in [17].

D. Mains Voltage Harmonics and Distortion Factor

Each line current harmonic produces a corresponding volt-age drop across the equivalent supply impedance. If a purely inductive mains is assumed, equal amplitudes of voltage harmonics occur according to the idealized harmonic law

C. Harmonic Line Current Distortion

The influence of dc ripple and commutation on the harmonic line current distortion is defined by and is outlined in Fig. 10 in the region $0.25 X d + 2x_N \leq 5$ for the two network reactances $X N = 7.5$ and 15% and the emf's $e = 0$ and 0.8 . For the upper limit of current harmonics, $N= 19$ is sufficient due to the strong decrease of the quadratic terms $(I_h/I_1)^2$ for higher harmonics. In comparison with the usual assumption of an ideal dc smoothing, i.e., since the real fundamental I_1 differs only slightly from the idealized value I_1 , even with dc ripple, the harmonics of the mains voltage $u_h = I_h X N$ may be estimated as follows This result means that the mains voltage harmonics can also be obtained from Figs. 6 and 7 or 8 and 9.

Finally, it is intended to specify the voltage distortion factor as the value that is frequently the most important one in assessing the voltage quality of the mains **network reactances $XN = 7.5\%$ (below) and 15% (above); emf $e = 0$ (o), 0.4 (U), 0.6 (0), 0.7 (O), 0.8 (+), and 0.85 (x).**

For this purpose, Fig. 11 shows the $DF, = f(X d + 2 X N)$ curves for the network reactance $X N = 7.5$ and 15% , with emf e as a parameter. The results are based on taking into account harmonics in a range up to $h = 50$ corresponding to the standard [1], i.e., $N = 49$ in (16). As the dc reactance $x d = X d/R_n = I d m X d / U N$ decreases, the voltage distortion factor passes through a minimum. This effect corresponds to the appropriate curves for the

line current harmonics of positive sequences, where the increase in the fifth and seventh current harmonics produce the rise for low dc smoothing.

The total voltage distortion factor represented here refers to the connection point of the converter bridge circuit. Otherwise, the corresponding voltage divider $X_s / (X_s + X_T)$ has to be taken into account, with the reactance X_s for source and X_T for transformer or line reactance. However, the investigation of more complex supply networks is based on the matrix equation

$U_{bus} = \mathbf{Z}_{bus} \cdot \mathbf{I}_{bus}$, where the spectral information of the injected currents considered here is required; for more details, see, e.g., [9] and [18].

E. Loci of the Complex Line Current Harmonics

The effect of emf $e = E/U_{dio}$ and dc reactance $X_d = x_{dIdm}/uN$ can be lined out in the complex plane; the loci describes the behavior of the pointer peaks of the harmonics. By limiting to the two lowest frequency harmonics $L5$ and $-I_5$, Figs. 12 and 13 show the normalized results I_h / I_{hi} as a function of the reactance sum $Z_d + 2X_N$, which is one of the dominant parameters determining the dc ripple; discrete values of the emf e are used as parameters. Here, the presentation of the influence of the dc reactance x_d results with sufficient accuracy in loci as straight lines.

Evaluation and Discussion Effect of DC Ripple and Commutation

The values marked with the symbol “0” correspond to the conventional behavior for good dc smoothing, and “()” in Fig. 12 applies to $x_d + 2X_N = 0.218$, i.e., operation at the pulsation limit for $e = 0$ according to (6) and (7). In the special case of $e = 0$, all pointer peaks lie on the imaginary axis; with increasing values of e , the straight lines are rotated around the origin proportionally to the reduction of the control angle α . It should be noted that according to Fig. 3, the positive sequence system $hp = 7$ shows a zero transition of the amplitude only for $e = 0$. For negative values of e , i.e., for inverted rotation immediately the relative deviations due to the commutation, and Fig. 3 lines out the results for dc ripple. With increasing emf, the approximation of the dc ripple by symmetrical sine tops [3], [4] leads to increasing errors, especially in the determination of the phase angle of the harmonics of positive sequence. An example of an asymmetry in the line current tops, which is neglected in this approximation, is shown in Fig. 14 and leads to a corresponding rotation of the straight lines away from the origin in the loci $L7/f7$ (in Figs. 12 and 13).

The evaluation proposed is based on the consideration of five dominant parameters, i.e., the operating point (I_{dm}, E) and the circuit data (X_d, X_N, U_N) . As a result of the cho-sen normalization, these five parameters are reduced to the following three: $e = E/U_d$; $x_d = X_d / (U_N I_{dm})$, and $X_N = X_N / (U_N / I_{dm})$. Note that the normalized reactances depend on the operating point $x_d, N N f d m$. The specified amplitude spectra refer to characteristic values of the network reactance in usual low- or medium-voltage supplies and thus permit a more realistic predetermination of the line current harmonics. It can be seen that these representations show differences from the usual assumption of a good-smoothed dc current, which are considerable in the case of higher dc ripple. Considering the results of Figs. 10 and 11, it becomes clear that the worst case for the voltage distortion factor DF , is given by the usual calculation, assuming ideal dc smoothing. In contrast with this, higher dc ripple leads to a significant enlarged current distortion D ; from the value with good smoothing both in amplitude and especially in phase. These deviations, which are considerable, in the of high dc lead to correspondingly modified line current and voltage distortion.

References

1. IEEE 519, *Guide for Harmonics Control and Reactive Compensation of Static Power Converters*. New York: IEEE, 1981.
2. DKE, “Electromagnetic compatibility,” *DINNDE 0839*, Draft, Feb. 9, 1990 (in German).
3. L. G. Dobinson, “Closer accord on harmonics,” *Electron. Power*, vol. 15, pp. 567-572, May 1975.
4. A. D. Graham and E. T. Schonholzer, “Line harmonics of converters with dc-motor loads,” *IEEE Trans. Ind. Applicat.*, vol. IA-19, pp. 849-853, Jan./Feb. 1983.

- 5.M. Sakui, A. Yanase, and H. Fujita, "Line harmonic current of three-phase thyristor bridge rectifier circuit with dc current ripple and over-lapping angle," *Elec. Eng.* Japan, vol. 105, no. 6, pp. 48-55, 1985.
- 6.S. De Haan, "Analysis of the effect of source voltage fluctuations on the power factor in three-phase controlled rectifiers," *IEEE Trans. Ind.Applicat.*, vol. IA-22, pp. 259-266, Mar./Apr. 1986.
- 7.M. Grotzbach and R. von Lutz, "Evaluation of converter harmonics in power systems by a direct and analytical based state variable approach," in *Proc. EPE* (Brussels), 1985, vol. 1, pp. 2.153-2.158.
- 8.K. R. Padiyar and P. K. Kalra, "Analysis of an HVDC converter with finite smoothing reactor," *EZec.. Power Syst. Res.*, vol. 11, pp. 171-184,1986.
- 9.J. Arrillaga, D. A. Bradley, and P. S. Podger, *Power System Harmonics*. Chichester: Wiley, 1985.
- 10.G. Moltgen, *Line commutated converters with thyristors*. Berlin-Miinchen: Siemens, 1974 (in German).
- 11.M. Grotzbach, T. StraOer, and L. Lorenz, "Line side harmonics of three-phase current controlled rectifiers in continuous and discontinuous operation mode," in *Proc. EPE* (Grenoble), 1987, vol. 2, pp. 701-712.
- 12.H. Arremann and G. Moltgen, "Line current harmonics of line commu-tated six-pulse bridge converters," *Siemens F.-u.E.-Ber.*, Bd. 7, no. 2, pp. 71-76, 1978 (in German).
- 13.J. Arrillaga, J. F. Eggleston, and N. R. Watson, "Analysis of the ac voltage distortion produced by converter-fed dc drives," *IEEE Trans. Ind. Applicat.*, vol. LA-21, pp. 1409-1417, Nov./Dec. 1985.
- 14.M. Grotzbach and R. von Lutz, "Unified modelling of rectifier-controlled dc-power supplies," *IEEE Trans. Power Electron.*, vol. PE-I, pp. 9CL100, Apr. 1986.
- 15.M. Grotzbach and G. Vogel, "Line current harmonics of three phase bridge-converters with dc ripple and variable emf," *etzdrchiv*, Bd. 8,
- 16.W. M. Grady, A. E. Emanuel, H. A. Khatib, and M. T. Doyle, "The effect of dc smoothing inductance on converter current distortion," *Proc. IEEE-ICHPS* (Budapest), pp. 214-217, 1990. G. T. Heydt. "The present status of harmonic power flow studies," in *Proc. EECPS-Symp.* (Caprintaly), invited paper W-IP.2, May 1989.

An Overview on Multiport DC-DC Converters for Integration and Energy Harvest from Renewable Energy Sources

Dr. C.R. Balamurugan
Department of EEE,
Karpagam College of Engineering, Coimbatore,
Tamil Nadu, India
crbalain2010@gmail.com

N. Ramadevi
Department of EEE,
GRT Institute of Engineering and Technology,
Tamil Nadu, India
nramadevi14@Gmail.com

Dr.T.Sengolrajan
Department of EEE
Kongunadu College of Engineering and Technology, Thottiam, Trichy, Tamilnadu
sengolmaha@gmail.com

Abstract

It is well known fact that dc loads are growing drastically in past two decades and at the same time the fossil fuels are getting exhausted rapidly. So there comes the need of efficient energy harvest systems from various renewable energy sources to meet the increased load demand. In recent past, as a solution to this, the researchers and academic scholars have developed and are still developing various DC-DC converter topologies. Multiport converters are more efficient, reliable and have minimal complex structures compared to other converter topologies. This paper surveys various Multiport DC-DC converters, its design structures used in integration of renewable energy sources in the process of efficient energy extraction from various renewable energy sources in the event of meeting the load demand. Since the literature reports huge number of topologies and design of Multiport DC-DC converters trying to achieve higher performance, reliability and efficiency with reduced cost in this field, it is quite confusing and challenging to select the desired Multiport DC-DC converter topology for a specified application. This article highlights the advantages and limitations of various topologies and design structures and gives clear idea of selection of the converter for the specific application.

Keywords— Multiport DC-DC converter, Renewable Energy Supply System, Isolation, Reliability, Gain.

Introduction

DC supply system is having its own advantageous nature of less transmission loss, absence of alternating magnetic fields, higher efficiency, easy to control the parameters like torque, speed, etc. in case of DC drive systems, lower set-up cost, more suitable for distributed renewable energy resources and many more. At the same time, human's life style and comfort living resulting in development of various DC domestic appliances. In overall, in real time applications DC loads are increased and increasing greatly. This made everyone to depend on renewable energy sources to meet the load demand. But the problem with Renewable Energy Supply systems (RESs) is its intermittency nature, which further impact on the reliability and applicability of the RESs. Another problem is mismatch of power generation and load demand in RESs concepts. Practically renewable energy supply will be sometimes higher and sometimes lower, not constant, not stable, will be fluctuating.

At the same time load demand is also varying type mostly in practice. As a solution to address these problems Energy Storage Systems (ESS) – batteries are used in the RESs. In this concept there will be two-way flow of power is made. When the supply is more than the demand, it can be stored in battery and when the demand is more, supply from both the renewable energy source and battery can be directed to load. Also as the load demand is higher, single unit of RES will not be sufficient to meet the load demand. So there comes the hybrid RESs, where different types of RESs are integrated along with ESSs. This system gives better reliable RESs named Hybrid RESs (HRESs). These RESs can be able to supply DC loads of fraction of Voltage to tens of kilo voltage and mill watts to megawatts for diverse applications.

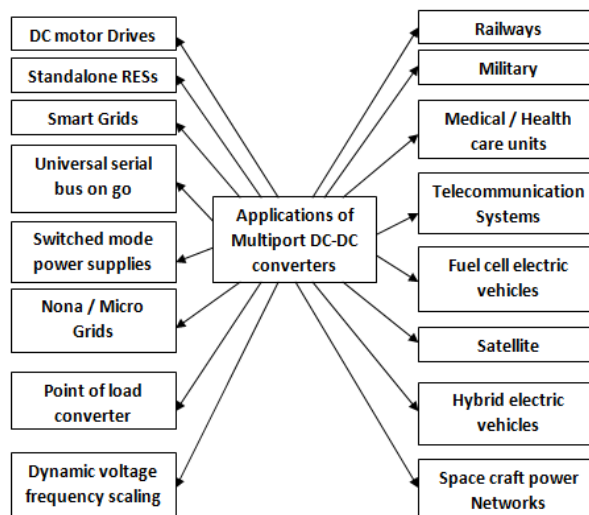


Fig.1. Applications of Multiport DC-DC Converters

In this article the various categorizations of the multiport converters, the need for various converter topologies, problematic issues faced and its various advantages, disadvantages are discussed in detail under section II. The various applications of different types of converters are highlighted in section III. The challenges faced in implementation of multiport converter is discussed in detail under section IV followed by conclusion of this article in section V.

I. CATEGORIZATION OF MULTI-PORT DC-DC CONVERTERS

A. Based on number of input and output ports

The classical model of DC-DC converter is simply addressed as Single-Input-Single-Output (SISO) converter, which is basically a two-port network configuration. According to the applications i.e. load demand, availability of source, nature and I-V characteristics of source and loads, the SISO converters [40] has to be modified and there comes the different converter structures. To meet the increased DC load demand, single unit of renewable energy source will not be sufficient. So more than one units of renewable energy source are need to be used. In such cases the immediate option is the implementation of multiple SISO converters. But this increases more components usage which is undesirable and it results more problematic issues like increased switching losses; voltage stress on components, driver and control units gets complex and many more issues arises. To overcome these problematic issues many designs of converter topologies were developed [11], [15], [22], [28]. The literature gives us many kinds of converter structures in recent past. These converters can be categorized in the name of multiport converters as Multi-Input-Single-Output (MISO) converters, Single-Input-Multi-Output (SIMO) converters and Multi-Input-Multi-Output (MIMO) converters as shown in Fig.2. MIMO converter is basically a Multi-port network configuration. The multiport converters has various advantages and more attracted for its key features of simple design, modular structure, lower component count, ease of control, less conversion stages. The applications of multiport converters are DC motor drive systems, switched mode power supplies, uninterrupted power supplies, nano grids / micro grids / smart grids, hybrid energy supply systems with and without battery energy storage systems, telecommunication systems, emitting diode display systems, satellites, healthcare units, railways, defence, space craft power networks, fuel electric vehicles / hybrid electric vehicles and many more applications. This article will discuss in detail about the problem faced and the need of modifications in basic SISO converters and also highlights the importance and applications of MISO, SIMO and MIMO converters. Fig.1. shows the various applications of Multiport DC-DC Converters.



Fig.2. Categorization of multiport DC-DC converter based on number of input and output ports.

The basic multiport converters are mostly the classic buck / boost / buck-boost / cuk converters. If the application is of low power or low voltage requirements then either SISO or MISO [1-5], [7], [8], [13-14], [21-25], [27], [28], [29], [30], [32] can be used. If the application demands various voltage levels then either SIMO [10], [12], [19], [20], [26], [31], or MIMO [6], [9], [17], [18] converters can be implemented with ESS [4], [7], [10], [11], [13], [15], [17], [23], [24], [27], [29].

B. Based on isolation demand

Converters can be provided with and without isolation transformer. Hence two types of converters are possible practically, namely isolated converters and non-isolated converters as shown in Fig.3. The major drawbacks of isolated DC-DC converters

are costly, bulky, circuit parameters dependency, complexity of control units [5-7], [9]. The non-isolated converters are advantageous like simple design, less cost, less weight, simple control features. Non-isolated converters are provided with and without magnetic coupling where high gain and cost effective is the major concern respectively [1], [2], [11], [13], [14], [15], [17], [19-23], [25], [31].

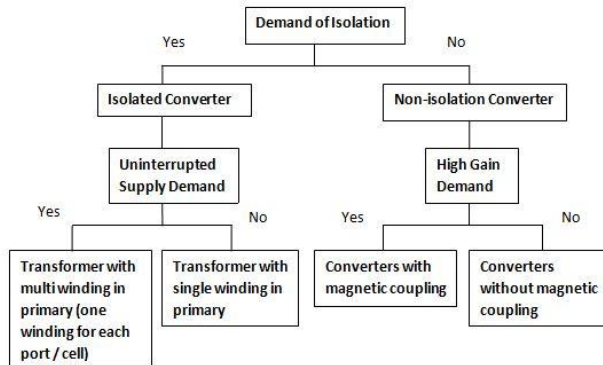


Fig.3. Categorization of multiport DC-DC converter based on demand of isolation.

C. Based on Gain value

If gain value is the major demand, the converters are modified in design to provide the required converters with specified gain value. The classification of converters based on gain value requirements is shown in Fig.4. The number of secondary coil turns in the transformer in isolated converters can be increased to achieve required gain value, so that the input voltage will to boost as per load demand where as in non-isolated converter with the converters with high gain factor can be used for voltage boosting. But limitations in case of high gain non-isolated converters are more number of semiconductor switches and passive elements are used to achieve the specified gain demand. Most of the converter topologies are given in literature which tries to enhance the voltage gain of the model [11], [13], [15], [16], [22], [23], [26], [28]. In case of low gain requirements the converter circuit are advantageous for its reduced voltage stress on components, less component count with increased efficiency, reliability and reduced cost.

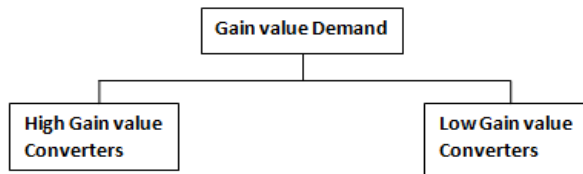


Fig.4. Categorization of multiport DC-DC converter based on Gain value.

D. Based on power flow direction

Converters are classified as unidirectional and bidirectional multiport converters as shown in Fig.4. In unidirectional multiport DC-Dc converters the power flows from source to load only whereas in the case of bidirectional multiport DC-DC converters the power flows in either direction i.e. from source to load also from load to source [13], [23], [24]. Unidirectional converters have advantages of simple control units and control methods and less component count. In unidirectional multiport DC-DC converters the loads receive supply from sources individually/simultaneously [17], [22]. In later case either bidirectional switches are employed or two individual unidirectional converts are employed. But in order to reduce the component count the bidirectional converter is preferred.

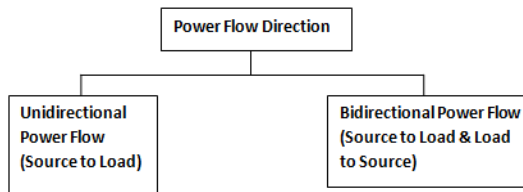


Fig.5. Categorization of multiport DC-DC converter based on power flow direction.

E. Based on converters in series/parallel connection with source

Converters can be connected either in series or parallel connection with source as referred in Fig.6. Former provides low gain [18], [24], [25] whereas later provides high gain [3], [4]. In multiport converters single output systems can be converted into multiple output converters by connecting the outputs in series, used mainly in applications where ESS units are implemented.

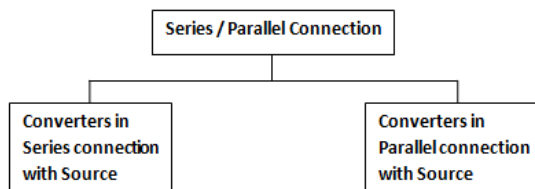


Fig.6. Categorization of multiport DC-DC converter based on converters in series/parallel connection with source.

In case of converters in parallel connection with source, loads can be connected in parallel to achieve high gain. Here the single output system can be converted to multiple voltage levels at load end by the use of optimum switching sequence and control units.

F. Based on modularity and non-modularity

Modularity feature of converter is mostly preferred for ease of addition and removal of sources without disturbing rest of units, it is highly reliable structure. In general modularity feature of the converter provide plug and play operation [7-9], [12]. Fig.7 indicates the classification of multiport converters as modular and non-modular structure. In case of MIMO converters modularity is applicable for both the source and load ends. The non-modular structure is one in which in some applications, ESS will be allowed to be charged by the source and the discharge processes will be dependent on the load requirements. ESS will be made to be connected in parallel to the sources and then independently/simultaneously discharged to meet the load demand.

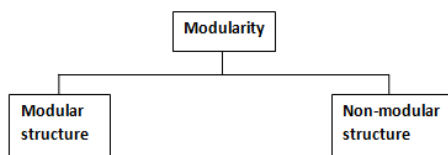


Fig.7. Categorization of multiport DC-DC converter based on modularity and non-modularity feature.

II. SELECTION OF MULTIPOINT DC-DC CONVERTERS FOR SPECIFIC APPLICATIONS

If the efficiency of the converter topology is higher, the reliability of the system will also be greater. The reliability of the system gets reduced due to increase in number of inputs, aging of the components / devices, due to increase in number of switches / diodes and operating temperature will cause increase in power loss in components which further cause reduction in reliability of the system [3], [5], [7], [8], [9-13], [17], [28], [29].

In case of low power applications like low voltage energy harvesting systems, RES, electric / hybrid vehicles, SISO and MISO are preferred. In case of applications like low power wireless sensors, smart devices which demands different voltage ranges SIMO or MIMO are preferred. The converters are generally classified as single stage converters and multi stage converters [31], based on the number of conversion stages involved in its implementation.

In grid connected applications, aerospace, critical health care units and medical fields, military applications uninterrupted supply is the major need, isolated converter with multi winding primary transformer is used. Isolated converters with single primary winding transformer are preferred where cost effectiveness is the major concern [5]. In high power / high gain applications where reliability and efficiency of the system is also the main concern, non-isolated converters with magnetic coupling can be used [25].

Converters with high gain value can be used for motor drive systems and grid connected RES [26], electric/hybrid electric vehicles, smart homes [13], [16] whereas converters with low gain value can be used in standalone RES applications [17], [30] and electrification of vehicles. Unidirectional converters are preferred in RESs without ESS, low power applications like safety equipments, sensors, etc., whereas bidirectional converters are preferred in RESs with ESS, electric/hybrid electric vehicles, smart home appliances [13] super-capacitors, micro/nano grids [23], [24], aerospace, drives like elevators and escalators, uninterrupted power supply.

Low gain RES and hybrid vehicle applications converters in series connection with source can be selected whereas high gain RES and hybrid vehicle, smart grid and ESS applications converters in parallel connection with source without isolation are employed [3], [4]. Modularity is most preferred feature of multiport converters. Mainly finds its application in micro/nano grids, ESS and electric vehicles, space craft [12] whereas non-modularity multiport converters find its application in systems involving ESS. It is noted that multiport convert topologies are absolutely selected based on the load, nature of source and load, availability of sources, cost and various other demands of the application.

III. CHALLENGES FACED IN IMPLEMENTATION OF MULTIPOINT CONVERTERS

Some of the converter topologies try to achieve continuous output current; if the output current is continuous the converter is more suitable for connecting to the inverter for further needs [14]. There are some topologies which aim to overcome the

cross-regulation problem in case of multiport converters [10], [18] Multiport converters also play a vital role in balancing power between the source and load. Some of paper works on load sharing as a solution to this issue [7].

As the years runs and in respect to duration of various operating modes of converters / rate of change of operating modes, the overall performance, efficiency and reliability of the converter system goes down. In literature survey it could be noted that some of the papers working on to analyse the converter life time under different operating conditions [8], [26]. Another key challenging factor is improvisation of fault tolerance capability and to eliminate the flow of circulating currents between the unequal voltage sources [23].

Obtaining a regulated output from highly variable and intermittent source is a big challenge. If the output is not stable and fixed in nature then it will not taken for implementation, so some topologies try to obtain regulated output from variable sources [1], [5], [7], [9], [21], [24], [25], [27]. In practice there will be issue of mismatch of source and load demand. For which Energy management is a key factor which has to be taken care in multiport converters, in some converter models it have been concentrated [1], [24], [25], [27]. Nut at the same time minimal operating modes, no limitations on switching duty cycles, less component usage are preferred [1].

It is preferred to have simple control system and algorithm [1], [9], [18]. The converter model should be having characteristics of flexibility [3], [18] and control flexibility [8]. At the same time output response should be high [4]. In concern to fast response, system-on-chip applications are also made in past [32]. Next focus is on reduction of size and cost of the converter models [1], [3], [4], [26], [27]. In related to this, in some converter topologies in order to reduce the installation and maintenance cost [8] battery energy storage units (BES) are eliminated [30]. In the case of improvisation of reliability and efficiency of the system, there is a need of implementation of maximum power point tracking system. This results in maximum energy extraction from the various renewable energy sources [3], [5], [27], [30].

Focus on the ripple cancellation, stability [4], accuracy with good output voltage range [10], [21] is also the needed one. Efficiency is directly related to reliability of the converter system which in turn directly related to the overall performance of the multiport converter topologies. So there is a need of focus on the improvisation of dynamic performance of the multiport converters [4], [6-8], [22], [27], [41].

IV. CONCLUSION

Focus on the ripple cancellation, stability [4], accuracy with good output voltage range [10], [21] is also the needed one. Efficiency is directly related to reliability of the converter system which in turn directly related to the overall By doing detail survey of various multiport converter topologies which is available in literature, it is noted that, the protection schemes are yet to be focused. And few parameters are still need to be given more focus namely minimizing operating modes, elimination of limitation on switching duty cycles, control flexibility, ripple cancellation, stability, load sharing, fault tolerance, elimination of cross-regulation problem, evaluation of life time of converters under different operating modes. The general focus of multiport converters found in past are higher efficiency, performance, regulation of output, implementation of maximum power point tracking & control systems with simple and effective algorithms and reduction of size and cost of the multiport converters. This paper aims to provide detail information of Multi- port converters, in the field of harvesting energy from renewable energy sources and better selection guide on multi-port converters for researcher scholars, designer engineers and application engineers. This article also highlights the various categorizations of multiport converters, its advantages and disadvantages and gives clear idea of selection of converter design for specific applications.

REFERENCES

- [1] Hassan AboReada, A.V.J.S Praneeth, Nimesh Vamanan, Vijay Sood, Sheldon S. Williamson, 'Design and Control of Non-isolated, Multi-input DC/DC Converter for Effective Energy Management', 2019 IEEE 28th International Symposium on Industrial Electronics (ISIE), 978-1-7281-3666-0/19 ©2019IEEE.
- [2] Hassan AboReada, Sheldon S. Williamson, Vijay Sood, 'Analysis and Control of Multi-input, Single-output, Non-isolated DC/DC Converter for Effective Renewable Energy Management', 2019 IEEE Transportation Electrification Conference and Expo (ITEC), 978-1-5386-9310-0/19 ©2019IEEE.
- [3] Rana Ahmed, Nahla E. Zakzouk, 'A Single-inductor MISO Converter with Unified Decoupled MPPT Algorithm for PV Systems Undergoing Shading Conditions', 2019 IEEE International Conference on Environment and Electrical Engineering and 2019 IEEE Industrial and Commercial Power Systems Europe (EEEIC / I&CPS Europe), 978-1-7281-0653-3/19 ©2019IEEE.
- [4] Farag S. Alargt, Ahmed S. Ashur, Ahmad H. Kharaz, 'Parallel Interleaved Multi-Input DC-DC Converter for Hybrid Renewable Energy Systems', 2019 54th International Universities Power Engineering Conference (UPEC), 978-1-7281-3349-2/19 ©2019IEEE.
- [5] Sara Alomari and Issam Smadi, 'Modeling and Control of Multi-Port DC/DC Converter', 2019 IEEE 28th International Symposium on Industrial Electronics (ISIE), 978-1-7281-3666-0/19 ©2019IEEE.
- [6] T.Anitha, N.Nachammai, 'Simulation of Single-Input Fuzzy Logic Control of Multi-output Zero-Voltage Switching Push-pull Quasi-resonant Converter', 2019 11th International Conference on Advanced Computing (ICoAC), 978-1-7281-5286-8/19 ©2019IEEE.
- [7] Ravi Vardhan Arya, Amrithes Kumar, Aditya Narula, 'Multi-Input Multi-Level Isolated DC-DC Converter for Enhanced Reliability of Renewable Sources', 2018 2nd IEEE International Conference on Power Electronics, Intelligent Control and Energy Systems (ICPEICES), 978-1-5386-6625-8/18 ©2018IEEE.
- [8] Allamsetty Hema Chander, Lalit Kumar Sahu, Manik Jalhotra, 'Reliability analysis of Multiple Input Converter', 2020 First International Conference on Power, Control and Computing Technologies (ICPC2T), 978-1-7281-4997-4/20 ©2020IEEE.
- [9] Yen-an Chen, Ping Wang, Youssef Elasser and Minjie Chen, 'LEGO-MIMO Architecture: A Universal Multi-Input Multi-Output (MIMO) Power Converter with Linear Extendable Group Operated (LEGO) Power Bricks', 2019 IEEE Energy Conversion Congress and Exposition (ECCE), 978-1-7281-0395-2/19 ©2019IEEE.

- [10] Zhiyuan Zhou, Nghia Tang, Bai Nguyen, Wookpyo Hong, Partha Pratim Pande, and Deukhyoun Heo, 'A Wide Output Voltage Range Single-Input-Multi-Output Hybrid DC-DC Converter Achieving 87.5% Peak Efficiency With a Fast Response Time and Low Cross Regulation for DVFS Applications', 2020 IEEE Custom Integrated Circuits Conference (CICC), 978-1-7281-6031-3/20 ©2020IEEE.
- [11] Rasoul Faraji, Hosein Farzanehfard, Georgios Kampitsis, Marco Mattavelli, Elison Matioli, Morteza Esteki, 'Fully Soft-Switched High Step-up Non-Isolated Three-Port DC-DC Converter Using GaN HEMTs', 0278-0046 ©2019IEEE.
- [12] Lorenzo Fontani, Mario Migliaro, Maurizio Inversi, Maurizio Bacci, Franco Bigongiari, Francesco Petroni, Elena Casali, Mariel Triggianese, David Levacq, 'DC2I, Configurable and compact isolated Multioutput DC-DC converter', 2019 European Space Power Conference (ESPC), 978-1-7281-2126-0/19 ©2019IEEE.
- [13] Behnam Zamanzad Ghavidel, Ebrahim Babaei and Seyed Hossein Hosseini, 'An Improved Three-Input DC-DC Boost Converter for Hybrid PV/FC/Battery and Bidirectional Load as Backup System for Smart Home', 2019 10th International Power Electronics, Drive Systems and Technologies Conference (PEDSTC), 978-1-5386-9254-7/19 ©2019IEEE.
- [14] Saman A. Gorji, Hosein G. Sahebi, Mahmood Movahed, Mehran Ektesabi, 'Multi-Input Boost DC-DC Converter with Continuous Input-Output Current for Renewable Energy Systems', 2019 IEEE 4th International Future Energy Electronics Conference (IFEEC), 978-1-7281-3153-5/19 ©2019IEEE.
- [15] Tohid Jalilzadeh, Naghi Rostami, Ebrahim Babaei, Seyed Hossein Hosseini, 'Multi-port DC-DC Converter with Step-up Capability and Reduced Voltage Stress on Switches/Diodes', 0885-8993 ©2020IEEE.
- [16] Sudarat Khwan-on, Kuagoon Kongkanjana, 'A Multi-input High Step-up Converter for Renewable Energy-Drive Systems', 2019 IEEE 2nd International Conference on Power and Energy Applications (ICPEA), 978-1-7281-1596-2/19 ©2019IEEE.
- [17] Kumaravel S, Arun Sarathi, Gangavarapu Guru Kumar, Sivaprasad A, 'Three inputs and Two Outputs Boost DC-DC Converter for DC Microgrid Applications', 2018 2nd IEEE International Conference on Power Electronics, Intelligent Control and Energy Systems (ICPEICES), 978-1-5386-6625-8/18 ©2018IEEE.
- [18] Xiaolu Lucia Li, Zheng Dong, Chi K. Tse, Dylan D-C. Lu, 'Single-Inductor Multi-Input Multi-Output DC-DC Converter with High Flexibility and Simple Control', IEEE Transactions on Power Electronics, 0885-8993 ©2020IEEE.
- [19] Sreeshma Markkassery, Arun D. Mahindrakar, Lakshminarasamma N, Ramkrishna Pasumarthy, 'Modelling of non-isolated single-input-multi-output DC-DC converter', 2018 IEEE International Conference on Power Electronics, Drives and Energy Systems (PEDES), 978-1-5386-9316-2/18 ©2018IEEE.
- [20] Sreeshma Markkassery, Akshit Saradagi, Arun D. Mahindrakar, Lakshminarasamma N, Ramkrishna Pasumarthy, 'Modelling, Design and Control of Non-isolated Single-input Multi-output Zeta-Buck-Boost Converter', IEEE Transactions on Industry Applications, 0093-9994 ©2020IEEE.
- [21] Fahim Nabil Mazelan, Ramani Kannan, Khairul Nisak Md.Hasan, Azuwa Ali, 'Multi-Input Power Converter for Renewable Energy Sources using Active Current Sharing Schemes', 2019 IEEE Student Conference on Research and Development (SCoREd), 978-1-7281-2613-5/19 ©2019IEEE.
- [22] Shahin Mohammadi, Morteza Dezhbord, Milad Babalou, Mahmoodreza Eskandarpour Azizkandi, Seyed Hossein Hosseini, 'A New Non-Isolated Multi-Input DC-DC Converter with High Voltage gain and Low Average of Normalized Peak Inverse Voltage', 2019 10th International Power Electronics, Drive Systems and Technologies Conference (PEDSTC), 978-1-5386-9254-7/19 ©2019IEEE.
- [23] Parham Mohammadi, Rahim Samanbakhsh, Fernando Davalos Hernandez, Peyman Koochi, Federico Ibanez, 'A Novel Non-Coupled Non-Isolated Double-Input Bidirectional High-Gain Converter for Hybrid Energy Storage System', 2019 IEEE 10th International Symposium on Power Electronics for Distributed Generation Systems (PEDG), 978-1-7281-2455-1/19 ©2019IEEE.
- [24] Gourab Mohanty, 'SEPIC Based Multi Input Dc-Dc Converter', 2019 5th International Conference for Convergence in Technology (I2CT) Pune, India. Mar 29-31, 2019. 978-1-5386-8075-9/19 ©2019IEEE.
- [25] Mounika A, Shankar S, J. Ramprabhakar, A Hybrid Energy Source Integration in a DC Microgrid using Multi-Input Buck-Boost Converter', 2018 4th International Conference for Convergence in Technology (I2CT) SDMIT Ujire, Mangalore, India. Oct 27-28, 2018, 978-1-5386-5232-9 ©2018IEEE.
- [26] Pathivada Priyanka, Shelas Sathyan, Manoranjan Sahoo, 'Current-fed Integrated Single-Input Multi-Output (SIMO) Switched Converter', 2018 15th IEEE India Council International Conference (INDICON), 978-1-5386-8235-7/18 ©2018IEEE.
- [27] Bhaskara Rao R, Narsa Reddy Tummuru, Bala Naga Lingaiah A, 'Photovoltaic-Wind and Hybrid Energy Storage Integrated Multi-Source Converter Configuration for DC Microgrid Applications', IEEE Transactions on Sustainable Energy, 1949-3029 ©2020IEEE.
- [28] Sajad Rostami, Vahid Abbasi, Masoumeh Parastesh, 'Proposing a Triple Input and Multi-Level DC-DC Converter for Using in Renewable Energy Applications', 2019 International Power System Conference (PSC), 978-1-7281-5273-8/19 ©2019IEEE.
- [29] Smrity, Abhishek Kumar, Nishtha Bajoria, Aftab Alam, 'Multiple-Input-Single-Output Converter for Hybrid Renewable Sources', 2019 International Conference on Vision Towards Emerging Trends in Communication and Networking (ViTECoN), 978-1-5386-9353-7/19 ©2019IEEE.
- [30] Anuradha Tomar, Sukumar Mishra, 'Grid Interactive MISO Converter Based PV System', 2nd IEEE International conference on power Electronics, Intelligent Control and Energy systems (ICPEICES-2018), 978-1-5386-6625-8/18 ©2018IEEE.
- [31] Rami TROUDI, Sandrine MOREAU, Gerard CHAMPENOIS, Monia BOUZID, Khaled JELASSI, 'A New Single-Input Dual-Output DC-DC Converter Modelled Using Small-Signal AC Approach for Micro-Grid Applications', The 10th International Renewable Energy Congress (IREC 2019), 978-1-7281-0140-8/19 ©2019IEEE.
- [32] Syed Abdul Yasin, Jagadeesh Kumar, Yeswhanth Kumar, Sivaprasad Athikkal, Joseph Peter, 'Analysis of A Dual Input DC-DC Converter Topology Based on SEPIC Configuration', 2019 International Conference on Power Electronics Applications and Technology in Present Energy Scenario (PETPES), 2019.

Zon-Linear Dynamical Forecasting of Electricity Demands

Justine Yasappan, Maria Wenisch and Arul Oli

Abstract

Forecasting is a powerful methodology to study the complexity of the real world and predict the possible future outcomes in a more scientific way. This paper presents the process of forecasting the electricity demand for each day from the given data, from the year 2000 to 2008, utilizing the ARIMA, Dynamic Regression and Non-linear model analysis. A comparison of all the three models is done with the original data. The purpose of this project is to forecast the electricity demand for each day.

Keywords: Forecasting, ARIMA, Dynamic Regression, Non-linear models, Autocorrelation, Multi-Layer Perceptron

1 Introduction

Electricity has become a vital necessity for the modern world. The demand and consumption of electricity is ever on the increase. It is essential for the producers to predict the real demand of electricity on a daily basis. In this paper, the demand of electricity is predicted taking into account the time, temperature and the working days. The given data is the electricity consumption from the year 2000 to 2008. The input variables are temperature, working days and time while the output variable is the demand of electricity for each day. Using ARIMA models, Dynamic Regression models and Non-linear models the future demand is forecasted by comparing the three models.

2 ARIMA model

ARIMA stands for Auto Regressive Integrated Moving Average. Box and Jenkins first introduced the ARIMA models. The ARIMA procedure was originally designed to analyze and forecast equally spaced univariate time series variables. The ARIMA procedure has three main stages. They are: IDENTIFY, ESTIMATE and FORECAST. Identifying stage signifies finding the time series, possibly differencing the series, finding ACF (autocorrelations), PACF (partial autocorrelation) and performing stationarity tests by differencing, if necessary. The analysis of the series would suggest one or more ARIMA models that could be fit. Options allow to test the stationarity or regularity of ARIMA identification. Once a model has been identified, it can be fitted to the series by estimating the coefficients of the model. In the third stage, future values of the series could be forecasted and confidence intervals could be estimated from the ARIMA model.

2.1 Analysis of electricity demand series

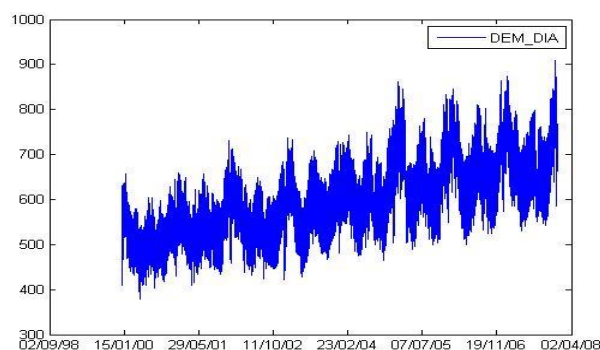


Figure 1. Time series of electricity demand

This is the time series of the demand for electricity for each day from the year 2000 to 2008. In the first phase, the analysis of the mean and variance of the given time series takes place. The plot exhibits a pattern of increase in the mean and variance. It raises eadily with the raise and fall pattern over the period of time. Therefore the plot exhibits a gradual increase in the mean and variance. The time series shows there are some leaps and bounds. It indicates that the forecasting model could be improved for a measure of accurate autocorrelation.

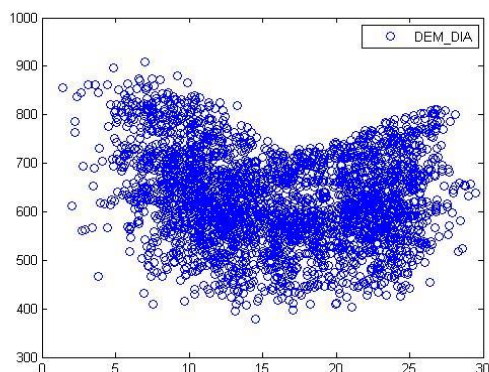


Figure 2. Scatter plot of electricity demand

The scatterplot has plotted the demand variable against the temperature. It shows the relationship between the demand and the temperature. Most of the values are found to be correlated to one another. The scatter plot shows that there is auto correlation in the data.

2.2 Stabilization of Variance

As the time series shows that it is varying in mean and variance, it is necessary to stabilize the mean and variance in the first place, by applying logarithm to the series. The Box-Cox value is found to be $\alpha = 0.78809$ and the value of the correlation coefficient is 0.50453.

2.3 Analysis for Regular or Stationarity

Stationarity means that it has a steady progress. The data fluctuate around a constant mean, independent of time and the variance of the fluctuation. It remains essentially constant over time. In the time series plotted, there is evidence of a change in the mean over the time, therefore the series is non-stationary in the mean. The plotted series shows obvious change in the variance over time, then we say the series is non-stationary in the variance. The mean changes and the variance is not reasonably constant over time. It is a non-stationary seasonal series of electricity demand. It has a period 7 and it has to be differenced.

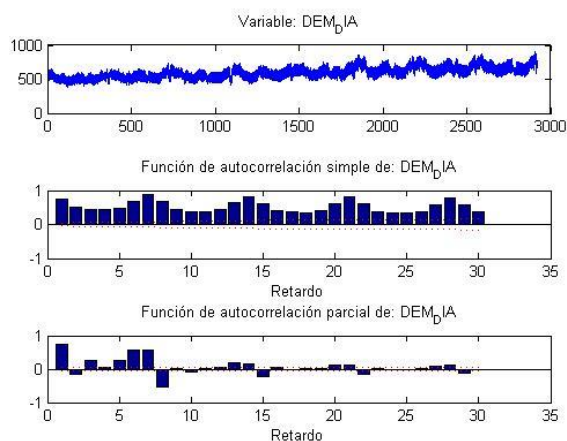


Figure 3. FAS of electricity demand

2.3.1 Auto-correlation function (ACF or FAS):

The key statistic in time series analysis is the autocorrelation coefficient, the correlation of time series with itself. The plot of autocorrelation function is a standard tool in explaining a time series. ACF or FAS helps us visualize the variables in general. We expect about 95% of all sample autocorrelation coefficients to be within $+1.96/\sqrt{n}$ to $-1.96/\sqrt{n}$

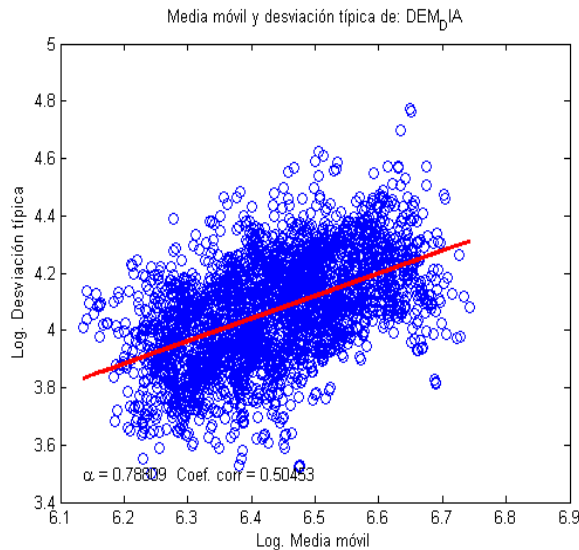


Figure 4. Coefficient of electricity demand

2.3.2 Partial autocorrelation(PACF or FAP)

Partial autocorrelations are used to measure the degree of association between the forecast variables Y_t and Y_{t-k} . Suppose there is a significant autocorrelation between Y_t and Y_{t-1} then there will be significant correlation between Y_{t-1} and Y_{t-2} . The partial autocorrelation coefficient of order k is denoted by α_k can be calculated by regressing Y_t against other variables.

$$Y_t = b_0 + b_1 Y_{t-1} + \dots + b_k Y_{t-k}$$

The partial autocorrelation α_k is the estimated coefficient b_k from this multiple regression. As with the autocorrelation function, the partial autocorrelation should all be close to zero for a white noise series.

2.4 Removing non-stationarity in a time series

One way of removing non-stationarity is through the method of differencing. We define the differenced series as the change between each observation in the original series.

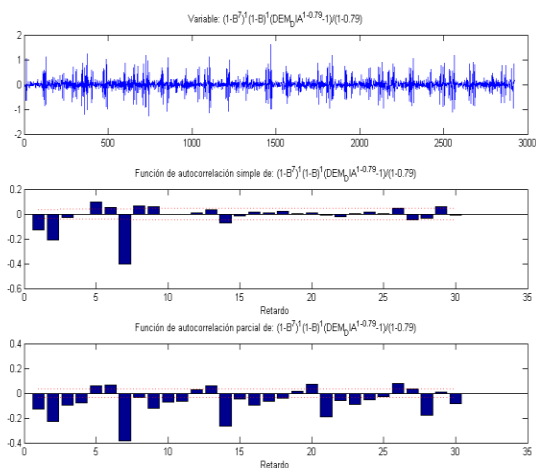


Figure 5. FAS of electricity demand after differencing

2.5 Identifying ARIMA Model

The general non seasonal model is known as ARIMA(p,d,q):

AR: p = order of the autoregressive part

I: d = degree of first differencing involved

MA: q = order of the moving average part

Correct identification of p , d and q is the key when fitting an ARIMA model. Patterns observed in the residual ACF and PACF will help a lot to determine the values of p and q . After plotting the time series, the major statistical tool is the autocorrelation coefficient which describes the relationship between various values of the time series that are lagged. The figure 5 shows the theoretical ACF and PACF for an AR (5, 0) model when the autocorrelation lags are found and that there are two non-zero partial autocorrelation at lag 5 and 6. The model was designed to be with coefficients (5, 1, 0) and (5, 1, 2).

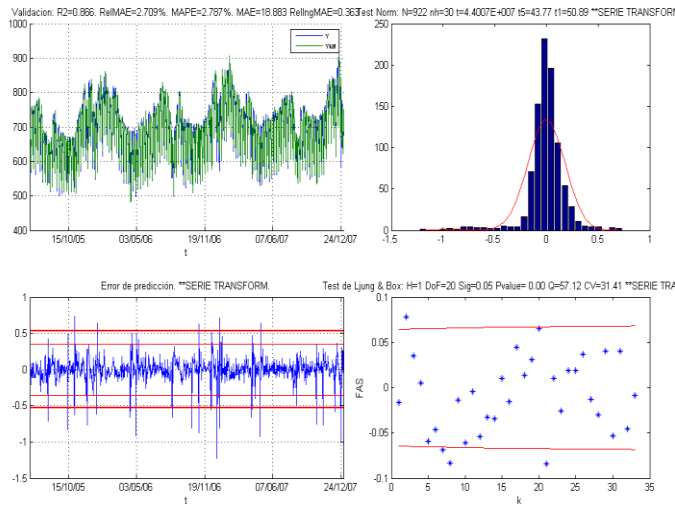


Figure 6. ARIMA model of electricity demand

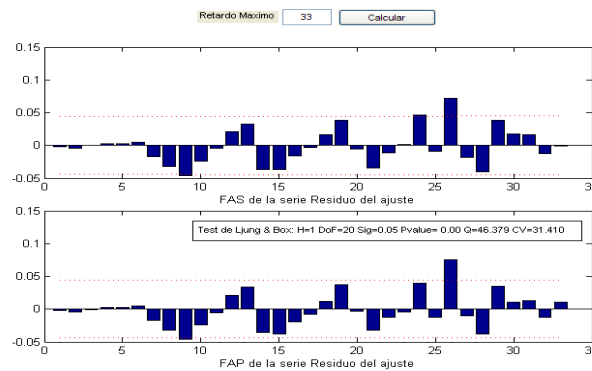


Figure 7. FAS and FAP for ARIMA model of electricity demand

Figure 7, the ACF and PACF obtained for the ARIMA model shows that most of the lags are well within the limit of the ratio, except at the point 9 and 26, which could be ignored because of the presumed presence of some outliers. Therefore it could be considered as a good ARIMA model.

2.6. Analysis of the residues

Although a selected model may appear to be the best among those models considered, it is also necessary to do diagnostic checking to verify that the model is adequate. This is done by studying the residuals to see if any pattern remains unaccounted for. For a good forecasting model, the residuals left over after fitting the model should be simply white noise. It is normal to standardize the residuals so that they have the same variance. The chosen model (5, 1, 0)₇ and (5, 1, 2)₇ shows that only a few outliers are there. This could be comparatively a good model to fit.

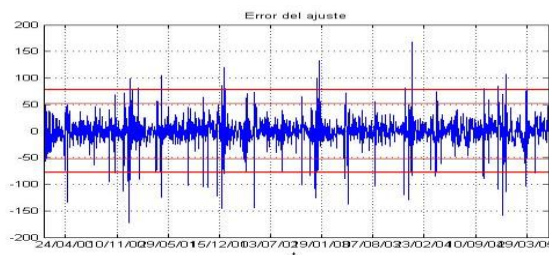


Figure 8. Residues of the ARIMA model of electricity demand

2.7. Analysis of the significance of the coefficients

Figure 9 shows that most of the coefficients are significant with P value being equal to zero. There are two P values that are greater than 0.05, with is a very high P value that are should be omitted. But the following coefficients are all very significant. Therefore they can be allowed as significant values.

Parametros del ajuste del modelo.
Función objetivo (algoritmo CLS) = 670.3408

| | Value | std. error | T-value | p-value |
|--------|--------|------------|---------|---------|
| ar_r_1 | -0.156 | 0.154 | -1.017 | 0.155 |
| ar_r_2 | -0.345 | 0.171 | -2.020 | 0.022 |
| ar_r_3 | 0.604 | 0.150 | 4.038 | 0.000 |
| ar_r_4 | 0.206 | 0.108 | 1.906 | 0.028 |
| ar_r_5 | -0.291 | 0.082 | -3.541 | 0.000 |
| ma_r_1 | -0.340 | 0.151 | -2.246 | 0.012 |
| ma_r_2 | -0.615 | 0.179 | -3.444 | 0.000 |
| ma_r_3 | 0.655 | 0.166 | 3.945 | 0.000 |
| ma_r_4 | 0.186 | 0.118 | 1.579 | 0.057 |
| ma_r_5 | -0.461 | 0.083 | -5.570 | 0.000 |
| ma_7_1 | -0.697 | 0.033 | -21.231 | 0.000 |
| ma_7_2 | -0.129 | 0.027 | -4.751 | 0.000 |

Figure 9. Significance of the Coefficients of the ARIMA model of electricity demand

The ARIMA model that we have obtained has significant P values. Therefore this model could be a good model for fitting.

2.8. Comparing with ARIMA model

We find that the actual time series and the expected prediction going in the same ratio. The given time series of electricity demand is compared with the ARIMA model time series with the horizontal value 7. Though both the series show a similar pattern of increase, there are times with the prediction is different from the actual.

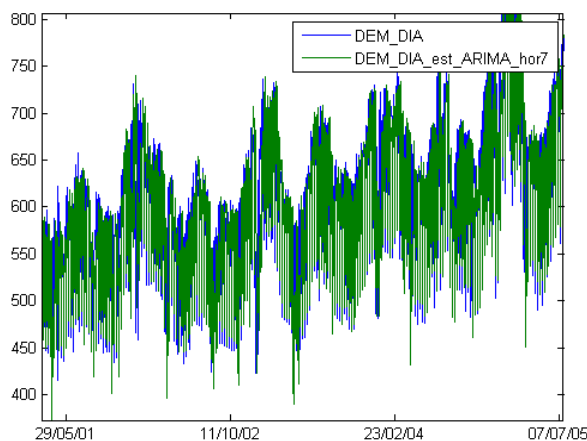


Figure 10. Comparing the Actual Time Series with the ARIMA model series of electricity demand

3. Dynamic Regression Model

The electricity demand time series the dynamic regression model include demand as an explanatory variable. By quantifying the relationship between temperature, working day and demand, the model allows to create forecasts under varying demand scenarios. What will happen if the temperature and working day is raised or lowered? Generating these alternative forecasts can help to determine an effective demand forecast strategy. Building a dynamic regression model is generally an iterative procedure, whereby one begins with an initial model and experiment with adding or removing independent variables and dynamic terms until one arrives upon an acceptable model.

3.1 Analysis of the Electricity Demand Time Series

In the first place, it is better to check the series for any outliers that should be eliminated before proceeding for further analysis and modeling. In the given electricity demand series there are not so many outliers. There is change in the mean and variance of the series but not many outliers.

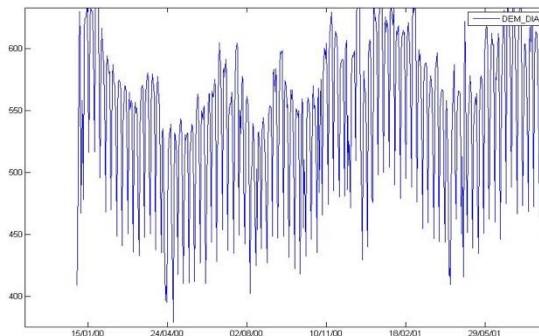


Figure 11. The sequence of the electricity demand time series.

Analyzing the correlation between the electricity demand and the temperature, working day is a preliminary step towards working with the variables. There seems to be a correlation between the explicative variable, the demand and the input variables, temperature and working day.

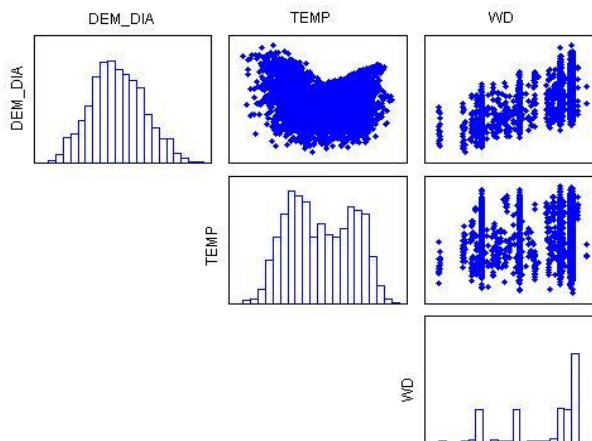


Figure 12. Correlation between demand, temperature and working day

3.2 Analyzing the Variance

The series shows that the mean and variance vary as the series progresses. In order to stabilize the variance, Box-Cox transformation was applied. The Box-Cox value is found to be $\alpha = 0.78809$.

3.3 Adjusting the Regression Dynamic model

The general procedure is: The first step in identifying the appropriate dynamic regression model is to fit a multiple regression model. To obtain the regression dynamic model, it is necessary to begin with adjusting an AR model with sufficient value of the explicative series, temperature and working day, to find the level of error in the dynamic regression. A model with error 10 delay of the explicative variable is an optimum option to begin the model. By doing this we get the regression model of the electricity demand variables with the successive temperature and working day variables. The error in this model seems to be so huge. It is necessary to differentiate the variables.

If the errors from the regression appear to be non-stationarity, and differencing appears appropriate, then difference the demand and temperature and working day.

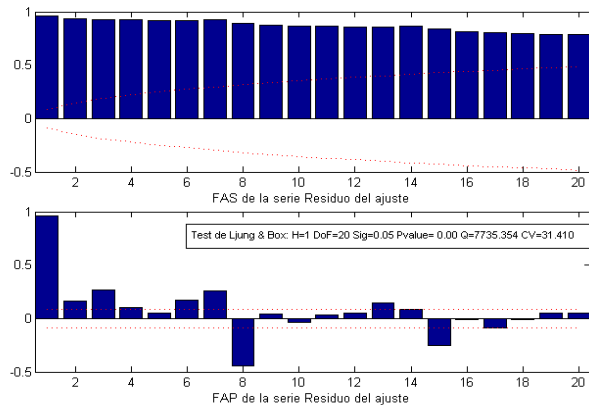


Figure 14. The auto-correlative function of the residue

Figure 14 shows that it is stational with period 7. We have to differentiate it for regular and stationarity by trying it out through different coefficients for regular and stationarity. The value of r determines the decay pattern in the remaining lags. If there is no decay pattern at all, but a group of spikes followed by a cutoff to zero, then choose $r = 0$. If there is simple exponential decay, then $r = 1$. If the lags show a more complex decay pattern like a sine-wave decay, then $r = 2$. The value of s is the number of non-zero lags before the decay.

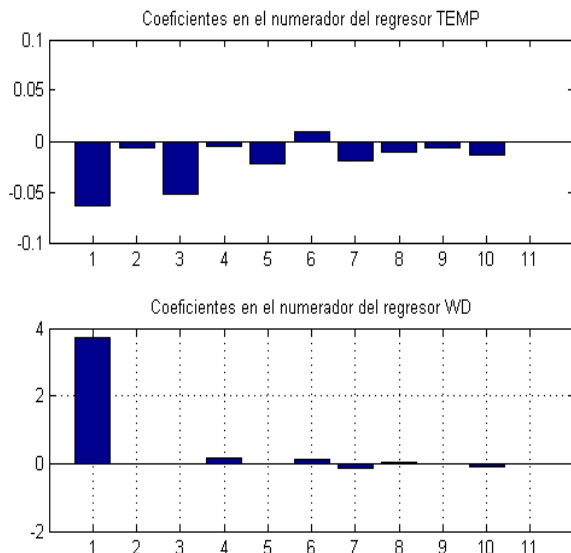


Figure 15. Coefficients of the explicative variables

To estimate the order of the transference function we have to analyze the coefficients. The coefficients of the regressive numerators of temperature and the coefficients of the regressive numerators of working day give us the values of s , b and r . Figure 15 shows that there two nonzero lags before the decay. Therefore the value of s may be One or two. There is no decay pattern at all in figure 6, but a group of spikes followed by a cutoff to zero, therefore $r = 0$. And the dead time $b = 0$. To further confirm the values of s , b and r , we have to look at the values of the coefficients. Analyzing the coefficients of the explicative variables in figure 16, for determining the values of s , b and r , we observe that the p -value is zero at two places before the AR value. Therefore the value of $s = 2$. Analyzing the figure 15 and figure 16, we fix the values of s , b and r as $s = 2$, $r = 0$ and $b = 0$.

Parametros del ajuste del modelo.
Función objetivo (algoritmo CLS) = 0.011335

| | Value | std. error | T-value | p-value |
|--------|--------|------------|---------|---------|
| w10 | -0.063 | 0.012 | -5.333 | 0.000 |
| w11 | -0.006 | 0.012 | -0.514 | 0.304 |
| w12 | -0.052 | 0.013 | -4.086 | 0.000 |
| w13 | -0.005 | 0.013 | -0.381 | 0.352 |
| w14 | -0.022 | 0.011 | -2.003 | 0.023 |
| w15 | 0.009 | 0.011 | 0.815 | 0.208 |
| w16 | -0.019 | 0.011 | -1.689 | 0.046 |
| w17 | -0.010 | 0.013 | -0.793 | 0.214 |
| w18 | -0.006 | 0.013 | -0.505 | 0.307 |
| w19 | -0.013 | 0.012 | -1.072 | 0.142 |
| w110 | -0.000 | 0.012 | -0.025 | 0.490 |
| w20 | 3.741 | 0.052 | 72.523 | 0.000 |
| w21 | 0.008 | 0.052 | 0.163 | 0.435 |
| w22 | -0.016 | 0.054 | -0.287 | 0.387 |
| w23 | 0.150 | 0.055 | 2.737 | 0.003 |
| w24 | 0.014 | 0.050 | 0.282 | 0.389 |
| w25 | 0.142 | 0.050 | 2.841 | 0.002 |
| w26 | -0.157 | 0.050 | -3.148 | 0.001 |
| w27 | 0.026 | 0.055 | 0.480 | 0.316 |
| w28 | 0.012 | 0.054 | 0.217 | 0.414 |
| w29 | -0.093 | 0.052 | -1.805 | 0.036 |
| w210 | -0.016 | 0.051 | -0.315 | 0.376 |
| ar_r_1 | 0.120 | 0.022 | 5.368 | 0.000 |

Figure 16. Coefficients of for determining s, b and r

Calculate the errors from the regression model and identify an appropriate ARMA model for the error series. Refit the entire model using the new ARMA model for the errors and the transfer function model for the input variables temperature and working day.

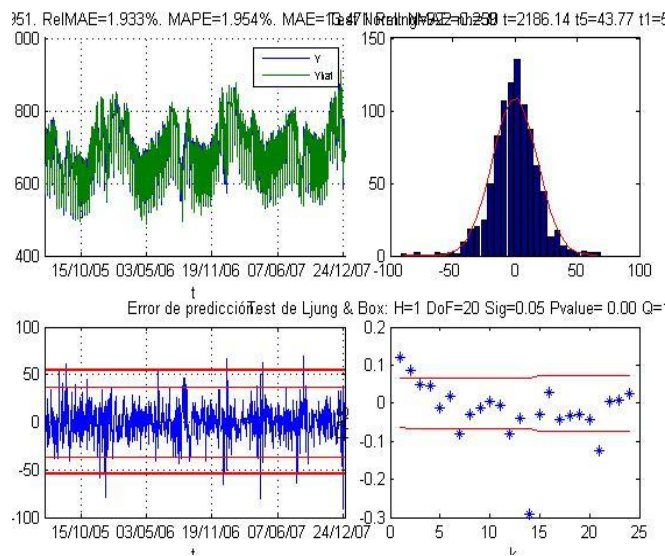


Figure17. The dynamic regression model after transference

Figure 17 is the Dynamic regression model error after differencing the explicative variables. The error predicted in this model is calculated to be nominal as the value of MAE = 1.933% and the value of MAPE = 1.954%. After differentiating the variables for regular and stationarity, the obtained coefficients are:

Parametros del ajuste del modelo.
Función objetivo (algoritmo CLS) = 259.5894

| | Value | std. error | T-value | p-value |
|--------|---------|------------|---------|---------|
| w10 | -1.225 | 0.249 | -4.921 | 0.000 |
| w11 | 0.434 | 0.258 | 1.683 | 0.046 |
| w12 | -1.164 | 0.249 | -4.668 | 0.000 |
| w20 | 605.872 | 7.566 | 80.078 | 0.000 |
| ar_r_1 | -0.741 | 0.031 | -24.234 | 0.000 |
| ma_r_1 | -0.908 | 0.020 | -45.573 | 0.000 |
| ar_7_1 | 0.410 | 0.022 | 18.752 | 0.000 |
| ma_7_1 | -0.888 | 0.011 | -77.280 | 0.000 |

Figure 18. The Coefficients after the transference

All the coefficients are significant in the series, even though the value of P at one place is 0.046 which is different from zero. This can be tolerated as it is less than 0.05 per cent of the error value. Therefore we accept all the values as significant values.

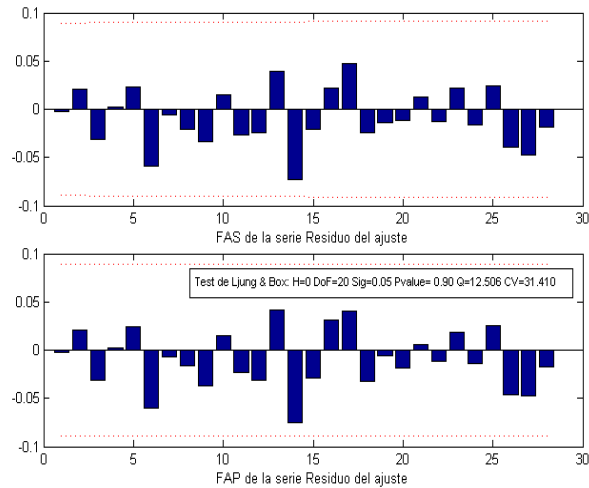


Figure 19. The Auto-correlation functions of the residues

Analyzing the autocorrelation function of the errors, we find that the lag at the second place is significantly large. But that could be allowed as it is the only significant lag in the entire autocorrelation function. The other lags are not significantly large as it is shown in the autocorrelation function. The simple and partial autocorrelation function of the residue obtained shows that there is no autocorrelation, except at one place. Therefore the model obtained for error is reasonably a good model.

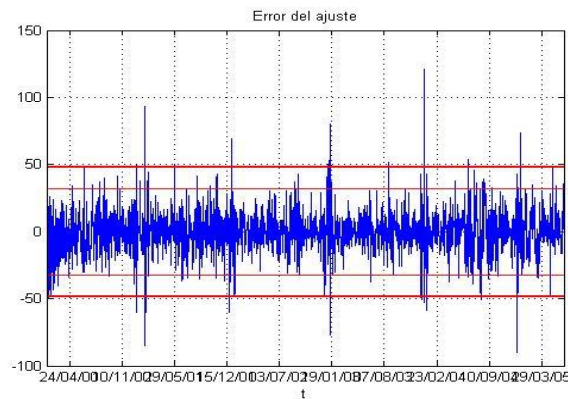


Figure 20 The adjusted residue of Error

The error residue of the adjusted explicative variables, temperature and working day shows that there are a few outliers. But these outliers could be ignored as they may be the product of error in the data. Therefore we can ascertain that the model obtained is a good model of dynamic regression, in which all that coefficients are significant with no autocorrelation between the explicative variables, temperature and working day with the values of $s=2$, $r = 0$ and $b = 0$ and the adjusted residue of an $ARIMA(2, 1, 1)(1, 1, 0)_7$ optimum to estimate the value of the electricity demand.

3.4 Comparison

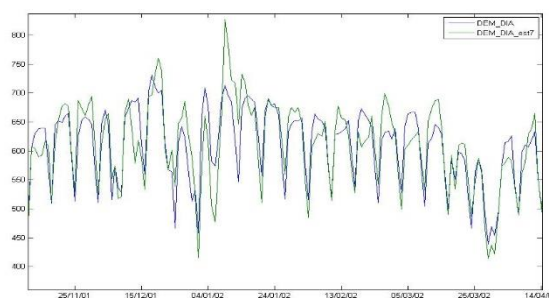


Figure 21. Comparison of actual time series with Dynamic Regression

The estimated Dynamic regression series has more sharp pointers than the actual series. The estimated series shows a standard pattern of rise and fall showing a clear estimation. Dynamic regression is a powerful forecasting technique that allows to incorporate the impact of explanatory variables into the forecasts. In addition to generating a forecast, a well-specified model can provide considerable insight onto the relationships between the independent variable and the dependent variables.

4. Identifying Non-linear model using MLP

Non-linear models are capable of reproducing some features in the time series such as chaotic behavior that are not able to be captured using linear models. It shows the relationship between the demand and the temperature. Most of the values are found to be correlated to one another. The scatter plot of temperature and electricity demand shows that it is strongly correlated. For the non-linear MLP analysis it has to be separated into two variables as Frio (cold), less than 15 degree Celsius and Calor (heat), more than 15 degree Celsius.

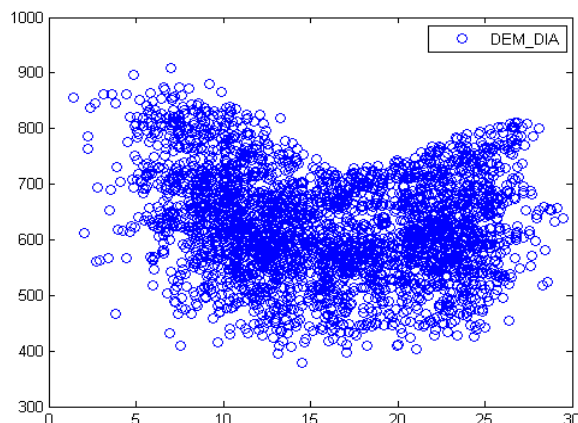


Figure 22. Correlation between electricity demand and temperature

In the analysis of the MLP model the input variables are Cold (frio), Hot (calor) and the working day. The output variable is the demand of electricity. First using the transference function, an ARIMA model for the errors was adjusted as it was done earlier.

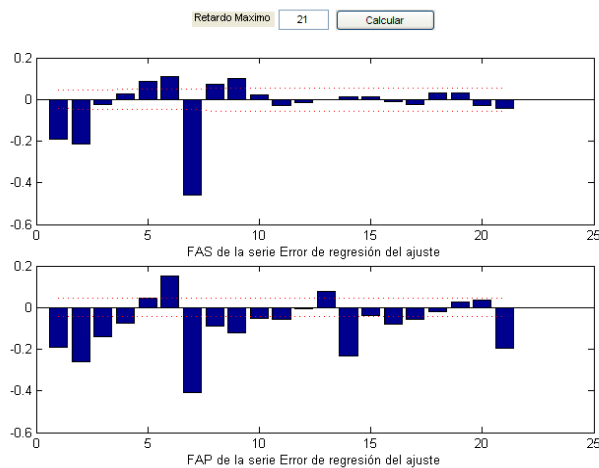


Figure 23. The Auto-correlation functions of the residues

The figure 23 shows the theoretical ACF and PACF for an AR (3, 0) model when the autocorrelation lags are found and that there are three non-zero partial autocorrelation at lag one, two and three. The model was designed to be with coefficients (2, 1,3) and (1, 1, 0) with a period 7.

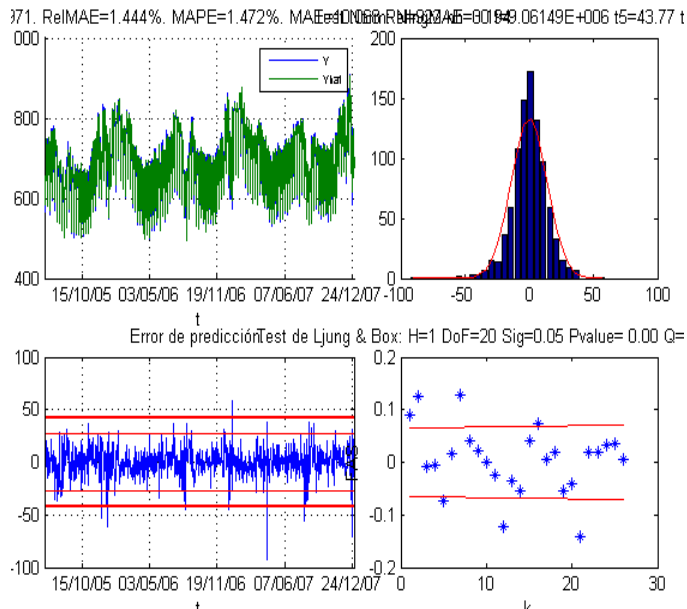


Figure 24. ARIMA model for the errors

To estimate the values of s , b , and r we have to analyze the coefficients. The coefficients of the regressive numerators of working day, Cold and Heat give us the values of s , b and r .

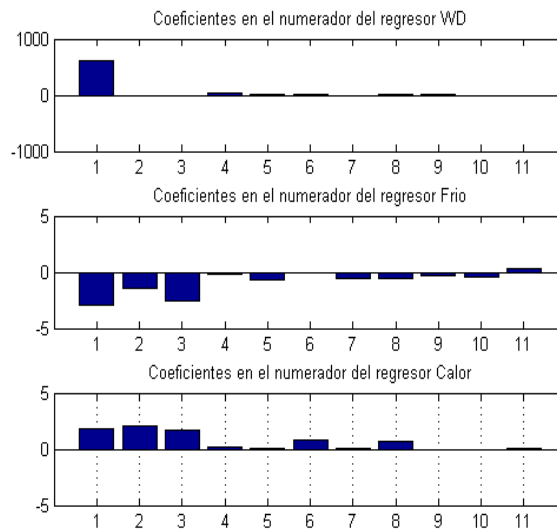


Figure 25. Coefficients of the numerator of WD, Frio, Calor

Figure 25 shows that there is one nonzero lag before the decay in Working day and three nonzero lags in Frio before the decay and there are three non-zero lags in Calor before the decay. Therefore the value of s may be one or two. And analyzing the coefficients of the explicative variables in figure 26, for determining the values of s , b and r , we observe that the value for working day will be $s=0$, $r=0$ and $b=0$ and the values for Frio and Calor will be $s=2$, $r=0$ and $b=0$.

Parametros del ajuste del modelo.
Función objetivo (algoritmo CLS) = 145.719

| | Value | std. error | T-value | p-value |
|--------|---------|------------|---------|---------|
| w10 | 623.295 | 7.255 | 85.915 | 0.000 |
| w20 | -2.757 | 0.301 | -9.155 | 0.000 |
| w21 | -1.460 | 0.322 | -4.535 | 0.000 |
| w22 | -2.726 | 0.300 | -9.094 | 0.000 |
| w30 | 1.505 | 0.367 | 4.101 | 0.000 |
| w31 | 1.844 | 0.410 | 4.495 | 0.000 |
| w32 | 1.337 | 0.367 | 3.645 | 0.000 |
| ar_r_1 | -1.147 | 0.086 | -13.323 | 0.000 |
| ar_r_2 | 0.368 | 0.055 | 6.724 | 0.000 |
| ar_r_3 | -0.181 | 0.024 | -7.543 | 0.000 |
| ma_r_1 | -1.434 | 0.085 | -16.950 | 0.000 |
| ma_r_2 | 0.441 | 0.072 | 6.147 | 0.000 |
| ma_7_1 | -0.823 | 0.014 | -60.513 | 0.000 |

Figure 26. The Coefficients after the transference

Figure 26 shows that all the coefficients are significant in the series, since the values of P for all the variables are zero. Therefore we accept all the values as significant values. And the model obtained is a very good model to fit.

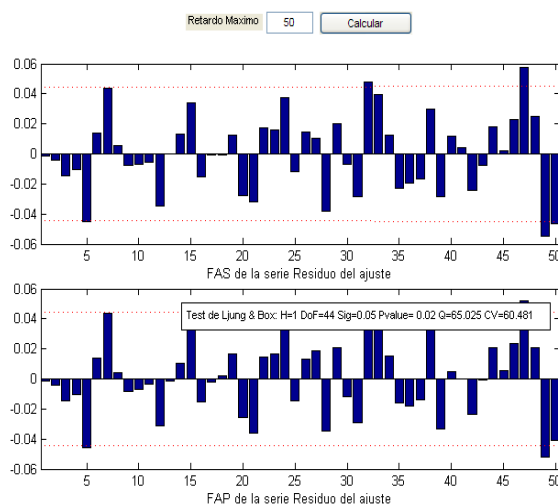


Figure 27. The Auto-correlation functions of the residues

Analyzing the autocorrelation function of the residues, we find that the lag at 32nd place is significantly large. But that could be allowed as it is the only significant lag in the entire autocorrelation function. The other lags are not significantly large as it is shown in the autocorrelation function. The simple and partial autocorrelation function of the residue obtained shows that there is no autocorrelation, except at one place. Therefore the model obtained for error is reasonably a good model. Figure 27, the FAS map ascertains with all the lags fitting well within the accepted range. Therefore the model is a good one to fit.

4.1. Multi-Layer Perceptron Analysis

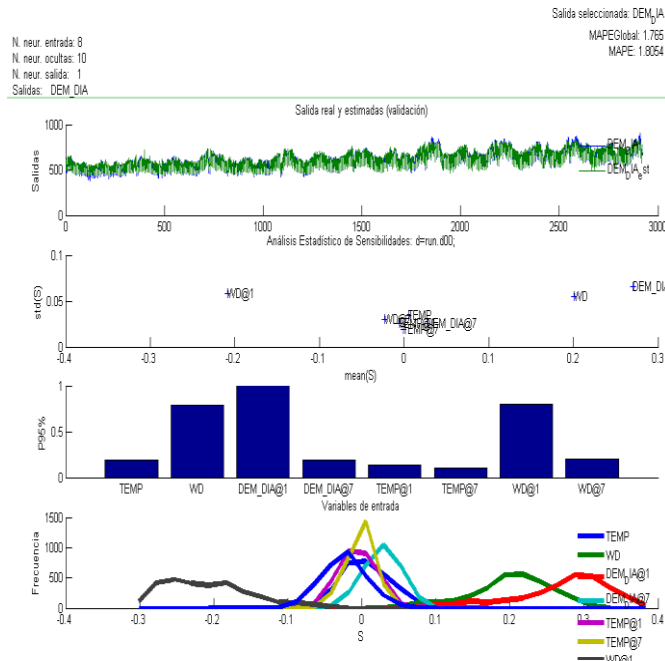


Figure 28 MLP model of the variables

In the MLP model, the output series, electricity demand and the estimated forecasted output series are given in Figure 28. We find that the estimated forecast is more close to the real series, which means that the actual series and the estimated series go well hand in hand. It is a close prediction. In the sensibility analysis we find that there are many variables like Temp@7, Temp@1, Temp and DEM-DIA@7 are found around the value of zero. All these variables close to zero are to be eliminated because these variables do not have any positive impact on the output series. All the series that are found to be far away from zero have positive impact on the output. Figure 29 shows that the working day series has a positive impact on the output electricity demand series.

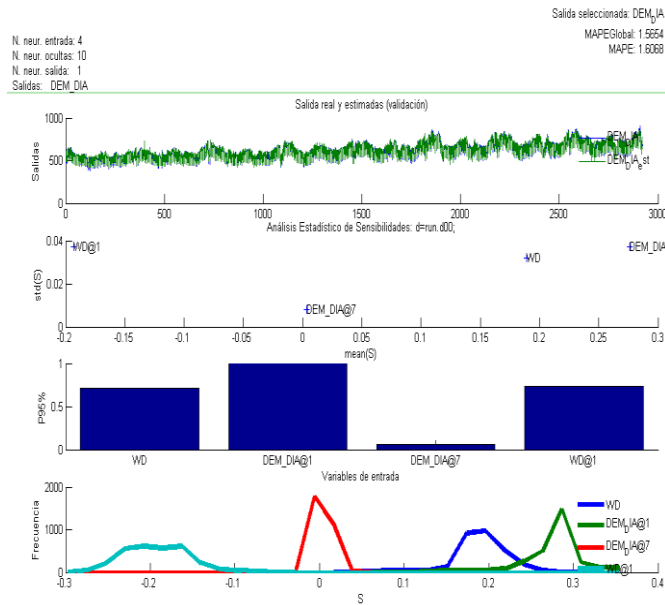


Figure 29 MLP model of the variables

Figure 29 shows the significant variables that have positive impact on the output series. The significant variables are WD, WD@1 which have a positive impact on the output variable, the electricity demand. These non-linear functions influence the electricity demand to a great extent.

5. Comparing the results

Comparison of the actual electricity demand series with the ARIMA model, Dynamic Regression model and MLP model gives very interesting results. The comparison is done for a period of three months, starting from 1.10.2002 to 19.01.2003. The ARIMA model forecasting takes into consideration the non-stationarity part of the series. In that aspect the ARIMA model forecast is only an

estimated forecast of the original series with non-stationarity removed. Therefore the ARIMA model forecast is in that sense, it is very close to the actual series. The Dynamic Regression model takes into consideration the error part of the series. The Dynamic Regression model forecast is devoid of the error in the original series. Comparing with ARIMA model forecast, Dynamic Regression model forecast is better because the forecast is devoid of the errors in the series.

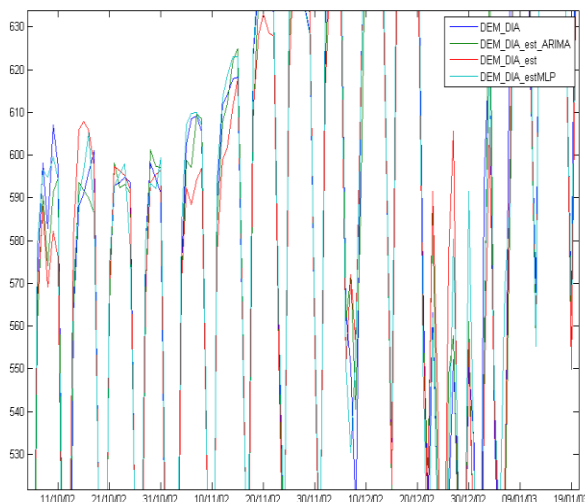


Figure 30. Comparing the Actual Demand Series with the ARIMA, Dynamic Regression model and MLP model

The Non-linear MLP model forecast takes into account all the errors and chaotic behaviours of the series. The Non-linear MLP model forecast is devoid of the errors and chaotic behaviour. Therefore we find that the Non-linear MLP model prediction gives more accurate forecast than the ARIMA model and dynamic Regression model prediction. Because the MLP model forecasting takes into account all the non-linear aspects of the variable. It takes into consideration of all the variables that have positive impact on the output. Therefore in comparison with ARIMA model and Dynamic Regression model, Non-linear MLP model forecast is more accurate as it has a positive influence on the electricity demand.

6. Conclusion

Forecasting electricity demand is a worthwhile task taking into consideration the aspects of working day and temperature. This process of forecasting is done using ARIMA, Dynamic Regression and Non-linear MLP functions in a satisfying manner. In particular, the Non-linear MLP model gives the accurate forecasting of the electricity demand.

References

- [1] Alan Pankratz, *Forecasting with Dynamic Regression Models*, Wiley-Interscience, 1991.
- [2] Alan Pankratz, *Forecasting with Univariate Box-Jenkins Models*, John Wiley and Sons, 1983.
- [3] Peter J. Brockwell and Richard A. Davies, *Introduction to Time series and Forecasting*, Springer, 1996.
- [4] Spyros Makridakis et al, *Forecasting Methods and Applications*, 3rd Edition, John Wiley and Sons, 1998.

Pesticide Spraying device using Raspberry Pi for Agricultural Application

M.Venkatesh, J.Rajesh,
AP/EEE,Priyadarshini Engineering College

Abstract

This paper presents the development of a smart sensor based environment monitoring system, in remote villages especially for crop fields. Basically, it is difficult to monitor the environment, weather all the time, so we proposed this project in Crop field, to monitor the weather and any environment changes using IOT which having some sensors like Temperature sensor, Moisture sensor, humidity which measures respective parameters throughout the day. And also parameters measured by sensors are sent through IOT. Using measured parameters we can detect and prevent from diseases by spraying pesticides.\

Keywords— IoT, monitoring, spraying, image processing.

Introduction

Beginning with the quote “SAVE THE AGRICULTURE”, main factor of agriculture is to predict the climatic changes, here we are using IOT for monitoring the weather as well as atmospheric changes throughout the crop field by having several systems in different fields as clients, which is getting reported every time to the server, about the current atmospheric change at that every certain place. So the watering and pesticides can be served based on the conditions of the field. Camera that captured image is processed then identified the disease affected plants and then pesticides to be sprayed.

In this system we are using Raspberry Pi to control the operation of the system. We use small tank in that we add pesticide and place motor to spray. Whenever the sensors detect the diseased plant, the signal is given to Raspberry Pi and it will turn on the motor and start to spray. By making some modification we can use for other applications also.

Features:

1. It can moves in forward direction.
2. It can moves in reverse direction.
3. It can suddenly turn right or left side direction.
4. It can even move sprayer up or down.

Technical Specification:

1. It operates on 9Vdc.
2. Low power consumption of 25 milli ampere current.
3. Operating Voltage of Raspberry Pi module 3V or 5Vdc.
4. Operating frequency of Raspberry Pi module 400 MHz

Hardware:

1. Robot module
2. Monitoring system.

SOFTWARE:

1. Python Program

Block Diagram Description

The block diagram of proposed system is shown in fig 1

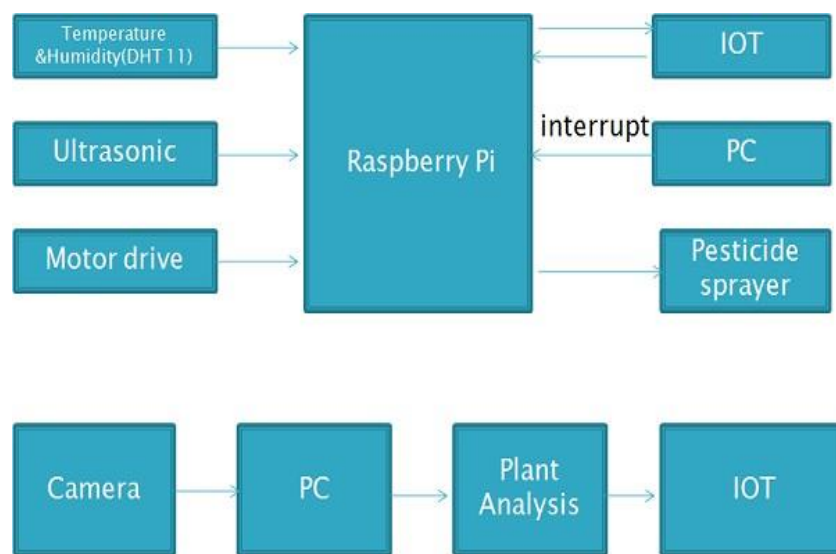


Fig 1. Block Diagram

This block diagram consist of Camera, Temperature & Humidity (DHT 11) sensor, Ultrasonic sensor, Sprayer, Motor drive (L293D) and Raspberry Pi Kit the description of each block is given in following subsections.

1 Camera:

A Webcam is a video camera that feeds or streams its image in real time to or through a computer to a computer network. When “captured” by the cam, the video stream may be saved, viewed or sent on to other network travelling through systems such as the internet, and wifi as an attachment. When send to remote location, the video stream may be saved, viewed or on sent there. Unlike an IP camera (which connects using Ethernet or wifi), a webcam is generally connected by a USB cable, or similar cable, or built into computer hardware, such as laptops.

2 Temperature & Humidity (Dht 11):

The DHT 11 Temperature and Humidity sensor features a calibrated digital signal output. It is integrated with a high performance 8-bit microprocessor. It ensure that high reliability And long term stability. This sensor includes a resistive element and a sensor for wet NTC temperature measuring devices. It has excellent quality, fast response, anti-interference ability and high performance.

Each DHT 11 sensor features extremely accurate calibration of humidity chamber. The calibration coefficients stored in the OTP program memory, internal sensors detect signals in the process, and we should call these calibration coefficients.

The single wire serial interface system integrated to become quick and easy. In Small size, low power, signal transmission distance up to 20 meters, enabling a variety of applications and even the most demanding ones. The product is 3-pin single row pin package. It has supply voltage of 5V, Temperature range is 0-50 C and Humidity ranges from 20-90% RH and it has digital interface.

3 Ultrasonic Sensor:

The Ultrasonic sensors measure distance by using ultrasonic waves. The sensor head emits an ultrasonic wave and receives the waves reflected back from the target. Ultrasonic sensors measure the distance to the target by measuring the time between the emission and reception.

An optical sensor has a transmitter and receiver, whereas ultrasonic sensor uses a single ultrasonic element for both emission and reception. In a reflective model ultrasonic sensor, a single oscillator emits and receives ultrasonic waves alternatively. This enables miniaturization of the sensor head.

The distance can be calculated with the formula: $Distance L = \frac{1}{2} * T * C$
Where L is the distance, T is the time between emission and reception, and C is the sonic speed. (The value is multiplied by $\frac{1}{2}$ because T is the time for go and return distance).

It has the following features such as Transparent object detectable, Resistance to mist and dust, Complex shaped objects detectable.

4 Sprayer:

Spray module consists of a spray head, pumps, relays, Servos, screw adjustable rod and DC machine. When an ordinary DC motor using L293D high-power motor drive circuit. Sprayer is mounted in a vertical adjustable rod to the driven by the DC motor to rotate the screw may be moved up and down to control the spray platform.

5 Motor Drive L293d:

L293D is a typical motor driver or motor driver IC which allows DC motor to drive on either direction. L293D is a 16-pin IC which can control a set of two DC motors simultaneously in any direction. It means that you can control two DC motor with a single L293D IC. Dual H-bridge motor drive integrated circuit(IC).

The L293D can drive small and quiet big motors as well, check the voltage specification. There are 4 input pins for l293d, pin 2, 7 on the left and pin 15, 10 on the right side of IC. Left input pins will regulate the rotation of motor connected across left side and right input for motor on the right hand side.

The motors are rotated on the basis of the inputs provided across the input pins as LOGIC 0 or LOGIC 1. VCC is the voltage that it needs for its own internal operation 5v; l293d will not use this voltage for driving the motor. For driving the motors it has a separate provision to provide motor supply VSS (V supply). L293D will use this to drive the motor.

It means if you want to operate a motor at 9v then you need to provide a supply of 9v across VSS motor supply. The maximum voltage for VSS motor supply is 36v. It can supply a max current of 600mA per channel. Since it can drive motor up to 36v hence you can drive pretty big motors with this l293d. VCC pin 16 is the voltage for its own internal operation. The maximum voltage ranges from 5v and upto 36v.

6 Raspberry Pi Kit:

Raspberry pi board is a miniature marvel, packing considerable computing power into a footprint no larger than a credit card. It's capable of some amazing things, but there are a few things you're going to need to know before you plunge head-first into the bramble patch.

The Raspberry Pi Compute Module (CM1), Compute Module 3 (CM3) and Compute Module 3 Lite (CM3L) are DDR2- SODIMM-mechanically-compatible System on Modules (SoMs) containing processor, memory, eMMC Flash (for CM1 and CM3) and supporting power circuitry. These modules allow a designer to leverage the Raspberry Pi hardware and software stack in their own custom systems and form factors. In addition these module have extra IO interfaces over and above what is available on the Raspberry Pi model A/B boards opening up more options for the designer.

The CM1 contains a BCM2835 processor (as used on the original Raspberry Pi and Raspberry Pi B+ models), 512MByte LPDDR2 RAM and 4Gbytes eMMC Flash. The CM3 contains a BCM2837 processor (as used on the Raspberry Pi 3), 1Gbyte LPDDR2 RAM and 4Gbytes eMMC Flash. Finally the CM3L product is the same as CM3 except the eMMC Flash is not suit, and the SD/eMMC interface pins are available for the user to connect their own SD/eMMC device. Note that the BCM2837 processor is an evolution of the BCM2835 processor.

The only real differences are that the BCM2837 can address more RAM (up to 1Gbyte) and the ARM CPU complex has been upgraded from a single core ARM11 in BCM2835 to a Quad core Cortex A53 with dedicated 512Kbyte L2 cache in BCM2837. All IO interfaces and peripherals stay the same and hence the two chips are largely software and hardware compatible. The pin out of CM1 and CM3 are identical. Apart from the CPU upgrade and increase in RAM the other significant hardware differences to be aware of are that CM3 has grown from 30mm to 31mm in height, the VBAT supply can now draw significantly more power under heavy CPU load, and the HDMI HPD N 1V8 (GPIO46 1V8 on CM1) and EMMC EN N 1V8 (GPIO47 1V8 on CM1) are now driven from an IO expander rather than the processor.

If a designer of a CM1 product has a suitably specified VBAT, can accommodate the extra 1mm module height increase and has followed the design rules with respect to GPIO46 1V8 and GPIO47 1V8 then a CM3 should work in a board designed for a CM1.

It is low in cost, reliable, low power consumption. Operating voltage is 3Vdc or 5Vdc.

Methodology And Testing

A. Digital Image:

A digital remotely sensed image is typically composed of picture elements (pixels) located at the intersection of each row i and column j in each K bands of imagery. Associated with each pixel is a number known as Digital Number (DN) or Brightness Value (BV) that depicts the average radiance of a relatively small area within a scene. A smaller number indicates low average radiance from the area and the high number is an indicator of high radiant properties of the area. The size of this area effects the reproduction of details within the scene. As pixel size is reduced more scene detail is presented in digital representation.

B. Image Acquisition and Preparation:

In this study, images of plant specimens are coated at high resolution of 700, 900, 1000 dpi using a line sensor camera with high spatial accuracy and fidelity. The image size was constrained to 1000*1000 pixels. Thus, one pixel is approximately 36, 28 and 25 micrometer for 700, 900 and 1000 dpi resolution respectively.

C. Image Enhancement Techniques:

Image enhancement techniques improve the quality of an image as perceived by a human. These techniques are most useful because many satellite images when examined on a colour display give inadequate information for image interpretation. There is no conscious effort to improve the fidelity of the image with regard to some ideal form of the image.

There exists a wide variety of techniques for improving image quality. The contrast stretch, density slicing, edge enhancement, and spatial filtering are the more commonly used techniques. Image enhancement is attempted after the image is corrected for geometric and radiometric distortions. Image enhancement methods are applied separately to each band of a multispectral image. Digital techniques have been found to be most satisfactory than the photographic technique for image enhancement, because of the precision and wide variety of digital processes.

D. Contrast:

Contrast generally refers to the difference in luminance or grey level values in an image and is an important characteristic. It can be defined as the ratio of the maximum intensity to the minimum intensity over an image.

Contrast ratio has a strong bearing on the resolving power and detects ability of an image. Larger this ratio, more easy it is to interpret the image. Satellite images lack adequate contrast and require contrast improvement.

E. Contrast Enhancement:

Contrast enhancement techniques expand the range of brightness values in an image so that the image can be efficiently displayed in a manner desired by the analyst. The density values in a scene are literally pulled farther apart, that is, expanded over a greater range. The effect is to increase the visual contrast between two areas of different uniform densities. This enables the analyst to discriminate easily between areas initially having a small difference in density.

F. Linear Contrast Stretch:

This is the simplest contrast stretch algorithm. The grey values in the original image and the modified image follow a linear relation in this algorithm. A density number in the low range of the original histogram is assigned to extremely black and a value at the high end is assigned to extremely white. The remaining pixel values are distributed linearly between these

extremes. The features or details that were obscure on the original image will be clear in the contrast stretched image. Linear contrast stretch operation can be represented graphically. To provide optimal contrast and colour variation in colour composites the small range of grey values in each band is stretched to the full brightness range of the output or display unit.

G. Non-Linear Contrast Enhancement:

In these methods, the input and output data values follow a non-linear transformation. The general form of the non-linear contrast enhancement is defined by $y = f(x)$, where x is the input data value and y is the output data value. The non-linear contrast enhancement techniques have been found to be useful for enhancing the colour contrast between the nearly classes and subclasses of a main class.

A type of non linear contrast stretch involves scaling the input data logarithmically. This enhancement has greatest impact on the brightness values found in the darker part of histogram. It could be reversed to enhance values in brighter part of histogram by scaling the input data using an inverse log function.

Histogram equalization is another non-linear contrast enhancement technique. In this technique, histogram of the original image is redistributed to produce a uniform population density. This is obtained by grouping certain adjacent grey values. Thus the number of grey levels in the enhanced image is less than the number of grey levels in the original image.

H. Spatial Filtering:

A characteristic of remotely sensed images is a parameter called spatial frequency defined as number of changes in Brightness Value per unit distance for any particular part of an image. If there are very few changes in Brightness Value once a given area in an image, this is referred to as low frequency area. Conversely, if the Brightness Value changes dramatically over short distances, this is an area of high frequency.

Spatial filtering is the process of dividing the image into its constituent spatial frequencies, and selectively altering certain spatial frequencies to emphasize some image features. This technique increases the analyst's ability to discriminate detail. The three types of spatial filters used in remote sensor data processing are: Low pass filters, Band pass filters and High pass filters.

I. Edge Enhancement in the Spatial Domain:

For many remote sensing earth science applications, the most valuable information that may be derived from an image is contained in the edges surrounding various objects of interest. Edge enhancement delineates these edges and makes the shapes and details comprising the image more conspicuous and perhaps easier to analyze. Generally, what the eyes see as pictorial edges are simply sharp changes in brightness value between two adjacent pixels. The edges may be enhanced using either linear or nonlinear edge enhancement techniques.

J. Linear Edge Enhancement:

A straightforward method of extracting edges in remotely sensed imagery is the application of a directional first-difference algorithm and approximates the first derivative between two adjacent pixels. The algorithm produces the first difference of the image input in the horizontal, vertical, and diagonal directions.

The Laplacian operator generally highlights point, lines, and edges in the image and suppresses uniform and smoothly varying regions. Human vision physiological research suggests that we see objects in much the same way. Hence, the use of this operation has a more natural look than many of the other edge-enhanced images.

K. Band rationing:

Sometimes differences in brightness values from identical surface materials are caused by topographic slope and aspect, shadows, or seasonal changes sunlight illumination angle and intensity. These conditions may hamper the ability of an interpreter or classification algorithm to identify correctly surface materials or land use in a remotely sensed image. Fortunately, ratio transformations of the remotely sensed data can, in certain instances, be applied to reduce the effects of such environmental conditions. In addition to minimizing the effects of environmental factors, ratios may also provide unique information not available in any single band that is useful for discriminating between soils and vegetation.

L. Training data:

Training fields are areas of known identity delineated on the digital image, usually by specifying the corner points of a rectangular or polygonal area using line and column numbers within the coordinate system of the digital image. The analyst must, of course, know the correct class for each area. Usually the analyst begins by assembling maps and aerial photographs of the area to be classified. Specific training areas are identified for each informational category following the guidelines outlined below. The objective is to identify a set of pixels that accurately represents spectral variation present within each information region

Various supervised classification algorithms may be used to assign an unknown pixel to one of a number of classes. The choice of a particular classifier or decision rule depends on the nature of the input data and the desired output.

Parametric classification algorithms assume that the observed measurement vectors X_c for each class in each spectral band during the training phase of the supervised classification are Gaussian in nature; that is, they are normally distributed. Nonparametric classification algorithms make no such assumption. Among the most frequently used classification algorithms are the parallelepiped, minimum distance, and maximum likelihood decision rules

This is a widely used decision rule based on simple Boolean "and/or" logic. Training data in n spectral bands are used in performing the classification. Brightness values from each pixel of the multispectral imagery are used to produce an n -dimensional mean vector, $M_c = (\mu_{c1}, \mu_{c2}, \mu_{c3}, \dots, \mu_{cn})$ with μ_{ck} being the mean value of the training data obtained for class c in band k out of m possible classes, as previously defined. S_{ck} is the standard deviation of the training data class c of band k out of m possible classes.

The decision boundaries form an n -dimensional parallelepiped in feature space. If the pixel value lies above the lower threshold and below the high threshold for all n bands evaluated, it is assigned to an

unclassified category. Although it is only possible to analyze visually up to three dimensions, as described in the section on computer graphic feature analysis, it is possible to create an n-dimensional parallelepiped for classification purposes.

The parallelepiped algorithm is a computationally efficient method of classifying remote sensor data. Unfortunately, because some parallelepipeds overlap, it is possible that an unknown candidate pixel might satisfy the criteria of more than one class. In such cases it is usually assigned to the first class for which it meets all criteria. A more elegant solution is to take this pixel that can be assigned to more than one class and use a minimum distance to means decision rule to assign it to just one class.

Minimum Distance to Means Classification Algorithm

This decision rule is computationally simple and commonly used. When used properly it can result in classification accuracy comparable to other more computationally intensive algorithms, such as the maximum likelihood algorithm. Like the parallelepiped algorithm, it requires that the user provide the mean vectors for each class in each band μ_{ck} from the training data. To perform a minimum distance classification, a program must calculate the distance to each mean vector, μ_{ck} from each unknown pixel (BV_{ijk}). It is possible to calculate this distance using Euclidean distance based on the Pythagorean theorem.

The computation of the Euclidean distance from point to the mean of Class-1 measured in band relies on the equation

$$\text{Dist} = \text{SQRT}\{ (BV_{ijk} - \mu_{ck})^2 + (BV_{ijl} - \mu_{cl})^2 \}$$

Where μ_{ck} and μ_{cl} represent the mean vectors for class c measured in bands k and l.

Many minimum-distance algorithms let the analyst specify a distance or threshold from the class means beyond which a pixel will not be assigned to a category even though it is nearest to the mean of that category.

Maximum Likelihood Classification Algorithm

The maximum likelihood decision rule assigns each pixel having pattern measurements or features X to the class c whose units are most probable or likely to have given rise to feature vector x . It assumes that the training data statistics for each class in each band are normally distributed, that is, Gaussian. In other words, training data with bi- or trimodal histograms in a single band are not ideal. In such cases, the individual modes probably represent individual classes that should be trained upon individually and labeled as separate classes. This would then produce uni-modal, Gaussian training class statistics that would fulfill the normal distribution requirement.

The Bayes's decision rule is identical to the maximum likelihood decision rule that it does not assume that each class has equal probabilities. A priori probabilities have been used successfully as a way of incorporating the effects of relief and other terrain characteristics in improving classification accuracy. The maximum likelihood and Bayes's classification require many more computations per pixel than either the parallelepiped or minimum-distance classification algorithms. They do not always produce superior results.

Classification Accuracy Assessment

Quantitatively assessing classification accuracy requires the collection of some in situ data or a priori knowledge about some parts of the terrain which can then be compared with the remote sensing derived classification map. Thus to assess classification accuracy it is necessary to compare two classification maps 1) the remote sensing derived map, and 2) assumed true map (in fact it may contain some error). The assumed true map may be derived from in situ investigation or quite often from the interpretation of remotely sensed data obtained at a larger scale or higher resolution.

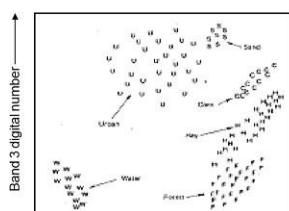


Figure 7a: Pixel observations from selected training sites plotted on scatter diagram

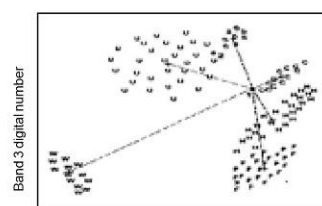


Figure 7b: Minimum Distance to Means Classification strategy

Classification Error Matrix

One of the most common means of expressing classification accuracy is the preparation of classification error matrix sometimes called confusion or a contingency table. Error matrices compare on a category by category basis, the relationship between known reference data (ground truth) and the corresponding results of an automated classification. Such matrices are square, with the number of rows and columns equal to the number of categories whose classification accuracy is being assessed.

Table 1 is an error matrix, an image analyst has prepared to determine how well a Classification has categorized a representative subset of pixels used in the training process of a supervised classification. This matrix stems from classifying the sampled training set pixels and listing the known cover types used for training

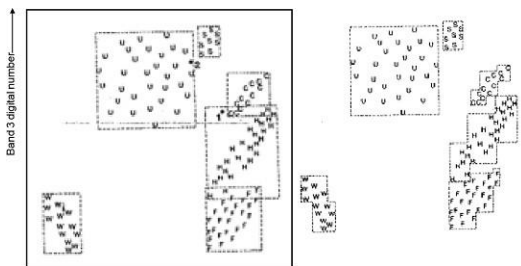


Figure 7c: Parallelepiped classification strategy

Figure 7d: Stepped parallelepipeds to avoid overlap

(columns) versus the Pixels actually classified into each land cover category by the classifier (rows).

Table 1. Error Matrix resulting from classifying training Set pixels

| | W | S | F | U | C | H | Row Total |
|--------------|-----|----|-----|-----|-----|-----|-----------|
| W | 480 | 0 | 5 | 0 | 0 | 0 | 485 |
| S | 0 | 52 | 0 | 20 | 0 | 0 | 72 |
| F | 0 | 0 | 313 | 40 | 0 | 0 | 353 |
| U | 0 | 16 | 0 | 126 | 0 | 0 | 142 |
| C | 0 | 0 | 0 | 38 | 342 | 79 | 459 |
| H | 0 | 0 | 38 | 24 | 60 | 359 | 481 |
| Column Total | 480 | 68 | 356 | 248 | 402 | 438 | 1992 |

Classification data Training set data (Known cover types) →

| Producer's Accuracy | Users Accuracy |
|---------------------|-------------------|
| W=480/480 = 100% | W= 480/485 = 99% |
| S = 052/068 = 16% | S = 052/072 = 72% |
| F = 313/356 = 88% | F = 313/352 = 87% |
| U = 126/241 = 51% | U = 126/147 = 99% |
| C = 342/402 = 85% | C = 342/459 = 74% |
| H = 359/438 = 82% | H = 359/481 = 75% |

Overall accuracy = (480 + 52 + 313+ 126+ 342 +359)/1992 = 84%

W, water; S, sand; F, forest; U, urban; C, corn; H, hay

Similarly data can be taken for plant only and image process is done and train the specific or all kind of plants in module. This data can be stored in database as a reference.

Thus the camera capture image is processed digital by following methodology as mentioned above.

Working of Autonomous Pesticide Sprayer

In this project, whenever our atmospheric condition changes sensors connected to Raspberry Pi sense and monitor weather throughout the day. If temperature becomes low and humidity is more than robot starts to move in crop field. The supply is given to motor by DC battery. According to logic programmed in L293D motor drive give commands to robot (Forward, Backward, Left Turn, Right Turn).

When an plant or object is detected by using ultrasonic sensor(within 50cm). If it is detected then it gives trip signal to motor drive and motor gets stop. The Camera connected to Raspberry Pi will capture image and it will undergo digital image processing. If plant is seem to be affected then this information is shared to L293D, the servomotor connected to L293D will turn on pesticide sprayer and its sprays.

After completion of spraying robot turns and go to next plant and starts image processing. When a plant is not affected by diseases then sprayer will not operate.

The overall setup is shown in figure below:

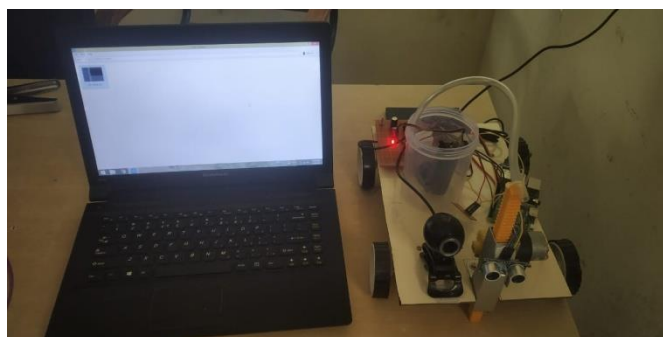


Fig: Robot Setup

Conclusion

According to this system, irrigation system becomes more autonomous with quick transmission of data by using IOT. The main advantage in IOT is, even when clients are not in the node network, data will be sent, whenever a client is connected with that node, they can able to see the data which has been sent already. So they can able to analyze the atmospheric change throughout every day and improve the crop production. It also reduce the usage of pesticides upto 30- 40%.

Reference

- [1] S. I. Cho and N. H. Ki, "Autonomous speed sprayer guidance using machine vision and fuzzy logic," *Trans. Amer. Soc. Agricult. Eng.*, vol. 42, no. 4, pp. 1137–1144, 1999.
- [2] S. Dasgupta, C. Meisner, D. Wheeler, K. Xuyen, and N. T. Lam, "Pesticide poisoning of farm workers—Implications of blood test results from Vietnam," *Int. J. Hygiene Environ. Health*, vol. 210, no. 2, pp. 121–132, 2007.
- [3] W. J. Rogan and A. Chen, "Health risks and benefits of bis(4- chlorophenyl)-1,1,1-trichloroethane(DDT)," *Lancet*, vol. 366, no. 9787, pp. 763–773, 2005.
- [4] S. H. Swan et al., "Semen quality in relation to biomarkers of pesticide exposure," *Environ. Health Perspect.*, vol. 111, no. 12, pp. 1478–1484, 2003.
- [5] Y. Guan, D. Chen, K. He, Y. Liu, and L. Li, "Review on research and application of variable rate spray in agriculture," in *Proc. IEEE 10th Conf. Ind. Electron. Appl. (ICIEA)*, Jun. 2015.
- [6] M. Pérez-Ruiz et al.,

“Highlights and preliminary results for autonomous crop protection,” *Comput. Electron. Agricult.*, vol. 110, pp. 150–161, Jan. 2015.

[7]. A. Mandow, J. M. Gomez-de-Gabriel, J. L. Martinez, V. F. Munoz, A. Ollero, and A. Garcia-Cerezo, “The autonomous mobile robot AURORA for greenhouse operation,” *IEEE Robot. Autom. Mag.*, vol. 3, no. 4, pp. 18–28, Dec. 1996.

Design of 7 Level Multilevel Inverter with Reduced Switches

Ms.S.Shobana, Ms.M.Saranya,Dr.K.Thenmalar

EEE,Vivekanandha College of Engineering forWomen,TamilNadu

Abstract

A Multilevel inverter is a force electronic gadget that is utilized for high voltage and high force applications and has numerous favorable circumstances like, low exchanging pressure, low absolute consonant twisting (THD). Thus, the size and cumbersomeness of detached channels can be diminished. This work proposes another geography of a 7-level fell staggered inverter with decreased number of switches than that of traditional sort which has 12 switches. The geographies comprise of circuit with 7 switches for a similar 7-level yield. Hence with less number of switches, there will be a decrease in door drive hardware and furthermore not many switches will lead for explicit timespans. The SPWM procedure is executed utilizing multicarrier wave signals. The circuit is displayed and recreated with the assistance of MATLAB/SIMULINK.

Keywords: *Cascaded Multilevel Inverter(CMLI), Diode Clamped Multilevel Inverter(DCMLI), Flying Capacitor, Pulse Width Modulation (PWM), Selective Harmonic Elimination*

1 Introduction

As of late, the requirement for high force mechanical assembly has been determined by various modern applications. Medium voltage engine drives and utility applications are a few models, since they require medium voltage and megawatt power level. Another application respects medium voltage matrices, where it is problematic to interface just one force semiconductor switch straightforwardly. Therefore, a few staggered power converter structures have been presented as an option in high force and medium voltage applications. Staggered converters accomplish high force appraisals, yet additionally empower the utilization of environmentally friendly power sources. This part examines about the kinds of staggered inverters and its preferences.

1.1 Multilevel Inverters

Multilevel converters not just create the yield voltages with low bending, yet in addition lessen the dv/dt stresses, henceforth electromagnetic compatibility (EMC) issues can be diminished. In addition, three diverse major staggered converter designs, for example, fell H-spans converter with isolated dc sources, diode clipped (nonpartisan clasped) and flying capacitors (capacitor braced) have been accounted for in the writing.

1.1.1 Cascaded Multilevel Inverter

A Cascaded Multilevel Inverter (CMLI) is a force electronic gadget intended to create an AC voltage from DC voltages of a few levels. This design of CMLI comprises of a progression of H-connect (single-stage full extension) inverter units in every one of its three stages. Every H-connect unit has its own dc source. Through various blends of the four switches, S1-S4, every converter level can produce three diverse voltage yields, +Vdc, - Vdc and zero. The AC yields of various full-connect converters in a similar stage are associated in arrangement with the end goal that the incorporated voltage waveform is the amount of the individual converter yields. Every H-connect unit creates a semi square waveform by stage moving its positive and negative stage legs exchanging time. Each exchanging gadget consistently leads for 180° paying little heed to the beat width of the semi square wave. This exchanging strategy causes current pressure of the whole exchanging gadgets as equivalent.

The number of output phase voltage levels in a cascade inverter is defined by

$$m = 2s + 1 \quad (1.1)$$

Where

m- Number of output voltage levels per phase s

- Number of dc sources.

A number of single-phase full bridges present in k-level CMLI is given by,

$$n = (k - 1) / 2$$

Where k- total level of CMLI.

A three-phase CMLI topology is essentially composed of three identical phase legs of the series- chain of H-bridge converters, which can possibly generate different output voltage waveforms and offers phase-balancing for AC system. This feature is impossible in other VSI topologies utilizing a common DC link. Since this topology consists of series power conversion cells, the voltage and power level may be easily scaled. The dc link supply for each full bridge converter is provided separately.

$$V_{an} = V_{dc1} + V_{dc2} + \dots + V_{dc(s+1)} + V_{dcs} \tag{5}$$

Operation of CMLI

A single-phase structure of an m-level cascaded inverter is illustrated in Figure 1.1. Each separate dc source is connected to a single-phase full-bridge, or H-bridge, inverter. Each inverter level can generate three different voltage outputs, +Vdc, 0 and -Vdc by connecting the dc source to the different combinations of the four switches, S1, S2, S3 and S4. To obtain +Vdc, switches S1 and S4 are turned on, whereas -Vdc can be obtained by turning on switches S2 and S3. By turning on S1 and S2 or S3 and S4, the output voltage is zero.

The ac outputs of each of the different full-bridge inverter levels are connected in series such that the synthesized voltage waveform is the sum of the inverter outputs.

The phase voltage waveform for an 5-level cascaded H-bridge inverter with 2 separate dc source voltage and 2 full bridges is shown in Figure 1.2.

Thus the output voltage of a phase is given as

$$V_{an} = V_{a1} + V_a$$

Thus, the predominant lower frequency harmonics such as 5th, 7th, 11th and 13th harmonics are eliminated while using this configuration.

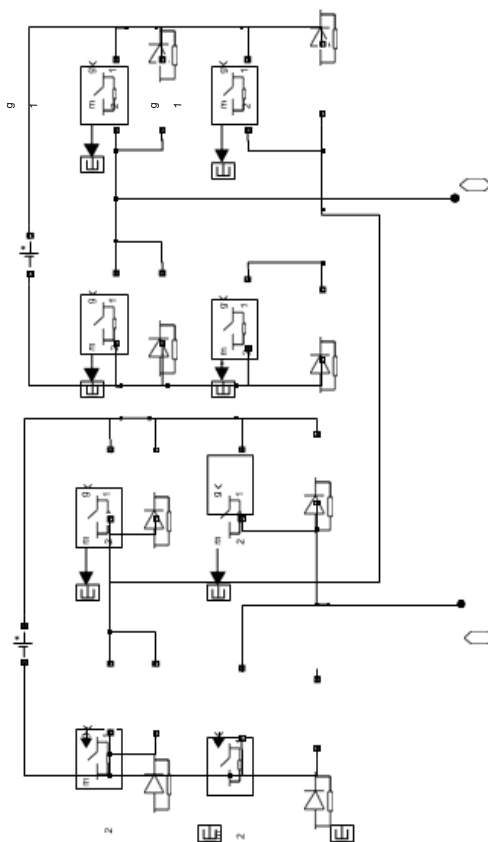


Figure 1 Topology of a cascaded multilevel inverter in one phase

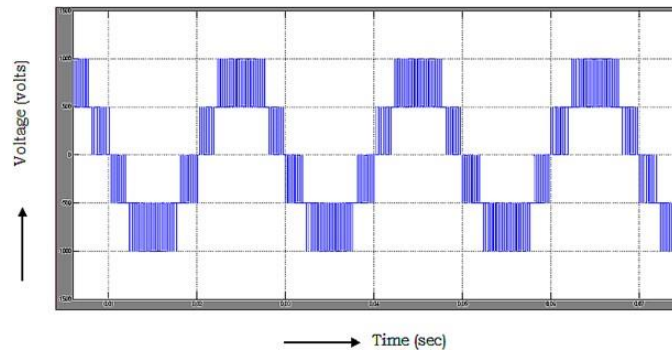


Figure 2 The output voltage waveform of H-bridge

Multilevel cascaded inverters have been proposed for the applications such as static var generation, an interface with renewable energy sources and for battery-based applications. Cascaded inverters are also proposed for use as the main traction drive in electric vehicles. Beside this, the applications of the cascaded inverters are as follows:

1. It is more suitable for high-voltage, high-power applications than the conventional inverters.
2. It generates a staircase voltage waveform approaching a sinusoidal output voltage thereby increasing the number of levels. It does not require any voltage balance circuits or voltage matching devices as it consists of a cascaded connection of many single-phase, full bridge inverter fed with a separate DC source.

1.1.2 Diode Clamped Multilevel Inverter

The general structure of the multilevel inverter is to synthesize a sinusoidal voltage from several levels of voltages typically obtained from capacitor voltage sources. A three level inverter, also known as a “neutral-clamped” inverter, consists of two capacitor voltages in series and uses the center tap as the neutral. Each phase leg of the three-level inverter has two pairs of switching devices in series. The center of each device pair is clamped to the neutral through clamping diodes. The output obtained from a three-level inverter is a quasi-square wave output if fundamental frequency switching is used. Multilevel inverters are being considered for an increasing number of applications due to their high power capability associated with lower output harmonics and lower commutation losses.

Multilevel inverters have become an effective and practical solution for increasing power and reducing harmonics of AC load. The main multilevel topologies are classified into three categories: diode clamped inverters, flying capacitor inverters, and cascaded inverters. In a three-phase inverter system, the number of main switches of each topology is equal. Comparing with the number of other components, for example, clamping diodes and dc-link capacitors having the same capacity per unit, diode clamped inverters have the least number of capacitors among the three types but require additional clamping diodes. Flying capacitor inverters need the most number of capacitors. But cascaded inverters are considered as having the simplest structure. The diode clamped inverter, particularly the three-level one, has drawn much interest in motor drive applications because it needs only one common voltage source. Also, simple and efficient PWM algorithms have been developed for it, even if it has inherent unbalanced dc-link capacitor voltage problem. However, it would be a limitation to applications beyond four-level diode clamped inverters for the reason of reliability and complexity considering dc-link balancing and the prohibitively high number of clamping diodes. Multilevel PWM has lower dv/dt than that experienced in some two-level PWM drives because switching is between several smaller voltage levels. Diode clamped multilevel inverter is a very general and widely used topology. DCMLI works on the concept of using diodes to limit voltage stress on power devices. A DCMLI typically consists of $(m-1)$

capacitors on the DC bus where m is the total number of positive, negative and zero levels in the output voltage. The phase a output voltage V_{an} has five states: $V_{dc}/2$, $V_{dc}/4$, 0 , $-V_{dc}/4$ and $-V_{dc}/2$.

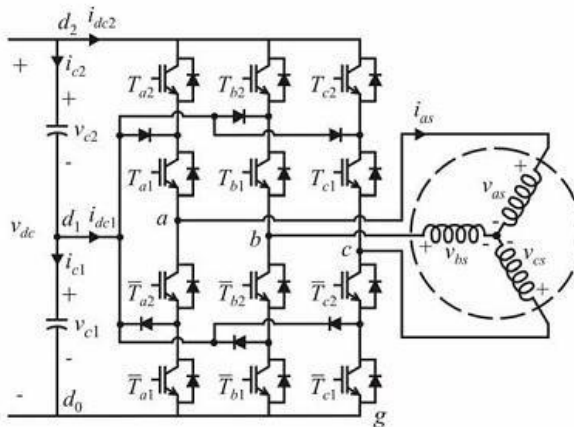
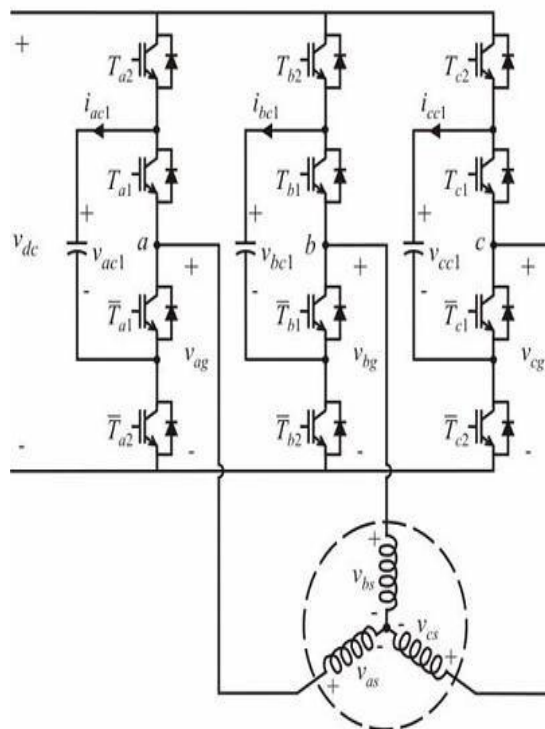


Figure 3 Diode clamped inverter topology

1.1.3 Flying capacitor structure

Another fundamental multilevel topology, the flying capacitor, involves series connection of capacitor clamped switching cells. This topology has several unique and attractive features when compared to the diode-clamped inverter. One feature is that added clamping diodes are not needed. Furthermore, the flying capacitor inverter has switching redundancy within the phase which can be used to balance the flying capacitors so that only one dc source is needed. Figure 4 shows the three-level flying capacitor inverter. The general concept of operation is that each flying capacitor is charged to one-half of the dc voltage and can be connected in series with the phase to add or subtract this voltage.



1.2 Modeling and Control of MLI

A scheme for finite state model predictive control-fed five-level cascaded MLI has been established. This proposed method uses 19 voltage vectors out of totally 125 voltage vectors of the cascaded MLI. Since this inverter has many switches and

Figure 4 Three level flying capacitor topology

reduces the average switching frequency which is a matter of great importance for high voltage applications, as they contribute to significant switching losses. Two schemes of Finite State Model Predictive Control (FSMPC) are proposed i.e. FSMPC-1 employing the current control of the cascaded MLI with 19 voltage vectors and FSMPC-2 aiming the control of inverter load current as well as reducing the average switching frequency using 19 vectors. The performance of the proposed schemes is compared with a conventional 61 voltage vector scheme of the cascaded inverter. The results show that both the proposed schemes perform well for steady state and dynamic operating conditions (Razia Sultana et al. 2016). A novel space-vector current-control strategy has been employed to maintain the desired number of voltage levels based on load current, in a newer five-level single-phase voltage source inverter. With the proper selection of the redundant inverter switching states, the deviation in neutral-point voltage is considerably minimized (Ammar Masaoud et al. 2014). To balance conduction losses in full-bridge and Multi-Level Cascade Inverters, a switching method has been proposed, and its effectiveness and validity have been examined (Hosseini Aghdam et al. 2008).

2.1 PWM Strategy

In 1999, Tolbert & Habetler found that the implementation of the existing control strategies for a DC-MLI impinges on the switch utilization, thus increasing the losses. In 2000, Mcgrath & Holmes obtained an analytical solution for PWM techniques and found that the harmonic components produced by APOD technique in DC-MLIs produce the same effect as that of the PSC in CHBMLIs. In 2001, Calais et al. reviewed the MCPWM methods. A few regular sampled control strategies apposite for MLIs are also available based on either solving complex equations or evolutionary computing. A general Space Vector PWM (SVPWM) method for MLI based on a generalization of dwell-times calculation has been achieved (Trabelsi et al. 2012).

The presented scheme is developed for CHBMLI in which the sectors are defined by two parameters serving for easy calculation of dwell-times. This paper introduced a new switching scheme for a new topology of MLI with reduced number of switches for interfacing fuel-cell with the grid. An unipolar PWM technique has been coined for the switching of MLI topology with reduced number of switches for interfacing fuel-cell with the grid (Kumar & Pal 2014). A level shifted PWM control string source-based MLI topology has been formulated. This topology works with the innovative PWM strategy in achieving the targeted output. In this case, the DC source is connected with controlled switch by level shifted PWM technique, which is connected across an anti-parallel diode and such types of controlled sources are placed in series (Subbarao et al. 2014).

The Third Harmonic Injection PWM (THIPWM) strategy of a seven-level Uniform Step Cascaded H-Bridge Asymmetrical Inverter (USCHBAI) has been detailed with the comparison of SPWM strategy (Taleb et al. 2015).

A single-phase modified H-Bridge seven-level inverter structure has been schemed suitable for stand-alone PV systems. Selective Harmonic Elimination (SHE) technique involving Newton-Raphson method has been used to solve the non-linear equations from the switching angles (Krismadinata et al. 2013). A Bacterial Foraging Algorithm (BFA) method is proposed for switching angle selection in PWM inverter. The problem of voltage harmonic elimination together with output voltage regulation is drafted as an optimization task and the solution is sought through the proposed method. Extensive simulations are carried out using MATLAB/SIMULINK environment under various operating points with different switching pulses per half cycle. To demonstrate the superiority of the proposed method, BFA results are compared with other existing techniques such as Genetic Algorithm (GA) and Particle Swarm Optimization (PSO) method (Sudhakar Babu et al. 2015).

A generalized Hybrid single-carrier sinusoidal modulation control for cascaded MLIs has been devised. This scheme combines the features of single-carrier sinusoidal and fundamental frequency modulations. The important characteristic of this modulation is better harmonic performance and reduced switching losses (Govindaraju & Baskaran 2011).

3.1 Pulse Width Modulation (PWM) Strategies

Mainly the power electronic converters are operated in the “switched mode” state. Thus, the switches within the converter are always in either one of the two states - turned off or turned on condition. To control the flow of power in the converter, the switches alternate between these two states (i.e. on and off). This happens rapidly so that the inductors and capacitors at the input and output averages or filters the switched signal. This process is called Pulse Width Modulation (PWM), since the desired average value is controlled by modulating the width of the pulses.

For maximum attenuation of the switching component, the switch frequency f_c should be higher than the frequency of the desired fundamental AC component.

This PWM can be realized using different techniques such as carrier based PWM, PWM with harmonics minimization and space vector PWM. The carrier PWM can be natural PWM, symmetric PWM and asymmetric PWM.

The most simple and well known PWM technique is the sinusoidal PWM. This technique uses a controller which determines the voltage reference of the inverter from the error between the measured current and its reference. This reference voltage is then compared with a triangular carrier signal. The output of this comparison decides the switching function of the VSI. The choice of the ratio between the frequency of the reference signal and the frequency of the carrier signal is very important in the case of symmetric and periodic reference. As a consequence, in the case of sinusoidal reference, the ratio between the two frequencies must be integer to synchronize the carrier with the reference. It is preferable that the carrier frequency be odd to conserve the reference symmetry. In all cases this ratio must be sufficiently high to ensure the fast switching and to take the switching harmonics away from the fundamental produced by the inverter.

3.2 Selective Harmonic Elimination (SHE) Method

In this technique, the switching angles are computed offline and are calculated in such a way that arbitrary harmonics, usually low order, up to $(a-1)$ harmonics are eliminated, where “a” is the number of switching angles. The switching angles must be lower than 90° . If the angles are larger than 90° than the actual output signal would not be achieved. Higher order harmonics can be filtered using additional filters between the inverter and the load.

This modulation operates at a very low switching frequency to reduce the semiconductor losses. To minimize harmonic distortion low frequency harmonics are chosen for elimination by properly selecting angles among different level inverters.

3.3 Space Vector Modulation (SVM) Technique

Each multilevel inverter has several switching states which generate different voltage vectors and can be used to modulate the reference. The reference signal is generated from its closest signals. SVM identifies each switching state of a multilevel inverter as a point in complex space. Then reference phasor rotating in the plane at the fundamental frequency is sampled within each switching period and the nearest three inverter switched states are selected with duty cycles calculated to achieve the same volt-second average as the sampled reference phasor. This directly controls the inverter line to line voltages and only implicitly develops the phase leg voltages (Massoud et al 2007a, Massoud et al 2007b, Massoud et al 2008).

Principle of Space Vector PWM

- a. Treats the sinusoidal voltage as a constant amplitude vector rotating at constant frequency
- b. This PWM technique approximates the reference voltage V_{ref} by a combination of the eight switching patterns (V_0 to V_7)
- c. Coordinate Transformation (abc reference frame to the stationary d-q frame): A three-phase voltage vector is transformed into a vector in the stationary d-q coordinate frame which represents the spatial vector sum of the three-phase voltage
- d. The vectors (V_1 to V_6) divide the plane into six sectors (each sector: 60 degrees)
- e. V_{ref} is generated by two adjacent non-zero vectors and two zero vectors

3.4 Carrier Based Pulse Width Modulation Techniques

The carrier frequency is the same as the switching frequency. If the modulation were reduced to zero or a DC quantity, then the PWM spectrum would consist of the carrier and its harmonics alone. As the amplitude of the modulating waveform is increased, sidebands appear and increase in amplitude on either side of the carrier and its harmonics. As the frequency of the modulating waveform is increased, the sidebands spread away from the central carrier frequency. The carrier frequency should be synchronous, that is an integer multiple of the fundamental frequency, if the pulse number is low (say $N < 21$). An odd multiple guarantees half and quarter wave symmetry and therefore no even harmonics occur in the carrier spectrum.

If the same carrier signal is used to generate all three phase leg PWM signals in a three phase inverter, the carrier spectral terms in the phase leg signals will also be identical. Thus the carrier spectral terms (but not the carrier sidebands or modulating terms) will be cancelled in the phase to phase waveforms. This is true regardless of the pulse number N . Although the phase relationship between the modulating and carrier waveforms can be arbitrary, it is suggested that the slopes of the triangular carrier and modulating waveform, if sinusoidal in character, should be of the opposite polarity at the coincident zero crossings, especially for low N . This has practical implementation advantages of preserving the accuracy of the edges in analog implementations and easing the transition between different pulse numbers in systems where this may change during operation. Additionally this 180 degree phase difference (phase relative to the carrier period) results in the minimization of the harmonic losses in an inductive load. This 180 degree out-of-phase relationship can only exist for odd N . Further, the reduction in harmonic losses due to a specific phase relationship between modulating function and carrier is only significant for odd N . To achieve this phase relationship in a three phase inverter for all three phases requires N to be an odd multiple of three ($N = 3, 9, 15, 21 \dots$), if the same carrier is to be used for all three phases to achieve carrier cancellation in the phase-phase output.

In a multi-level converter with an integer pulse number, only one carrier can ever meet this requirement, as the other carriers are usually phase shifted relative to it. However, if a non-integer synchronous pulse number is used in a multilevel converter, this phase relationship once again becomes valid.

(i) Carrier Switching Frequency Sub Harmonic Pulse Width Modulation (CSFSHPWM)

For an m -level inverter, this technique uses $(m-1)$ triangular carrier signals with the same frequency (f_c), same peak-to-peak amplitude (A_c) and same phase which are disposed such that the bands they occupy are contiguous. The sinusoidal modulation waveform is centered in the middle of the carrier set and is continuously compared with each of the carrier signals. If the reference is greater than a carrier signal, then the active device corresponding to that carrier is switched on and if the reference is less than a carrier signal, then the active device corresponding to that carrier is switched off. This method is also known as sinusoidal pulse width modulation (SPWM). In multilevel inverters, the amplitude modulation index m_a and the frequency ratio m_f are defined as given as

$$m_a = A_m / (m-1) \cdot A_c \quad (3.1)$$

$$m_f = f_c / f_m \quad (3.2)$$

The CSFSHPWM control method along with carrier and modulating wave forms are shown in Figure 5.

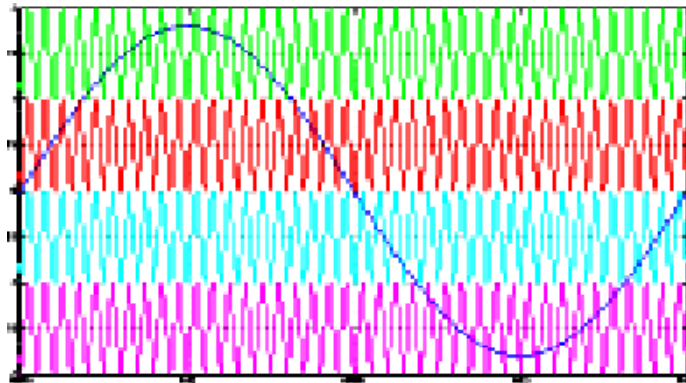


Figure 5 Waveform of CSFSHPWM

(ii) Carrier Switching Frequency Optimal Pulse Width Modulation (CSF-O-PWM)

Another carrier based method for multilevel applications is termed as switching frequency optimal PWM (SFO-PWM) and it is similar to SH-PWM except that a zero sequence (triplen harmonic) voltage is added to each of the carrier waveforms. This method takes the instantaneous average of the maximum and minimum of the three reference voltages (V_{a^*} , V_{b^*} and V_{c^*}) and subtracts this value from each of the individual reference voltages to obtain the modulation waveforms. The CSF-O-PWM control method along with carrier and modulating wave forms are shown in Figure.

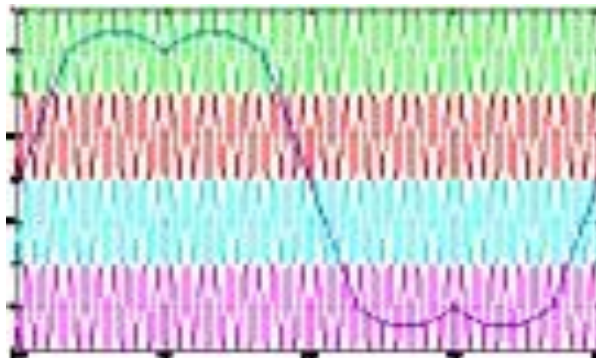


Figure 6 Waveform of CSF-O-PWM

(iii) Variable Switching Frequency Multi-Carrier Sub Harmonic Pulse Width Modulation (VSFMC-SH-PWM)

In this technique for a multi-level inverter, $(m-1)$ carrier signals with different switching frequencies are used with sinusoidal reference signals.

(iv) Variable Switching Frequency Multicarrier Optimal Pulse Width Modulation (VSFMC-O-PWM)

For a multilevel inverter, if the levels are 'm' there will be ' $(m-1)$ ' carrier set with variable switching frequency multi carrier pulse width modulation.

(v) Carrier Phase Shifted Sub Harmonic PWM (CPS-SHPWM)

In the phase shifted multicarrier modulation, all triangular carriers have same frequency and the same peak to peak amplitude but there is a phase shift between any two adjacent carrier waves. Gate signals are generated by comparing the

modulating wave with the carrier waves. In this PWM method the equivalent switching frequency of the whole converter is $(m-1)$ times the switching frequency of each power device. This means CPS-PWM can achieve a high equivalent switching frequency effect at very low real device switching frequency which is most useful in high power applications.

(vi) Alternate Phase Opposition Disposition (APOD) PWM

In this modulation, alternative carrier waves are phase displaced by 180° . The APOD-PWM control method along with carrier and modulating wave forms are shown in Fig. The rules for APOD method,

i) The converter switches to $+V_{dc} / 2$ when the reference is greater than all the carrier waveforms.

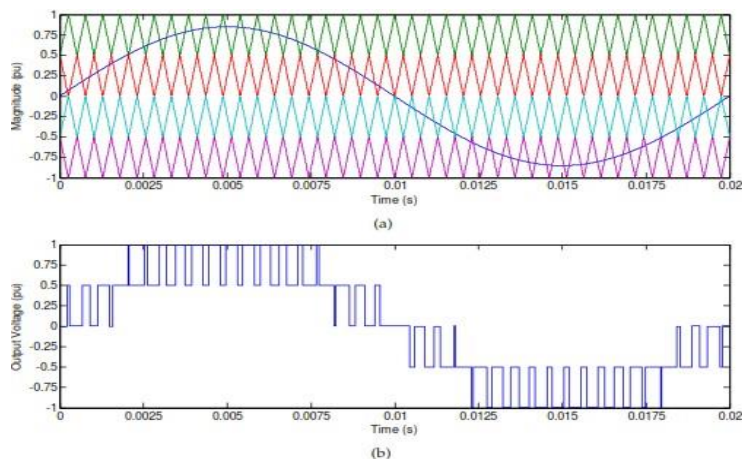


Figure 7 APOD-PWM technique: a) Reference and carrier signals, b) Output phase voltage waveform

(vii) Phase Opposition Disposition PWM (POD-PWM)

In POD-PWM control technique, the carrier signals which are above the zero level are in phase and the carrier signals which are below the zero level are in phase of each other and out of phase by 180° to above signals which is shown in Figure 3.4.

The rules for the phase opposition disposition method for a multilevel inverter are

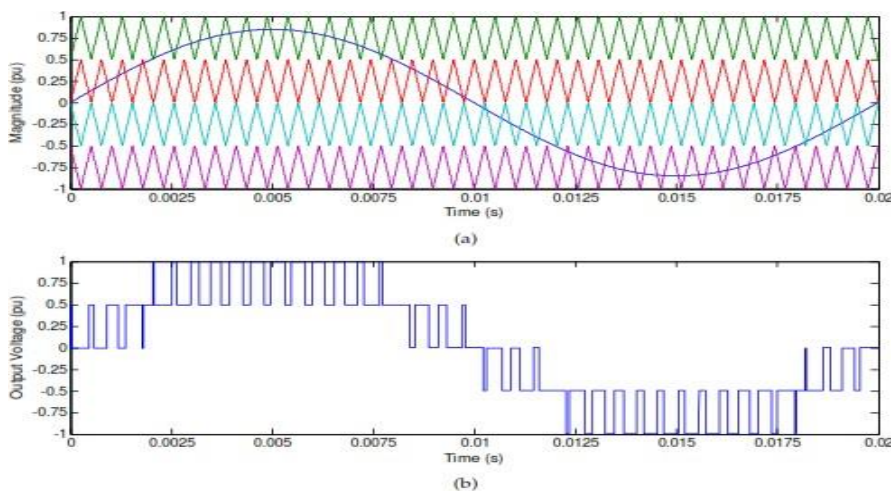


Figure 7 POD-PWM technique: a) Reference and carrier signals, b) Output phase voltage waveform

(viii) Phase Disposition PWM (PD-PWM)

In PD-PWM modulation, all the carrier signals are in phase. In this method, the major feature of the phase voltage spectrum is the significant first carrier harmonic. This feature gives the PD-PWM excellent line voltage performance, since this carrier harmonic is a common-mode component across the phase voltages of a three phase inverter and therefore cancels in the output line voltage reducing harmonics in line voltage. This technique is similar to APOD except the carriers are in phase as shown in Figure 3.5.

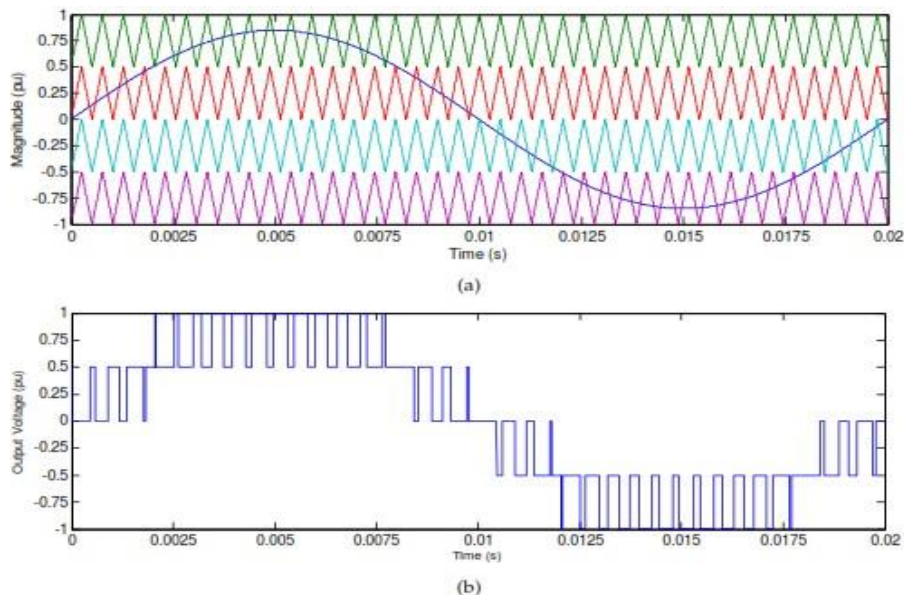


Figure 8 PD-PWM technique: a) Reference and carrier signals, b) Output phase voltage waveform

4.1 Analysis and Design of 7 - Level Cascaded Inverter with 6 Switches

Multilevel inverters (MLI) are being considered as the most popular method to synthesize almost sinusoidal waveforms using multi steps. Out of three conventional topologies cascaded H- bridge type of MLIs with different dc sources are proven to be more reliable in generating higher voltage with comparatively less harmonics due to its modular nature. These types of MLIs are also very suitable for solar applications as the separate dc sources requirement is naturally available. However, there are certain drawbacks of these MLIs such as the use of large number of switches and the related gate drive circuit design as required by the corresponding semiconductor switches which create more complexity in electrical and mechanical design of the inverters.

4.1.1 Proposed 7-Level Configuration

The design of cascaded MLIs can be made simple by designing a simple gate pulse generation scheme. The cascaded MLIs use bridges cascaded with each other. For a five level inverter, two bridges are required, for a seven level inverter three bridges are required and for a nine level inverter four bridges are required and so on. One bridge consists of four semiconductor switches, so the number of switches increase with the level and voltage steps. Hence the switching losses and the cost of the MLIs also increase accordingly. Therefore, an initiative is taken to reduce the number of semiconductor switches and hence the cost of MLI and a simpler switching technique is developed to control the MLIs. In this section, a method is developed to reduce the switches for a seven level inverter by using 6 switches.

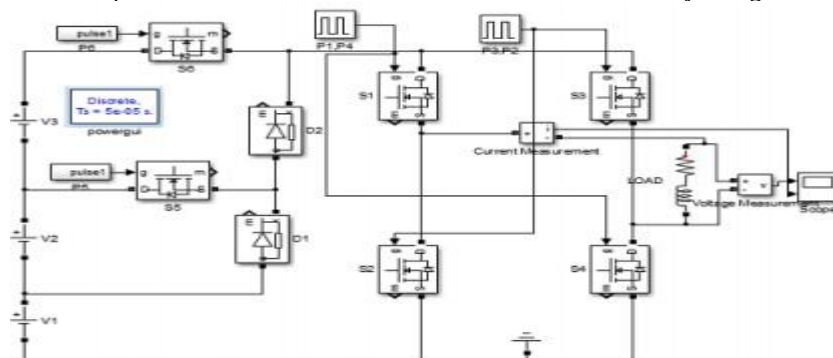


Figure 9 Seven Level Inverter with Six Switches

In this topology six MOSFETS are used. Four MOSFETS are used in H-bridge for changing the polarity and two MOSFETS are used for level generation. Two diodes are used to generate voltage $\pm V$. The switching scheme is given in Table-1. It has 7 output voltage levels that is 3V, 2V, V, 0, -V, -2V, -3V. For 3V output voltage, MOSFETS S1, S4 & S7 are switched on and others are switched off. For 2V output voltage, MOSFETS S1, S4 & S6 are switched on and others

are switched off. For V output voltage, two MOSFETS S1 and S4 are only switched on and others are switched off. For 0 output voltage all the MOSFETS are switched off. For $-V$ output voltage, two MOSFETS S2, S3 are only switched on and others are switched off. For $-2V$ output voltage, MOSFETS S2, S3 & S6 are switched on and others are switched off. For $-3V$ output voltage, MOSFETS S2, S3 & S7 are switched on and others are switched off. It can be observed that the switching devices for the proposed seven level seven switch inverter at the time of conduction are three and for seven level six switch inverter is 2 or 3. So switching loss is greatly reduced. Table 4.1 represents the switching scheme of the proposed topology

Table 1 Switching scheme for 7-level 6-switch topology

| SL no. | S1 | S2 | S3 | S4 | S5 | S6 | Output voltage |
|--------|-----|-----|-----|-----|-----|-----|----------------|
| 1 | OFF | OFF | ON | OFF | ON | OFF | +Vdc |
| 2 | OFF | ON | OFF | OFF | ON | OFF | +2Vdc |
| 3 | ON | OFF | OFF | OFF | ON | OFF | +3Vdc |
| 4 | OFF | OFF | OFF | OFF | OFF | ON | 0 |
| 5 | ON | OFF | OFF | ON | OFF | OFF | -Vdc |
| 6 | OFF | ON | OFF | ON | OFF | OFF | -2Vdc |
| 7 | OFF | OFF | ON | ON | OFF | OFF | -3Vdc |

4.2 PWM Generation

The pulse generation is essential in order to trigger the switches with appropriate pulse pattern to produce the desired 7-level output. It is inevitable to analyse which PWM suits the new topology. The simplest PWM technique is the carrier-based PWM (CBPWM) technique. It can be further categorized into level and phase shifting CBPWMs, respectively. Since the phase shifting CBPWM yields more harmonics comparatively, the level shifting CBPWM is preferred over it.

The reference signal comparing with carrier generating pulse which is then modified feeding to logic gates in order to get the required pattern to trigger the switches at the proper instant. For examples switches S1 needs to have a pulse so as to obtain +Vdc and -3Vdc and S2 requires +2Vdc and -2Vdc. S3 conducts +3Vdc and -Vdc. Also, switches S5 and S4 conduct positive and negative half cycles, respectively. Figure 4.2 represents the CBPWM technique proposed in this work.

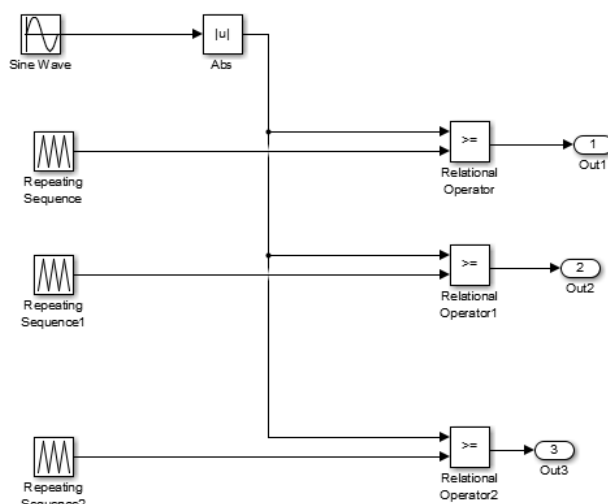


Figure 11 PWM generation scheme

5.1 Experimental Results

The simulation result and THD of the proposed topology is shown below. Here the input voltage is about 77V and the resistive load is taken. Figure 4.3 shows the output voltage waveform of the 7 level symmetrical CHB configuration. The

magnitude of the voltage is about 230 volts. The total harmonic distortion (THD) for the output voltage wave form is measured 17.98% and is shown in figure 4.4.

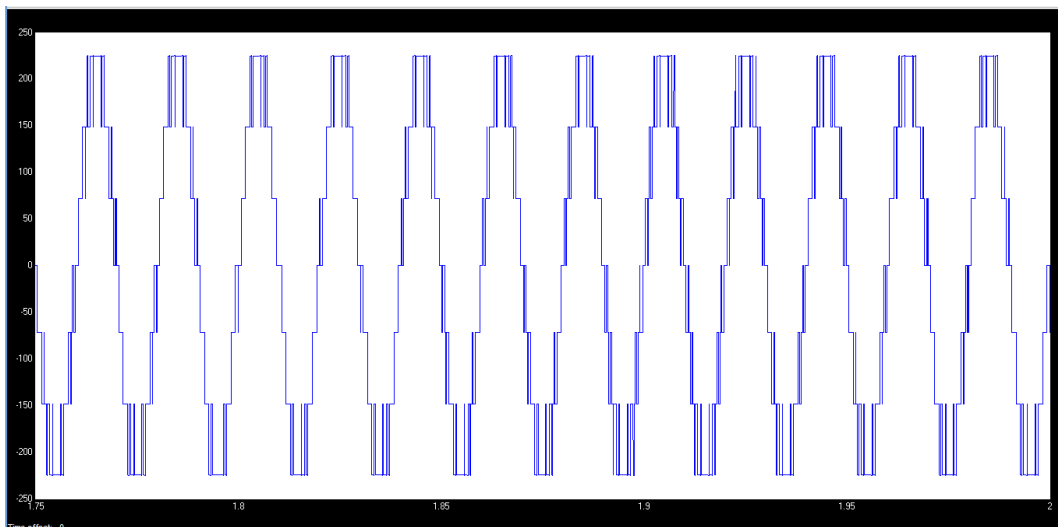


Figure 12 Output Voltage

Table 2 : THD results obtained for conventional & modified 7 level inverter configurations

| | |
|--|---------------------------------------|
| Symmetric conventional cascaded 7-level MLI | Proposed (7-level, 6 switches) |
| 24.26 | 17.98 |

Simulation results presented in table 2 (reveals that the total harmonic distortion is reduced to 17.98%)

Table 3 Voltage stress in proposed topology across switches

| Parameter | Conventional CMLI | Proposed topology |
|----------------|----------------------|--|
| Voltage stress | 5V (All switches) | 3.33V (S3) 13.3V (S2) 23.3V (S1) |

Table 4 Comparison of proposed 7-level with other topology

| Inbuilt structure | Flying capacitor | Diode clamped | Cascaded 7-level | 7-level, 6 switches |
|-------------------|------------------|---------------|------------------|---------------------|
| No. of capacitors | 14 | 6 | — | — |
| No. of diodes | — | ≥8 | — | — |
| No. of switches | 10 | 10 | 12 | 6 |
| No. of dc sources | — | — | 3 | 4 |

6.1 Conclusion

In this chapter, the overall conclusion along with the suggestions for future work is presented. In recent days MLI has drawn large interest in high power industry. They present a latest set of aspects to facilitate and utilized in reactive power compensation. The unique arrangement of multilevel voltage source inverters allow them to achieve high voltages with the low harmonics not including the utilization of transformers or series connected synchronized switching devices.

The Diode clamped, Flying capacitor, Cascaded H-bridge inverter are the three main different multilevel inverter structures which are used in industrial applications with separate dc sources. In flying capacitor and diode-clamped inverter there is a problem of capacitor voltage balancing and this problem is overcome by cascaded H-bridge inverter. However, the main drawback in Conventional cascaded is that when levels are increasing it requires more number of semiconductor switches. As a result some alternations are to be made in order to reduce the size and switch of the inverter.

A single phase 7 level reduced switch MLI topology is introduced and its various modes of operation are studied. A novel modulation approach is presented and utilized in the proposed topology. From the results, it is evident that this proposed system reduces switching losses with less THD. Thus, the overall cost reduction and effective reduction of total harmonics distortion is achieved.

7.1 References

1. Adam, GP, Anaya-Lara, O, Burt, GM, Telford, D, Williams, BW & McDonald, JR 2010, 'Modular multilevel inverter: pulse width modulation and capacitor balancing technique', *IET Power Electronics*, vol. 3, no. 5, pp. 702–715.
2. Ammar Masaoud, Hew Wooi Ping, Saad Mekhilef & Hamza Omar Belkamel 2014, 'A New Five- level Single-phase Inverter Employing a Space Vector Current Control', *Electric Power Components and Systems*, vol. 42, no. 11, pp. 1121-1130.
3. Anup Kumar Panda & Sushree Sangita Patnaik 2015, 'Analysis of cascaded multilevel inverters for active harmonic filtering in distribution networks', *Electrical Power and Energy systems*, vol. 66, pp. 216-226.
4. Ataollah Mokhberdorran & Ali Ajami 2014, 'Symmetric and Asymmetric Design and Implementation of New Cascaded Multilevel Inverter Topology', *IEEE Transactions on Power Electronics*, vol. 29, no. 2, pp. 6712-6724.
5. Bakhshizadeh Dowlatabadi, M, Iman-Eini, H & Blaabjerg, F 2015, 'Selective Harmonic Elimination in Asymmetric Cascaded Multilevel Inverters Using a New Low-frequency Strategy for Photovoltaic Applications', *Electric Power Components and Systems*, vol. 43, no. 8-10, pp. 964- 969.
6. Banerjee, P, Biswarup Das & Agarwal, P 2010, 'Distribution Grid Voltage Control Using Cascaded Multi-level Inverter based Static Synchronous Compensator', *Electric Power Components and Systems*, vol. 38, pp. 1389-1405.
7. Basavaraja, DS, Kulkarni, AD & Anandhapadmanabha, T 2015, 'A Modular Single-Phase Multistring Multilevel Inverter Topology for Distributed Energy Resources', *Procedia Technology*, vol. 21, pp. 569- 574.
8. Calais, M, Borle, LJ & Agelidis, VG 2001, 'Analysis of multi carrier PWM methods for single- phase five level inverter', *Proceedings of 32nd Annual IEEE International Power Electronics Specialists Conference (PESC'2001)*, pp. 1351-1356, Vancouver, BC.
9. Charles Ikechukwu Odeh 2014, 'A cascaded Multi-level inverter Topology with Improved Modulation Scheme', *Electric Power Components and systems*, vol. 42, no. 7, pp. 768-777
10. Ebrahim Babaei, Mohammad Farhadi Kangarlu & Mehran Sabahi 2014, 'Dynamic voltage restorer based on Multilevel Inverter with adjustable Dc-link voltage', *IET Power Electronics*, vol. 7, no. 3, pp. 576-590.
11. Ebrahim Babaei, Sara Laali & Sepideh Bahravar 2015, 'A new Cascaded Multi –level Inverter Topology with Reduced Number of Components and Charge Balance Control Methods Capabilities', *Electric Power Components and systems*, vol. 43, no. 19, pp. 2116- 2130.
12. Ebrahim Babaei, Sara Laali & Zahra Bayat 2015, 'A Single – Phase Cascaded Multilevel Inverter Based on a New Basic Unit With Reduced Number of Power Switches', *IEEE Transactions on Industrial Electronics*, vol. 62, no. 2, pp. 922-929.
13. Fei Jiang, Chunming Tu, Zhikang Shuai, Miaomiao Cheng, Zheng Lan & Fan Xiao 2016, 'Multilevel Cascaded -Type Dynamic Voltage Restorer With Fault Current- Limiting Function', *IEEE Transaction on Power Delivery*, vol. 31, no. 3, pp. 1261-1269.
14. Fernao Pires, V, Joao Fialho & Fernando Silva, J 2015, 'HVDC transmission system using multilevel power converters based on dual three-phase two-level inverters', *Electrical Power and Energy systems*, vol. 65, pp. 191-200.
15. Gayathri Devi, KS, Arun, S & Sreeja, C 2014, 'Comparative Study on different five level inverter topologies', *Electrical Power and Energy Systems*, vol. 63, pp. 362-372.
16. Govindaraju, G & Baskaran, K 2011, 'Sequential Switching Hybrid Single- Carrier Sinusoidal Modulation for Cascaded Multi-level Inverter', *Electric Power Components and systems*, vol. 39, no. 4, pp. 303-316.
17. Gowande, SP & Ramteke, MR 2014, 'Three-level NPC inverter based new DSTATCOM topologies and their performance evaluation for load compensation', *Electrical Power and Energy systems*, vol. 61, pp. 576-584.
18. Gupta, KK & Jain, S 2012, 'Topology for multilevel inverters to attain maximum number of levels from given DC sources', *IET Power Electronics*, vol. 5, no. 4, pp. 435-446.

19. Hosseini Aghdam, MG, Fathi, SH & Gharehpetian, GB 2008, 'A Novel Switching Algorithm to Balance Conduction Losses in Power Semiconductor Devices of Multi-level Cascade Inverters', *Electric Power Components and Systems*, vol. 36, no. 12, pp. 1253-1281.
20. Junfeng Liu, Cheng, KWE & Yuanmao Ye 2014, 'A Cascaded Multilevel Inverter Based on Switched- Capacitor for High- Frequency AC Power Distribution System', *IEEE Transactions on Power Electronics*, vol. 29, no. 8, pp. 4219-4230.
21. Khounjahan, H, Banaei, MR & Amir Farakhor 2015, 'A new low cost cascaded transformer multilevel inverter topology using minimum number of components with modified selective harmonic elimination modulation', *Ain Shams Engineering Journal*, vol. 6, pp. 67-73

International Conference on Research and Developments in Science, Engineering and Technology
ICRDSET - 2021

International Conference on Recent Developments in Science, Engineering and Technology

International Conference on Recent Developments in Science, Engineering and Technology

22. Krishna Kumar Gupta, Alekh Ranjan, Pallavee Bhatnagar, Lalit Kumar Sahu, & Shallendra Jain 2016, 'Multilevel Inverter Topologies With Reduced Device Count: A Review', IEEE Transactions on Power Electronics, vol. 31, no. 1, pp. 135-151.
 23. Krismadinata, Nasrudin Abd Rahim, Hew Wooi Ping & Jeyaraj Selvaraj 2013, 'Elimination of harmonics in photovoltaic seven-level inverter with Newton-Raphson optimization', Procedia Environmental Sciences, vol. 17, pp. 519-528.
 24. Kumar, GKN & Pal, Y 2014, 'A modified switching scheme for a new multi level inverter topology for fuel-cell microgrid', Proceedings of IEEE 6th India International Conference on Power Electronics (IICPE), Kurukshetra, pp. 1-6.
 25. Law Kah Haw, Mohammad SA Dahidah & Haider AF Almurib 2014, 'SHE-PWM Cascaded Multilevel Inverter with Adjustable DC Voltage Levels Control for STATCOM Applications', IEEE Transactions on Power Electronics, vol. 29, no. 12, pp. 6433-6444.
 26. Mahalakshmi, R & Sindhu Thampatty, KC 2015, 'Grid Connected Multilevel Inverter for Renewable Energy Applications', Procedia Technology, vol. 21, pp. 636-642.
 27. Mahmoud El-Bakry 2014, 'A 43 -Level filterless CMLI with very low harmonics values', Journal of Electrical systems and Information Technology, vol. 1, pp. 175-186.
- McGrath BP & Holmes DG 2000, 'A comparison of multi carrier PWM strategies for cascaded and neutral point clamped multilevel inverters', Proceedings of 31st IEEE International Power Electronics Specialists Conference (PESC'2000), pp. 674-679, Galway.

Group Leader Optimisation Algorithm Based Optimal Reconfiguration Of Distribution Feeder For Loss Reduction

Sriram K
Assistant Professor
St. Anne's College of Engineering and
Technology
Panruti

Dr. S.P. Mangaiyarkarasi
Assistant Professor
University College of Engineering Panruti

Abstract

This paper proposes the method of reconfiguration for loss reduction in distribution system in order to achieve the loss reduction for maximizing the operation of power system at a reduced cost. Reconfiguration is the process of re-routing the power flow in the distribution network. The process of reconfiguration is achieved by changing the on off status of circuit breakers in distribution network. Here Group leader optimization algorithm is used to determine the optimal status of network switches for maximum loss reduction. The proposed system is tested in IEEE 33 bus system and simulated in MATLAB software.

1. Introduction

The distribution system is a largest portion of network in electrical power system. It can be defined as the part of power system this distributes power to various customers in ready-to-use form at their place of consumption. Hence, utilities have to ensure reliable and efficient cost effective service, while providing service voltages and power quality within the specified range. This is a very challenging task. Utilities, traditionally determine future system developments based on a top down approach, all over the world are competing for improvement in service to consumers.

Mostly the power utilities emphasize on power generation and transmission system to reduce the overall cost of the system. Many of the distribution systems experience uncontrolled expansion, minimum monitoring, under/over utilization and development in unplanned manner.

The distribution networks typically located at every nook and corner to provide the electric power supply for all the individual customers. Obviously the distribution system is the most suitable system to meet the individual consumer requirements such as the electricity demand, reliability, power quality etc. As an example, certain load centers need high level of reliability and different load centers have different demand growth etc. Therefore the process of optimal planning shall begin from distribution system.

In this process work out the system needs, i.e., identifying the network reinforcements/expansions, additional substations, augmentation of the existing substations and expansion of transmission line to meet the need of substation, in the upward direction to achieve the final objective and techno-economic solution. Nowadays advanced computer aided techniques and analysis tools available to carry out the optimal planning process. The power engineers need to overcome some of the challenges while applying the techniques.

2. Distribution Network reconfiguration

Optimal planning and design of the distribution systems involves network reconfiguration for distribution loss minimization, load balancing under normal operating conditions and fast service restoration to minimize the zones without power under failure conditions. Most of the distribution networks are configured radially which simplifies over-current protection of the feeders.

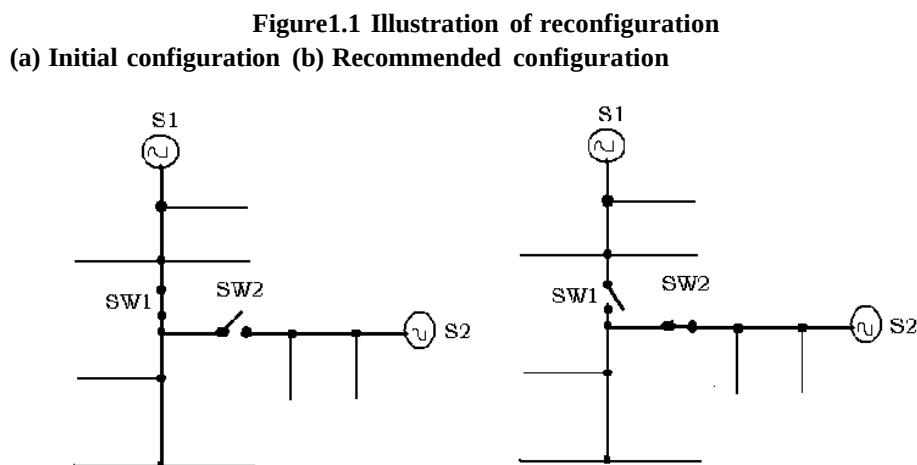
The manual or automatic switching operations are performed to vary the configurations. As the operating conditions change, the purpose of network reconfiguration is: (i) to minimize the system power loss and (ii) to balance the loads in the network. Reconfiguration problem of large scale distribution systems is essentially a combinatorial optimization problem since various operational constraints are to be considered. Therefore it is difficult to obtain a true and fast solution for a real system.

Two types of switches, normally open switches (tie switches) and normally closed switches (sectionalizing switches), are used in primary distribution systems for protection and configuration management. The distribution network reconfiguration is obtained by closing tie (normally open) switches and opening sectionalizing (normally closed) switches in the network. The structure of the distribution network is maintained radial and all loads are energized while switching operations are performed. Obviously, the possibilities of network reconfiguration are greater when large number of switches is present.

The network reconfiguration is illustrated through a simple system as shown in figure1.1. Consider two switches, SW1 (sectionalized) and SW2 (tie) and two substations, S1 and S2 as shown in figure 1.1(a). A reconfiguration to reduce the system losses can be obtained by altering the system topology as shown in figure 1.1(b). It is recommended to open SW1 and close SW2 for the reconfiguration of the system.

The effect of constraints on reconfiguration must be thoroughly studied before changing the basic configuration. One of the major constraints to be considered is that the network must have radial structure.

Some of the general optimization algorithms fail in satisfying this radial constraint directly. Particularly a meshed network containing all switches closed will have less loss, but the radial constraint is violated.



A method, by not closing any switches forming a loop, that builds the network from scratch can easily enforce the radial constraint. The line current carrying capacity and voltage limits are the other major constraints in reconfiguration. However, these constraints are closely related because a line carrying current close to its thermal capacity will also have a larger resistive voltage drop. Solutions, heuristically, with a good voltage profile have low losses and the line currents within limits. Either the voltage or the current constraint may be reached first in a particular situation. The current constraints can be alleviated by switching or re-conductoring the feeder in the longer term or installing a larger substation transformer. The voltage constraints can be alleviated by switching or installing capacitor banks or by adjusting voltage regulators.

Energy policies are major arguments of the international politics. The energy has a vital role for all countries and the main goal is reaching cost effective and sustainable energy sources. Since conventional energy sources are limited and energy saving is the most cost effective energy source, energy efficiency is regarded as a major topic for many countries. Distribution system losses constitute a significant part in total electrical losses. Network reconfiguration is one of the fundamental methods of loss reduction in distribution systems.

Electrical distribution systems aim a single direction power flow from the source to the load to minimize operation difficulty and costs. However, designing the system as a mesh offers the possibility to achieve alternative network configurations in order to maintain the continuity of supply under failures. As a result the conventional distribution systems are constructed as a weak mesh with closed rings but operated radially.

Radial operation constraint makes it compulsory to open the distribution feeders connected to multiple sources or to a single source with a ring configuration from a suitable switching location. Meshed networks offer many alternative configuration options and it is possible to reconfigure the network by interchanging the switching locations. Different configurations alternate the existing feeder lengths, voltage and current rates, loading levels and amount of losses. Accurate selection of switching locations would reduce losses, increase the lifetime of equipment and improve system reliability by balancing the system loading.

Distribution system configurations are usually chosen during planning of the system according to normal operation conditions and average loading levels. Nevertheless the load flows are not constant and they vary with different factors including changing demand, failures, maintenance operations or additional loads and sources connecting to the network.

In a very fast growing city such as Istanbul, the electricity demand increase and network growth rate is also high. As a result it is not quite probable for the initial network configuration to maintain the optimum system loading for a long time under such conditions.

Locations of tie switches in a network providing minimum loss configuration can be determined by optimum distribution system reconfiguration methods. Most of the optimum reconfiguration methods are based on heuristics. Consecutively opening switches from meshed network and branch exchange methods are used in many different reconfiguration studies. Recently probabilistic methods including genetic algorithms, particle swarm optimization, ant colony optimization and artificial bee colony are also applied to optimum reconfiguration algorithms. Studies evaluating the use of heuristic methods on distribution system reconfiguration are also presented in recent years.

The objective function of reconfiguration optimization is defined as minimization of the resistive losses in most of the previous studies. However the optimization function can be defined as maximization of reliability, balancing feeder lengths and loadings, minimization of voltage drop or overloads and integration of distributed generation.

To determine a new network configuration on the chosen network section from Istanbul, to reduce the system losses by evaluating the fitness of present configuration and simulating alternative switching operations.

As a result, the chosen network section is modelled and a reconfiguration algorithm is generated on Mat lab, based on opening switches consecutively according to optimum flow pattern.

3. Problem Formulation

The reconfiguration method utilized in this study to reduce resistive losses of the distribution system starts with analyzing the load flow of the meshed system by closing all the switches in the network. According to the Kirchoff's laws, current favors to flow through the path with minimum losses. Whereas the system is operated as a meshed network, the resistive losses would be minimum and opening a line carrying high amount of current would force the current to flow through paths with higher losses.

With the acceptance of opening the minimum current carrying switch would interfere the optimum flow least, the increase in losses by opening the switches would be minimized. This switch opening step is repeated until the network is radial in order to achieve a low loss configuration.

The method uses a meshed network with all switches closed in the beginning of the reconfiguration process, thus the resulting configuration would be independent of the initial state of the network. However all the switch selections of network reconfiguration methods have impact on selection of other switches, due to their influence on the load flows. Therefore the sequential switching method used in this study would not guarantee a global optimum solution to the minimum loss network reconfiguration problem.

Ensuring radiality is one of the main constraints and challenges of distribution system reconfiguration. In order to achieve radial configuration there has to be only one electrical path from any given point of the network to another. In graph theory a connected graph without any loops is defined as a tree. A graph can be a tree if the number of edges, e is one less than the number of vertices, v .

The edges and vertices can be defined as graphical equivalents of nodes and branches of a network. As a result, the number of connected lines, n_{line} has to be one less than the number of nodes in a network to have a radial configuration.

The number of edges e given by

$$e = v - 1 \quad (1)$$

n_{line} is number of lines given by

$$n_{line} = n_{branch} - 1 \quad (2)$$

where v, n_{node} are numbers of vertices and nodes respectively.

The number of tie switches need to be opened can be calculated according to (3.7). During switching, radially of the network is checked by comparing the number of open switches with the number of tie switches.

n_{Tsw} is number of tie switches that has to be opened, represented by

$$n_{Tsw} = n_{branch} - n_{bus} - 1 \quad (3)$$

where n_{branch} and n_{bus} represent the number of branches and buses in the network respectively.

In order to keep all the loads supplied by the source, only one switch can be opened on the same feeder. Only operable switches are evaluated during reconfiguration. When a switch is chosen as tie switch, rest of the switches on the same feeder are defined as non operable switches, and added to a blacklist. Thus the next switch is certainly chosen from other feeders. When entire tie switches are chosen, none of the remaining switches will be operable and radial network will be obtained. Flowchart of the optimization algorithm can be seen in figure 3.1.

Group Leader Optimization Technique

Inspired by leaders in social groups and cooperative co evolutionary algorithms, we have designed a new global optimization algorithm in which there are separate groups and leaders for each group. Initially forming groups does not require members to have some similar characteristics. Instead, it is based on random selection. While CCGA and other similar algorithms decompose the solution space, and each group represents a solution for a part of the problem, in our algorithm each group tries to find a global solution by being under the influence of the group leaders which are the closest members of the groups to local or global minima. The leaders are those whose fitness values are the best in their groups, and a leader can lose its position after an iteration if another member in the same group then has a better fitness value. Since in social networks, leaders have effects on their peers, thusly the algorithm uses the some portion of leaders while generating new group members. Hence, a leader, (in most cases a local optimum) dominates all other solution candidates (group members) surrounding it, and the members of a group come closer and resemble their leader more in each iteration. In this way, the algorithm is able to search the solution space between a leader and its group members thoroughly, and so is able to search the area for a local or a global optimum (or an approximation of it) in a fast way. After a certain number of evolutions, it is obvious that the members may become too similar to their leaders. To maintain the diversity of the group, for each group, we transfer some variables from different groups by choosing them randomly. In addition to providing diversity, this one-way crossover helps a group to jump out of local minima and search new solution spaces.

3.3.2 Algorithm steps

In this section, algorithm steps are described with their reasons in sequence and are shown in Figures 1.

Step 1: Generate p number of population for each group randomly

The total population for each group is p, hence, the whole population is $n * p$ where n is the number of groups. Creation of the groups and the members are totally random.

Step 2: Calculate fitness values for all members in all groups

All solution candidates, group members, are evaluated in the optimization problem and their fitness values are assigned.

Step 3: Determine the leaders for each group:

Each group has one leader and the leaders are ones whose fitness values are the best within their respective groups.

Step 4: Mutation and recombination:

Create new member by using the old one, its group leader, and a random element. If the new member has better fitness value than the old one, then replace the old one with the new one. Otherwise, keep the old member. For numerical problems, the expression simply reads;

$$\text{new} = (r1 * \text{old}) + (r2 * \text{leader}) + (r3 * \text{random})$$

In Equation (1), r1, r2, and r3 are the rates determining the portions of old (current) member, leader, and random while generating the new population. Although in this paper, r1, r2, and r3 will always sum to 1, it is not a requirement for the algorithm in general. For instance, let the current element be 0.9, the leader 1.8, and the generated random element 1.5, and suppose $r1=0.8$, $r2=0.19$, and $r3=0.01$. In this case, the new element is equal to 1.077. Then fitness values of the old and the new element are checked. If fitness (1.077) is better than the fitness (0.9), then the old element is replaced by the new one.

The expression in the inner loop is the general formula of recombination and mutation for numerical optimization problems. Depending on the value of r1 an element keeps its original characteristics, and depending on the value of r2 it becomes more like its leader during iterations. Thus, in some cases, choosing the right values for r1, r2 and r3 may play an important role for the algorithm to get better results during the optimization. However, choosing these parameters by obeying the property, $r3, r2 \leq 0.5, r1$ allows one to perform a thorough search of a solution space. Hence, this minimizes the effect of these parameters on the results. The main benefit of this evolution is that the algorithm becomes able to search the solution space surrounding the leaders (which are possibly local or global minima). Therefore, this allows the population to converge upon global minima in a very fast way. The members of the groups are not subjected to a local minimization; however, an implementation of Lamarckian concepts of evolution for the local minimization [28] gives a more stable and efficient algorithm. It is also important to note that Equation (1) looks similar to the updating equation of PSO [17]. The difference is that a member is always at its best position and the best position of a member is not saved in a parameter as is done in PSO, hence there are no information about the member's (or the particles) previous positions (values).

Step 5: Parameter transfer from other groups (One way crossover)

Choose random members starting from the first group, and then transfer some parameters by choosing another random member from another group. If this transfer makes a member have a better fitness value, then change the member, otherwise keep the original form. This process is shown in Figure 2 via pseudo code. This one-way crossover has similarities with the difference vector of Differential Evolution [29]. The difference is that the transfer operation is between the members which are in different groups. In this step, it is important to determine correct transfer rate, otherwise all populations may quickly become similar. In our experiments, transfer operation rate was taken t times [t is a random number between 1 and half of the number of total parameters (variables) plus one $(1 + \lfloor \text{parameter}/2 \rfloor)$] for each group (not for each member). And each time, only one parameter is transferred.

Figure 1. Step 5 of the algorithm: one way crossover: prth variable of an element, member of the i th group, is replaced by path variable of the k th member of the xth group. The same operation is repeated t times for each group (maximum – half of the number of variables plus one – times for each group). The arrow at the bottom of the figure shows the direction of transfer.

Step 6: Repeat step 3–step 5 number of given iteration times

Since each group looks for the solution in mostly different spaces, Group Leaders Optimization Algorithm (GLOA) is able to search different solution spaces simultaneously. We did not place any constraint for groups

to only search in subspaces, so a few groups may also search the same places. However, this does not make them redundant as they allow GLOA to find different local or global minima within the same subspace. Since each group has a leader and the leaders direct the other members of the group in order to search the area between the leader and the members of the group, it is able to search for a good solution (around the leader of the group). In addition to increasing the level of diversity of the groups, transferring some parameters (crossover) between groups allows the algorithm to direct the members of a group to search different spaces. Therefore, if a group has found some parameters correctly or very close to correct, then transferring parameters between groups allows other groups to get these parameters and find their solutions faster. Since only parameters are transferred which make the member have better fitness value, the spreading of a member who has a bad fitness value is avoided. In terms of optimization problems requiring highly diverse populations, choosing to do crossover and mutation-recombination steps without comparing fitness values may be wise and may improve the effectiveness of the algorithm.

Test System

The network used in this study is a section from 34.5kV distribution system of Istanbul. The network consists of 95 buses, 107 branches and 58 switches connected with 7.2km of 150mm² three core, 38.5km of 240mm² three core and 15km of 240mm² single core, armored copper cables with XLPE insulation. Total length of the network is 60.7km with 86 distribution transformers connected to the network.

Distribution transformers are modeled as medium voltage loads with 97.6MVA apparent power in total. The power factor is taken as 0.85, at the reactive power penalty limit to be conservative. The minor unbalances between phases are neglected for calculation simplicity.

The resulting power losses from actual configuration, meshed network, and the configuration achieved by the reconfiguration algorithm are analyzed in this section.

The meshed configuration of the network with all switches closed has total resistive loss of 94kW. The actual configuration of the network is with switches s1, s8, s10, s19, s28, s29, s36, s38, s39, s40, s49, s54 and s58 open and the resistive losses are calculated as 169kW.

The configuration achieved by the reconfiguration algorithm has switches s3, s7, s10, s18, s20, s30, s35, s38, s39, s40, s48, s51 and s55 open resulting total resistive losses of 124kW. The mentioned configurations, open switches and resistive losses are shown in Table 3.1.

4. Results and Discussion

The proposed method was tested on IEEE 33-bus radial distribution systems and results have been obtained to evaluate its effectiveness. For all these systems, the substation voltage is considered as 1.0 p.u. and all the tie and sectionalizing switches are considered as candidate switches for reconfiguration problem.

The algorithm of this method was programmed in MATLAB R2013a environment and run on intel i3 - 3rd Generation , 2.4 GHz personal computer with 4GB RAM.

The 33-bus, 12.66 kV, radial distribution system consists of five tie lines and 32 sectionalize switches. The normally open switches are 33, 34, 35, 36 and 37 and the normally closed switches are 1 to 32. The total real and reactive power loads on the system are 3715 kW and 2300 KVAR. The initial power loss this system is 208.4592 kW. The lowest bus bar voltage limit is 0.91075 p.u which occurs at node 18.

Simulations are carried from 10 to 100 iterations and all are converged to same solution after 8 iterations. The CPU time used to get optimal solution is 49.7 seconds. The optimal configuration obtained by the proposed algorithm is 7,9,14,32 and 37 which has a real power loss of 138.92 kW. This amounts to a reduction of 33.35 % in total power loss. The minimum node voltage of the system after reconfiguration improved to 0.94234 p.u (node 33). The results of the proposed algorithm are compared with Genetic Algorithms is presented in Table 6.1. From the results, it is observed that the optimal power loss obtained by the proposed method is 1.68 kW less than GA. The CPU time used by the proposed method is 49.7 sec only but it is 55.2 in case of GA methods.

| Item | Tie Switches | Power Loss (kW) | Min.Node Voltage (p.u) | Power Loss Reduction (%) | CPU Time (s) |
|------------------------|-----------------|-----------------|------------------------|--------------------------|--------------|
| Original Configuration | 33,34,35,36, 37 | 208.4592 | 0.91075 (Node 18) | -- | -- |

| | | | | | |
|------------------------|------------------|----------|----------------------|-------|------|
| GA | 33,9,34,28 36 | 140.6 | 0.9371 (Node 33) | 30.6 | 55.2 |
| Proposed System | 7,9,14,32,37 | 138.9275 | 0.94234 (Node 33) | 33.35 | 49.7 |

Table 6.1 Simulation Result of 33-Bus System

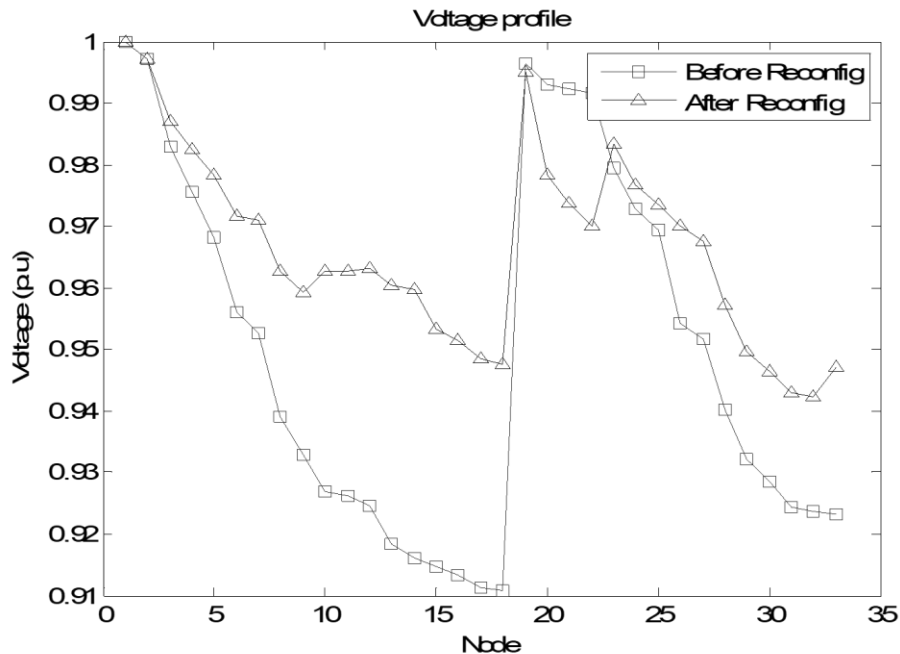


Figure 6.1 Convergence characteristics of GLO for 33 bus radial distribution system

5. Conclusion

In this paper, a new population based group leader optimization (GLO) was utilized to solve the network reconfiguration problem in a radial distribution system. The main objectives considered in the present problem are minimization of real power loss and voltage profile improvement subject to the radial network structure in which all loads must be energized. Simulations are carried on IEEE - 33 bus systems and results are compared with the other populations based method such as GA. The results obtained by the proposed method out perform the other methods in terms of quality of the solution and computation efficiency.

The main advantage of GLO algorithm is that it does not require external parameters such as cross over rate and mutation rate etc., as in case of genetic algorithms, differential evolution and other evolutionary algorithms and these are hard to determine in prior. The other advantage is that the global search ability in the algorithm is implemented by introducing neighborhood source production mechanism which is a similar to mutation process. This project illustrates the capability of group leader optimization algorithm in solving network reconfiguration problem.

References

- [1]. S. Sehgal, A. Swarnkar, N. Gupta, and K. R. Niazi, "Reconfiguration of distribution network for loss reduction at different load schemes," in *Proc. IEEE Students' Conference on Electrical, Electronics and Computer Science SCECS*, Mar. 2012, pp. 1-4.

- [2]. H. L. Willis, H. Tram, M. V. Engel, and L. Farley, "Optimization applications to power distribution," *IEEE Computer Applications in Power*, vol. 8, no. 4, pp. 12-17, Oct. 1995.
- [3]. T. E. McDermott, I. Drezga, and R. P. Broadwater, "A heuristic nonlinear constructive method for distribution system reconfiguration," *IEEE Trans. Power Syst.*, vol. 14, no. 2, pp. 478- 483, May 1999.
- [4]. H. R. Esmaeilian, R. Fadaeinedjad, and S. M. Attari, "Distribution network reconfiguration to reduce losses and enhance reliability using binary gravitational search algorithm," in *Proc. 22nd International Conference on Electricity Distribution*, 2013.
- [5]. P. Zhang, L. Wenyuan, and W. Shouxiang, "Reliability-Oriented distribution network reconfiguration considering uncertainties of data by interval analysis," *International Journal of Electrical Power and Energy Systems*, vol. 34, no. 1, pp. 138-144, Jan. 2012.
- [6]. D. Shirmohammadi and H. W. Hong, "Reconfiguration of electric distribution for resistive line loss reduction," *IEEE Trans. Power Del.*, vol. 4, no. 2, pp. 1492-1498, Apr. 1989.
- [7]. S. Civanlar, J. J. Grainger, H. Yin, and S. S. H. Lee, "Distribution feeder reconfiguration for loss reduction," *IEEE Trans. Power Del.*, vol. 3, no. 3, pp. 1217-1223, Jul. 1988.
- [8]. S. K. Goswami and S. K. Basu, "A new algorithm for the reconfiguration of distribution feeders for loss minimization," *IEEE Trans. Power Del.*, vol. 7, no. 3, pp. 1484-1491, Jul. 1992.
- [9]. R. J. Sarfi, M. Salama, and A. Chikhani, "A survey of the state of the art in distribution system reconfiguration for system loss reduction," *Electric Power Systems Research*, vol. 31, pp. 61-70, 1994.
- [10]. L. F. Ochoa, R. M. Ciric, A. Padilha-Feltrin, and G. P. Harrison, "Evaluation of distribution system losses due to load unbalance," in *Power Systems Computation Conference (PSCC)*, Liege, Belgium, 2005, pp. 1-4.
- [11]. S. P. Singh, G. S. Raju, G. K. Rao, and M. Afsari, "A heuristic method for feeder reconfiguration and service restoration in distribution networks," *International Journal of Electrical Power & Energy Systems*, vol. 31, pp. 309-314, 2009.
- [12]. K. L. Butler, N. Sarma, and V. Ragendra Prasad, "Network reconfiguration for service restoration in shipboard power distribution systems," *Power Systems, IEEE Transactions on*, vol. 16, pp. 653-661, 2001.
- [13]. Hai shen, Yunlong Zhu, Wenping Zou, Zhu Zhu, "Group Search Optimizer Algorithm for constrained Optimization," *Computer Science for Environmental Engineering & Eco Information*, vol. 159, pp. 48-45.
- [14]. D. Das, "A fuzzy multi-objective approach for network reconfiguration of distribution systems," *IEEE Trans. Power Del.*, vol. 21, no. 1, pp. 202-209, Jan. 2006.
- [15]. C. T. Su and C. S. Lee, "Network reconfiguration of distribution systems using improved mixed-integer hybrid differential evolution," *IEEE Trans. on Power Delivery*, Vol. 18, No. 3, July 2003.
- [16]. Y. C. Huang, "Enhanced genetic algorithm-based fuzzy multi-objective approach to distribution network reconfiguration," *Proc. Inst. Elect. Eng.*, vol. 149, no. 5, pp. 615-620, 2002.
- I. Z. Zhu, "Optimal reconfiguration of electrical distribution network using the refined genetic algorithm," *Elect. Power Syst. Res.*, vol. 62, pp. 37-42, 2002.
- [17]. Y. Y. Hong and S. Y. Ho, "Determination of network configuration considering multi-objective in distribution systems using genetic algorithms," *IEEE Trans. Power Syst.*, vol. 20, no. 2, pp. 1062-1069, May 2005.
- [18]. K. Prasad, R. Ranjan, N. C. Sahoo, and A. Chaturvedi, "Optimal reconfiguration of radial distribution systems using a fuzzy mutated genetic algorithm," *IEEE Trans. Power Del.*, vol. 20, no. 2, pp. 1211- 1213, Apr. 2005.
- [19]. J. Z. Zhu, "Optimal reconfiguration of electrical distribution network using the refined genetic algorithm," *Elect. Power Syst. Res.*, vol. 62, no. 1, pp. 37-42, May 2002.
- [20]. M. E. Baran and F. Wu, "Network reconfiguration in distribution system for loss reduction and load balancing," *IEEE Trans. Power Del.*, vol. 4, no. 2, pp. 1401-1407, Apr. 1989.
- [21]. Y. Mishima, K. Nara, T. Satoh, T. Ito, "Method for minimum-loss reconfiguration of distribution system by tabu search," *Electrical Engg. Japan*, Vol. 152, No. 2, July 2005.
- [22]. D. Zhang, Z. Fu, L. Zhang, "An improved TS algorithm for Loss minimum reconfiguration in large-scale distribution systems," *Electric Power Systems Research*, Vol. 77, pp. 685-694, 2007.

PV Based Switched Capacitor Converter for NPC Inverter in Grid Connected Applications

M. Meenalochani¹, A. Albert Martin Ruban², R. Santhiya³

¹Assistant Professor, Department of EEE, Kings College of Engineering, Punalkulam, Pudukkottai

²Associate Professor, Department of EEE, Kings College of Engineering, Punalkulam, Pudukkottai

³PG student, Department of EEE, Kings College of Engineering, Punalkulam, Pudukkottai

Email:rsanthiyaa97@gmail.com

Abstract

This paper proposes a grid connected solar Photovoltaic (PV) Systems with a new voltage balancing converter suitable for Neutral-Point-Clamped (NPC) Multilevel Inverter (MLI). The switched capacitors used in the proposed converter are able to balance the DC link capacitor voltage effectively by using proper switching states. The proposed balancing converter can be extended to any higher levels and it can boost the DC input voltage to a higher voltage levels without using any magnetic components. This feature allows the converter to operate with the boosting capability of the input voltage to the desired output voltage while ensuring the self-balancing. In this paper, the proposed converter is used for a grid connected solar PV system with NPC multilevel inverter, which is controlled using vector control scheme. The proposed grid connected solar PV system with associated controllers and maximum power point tracking (MPPT) is implemented in Matlab/Sims Power System and experimentally validated using dSPACE system and designed converters. The simulation and experimental results show that the proposed topology can effectively balance the DC link voltage extract maximum power from PV module and inject power to the grid under varying solar irradiances with very good steady state and dynamic performances.

Index Terms Solar photovoltaics, NPC multilevel inverter, balancing circuit, dc-link voltage balancing, grid connected PV system

Introduction

Due to the use of fossil fuels for energy generation, adverse effects are occurred on the environment such as ozone depletion, greenhouse gas emission and acid rain. Now-a-days, the policies for renewable power generation support the capital subsidies to promote its applications and to provide subsidies in taxes. Due to innovation in research and technology improvement in manufacturing, the cost of photovoltaic (PV) array is decreasing day by day. Hence, reliability of PV array in miniature scale applications is improved. Various methods are available to model and simulate the PV array. Kaplani et. al have examined the effects of humidity, inclination and orientation of PV modules, rapid change in solar insolation on output of PV array, which are analysed for various conditions. Therefore, maximum power point tracking (MPPT) algorithm must be fast, reliable, less complex and adaptive at varying atmospheric conditions, which enhances the penetration of PV array-based generation into the grid by extracting maximum power from PV array. Various classical and Artificial Neural Network techniques for standalone system, combination of these techniques with classical MPPT algorithms and hybrid techniques are analysed with their complexity, convergence speed and accuracy. Moreover, an implementation of various MPPT methods is described. The power loss analysis is carried out for different operating conditions such as fast insolation variation and double line frequency voltage ripple. Different compositions of it are analysed for single-stage and double-stage topologies for three phase grid interfaced PV system and variety of advantages over double-stage topology, are as follows:

- i. Numbers of components used in single-stage topology (diodes and capacitors etc.) are less. Therefore, weight, complexity and cost of topology are reduced.
- ii. Efficiency of the single-stage topology is high due to reduced losses. Moreover, various conventional algorithms such as generalized integrators enhanced phase locked loop are to extract fundamental component from the distorted signal.

Many algorithms such as quadrature-phase locked loop, least mean fourth (LMF), variable step size least mean square (VSSLMS), peak estimation are demonstrated for interaction between PV system with three-phase grid with active shunt filtering capabilities. Owing to the double frequency oscillation problem and poor dynamic

response carried by low pass filter in synchronous reference frame (SRF)-based phase locked loop, the performance of the system is degraded. However, second-order generalized integrator and second-order generalized integrator quadrature have lower harmonics and DC offset filtering capabilities, respectively. Due to slow convergence during steady state operations, performance of the solar PV system is not reliable for conventional LMF and VSS-LMS algorithms, respectively. The behavior of system using peak estimation technique is not reliable due to poor dynamic response as the low pass filter is used in path of fundamental extraction of non-linear load current. The single layer neural network-based control scheme is proposed for double-stage grid interfaced solar PV array system to improve power quality of the system. The double-stage topology has low power transfer efficiency due to additional losses in the boost converter. The parallel operation of two single-stage solar PV system is modelled and analysed in to improve the power quality of the distribution network along with droop characteristics. The ideal magnitude and phase characteristics of notch filter make it complex in real-time implementation of solar PV grid interfaced system. Moreover, sensitive performance parameters variations of the system make it least feasible for the practical applications of solar PV grid interfaced system. Therefore, there is a need for adaptive filtering algorithm, which can enhance the system performance without affecting system topology.

Related Work

Multilevel inverters (MLIs) are broadly used for the grid integration of solar photovoltaic (PV) systems due to several advantages such as lower harmonic distortions, less electromagnetic interference (EMI), less standing voltage on semiconductors, high output waveform quality and smaller lter size [1], [2]. Three principal types for MLIs are Cascaded H-Bridge (CHB), Neutral-Point-Clamped (NPC), and Flying Capacitors (FC) [3]. These MLIs have several drawbacks and limitations such as: 1) CHB converters require large number of separate input DC-link sources [4], 2) FC MLIs have both balancing and large number of capacitors problems in high output voltage levels [5], and 3) NPC MLIs also require separate DC source and have balancing problems due to the use of capacitors which necessitate an additional balancing circuit [6]. The Neutral-Point-Clamped Multilevel Inverter (NPC-MLI) is initially suggested by Nabae in 1981 [7] which has numerous applications such as electric motor drives [8], grid integration of renewable energy sources (PV, fuel cell, and wind turbine) [9], [10] and utility applications [11], [12]. The main drawback of this type of converter is capacitor voltage balancing at the input of MLI in solar PV system which causes problems with the grid connected solar PV system [13]. In the existing literature, several methods have been suggested to solve the problem of capacitor voltage balancing of NPC-MLIs [14]. The adjacent switching technique is used in [15] to balance the capacitors' voltage where redundant states are used for voltage balancing and maintaining the output voltage at the acceptable range. However, the external circuit used to balance the capacitors' voltage increases the inductor size at higher voltage levels which introduces challenges in implementation. A voltage balancing technique for DC-link capacitors in parallel three-phase and single-phase NPC MLIs is presented in [16]. In this method, the voltage balancing capability is achieved where NPC-MLIs are connected in parallel. In this system, at least one of the inverters generates opposite voltage which limits the output voltage levels and increases the number of power semiconductors in higher voltage levels. A carrier-based pulsed-width modulation (CB-PWM) using zero-sequence voltage injection proposed in [17]. The switching frequency under this method is low and can balance the capacitors' voltage without using any extra control. However, the above mentioned methods are computationally intensive. Another DC-link voltage balancing method is proposed. This method uses a passive RLC circuit which requires magnetic elements. Some topologies are suggested in for the balancing capacitors' voltage at higher voltage levels, which are derived from 3L NPC. Although these topologies can be used for more than two levels; however, they have difficulties for balancing capacitors in more than five voltage levels. It is worth mentioning that in NPC-MLIs, the series connection of the DC-link capacitors is used to charge the capacitors through the PV unit in order to produce high voltage levels at the output. However, these converters with series capacitors are more vulnerable to capacitors are unbalancing and voltage dynamics instability as compared to the converters using capacitors in parallel.

Another concern in NPC-MLIs is voltage boosting in capability which causes the use of massive magnetic components. This condition is dealt using DC-DC boost converter. A multi output boost (MOB) DC-DC converter is suggested as an additional circuit to balance the DC-link capacitors while boosting the voltage. A new power conversion system for wind turbine application is proposed and validated. In this system a four-level boost converter has been proposed as an alternative to the traditional DC-DC boost converters. Another boost-type grid-connected inverters are proposed in magnetic elements are used to boost the input voltage to its chosen value at

the output. However, in these topologies, the drawback is using magnetic elements at the input, which increase size, volume and complexity, and reduces the efficiency of the system.

In this paper,

*A new step-up switched capacitor voltage balancing converter for NPC multilevel converter based solar PV system is proposed. The proposed converter is able to balance the DC link capacitor voltage effectively by using proper switching states.

*The proposed topology can boost the input DC voltage at the desired output voltage level without using any magnetic elements. It also requires only one DC source or PV array output to produce multi-level output, which reduces the number of input voltage sources required in such system. The proposed topology is cost effective than the traditional dc-dc converter and produce better output.

*The proposed grid connected solar PV system with associated controllers is implemented in Matlab Sim Power System and experimentally validated using dSPACE DSP (digital signal processor) system and designed converters. Results confirm that the proposed topology can effectively balance the DC link voltage, extract maximum power from PV module and inject power to the grid effectively.

Proposed System

Solar photovoltaic systems provide an attractive alternative source of power generation. As it can be placed near to the load centres when compared with other renewable source of generation. The rooftop PV system in general is grid connected and supports the off grid load with battery backup. A maximum power point is tracked using converter with variation in the irradiations all throughout the year. This paper proposes single phase synchronous reference frame (SRF) theory based current controlled PWM controller for the voltage source converter (VSC) to realize maximum generated power evacuation by maintaining the DC link voltage constant without battery support, low THD sinusoidal line synchronized current output, and limited reactive power compensation based on the unutilized capacity of the inverter. Stable converter (Buck-boost) acts as a better alternative to MPPT has been proposed. MATLAB based simulation results shows the efficient working of rooftop PV with proposed control methodologies in grid connected mode with limited reactive power conditioning.

The proposed grid connected solar PV System with a new voltage balancing converter is presented in , which include (i) PV array, (ii) proposed step-up converter for balancing the capacitors' voltage, (iii) a three-phase Inverter along with its controllers (iv) LC filter to improve total harmonic distortion (THD) and converting the staircase voltage to a near sinusoidal waveform by reducing the THD, (iv) grid interface transformer and (v) power grid. The PV array output is fed to the proposed step-up voltage balancing converter.

Electric utilities and end users of electric power are becoming increasingly concerned about meeting the growing energy demand. Seventy five percent of total global energy demand is supplied by the burning of fossil fuels. But increasing air pollution, global warming concerns, diminishing fossil fuels and their increasing cost have made it necessary to look towards renewable sources as a future energy solution. Since the past decade, there has been an enormous interest in many countries on renewable energy for power generation. The market liberalization and government's incentives have further accelerated the renewable energy sector growth. Renewable energy source (RES) integrated at distribution level is termed as distributed generation (DG). The utility is concerned due to the high penetration level of intermittent RES in distribution systems as it may pose a threat to network in terms of stability, voltage regulation and power-quality (PQ) issues. It is therefore Distributed Generation (DGs) particularly single phase Solar PV systems which are major research area for grid integration, since these sources have huge opportunity of generation near load terminal.

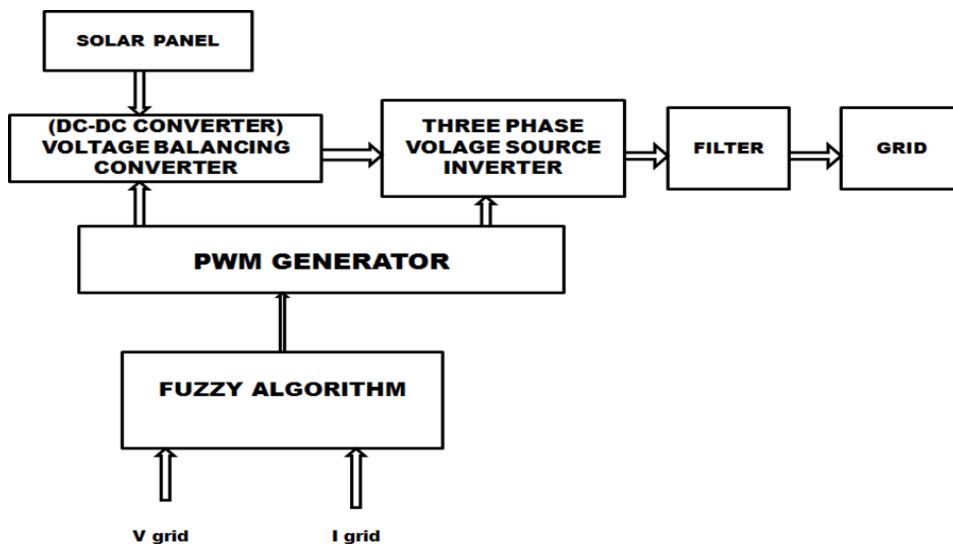


Fig 1: Proposed system block diagram

The single phase DG's fed with PV source can be not only utilized for household use but the excess energy can be transferred to the grid through proper control scheme and adequate hardware. Control scheme based on instantaneous PQ theory has been presented in some literatures for single phase system. Other control scheme such as Synchronous Reference Frame (SRF) is mainly used with three phase system in which sinusoidal varying quantities are being transferred to dc quantities that provides better and precise control than PQ based control even under distorted condition of mains. But SRF based control scheme can be customized for single phase which can't be utilized to get the desired dc quantity to generate required reference command. PV sources are interfaced with the grid through Voltage Source Converters (VSC's). VSC's can be controlled either in PWM based voltage control method or Hysteresis based Current Controlled method (HCC). HCC based controller gives fast response and better regulation but its major drawback lies with variable frequency.

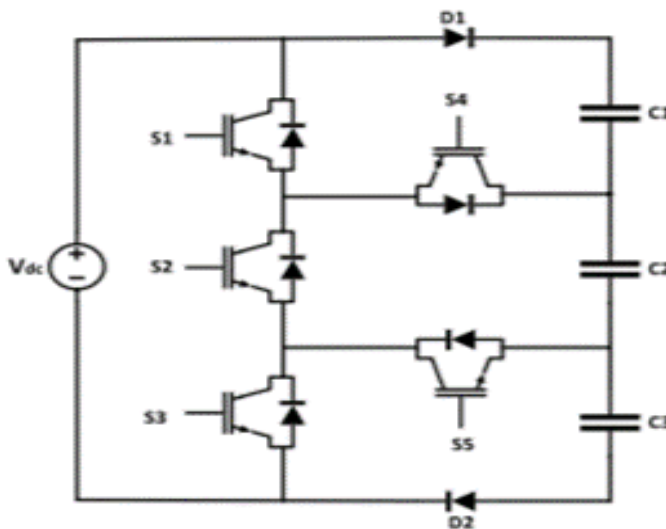


Fig 2: Proposed System circuit diagram

Simulation Results

This section presents a thorough validation of the proposed converter in interfacing solar PV system with the utility grid through a comprehensive simulation study using MATLAB/SimpowerSystem toolbox. This simulation studies a grid connected 1.14 kw solar PV system using the proposed converter topology. This simulation study

thoroughly investigates the effectiveness of the proposed converter topology in harvesting maximum possible solar power under varying irradiation condition. The incremental conductance MPPT algorithm along with vector control approach has been considered in this simulation study to facilitate harvest of maximum solar power transfer to the grid. The other relevant parameters of the simulation study are as follows: PVmodule: BIPV BIPV054-T86, 28.8V voltage at maximum power point (VMPP), 6.6A MPP current (IMPP), string comprising 6 modules and the whole PV array includes 1 string with MPP power of 1.14kW at 172.8 V, switching frequency: 5 kHz, the sampling time is 50s, output frequency: 50 Hz, capacitor value: of 4700 f, output filter with LD 12 my and C D 2.5 f. In the simulation study, the irradiations are varied (at room temperature) as follows (refer to (A)): 200 W/m² (0<t<1.2s), 400 W/m² (1.2s<t<2.4s), 600 W/m²(2.4s<t<3.6s), 800 W/m² (3.6s< t<4.8), 1000 W/m²(4.8s<t<6s), 800 W/m² (6s<t<7.2s), 600 W/m² (7.2s<t<8.4s), 400 W/m² (8.4s<t<9.6s), 200 W/m² (9.6s<t<10s).

The figure 3 shows the input voltage to the BALANCING converter, the temperature and irradiation variation causes oscillation in the output voltage.

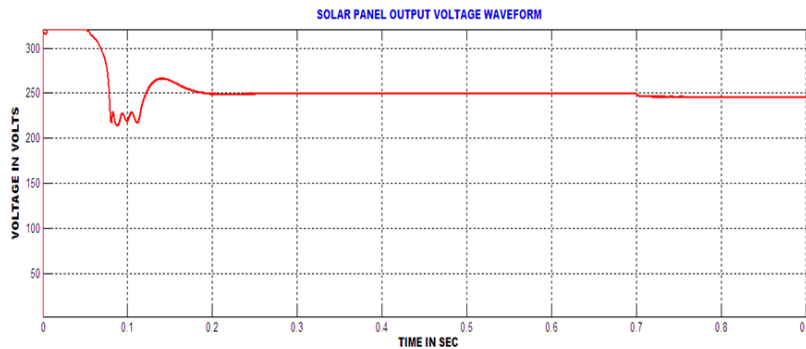


Fig 3: Solar panel output voltage waveform

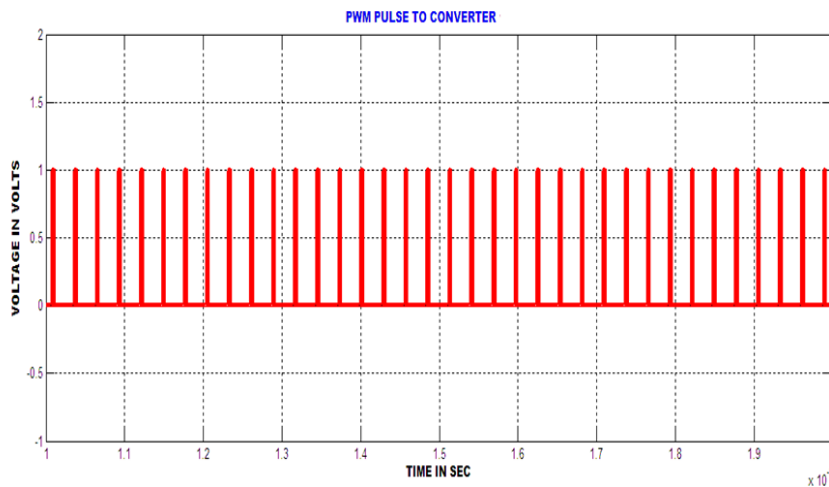


Fig 4: PWM Pulse waveform

The fig 4 shows the PWM pulses waveform to the Balancing converter, this PWM pulses has produced by incremental conductance algorithm.

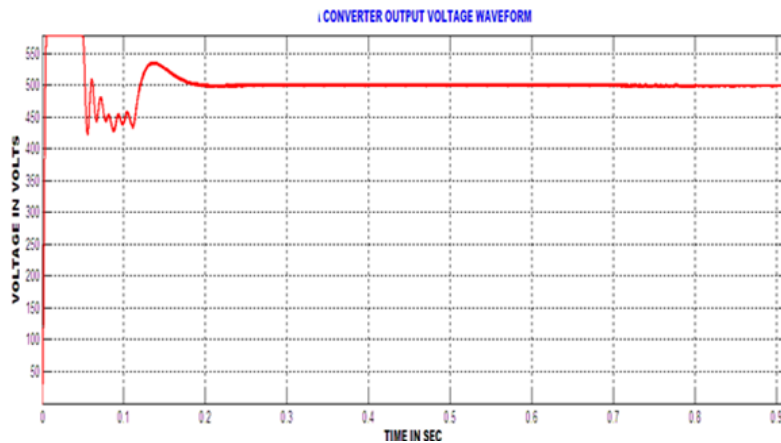


Fig 4: Three phase inverter voltage waveform

From the fig 4 we can observe that the three phase inverter voltage waveform. It can be seen from the figure that voltage stresses on all semiconductors are equal to voltage of the PV module at any instant. It is worth nothing that the entire DC link capacitors are required to be connected in parallel to ensure charging of the capacitors, which may cause high current spike that can potentially damage the switches.

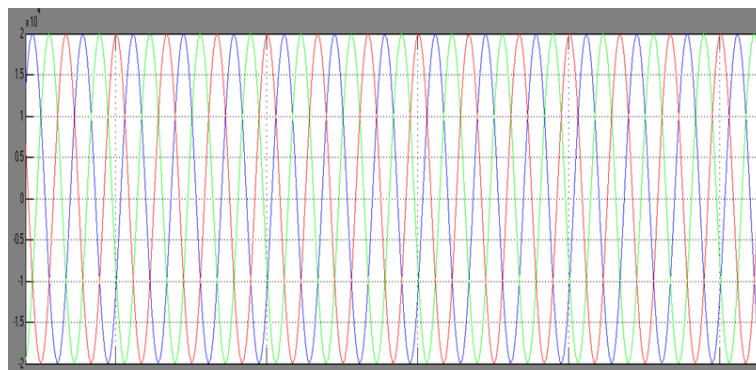


Fig 5: Three phase grid voltage waveform

From the fig 5, we can observe that the three phase grid voltage waveform. It can be seen from the current response that the ac current flowing to the grid is varying in correspondence to different irradiation level and ensure export of maximum possible solar power under varying weather condition.

Conclusion

The ability of the proposed control scheme to evacuate MPP tracked power from the PV array and provide limited reactive power compensation with grid connected mode. The current controlled PWM controller inject adequate generated current for self-support of capacitor at DC bus and thereby providing storage less operation. Single phase SRF (Synchronous Reference Frame) based estimation is employed which provides rugged control with cost effective solution. The proposed SRF based approach enable the control for providing limited compensation of reactive power depending on available unutilized capacity of VSC. Incremental Conductance algorithm is used to track the maximum power from the PV system. Power Factor is maintained near to unity even though there are changes in irradiations and also the limited reactive power compensation is provided by DG with Balancing converter.

References

[1] IEA: 'Transition to sustainable buildings: strategies and opportunities to 2050' (International Energy Agency (IEA), Paris, France, 2013)

- [2] Hsu, C.W.: 'Using a system dynamics model to assess the effects of capital subsidies and feed-in tariffs on solar PV installations', *Appl. Energy*, 2012, 100, pp. 205–217
- [3] 'Solar rooftop-grid connected', Ministry of New and Renewable Energy (MNRE), Government of India. Available at <http://www.mnre.gov.in/schemes/decentralized-systems/solar-rooftop-grid-connected/>, accessed November 15 2016
- [4] Shongwe, S., Hanif, M.: 'Comparative analysis of different single-diode PV modeling methods', *IEEE J. Photovoltaics*, 2015, 5, (3), pp. 938–946
- [5] Villalva, M.G., Gazoliand, J.R., Filho, E.R.: 'Comprehensive approach to modelling and simulation of photovoltaic arrays', *IEEE Trans. Power Electron.*, 2009, 24, (5), pp. 1198–1208
- [6] Kaplani, E., Kaplansis, S.: 'Thermal modelling and experimental assessment of dependence of PV module temperature on wind velocity and direction, module orientation and inclination', *Sol. Energy*, 2014, 107, pp. 443–460
- [7] Subudhi, B., Pradhan, R.: 'A comparative study on maximum power point tracking techniques for photovoltaic power systems', *IEEE Trans. Sustain. Energy*, 2013, 4, (1), pp. 89–98
- [8] Elobaid, L.M., Abdelsalam, A.K., Zakzouk, E.E.: 'Artificial neural network based photovoltaic maximum power point tracking techniques: a survey', *IET Renew. Power Gener.*, 2015, 9, (8), pp. 1043–1063
- [9] Wu, T.F., Chang, C.H., Lin, L.C., et al.: 'Power loss comparison of single and two-stage grid-connected photovoltaic systems', *IEEE Trans. Energy Convers.*, 2011, 26, (2), pp. 707–715
- [10] Gao, S., Barnes, M.: 'Phase-locked loop for AC systems: analyses and comparisons'. *Proc. IET Int. Conf. on Power Electronics, Machines and Drives*, 2012, pp. 1–6
- [11] Timbus, A.V., Ciobotaru, M., Teodorescu, R., et al.: 'Adaptive resonant controller for grid-connected converters in distributed power generation systems'. *Proc. IEEE Applied Power Electronics Conf. and Exposition*, 2006, pp. 1601–1606
- [12] Agarwal, R., Hussain, I., Singh, B.: 'LMF based control algorithm for single stage three-phase grid integrated solar PV system', *IEEE Trans. Sustain. Energy*, 2016, 7, (4), pp. 1379–1387
- [13] Pradhan, S., Hussain, I., Singh, B.: 'Modified VSS-LMS-based adaptive control for improving the performance of a single-stage PV-integrated grid system'. *IET Science and Measurement Technology*, Early Access.
- [14] Jain, C., Singh, B.: 'Single-phase single-stage multifunctional grid interfaced solar photo-voltaic system under abnormal grid conditions', *IET Gener. Transm. Distrib.*, 2015, 9, (10), pp. 886–894.
- [15] Singh, B., Shahani, D.T., Verma, A.K.: 'Neural network controlled grid interfaced solar photovoltaic power generation', *IET Power Electron.*, 2014, 7, (3), pp. 614–626
- [16] Liu, J., Miura, Y., Ise, T.: 'Power quality improvement of microgrids by virtual synchronous generator control', *Electr. Power Qual. Supply Reliab.*, Tallinn, Estonia, 2016, pp. 119–124
- [17] Deo, S., Jain, C., Singh, B.: 'A PLL-less scheme for single-phase grid interfaced load compensating solar PV generation system', *IEEE Trans. Ind. Inf.*, 2015, 11, (3), pp. 692–699

IOT Based Monitoring and Control of Distribution Transformer & Transmission Lines

Mr.S.R.Karthikeyan¹ Mr.J.Arokiaraj² Mr.R.Divyabharath³ Mr.E.Ganesan⁴ Mr.P.Gopinath⁵ Mr.R.Hariharan⁶
^{1, 2} – Assistant Professor and ^{3,4,5,6} - UG Final Year Student
Department of EEE, Kings College of Engineering, Punalkulam.

Abstract

To maintain the reliability in grid operation it is important to monitor real time transformer health and faults in the transmission lines. We know the importance of transformers in electricity distribution and transmission. They are the main components and constitute the large portion of capital investment of the distribution grid. Real time transformer health and transmission line fault detection systems help to replace the equipment before failure and continuity of the power will not be disturbed and also reducing the potential dangers that are caused due to any unforeseen circumstances. So we need a system that can monitor the health of the transformer as well as the faults in the transmission line in real-time. So, that we can easily identify the faults and ensure the safety and reliability of the overall power grid.

Introduction

The power transformer plays important role in power transmission and distribution sections. In this system, the internet of things based monitoring and controlling may be suitable for manual operating system. For example in case of manual operating system it is not possible to monitor the oil level and temperature level by means of man power. So our system is designed based upon the online monitoring which provide useful data and information the health of transformers and help the utility services to use optimistic for long period of time.

Power system is classified into power generation, transmission and distribution. Transmission network is considered to be one of the vital parts of power system, as it connects the supply and the demand. The loss in transmission and distribution network is considered to be very high, compared to other parts of power system. The fault in the transmission network obstruct the supply of power to the consumer. Hence the transmission network fault identification and clearance should be very fast. Additionally, there is an impending need to equip the age old transmission line infrastructure with a high performance data communication network that supports future operational requirements like real time monitoring and control necessary for smart grid integration.

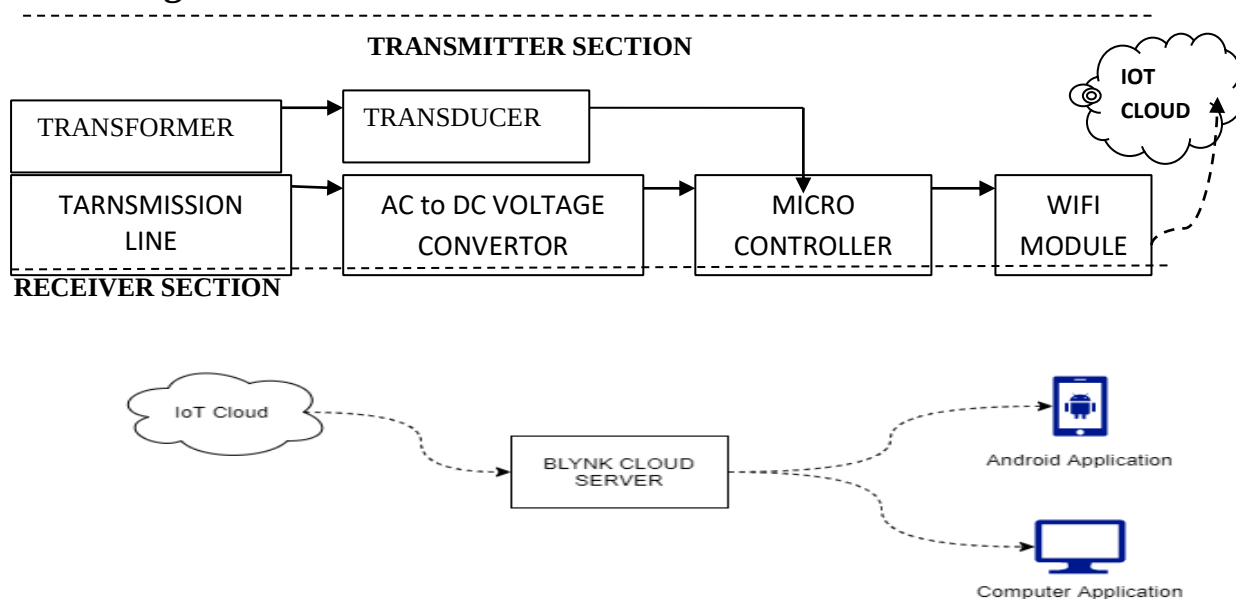
Existing System

- ❖ Most of the distribution transformers are remotely located in a rural area, where regular monitoring by human observation is difficult to perform due to insufficient manpower.
- ❖ Our existing monitoring systems are not supported for real time operations. There is too many transformer failure cases are detected every day.
- ❖ The Existing fault Detection system can only detect a fault and cannot identify the fault and fault location in a transmission line. As the conventional systems are not real-time in nature, the operators cannot devise any quick action to solve the fault cased in the transmission line or the transformer.
- ❖ The Existing Systems are analog in nature and not digital so they are not accurate and always have a miss in the range of +/- 10 %.

Proposed System:

To overcome the existing system drawbacks we need a smart and reliable solution to monitor the distribution transformer parameter, transmission line faults and send it to the IOT platforms in real time. It enables the grid operator to define the performance of the grid. It also provides important information about transformer health and transmission line state. IOT Based Transformer Monitoring System will allow the utilities to optimally run the transformer and keep this equipment in operation for a longer period.

Block Diagram



Equipment & Software Tools Required

Hardware Components:

1. MICRO CONTROLLER
2. VOLTAGE SENSOR
3. CURRENT SENSOR.
4. GAS SENSOR
5. OIL LEVEL SENSOR.
6. TEMPERATURE SENSOR
7. BUZZER
8. EXHAUST FAN
9. RELAY (3Channel)

Software Requirement:

1. Blynk Library.
2. ESPyTool-3.4.1A.
3. RPGPIO Module.
4. Arduino-IDE

Conclusion

Proper monitoring and maintenance can ensure a smooth service life for distribution transformer. The IOT based solution for monitoring and controlling of distribution transformers is quite easy and effective compared to manual monitoring method. Reliable power distribution system must use protective devices which will essentially reduce running cost. Continuous monitoring of Distribution transformer, timely alerts to rectify the abnormality if any, there by extending the lifetime of distribution transformers This study will help in cost minimization by reducing the workforce in maintenance. IOT based transformer & transmission line fault monitoring system in proposed. The prototype will be done.

References:

1. R. R. Pawar, P. A. Wagh and S. B. Deosarkar, "Distribution transformer monitoring system using Internet of Things (IoT)," 2017 International Conference on Computational Intelligence in Data Science (ICCIDS), Chennai, 2017, pp. 1-4, doi: 10.1109/ICCIDS.2017.8272671.
2. W. K. A. Hasan, A. Alraddad, A. Ashour, Y. Ran, M. A. Alkelsh and R. A. M. Ajele, "Design and Implementation Smart Transformer based on IoT," 2019 International Conference on Computing, Electronics & Communications Engineering (iCCECE), London, United Kingdom, 2019, pp. 16-21, doi: 10.1109/iCCECE46942.2019.8941980.

3.D. Srivastava and M. M. Tripathi, "Transformer Health Monitoring System Using Internet of Things," 2018 2nd IEEE International Conference on Power Electronics, Intelligent Control and Energy Systems (ICPEICES), Delhi, India, 2018, pp. 903-908, doi: 10.1109/ICPEICES.2018.8897325.

4.F. Haghjoo, M. Mostafaei and H. Mohammadi, "A New Leakage Flux-Based Technique for Turn-to-Turn Fault Protection and Faulty Region Identification in Transformers," in IEEE Transactions on Power Delivery, vol. 33, no. 2, pp. 671-679, April 2018, doi: 10.1109/TPWRD.2017.2688419.

5.Md. Sanwar Hossain, Mostafizur Rahman, Md. Tuhin Sarker, Md. Ershadul Haque, Abu Jahid, A smart IoT based system for monitoring and controlling the sub-station equipment, Internet of Things, Volume 7,2019,100085,ISSN 2542-6605,https://doi.org/10.1016/j.iot.2019.100085.

IoT Based Non Intrusive Power Monitoring and Energy Alert

R.Raghuraman¹, Dr.S.Saravanan²,Dr.A.Arulvizhi³, D.Venkatesan⁴

^{1,4} Assistant Professor / EEE, ² Principal, ³ Associate Professor & Head,
¹²³⁴ CK College of Engineering & Technology, Cuddalore

Abstract

The advancement in automation of every activity is to a large extent and one such IoT (Internet of Things) based automation in the electrical distribution sector is proposed in this work. The consumption of electrical energy by all types of consumers is being recorded on a regular basis and the consumers are made to pay accordingly to their tariff slab. The process currently being adopted requires a human operator to record the readings of the energy meters located at the consumers premises that incur losses to either the utility or the consumer. IoT based non intrusive load monitoring technique is proposed for commercial and domestic applications. The meter continuously measures the energy consumption and send the cumulative usage to the consumers on a daily basis so as to caution their usage. This recorded cumulative consumption over the billing period is also sent to the utility's centralized database. In addition, an online dashboard is made available to the user through internet that allows live monitoring of the energy consumption and the cumulative cost incurred during the billing cycle. The defaulters' electricity supply can be automatically terminated remotely from the service provider's office premises itself through internet.

Keywords:IoT, PZEM sensor, ESP8266, Adafruit

1 Introduction

The advancement in technologies related to all field is to a larger extent especially pertaining towards automation of every activity. At the same time, high security is also preferred. One such automation in the electrical distribution sector is proposed in this paper. The consumption of electrical energy by all types of consumers is being recorded on a regular basis and the consumers are made to pay accordingly to their slab of tariff. The process currently being adopted by the TANGEDCO -Tamilnadu Electricity board requires a human operator to record the readings of the energy meters located at the consumers premises. This system requires huge number of manpower as the meter recordings need to be carried out from houses to houses and building to buildings. Hence this process turns out to be time consuming one. As it depends on the human operator, the readings are also prone to errors which may incur losses to either the consumer or to the utility. This traditional billing is also slowed down during the bad weather conditions.

In Tamilnadu, the electricity tariff is under the slab system wherein a consumer may be charged on very high scale if the consumption falls on the next slab. The consumer has no clue / notifications till the final recordings of how much units of electricity that has been used. This will take a toll on the consumers who merely crossed the slab. Hence periodic notifications about their usage to consumers are essential. Also certain consumers stay lethargic in paying their electricity bill before the due date as there is no provision for immediate action to be taken on the defaulters. Moreover it would be very much at ease if the consumers are able to monitor their consumption and cumulative tariff for the billing cycle in either their mobile or laptops.

To overcome the aforementioned statements, an IoT based electricity meter is designed for commercial and domestic appliances. The meter continuously measures the consumption and sends the cumulative data to the consumers on a daily basis so as to caution their usage and send the cumulative consumption over the billing period to the utility's centralized (say TANGEDCO for instance) database. The defaulters' electricity supply can be terminated remotely by a single operator from the office premises itself. The proposal will evolve a new era in the automation of electricity billing that leads to better consumer – utility relationship. Timely billing and better service from the utilities will lead to effectiveness in the system and encourages the use of electricity.

2 Problem Formulation

2.1 Preamble

In existing system of electricity meter recording man power is used to record the energy meter reading for consumers. It is prone to human errors and also the process is affected during bad weather conditions. Hence timely billing cannot be done. The electricity tariff is under the slab system wherein a consumer may be charged on very high scale if the consumption falls on the next slab. The consumer has no clue / notifications till the final recordings of how much units of electricity that has been used. This will take a toll on the consumers who

merely crossed the slab Certain consumers stay lethargic in paying their electricity bill before the due date as there is no provision for immediate action to be taken on the defaulters.

2.2 Problem Statement

Consider the example shown in Fig. (1).that illustrates the tariff comparison of a domestic customer for different units. It can be visualized from the calculation that Rs 716 has to be paid more for just crossing the slab by mere six units. The energy consumption of 506 units will be rounded to 510 units and the cost is calculated accordingly. The calculation show below is from the TNEB online bill calculation web page.

| | | | |
|---------------------------|--------|---------------------------|--------|
| Consumed Units: | 500.0 | Consumed Units: | 510.0 |
| Total Current Charges Rs. | 1400.0 | Total Current Charges Rs. | 2046.0 |
| Subsidy Rs.(-) | 50.0 | Current Charges Rs. | 2046.0 |
| Current Charges Rs. | 1350.0 | Fixed Cost Rs.(+) | 50.0 |
| Fixed Cost Rs.(+) | 30.0 | Subsidy Fixed Cost Rs.(-) | 0.0 |
| Subsidy Fixed Cost Rs.(-) | 0.0 | New Subsidy Rs.(-) | 250.0 |
| New Subsidy Rs.(-) | 250.0 | Net Amount Rs. | 1846.0 |
| Net Amount Rs. | 1130.0 | | |

Figure 1:Tariff Comparison between two immediate next Slabs

The domestic consumers of tamilnadu, pay TNEB bimonthly for their electricity usage. The number of units is billed only at the end of every two months by a TNEB official. We do not know how much electricity we use on a daily basis. As our electricity bill is slab tariff based structure, the tariff rates increases very much when the consumption for the entire units fall on the higher slab.

To address these problems, energy should be monitored and the cumulative consumption of units & cost is intimated to the consumers on a daily basis through an automated system. In addition, notification shall also be sent on nearing the slabs.

3 Proposed Methodology

The total energy consumed by a customer is continuously sensed through PZEM sensor and the recordings are pushed to the microcontroller. From the recordings, the number of units and the cost are calculated by the NodeMCU. The cost and units consumption are logged in the internet cloud (Adafruit I/O) space by the NodeMCU. In addition, the tracked power consumption is made available as a live dashboard in the adafruit i/o that can be accessed by the user. The power to all the loads can also be disconnected remotely by commanding the NodeMCU through internet and causing the relay to disconnect the loads from the mains. The daily and the slab crossing alerts are issued to the user via sms.

3.1 PZEM Sensor Description

PZEM004T-V3 sensor is shown in the below Fig. (2).PZEM004T is most appropriate to measure the voltage, current, power, energy, frequency, Power factor (frequency and PF is extra added in the new version)using Arduino/ESP8266/Raspberry Pi like open source platform. The sensor comes with the following advantages

- High galvanic isolation
- Parameter display
- Direct communication with computer
- Data acquisition and storage with subsequent viewing or copying to the computer.

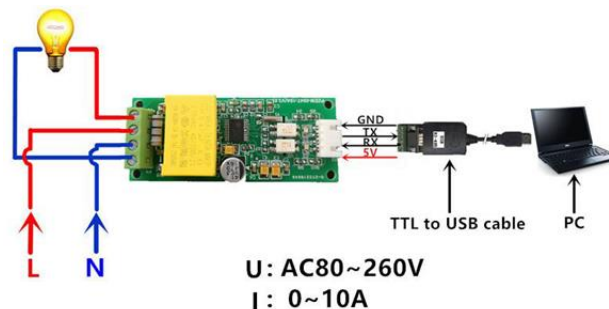


Figure 2 :PZEM Sensor and its Interfacing Schematics

3.2. Adafruit IO

Adafruit IO is a system that makes data useful. It mainly focuses on ease of use, that allows simple data connections and with less programming logic data can be pushed in and out from the database,. IO includes client libraries that wrap our REST and MQTT APIs. IO is built on Ruby on Rails, and Node.js. It provide feeds to store the pushed data continuously from the sensors and dash board for live monitoring of all / selected feeds in order to visualize the data. Based on the data and the conclusions drawn, certain events can also be triggered from the IO. The event can either be triggered from the IO or the data can be subscribed from the feeds and the event sequence can be triggered by the controller action also. Thus through MQTT protocol, Adafruit allows one of the best publish and subscribe phenomenon of the data.

4 Schematic of the System & Circuit Connection

The schematic of the system and the circuit connection are shown below Fig. (4) and Fig. (5) respectively. +5V Power supply (common ground to microcontroller relay and sensor --not shown) is provided through a SMPS.

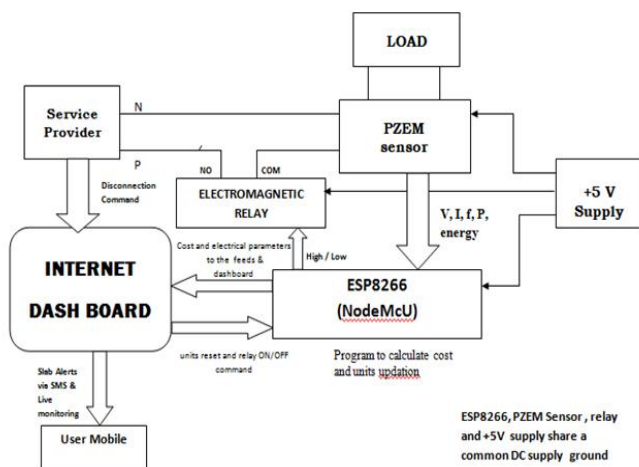


Fig.4: Schematic of the Proposed System

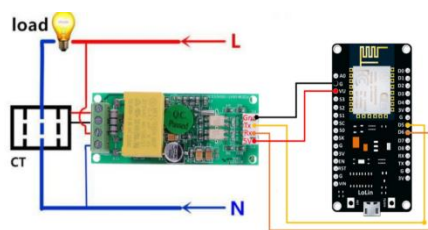


Fig.5: Circuit Connection

5 Experimental Setup

The below Fig.(6) depicts the hardware prototype that has been developed to realize the proposed methodology. The tests were conducted using the below experimental setup. The power consumed by the CFL is sensed by the PZEM sensor and it transfers the values of voltage, current, real power, power factor, frequency and the units consumed to the NodeMCU. The NodeMCU is programmed to calculate the cumulative units and the cost accordingly. The NodeMCU also pushes the power consumption and other necessary electrical parameters along with the cumulative units and cost into adafruit i/o feeds. The selected data alone can be made available in the dashboard. A button is provided in the dashboard that enables the disconnection of the relay. This button control is only enabled for the service provider.



Fig.6: Experimental Setup

6 Results and Discussions

6.1 Validation of the Sensor

The readings of the PZEM sensor for a sample load has been compared with a standard energy meter and the performance of the sensor accuracy is determined. The readings of the PZEM sensor are made available through IoT in a mobile application and compared. The comparison between them is shown in the Fig.(7). It is found that for a given sample load the readings of the PZEM sensor and the energy meter readings are same which reveals the PZEM is calibrated against the standard energy meter. The study gives assurance to deploy the PZEM sensor for the energy recordings.



Fig.7: Validation of the Sensor

6.2 Live Monitoring Dashboard

The power consumption, cumulative number of units consumed and the corresponding cost incurred during the current billing cycle is made available in the adafruit dashboard through the MQTT protocol available in the adafruit i/o service provider by the NodeMCU. The result is shown below in Fig.(8).



Fig.(8). Live Monitoring Dashboard

6.2 SMS Alerts

The built automated system provides SMS alerts on a daily basis and during the times when a particular slab is crossed to user. The slab crossing is simulated manually in the software program & the status of alert is verified. It is found the user mobile is receiving alerts whenever the number of units consumed have crossed a predefined slab. The output is shown in the below Fig.(9)

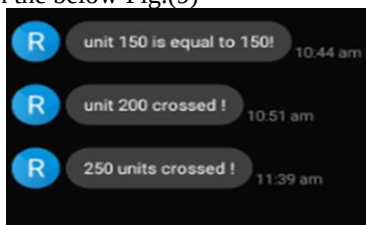


Fig.(9). SMS Alerts

A fundamental control of home automation using IoT can be adopted to disconnect the loads in the customer home in the event of electricity bill payment default.

6.3 Conclusion

Thus a successful power monitoring scheme is designed where the live power consumption & the electricity bill for the current cycle are made known to the customer in a simple elegant user interface dashboard. A remote action of disconnection can also be performed by the service providers with certain access restriction meant only to them. . With the proposed system the consumer have an awareness about the energy consumption on a daily basis and hence forth it will inherently force the consumer to avoid the excess usage of

electricity.. Thus the developed system found to be highly beneficial for both the customer and service providers. The proposed scheme can be extended to any type of single phase power monitoring. The work has a scope of extending to three phase systems. It also paves way for the need of an intelligent controller to optimize the energy consumption i.e to perform the energy management without the compromise of the sophistication of the customer automatically and claim to be energy efficient thereby reducing the electricity bill of the consumers.

References

- [1] Fangyu Li, Yang Shi, Aditya Shinde, Jin Ye, WenZhan Song. ,*"Enhanced Cyber-Physical Security in Internet of Things through Energy Auditing "*, IEEE Internet of Things Journal (Volume: 6 , Issue: 3 , June 2019) 5224 - 5231.
- [2] Bharath,S., Pasha, M.Y., & Deepth, J.(2017, April). *IoT-Home Automation. International Journal of Computer Technology and Research*, 5, 4-6. April 2017
- [3] Sahil Garg, Kuljeet Kaur, Georges Kaddoum, Francois Gagnon, Syed Hassan Ahmed, Dushantha Nalin K. Jayakody, *"LiSA: A Lightweight and Secure Authentication Mechanism for Smart Metering Infrastructure"*, Global Communications Conference (GLOBECOM) 2019 IEEE, pp. 1-6, 2019
- [4] Rijo Jackson Tom, Suresh Sankaranarayanan, Joel J. P. C. Rodrigues. *"Smart Energy Management and Demand Reduction by Consumers and Utilities in an IoT-Fog-Based Power Distribution System,"* IEEE Internet of Things Journal (Volume: 6 , Issue: 5) 7386 - 7394, , Oct. 2019.

Analysis of a 21 level Inverter with reduced switch count

A. Annai Theresa
Assistant Professor

Department of Electrical and Electronics Engineering
St. Anne's College of Engineering and Technology, Panruti

Abstract

In recent day's Multilevel inverter (MLI) technologies become a incredibly main choice in the area of high power medium voltage energy control. Though multilevel inverter has a number of advantages it has drawbacks in the vein of higher levels because of using more number of semiconductor switches. This may leads to vast size and price of the inverter is very high. So in order to overcome this problem the new multilevel inverter is proposed with reduced number of switches. The proposed topology results in reduction of the number of switches, losses, installation area, and converter cost. These are accomplished by using asymmetrical cascaded-H- Bridge type and Selective Harmonic Elimination (SHE) technique. In this paper, the hardware implementation of the multilevel inverter in 21 levels has been done after verifying in MATLAB/ SIMULINK.

Keywords: *multilevel inverters, cascaded MLI, total harmonic distortion (THD), Selective Harmonic Elimination (SHE).*

1 Introduction

Generally, the voltage source inverters generate an output voltage with a two level, so they are also called the two-level inverter. To obtain a quality output voltage or a current waveform with a minimum amount of ripple content, they require a high switching frequency along with various PWM techniques. For the high power and medium power application, these two-level inverters have some disadvantages, like switching losses due to high frequency operation, the distorted output voltage and current waveforms and the large total harmonic distortion of the voltage and current. Hence multi-level inverters are used to mitigate the overall THD [1]. The multilevel inverter can be classified as flying capacitor, Cascaded H-Bridge and diode clamped multilevel inverters. Out of these technologies Cascaded H-Bridge multilevel inverter is one of the well-known, most advantageous, much simpler and basic method of multilevel inverter [2]. High voltages with the low harmonics can be achieved with the special organisation of multilevel voltage source [3].

The first topology introduced was the series H-bridge design [4], but several configurations have been obtained for this topology as well [5], [6]. Since this topology consists of series power conversion cells, the voltage and power levels may be scaled easily. An apparent disadvantage of this topology is the large number of isolated voltages required to supply each cell. The H-bridge topology was followed by the diode-clamped converter that utilized a bank of series capacitors [7]. Another fundamental multilevel topology, the flying capacitor, involves series connection of capacitor-clamped switching cells [8]. When compared to the diode-clamped inverter, this topology has several distinctive features. One quality is that additional clamping diodes are not looked-for. Moreover, only one dc source is desired, because the flying capacitor inverter has switching redundancy inside the phase that can be utilised to balance the flying capacitors. The inverter phases are paralleled through interphase reactors in another multilevel design [9]. In this design, the entire dc voltage is blocked by the semiconductors, but the load current is shared. Quite a lot of combinational designs have also appeared, some including, cascading the fundamental topologies [10], [11]. A higher power quality than the fundamental topologies could be achieved with these designs for a given number of semiconductor devices owing to a increasing effect of the number of levels. Some new configurations have also been suggested to lessen the number of separate dc sources for high-voltage, high-power applications that are discussed in [12], [13].

Regrettably, multilevel inverters do have some shortcomings. One specific drawback is the requirement of a huge quantity of power semiconductor switches. Though low-voltage-rated switches can be employed in a multilevel converter, each switch necessitates the associated gate driver and protection circuits. This may cause the overall system to be more expensive and complex. An effort has been taken to introduce a new topology for multilevel converters to reduce the power electronics switches and dc voltage sources compared to traditional multilevel converters [14]. All odd and even step levels could not be created at the output voltage by the recommended algorithm in [14] and [15]. Also, for creating the output voltage with a constant number of step levels, the converter required many great quantities of bidirectional switches.

This paper proposes a new topology for multilevel converters with a high number of step levels associated with a lesser quantity of power switches after evaluating the downsides of the present topologies.

The proposed topology is designed with four dc sources, twelve switches and twelve driver circuits. The proposed Selective Harmonic Elimination (SHE) technique is effective in eradicating the lowest order harmonics and making a higher quality sinewave output waveform with an improved harmonic profile.

2 Multilevel Inverter

Multilevel power conversion technology developed initially from the need for reducing the harmonic content in inverter output voltage. Subsequently, it has been practically implemented to serve the need for realizing the inverters driven for high voltage dc buses. The state of the art switching devices have been either highly stressed or lacking sufficient voltage rating to realize high voltage and high power inverters. By using multilevel structures, the stress on switching device will be proportionately reduced. Thus a high dc bus voltage level can be handled without the use of bulky and lossless step-up/down transformers.

Multilevel inverters include an array of the power semiconductor devices and number of voltage sources, the output of which generate voltages with many levels in the waveforms.

2.1 Cascaded H- Bridge Topology

In recent years the electrical engineering researchers pay their attention on MLI to obtain quality and reliable power for many industrial applications. The Cascaded H- Bridge inverter overcomes the shortcomings of conventional two level inverter by combining more than one H- Bridge modules together because of its level increasing ability.

The term H Bridge arrived from the typical graphical demonstration of a circuit. An H bridge is erected with 4 switches. One of the simple and popular topologies amongst all multilevel inverter is cascaded H-bridge multilevel inverter. It can be applied for the conversion of both single phase and three phase voltage. More quantity of H-Bridges are organised in series in Cascaded H-Bridge multilevel inverter. Each H-Bridge has isolated DC source which is to be obtained from any natural sources, ultra-capacitors, fuel cells or batteries to produce inverted ac output [16].

3 Proposed System

A new multilevel inverter is proposed here with reduced number of switches and the output voltage level is increased up to 21 level with reduced (THD). Since we use less number of switches the switching losses also get reduced. The proposed Asymmetrical Cascaded Multilevel Inverter (ACMLI) topology for 21-level inverter involves twelve semiconductor switches and four separate DC sources. Output voltage is separated into two parts. The left side part is termed as level generation part and it is accountable for producing levels in positive polarity and negative polarity. The right side part is termed as polarity generation part and it is accountable for producing the polarity (+ or -) of the output voltage. The proposed topology chains the left part and right part to generate the multilevel output voltage waveform. The main determination of the proposed ACMLI topology is to reduce the electromagnetic interference, lower the total harmonic distortion with SHE technique and also to lessen the power semiconductor switches than traditional multilevel inverter. For a traditional single-phase 21-level inverter, it uses 40 switches, whereas the proposed topology uses only 12 switches with the similar principle. Gate pulses for Switches are generated by using PIC microcontroller PIC16F877A. In this suggested scheme, the SHE technique is used and by which the lower order harmonics are eradicated and the efficiency of the MLI is increased.

3.1 Operation of the proposed topology

The proposed single-phase asymmetrical cascaded 21-level inverter is shown in figure 2. With this inverter, 21 levels (0, ± 10 level) of output voltage as a stepped waveform is attained. The different switching states (i.e) ON, OFF states of different switches for attaining different voltage levels are given in the table.1

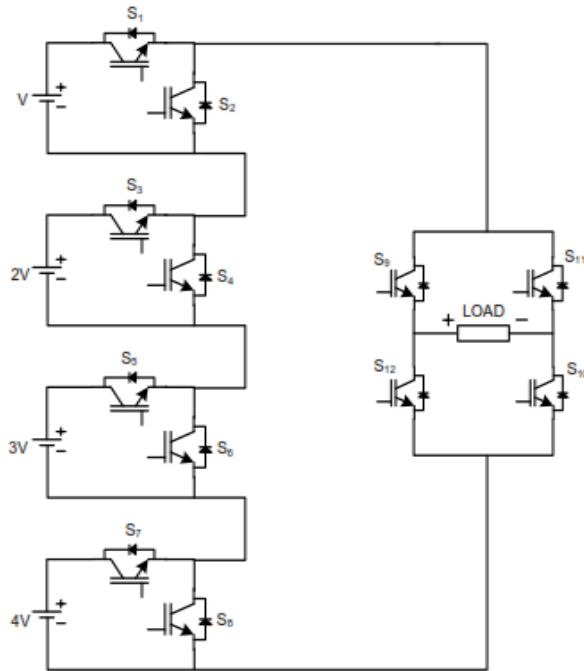


Figure 1: The proposed single-phase asymmetrical cascaded 21-level inverter

The number of output voltage levels achieved from the conventional method is given by the equation: $m = 2N_s + 1$ where m represents the output voltage levels and N_s is the individual inverter stages. The number of switches (l) required to achieve m levels is given by the equation: $l = 2(m - 1)$ for the implementation of 21-level CMLI and therefore the number of switches required in the conventional method is 40.

The proposed ACMLI topology for 21-level inverter requires twelve semiconductor switches and four isolated dc sources. So, a conventional single-phase 21-level inverter uses 40 switches, whereas the proposed topology uses only 12 switches with the same principle. PIC microcontroller PIC16F877A is used to generate pulse for Switches.

Table 1: Switching States

| Voltage level | Switching State | | | | | | | | | | | | Output Voltage |
|---------------|-----------------|----------------|----------------|----------------|----------------|----------------|----------------|----------------|----------------|-----------------|-----------------|-----------------|----------------|
| | S ₁ | S ₂ | S ₃ | S ₄ | S ₅ | S ₆ | S ₇ | S ₈ | S ₉ | S ₁₀ | S ₁₁ | S ₁₂ | |
| +10 | 1 | 0 | 1 | 0 | 1 | 0 | 1 | 0 | 1 | 1 | 0 | 0 | 10V |
| +9 | 0 | 1 | 1 | 0 | 1 | 0 | 1 | 0 | 1 | 1 | 0 | 0 | 9V |
| +8 | 1 | 0 | 0 | 1 | 1 | 0 | 1 | 0 | 1 | 1 | 0 | 0 | 8V |
| +7 | 0 | 1 | 0 | 1 | 1 | 0 | 1 | 0 | 1 | 1 | 0 | 0 | 7V |
| +6 | 1 | 0 | 1 | 0 | 1 | 0 | 0 | 1 | 1 | 1 | 0 | 0 | 6V |
| +5 | 1 | 0 | 0 | 1 | 0 | 1 | 1 | 0 | 1 | 1 | 0 | 0 | 5V |
| +4 | 0 | 1 | 0 | 1 | 0 | 1 | 1 | 0 | 1 | 1 | 0 | 0 | 4V |
| +3 | 1 | 0 | 1 | 0 | 0 | 1 | 0 | 1 | 1 | 1 | 0 | 0 | 3V |
| +2 | 0 | 1 | 1 | 0 | 0 | 1 | 0 | 1 | 1 | 1 | 0 | 0 | 2V |

| | | | | | | | | | | | | | |
|-----|---|---|---|---|---|---|---|---|---|---|---|---|-------|
| +1 | 1 | 0 | 0 | 1 | 0 | 1 | 0 | 1 | 1 | 1 | 0 | 0 | 1 V |
| 0 | 0 | 1 | 0 | 1 | 0 | 1 | 0 | 1 | 1 | 1 | 0 | 0 | 0 V |
| -1 | 1 | 0 | 0 | 1 | 0 | 1 | 0 | 1 | 0 | 0 | 1 | 1 | -1 V |
| -2 | 0 | 1 | 1 | 0 | 0 | 1 | 0 | 1 | 0 | 0 | 1 | 1 | -2 V |
| -3 | 1 | 0 | 1 | 0 | 0 | 1 | 0 | 1 | 0 | 0 | 1 | 1 | -3 V |
| -4 | 0 | 1 | 0 | 1 | 0 | 1 | 1 | 0 | 0 | 0 | 1 | 1 | -4 V |
| -5 | 1 | 0 | 0 | 1 | 0 | 1 | 1 | 0 | 0 | 0 | 1 | 1 | -5 V |
| -6 | 1 | 0 | 1 | 0 | 1 | 0 | 0 | 1 | 0 | 0 | 1 | 1 | -6 V |
| -7 | 0 | 1 | 0 | 1 | 1 | 0 | 1 | 0 | 0 | 0 | 1 | 1 | -7 V |
| -8 | 1 | 0 | 0 | 1 | 1 | 0 | 1 | 0 | 0 | 0 | 1 | 1 | -8 V |
| -9 | 0 | 1 | 1 | 0 | 1 | 0 | 1 | 0 | 0 | 0 | 1 | 1 | -9 V |
| -10 | 1 | 0 | 1 | 0 | 1 | 0 | 1 | 0 | 0 | 0 | 1 | 1 | -10 V |

3.2 Harmonic Elimination Technique

In this proposed scheme, the selected harmonic elimination technique is used and by which the lower order harmonics are eliminated. The harmonic elimination is performed for several reasons. The first reason is that harmonics are the source of EMI. Without harmonic elimination, designed circuits would need more protection in the form of snubbers or EMI filters [17], as result, designed circuits would cost more. The second reason is that EMI can interface with control signals used to control power electronics devices and radio signals. The third reason is that harmonics can create losses in power equipment. The fourth reason is that harmonics can lower the power factor of a load. Increased harmonic content will decrease the magnitude of the fundamental relative to the magnitude of the entire current, as a result the power factor would decrease. There are four kinds of control methods for multilevel converters. They are the traditional PWM control method, selective harmonic elimination method, space vector control method and space vector PWM control. The traditional PWM, space vector PWM and space vector modulation methods cannot completely eliminate harmonics. Of these four kinds we use here the selective harmonic elimination technique which is very important and efficient method. This technique is widely used in control of the conventional VSIs, in order to improve much more the quality of their output voltages. [18]

Selective Harmonic Elimination technique SHE is used to increase MLI efficiency by reducing output Total Harmonic Distortion THD associated with MLI switched output [19], [20]. It is rather simple to be applied to proposed topology by selecting suitable switching angles.

4 Result Analysis

The circuit for 21 level inverter is simulated in MATLAB/ SIMULINK and its outputs (i.e) load current and voltage are verified with the hardware implementation.

4.1 Simulation Results

The simulation circuit diagram its output and THD analysis is shown in figures 2,3 and 4.

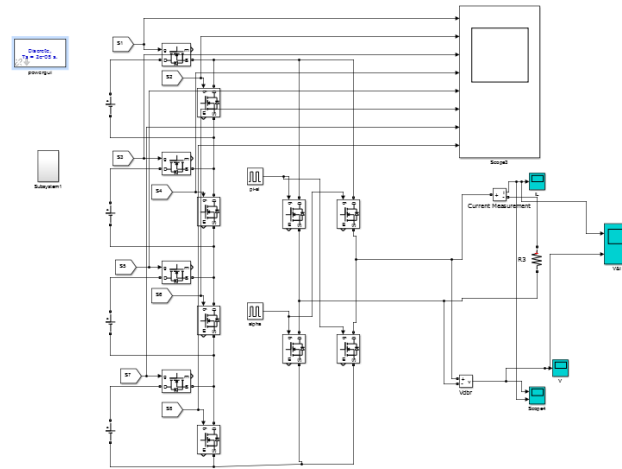


Figure2: Simulation Circuit Diagram of the Proposed 21 level Inverter

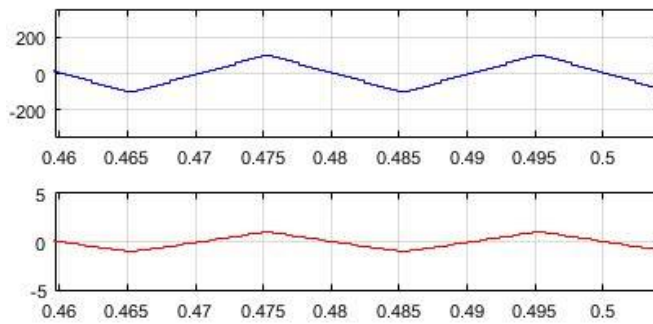


Figure 3: Output Voltage and Output Current of the Proposed 21 level Inverter

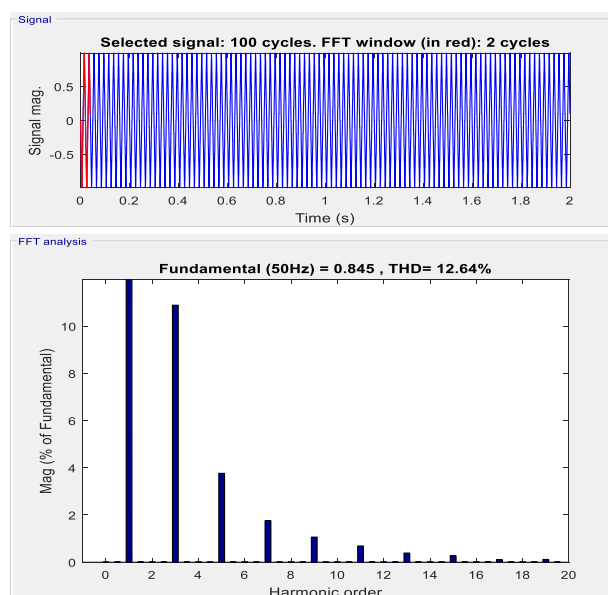


Figure 4: THD of the Proposed 21 level Inverter

4.2 Hardware Result

. The output obtained as a result of hardware setup is shown in figure 5.

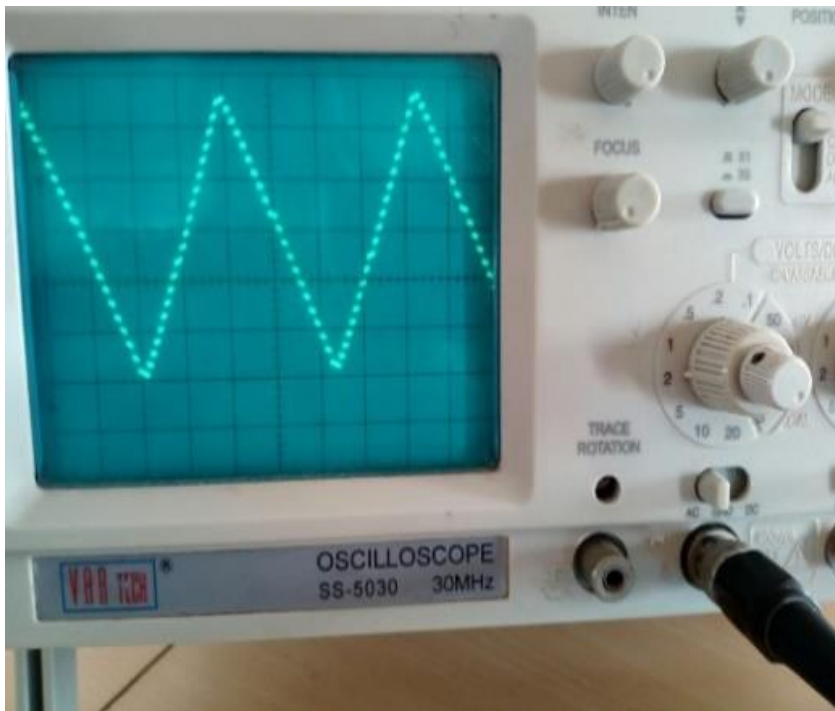


Figure 5: Output voltage of the Proposed 21 level Inverter in the experimental setup

5 Conclusions

This paper introduces a new MLI topology based on conventional asymmetric cascaded H-bridge inverter. Asymmetric DC sources configuration is utilized in order to maximize number of output voltage levels. DC sources are sized and interconnected in order to allow the proposed topology to produce both negative and positive half cycles. Thus, this eliminates the need for conventional polarity changer H-bridge. And also, instead of using 40 switches, the number of switches are reduced to 12 so that the switching losses are getting reduced and the cost required for the devices becomes less. In addition to that the THD is reduced to a reasonable value by using selective harmonic elimination (SHE) technique. Harmonic analysis is carried out using MATLAB/SIMULINK software. The scheme has successfully been implemented and the result is also verified through the hardware arrangement.

References

- [1] Dr. Asha Gaikwad, Pallavi Appaso Arbune (2016). Study of Cascaded H-Bridge Multilevel Inverter. In: International Conference on Automatic Control and Dynamic Optimization Techniques (ICACDOT).
- [2] Mohammad Ahmad and B.H. Khan, Senior Member, IEEE (2012). New Approaches for harmonic reduction in solar inverters.
- [3] P Palanivel, SS Dash. Analysis of THD and output voltage performance for CMLI using carrier PWM. IET Power Electronics. 2011.
- [4] R. H. Baker and L. H. Bannister, "Electric power converter," U.S. Patent 3 867 643, Feb. 1975.
- [5] Y. Khersonsky, "Step switched PWM sine generator," U.S. Patent 06 556 461, Apr. 2003.

- [6] E. Babaei, M. T. Haque, and S. H. Hosseini, "A novel structure for multilevel converters," in Proc. ICEMS, vol. II, pp. 1278–1283, 2005.
- [7] A. Nabae, I. Takahashi, and H. Akagi, "A new neutral-point clamped PWM inverter," IEEE Trans. Ind. Appl., vol. IA-17, no. 5, pp. 518–523, Sep./Oct. 1981.
- [8] T. A. Meynard and H. Foch, "Multi-level conversion: High voltage choppers and voltage-source inverters," in Proc. IEEE PESC, pp. 397–403, 1992.
- [9] S. Ogasawara, J. Takagaki, H. Akagi, and A. Nabe, "A novel control scheme of a parallel current-controlled PWM inverter," IEEE Trans. Ind. Appl., vol. 28, no. 5, pp. 1023–1030, Sep./Oct. 1992.
- [10] T. Kawabata, Y. Kawabata, and K. Nishiyama, "New configuration of high-power inverter drives," in Proc. ISIE, vol. 2, pp. 850–855, 1996.
- [11] M. R. Baiju, K. Gopakumar, K. K. Mohapatra, V. T. Somasekhar, and L. Umanand, "A high resolution multilevel voltage space phasor generation for an open-end winding induction motor drive," Eur. Power Electron. Drive J., vol. 13, no. 4, pp. 29–37, Sep.–Nov. 2003.
- [12] M. Manjrekar, P. K. Steimer, and T. Lipo, "Hybrid multilevel power conversion system: A competitive solution for high-power applications," IEEE Trans. Ind. Appl., vol. 36, no. 3, pp. 834–841, May/Jun. 2000.
- [13] Z. Du, L. M. Tolbert, J. N. Chiasson, and B. Ozpineci, "A cascade multilevel inverter using a single dc power source," in Proc. IEEE APEC, pp. 426–430, 2006.
- [14] E. Babaei, S. H. Hosseini, G. B. Gharehpetian, M. T. Haque, and M. Sabahi, "Reduction of dc voltage sources and switches in asymmetrical multilevel converters using a novel topology," Elsevier J. Electr. Power Syst. Res., vol. 77, no. 8, pp. 1073–1085, Jun. 2007.
- [15] M. T. Haque, "Series sub-multilevel voltage source inverters (MLVSI) as a high quality MLVSI," in Proc. SPEEDAM, pp. F1B-1–F1B-4, 2004.
- [16] Pravin T. Jadhav Swapnil Y. Gadgune, and Lohit R. Chaudhary "Implementation of Shunt APF based on Diode Clamped and Cascaded H-Bridge Multilevel Inverter" IEEE 2015.
- [17] K.J.Mckenzie, onverter using resultant theory, Symmetric polynomials, and Power Sums "; Master thesis, 2004.
- [18] A. Annai Theresa, Sinu Cleetus, A. Abinesh, C. Thamizharasan and S. Shanmuganatham, "21 Level Staircase Sine Wave Inverter with Reduced Switches And THD" Journal of Emerging Technologies and Innovative Research (JETIR) Volume 7, Issue 3, March 2020.
- [19] Kamaldeep, J. Kumar, Performance analysis of H-Bridge multilevel inverter using Selective Harmonic Elimination and Nearest Level Control technique, in: 2015 International Conference on Electrical, Electronics, Signals, Communication and Optimization (EESCO), pp. 1–5, 2015.
- [20] L.M. Tolbert, F.Z. Peng, T.G. Habetler, Multilevel converters for large electric drives, IEEE Trans. Ind. 36–44, Appl. 35 (1) (1999).

Optimizing Combined Emission Economic Dispatch for Solar Integrated Power Systems

Richard Pravin A¹

¹Assistant Professor,
St. Anne's College of Engineering and Technology.

Abstract

The dispatch of power at minimum operational cost of thermal energy sources has been a significant part of research since decades. Recently, with increasing interests in renewable energy resources, the optimal economic dispatch has become a challenging issue. This paper presents combined emission economic dispatch model for a solar photo voltaic integrated power system with multiple solar and thermal generating plants. We formulate mixed integer binary programming problem subject to various practical constraints. A decomposition framework is proposed where the original problem is split into two sub-problems. Particle swarm optimization, Newton–Raphson method, and binary integer programming techniques are exploited to find the joint optimization solution. The proposed model is tested on the IEEE 30 bus system. The simulation results demonstrate the effectiveness of the proposed model.

Keywords: *Economic dispatch, power systems, photo voltaic, PSO*

1.Introduction

The distribution system is a largest portion of network in electrical power system. It can be defined as the part of power system this distributes power to various customers in ready-to-use form at their place of consumption. Hence, utilities have to ensure reliable and efficient cost effective service, while providing service voltages and power quality within the specified range. This is a very challenging task. Utilities, traditionally determine future system developments based on a top down approach, all over the world are competing for improvement in service to consumers.

Mostly the power utilities emphasize on power generation and transmission system to reduce the overall cost of the system. Many of the distribution systems experience uncontrolled expansion, minimum monitoring, under/over utilization and development in unplanned manner.

The distribution networks typically located at every nook and corner to provide the electric power supply for all the individual customers. Obviously the distribution system is the most suitable system to meet the individual consumer requirements such as the electricity demand, reliability, power quality etc. As an example, certain load centers need high level of reliability and different load centers have different demand growth etc. Therefore the process of optimal planning shall begin from distribution system.

In this process work out the system needs, i.e., identifying the network reinforcements/expansions, additional substations, augmentation of the existing substations and expansion of transmission line to meet the need of substation, in the upward direction to achieve the final objective and techno-economic solution. Nowadays advanced computer aided techniques and analysis tools available to carry out the optimal planning process. The power engineers need to overcome some of the challenges while applying the techniques.

2. Distribution Network reconfiguration

Optimal planning and design of the distribution systems involves network reconfiguration for distribution loss minimization, load balancing under normal operating conditions and fast service restoration

to minimize the zones without power under failure conditions. Most of the distribution networks are configured radially which simplifies over-current protection of the feeders.

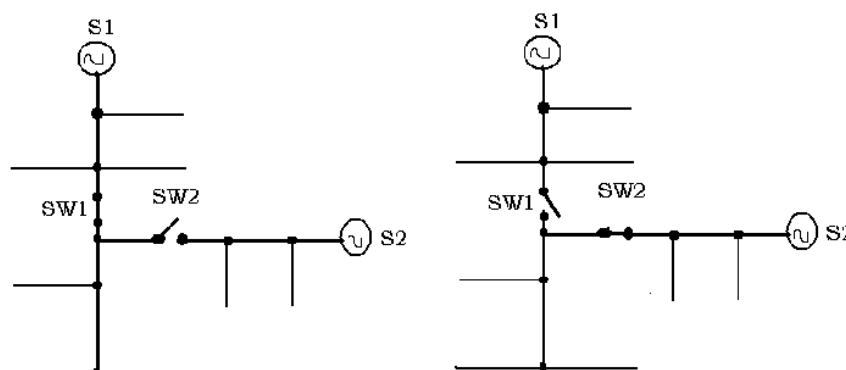
The manual or automatic switching operations are performed to vary the configurations. As the operating conditions change, the purpose of network reconfiguration is: (i) to minimize the system power loss and (ii) to balance the loads in the network. Reconfiguration problem of large scale distribution systems is essentially a combinatorial optimization problem since various operational constraints are to be considered. Therefore it is difficult to obtain a true and fast solution for a real system.

Two types of switches, normally open switches (tie switches) and normally closed switches (sectionalizing switches), are used in primary distribution systems for protection and configuration management. The distribution network reconfiguration is obtained by closing tie (normally open) switches and opening sectionalizing (normally closed) switches in the network. The structure of the distribution network is maintained radial and all loads are energized while switching operations are performed. Obviously, the possibilities of network reconfiguration are greater when large number of switches is present.

The network reconfiguration is illustrated through a simple system as shown in figure 1.1. Consider two switches, SW1 (sectionalized) and SW2 (tie) and two substations, S1 and S2 as shown in figure 1.1(a). A reconfiguration to reduce the system losses can be obtained by altering the system topology as shown in figure 1.1(b). It is recommended to open SW1 and close SW2 for the reconfiguration of the system. The effect of constraints on reconfiguration must be thoroughly studied before changing the basic configuration. One of the major constraints to be considered is that the network must have radial structure.

Some of the general optimization algorithms fail in satisfying this radial constraint directly. Particularly a meshed network containing all switches closed will have less loss, but the radial constraint is violated.

Figure 1.1 Illustration of reconfiguration
(a) Initial configuration (b) Recommended configuration



A method, by not closing any switches forming a loop, that builds the network from scratch can easily enforce the radial constraint. The line current carrying capacity and voltage limits are the other major constraints in reconfiguration. However, these constraints are closely related because a line carrying current close to its thermal capacity will also have a larger resistive voltage drop. Solutions, heuristically, with a good voltage profile have low losses and the line currents within limits. Either the voltage or the current constraint may be reached first in a particular situation. The current constraints can be alleviated by switching or re-conductoring the feeder in the longer term or installing a larger substation transformer. The voltage constraints can be alleviated by switching or installing capacitor banks or by adjusting voltage regulators.

Energy policies are major arguments of the international politics. The energy has a vital role for all countries and the main goal is reaching cost effective and sustainable energy sources. Since conventional energy sources are limited and energy saving is the most cost effective energy source, energy efficiency is regarded as a major topic for many countries. Distribution system losses constitute a significant part in total electrical losses. Network reconfiguration is one of the fundamental methods of loss reduction in distribution systems.

Electrical distribution systems aim a single direction power flow from the source to the load to minimize operation difficulty and costs. However, designing the system as a mesh offers the possibility to achieve alternative network configurations in order to maintain the continuity of supply under failures. As a result the conventional distribution systems are constructed as a weak mesh with closed rings but operated radially.

Radial operation constraint makes it compulsory to open the distribution feeders connected to multiple sources or to a single source with a ring configuration from a suitable switching location. Meshed networks offer many alternative configuration options and it is possible to reconfigure the network by interchanging the switching locations. Different configurations alternate the existing feeder lengths, voltage and current rates, loading levels and amount of losses. Accurate selection of switching locations would reduce losses, increase the lifetime of equipment and improve system reliability by balancing the system loading.

Distribution system configurations are usually chosen during planning of the system according to normal operation conditions and average loading levels. Nevertheless the load flows are not constant and they vary with different factors including changing demand, failures, maintenance operations or additional loads and sources connecting to the network.

In a very fast growing city such as Istanbul, the electricity demand increase and network growth rate is also high. As a result it is not quite probable for the initial network configuration to maintain the optimum system loading for a long time under such conditions.

Locations of tie switches in a network providing minimum loss configuration can be determined by optimum distribution system reconfiguration methods. Most of the optimum reconfiguration methods are based on heuristics. Consecutively opening switches from meshed network and branch exchange methods are used in many different reconfiguration studies. Recently probabilistic methods including genetic algorithms, particle swarm optimization, ant colony optimization and artificial bee colony are also applied to optimum reconfiguration algorithms. Studies evaluating the use of heuristic methods on distribution system reconfiguration are also presented in recent years.

The objective function of reconfiguration optimization is defined as minimization of the resistive losses in most of the previous studies. However the optimization function can be defined as maximization of reliability, balancing feeder lengths and loadings, minimization of voltage drop or overloads and integration of distributed generation.

To determine a new network configuration on the chosen network section from Istanbul, to reduce the system losses by evaluating the fitness of present configuration and simulating alternative switching operations.

As a result, the chosen network section is modelled and a reconfiguration algorithm is generated on Mat lab, based on opening switches consecutively according to optimum flow pattern.

3. Problem Formulation

The reconfiguration method utilized in this study to reduce resistive losses of the distribution system starts with analyzing the load flow of the meshed system by closing all the switches in the network. According to the Kirchoff's laws, current favors to flow through the path with minimum losses. Whereas the system is operated as a meshed network, the resistive losses would be minimum and opening a line carrying high amount of current would force the current to flow through paths with higher losses.

With the acceptance of opening the minimum current carrying switch would interfere the optimum flow least, the increase in losses by opening the switches would be minimized. This switch opening step is repeated until the network is radial in order to achieve a low loss configuration.

The method uses a meshed network with all switches closed in the beginning of the reconfiguration process, thus the resulting configuration would be independent of the initial state of the network. However all the switch selections of network reconfiguration methods have impact on selection of other switches, due to their influence on the load flows. Therefore the sequential switching method used in this study would not guarantee a global optimum solution to the minimum loss network reconfiguration problem.

Ensuring radiality is one of the main constraints and challenges of distribution system reconfiguration. In order to achieve radial configuration there has to be only one electrical path from any given point of the network to another. In graph theory a connected graph without any loops is defined as a tree. A graph can be a tree if the number of edges, e is one less than the number of vertices, v .

The edges and vertices can be defined as graphical equivalents of nodes and branches of a network. As a result, the number of connected lines, n_{line} has to be one less than the number of nodes in a network to have a radial configuration.

The number of edges e given by

$$e = v - 1 \quad (1)$$

n_{line} is number of lines given by

$$n_{line} = n_{branch} - 1 \quad (2)$$

where v, n_{node} are numbers of vertices and nodes respectively.

The number of tie switches need to be opened can be calculated according to (3.7). During switching, radially of the network is checked by comparing the number of open switches with the number of tie switches.

n_{Tsw} is number of tie switches that has to be opened, represented by

$$n_{Tsw} = n_{branch} - n_{bus} - 1 \quad (3)$$

where n_{branch} and n_{bus} represent the number of branches and buses in the network respectively.

In order to keep all the loads supplied by the source, only one switch can be opened on the same feeder. Only operable switches are evaluated during reconfiguration. When a switch is chosen as tie switch, rest of the switches on the same feeder are defined as non operable switches, and added to a blacklist. Thus the next switch is certainly chosen from other feeders. When entire tie switches are chosen, none of the remaining switches will be operable and radial network will be obtained. Flowchart of the optimization algorithm can be seen in figure 3.1.

Group Leader Optimization Technique

Inspired by leaders in social groups and cooperative co evolutionary algorithms, we have designed a new global optimization algorithm in which there are separate groups and leaders for each group. Initially forming groups does not require members to have some similar characteristics. Instead, it is based on random selection. While CCGA and other similar algorithms decompose the solution space, and each group represents a solution for a part of the problem, in our algorithm each group tries to find a global solution by being under the influence of the group leaders which are the closest members of the groups to local or global minima. The leaders are those whose fitness values are the best in their groups, and a leader can lose its position after an iteration if another member in the same group then has a better fitness value. Since in social networks, leaders have effects on their peers, thusly the algorithm uses the some portion of leaders while generating new group members. Hence, a leader, (in most cases a local optimum) dominates all other solution candidates (group members) surrounding it, and the members of a group come closer and resemble their leader more in each iteration. In this way, the algorithm is able to search the solution space between a leader and its group members thoroughly, and so is able to search the area for a local or a global optimum (or an approximation of it) in a fast way. After a certain number of evolutions, it is obvious that the members may become too similar to their leaders. To maintain the diversity of the group, for each group, we transfer some variables from different groups by choosing them randomly. In addition to providing diversity, this one-way crossover helps a group to jump out of local minima and search new solution spaces.

3.3.2 Algorithm steps

In this section, algorithm steps are described with their reasons in sequence and are shown in Figures 1.

Step 1: Generate p number of population for each group randomly

The total population for each group is p, hence, the whole population is $n * p$ where n is the number of groups. Creation of the groups and the members are totally random.

Step 2: Calculate fitness values for all members in all groups

All solution candidates, group members, are evaluated in the optimization problem and their fitness values are assigned.

Step 3: Determine the leaders for each group:

Each group has one leader and the leaders are ones whose fitness values are the best within their respective groups.

Step 4: Mutation and recombination:

Create new member by using the old one, its group leader, and a random element. If the new member has better fitness value than the old one, then replace the old one with the new one. Otherwise, keep the old member. For numerical problems, the expression simply reads;

$$\text{new} = (r1 * \text{old}) + (r2 * \text{leader}) + (r3 * \text{random})$$

In Equation (1), r1, r2, and r3 are the rates determining the portions of old (current) member, leader, and random while generating the new population. Although in this paper, r1, r2, and r3 will always sum to 1, it is not a requirement for the algorithm in general. For instance, let the current element be 0.9, the leader 1.8, and the generated random element 1.5, and suppose $r1=0.8$, $r2=0.19$, and $r3=0.01$. In this case, the new element is equal to 1.077. Then fitness values of the old and the new element are checked. If fitness (1.077) is better than the fitness (0.9), then the old element is replaced by the new one.

The expression in the inner loop is the general formula of recombination and mutation for numerical optimization problems. Depending on the value of r1 an element keeps its original characteristics, and depending on the value of r2 it becomes more like its leader during iterations. Thus, in some cases, choosing the right values for r1, r2 and r3 may play an important role for the algorithm to get better results during the optimization. However, choosing these parameters by obeying the property, $r3, r2 \leq 0.5, r1$ allows one to perform a thorough search of a solution space. Hence, this minimizes the effect of these parameters on the results. The main benefit of this evolution is that the algorithm becomes able to search the solution space surrounding the leaders (which are possibly local or global minima). Therefore, this allows the population to converge upon global minima in a very fast way. The members of the groups are not subjected to a local minimization; however, an implementation of Lamarckian concepts of evolution for the local minimization [28] gives a more stable and efficient algorithm. It is also important to note that Equation (1) looks similar to the updating equation of PSO [17]. The difference is that a member is always at its best position and the best position of a member is not saved in a parameter as is done in PSO, hence there are no information about the member's (or the particles) previous positions (values).

Step 5: Parameter transfer from other groups (One way crossover)

Choose random members starting from the first group, and then transfer some parameters by choosing another random member from another group. If this transfer makes a member have a better fitness value, then change the member, otherwise keep the original form. This process is shown in Figure 2 via pseudo code. This one-way crossover has similarities with the difference vector of Differential Evolution [29]. The difference is that the transfer operation is between the members which are in different groups. In this step, it is important to determine correct transfer rate, otherwise all populations may quickly become similar. In our experiments, transfer operation rate was taken t times [t is a random number between 1 and half of the number of total parameters (variables) plus one ($1 + t * (\lfloor \text{parameter}/2 \rfloor + 1)$)] for each group (not for each member). And each time, only one parameter is transferred.

Figure 1. Step 5 of the algorithm: one way crossover: prth variable of an element, member of the i th group, is replaced by path variable of the k th member of the xth group. The same operation is repeated t times for each

group (maximum – half of the number of variables plus one – times for each group). The arrow at the bottom of the figure shows the direction of transfer.

Step 6: Repeat step 3–step 5 number of given iteration times

Since each group looks for the solution in mostly different spaces, Group Leaders Optimization Algorithm (GLOA) is able to search different solution spaces simultaneously. We did not place any constraint for groups to only search in subspaces, so a few groups may also search the same places. However, this does not make them redundant as they allow GLOA to find different local or global minima within the same subspace. Since each group has a leader and the leaders direct the other members of the group in order to search the area between the leader and the members of the group, it is able to search for a good solution (around the leader of the group). In addition to increasing the level of diversity of the groups, transferring some parameters (crossover) between groups allows the algorithm to direct the members of a group to search different spaces. Therefore, if a group has found some parameters correctly or very close to correct, then transferring parameters between groups allows other groups to get these parameters and find their solutions faster. Since only parameters are transferred which make the member have better fitness value, the spreading of a member who has a bad fitness value is avoided. In terms of optimization problems requiring highly diverse populations, choosing to do crossover and mutation-recombination steps without comparing fitness values may be wise and may improve the effectiveness of the algorithm.

Test System

The network used in this study is a section from 34.5kV distribution system of Istanbul. The network consists of 95 buses, 107 branches and 58 switches connected with 7.2km of 150mm² three core, 38.5km of 240mm² three core and 15km of 240mm² single core, armored copper cables with XLPE insulation. Total length of the network is 60.7km with 86 distribution transformers connected to the network.

Distribution transformers are modeled as medium voltage loads with 97.6MVA apparent power in total. The power factor is taken as 0.85, at the reactive power penalty limit to be conservative. The minor unbalances between phases are neglected for calculation simplicity.

The resulting power losses from actual configuration, meshed network, and the configuration achieved by the reconfiguration algorithm are analyzed in this section.

The meshed configuration of the network with all switches closed has total resistive loss of 94kW. The actual configuration of the network is with switches s1, s8, s10, s19, s28, s29, s36, s38, s39, s40, s49, s54 and s58 open and the resistive losses are calculated as 169kW.

The configuration achieved by the reconfiguration algorithm has switches s3, s7, s10, s18, s20, s30, s35, s38, s39, s40, s48, s51 and s55 open resulting total resistive losses of 124kW. The mentioned configurations, open switches and resistive losses are shown in Table 3.1.

4. Results and Discussion

The proposed method was tested on IEEE 33-bus radial distribution systems and results have been obtained to evaluate its effectiveness. For all these systems, the substation voltage is considered as 1.0 p.u. and all the tie and sectionalizing switches are considered as candidate switches for reconfiguration problem.

The algorithm of this method was programmed in MATLAB R2013a environment and run on intel i3 - 3rd Generation , 2.4 GHz personal computer with 4GB RAM.

The 33–bus, 12.66 kV, radial distribution system consists of five tie lines and 32 sectionalize switches. The normally open switches are 33, 34, 35, 36 and 37 and the normally closed switches are 1 to 32. The total real and reactive power loads on the system are 3715 kW and 2300 KVA_r. The initial power loss this system is 208.4592 kW. The lowest bus bar voltage limit is 0.91075 p.u which occurs at node 18.

Simulations are carried from 10 to 100 iterations and all are converged to same solution after 8 iterations. The CPU time used to get optimal solution is 49.7 seconds. The optimal configuration obtained by the proposed algorithm is 7,9,14,32 and 37 which has a real power loss of 138.92 kW. This amounts to a reduction of 33.35 % in total power loss. The minimum node voltage of the system after reconfiguration improved to 0.94234 p.u (node 33). The results of the proposed algorithm are compared with Genetic Algorithms is presented in Table 6.1. From

the results, it is observed that the optimal power loss obtained by the proposed method is 1.68 kW less than GA. The CPU time used by the proposed method is 49.7 sec only but it is 55.2 in case of GA methods.

| Item | Tie Switches | Power Loss (kW) | Min.Node Voltage (p.u) | Power Loss Reduction (%) | CPU Time (s) |
|------------------------|------------------|-----------------|------------------------|--------------------------|--------------|
| Original Configuration | 33,34,35,36, 37 | 208.4592 | 0.91075 (Node 18) | -- | -- |
| GA | 33,9,34,28 36 | 140.6 | 0.9371 (Node 33) | 30.6 | 55.2 |
| Proposed System | 7,9,14,32,37 | 138.9275 | 0.94234 (Node 33) | 33.35 | 49.7 |

Table 6.1 Simulation Result of 33-Bus System

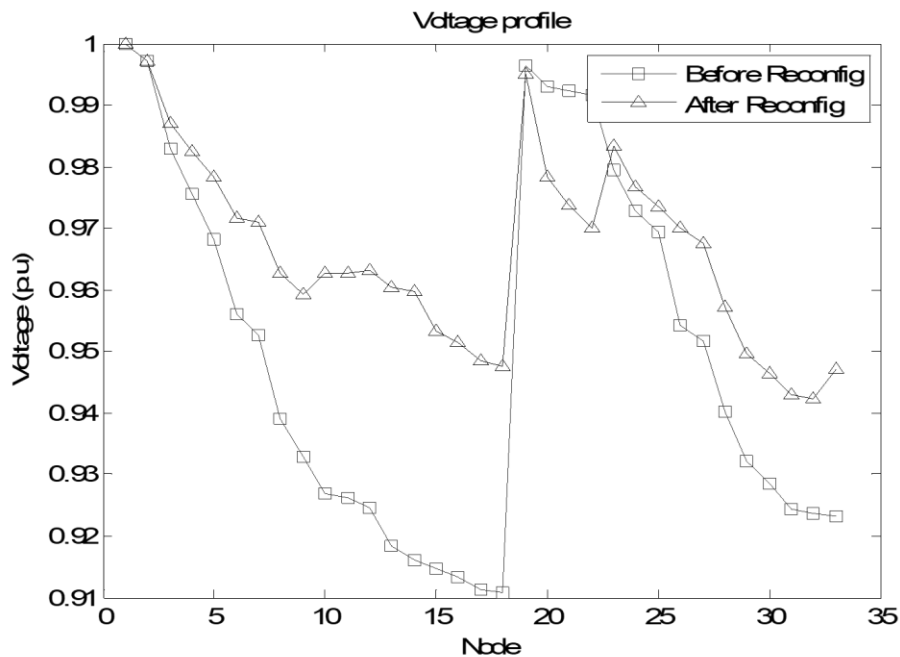


Figure 6.1 Convergence characteristics of GLO for 33 bus radial distribution system

5. Conclusion

In this paper, a new population based group leader optimization (GLO) was utilized to solve the network reconfiguration problem in a radial distribution system. The main objectives considered in the present problem

are minimization of real power loss and voltage profile improvement subject to the radial network structure in which all loads must be energized. Simulations are carried on IEEE - 33 bus systems and results are compared with the other populations based method such as GA. The results obtained by the proposed method out perform the other methods in terms of quality of the solution and computation efficiency.

The main advantage of GLO algorithm is that it does not require external parameters such as cross over rate and mutation rate etc., as in case of genetic algorithms, differential evolution and other evolutionary algorithms and these are hard to determine in prior. The other advantage is that the global search ability in the algorithm is implemented by introducing neighborhood source production mechanism which is a similar to mutation process. This project illustrates the capability of group leader optimization algorithm in solving network reconfiguration problem.

References

- [1]. S. Sehgal, A. Swarnkar, N. Gupta, and K. R. Niazi, "Reconfiguration of distribution network for loss reduction at different load schemes," in *Proc. IEEE Students' Conference on Electrical, Electronics and Computer Science SCEECs*, Mar. 2012, pp. 1-4.
- [2]. H. L. Willis, H. Tram, M. V. Engel, and L. Farley, "Optimization applications to power distribution," *IEEE Computer Applications in Power*, vol. 8, no. 4, pp. 12-17, Oct. 1995.
- [3]. T. E. McDermott, I. Drezga, and R. P. Broadwater, "A heuristic nonlinear constructive method for distribution system reconfiguration," *IEEE Trans. Power Syst.*, vol. 14, no. 2, pp. 478- 483, May 1999.
- [4]. H. R. Esmaeilian, R. Fadaeinedjad, and S. M. Attari, "Distribution network reconfiguration to reduce losses and enhance reliability using binary gravitational search algorithm," in *Proc. 22nd International Conference on Electricity Distribution*, 2013.
- [5]. P. Zhang, L. Wen Yuan, and W. Shouxiang, "Reliability-Oriented distribution network reconfiguration considering uncertainties of data by interval analysis," *International Journal of Electrical Power and Energy Systems*, vol. 34, no. 1, pp. 138-144, Jan. 2012.
- [6]. D. Shirmohammadi and H. W. Hong, "Reconfiguration of electric distribution for resistive line loss reduction," *IEEE Trans. Power Del.*, vol. 4, no. 2, pp. 1492-1498, Apr. 1989.
- [7]. S. Civanlar, J. J. Grainger, H. Yin, and S. S. H. Lee, "Distribution feeder reconfiguration for loss reduction," *IEEE Trans. Power Del.*, vol. 3, no. 3, pp. 1217-1223, Jul. 1988.
- [8]. S. K. Goswami and S. K. Basu, "A new algorithm for the reconfiguration of distribution feeders for loss minimization," *IEEE Trans. Power Del.*, vol. 7, no. 3, pp. 1484-1491, Jul. 1992.
- [9]. R. J. Sarfi, M. Salama, and A. Chikhani, "A survey of the state of the art in distribution system reconfiguration for system loss reduction," *Electric Power Systems Research*, vol. 31, pp. 61-70, 1994.
- [10]. L. F. Ochoa, R. M. Ciric, A. Padilha-Feltrin, and G. P. Harrison, "Evaluation of distribution system losses due to load unbalance," in *Power Systems Computation Conference (PSCC)*, Liege, Belgium, 2005, pp. 1-4.
- [11]. S. P. Singh, G. S. Raju, G. K. Rao, and M. Afsari, "A heuristic method for feeder reconfiguration and service restoration in distribution networks," *International Journal of Electrical Power & Energy Systems*, vol. 31, pp. 309-314, 2009.
- [12]. K. L. Butler, N. Sarma, and V. Ragendra Prasad, "Network reconfiguration for service restoration in shipboard power distribution systems," *Power Systems, IEEE Transactions on*, vol. 16, pp. 653-661, 2001.
- [13]. Hai shen, Yunlong Zhu, Wenping Zou, Zhu Zhu, "Group Search Optimizer Algorithm for constrained Optimization," *Computer Science for Environmental Engineering & Eco Information*, vol. 159, pp. 48-45.
- [14]. D. Das, "A fuzzy multi-objective approach for network reconfiguration of distribution systems," *IEEE Trans. Power Del.*, vol. 21, no. 1, pp. 202-209, Jan. 2006.
- [15]. C. T. Su and C. S. Lee, "Network reconfiguration of distribution systems using improved mixed-integer hybrid differential evolution," *IEEE Trans. on Power Delivery*, Vol. 18, No. 3, July 2003.
- [16]. Y. C. Huang, "Enhanced genetic algorithm-based fuzzy multi-objective approach to distribution network reconfiguration," *Proc. Inst. Elect. Eng.*, vol. 149, no. 5, pp. 615-620, 2002.
- [17]. I. Z. Zhu, "Optimal reconfiguration of electrical distribution network using the refined genetic algorithm," *Elect. Power Syst. Res.*, vol. 62, pp. 37-42, 2002.
- [17]. Y. Y. Hong and S. Y. Ho, "Determination of network configuration considering multi-objective in distribution systems using genetic algorithms," *IEEE Trans. Power Syst.*, vol. 20, no. 2, pp. 1062-1069, May 2005.

- [18]. [K. Prasad, R. Ranjan, N. C. Sahoo, and A. Chaturvedi, "Optimal reconfiguration of radial distribution systems using a fuzzy mutated genetic algorithm," *IEEE Trans. Power Del.*, vol. 20, no. 2, pp. 1211–1213, Apr. 2005.
- [19]. J. Z. Zhu, "Optimal reconfiguration of electrical distribution network using the refined genetic algorithm," *Elect. Power Syst. Res.*, vol. 62, no. 1, pp. 37–42, May 2002.
- [20]. M. E. Baran and F. Wu, "Network reconfiguration in distribution system for loss reduction and load balancing," *IEEE Trans. Power Del.*, vol. 4, no. 2, pp. 1401–1407, Apr. 1989.
- [21]. Y. Mishima, K. Nara, T. Satoh, T. Ito, "Method for minimum-loss reconfiguration of distribution system by tabu search", *Electrical Engg. Japan*, Vol. 152, No. 2, July 2005.
- [22]. D. Zhang, Z. Fu, L. Zhang, "An improved TS algorithm for Loss minimum reconfiguration in large-scale distribution systems", *Electric Power Systems Research*, Vol. 77, pp. 685–694, 2007.

A Single Phase Bidirectional Electric Drive Reconstructed Onboard Converter for Electric Vehicles Applications

N.Rajeswari¹, A. Albert Martin Ruban², S.Nalini³

¹Assistant Professor, Department of EEE, Kings College of Engineering, Punalkulam, Pudukkottai

²Associate Professor, Department of EEE, Kings College of Engineering, Punalkulam, Pudukkottai

³PG student, Department of EEE, Kings College of Engineering, Punalkulam, Pudukkottai

Email:nalini.nathiya87@gmail.com

Abstract

In this paper, an Electric-drive-reconstructed onboard converter (EDROC) based on a switching network in the DC side is proposed. The system can utilize the existing hardware of electric vehicles and does not need extra equipment. When the EDROC connects to the power grid through the power outlet at the office or home, there is not by additional equipment (relay) on the AC side. Compare with traditional EDROC, the proposed EDROC has advantages in cost and volume. The EDROC can realize the unity power factor in the charging mode and discharges to drive the motor in the driving mode. A proof-of-concept prototype has been built to verify the charging function and driving function of the proposed EDROC.

INDEX TERMS Power conversion, electric vehicles, bidirectional converters, electric-drive-reconstructed systems.

Introduction

An electric vehicle charging station, also called EV charging station, electric recharging point, charging point, charge point, electronic charging station (ECS), and electric vehicle supply equipment (EVSE), is an element in an infrastructure that supplies electric energy for the recharging of plug-in electric vehicles including electric cars, neighbourhood electric vehicles and plug-in hybrids for charging at home or work, some electric vehicles have converters on board that can plug into a standard electrical outlet or a high-capacity appliance outlet. Others either require or can use a charging station that provides electrical conversion, monitoring, or safety functionality. These stations are also needed when traveling, and many support faster charging at higher voltages and currents than are available from residential EVSEs. Public charging stations are typically on-street facilities provided by electric utility companies or located at retail shopping station, restaurants and parking places, operated by a range of private companies, charging stations provides range of heavy duty or special connectors that conform to the variety of standards. For common DC rapid charging, multi-standard chargers equipped with two or three of the Combined Charging System (CCS), CHAdeMO, and AC fast charging has become the de facto market standard in many regions.

Related Work

With the depletion of fossil fuel, electric vehicles are gaining popularity. Owing to cleanliness and environmental protection, plug-in electric vehicle (PEV) sales will be expected to grow in the future [1]. The electrical drive system and charging system in PEV will replace the conventional drive system of the internal combustion engine (ICE) because the electric drive can achieve zero emissions [2]_[4]. Usually, the PEV is consisted of the charging system and the drive system, independently. The charging system is an important part of the electric drive, which contains two stages bi-directional converters [5], [6]. The drive system contains motor and driver circuit. The system has large size and high cost. The electric-drive-reconstructed onboard converter (EDROC) has been proposed to reduce the size and increase the power density by integrating the drive system and charging system in PEV [7]. So the converter can operation drive mode or charging mode, independently. Meanwhile, the EDROC can be classified as three types based on the number of converters [8]: the composite converter system, the double-stage converter system, and the single-stage converter system. There are multiple motors and multiple power converters in the composite converter system, and the system is often applied to the four-wheel-drive EV or a series hybrid electric vehicle [9], [10]; Composite converter system is not suitable for a single-motor EV such as PEV. Owing to only one motor is needed, the double-stage converter system and the single-stage converter system can be applied to most types of electric vehicles. The double-stage converter system is usually applied to three-phase fast charging. It has more components than the single-stage converter system, so the single-stage converter

system has advantages in terms of cost and size. Generally, the EDROC uses the motor windings as inductors in the charging mode. However, the conventional motor in PEV is the permanent magnet synchronous motor (PMSM) [11], [12], which is not conducive to reconfiguring the converter as a charger. Some specially designed motors are used as charger in [14]- [20]. The EDROC with a split-winding AC motor has been proposed in [14]-[16]. In the charging mode, the motor winding and 3 H-bridge inverters are reconfigured as two 3-phase boost converters sharing a DC bus. The AC power supply connected to the middle point of the stator winding. This converter is complicated as it must control three independent currents in the driving mode. The motor with two sets of three-phase windings is used in [17], [18]. In the driving mode, the motor work as a three-phase motor; In the charging mode, the motor work as a transformer. The other EDROCs with specially designed motors are connected AC source to the neutral point of the motor in [19], [20]. The proposed converter can be onboard without additional AC inductor. The proposed converter can directly utilize the socket power outlet at the office or home.

Proposed System

In this work, an Electric-drive-reconstructed onboard converter (EDROC) based on a fuzzy switching network in the DC side is proposed. The system can utilize the existing hardware of electric vehicles and does not need extra equipment. When the EDROC connects to the power grid through the power outlet at the office or home, there is not any additional equipment (relay) on the AC side. Compare with traditional EDROC, the proposed EDROC has advantages in cost and volume. The EDROC can realize the unity power factor in the charging mode and discharges to drive the motor in the driving mode

Topology and analysis of electric-drive-reconstructed Converter

The proposed electric-drive-reconstructed onboard converter in PEV is realized by connecting an auxiliary circuit between battery and traction hardware, as shown in figure. The auxiliary circuit and the inverter of traction hardware forma switching network to reconstruct converter. And the proposed fuzzy control method is applicable for any traction hardware with the three-phase inverter, and there is no need specially designed motor. The converter only uses a single phase power supply without additional equipment such as inductance or relay

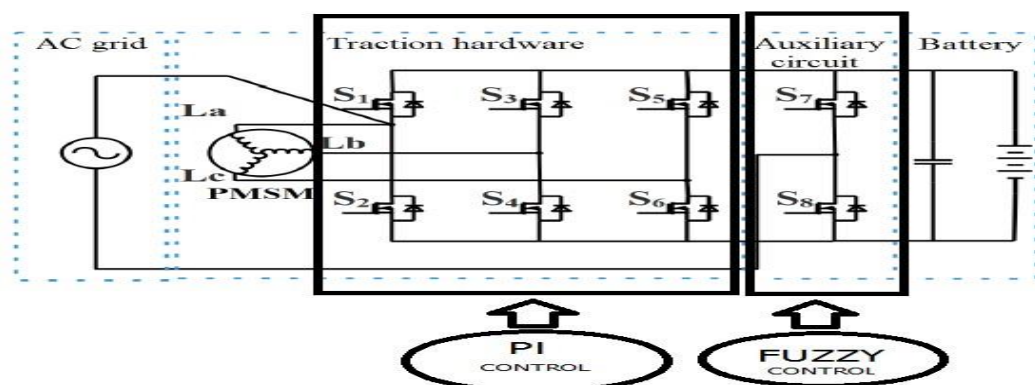


Fig1. Proposed System

AC side. The system has two working modes, which are charging mode and driving mode.

A.CHARGING MODE

During the charging mode, the switches S3-S8 are enabled. The switches S1 and S2 are disabled. The switching states are divided into eight states, as shown in figure. When the grid voltage is positive, the system work in states I - IV. When the grid voltage is negative, the system work in states V- VIII. In states I, the switch S7 is turned off, and the switch S8 is turned on, the switches S4 and S5 are turned on and switches S3 and S6 are turned off. The current flows back to the grid through switch S8, as shown in Fig 1. The state equation of the system can be written as

$$\begin{cases} L_s \frac{di_{La}^I}{dt} = \frac{2V_{in} - V_B}{3} \\ L_s \frac{di_{Lb}^I}{dt} = \frac{-V_{in} - V_B}{3} \\ L_s \frac{di_{Lc}^I}{dt} = \frac{-V_{in} + 2V_B}{3} \end{cases} \text{----- (1)}$$

Where V_{in} is input voltages of AC side; V_B is battery voltages; i_{La} , i_{Lb} , and i_{Lc} is the inductive current of the three-phase motor in state I, respectively. L_s is stator inductance. In states I, inductor L_b stores energy; the inductor L_c discharge the stored energy to the battery by the switch S5. In states II, the switches S3, S6; and S8 are turned on, and the switch S4,S5; and S7 are turned off; as shown in fig

state equation can be expressed as in states II, the inductor L_b is discharged the stored

$$\begin{cases} L_s \frac{di_{La}^{II}}{dt} = \frac{2V_{in} - V_B}{3} \\ L_s \frac{di_{Lb}^{II}}{dt} = \frac{-V_{in} + 2V_B}{3} \\ L_s \frac{di_{Lc}^{II}}{dt} = \frac{-V_{in} - V_B}{3} \end{cases} \text{----- (2)}$$

energy to the battery by the switch S3; inductor L_c stores energ

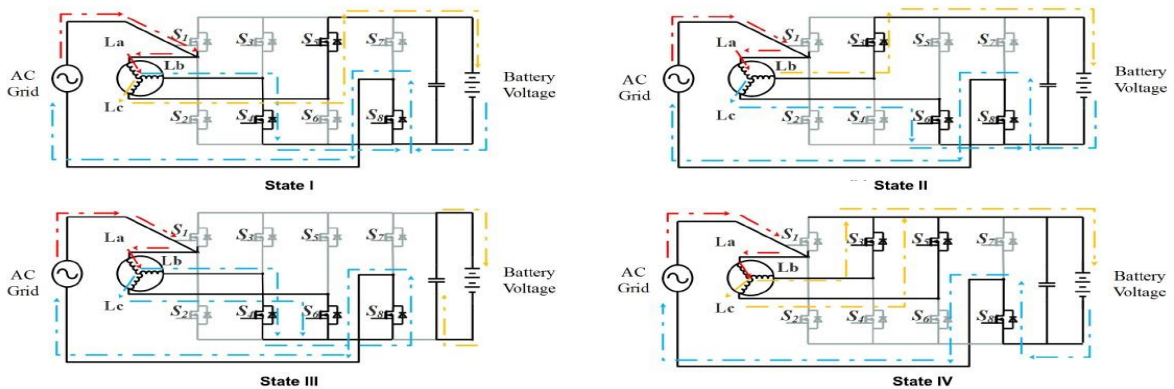


Fig 2. Switching states of the proposed EDROC in charging mode.

During the grid voltage is positive, the proposed converter has two ways of working operation, according to the duty cycle (D) of switch S4 & S6. When $0 < D < 0.5$, the circuit operation has a switching sequence of states I states III - states II - states III - states I. When $0.5 < D < 1$, the switching sequence changes to states I - states IV - states II - states IV - states I. During the grid voltage is negative, the working operation is similar that in positive grid voltage.

B.DRIVING MODE

During the driving mode, the switches S1-S6 are enabled; the switches S7 and S8 are disabled. The converter can work in eight vector states of PMSM similar traditional fuzzy control method, as shown in figure. The proposed converter can be controlled by fuzzy. The state equation and produced electromagnetic torque of PMSM in the d-q frame is expressed as follows:

$$\begin{cases} u_d = R_s i_d + P \psi_d - \omega_r \psi_q \\ u_q = R_s i_q + P \psi_q + \omega_r \psi_d \\ T_e = P (\psi_d i_q - \psi_q i_d) \end{cases} \text{----- (3)}$$

Where R_s is the stator resistance; i_d and i_q are d-axes stator currents and q-axes stator currents respectively; d and q are the permanent magnet flux linkage in d-axes and q-axes, respectively.

IV. SIMULATION RESULTS

MATLAB (Matrix Laboratory) is a multi-paradigm numerical computing environment and proprietary programming language developed by Math Works. MATLAB allows matrix manipulations, plotting of functions and data, implementation of algorithms, creation user. The MATLAB model simulated to verify the charging function and driving function of the proposed EDROC. The proposed EDROC has a good suppression effect on the ripple of the input current.

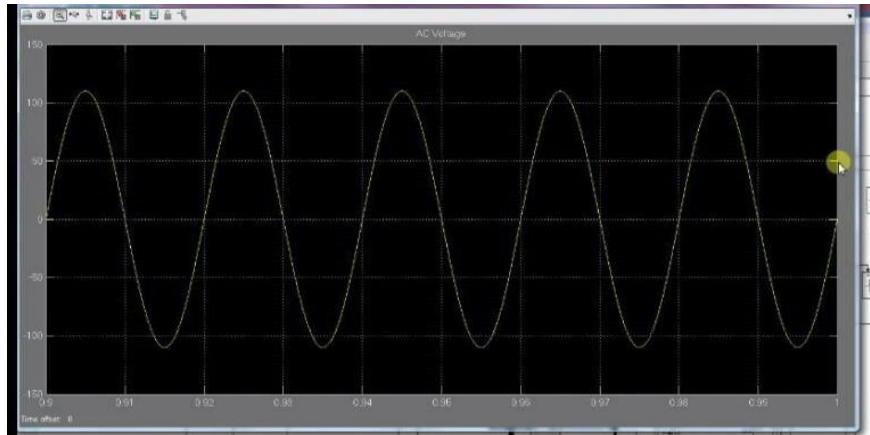


Fig3.Input AC waveform

The following figure4 shows the simulations result of battery voltage waveform. The voltage charging is a widely used charging method involving constant voltage between the battery poles. The starter battery uses constant voltage charging when the vehicle is running.

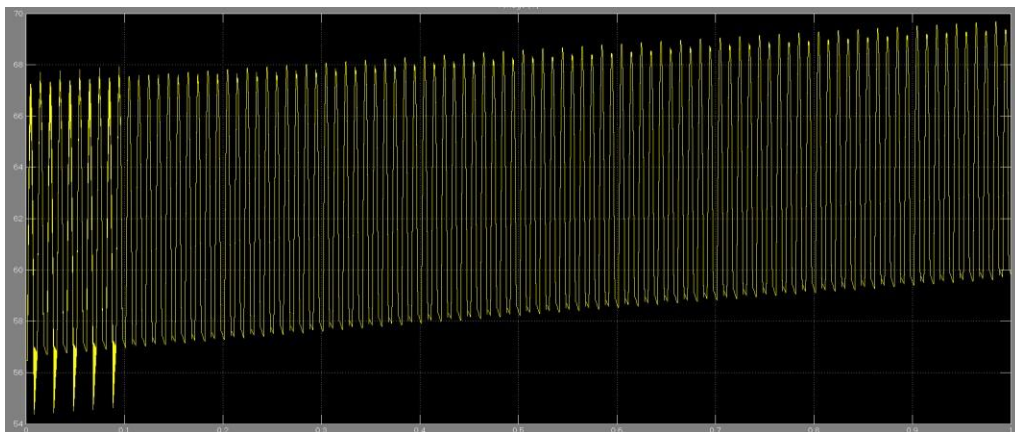


Fig 4 Battery voltage

If specified voltage constant value is appropriate, it can ensure that the battery is fully charged, while also minimizing gas and water loss. Standard power lead plugged into normal outlet. Charger in vehicle converts AC to DC and controls battery charging

The following figure 5 shows the simulations result of motor speed. The significant even after the completion of the transient part of the required feed forward contribution to make the vehicle follow the reference understeer characteristic, different from the one of the baseline vehicle.

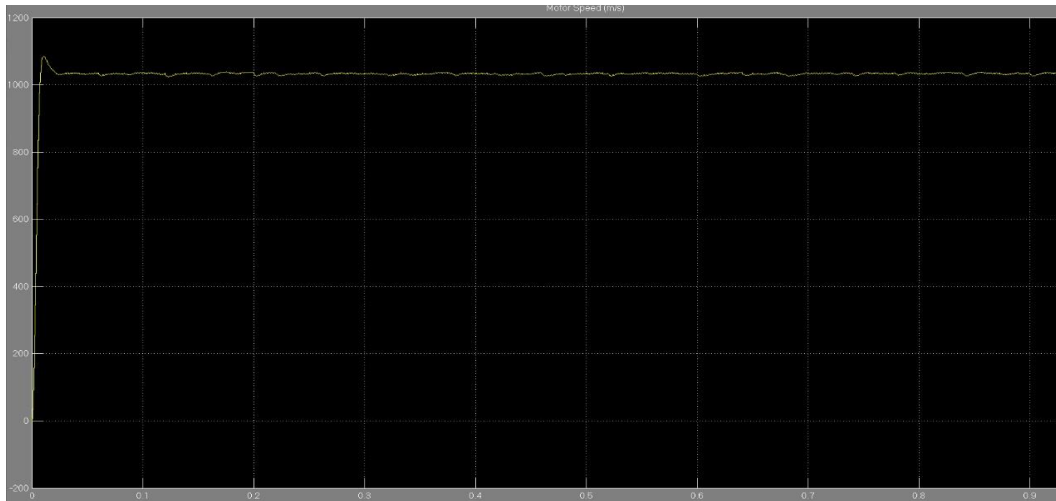


Fig 5 Motor speed

In general, for same steering wheel angle and vehicle velocity, the vehicle in sport mode, driving mode requires more input power than the vehicle in normal mode, because of the higher lateral acceleration values, the results were obtained from a sequence of sinusoidal tests with an amplitude.



Fig 6 Controlling pulses

If we switch the power on and off quickly enough, the motor will run at some speed part way between zero and full speed. This is exactly what a PWM controller does it switches the motor on in a series of pulses. To control the motor speed it varies (modulates) the width of the pulses hence Pulse Width Modulation. As the figure shows the simulations result of PWM

V.CONCLUSION

In the paper, a fuzzy and PI controlled Electric-Drive-Reconstructed Onboard Converter is proposed for PEVs. The proposed reconstructed converter is simple without specially designed motor or ac additional equipment. The proposed converter is modified from the three-phase motor drive converter. It only needs a set of auxiliary switches in the DC side. The proposed EDROC can be connected to the power outlet at the office or home without extra power supply equipment. The ripples were reduced by using interleaving control. The effect of ripple suppression is better than that of the traditional converter. Compared with the existing EDROCs, the proposed EDROC has some advantages include small size and low cost. The proposed EDROC is verified through workbench, the functions of motor drive and charger are realized.

REFERENCES

- [1] C. Chan, A. Bouscayrol, and K. Chen, "Electric, hybrid, and fuel-cell vehicles: Architectures and modeling," *IEEE Trans. Veh. Technol.*, vol. 59, no. 2, pp. 589_598, Feb. 2010.
- [2] S. Kumar and A. Usman, "A review of converter topologies for battery charging applications in plug-in hybrid electric vehicles," in *Proc. IEEE Ind. Appl. Soc. Annu. Meeting (IAS)*, Portland, OR, USA, Sep. 2018, pp. 1_9.
- [3] F. Berthold, A. Ravey, B. Blunier, D. Bouquain, S. Williamson, and A. Miraoui, "Design and development of a smart control strategy for plugin hybrid vehicles including vehicle-to-home functionality," *IEEE Trans. Transport. Electri_c.*, vol. 1, no. 2, pp. 168_177, Aug. 2015.
- [4] A. Rezaei, J. B. Burl, M. Rezaei, and B. Zhou, "Catch energy saving opportunity in charge-depletion mode, a real-time controller for plugin hybrid electric vehicles," *IEEE Trans. Veh. Technol.*, vol. 67, no. 11, pp. 11234_11237, Nov. 2018.
- [5] F. Ahmadi, E. Adib, and M. Azari, "Soft switching bidirectional converter for re_ex charger with minimum switches," *IEEE Trans. Ind. Electron.*, to be published.
- [6] U. Yilmaz, O. Turksoy, and A. Teke, "Intelligent control of high energy ef_cient two-stage battery charger topology for electric vehicles," *Energy*, vol. 186, Nov. 2019, Art. no. 115825.
- [7] F. Yu, W. Zhang, Y. Shen, and J. Mao, "A nine-phase permanent magnet electric-drive-reconstructed onboard charger for electric vehicle," *IEEE Trans. Energy Convers.*, vol. 33, no. 4, pp. 2091_2101, Dec. 2018.
- [8] M. Yilmaz and P. T. Krein, "Review of battery charger topologies, charging power levels, and infrastructure for plug-in electric and hybrid vehicles," *IEEE Trans. Power Electron.*, vol. 28, no. 5, pp. 2151_2169, May 2013.
- [9] S. Haghbin, K. Khan, S. Lundmark, M. Alakla, O. Carlson, M. Leksell, and O. Wallmark, "Integrated chargers for EV's and PHEV's: Examples and new solutions," in *Proc. 19th Int. Conf. Elect. Mach.-ICEM*, Sep. 2010, pp. 1_6.
- [10] M. Grenier, T. Thiringer, and M. Aghdam, "Design of on-board charger for plug-in hybrid electric vehicle," in *Proc. 5th IET Int. Conf. Power Electron., Mach. Drives (PEMD)*, 2010, pp. 1_6.
- [11] S. Morimoto, S. Ooi, Y. Inoue, and M. Sanada, "Experimental evaluation of a rare-Earth-free PMASynRM with ferrite magnets for automotive applications," *IEEE Trans. Ind. Electron.*, vol. 61, no. 10, pp. 5749_5756, Oct. 2014.
- [12] J. Nerg, M. Rilla, V. Ruuskanen, J. Pyrhonen, and S. Ruotsalainen, "Direct-driven interior magnet permanent-magnet synchronous motors for a full electric sports car," *IEEE Trans. Ind. Electron.*, vol. 61, no. 8, pp. 4286_4294, Aug. 2014.
- [13] Y. Tang, W. Ding, and A. Khaligh, "A bridgeless totem-pole interleaved PFC converter for plug-in electric vehicles," in *Proc. IEEE Appl. Power Electron. Conf. Expo. (APEC)*, Mar. 2016, pp. 440_445.
- [14] L. De Sousa, B. Silvestre, and B. Bouchez, "A combined multiphase electric drive and fast battery charger for electric vehicles," in *Proc. IEEE Vehicle Power Propuls. Conf.*, Sep. 2010, pp. 1_6.
- [15] A. Bruyère, L. De Sousa, B. Bouchez, P. Sandulescu, X. Kestelyn, and E. Semail, "A multiphase traction/fast-battery-charger drive for electric or plug-in hybrid vehicles: Solutions for control in traction mode," in *Proc. IEEE VPPC*, Sep. 2010, pp. 1_7.
- [16] S. Lacroix, E. Laboure, and M. Hilairet, "An integrated fast battery charger for electric vehicle," in *Proc. IEEE Vehicle Power Propuls. Conf.*, Sep. 2010, pp. 1_6.
- [17] S. Haghbin, S. Lundmark, M. Alakula, and O. Carlson, "An isolated highpower integrated charger in electric-vehicle applications," *IEEE Trans. Veh. Technol.*, vol. 60, no. 9, pp. 4115_4126, Nov. 2011.
- [18] S. Haghbin, S. Lundmark, M. Alakula, and O. Carlson, "Grid-connected integrated battery chargers in vehicle applications: Review and new solution," *IEEE Trans. Ind. Electron.*, vol. 60, no. 2, pp. 459_473, Feb. 2013.

Enhancing LVAD Device Performance Using BLDC Motor

V.Vasugi , M.Srividhya , G.Sasikala , V.Suganya

Abstract

Nowadays , Left Ventricular Assist Devices(LVADs) have extremely used clinically to treat heart failure patients. Even though , it has major limitations of LVAD method. Meanwhile using a Blood Shear Stress Device(BSSD),it shows experimental development in reliable and quantifiable blood pressure .In this prevail system , enlarged air-gap drive motor in Blood Shear Stress Device , vital to avoid blood shear stress and reduce the motor torque which may lead to inadequate force to drive the entire system. Spick and span overcome those liability , Brushless DC(BLDC)motor was implemented in the proposed system to get various air-gap was evaluated on the torque speed constant changes . There by the simulation was experimental by Proteus software.

Keywords: LVAD , BLDC , BSSD , Proteus.

1 Introduction

Clinically, left ventricular assist devices (LVADs) are indicated for New York Heart Association (NYHA) Class IV heart failure (HF), so they are used as both destination therapy and bridge-to-transplant devices [1-6]. With the advancement of minimally invasive cardiac interventions, focus is being placed on miniature LVADs that partially support the LV [7- 10]. Long-term LVAD use is becoming more common in clinical use; however, hemolysis, pump thrombosis, infection and bleeding still persist as major limitations of VAD technology [11-14]. To assist the development and application of blood-contacting VADs, different methods have been developed to study the quantitative relationship between total blood damage and shear-dependent parameters [15-18]. Hemocompatibility of a new device is priority key consideration for blood pump designers, and it should be learned from *in vitro* work before animal implants to prevent unnecessary animal sacrifice, lost time, and excess costs.

Since good hemocompatibility is essential for long-term LVAD implant, a blood shear stress device (BSSD) was designed to evaluate the hemocompatibility profile to the LVAD to determine high blood shear region, unwanted platelet activation and von Willebrand Factor (vWF) cleavage before testing the LVAD *in vivo*. A BSSD that can evaluate individual components of the LVADs will identify specific sources of blood trauma, enabling rapid iteration and refining of pump components. In many LVADs, the blood is exposed to high shear stresses (>100 Pa) repeatedly for short periods of time (<1 s). A controllable shear stress device with a short blood exposure time and no seals or contact bearings is required to accurately study shear stress' impact on blood trauma levels of the 2- dimensional form of the standard fluid dynamics shear stress calculation, an exposure time calculation, and the index of hemolysis (IH) prediction from Zhang [19]. The application of these formulae suggests that at 20,000 rpm, a motor stator inner diameter (ID) of 10 mm and motor rotor outer diameter (OD) of 8 mm with a length of 55 mm will have an IH of 0.02% with a 100 mL/min washout flow rate. However, the air-gap size is essential for the BLDC motor efficiency. Commercial BLDC motors normally have an air- gap of approximately 0.1-0.2 mm at such motor dimension For this reason, we propose a novel BSSD that can evaluate the hemocompatibility of each component of the LVAD.

To address blood exposure time in the BSSD, the BSSD was designed to subject blood to controllable shear stress and exposure times to mimic the flow regime of the LVAD. The BSSD (Fig.1) features an exchangeable rotor (Test Rotor and Test Stator in Fig. 1) to evaluate each individual component of the LVAD. To serve as a blood trauma testing platform the BSSD should not induce blood trauma inherently, therefore a magnetic levitation system (Axial PM and Axial Maglev Coil in Fig. 1) was proposed to replace the conventional contact bearing, and the whole system will be driven by a blushless DC (BLDC) motor. .

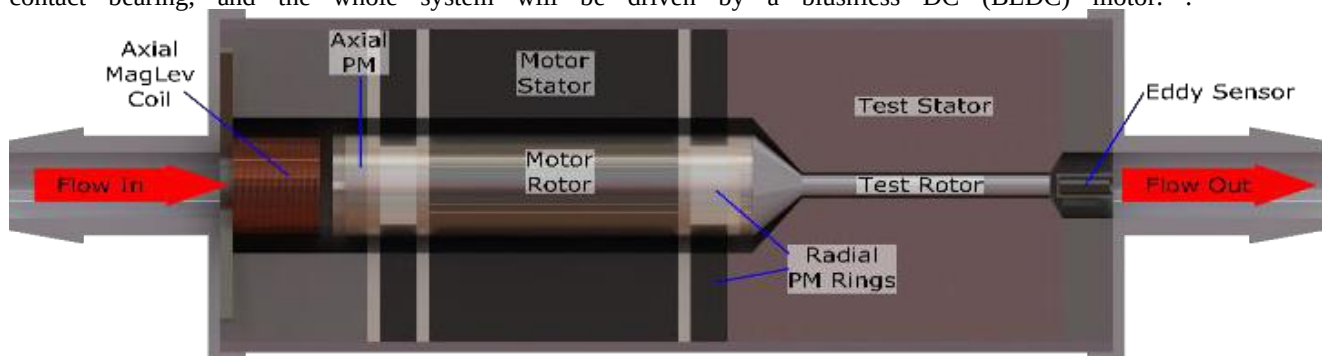


Figure 1. Blood shear test rig.

Enlarged air-gap would significantly reduce the motor torque, which may result in inadequate force to drive the entire system. Therefore, it is important to analyze and optimize the motor air-gap in the BSSD, to ensure adequate motor torque as well as acceptable range for blood exposure time and shear stress.

In this study, a BLDC motor test rig was designed to characterize the motor parameters, meanwhile, a numerical model was established based on a stock motor using FEM in numerical simulation software proteus (Inc., Burlington, MA, USA). As the data between experimental and numerical corroborate each other, the BLDC motor with different air-gap was then evaluated to effectively select the prototype that can best balance the motor efficiency and blood shear stress for the BSSD.

2 Materials & Methods

2.1 Experimental Setup for BLDC Motor Testing

Fig. 2 shows the setup for the motor test rig. The Maxon ECX22 BLDC motor (Maxon Precision Motors, Inc., Taunton, MA, USA) was driven by a pulse width modulation (PWM) amplifier (Koford Inc., S24V10A-H3) and the power source (TKD-Lambda Inc., CME350A-24). The PWM amplifier can specify the motor target speed by the reference input voltage from 0 V to 5 V as motor speed ranges from 0 min^{-1} to about 26,000 min^{-1} . The PWM amplifier fed the control current to the BLDC motor via the terminal box. The terminal box connected the power meter (Yokogawa Inc., WT-1800) to the BLDC motor and PWM amplifier. The motor mounting jig fixed the motor to the base with the motor coupling connected the motor and the torque meter (Sugawara laboratory, TB-200NM). The controller (Sugawara laboratory, DMC-2) controls the torque meter, which specifies the automatic measurement sequence.

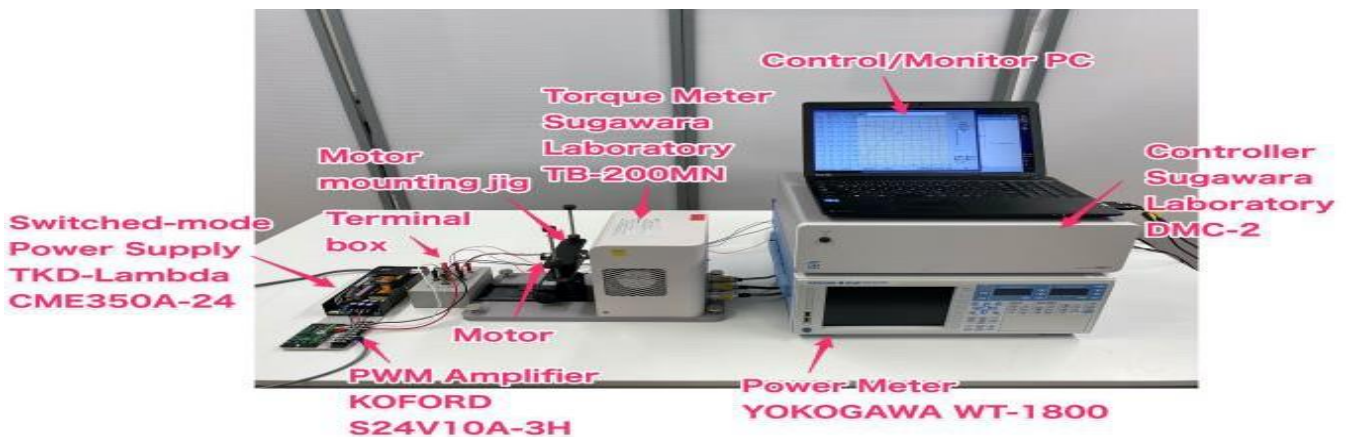


Figure 2. BLDC Motor Experimental Test

The motor was driven at a constant speed (ϵ) of about 20,000 min^{-1} in this study, and the braking torque, σ , was applied from 10 mNm to 60 mNm with an interval of 10 mNm. The motor current, I , and voltage, U , were then measured by using the power meter. The motor experimental speed constant, $KS(E)$, and speed constant.

2.2 Numerical Modeling for BLDC Motor with Different Air- gap

Based on the data sheet from ECX 22 BLDC motor, a 2- dimensional geometry was built in 5.4. The BLDC 2D model consists of a stationary stator with an inner layer of copper winding and a rotating rotor inside this layer. The OD and ID of the stator are set to 20.8 mm and 10.7 mm with the winding layer of 30 coils, each of 0.33 mm diameter. The rotor comprises a 4.0 mm diameter shaft and two semi-circular 10.4 mm diameter permanent magnet (PM) encapsulating the shaft. This rotor assembly was set as rotating domain at 20,000 rpm. The stator and the shaft were assigned soft iron as the material from the material data base, whereas the permanent magnets are treated as air. A user defined fine mesh was created using tetrahedrons with maximum and minimum element size of 0.1 mm and 0.001 mm, respectively. The mesh was calibrated for general physic with maximum element growth rate of 1.1

$$B = \mu_0 \mu_r H + B_r \quad (1)$$

$$H = f(|B|) \frac{B}{|B|} \quad (2)$$

$$K_s(N) = \epsilon \backslash (\text{Back EMF}) \text{min}^{-1} \text{V}^{-1} \quad (3)$$

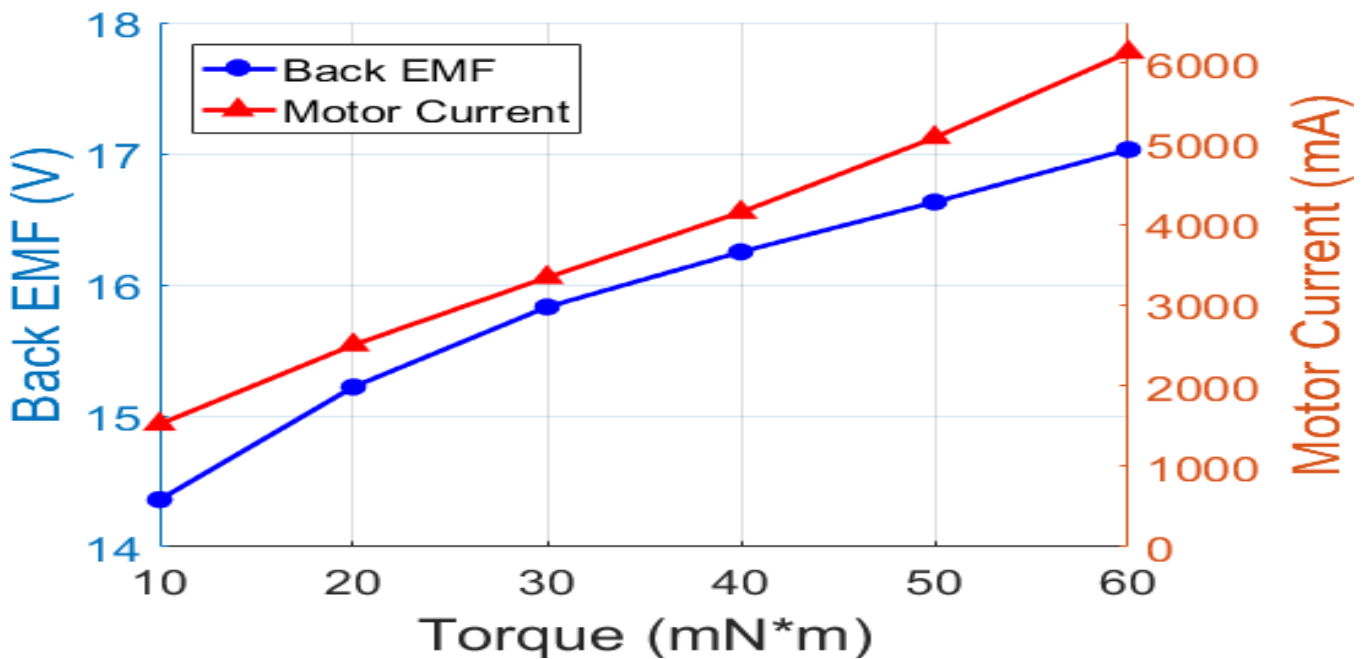
$$K_T(N) = 6 * 10^4 \backslash (2\pi * K_s(N)) \text{mNmA}^{-1} \quad (4)$$

3 Results

3.1 Validation of the Numerical Model for BLDC Motor

The motor test rig result shows that when the brake torque was applied from 10 mNm to 60 mNm to the BLDC motor, both motor voltage and current increased linearly (Fig. 4). The mean value for the speed and torque constant was calculated by Equation (1) and (2), resulting $1266 \pm 82 \text{ min}^{-1} \text{V}^{-1}$ and $8.77 \pm 1.37 \text{ mNmA}^{-1}$, respectively.

Figure 4. Back EMF and motor current generated at different torque under 20,000 rpm motor speed



rotor diameter of 10.4 mm. In the motor specification sheet, the speed constant and torque constant were $1090 \text{ min}^{-1} \text{V}^{-1}$ and

8.77 mNmA^{-1} , respectively. In the numerical model for this stock motor, the back EMF value was calculated as 18.4V at the motor speed of 20,000rpm, resulting the speed constant and torque constant as $1015 \text{ min}^{-1} \text{V}^{-1}$ and 8.81 mNmA^{-1} , respectively. The torque constant and speed constant from the experiment results and motor specification sheet were each compared to those found numerically (Table 1). The torque constant errors were both 0.5%, and the speed constant errors were 6.9% compared to data sheet and 19.8% compared to experimental data.

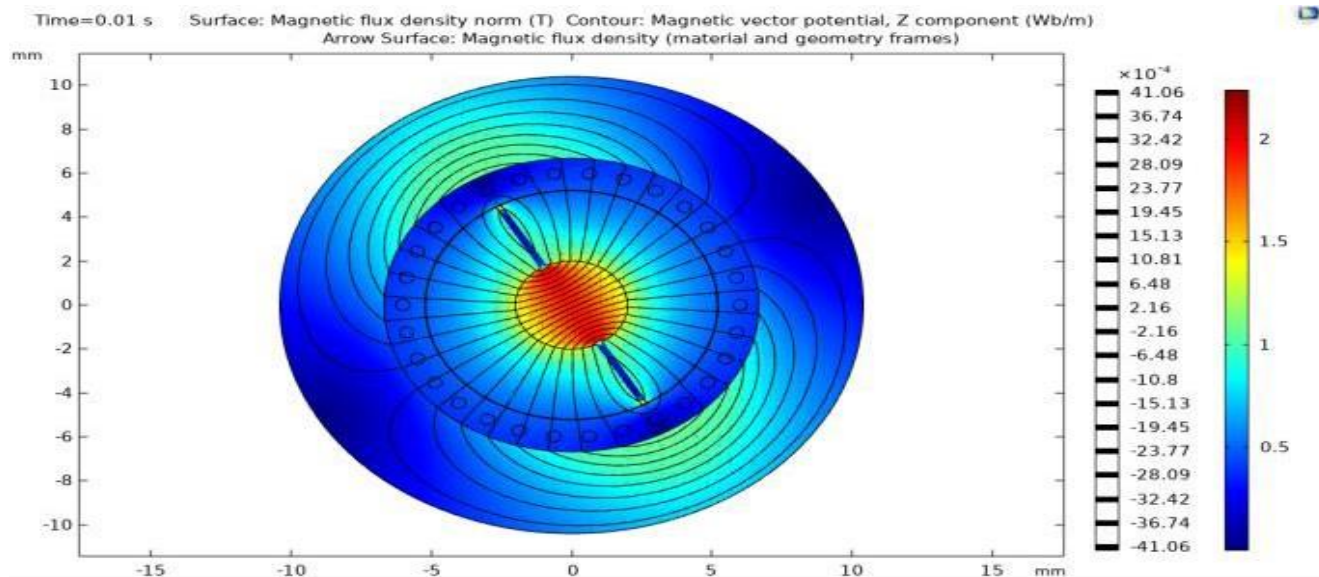


Figure5.Fluxdistribution

TABLE 1 COMPARISON AMONG MOTOR SPECIFICATION SHEET, EXPERIMENTAL AND NUMERICAL RESULTS

| | <i>Motor specification sheet</i> | <i>Experimental Results</i> | <i>Numerical Results</i> |
|---------------------------------------|----------------------------------|-----------------------------|--------------------------|
| Speed Constant (min-1v-1) | 1090 | 1266 ±82 | 1015 |
| Error (%) | 6.9 | 19.8 | 0 |
| Torque Constant (mNmA ⁻¹) | 8.77 | 8.77 ±1.37 | 8.81 |
| Error(%) | 0.5 | 0.5 | 0 |

3.2 Characteristic Different Air-gap BLDC Motor via Numerical Approach

Fig. 6 shows that the average back EMF generated in each motor geometry at 20,000 rpm motor speed for different rotor OD. The back EMF value decreased from 17.37 V to 5.46 V as the rotor OD reduced from 10.0 mm to 6.0 mm. The back EMF changes linearly with the rotor OD with a Figure 6. Change in back EMF with BLDC motor rotor slope of 3 ($R^2 = 0.9998$).

The speed constant, $KS(N)$, was obtained by using Equation (5), showing an approximate decrease between 85% - 90% as the rotor OD, r , increased from 6.0 mm to 10.0 mm. The values depreciate from 3665 min-1V-1 to 1085 min-1V-1 (Fig. 7a). Using a polynomial equation to fit the $KS(N)$ curve, the $KS(N)$ (r) at each r value can be expressed as below with $R^2=0.9992$.

$$(N)(r) = -34.898r^3 + 1001.5r^2 - 9801r + 33929 \quad (5)$$

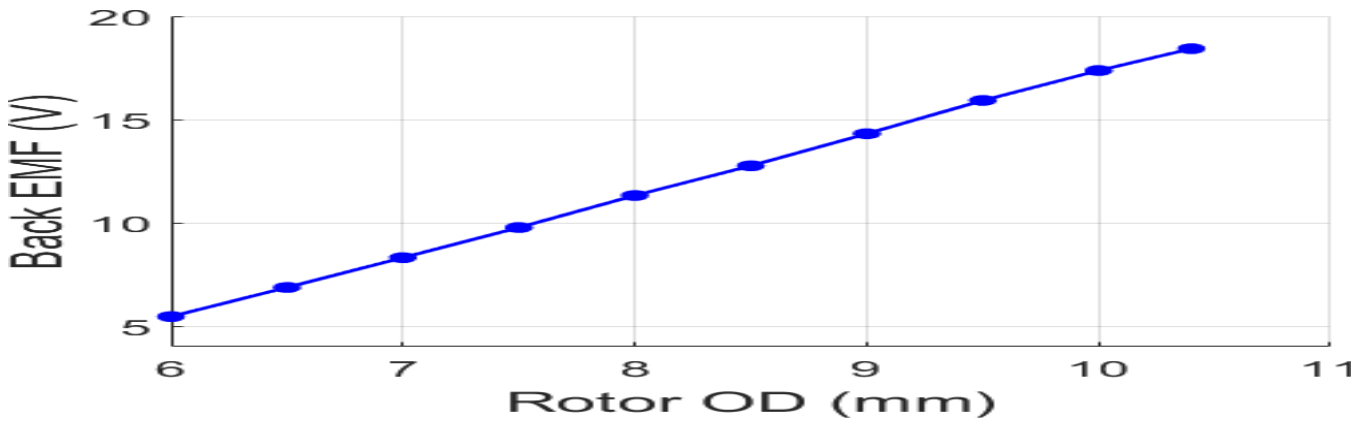


Figure 6. Change in back EMF with BLDC motor rotor size

The torque constant, $K_T(N)$ was obtained by using Equation (6), showing a linear relationship with the rotor OD change (Fig. 7). The torque constant, $K_T(N)$, increased as the rotor OD increased, which indicates smaller air-gap results in higher torque constant for the BLDC motor. A linear equation was used to fit the $K_T(N)$ curve, so the $K_T(N)$ (r) at each r value can be expressed as below with $R^2=0.9998$.

$$(N)(r) = 1.4253r - 5.9877 \quad (6)$$

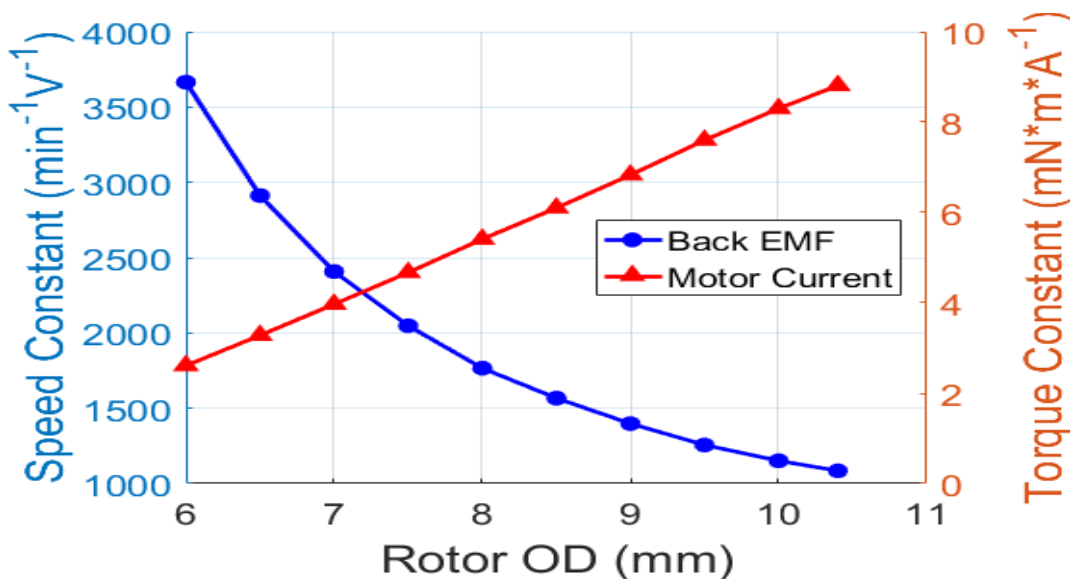


Figure 7. Changes in speed constant, and torque constant, with the increase of motor rotor outer diameter

4 Conclusion

In this study, a numerical BLDC motor model was established based on the data sheet from a stock motor (ECX22) and then validated by comparing the motor specification with that from the experimental motor test result. In order to effectively select the prototype that can best balance the motor efficiency and blood shear stress for the BSSD, the numerical BLDC motor model with different rotor OD was evaluated on the torque and speed constant changes. Two equations were generated based on the curves derived from the torque and speed constant calculations. These analytical relationships between motor specification and the motor air-gap will help identify the drive motor performance in our future BSSD design, which will improve the field's understanding of how motor geometry can be tuned to reduce trauma.

5 References

- [1] H. R. Mallidi, J. Anand, and W. E. Cohn, "State of the art of mechanical circulatory support," *Texas Heart Institute Journal*, vol. 41, no. 2, pp. 115-120, 04/01, 2019.
- [2] C. R. Bartoli, and R. D. Dowling, "The future of adult cardiac assist devices: novel systems and mechanical circulatory support strategies," *Cardiology clinics*, vol. 29, no. 4, pp. 559-582, 2019.
- [3] X. Song, A. L. Throckmorton, A. Untaroiu, S. Patel, P. E. Allaire, H. G. Wood, and D. B. Olsen, "Axial flow blood pumps," *ASAIO J*, vol. 49, no. 4, pp. 355-64, Jul-Aug, 2019.
- [4] D. Timms, "A review of clinical ventricular assist devices," *Medical Engineering & Physics*, vol. 33, no. 9, pp. 1041-1047, 2019.
- [5] P. Diehl, M. Aleker, T. Helbing, V. Sossong, F. Beyersdorf, M. Olschewski, C. Bode, and M. Moser, "Enhanced microparticles in ventricular assist device patients predict platelet, leukocyte and endothelial cell activation," *Interactive cardiovascular and thoracic surgery*, vol. 11, no. 2, pp. 133-137, 2010.
- [6] C. H. H. Chan, I. L. Pieper, S. Fleming, Y. Friedmann, G. Foster, K. Hawkins, C. A. Thornton, and V. Kanamarlapudi, "The effect of shear stress on the size, structure, and function of human von Willebrand factor," *Artificial organs*, vol. 38, no. 9, pp. 741-750, 2014.
- [7] Z. Chen, N. K. Mondal, J. Ding, S. C. Koenig, M. S. Slaughter, and Z. J. Wu, "Paradoxical effect of nonphysiological shear stress on platelets and von Willebrand factor," *Artificial organs*, vol. 40, no. 7, pp. 659-668, 2016.
- [8] F. Boehning, T. Mejia, T. Schmitz-Rode, and U. Steinseifer, "Hemolysis in a Laminar Flow-Through Couette Shearing Device: An Experimental Study," *Artificial organs*, vol. 38, no. 9, pp. 761-765, 2014.
- [9] J. Sheriff, P. L. Tran, M. Hutchinson, T. DeCook, M. J. Slepian,
- [10] D. Bluestein, and J. Jesty, "Repetitive Hypershear Activates and Sensitizes Platelets in a Dose-Dependent Manner," *Artificial organs*, vol. 40, no. 6, pp. 586-595, 2016.
- [11] T. Zhang, M. E. Taskin, H. B. Fang, A. Pampori, R. Jarvik, B. P. Griffith, and Z. J. Wu, "Study of Flow-Induced Hemolysis Using Novel Couette-Type Blood-Shearing Devices," *Artificial organs*, vol. 35, no. 12, pp. 1180-1186, 2011.
- [12] P. A. Smith, Y. Wang, S. A. Bieritz, L. C. Sampaio, W. E. Cohn, R. W. Metcalfe, and O. H. Frazier, "Design Method Using Statistical Models for Miniature Left Ventricular Assist Device Hydraulics," *Annals of biomedical engineering*, vol. 47, no. 1, pp. 126-137, 2019.
- [13] P. A. Smith, Y. Wang, R. W. Metcalfe, L. C. Sampaio, D. L. Timms, W. E. Cohn, and O. H. Frazier, "Preliminary design of the internal geometry in a minimally invasive left ventricular assist device under pulsatile-flow conditions," *Int J Artif Organs*, vol. 41, no. 3, pp. 144-151, Mar, 2018.

Voltage Reference Control for Standalone PV Systems

S.Subitha¹, Dr.S.Krishnan², M.Sidheswaran³

1. Second Year ME-Control Systems, Dept. of EEE, Mahendra Engineering College, Tiruchengode, Namakkal Dt.
2. Associate Professor, Dept. of EEE, Mahendra Engineering College, Tiruchengode, Namakkal Dt.
3. Assistant Professor, Dept. of EEE, Mahendra Engineering College, Tiruchengode Namakkal Dt.

Abstract

The fast depleting rate of fossil fuels necessitates the need for alternate renewable energy sources to generate electricity. Electricity plays a pivotal role in the country's economic development and has a pre-eminent role to play. One way of converting the incident sunlight into electricity is by using PV cells. This proposed paper focuses on using the power generated from PV cells for supplying single phase AC loads. A boost converter with 0.5 duty cycle was fabricated and tested. The results obtained from hardware and software simulation is shown to have better efficiency. This concept is simulated using PLECS software. The boost converter fabricated has specifications of 24-48 V conversion and power rating of 96W. The efficiency was found to be 93%.

Keywords: *Multi-level inverter, Harmonics, Total Harmonic Distortion (THD), Lower Order Harmonic (LOH), Fuzzy Logic Controller (FLC).*

1. Introduction

Non renewable energy sources are on the verge of depletion and pollutes the environment. There is an urgent need to switch to a cleaner form of energy sources like wind, solar and hydro power. The major problems faced in the renewable energy utilization are low yield, variable output, distribution and direct use for appliances. These problems discourage the complete switch over to renewable energy sources. In solar energy the amount of power generated depends on the incident sunlight, which in turn varies through the day and region. Voltage multiplier circuits can be used to obtain output voltage with high gain. In circuit Voltage Multiplier Cell (VMC) can be implemented in the middle of a circuit and thus reduce voltage stresses. Voltage multiplier rectifier (VMR) are used at the output stage of Transformer and coupled inductor-based structures, which rectifies the AC or pulsating DC voltage, and it meanwhile also acts as a voltage multiplier. The hysteresis voltage controller consists of a comparison between the output voltage V_o and the tolerance limits (V_H , V_L) around the reference voltage V_{ref} . Hysteresis control improves voltage sag condition efficiently. The design of the boost converter is under closed loop so that a constant output is obtained is fed to a single-phase inverter to get an AC output for driving small loads. Calculation of current Total Harmonic Distortion (THD) for a single-phase multilevel PWM inverter with LCL-filter is presented. The single phase inverter switch is triggered using gate pulse generator, SPWM and Relay with hysteresis.

2. Existing System

An interleaved high step-up dc/dc converter is derived by inserting a voltage multiplier cell into the conventional interleaved boost converter. Interleaved structure is employed in the input side to reduce the input current ripple and improve the power level. Moreover, the voltage multiplier cell is adopted in the output side to achieve a high step-up voltage gain and simplify the circuit structure. The voltage multiplier cell is composed of a capacitor, two diodes, and the second windings of the coupled inductors, which can extend the voltage gain and minimize the current ripple without extreme duty cycle. Moreover, the switch voltage stress is reduced as the turn's ratio of the coupled inductors increases, which makes low-voltage-rated MOSFETs with low RDS ON available to improve the circuit performance. The diode reverse recovery problem can be alleviated by the leakage inductance of the coupled inductors, which reduces the reverse recovery losses. Furthermore, zero-current-switching (ZCS) turnon soft-switching performance for the switches is realized, which reduces the switching losses and electromagnetic interference (EMI) noises. The circuit is simple and easy to design because there is no additional active power devices in this converter

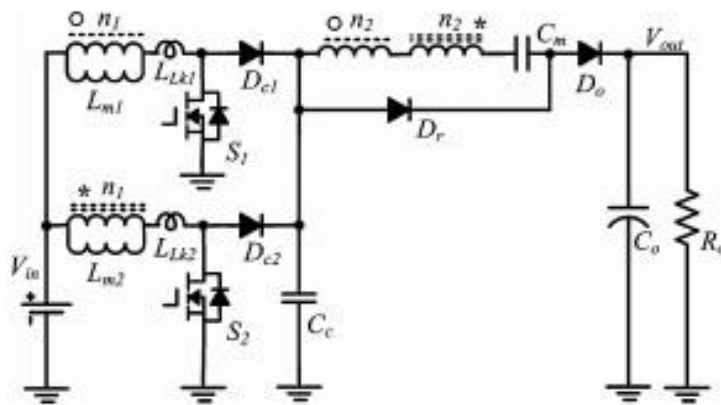


Figure 1: Existing system circuit diagram

3. Proposed System

An integrated system with voltage multiplier cell is introduced in this system with PI controller. The output of the boost converter with multiplier cell is made constant for a variable input source by tuning the PI controller by Zeigler Nicholas tuning method. The design of the boost converter is under closed loop so that a constant output is obtained. Hysteresis control improves voltage sag condition efficiently. A constant voltage supply is obtained using this technique and can be feed to any type of single-phase load. The design of the boost converter is under closed loop so that a constant output is obtained. Hysteresis control improves voltage sag condition efficiently. A constant voltage supply is obtained using this technique and can be feed to any type of single-phase load.

PROPOSED BLOCK DIAGRAM

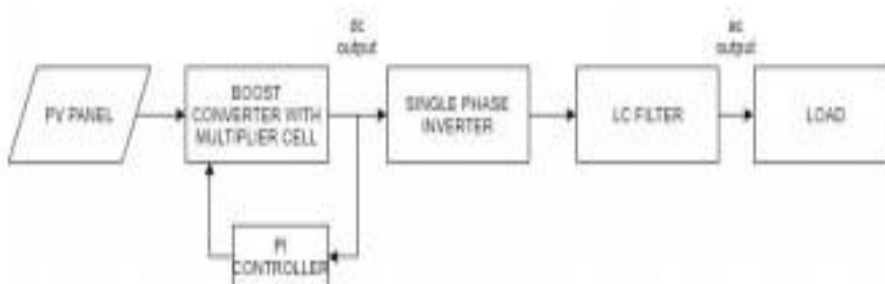


Figure 2: Block diagram of proposed system

4. Design of Proposed System

The voltage multiplier cell (M=1) with diodes D1 and D2, capacitors C1 and C2 and an inductor L_r are integrated with the conventional boost converter

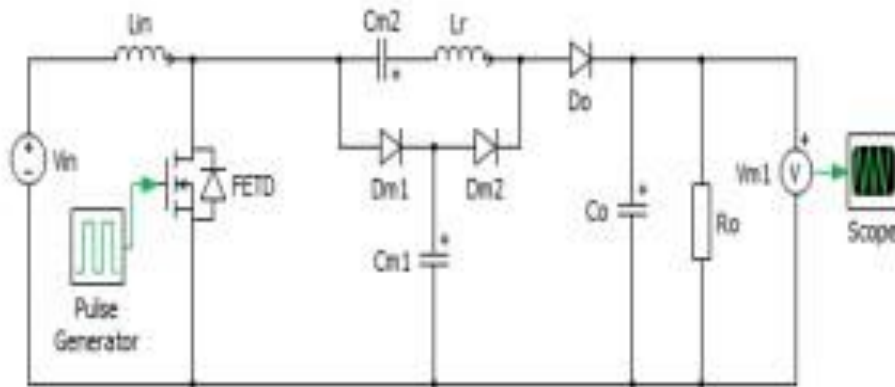


Figure 3: Proposed circuit diagram

5. Modes of Operation

The modified boost converter has five operating stages. All the operating stages are in Continuous Conduction Mode, since it is found to have better operating characteristics.

5.1 Stage 1

Initially in Fig.4, when the switch S is off, the input inductor L_{in} stores energy from the source. The energy stored in the inductor L_{in} gets transferred to multiplier cell capacitor C_1 and output capacitor C_o through the diodes D_1 and D_o respectively.

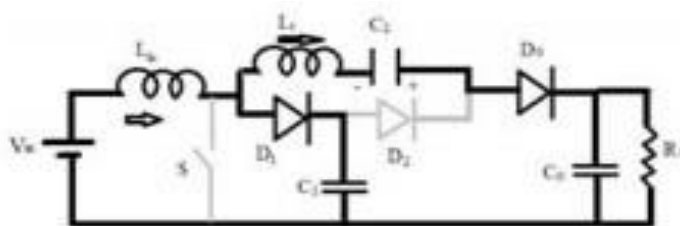


Figure 4: Stage 1 circuit diagram

Stage 2

It shows that the switch S is still off and the diode current in D_1 is 0. The currents in the input inductor (L_{in}) and the multiplier cell inductor (L_t) are equal and this stored energy is transferred to the load via diode D_o .

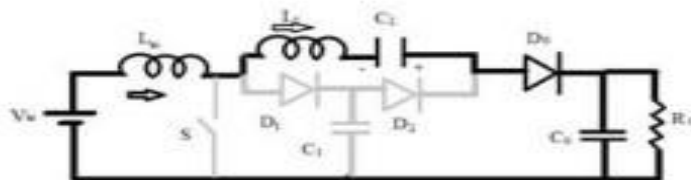


Figure 5: Stage 2 circuit diagram

5.2 Stage 3

It when the switch S is turned on and the current from the input inductor gets split into two, one through the short circuit path and the other to the resonant inductor L_t . As maximum current flows through the least resistive path (Short circuit path), the current through the resonant inductor and diode D_o reduces to zero linearly.

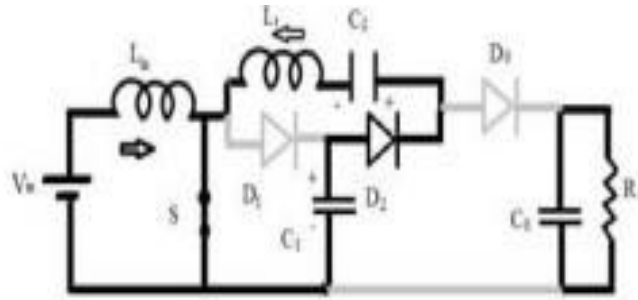


Figure 6: Stage 3 circuit diagram

5.3 Stage 4

It shows the energy stored in the capacitor C1 is transferred to the capacitor C2 forward biasing the diode D2 when the output diode D0 is blocked.

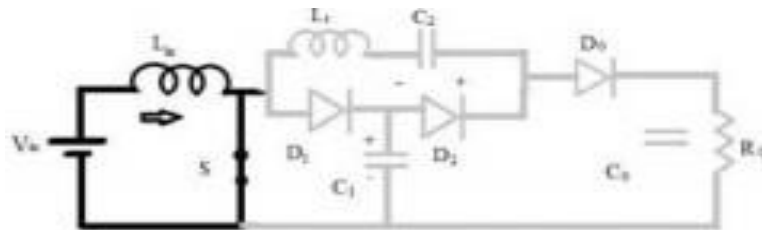


Figure 7: Stage 4 circuit diagram

5.4 Stage 5

It shows that the cell diode D2 is blocked and the current in the resonant inductor, L_r becomes 0. Once the switch turns off, the operation returns back to stage 1.

6. Control Technique

The output of the boost converter with multiplier cell is made constant for a variable input source by tuning the PI controller by Zeigler Nicholas tuning method. This output from the PI controller is compared with a triangular wave generator using relational operator to get gate pulses of desired duty cycle. The controlled gate pulses obtained are supplied to the switch to get the required output. the values of ultimate gain K_u and ultimate period P_u are obtained

Stanard Formula for Calculating Parameters in Zeighlor Nicols' Method

| Control Type | K_p | K_i | K_D |
|--------------|-----------|---------------|---------------|
| P | $0.5 K_u$ | - | - |
| PI | $0.45K_u$ | $1.2 K_p/P_u$ | - |
| PID | $0.6K_u$ | $2 K_p/P_u$ | $K_c * K_p/8$ |

Table 1: calculating in zeighlor method

Formula for parameters nicols'

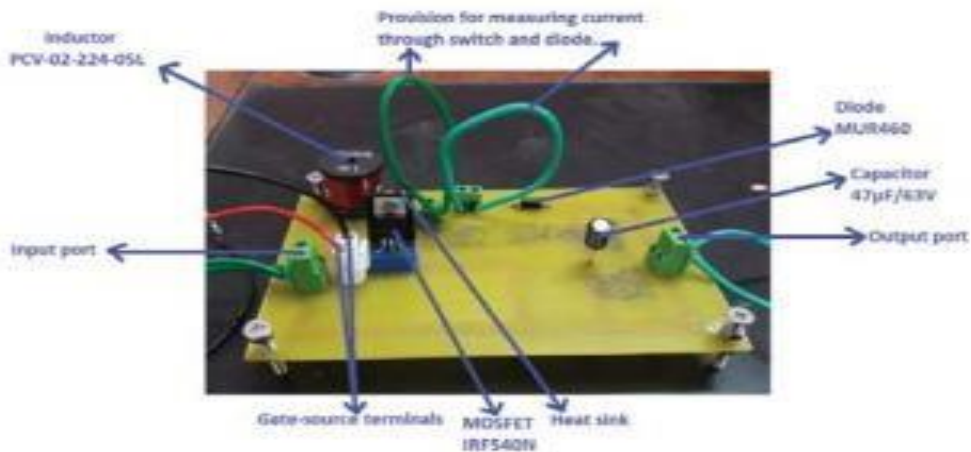


Figure 8: Prototype of fabricated converter

7. Output of Proposed System

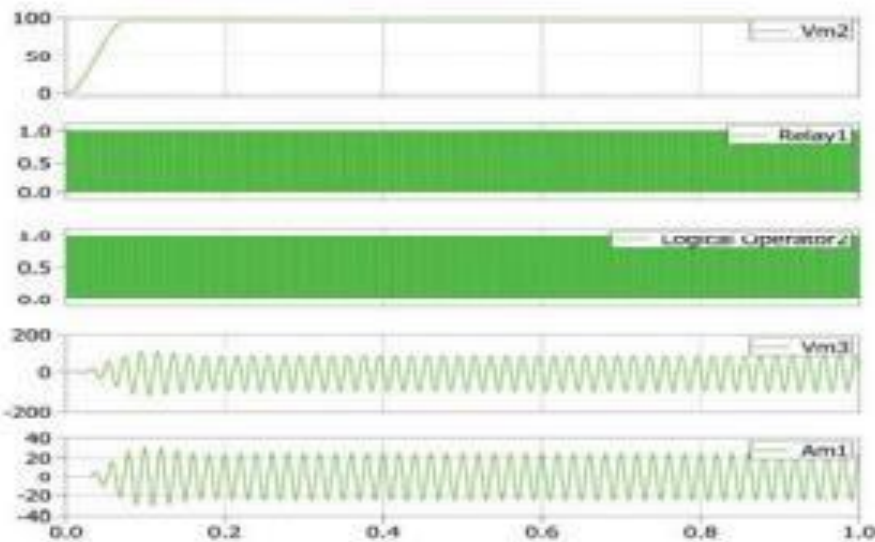


Figure 9: Simulation Output

8. Conclusion

The integration of conventional boost converter with the voltage multiplier cell on feeding to a single-phase inverter has been designed, simulated and experimentally verified. The advantages of this modified boost converter are low voltage and current stresses on the switch and transformer less high static gain which allows reduction of weight and volume. A voltage gain of 4 is obtained at the output of the inverter without using a power transformer and the THD of the obtained output AC voltage is minimized by designing an LC filter. The output of the inverter cannot just be used for a load but can also be integrated to the grid after voltage conditioning.

| Parameter | Pulse Generator | SPWM | Relay with hysteresis |
|------------------------|-----------------|-------|-----------------------|
| Output RMS Voltage (V) | 67.18 | 67.89 | 67.48 |
| Output RMS Current (A) | 17.42 | 17.59 | 17.51 |

| | | | |
|-----------------------|-------|--------|---------|
| THD of Output Voltage | 1.348 | 0.28 % | 0.211 % |
|-----------------------|-------|--------|---------|

Table 2: Observation Table

9. References

- [1] Muhammad H. Rashid, "Power Electronics: Circuits, Devices, and Application", third edition.
- [2] Ramazan Abdikarimuly, Yakov L. Familiant and Alex Ruder man , " Calculation of Current Total Harmonic Distortion for a Single-Phase Multilevel Inverter with LCL-Filter", Conference Paper September 2016 DOI: 10.1109/EPEPEMC.2016.7751975.
- [3] Mojtaba Forouzesheh¹, Yam P. Siwakoti, Saman A. Gorji, Frede Blaabjerg, Brad Lehman, " A Survey on Voltage Boosting Techniques for Step-Up DC-DC Converters", Conference Paper September 2016 DOI: 10.1109/ECCE.2016.7854792.[4] S.Saravanan¹,
- [4] M.Solaimanigandan², T.Tharaneetharan³, V.Varunraj⁴, S.Parthasarathy, "Dynamic Voltage Restorer for Distribution System", International Journal of Engineering Research and Development e-ISSN: 2278-067X, p-ISSN: 2278-800X, www.ijerd.com, Volume 7, Issue 1 (May 2013), PP. 14-24
- [5] Divya Navamani.J, Vijayakumar.K, Jegatheesan.R, " Study on High Step-up DCDC Converter with High Gain Cell for PV Applications", Procedia Computer Science 115 (2017) 731–739, 7th International Conference on Advances in Computing & Communications, ICACC- 2017, 22-24 August 2017, Cochin, India.

A Review of Non Conventional Energy Systems and Energy Regulation Technologies

C.Dinakaran^{1*}, Research Scholar

Dr.T.Padmavathi², Assistant Professor

Dr.K.Sri Chandan³, Assistant Professor

^{1,2,3}Department of Electrical and Electronics Engineering, GITAM Institute of Technology, GITAM (Deemed to be University), Visakhapatnam, Andhra Pradesh, India

dina4karan@gmail.com^{1*}, ptadi@gitam.edu², skondamu@gitam.edu³

Abstract – A majority of the communities in the region of the globe rely a lot on oil, natural gas along with coal for their energy requirements. These fuels represent on plenty of resources to facilitate ultimately reduce, which in turn makes them too costly or too environmentally harmful to recuperate. This analysis commentary discusses the merits as well as demerits of non-conventional energies, consequently based on the benefits of these energy resources, the utilize of renewable energies as an alternative of fossil fuels will be a fine resolution in favor of the control of the ecological, societal along with cost-effective troubles of our communities. The globe is prompt appropriate a universal village suitable to the growing day by day necessity of energy with all population across the world though the earth in its appearance cannot modify. The need for energy with its correlated services to satisfy human social moreover economic growth, welfare as well as health is increasing. Persistent to renewable to assist mitigate weather change is an excellent approach which needs to be sustainable in order to meet energy demand of upcoming generations.

Keywords: Renewable Energy Sources, Clean Energy, Environment, Sustainability issues, Green Energy, Clean Technologies, Solar Radiation.

1. Introduction

Renewable energy uses energy sources to facilitate constantly replenished by environment is the sun, wind, water, the Earth's heat plus plants [1]. Renewable energy technologies revolve these fuels into utilizable forms of energy the majority often electricity other than also heat, chemicals or mechanical power. In the present day we primarily utilize fossil fuels to heat as well as power our homes moreover fuel our cars [2]. It's convenient to employ coal, oil as well as natural gas intended for meeting our energy needs, although we have an inadequate supply of these fuels on the globe. We are using them a lot further quickly than they are being created [3].

Still if we have a limitless contribute of fossil fuels, by means of renewable energy is superior for the environment. We frequently entitle renewable energy technologies clean or green for the reason that they produce few if any pollutants. Burning fossil fuels though sends greenhouse gases into the environment, trapping the sun's heat in addition to contributing to global warming [4]. Weather scientists usually agree that the Earth's average temperature has risen in the precedent century. If this trend continues, sea levels will rise with scientists predict that floods, heat waves, droughts moreover other extreme weather circumstances might occur more often [5].

Other pollutants are released addicted to the air, soil along with water, when fossil fuels are burned. These pollutants acquire a dramatic toll on the environment also on humans [6]. Air contamination contributes to diseases in the vein of asthma. Acid rain commencing sulfur dioxide as well as nitrogen oxides troubles plants along with fish. Nitrogen oxides as well throw in to smog [7].

Renewable energy is consequential commencing natural processes to facilitate are replenished constantly. In its various forms, it derives directly commencing the sun, wind, rain, tides of ocean, biomass furthermore geothermal resources commencing heat generated deep contained by the earth [8]. The selection of energy has worldwide implications so as to involve greenhouse gas emissions, water resource distribution, mineral consumption along with equipment developed as well as transportation. There is a necessitate for confirmation of the sustainability of renewable energy, which can easily be done with resource and use optimization, techno-economic achievability along with cost analysis, life cycle assessment, ecological externalities investigation, cost benefits analysis, manufacturing cost examination, research and development targets with barrier recognition with water supplies along with distribution analysis [9].

1.1 History and Projections of World Energy Utilization

In the year 2021, the Earth's human being population consumed an all-time high of 620 quadrillion Btu of energy as well as energy utilization is estimated to enhance by ~30% more than the next 20 years. The rise in

worldwide energy demand is estimated to be fulfilled not only by means of traditional, non-renewable energy resources, (e.g., coal, oil, natural gas and nuclear fuel) although by means of renewable energy resources (e.g., solar irradiance as well as wind). In reality as a result of 2040, renewable energy production is estimated to enhance by ~80% though supplying ~20% of the world’s energy demand represented in figure 1. On the contrary, energy production by the use of oil as well as coal are each only estimated to enhance by ~30% although supplying ~3% fewer of the world’s energy demand than they accomplish at the moment [10].

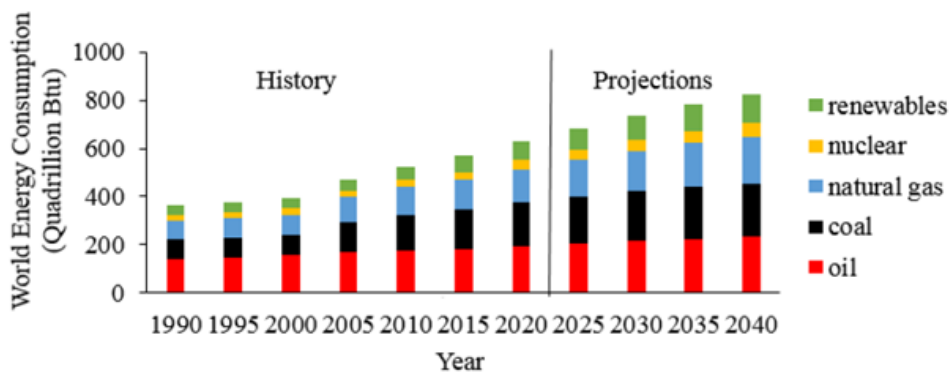


Figure 1. History and projections of global energy utilization by fuel type (Renewables, nuclear, natural gas, coal and oil)

The change in upcoming energy resource utilize is to some extent propelled through the inherent demerits of conventional energy resource [11]. The price of oil, coal, natural gas as well as nuclear fuel. For example, is estimated to enhance by an average of ~70% more than the next 10 years, through expenditure enduring to increase further into the future exposed in figure 2. In addition, non-renewable energy resources are a foremost supplier towards greenhouse gas emissions (e.g., CO₂, NO_x, SO_x etc.), which are responsible for the Earth’s climate change to some extent [12]. Finally, it is recognized to facilitate the supply of non-renewable energy reserves is limited as well as continues to diminish.

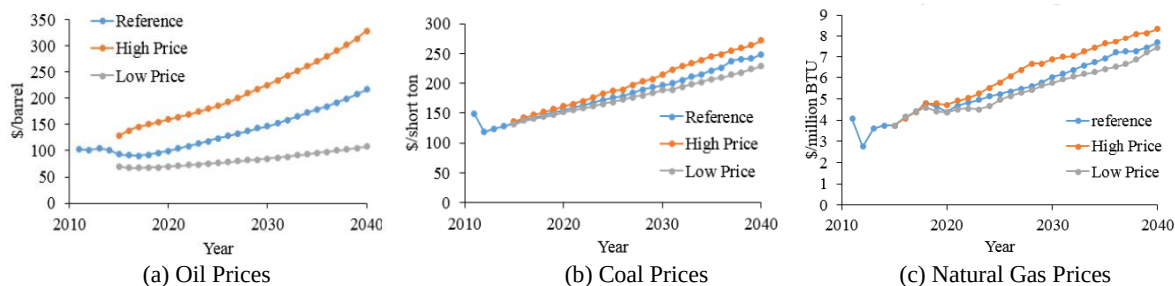


Figure 2. Historical and projected prices for various Non-Renewable Fuel Types (i.e., Prices with Projections through 2040)

Another contributing aspect towards the estimated enhance during utilize of renewable is the merits of systems to facilitate exploit renewable energy resources [13]. For instance, photovoltaic’s as well as wind turbines are predictable to be ~20% cheaper in 10 years than they are at the moment as illustrated in figure 3. Moreover, low-emission renewable energy systems, such as Photovoltaic’s as well as Wind Turbines, generate zero greenhouse gas emissions with their energy resources are almost infinite [14].

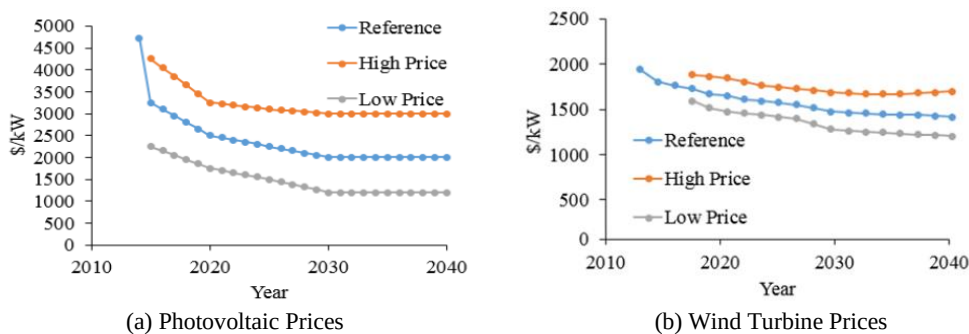


Figure 3. Historical and projected prices for various Renewable Energy Systems (i.e., Prices and Projections through 2040)

2. Renewable Energies

This manuscript reviews merits and demerits of little common renewable energies are hydropower, solar power, wind power, geothermal power as well as biomass. Expectantly after studying this analysis article, the community has a better

2.1 Hydro Power

Hydropower is a clean as well as renewable energy source. Considering the financially viable, technological as well as ecological benefits of hydropower, the majority countries provide main concern to its growth. Hydropower is generated by means of the mechanical energy of flowing water with forcing it through piping called a penstock, which subsequently turns a generator in order to generate electricity. Water power besides consists of wave as well as tidal energy, which are in cooperation in the infant stage of investigate, as scientists make an effort to determine how to exploit the energy created from association of the ocean.

Hydropower has numerous merits over the majority other sources generating electrical power. These consist of a high level of consistency, proven technology, high efficiency, very low operating as well as maintenance costs and the ability to easily regulate to load changes. Normally many hydropower plants are situated in coincidence with reservoirs, which supply water, flood control as well as recreation profit in favor of the public. In addition, hydropower does not create waste products to facilitate cause acid rain as well as greenhouse gases.

Demerits of hydropower consist of high initial costs of amenities, dependence on precipitation changes in stream regimens, stream of property along with wildlife habitat and displacement of community living in the reservoir area.

2.2 Solar Power

Solar power is the majority plentiful renewable resource on our planet. In spite of this plenty, merely 0.04% of the basic power used by means of humans comes directly from solar sources because using a photovoltaic (PV) panel costs more than burning fossil fuels. Organic resources have recently been intensively study for PV applications, not for the reason that of harvesting the sun's power more efficiently, although because power generation commencing organic photovoltaic resources will cost significantly less than other PV technologies. Concentrating solar power uses the heat from the sun to generate steam, which in turn powers a generator that creates electricity. This also has low operating costs as well as high efficiency in addition to generate a reliable supply of energy by using thermal storage.

Solar energy is a accurate renewable resource. The majority of global earth has the ability to bring together a quantity of amount of solar power. Solar energy is non-polluting, does not generate greenhouse gases, such as oil based energy does, nor does it produce waste that must be stored, such as nuclear energy. It is also far quieter to produce moreover harness, considerably reducing the noise contamination necessary converting power to a valuable form. Residential size solar energy systems besides contain very little impact on the neighboring atmosphere, in contrast with further renewable energy sources such as wind along with hydro electric power. Solar panels contain no moving parts as well as involve very little maintenance beyond regular cleaning. Exclusive of moving parts to break and replace, after the initial costs of installing the panels, maintenance in addition to repair costs are very realistic. It must also be prominent that photovoltaic solar panels are the solitary resource measured with the impending to satisfy existing demand.

The major problem of using solar energy is the expenditure concerned. Although advances in technology, solar panels remain almost prohibitively expensive. Even when the cost of the panels is ignored, the system essential to accumulate the energy for exploit can also be pretty expensive. Even though a little solar energy can be composed for the duration of cloudiest of days, competent solar energy collection is dependent on sunshine. Still a few cloudy days are able to have a enormous effect on an energy system, predominantly once the fact that solar energy cannot be collected at night is taken into account.

2.3 Wind Power

Wind power is a very easy process. A wind turbine converts the kinetic energy of wind into mechanical energy with the intention of used to generate electricity. The energy is fed through a generator transformed a succeeding instance into electrical energy as well as then fed into the grid to be transmitted to a power station.

Similar to other renewable energy sources, wind energy has numerous merits. It reduces greenhouse gas emissions by using turbines, which create energy furthermore electricity when stirred by the wind furthermore

can condense electrical energy expenses. All the turbines necessitate in order to function is wind, which is presently air in natural motion as well as air is universally. Wind signifies a free, abundant moreover sustainable energy that will not depreciate if we take merits of it.

Wind power has been harnessed for thousands of years, however merely in the previous decade has it generated momentous amounts of commercial energy. A lot of the windiest areas in the region of the world are situated far from population centers. The intermittent as well as unpredictable nature of the wind power would limit its involvement to any constituency, unless large-scale energy storage or intercontinental transmission is obtainable. Environmental constrains, such as the existence of forests along with protected areas, further limit the position of the wind turbines. Wind farms are not essential attractive as well as they have generated complaints regarding noise, interference with radio and TV signals and also interfering with migratory birds.

2.4 Geothermal Power

The geothermal method involves trapping heat underground, then building energy to facilitate rises close to the surface in the form of heat. When this heat naturally creates hot water or steam, it is harnessed along with used to turn a steam turbine to produce electricity.

Geothermal energy derived from heat impending from the earth's interior, has a lot of different uses. These uses be able to be grouped into three categories are for heating systems, for generation of electricity as well as for use in geothermal heat pumps. Moreover these convenient uses of geothermal energy, there are a lot of other things that make geothermal energy an extremely precious energy resource. Since the earth's core constantly produces heat with the radioactive decompose of elements such as potassium and uranium, geothermal energy turns out to be a renewable, abundant as well as reliable energy source. A geothermal energy plant does not compose of fuel, it is in cooperation sustainable as well as secure for the environment. Emissions of geothermal energy operations are low. These operations neither pollute the air nor contribute to global warming.

The demerits of geothermal energy power plants are its locality for the reason that finding appropriate locations for these power plants is not a simple task. The quantity of locations with the intention to provide accommodation geothermal power plants is extremely limited. The locality must have hot rocks so they preserve easily be drilled. Besides the rarity of appropriate geothermal power plant locations, there is furthermore the concern of safety. The concentration of geothermal energy can typically be found along plate boundaries, where volcanoes are concentrated along with earthquakes are most frequent. Once in a despite the fact that geothermal energy locations run out of steam for a couple of months, for the duration of which the power plant is not capable to produce electricity.

2.5 Biomass

People have used biomass energy or bioenergy as long as one can imagine, Wood is still the major biomass energy resource nowadays, although other sources of biomass be able to be used. These comprise food crops, grassy as well as woody plants, residues from cultivation otherwise forestry, oil-rich algae along with the organic constituent of municipal as well as industrial wastes. Even the methane fume from landfills be able to be used as a biomass energy source.

The use of biomass energy have the potential to significantly reduce greenhouse gas emissions, dependence on foreign oil, landfills as well as at last supports local agricultural along with forest product industries. The most important biomass feed stocks for power is paper mill residue, lumber mill scrap as well as municipal waste. For biomass fuels the majority common feed stocks used nowadays is corn grain moreover soybeans for biodiesel. Long-term strategy comprises growing as well as using enthusiastic energy crops, such as fast-growing trees as well as grasses along with algae. These feed-stocks are able to grow sustainably on land so as to sustain rigorous food crops. Another advantage of biomass is its ability to exchange into a collection of valuable fuels, chemicals, materials along with products much like crude oil,

- Biofuel – Converting biomass into liquid fuels intended for transportation
- Biopower - Burning biomass directly otherwise converting it into gaseous or liquid fuels that burn more efficiently in the direction of produce electricity
- Bioproducts - Converting biomass into chemicals for making plastics as well as other products that typically are made from petroleum.

Biomass in the midst of all of its benefits may cause destruction for the environment, if one does not choose its crop for the production of biomass energy from the subsequent list,

- Energy crops that do not compete with food crops for land
- Portions of crop residues such as wheat straw or corn Stover
- Sustainably harvested wood as well as forest residues
- Clean municipal along with industrial wastes

3. Basic Solar Components (i.e., Solar Angles)

3.1 Declination Angle (δ)

Declination is the angular distance from the sun north or south to the earth’s equator. As schematically illustrated in Figure 4, the maximum and minimum declination angle standards of the earth’s orbit produce seasons. Declination range between 23.45° North as well as 23.45° South. The northern hemisphere is inclined 23.45° far away from the sun for a moment around 21 December, which is the summer solstice for the southern hemisphere as well as the winter solstice for the northern hemisphere. In the northern hemisphere along with through 21 June, starting around 21 June, the southern hemisphere is situated in a way that it is 23.45° away from the sun. For the moment, it is winter solstice in the northern hemisphere. During the fall and spring equinoxes, which begin on 21 March and 21 September correspondingly, the sun passes directly over the equator.

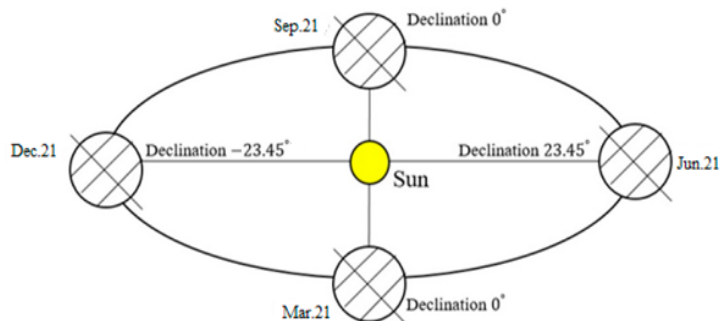


Figure 4. Maximum and Minimum value of Declination angle

The declination angle can be considered by the equation

$$\delta = 23.45 \sin[(360 \times (284 + n))/365]$$

Where n is the day of the year with January 1 as n = 1, February 20 as n = 51

3.2 Solar Hour Angle (ω)

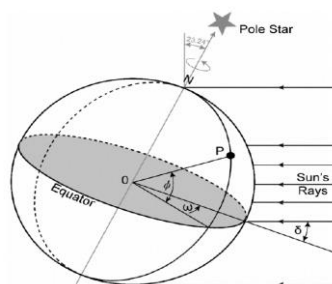


Figure 5. Hour Angle (ω) for point P

The concept of hour angle is used for describing the rotation of the earth around its polar axis which is equivalent to $+15^{\circ}$ per hour throughout the morning and -15° in the afternoon. It is the angular distance between the observer’s meridian as well as the meridian whose plane contains the sun as illustrated in figure 5. The following equation can be used to determine the hour angle in degrees. It should be eminent that at noon the hour angle ω is zero.

$$\omega = 15(12 - ST)$$

Where, ST is the local solar time

3.3 Solar Azimuth Angle (γ_s)

The angular displacement commencing the south of the beam radiation projection on the horizontal plane is defined as the solar azimuth angle. This is schematically represented in figure 6.

$$\cos \gamma_s = \sec \alpha [\cos \phi \sin \delta - \cos \delta \sin \phi \cos \omega]$$

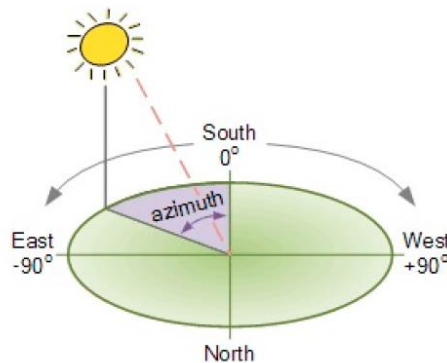


Figure 6. Sun's Azimuth Angle

3.4 Latitude (φ)

The latitude of a region is the location with significance north otherwise south of the Equator. The variation of the latitude is from 0^0 to $\pm 90^0$ (positive for northern as well as negative for the southern hemisphere), 0^0 at the Equator and $\pm 90^0$ at the Poles.

3.5 Hourly Global Solar Radiation on an Inclined Surface (I_{β})

Beam radiation ($I_{b\beta}$), Reflected radiation (I_r) as well as diffuse radiation ($I_{d\beta}$) are the three components of the global solar radiation on an inclined surface (I_{β}). The fraction of incident radiation reflected by the ground is called reflected radiation.

$$I_{\beta} = I_{d\beta} + I_{b\beta} + I_r$$

Normally, diffuse radiation models for inclined surfaces can be classified into two group's isotropic and anisotropic models. They differ in the division of the sky addicted to regions with standard as well as elevated diffuse radiation intensities. Isotropic models presuppose there is consistency in the circulation of diffuse radiation intensity over the sky. Anisotropic models consist of suitable modules for representing areas of elevated diffuse radiation.

4. I-V Characteristics of a Solar Cell

Solar cell is the essential unit of solar energy production system where electrical energy is extracted directly from light energy exclusive of any intermediate process. The working of a solar cell exclusively depends upon its photovoltaic effect, therefore a solar cell as well recognized as photovoltaic cell. A solar cell is essentially a semiconductor p-n junction device. It is produced by joining p type and n-type semiconductor material. At the junction surplus electrons from n-type try to diffuse to p-side and vice-versa. Movement of electrons to the p-side exposes positive ion cores in n side, whereas movement of holes to the n-side exposes negative ion cores in the p-side. This results in an electric field at the junction as well as forming the depletion region.

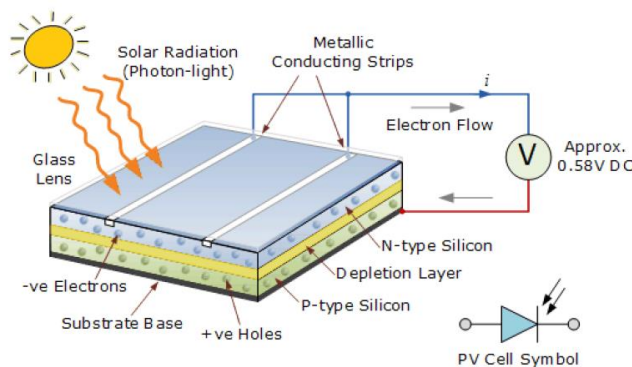


Figure 7. Construction of a Solar Cell

When sunlight falls on the solar cell, photons with energy greater than band gap of the semiconductor are absorbed by the cell and produce electron-hole (e-h) pair. These e-h pairs migrate correspondingly to n-side and p- side of the pn junction owing to electrostatic force of the field transversely the junction. In this way a

potential difference is recognized between two sides of the cell. Typically a solar or photovoltaic cell has negative front contact as well as positive back contact. A semiconductor p-n junction is in the middle of these two contacts like a battery. If these two sides are associated by an external circuit, current will start flowing from positive to negative terminal of the solar cell. This is basic working principle of a solar cell. For silicon, the band gap at room temperature is $E_g = 1.1 \text{ eV}$ as well as the diffusion potential is $U_D = 0.5 \text{ to } 0.7 \text{ V}$. Construction of a Si solar cell is depicted in figure 7.

Solar Cell I-V Characteristics Curve is the superposition of the I-V curves of the solar cell diode in absence (dark) and in presence of light. Illuminating a cell adds to the normal dark currents in the diode so that the diode law becomes,

$$I = I_0 \left[\exp\left(\frac{qV}{nkT}\right) - 1 \right] - I_L$$

Where, I_0 = Dark saturation current or diode leakage current in absence of light

q = Electronic Charge

V = Applied voltage across the terminals of the diode

n = Ideality factor

k = Boltzmann's Constant

T = Temperature

I_L = Light generated current

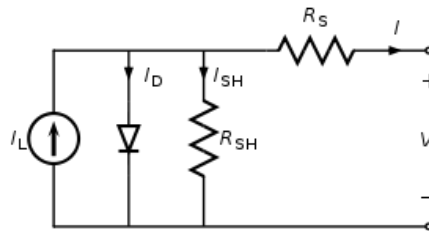


Figure 8. Equivalent Circuit of a Solar Cell

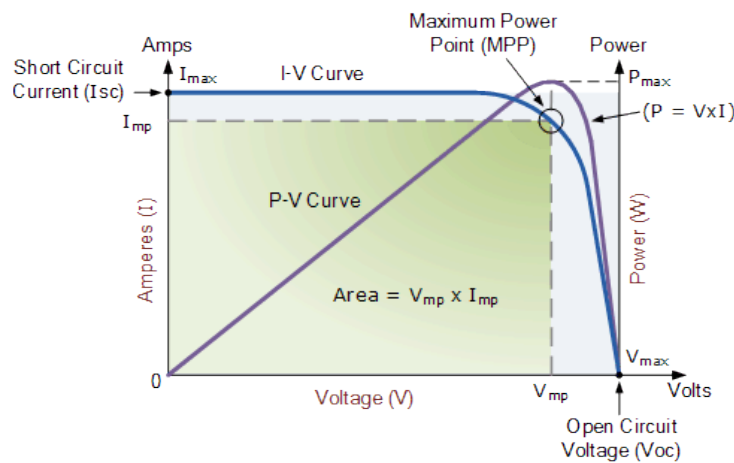


Figure 9. A Typical I-V Curve and Power Curve of a Solar Cell

Figure 8 represents the equivalent circuit of solar cell. The efficiency is the majority commonly used parameter to evaluate the performance of one solar cell to another. Efficiency is definite as the ratio of energy output from the solar cell to input energy from the sun. In accumulation to reflecting the performance of the solar cell itself, the efficiency depends on the spectrum as well as intensity of the incident sunlight along with the temperature of the solar cell.

The figure 9 shows the current-voltage (I-V) characteristics of a typical silicon PV cell operating under standard conditions. The power delivered by a solar cell is the product of current and voltage ($I \times V$). If the reproduction is done, point for point for all voltages from short-circuit to open-circuit conditions, the power curve above is obtained for a given radiation level. With the solar cell open-circuited that is not connected to any load the current will be at its minimum as well as the voltage across the cell is at its maximum recognized as the solar cells open circuit voltage (V_{oc}). At the further extreme, when the solar cell is short circuited so as to the positive and negative leads connected together, the voltage across the cell is at its minimum except the current flowing out of the cell reaches its maximum recognized as the solar cells short circuit current (I_{sc}).

5. Hybrid Power System

Off grid renewable energy technologies convince energy demand directly furthermore avoid the need for long distribution infrastructures. A combination of different but complementary energy generation systems based on renewable energies or mixed is known as a hybrid power system as illustrated in figure 10.

Hybrid systems capture the best features of each energy resource as well as provide grid-quality electricity, with a power range between 1 kW to several hundred kilowatts. They can be developed as innovative integrated designs contained by small electricity distribution systems and also be retrofitted in wind power systems.

Hybrid systems are able to afford a steady community-level electricity service, such as village electrification, contribution to the opportunity to be upgraded during grid connection in the future. Furthermore, due to their high levels of efficiency, reliability as well as long term performance, these systems can also be used as an efficient backup solution to the public grid in case of blackouts or weak grids also for proficient energy solutions, such as telecommunication stations otherwise emergency rooms at hospitals.

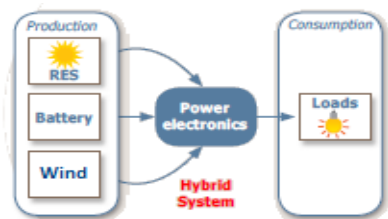


Figure 10. Hybrid Power Generation System

5.1 Technological Configurations for Hybrid Systems

5.1.1 Electricity Generation Coupled at DC bus line

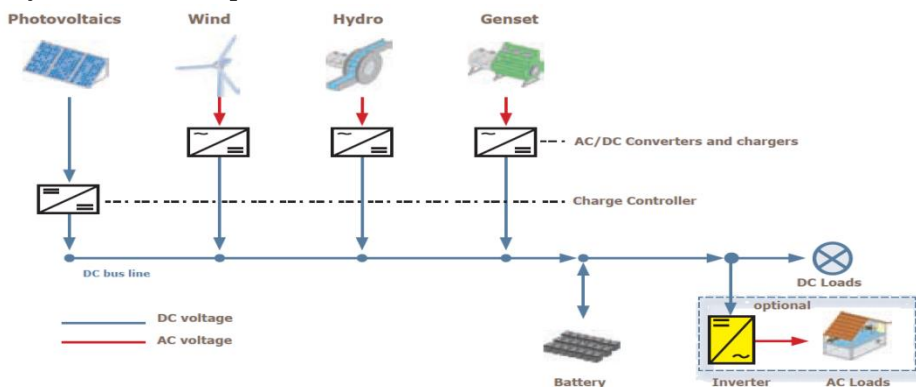


Figure 11. Hybrid System (DC Coupled)

All electricity generating apparatus are associated to a DC bus line from which the battery is charged. AC generating components require an AC/DC converter. The battery controlled as well as protected from over charge along with expulsion by a charge controller, then supplies power to the DC loads in reaction to the demand. AC loads be able to be optionally supplied by an inverter as represented in figure 11.

5.1.2 Electricity Generation Coupled at AC bus line

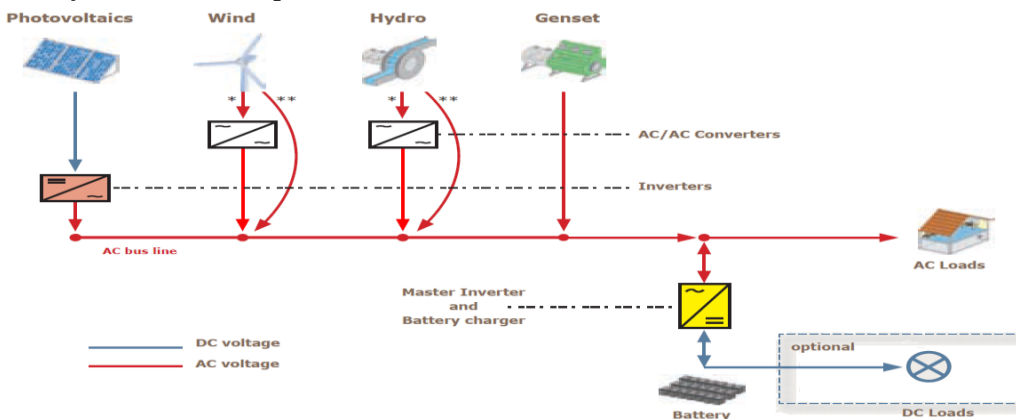


Figure 12. Hybrid System (AC Coupled)

All electricity generating apparatus are associated to an AC bus line. AC generating components may be directly linked to the AC bus line or may need an AC/AC converter to allow stable coupling of the components. In both options, a bidirectional master inverter controls the energy supply for the AC loads as well as the battery charging. DC loads be able to be optionally supplied through the battery as illustrated in figure 12.

5.1.3 Electricity Generation Coupled at AC/DC bus lines

DC and AC electricity generating apparatus are associated at mutually of a master inverter, which controls the energy contributes of the AC loads. DC loads can be optionally supplied by the battery. On the AC bus line, AC generating apparatus might be directly connected to the AC bus line otherwise might require an AC/AC converter to enable stable coupling of the mechanism as shown in figure 13.

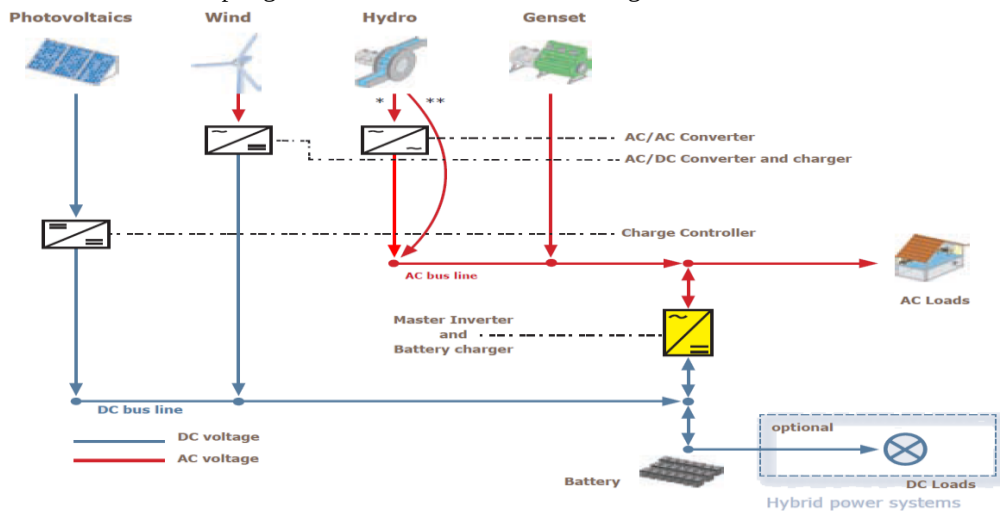


Figure 13. Hybrid System (AC/DC Coupled)

6. Renewable Energy Sources and Sustainability

Renewable energy sources reload themselves in nature without being exhausted in the earth they comprise bioenergy, hydropower, geothermal energy, solar energy, wind energy and ocean energy. The major renewable energy forms with their uses are obtainable in Table 1.

The world’s growing energy need, along with growing population led to the persistent utilize of fossil fuel based energy sources (Coal, Oil and Gas) which became problematic by creating numerous challenges such as, exhaustion of fossil fuel reserves, greenhouse gas emissions moreover further environmental concerns, geopolitical as well as military conflicts along with the continual fuel price fluctuations. These troubles will make unsustainable situations which will ultimately outcome in potentially irreversible threat to human societies. Even though renewable energy sources are the majority exceptional alternative with the only resolution to the increasing challenges.

Reliable energy supply is necessary in all economy for heating, lighting, industrial equipment, transport, etc., Renewable energy supplies diminish the emission of greenhouse gases considerably if replaced with fossil fuels. Since renewable energy supplies are obtained naturally from continuing flows of energy in our environment, it should be sustainable. For renewable energy to be sustainable, it should be immeasurable also provide non-harmful deliverance of ecological goods and services. For occurrence, a sustainable biofuel be supposed to not enhance the net CO₂ emissions, be supposed to not unfavorably concern food security nor intimidate biodiversity.

Table 1. Renewable Energy Sources and their exploit

| Energy Sources | Energy Conversion and Usage Options |
|----------------|---|
| Hydro Power | Power Generation |
| Modern Biomass | Heat and Power Generation, Pyrolysis, Gasification, Digestion |
| Geothermal | Urban heating, Power generation, Hydrothermal, Hot dry rock |
| Solar | Solar home systems, Solar dryers, Solar cookers |
| Direct Solar | Photovoltaic, Thermal power generation, Water heaters |
| Wind | Power generation, Wind generators, Windmills, Water pump |
| Wave and Tide | Numerous design, Barrage, Tidal stream |

Renewable technologies are measured as clean sources of energy as well as most favorable use of these resources decreases environmental impacts produces minimum secondary waste furthermore are sustainable based taking place the current also future economic moreover social needs. Renewable energy technologies make available an incomparable opportunity for mitigation of greenhouse gas emission with reducing global warming during substituting conventional energy sources.

7. Conclusion

It is essential that we take safety measures once distributing moreover consuming the earth's resources. The current use of natural gas as well as fossil fuels collective with growing global population has caused the earth's resources to be abused moreover exhausted. The possessions on the atmosphere are exhausting with threatening to the sustainability of the earth. The technique we contain consuming fossil fuels is very scary furthermore the scarier point is the fact so as to during last couple of decades the consumption of fossil fuels has gone up. The oil reserves across the world are diminishing along with energy production at present depends too extremely on oil as well as fuels, which contribute to the emission of conservatory gases. Release of pollutants into the environment has dire consequences. Including global warming consequently it is required to protect globe earth by incorporate renewable, ecological energy sources in our everyday lives.

References

- [1] Gueymard, C.A, "A review of validation methodologies and statistical performance indicators for modeled Solar radiation data: Towards a better bankability of solar projects", *Renew. Sustain. Energy Rev*, Vol. 39, PP. 1024-1034, 2014.
- [2] El-Sebaili, A.A, Al-Hazmi, F.S, Al-Ghamdi, A.A, Yaghmour, S.J, "Global, direct and diffuse solar radiation on horizontal and tilted surfaces in Jeddah, Saudi Arabia," *Appl. Energy*, Vol. 87, PP. 568-576, 2010.
- [3] Khatib, T, Mohamed, A, Mahmoud, M., Sopian, K, "Optimization of the Tilt Angle of Solar Panels for Malaysia," *Energy Sources A Recover. Util. Environ. Eff.*, Vol. 37, PP. 606-613, 2015.
- [4] Erbs, D.G., Klein, S.A., Duffie, J.A, "Estimation of the diffuse radiation fraction for hourly, daily and monthly-average global radiation," *Sol. Energy*, Vol. 28, PP. 293-302, 1982.
- [5] Shukla, K.N., Rangnekar, S., Sudhakar, K, "Comparative study of isotropic and anisotropic sky models to estimate solar radiation incident on tilted surface: A case study for Bhopal, India," *Energy Rep.*, Vol.1, PP. 96-103, 2015.
- [6] Padovan, A., Col, D. Del, "Measurement and modeling of solar irradiance components on horizontal and tilted planes," *Sol. Energy*, Vol. 84, PP. 2068-2084, 2010.
- [7] Khatib, T, "A Review of Designing, Installing and Evaluating Standalone Photovoltaic Power Systems," *J. Appl. Sci.*, Vol. 10, PP. 1212-1228, 2010.
- [8] K. Agbossou, M. Kolhe, J. Hamelin, and T. K. Bose, "Performance of a standalone renewable energy system based on energy storage as hydrogen," *IEEE Trans. Energy Convers.*, vol. 19, no. 3, pp. 633–640, Sep. 2004.
- [9] Schaeffer R, Szklo AS, Pereira de Lucena AF, Moreira Cesar Borba BS, Pupo Nogueira LP, Fleming FP, et al. "Energy sector vulnerability to climate change: a review," *Energy*, Vol. 38, PP. 1-12, 2012.
- [10] Boehlert B, Strzepek KM, Gebretsadik Y, Swanson R, McCluskey A, Neumann JE, et al., "Climate change impacts and greenhouse gas mitigation effects on U.S. hydropower generation," *Applied Energy*, Vol 183, PP. 1511–1519, 2016.
- [11] P. Trop and D. Goricanec, "Comparisons between energy carriers' productions for exploiting renewable energy sources," *Energy*, vol. 108, pp. 155-161, Aug. 2015.
- [12] C. Bhowmik, S. Bhowmik, A. Ray, and K. M. Pandey, "Optimal green energy planning for sustainable development: A review," *Renew. Sustain. Energy Rev.*, vol. 71, pp. 796-813, May 2017.
- [13] W. Al-Marri, A. Al-Habaibeh, and M. Watkins, "An investigation into domestic energy consumption behavior and public awareness of renewable energy in Qatar," *Sustain. Cities Soc.*, vol. 41, pp. 639-646, Aug. 2018.
- [14] T. M. Nisar, G. Prabhakar, and L. Strakova, "Social media information benefits, knowledge management and smart organizations," *J. Bus. Res.*, vol. 94, pp. 264-272, Jan. 2018.

A Novel Design and Fabrication of Road Sweeper by using Photo-voltaic system.

S. Prasanna, R. Amaresh & A. Mohamed Suhaib

Final Year, Department of Electrical and Electronics Engineering Krishnasamy College of Engineering and Technology, Cuddalore

Mr. J. Jayakumar, Assistant professor, Department of Electrical and Electronics Engineering Krishnasamy College of Engineering and Technology, Cuddalore

Abstract

In our country, Governments are taking some actions towards the avoidance of accidents by placing dividers on the major roads of the city. But there is a usage of heavy trucks and loaded vehicles are polluting the roads by dust which is not a major concern but one of the issues that the bikers are skidded by the dust-sand enclosed along the dividers. Multinational companies are concentrating on this with high cost of Sweepers with Diesel Engines but this proposed scheme would help to solve in the case of low cost of manufacturing and effective way of renewable energy resource. This Photovoltaic based sweeper come with solar powered vacuum cleaner with spiral sweepers, automated divider tracker and a loader bag thus this total system is operated only using the renewable energy resource. This would make the platform that all the corners of the roads are clean with less traffic accidents and economical to the municipalities to change over with this efficient system.

Keywords: PV-Photo Voltaic, PM-Particulate Matter.

1. Introduction

1.1. History Of Sweepers

The very first street sweeping machine was patented in 1849 by an inventor named C. S.Bishop. For a long time, since street sweepers were made of rotating disks with the wire bristles.

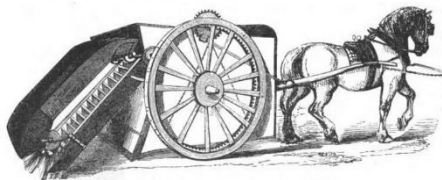


Figure 1 First Invented Sweeper

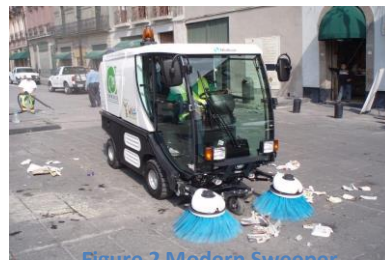


Figure 2 Modern Sweeper

The Rotating disks served as the mechanical brooms that were swept the dirt on the streets. In the fall of 1913, the city of Boise, Idaho, purchased the first Elgin Sweeper, the following a demonstration Boise Street Commissioner, Thomas Finegan made a comparison showing a saving of \$ 2,716,77 from Elgin motorized sweeper when used rather than a horse drawn sweeper.

Never street sweepers are capable of collecting small particles of debris. Many street sweepers produced from today are PM 10 and PM 2.5 certified. Thus, the meaning that they are capable of collecting and holding particulate matters sized less than that 10 micro meter and evendown to 2.5 micro meter. Despite advancement in street sweeping technology, the mechanical broom type street sweepers accounts for approximately 90 % of all street sweepers used in the United States today.

1.2. Need For Solar Energy

Earth has limited amount of energy resources which is very soon going to extinct. Fortunately, population models have suggested that the world's population will probably level out at about two to three times the present numbers over the next hundred years. As the population is increasing the demands of people is also increasing. The question is whether the earth's resources are sufficient to sustain that population at a high standard of living for all. In this the key issue is energy.

Now-a-days, dealers of natural resources like fuel, coal etc. are facing a hard time to keep pace with the increasing demand. At one hand, there are more cars or motor vehicles are dominating the transport medium, on the other hand these cars are being dominated by the fuel. As a result, the limited resources are being quashed by the producers and dealers to satisfy this need which is leading us to an uncertain future with having the scarcity of fuel and minerals. So, it is clear that present trends in energy consumption, especially oil, cannot be sustained much longer. Also, these are responsible for Global Warming, Environmental Imbalance, Ozone layer depletion etc. which in turn is a big threat to the future human race.

Again, in view of the possibility of global warming, these resources are playing a negative role. Therefore, under this circumstance, it is quite necessary to make a new exploration of natural resource of energy and power. But why exploration when the resource is in front of our bear eye. It is effective, less expensive and above all, it is an endless source of energy. With greatly improved energy efficiency, a transition to this energy-based economy capable of sustaining the anticipated growth in the world economy is possible. This effective source is- Solar Energy.

2. System Description

2.1. Existing System

The Road sweepers used now-a-days are made of large multinational companies with the high cost of local Municipal Responsible for the sanitary cannot afford the rate of cost to buy for the purpose of cleaning. They are operated at fossil fuel with the heavy usage of energy. The Existing system is of a vehicle which looks like a truck with the storage and it to be operated manually using a Driver. And there will be huge level of Maintenance is required.

3. Proposed System

3.1. Detailed Description Of Proposed System

3.1.1. Components

Solar Photovoltaic Module

A Solar PV module can be considered to be a big solar cell. That is array of many solar cells are connected in series and parallel with larger voltage and current generated by a solar module depends on its efficiency. The power generated per unit area is usually of $10\text{mW}/\text{cm}^2$ to $25\text{mW}/\text{cm}^2$ which corresponds to 10% to 25% cell efficiency.

LITHIUM-ION BATTERY

The lithium-ion battery was introduced in the market in 1991, is the choice in most consumer electronics, having the best energy density and a very slow loss of charge when not in use. Such incidents are rare and according to experts, they can be minimized by "via appropriate design, installation, procedures and layers for safeguards" so the risk is acceptable.

CHARGING CIRCUIT

Solar chargers convert light energy into low voltage DC current.

Although portable solar chargers obtain energy from the Sun only, they still can (depending on the technology) be used in low light (i.e., cloudy) applications. Portable solar chargers are often used for trickle charging, although some solar chargers (depending on the wattage), can completely recharge batteries. Other devices may exist, which combine this with other sources of energy for added recharging efficacy.

POWER CONVERTER

A DC-to-DC converter is used an electronic circuit or electromechanical device that converts a source of direct current (DC) from one voltage level to another. It is a type of electric power converter. Power levels range from very low (Lithium-ion Batteries) to very high (High voltage Operating Drives).

MOTOR DRIVES

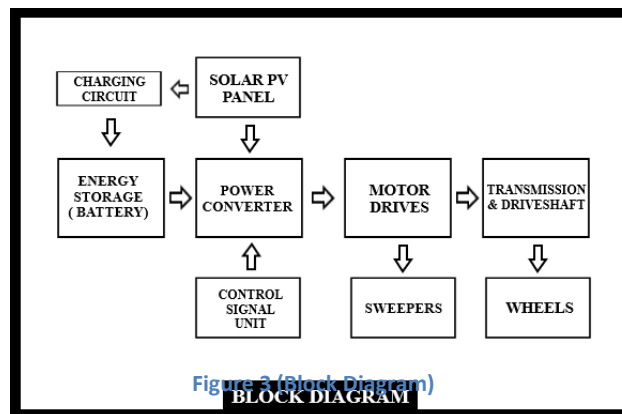
The Motor Drivers are used for the system of which the Sweepers and Wheels are controlled by using the motor drives which are powered using Battery of Solar charged. The motors used in the proposed system is of various voltage specifications, but the battery is of 12V and 8 Ah specification. So that the power converter is used for the system to drive.

SWEEPING BRISTLES

There are two conventional sweepers are used in the system for the linear flow of sweeping on the road. And a Single arm provided sweeper used with the vacuum tube for the absorption of Dust around the Indicators present on the road.

3.1.2 System Model & Working

The Drawbacks of the existing system is overcome through the system by which the use of alternative source of energy. Solar Photovoltaic panels is the important source for the system to be operated. The below block diagram shows the schematic representation of this proposed system.



The charging and discharging circuit are of related with the energy storage device Battery. Thus, the solar Photovoltaic panel exhibits as the energy source to perform the charging source of the battery. The Power converting system is used in the proposed system that the charge stored in the battery is used for the sweepers and wheels to rotate. They are controlled by using the arduino which are an In-build one to perform the drive system through the control signals.

4. Circuit Flow Representation

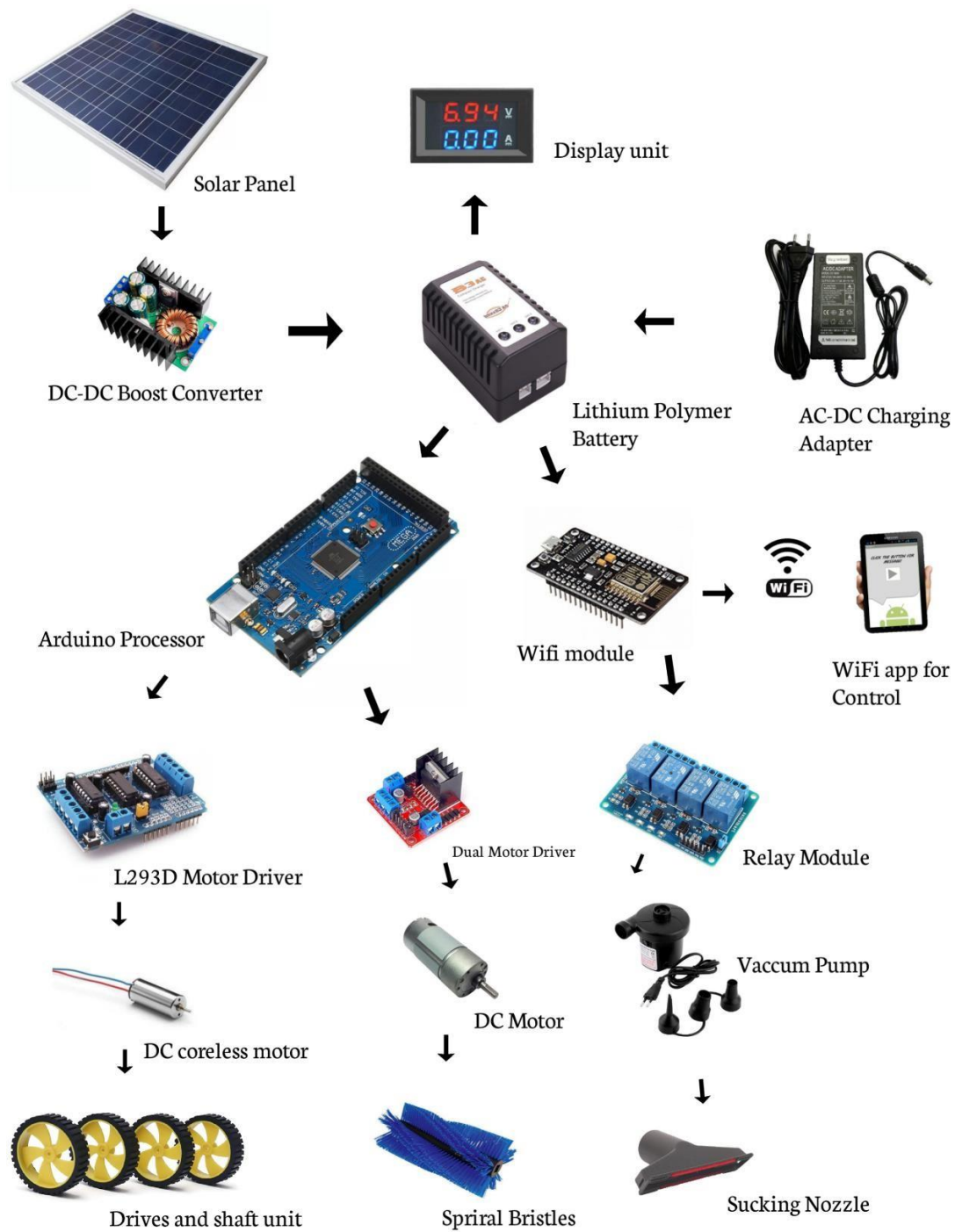


Figure 4 (Flow of Components)

5. Advantages

Solution: The system is semi-automatically clean the sides of the dividers in the mid of the road along the moving vehicles with the supervisor.

Need: To reduce Man-Power in risk areas with Efficient solution on cleaning with roads.

Impact: Conventional forms of High Energy consuming sweepers will be replaced with the Renewable sources.

Control: Integration of Photo-voltaic leads to reduction of Green-House Effect and control the emission of CO₂.

6. Conclusion

Our Photovoltaic Based road sweeper solves many problems related to the environment and is the best pollution free method. We need to make use of this proposed system so that we can reduce our dependence on fossil fuel. This Photo-voltaic based road sweeper will become the new era on cleaning the roads by local municipalities with low cost of Investment.

7. References

- [1]. "Electric and Hybrid Vehicles Design Fundamentals"- Iqbal Husain.
- [2]. "Solar Photovoltaic Fundamentals, Technologies and Applications"- Chetan Singh Solanki.

Plant Growth Algorithm based Load forecasting of a power System

Mrs. J. Arul Martinal
Assistant Professor,
Department of Electrical and Electronics Engineering,
St. Anne's College of Engineering and Technology,
Anguchettypalayam, Panruti – 607106.

Abstract

In power system energy management system Load forecasting is the major part of the system. The exact load forecasting helps the electric utility to make unit commitment decisions, reduce spinning reserve capacity and schedule device maintenance plan properly. Apart from its plays a key role in reducing the generation cost, it is also essential to the reliability of power systems. In current scenario Load forecasting plays an important role in power system planning, operation and control. But for the proper Planning and precise operational applications of load forecasting requires a certain 'lead time' which is called as forecasting intervals. On the basis of lead time, load forecasting types fall into four different categories: very short-term forecasts, short-term forecasts, medium-term forecasts and long-term forecasts. In the present paper STLF model is developed and executed using Matlab 8.6 with a new optimization algorithm called Plant Growth Algorithm for the Andhra Pradesh Grid. By using the five year load pattern of Andhra Pradesh Grid from the year 2007 to 2011 the forthcoming year's load pattern will be forecasted by using (PGOA) Plant Growth Optimization Algorithm.

Index Terms— PGOA, STLF, Load Forecasting.

I. Introduction

Load forecasting is the process used to predict the future demand from the past load data and environment data. Till now numerous models have been adapted to predict the electrical demand more precisely. There are three different types of Load forecasting:

A. Long-term electric load forecasting (LTLF): is helpful for the power utility to plan the forthcoming projects, altering the existing project in order to increase power generation, hiring of man power for smooth operation. The time period for long time demand prediction is more than 10 years.

B. Medium-term load forecasting (MTLF): is helpful in making necessary arrangement of fuel reserves and planning equipment as well as plant maintenance. The time range for medium term load forecasting is 3 to 5 years.

C. Short-term load forecasting (STLF): is helpful in providing essential data for the daily operation and energy scheduling. The time range is from hour to a month.

In current deregulated power scenario forecasting of electrical power gained much more attention. In the power bid market the precise forecasting helps in buying the ample amount of power at a minimal cost. The inaccurate predicted data leads to wrong bidding of price for the required power which leads to increase in electricity pricing. Hence in this paper, the important focus is narrow down the difference between the predicted data and actual data therefore prediction accuracy increases which lead to most accurate electricity price bidding.

II. Electrical Load Forecasting

2.1 Load Characteristics:

In load forecasting problem the aim is to predict the load, hence it is very important to know the load behavior. It is known that electrical load is the dynamic one which changes with respect to time and also influenced by external factors like time, seasonal changes and currency value etc.

2.2 Necessities of the Load Forecasting Process

- Precise
- Fast Convergence
- Simple GUI
- Self erroneous value detection
- Continuous Data Access

III. Plant Growth Optimisation Algorithm

An effective algorithm is presented to simulate plant growth realistic in this paper, taking into account branching, phototropism, leaf growth and spatial occupancy. The major focus of the model is to select the activated points by equate the concentration of their morphogen to augment the L system.

The PGOA takes the growth area of artificial plant as solution space, the best node of the plant considered as the best solution to the problem. The PGOA searches the optimal node in the solution search space based on two criteria.

1. Generating new nodes by branching to search the solution space in order to find the best solution.
 2. Growing leaves around the branch points to find the precise solution in the local solution space.
0. Start
 1. Initialize
 - Set $NG=0$ {NG is the generations counter}
 - Set $NC=0$ {NC is the convergence counter}
 - Set $NM=0$ {NM is the Mature points counter}
 - Set the upper limit of the branch points N and initialize other parameters.
 - Select N_0 branch points at random and perform leaf growth.
 2. Assign Morphogen
 - Calculate the eligibility of the leaf point.
 - Assign the concentration level of the morphogen of each branch point by Eq.1.
 3. Branching
 - Select two critical values between 0 and 1 randomly and dispose by Eq.3.
 - Produce new points by branching in four modes.
 4. Selection Mechanism
 - Perform leaf growth in all of the points.
 - Pick out the mature branch points, the number of which is k ($0 \leq k \leq N$), by the maturity mechanism.
 - Set $NM = NM + k$
 - Generate new point in the amidst of the crowded area and choose the best point in order to substitute the crowded points.
 - Eliminate the lower competition ability branch points and select N branch points for next generation.
 5. Competition
 - Compare the current points with the mature points and get the best fitness value f_{max}
 6. Check the Termination Criteria
 - If ($NG < NG_{max}$ && $NC < NC_{max}$ && $NM < NM_{max}$)
 - Go to step2
 - else
 - Exit
 7. Stop
 - One execution of the procedure from step2 through step6 is called a generation or a cycle.

IV. Result Analysis

A Matlab code was developed to perform the load forecasting for the Andhra Pradesh Grid using Plant Growth Optimisation Algorithm. Using the actual data for the years 2007 - 11 the load demand for the years 2012 -2016 is forecasted.

| YEAR | ACTUAL | FORECASTED |
|------|--------|------------|
| 2007 | 8157 | 8984 |
| 2008 | 8482 | 9498 |
| 2009 | 9309 | 10023 |
| 2010 | 9683 | 10559 |
| 2011 | 10453 | 11106 |

Table.4.1 Predicted Load (in MW) with actual load for the years (2007 - 11)

| YEAR | MONTH | PSO | DE | PGOA |
|------|-------|-------|-------|-------|
| 2012 | DEC | 11980 | 11771 | 11665 |
| 2013 | DEC | 12913 | 12281 | 12235 |
| 2014 | DEC | 13550 | 12968 | 12816 |
| 2015 | DEC | 14360 | 13850 | 13408 |

| | | | | |
|------|-----|-------|-------|-------|
| 2016 | DEC | 15175 | 14890 | 14012 |
|------|-----|-------|-------|-------|

Table. 4.2 Predicted load (in MW) for the December month from (2012 – 16) using PSO, DE and PGOA

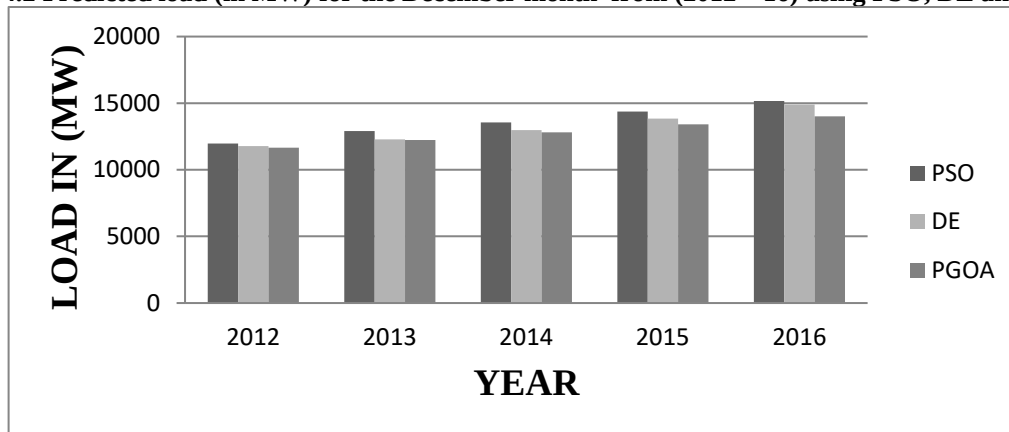


Fig. 4.1 Comparison of Forecasted load in (MW) for the year (2012 – 16) using PSO, DE and PGOA

V. Conclusion

The main objective of this work is to implement the Plant Growth Optimization Algorithm in order to predict the future load for planning and hassle free operation of power system. Also by using the PGOA we narrowed the difference between the predicted data and actual data which increases the computational efficiency of developed load forecasting model when compared to existing models with minimal time and better convergence.

References

1. G. Gross, F. D. Galiana Short term load forecasting Proceedings of the IEEE, 1987, 75(12), 1558 – 1571.
2. J.Y. Fan, J.D. McDonald, ‘A real-time implementation of short – term load forecasting for distribution power systems’, IEEE Transactions on Power Systems, 1994, 9, 988 – 994.
3. M.Y. Cho, J.C. Hwang, C.S. Chen, ‘Customer short-term load forecasting by using ARIMA transfer function model’, Proceedings of the International Conference on Energy Management and Power Delivery, EMPD, 1995, 1, 317 – 322.
4. E.A. Feinberg and D. Genethliou (2005) ‘Load forecasting In: Applied Mathematics for Restructured Electric Power Systems’: Optimization, Control, and Computational Intelligence, J.H. Chow et al. (eds.), Springer.
5. M. EL-Naggar, and A. AL-Rumaih (2005) ‘Electric Load Forecasting using Genetic Based Algorithm, Optimal Filter Estimator and least error squares Technique’, Comparative study, PWASET, pp. 138 -142.
6. Ping-Feng Pai (2006) ‘Hybrid ellipsoidal fuzzy systems in forecasting regional electricity loads’ Energy Conversion and Management, Volume 47, Issues 15-16, September 2006, Pages 2283-2289
7. D.W. Bunn and E.D. Farmer (1985) ‘Comparative models for electrical load forecasting’, John Wiley and Sons, New York. pp.232
8. Gross, G and Galiana, F.D (1987), ‘Short-Term Load Forecasting’, Proceedings of the IEEE, Vol.75, No.12, pp. 1558-1572.
9. Mohsen Hayati and Yazdan Shirvany (2007) ‘Artificial Neural network Approach for Short-term load forecasting for Illam Region’, Volume1 Number 2, WASET ORG
10. S.S. Sharif and J.H. Taylor (2000) ‘Short-term Load Forecasting by Feed Forward Neural Networks’, Proc. IEEE ASME First Internal Energy Conference (IEC), Al Ain, United Arab Emirate, <http://www.ee.unb.ca>
11. S.S. Sharif and J.H. Taylor (2000) ‘Real-time Forecasting by Artificial Neural Networks’ Proc. IEEE Power Engineering Society Summer Meeting (PES), Seattle, Washington
12. K. Y. Lee and J. H. Park (1992) ‘Short-Term Load Forecasting Using an Artificial Neural Network’ IEEE Trans. Power Systems, vol. 7, no. 1.

Minimization of Reactive power in Power System using Group Leader Optimization Algorithm

Ms.M. Premaltaha
Assistant Professor,
Department of Electrical and Electronics Engineering,
St. Anne's College of Engineering and Technology
Panruti – 607106

Abstract

In this paper the MRPG problem is solved to make smooth real power flow in supporting to generators requirement with the help of GLO technique for IEEE 14-bus system. According to the problem criteria, minimization of reactive power generation brings a new corner in the field of deregulated power environment. MRPG problem is a very important aspect for the power generating companies as reward in terms of money is related to this. GLO is a very well-known soft-computing technique which is applied previously to solve similar problem like optimal power flow, reactive power dispatch etc. The application of GLO technique to solve MRPG problem raising a value of 3.5000MVAR from the base value of 5.89MVAR shows credibility. Due to sake of simplicity some parameters are neglected during the network analysis like voltage index and sensitivity analysis which may be included in future study. Furthermore, MRPG problem is considered as single objective problem which can be improved as multi-objective problem by incorporating cost or real power loss minimization in the future study. On account of novelty of the proposed issue, GLO based MRPG problem solved in this paper shows satisfactory performance.

Keywords: MRPG; Group Leader Optimization

1. Introduction

We present a new global optimization algorithm in which the influence of the leaders in social groups is used as an inspiration for the evolutionary technique which is designed into group architecture. To demonstrate the efficiency of the method, a standard suite of single and multi-dimensional optimization functions along with the energies and the geometric structures of Lennard-Jones clusters are given as well as the application of the algorithm on quantum circuit design problems. We show that as an improvement over previous methods, the algorithm scales as $N^{2.5}$ for the Lennard-Jones clusters of N -particles. In addition, an efficient circuit design is shown for a two-qubit Grover search algorithm which is a quantum algorithm providing quadratic speedup over the classical counterpart. Global optimization is one of the most important computational problems in science and engineering. Because of the complexity of optimization problems and the high dimension of the search space, in most cases, using linear or deterministic methods to solve them may not be a feasible way. Wille and Vennik argued that global optimization of a cluster of identical atoms interacting under two-body central forces, belong to the class of NP-hard problems. This means that as yet no polynomial time algorithm solving this problem is known. Recently, Adib reexamined the computational complexity of the cluster optimization problem and suggested that the original NP level of complexity does not apply to pair wise potentials of physical interest, such as those that depend on the geometric distance between the particles. A geometric analogue of the original problem is formulated and new sub problems that bear more direct consequences to the numerical study of cluster optimization were suggested. However, the intractability of this sub problem remains unknown, suggesting the need for good heuristics. Many optimization methods have been developed and these can be largely classified into two groups, deterministic and stochastic. Deterministic methods include variations on Newton's method such as discrete Newton, quasi Newton and truncated Newton, tunneling method and renormalization group methods. Stochastic methods include simulated annealing, quantum annealing, J-walking, tabu search, genetic algorithms (GA) and basin-hopping approach. More recent work on probabilistic techniques have been proposed to solve these optimization problems by observing nature and modeling social behaviors and characteristics, including GA, evolutionary algorithms (EA), such as the particle swarm optimization algorithm (PSO), and the Pivot methods. Implementation of many of these algorithms on complex problems requires exhausting computational time and a growing need for more computer resources depending upon: the dimension, the solution space and the type of problem. The key to speed up the optimization process is reducing the number of computations in the algorithms while keeping the amount of iterations low and the success rate of the algorithms high. This paper introduces a new global optimization algorithm which reduces the optimization time, and is both simple and easy to implement. In the following sections, the inspiration and the implementation of the algorithm will be explained and test results will be given for some of the most famous optimization test problems; for the global optimization

of the minimum energy structures of complex Lennard-Jones clusters; and for the quantum circuit design of the Grover search algorithm.

II. Inspirations And Related Works

Leaders in social groups affect other members of their groups by influencing either the number of members or each member intensively. Therefore, the effect of group leaders inclines the groups to have uniform behavior and characteristics similar to the leader. These new behaviors and characteristics may improve or worsen the quality of the members of a group. A leader represents the properties of its group. To become a leader for a group requires a person to have some better abilities than others in the group. Similar ideas to using leaders or/and grouping solution population have been the inspiration for optimization algorithms such as Cooperative Co-evolutionary Genetic Algorithms (CCGA), Cooperative Co-evolutionary Algorithms (CCEAs), and Parallel Evolutionary Algorithms (PEAs) [2]. However, instead of trying to fully simulate the influence of leaders on their peers in social groups by constructing a population which includes small, interacting groups with their leaders, most of these and other similar algorithms have attempted the decomposition of big and complex problems into subcomponents or divide the whole population into multiple subpopulations with a parallel structure. In CCGAs, as described by Potter and Jong, each species – which are evolved into subcomponents by using a standard genetic algorithm – represents a subcomponent of the potential solution, and each representative member of the species is used to form the complete solution of the optimization problem. In a general architecture for the evolving co-adapted subcomponents was presented in order to apply evolutionary algorithms to complex problems. Therefore, instead of GA, the PSO Algorithm has been used for the subcomponents of Potter's CCGA structure by van den Bergh and Engelbrecht [3]. Briefly, the general framework of cooperative co evolutionary algorithms has three main steps: problem decomposition, subcomponent optimization, and subcomponent adaptation. In PEAs the whole population forms in a distributed way and consists of a multiple subpopulation. Single-population master-slaves, multiple populations, fine-grained and hierarchical combinations are the main types of PEAs. The proposed algorithm in this paper differs from the PEAs in that all members of the population are interacting and there is a mutual effect between the members of the population in addition to the leaders' effect on individuals in their groups. The sum of all these interactions forms the evolutionary technique. However, in PEAs, in most cases, the interaction between subpopulations is made with the migration of individuals and evolutionary techniques used for subpopulations can be independent from each other.

III Group Leader Optimization Algorithm

3.1 General idea

Inspired by leaders in social groups and cooperative co evolutionary algorithms, we have designed a new global optimization algorithm in which there are separate groups and leaders for each group. Initially forming groups does not require members to have some similar characteristics. Instead, it is based on random selection. While CCGA and other similar algorithms decompose the solution space, and each group represents a solution for a part of the problem, in our algorithm each group tries to find a global solution by being under the influence of the group leaders which are the closest members of the groups to local or global minima. The leaders are those whose fitness values are the best in their groups, and a leader can lose its position after an iteration if another member in the same group then has a better fitness value. Since in social networks, leaders have effects on their peers, thusly the algorithm uses the some portion of leaders while generating new group members. Hence, a leader, (in most cases a local optimum) dominates all other solution candidates (group members) surrounding it, and the members of a group come closer and resemble their leader more in each iteration. In this way, the algorithm is able to search the solution space between a leader and its group members thoroughly, and so is able to search the area for a local or a global optimum (or an approximation of it) in a fast way. After a certain number of evolutions, it is obvious that the members may become too similar to their leaders. To maintain the diversity of the group, for each group, we transfer some variables from different groups by choosing them randomly. In addition to providing diversity, this one-way crossover helps a group to jump out of local minima and search new solution spaces.

3.3.2 Algorithm steps

In this section, algorithm steps are described with their reasons in sequence and are shown in Figures 1.

Step 1: Generate p number of population for each group randomly

The total population for each group is p, hence, the whole population is $n * p$ where n is the number of groups. Creation of the groups and the members are totally random.

Step 2: Calculate fitness values for all members in all groups

All solution candidates, group members, are evaluated in the optimization problem and their fitness values are assigned.

Step 3: Determine the leaders for each group:

Each group has one leader and the leaders are ones whose fitness values are the best within their respective groups. The algorithm steps 1–3 are shown in Figure 1.

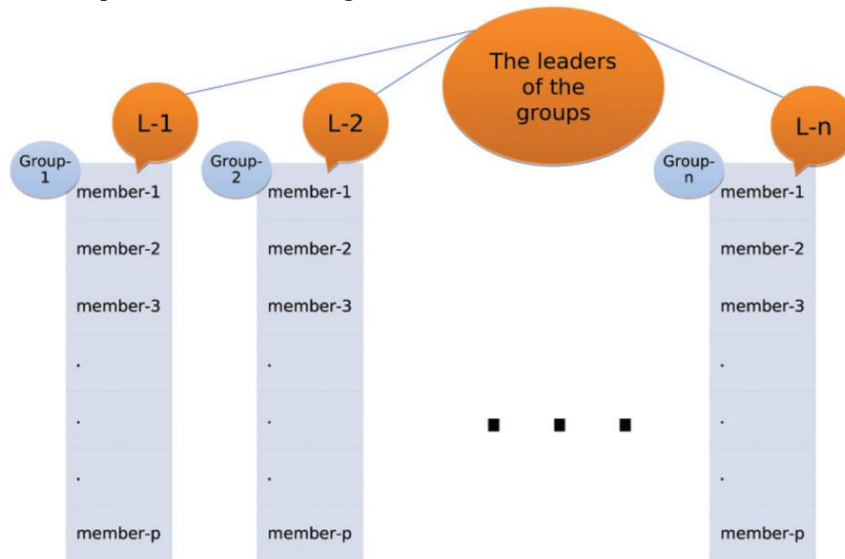


Figure 1. Steps 1–3 of the algorithm; groups consisting of p number of members are created, and their leaders are chosen based on the fitness values.

Step 4: Mutation and recombination:

Create new member by using the old one, its group leader, and a random element. If the new member has better fitness value than the old one, then replace the old one with the new one. Otherwise, keep the old member. For numerical problems, the expression simply reads;

$$\text{new} = (r1 * \text{old}) + (r2 * \text{leader}) + (r3 * \text{random})$$

In Equation (1), $r1$, $r2$, and $r3$ are the rates determining the portions of old (current) member, leader, and random while generating the new population. Although in this paper, $r1$, $r2$, and $r3$ will always sum to 1, it is not a requirement for the algorithm in general. For instance, let the current element be 0.9, the leader 1.8, and the generated random element 1.5, and suppose $r1=0.8$, $r2=0.19$, and $r3=0.01$. In this case, the new element is equal to 1.077. Then fitness values of the old and the new element are checked. If fitness (1.077) is better than the fitness (0.9), then the old element is replaced by the new one. Pseudo-code for this step is as follows:

```

for i=1 to n do
for j=1 to p do
 $\text{new}_{ij} = r1 * \text{member}_{ij} + r2 * L_i + r3 * \text{random};$ 
if fitness( $\text{new}_{ij}$ ) better than fitness( $\text{member}_{ij}$ )
then
 $\text{member}_{ij} = \text{new}_{ij};$ 
end if
end for
end for

```

In the pseudo-code: n is the number of groups, p is the number of population in each group, $r1$, $r2$ and $r3$ are the rates of the old value for the members of groups, leaders, and the random part. The expression in the inner loop is the general formula of recombination and mutation for numerical optimization problems. Depending on the value of $r1$ an element keeps its original characteristics, and depending on the value of $r2$ it becomes more like its leader during iterations. Thus, in some cases, choosing the right values for $r1$, $r2$ and $r3$ may play an important role for the algorithm to get better results during the optimization. However, choosing these parameters by obeying the property, $r3, r2_{0.5_r1}$ allows one to perform a thorough search of a solution space. Hence, this minimizes the effect of these parameters on the results. The main benefit of this evolution is that the algorithm becomes able to search the solution space surrounding the leaders (which are possibly local or global minima). Therefore, this allows the population to converge upon global minima in a very fast way. The members of the groups are not subjected to a local minimization; however, an implementation of Lamarckian concepts of evolution for the local minimization [28] gives a more stable and efficient algorithm. It is also important to note that Equation (1) looks similar to the updating equation of PSO [17]. The difference is that a member is always at its best position and the best position of a member is not saved in a parameter as is done in PSO, hence there are no information about the member's (or the particles) previous positions (values).

Step 5: Parameter transfer from other groups (One way crossover)

Choose random members starting from the first group, and then transfer some parameters by choosing another random member from another group. If this transfer makes a member have a better fitness value, then change the member, otherwise keep the original form. This process is shown in Figure 2 via pseudo code. This one-way crossover has similarities with the difference vector of Differential Evolution [29]. The difference is that the transfer operation is between the members which are in different groups. In this step, it is important to determine correct transfer rate, otherwise all populations may quickly become similar. In our experiments, transfer operation rate was taken t times [t is a random number between 1 and half of the number of total parameters (variables) plus one ($1 + \lfloor \text{parameter}/2 \rfloor$)] for each group (not for each member). And each time, only one parameter is transferred.

Figure 1. Step 5 of the algorithm: one way crossover: p th variable of an element, member of the i th group, is replaced by p th variable of the k th member of the x th group. The same operation is repeated t times for each group (maximum – half of the number of variables plus one – times for each group). The arrow at the bottom of the figure shows the direction of transfer.

Step 6: Repeat step 3–step 5 number of given iteration times

Since each group looks for the solution in mostly different spaces, Group Leaders Optimization Algorithm (GLOA) is able to search different solution spaces simultaneously. We did not place any constraint for groups to only search in subspaces, so a few groups may also search the same places. However, this does not make them redundant as they allow GLOA to find different local or global minima within the same subspace. Since each group has a leader and the leaders direct the other members of the group in order to search the area between the leader and the members of the group, it is able to search for a good solution (around the leader of the group). In addition to increasing the level of diversity of the groups, transferring some parameters (crossover) between groups allows the algorithm to direct the members of a group to search different spaces. Therefore, if a group has found some parameters correctly or very close to correct, then transferring parameters between groups allows other groups to get these parameters and find their solutions faster. Since only parameters are transferred which make the member have better fitness value, the spreading of a member who has a bad fitness value is avoided. In terms of optimization problems requiring highly diverse populations, choosing to do crossover and mutation-recombination steps without comparing fitness values may be wise and may improve the effectiveness of the algorithm.

IV Optimization Results

The parameters for the algorithm have effects on the quality of results. As stated in the previous section, choosing $r3$, $r2$ less than and $r1$ greater than 0.5 makes the algorithm more stable and minimizes the effects of these parameters. The number of groups and the population of the groups should be chosen to be large enough depending on the complexity of the problem. Therefore, while generating new elements, the rate of crossover between groups and the portions of elements, leaders, and random elements should be carefully adjusted for the type and the complexity of the optimization problem. For instance, if one takes crossover rate or the portion of the leaders too high in relation to the chosen group and population number, this may cause the whole population to become uniform very quickly. Hence, the algorithm may get stuck in a local solution, and not search the whole solution space. The algorithm was tested on different types of optimization problems, one-dimensional and multidimensional optimization test functions, and it was also used to find the minimum energy structures of Lennard-Jones clusters.

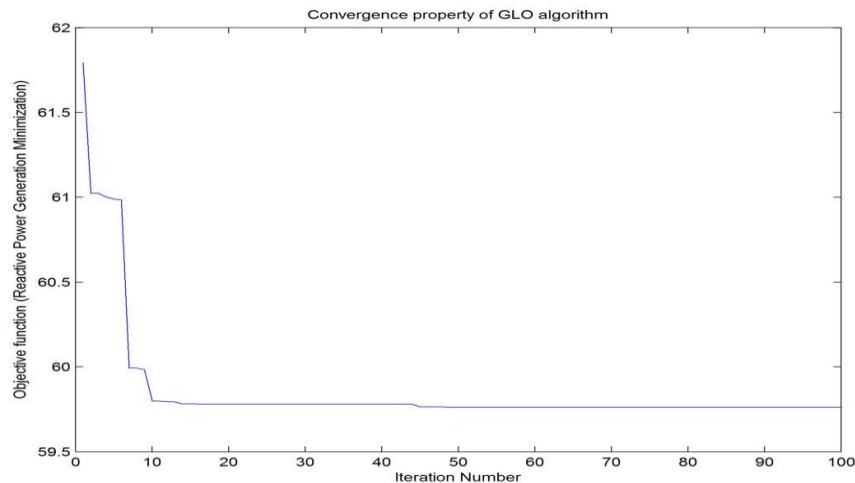
| Bus No | V | Angle | Injection | | Generation | | Load | |
|--------|--------|---------|-----------|---------|------------|--------|--------|--------|
| | PU | Degree | MW | MVar | MW | MVar | MW | MVar |
| 1 | 1.0000 | 0.0000 | 10.545 | 2.140 | 10.545 | 2.140 | 0.000 | 0.000 |
| 2 | 1.0000 | 0.0024 | 40.822 | 4.943 | 62.522 | 17.643 | 21.700 | 12.700 |
| 3 | 1.0000 | -0.8627 | 5.335 | 7.579 | 99.535 | 26.579 | 94.200 | 19.000 |
| 4 | 0.9769 | -1.781 | -47.800 | 3.900 | -0.000 | -0.000 | 47.800 | -3.900 |
| 5 | 0.9784 | -1.157 | -7.600 | -1.600 | 0.000 | 0.000 | 7.600 | 1.600 |
| 6 | 1.0000 | -0.239 | 54.906 | -4.685 | 66.106 | 2.815 | 11.200 | 7.500 |
| 7 | 0.9821 | -1.9916 | 0.000 | 0.000 | 0.000 | 0.000 | 0.000 | 0.000 |
| 8 | 1.0000 | 0.2969 | 22.263 | 10.584 | 22.263 | 10.584 | 0.000 | 0.000 |
| 9 | 0.9630 | -3.5902 | -29.50 | -16.600 | 0.000 | 0.000 | 29.500 | 16.600 |

| | | | | | | | | |
|-------|--------|---------|---------|--------|---------|--------|---------|--------|
| 10 | 0.9608 | -3.319 | -9.000 | -5.800 | 0.000 | 0.000 | 9.000 | 5.800 |
| 11 | 0.9756 | -1.9238 | -3.500 | -1.800 | 0.000 | -0.000 | 3.500 | 1.800 |
| 12 | 0.9827 | -1.409 | -6.100 | -1.600 | 0.000 | 0.000 | 6.100 | 1.600 |
| 13 | 0.9750 | -1.6598 | -13.500 | -5.800 | 0.000 | -0.000 | 13.500 | 5.800 |
| 14 | 0.9483 | -3.929 | -14.900 | -5.000 | 0.000 | 0.000 | 14.900 | 5.000 |
| Total | | | 1.972 | -13.73 | 260.972 | 59.762 | 259.000 | 73.500 |

Table : 1 Real & Reactive Power Generation of IEEE 14 under Base Cases

| From Bus | To Bus | P | Q | From Bus | To Bus | P | Q | Line Loss | |
|------------|--------|--------|--------|----------|--------|---------|--------|-----------|-------|
| | | MW | MVar | | | MW | Mvar | MW | MVar |
| 1 | 2 | -0.064 | 0.021 | 2 | 1 | 0.064 | -0.021 | 0.000 | 0.000 |
| 1 | 5 | 10.609 | 7.219 | 5 | 1 | -10.520 | -6.852 | 0.089 | 0.367 |
| 2 | 3 | 7.233 | -1.659 | 3 | 2 | -7.207 | 1.768 | 0.026 | 0.109 |
| 2 | 4 | 19.524 | 6.911 | 4 | 2 | -19.275 | -6.155 | 0.249 | 0.756 |
| 2 | 5 | 14.000 | 7.972 | 5 | 2 | -13.853 | -7.521 | 0.148 | 0.451 |
| 3 | 4 | 12.543 | 8.641 | 4 | 3 | -12.387 | -8.244 | 0.155 | 0.397 |
| 4 | 5 | -23.37 | 4.241 | 5 | 4 | 23.449 | -3.992 | 0.079 | 0.249 |
| 4 | 7 | 1.722 | -2.479 | 7 | 4 | -1.722 | 2.499 | 0.000 | 0.020 |
| 4 | 9 | 5.510 | 2.608 | 9 | 4 | -5.510 | -2.398 | 0.000 | 0.210 |
| 5 | 6 | -6.676 | -8.958 | 6 | 5 | 6.676 | 9.264 | -0.00 | 0.306 |
| 6 | 11 | 16.603 | 4.573 | 11 | 6 | -16.321 | -3.983 | 0.282 | 0.590 |
| 6 | 12 | 9.040 | 2.489 | 12 | 6 | -8.932 | -2.265 | 0.108 | 0.225 |
| 6 | 13 | 22.587 | 7.938 | 13 | 6 | -22.208 | -7.192 | 0.379 | 0.747 |
| 7 | 8 | -22.26 | -9.514 | 8 | 7 | 22.263 | 10.584 | 0.000 | 1.070 |
| 7 | 9 | 23.985 | 17.391 | 9 | 7 | -23.985 | -16.39 | -0.00 | 1.001 |
| 9 | 10 | -3.666 | 3.985 | 10 | 9 | 3.676 | -3.958 | 0.010 | 0.027 |
| 9 | 14 | 3.661 | 3.538 | 14 | 9 | -3.625 | -3.462 | 0.036 | 0.076 |
| 10 | 11 | -12.67 | -1.842 | 11 | 10 | 12.821 | 2.183 | 0.146 | 0.341 |
| 12 | 13 | 2.832 | 0.665 | 13 | 12 | -2.813 | -0.647 | 0.019 | 0.018 |
| 13 | 14 | 11.521 | 2.039 | 14 | 13 | -11.275 | -1.538 | 0.246 | 0.501 |
| Total Loss | | | | | | | | 1.972 | 7.461 |

Table: 2 Optimized Reactive Power using Group Leader Optimization



v. Conclusion

The proposed algorithm is developed using MATLAB-7.10 software. In this paper GLO algorithm is applied to solve minimal reactive power generation by controlling VG keeping all the equality and inequality constraints under deregulated power system operating range. Optimization process stops whenever preset convergence criteria matches. In this paper, as test case IEEE 14-bus system is considered where four generator buses are there for which minimal reactive power generation is tried to be implemented.

References

- [1] L. L. Lai. **“Power system restructuring and deregulation”**, Fourteenth reprint, John Wiley and Sons Limited, april, 2002.
- [2] H. Yang, H. Chao and C. Kun-wei, “Optimal power flow in deregulated electricity markets”.
- [3] V.L. Paucar and M.J. Rider, “Reactive power pricing in deregulated electrical market using a methodology based on the theory of marginal costs”, IEEE Proc, 2001
- [4] Saini and A. K. Saxena, “Optimal power flow based congestion management methods for competitive electricity markets”, IJCEE, vol. 2(1), pp. 1793-81633, 2010.
- [5] H. Wu, C. W. Yu, N. Xu and X. J. Lin, “An OPF based approach for assessing the minimal reactive power support for generators in deregulated power systems”, Electric Power & Energy Systems, vol. 30, pp. 23-30, 2008.
- [6] H. Sadat. “Power system analysis”, Fourteenth reprint, Tata McGraw-Hill Publishing Company limited, 2008.
- [7] Saini and A. K. Saxena, “Optimal power flow based congestion management methods for competitive electricity markets”, IJCEE, vol. 2(1), pp. 1793-81633, 2010
- [8] V.L. Paucar and M.J. Rider, “Reactive power pricing in deregulated Electrical market using a methodology based on the theory of marginal Costs”, IEEE Proc, 2001.
- [9] Dommel H.W. and Tinney W.F “Optimal power flow solutions“IEEE Transactions on Power Apparatus and Systems, PAS- 87, pp. 1866– 1876, October 1968.
- [10]Barbosa HJC and Lemonge ACC. “A new adaptive penalty scheme for genetic algorithms” Information Sciences 2003; 156(3–4):215–251.
- [11]Neumaier A. “Complete search in continuous global optimization and constraint satisfaction” ACTA NUMERICA, 2004; 13:271–370.
- [12]Griewank A and Walther A. “Evaluating Derivatives: Principles and Techniques of Algorithmic Differentiation” (2nd edition). SIAM, 2008.
- [13]Venter G and Haftka RT. “Constrained particle swarm optimisation using a multi-objective formulation”. In Proceedings of the 9th International Conference on Computational Structures Technology, Athens, Greece, Sep 2–5 2008.
- [14]T. Weise, “Global Optimization Algorithms – Theory and Application (Thomas Weise, University of Kassel, Germany, 2007)”, <http://www.it-weise.de/projects/book.pdf4>
- [15]E. Cantu-Paz, Efficient and Accurate Parallel Genetic Algorithms (Kluwer Academic Publishers, Norwell, MA, 2000).

Advanced Embedded Design Based Power System Maximum Demand Prediction and Controller for Efficient Power Management by Using Proteus

Ramesh J ¹, Balaji J ²

Assistant Professor, EEE Department, St. Anne's College of Engg. & Technology, Panruti, India ¹

Lecturer, EEE Department, Annai Velankanni Polytechnic College, Panruti, India ²

Abstract

The demand for energy is increasing as a result of the growth in both population and industrial development. To improve the energy efficiency, consumers need to be more aware of their energy consumption. In recent years, utilities have started developing new electric energy meters which are known as smart meters. A smart meter is a digital energy meter that measures the consumption of electrical energy and provides other additional information as compared to the traditional energy meter. The aim is to provide the consumer and supplier an easy way to monitor the energy. Smart energy meters can also store and review our consumer energy consumption according to day, month and year wise. Smart energy meters can also sense and protect some electrical interference like, Magnetic interference, phase reversal, phase over voltage, phase over current. Smart meters will enable two-way and real-time communication between the consumers and the provider.

Keywords: MDI, Power factor, Penalty, Load management

I. Introduction

Power is measured in monetary amounts, while energy is the vital of power over the long run. For instance, a 100 W light retains 100 W of power. On the off chance that worked for one hour, that light ingests 100 W - hours of energy. Greatest demand is the most extreme quick power devoured over a detailed window of time. On account of that 100 W bulb, as it is exchanged on and off, the immediate demand goes from zero to 100 W to zero, and so on. Not exceptionally intriguing. At the same time if that bulb is worked in parallel with a second 100 W light that is left on constantly, the demand will switch promptly between 100 W and 200 W, and the greatest demand of the blend will be 200 W. Presently, the way this is connected is that electric appropriation utilities frequently incorporate demand as one of the components used to focus the charge the buyer gets. Notwithstanding measuring incorporated energy utilization over the charging period (regularly a month), they additionally measure demand. Instead of measuring genuinely immediate qualities, they really measure energy over a short window of time, and after that partition the energy devoured amid that interim by the length of the interim to touch base at successful peak esteem for the interim.

The best normal estimation of the power, apparent power, or current devoured by a client of an electric power system, the midpoints being assumed control progressive time periods, normally 15 or 30 minutes long and It is the best demand of burden on the power station amid a given period, i.e., the most extreme of every last one of demands that have happened amid a given period (may be a day, may be an hour, and so forth).

- Need maximum demand in the Electricity bill?

When the rate of electrical energy is charged on the basis of maximum demand of the consumer and the units consumed, it is called a two-part tariff.

- In this total charge is divided into two.

1. Fixed charge depends on the maximum demand of the consumer.

2. Running charge depends on no. of units consumed. It is measured by installing a maximum demand meter. Charges are made on the basis of maximum demand in KVA and not in kW.

- The maximum demand is further split into four types, namely:

1. Daily maximum (0530h to 1630h and 1830h to 2100h).

2. Restricted maximum (1630h to 1830h).

- 3. Night maximum (2100 h to 0500h).
- 4. Weekend maximum (Saturday 0500h to Monday 0500h).

Each type of maximum demand has a different tariff. Maximum demand is usually measured as an average over a half hour period. The maximum half hour average reached during the month gives the monthly maximum demand charge (Gaggioli 1983; and Clive Beggs, 2002).

It is important to note that while maximum demand is recorded, it is not the instantaneous demand drawn, as is often misunderstood, but that integrated demand over the predefined recording cycle.

As example, in an industry, if the drawl over a recording cycle of 30 minutes is:

2500 KVA for 4 minutes

3600 KVA for 12 minutes

4100 KVA for 6 minutes

3800 KVA for 8 minutes

The MD recorder will be computing MD as:

$$\frac{(2500 * 4 + 3600 * 12 + 4100 * 6 + (3800 * 8))}{30}$$

30

$$= 3606.7 \text{ KVA}$$

As can be seen from the Figure 1 below, the demand varies from time to time. The demand is measured over a predetermined time interval and averaged out for that interval as shown by the horizontal dotted line.

II.MDI Penalty

The MDI penalty can be avoided by improving the power factor and by using more efficient appliances.

The MDI penalty can be avoided by improving the power factor and by using more efficient appliances. Another option of avoiding MDI penalty is by shifting your peak load to a time of day when your load is less.

There are 2 methods of calculating MD (Maximum Demand):

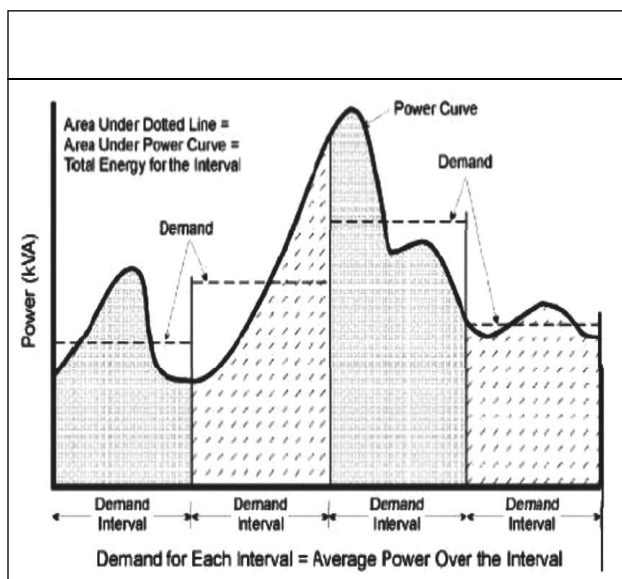


Figure 1: Power and Demand Curve

III. Normal Or Block Method

Toward the end of each one fix integrating period, normal power for that period is ascertained. On the off chance that this quality is more noteworthy than officially existing esteem then this is put away as the MD.

IV. Sliding window method

Toward the end of a sub incorporating period the average power is ascertained for one coordinating period. In the event that this quality is more prominent than the officially existing esteem then this is put away as MD. The incorporating period slides by a window of the sub incorporating period (Capasso and so forth every one of the., 1994; and World Bank, 2012).

| MO No. | MO No. | MO No. | MO No. |
|--------|--------|--------|--------|
| MD 1 | MD 1 | MD 1 | MD 1 |
| MD 2 | MD 2 | MD 2 | MD 2 |

Assume a load pattern of following type:

$T = 09.00, T = 09.15, T = 09.30, T = 09.45,$
 $T = 10.00$

20 KVA, 30 KVA, 30 KVA, 20 KVA

15 mins, 15 mins, 15 mins, 15 mins

For MD 1 (Sliding window method) Demand - 09.00 to 09.30 block

$$\frac{(20 * 15 + 30 * 15)}{30} = 25\text{KVA}$$

Demand - 09.15 to 09.45 block

$$\frac{(30 * 15 + 30 * 15)}{30} = 30\text{KVA}$$

Demand - 09.30 to 10.00 block

$$\frac{(30 * 15 + 20 * 15)}{30} = 25\text{KVA}$$

MD 1 at the end of 10.00 = 30 KVA.

For MD 2 (Block method)

Demand - 09.00 to 09.30 block

$$= \frac{(20 * 15 + 30 * 15)}{30} = 25\text{KVA}$$

Demand - 09.30 to 10.00 block

$$= \frac{(30 * 15 + 20 * 15)}{30} = 30\text{KVA}$$

MD 2 at the end of 10.00 = 25 KVA Normally MD is reset on the first of every month, i.e., on a Monthly basis.

V. Microcontroller based mdi

The conventional greatest demand metering utilized conventional meters with current transformers and the meter dealt with a 15 moment normal with a pointer which showed the most extreme arrived at since the last time the pointer was reset.

It has several drawbacks, as:

The meter did not correspond precisely to the supply authority's meter values because of differences in the averaging times and differences in reset time.

This meter couldn't be monitored continuously and high greatest demand values were regularly recorded when problems happened in the factory and the administrator had neglected to recognize the excessive most extreme demand.

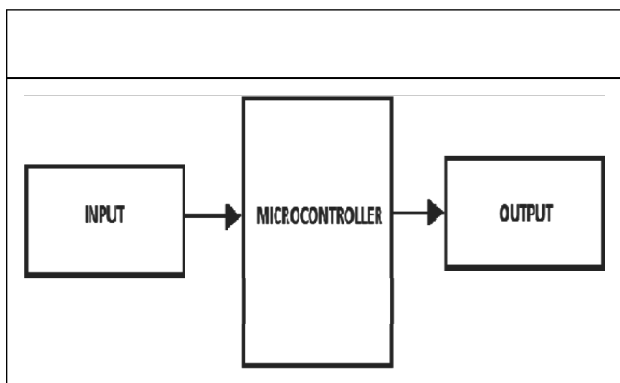


Figure 2: Microcontroller Based MDI

- It was very difficult to discover exactly when the maximum demand had been exceeded due to a lack of any recording.
- It was difficult to predict the effects of adding or removing load.

It was difficult to predict the effects of adding or removing load. So, a microcontroller based MDI and Controllers are introduced.

It calculates the KVA and kW values approximately every minute and displays these on the VDU for the power station attendant or shift electrician to see. Every half hour, at the end of each metering period (after a reset has occurred), the KVA, kW and power factor recorded during that time, is printed by the printer together with a simple graph comparing the actual KVA with the set point (Cobus,2003; and IOSR, 2012).

The load shedding of the feeders can be based on several logics which lead to the development of different strategies for the demand controllers.

For designing the MDI there are three main strategies for calculation of MDI As:

A. Rotating Strategy

In a rotating strategy, an equal distribution of power is provided to all controlled loads. This strategy is suitable when all areas require an equal share of power.

B. *Fixed Priority Strategy*

A Fixed priority strategy not just sheds the slightest imperative loads first and the most essential burden last. The altered priority strategy has the preference of keeping high priority ranges supply "ON" while low priority territories will be "OFF" amid crest demand periods.

C. *Combination Fixed/Rotate Strategy*

It is the most versatile and powerful strategy because there are so many possible combinations A combination load strategy allows groups of rotating loads to be programmed with or without fixed priority loads. This can result in the maximum efficiency and energy cost savings.

It is the most versatile and powerful strategy because there are so many possible combinations. A combination load strategy allows groups of rotating loads to be programmed with or without fixed priority loads. This can result in the maximum efficiency and energy cost savings.

In addition to the measurement of the MDI this project has a capability of detection and indication as there is a close relationship between the frequency and the power (demand/supply) which is shown in Figure 3 below.

Vi. **Electrical load management**

Need for Electrical Load Management

In a macro perspective, the growth in the electricity use and diversity of end use segments in time of use has led to shortfalls in capacity to meet demand. As capacity addition is costly and only a long time prospect, better load management at user end helps to minimize peak demands on the utility infrastructure as well as better utilization of power plant capacities.

The utilities (State Electricity Boards) use power tariff structure to influence end users in better load management through measures like time of use tariffs, penalties on exceeding allowed maximum demand, night tariff concessions, etc. Load management is a powerful means of efficiency improvement both for the end user as well as utility.

As the demand charges constitute a considerable portion of the electricity bill, from a user angle too there is a need for integrated load management to effectively control the maximum demand (Brown, 2008; and Steve *et al.* 2010).

VII. **Maximum demand control**

Step By Step Approach for Maximum Demand Control:

A. *Load Curve Generation*

Presenting the load demand of a consumer against time of the day is known as a 'load curve'. If it is plotted for the 24 hours of a single day, it is known as an 'hourly load curve' and if daily demands are plotted over a month, it is called daily load curves.

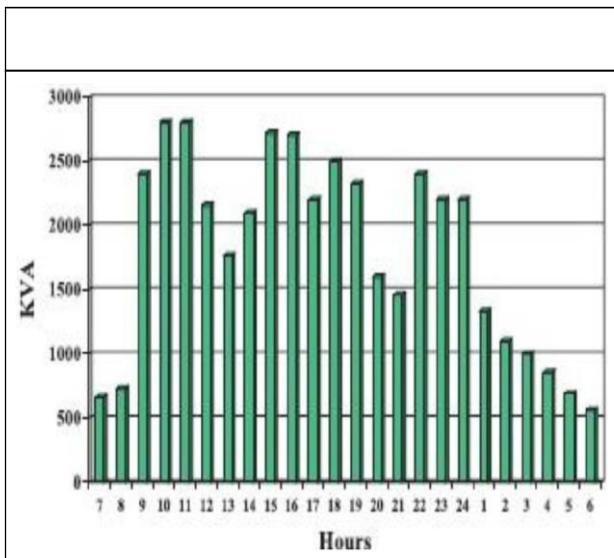


Figure 4: Load Curve

These types of curves are useful in predicting patterns of drawl, peaks and valleys and energy use trends in a section or in an industry or in a distribution network as the case may be.

B. *Rescheduling of Loads*

Rescheduling of large electric loads and equipment operations, in different shifts can be planned and implemented to minimize the simultaneous maximum demand. For this purpose, an operation flow chart and a process chart are prepared. Analyzing these charts and with an integrated will help to improve the load factor which in turn reduces the maximum demand approach.

C. *Storage of Products/in Process Material/Process Utilities Like Refrigeration*

It is possible to reduce the maximum demand by building up storage capacity of products materials, water, chilled water and hot water, using electricity during off peak periods.

D. *Shedding of Non-Essential Loads*

When the maximum demand tends to reach a preset limit, shedding some of non- essential loads temporarily can help to reduce it. Sophisticated microprocessor controlled systems are also available, which provide a wide variety of control options like:

- Accurate prediction of demand.
- Graphical display of present load, available load, demand limit.
- Visual and audible alarm.
- Automatic load shedding in a predetermined sequence.
- Automatic restoration of load.
- Recording and metering

E. *Operation of Captive Generation and Diesel Generation Sets*

When diesel generation sets are used to supplement the power supplied by the electric utilities, it is advisable to connect the DG sets for durations when demand reaches the peak value. This would reduce the load demand to a considerable extent and minimize the demand charges.

F. *Reactive Power Compensation*

The maximum demand can also be reduced at the plant level by using capacitor banks and maintaining the optimum power factor. Capacitor banks are available with microprocessor based control systems. These systems switch on and off the capacitor banks to maintain the desired Power factor of the system and optimize maximum demand thereby (Calcutta *et al.*, 1998; and Collabus, 2003).

VIII. Power Factor Improvement And Benefits

A. Power Factor Basics

In all industrial electrical distribution systems, the major Loads are resistive and inductive. Resistive loads are incandescent lighting and resistance heating. In case of pure resistive loads, the voltage (V), current (I), resistance (R) relations are linearly related,

i.e.,

$$\text{Voltage (V)} = IR$$

$$\text{And Power (kW)} = VI$$

Typical inductive loads are AC Motors, induction furnaces, transformers and ballast- type lighting.

Inductive loads require two kinds of power:

1. Active (or working) power to perform the work, and
2. Reactive power to create and maintain electromagnetic fields.

Active power is measured in kW (Kilo Watts). Reactive power is measured in KVAR (Kilo Volt-Amperes Reactive).

The vector sum of the active power and reactive power make up the total (or apparent) power used. This is the power generated by the SEBs for the user to perform a given amount of work. Total Power is measured in KVA (KiloVolts-Amperes).

The active power (shaft power required or true power required) in kW and the reactive power required (KVAR) are 90° apart in a pure inductive circuit,

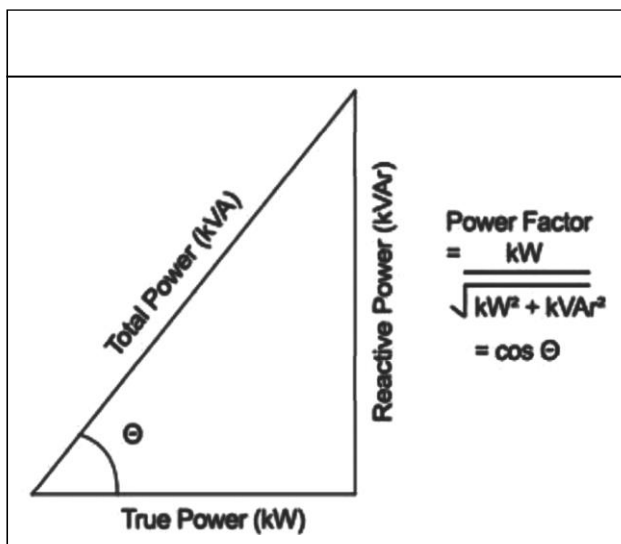


Figure 5: Power Triangle

The active power (shaft power required or true power required) in kW and the reactive power required (KVAR) are 90° apart vectors in a pure inductive circuit, i.e., reactive power KVAR lagging the active kW. The vector sum is called the apparent power or KVA, as illustrated above and the KVA reflects the actual electrical load on the distribution system (Brown, 2008).

The ratio of kW to KVA is called the power factor, which is always less than or equal to unity. Theoretically, when electric utilities supply power, if all loads have unity power factor, maximum power can be transferred for the same

distribution system capacity. However, as the loads are inductive in nature, with the power factor ranging from 0.2 to 0.9, the electrical distribution network is stressed for capacity at low power factors.

B. Improving Power Factor

The solution to improve the power factor is to add power factor correction capacitors to the plant power distribution system.

They act as reactive power generators, and provide the needed reactive power to accomplish kW of work. This reduces the amount of reactive power, and thus total power, generated by the utilities.

IX. Advantages of PF Improvement By Capacitor Addition

- Reactive component of the network is reduced and so also the total current in the system from the source end.
- I²R power losses are reduced in the system because of reduction in current.
- Voltage level at the load end is increased.
- KVA loading on the source generators as also on the transformers and lines up to the capacitors reduces giving capacity relief. A high power factor can help in utilizing the full capacity of your electrical system (Calcutta *et al.*, 1998; and Mc Donald, 2003).

X. Cost Benefits of PF Improvement

While costs of PF improvement are in terms of investment needs for capacitor addition the benefits to be quantified for feasibility analysis are:

- Reduced KVA (Maximum demand) charges in utility bill.
- Reduced distribution losses (KWH) within the plant network.
- Better voltage at motor terminals and improved performance of motors.
- A high power factor eliminates penalty charges imposed when operating with a low power factor.
- Investment on system facilities such as transformers, cables, switchgears, etc., for delivering load is reduced

Xi. Maximum Demand Controller

High-Tension (HT) consumers need to pay a maximum demand charge notwithstanding the usual charge for the number of units expended. This charge is generally taking into account the most astounding measure of force utilized amid some period (say 30 minutes) amid the metering month. The maximum demand charge regularly speaks to an extensive extent of the total bill and may be in view of one and only segregated 30 moment episode of high power utilization.

Considerable savings can be realized by monitoring power use and turning off or reducing non-essential loads during such periods of high power use.

Maximum Demand Controller is a device designed to meet the need of industries conscious of the value of load management. Alarm is sounded when demand approaches a preset value. If corrective action is not taken, the controller switches off non-essential loads in a logical sequence.

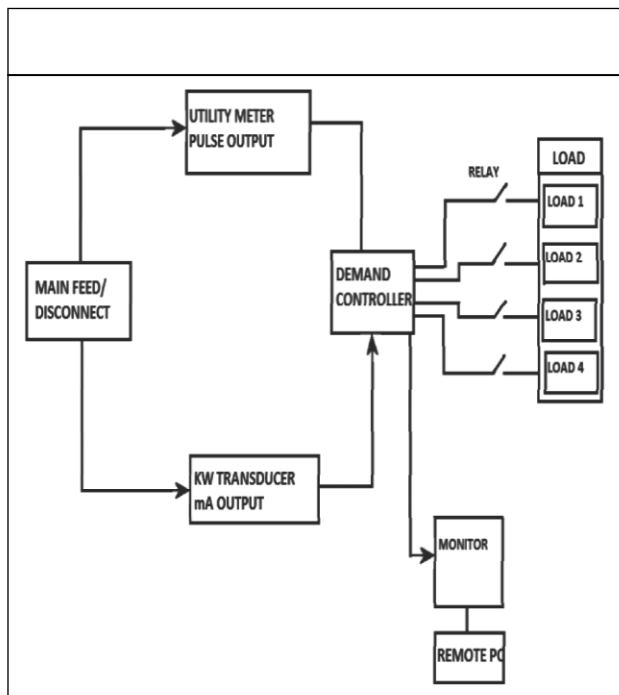


Figure 6: Demand Controller

This sequence is predetermined by the user and is programmed jointly by the user and the supplier of the device. The plant equipment selected for the load management are stopped and restarted as per the desired load profile.

Demand control scheme is implemented by using suitable control contactors. Audio and visual annunciations could also be used.

XII. Conclusion

A good record of the load pattern is obtained which enables accurate predictions and better load distribution. The capital outlay for maximum demand control is low. With a good maximum demand indicator, it is possible to create awareness of where and when power is used and consequently gets greater power utilization. The data obtained from the MDI controller may be used for the design and development of Smart Grid and helpful for prediction of estimated load in large load dispatch centres.

Proper utilization of electrical power during off peak period and the data obtained from the MDI controller is useful for the automation of the Distribution system.

References

- [1] Mc Donald John D (2003), Electric Power Substation on Engineering, pp. 124-192.
- [2] Cobus S (2003), Electrical Network Automation and Communication Systems, pp. 142-153.
- [3] Calcutta David M, Cowan J Frederick and Parchizadeh Hassan G (1998), 8051Microcontrollers Hardware, Software and Applications, pp. 1-13.
- [4] Mostafa Al Mamun, Ken Nagasaka and Salim Reza S (2004), 3rd International Conference on Electrical & Computer Engineering, ICECE 2004, December 28-30, Dhaka, Bangladesh.
- [5] El-Sayed Y M (1999), "Revealing the Cost Efficiency Trends of the Design Concepts of Energy-Intensive Systems", Energy Conversion and Management, Vol. 40, pp. 1599-1615.
- [6] Capasso A, Grattieri W *et al.* (1994), "A Bottom-Up Approach to Residential Load Modeling", IEEE Transactions on Power Systems, Vol. 9, No. 2, May.
- [7] Brown Richard (2008), Electrical Power Distribution Reliability, pp. 17-34.
- [8] World Bank, World Development Indicators – Last Updated March 2, 2011 Energy Statistics 2012 (19th Issue), Issued by Central Statistics Office, Ministry of Statistics and Programmed Implementation, Govt. of India, New Delhi.
- [9] Microcontroller Based Substation Monitoring and Control System with GSM Modem", IOSR Journal of Electrical and Electronics Engineering (IOSRJEEE).

- [10] Steve Hsiung, John Ritz, Richard Jones and Jim Eilan (2010), "Design and Evaluation of a Microcontroller Training System for Hands-on Distance and Campus-Based Classes", Journal of Industrial Technology, Vol. 26, No. 4.
- [11] Gaggioli R (Ed.) (1983), Efficiency and Costing, ACS Symposium Series 235.
- [12] Clive Beggs (2002), Energy Management Supply and Conservation, Butterworth Heinemann.

Optimal Design of Energy Saving for Single Phase Induction Motor

A.Sundara Pandiyan
Assistant Professor,EEE department.
ST.Anne's college of Engineering and Technology

Abstract

This project presents the energy conservation and speed control of single phase induction motor using microcontroller. In this project we are designing a circuit for energy conservation for partial load machines. We can implement soft starting and speed control can also be achieved besides doing energy conservation. The advantages of this project are mainly 45-50 percent of energy conservation. Smooth starting of motor is also achieved. Speed control can also be done using this circuit. Our project deals with single phase induction motors, since they are mostly subjected to partial loads. By controlling the amount of voltage supplied to the induction motor and using a microcontroller it is possible to achieve energy saving and speed control. The energy conservation on single phase induction motors is simulated using MATLAB. The circuits for NO LOAD and FULL LOAD are simulated. The simulated results coincide with the experimental results. The voltage supplied to the induction motor is chopped off using the MOSFET, whose firing angle is determined by the microcontroller. The control circuit, power circuit & driver circuit are fabricated on general purpose PCB. The required amount of voltage which needs to be supplied when the motor is running at NO LOAD and FULL LOAD can be obtained from the circuits. Also, the simulation results coincide with the hardware results.

Index Terms— induction motor, microcontroller, chopper , optical sensor

I. Introduction

In electrical power intensive industries like cement, glass, paper, metal etc., where the electricity bill costs more than 30% of raw material cost, it is necessary to benchmark the unit consumption per ton of final product output.AC variable speed drive is one of the many well-known solutions to achieve this goal. The growing popularity of ac drives is chiefly due to its ability to control the speed of induction motor, which is most commonly used in industry. Induction motor is the most cost effective motor. It is considerably smaller, lighter, and more readily available. It is rugged, and virtually maintenance free motor. In Industrial complexes many induction motors may often be running at no or low partial loads. Irrespective of the load conditions, these motors are however always connected to the mains.

Due to the applied rated voltage at stator terminals, rated iron losses have to be supplied constantly to the motors. If it were possible by means of an additional switching device to reduce the terminal voltage of induction motors at no and low partial load, some electrical energy might be saved. Three phase induction motors have high efficiency to less than 50% of load. Large induction motors are inherently very efficient with efficiency as high as 95% at full load. Experiments have revealed that there can be very little advantage in using an energy saving algorithm on anything other than a small inefficient motor. The potential to save energy with a solid-state energy saving device, only becomes a reality when the motor efficiency has fallen. So we have chosen single-phase induction motor.

Literature Review

This project is based on the IEEE paper “Energy saving operation of Induction motor by voltage reduction at no and low partial load”, by Basanta B.Palit, Basle of technology. It gives us the information about the various methods for reducing the terminal voltages to save energy.

Objective Of This

The aim of the project deals with energy saving scheme for single-phase induction motor. It includes the following, Control of output voltage by varying the firing angle. Calculation of energy that is being saved.

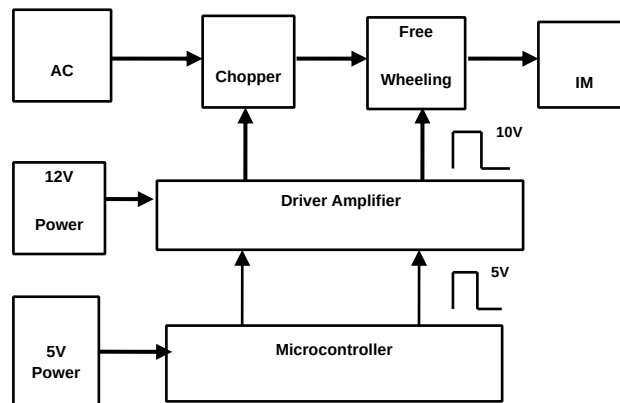
Aim And Scope Of Investigation

The aim of this project to simulate AC Chopper system with Induction motor load in closed loop. This is implemented in Hardware with the help of microcontroller.

Advantages:

1. Speed can be varied using firing angle delay.
2. Fast response
3. Input power factor can be improved.

Block Diagram



AC Source

AC source is given to the AC Chopper circuit. According to the pulses obtained from the Driver amplifier the Thyristor switch connected between the ac supply and load varying the voltage applied to the Induction motor can controls the power flow in which the motor rotates. When the Thyristor switch starts conduction the current flows in the circuit produces negative pulses which decays the circuit. So to avoid this occurrence Free wheeling diode is used which avoids the unwanted pulses which avoids damage to the motor. Microcontroller is the programming device used here to produce the pulses. 5V power supply is given to the microcontroller. The microcontroller used here is 89C51. It is used to produce the delay to firing pulse of the thyristor. The output of the microcontroller is given to the driver circuit. Driver circuit consists of Opto Coupler which acts as an isolator. The LED of driver circuit initiates Opto Coupler to produce pulses and the output of this OptoCoupler is given to the gate of the Thyristor switch. According to the firing angle thyristor switch of the AC chopper circuit controls the power flow which is used to save the energy.

3.1.2. AC Chopper Circuit

When a Thyristor Switch is connected between the AC Supply and load varying the voltage applied to the load can control the power flow, and this type of power circuit is known as ac chopper.

The most common applications of this are

- Industrial heating
- On-load Transformer connection charging
- Light control Speed control of polyphase induction motors
- AC magnet controls

Induction Motor

Single-Phase Induction Motor is used here. Single-Phase Induction Motor is not Self-starting. However, if the rotor of such a machine is given an initial start in either direction, then immediately a torque arises and the motor accelerates to its final speed.

Advantages of using single-phase induction motor are the following

- Easy erection and installation
- Rugged in construction
- Low maintenance
- Environmental Compact ability

Single-phase induction motor is used for the following

- Fans, grinders, blowers
- Centrifugal Pumps
- Washing machines
- Refrigerators and air conditioners etc.

Free-Wheeling Circuit

When Thyristor switch conducts the current flows through the circuit produces negative going pulses. To avoid the unwanted negative going pulses free wheeling circuit is used.

Microcontroller

The Microcontroller used here is 89c51. It is used to produce delay to the firing pulse of the thyristor. 5V power supply is given to the Microcontroller.

driver amplifier

The output of Microcontroller is given to the Driver circuit which has Opto Coupler. Opto Coupler is used as an isolator. Opto coupler combines an infrared light-emitting diode. According to the LED Glows the Opto Coupler produces the output pulses. The output of the Opto Coupler is given to the gate of the thyristor.

Analysis Of Power Circuit And Its Load

No load operation:

Under no load condition of the Induction Motor the voltage is changed in steps from 20% up to 100% of the rated voltage. At each voltage level the motor is run for sometime, during which the energy is measured. It is clear from the results that the energy consumption is reduced by nearly 50% as the voltage is decreased from rated value to 20% of the rated value.

Low partial-load operation:

The Energy saving at partial loads will be modest. However, by decreasing the terminal voltage energy can be saved at partial loads between 0 and 20% of the rated value. This, of course is at the cost of the speed, which decreases. On the other hand, there is an improvement in the power factor and the efficiency as we decrease the terminal voltage

Calculation Of Induction Motor

Under No load Condition

For Speed=1450 rpm; Slip=0.33

$$Z1=3.46+j2.4 \Omega$$

$$Z2= (j40.55*(52.42+j1.2))/(52.42+j40.55+j1.2)$$

$$=2126.187L91.311/67.0143L38.535$$

$$=19.192+j25.263 \Omega$$

$$Z3= (j40.55*(.88+j1.2))/(.88+j40.55_j1.2)$$

$$=60.327L143.76/41.758L88.793$$

$$=0.8494+j1.167 \Omega$$

$$Z=Z1+Z2+Z3$$

$$=23.5014+j28.83$$

$$=37.159L50.814 \Omega$$

$$V=230*(((3.6066-2.513).5*\sin (2*2.513)- 5*\sin (2*3.6066)))/3.14)^.5)$$

$$=60.4875V$$

$$\text{Stator Current } I_s = V/Z$$

$$=60.4875/37.159$$

$$=1.6278A$$

$$\text{Stator copper loss} = (1.6278)^2 \times 3.46$$

$$=9.168 \text{ watts}$$

$$\text{Rotor current } I_r = I_s \times Z_a / (Z_a + Z_b)$$

$$S = (1.6278 \times j40.55) / (j40.55 - j1.2_52.42)$$

$$=j66.0073/52.42 - j41.75$$

$$=.985L51.485$$

$$\text{Rotor copper loss} = (.985)^2 \times 3.46$$

$$=3.357 \text{ watts}$$

$$\text{Iron loss} = 1.732 \times 60.4875 \times 1.6278 \times \cos(50.814) - 9.168 - 3.357$$

$$=95.253W$$

$$\text{Total loss} = 9.168 + 3.357 + 95.253$$

$$=107.77 \text{ Watts}$$

Energy Saving Calculation

From experiment conducted at no load when V=220 volts, the power was found to be 212 watts.

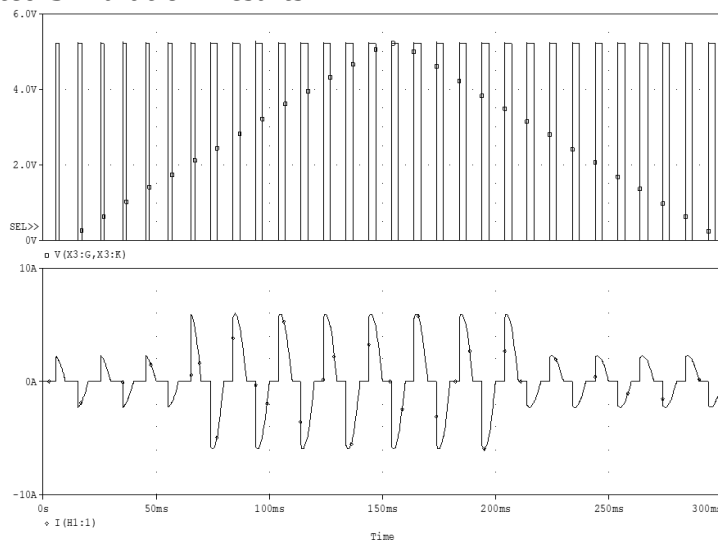
$$\text{Energy saved} = ((W_{\text{rated}} - W_{\text{reduced}}) / W_{\text{rated}}) \times 100$$

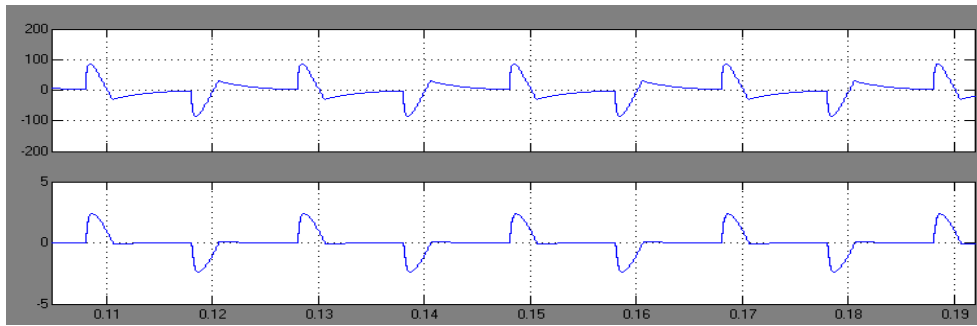
$$= ((212 - 107.77) / 212) \times 100\%$$

$$=49.17\%$$

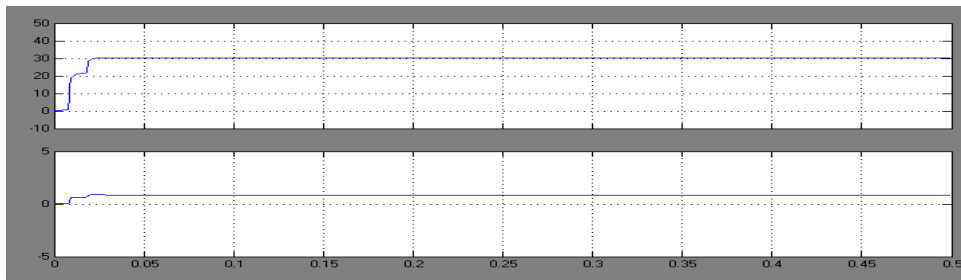
which is 50% of energy is saved.

Expected Simulation Results

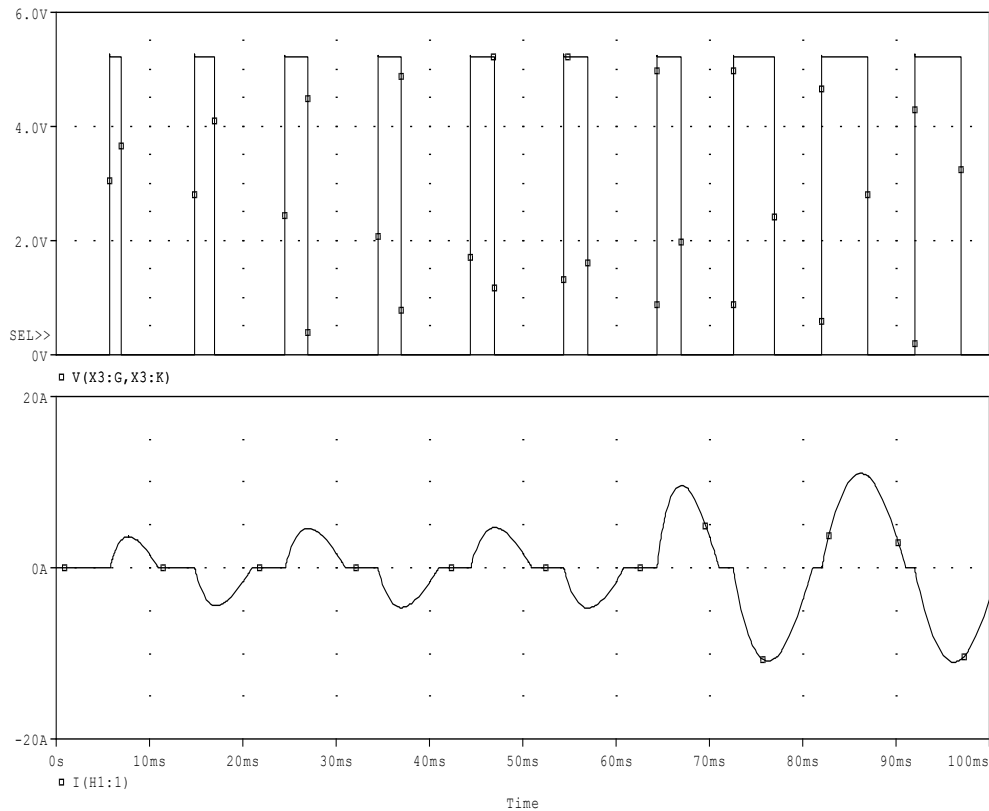




Voltage and Current Output at $\alpha=144$ Degree



RMS Voltage and Current Output at $\alpha=144$ Degree



Output Current and Voltage Waveform

Conclusion

Energy saver circuit for Induction Motor is simulated using ORCAD PSPICE. A circuit model is developed for simulating closed loop system. This circuit can provide Soft Starting, Speed Control and Energy Saving. The circuit is simulated under no load and full load conditions.

The driver circuit, synchronization circuit and power circuit are fabricated on PCB and tested. Later the circuit is tested using PCB system. The experimental waveforms coincide with the simulation results. The energy saving of 50% can be obtained only on no-load. The energy saving is applicable only for duty loads. Thus the energy saving is possible only under no-load condition.

References

1. H. Huang, E. F. Fuchs, and J. C. White, "Optimal placement of the run capacitor in single-phase induction motor designs", *IEEE Trans. Energy Convers.*, vol. 3, no. 3, pp.647 -652 1988
2. H. Huang, E. F. Fuchs, and J. C. White, "Optimization in single-phase induction motor design, part II: the maximum efficiency and minimum cost of an optimal design", *IEEE Trans. Energy Convers.*, vol. 3, no. 2, pp.357 -366 1988
3. D. E. Cattermole and R. M. Davis, "A triac voltage (speed) control for improved performance of split-phase fan motors", *IEEE Trans. Power App. Syst.*, vol. PAS-94, no. 3, pp.786 -791 1975
4. D. E. Cattermole, R. M. Davis, and A. K. Wallace, "The design optimization of a split phase fan motor with triac voltage (speed) control", *IEEE Trans. Power App. Syst.*, vol. PAS-94, no. 3, pp.778 -785 1975
5. J. D. Law and T. A. Lipo, "A single phase induction motor voltage controller with improved performance", *IEEE Trans. Power Electron.*, vol. PE-1, no. 4, pp.240 -247 1986
6. T. A. Lettenmaier, D. W. Novotny, and T. A. Lipo, "Single-phase induction motor with an electrically controlled capacitor", *IEEE Trans. Ind. Appl.*, vol. 27, no. 1, pp.38 -43 1991
7. E. Muljadi, Y. Zhao, T. H. Liu, and T. A. Lipo, "Adjustable ac capacitor for a single-phase induction motor", *IEEE Trans. Ind. Appl.*, vol. 29, no. 3, pp.479 -485 1993
8. T. H. Liu, "A maximum torque control with a controlled capacitor for a single-phase induction motor", *IEEE Trans. Ind. Electron.*, vol. 42, no. 1, pp.17 -24 1995
9. K. Sundaraseswaran, "An improved energy-saving scheme for capacitor-run induction motor", *IEEE Trans. Ind. Electron.*, vol. 48, no. 1, pp.238 -240 2001
10. E. R. Collins, "Torque and slip behavior of single-phase induction motors driven from variable-frequency supplies", *IEEE Trans. Ind. Appl.*, vol. 28, no. 3, pp.710 -715 1992
11. C. C. Liu, C. M. Young, and C. H. Liu, "New inverter-driven design and control method for two-phase induction motor drives", *Proc. Inst. Elect. Eng., Electr. Appl.*, vol. 143, no. 6, pp.458 -466 1996
12. M. B. R. Corrêa, C. B. Jacobina, A. M. N. Lima, and E. R. C. Silva, "Rotor-flux-oriented control of a single-phase induction motor drive", *IEEE Trans. Ind. Electron.*, vol. 47, no. 4, pp.832 -841 2000
13. M. M. Morcos, J. A. Mowry, and A. J. Heber, "A solid-state speed controller for capacitor motors driving ventilation fans", *IEEE Trans. Ind. Appl.*, vol. 30, no. 3, pp.656 -662 1994
14. A. L. Julian, R. S. Wallace, and P. K. Sood, "Multi-speed control of single-phase induction motors for blower applications", *IEEE Trans. Power Electron.*, vol. 10, no. 1, pp.72 -77 1995
15. E. F. Fuchs, A. J. Vandenput, J. Höll, and J. C. White, "Design analysis of capacitor-start, capacitor-run single-phase induction motors", *IEEE Trans. Energy Convers.*, vol. 5, no. 2, pp.327 -336 1990
16. S. D. Umans, "Steady-state, lumped-parameter model for capacitor-run, single-phase induction motors", *IEEE Trans. Ind. Appl.*, vol. 32, no. 1, pp.169 -179 1996

Design and Implementaion of Solar Tracking System with Improvement of Voltage and Current Using Labview

V.Devi Priya, J.R.Lydia Jenifer,C.Jansi Sophia Mary

Abstract

As the world population is increasing gradually the need for energy is increasing equally. Every day people depend on energy for the purpose of electricity, hot water and fuel for automobiles. Majority of this energy come from fossil fuels, such as coal, oil and natural gas. The energy from fossil fuels are a non-renewable energy source, which means that if people use them all up, they can never get more during our life time, so it is important that they use other energy sources, like renewable energy sources these are energies that can be used again and again such as sunlight, water and wind. The main aim of this project is to absorb maximum solar energy from the solar panel. The solar tracker is the one which traces the sun's movement continuously, such that maximum amount of sunlight falls on the solar panel which we have designed. The design of hardware and the software are incorporated in this project. The hardware part includes servo motor, Arduino Uno, solar panel, LDR, Resistor and battery. PV (Photovoltaic) systems are one of in real-time manner is essential. The monitoring controller for solar cell with the use of Lab view

System is proposed in this project. It is a graphical representation and differs from other languages like C, C++, and JAVA etc. By using the Lab View software the system can monitor the function of solar tracking system and other parameters. It will reduce the man power and cost. This will improve the efficiency of the generation by orienting this PV cells in the correct direction to receive maximum sunlight from the sun.

Keywords: SolarPanel, CurrentSensor, LDR (Light Dependent Resistor), Arduino, DC Gear Motor, DC Supply System.

1 Introduction

The energy crisis has been one of the most important issues in today's world. Renewable energy sources have earned a high priority in reducing dependency on conventional sources. Solar energy system are quickly becoming the major renewable source to replace the conventional energy sources due to its inexhaustibility, its environmental implications. Humans have used fossil fuels which took millions of years to form and was stored in the ground in various places. Humans now must put an extreme effort, technologically and politically, into finding new energy systems that uses solar energy more directly. Being one of the most inspiring challenges facing engineers and scientists today, Photovoltaic (PV) is one of the exciting new technologies that is already helping us towards a solar future. (Lynn, P., 2010). Global primary energy consumption increased by 2.3% in 2013, and by 1.8% in 2012. Growth in 2013 resulted from the consumption of oil, coal, and nuclear power, but global growth remained below the 10-year average of 2.5%. All fuels except oil, nuclear power and renewable in power generation grew at below-average rates. All regions, except North America, were below the growth average. Oil remains the world's leading fossil fuel, comprising 32.9% of global energy consumption, although it continued to lose its market share for the fourteenth consecutive year and the current market share remains the lowest in the data set, which began in 1965. (BP Statistical Review of World Energy 2014, 2014). PV's earliest applications were in situations where there was a lack of electricity. While the cost has decreased and the efficiency of PV has increased, more applications involving PV have emerged. With greater demands on developing the technology and increasing, the production of PV systems has been implicated toward cost performance in a wide range of PV applications. In the new solar age, people apply PV applications to places that need electricity. Being versatile, PV applications also support AC circuits and DC circuits, can also be grid-connected. Current PV systems include photovoltaic modules, inverters modules, storage batteries, and control components. Supply chain refers to the procurement of all required inputs, conversion into finished PV products, distribution, and installation of these products for customers. The value chain looks at how increased customer value can be created across a company's business activities, which can include design, production, marketing, delivery, and support functions. (TRENDS in Photovoltaic Applications – 2013.) In existing system there is no consideration for the faults occurred in the Solar system. There is no monitoring system for solar to monitor it 24hrs so any over voltage or over current occur, the solar system will damage.

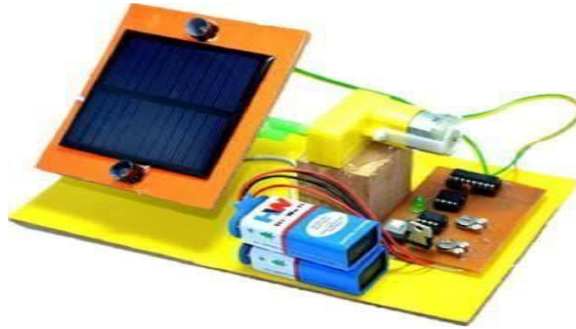


Fig : Single traction of solar PV system

II. Proposed System

2.1 Solar Panel

Solar panel refers to a panel designed to absorb the sun's rays as a source of energy for generating electricity or heating. Photovoltaic modules use light energy (photons) from the Sun to generate electricity through the photovoltaic effect. The majority of modules use wafer-based crystalline silicon cells or thin-film cells. The structural (load carrying) member of a module can either be the top layer or the back layer. Cells must also be protected from mechanical damage and moisture. Most modules are rigid, but semi-flexible ones are available, based on thin-film cells. The cells must be connected electrically in series, one to another. Externally, most of photovoltaic modules use MC4 connectors type to facilitate easy weatherproof connections to the rest of the system. Modules electrical connections are made in series to achieve a desired output voltage and/or in parallel to provide a desired current capability. The conducting wires that take the current off the modules may contain silver, copper or other non-magnetic conductive transition metals. Bypass diodes may be incorporated or used externally, in case of partial module shading, to maximize the output of module sections still illuminated.



Fig: solar panel

2.2 Arduino UNO

Arduino UNO is an open source, computer hardware and software company, project, and user community that designs and manufactures microcontroller kits for building digital devices and interactive objects that can sense and control objects in the physical world. The project's products are distributed as open-source hardware and software, which are licensed under the GNU Lesser General Public License (LGPL) or the GNU General Public License (GPL) permitting the manufacture of Arduino boards and software distribution by anyone. Arduino boards are available commercially in preassembled form, or as do-it yourself kits. Arduino board designs use a variety of microprocessors and controllers. The boards are equipped with sets of digital and analog input/output (I/O) pins that may be interfaced to various expansion boards (shields) and other circuits. The boards feature serial communications interfaces, including Universal Serial Bus (USB) on some models, which are also used for loading programs from personal computers. The microcontrollers are typically programmed using a dialect of features from the programming languages C and C++. In addition to using traditional compiler tool chains, the Arduino project provides an integrated development environment (IDE) based on the Processing language project. Arduino Uno is a microcontroller board based on the ATmega328P. It has 14 digital input/output pins (of which 6 can be used as PWM outputs), 6 analog inputs, a 16 MHz quartz crystal, a USB connection, a power jack, an ICSP header and a reset button. It contains everything needed to support the microcontroller; simply connect it to a computer with a USB cable or power it with a AC to- DC adapter or battery to get started.. You can tinker with your UNO without worrying too much about doing something wrong, worst case scenario you can replace the chip for a few dollars and start over again.



Fig: Arduinio UNO

2.3 LDR

A Light dependent sensor (LDR) or a photo resistor is a device whose resistivity is a function of the incident electromagnetic radiation. Hence, they are light sensitive devices. They are also called as photo conductors, photo conductive cells or simply photocells. They are made up of semiconductor materials having high resistance. A photo resistor is made of a high resistance semiconductor. In the dark, a photo resistor can have a resistance as high as several mega ohms ($M\Omega$), while in the light, a photo resistor can have a resistance as low as a few hundred ohms. If incident light on a photo resistor exceeds a certain frequency, photons absorbed by the semiconductor give bound electrons enough energy to jump into the conduction band. The resulting free electrons (and their hole partners) conduct electricity, thereby lowering resistance. The resistance range and sensitivity of a photo resistor can substantially differ among dissimilar devices. Moreover, unique photo resistors may react substantially differently to photons within certain wavelength bands



Fig: LDR

Current sensor is used for sensing the current in the solar cell. Using the LDR sensor for solar tracking system. With the use of a motor it will track the sun, so it will get maximum radiation in entire day. The sensed values at different times, we can display by use of LABVIEW. It can monitor 24 hrs using this system

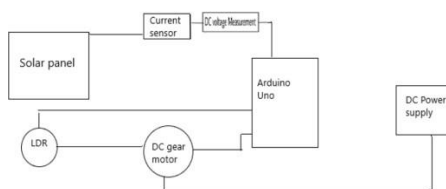


Fig: Block Diagram of solar tracking system

III. Control Techniques

3.1. Current Sensor

Measuring a voltage in any system is a “passive” activity as it can be done easily at any point in the system without affecting the system performance. However, current measurement is “intrusive” as it demands insertion of some type of sensor which introduces a risk of affecting system performance. Current measurement is of vital importance in many power and instrumentation systems. Traditionally, current sensing was primarily for circuit protection and control. However, with the advancement in technology, current sensing has emerged as a method to monitor and enhance performance. A current sensor is a device that detects and converts current to an easily measured output voltage, which is proportional to the current through the measured path. When a current flows through a wire or in a circuit, voltage drop occurs. Also, a magnetic field is generated surrounding the current carrying conductor. Both of these phenomena are

made use of in the design of current sensors. Thus, there are two types of current sensing: direct and indirect. Direct sensing is based on Ohm's law, while indirect sensing is based on Faraday's and Ampere's law. Direct Sensing involves measuring the voltage drop associated with the current passing through passive electrical components.



Fig: Current sensor

3.2 L293D Drive

The Device is a monolithic integrated high voltage, high current four channel driver designed to accept standard DTL or TTL logic levels and drive inductive loads (such as relays solenoids , DC and stepping motors) and switching power transistors. To simplify use as two bridges each pair of channels is equipped with an enable input. A separate supply input is provided for the logic, allowing operation at a lower voltage and internal clamp diodes are included. This device is suitable for use in switching applications frequencies up to 5 kHz. The L293D is assembled in a 16 lead plastic package which has 4 center pins connected together and used for heat sinking The L293DD is assembled in a 20 lead surface mount which has 8 center pins connected together and used for heat sinking



Fig: L293D Drive

3.3 DC Gear Motor

A gear motor is an all-in-one combination of a motor and gearbox. The addition of a gear head to a motor reduces the speed while increasing the torque output. The most important parameters in regards to gear motors are speed (rpm), torque (lb-in) and efficiency (%). In order to select the most suitable gear motor for your application you must first compute the load, speed and torque requirements for your application. ISL Products offers a variety of Spur Gear Motors, Planetary Gear Motors and Worm Gear Motors to meet all application requirements. Most of our DC motors can be complimented with one of our unique gear heads, providing you with a highly efficient gear motor solution.

Design Requirements – A design assessment phase where the product development requirements, design parameters, device functionality, and product optimization are studied.

Design Calculations – Calculations used to determine which motor would be the best solution for your application. Design calculations determine gear ratio, torque, rotating mass, service factor, overhung load, and testing analysis.

Types of DC Motors/Gear motors – The most common electrical motors convert electrical energy to mechanical energy. These types of motors are powered by direct current (DC)

- Brushed
- Brushless (BLDC)
- Planetary Gear Motors
- Spur Gear Motors
- Stepper
- Coreless & Coreless Brushless
- Servo
- Gear heads



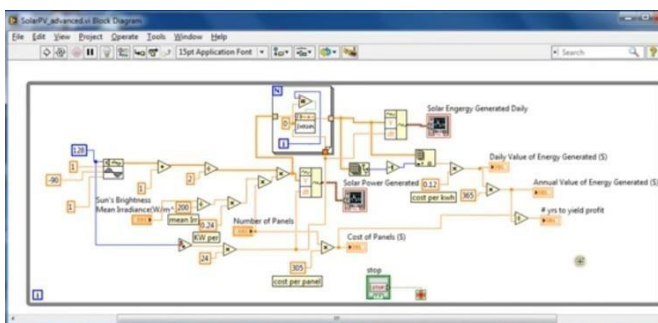
Fig: DC gear motor

| | |
|---------------|-----------------|
| Rated voltage | 24 VDC |
| Rated speed | 50rpm |
| Rated Load | 60Watts |
| Rated Torque | 6N-m(4.4 ft-lb) |

Table 1: Rating of DC geared motor

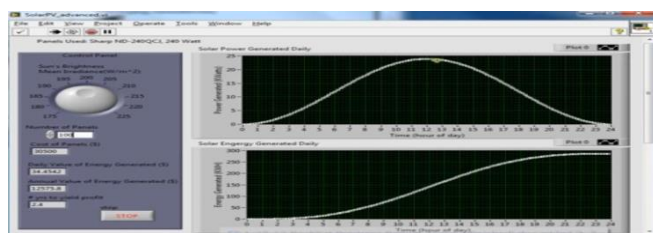
IV. Simulation and results

4.1 Solar tracking module



The components to be added in the module is designed in the software and the simulink is modeled. Here the solar system is traced with the help of multiple sensors and drives.

4.2 Graphical Presentation



The simulation of solar tracking system with LABVIEW is predicted graphically. The tracking range is limited using the drive and regulator of the system software.

V. Hardware Description

The solar panel receives the sunlight and converts it to electrical energy which stores in the PV cell. It is then sensed in the current sensor and voltage is measured in DC voltage measurement. Then the current sensor is connected to Arduino micro controller which makes the solar panel to act according to the perfect flow of sunlight in all directions with the help of motor. Again the motor is sensed with the LDR sensor which is also connected to Arduino Micro-Controller for their perfect working of the system. Finally the whole set up modulates the solar panel and get the high power production with less loss. The system is finally connected to

DC supply system.



Fig: Hardware Model Of Solar Tracking System

VI. Conclusion

- Current sensor senses the current in the solar cell.
- Using the LDR sensor the drive and the solar system could be tracked with absolute values.
- With the use of a motor it will track the sun, so it will get maximum radiation in entire day
- The sensed values of power at different times is displayed by use of LABVIEW.
- The LABVIEW can monitor 24 hrs in which the solar tracking could be done.

References

- [1] Regine Mallwitz, "First 99% PV Inverter with SiC JFETs on the market – future role of SiC", Power Conversion Intelligent Motion Conference, PCIM Europe 2012, 8-10 May 2012, Nuremberg, Germany.
- [2] Rabkowski, J.; Pefitsis, D.; Nee, H.-P.; "Design steps towards a 40-kVA SiC inverter with an efficiency exceeding 99.5%", Twenty-Seventh Annual IEEE Applied Power Electronics Conference and Exposition (APEC 2012), pp.1536-1543, 5-9 Feb. 2012.
- [3] Badstuebner, U.; Biela, J.; Kolar, J.W.; "Design of an 99%-efficient, 5kW, phase-shift PWM DC-DC converter for telecom applications", Twenty-Fifth Annual IEEE Applied Power Electronics Conference and Exposition (APEC 2010), pp.773-780, 21-25 Feb. 2010.
- [4] Kirubakaran, K.; Jain, S.; Nema, R.K.; "DSP-Controlled Power Electronic Interface for Fuel-Cell-Based Distributed Generation", IEEE Transactions on Power Electronics, vol.26, no.12, pp.3853-3864, Dec. 2011.
- [5] Sugahara, K.; Oida, S.; Yokoyama, T.; "Highperformance FPGA controller for digital control of power electronics applications", IEEE 6th International Power Electronics and Motion Control Conference, 2009 (IPEMC '09), pp.1425-1429, 17-20 May 2009.
- [6] Li Weichao; Hu An; Geng Shiguang; Sun Chi, "Rapid control Prototyping of fifteen-phase induction motor drives based on dSPACE," International Conference on Electrical Machines and Systems (ICEMS 2008), pp.1604-1607, 17-20 Oct. 2008.
- [7] Sarik, J.; Kymissis, I.; "Lab kits using the Arduino prototyping platform," IEEE Frontiers in Education Conference (FIE), 2010, pp.T3C-1-T3C-5, 27-30 Oct. 2010.
- [8] Buechley, L.; Eisenberg, M.; "The LilyPad Arduino: Toward Wearable Engineering for Everyone," IEEE Pervasive Computing, vol.7, no.2, pp.12-15, April-June 2008.
- [9] Kioumars, A.H.; Liqiong Tang; "Wireless network for health monitoring: heart rate and temperature sensor", Fifth International on Sensing Technology (ICST 2011), pp.362-369, Nov. 28 2011-Dec. 1, 2011.

Grasshopper Optimization Algorithm for Multi-Fuel Power Dispatch

K. Karthikeyan^{#1}, S. Ganesan^{#2}, and N. Jayakumar^{#3}

^{#1}Research Scholar, Department of Electrical Engineering, Annamalai University, Annamalai Nagar – 608002, Tamil Nadu, India.

^{#2}Assistant Professor, Department of Electrical & Electronics Engineering, Government College of Engineering, Salem – 636011, Tamil Nadu, India.

^{#3}Lecturer, Department of Electrical & Electronics Engineering, Government Polytechnic College, Uthangarai – 635207, Tamil Nadu, India.

Abstract

–Electric power utilities aim to increase their economic efficiency for being more economical in the energy market and also aim for adhering to the environmental norms. This operational task is inevitable and the best way to achieve this operation situation is to schedule the generating units on their optimum output levels. In contrast with the existing multi-fuel option (MFO) power system models, a accurate operational is proposed by incorporating valve point loadings, CO₂ emission and restricted operating zones in the optimization framework. As the developed model is a bi-objective, nonlinear and non-convex optimization problem, a stochastic optimization tool is needed to fetch the best compromise solution. Grasshopper optimization algorithm (GOA) is chosen as the prime optimization tool and is applied for the first time to address the optimal operation of the MFO power system. The intended optimization tool is implemented on standard 10-unit system. The applicability of GOA is verified by comparing the numerical results against other challenging methods and the statistical indices confirm the consistency and solution quality.

Keywords: *Multiple fuel option, Valve point loadings, Co₂ emission, Restricted operating zone, Grasshopper optimization algorithm*

1. Introduction

Optimal operation of modern electric power industries is crucial due to the ever-increasing load demands, scarcity of fossil fuels and pollutant norms. Hence, the power companies aim to meet the real power demands at the cheapest price with minimum pollutant emission. This operation is modeled as an optimization problem. The fuel cost and pollutant emission are characterized as piecewise quadratic functions if the generators have multiple fuel option (MFO). The fuel cost function has become non-linear if the valve-point loadings are included. The realistic operational model comprises of these conflicting operational objectives and the best compromise schedule can be determined by optimizing the real power output levels of generators. Thus, this operational task is modeled as a constrained, non-linear and multi-objective optimization problem.

1.1. Research Gap and Motivation

Numerical optimisation tools have been reported for solving the economic dispatch considering MFO (ED_MFO) and are categorised as analytical, meta-heuristic and hybrid methods. The hierarchical method which utilises the composite cost function, Hopfield neural network and its improved versions were reported for solving ED_MFO problem [1-4]. The population-based nature-inspired and bio-inspired meta-heuristic techniques such as genetic algorithm (GA) [5], evolutionary programming (EP) [6], particle swarm optimisation (PSO) [7,10], artificial immune system (AIS) [9], artificial bee colony (ABC) [11], biogeography-based optimisation [12], kinetic gas molecule optimisation (KGMO) [19], criss-cross optimisation (CCO) [20], grey wolf optimisation (GWO) [21], synergic predator-prey optimisation (SPPO) [26], lightning flash algorithm (LFA) [27], ant lion optimiser (ALO) [30-31] and the improved and hybrid versions of meta-heuristic algorithms [13-18, 22-25, 28-29, 32-35] were also been implemented for solving ED_MFO problems considering valve-point loadings (EDVP_MFO).

It is observed that the ED_MFO and EDVP_MFO are well explored in a static environment but research scope still exists in the research avenues as improving solution quality; multi-objective operational framework by combining pollutant emission and including the operational challenges such as valve point loadings and restricted operating zones (ROZ). Though, the meta-heuristic algorithms exploring the search space better than the analytical techniques, their search process is restricted by their algorithmic parameter settings. Exploring new optimization algorithms or improving the search mechanism of the existing techniques is also an interesting research field. The modern bio-inspired algorithm namely, grasshopper optimization algorithm (GOA) has been chosen as an optimization tool and is applied for enhancing the various MFO power system operations. The research objectives of the present work are summarized as: a realistic operational model is developed by incorporating valve-point loading effects and restricted operating zones in the multi-objective operational framework and the GOA is applied for the first time to solve power system operational cases having MFO.

2. Optimization Model of a Multi-fuel Power System

The economic and environmental norms compromised operation of the multi-fuel power system (MFPS) is formulated as a nonlinear, constrained and bi-objective optimization problem and is detailed as follows.

2.1 Total Fuel Cost

A piecewise quadratic cost function represents the fuel input- power output characteristics of a generating unit with MFO. The piecewise quadratic function considering the valve-point loadings of a generator 'i' with multi-fuel option 'j' is defined in Equation (1).

$$F_i(P_i) = a_{ij} + b_{ij}P_i + c_{ij}P_i^2 + |e_{ij} \sin(f_{ij}(P_i^{\min} - P_i))| \quad (1)$$

where, a_{ij} , b_{ij} , c_{ij} , e_{ij} , f_{ij} are the fuel cost coefficients of generating unit i for the fuel j , P_i is the real power output of generator i in MW and P_i^{\min} and P_i^{\max} are the real power limits of generator i in MW.

Consider a power system comprises of N generating units and the total fuel cost of MFO is computed as,

$$FC = \text{Min} \sum_{i=1}^N F_i(P_i) \quad \$ / h \quad (2)$$

2.2 Total CO2 Emission

The emission characteristics of a generating unit 'i' with multiple fuel options 'j' is also expressed as a piecewise segment function and is stated as,

$$E_i(P_i) = \alpha_{ij} + \beta_{ij}P_i + \gamma_{ij}P_i^2 \quad (3)$$

where, α_{ij} , β_{ij} , γ_{ij} are the fuel cost coefficients of generating unit i for the fuel j .

The total CO₂ emission for a power system comprises of N generators, is expressed as,

$$EC = \text{Min} \sum_{i=1}^N E_i(P_i) \quad \text{kg} / h \quad (4)$$

2.3 Economic-Environmental Operational Model of MFPS

The most realistic operational model can be formulated by combining the design objectives FC and EC detailed as Equation (2) and Equation (4) in single framework. Thus, the model proposed in Equation (5) aims to optimize the conflicting objectives simultaneously.

$$\text{Min} \left(\sum_{i=1}^N F_i(P_i), \sum_{i=1}^N E_i(P_i) \right) \quad (5)$$

2.4 Constraints

Power Balance

The total generation by all the generators must be equal to the local power demand (P_d) and network loss

(P_L) .

$$\sum_{i=1}^N P_i = P_d + P_L \quad (6)$$

$$P_L = \sum_{j=1}^N \sum_{l=1}^N P_j B_{jl} P_l + \sum_{j=1}^N B_{0j} P_j + B_{00} \quad (7)$$

Generation Limits

The real power generation of each generator is to be controlled within its upper (P_i^{max}) and lower (P_i^{min}) operating limits.

$$P_i^{min} \leq P_i \leq P_i^{max} \quad i = 1, 2, \dots, N \quad (8)$$

Restricted Operating Zones

The restricted operating regions of generating units decompose the entire feasible operating regions into a number of feasible sub-regions and the operating point of a generator should lie in any one of the sub-regions as follows:

$$\begin{aligned} P_i^{min} &\leq P_i \leq P_{i,1}^l \\ P_{i,j-1}^u &\leq P_i \leq P_{i,j}^l \quad j = 2, 3, \dots, n_i \\ P_{i,n_i}^u &\leq P_i \leq P_i^{max} \end{aligned} \quad (9)$$

The economic, emission and economic-environmental operations are performed by minimizing the operational objectives detailed in Equations (2), (4) and (5) respectively subject to inevitable system and operational constraints detailed in Equations (6)-(9).

3. Application of GOA to MFS

3.1. Grasshopper Optimisation Algorithm [36]

Grasshopper is a kind of insects and is cause damage to crop production and agriculture; hence they are treated as a pest. Although grasshopper is usually seen individually in nature, they join in one of the largest swarms of all creatures. The life cycle of a grasshopper is as follows: larvae, nymph and adulthood. The unique aspect of the grasshopper swarm is that swarming behaviour is found in both nymph and adulthood. The nymph grasshopper's jump and move like a rolling cylinder and eat almost all vegetations in their path. After this stage, the nymph has grown as an adult and forms a swarm in the air. The swarm behaviour in the larvae phase is slow movement and small in steps and it is long-range and abrupt movement in the adulthood phase. Thus, the swarm behaviour of grasshoppers naturally comprises of exploration and exploitation tendencies and target seeking behaviour. As these characteristics coincide with the search process of stochastic optimisation algorithms, the mathematical model of the swarm behaviour of grasshopper is highly suitable to develop a novel design of bio-inspired stochastic optimisation algorithm.

The mathematical model to simulate the position of grasshopper comprises of social interaction, gravity force and wind advection. To provide the random positions, three random numbers varying between 0 and 1 are used. The social interaction behaviour is developed by using the social force and distance between the two grasshoppers. The distance impacts on social interaction such as attraction and repulsion of grasshoppers. The comfort zone or comfortable distance is defined as the distance between two grasshoppers do not provide attraction or repulsion. It is identified that the attraction increases from 2.079 to 4 and then gradually decreases. The social force is a function of the intensity of attraction and attractive length of the scale, changing these parameters result in different social behaviour. It is identified that the intensity of attraction (f) and attractive length of scale (l) are chosen as 1.05 and 0.5 respectively. The weak social force is experienced with the long distance between the grasshoppers and it is mapped in the interval between 1 and 4. Nymph grasshoppers have no wings and land on the ground. Hence, their position should not go below a threshold value and their movements are highly correlated with wind direction. These swarm behaviour of grasshoppers is modelled in free space.

However, the developed mathematical model cannot be directly used for solving optimisation problems as the grasshoppers reach the comfort zone quickly and the swarm does not converge to a specific point. Hence, a modification is introduced in the grasshopper position equation. The boundary limits of each dependent

variable, the value of the best solution found so far (target) and decreasing coefficient to shrink the comfort, repulsion and attractive zones. Moreover, the gravity component is neglected and wind direction is assumed that always towards a target. The adaptive parameters have been used to balances exploration and exploitation of the entire swarm around the target (i.e. reduces the search convergence around the target as the iteration count increases) and to reduce the comfort, attraction and repulsion zones (i.e. reduces the repulsion/attraction forces between grasshoppers proportional to the number of iterations).

In a nutshell, the GOA optimisation mechanism involves creating a set of random initial solutions, updating the positions of search agents, the position of the best target obtained so far is updated in each iteration, calculating the adaptive parameters and the distances between the grasshoppers are normalised. The grasshopper positions are updated iteratively until satisfying the stopping criterion. The mathematical model of GOA is first proposed in the literature [36].

3.2. Fuzzy Decision Making - GOA

In multi-objective optimization problems, two or more objectives are optimized simultaneously subject to equality and inequality constraints. Many feasible solutions are obtained rather than a single solution and these solutions are contradictory. As an initial population of GOA is randomly generated for the chosen problem domain variables and to obtain the best-compromised solution (BCS), the objective function values of each candidate solution are normalized. The membership value indicates the degree of satisfaction of the solution for an objective function. The decision-maker is fully satisfied with the objective function value if the fuzzy membership value is 1, and not satisfied at all if the membership value is 0. The membership function can be defined as in Equation (10). For each non-dominated solution k , the normalized membership value is calculated using Equation (11).

$$\mu_i = \begin{cases} 1 & \text{if } F_i < F_i^{\min} \\ \frac{F_i^{\max} - F_i}{F_i^{\max} - F_i^{\min}} & \text{if } F_i^{\min} \leq F_i \leq F_i^{\max} \\ 0 & \text{if } F_i > F_i^{\max} \end{cases} \quad (10)$$

$$\mu^k = \frac{\sum_{i=1}^{N_{obj}} \mu_i^k}{\sum_{k=1}^{M_{nd}} \sum_{i=1}^{N_{obj}} \mu_i^k} \quad (11)$$

The fuzzy decision-making mechanism has been incorporated into the GOA algorithm to develop FDM-GOA.

3.3. FDM-GOA for solving MFPS Problems

The real power outputs of generating units are treated as control variables. The penalty function method is adopted to handle the remaining constraints. The computational flow of FDM-GOA for solving MFS problem is as follows.

Step 1: Read the system data and initialise the algorithm domain parameters such as search agents (P_s), limits of the adaptive parameter (c_{max} and c_{min}), maximum number of iterations ($iter_{max}$), number of decision variables (N_d) and their limits (ub and lb).

Step 2: The decision variables such as real power outputs of generating units and tie-line flow limits are generated randomly within the lower and upper bounds to initialise the positions of search agents.

Step 3: Multi-objective Strategy:

a. Compute the objective function values and normalise their values by using fuzzy decision-making mechanism.

b. Evaluate the normalised membership value.

c. Determine the BCS.

Step 4: The fitness of each individual is evaluated subject to constraints.

Step 5: The individual having the best fitness is assumed as target.

Step 6: Set $iter = 1$.

Step 7: Update the adaptive parameter using the following equation.

$$c = c_{max} - \left[\frac{c_{max}}{iter} \right] \quad (12)$$

Step 8: Set $P_s = 1$.

Step 9: Normalise the distances between the grasshoppers in $[1,4]$.

Step 10: Update the position of the current search agent by using the following equations.

$$s(r) = f e^{-\frac{r}{l}} \quad (13)$$

$$X_i^j = c \left(\sum_{k=1, k \neq i}^{Nd} c \frac{ub_j - lb_j}{2} s(|X_i^j - X_k^j|) \frac{x_k - x_i}{d_{ik}} \right) \quad (14)$$

Step 11: Bring the current search agent back if any decision variables go outside the boundaries.

Step 12: Perform a multi-objective strategy.

Step 13: The fitness of each individual is evaluated subject to constraints.

Step 14: Go to Step 8 and repeat Step 8- Step 13 for all search agents.

Step 15: Update the target if there is a better solution.

Step 16: Check for max iterations. Otherwise, $iter = iter + 1$ and go to Step 5.

Step 17: Print the best individual.

4. Results and Discussions

The GOA is coded in MATLAB 7 platform and is executed in a personal computer with the hardware configuration of Intel Core i3 2.4 GHz processor and 4 GB RAM. The algorithmic parameters are determined based on the sensitivity analysis and is executed for 100 trails to validate its consistency. The desirable algorithm domain parameters are: Number of search agents=40 and maximum number of iteration = 200. The network loss in each area is computed by using Kron's formula. The following case studies have been carried out.

Scenario 1: EDVP_MFO

Scenario 2: EDVP_MFO considering ROZ

Scenario 3: Emission dispatch (EmD_MFO)

Scenario 4: EmD_MFO considering ROZ

Scenario 5: EDVP-EmD_MFO

Scenario 6: EDVP-EmD_MFO considering ROZ

The intended algorithm has been implemented on the standard ten-unit system for solving the economic dispatch problem. This test system comprises of ten generating units in which generator 1 has two fuel options and the remaining generating units have three fuel options. The fuel cost and CO₂ emission functions of the generating units are expressed as piecewise quadratic functions. The cost coefficients including valve-point loadings, emission coefficients and ROZ are detailed in the literature [2, 8, 16, 17].

4.1 Scenario 1: EDVP_MFO

The GOA is implemented on for determining the economic schedules for load demands varies from 2400 MW to 2700 MW. The attained best feasible dispatch schedules achieving minimum fuel cost for 2400MW,

2500MW, 2600MW and 2700MW are presented in Table 1.

Table 1. Cost-Effective Schedules for Scenario 1

| Unit No. | $P_d = 2400$ MW | $P_d = 2500$ MW | $P_d = 2600$ MW | $P_d = 2700$ MW |
|-----------|--------------------|--------------------|--------------------|--------------------|
| | P_i (MW) | P_i (MW) | P_i (MW) | P_i (MW) |
| P_1 | 189.2870 | 206.2830 | 217.9991 | 218.613 |
| P_2 | 200.2100 | 206.0042 | 209.9991 | 211.216 |
| P_3 | 254.4583 | 266.2460 | 278.1010 | 280.656 |
| P_4 | 234.0337 | 235.6046 | 236.9999 | 239.3707 |
| P_5 | 241.3677 | 258.3711 | 274.9999 | 279.934 |
| P_6 | 233.0557 | 235.3679 | 239.9120 | 239.3707 |
| P_7 | 253.6068 | 268.6971 | 285.9999 | 287.7275 |
| P_8 | 233.4948 | 235.9969 | 238.9998 | 239.4951 |
| P_9 | 320.6885 | 331.6017 | 342.9898 | 427.7583 |
| P_{10} | 239.7971 | 255.8573 | 273.9990 | 275.865 |
| FC (\$/h) | 482.4118 | 526.7945 | 575.0494 | 623.8269 |
| EC (kg/h) | 4896.08 | 5336.92 | 5836.18 | 6264.25 |
| | Fuel 1 | Fuel 2 | Fuel 3 | |

For the sake of comparison, the total fuel cost for load demand of 2700MW is compared against the other competitive methods and the comparison is presented in Table 2. It is observed that the intended tool is highly competitive with other methods and provide considerable savings in total fuel cost.

Table 2. Total Fuel Cost (\$/h) Comparison for Scenario1

| Methods | $P_d = 2400$ MW | $P_d = 2500$ MW | $P_d = 2600$ MW | $P_d = 2700$ MW |
|------------|--------------------|--------------------|--------------------|--------------------|
| IGA-MU | NA | NA | NA | 624.5178 |
| GA-MU | NA | NA | NA | 624.7193 |
| NPSO | NA | NA | NA | 624.1624 |
| NPSO-LRS | NA | NA | NA | 624.1273 |
| PSO-LRS | NA | NA | NA | 624.2297 |
| RGA | 482.5114 | 527.0189 | 575.1610 | 624.5081 |
| DE | 482.5275 | 527.0360 | 575.1753 | 624.5146 |
| PSO | 482.5088 | 527.0185 | 575.1606 | 624.5074 |
| RCGA | NA | NA | NA | 623.8281 |
| ABC | NA | NA | NA | 609.2250* |
| BBO | NA | NA | NA | 605.6387* |
| NAPSO | NA | NA | NA | 623.6217* |
| AA | NA | NA | NA | 623.9524 |
| DSD | NA | NA | NA | 623.8325 |
| GWO | NA | NA | NA | 605.6818* |
| KGMO | NA | NA | NA | 608.1096* |
| OGHS | NA | NA | NA | 623.8240* |
| CCDE | NA | NA | NA | 623.8288 |
| ALO | 482.4127 | 526.8142 | 575.0544 | 623.8278 |
| GOA | 482.4118 | 526.7945 | 575.0494 | 623.8269 |

*-Not feasible NA- Not Applicable

4.2 Scenario 2: EDVP_MFO considering ROZ

The ROZ is an operational constraint and is included in the optimization frame. The inclusion of the ROZ constraint increases further the complexity. The generating units 3, 5, 7 and 10 having restricted operating

regions are detailed in the literature [16]. The intended optimization tool is applied for the least cost schedules for various load demands and is detailed in Table 3.

Table 3. Cost-Effective Schedules for Scenario 2

| Unit No. | $P_d = 2400$ MW | $P_d = 2500$ MW | $P_d = 2600$ MW | $P_d = 2700$ MW |
|-----------|--------------------|--------------------|--------------------|--------------------|
| | P_i (MW) | P_i (MW) | P_i (MW) | P_i (MW) |
| P_1 | 189.7444 | 206.4992 | 219.2200 | 221.0370 |
| P_2 | 202.3431 | 206.4769 | 212.0940 | 212.8995 |
| P_3 | 253.8900 | 265.6989 | 281.9526 | 284.2837 |
| P_4 | 233.0457 | 235.9534 | 239.8460 | 240.5154 |
| P_5 | 241.8289 | 258.1081 | 260.0000 | 260.0000 |
| P_6 | 233.0461 | 235.9529 | 239.9558 | 240.4955 |
| P_7 | 253.2810 | 268.8637 | 290.2970 | 293.2792 |
| P_8 | 233.0420 | 235.9329 | 239.9362 | 240.4953 |
| P_9 | 320.3810 | 331.5075 | 346.6984 | 436.9954 |
| P_{10} | 239.3909 | 255.0065 | 270.0000 | 269.9999 |
| FC (\$/h) | 481.7197 | 526.2282 | 574.6999 | 624.310 |
| EC (kg/h) | 4897.78 | 5337.71 | 5830.24 | 6263.56 |
| Fuel 1 | | Fuel 2 | | Fuel 3 |

4.3 Scenario 3: Emission dispatch

The GOA is applied for minimum emission operation which aims for determining the dispatch schedules with least CO₂ emission. The pollutant emission of generating unit is characterized as piecewise quadratic function and the coefficients are taken from the literature [17]. The extreme points in the search space are identified through the single-objective optimization. The minimum pollutant emission schedules for various load demands are presented in Table 4 and the comparison is presented in Table 5.

Table 4. Emission Dispatch Schedules for Scenario 3

| Unit No. | $P_d = 2400$ MW | $P_d = 2500$ MW | $P_d = 2600$ MW | $P_d = 2700$ MW |
|-----------|--------------------|--------------------|--------------------|--------------------|
| | P_i (MW) | P_i (MW) | P_i (MW) | P_i (MW) |
| P_1 | 169.8432 | 196.0695 | 196.0024 | 196.7149 |
| P_2 | 199.9977 | 209.694 | 209.905 | 211.3997 |
| P_3 | 270 | 281.0124 | 298.0023 | 301.2075 |
| P_4 | 248.7711 | 254.0253 | 255.0274 | 257.0964 |
| P_5 | 269.9987 | 297.0978 | 299.0007 | 288.9928 |
| P_6 | 157.9886 | 159.9894 | 159.4945 | 167.52 |
| P_7 | 290.5958 | 271.4934 | 291.9906 | 365.069 |
| P_8 | 252.2193 | 243.4808 | 250.4337 | 258 |
| P_9 | 340.5856 | 388.9167 | 439.9585 | 439.9946 |
| P_{10} | 200 | 200.2175 | 200.1856 | 214.0087 |
| EC (kg/h) | 4692.52 | 5136.20 | 5571.86 | 6042.43 |
| FC (\$/h) | 501.24 | 547.84 | 599.01 | 651.68 |
| Fuel 1 | | Fuel 2 | | Fuel 3 |

Table 5. Total CO₂ Emission (kg/h) Comparison

| Methods | $P_d = 2400$ MW | | $P_d = 2500$ MW | | Methods | $P_d = 2400$ MW | | $P_d = 2500$ MW | |
|---------|-----------------|----|-----------------|----|---------|-----------------|----|-----------------|----|
| | FC | EC | FC | EC | | FC | EC | FC | EC |

| | | | | | | | | | |
|-----|--------|---------|--------|---------|-----|--------|---------|--------|---------|
| | (\$/h) | (kg/h) | (\$/h) | (kg/h) | | (\$/h) | (kg/h) | (\$/h) | (kg/h) |
| ALO | 501.25 | 4692.54 | 548.29 | 5137.02 | ALO | 599.38 | 5572.28 | 599.38 | 5572.28 |
| GOA | 501.24 | 4692.52 | 547.84 | 5136.20 | GOA | 599.01 | 5571.86 | 599.01 | 5571.86 |

4.4 Scenario 4: Emd_MFO considering ROZ

Further, the ROZ is incorporated in the optimisation model and the GOA is applied for determining minimum emission dispatch schedules. The attained schedules for various load demands presented in Table 6.

Table 6. Emission Effective Schedules for Scenario 4

| Unit No. | $P_d = 2400$ MW | $P_d = 2500$ MW | $P_d = 2600$ MW | $P_d = 2700$ MW |
|-----------|--------------------|--------------------|--------------------|--------------------|
| | P_i (MW) | P_i (MW) | P_i (MW) | P_i (MW) |
| P_1 | 170.99 | 206.4751 | 206.2431 | 216.3542 |
| P_2 | 200.4852 | 215.4571 | 219.8645 | 213.6571 |
| P_3 | 269.4734 | 296.9875 | 303.5431 | 302.8835 |
| P_4 | 250.5234 | 257.5432 | 255.5634 | 259.1586 |
| P_5 | 260 | 259.9999 | 260 | 260 |
| P_6 | 158.5421 | 159.2453 | 162.6674 | 168.2476 |
| P_7 | 291.5419 | 271.2654 | 298.9875 | 365 |
| P_8 | 252.1974 | 243.3542 | 250.4677 | 259.6576 |
| P_9 | 345.5324 | 388.8065 | 439.6674 | 439.8035 |
| P_{10} | 200.7142 | 200.8654 | 202.9921 | 215.2461 |
| EC (kg/h) | 4690.6603 | 5158.7313 | 5594.931 | 6073.83 |
| FC (\$/h) | 500.6173 | 547.9734 | 597.1259 | 651.1233 |
| | Fuel 1 | Fuel 2 | Fuel 3 | |

4.5 Scenario 5: EDVP-EmD_MFO

The FDM-GOA is extended to the multi-objective optimization model considering valve point loadings. The algorithm is implemented for determining the best-compromised dispatch schedules for load demands of 2400 MW, 2500 MW, 2600 MW and 2700 MW and the corresponding power outputs are presented in Table 7.

The attained numerical results are compared with the earlier reports such as Hopfield Neural Network (HLN) [17], Lambda Iteration Method (LIM) [17], ABC [30], teaching-learning based optimization (TLBO)[31] and GWO[31] and the comparison is presented in Table 8.

Table 7. BCS Schedules for Scenario 5

| Unit No. | $P_d = 2400$ MW | $P_d = 2500$ MW | $P_d = 2600$ MW | $P_d = 2700$ MW |
|-----------|--------------------|--------------------|--------------------|--------------------|
| | P_i (MW) | P_i (MW) | P_i (MW) | P_i (MW) |
| P_1 | 166.6745 | 196.1525 | 196.0925 | 204.0301 |
| P_2 | 199.2836 | 205.654 | 208.014 | 209.9991 |
| P_3 | 259.6255 | 285.0077 | 296.6024 | 302.4366 |
| P_4 | 245.5248 | 254.0200 | 246.2223 | 249.0655 |
| P_5 | 251.8932 | 297.1178 | 298.0178 | 292.2943 |
| P_6 | 156.0649 | 164.9894 | 167.4994 | 167 |
| P_7 | 283.5863 | 271.4834 | 297.9934 | 368.2974 |
| P_8 | 244.7472 | 236.5108 | 249.4908 | 258 |
| P_9 | 392.5025 | 388.8667 | 439.8467 | 438.8752 |
| P_{10} | 200.1811 | 200.1775 | 200.2175 | 210.0021 |
| FC (\$/h) | 499.0621 | 546.8059 | 595.50 | 650.08 |
| EC (kg/h) | 4693.517 | 5142.876 | 5571.37 | 6046.13 |

Table 8. BCS Comparison for Scenario 5

| Methods | $P_d = 2400$ MW | | $P_d = 2500$ MW | | $P_d = 2600$ MW | | $P_d = 2700$ MW | |
|--------------|-----------------|----------------|-----------------|----------------|-----------------|----------------|-----------------|----------------|
| | FC (\$/h) | EC (kg/h) | FC (\$/h) | EC (kg/h) | FC (\$/h) | EC (kg/h) | FC (\$/h) | EC (kg/h) |
| ABC | 501.83 | 4701.45 | 546.875 | 5143.02 | 596.572 | 5587.21 | 650.317 | 6044.81 |
| TLBO | 501.71 | 4701.67 | 546.804 | 5143.04 | 596.411 | 5586.52 | 650.490 | 6044.83 |
| GWO | 500.94 | 4701.96 | 547.038 | 5143.05 | 596.323 | 5585.68 | 650.661 | 6044.86 |
| FSALO | 499.06 | 4693.51 | 546.836 | 5142.89 | 595.804 | 5571.48 | 650.617 | 6046.56 |
| FSGOA | 499.06 | 4693.51 | 546.805 | 5142.87 | 595.50 | 5571.37 | 650.08 | 6046.13 |

4.6 Scenario 6: EDVP-EmD_MFO considering ROZ

Further, the ROZ is incorporated in the multi-objective optimization operational model. The FDM-GOA is applied for determining the best-compromised solution and the attained real power settings for various load demands are presented in Table 9.

Table 9. BCS Dispatches of 10-unit System with ROZ with VP

| Unit No. | $P_d = 2400$ MW | $P_d = 2500$ MW | $P_d = 2600$ MW | $P_d = 2700$ MW |
|-----------|-----------------|-----------------|-----------------|-----------------|
| | P_i (MW) | P_i (MW) | P_i (MW) | P_i (MW) |
| P_1 | 173.5036 | 215.1457 | 229.2455 | 226.3642 |
| P_2 | 206.3945 | 195.4572 | 216.6424 | 203.8562 |
| P_3 | 259.5376 | 290.1475 | 279.5627 | 294.8874 |
| P_4 | 231.6166 | 259.1287 | 238.8854 | 263.5562 |
| P_5 | 251.7806 | 260 | 260 | 260 |
| P_6 | 156.178 | 159.7541 | 165.5623 | 174.4265 |
| P_7 | 283.8592 | 275.2214 | 298.3032 | 365 |
| P_8 | 244.4789 | 253.5745 | 259.9745 | 243.3621 |
| P_9 | 385.6515 | 388.4571 | 439.3645 | 438.1856 |
| P_{10} | 207 | 203.1134 | 212.4572 | 230.3645 |
| FC (\$/h) | 499.64 | 549.7779 | 594.9237 | 647.389 |
| EC (kg/h) | 4717.18 | 5162.832 | 5631.0645 | 6104.2375 |

5. Performance Characteristics

The GOA method can reach an optimum solution quickly. Over 200 iterations with several initial random solutions, the GOA has confirmed as a trustworthy toll for solving MFS problems. Due to the randomness of the heuristic algorithms, their performance cannot be analyzed by the result of a single run. Many trials with different initializations should be made to acquire a useful conclusion about the performance of the algorithm. An algorithm is robust, if it gives consistent result during all the trials. The performance of GOA for solving the chosen problem is detailed below.

The number of search agents is a crucial algorithm domain parameter which influences the solution quality. Referring to Table 10, the economic operation has been performed for the different number of search agents and is identified that the number of search agent 40 provides the least cost solution with reasonable execution time.

The convergence characteristic of GOA is illustrated in Fig. 1. The intended method reaches the optimal solution quickly that confirms the good convergence behaviour for solving MFO operational problems. Over 200 iterations with several initial random solutions, the GOA has confirmed as a trustworthy solution procedure by generating the global best solution.

Table 10. Effect of population size for various demands

| P_d (MW) | P_s | Total Fuel Cost (\$/h) | | | SD | P_d (MW) | P_s | Total Fuel Cost (\$/h) | | | SD |
|---------------|-------|------------------------|---------|---------|------------|---------------|-------|------------------------|---------|---------|-------|
| | | Best | Average | Worst | | | | Best | Average | Worst | |
| Scenario 1 | | | | | Scenario 2 | | | | | | |
| 2400 | 10 | 483.259 | 490.475 | 499.954 | 4.442 | 2400 | 10 | 482.978 | 488.024 | 499.992 | 4.297 |
| | 40 | 482.411 | 487.872 | 497.210 | 4.002 | | 40 | 482.136 | 487.124 | 497.021 | 4.124 |
| | 60 | 482.411 | 489.991 | 498.557 | 4.351 | | 60 | 482.136 | 487.354 | 498.004 | 4.204 |
| | 100 | 482.411 | 489.224 | 498.014 | 4.125 | | 100 | 482.136 | 487.297 | 497.458 | 4.156 |
| 2500 | 10 | 527.322 | 533.924 | 544.987 | 4.354 | 2500 | 10 | 527.045 | 532.999 | 543.045 | 4.022 |
| | 40 | 526.794 | 532.550 | 541.739 | 4.050 | | 40 | 526.228 | 531.875 | 540.568 | 3.914 |
| | 60 | 526.794 | 533.004 | 543.004 | 4.265 | | 60 | 526.228 | 532.245 | 542.879 | 3.995 |
| | 100 | 526.794 | 532.971 | 542.568 | 4.127 | | 100 | 526.228 | 531.997 | 541.457 | 4.012 |
| 2600 | 10 | 575.996 | 582.694 | 593.842 | 4.299 | 2600 | 10 | 576.213 | 581.998 | 593.014 | 4.223 |
| | 40 | 575.049 | 580.515 | 590.340 | 4.034 | | 40 | 575.262 | 579.854 | 589.221 | 4.012 |
| | 60 | 575.049 | 581.954 | 592.006 | 4.265 | | 60 | 575.262 | 581.245 | 591.586 | 4.234 |
| | 100 | 575.049 | 581.245 | 591.784 | 4.156 | | 100 | 575.262 | 580.012 | 590.548 | 4.154 |
| 2700 | 10 | 624.679 | 631.257 | 643.257 | 4.125 | 2700 | 10 | 626.558 | 632.004 | 644.547 | 4.321 |
| | 40 | 623.826 | 629.222 | 639.241 | 3.992 | | 40 | 625.651 | 630.025 | 639.698 | 4.014 |
| | 60 | 623.826 | 630.047 | 641.247 | 4.024 | | 60 | 625.651 | 631.584 | 642.336 | 4.312 |
| | 100 | 623.826 | 629.845 | 640.987 | 3.999 | | 100 | 625.651 | 630.996 | 641.984 | 4.245 |

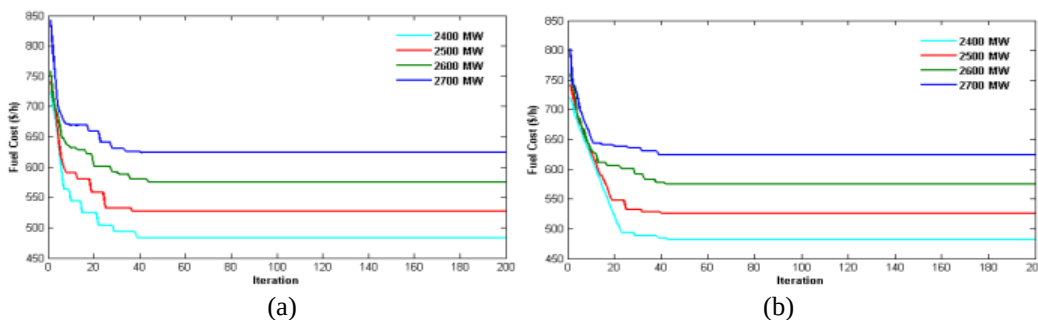


Fig. 1. Convergence characteristics of GOA for various demands (a) Scenario 1 (b) Scenario 2

To view further insights into the solution quality attained by GOA, the statistical indices such as standard deviation, best, worst and average values are computed and are presented in Table 10. The statistical indices confirm that the solution attained by GOA for different trails is a close agreement to the best solution. It also indicates that the GOA can attain reliable and best feasible solution with higher probability. Further, three criteria of goodness such as “Epsilon”, “Iter”, and “Sol Iter” are considered and listed in Table 11. The success rate of the intended algorithm for all case studies is above 80% that confirms the algorithm has a satisfactory success rate.

Table 11. Performance indices of GOA

| Scenario | P_d (MW) | Epsilon | Iter | Sol Iter |
|------------|------------|----------|------|----------|
| Scenario 1 | 2400 | 482.5114 | 39 | 39 |
| | 2500 | 527.0189 | 35 | 37 |
| | 2600 | 575.161 | 43 | 44 |
| | 2700 | 624.5081 | 39 | 41 |
| Scenario 2 | 2400 | 486.719 | 44 | 46 |
| | 2500 | 534.759 | 43 | 49 |
| | 2600 | 575.552 | 39 | 45 |
| | 2700 | 624.852 | 38 | 44 |

(a)

(b)

6. Conclusion

This paper details the application of GOA for solving economic, emission and combined economic emission operation of the power system with multiple fuel option. The realistic optimisation framework is developed by incorporating the valve point loading effects in the existing cost model, CO₂ emission and restricted operating zones of generating units. These realistic operations are formulated as nonlinear and constrained optimisation problems and GOA is used as an optimisation tool. The fuzzy decision-making mechanism is incorporated in the GOA search mechanism to handle the conflicting operational objectives simultaneously. The optimisation tool is implemented on the standard ten-unit system for six different operational scenarios. The attained numerical results are compared with the recent reports and are observed that the intended tool is highly competitive in providing the global best feasible solution. The performance analysis also indicates that it has quick convergence behaviour and highly robust characteristics. The statistical indices also confirm that the GOA can provide the best feasible solution consistently.

References

- [1] R.R. Shoults, S.K. Chang, S. Helmick and W.M. Grady, "A practical approach to unit commitment, economic dispatch and savings allocation for multiple-area pool operation with import/export constraints", *IEEE Transactions on Power Apparatus and Systems*, vol. PAS 99, no. 2, pp. 625-635, 1980.
- [2] C. E. Lin and G. L. Viviani, "Hierarchical economic dispatch for piecewise quadratic cost functions", *IEEE Transactions on Power Apparatus and Systems*, vol. PAS-103, no. 6, pp. 1170-1175, 1984.
- [3] J. H. Park, Y.S. Kim, I. K. Eom and K.Y. Lee, "Economic load dispatch for piecewise quadratic cost function using Hopfield neural network", *IEEE Transactions on Power Systems*, vol. 08, no. 3, pp. 1030-1038, 1993.
- [4] K. Y. Lee, A. Sode-Yome and J. H. Park, "Adaptive Hopfield neural networks for economic load dispatch", *IEEE Transactions on Power Systems*, vol. 13, no. 2, pp. 519-526, 1998.
- [5] S. Baskar, P. Subbaraj and M.V.C. Rao, "Hybrid real coded genetic algorithm solution to economic dispatch problem" *Computers & Electrical Engineering*, vol. 29, no. 3, pp. 407-419, 2003.
- [6] T. Jayabarathi, K. Jayaprakash, D. N. Jeyakumar and T. Raghunathan, "Evolutionary programming techniques for different kinds of economic dispatch problems", *Electric Power System Research*, vol. 73, no. 2, pp. 169-176, 2005.
- [7] J. B. Park, K.S. Lee, J. R. Shin and K. Y. Lee, "A particle swarm optimization for economic dispatch with non smooth cost functions", *IEEE Transaction on Power Systems*, vol. 20, no.1, pp. 34-42, 2005.
- [8] C. L. Chiang, "Improved genetic algorithm for power economic dispatch of units with valve-point effects and multiple fuels", *IEEE Transaction on Power Systems*, vol. 20, pp.1690-1699, 2005.
- [9] B. K. Panigrahi, S. R. Yadav, S. Agarwal and M. K. Tiwari, "A clonal algorithm to solve economic load dispatch", *Electric Power System Research*, vol. 77, pp. 1381-1389, 2007.
- [10] A. I. Selvakumar and K. Thanushkodi, "A new particle swarm optimization solution to non convex economic dispatch problems", *IEEE Transactions on Power Systems*, vol. 22, pp. 42-51, 2007.
- [11] S. Hemamalini and S.P. Simon, "Artificial bee colony algorithm for economic load dispatch problem with non-smooth cost functions", *Electric Power Components and Systems*, vol. 38, pp. 786-803, 2010.
- [12] A. Bhattacharya and P. K. Chattopadhyay, "Hybrid differential evolution with biogeography-based optimization for solution of economic load dispatch" *IEEE Transaction on Power Systems*, vol. 25, pp. 1955-1964, 2010.
- [13] T. Niknam, H. D. Mojarrad and H. Z. Meymand, "Non-smooth economic dispatch computation by fuzzy and self-adaptive particle swarm optimization", *Applied Soft Computing*, vol.11, pp. 2805-2817, 2011.
- [14] D. N. Vo and W. Ongsakul, "Economic dispatch with multiple fuel types by enhanced augmented lagrange hopfield network", *Applied Energy*, vol. 91, pp. 281-289, 2012.
- [15] V. N. Dieu, W. Ongsakul and J. Polprasert, "The augmented Lagrange Hopfield network for economic dispatch with multiple fuel options", *Mathematical and Computer Modelling*, vol. 57, pp. 30-39, 2013.

- [16] V. N. Dieu and P. Schegner, "Augmented Lagrange Hopfield network initialized by quadratic programming for economic dispatch with piecewise quadratic cost functions and prohibited zones", *Applied Soft Computing*, vol. 13, pp. 292-301, 2013.
- [17] Nguyen Trung Thang, "Economic emission load dispatch with multiple fuel options using Hopfield Lagrange network" *Int Journal of Advance Science and Technology*, vol. 57, pp.9-24, 2013.
- [18] J. Zhan, Q. H. Wu, C. Guo and X. Zhou, "Economic dispatch with non-smooth objectives—part II: dimensional steepest decline method. *IEEE Transactions on Power Systems*, vol. 30, pp. 722-733, 2014.
- [19] M. Basu, "Kinetic gas molecule optimization for nonconvex economic dispatch problem", *International Journal of Electric Power and Energy System*, vol. 80, pp. 325-332, 2016.
- [20] A. Meng, J. Li and H. Yin, "An efficient crisscross optimization solution to large-scale non-convex economic load dispatch with multiple fuel types and valve-point effects", *Energy*, vol. 113, pp. 1147-1161, 2016.
- [21] M. Pradhan, P.K Roy and T. Pal, "Grey wolf optimization applied to economic load dispatch problems", *International Journal of Electric Power and Energy System*, vol. 83, pp. 325-334, 2016.
- [22] M. Modiri-Delshad, S.H.A. Kaboli, E. Taslimi-Renani and N. A. Rahim, "Backtracking search algorithm for solving economic dispatch problems with valve-point effects and multiple fuel option", *Energy*, vol. 116, pp. 637-649, 2016.
- [23] M. Singh and J.S. Dhillon, "Multiobjective thermal power dispatch using opposition-based greedy heuristic search", *Int Journal of Electric Power and Energy System*, vol. 82, pp. 339-353, 2016.
- [24] R. P. Parouha and K.N. Das, "A novel hybrid optimizer for solving economic load dispatch problem", *International Journal of Electric Power and Energy System*, vol. 78, pp. 108-126, 2016.
- [25] M. Ghasemi, M. Taghizadeh, S. Ghavidel and A. Abbasian, "Colonial competitive differential evolution: an experimental study for optimal economic load dispatch", *Applied Soft Computing*, vol. 40, pp. 342-363, 2016.
- [26] N. J. Singh, J. S. Dhillon and D.P. Kothari, "Synergic predator-prey optimization for economic thermal power dispatch problem", *Applied Soft Computing*, vol. 43, pp. 298-311, 2016.
- [27] M. Kheshti, X. Kang, Z. Bie, Z. Jiao and X. Wang, "An effective lightning flash algorithm solution to large scale non-convex economic dispatch with valve-point and multiple fuel options on generation units", *Energy*, vol. 129, pp. 1-15, 2017.
- [28] A. Shukla and S.N. Singh, "Pseudo-inspired CBA for ED of units with valve-point loading effects and multi-fuel options", *IET Generation Transmission and Distribution*, vol. 11, No. 4, pp. 1039-1045, 2017.
- [29] N. J. Singh, J. S. Dhillon and D. P. Kothari, "Surrogate worth trade-off method for multi-objective thermal power load dispatch", *Energy*, vol. 138, pp. 1112-1123, 2017.
- [30] P. Balachandar, S. Ganesan, N. Jayakumar and S. Subramanian, "Multi-fuel power dispatch in an interconnected power system using ant lion optimizer", *International Journal of Energy Optimization and Engineering*, vol. 6, No. 3, pp. 29-54, 2017.
- [31] P. Balachandar, S. Ganesan, N. Jayakumar and S. Subramanian, "Multi-fuel energy dispatch considering bi-objectives using ant lion algorithm" *International Journal of Energy Sector and Management*, vol. 12, pp. 2-27, 2017.
- [32] M. Kheshti, L. Ding, S. Ma and B. Zhao, "Double weighted particle swarm optimization to non-convex wind penetrated emission/economic dispatch and multiple fuel option systems", *Renewable Energy*, vol. 125, pp. 1021-1037, 2018.
- [33] N. J. Singh, J. S. Dhillon and D. P. Kothari, "Multi objective thermal power load dispatch using adaptive predator-prey optimization", *Applied Soft Computing*, vol. 66, pp. 370-383, 2018.
- [34] Hosseoin Narimani, Seyed Ehsan Razavi, Ali Azizivahed, EshanNaderi, Mehdi Fathi, Mohammad H. Ataei and Mohammad RasoulNarimani, "A multi-objective framework for multi-area economic emission dispatch", *Energy*, vol. 154, pp. 126-142, 2018.
- [35] H. Nourianfar and H. Abdi, "Solving the multi-objective economic emission dispatch problems using fast non-dominated sorting TVAC-PSO combined with EMA", *Applied Soft Computing*, vol. 85, pp. 105770, 2019.
- [36] S. Saremi, S. Mirjalili and A. Lewis, "Grasshopper optimisation algorithm: Theory and application", *Advances in Engineering Software*, vol. 105, pp. 30-47, 2017.

Optimal Setting of FACTS Devices using BAT Optimization Algorithm for Congestion Management Problem in Deregulated Power System

M.Gnanaprakash¹, S.P.Mangaiyarkarasi²

¹Research Scholar, Department of Electrical and Electronics Engineering,
University College of Engineering, Panruti, Tamil Nadu. India.
(e-mail: gnanam.au@gmail.com).

²Assistant Professor, Department of Electrical and Electronics Engineering,
University College of Engineering, Panruti, Tamil Nadu.
India (e-mail: mangaisowmeya@gmail.com).

The Bat Algorithm (BA), which is a global optimization method, performs poorly on complex continuous optimization problems due to BA's disadvantages such as the premature convergence problem. In this paper, we propose a novel Bat Algorithm (BA) to improve the performance. Congestion Management (CM) is one of the technical challenges in power system deregulation. This project proposes a Congestion Management approach to relieve congestion and to improve the voltage stability in a system with Flexible AC Transmission System (FACTS) controller in the restructured power system. The optimal choice, location and size of Static Var Compensators (SVC) and Thyristor Controlled Series Compensators (TCSC) in deregulated power system to improve branch loading (minimize congestion, improve voltage stability and reduce line losses). Though FACTS controllers offer many advantages their installation cost is very high. Hence Independent System Operator (ISO) has to locate them optimally to satisfy a desired objective. This project presents optimal location of FACTS controller considering Branch Loading (BL), Voltage Stability (VS) and Loss Minimization (LM) as objectives at once using BAT algorithm. It is observed that the locations that are most favorable with respect to one objective are not suitable locations with respect to other two objectives. The proposed optimization problem is solved using the BAT algorithm. The effectiveness of the proposed CM approach is examined on IEEE 30 bus test system.

Keywords: *Hybrid algorithm; Bat algorithm; Extremal optimization; Continuous optimization problems*

1 Introduction

There are many multimodal optimization problems in engineering and science. Therefore, an algorithm must be able to deal with these problems in addition to unimodal optimization problems. Evolutionary Computing (EC), which is based on the biological concept of populations and iterative improvements, is a powerful optimization method, despite its slow convergence speed [1-3]. EC mainly involves Evolutionary Algorithms (EAs) and Swarm Intelligence (SI). EAs are effective optimization techniques for finding global solutions to complex problems with several decision variables and constraints [4]. Genetic Algorithm (GA) [5], Evolutionary Programming (EP) [6], Evolutionary Strategies (ESs) [7, 8], Genetic Programming (GP) [9], Differential Evolution (DE) [10], Estimation of Distribution Algorithm (EDA) [11], and Immune System Optimization [12] are the most representative implementations of the EA concept. However, their evolutionary patterns and principles are not the same. SI is inspired by animal behavior patterns and has aroused the attention of scientists. Many biological metaphors were used when proposing new metaheuristic methods for solving optimization problems. The typical examples of SI include Particle Swarm Optimization (PSO) [13], Fruit Fly Optimization Algorithm (FOA) [14], Artificial Bee Colony Algorithm (ABC) [15], Cuckoo Search (CS) [16], Ant Colony Optimization (ACO) [17], Cat Swarm Optimization (CSO) [18], Firefly Algorithm (FA) [19], Artificial Fish Swarm Algorithm (AFSA) [20], and Shuffled Frog Leaping Algorithm (SFLA) [21]. Most of these traditional optimization algorithms achieve excellent performance on a small number of instances that are very small in size. However, as the complexity of the problems increases, their adaptability deteriorates [22].

2 Congestion Management (CM)

3.1 Introduction:

In this chapter, we look at congestion management methodologies and how they get modified in the new competitive framework of electricity power markets. A simple example is given for the calculation of congestion charges in a scenario where the objective of optimization is to maximize societal benefit.

3.2. Congestion:

Congestion is a technical problem which occurs when power producers and consumers of electrical energy desire to produce and consume in total amount that would cause the transmission system to operate at or beyond one or more transfer limits. Congestion does not occur in both electrically bundled and unbundled systems, but the management in the bundled system is relatively simple and it is more complex in competitive power markets.

3. Bat Algorithm:

If we idealize some of the echolocation characteristics of microbats, we can develop various bat-inspired algorithms or bat algorithms. For simplicity, we now use the following approximate or idealized rules:

1. All bats use echolocation to sense distance, and they also 'know' the difference between food/prey and background barriers in some magical way;
2. Bats fly randomly with velocity V_i at position X_i with a fixed frequency f_{MIN} , varying wavelength λ and loudness A_0 to search

for prey. They can automatically adjust the wavelength (or frequency) of their emitted pulses and adjust the rate of pulse emission $r \in [0, 1]$, depending on the proximity of their target;

3. Although the loudness can vary in many ways, we assume that the loudness varies from a large (positive) A_0 to a minimum constant value A_{MIN} .

Another obvious simplification is that no ray tracing is used in estimating the time delay and three dimensional topography. Though this might be a good feature for the application in computational geometry, In addition to these simplified assumptions, we also use the following approximations, for simplicity. In general the frequency f in a range $[f_{MIN}, f_{MAX}]$ corresponds to a range of wavelengths $[\lambda_{MIN}, \lambda_{MAX}]$. For example a frequency range of $[20\text{kHz}, 500\text{kHz}]$ corresponds to a range of wavelengths from 0.7mm to 17mm. For a given problem, we can also use any wavelength for the ease of implementation. In the actual implementation, we can adjust the range by adjusting the wavelengths (or frequencies), and the detectable range (or the largest wavelength) should be chosen.

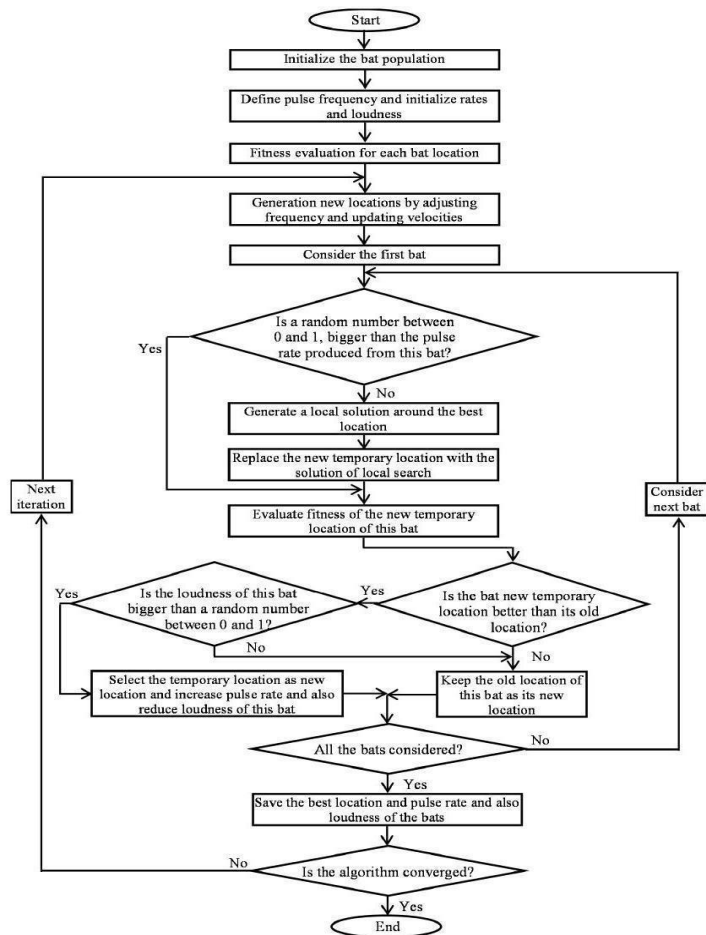
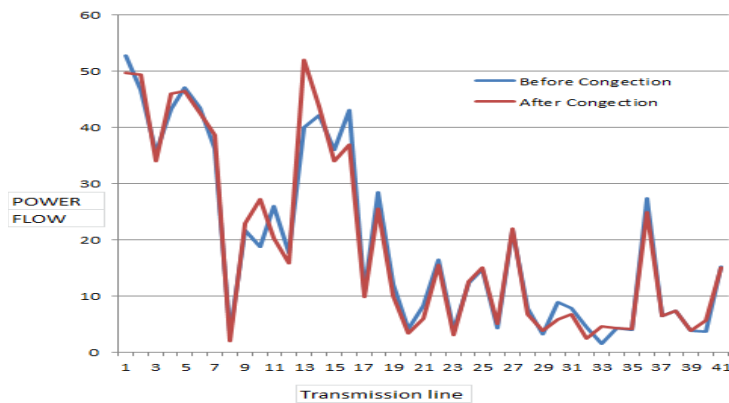
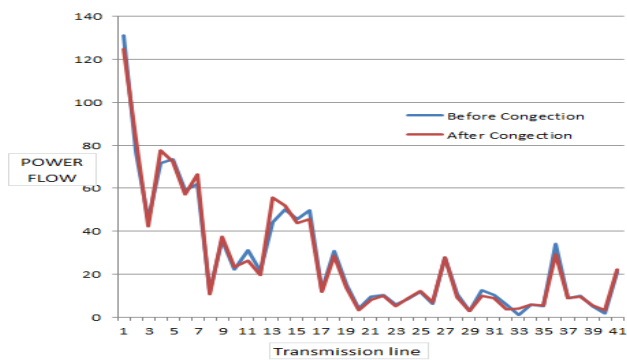


Figure 3.1 Flowchart for bat algorithm

4 Results and Discussion



| BEST LOCATION OF FACTS DEVICE STANDARD IEEE 30 BUS SYTEM | TRANSMISSION LINE | SIZE |
|--|-------------------|---------|
| | 2 | -0.1345 |
| | 13 | -0.5226 |
| | 19 | 5.2578 |
| | 24 | 9.3420 |



| BEST LOCATION OF FACTS DEVICE BY INCREASING LOAD BY 135% | TRANSMISSION LINE | SIZE |
|--|-------------------|---------|
| | 2 | -0.1654 |
| | 13 | -0.4230 |
| | 25 | 7.4612 |
| | 29 | 5.2955 |

5 Conclusion

In this paper an algorithm is developed for optimal choice and location of FACTS controllers for congestion management in deregulated power systems. Bat algorithm are best suitable for solution of objective optimization problems. In this work congestion is created in the system using i) uniform loading ii) line outage iii) bilateral transaction and iv) multilateral transactions. Optimal location of FACTS to relieve line congestion is treated as a single objective optimization problem considering i) BL ii) VS and iii) TL as objectives. It is observed that the locations which present favorable solution with respect to one of the objectives are not effective with respect to other objectives. The results obtained for various cases studied for IEEE 30 bus system reveal that, single objective optimization algorithms do not provide attractive solutions when all objectives considered are to be given equal priority. Therefore, multi objective with Bat algorithm is developed for simultaneous optimization of BL, VS and LM. Further, simultaneous optimization of three objectives considered presents optimal location of FACTS devices, which reduce line congestion, improved system voltage profile and reduce system losses. The proposed Bat algorithm with SVC, TCSC models evolves as a good optimization algorithm for single objective optimization and SPEA for multi-objective optimization studies of optimal location of FACTS controllers’ problem.

References

[1] M. Ergezer, D. Simon, Probabilistic properties of fitness-based quasi-reflection in evolutionary algorithms, *Comput. Oper. Res.* 63(C) (2015) 114-124.

[2] M. Borrotti, G. Minervini, D.D. Lucrezia, I. Poli, Naïve Bayes ant colony optimization for designing high

- dimensional experiments, *Appl. Soft Comput.* 49(2016) 259-268.
- [3] M.M. Noel, A new gradient based particle swarm optimization algorithm for accurate computation of global minimum, *Appl. Soft Comput.* 12(1) (2012) 353–359.
- [4] J. Galletly, Evolutionary algorithms in theory and practice, *Complexity*, 2(8) (1996) 26–27.
- [5] J.H. Holland, Adaptation in natural and artificial systems: an introductory analysis with applications to biology, control, and artificial intelligence, *Q. REV. BIOL.* 6(2) (1992)126-137.
- [6] A.E. Eiben, J.E. Smith, Evolutionary programming, in: *Proceedings of the IEEE International Conference on Evolutionary Computation*, 'Vol.' 6, IEEE, 2011, pp. 443-446.
- [7] H.G. Beyer, The theory of evolution strategies, *Springer*, 33(4) (2001) 266-74.
- [8] H.G. Beyer, B. Sendhoff, Covariance matrix adaptation revisited—the CMSA evolution strategy, *International Conference on Parallel Problem Solving From Nature: PPSN X*, Springer, Berlin, Heidelberg, 2008, pp.123-132.
- [9] M.A. Haeri, M.M. Ebadzadeh, G. Folino, Statistical genetic programming for symbolic regression, *Appl. Soft Comput.* 60(2017) 447-469.
- [10] S. Das, P.N. Suganthan, Differential evolution: a survey of the state-of-the-art, *IEEE T. Evolut. Comput.* 15(1) (2011)
- [11] P. Larrañaga, J.A. Lozano, Estimation of distribution algorithms, *Springer US*, 192(5) (2002)454-468.
- [12] S.A. Hofmeyr, S. Forrest, Architecture for an artificial immune system, *Evol. Comput.* 8(4) (2000) 443-473.
- [13] J. Kennedy, R.C. Eberhart, Particle swarm optimization, in: *Proceedings of the IEEE International Conference on Neural Networks*, 'Vol.' 4, Perth, Australia, IEEE Service Center, Piscataway, NJ, 1995, pp. 1942-1948.
- [14] W. Pan, A new Fruit Fly Optimization Algorithm: Taking the financial distress model as an example, *Knowl-Based Syst.* 26(2) (2012) 69-74.
- [15] Karaboga, B. Akay, A comparative study of Artificial Bee Colony algorithm, *Appl. Math. Comput.* 214(1) (2009) 108-132.
- [16] X.S. Yang, S. Deb, Cuckoo Search via Levy Flights, in: *Proceedings of the World Congress on Nature and Biologically Inspired Computing*, IEEE, 2009, pp. 210-214.
- [17] M. Dorigo, L.M. Gambardella, Ant colonies for the travelling salesman problem, *Biosystems*, 43(2) (1997) 73-81.
- [18] S.C. Chu, P. Tsai, J.S. Pan, Cat swarm optimization, *Trends in Artificial Intelligence*, Springer, Berlin, Heidelberg, 2006, pp.854-858.
- [19] X.S. Yang, X. He, Firefly algorithm: Recent advances and applications, *Int. J. Swarm Intelligence*, 1(1) (2013) 36-50, doi: 10.1504/IJSI.2013.055801.
- [20] M. Neshat, G. Sepidnam, M. Sargolzaei, A.N. Toosi, Artificial fish swarm algorithm: a survey of the state-of-the-art, hybridization, combinatorial and indicative applications, *Artif. Intell. Rev.* 42(4) (2014) 965-997.

Behaviour Modelling of Composite Glass Fibre and Epoxy Matrix in different angles

K. Rajendran ¹, S. Muthukumar ²

¹ Senior Lecturer, Department of Mechanical Engineering, P.A.C. Ramasamy Raja Polytechnic College, Rajapalayam, Tamil Nadu - 626 108

² Project Engineer, Bluesky Projects, Chennai - 600 028

Abstract

A tremendous usage of composite materials in our day-to-day life is going on rising trend. Because of advantages like light weight, high strength to weight ratio, the composite materials are plays vital role in Automobile sectors, Home appliances, Electronic gadgets etc., we are going to make composite sheets using Glass Fibre and Epoxy materials. Since composite materials are orthotropic, the prediction of material properties varies with direction and orientation of fibre. Determining bending and tensile stresses for various orientation of fibre will becomes challenging process. To reduce this exertion, we will have proposed to generate a behaviour equation by interpreting the ANSYS results of bending stress and tensile stress. From the regression analysis, we will formulate a general mathematical equation having variable as orientation angles of different layers. This equation gives bending stress and tensile stress directly by applying orientation angles of each layer without conducting test. Thus the prediction regression equation eliminates the time involved in testing the composites at different orientation angles. The prepared composites are tested in UTM to validate the equation.

Keywords: Glass fibre, Epoxy, Regression, Ansys

1 Introduction

Generally, the composites are classified according to their reinforcement types as particle reinforced composites and fibre reinforced composites. But more commonly, the classification is based on the matrix types i.e., metal matrix composites (MMCs), ceramic matrix composites (CMCs) and polymer matrix composites (PMCs) as shown in the Fig. (1).

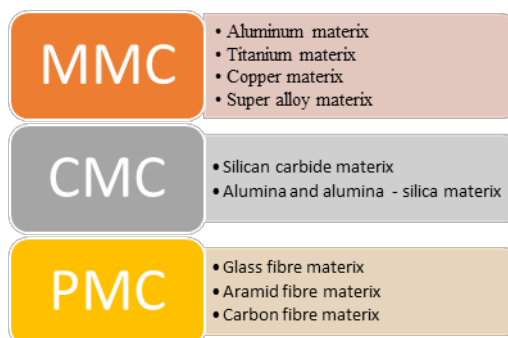


Figure 1: Classifications of matrix components. Also various types of matrix components are listed here.

PMCs used in boat bodies, canoes, sport kids, automobile components, and bullet proof vests etc., CMCs used in heat exchangers, and burner components, turbine blades, engine exhaust nozzle, cutting tools, wear components etc., MMCs used in prototypes of space shuttle and commercial airlines, electronic substrates, bicycles, automobile parts, etc.,

This article we choose PMCs as glass fibre for reinforcement and epoxy resin as resin matrix. In glass fibre, we have various types as A-glass fibre, E-CR-glass fibre, C- glass fibre, D- glass fibre, - glass fibre, and S- glass fibre. Depending upon application glass fibres will be chosen. Further, glass fibres are used in making of wind turbine blades, medical instruments like form instruments enclosures to X-ray beds, Home applications like shower tray, furniture and spa tubs etc., and automobiles fibreglass has a big presence in the replacement body parts, custom and kit auto markets.

The most demanding strength/weight applications, we use epoxy almost exclusively. It has excellent strength, hardness, very good chemical heat and electrical resistance and also it has disadvantages like higher cost, processing difficulty. Epoxy systems are used in applications like aerospace, defence, marine, sports equipment, adhesives, sealants, coatings, architectural, flooring and many others.

In the mechanical properties of any resin system, tensile strength and stiffness are very vital. The following two figures Fig. (2) and Fig. (3) show the results for tests carried out on commercially available polyester, vinyl ester and epoxy resin systems cured at 20°C and 80°C.

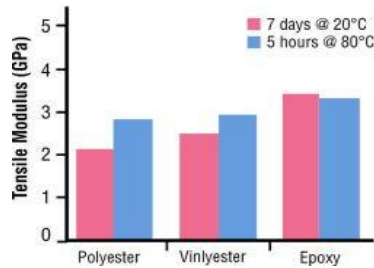


Figure 2: Comparison of Resin and Tensile Modulus. Polyester, Vinyl ester and Epoxy resins are compared with respect to the Tensile Modulus at standard curing time and temperature.

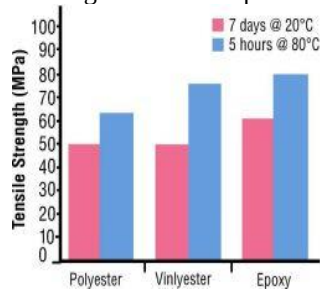


Figure 3: Comparison of Resin and Tensile Strength. Polyester, Vinyl ester and Epoxy resins are compared with respect to the Tensile Strength at standard curing time and temperature.

We have chosen epoxy resin for better higher properties than a typical polyester and vinyl ester for both strength and stiffness under various curing time and temperatures.

2 Methodology

Now-a-days lot of technology improvements in composites has been taken place. By upgrading that, we have to generate general equation for finding the tensile stress and bending stress. This above said equation is generated by regression analysis. The GFRP composite sheets is proposed to fabricated by the hand lay-up process because out of various polymer matrix manufacturing process this process have the more advantages and most suitable for sheets. Glass fibre and epoxy matrix used as composite material. Different orientation angles as 0° , 30° , 45° , 60° taken and their different combinations made. First 0° taken as constant the other 3 various degrees as variable (1) 0° , 45° , 30° , 60° . (2) 0° , 60° , 30° , 45° . (3) 0° , 30° , 60° , 45° .

Repeat this for 30, 45, 60 degrees. So totally we have 24 various combinations of angles. Testing the composites for bending stress and tensile stress at different orientation angles is difficult process. That is, every time the orientation angles are varied and hand layup process is done. For all this combinations bending and tensile test will be done in ANSYS software. General equation will be generated by using regression analysis by interrupt the results from bending stress and tensile stress values from ANSYS. After this, equation is validated by fabricating composite sheet and test it. Also validate by finding the bending stress and tensile stress values from ANSYS for other orientation angles. That equation gives bending stress and tensile stress directly by applying orientation angles of each layer without conducting test. Thus the prediction regression equation eliminates the time involved in testing the composites at different orientation angles.

2.1. Fabrication of GFRP Sheet by Hand Lay-Up:

We choose Hand lay-up process for making composite sheet fabrications. Before lay-up, glass fibres cut into first combination of angles 0° 45° 30° 60° , also placed in the mould. Resin must then be catalysed and added to the fibres. Fig. (4). shows the basic process of hand lay-up.

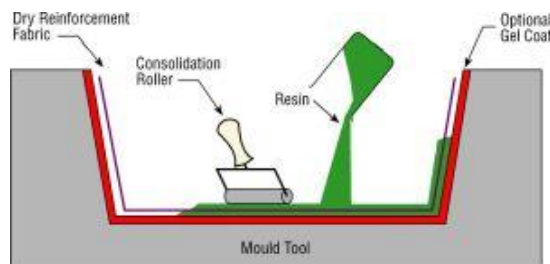


Figure 4: Schematic diagram of Hand Lay Up process. Using this working principle the glass fibre and resin components are made into composite sheet.

2.2. Weight Calculation for Fabrication:

| | |
|-----------------------------|---------------------------------|
| Weight of glass fibre mat 1 | = 24.79 g |
| Weight of glass fibre mat 2 | = 28.30 g |
| Weight of glass fibre mat 3 | = 27.90 g |
| Weight of glass fibre mat 4 | = 28.10 g |
| Total weight of fibre mat | = 109.09g |
| Amount of resin required | = 2 x weight of mat = 220 g |
| Amount of hardener required | = 0.5 x weight of resin = 110 g |



Figure 5: Glass fibre cut into required angles are weighed in weight measuring machine and weights of corresponding fibres are noted.



Figure 6: Resin is weighed in weight measuring machine and weight corresponding to the resin is noted.

The glass fibre mat was cut into the dimension of 300 x150 mm size at the angle of 0 degree. Then the angle is marked on the mat by using protractor as 30 degree and size of 300 x150 mm marked. Repeat these also for 45 and 60 degrees. Finally, all marked mats are cut by using cysers. Weight of the glass fibre is weighed in weight measuring machine as shown in the Fig. (5). Weight calculated for the resin and hardener are taken in bowls at correct quantity measured by a weighing machine as shown in the Fig. (6). Both resin and hardener are mixed thoroughly. Paste the wax on the glass plate where the process is to be done.

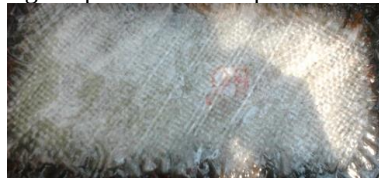


Figure 7: After measuring weights, fibre and resins are made to generate composite sheet by hand lay-up process and allowed to curing of composite sheet.

Then place mat-1 0 degree on the wax pasted surface. After mixed resin and hardener should have applied on the mat-1 fully. Place the mat-2 30 degree mat over resin coated surface and give light pressure on mat-2 to ensure mat is completely placed over coated surface Repeat these for 45 and 60 degree mats. After placing mat-4 60-degree resin coated over these mat also. Then the composite sheet allowed to cure as shown in the Fig. (7).

3 ANSYS Testing

By using ANSYS software, the various combinations of angles are analysed for the following bending test and tensile test. we use ANSYS Mechanical APDL. This composite matrix consists of 4 layers i.e., 24 combinations angles are to be analysed. After analysis, results are plotted as following figures from Fig. (8) to Fig. (15).

3.1. ANSYS Results Tensile test:

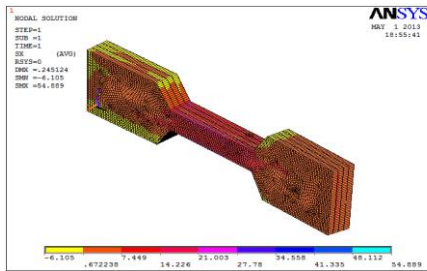


Figure 8: ANSYS Tensile Test results for 0°, 45°, 30°, 60° angles

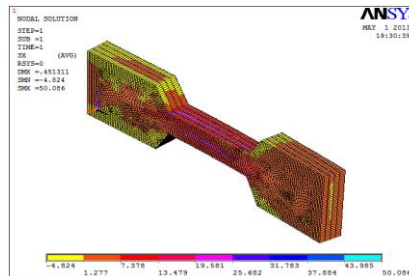


Figure 9: ANSYS Tensile Test results for 30°, 45°, 60°, 0° angles

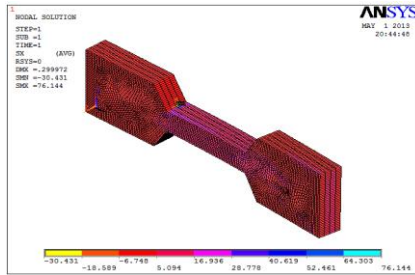


Figure 10: ANSYS Tensile Test results for 45°, 0°, 30°, 60° angles

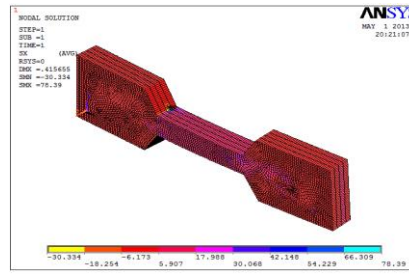


Figure 11: ANSYS Tensile Test results for 60°, 0°, 30°, 45° angles

3.2 ANSYS Results Bending Test:

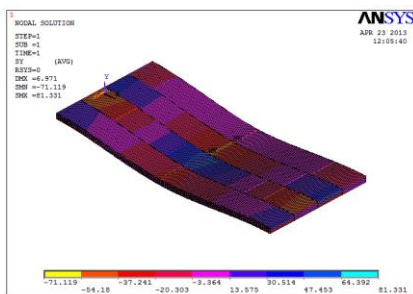


Figure 12: ANSYS Bending Test results for 0°, 30°, 45°, 60° angles

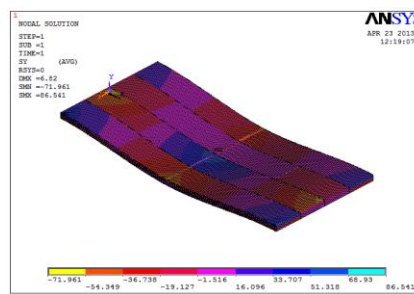


Figure 13: ANSYS Bending Test results for 30°, 0°, 60°, 45° angles

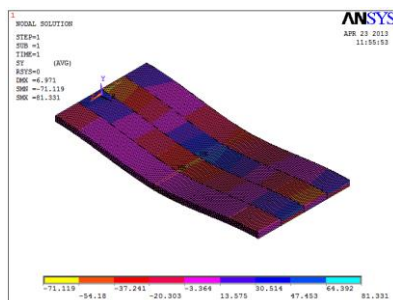


Figure 14: ANSYS Bending Test results for 45°, 60°, 30°, 0° angles

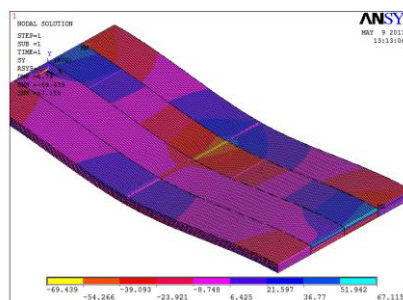


Figure 15: ANSYS Bending Test results for 60°, 30°, 45°, 0° angles

Table 1: ANSYS Result

| Angle combinations in Degrees | | | | Bending Stress | Tensile Stress |
|-------------------------------|------------|------------|------------|----------------|----------------|
| θ_1 | θ_2 | θ_3 | θ_4 | N/mm^2 | N/mm^2 |
| 0 | 30 | 45 | 60 | 61.678 | 58.901 |
| 0 | 30 | 60 | 45 | 81.331 | 61.326 |
| 0 | 45 | 30 | 60 | 67.115 | 54.889 |

| | | | | | |
|----|----|----|----|--------|--------|
| 0 | 45 | 60 | 30 | 96.9 | 51.248 |
| 0 | 60 | 30 | 45 | 70.23 | 48.503 |
| 0 | 60 | 45 | 30 | 73.847 | 50.086 |
| 30 | 0 | 45 | 60 | 67.789 | 60.685 |
| 30 | 0 | 60 | 45 | 86.541 | 55.541 |
| 30 | 45 | 0 | 60 | 55.958 | 57.23 |
| 30 | 45 | 60 | 0 | 73.847 | 50.086 |
| 30 | 60 | 0 | 45 | 73.847 | 55.277 |
| 30 | 60 | 45 | 0 | 96.9 | 51.248 |
| 45 | 0 | 30 | 60 | 68.308 | 76.144 |
| 45 | 0 | 60 | 30 | 80.641 | 75.334 |
| 45 | 30 | 0 | 60 | 62.727 | 78.39 |
| 45 | 30 | 60 | 0 | 70.402 | 65.171 |
| 45 | 60 | 0 | 30 | 86.541 | 81.594 |
| 45 | 60 | 30 | 0 | 81.331 | 61.326 |
| 60 | 0 | 30 | 45 | 62.727 | 78.39 |
| 60 | 0 | 45 | 30 | 55.808 | 84.443 |
| 60 | 30 | 0 | 45 | 68.308 | 76.144 |
| 60 | 30 | 45 | 0 | 67.246 | 60.599 |
| 60 | 45 | 0 | 30 | 67.789 | 84.296 |
| 60 | 45 | 30 | 0 | 61.771 | 59.085 |
| 0 | 15 | 30 | 45 | 46.84 | 55.23 |
| 0 | 15 | 45 | 30 | 41.75 | 51.76 |

4 Testing of composites:

FRP sheet is cut into as per ASTM standard size. The tensile and bending tests are carried out in UTM machine and results are tabulated. Tensile stress for 0° 45° 30° 60° combination of angle is calculated as 54.16 N/mm². Bending stress 0° 30° 45° 60° combination of angle is calculated as 59.3 N/mm²



Figure 16: Specimen before tensile test



Figure 17: Specimen During Tensile Test (UTM)



Figure 18: Specimen after tensile test



Figure 19: Specimen before Bending test

Figure 20: Specimen after Bending test

5 Regression Analysis:

5.1. Bending stress:

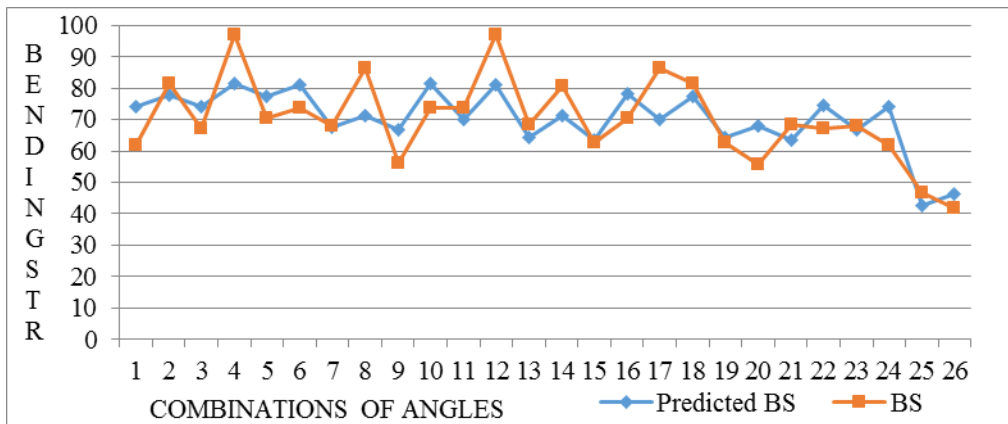


Figure 21: Comparison of ANSYS and Predicted Bending Stress values. The chart shows closeness of Predicted Bending stress value and ANSYS Bending stress value.

We are going to use statistical method to investigate the relationship between a dependent variable y and one or more independent variable x, independent variable is usually called as regressor or predictor variable. In excel regression, taking bending stress values from ANSYS as Y variable and $\theta_1, \theta_2, \theta_3, \theta_4$ angle of first, second, third, fourth layers taking as X variables and give OK. The result of regression analysis has following equation Eq. (1).

$$-17.83378 + 0.554867\theta_1 + 0.774001\theta_2 + 0.795658\theta_3 + 0.551506\theta_4 \quad \text{Eq. (1)}$$

5.2 Tensile stress:

In excel, Go to regression, taking tensile stress values from ANSYS as Y variable and $\theta_1, \theta_2, \theta_3, \theta_4$ angle of first, second, third, fourth layers are taking as X variables and give OK. Result of regression analysis has following equation Eq. (2).

$$51.20705 + 0.37091 \theta_1 - 0.08826 \theta_2 - 0.06385 \theta_3 + 0.1601 \theta_4 \quad \text{Eq. (2)}$$

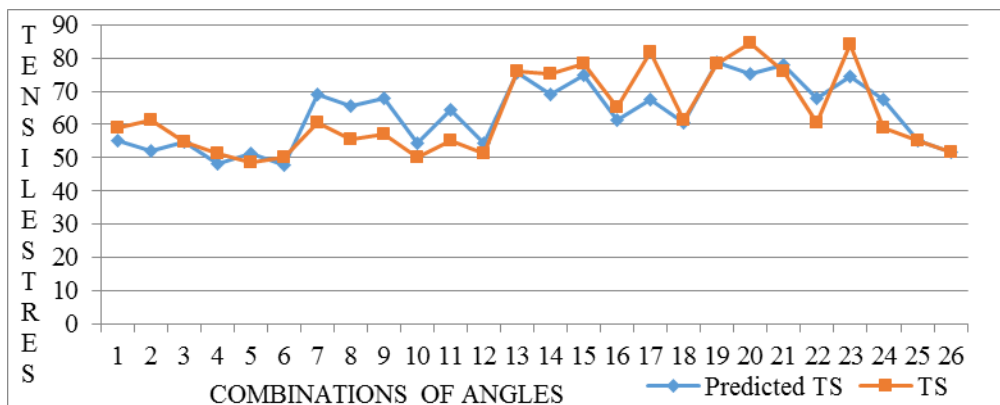


Figure 22: Comparison of ANSYS and Predicted Tensile Stress values. The chart shows closeness of Predicted Tensile stress value and ANSYS Tensile stress value.

6 Validation of Regression Results

6.1 Validation of Tensile Stress Equation:

From ANSYS table for the following combination of angles 0° 45° 30° 60° the tensile stress is noted and actual value gets from equation by substituting angles.

- ANSYS table value = 54.889 N/mm²
- Actual value (Equation) = 54.9283 N/mm²
- Tensile test = 54.66 N/mm²

From ANSYS another combination of 15°, 30°, 45°, 60°

- ANSYS table value = 82.31 N/mm²
- Actual value (Equation) = 82.295 N/mm²

From ANSYS another combination of 15°, 45°, 30°, 60°

- ANSYS table value = 81.409 N/mm²
- Actual value (Equation) = 81.92 N/mm²

6.2 Validation of Bending Stress Equation:

From ANSYS table for the following combination of angles 0° 30° 45° 60° the tensile stress is noted and actual value gets from equation by substituting angles.

- ANSYS table value = 61.678 N/mm²
- Actual value (Equation) = 62.281N/mm²
- Bending test = 61.3 N/mm²

From ANSYS another combination of 15°, 30°, 45°, 60°

- ANSYS table value = 61.93 N/mm²
- Actual value (Equation) = 61.07 N/mm²

From ANSYS another combination of 15°, 45°, 30°, 60°

- ANSYS table value = 61.93 N/mm²
- Actual value (Equation) = 60.83 N/mm²

Hence, above two equations Eq. (1) and Eq. (2) offered nearer value by ANSYS value. Therefore, Equation from regression provides less margin of gap within acceptable range. But fine tuning of gap will be reduced further research works by fabrication and testing of other angles.

7 Conclusion

The model equation is generated from regression analysis for the four layered glass fibre-epoxy matrix composite. This equation validated by testing of composite plates and results are in acceptable range. The equation can be used for calculating bending stress and tensile stress directly by substituting the values of different fibre orientation layer angles. Thus it reduces the time involved in testing the glass fibre-epoxy matrix composite with different orientation layer angles. This work also helps the researchers to get the optimum combination of layer orientation angle. This work can be extended to impact test and shear test in future. This proposed method is also extended to predict the mechanical properties of composites by increasing layers.

References:

- [1] M.A. Azmir, A.K. Ahsan, "Investigation on glass/epoxy composite surfaces machined by abrasive water jet machining" *Journal of materials processing technology*, 198, pp 122-128, 2008.
- [2] Doreswamy, Hemanth K S and Manohar M, "Linear regression model for knowledge discovery in engineering materials", *Computer Science & Information Technology*, pp 4-10, 2009.
- [3] Miss Priya Dongare and Prof. Dr. Suhas Deshmukh, "Static and modal analysis of composite drive shaft and development of regression equations" *International Journal of Engineering Research & Technology*, vol-1, pp 2-6, 2012.
- [4] Chensong Dong, Chuck Zhang, Zhiyong Liang, Ben Wang, "Dimension variation prediction for composites with finite element analysis and regression modeling", *Composites Part A* 35, pp 2-6, 2004.
- [5] Alisa Dahl Andy Bertsch, "Regression Model Building with MS Excel: Using Excel's Multiple Regression Tool to Explore the Correlation Between Advertising Dollars and Sales Volume", *Journal of Applied Business and Economics*, pp 4-10, 2008.

Experimental investigation of the correlation between FDM process parameters and dimensional accuracy for nylon parts

C. R. Sanghani, V. R. Vaghani

Department of Mechanical Engineering, Tapi Diploma Engineering College, Surat, India

Abstract

For the last few decades, additive manufacturing is drawing the attention of researchers and industry professionals working in different fields. Fused deposition modeling (FDM) is a well known additive manufacturing process for polymer parts. To improve the performance of any process, it is necessary to study the influence of various process parameters on performance measures. Hence, the effects of FDM process parameters like layer thickness, printing speed, raster angle, and % infill on the dimensional accuracy of nylon parts are investigated and discussed in this paper. Taguchi's L16 orthogonal array was used for the design of experiment and the significance of each parameter was identified by analysis of variance (ANOVA). It was found that print speed is the most significant parameter for the dimensional accuracy of nylon parts.

Keywords: Dimensional accuracy, FDM, infill, layer thickness, print speed, raster angle, nylon

1 Introduction

Additive manufacturing (AM) has certain advantages over conventional manufacturing methods and hence, the world's well-known companies are taking interest in this technology. Fused deposition modeling is one of the most used AM techniques for producing complex geometrical parts in less time. The quality of parts produced by any technique depends on its process parameters. Hence, many researchers have tried to investigate the effect of FDM parameters on performance measures like tensile strength, compressive strength, flexural strength, impact strength, dimensional accuracy, surface roughness, hardness, etc. for different materials like Acrylonitrile Butadiene Styrene (ABS), Polylactic Acid (PLA), Polyethylene Terephthalate Glycol (PETG), etc. A summary of some of the literature related to parametric analysis is shown in Table 1. The literature study showed a lack of work on parametric analysis for nylon parts made by the FDM process. Hence, the objective of this paper is to present the correlation between process parameters namely layer thickness, printing speed, raster angle, and % infill and dimensional accuracy of nylon parts fabricated by the FDM process.

Table 1: Summary of literature

| Author | Material | Process parameters | Performance characteristics | Remarks |
|---------------------------|---------------|---|---|---|
| Letcher and Waytashek [1] | PLA | Raster orientation | Tensile strength, Bending strength, Fatigue strength | The 45° raster orientation gives the highest tensile, flexural, and fatigue strength. |
| Christiyan et al. [2] | ABS composite | Layer thickness, Printing speed, Nozzle diameter | Tensile strength, Flexural strength | Lower printing speed and layer thickness showed good tensile and flexural strength due to better bonding. |
| Basavaraj and Vishwas [3] | Nylon | Layer thickness, Orientation angle, Shell thickness | Ultimate tensile strength, Dimensional accuracy, Manufacturing time | The lower layer thickness gives good axial loading capability. |
| Vishwas and | ABS | Orientation angle, | Tensile Strength, | The layer thickness is |

| | | | | |
|---------------------------|----------|---|--|---|
| Basavaraj [4] | | Layer thickness, Shell thickness | Dimensional Accuracy, Manufacturing Time | found the most influential parameter for all the performance measures. |
| Rajpurohit and Dave [5] | PLA | Raster angle, Layer height, Raster width | Tensile strength | Raster angle is the most influential factor for the tensile strength of the specimen. |
| Miranda et al. [6] | PETG | Extrusion temperature | Young's modulus | Lower printing temperature gives better part finishing as it prevents warping. |
| Barrios and Romero [7] | PETG | Layer height, Printing temperature, Printing speed, Printing acceleration, Flow rate | Surface roughness, Sliding angle, Contact angle | The flow rate and print acceleration are responsible for the circularity of the deposited filament section and uniformity along the printing road respectively. |
| Abdelrhman et al. [8] | PLA | Part orientation | Dimensional accuracy, Tensile strength, Surface quality | The part orientation for good dimensional accuracy and tensile strength is X0°Y0° while X90°Y0° for good surface quality. |
| Dave et al. [9] | PLA | Orientation, Infill pattern, Infill density | Tensile strength | The flat part orientation and concentric pattern showed maximum tensile strength. |
| Mendricky and Fris [10] | PLA | Layer height, Extruded line width, Number of walls, Top layer thickness, Percentage of fill, Fill shape, Fill print speed, Wall print speed, Top layer print speed, Orientation, % of extruded material | Printing time, Material consumption, Surface quality, Accuracy | The material consumption is influenced by percentage fill, layer height, and no. of walls. The layer height affects mostly to surface roughness and dimensional accuracy of the part. |
| Rajurkar and Thesiya [11] | PLA, ABS | Layer height, Infill pattern, Infill density, | Tensile strength, Impact | ABS parts exhibited more shrinkage and |

| | | | | |
|--|--|--------------|------------------------|---|
| | | Raster angle | strength, Shrinkage | warpage as compared to PLA parts due to thermal problems. |
|--|--|--------------|------------------------|---|

2 Experimental Details

2.1 Material

In this study, a wire filament of nylon 6 material is used for printing different specimens. Nylon 6 is a very famous and extensively used polyamide material in industries due to its combination of strength and toughness. Durability, flexibility, and abrasion resistance make it suitable to be used for jigs, fixtures, guides, sports goods, and functional prototypes.

2.2 Process parameters

In this study, four FDM process parameters namely layer thickness, printing speed, percentage infill, and raster angle were considered with four levels. Layer thickness can be defined as the height of a single layer of material deposited by an extruder. Print speed is the traveling speed of the extruder during the deposition of the material. Infill refers to the percentage of total cavity volume that will be printed inside the shell boundary. Raster angle is the inclination of material deposition direction with respect to the x-axis of the printer bed. The values of parameters at each level are shown in Table 2.

Table 2: Process Parameters and their levels

| Parameters | Code | Levels |
|---------------------------|------|------------------------|
| Layer thickness (mm) | LT | 0.10, 0.15, 0.20, 0.25 |
| Print speed (mm/s) | PS | 30, 40, 50, 60 |
| Infill (%) | PI | 70, 80, 90, 100 |
| Raster angle (°) | RA | 0, 45, 60, 90 |
| Extruder temperature (°C) | - | 250 |
| Bed temperature (°C) | - | 80 |
| Shell wall thickness (mm) | - | 2 |

2.3 Design of experiment

To explore the relationship of FDM parameters with dimensional accuracy, Taguchi's L16 orthogonal array was used based on four factors and four levels. Total 16 different combinations of FDM process parameters were selected for preparing specimens as shown in Table 3.

2.4 Preparation of test specimens

The dimensions of the target specimen were considered from reference [1] as depicted in Fig. (1). A 3D model of the test specimen was prepared using CAD software 'Solidworks'. The file of the 3D model was exported with .stl format and that file was imported in 3D printing software 'Ultimaker Cura' to generate G-code for the toolpath. Based on Taguchi's L16 array, total 16 specimens were prepared with the FDM 3D printer having chamber volume 550 x 550 x 550 mm and nozzle diameter 0.3 mm. Figure 2 shows all the printed specimens using FDM based 3D printer.

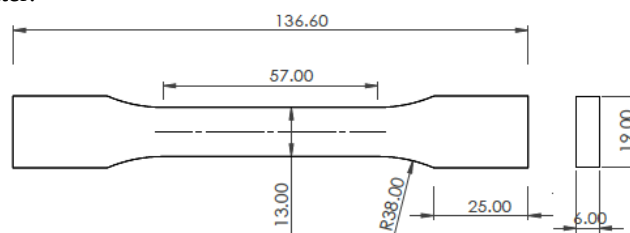


Figure 1: Test specimen dimensions [mm]

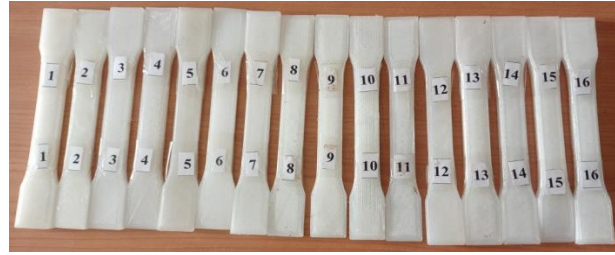


Figure 2: 3D printed specimens

2.5 Evaluation of dimensional accuracy

To measure different dimensions of test specimens and hence to evaluate dimensional accuracy, a Mitutoyo digital vernier caliper having measuring range 0-150 mm and resolution 0.01 mm was used. To check the effect of different parameters on the dimensional accuracy of 3D printed specimens, total five dimensions (d1-d5) were considered as shown in Fig. (3).

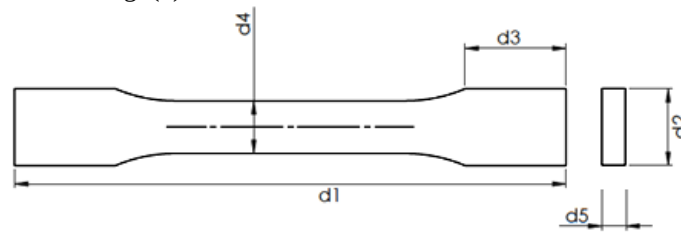


Figure 3: Dimensions for checking the accuracy

The dimensional accuracy is calculated based on measured dimensions and nominal dimensions of the CAD model.

3 Results and Discussion

Taguchi's design of experiment for the present investigation and the values of average dimensions observed from the measurements are shown in Table 3. Three readings of each dimension have been taken for all the specimens and their average values have been considered for the calculation of dimensional accuracy (DA).

Table: 3 Result of dimension measurement

| Exp. No. | LT | PS | PI | RA | Average dimensions (mm) | | | | | DA (%) | S/N ratio |
|----------|------|----|-----|----|-------------------------|-------|-------|-------|------|--------|-----------|
| | | | | | d1 | d2 | d3 | d4 | d5 | | |
| 1 | 0.1 | 30 | 70 | 0 | 135.32 | 19.38 | 25.75 | 13.65 | 6.38 | 96.69 | 39.708 |
| 2 | 0.1 | 40 | 80 | 45 | 134.62 | 19.17 | 25.70 | 13.47 | 5.62 | 97.04 | 39.739 |
| 3 | 0.1 | 50 | 90 | 60 | 135.40 | 19.17 | 25.45 | 13.54 | 5.93 | 98.27 | 39.848 |
| 4 | 0.1 | 60 | 100 | 90 | 135.61 | 19.35 | 25.56 | 13.53 | 6.22 | 97.57 | 39.786 |
| 5 | 0.15 | 30 | 80 | 60 | 135.15 | 19.34 | 25.47 | 13.27 | 5.79 | 97.96 | 39.821 |
| 6 | 0.15 | 40 | 70 | 90 | 135.23 | 19.48 | 25.52 | 13.54 | 5.63 | 96.87 | 39.724 |
| 7 | 0.15 | 50 | 100 | 0 | 134.96 | 19.05 | 25.46 | 13.30 | 5.86 | 98.43 | 39.862 |
| 8 | 0.15 | 60 | 90 | 45 | 134.74 | 18.87 | 25.51 | 13.15 | 5.66 | 97.84 | 39.810 |
| 9 | 0.2 | 30 | 90 | 90 | 135.03 | 19.14 | 25.77 | 13.37 | 6.14 | 98.02 | 39.826 |
| 10 | 0.2 | 40 | 100 | 60 | 135.38 | 18.99 | 25.91 | 13.28 | 6.75 | 96.45 | 39.686 |
| 11 | 0.2 | 50 | 70 | 45 | 135.43 | 19.08 | 25.87 | 13.29 | 6.03 | 98.54 | 39.872 |
| 12 | 0.2 | 60 | 80 | 0 | 135.61 | 19.34 | 25.80 | 13.22 | 5.87 | 98.12 | 39.835 |
| 13 | 0.25 | 30 | 100 | 45 | 135.34 | 19.19 | 25.81 | 13.33 | 6.23 | 97.76 | 39.803 |

| | | | | | | | | | | | |
|----|------|----|----|----|--------|-------|-------|-------|------|-------|--------|
| 14 | 0.25 | 40 | 90 | 0 | 134.60 | 19.30 | 25.79 | 13.64 | 6.05 | 97.67 | 39.796 |
| 15 | 0.25 | 50 | 80 | 90 | 134.97 | 19.08 | 25.58 | 13.20 | 5.99 | 98.90 | 39.904 |
| 16 | 0.25 | 60 | 70 | 60 | 135.03 | 18.75 | 25.86 | 13.16 | 5.79 | 97.89 | 39.815 |

Figure 4 shows the dimensional accuracy of each specimen by taking the mean of the accuracy of dimensions d1 to d5 in form of a bar chart. The process parameters corresponding to a higher S/N ratio gives the best output response (Table 3). The specimen 15 is having the highest accuracy of 98.90 %. The deviations of each dimension for all the specimens are depicted in form of a radar chart in Fig. (5). The maximum deviation was found 2 mm in dimension d1 of specimen 14 while the minimum deviation was 0.01 mm in dimension d2 and d5 of specimen 10 and 15 respectively.

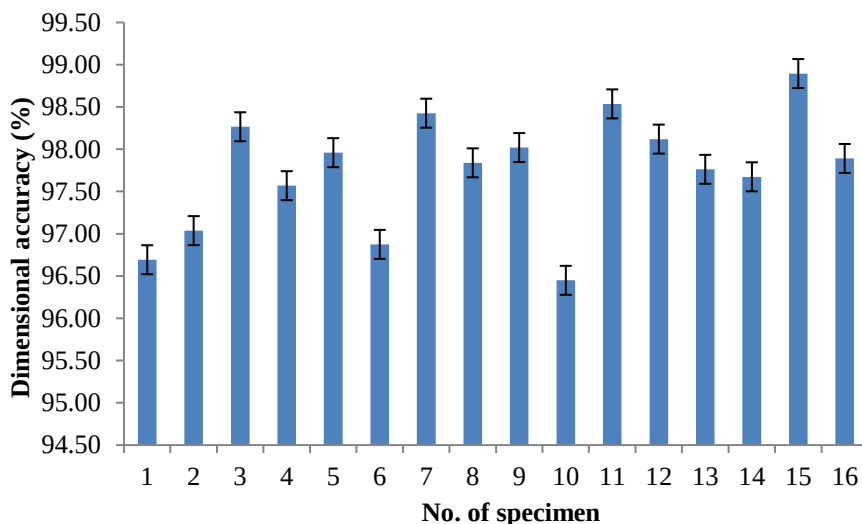


Figure 4: Dimensional accuracy of test specimens

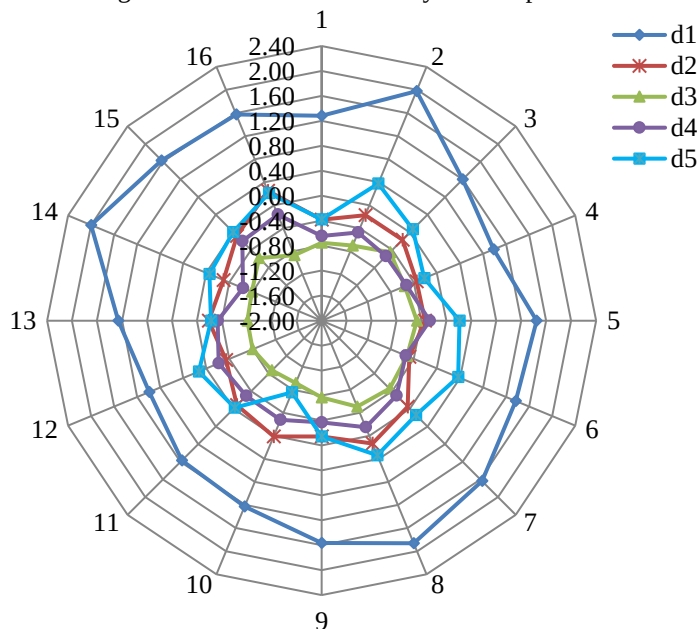


Figure 5: Dimensional deviation in test specimens

Table 4 shows an analysis of variance (ANOVA) for dimensional accuracy. From Table 5, it can be seen that print speed (67.47%) is the most influential parameter for dimensional accuracy followed by layer thickness (12.68%), % infill (11.69%), and raster angle (1.26%). To observe the significance of each process variable, a 95% confidence interval has been considered. To investigate the individual effect of each parameter on the dimensional accuracy of nylon parts fabricated by the FDM process, the main effect is plotted using mean data as shown in Fig. (6).

Table 4 Analysis of variance (ANOVA) for dimensional accuracy

| Source | DF | Adj SS | Adj MS | F-Value | P-Value | % Contribution |
|-----------------|----|---------|---------|---------|---------|----------------|
| Layer thickness | 3 | 0.89509 | 0.29836 | 1.84 | 0.315 | 12.68 |
| Print speed | 3 | 4.76196 | 1.58732 | 9.78 | 0.047 | 67.47 |
| % Infill | 3 | 0.82542 | 0.27514 | 1.69 | 0.338 | 11.69 |
| Raster angle | 3 | 0.08889 | 0.02963 | 0.18 | 0.902 | 1.26 |
| Error | 3 | 0.48704 | 0.16235 | | | 6.9 |
| Total | 15 | 7.05839 | | | | 100 |

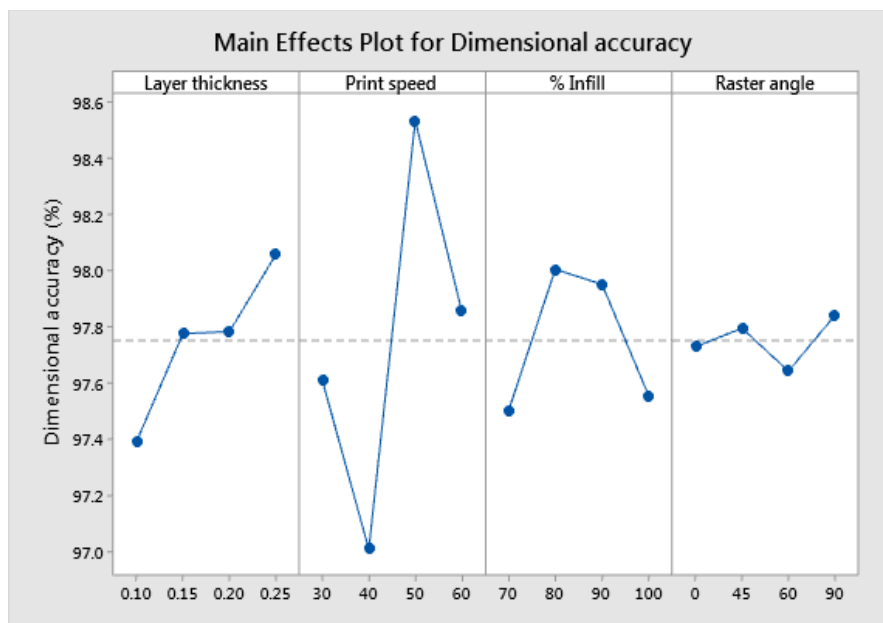


Figure 6: Main effect plot for dimensional accuracy

As shown in Fig. 6, the dimensional accuracy increases with the increment in layer thickness. The value of dimensional accuracy fluctuates with an increase in print speed. With an increase in infill up to 80%, the dimensional accuracy increases and then it decreases. An increase in raster angle shows the same behavior as that of print speed. From the Fig. (6), it can be observed that highest dimensional accuracy is achieved at setting: layer thickness 0.25 mm, print speed 50 mm/s, infill 80%, and raster angle 90°.

4 Conclusion

In the present work, the effect of layer thickness, print speed, % infill, and raster angle on dimensional accuracy has been investigated for nylon parts fabricated by the FDM process. The highest dimensional accuracy has been observed at 0.25 mm layer thickness, 50 mm/s print speed, 80% infill, and 90° raster angle. The maximum and minimum deviations have been found 2 mm and 0.01 mm respectively. The print speed has been found the most influential parameter for the dimensional accuracy of the specimen as per the ANOVA table. The dimensional accuracy increased with increasing layer thickness because higher layer thickness reduces no. of layers required to prepare a specimen which results in less possibility of uneven shrinkage/distortion after layer solidification. The results can be helpful in optimization of process parameters. This investigation can be further extended by exploring the influence of other process parameters namely extrusion temperature, bed temperature, number of shell boundaries, etc. on the dimensional accuracy of nylon parts.

References

- [1] T. Letcher, M. Waytashek, "Material property testing of 3D-printed specimen in PLA on an entry-level 3D printer," Proceedings of the ASME 2014 International Mechanical Engineering Congress & Exposition IMECE2014, Montreal, Quebec, Canada, November 14-20, 2014.
- [2] K.G. Jaya Christiyan, U. Chandrasekhar, K. Venkateswarlu, "A study on the influence of process parameters on the Mechanical Properties of 3D printed ABS composite," IOP Conference Series: Materials Science and Engineering, vol. 114, 012109, 2016.
- [3] C.K. Basavaraj, M. Vishwas, "Studies on Effect of Fused Deposition Modelling Process Parameters on Ultimate Tensile Strength and Dimensional Accuracy of Nylon," IOP Conference Series: Materials Science and Engineering, vol. 149, 012035, 2016.
- [4] M. Vishwas, C.K. Basavaraj, "Studies on Optimizing Process Parameters of Fused Deposition Modelling Technology for ABS," Materials Today: Proceedings, vol. 4, pp. 10994–11003, 2017.
- [5] S.R. Rajpurohit, H.K. Dave, "Effect of process parameters on tensile strength of FDM printed PLA part", Rapid Prototyping Journal, vol. 24, issue: 8, pp.1317-1324, 2018.
- [6] M.F.O. de Miranda, F.J.O. Ribeiro, N.S. Saad, A.Z. Guarato, "Experimental analysis on the mechanical properties of PETG parts made with fused deposition modeling manufacturing," 25th ABCM International congress of Mechanical engineering, Uberlandia, MG, Brazil, October 20-25, 2019.
- [7] J.M. Barrios, P.E. Romero, "Improvement of Surface Roughness and Hydrophobicity in PETG Parts Manufactured via Fused Deposition Modeling (FDM): An Application in 3D Printed Self-Cleaning Parts," Materials, vol. 12, issue 15, 2499, 2019.
- [8] A.M. Abdelrhman, W.W. Gan, D. Kurniawan, "Effect of part orientation on dimensional accuracy, part strength, and surface quality of three dimensional printed part," IOP Conference Series: Materials Science and Engineering, vol. 694, 012048, 2019.
- [9] H.K. Dave, N.H. Patadiya, A.R. Prajapati, S.R. Rajpurohit, "Effect of infill pattern and infill density at varying part orientation on tensile properties of fused deposition modeling-printed poly-lactic acid part," Proceedings of the Institution of Mechanical Engineers Part C: Journal of Mechanical Engineering Science, vol. 203, pp. 1–17, 2019.
- [10] R. Mendricky, D. Fris, "Analysis of the Accuracy and the Surface Roughness of FDM/FFF Technology and Optimisation of Process Parameters," Technical Gazette, vol. 27, issue 4, pp. 1166-1173, 2020.
- [11] A. Rajurkar, D. Thesiya, "Effect of Deposition Strategies and Printing Parameters on Dimensions and Strength of 3D Printed Parts: A Comparative Analysis," 1st International Virtual Conference on Recent Advancements in Design and Manufacturing (ICRADM-2020), Sardar Vallabhbhai National Institute of Technology, Surat, July 16-17, 2020.

Microstructural Investigations by using Friction Stir Processing

Bazani Shaik^{1*}, G. Harinath Gowd², B. Durga Prasad³

^{1*} Professor, Department of Mechanical Engineering,
Ramachandra College of Engineering-534007, A.P, INDIA.

² Department of Mechanical Engineering, Madanapalle Institute of Technology and Science-517325, A.P,
INDIA.

³ Department of Mechanical Engineering, JNTUA, Ananthapuramu-515002, A.P.,

Abstract

This work mainly focused on finding the optimal conditions for improving the efficiency of the dissimilar welded joints that were prepared using the Friction stir process. To carry out further research on Friction Stir Process, it is very much required to know the significant process parameters. As per the literature, tool rotational speed, weld speed and tilt angle are proved to be most significant hence are taken in the current investigations. Experimental design and Micro structural investigations is planned as per the Taguchi L9 orthogonal array. After doing the experiments, each output responses are measured at all the welding conditions and are tabled. This experimental data is used for optimizing the multi responses with the application of this method, it is quite possible to optimize the output responses more than one. So this method proved to be very effective in finding the multi responses which can yield the optimal results.. Overall this method finds suitable for optimizing the multi responses in FSW process.

Keywords: Dissimilar Joints, Friction Stir Process, Microstructural Investigations.

1 Introduction

The advanced manufacturing process or other popular destructive welding methods of friction stir welding is controllable and inexpensive. The direction of large welding joint composition[1] is available and due to external heating low power consumption and fine grain size. The similar and dissimilar metals can be weld and here not use of filler metals, flux etc. The main advantage of friction stir welding has no environmental pollution and now a day's friction stir welding process is used for industries prefer marine, automotive and aerospace for particular properties. The principle of operation is for without reaching melting point of material for soften tool pin and tool shoulder enable deformation of heat for low plasticized material. The work piece material and rotating tool generates friction and joining the work pieces non consumable tool is used shown in Fig[1].

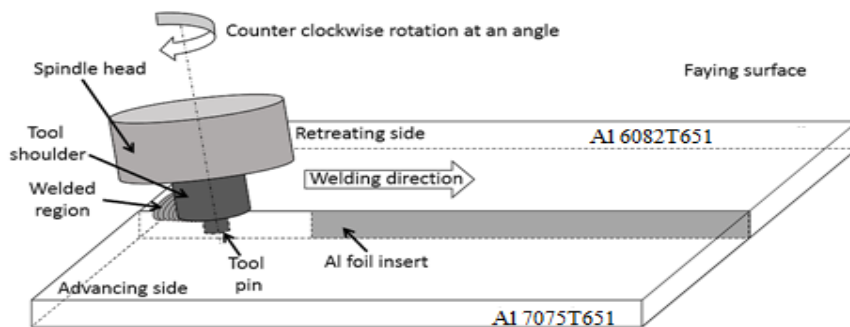


Figure 1. Typical schematic view of friction stir welding setup

[2] Studied in detail on the Taguchi modeling process with the composition factor method, grey relation analysis, response surface methodology observed and Design experiments are capable reliable tools. Investigated dissimilar friction stir welding (FSW) of an Al-Mg alloy (AA5083) to austenitic stainless steel (A316L) by using nano-sized SiC reinforcement was examined. Two optimized traverse velocities of 16 and 20 mm/min (and a constant rotational speed of 250 rpm) with the intact joint appearance were considered for investigating the effect of the number of passes on microstructural and mechanical properties[3]. It was noticed that the average wave reflection generated when the wave crossed from the AZ31B to the AA6061-T6 base metal was around 35% of the incident signal, but is reduced to 25% when the wave propagation direction was reversed[4]. Investigated 6mm, thick copper and bronze plates are friction stir welded at different tool rotational

speeds [5] of 800, 1000 and 1200 RPM, with a constant travel speed of 40 mm/min and an axial force of 10 kN. Provides a review of FSW of both similar and dissimilar titanium alloys focusing on the surface, and subsurface properties, such as microstructural, and mechanical properties, texture evolution, current challenges summarizing a possible remedy, encompassing the recent development and research in the field[6,7]. The extent of continuous dynamic recrystallization in the thermomechanically affected zone (TMAZ) of the advanced side was lower than that of the retreating side and the recrystallized grains were rarely seen on the advancing side. Microhardness profile on the advancing side was almost identical, while the profile revealed three distinguishable regions on the retreating side [8]. Studied The welding joint of AA2024T6 and AA6061T6 plates of 4mm thickness and taper threaded tool were used, welding speed 100 mm/min, rotational speed 1000 rpm with [9]precipitation taken place at heat treatment hardening effects at advancing side and retreating side.

2 Experimental procedure and operating parameters

AA7075T651 and AA6082T651 plate of thickness 6 mm is used as work piece material. The material is penetrated by Friction Stir Processing The experiments were carried out Dissimilar AA7075T651 and AA6082T651 aluminium alloys having 6mm thickness of each on a computer numerically controlled Friction Stir Welding it's a special purpose machine done at Annamalai university . The chemical compositions of base material are shown in table 1. The plates were finished to a dimension of 100mm × 50mm×6mm. A butt weld is been made by clamping the materials using fixtures by placing AA 7075T651 on advancing side and AA 6082T651 retreating Side using M2Grade SHSS tool of shoulder dia 18 mm and probe length 6 mm. The test specimens are prepared according to the ASTM standards. The side where the spindle rotation direction is in the same direction with the tool traversing is called the advancing side and the opposite side is called the retreating side. AA7075T651 was placed in the advancing side and AA6082T651 was placed in the retreating side in order to improve mechanical properties of Joint. Based on the literature and previous studies, the parameters with greater influence on the mechanical properties of dissimilar FSW were selected, with their notations and units described in Table 2. After the welding process, all the welded specimens were cut at transverse sections are appropriately prepared for metallurgical examination. The dissimilar welds of 7075 aluminum alloy and 6082 aluminum alloy was etched with Hydro Fluoric Solution. Microstructural examination and material mixing observation were carried out using optical microscope.

| Al alloy | | |
|----------|-----------|-------|
| Elements | 7075-T651 | 6082- |
| Si | 0.12 | 1.05 |
| Fe | 0.2 | 0.26 |
| Cu | 1.4 | 0.04 |
| Mn | 0.63 | 0.68 |
| Mg | 2.53 | 0.8 |
| Cr | 0.2 | 0.1 |
| Ni | 0.004 | 0.005 |
| Zn | 5.62 | 0.02 |
| Ti | 0.03 | 0.01 |
| Al | bal | bal |

Table 1. chemical compositions of base material

| No. | Parameters | Notations | Unit | Levels | | |
|-----|------------------|-----------|--------|--------|------|------|
| | | | | 1 | 2 | 3 |
| 1 | Rotational speed | RS | rpm | 1150 | 1250 | 1350 |
| 2 | Welding speed | WS | mm/min | 40 | 50 | 60 |

| No. | Parameters | Notation | Unit | Levels | | |
|-----|------------|----------|--------|--------|---|---|
| | | | | 1 | 2 | 3 |
| 3 | Tilt angle | TA | Degree | 1 | 2 | 3 |

Table 2. The coded and actual values of input variables

3 Micro structural Investigations of Friction Stir processing for samples

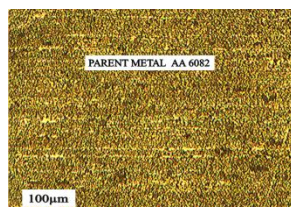


Fig. (3.a). Parent Metal

The Figure 3.a. Shows microstructures of magnification 100 x and etchant Keller's Reagent solution are used it has a microstructure of parent metal AA6082 in the annealed condition with precipitated Mg_2Si particles in primary aluminum alpha solid solution. The grains of eutectics flow with rolling direction. The primary grains are elongated and the eutectics are precipitated.

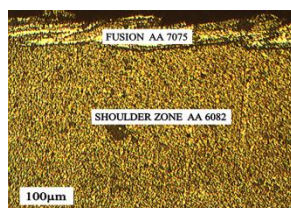


Fig. (3.b). Shoulder Zone of dominant AA6082 Constituents on FSW by using taper threaded tool for samples

The Figure 3.b The Shoulder Zone of dominant AA6082 Constituents for taper threaded tool sample shows the shoulder zone of the FSW process with fine fragmented particles of dominant AA6082 constituents. The top layer shows a fusion of AA7075 materials.

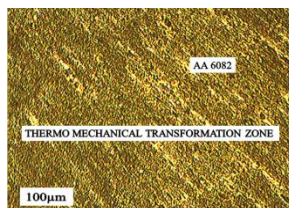


Fig. (3.c). TMT zone of the retreating side of AA6082 on FSW by using taper threaded tool for samples

The Figure 3.c shows TMT zone of the retreating side of AA6082 for taper threaded tool sample Shown AA6082 has a thermomechanical transformation zone with the directional flow of grains of primary and secondary phase grains. The direction of parent metal has changed.

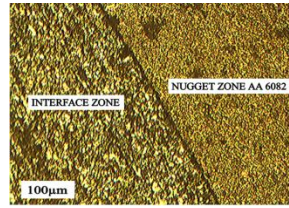


Fig. (3.d). Interface zone of AA6082 with nugget zone on FSW by using taper threaded tool for samples

The Figure 3.d Shows AA6082 has a nugget and interface zone. Parent metal shows the vertical flow of grains and the nugget zone at the left shows fragmented particles of the two-alloy used along the same vertical direction.

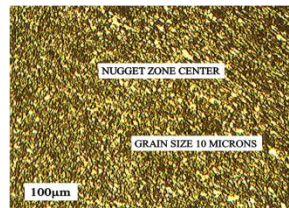


Fig. (3.e). Nugget zone center for on FSW by using taper threaded tool for samples

The Figure 3.e Shows the nugget zone center with fragmentation and dynamic recrystallization. An alternate layer of both the metals has formed. Shows the top zone of the FSW with fragmented grains and re-crystallization and the grain size is 10 microns. The constituents of two alloys have undergone fragmentation and dynamic recrystallization.

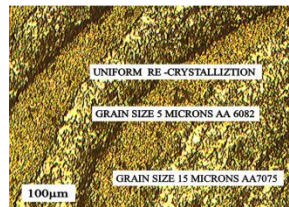


Fig. (3.f). Effective plasticity of both constituents on FSW by using taper threaded tool for samples

The Figure 3.f Shows Alternate layer of both the metals have formed with the effective plasticity of both the constituents of the alloys. Both the constituents show fusion and uniform re-crystallization to give grain size of 15 microns of AA7075 and 5 microns of AA6082 as average as per grain size measurements.

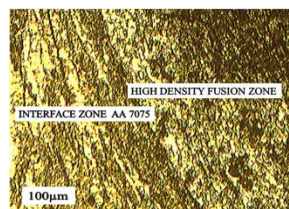


Fig. (3.g). Interface zone of AA7075 on FSW by using taper threaded tool for samples

The Figure 3.g Shows the interface zone of AA7075 at the left and nugget zone at the right side at the advancing side process that shows the microstructure of nugget very close to the interface zone AA7075 and nugget zone. The high-density Fusion zone of the nugget with AA7075 at the bottom has taken place.

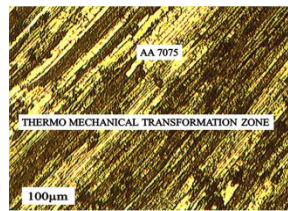


Fig. (3.h). TMT zone of AA7075 on FSW by using taper threaded tool for samples

The Figure 3.h Shows AA7075 has a thermomechanical transformation zone that had undergone higher plasticity due to the heat and stress of the process. This has led to the thermomechanical transformation with the partial dissolution of the constituents of AA7075.

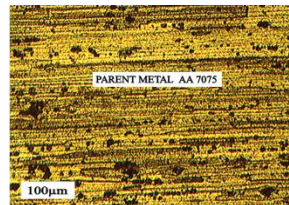


Fig. (3.i). AA7075 parent metal at advancing side on FSW by using taper threaded tool for samples

The Figure 3.i Shows AA7075 parent metal at the advancing side of the FSW process. The parent metal has microstructure in rolled temper condition. The sheet has been cold worked by a rolling process, primary grains of alpha aluminum is elongated along with the direction forming. The eutectic constituents like Cu-Al₂, Mg₂Si, Zn-Al₂, and Mg-Al₂ elongated with the rolling direction of precipitation.

4 Conclusions

In this paper, Friction Stir Processing of experiments based on central composite design and microstructural investigations are done led to the following conclusions.

1. The CNC-Friction stir welding framework has proved to be efficient in performing the welding operations.
2. It can be inferred that the process parameters can be ideally controlled for attaining the better quality weld in Friction stir welding process.
3. The results presented in the work can be used for further analysis. Overall this method proved to be very successful in optimizing the FSP process.
4. With the application of this method, it is quite possible to optimize the output responses more than one. So this method proved to be very effective in finding the multi responses which can yield the optimal results.
5. Then the problem can be solved by using any optimization algorithm after formulating the objective function.
6. Later the entire process can be automated which helps to increase the product rate without increasing the unit cost of the welded joints.

Acknowledgement

The authors would like to express their deep gratitude to Prof.V.Balasubramanian from Department of Manufacturing Engineering, Annamalai University for providing equipment facilities.

References

- [1] Angelos P. Markopoulos, Witold Habrat, Nikolaos I. Galanis and Nikolaos E. Karkalos, Modelling and Optimization of Machining with the Use of Statistical Methods and Soft Computing, Springer International Publishing Switzerland 2016 J.P. Davim (ed.), Design of Experiments in Production Engineering, Management and Industrial Engineering, DOI 10.1007/978-3-319-23838-8_2.
- [2] A.A. Fallahi, A. Shokuhfar, A. Ostovari Moghaddam, A. Abdolazadeh, Analysis of SiC nano-powder effects on friction stir welding of dissimilar Al-Mg alloy to A316L stainless steel, Journal of Manufacturing Processes 30 (2017) 418–430.
- [3] Tara J, Mustapha S, Fakir MA, Herb M, Wang H, Ayoub G, Hamade R, Application of Ultrasonic Waves Towards the Inspection of Similar and Dissimilar Friction Stir Welded Joints, Journal of Materials Processing Technology, <https://doi.org/10.1016/j.jmatprotec.2018.01.006>
- [4] R Morgan, N Thirumalaisamy, Experimental and numerical analysis of friction stir welded dissimilar copper and bronze plates, Materials Today: Proceedings 5 (2018) 803–809
- [5] KepiGangwar, M. Ramulu, Friction stir welding of titanium alloys, Jade (2017), <https://doi.org/10.1016/j.matdes.2017.12.033>.
- [6] Mohammad Mahdi Moradi, Hamed Jamshidi Aval, Roohollah Jamaati, Sajjad Amir Khanlo, Shouxun Ji, Microstructure and texture evolution of friction stir welded dissimilar aluminum alloys: AA2024 and AA6061, Journal of Manufacturing Processes 32 (2018) 1–10
- [7] Hussein Karami, Abandon, Hamed Reza Jashnani, Moslem Payday, Effect of precipitation hardening heat treatment on mechanical and microstructure features of dissimilar friction stir welded AA2024-T6 and AA6061-T6 alloys, Journal of Manufacturing Processes 31 (2018) 214–220
- [8] Mojtaba Rezaee Hajideh, Mohammadreza Farahani, Navid Molla Ramezani, Reinforced Dissimilar Friction Stir Weld of Polypropylene to Acrylonitrile Butadiene Styrene with Copper Nanopowder, Journal of Manufacturing Processes 32 (2018) 445–454
- [9] S. Fey X, Ye Y, Jin Lowing H, Live S, Special welding parameters study on Cu/Al joint in laser-heated friction stir welding, Journal of Materials Processing Technology, <https://doi.org/10.1016/j.jmatprotec.2018.02.004>.

Design And Analysis Of Internal Combustion Engine Manifold Using CFD Analysis

P.Saravanan¹ , S.Senthil² ,R.Rajappan³ & V.Pugazhenthithi⁴

^{1,2 & 3} Professor, Department of Mechanical Engineering, Mailam Engineering College, Mailam, Villupuram District, Tamilnadu, India.

⁴ Assistant Professor, Department of Mechanical Engineering, Mailam Engineering College, Mailam, Villupuram District, Tamilnadu, India.

Email id: ¹psaravanan125@gmail.com, ²principalmailam@gmail.com, ³ssraj2k@gmail.com, ⁴vpmech88@gmail.com

Abstract

In today's world, major objectives of engine designers are to achieve the twin goals of best performance and lowest possible emission levels. Excellent engine performance requires the simultaneous combination of good combustion and good engine breathing. An internal combustion engine (ICE) is a heat engine where the combustion of a fuel occurs with an oxidizer (usually air) in a combustion chamber that is an integral part of the working fluid flow circuit. In an internal combustion engine the expansion of the high-temperature and high-pressure gases produced by combustion apply direct force to some component of the engine. The designing of exhaust manifold is a complex procedure and is dependent on many parameters viz. back pressure, exhaust velocity, mechanical efficiency etc. Preference for any of this parameter varies as per designer needs. Usually fuel economy, emissions and power requirement are three different streams or thought regarding exhaust manifold design. In this paper, an existing model of an engine Exhaust Manifold is modeled in 3D modeling software. The design of the exhaust manifold is changed. In existing model the bend radius is 48 mm and exhaust is on one side, Modified model has bend radius of 48mm and exhaust is at the centre of header, the models are model in CATIAV5R20.

KEYWORDS: Exhaust Manifold, Back Pressure, Exhaust Velocity, Mechanical Efficiency, CFD

1. Introduction:

The Exhaust Manifold is the key component in the exhaust system on a vehicle. It is responsible for collecting the exhaust gas from the engine's cylinder heads and sending it down to the exhaust pipe. At the same time, it prevents any toxic exhaust fumes from leaking into the passenger area of the vehicle. Exhaust manifolds come in two main design styles, commonly referred to as four-into-one and four-into-two exhaust manifolds. Most exhaust manifolds are made from cast iron, but aftermarket versions are often made from welded tubular steel. A damaged exhaust manifold should be replaced immediately, and car owners in the market for one need to know which features to pay attention to in order to find the right one. An exhaust manifold is a series of connected pipes that bolt directly onto the engine head. It is an integral part of the exhaust system. Hot exhaust gas from the exhaust ports on the engine's cylinder head is funneled through the pipes and into a single collector pipe. From there, it is sent to the exhaust pipe. Exhaust manifolds are a necessary component of the exhaust system. Their design is optimized to ensure exhaust gases flow efficiently from the engine combustion chamber without creating any back pressure. A properly functioning exhaust manifold is important to prevent uneven power and engine vibrations.

2. Exhaust Manifold Design Considerations and Criteria

Present day engines are required to have more engine power and are also required to meet the strict pollution standards. To improve the exhaust system performance, many design specifications are must required. Exhaust gases should be led from the piston chambers to the exhaust manifold smoothly. This will ensure to

maximize the engine power at high speeds. The catalyst will absorb more pollutant at high temperatures. Hence, the exhaust gases should be kept at high temperature in the exhaust pipe even during low speeds as shown in figure.

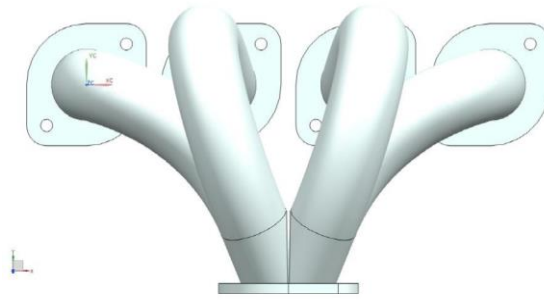


Fig: 2 Top view of the exhaust manifold

The exhaust system has to be “turned” for optimal efficiency. A tuned exhaust system should have geometry which will reflect the pressure waves of the exhaust gases which are emitted, as per engine firing order as shown in figure.

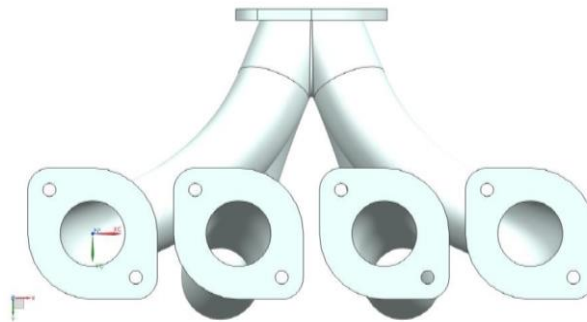


Fig: 1 Bottom view of the exhaust manifold

3. Computational Fluid Dynamics (CFD) Analysis

Nowadays, Computational fluid dynamics (CFD) has become a progressively handy and robust tool for the numerical analysis involving transport processes. CFD provides understanding into flow design, which is laborious, costly or impossible to investigate using conventional techniques. It consists of simulation of multiphase flow, heat transfer, chemical reactions and particulate processes. In CFD simulations, accuracy and reliability are the main factors upon. Which emphasize is given. It is broadly accepted that simulations performed by CFD are very susceptible to the various computational parameters that have to be set by the user. Consequently, CFD verification and validation studies are crucial, as well as comprehensive sensitivity studies that can deliver effective guidance in the selection of computational variables for future CFD studies. In this paper, CFD analysis has been done to study the fluid flow analysis through nozzle injector. By using CFD tools it is possible to obtain unlimited level of details about the behavior of the flow.

3.1 Concept of Computational Fluid Dynamics

Computational Fluid Dynamics (CFD) is the simulation of fluids engineering systems using modeling (mathematical physical problem formulation) and numerical methods. First, we have a fluid problem. To solve this problem, we should know the physical properties of fluid by using Fluid Mechanics. Then we can use mathematical equations to describe these physical properties. As the Navier-Stokes Equation is analytical, human can understand it and solve them on a piece of paper.

The translators are numerical discretization methods, such as Finite Difference, Finite Element, Finite Volume methods. Consequently, we also need to divide our whole problem domain into many small parts because our discretization is based on them. Then, we can write programs to solve them. The typical languages are FORTRAN and C. We can compare and analyse the simulation results with experiments and the real problem. If the results are not sufficient to solve the problem, we have to repeat the process until find satisfied solution.

3.2 Background and History

The fundamental basis of almost all CFD problems is the Navier–Stokes equations, which define many single-phase (gas or liquid, but not both) fluid flows. These equations can be simplified by removing terms describing viscous actions to yield the Euler equations. Further simplification, by removing terms describing vortices yields the full potential equations.

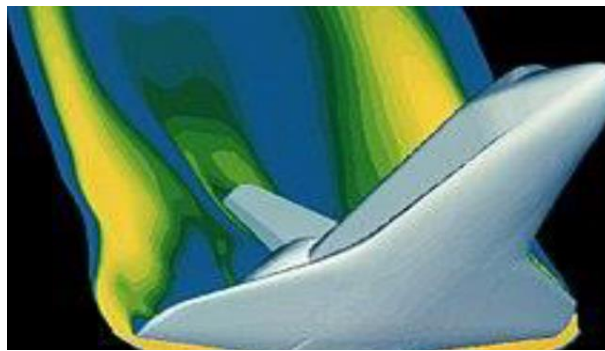


Fig: 3 A computer simulation of high velocity air flow around the Space Shuttle during re-entry.

Finally, for small perturbations in subsonic and supersonic flows (not transonic or hypersonic) these equations can be linearized to yield the linearized potential equations. Historically, methods were first developed to solve the linearized potential equations. Two-dimensional (2D) methods, using conformal transformations of the flow about a cylinder to the flow about an air foil were developed in the 1930s.

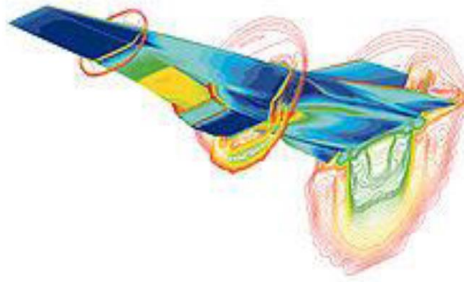


Fig: 4 A simulation of the Hyper-X scramjet vehicle in operation at Mach7

One of the earliest types of calculations resembling modern CFD are those by Lewis Fry Richardson, in the sense that these calculations used finite differences and divided the physical space in cells. Although they failed dramatically, these calculations, together with Richardson's book "Weather prediction by numerical process", set the basis for modern CFD and numerical meteorology. In fact, early CFD calculations during the 1940s using ENIAC used methods close to those in Richardson's 1922 book.

3.3 Boundary Conditions

To solve the equation system, we also need boundary conditions. The typical boundary conditions in CFD are No-slip boundary condition, axisymmetric boundary condition, Inlet, outlet boundary condition and Periodic boundary condition.

The fluid flows from left to right. We can use inlet at left side, which means we can set the velocity manually.

At the right side, we use outlet boundary condition to keep all the properties constant, which means all the gradients are zero. At the wall of pipe, we can set the velocity to zero. This is no-slip boundary condition. At the centre of pipe, we can use axisymmetric boundary condition.

3.4 Post Processing

Post processing of the simulation results is performed in order to extract the desired information from the computed flow field

- Calculation of derived quantities (stream function, vortices)
- Calculation of integral parameters (lift, drag, total mass)
- Visualization (representation of numbers as images)
- Systematic data analysis by means of statistical tools
- Debugging, verification, and validation of the CFD mode
 - 1D data : function values connected by straight lines
 - 2D data : streamlines, contour levels, colour diagrams
 - 3D data : cutlines, cutplanes, isosurfaces, isovolumes – arrow plots, particle tracing, animations.

4. Design Setup of Manifold

The geometry specification is important in any kind of CFD simulation. It is fascinating to report the physical boundaries that contain the fluid as accurately as possible, particularly for engineering issues, wherever sometimes the impact of one or more synthetic, or design, objects are to be predicted. Any inaccurate specification of the boundary surfaces may give erroneous result. Geometric setup and grid generation used to take a month or longer to perform. Presently, the geometry setup and grid generation processes have been made effortless, since almost all the packages have CAD system.

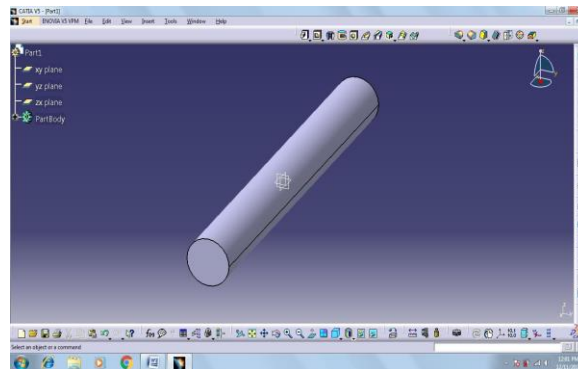


Fig: 5 HEADER OF EXISTING MODEL

The dimensions of a simple intake manifold are taken. The manifold has been tested by blowing air at different velocities through it and when we have the results from its physical testing we can compare these results by using these basic dimensions.

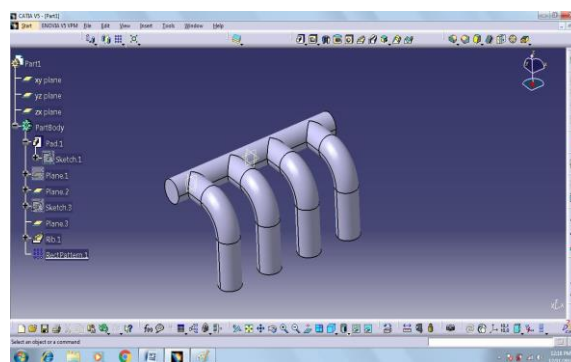


Fig: 6 INLET PORTS OF EXHAUST MANIFOLD

Under certain circumstances which could potentially create a high-pressure impulse inside the manifold or backfire due to the mistimed spark events occur, that's why it is necessary for a designer to design a suitable one for tolerating the effect of backfire. Manifold geometry is a factor in the magnitude of a backfire event. Simple four cylinder log type manifolds at atmospheric pressure typically generate pressures of approximately five bars.

5. Analysis Result

5.1 Inlet Port of Exhaust Manifold Existing Model

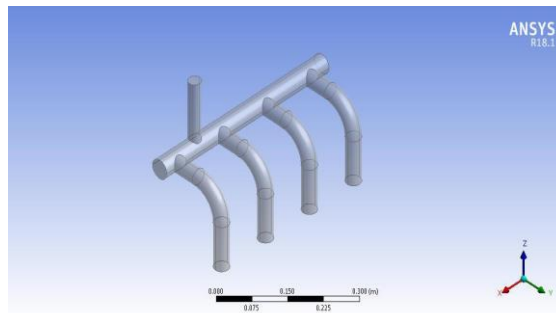


Fig: 7 DESIGNER MODELS

Pressures of eight bars have been seen with complex manifolds incorporating long runners and multiple plenums under the same conditions. Intake material properties are very important factor while choosing an intake manifold for car. Most of IM manufacturer using aluminium alloys due to its high strength and high temperature resistance properties. Sometime ribs and fillets are used in intake manifolds but ribs and fillets to the model give no improvement to the stress state, so it is necessary to review all parameters in manufacturing process. For finding out losses and optimized geometry, study will take place on following three models of same intake manifold with small modifications.

5.2 Inlet Port of Exhaust Manifold Modified Model

Exhaust manifolds are made either from cast iron or one of a few types of steel. The majority of exhaust manifolds are made from cast iron, as it is relatively inexpensive and lasts a long time. The drawbacks to cast iron manifolds are that they are quite heavy and tend to get brittle with age and exposure to the heat cycles of an engine. Tubular steel exhaust manifolds are known for having better exhaust flow and are, therefore, found on many performance vehicles. Stainless steel exhaust manifolds are the most expensive and benefits of stainless ones, but will rust if the outer layer is scratched. Exposure to the normal heat cycles of an engine can cause cracks in an exhaust manifold. As the vehicle continues to age, the cracks turn into holes. Once this happens, the vehicle engine sounds extremely loud and there is a likely chance that toxic fumes are entering the cabin of the vehicle. The gaskets on the exhaust manifold are equally important, and their failure has the same results. Other exhaust manifold components that are subject to failure include the exhaust system hangers, which are designed to hold up the entire system.

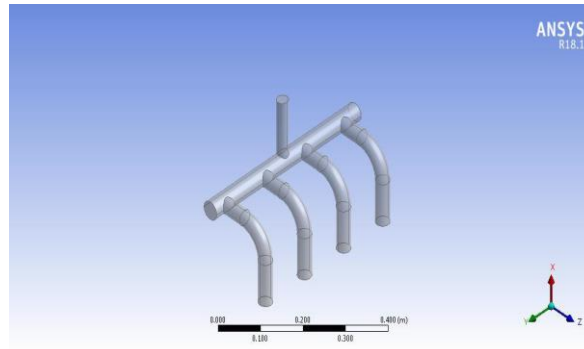


Fig: 8 Designer model

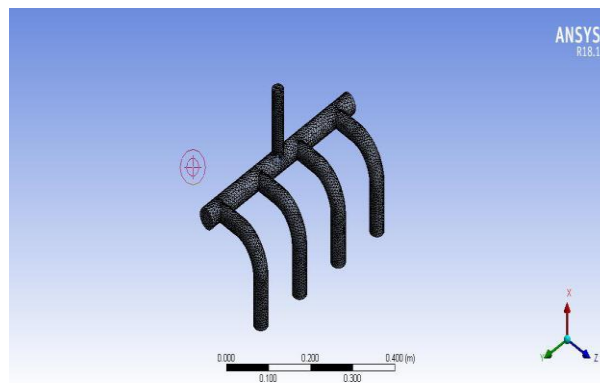


Fig: 9 Meshed model

The Designer model and Meshed model of a manifold is shown in figure. The manifold system is the most important to design for this engine, as it has to be completely altered for the stock system. Having it is too small of a throttle will choke the engine, while having too large of a throttle will make it very sensitive.

6. Result and Discussion

The result data from needed to be found from the CFD simulation is the Momentum and Mass Graph , Turbulence graph, Heat Transfer Graph, Contour Plot for Velocity Variations, Contour Plot for Pressure Variations and Contour plot for Temperature Variations drop from each outlet.

Design is done on both models of the exhaust manifold. In this paper, an existing model of an engine Exhaust Manifold is modeled in 3D modelling software. The design of the exhaust manifold is changed. In existing model, the bend radius is 48 mm and exhaust is on one side, Modified model has bend radius of 48mm and exhaust is at the centre of header, the models are model in CATIAV5R20.

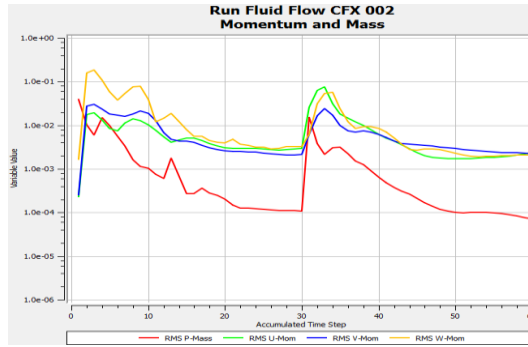


Fig: 10 Momentums and Mass Graph

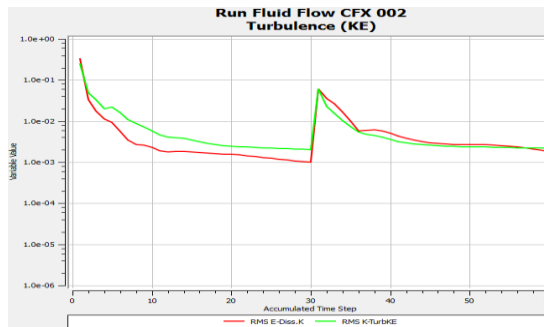


Fig: 11 Turbulence graph

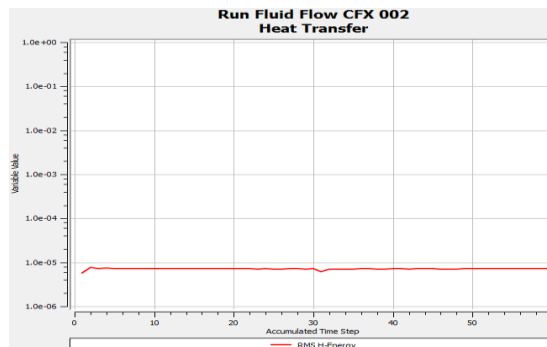


Fig: 12 Heat Transfer Graph

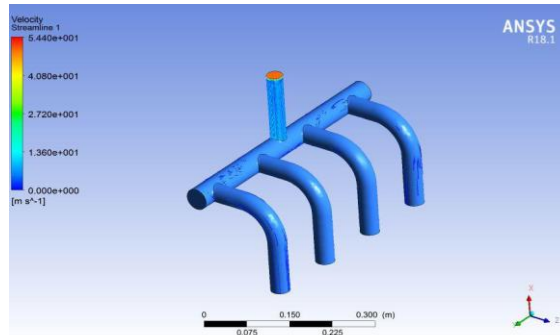


Fig: 13 Contour Plots for Velocity Variations

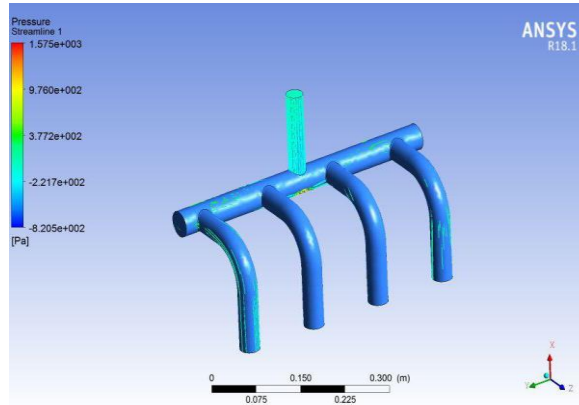


Fig: 14 Contour Plots for Pressure Variations

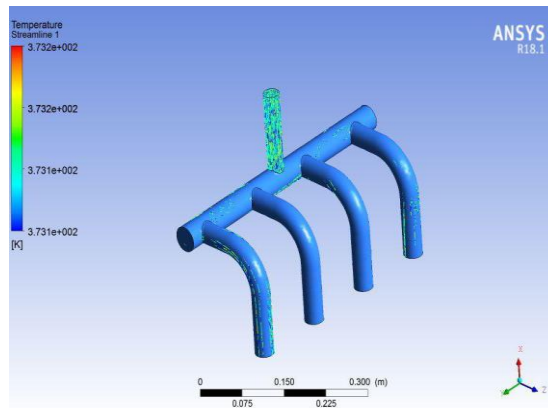


Fig: 15 Contour plots for Temperature Variations

From this project an unwanted projection of inside plenum to be avoided and Stiffeners of runners and nut projection inside plenum to be reduced. The Depth cuts at extreme side of plenum are newly designed. The curved

design is perfect to obtain, equal flow and no alteration is required. The geometry of good configuration obtains which giving nearly equal velocity in all runners but also discharge air at high velocity compare to previous design.

Conclusion

CFD analysis is done on both the model at different mass flow rates. By observing the CFD analysis results, the outlet pressure, velocity and total heat transfer rates are increasing by increasing the mass flow rates and they are more for modified model when compared with that of original model.

References

- [1] Muthaiah PLS, Kumar MS, Sendilvelan S. CFD Analysis of catalytic converter to reduce particulate matter and achieve limited back pressure in diesel engine. Global journal of researches in engineering A: Classification (FOR) 091304,091399, 2010; 10(5).
- [2] Suresh Aadepu, I.S.N.V.R.Prasanth&JarapalaMurali Naik, Design of intake manifold of IC engines with improved volumetric efficiency, IJMETMR, <http://www.ijmetmr.com/oljune2014/Article6.pdf>, Volume No: 1(2014), Issue No: 6 (June), ISSN No: 2348-4845
- [3] Beardsley MB et al. Thermal Barrier Coatings for Low Emission, High Efficiency Diesel Engine Applications, SAE Technical Paper 1999; 1: 2255.
- [4] JacobE, Lammermann R, Pappenherimer A, Rothe D. Exhaust Gas After treatment System for Euro 4: Heavy Duty Engines – MTZ 6/2005.
- [5] Jacobs T, Chatterjee S, Conway R, Walker A, Kramer J, Mueller-Haas K. Development of a Partial Filter Technology for Hdd Retrofit, Sae Technical Paper 2006-01-0213.
- [6] Lahousse C, Kern B, Hadrane H, Faillon L. Backpressure Characteristics of Modern Three-way Catalysts, Benefit on Engine Performance, SAE Paper No. 2006011062,2006 SAE World Congress, Detroit, Michigan , April 36, 2006.
- [7] Muramatsu G, Abe A, Furuyama M. Catalytic Reduction of Nox in Diesel Exhaust, SAE 930135, 1993.
- [8] Heywood JB, Internal Combustion Engine Fundamentals (Tata McGrah Hill).
- [9] Labhsetwar NK, Watanabe A, Mitsushashi T.Possibilities of the application of catalyst technologies for the control of particulate emission for diesel vehicles, SAE Transaction 2001.
- [10] Biniwale R, Labhsetwar NK, Kumar R, Hasan MZ. A non-noble metal based catalytic converter for two strokes, two-wheeler applications, SAE.
- [11] M.A. Ceviz *, M. Akin (2010), ‘Design of a new SI engine intake manifold with variable length plenum’, An article presented in Energy Conversion and Management, Elsevier Ltd.
- [12] S. A. Sulaiman, S. H. M. Murad, I. Ibrahim and Z. A. Abdul Karim (2010), ‘study of flow in air-intake system for a single-cylinder Go-kart engine’, International Journal of Automotive and Mechanical Engineering (IJAME) Volume 1, pp. 91-104.
- [13] Hiren R Patel, Prof. V.H.Chaudhari (2013), ‘Optimization of Intake Manifold of Dual Fuel Gasoline Engine - A Review’, International Journal of Latest Trends in Engineering and Technology (IJLTET), Vol. 2 Issue 2 March 2013, pp. 99-105.
- [14] B.M.Angadi, Anandkumar S Malipatil., V.V.Nagathan, R.S.Kattimani., ‘Modelling and Analysis of Intake manifold of a Multi-cylinder SI engine’, the 37th National & 4th International Conference on Fluid Mechanics and Fluid Power December 16-18, 2010, IIT Madras, Chennai, India, FMFP10 - NE – 04.

- [15]Negin Maftouni , Reza Ebrahimi, 'Intake manifold optimization by using 3-d cfd analysis with Observing the effect of length of runners on volumetric Efficiency', Proceedings of the 3rd BSME-ASME International Conference on Thermal Engineering, 20-22 December, 2006, Dhaka, Bangladesh.
- [16]Long Xie, Harutoshi Ogai, and Yasuaki Inoue, 'Modeling and solving an engine intake manifold With turbo charger for predictive control', Asian Journal of Control, Vol. 8, No. 3, pp. 210-218, September 2006.
- [17]D.Ramasamy, Zamri.M, S. Mahendran, S.Vijayan "Design Optimization of Air Intake System (AIS) of 1.6L Engine", IMECS, vol. 2, pp.19-20, 2010.
- [18]Martínez-Sanz A., Sánchez-Caballero S, Viu A. and Pla-Ferrando R. "Design and Optimization Of Intake Manifold In A Volkswagen Car", ANNALS of the Oradea University, fascicle of management and technological engineering Vol X(XX) ,NR2, 2011.
- [19]Mardani Ali Sera, Rosli Abu Bakar and Azhar Abdul Aziz "Effect Of Air Fuel Mixer Design On Engine Performance And Exhaust Emission of A CNG Fuelled Vehicles" 2nd world engineering congress Sarawak, Malaysia,22-25, July2002.
- [20]Jemni M .A, Kantchev G, Abid M. S, "Intake Manifold Design Effect On Air Fuel Mixing And Flow For an LPG Heavy Duty Engine", IJEE, Vol. 3, Issue1,pp.61-72,2011.
- [21]Benny Paul, Ganesan V, "Flow Field Development In a Direct Injection Diesel Engine With Different Manifolds", IJEST, Vol.2, No. 1, pp. 80-91, 2010.
- [22]S. Karthikeyan, R.Hariganesh, M.Sathyanadan, S.Krishnan,P. Vadivel,D.Vamsidhar "Computational Analysis of intake manifold Design and experimental investigation on Diesel Engine for LCV" International Journal of Engineering Science and Technology (IJEST) Vol. 3 No.4, pp- 2359-2367 , 2011.
- [23]Ismail, A.R., Bakar, R.A. and Semin (2008) An Investigation of Valve Lift Effect on Air Flow and CD of Four Stroke Engines Based on Experiment. American Journal of Applied Sciences, 5: 963–971.
- [24]Kondapalli PS. General guidelines for improving burst pressure strength of welded nylon air intake manifolds. SAE Paper No 2000-01-0040; 2000.
- [25]Brady JM. A simple high-efficiency S.I. engine design. SAE Paper No: 2003-01-0923;2003.

Investigating the Sliding Wear Characteristics of ZAMAK 5 Alloy Under Dry and Wet Lubricating Conditions

Udhayakumar S¹, Kalidas K², Saravanakumar P T³

¹Assistant Professor, Department of Automobile Engineering, Hindusthan Institute of Technology, Coimbatore.

²Assistant Professor, Department of Mechanical Engineering, Hindusthan Institute of Technology, Coimbatore.

³Professor and Head, Department of Automobile Engineering, Hindusthan Institute of Technology, Coimbatore.

ABSTRACT

Zamak is a group of alloys with Zinc as a base metal having various alloying elements like aluminum, magnesium, and Copper. Although, Zamak alloy is part of the ZA alloy family it constantly has 4% aluminum composition. Zamak alloy can be electroplated, wet painted, and chromate change covered. So ZAMAK alloy can be used as a replacement for aluminum alloys in various automobile applications. In the present study, the tribological characteristics of Zamak alloy were investigated by weight loss method with a use of Pin-on Disc apparatus. Zamak 5 samples were produced by Mechanical molding and machining. For a temperature study the samples were made with blind hole at the bottom. The experimental study is conducted on dry, wet and Nano lubrication conditions under various loads, Displacement and Speeds.

Key words : ZAMAK 5 Alloy, Pin on Disc, Dry and Wet Lubrication.

1 Introduction

Zinc composites are prominently alloyed as pot metal or white metal. Zamak 5 is considered over other Zamak alloys, when greater hardness, strength and creep resistance is required. Zamak 5 has a similar composition as Zamak 3 with the extra of 1% copper so as to build the properties of hardness and ductility (by around 10%), but it decreases ductility. Zamak 5, or Zinc compound 5, is the most broadly utilized Zinc alloy in European countries. It has higher strength and less ductility compared to the Zamak alloys. The wear rate for Zamak 5 alloy was very low when compared to Aluminium alloy. This paper studies the tribological characteristics of Zamak5 alloy under dry condition and lubricated condition. Pin-on-disc apparatus is used to study the Sliding wear test under various loads and sliding speed. Zamak5 alloy has the highest damping character among other zinc alloy, has nearly ten times greater damping capacity than A380 aluminium or mild steel. Zinc's phenomenon projects smoothness, licenses more slender blade and cooling pin configuration to more readily disseminate heat. All zamak alloys, particularly Zamak-3 and Zamak-5, demonstrate excellent wear resistance qualities thanks to their high hardness (**Table 1**) and natural lubrication characteristics.

Table 1
Mechanical properties of Zamak 5 alloy

| S.No | Property | Metric Value |
|------|---|------------------------|
| 1 | Ultimate tensile strength | 331 MPa (270 MPa aged) |
| 2 | Yield strength (0.2% offset) | 295 MPa |
| 3 | Impact strength | 52 J (56 J aged) |
| 4 | Elongation at F _{max} | 2% |
| 5 | Elongation at fracture | 3.6% (13% aged) |
| 6 | Shear strength | 262 MPa |
| 7 | Compressive yield strength | 600 MPa |
| 8 | Fatigue strength (reverse bending 5x10 ⁸ cycles) | 57 MPa |
| 9 | Hardness | 91 BHN |
| 10 | Modulus of elasticity | 96 GPa |

2 Properties of ZAMAK 5

Zamak 5 castings are barely more grounded and harder than Zamak 3. In any case, these enhancements are tempered with a decrease in pliability which can influence formability during auxiliary twisting, riveting, swaging or pleating tasks. Zamak 5 contains an addition of 1% copper (**Table 3**) which accounts for these property changes. The alloy is widely die cast in Europe and does exhibit excellent castability characteristics, as well as, improved creep performance over Zamak 3. Because of Zamak 3's wide availability, material specifiers often strengthen components by design modifications instead of using Zamak 5. However, when an extra measure of tensile performance is needed, Zamak 5 alloy castings are recommended. The alloy is readily plated, finished and machined, comparable to Zamak 3 alloy.

Table 2
Physical properties of Zamak 5 alloy

| S.No | Property | Metric Value |
|------|----------------------------------|-----------------------|
| 1 | Density | 6.6 g/cm ³ |
| 2 | Melting point | 383°C |
| 3 | Thermal conductivity | 109W/mK |
| 4 | Coefficient of thermal expansion | 27.4µm/m°C |
| 5 | Electrical Conductivity | 26µm/m ⁰ k |
| 6 | Thermal conductivity | 109 W/mK |

3 Experimental Study

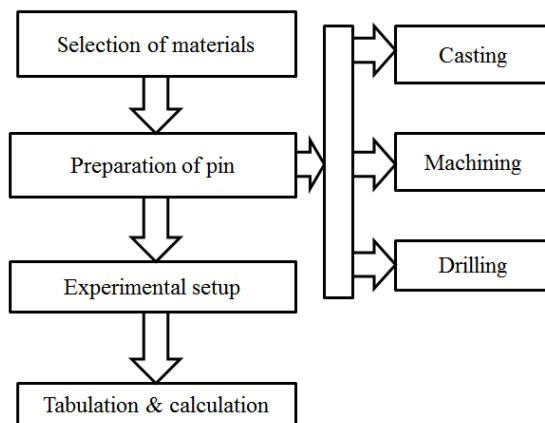


Fig 1 Methodology

3.1 Specimen Preparation

Zamak 5 alloy is used as the specimen material in the present investigation and has the chemical composition as shown in **Table 3**. It is prepared through mechanical molding. The melting process for Zamak5 alloy was carried out in the temperature controlled electrical crucible furnace.

Table 3
Chemical composition of the ZAMAK 5

| S.No | Materials | Weight % |
|------|-----------|----------|
| 1 | Aluminum | 3.5-4.3 |

| | | |
|---|---------------|-----------|
| 2 | Copper | 0.75-1.25 |
| 3 | Magnesium | 0.03-0.08 |
| 4 | Iron (max) | 0.1 |
| 5 | Lead (max) | 0.005 |
| 6 | Cadmium (max) | 0.004 |
| 7 | Tin (max) | 0.003 |
| 8 | Zinc | Balance |

With the use of CNC turning the specimen was machined to 6mm dia and 35mm length as per required size of pin on disc apparatus. For temperature measurements the specimen has a blind hole at the bottom of the specimen. The sample of the pins was shown in Figure 2a&b.



Fig 2(a) 3D view of specimen Fig 2(b) Tested specimen

3.2 Experimental Procedure

In this study, dry and wet sliding wear behavior of ZAMAK 5 alloy has been investigated. Sliding wear tests were conducted by using a pin-on-disc apparatus under both dry and wet lubricated conditions. The wear rate of the **ZAMAK-5** alloy is to be calculated by weight loss method with the help of **PIN ON DISC** apparatus.



Fig 3 Pin on Disc Apparatus

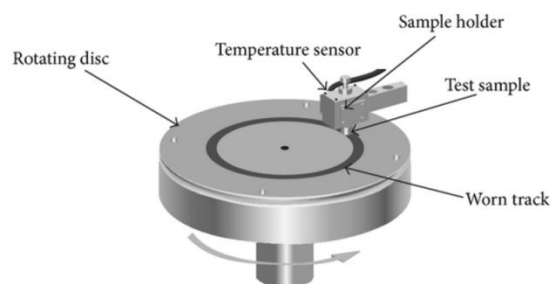


Fig 3 working of Pin on Disc Apparatus

Friction and Wear test is to be conducted in Pin-on-disc Equipment. The ZAMAK-5 sample pin material is taken in cylindrical shape in 15mm diameter & 30mm length. The experiments were carried out with various loads, various speeds. Frictional forces are taken from tribometer. The weight loss is taken from mettler weighing balance machine. The wear rate and co-efficient of friction is calculated by using formula. By using of below formulas calculate the wear rate and co-efficient of friction for zamak-5 material.

$$\text{Sliding velocity} = \pi DN/60$$

Where

‘D’=track diameter in m, ‘N’=disc speed in rpm

$$\text{Time} = \frac{\text{Distance}}{\text{Sliding Velocity}}$$

$$\text{Volume loss} = \frac{\text{Weight Loss}}{\text{Density}}$$

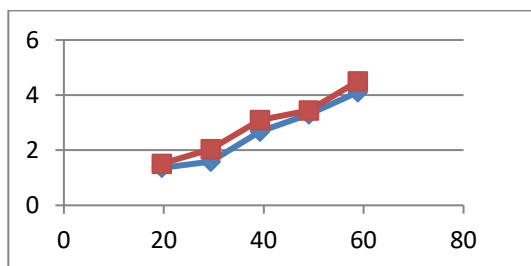
$$\text{Wear rate} = \frac{\text{Volume Loss}}{\text{Distance}}$$

$$\text{Co-efficient of friction} = \frac{\text{Frictional force}}{\text{Applied load}}$$

4 Results and Discussions

Table 4
Wear rate of Zamak 5 under Dry Lubrication

| LOAD (N) | SPEED (RPM) | WEAR RATE OF ZAMAK-5 ALLOY (mm ³ /m) | WEAR RATE OF ALUMINIUM ALLOY (mm ³ /m) |
|----------|-------------|---|---|
| 19.62 | 600 | 1.361x10 ⁻⁰⁶ | 1.51x10 ⁻⁰⁶ |
| 29.43 | 600 | 1.597x10 ⁻⁰⁶ | 2.04x10 ⁻⁰⁶ |
| 39.24 | 600 | 2.681x10 ⁻⁰⁶ | 3.10x10 ⁻⁰⁶ |
| 49.05 | 600 | 3.306x10 ⁻⁰⁶ | 3.41x10 ⁻⁰⁶ |
| 58.86 | 600 | 4.108x10 ⁻⁰⁶ | 4.50x10 ⁻⁰⁶ |

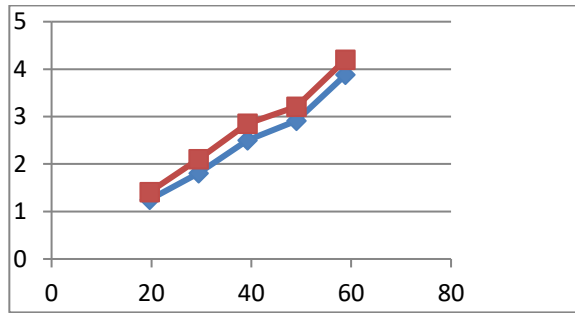


Graph1Wear rate of Zamak 5 under Dry Lubrication

Table 5
Wear rate of Zamak 5 under Wet Lubrication

| LOAD (N) | SPEED (RPM) | WEAR RATE OF ZAMAK-5 ALLOY | WEAR RATE OF ALUMINIUM ALLOY |
|----------|-------------|----------------------------|------------------------------|
|----------|-------------|----------------------------|------------------------------|

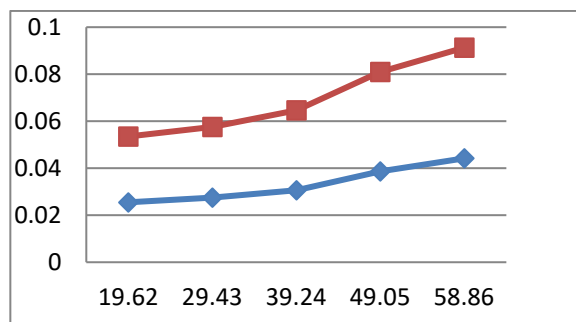
| | | (mm^3/m) | (mm^3/m) |
|-------|-----|--------------------------|--------------------------|
| 19.62 | 600 | 1.251×10^{-07} | 1.41×10^{-07} |
| 29.43 | 600 | 1.807×10^{-07} | 2.104×10^{-07} |
| 39.24 | 600 | 2.501×10^{-07} | 2.85×10^{-07} |
| 49.05 | 600 | 2.91×10^{-07} | 3.21×10^{-07} |
| 58.86 | 600 | 3.88×10^{-07} | 4.20×10^{-07} |



Graph 2 Wear rate of Zamak 5 under Wet Lubrication

Table 6
Coefficient of Friction of Zamak 5 under Dry Lubrication

| LOAD (N) | SPEED (RPM) | COEFFICIENT OF FRICTION OF ZAMAK-5 | CO-EFFICIENT OF FRICTION OF ALUMINIUM ALLOY |
|----------|-------------|------------------------------------|---|
| 19.62 | 600 | 0.132 | 0.172 |
| 29.43 | 600 | 0.163 | 0.201 |
| 39.24 | 600 | 0.193 | 0.242 |
| 49.05 | 600 | 0.234 | 0.276 |
| 58.86 | 600 | 0.278 | 0.304 |

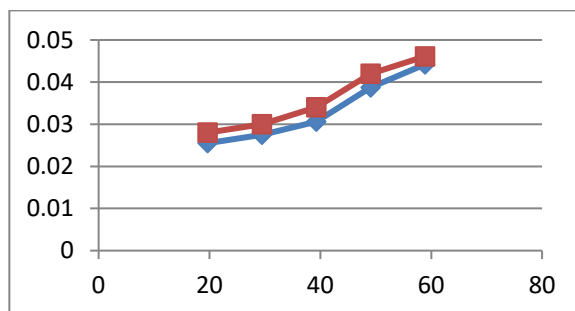


Graph 3 Coefficient of Friction of Zamak 5 under Dry Lubrication

Table 7
Coefficient of Friction of ofZamak 5 under Wet Lubrication

| Load (N) | Speed (RPM) | Coefficient of Friction of Zamak-5 | Co-Efficient of Friction of |
|----------|-------------|------------------------------------|-----------------------------|
| 19.62 | 600 | 0.132 | 0.172 |
| 29.43 | 600 | 0.163 | 0.201 |
| 39.24 | 600 | 0.193 | 0.242 |
| 49.05 | 600 | 0.234 | 0.276 |
| 58.86 | 600 | 0.278 | 0.304 |

| | | | Aluminium Alloy |
|-------|-----|--------|------------------------|
| 19.62 | 600 | 0.0255 | 0.028 |
| 29.43 | 600 | 0.0275 | 0.030 |
| 39.24 | 600 | 0.0306 | 0.034 |
| 49.05 | 600 | 0.0387 | 0.042 |
| 58.86 | 600 | 0.0442 | 0.0461 |



Graph 4 Coefficient of Friction of Zamak 5 under Wet Lubrication

5 CONCLUSION

By using of ZAMAK-5 alloy will be reduce the wear rate and also improves lubrication. At dry and wet lubrication condition zamak-5 alloy has 9 to 11% less wear rate and co-efficient of friction than the existing aluminium –silicon alloy. And it can also use at high temperature. Though the zamak-5 alloy is not economical but it offers longer life even at high temperatures on wet and dry conditions.

References

- [1] Kwangho lee, Yujinhwang , Seongircheong ,Youngminchoi , Laeun kwon (2009) “Understanding the role of nanoparticles in nano-oil lubrication” tribollett (2009) 35:127 131
- [2] Chang-gunlee, yu-jinhwang, young-min choi (2009) “A study on the tribological characteristics of graphite nano lubricants” International journal of precision engineering and manufacturing vol. 10, no. 1, pp. 85-90
- [3] Y.Y. Wu ,W.C.Tsui, T.C.Liu (2006) “Experimental analysis of tribological properties of lubricating oils with nanoparticle additives” Elsevier wear 262 (2007) 819–825
- [4] B.K. Prasad(2006) “Investigation into sliding wear performance of zinc- based alloy reinforced with sic particles in dry and lubricated conditions” Elsevier wear 262 (2007) 262–273
- [5] Stephen M. Hsu(2004) “Nano-lubrication: concept and design” Tribology international 37 (2004) 537–545
- [6] L. Joly-pottuz B. Vacher n. Ohmae J. M. Martin t. Epicier(2008) “ Anti-wear and friction reducing mechanisms of carbon nano-onions as lubricant additives” Tribollett (2008) 30:69–80
- [7] Sushil Kumar Srivastava “Oils lubricants and Lubrication” Oxford & IBH publications
- [8] M.S. Yadav, S. Rathod ,B.K. Prasad, and O.P. Modi (2010) “ Sliding wear behavior of cast iron: influence of mos₂ and graphite addition to the oil lubricant ” ASM international 1059-9495
- [9] B.K. Prasad (2003) “ Sliding wear behaviour of bronzes under varying material composition, microstructure and test conditions ” wear 257 (2004) 110–123
- [10] Desmond F. Moore “Principles and applications of tribology” Pergamon publications (ISBN 0-08-017902-9)

Analysis and Performance Characteristics of Various Fluids Used In Cooling System of Electric Car Battery With CFD Analysis Software

P.Saravanan¹, S.Senthil², R.Rajappan³ & P.Paramadayalan⁴

^{1,2 & 3} Professor, Department of Mechanical Engineering, Mailam Engineering College.

⁴Assistant Professor, Department of Mechanical Engineering, Mailam Engineering College.

Abstract

Electric cars are initially developed as an alternative option for the existing gas powered cars. It also shown good results in both performance and energy utilization. Usage of electric cars are encouraged due to its effect over global warming as there is no emission of harmful gases like CO, CO₂, NOX. Electric car is an automobile which is propelled by one or more electric motors, using energy stored in rechargeable batteries. This idea as coined in late 18th century, But it was in the 20th century when it started to roll on in roads. Even though we use battery as the energy source, we need a cooling system. It is to ensure the proper dissipation of heat which is emitted from the battery while transmission. Here we discuss about the cooling system of the battery in an electric car. We use three different liquids to analyze its effectiveness. Those fluids are Glycol, Fluorinert FC72 and NOVEC7200 (Ethoxy nonaflurobutane). We designed and drawn the model using CATIA V5 software and analyzed using ANSYS FLUENT software. This analyzed best Coolant for the battery cooling system.

Keywords: *Glycol, Ethoxy nonaflurobutane, Fluorinert FC72, CATIA V5, ANSYS FLUENT.*

1 Introduction:

Automobiles throughout the world are the primary consumers of fossil fuels, which emit toxic gases when burnt such as CO, CO₂ and NOX. This resulted in Increase of Global Warming. To reduce this factor Electric Vehicles were invented. Electric cars are a variety of electric vehicle (EV). The term "electric vehicle" refers to any vehicle that uses electric motors for propulsion, while "electric car" generally refers to highway-capable automobiles powered by electricity. Low-speed electric vehicles classified as NEVs in the United States and as electric motorised quadricycles in Europe are plug-in electric- powered micro cars or city cars with limitations in terms of weight, power and maximum speed that are allowed to travel on public roads and city streets up to a certain posted speed limit, which varies by country.

While an electric car's power source is not explicitly an on-board battery, electric cars with motors powered by other energy sources are typically referred to by a different name. An electric car carrying solar panels to power it is a solar car, and an electric car powered by a gasoline generator is a form of hybrid car. Thus, an electric car that derives its power from an on-board battery pack is a form of battery electric vehicle (BEV). Most often, the term "electric car" is used to refer to battery electric vehicles, but may also refer to plug-in hybrid electric vehicles (PHEV). Although it is an electric vehicle it needs a cooling system. It is due to its optimal usage of battery which dissipates heat heavily. So we analysis the different types of fluids and its performance in this project.

2 Literature review

The vehicles emitting organic compounds, Pd, nitrogen oxide and carbon monoxide have done significant pollution of air. World population is growing by an extremely high rate so that the vehicle usage is also rising with the rise of the population.

Fossil fuel is the main energy resource of these vehicles. In 21th century oil production reached a peak. Estimates indicate that petroleum and natural gas will be run out by the year 2042 (Shafiee. S and Topal. E, 2009).

After inventing the lead acid batteries and the electric motors in late 1800s, the first electric vehicles were invented. In the early 1900s, electric vehicles were very popular and that time is called the golden period of electric vehicles.

After the arriving of gasoline powered vehicles almost every electric vehicle was disappeared due to limitation of range, long charging time, heavy weight and poor durability of batteries (Young, K., Wang, C. and Wang, L.Y., 2013) (Kulkarni. A, Kapoor. A, and Arora. S, 2015).

Because of gas emission laws and air pollution automobile manufactures were forced to manufacture low carbon emission vehicles so the electric vehicle manufacturing is increasing today (Sagar. A.D, 1995) (Kulkarni. A, Kapoor. A, and Arora. S, 2015).

Electric vehicles present an excellent alternative to the current fossil fuel powered vehicles due to several reasons. Low noise and zero emission are some main reasons why people buy electric car now days. Electric vehicles are perfectly suitable for urban environment thus they are very compact, not as wasteful as internal combustion engines in traffic and the limited range is not a matter in the urban environment (Sagar. A.D, 1995). Internal operation of electric vehicles is similar to the internal combustion vehicles. Like in combustion vehicles, electric vehicles have an electric motor, an ECM, a battery, battery management system with regenerative braking system a charger and a cooling and heating system.

There are two types of motors used in electric vehicles AC motors, and DC motors. DC motors are easily control when comparing with AC motors and also less expensive than AC motors. However, DC motors are larger and heavier than the AC motors. Hence the electric motors have high torque acceleration of an electric vehicle is quicker than the internal combustion engine. That property can use to build fast electric racing cars because in races instant torque is much help full.

Electric vehicle also has a feature called regenerative breaking and by using that feature the vehicle can generate electricity by own kinetic energy that can be stored in super capacitors. Electric vehicles sales are increasing rapidly when we compare the sales data for previous years. That shows that the demand for electric vehicles are higher now days. With the rise of the demand, much more research must be done to develop the EV technology.

A cell of a battery is consisting of an anode and a cathode and all the chemical process happen between those two. Other than the electrodes a battery has separators, terminals, electrolyte and a case (Dhameja, S. and Dhameja, eep, 2000).

A battery has one negative terminal and a one positive terminal. The electrolyte can be a gel, solid or liquid according to the battery type and it can be acidic or alkaline (Dhameja, S. and Dhameja, eep, 2000).

For an example electrolyte of a lead-acid battery is sulphuric acid and the negative terminal is made by pure lead and the positive terminal is made by lead-dioxide. In late 80's there were electric vehicles but failed, in early 90's due to lack of battery technology (Kulkarni. A, Kapoor. A, and Arora. S, 2015). Nevertheless, in 1990s due to climate change governments looked forward to develop electric vehicle.

For example, the U.S. Advanced battery consortium (USABC) was formed to develop electric vehicle batteries (Dhameja, S and Dhameja, eep, 2000). Therefore, the electric vehicle battery technology was developed up to now passing so many stages.

Electric vehicle batteries should have some special properties rather than the normal batteries like laptop and cell phone batteries. The battery should have high energy density to travel long range. The battery should give a stable output with different acceleration and it should have a higher C rate. Long life cycle is more important for electric vehicle battery and the maintenance cost also should be low. Also the battery must be environmental friendly and recycling must be possible (Dhameja, S. and Dhameja, eep, 2000).

There are a vast range of EV vehicle battery available on the market. Most of the electric vehicle manufacturers are using Li-ion or Ni-MH batteries for their EV's. Normally NiMH battery is used in electric vehicles as a secondary power source. Ni-MH batteries are safer than the Li-ion battery but Li-ion is preferred as the power source of electric vehicles (Kulkarni. A, Kapoor. A, and Arora. S, 2015).

3 Proposed Methodology

3.1 PCM-Based Cooling battery Thermal management System

It is one of the types of Phase Change Material based cooling system. Compared with traditional thermal management methods such as air cooling and liquid cooling, the research on applying phase change materials to battery thermal management system started late. However, PCM battery thermal management system has broad application prospects and outstanding comprehensive performance. Many related scholars have made in-depth research on this technology.

Initially proposed using phase change materials in battery thermal management system, and found that the temperature in the battery module controlled by PCM is more uniform than that cooled by air at different discharge rates. Which proved that PCM temperature control effect is effective. RAO found that PCM with a melting point below 45°C is more effective in decreasing battery temperature.

In practical applications, more attention should be paid to the PCM packaging. Design details such as leakage, volume change of PCM, and proper quality of PCM based on load should be taken into consideration. The breakthrough of these practical problems is crucial for the PCM-based BTMS future development.

3.2 Heat Pipe-Based Cooling Battery Thermal Management System

As an efficient heat transfer element, heat pipe is favoured by the energy industry due to its high thermal conductivity and low thermal resistance. It is widely used in aerospace, military industry, micro-electronics heat dissipation, building materials, metallurgy, solar energy and other fields. Thanks to the variable structure, the heat pipe can move a large amount of heat inside the battery pack to keep the battery within the required operating temperature range. The temperature difference inside the battery pack can also be significantly reduced. It can also significantly reduce the temperature difference inside battery cells.

3.3 Thermoelectric Element-Based Cooling Battery Thermal Management System

Thermoelectric refrigeration technology is an electronic refrigeration technology with high efficiency and low energy consumption. Thermoelectric elements are characterized by compact structure, fast response, and integration of refrigeration and heating, providing new ideas for BTMS. The thermoelectric elements can be divided into two categories, one is a thermoelectric generator (TEG) based on Seebeck effect, which converts heat into electricity and uses waste heat as energy. The other is a thermoelectric cooler (TEC) based on Peltier effect, which converts electricity into heat for cooling and heating. The most direct representative is semiconductor refrigeration. Based on the thermoelectric elements characteristics, a large number of experiments and simulations have been done to prove feasibility of thermoelectric elements in BTMS.

3.4 Designing Process

The Battery Arrangement was designed using CATIA software (an acronym of computer-aided three-dimensional interactive application) is a multi-platform software suite for computer-aided design (CAD), computer-aided manufacturing (CAM), computer-aided engineering (CAE), PLM and 3D, developed by the French company Dassault Systèmes.

Since it supports multiple stages of product development from conceptualization, design and engineering to manufacturing, it is considered a CAx-software and is sometimes referred to as a 3D Product Lifecycle Management software suite. Like most of its competition it facilitates collaborative engineering through an integrated cloud service and have support to be used across disciplines including surfacing & shape design, electrical, fluid and electronic systems design, mechanical engineering and systems engineering.

Besides being used in a wide range of industries from aerospace and defence to packaging design, CATIA has been used by architect Frank Gehry to design some of his signum curvilinear buildings and his company Gehry Technologies was developing their Digital Project software based on CATIA.

Fig.1 shows an isometric view of an our proposed model it gives clear view about the structure of the model.

Fig.2 represents the top view of the model and fig.3 represents the front view of the model which has been used in our work.

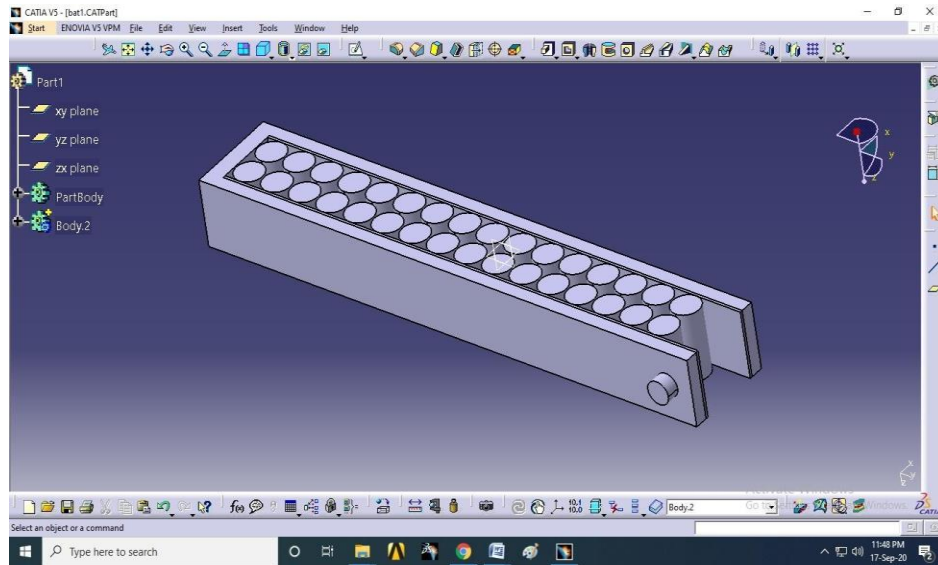


Fig.1 Proposed model Isometric view

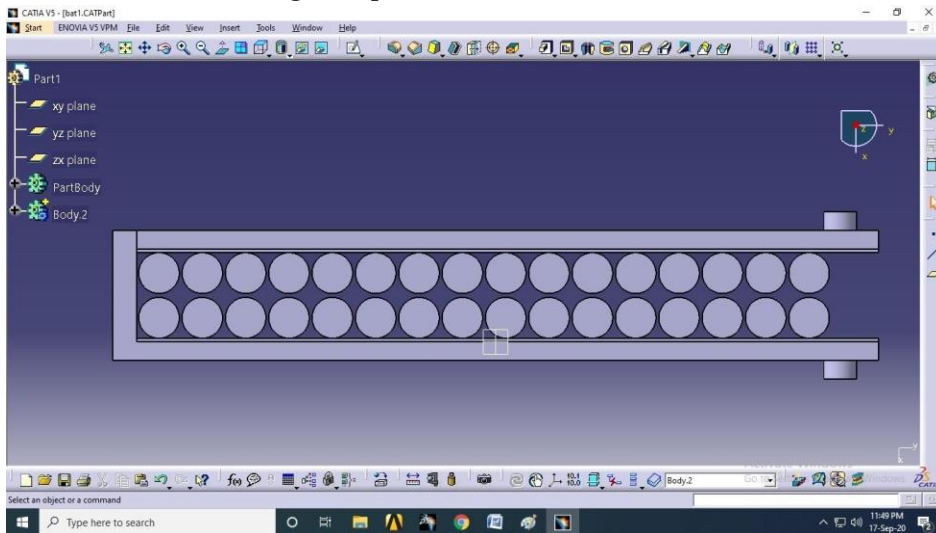


Fig.2 Proposed model Top view

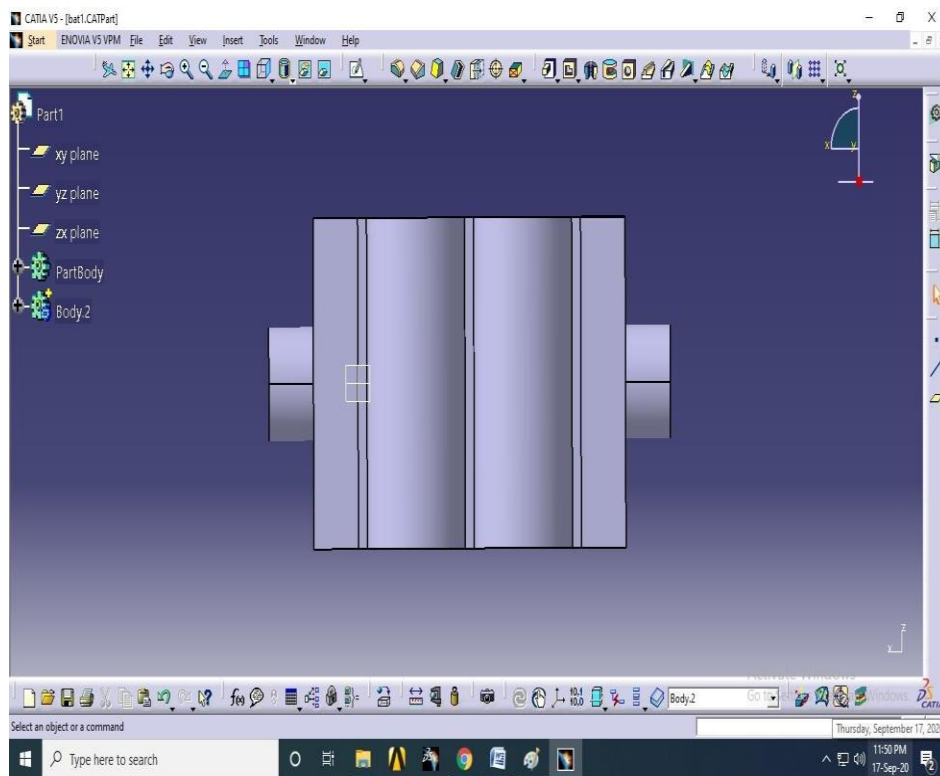


Fig.3 Proposed model Side view

4 Results and Discussion

The Results of the CFD Analysis of a single battery in a container (fluid flow surface) for all three fluids were compared with various aspects. Single battery is used here for analyzing convenience.

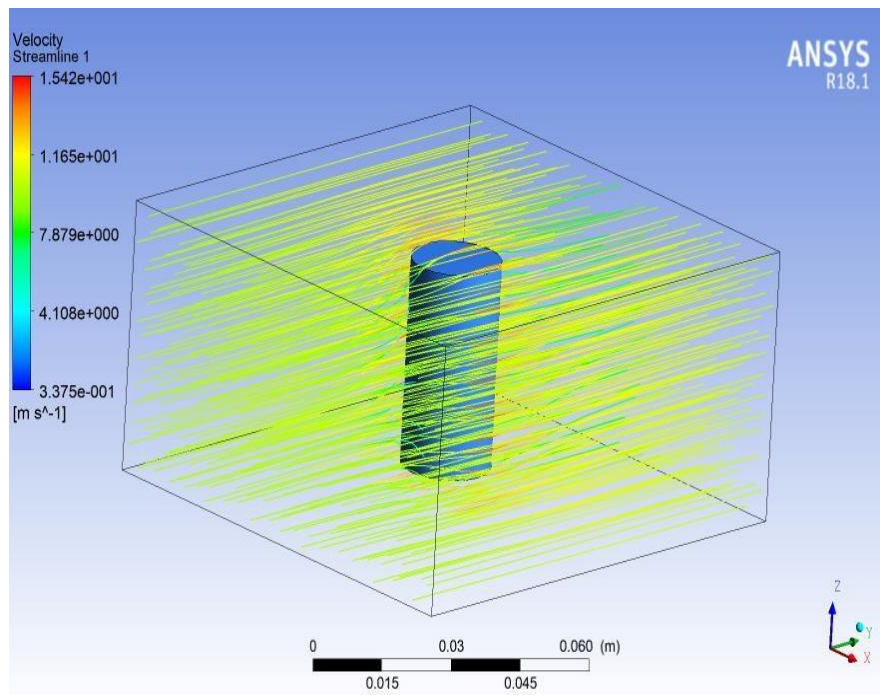


Fig.4 Streamline flow for battery cooling management system

Streamline flow of battery cooling setup is clearly shown in fig.4 and fig.5 represents the Velocity flow for battery cooling management system. This explains range of velocity which occurred in battery cooling management system.

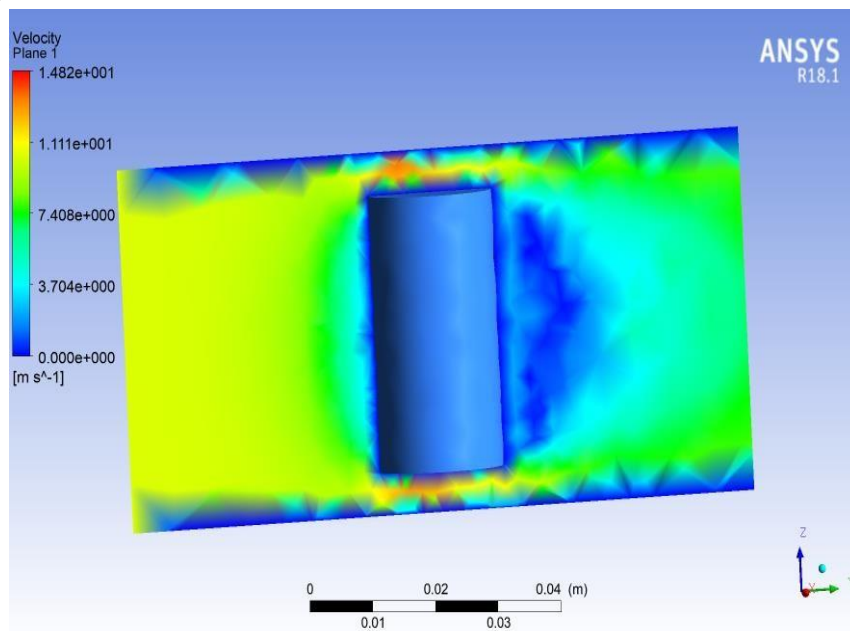


Fig.5 Velocity flow for battery cooling management system

Fig.6 represents the pressure flow for battery cooling management system. In this diagram we can see the left side of cooling system is has high range of values in battery cooling management system.

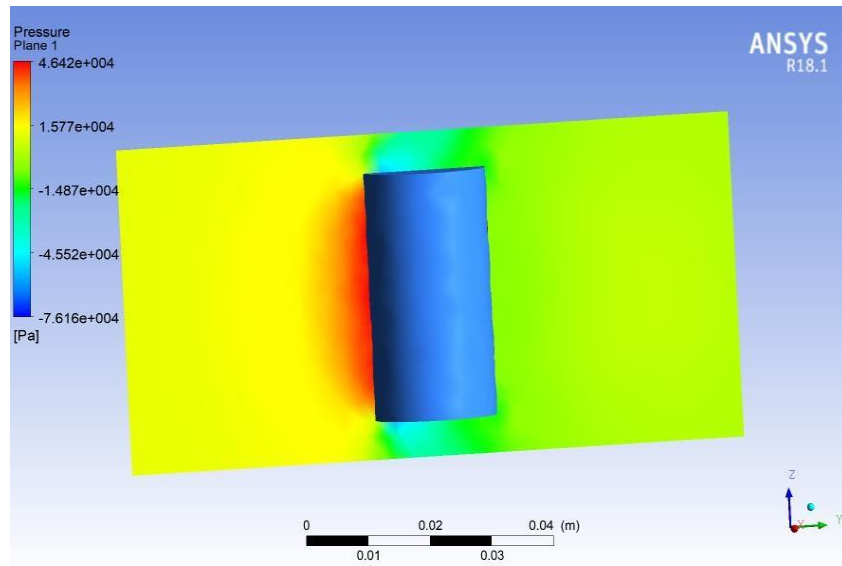


Fig.6 Pressure flow for battery cooling management system

In fig. 7 shows the temperature variation of setup which uses the Ethylene glycol. The surrounding temperature value of battery setup is shown in various colour variations.

Fig. 8 shows the momentum and mass graph for Ethylene glycol and fig. 9 represents turbulence graph for Ethylene glycol.

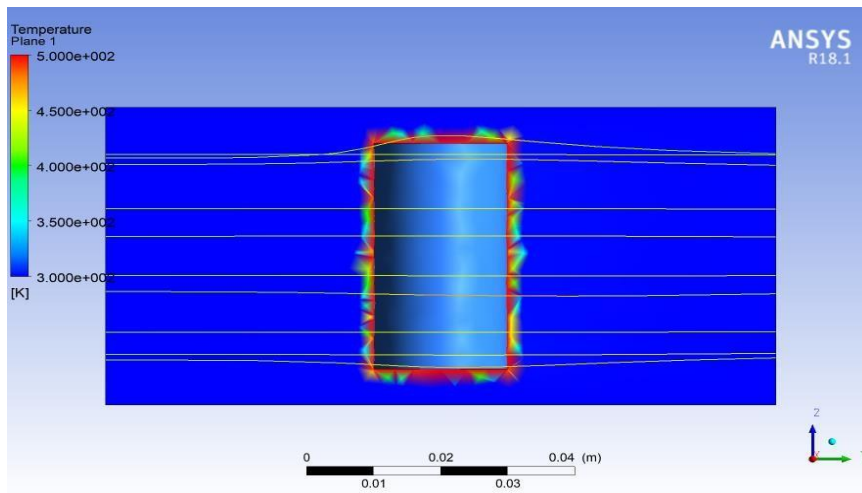


Fig.7 Temperature variations for Ethylene glycol

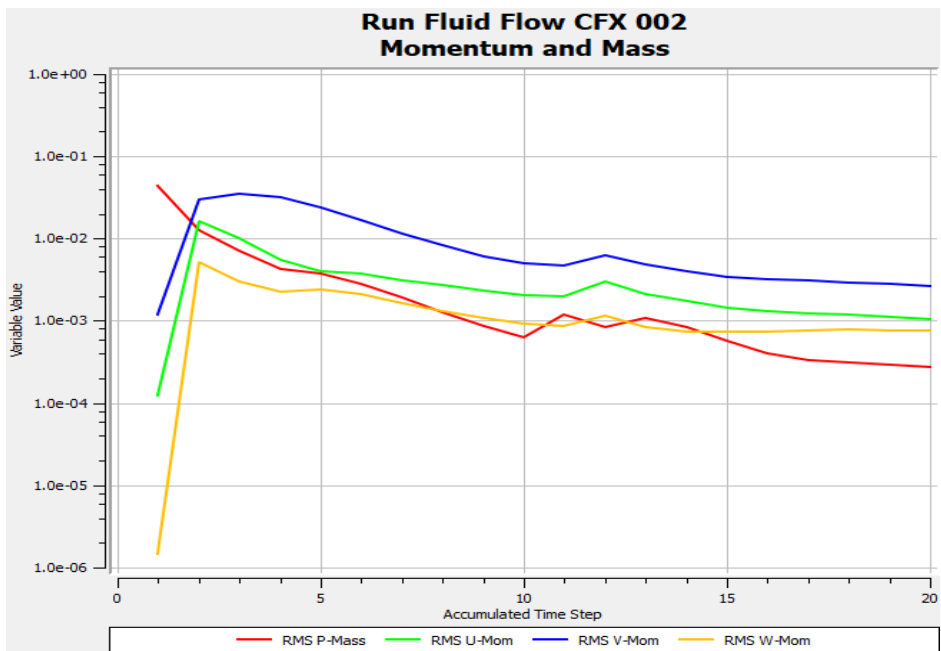


Fig.8 Momentum and mass graph for Ethylene glycol

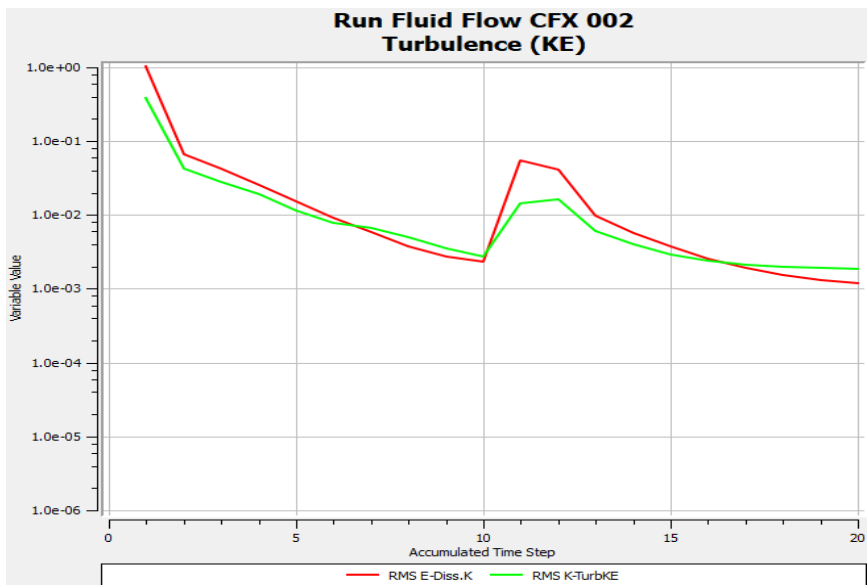


Fig.9 Turbulence graph for Ethylene glycol

In fig. 10 shows the temperature variation of setup which uses the Fluorinert FC72. The surrounding temperature value of battery setup is shown in various colour variations.

Fig. 11 shows the momentum and mass graph for Fluorinert FC72 and fig. 12 represents turbulence graph for Fluorinert FC72.

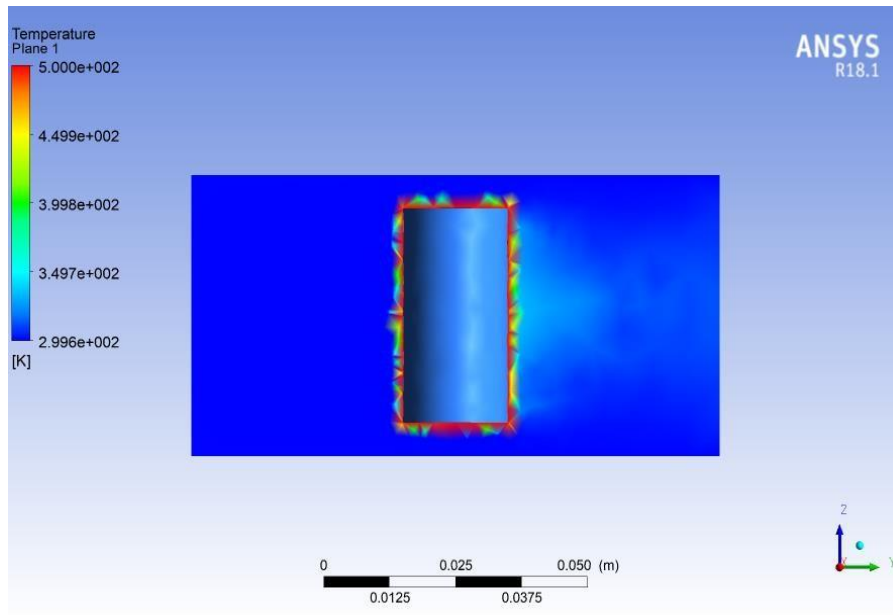


Fig.10 Temperature variations for Fluorinert FC72

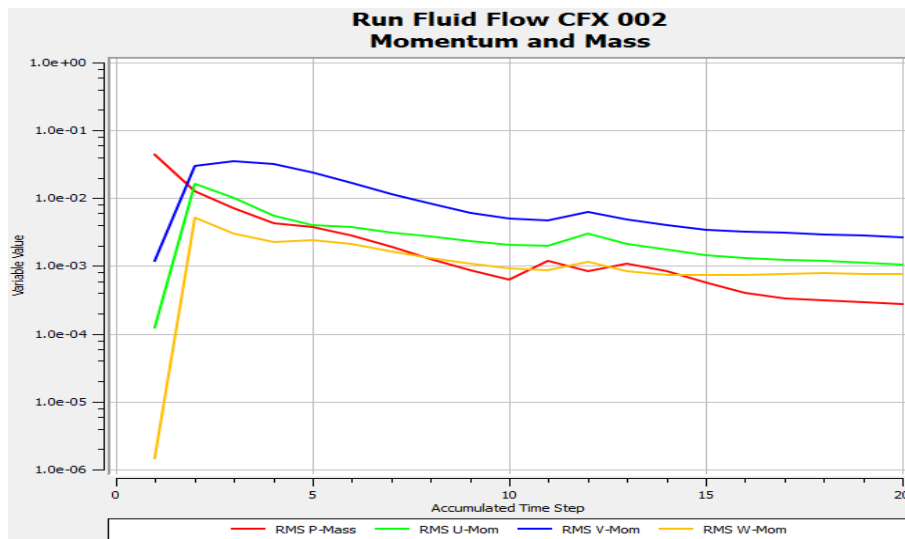


Fig.11 Momentum and mass for Fluorinert FC72

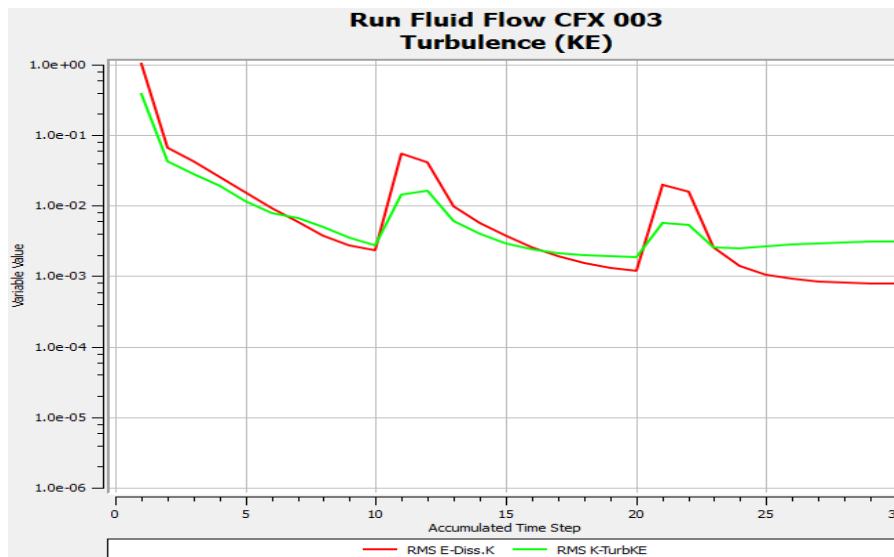


Fig.12 Turbulence graph for Fluorinert FC72

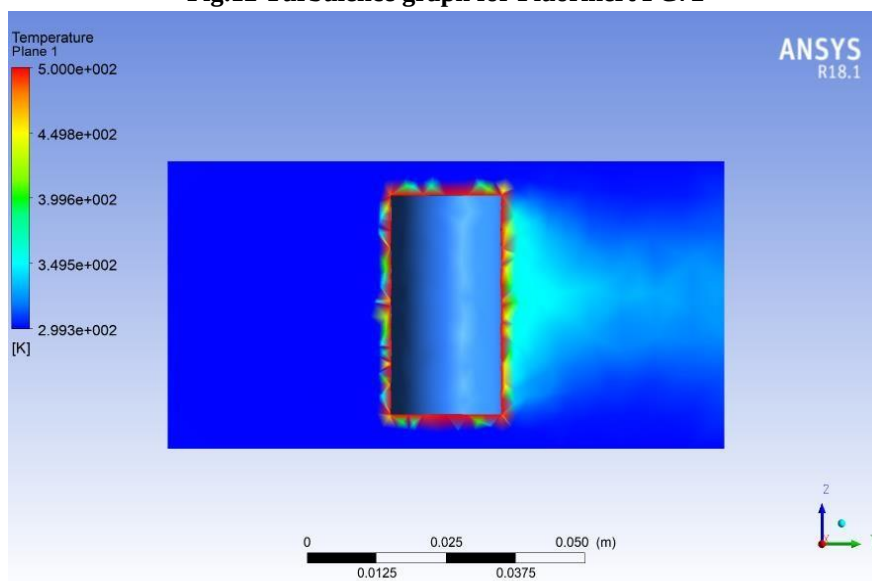


Fig.13 Temperature variations for Ethoxy Nonfluorobutane

In fig. 13 shows the temperature variation of setup which uses the Ethoxy Nonfluorobutane. The surrounding temperature value of battery setup is shown in various colour variations.

Fig. 11 shows the momentum and mass graph for Ethoxy Nonfluorobutane and fig. 12 represents turbulence graph for Ethoxy Nonfluorobutane.

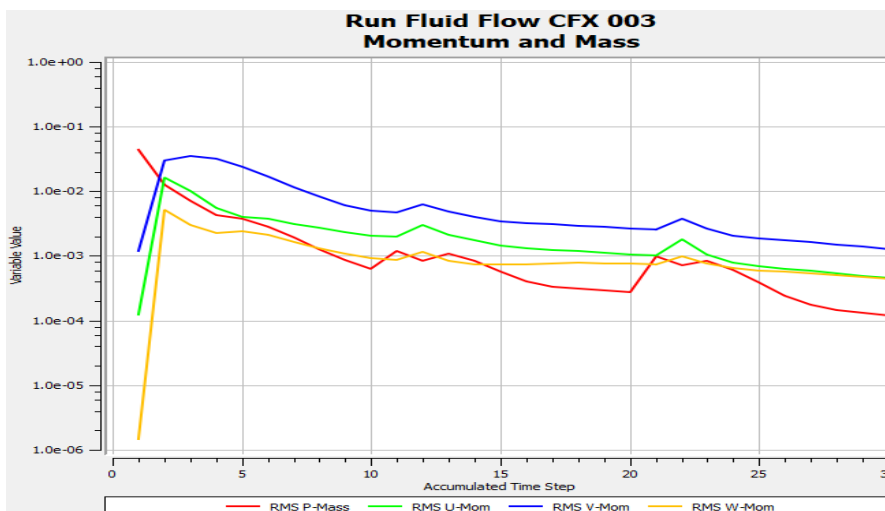


Fig.14 Momentum and mass for Ethoxy Nonfluorobutane

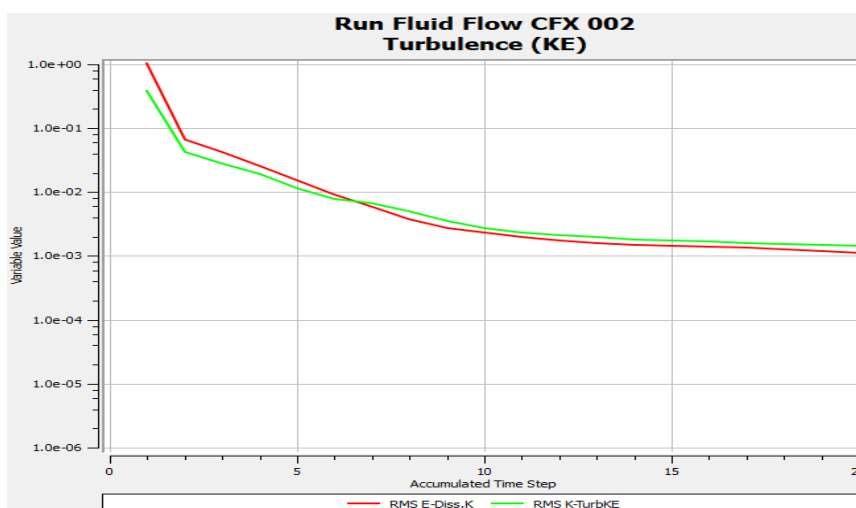


Fig.15 Turbulence graph for Ethoxy Nonfluorobutane

Conclusions

This project work has provided us an excellent opportunity and experience, to use our limited knowledge. We gained a lot of knowledge about electric cars, its working techniques, charging methods and cooling systems.

We had used Ethylene Glycol, Fluorinert FC72 and Ethoxy Nonfluorobutane fluids for analysing. We used ANSYS FLUENT for the analysis. At the end the Ethoxy Nonfluorobutane, an Engineering Fluid had shown enormous result compared to the other fluids. It had a greater heat conduction when compared to other fluids. So we conclude this project as the ETHOXY NONAFLUROBUTANE as the best coolant fluid.

References

- [1] Z. Lu, X.Z. Meng, L.C. Wei, et al., Thermal management of densely-packed EV battery with forced air cooling strategies, Energy Procedia 88 (2016) 682– 688.

- [2] K. Chen, M. Song, W. Wei, et al., Structure optimization of parallel air-cooled battery thermal management system with U-type flow for cooling efficiency improvement, *Energy* 145 (2018) 603–613.
- [3] J. Xun, R. Liu, K. Jiao, Numerical and analytical modelling of lithium ion battery thermal behaviours with different cooling designs, *Power Sources* 233 (2013) 47–61.
- [4] Y.S. Choi, D.M. Kang, Prediction of thermal behaviours of an air-cooled lithium-ion battery system for hybrid electric vehicles, *Power Sources* 270 (2014) 273–280.
- [5] C. Forgez, D.V. Do, G. Friedrich, et al., Thermal modelling of a cylindrical Li Fe PO₄/graphite lithium-ion battery, *J. Power Sources* 195 (2010) 2961–2968.
- [6] Y. Inui, Y. Kobayashi, Y. Watanabe, et al., Simulation of temperature distribution in cylindrical and prismatic lithium ion secondary batteries, *Energy Convers. Manage.* 48 (2007) 2103–2109.
- [7] C. Zhu, X. Li, L. Song, et al., Development of a theoretically based thermal model for lithium ion battery pack, *J. Power Sources* 223 (2013) 155–164.
- [8] W. Wu, S. Wang, W. Wu, et al., A critical review of battery thermal performance and liquid based battery thermal management, *Energy Convers. Manage.* 182(2019) 262–281.
- [9] Q. Zhang, R.E. White, Capacity fade analysis of a lithium ion cell, *Power Sources* 179 (2008) 793–798.
- [10] Y. Huo, Z. Rao, X. Liu, et al., Investigation of power battery thermal management by using mini-channel cold plate, *Energy Convers. Manage.* 89 (2015) 387–395.
- [11] Z. Rao, Q. Wang, C. Huang, et al., Investigation of the thermal performance of phase change material/mini-channel coupled battery thermal management system[J], *Appl. Energy* 164 (2016) 659–669.
- [12] L.W. Jin, P.S. Lee, X.X. Kong, et al., Ultra-thin mini channel LCP for EV battery thermal management, *Appl. Energy* 113 (2014) 1786–1794.
- [13] Y. Lai, W. Wu, K. Chen, et al., A compact and lightweight liquid-cooled thermal management solution for cylindrical lithium-ion power battery pack, *Int. J. Heat Mass Transf.* 144 (2019) 118581.
- [14] Y. Deng, C. Feng, E. Jiaqiang, et al., Effects of different coolants and cooling strategies on the cooling performance of the power lithium ion battery system: are view, *Appl. Therm. Eng.* 142 (2018) 10–29.

Micro Hardness and Surface Analysis of Polysiloxane Coating on Alloy Steel Substrate

1. M. Sivamanikandan Assistant Professor, 2. R. Jayakumar. Assistant Professor
Mechanical Department, St. Anne's college of Engineering & Technology

Abstract

This project deals about developing anti-scratch coating for automotive body. Automobiles undergo severe scratches on body and to some extend on the wind shields. An experimental investigation is carried out over automotive body to improve the scratch resistant using the newly developed polysiloxane coating. The coating process used is spray coating. Polysiloxane coatings are industrial protective and maintenance coating which is characterized by abrasion, chemical, extreme UV and high temperature. Scratch properties of polysiloxane coatings are critical in their application in many fields which require long-term protection and aesthetics. Critical input parameters of spray coating process such as nozzle distance, spraying time and pressure is optimized and corresponding output parameters are coating thickness, surface roughness, coating micro hardness, abrasion rate are studied. Taguchi's L9 orthogonal array and Analysis of variance is used to conduct the experiment for finding the optimum process parameter. The coated samples will be examined using scanning electron microscopy (SEM) for micro structure analysis. Phase and chemical composition will be carried out using XRD and energy dispersive x-ray spectroscopy (EDAX). Optical microscopy is used to examine the microstructure of the coated samples. The Vickers Hardness Test will be taken to measure the micro hardness of the coating. In addition to it the adhesion, corrosive, wear test will be studied.

Keywords: *Substrate coating, Spray coating, Polysiloxane coating, Optical Microscope, SEM, Vickers's hardness test.*

1 Introduction

The modern automobile is a grand assemblage of parts made from a variety of materials. Many of these parts have a protective coating applied to improve the appearance or provide additional durability to the substrate. In many coating systems the uppermost layer is a clear coating (ranging between 5–50 μm in thickness), which not only protects the underlying layers or substrate from chemical and UV degradation, but also provides protection from mechanical damage that can result in surface scratches.

2 Substrate for Coating:

A part of the car bonnet is used for this experiment to coat and analyze the scratch resistivity. The substrate is cut from the bonnet with respective dimensions 80x80 mm. The test samples has the dimension of 20x20 mm.



Fig 1.1-Substrate

3 Modern Automotive Coating Processes:

Modern automotive coating methods consist of five main steps. They include the following:

Pre-Treatment:

It removes and cleans excess metal and forms an appropriate surface structure enabling bonding of a corrosion

protection layer.

Electro Deposition: (Ed)

The metal underbody and frames of automobiles are coated to prevent corrosion, whereas other areas like the roof are not rust proofed.

Rust-Proof Materials: Sealer / Pvc

The third step is underbody coating and seam sealing using PVC (Polyvinyl Chloride) and urethane. Recently, PVC and acryl/urethane sealants have also been used in the underbody areas, a process called the Dampening Coat (DC), to impart noise-proofing and vibration-deadening. The noise and vibration are transferred from the engine, drive train, suspension system, road noise of the tires, and flowing air, and the underbody sealants reduce noise transfer into the passenger compartment of the automobile. A sealer like Poly Vinyl Chloride (PVC) is applied for anti-corrosion, elimination of water leaks, and minimization of chipping and vibrational noise.

Primer:

The fourth coating step is the application of a primer surface or simply primer. It can be water-borne, solvent-borne, or a powder. The main reason for primer application was to improve weather resistance, appearance, and chipping resistance

Top Coat:

The final step in the body coating process is to apply the topcoat, which consists of two layers-the base coat and clear coat. The base coat contains the primary coloring pigment, and the clear coat provides a protective coating against environmental effects, corrosion, and UV light degradation.

Spray Coating:

It is a painting technique where a device sprays a coating (paint, ink, varnish, etc.) through the air onto a surface. The most common types employ compressed gas usually air to atomize and direct the paint particles.

Air Gun Spraying:

This process occurs when paint is applied to an object through the use of an air-pressurized spray gun. The air gun has a nozzle, paint basin, and air compressor. When the trigger is pressed the paint mixes with the compressed air stream and is released in a fine spray. Due to a wide range of nozzle shapes and sizes, the consistency of the paint can be varied. The shape of the workpiece and the desired paint consistency and pattern are important factors when choosing a nozzle. The three most common nozzles are the full cone, hollow cone, and flat stream. There are two types of air-gun spraying processes. In a manual operation method the air-gun sprayer is held by a skilled operator, about 6 to 10 inches (15–25 cm) from the object, and moved back and forth over the surface, each stroke overlapping the previous to ensure a continuous coat. In an automatic process the gun head is attached to a mounting block and delivers the stream of paint from that position. The object being painted is usually placed on rollers or a turntable to ensure overall equal coverage of all sides.

Objectives

In this work, the automobile coatings are performed by the progress in controlling droplets and their deposition attributes, and by the development of new technologies and paint chemistries, a comprehensive and up-to-date review of automobile coatings and coating technologies was considered to be of value to industrial practitioners and researchers.

In this work the combination of Phenyl trimethoxysilane (PTMS), Dimethoxy dimethylsilane (DMDS), 3-Glycidoxypropyl methyl dimethoxysilane is used for coating over the substrate using the spray coating process.

4 Experimental Setup for Spray Coating:

The air inflator is connected to the input valve of the cylindrical tank and make tight, from the output valve the pipe is connected with the help of the pipe tightening clip. Pressure regulator is fixed at the end of the pipe by fixing the nipple in it. The nipple is connected to the inlet side of the regulator. The pressurized air is taken from the outlet of the regulator. Another piece of pipe is connected to the airbrush (spray gun) and made tight with the clip. The air inflator is given power supply with Switched-Mode Power Supply (SMPS) and switched on. The air flows from the inflator to the tank and get compressed. The required pressure is set with the help of the knob in the regulator and by pressing the trigger in the spray gun the compressed air is released for setting the pressure. The polysiloxane chemical is poured into the storage cup in the spray gun so that atomized air mixes with the polysiloxane.

Coated Substrate:

According to the parameters included the substrate are coated with different pressure, substrate distance and spraying time. There are totally nine substrate with different composition parameters used for optimizing it.

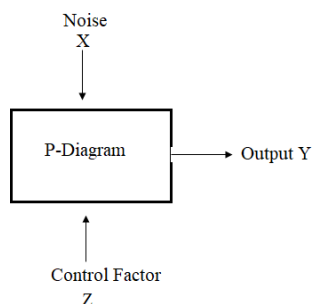
5 Taguchi Method Treats Optimization Problems in Two Categories:

(i) Static Problems:

Generally, a process to be optimized has several control factors which directly decide the target or desired value of the output. The optimization then involves determining the best control factor levels so that the output is at the the target value. Such a problem is called as a "STATIC PROBLEM".

This is best explained using a P-Diagram which is shown below ("P" stands for Process or Product). Noise is shown to be present in the process but should have no effect on the output! This is the primary aim of the Taguchi experiments - to minimize variations in output even though noise is present in the process. The process is then said to have become ROBUST.

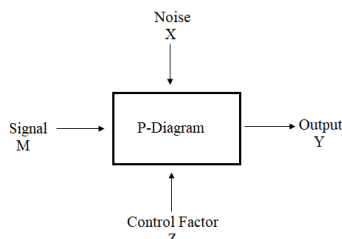
Fig 3.15 P-Diagram for Static Problems



ii) Dynamic Problems:

If the product to be optimized has a signal input that directly decides the output, the optimization involves determining the best control factor levels so that the "input signal / output" ratio is closest to the desired relationship. Such a problem is called as a "DYNAMIC PROBLEM".

This is best explained by a P-Diagram which is shown below. Again, the primary aim of the Taguchi experiments -



to minimize variations in output even though noise is present in the process- is achieved by getting improved linearity in the input/output relationship.

Fig 3.16 P-Diagram for Dynamic Problems

Spray Coating Process Parameters and their Levels:

Table 3.2

| Parameters | Level 1 | Level 2 | Level 3 |
|--------------------------------|---------|---------|---------|
| Pressure (kg/cm ²) | 1.10 | 1.50 | 1.85 |
| Substrate distance (cm) | 10 | 15 | 20 |

| | | | |
|---------------------|---|----|----|
| Spraying time (sec) | 5 | 10 | 15 |
|---------------------|---|----|----|

Experimental Plan for Spray Coating As Per L9 Orthogonal Array:

| Specimen | Pressure (kg/cm ²) | Substrate distance(cm) | Spraying time (sec) |
|----------|--------------------------------|------------------------|---------------------|
| 1 | 1.10 | 10 | 5 |
| 2 | 1.10 | 15 | 10 |
| 3 | 1.10 | 20 | 15 |
| 4 | 1.50 | 10 | 10 |
| 5 | 1.50 | 15 | 15 |
| 6 | 1.50 | 20 | 5 |
| 7 | 1.85 | 10 | 15 |
| 8 | 1.85 | 15 | 5 |
| 9 | 1.85 | 20 | 10 |

Table 3.3

The column of orthogonal array represents experimental parameters are to be optimized. Row of orthogonal array represents the level of each parameter. S/N ratio will be calculated in the MINITAB software using Taguchi method. After experimentation and testing the response value such as coating thickness, surface roughness coating micro hardness to determine the optimal process parameters. ANOVA will be performed to estimate the magnitude of factors effects on the response characteristics.

6 Result and Discussion

| SAMPLE | SURFACE ROUGHNESS(μm) | COATING THICKNESS(μm) |
|--------|------------------------------------|------------------------------------|
| 1 | 0.503 | 44 |
| 2 | 0.543 | 51.3 |
| 3 | 0.56 | 77 |
| 4 | 0.601 | 101 |
| 5 | 0.633 | 129 |
| 6 | 0.619 | 104 |
| 7 | 0.556 | 144 |
| 8 | 0.508 | 173 |
| 9 | 0.476 | 221 |

Table 4.1- Measurement of Surface Roughness and Coating Thickness

The coating thickness of the coated samples is measured by using the samples which is masked on one side, the stylus profilometer probe slides over the sample which shows the difference in the thickness. Surface Roughness is measured by rolling the probe over the coated surface of the sample over three different place, the average is taken to know the overall roughness of the particular sample.

Main Effect Plot For Coating Thickness:

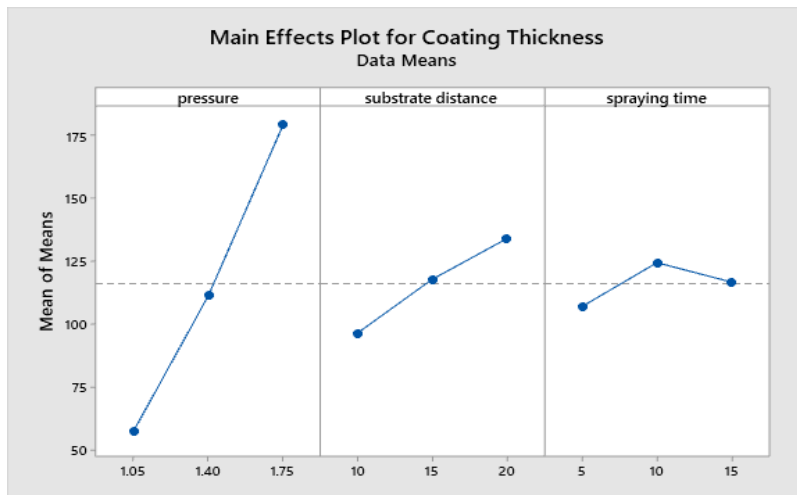


Fig 4.1 Mean Effect Plot for Coating Thickness

As the pressure increases the flow velocity of the polysiloxane fluid increases and condenses on the substrate, so the pressure is directly proportional to the coating thickness. The coating thickness is decreased when the substrate distance is low, it increases when the distance is increased. The spraying time increases with respect to the pressure the amount of fluid will be ejected from the nozzle and thus the coating thickness varies accordingly.

Main Effect Plot for Surface Roughness:

As the pressure increases the surface roughness is decreased. In the substrate distance initially the surface roughness remains constant. As the spraying time is increased the surface roughness is also increases but initially the roughness is low due the decrease in the spraying time.

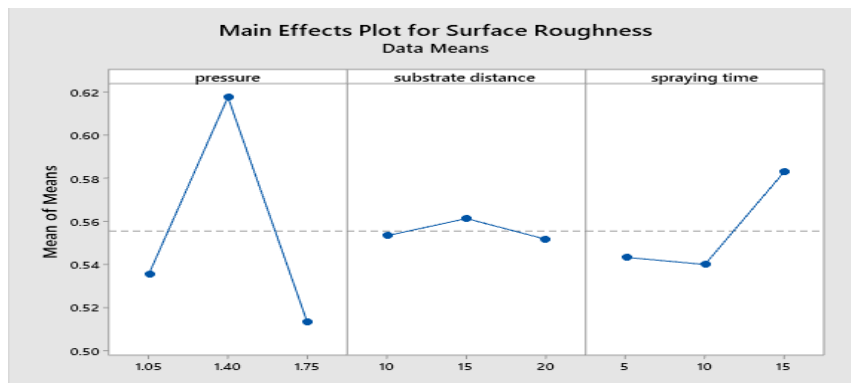


Fig 4.2 Mean Effect Plot For Surface Roughness

Measurement of Micro-Hardness:

| SAMPL E | VICKERS HARDNESS |
|---------|------------------|
| 1 | 18.65 |
| 2 | 19.03 |
| 3 | 21.30 |
| 4 | 22.01 |

| | |
|---|-------|
| 5 | 61.03 |
| 6 | 70.66 |
| 7 | 71.14 |
| 8 | 73.56 |
| 9 | 74.23 |

Table 4.2- Measurement of Vickers Hardness

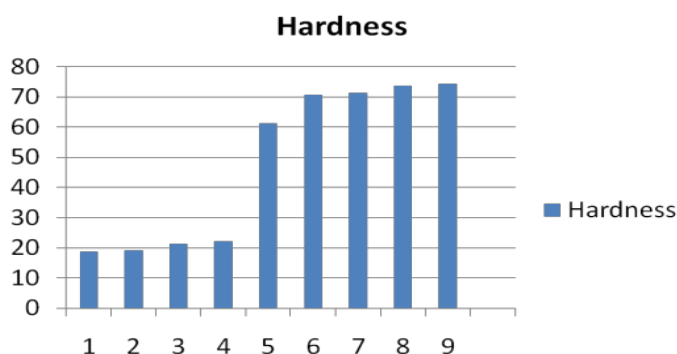


Fig 4.6 Hardness Graph

Initially the Micro-hardness value for the uncoated steel substrate is 9.8HV. The micro- hardness value for the polysiloxane coated substrate increases gradually from 18.85HV based on the influence of the parameters, as the thickness of the film increases the hardness value increased drastically to 74.73HV.

7 Conclusion

The conclusion drawn from the present investigation are as follows:

The polysiloxane coating was successfully coated over the substrate by spray coating technique. The input parameters such as pressure, substrate distance and spraying time of coating process was optimized using Taguchi's L9 orthogonal array method. The coating properties such as coating thickness and surface roughness were measured by Stylus Profilometer, the coating thickness was increased from 44 μ m to 221 μ m and surface roughness was decreased to 0.476 μ m from 0.503 μ m. The physical and surface characteristics were measured successfully.

The Morphological analysis was carried out by FE-SEM the good dispersion of the polysiloxane on the substrate with a distance of 20cm and the elemental composition was confirmed by the EDS. The physical characteristics was carried out by XRD, it shows that the coating to be in crystalline nature having silicon, carbon and oxygen as the component. The Mechanical properties were studied using Vickers Hardness Test. We observed that the hardness was increased from 18.85HV to 74.73HV and 296.552% was the increase in micro hardness. Due to the features of facile and eco friendly preparation, the coatings are potential in the application of automobiles

Reference

[1] L.Q. Feng, B. Benhamida, C.Y. Lu, L.P. Sung, P. Morel, A.T. Detwiler, J.M. Skelly, L.T. Baker, D. Bhattacharya, Fundamentals and characterizations of scratch resistance on automotive clearcoats, Prog. Org. Coat. 125 (2018)339–347

- [2] N.D. Vietroa, L. Belforteb, V.G. Lambertinib, F. Fracassi, Low pressure plasmamodified polycarbonate: A transparent, low reflective and scratch resistant material for automotive applications, *Appl. Surf. Sci.* 307 (2014)698–703
- [3] P. Munzert, N. Danz, A. Sinibaldi, F. Michelotti, Multilayer coatings for Bloch surface wave optical biosensors, *Surf. Coat. Technol.* 314 (2017)79–84
- [4] K. Taeschner, H. Bartzsch, P. Frach, E. Schultheiss, Scratch resistant optical coatings on polymers by magnetron-plasma-enhanced chemical vapor deposition, *Thin Solid Films* 520 (2012)4150–4154
- [5] L.F. Yi, Y. Xu, D. Li, J.B. Shen, S.Y. Guo, H.J. Sue, Fabrication of Scratch Resistant Polylactide with Multilayered Shishkebab Structure through Layer-Multiplying Co extrusion, *Ind. Eng. Chem. Res.* 57 (2018) 4320–4328
- [6] H. Jiang, Y.F. Wei, Q. Cheng, Z.M. Zhu, Scratch behavior of low density polyethylene film: Effects of pre-stretch and aging, *Mater. Des.* 157 (2018) 235–243
- [7] M.M. Hossain, S. Xiao, H.J. Sue, M. Kotaki, Scratch behavior of multilayer polymeric coating systems, *Mater. Des.* 128 (2017)143–149
- [8] M. Zouari, M. Kharrat, M. Dammak, M. Barletta, Scratch resistance and tribological performance of thermosetting composite powder coatings system: A comparative evaluation, *Surf.Coat. Technol.* 263 (2015) 27–35

Wear Simulation of Aluminum-Silicon Carbide Metal Matrix Composites

Hareesha G^{1*}, Chikkanna N², Saleemsab Doddamani³

¹ Dept of Mechanical Engineering, Government Engineering College, HuvinaHadagali, India

² Dept of Aerospace Propulsion Technology, VTU, VIAT, Muddenahalli, Chickballapur, India

³ Dept of Mechanical Engineering, Jain Institute of Technology, Davangere, India

*

Abstract

The main objective of this work is to find the wear rate using Archard's model in a finite element tool. The finite element model for the contact analysis of the disc and pin is built using ansys workbench. The material for the disc used is stainless steel and the pin material used is an aluminum alloy and its composites. A 3D surface-to-surface body-ground connection and revolute type element was utilized, under various circumstances, to display the behavior of the contact surfaces. Archard's model is utilized to simulate the wear using ansys. Outcomes demonstrated that the wear behavior can be simulated and the method can be used to anticipate wear issues for designing. The comparison of results of the wear simulation and experimental wear analysis has been carried out. From the comparison of results it is observed that, the experimental outcomes support the analytical outcomes.

Keywords: Al6061/SiC, Wear simulation, Dry sliding wear, Archard's model, ANSYS.

1 Introduction

Nowadays, in the design of mechanical structures, the dynamic behavior gets more attention. Lifetime under cyclic loading, levels of vibration or noise radiation, the interaction between control systems & structure vibrations, are often important constraints for the designer. The dynamic behavior analysis is on the other hand not straightforward. Designers can easily determine a modal parameter of a mechanical structure by mathematical techniques. The outcomes of the investigation are predicted to correlate with experimental results. ANSYS is universally useful FEM software for numerically resolving a broad range of structural, mechanical issues. Following are the set of a general guideline that can be utilized for solving of any FEM problem. (1) Problem definition, (2) Assigning loads, constraints & solving, (3) Post-processing and presentation of the results.

Different author's were used finite element analysis to simulate or to compare the experimental results. Rullkoetter, P.J et al [1] conducted finite element analysis of Musculoskeletal for its wear behaviour. Author indicate that potential wear cherecteristics include contact pressure and the contact area. Priit Po~dra et al [2] presented the approach to simulate the wear using finite element software called ANSYS. Authors conducted the wear simulation using linear wear law to simulate the pin-on-disc dry sliding wear regime. It was reported that the FEA wear simulation using ANSYS is best suited to analyse the contact issues and wear behaviour. John M. Thompson et al [3] used finite element method to simulate the wear mechanism. The well known commercially available software ANSYS has been utilized to analyze the dry sliding wear. Archard's model was used to calculate the wear depth and contact pressure. Y.S. Lee et al [4] proposed model to predict the wear depth and wear volume. Michael P. Pereira

et al [5] proposed a finite element model to explain the contact pressure growth and its distribution over the die radius, all through the duration of a channel forming process.

Rachit N. Singh et al [6] presented the general finite element model to predict the wear behaviour using rolling and sliding contacts. Ahmed Hadi Abood et al [7] investigated the contact surface analysis to calculate wear rate. Archard's wear simulation model has been utilized to analyze the wear behaviour. Pin-on-disc dry sliding wear test was modeling using ANSYS and evaluated wear depth and contact pressure. Outcomes of the investigations shows the simulation of wear behaviour can be done using finite element method and can be used widely to forecast the engineering wear issues.

Rajesh A M et al [8-11, 13-16] conducted experimentations like hardness, wear behavior at as-cast and age hardened conditions etc on aluminum hybrid metal matrix composites. The matrix material considered is Al6061, and reinforcement material is SiC and alumina. From the results it is clear that the HAMMCs have better properties as compared to unreinforced aluminum alloy.

Saleemsab Doddamani et al [12] conducted experimentation on wear behaviour of Aluminum-graphite MMC. From the results it is found that the adding of particles of graphite has increased the resistance to wear of the MMC. Also it is reported that addition of particles of graphite in aluminum reduces the friction then that of the base alloy.

The main objective of this work is to find the wear rate using Archard's model in a finite element tool. ANSYS software has been utilized to estimate the wear rate of the composite. Also validations of wear simulation using FEA with the experimental results has been carried out.

2 Contact Analyses by ANSYS

The various models and approaches are controlling the finite element wear simulations, such as Archard's model, accommodating the linear wear law equation 1. The disc is assumed to be the harder one and the only the pin endure the wear while in the analysis. During the analysis for design application, the wear depth is considered to be most significant than the wear volume. Thus the Archard's proposed equation.1 can be given as,

$$\frac{V}{sA} = \frac{h}{s} = kp \quad \text{----- 1}$$

where V is the volumetric rate of wear in m³, 's' = sliding distance, 'A' is the apparent contact area in sq.m. h = wear depth in m, K = coefficient of wear in Pa⁻¹ and p = contact pressure in Pa.

The finite element simulation results can be validated by comparing them with the will known values or experimental values. ANSYS is one of the finite element tool, which is additionally fitted with the energy error estimation technique, in order to examine the results in a field of continuous displacement from component to component. By considering the linear wear law, the wear analysis using FE simulation is dealt with the sliding

distance, wear coefficient which depend on the wear depth. The product of coefficient of wear and sliding distance is not changed with the estimation of k and s , than the wear depth won't change with specified load.

3 Model Generations

The ANSYS workbench is used to create the three dimensional disc-on-pin model by giving the contact constraint. The material selected for the disc is stainless steel by considering the built-in properties. The pin material is Al6061-SiC particulate composite with various compositions of reinforcement. Both the pin and the disc have contact type of elements. The frictional type of contact between the disc and pin elements have modeled. The joint between the pin and disc is the Body-Ground connection and revolute type. The ANSYS programming will simulate the wear between the pin and the disc will progressively accumulate the wear between them. This type of simulation can be utilized to solve the wear problems in structural design. The finite element dry sliding wear simulation model is generated in ANSYS workbench as appeared in Fig. 1.

The three dimensional surface contact revolute type, and body-ground connection element is utilized, for various process parameters, to demonstrate the behaviour of the contact surfaces. The contact-pair comprises of two elements, one is considered to be target surface (Pin), and other is counterface surface considered to be contact surface (Disc).

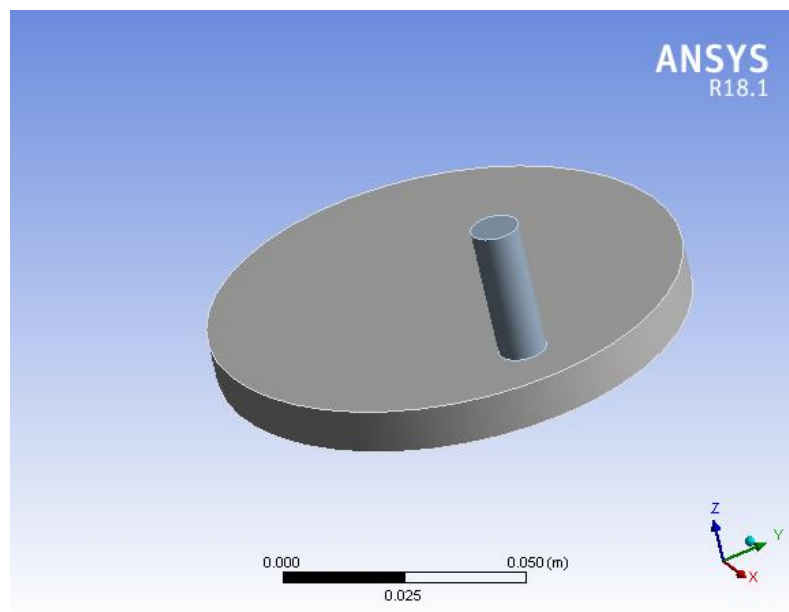


Fig.1 3D model of Disc and Pin in a wear testing

The created 3D model is meshes to a coarse mesh to a mesh size of 3mm. The FE simulation model i.e meshed model is showed in Fig. 2.

The FE simulation model is generated for the contact analysis of the disc and pin. The Archard's wear simulation analysis was carried out for the various process parameters such as sliding distance, speed, composition of the composite. The FE simulation analysis is conducted for the Taguchi's design of experiments as mentioned in the Table 1. During the FE simulation analysis, the contact pressure, wear depth of the pin material has to be recorded to calculate the wear rate of the composite. The sample of the induced contact pressure in pin material, for the given parameters, is shown in the Fig.3

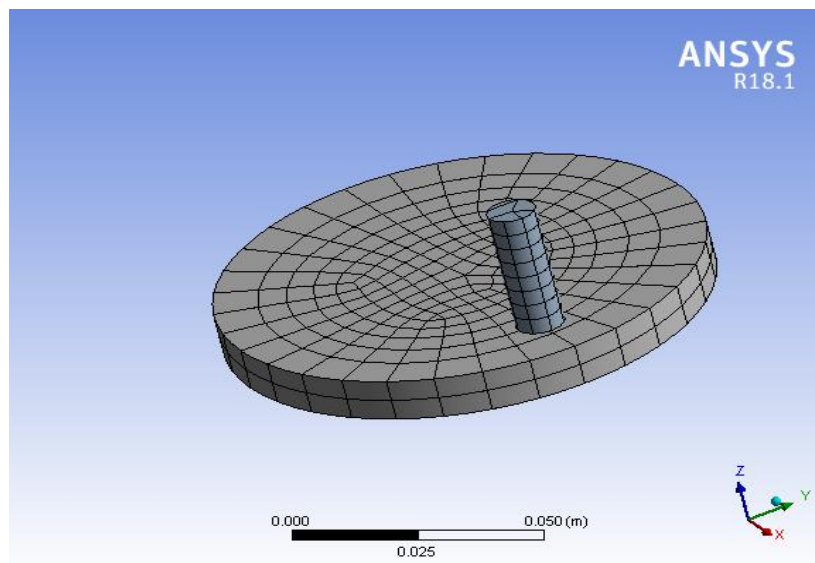


Fig. 2 Meshed Finite Element Model of Disc and Pin

4 Results and Discussions

The FE model is built using ANSYS Workbench, for the contact analysis of the disc and pin. Archard's model is utilized to simulate the contact analysis of disc and pin. The Archard's analysis was carried out and the result of the analysis shown in Fig.3. The contact pressure induced by the contact analysis is given in the Fig.3. The maximum pressure of 0.59MPa is induced is in the pin material.

From the experimental results [14], it is observed that as load increases the wear rate of the composite increases. As composition increases wear rate reduces up to 9% of SiC reinforcement in the Al6061 matrix and increases for 12% SiC. It has been observed that as sliding distance increases wear rate of the composite decreases. It is obvious that as the increment in the applied load gives the increment in the wear. As composition increases wear rate decreases for 9% of SiC and increases by 12% of SiC. The optimize composition is at 9% of SiC based on load, sliding distance,

and composition of the Al6061- SiC composites. From the Taguchi analysis, on the specimens, 9% of SiC is the optimized composition and wear rate reduces for the optimized composition. The analytical wear analysis is done successfully by using ANSYS. Wear analysis is carried out using ANSYS and there is a good correlation between the results obtained by experiment and ANSYS. From the comparison of results, it is observed that, the experimental results back up the analytical results.

Model of Disc and Pin

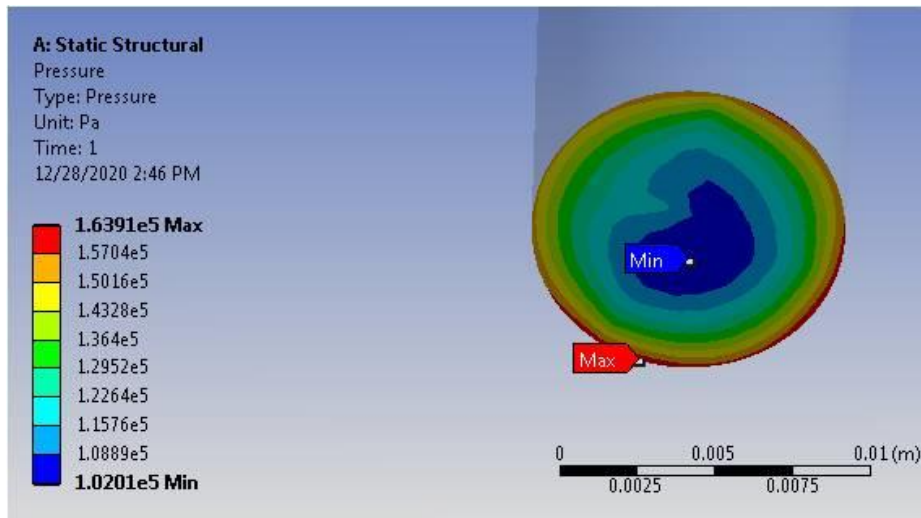


Fig. 3 Pressure induced in the Al6061-9wt% of SiC.

The maximum pressure of 0.1639MPa is induced is in the pin material of 9wt% of reinforcement.

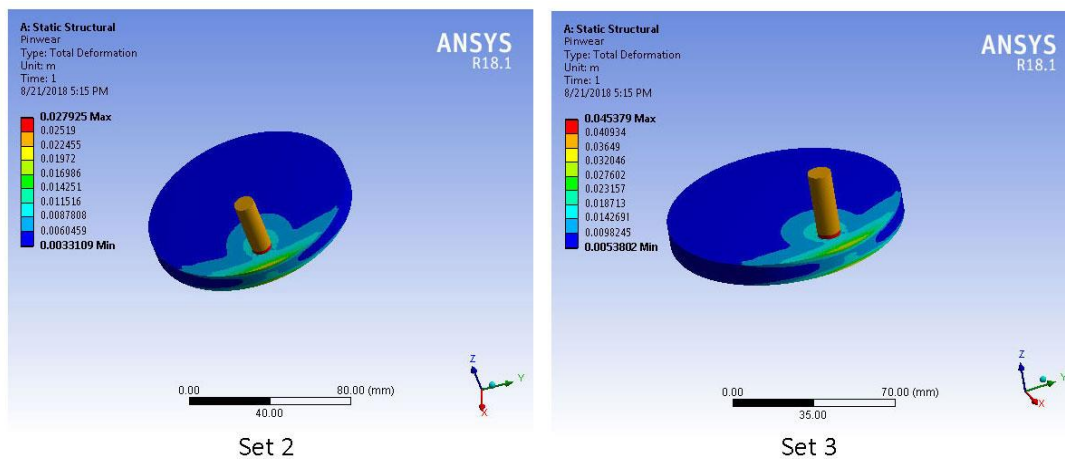


Fig. 4 Wear depth of pin material for different process parameters

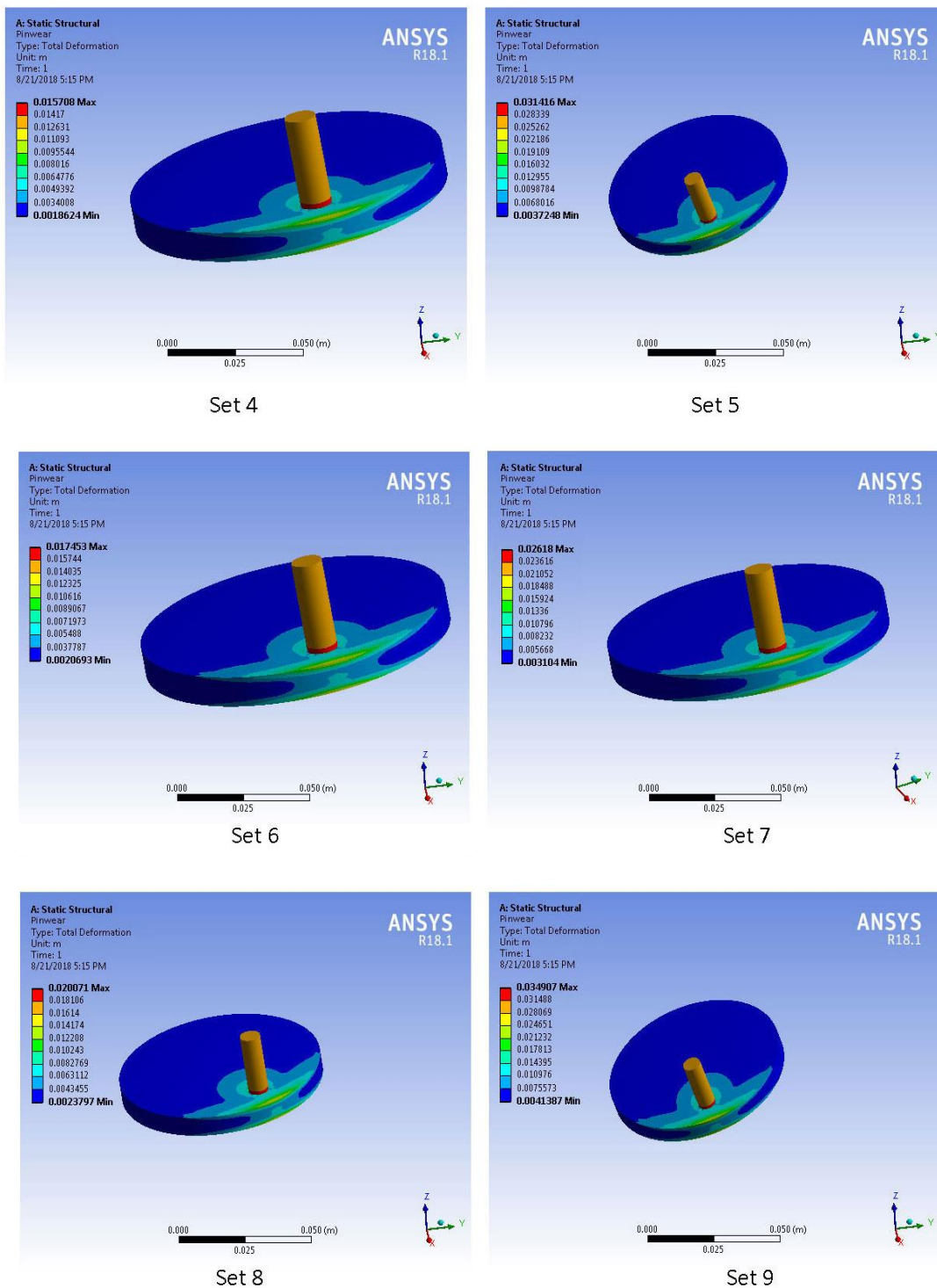


Fig.5 Wear depth of pin material for different parameters

Fig.5 shows the wear depth (h) for the pin material for different process parameters. Using wear depth and contact pressure, wear coefficient value has been calculated. Archard's wear model was extensively used to calculate the wear rate using Eq 1. Using ANSYS, wear simulation model will use Archard's law to calculate the wear rate. Wear rate has been determined from the data available from the Archard's model contact pressure analysis and listed in Table 1.

Table 1 FEM results for different process parameters

| Sl no | Composition | Speed m/s | Sliding distance m | Wear depth m | Contact pressure MPa | Wear coefficient $\times 10^{-11}$ | Wear rate $\times 10^{-6}$ |
|-------|---------------|--------------|--------------------------|--------------------|----------------------------|--|----------------------------------|
| 1 | Al6061-3%SiC | 1 | 400 | 0.02792 | 0.5936 | 8.318 | 4.937 |
| 2 | Al6061-3%SiC | 2 | 600 | 0.04538 | 0.8901 | 6.010 | 5.350 |
| 3 | Al6061-6%SiC | 1 | 400 | 0.01571 | 0.2953 | 9.407 | 2.778 |
| 4 | Al6061-6%SiC | 2 | 600 | 0.03142 | 0.5906 | 6.272 | 3.704 |
| 5 | Al6061-9%SiC | 1 | 400 | 0.01745 | 0.8865 | 6.970 | 6.179 |
| 6 | Al6061-9%SiC | 2 | 600 | 0.02618 | 0.2941 | 10.494 | 3.086 |
| 7 | Al6061-12%SiC | 1 | 400 | 0.02007 | 0.5886 | 12.072 | 7.106 |
| 8 | Al6061-12%SiC | 2 | 600 | 0.03491 | 0.8827 | 6.994 | 6.173 |

5 Conclusions

In this work, we discussed the 3D finite element modeling for wear analysis. For analysis of wear behavior, ANSYS software has been utilized. The result of the investigation is a FEM that is more reliable for further predictions. The FE model is built using ANSYS Workbench, for the contact analysis of the disc and pin. Archard's model is utilized to simulate the contact analysis of disc and pin. The Archard's analysis was carried out and the result of the analysis shown. The analytical wear analysis is done successfully by using ANSYS. Wear analysis is carried out using ANSYS and there is a good correlation between the results obtained by experiment and ANSYS. From the comparison of results it is observed that, the experimental outcomes support the analytical outcomes. The outcomes obtained by experimental and analytical method agree with each other with a deviation of about 1% – 25%. There is a good correlation between experimental and FEA values of the wear analysis are obtained.

References

- [1] Rullkoetter, P.J., Gabriel, S.M., Colleran, D.P., and Zalenski, E.B, “The relationship between contact stress and contact area with implications for TKR evaluation and design”, 45th Annual Meeting, Orthopaedic Research Society, Anaheim, California, February 1-4, 1999.
- [2] Priit Poõdra and Soõren Andersson, “Simulating sliding wear with finite element method”, *Tribology International* 32 (1999) 71–81.
- [3] John M. Thompson, “A Proposal for the Calculation of Wear”, -International ANSYS Conference 2006, pp 286-300.
- [4] Y.S. Lee, C.Y. Park, T.S. Kim, H.D. Kim, “The method to predict wear depth and wear volume of tube at near-distant future from measured or prescribed depth at present time”, *Nuclear Engineering and Design* 225 (2003) 99–108.
- [5] Michael P. Pereira, Wenyi Yan, Bernard F. Rolfe, “Contact pressure evolution and its relation to wear in sheet metal forming”, *Wear* 265 (2008) 1687–1699.
- [6] Rachit N. Singh, Dr. A. V. Vanalkar, “Analysis of Wear Phenomena in Sliding Contact Surfaces”, *International Journal of Engineering Research and Applications*, Vol. 2, Issue 3, May-Jun 2012, pp.2403-2409.
- [7] Ahmed Hadi Abood, “Effect of Asperity Height on Wear Behavior by Finite Element Method”, *Journal of Babylon University, Engineering Sciences*, No.(4), Vol.(20), 2012.
- [8] Rajesh A M, Mohammed Kaleemulla, Experimental investigations on mechanical behavior of aluminium metal matrix composites, *Materials Science and Engineering* 149, 2016. Doi:10.1088/1757-99X/149/1/012121.
- [9] Rajesh A M, Mohammed Kaleemulla, Experimental investigations on mechanical and wear behavior of hybrid aluminium alloy, *IJERT*, Volume: 05, Issue: 13, pp 128-131, Sep-2016.
- [10] Rajesh A M, Mohammed Kaleemulla, Effect of heat treatment on hybrid aluminum metal matrix composites, *International Journal of Emerging Research in Management &Technology*, Volume-6, Issue-5, pp 548-551, 2017.
- [11] Rajesh A M, Mohamed Kaleemulla, Doddamani Saleemsab, “Effect of addition of SiC and Al₂O₃ on wear behavior of hybrid aluminum metal matrix composites”, *ACTA TECHNICA CORVINIENSIS – Bulletin of Engineering*, 12 (1), 2019, pp 43-52.
- [12] Saleemsab Doddamani, Mohamed Kaleemulla, Yasmin Begum, Anand K J, “An Investigation on Wear Behavior of Graphite Reinforced Aluminum Metal Matrix Composites”, *JoRSTEM*, Sp issue; 2017: pp. 1-6.
- [13] Rajesh A M, Mohamed Kaleemulla, Doddamani Saleemsab, KN Bharath,, “Development And Characterization Of Hybrid Aluminum Metal Matrix Composites”, *ACTA TECHNICA CORVINIENSIS – Bulletin of Engineering*, Vol. 12, Fascicule 3, 2019, pp 63-66.
- [14] Rajesh A M, Mohamed Kaleemulla, Doddamani Saleemsab, “Effect of heat treatment on wear behavior of hybrid aluminum metal matrix composites”, *Tribology in Industry*, vol.41, iss.3, pp.1-11, 2019. DOI: 10.24874/ti.2019.41.03.04.
- [15] Rajesh A M, Mohamed Kaleemulla, Doddamani Saleemsab, KN Bharath,, “Material characterization of SiC and Al₂O₃ reinforced hybrid aluminum metal matrix composites on wear behavior”, *Advanced Composite Letters*, SAGE, vol.28, pp.1-10, 2019. DOI: 10.1177/0963693519856356.
- [16] Rajesh A M, Mohamed Kaleemulla, Doddamani Saleemsab, KN Bharath, “Generation of Mechanically Mixed Layer (MML) in Hybrid Aluminum Metal Matrix Composites under As-cast and Age Hardened Conditions”, *SN Applied Science*, Springer, Vol. 1, Iss 8, 2019, pp.. DOI:10.1007/s42452-019-0906-5
- [17] Rajesh A M, Mohamed Kaleemulla, “Wear behavior of aluminum matrix composites under conditions that generate mechanically mixed layer”, Ph.D Thesis, Visvesvaraya Technological University, Belagavi, India. 2019.
- [18] Saleemsab Doddamani, Rajesh A M, Mohammed Kaleemulla, “Dry sliding wear simulation of hybrid aluminium metal matrix composites”, *Advanced Composites and Hybrid Materials*, Springer, Vol.3, iss.1, pp.120–126, (2020). <https://doi.org/10.1007/s42114-020-00133-9>.

Experimental Investigation of EDM For Surface Roughness and MRR In Machining of Aluminium 2024

Aravintha raj A, Arun S ,Aravindhnan D

ABSTRACT

Electrical discharge machining (EDM) process is a non-conventional and non-contact machining operation which is used in industry for high precision products. EDM is known for machining hard and brittle conductive materials since it can melt any electrically conductive material regardless of its hardness. The work piece machined by EDM depends on thermal conductivity, electrical resistivity, and melting points of the materials. The tool and the work piece are adequately both immersed in a dielectric medium, such as, kerosene, deionized water or any other suitable EDM fluid. This project provides an important review on different types of EDM operations. A brief discussion is also done on the machining responses and time taken to finish the process. Al 2024 alloy is widely used in aerospace applications.

The aerospace application required close tolerances and accuracy in the machined parts. Henceforth non-conventional machining processes are widely used for different machining operations such as drilling through holes. In the present study, the Electrical Discharge Machining (EDM) process is used to drill through holes in 2mm thick Aluminium 2024 alloy material. With the aim of getting high accuracy and finish of the metal different parameters necessary set accordingly. Three input parameters such as Peak current (IP), Spark Gap voltage (SV) and Pulse on time were selected and the input values were given on required bases.

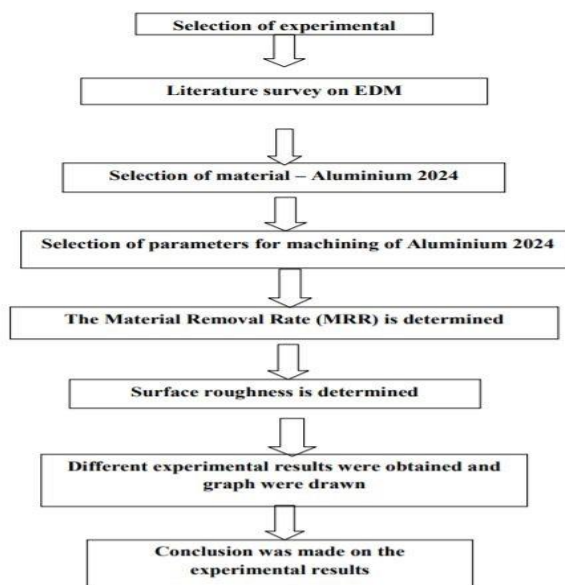
Keywords :

Aluminium (2024),aluminium plate,copperelectrode,edm machine,workingof edm,roughness.

INTRODUCTION

Aluminium compound is generally favoured in the business because of its low weight and extensively high strength. The avionic business broadly utilizes this property of aluminium, making it an essential competitor as a basic material. With the end goal to abuse the utilization of these combinations, the aviation businesses request high exactness and precision of the machined parts. A minor misalignment or blunder in the parts can result in deadly outcomes. In this way, non-ordinary machining techniques are for the most part favoured for various machining activities, for example, penetrating openings, making weld edge readiness and so forth. Electrical Discharge Machining (EDM) is the for the most part generally utilized non-customary machining process, especially to bore openings and spaces. Out of various variations of EDM, start disintegration EDM process includes material expulsion from the work piece with a progression of progressive electric sparkles which dissolves the work piece material. The device and work piece are inundated in dielectric medium which likewise always streams and aids in flushing the dissolved material. As there is no contact among instruments and work pieces, the procedure is most favoured for accuracy machining. Be that as it may, similar to every mechanical procedure, the quality and exactness of the last item is specifically influenced by the info procedure parameters.

1 METHODOLOGY



1.1 MATERIALS AND ITS DESCRIPTIONS

1.1.1 ALUMINIUM 2024

Aluminium 2024 alloy is an aluminium alloy, with copper as the primary alloying element. It is used in applications requiring high strength to weight ratio, as well as good fatigue resistance. It is weldable only through friction welding, and has average machinability. Due to poor corrosion resistance, it is often clad with aluminium or Al-1Zn for protection, although this may reduce the fatigue strength. Aluminium 2024 is heat-treatable aluminium alloy with copper as the primary alloying element. It is used in applications requiring high strength to weight ratio, as well as good fatigue resistance. Due to its high strength and fatigue resistance, 2024 is widely used in aircraft structures.

| | Si | Fe | Cu | Mn | Mg | Cr | Zn | Ti | Others-Each | Others Total | Al |
|------|------|------|---------|----------|---------|------|------|------|-------------|--------------|-----------|
| 2024 | 0.50 | 0.50 | 3.8-4.9 | 0.30-0.9 | 1.2-1.8 | 0.10 | 0.25 | 0.15 | 0.05 | 0.15 | Remainder |

Fig.No.1 – Composition of Aluminium(2024)



Fig.No.2 – Aluminium Plate

1.2 ELECTRICAL DISCHARGE MACHINE:

1.2.1 COPPER ELECTRODE

Copper and copper alloys have better EDM wear resistance than brass, but are more difficult to machine than either brass or graphite. It is also more expensive than graphite. Copper is, however, a common base material because it is highly conductive and strong. It is useful in the EDM machining of tungsten carbide, or in applications requiring a fine finish.



Fig.No.3 – Copper Electrode

1.3 EDM MACHINE

The essential EDM process is extremely very straightforward. An electrical start is made between a cathode and a workpiece. The start is unmistakable proof of the stream of power. This electric start produces exceptional warmth with temperatures achieving 8000 to 12000 degrees Celsius, softening nearly anything. The start is deliberately controlled and limited with the goal that it just influences the surface of the material. The EDM procedure typically does not influence the warmth treat beneath the surface. With wire EDM the start dependably happens in the dielectric of deionized water. The conductivity of the water is deliberately controlled making an astounding domain for the EDM procedure.

The water goes about as a coolant and flushes away the disintegrated metal particles.



Fig.No.4 - EDM Machine

2.PRINCIPLE OF ELECTRIC DISCHARGE MACHINE

2.1WORKING :

The working of EDM process is based on the thermoelectric energy. This energy is created between a workpiece and an electrode submerged in a dielectric fluid with the passage of electric current. The workpiece and the electrode are separated by a specific small gap called spark gap. Pulsed arc discharges occur in this gap filled with an insulating medium, preferably a dielectric liquid like hydrocarbon oil or de- ionized water. Electrical discharge machining is a machining method primarily used for hard metals or those that would be very difficult to machine with traditional techniques.

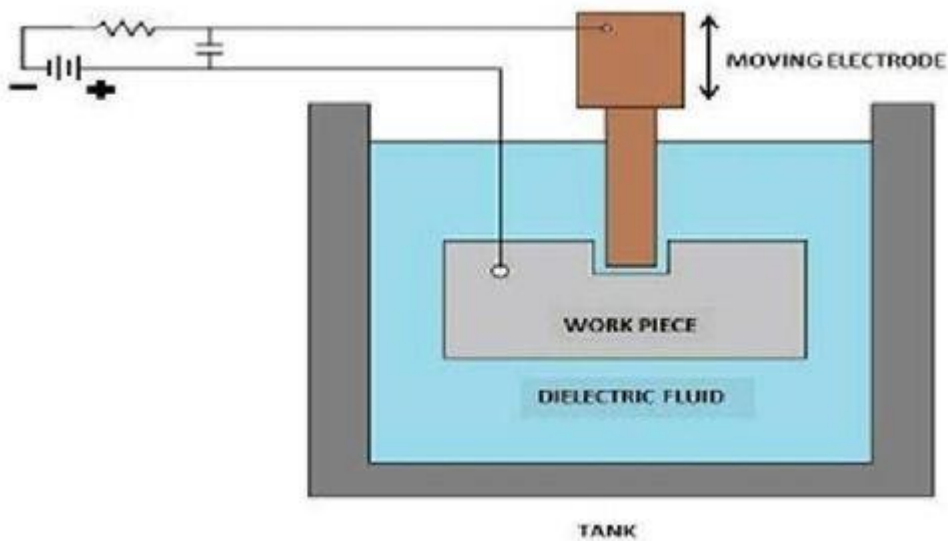


Fig.No.5 - Working of electrical discharge machine

2.2 ROUGHNESS VARIATION:

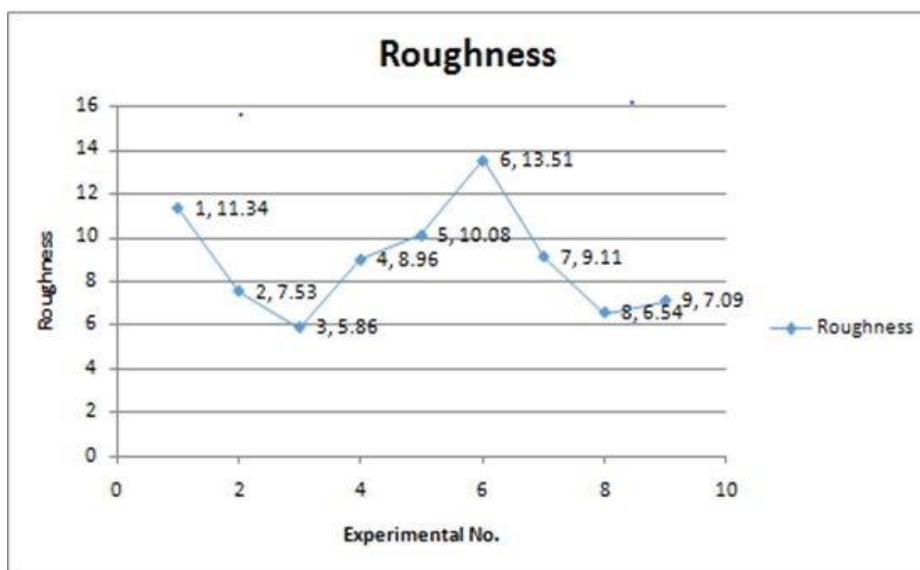


Fig. No.6 - Roughness Variation

Surface roughness value is measured using a surface roughness device. Surface roughness is an important parameter in machining operation. In this pulse on time (TON) is less the roughness is high because spark strike on metal is huge. Peak current is high, the surface roughness is low, because the spark produced is evenly distributed. Good level of roughness is obtained when an optimum value of three parameters is maintained.

2.3 METAL REMOVE RATE VARIATION:

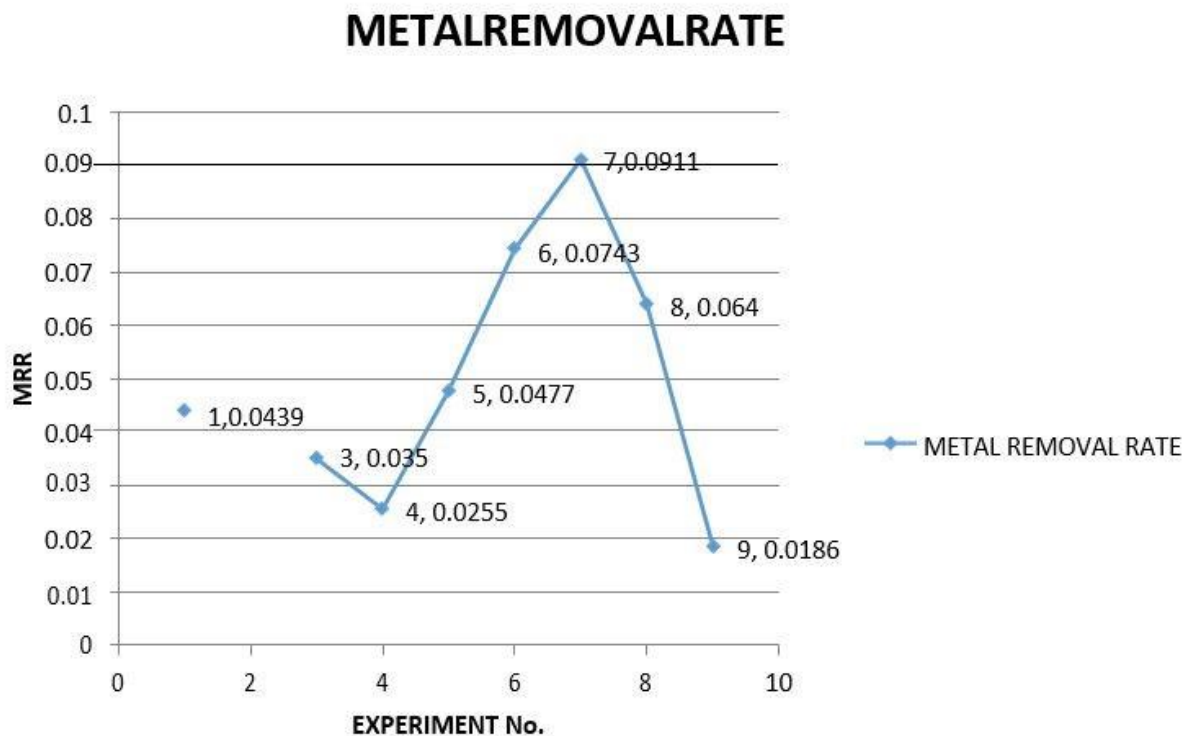


Fig 7- Metal removal rate variation

MRR is high when the gap voltage is low because voltage difference is high. Voltage applied from 200V to 25V. This causes huge power to flow through the electrode and MRR is maintained at high level and surface roughness is also good.

$$\text{MRR} = \frac{\text{mass before machining} - \text{mass after machining}}{\text{Time taken for machining}}$$

2.4 DESIGN:

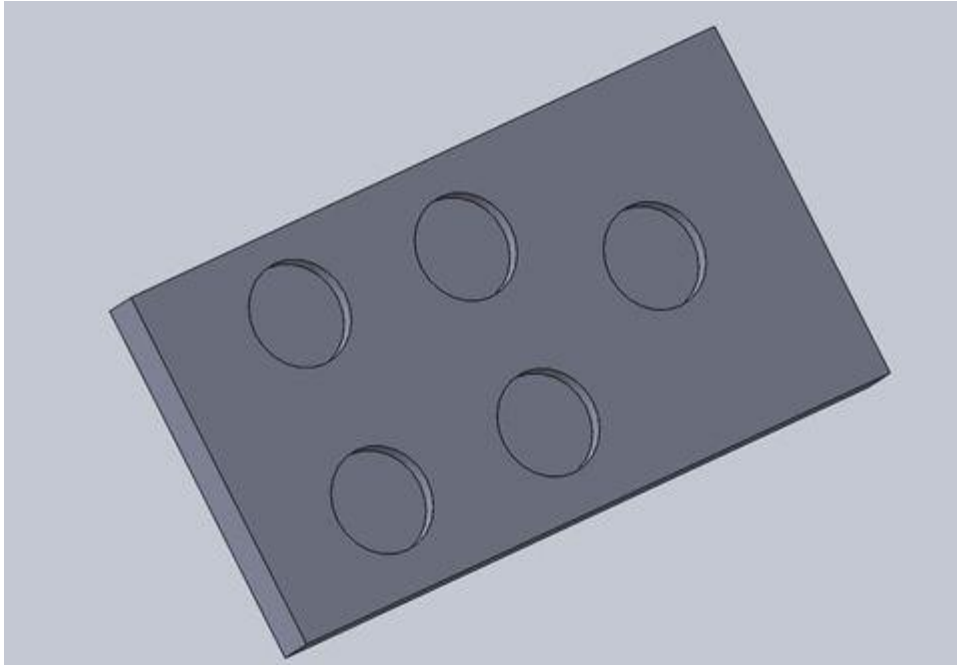


PLATE 1(3D-ISOMETRIC VIEW)

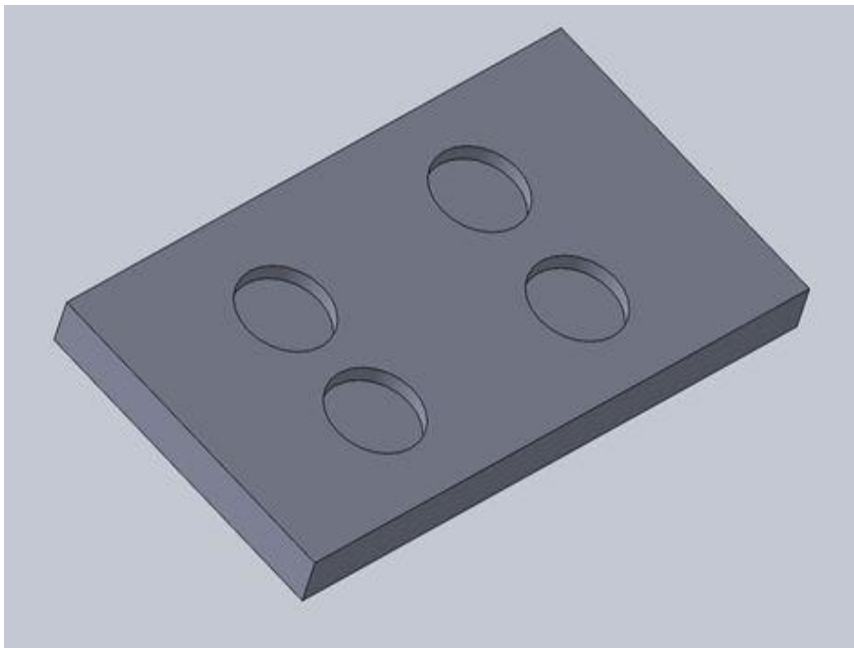


PLATE 2(3D-ISOMETRIC VIEW)

3.CONCLUSION

A review of electrical discharge machining process and research work done in EDM on aluminium metal matrix composites (AMMCs) is presented in this paper. When peak current is in moderate range with low gap voltage both metal removal rate and roughness of aluminium 2024 is good for machining using the EDM. The appropriate parameters set will determine the removal rate and as well the surface roughness and exhibits a better enhanced result.

4.FUTURE SCOPE

Surface integrity is characterized by surface roughness, residual stresses, white layer, surface morphology, altered composition of the surface, corrosion resistant, mechanical properties. All the above tests are to be performed on the same material, in order to establish a relation between the parameters.

REFERENCES

- [1] Chen Yuang (1999) "Investigation of effects of cutting parameters on surface roughness in the EDM process" Vol.5, pp.1387-395
- [2] Kaminski and Capuano (2003) "Productivity and Workpiece Surface Integrity When WEDM Aerospace Alloys Using Coated Wires, Proceedings Engineering" vol.4.pp.127-129.
- [3] Mahapatra and Amar Patnaik (2001) "Influence of machining parameters on surface roughness in finish cut of EDM" vol.8.pp.695- 701.
- [4] Mustafa Ilhan Gokler and Alp Mithat Ozanozu(2005)"Choosing High Performance EDM"vol.4 pp.279.
- [5] Nagahanumaiyah et al. (2009) " An investigation on wire wear in WEDM, Journal of Materials Processing Technology" vol.3.pp.556-559.
- [6] Yeo et al. (1999) Optimization of wire electrical discharge machining (WEDM) process parameters using Taguchi method, The International Journal of Advanced Manufacturing Technology vol.5.pp.121-138.
- [7] <http://www.xactedm.com/edm-capabilities/how-edm-works/>, viewed on 23/10/2018.

Optimization of Injection Molding Process Parameters for Improvement of Tensile Strength using the Taguchi Experimental Design

Tapas Chakraborty ¹

¹ Asst. Professor, Department of Mechanical Engineering, Saroj Mohan Institute of Technology, Guptipara, Hooghly-712512, West Bengal, India.

Email: tapas260465@gmail.com

Abstract

Tensile strength is an essential parameter for improving the quality of Injection-molded products. This thesis presents an experimental investigation into the impact of input variables of plastic injection molding process on the ultimate tensile strength of High Density Polyethylene. Depending on Taguchi quality design concept, a L₁₆ mixed-level array was implemented to evaluate the S/N ratio (dB), analysis of variance (ANOVA) and the 'F' test values for detecting dominant process variables influencing the injection molding performance and product quality. The ultimate tensile strength was improved with the optimum setting of input parameters. The input parameters were Injection Pressure, Melt Temperature, Cooling Time, Mold Temperature, Injection Speed, Holding Time, and Holding Pressure. Here, the room temperature was selected as a noise factor whereas the output response was ultimate tensile strength. Based on the experimental results and through ANOVA and 'F' test values, all the control parameters were observed to be significant but the room temperature was insignificant (P value .054). Considering these significant parameters, verification of the improvement in the quality characteristics of the product has been made through confirmation test concerning the selected initial parameter setting.

Keywords: S/N ratio, Taguchi, ANOVA, F-test

1 Introduction

From the birth of Injection-molding machine in the year 1872 by the patent of John and Isaiah Hyatt, to the present time, the injection molding industry has grown rapidly with steady rate. Moreover, plastic materials are relatively cheaper and light in weight, having good mechanical properties. The uses of plastic materials are increasing rapidly in a various engineering applications due to the advancement of material science technology. Among polymer materials high density polyethylene is a recycled, eco-friendly and economical [1]. There are so many different variables which affect the injection-molding process. It is not impossible to get control of the injection molding process. Even items such as humidity and ambient temperature may also have significant or insignificant effect on the injection molding process outcome. Based on requirement, it is more practical approach to identify all of these variables and targeting those that have the greatest effect on the overall quality and cost-effectiveness of the molded product. An effectual approach of solving such a problem is to establish the relationship among controllable input variables and the process outcome and optimize the variables for a given set of conditions. The Taguchi method is very effective to deal with response influenced by several variables. This approach acts as a powerful instrument for the design of experiments, which confers a simple, effective, and methodical approach of deciding optimal process parameters. Compared to the standard approach to experimentation, Taguchi technique drastically declines the number of experimental runs that are necessary to model the response function. But traditional one factor at a time experiment is very much tedious, time consuming and even in some cases it is impossible to conduct all the experiments. In those cases, Taguchi method gives the best result with minimum cost and time. This process results in a fast and efficient bulk manufacturing process of complicated 3D parts with considerably low cost of production. However, it remains a complex process and includes various factors that can affect the quality of final product, such as materials, part and mold design, and processing parameters [2, 3]. Several works have been done in plastic injection molding research with the variation of different control process parameters. Wu and Liang used six process parameters such as mold temperature, filling pressure, melt temperature, injection speed, injection acceleration and filling time to measure their results on the weld-line width of injection-molded plastic production [4]. Tensile property of plastic is one of the most important factors in deciding the quality of plastic injection-molded products. Fung et al. worked on short glass fiber-induced polybutylene terephthalate material and observed the improvement of tensile properties of this material with the variation of injection molding process variables. They became confirmed that the strength of PBT is dependent on the thickness of the layer where fibers were systematized in the loading direction [5]. Campbell et al. investigated the influence of injection molding process parameters on the tensile and impact strength of polypropylene, and concluded that the processing parameter interactions had significant effect on the product's mechanical properties [6]. Chen, et al. studied the result of processing factors

including melt temperature, mold temperature, injection speed, and packing pressure on the tensile properties of polycarbonate thin-wall parts, and concluded that the tensile strength was improved with the rise in melt temperature, mold temperature and injection speed [7]. Conversely, unfavorable combination of process variables can produce a product with poor tensile strength or lower quality. So, the fixation of appropriate set-points for the processing parameters is necessary for optimizing injection molding operations. Several methods are there which are used for controlling process parameters. Many expert systems have been used by different experimenters to assist in determining the set-points for the processing parameters to improve the mechanical strength [8-11]. But, these systems are not sufficient for situations requiring a quantitative value for the processing parameters. Another approach is to apply optimization techniques such as design of experiment methods to detect the most significant factors that offer suitable conditions for obtaining the best tensile properties. Gao et al applied novel intelligent methods with a view to selection of important process parameters for injection molding process [12]. Dr. Taguchi of Japan refined the technique intending to achieve robust product design against sources of variation. Experimental design techniques are a strong approach in product and process development and are frequently used in the engineering areas. Potential uses include product design optimization, process design development, process optimization, material selection and many others. Many researchers and experimenters gained several benefits by using the experimental techniques. In the Process development of injection molding, DOE can be used to find out the process parameters which have significant effect in the injection molding process output [13, 14]. The Taguchi Parameter Design is another technique similar to DOE. This method offers the same effectiveness as traditional DOE but with far fewer experimental runs [15]. The important first step in Taguchi's approach is the design of a matrix experiment based on an orthogonal array. Orthogonal arrays ensure unbiased estimation of the effects of various factors on the responses and form a basic feature of all Taguchi experiments. The general method for building these arrays was developed by Rao [16, 17]. Orthogonal array dictates the combination of factors and levels to be tested. Using orthogonal arrays, pro a huge amount of data about the effects of many processing parameters can be acquired from comparatively fewer experimenters [18, 19]. Experimenters can simultaneously optimize quality, mechanical properties, and cycle time by decreasing the number of experiments. Many research studies of recent era have proven that the Taguchi Parameter Design is effective in setting the optimum processing parameters in injection molding to obtain good tensile or impact strength, weld line strength and better product quality [20, 21]. Zhu, et al. also optimized the process parameters of PIM by Taguchi method and found out the maximum tensile strength of General Purpose Polystyrene (GPS). He selected mixed a level array for his experimentation [22]. In another work Tang et al studied the effects of the process parameters to minimize the warpage problem in the injection moulding process employing Taguchi experimental design. [23]. Hussin et al and Sanap et al conducted optimization for warpage problem. Here, the melt temperature was observed to be the most significant factor on warpage defect [23,24,25]. Puzari et al and Sreedharan et al in their study optimized to control percent defects and shrinkage defects respectively by using Taguchi experimental design. The melt temperature was detected to be the most significant factor [26, 27]. Singh et al studied the shrinkage effect of polypropylene and optimized the factors by Taguchi approach [28]. Abohashima et al in their work perceived the injection pressure and baking pressure as the most significant factors on partial filling defect of molten material [29]. In optimization of input parameters in injection molding for minimizing of short shot Mold closing speed was detected as the most significant factor [30].

Several past research papers have explored that how the injection molding processing parameters of Plastic Injection-Molding process affect the tensile properties of different plastic materials such as short glass fiber-reinforced Polybutylene Terephthalate, Polypropylene, Polycarbonate thin wall parts, General Purpose Polystyrene. This paper employed Taguchi Parameter Design to systematically investigate the influence of injection molding processing parameters and optimized them to maximize the ultimate tensile strength of HDPE.

2 Experimental Procedure

High density polyethylene (HDPE) plastic granules (grade-M6007L) made by Haldia Petrochemicals Ltd. (HPL) were used in Injection molding for this experiment. The experiment was performed in Advanced Research Development Centre of Haldia Petrochemicals Ltd. A two cavity mold was used to generate dumbbell-shaped specimen for testing the ultimate tensile strength as recommended in ASTM D-638-03. An 80 ton capacity injection molding machine FERROMATIC MILACRON, Model - SIGMA 80 (shown in Figure 1) was used to produce test samples in different factor-level combinations. Room temperature was taken as the noise factor in this study. The selected control factors and the noise factor are shown below in fig 2. The starting level (before conducting the matrix experiment) was **A₂B₁C₄D₃E₁F₁G₂**. The bold lettered numbers shown in **Table 1** indicate the starting factor-level combination. These factor levels define the experimental region or the region of interest. The best combined setting for each parameter was determined so that the ultimate tensile

strength was maximum. The experiment was conducted based on L_{16} Mixed Level Array given in **Table 2 & Table 3**. It consists of sixteen individual experiments corresponding to sixteen individual rows. The seven columns of the matrix represent the seven factors as indicated in the **Table 2**. The entries in the matrix represent the level of the factors. Thus experiment 1 was conducted with each factor at the first levels. Similarly the setting of experiment 3 is $A_1 B_3 C_3 D_3 E_2 F_1 G_2$. The temperature 30°C was selected to stimulate normal working condition and 20°C to stimulate lower-temperature working condition. During experiment at least 20 minutes was given to each processing condition to be stable. Five samples were collected in each run and three samples of defect less (without any blow holes, flash, distorted, short shot) were collected separately for ultimate tensile strength testing. Next the ultimate tensile strength was found out for each specimen separately. The samples were tested in a Lloyd tensile tester (Model – EZ20KN of XLC series) at the laboratory of Science College & University (Calcutta University) following the ASTM standard test method (ASTM D638-03, type IV), grip length = 65 mm, speed 50mm/min (shown in Fig. 5) and the results were recorded accordingly.



Figure 1: Automatic Injection moulding machine FERROMATIC MILACRON

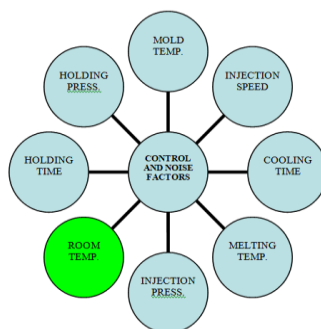


Figure 2: Control and Noise Factors



Figure 3: Samples produced



Figure 4: Samples in the mold

2.1 Control Factors, Noise Factor and their Levels

The control factors such as injection pressure, melt temperature, cooling time and mold temperature were at four levels and injection speed, holding time and holding pressure at two levels. Room temperature was selected as the noise factor in this study. A temperature of 30°C was selected to simulate normal working condition and 20°C for lower temperature working condition. The control factors and noise factor along with their levels are provided in the Table 1

| FACTOR | LEVELS | | | |
|--|-------------|-----------|-----------|-----------|
| | 1 | 2 | 3 | 4 |
| A = Injection pressure (bar) | 30 | 35 | 40 | 45 |
| B = Melt temperature ($^{\circ}\text{C}$) | 225 | 230 | 235 | 240 |
| C = Cooling time (sec.) | 27 | 30 | 33 | 36 |
| D = Mold Temperature ($^{\circ}\text{C}$) | 31 | 32 | 33 | 34 |
| E = Injection speed (mm/s) | 50 | 55 | - | - |
| F = Holding time (sec.) | 0.35 | 0.45 | - | - |
| G = Holding pressure (bar) | 20 | 25 | - | - |
| Noise factor/room temperature ($^{\circ}\text{C}$) | 20 | 30 | - | - |

Table 1: HDPE seven control factors, noise factor and their settings

2.2 L₁₆ Mixed Level Orthogonal Array and Factor Assignment

MINITAB software has been used for the design of this orthogonal array (mixed level). The L₁₆ mixed level orthogonal array has been used for the Taguchi experimental design. The minimum numbers (**sixteen**) of experimental runs have been selected.

Table 2: L₁₆ Orthogonal Array Assignment

| Inner Control Factor Array | | | | | | | |
|----------------------------|---|---|---|---|---|---|---|
| Run | A | B | C | D | E | F | G |
| 1 | 1 | 1 | 1 | 1 | 1 | 1 | 1 |
| 2 | 1 | 2 | 2 | 2 | 1 | 2 | 2 |
| 3 | 1 | 3 | 3 | 3 | 2 | 1 | 2 |
| 4 | 1 | 4 | 4 | 4 | 2 | 2 | 1 |
| 5 | 2 | 1 | 2 | 1 | 2 | 2 | 1 |
| 6 | 2 | 2 | 1 | 2 | 2 | 1 | 2 |
| 7 | 2 | 3 | 4 | 4 | 1 | 2 | 2 |
| 8 | 2 | 4 | 3 | 3 | 1 | 1 | 1 |
| 9 | 3 | 1 | 3 | 4 | 1 | 2 | 2 |
| 10 | 3 | 2 | 4 | 3 | 1 | 1 | 1 |
| 11 | 3 | 3 | 1 | 2 | 2 | 2 | 1 |
| 12 | 3 | 4 | 2 | 1 | 2 | 1 | 2 |
| 13 | 4 | 1 | 4 | 2 | 2 | 1 | 2 |
| 14 | 4 | 2 | 3 | 1 | 2 | 2 | 1 |
| 15 | 4 | 3 | 2 | 4 | 1 | 1 | 1 |
| 16 | 4 | 4 | 1 | 3 | 1 | 2 | 2 |

Mixed Level and Factor

2.3 Design

Experimental

| Run No. | Inner Control Factor Array | | | | | | | Noise factor | |
|---------|----------------------------|-----------------|---------------------|------------------|-------------------|----------------------|--------------------|-----------------|----|
| | Injection Pressure (bar) | Melt Temp. (°C) | Cooling Time (sec.) | Mould Temp. (°C) | Inj. Speed (mm/s) | Holdin g Time (sec.) | Holdin g Pr. (bar) | Room Temp. (°C) | |
| | A | B | C | D | E | F | G | | |
| 1. | 30 | 225 | 27 | 31 | 50 | 0.35 | 20 | 20 | 30 |
| 2. | 30 | 230 | 30 | 32 | 50 | 0.45 | 25 | | |
| 3. | 30 | 235 | 33 | 33 | 55 | 0.35 | 25 | | |
| 4. | 30 | 240 | 36 | 34 | 55 | 0.45 | 20 | | |
| 5. | 35 | 225 | 30 | 31 | 55 | 0.45 | 20 | | |
| 6. | 35 | 230 | 27 | 32 | 55 | 0.35 | 25 | | |
| 7. | 35 | 235 | 36 | 34 | 50 | 0.45 | 25 | | |
| 8. | 35 | 240 | 33 | 33 | 50 | 0.35 | 20 | | |
| 9. | 40 | 225 | 33 | 34 | 50 | 0.45 | 25 | | |
| 10. | 40 | 230 | 36 | 33 | 50 | 0.35 | 20 | | |
| 11. | 40 | 235 | 27 | 32 | 55 | 0.45 | 20 | | |
| 12. | 40 | 240 | 30 | 31 | 55 | 0.35 | 25 | | |
| 13. | 45 | 225 | 36 | 32 | 55 | 0.35 | 25 | | |
| 14. | 45 | 230 | 33 | 31 | 55 | 0.45 | 20 | | |
| 15. | 45 | 235 | 30 | 34 | 50 | 0.35 | 20 | | |
| 16. | 45 | 240 | 27 | 33 | 50 | 0.45 | 25 | | |

Table 3: Injection Molding Experimental Design

3 Results and Analysis

The goal of the experiment is to establish the optimum setting of parameters for Injection Molding Process to increase the ultimate tensile strength. The experimental data have been analyzed using the statistical MINITAB 13 software. Here Taguchi's larger-the-better criterion has been considered.

3.1 Analysis of Signal to Noise Ratio

The result for each experimental run separately for each individual temperature was evaluated. Mean of the two replicates for each experimental run was estimated and then S/N ratio for each mean was evaluated which have been shown.

| Inner Control Factor Array | | | | | | | Outer Noise Array | | | | |
|----------------------------|---|---|---|---|---|---|-------------------|--------------------------|--------------------------|----------------|-----------|
| Run | A | B | C | D | E | F | G | Temperature | | Average UTS | S/N ratio |
| | | | | | | | | UTS at 30 ^o C | UTS at 20 ^o C | | |
| | | | | | | | | In psi | In psi | In psi | In dB |
| 1 | 1 | 1 | 1 | 1 | 1 | 1 | 1 | 2983.4 | 2799.1 | 2891.25 | 69.2085 |
| 2 | 1 | 2 | 2 | 2 | 1 | 2 | 2 | 2968.6 | 2746.6 | 2857.60 | 69.1004 |
| 3 | 1 | 3 | 3 | 3 | 2 | 1 | 2 | 2988.9 | 2748.4 | 2868.65 | 69.1307 |
| 4 | 1 | 4 | 4 | 4 | 2 | 2 | 1 | 3020.3 | 2749.6 | 2884.95 | 69.1741 |
| 5 | 2 | 1 | 2 | 1 | 2 | 2 | 1 | 2730.1 | 2776.5 | 2753.30 | 68.7961 |
| 6 | 2 | 2 | 1 | 2 | 2 | 1 | 2 | 2648.5 | 2783.1 | 2715.80 | 68.6700 |
| 7 | 2 | 3 | 4 | 4 | 1 | 2 | 2 | 2918.7 | 2757.8 | 2838.25 | 69.0505 |
| 8 | 2 | 4 | 3 | 3 | 1 | 1 | 1 | 2703.8 | 2766.3 | 2735.05 | 68.7376 |
| 9 | 3 | 1 | 3 | 4 | 1 | 2 | 2 | 2854.8 | 2818.2 | 2836.50 | 69.0551 |
| 10 | 3 | 2 | 4 | 3 | 1 | 1 | 1 | 2874.2 | 2852.1 | 2863.15 | 69.1367 |
| 11 | 3 | 3 | 1 | 2 | 2 | 2 | 1 | 2807.6 | 2812.2 | 2809.90 | 68.9738 |
| 12 | 3 | 4 | 2 | 1 | 2 | 1 | 2 | 2820.9 | 2821.3 | 2821.10 | 69.0084 |
| 13 | 4 | 1 | 4 | 2 | 2 | 1 | 2 | 2792.7 | 2867.6 | 2830.15 | 69.0339 |
| 14 | 4 | 2 | 3 | 1 | 2 | 2 | 1 | 2955.7 | 2860.2 | 2907.95 | 69.2682 |
| 15 | 4 | 3 | 2 | 4 | 1 | 1 | 1 | 2878.5 | 2821.1 | 2849.80 | 69.0950 |
| 16 | 4 | 4 | 1 | 3 | 1 | 2 | 2 | 2791.4 | 2815.5 | 2803.45 | 68.9536 |

Table 4: Modified L₁₆ orthogonal array

3.2 Individual Factor Effects

For the performance analysis of injection molding, higher tensile strength of the material is desired and larger-the-better criterion has been applied for obtaining the optimal parameter setting. The results of mean response variable effects and S/N ratio effects for all seven factors at different levels along with the difference between the highest and the lowest level and their ranks respectively are shown in Table 5 and Table 6. The relation of the individual factor effects at each level has been shown by graphical plots in Figure 6.

| Level | A | B | C | D | E | F | G |
|-------|---------|---------|---------|---------|---------|---------|---------|
| 1 | 2875.61 | 2827.80 | 2805.10 | 2843.40 | 2834.38 | 2821.87 | 2836.92 |
| 2 | 2760.60 | 2836.12 | 2820.45 | 2803.36 | 2823.98 | 2836.49 | 2821.44 |
| 3 | 2832.66 | 2841.65 | 2837.04 | 2817.58 | | | |
| 4 | 2847.84 | 2811.14 | 2854.12 | 2852.38 | | | |
| Delta | 115.01 | 30.51 | 49.02 | 49.01 | 10.41 | 14.62 | 15.48 |
| Rank | 1 | 4 | 2 | 3 | 7 | 6 | 5 |

Table 5: Response Table for Means

Table

| Level | A | B | C | D | E | F | G |
|-------|---------|---------|---------|---------|---------|---------|---------|
| 1 | 69.1534 | 69.0234 | 68.9515 | 69.0703 | 69.0422 | 69.0026 | 69.0487 |
| 2 | 68.8136 | 69.0438 | 69.0000 | 68.9445 | 69.0069 | 69.0465 | 69.0003 |
| 3 | 69.0435 | 69.0625 | 69.0479 | 68.9896 | | | |
| 4 | 69.0837 | 68.9684 | 69.0988 | 69.0937 | | | |
| Delta | 0.3398 | 0.0941 | 0.1473 | 0.1492 | 0.0353 | 0.0439 | 0.0484 |
| Rank | 1 | 4 | 3 | 2 | 7 | 6 | 5 |

6:

Response Table for Signal to Noise Ratios (Larger is better)

3.3 Main Effect plots:

Figure 6 shows the effect of each of the seven control factors on tensile strength changes at different levels. Figure 6 & 7 explain the best levels to be chosen as optimal process parameters for both larger-the-better stress and the ideal S/N ratio, which we desire to be as large as possible.

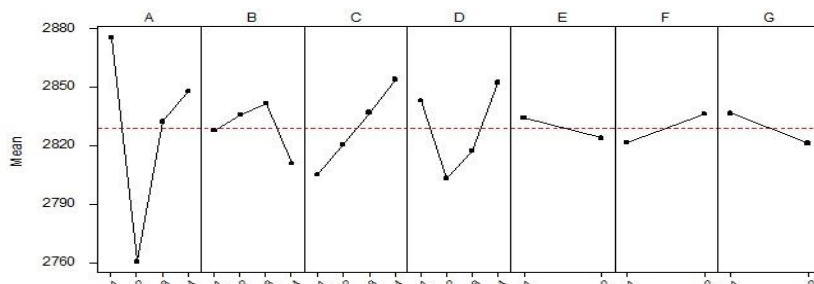


Figure 6: Main Effects Plot for Means

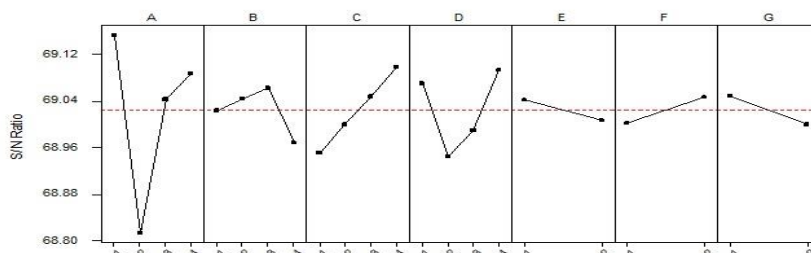


Figure 7: Main Effects Plot for S/N Ratios

The optimal process parameter settings from this Taguchi Parameter Design experiment was determined from figure 6. and figure 7. Since there was no conflict found in fig.6 and fig.7 between tensile strength and S/N ratio, the optimal combination of all the factors is A1-B3-C4-D4-E1-F2-G1.

3.4 Analysis of Variance (ANOVA) for control factors and noise factor

Analysis of variance (ANOVA) is an important step for parametric optimization by Taguchi method. So, ANOVA table was formed to check the significance of the process parameters. The table reveals that all the factors are significant at 95% confidence level. It is observed that the P values (Table-7) for all the factors are below 0.05. This means that all these parameters have significant influence on the tensile strength.

| Source | DF | Sum of squares | Variance | F- Ratio | % contribution | P value |
|----------------|----|----------------|------------|----------|----------------|---------|
| A | 3 | 0.26179704 | .08726568 | 136.843 | 62.343 | 0.0000 |
| B | 3 | 0.01985964 | .00661988 | 10.381 | 4.729 | 0.0005 |
| C | 3 | 0.0479892 | .0159964 | 25.084 | 11.428 | 0.0000 |
| D | 3 | 0.05801716 | .019339053 | 30.326 | 13.816 | 0.0000 |
| E | 1 | 0.0049844 | .0049844 | 7.816 | 1.187 | 0.0129 |
| F | 1 | 0.00770888 | .00770888 | 12.088 | 1.836 | 0.0031 |
| G | 1 | 0.00937024 | .00937024 | 14.694 | 2.232 | 0.0015 |
| Residual Error | 16 | 0.01020328 | .000637705 | | | |
| Total | 31 | 0.41992984 | | | | |

Table 7: ANOVA table for control factors

| Source | DF | SS | MS | F | P |
|--------|----|--------|-------|------|-------|
| Temp. | 1 | 27760 | 27760 | 4.04 | 0.054 |
| Error | 30 | 206328 | 6878 | | |
| Total | 31 | 234088 | | | |

Table 8: ANOVA table for noise factor

The Table-8 shows the F value for room temperature (noise factor). The P value was detected slightly greater than 0.05 (with 95% confidence). So, the noise-factor had no significant effect on tensile strength. Thus, the small effect of room temperature may be ignored.

3.5 Additive Equation

The predicted value can be approximated by the following additive equation.

$$Y_{\text{predicted}} = M + (y_A - M) + (y_B - M) + (y_C - M) + \dots + (y_G - M)$$

Where M is the overall average response and $y_A, y_B, y_C, y_D, y_E, y_F, y_G$ are the factor effects for factor A,B,C,D,E,F,G respectively corresponding to the optimum levels.

$Y_{\text{predicted}}$ value was obtained 2956.47 psi

3.6 Verification Experiment

Sixteen specimens were collected using the optimal combined setting of the control factors. The experiment was conducted at a room temperature 30°C because room temperature does not significantly affect the results. The results of the verification experiment are shown below in Table 9. The individual tensile strength σ , the overall mean value M of tensile strength, Overall standard deviation S.D was evaluated by using MINITAB software. The mean of UTS = 2970.5 (psi) and standard deviation = 110.12 Since the optimum configuration bestows the mean value close to the predicted result, the verification test is concluded successful. So, the prediction model is successful and there are no significant interactions among the control factors.

| | | | | | | | | |
|--------------|--------|--------|--------|--------|--------|--------|--------|--------|
| Specimen No. | 1 | 2 | 3 | 4 | 5 | 6 | 7 | 8 |
| UTS (psi) | 2842.6 | 2978.4 | 3032.8 | 2830.2 | 2952.6 | 3136.0 | 3088.8 | 3172.4 |
| Specimen No. | 9 | 10 | 11 | 12 | 13 | 14 | 15 | 16 |
| UTS (psi) | 2992.8 | 2888.4 | 2946.2 | 2776.0 | 3010.8 | 2890.0 | 3042.4 | 2948.2 |

Table-9 Verification Test results

| Level | $A_3B_1C_3D_4E_1F_2G_2$ (at initial factor setting) | Predicted value $A_1B_3C_4D_4E_1F_2G_1$ (at optimal setting) | Experimented value $A_1B_3C_4D_4E_1F_2G_1$ (at optimal setting) |
|------------------------|---|---|--|
| Tensile Strength (psi) | 2836.50 | 2956.47 | 2970.5 |
| S/N ratio | 69.0551 | | 69.4566 |

Table 10: Validation Experiment

Improvement of tensile strength = $(2970.5 - 2836.50) = 134$ psi
 Hence, % improvement = $(134.0 / 2836.50) \times 100 = 4.724\%$

Comparing the results between prediction and verification run from the optimal combined setting of factors, it is cleared that the strongest tensile strength samples can be produced by using Taguchi Parameter Design.

For 95% confidence interval confidence limits are

$$\begin{aligned} & \text{Mean} \pm t_{.025} \times (SD/\sqrt{n}) \\ & = 2970.5 \pm 2.13 \times 110.12/4 \\ & = 2970.5 \pm 58.64 \end{aligned}$$

So, UL = 3029.14 psi

LL = 2911.86 psi

Degree of Freedom (DF) = $(n-1) = (16-1) = 15$

Where n = number of replicates, SD= standard deviation UL = Upper limit,
LL = Lower limit

From the tables of t distribution, we find for 15 DF the percentage points t are respectively. $t_{.025} = 2.13$
So, the predicted value 2956.47 psi exists within the confidence limits.

4 Conclusions

- It was observed from the Table 4 that lower room temperature has increased the tensile strength data in some of the experimental runs and also reduced in some cases. So, it is ensured that the room temperature (noise factor) had insignificant effect on the response data for all the control factors.
- Mean response variable effects and S/N ratio effects for all seven factors at different levels are shown in Table 5 and Table 6 respectively. Figure 6 and figure 7 exhibit their effects. The optimal combination of all the factors obtained is A1-B3-C4-D4-E1-F2-G1.
- Table 7 shows that all the control factors are significant at 95% confidence level.
- Table 8 also shows that the room temperature had insignificant effect on response data. F test for the noise-factor of room temperature ensured this result. The P – value was evaluated slightly more than 0.05 (with 95% confidence level). So, the small effect of room temperature was ignored.
- Figure 6 shows that tensile strength increases with the increase of cooling time and holding time. Gradual increase of cooling time from level 1 to level 4 (27 sec. to 36 sec.) can produce the strongest specimen. Decreasing of injection pressure and mold temperature from level 1 to 2, decreases tensile strength, then increases with tensile strength from level 2 to 4. Melt temperature increases with tensile strength from level 1 to 3, then decreases. Injection speed and Holding pressure decreases with tensile strength from level 1 to 2. The statistical analysis showed that Injection pressure, Cooling time and Mold temperature are highly significant to tensile strength.

Acknowledgement

I would like to express my deep sense of gratitude to Prof. Samit Kr. Roy and Mr. Sujoy Debnath, Polymer Science and Engineering Department, Science College and University, Kolkata, for constant encouragement for the successful completion of this thesis and allowing me to work in their laboratory. I am taking this opportunity to express my gratitude and hearty thanks to Dr. Rajkumar Dutta, General manager, HDPE and Dr. Arup Chakraborty, General Manager, Polypropylene and Mr. Susanta Pai, Injection Moulding Machine Operator, ARDC, Haldia Petrochemicals Ltd., Kolkata for their valuable suggestions and allowing me to conduct the experiment in their organization. I am also thankful to Dr. Nilambar Mangal and Dr. Sanjoy Roy, Research and Development, Nicco Cables Ltd., Kolkata for their assistance, guidance and whole hearted support to conduct experiment in Haldia Petrochemicals Ltd.

References:

1. G. Scott, *Polymers and the Environment: Polymers in modern life*. The Royal Society of Chemistry, Cambridge, 1999, doi:10.1039/9781847551726-00001
2. Total Petrochemicals USA, INC., Technical Bulletin, Injection Molding.
3. W. He, Y.F Zhang, K.S. Lee, J.Y.H. Fuh, and A.Y.C.Nee, “Automated Process Parameter Resetting for Injection Molding: A Fuzzy-Neuro Approach,” *Journal of Intelligent Manufacturing*, Vol. 9, pp.17-27, 1998,
4. C H. Wu, and W J. Liang, “Effects of Geometry and Injection-Molding Parameters on Weld-line Strength,” *Polymer Engineering and Science*, 45(7), 1021-1030, 2005.
5. C P. Fung, J R Hwang and C.Hsu, “The effect of Injection Molding Process Parameters on the Tensile Properties of Short Glass Fiber- Reinforced PBT,” *Polymer-plastics Technology and Engineering*, Vol.42, No. 1, pp. 45-63, 2003.
6. G A. Campbell, S.E. Campbell, M. Bullwinkel, J. Savoka, L. Ragona, and C.Moiser, “Effect of Oil Additives and Injection Molding Process Parameters on the Tensile and Impact Energy of Polypropylene.” *Proceedings, 59th Annual Technical Conference of the Society of Plastic Engineers*, Vol. 1, pp.466 – 470, 2001.

7. S. C. Chen, H.S. Peng, L.T. Huang and M.S.Chung, "Investigations of the Tensile Properties on Polycarbonate Thin-Wall Injection Molded Parts," *Journal of Reinforced Plastics and Composites*, Vol.22, No. 5, pp. 479-494, 2003.
8. J. L. Wu, S. J. Chen and R. Malloy, "Development of an on-Line Cavity Pressure-Based Expert System for Injection Molding Process," *Proceedings from the Annual Technological Conference of the Society of Plastic Engineers*, Vol.49, pp. 444-449, 1991.
9. W. He, Y. F. Zhang and K..S. Lee, "Development of Fuzzy-Neuro System for Parameter Resetting of Injection Molding," *Journal of Manufacturing Science and Engineering*, Vol.123, pp.110-118, 2001.
10. R.E. Farrell and L.Dzeskiewicz, "Expert system for Injection Molding," *Proceedings from the Annual Technological Conference of the Society of Plastic Engineers*, Vol.52, pp. 692-695, 1994.
11. G. H. Choi, K.-D. Lee, N. Chang,, S.G. Kim, "Optimization of Process Parameters of Injection Molding with Neural Network Application in a Process Stimulation Environment," *Annals of the CIRP*, Vol.43, No. 1, pp.449-452, 1994.
12. H. Gao, Y. Zhang,. X. Zhou and D. Li, "ZIntelligent methods for the process parameter determination of plastic injection molding," *Frontiers of mechanical engineering*, 13: 85-95, 2018.
13. J.S. Antony, Warwood, K.Fernandes, and H.Rowlands,"Process Optimization Using Taguchi Methods of Experimental Design," *Work Study*, 50 (2), 2001.
14. D.C. Montgomery, *Design and Analysis of Experiments*, John Wiley and Sons, Fourth Edition, 1997.
15. L. Ealey, *Quality by Design: Taguchi Methods and U.S. Industry*, Dearborn, Michigan: ASI Press, 1998.
16. N. Logothetis, H.P. Wynn, *Quality through Design: Experimental Design, Of-line Quality Control and Taguchi's Contributions*, Clarendon press, Oxford, 1989.
17. C.R.Rao, "Factorial Experiments Derivable from Combinatorial Arrangements of Arrays," *Journal of the Royal Statistical Society, Series B*, 9: 128-139, 1947.
18. W.Y. Fowlkes and C.M. Creveling, *Engineering Methods for Robust Product Design: Using Taguchi Methods in Technology and Product Development*, Reading, Massachusetts: Addison-Wesley Publishing Co., 1995.
19. C.R. Hicks, *Fundamental Concepts in the Design of Experiments*, Holt-Saunders International Editions, 3rd Edition, 1983.
20. S. J. Liu, J. Y. Wu and J. H. Chang, "Design of Experiments to optimize the Weld Line Strength in Injection Molded Thermoplastics," *Proceedings*, 59th Annual Technical Conference of the Society of Plastic Engineers, Vol.1, pp.508-511, 2001.
21. J.C. Viana, P.Kearney and A. N. Cunha, "Improving Impact Strength of Injection Molded Plates through Molding Conditions optimization: A Design of Experiments Approach," *Proceedings*, 56th Annual Technical Conference of the Society of Plastic Engineers, Vol.1, pp. 646-650, 1998.
22. J. Zhu, J. C Chen and E.D Kirby, "Tensile Strength and Optimisation of Injection Molding Processing Parameters Using the Taguchi Method," *The International Journal of Modern Engineering*, Vol.4, No.2, 2004.
23. S. H. Tang, Y. J. Tan, S. M. Sapuan and S. Sulaiman, "The use of Taguchi method in the design of plastic injection mould for reducing warpage," *J material Process technology*, 182 (1-3):418-426, 2007.
24. R. Hussin, R. M. Saad, R. Hussin and I. M. Dawi, "An optimization of plastic injection molding parameters using Taguchi optimization method," *Asian transactions on engg.*, 2(5) : 74-80, 2012.
25. P. Sanap, H. M. Dharmadhikari and A. J. Keche, "Optimization of plastic moulding by reducing warpage with the application of Taguchi optimization technique & addition of ribs in washing machine wash lid component," *IOSR J of mech. & civil engg.*, 13(5): 61-68, 2016.
26. G. V. Puzari and V. R. Naik, "Process parameters optimization for development of defect free injection molded component," *Int J Science Technology and Management*, 4(10): 56-62, 2015.
27. J. Sreedharan and A. K. Jeevanantham, Analysis of shrinkages in ABS injection molding parts for automobile applications, *Materials Today: Proceedings*, International Conference on Materials Manufacturing and Modelling , 2018.
28. T. Singh, M. P. Singh and M. M. Alam, "Taguchi and ANOVA analysis of shrinkage of Injection moulded polypropylene Component," *Int J Scientific & engg. research*, 5(7): 750-756, 2014.
29. H. S. Abohashima, M. F. Aly, A. Mohib and H. A. Attia, "Minimization of defects percentage in injection molding process using design of experiments," *Industrial engg. & management*, 2015, DOI: 10.4172/2169-0316.1000179
30. L. D. Mahajan and P. N. Ulhe, "Analysis of injection molding process to reduced defects (Short-shot)," *Int J Engg. Technol & Mgmt. Res*, 5(6):113-119, 2018.

A Review of Multifunctional Composite Materials With Their Applications

T.Elangovan¹, K.saravanan².

Assistant Professor, Department of mechanical Engineering, St.Anne's College of Engineering And Technology, Panruti

Associate Professor, Department of mechanical Engineering, St.Anne's College of Engineering And Technology, Panruti

Abstract

Multifunctional composite materials and structures (MFCMS) is remarkably increased in the last decades. Multifunctional composite materials and structures review paper is done by many journal publications related to this title. Multifunctional composite means 'made of two or more materials that perform two or more functions in a manner that is constructive to the overall purpose of the structure' where there is no differentiation between structural or non-structural functions. Many of the recent developments focused on the applications of MFCMS such as High Altitude Airship (HAA), morphing aircraft wings, energy harvesting, nonmaterial's & nanostructures, smart structures, coupled field analysis, biomechanical etc. This paper also focused on the nonlinear mechanics of MFCMS because High Altitude Airship type of problems comes under geometrically and materially nonlinear case, so to analyze this type of problems one of the effective method called Variational Asymptotic Method is used. (VAM) is a powerful mathematical approach to simplify the process of finding stationary points for a described functional by taking an advantage of small parameters. Thus, approximate stationary points in the functional can be utilized to obtain the original functional. This paper concludes with a discussion of future scope and difficulties in design and analysis of multifunctional composite structures.

Keywords: Multifunctional composite materials and structures, Variational Asymptotic Method, Carbon fiber reinforced polymer

1. Introduction

Multifunctional composite structures are meant for performing a variety of functions apart from the primary functions. Multifunctional materials (MFS), Multifunctional composites (MFC) and Multifunctional structures (MFS) are the sub branches of Multifunctional material systems (MFMS) [1]. The need of excess components is eliminated by combining of one or more functional capabilities of subsystems with the total structure so that the total system mass and volume can be reduced and improves the overall efficiency of the system [2]. In the recent years the need of multifunctional materials and structures is increased in many fields due to its multiple structural functions or both structural and non-structural functions [3], Fig [1] represents the functional capabilities of Multi- functional composite materials and structures as shown in below Table 1

Table 1. Illustration of MFM, MFC and MFS [1, 2]

| source | MFM | MFC | MFS |
|-----------|-----------------------|---|--|
| Examples | PZT | Epoxy/Carbon fiber | Shark denticles |
| Functions | Sensing and actuation | Mechanical strength and electrical conductivity | Reduce the drag by providing anti-biofouling |

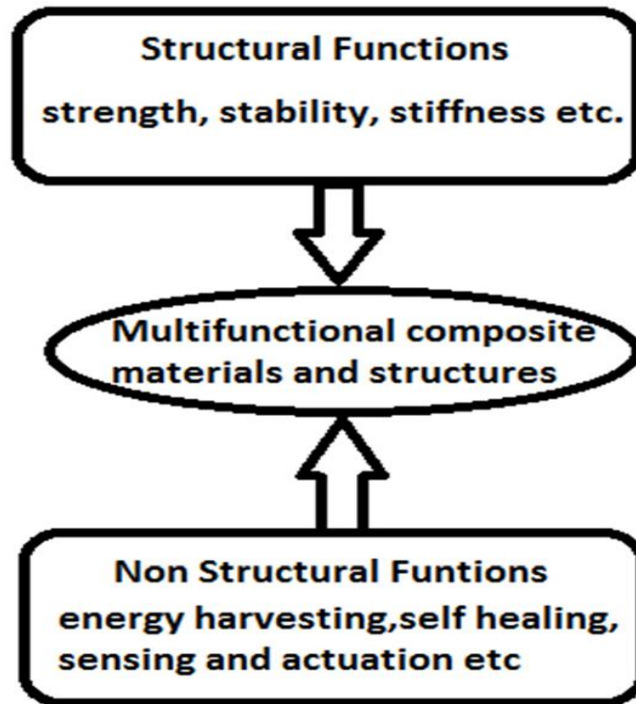


Fig 1. Structural and non-structural functions of MFCMS

2. Design and fabrication

The design of MFCMS is a challenging task because of its complex structures whereas the selection of materials for the fabrication and the process of fabrication plays very important role to get the required functional capabilities, by preserving the initial structural functions and adding the additional non-structural functions [3]. The design of multifunctional materials and structures

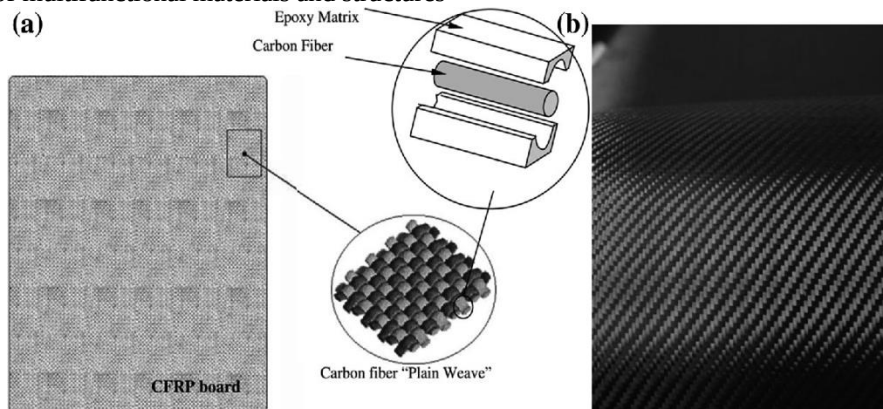


Fig.2 Carbon fiber reinforced polymer (CFRP) composite material

M. Akbar and J. L. Curiel-Sosa[5] presented the piezoelectric embedded aircraft wing box used to harvest the energy for large scale structures by the dynamic bending responses. This design is implemented on jet aircraft wing box which is having piezo electric layer stacked in the laminated composite. The difficulty for the structure is the weight increment by the addition of piezo layer this problem is handled by the appropriate optimization method. The result showed the improved electric power of 25.24 KW is generated for 14.5 m wing span when compared to previous literature result. M.U. Saeed, B.B. Li et al. [6] designed the micro channels which are embedded within the laminated composite structure (see Fig 3). These channels are used to store and transport or circulate the fluid to the desired location. The micro channel exhibits non-structural functions such as cooling and sensing. The design of micro channel developed by two methods one is by removal of solid wired within the structure to form the hollow holes and the other one is non-removal of hollow tubes. The non-

removable hollow tubes results showed good fracture resistance or in simple words fracture is deviated from the hollow micro channel when compared to the othertype of design process (see Fig 4).

P. Ladpli, R. Nardari et al. [7]presented the embedded lithium ion battery materials in CERP (composite reinforced polymers) which maximizes the utilization of material when compared to standard lithium ion pouch cells (see Fig 5). R. D. Farahani, M. Dub  et al. [8] reviewed the 3-D printing techniques for multifunctional composites which include the methods such as micro stereo lithography, extrusion based, powder based and inject printing techniques by using metal and carbon based nanomaterials (see Fig 6 (a) (b)). These methods improved the printability and functional capabilities such as electromechanical sensitivity, mechanical strength and electrical conductivity.

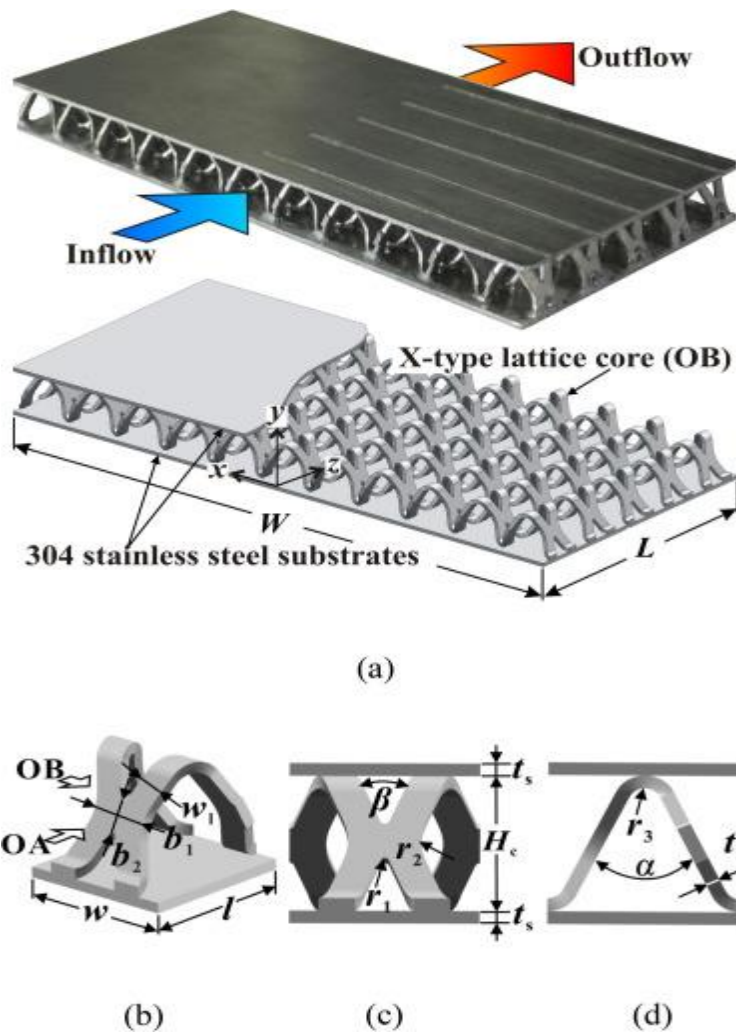


Fig.3 convective heat transfer in a lightweight multifunctional sandwich panel

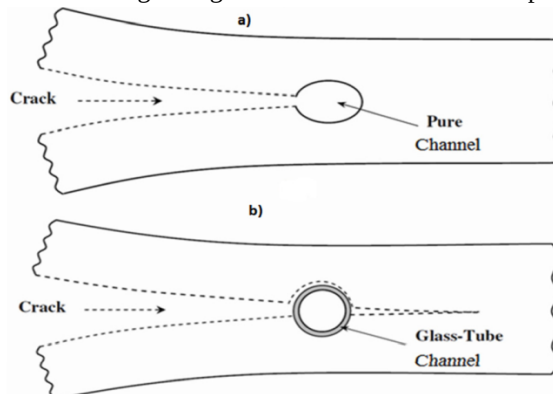


Fig 4.a) crack tip blunting ; b) crack tip deflection [6]

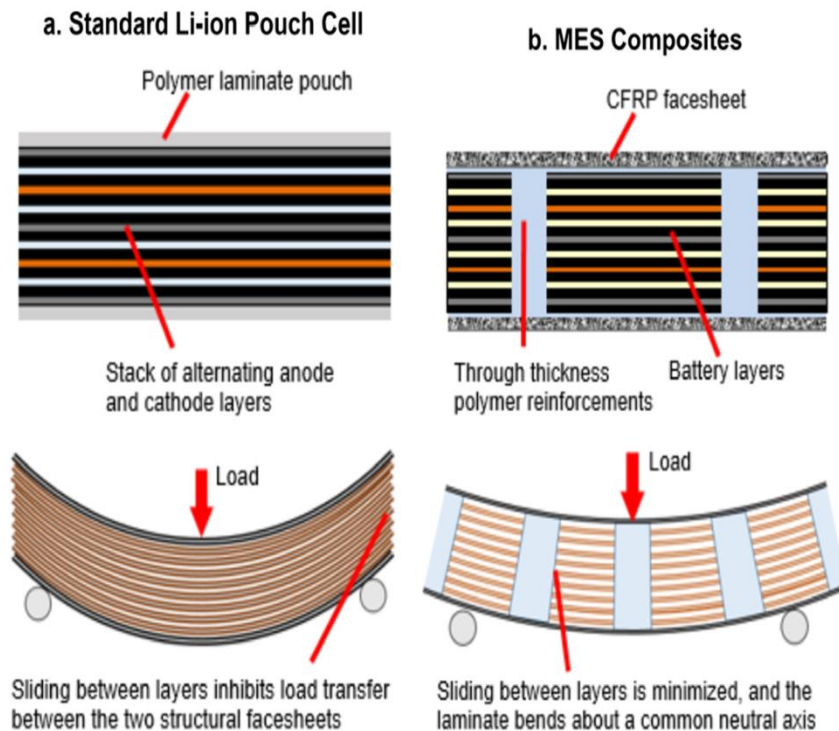


Fig 5. Comparison of standard Li-ion pouch cells with MES Composites (Multifunctional Energy Storage Composites (MES) improve the shearresistance of the battery core) [7]

C. J. C. Heath, I. P. Bond et al. [9] introduced the electronic adhesion by creating the very high potential difference in the electrodes which generates attractive force providing good attachment and exhibits good structural functions in the fibre reinforced polymer composite structures. M. Zhang, C. Hou et al. [10] presented the synthesis methods of on-pot green to fabricate interlocked graphene Prussian blue composites (PB) which are useful for biosensors and super capacitor electrodes as high performance materials. PB composite material is used because of its low toxic nature and low cost which are suitable for the large scale industries. Graphene oxide is reduced to control the toxicity by using iron and glucose as co-reducing agents. M. H. Gabr and K. Uzawa [11] described the usage of sub- micro titanium/alumina (TIAL) particle as reinforcement which can produce the polyamide multifunctional composites. The properties vary with the concentration of alumina/titanium, by incorporating TIAL the strength and flexural modulus are improved by 22% and 75% respectively.

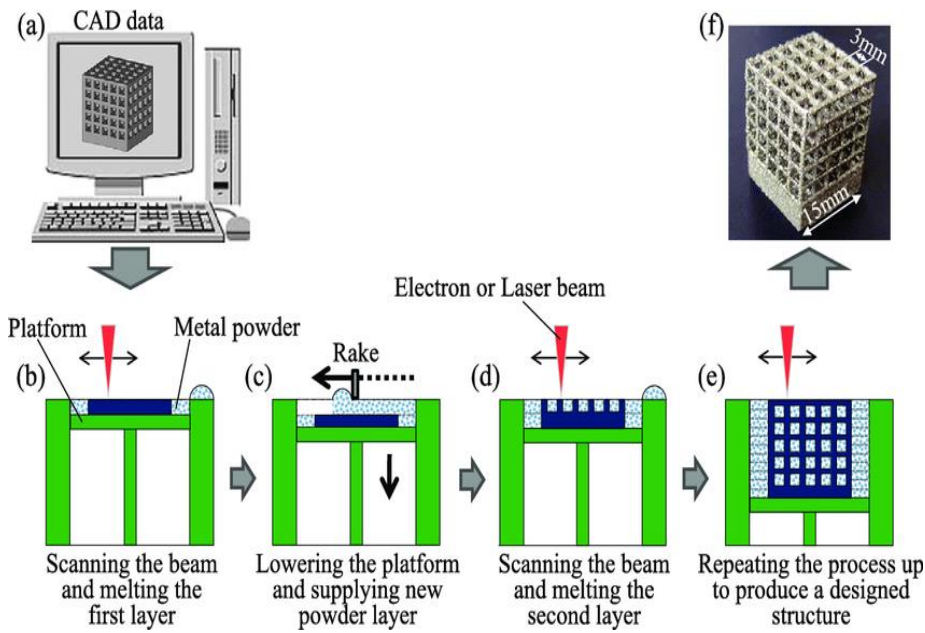
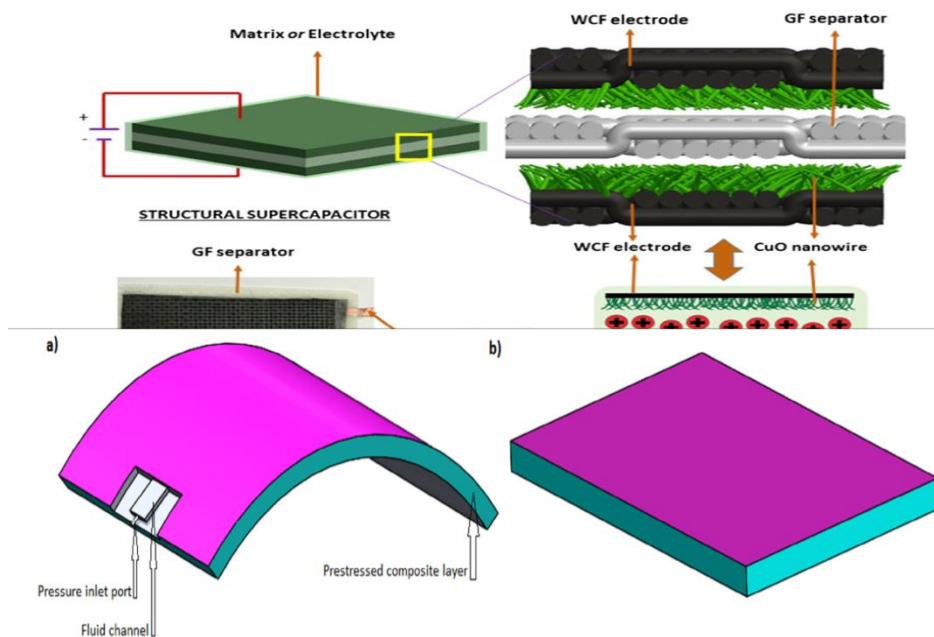


Fig 6. Powder-bed technology through layer-by-layer fabrication of a 3D structure

3. Structural and non-structural functions

M. H. Malakooti, B. A. Patterson et al. [12] reported the zinc oxide (Zno) nanowires growth on the surface of a woven aramid fabric which are aligned vertically. Zno provides the significant improvement in elastic modulus and tensile strength of the composites by 34.3% and 18.4% respectively. The large deformation of nanowires leads to electric charge accumulation between the carbon electrodes and creates a potential difference. B. K. Deka, A. Hazarika et al. [13] described the growing of CuO (copper oxide) nanowires on the surface of woven carbon fiber (WCF) to improve the capacitance (as a supercapacitor) and mechanical properties (see Fig 7). The specific capacitance of CuO-WCF based super capacitor is increased drastically when compared to base WCF based supercapacitor.



V. S. C. Chillara, L. M. Headings [14] introduced the Multifunctional laminated composite structures having pressurized fluid layer as one of its laminae (see Fig 8 (a) (b)). This layer is used to change the shape of

structure from curved geometry to flat by applying pressure on pre-stress fluid layer. This methodology is used in aircraft morphing wings and automobiles by incorporating the morphing panels into the vehicle body to reduce the additional components of total structure there by decreasing the mass and volume of the composite structure.

Fig 7.(a) Unactuated state of a fluidic pre-stressed composite; (b) actuated shape of the composite when the fluid channels are pressurized. (EMC- elastomeric matrix composite)

D. J. Hartl, G. J. Frank et al. [15] described the embedded microvascular networks as multifunctional structure which exhibits additional functions such as self-healing, thermal management. The performance depends on the space between channels, channel orientation, aspect ratio of channel cross section etc. P. B. Kaul, M. F. P. Bifano et al. [16] introduced the tin capped multi walled carbon nanotube array composites aligned vertically, which are used for thermal management. Thermal conductivity is increased by the vertically aligned carbon nanotube when compared to normal thermal interface materials as shown in below Table 2.

4. Mechanics of multi-functional composite materials and structures

S. Agrawal and D. Harursamath et al. [23] introduced the variational asymptotic method (VAM) to solve coupled problem of multi layered piezo composite beam. VAM is a novel tool to solve various multi physics problems it simplifies the problem and solves the problem without considering ad-hoc assumptions. VAM provides way to get asymptotically correct solution by taking the advantage of small parameters. VAM breaks down the problem of 3-D

elastic beam into 2-D nonlinear cross sectional analysis and 1-D nonlinear analysis. Total energy of elastic body is integrated over cross section to obtain 1-D behavior then 1-D generalized variables are solved by using geometrically exact equilibrium equations of motion and 1-D kinematic equations which are obtained by substituting of constitutive law from cross sectional analysis in to 1-D analysis.

S. Banerjee and S. Roy [24] Presented the analysis of piezoelectric cantilever sensor under static and dynamic load by using variational asymptotic method (VAM). Electro mechanical response is captured effectively under static and dynamic load of piezo sensor. This study is carried out on a single layer of piezo sensor and double layer of piezo sensor. VAM results showed a good agreement with ABAQUS 3-D simulation results.

K. Chau Leet al. [25] developed a first order 2-D theory for functionally graded piezo electric shells (FGP) by using VAM. Dimensional reduction is carried out by using small parameters. The electro static fields of FGP shells vary through the thickness and differ essentially from homogeneous piezoelectric shells. S. Sawarkar, S. Pendhari et al. [26] analyzed the displacement and stress for piezoelectric laminate by using new approach with the mathematical integration through the thickness direction which is free from all assumptions and the model is mixed with first order differential equations.

V. M. Sreehari, L. J. George et al. [27] analyzed bending and buckling of smart composite plate by using inverse hyperbolic shear deformation theory (IHSDT). Hamilton principle is used to form the governing equations of laminated plate which is perfectly bonded with piezoelectric material on the top and bottom surface of the structure. MATLAB program is developed based on the finite element formulation. The effectiveness of piezo patch attached at center instead of piezo layers are presented.

Li, Eric, Zhongpu Zhanget al. [28] demonstrated the SFEM (smoothed finite element method) to analyze multifunctional structural composite by asymptotic homogenization technique. SFEM computational efficiency is high compared to conventional FEM. M. N. Rao, S. Tarun et al. [29] presented a shell element for nonlinear analysis of piezo electric laminated composite plates and shells. Second order nonlinear constitutive equations are used in the variational approach for finite element model. The analysis showed the difference between linear and nonlinear constitutive models when the applied electric field is large. Shell four-node piezo linear element (SH4PL) and shell four-node piezo nonlinear element (SH4NPL) are used to analyze the structure and compared results showed that transverse bending and twisting deflections are better predicted by the present nonlinear theory. M. C. Ray [30] developed the governing equations and boundary conditions for the smart nano beams which are integrated with flexo-electric nano actuator layer.

5. Characteristics

H. Kim and M. Gonzalez et al. [31] demonstrated the use of mimic printed circuit board which carries both structural load and electric current within the system. The failure modes and fatigue life are measured experimentally to investigate the capability of these embedded systems within the composite structures. Dog bone model with copper traces specimens are used to measure the fatigue life which is a function of loading level. S. Yoo, E. Kandare et al. [32] reviewed the thermo-physical properties of polymer based composite materials (PCM). Thermal conductivity and thermal expansion coefficients are determined. The inter-laminar properties of these laminated composites which are fabricated with micro-PCM and epoxy showed very good physical and thermal properties. Thermal conductivity varies with loading values of PCM. Crystallization properties are determined by using differential scanning calorimeter (DSC).

L. de Castro Folgueras et al. [33] investigated the electromagnetic properties of multilayered multi-functional composites which are used as conductors or radiation absorbing materials. The electromagnetic properties are evaluated by using waveguide technique in the X-band (8.2 to 12.4 HZ) which measures the reflection of microwave radiation and 90 to 99% energy of the incident radiation is being absorbed in the multi-functional material made up of nonwoven glass fiber pre-impregnated with formulation based carbon block.

6. Applications

Y. Ding, J. Zhu et al. [44] demonstrated the use of multifunctional materials in nanocomposites. Graphene nanoribbons are introduced into polyurethane sponges which are used in supercapacitor applications. X. W. Yin, L. F. Cheng et al. [45] presented the ceramic matrix composites which are useful in the application of hot engine structures, electronic devices and exhibits multifunctionalities such as crack healing, electromagnetic shielding, self lubrication and energy absorption. Perez-Rosado, Ariel et al. [46] introduced the robotic birds or flapping wing aerial vehicles. The wings deform while flapping and generate necessary aerodynamic forces which are required to flight. The solar cells used to increase the payload capacity by harvesting the electrical energy. This type of mechanism is one of the advanced technology used in aerospace application.

J. Wilson et al. [47] developed the concept of multifunctional foot in athletic moment. The structure design helpful to bear impact load and provides flexible movements. S. Seyedin, J. M. Razal et al. [48] introduced the elastomeric fibers which are electrically conductive. This type of structures or materials are used in intelligent textiles which is a strain sensing component of the structure.

A. D. Alessandro et al. [53] presented nano-modified materials that cover a wide range of applications such as radiant systems, structural members, floors, geothermal plies etc. C. Wang, Y. Ding et al. [54] introduced polypyrrole foam materials which has excellent thermal, electrical and optical properties and used in various applications such as sensors, supercapacitors. S. Torquato et al. [55] Stated biological materials are unique nature's multifunctional materials. The different optimization techniques are used to maximize the transport of heat and electricity and it is useful in electrical and thermal applications. Baum, Thomas C. et al. [56] developed Egyptian axe dipole (EAD) antenna using sandwich structure which improved the performance in the structural applications. Iannone, Michele et al. [57] described the multifunctional materials by using Fin-mechanics, the improved functionalities such as self-diagnostic capability, process ability and environment effects are useful in aircraft applications. S. Kumar et al. [58] presented the polymer nano composites as multifunctional materials by improving the electrical conductivity and modulus of elasticity. These materials are used in bio medical applications.

7. Conclusion

This paper reviewed the multifunctional composite materials and structures which includes different structural designs, new fabrication processes, multi structural functions, nonstructural functions, characteristics and mechanics of laminated structures by using different methods (Example VAM, SFEM). This paper also presented the different type of multifunctional materials such as Nano materials, polymer based composites, carbon/epoxy fiber composites. Addition of functional and non-structural functions improves the efficiency of the system and reduces the mass and volume of the total structure. The characteristics allow us to analyze the output results of the system. The future research on multifunctional structures and multifunctional composite materials is not limited to particular application such as automobile, aircraft structures because the requirement of multifunctional components are also more in the bio-mechanical, bio-medical, and space applications. In the space applications solar energy utilization, electromagnetic shielding and reduction of mass and volume of the

system are the major additional functions which take the research further in this field. The journals published for experimental work and design work of multifunctional area are less compared to the analytical work. So there is a need to work on the mechanics of multifunctional composite materials and structures because based on the analytical results we can interpret the experimental work as well as the numerical simulation work and also useful in the optimization of the multifunctional system based on the required application.

References

- [1] A. D. B. L. Ferreira, P. R. O. Nóvoa, and A. T. Marques, "Multifunctional Material Systems: A state-of-the-art review," *Compos. Struct.*, 2016.
- [2] K. K. Sairajan, G. S. Aglietti, and K. M. Mani, "A review of multifunctional structure technology for aerospace applications," *Acta Astronaut.*, vol. 120, pp. 30–42, 2016.
R. F. Gibson, "A review of recent research on mechanics of multifunctional composite materials and structures," *Compos. Struct.*, vol. 92, no. 12, pp. 2793–2810, 2010
- [3] Y. Xiao, W. Qiao, H. Fukuda, and H. Hatta, "The effect of embedded devices on structural integrity of composite laminates," *Compos. Struct.*, vol. 153, pp. 21–29, 2016.
- [4] M. Akbar and J. L. Curiel-Sosa, "Piezoelectric energy harvester composite under dynamic bending with implementation to aircraft wingbox structure," *Compos. Struct.*, vol. 153, pp. 193–203, 2016.
- [5] M. U. Saeed, B. B. Li, and Z.-F. Chen, "Mechanical effects of microchannels on fiber-reinforced composite structure," *Compos. Struct.*, vol. 154, pp. 129–141, 2016.
- [6] P. Ladpli, R. Nardari, R. Rewari, H. Liu, M. Slater, K. Kepler, Y. Wang, F. Kopsaftopoulos, and F. K. Chang, "Multifunctional energy storage composites – Design, fabrication, and experimental characterization," *Proc. ASME 2016 Power Energy Conf.*, no. June 26–30, pp. 1–9, 2016.
- [7] R. D. Farahani, M. Dubé, and D. Therriault, "Three-Dimensional Printing of Multifunctional Nanocomposites: Manufacturing Techniques and Applications," *Adv. Mater.*, pp. 5794–5821, 2016.
- [8] C. J. C. Heath, I. P. Bond, and K. D. Potter, "Electrostatic adhesion for added functionality of composite structures," *Smart Mater. Struct.*, vol. 25, no. 2, p. 025016, 2016.
- [10] M. Zhang, C. Hou, A. Halder, J. Ulstrup, and Q. Chi, "Interlocked graphene-Prussian blue hybrid composites enable multifunctional electrochemical applications," *Biosens. Bioelectron.*, pp. 1–8, 2015.
- [11] M. H. Gabr and K. Uzawa, "Novel multifunctional polyamide composites produced by incorporation of AlTi sub-microparticles," *J. Compos. Mater.*, no. Icc, 2016.
- [12] M. H. Malakooti, B. A. Patterson, H.-S. Hwang, and H. A. Sodano, "ZnO nanowire interfaces for high strength multifunctional composites with embedded energy harvesting," *Energy Environ. Sci.*, vol. 2, no. 9, pp. 634–643, 2016.
- [13] B. K. Deka, A. Hazarika, J. Kim, Y. Bin Park, and H. W. Park, "Multifunctional CuO nanowire embodied structural supercapacitor based on woven carbon fiber/ionic liquid-polyester resin," *Compos. Part A Appl. Sci. Manuf.*, vol. 87, pp. 256–262, 2016.
- [14] V. S. C. Chillara, L. M. Headings, and M. J. Dapino, "Multifunctional Composites with Intrinsic Pressure Actuation and Prestress for Morphing Structures," *Compos. Struct.*, vol. 157, pp. 265–274, 2016.
- [15] D. J. Hartl, G. J. Frank, and J. W. Baur, "Effects of microchannels on the mechanical performance of multifunctional composite laminates with unidirectional laminae," *Compos. Struct.*, vol. 143, pp. 242–254, 2016.
- [16] P. B. Kaul, M. F. P. Bifano, and V. Prakash, "Multifunctional carbon nanotube–epoxy composites for thermal energy management," *J. Compos. Mater.*, vol. 47, no. 1, pp. 77–95, 2013.
- [17] Olawale, David O., Jin Yan, Divyesh H. Bhakta, Donovan Carey, Tarik J. Dickens, and Okenwa I. Okoli. "In pursuit of bio-inspired triboluminescent multifunctional composites," In *Mechanics of Composite and Multifunctional Materials, Volume 7*, pp. 55–65, 2016.
- [18] D. Micheli, A. Vricella, R. Pastore, A. Del, A. Giusti, M. Albano, M. Marchetti, F. Moglie, and V. M. Primiani, "Ballistic and electromagnetic shielding behaviour of multifunctional Kevlar fiber reinforced epoxy composites modified by carbon nanotubes," vol. 104, pp. 141–156, 2016.
- [19] J. Lou, Y. Liu, Z. Wang, D. Zhao, C. Song, J. Wu, N. Dasgupta, W. Zhang, D. Zhang, P. Tao, W. Shang, and T. Deng, "Bioinspired Multifunctional Paper-Based rGO Composites for Solar-Driven Clean Water Generation," *ACS Appl. Mater. Interfaces*, vol. 8, no. 23, pp. 14628–14636, 2016.
- [20] Y. Ito, Y. Tanabe, J. Han, T. Fujita, K. Tanigaki, and M. Chen, "Multifunctional Porous Graphene for High-Efficiency Steam Generation by Heat Localization," *Adv. Mater.*, vol. 27, no. 29, pp. 4302–4307, 2015.

- [21]Wang, Yishou, Xinlin Qing, Liang Dong, and Sourav Banerjee. "Multi-field coupled sensing network for health monitoring of composite bolted joint." In *SPIE Smart Structures and Materials Non-destructive Evaluation and Health Monitoring*, pp. 98052L-98052L. International Society for Optics and Photonics, 2016.
- [22]R. Wagner, "A Multifunctional Hot Structure Heatshield Concept for planetary entry " *20th AIAA Int. Sp. Planes Hypersonic Syst. Technol. Conf.*, no. November 2013, pp. 1–22, 2015.
- [23]S. Agrawal and D. Harursamath, "Computational Modeling of a Multi-Layered Piezo-Composite Beam Made up of MFC," no. WCCM Xi, pp. 1–7.
- [24]S. Banerjee and S. Roy, "Multiphysics analysis of an asymptotically correct piezoelectric sensor under static and dynamic load," *Int. J. Solids Struct.*, vol. 92–93, no. April, pp. 64–75, 2016.
- [25]K. Chau Le and J. H. Yi, "An asymptotically exact theory of smart sandwich shells," *Int. J. Eng. Sci.*, vol. 106, pp. 179–198, 2016.
- [26]V. M. Sreehari, L. J. George, and D. K. Maiti, "Bending and buckling analysis of smart composite plates with and without internal flaw using an inverse hyperbolic shear deformation theory," *Compos. Struct.*, vol. 138, pp. 64–74, 2016.
- [27]S. Sawarkar, S. Pendhari, and Y. Desai, "Semi-analytical solutions for static analysis of piezoelectric laminates," *Compos. Struct.*, vol. 153, pp. 242–252, 2016.
- [28]Li, Eric, Zhongpu Zhang, C. C. Chang, Shiwei Zhou, G. R. Liu, and Q. Li. "A New Homogenization Formulation for Multifunctional Composites," *International Journal of Computational Methods* 13, no. 02 (2016): 1640002.
- [29]M. N. Rao, S. Tarun, R. Schmidt, and K.-U. Schröder, "Finite element modeling and analysis of piezo-integrated composite structures under large applied electric fields," *Smart Mater. Struct.*, vol. 25, no. 5, p. 055044, 2016.
- [30]M. C. Ray, "Analysis of smart nanobeams integrated with a flexoelectric nano actuator layer," *Smart Mater. Struct.*, vol. 25, no. 5, p. 055011, 2016.

Patient Health Monitoring System in Ambulance for Accident Management using Internet of Vehicles

N. Dhavaneeswaran, A. Thiyagarajan

Abstract

Road accidents being a genuine general wellbeing challenge which builds the quantity of deadly and handicaps step by step. Accidents some of the time become a significant compromising component for living souls in which street mishap is generally unmistakable. With the expanding traffic on roads, emergency vehicle has an intense errand in taking the patient to clinic on time this prompts tolerant misfortune because of the substantial blood misfortune declining heart beat rate and so on, which prompts the reason for death likewise the truth of the matter is that Thousands of individuals are biting the dust since ambulances take excessively long to reaction to a crisis circumstance. We address this issue by proposing an answer utilizing the Internet of Things which is an advancing innovation. Here, we are associating the emergency vehicle with the IOT which has biomedical sensors like pulse rate sensor, heartbeat rate sensors, temperature sensor that will detect constantly the harmed person's health conditions and update these data to the close by clinic worker. This system helps in reducing the mortality rate caused due to road accidents by reducing the preliminary treatment time.

Keywords: *Patient monitoring system, accidents, mortality rate, Internet of Things, ambulance.*

1 Introduction

Road safety is an arising pattern these days. Road accidents is a worldwide calamity hampering the existence of millions. Consistently 414 assets lives are lost because of street mishaps. Street wellbeing mirrors the personality of an individual. After numerous street security missions and mindfulness programs, there is as yet an expansion in passings in India, positioning first in the quantity of street mishap passings across the 199 nations and representing practically 11% of the mishap related passings in the World. Not just in India, Road traffic keeps on being a significant formative issue, a general wellbeing concern, and is a main source of death and injury across the World slaughtering more than 1.35 million internationally as detailed in the Global Status report on Road Safety 2018 with 90% of these setbacks occurring in the developing nations. According to Planning Commission of India, estimated that accident results in an annual monetary loss of rupees 1 trillion, so its reduces our countries GDP by 4%.

Accidents being a real public health challenge which increases the number of fatalities day by day. The most likely reason for an individual's death in an accident is lack of the first aid provision that is because of emergency services not receiving information about accident on time. Even though, there are lot of accident preventive mechanisms, we are lagging in accident management system in automobiles. Investigation shows that in the event that we decline only 1-minute in mishap reaction time that can expand odds of saving a person's life up to 6%. So, the aim of this paper is to build a patient monitoring system in ambulance to reduce the mortality rate by sending the basic parameters of the patient from the ambulance to the hospital. This patient essential data will be useful to decrease the time taken for fundamental tests in clinics, in light of the fact that the clarification behind an individual's destruction in a disaster is nonappearance of clinical guide game plan that is a consequence of emergency organizations not tolerating information about the setback true to form.

2 Related Work

The management of accident is a very much considered region, where various analysts utilized various techniques to sort out the mishap occasion.

Alagumeenaakshi Muthiah et al proposed Maternal health monitoring System utilizing Lora Technology. The Proposed System interfaces the Maternal Monitoring System (MMS) and Traffic Monitoring System (TMS) utilizing a Lora Gateway to help the decrease in Maternal Death Rate. The MMS accessible in the rescue vehicle gauges the crucial boundaries of a maternal lady, for example, internal heat level, pressure, glucose level, beat rate and development of the baby and are conveyed to the clinic for the pre-arranging of work/crisis ward as per patient's conditions [1].

Shiny Amala et.al proposed IOT based wellbeing checking for provincial Pregnant ladies to screen the wellbeing boundary of the pregnant ladies. The proposed framework quantifies the development of embryo utilizing accelerometer sensor and boundaries like temperature, glucose level, heart beat and pulse utilizing various sensors. The deliberate boundaries are moved to cell phone through IOT [2].

Khushboo Bhagchandani et.al proposed an IOT based heart checking framework and overseeing traffic for rescue vehicle. This framework means to give an answer for the heart patients utilizing IOT and information investigation. IOT assists with gathering the information from the sensors. It investigations the information gathered from the sensors of the cardiovascular patients. In view of the information gathered from the sensors it assists with offering alarm to their family members. It additionally finds briefest way for rescue vehicle to arrive at the clinic [3].

The previously mentioned contents give a short presentation of patient checking framework. In spite of the fact that the substance and strategies were opposite among different creators, the center plan stays to be the equivalent. The strategies utilized in the previously mentioned surveys are thought about for the plan and manufacture quiet observing framework in emergency vehicle.

3 Methodology

3.1 Method of Concept Development

This framework will be founded on plan of item and its advancement techniques. The current system, working and parts were broken down with its effectiveness. The ideas of existing framework were joined together in a solitary unit for mishap recognition and the executives. The Steps in the planning stage is appeared in the fig. (1).

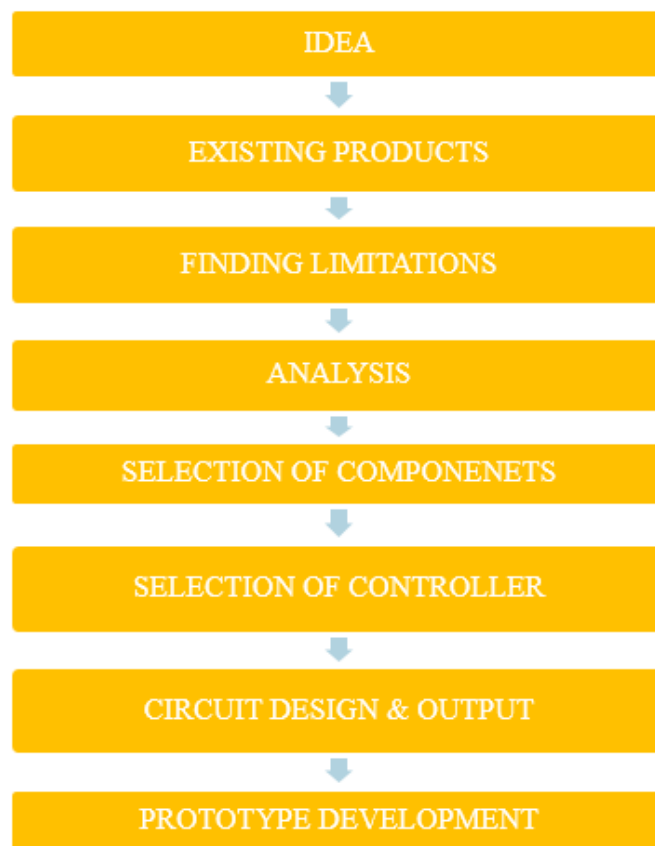


Figure 1: Method of concept development.

3.2 Accident Management System

This administration framework comprise of sensors like heartbeat oximeter (MAX30100), Temperature sensor associated with the focal microcontroller through Nodemcu ESP8266, which is loaded with the code to deliver a yield constantly with the estimations of heartbeat, oxygen level and temperature to the IP address of Nodemcu. This IP address stage will be taken care of to the site for medical clinic getting to and observing the overall usefulness of the patient while arriving at medical clinic and this will help the emergency clinic help to make earlier courses of action.

3.3 Functional Diagram of the proposed system

The block diagram of patient monitoring system in ambulance is shown in fig. (2).

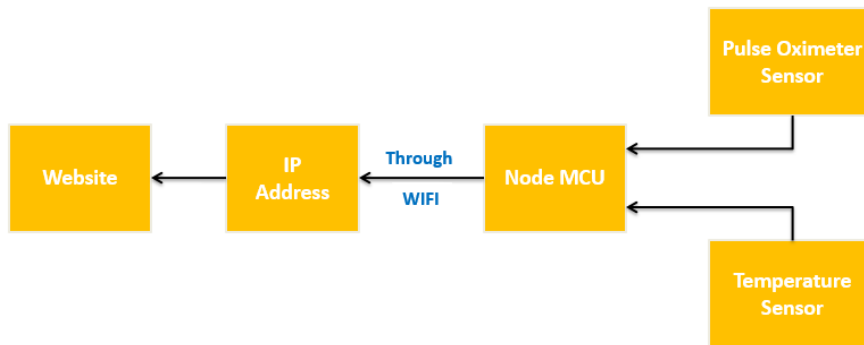


Figure 2: Block diagram of patient monitoring system

4 System Architecture and Flowchart

Fig. (3) clarifies the proposed framework engineering of the patient observing framework in emergency vehicle. After the patient is taken into the rescue vehicle, essential crucial boundaries, for example, internal heat level, blood oxygen level and heartbeat rate will be observed by the emergency clinic help from the rescue vehicle through website page. By utilizing these boundaries, emergency clinic may orchestrate treatment measure without stepping through any primer exams from the mishap casualty. So the time taken for the tests can be diminished in crisis circumstance, by this death rate caused because of street mishaps can be decreased.

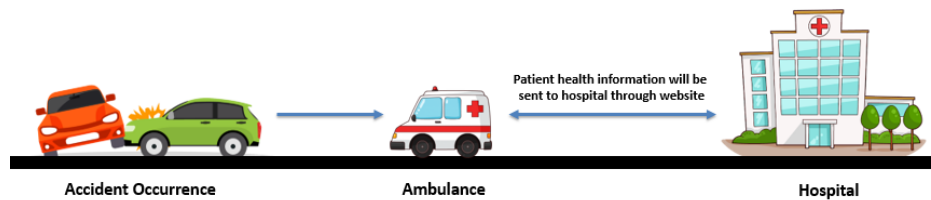


Figure 3: System architecture of the proposed system.

Flow chart of the of the proposed system is shown in Fig. (4). It explains the complete process of the system.

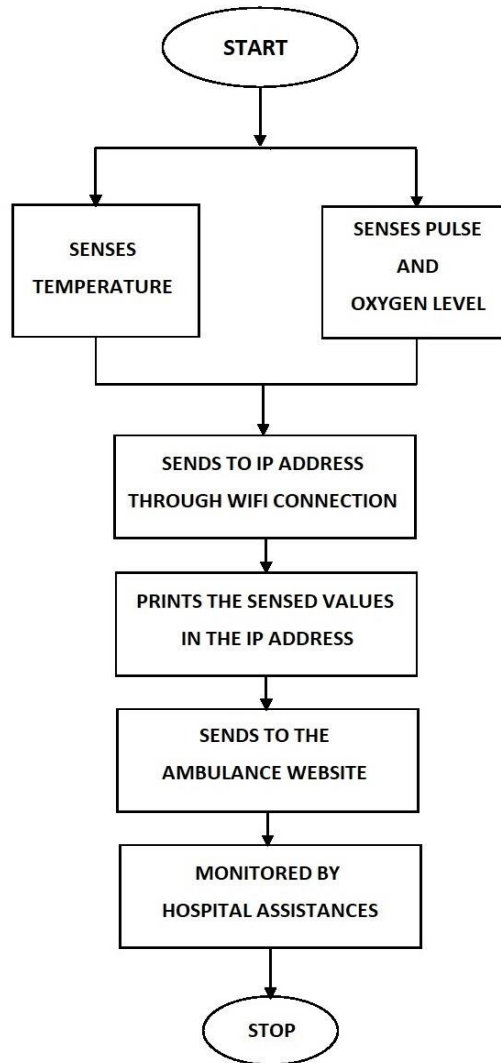


Figure 4: Flowchart of the proposed system.

5 Hardware Output

The framework is created to get the live status of the essential functionalities like temperature, beat rate, oxygen level of patients which is ship off emergency clinic reconnaissance through a particular IP address allocated for a rescue vehicle and afterward took care of to a basic site for getting to. This causes the clinic to be ready for the treatment of that tolerant. Fig. (5) shows the equipment yield of the mishap the board framework and the patient status yield is appeared in Fig. (6) and Fig. (7).

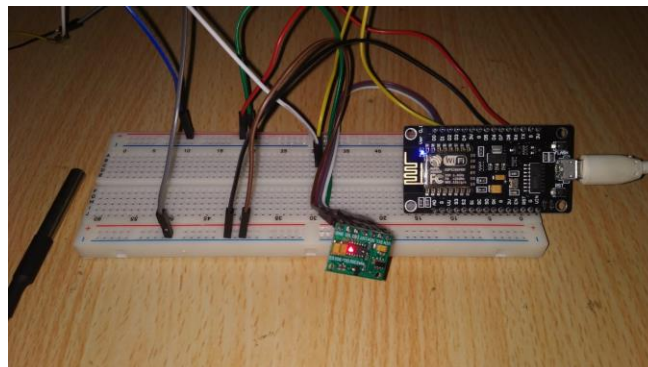


Figure 5: Hardware setup – Accident Management System.

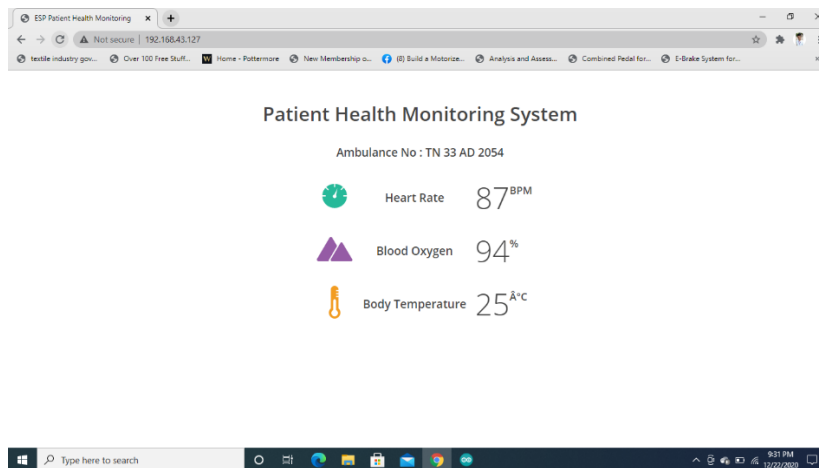


Figure 6: Patient Status in IP address.

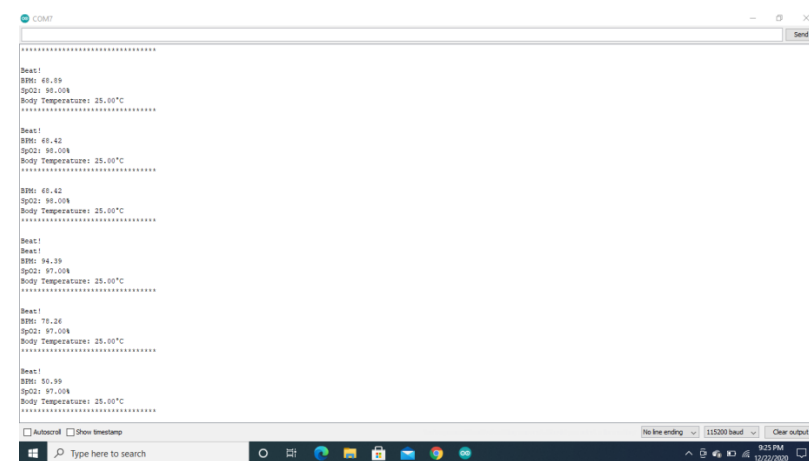


Figure 7: Arduino IDE Serial Monitor Output.

6 Conclusion

The patient checking framework can distinguish the essential boundaries like temperature, beat rate, blood oxygen level of the patient and shipped off the clinic through site to screen the overall usefulness of the patient while arriving at emergency clinic and this will help the clinic help to make earlier courses of action. The proposed framework will cause the local area to decrease the death rate coming about because of vehicle mishaps.

Numerous further upgrades can be made in the framework to improve it and effectively versatile, for example, adding traffic the board framework to diminish the vehicle traffic and this framework can be actualized through android application for adaptability. Empowering web in every single vehicle out and about can clear path for complete mechanization of vehicles and traffic. The idea of Internet of Vehicles (IoV) can be stretched out to all methods of transport having a huge effect in the manner that correspondence happens between various media of transport.

References

- [1] A. Muthiah, S. Ajitha, M. Thangam K.S., V. Vikram K., K. Kavitha and R. Marimuthu, "Maternal ehealth Monitoring System using LoRa Technology", 2019 IEEE 10th International Conference on Awareness Science and Technology (iCAST), Morioka, Japan, 2019, pp. 1-4.
- [2] ShinyAmala, S, Mythili, S, "IoT Based Health Care Monitoring System for Rural Pregnant Women", International Conference of Scientific research and Reviews, 2018, pp. 763-771.

- [3] Khushboo Bhagchandani, D. Peter Augustine, "IoT based heart monitoring and alerting system with cloud computing and managing the traffic for an ambulance in India", *International Journal of Electrical and Computer Engineering (IJECE)*, vol 9, no 6, pp. 5068-5074, 2019.
- [4] Montes, N. Tiglao, R. Ocampo, C. Festin, "Delay Based End-to-End Congestion Control for Wireless Sensor Networks", in *ICUFN 2015*, pp 497-502, 2015
- [5] Ghaffari, "Congestion control mechanisms in wireless sensor networks: A survey", in *Jour. of NW and Comp Applications*, vol. 52, pp 101–115, Mar. 2015
- [6] G. Huang, D. Chen, X. Liu, Member IEEE, "A Node Deployment Strategy for Blindness Avoiding in Wireless Sensor Network", in *IEEE COMMUNICATIONS LETTERS*, vol. 19, no. 6, pp 1005–1008, 2015.
- [7] C. Sergious, V. Vassilious, A. Paphitis, "Congestion Controlling Wireless Sensor Networks through Dynamic alternative path selection" in Elsevier, *Jour. on computer networks*, vol 75, pp 226- 238, Oct. 2014.
- [8] AliRezaee, M. Yaghmaee, "HOCA: Healthcare Aware Optimized Congestion Avoidance and control protocol for wireless sensor networks" in Elsevier, *Jour. on Network and Comp Applications*, vol 37, pp 216-228, Mar 2013.
- [9] Dattatray S. Waghole & Vivek. S. Deshpande, "Characterization of Wireless Sensor Networks for Traffic & Delay," *IEEE, International Conference on CUBE, Pune*, pp.69-72, Nov-2013.
- [10] Dattatray S. Waghole & Vivek S. Deshpande, "Reducing Delay Data Dissemination Using Mobile Sink in Wireless Sensor Networks." *IJSCE, Vol-3, Issue-1, ISSN 22312307* pp.305-308, Mar. 2013.

Impact behavior of Nano SiC reinforced AA7075 metal matrix composites, by FE simulation tests

AnilKumar kallimani S^{*1}, Chikkanna N², Thirtha Prasad³, Rukmangada⁴

¹Assistant Professor & Head of the Dept.in Mechanical Engineering. Government Engineering College
Huvinahadagali-583219, Karnataka, India

²Professor & Chairman Dept. of Aerospace & Propulsion Technology, Visvesvaraya Institute of Advanced
Technologies, VTU, Muddenahalli-562101, Karnataka India

³Associate Professor Dept. of CAE, Visvesvaraya Institute of Advanced Technologies, VTU,Muddenahalli-
562101, Karnataka India

⁴Professor & Head Dept.of Mechanical Engineering, SJCIT, Chikkaballapur, Karnataka, India

Abstract

The aluminum alloy is having one of the superior material properties which is used in different industrial sectors like aerospace, automobile and general engineering industries because of their favorable microstructure and mechanical behavior. Research shows that The Metal matrix composites of aluminum alloy reinforced with silicon carbide reinforcement have exhibited enhanced mechanical properties. In this work, Composites of aluminum alloy AA7075 reinforced with 500nm silicon carbide were fabricated by using popular method of stir casting techniques. Addition of Silicon carbide was made in weight percentage in the range of 0 to 8% respectively. Charpy Impact test was carried out for the MMC specimens. Results showed increase in energy and Toughness for the increased SiC content in the Specimens. FEM Analysis was carried out using Johnson cook material model for the MMC's, and Experimental and FEM results were compared in this work.

Keywords: 500nmSiC, AA7075, MMC's Fabrication, Charpy Impact test with FEA by using ABAQUS software, Johnson Cook Material constants

1. Introduction

Metal matrix composites are popular choice when it comes to selection of materials for structure design of Aircraft and marine,automobile applications. Lot of research has undergone and has been undergoing in the field of metal matrix composites. The experiments and results of the researchers have shown improved and enhanced Mechanical and wear properties for the reinforced metal matrix materials these metal matrix composites have been classified into fiber reinforced, particle reinforced and whisker reinforced composites. Particle reinforced metal matrix (PAMC) are popular choice for the researchers because of ease of the fabrication of samples. Reinforcements like Silicon carbide (SiC), alumina (Al₂O₃) are most commonly used reinforcements with aluminum alloys available in the series like 2XXX, 3XXX, 6 XXX & 7XXX series etc. Aluminum alloys are first choice in the field of Aircraft structure design due to their High strength and weight ratio. When these aluminum alloys are reinforced with particles it has been observed from the research that they shown better mechanical properties. Compared to as cast alloys. AA7075 is aluminum zinc alloy which is used in the landing gear struts, wing attachments, engine mountings, and also used for the Bulkheads which carry concentrated masses in the aircraft.

2. Experimental details

2.1 Materials

Present work describes the production of MMC's by using stir casting technique tensile test with FEA, analysis and density and porosity of Al7075 Aluminum alloy with reinforced with silicon carbide with %wt in the range of 0-8%. Compositions of AA7075 as shown in table 1

Table 1. Composition AA7075

| Element | Wt.% | Element | Wt% |
|-----------|------|----------|---------|
| Copper | 1.6 | Zinc | 5.5 |
| Magnesium | 2.5 | Chromium | 0.15 |
| Silicon | 0.4 | Titanium | 0.2 |
| Iron | 0.5 | aluminum | Balance |
| Manganese | 0.3 | | |

2.2 Fabrication of Composites

The MMC's were fabricated by using the stir casting techniques. Fig.1.shows the schematic of stir casting setup. And Fig.2. Shows the cast samples prepared using this method. The AA 7075 is kept into the crucible furnace and heat is supplied by using the electric heating source, when temperature reaches 600°C -750°C the AA7075 is melted in crucible then SiC Powder is poured as per the weight %. The molten metal and SiC are mixed and the mixture is stirred by a electric operated stirrer at a constant speed. Mixture is poured in to the mould and allowed to cool for few minutes. Finally the cast samples are taken out of the mould.

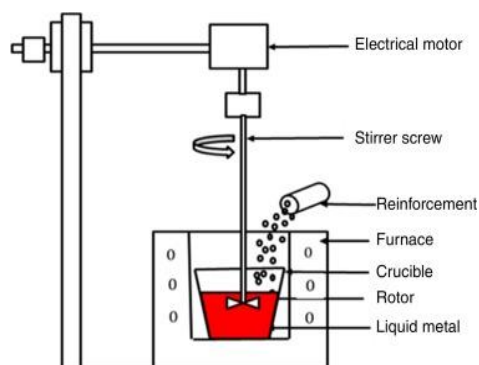


Fig.1 Stir casting set up



Fig.2.Stir cast samples

2.3 Experimental work

Stir cast samples were machined & made into different specimens as per ASTM standards to carryout mechanical tests. Before conduction of the tests the samples were tested using X-ray diffraction (XRD) peak intensities and peak positions were obtained for the 0%,2%,4%,6%,8% samples respectively from the X-ray diffractometer. Specimens for Impact testing were machined as per ASTM standards to test using Impact testing set up Fig.3,4,5&6 shows the Impact specimens and Impact testing machine.

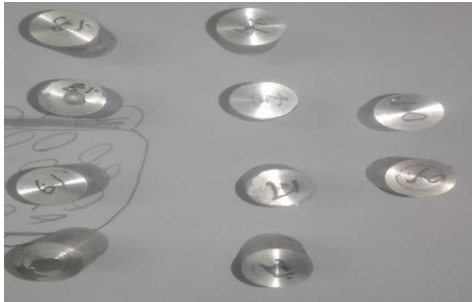


Fig.3 specimens for XRD



Fig.4 Specimens for Charpy Impact test

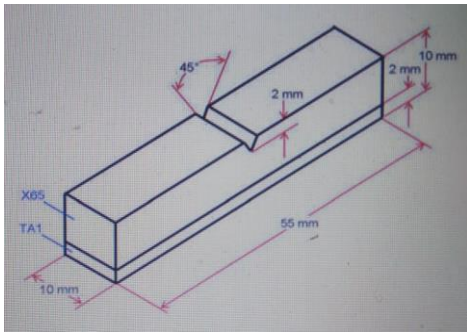


Fig.5 Charpy Impact specimen size



Fig.6 Impact testing machine

2.4 Estimation of Volume Fractions & Young's Modulus

Density, Volume fractions, Mass fractions & Young's modulus were estimated by using rule of mixture empirical relations and used for the FEM analysis.

Density of the composites is given by equation

$$\rho_c = f_m \rho_m + f_r \rho_r \quad (1)$$

Where

ρ_c = Density of the composite

ρ_m = Density of the matrix

ρ_r = Density of the matrix

M_m = Mass of matrix

M_r = Mass of reinforcement

f_m = Mass fraction of the matrix

f_r = Mass fraction of the reinforcement

The following equations were used to measure the mass fraction of matrix and reinforcement also volume fractions of SiC finally young's modulus is estimated by kerner equation

$$f_m = \frac{M_m}{(M_m + R_m)} \quad (2)$$

$$f_r = \frac{R_m}{(M_m + R_m)} \quad (3)$$

$$V_{SiC} = \frac{\frac{m_{SiC}}{\rho_{SiC}}}{\left[\frac{m_c - m_{SiC}}{\rho_{Al}}\right] + \frac{m_{SiC}}{\rho_{SiC}}} \quad (4)$$

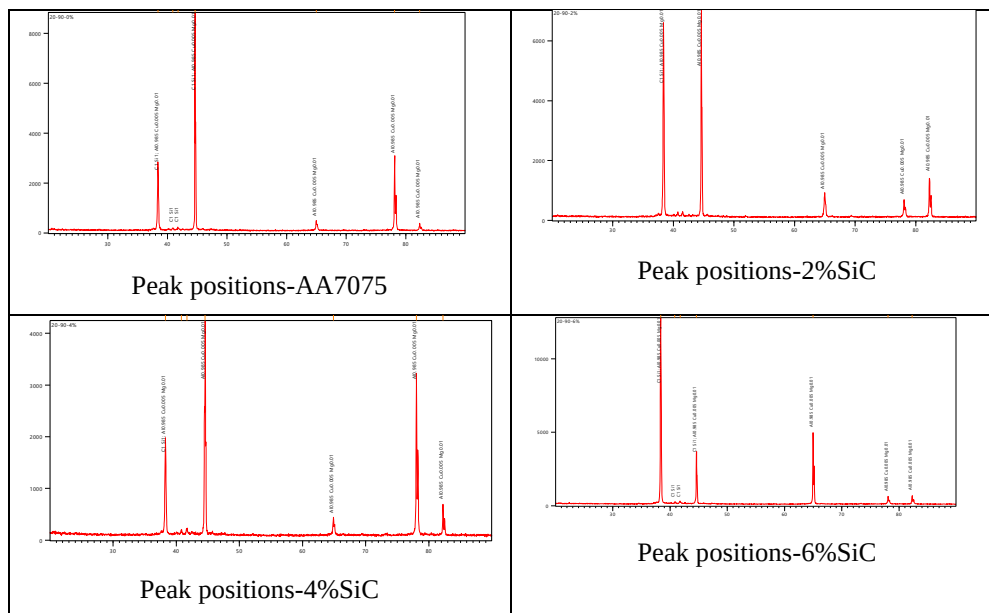
$$E_c = E_m \left[1 + \frac{v_p}{1 - v_p} \times \frac{15(1 - m_m)}{8 - 10m_m} \right] \quad (5)$$

Table 2. Young's Modulus

| S.No | MMC Samples | Young's Modulus (GPa) |
|------|----------------|-----------------------|
| 1 | $E_{as\ cast}$ | 71.7 |
| 2 | $E_{2\%SiC}$ | 74.5 |
| 3 | $E_{4\%SiC}$ | 77.3 |
| 4 | $E_{6\%SiC}$ | 80.3 |
| 5 | $E_{8\%SiC}$ | 83.4 |

These results shows that young's modulus of the MMC increases as the weight percentage of reinforcement (Silicon carbide) increases research also reveals that young's modulus linearly increases with addition of particle, whiskers, and fiber reinforcements.

2.6 XRD Analysis



XRD Patterns list and peak intensities, positions were obtained from Diffractometer system=XPERT-3.for the MMC samples. Fig (4) to Fig.(7) show the peak intensities and positions and Table.(2) to Table (6) show the corresponding

Full width half max and the spacing of the crystals XRD tests confirmed the crystallite size of the SiC and its cubic structure.

2.6 Johnson Cook Material Constants

The flow stress is defined as

$$\sigma = (A + B\varepsilon^n)(1 + C \ln \varepsilon^*)(1 - T^m) \quad (6)$$

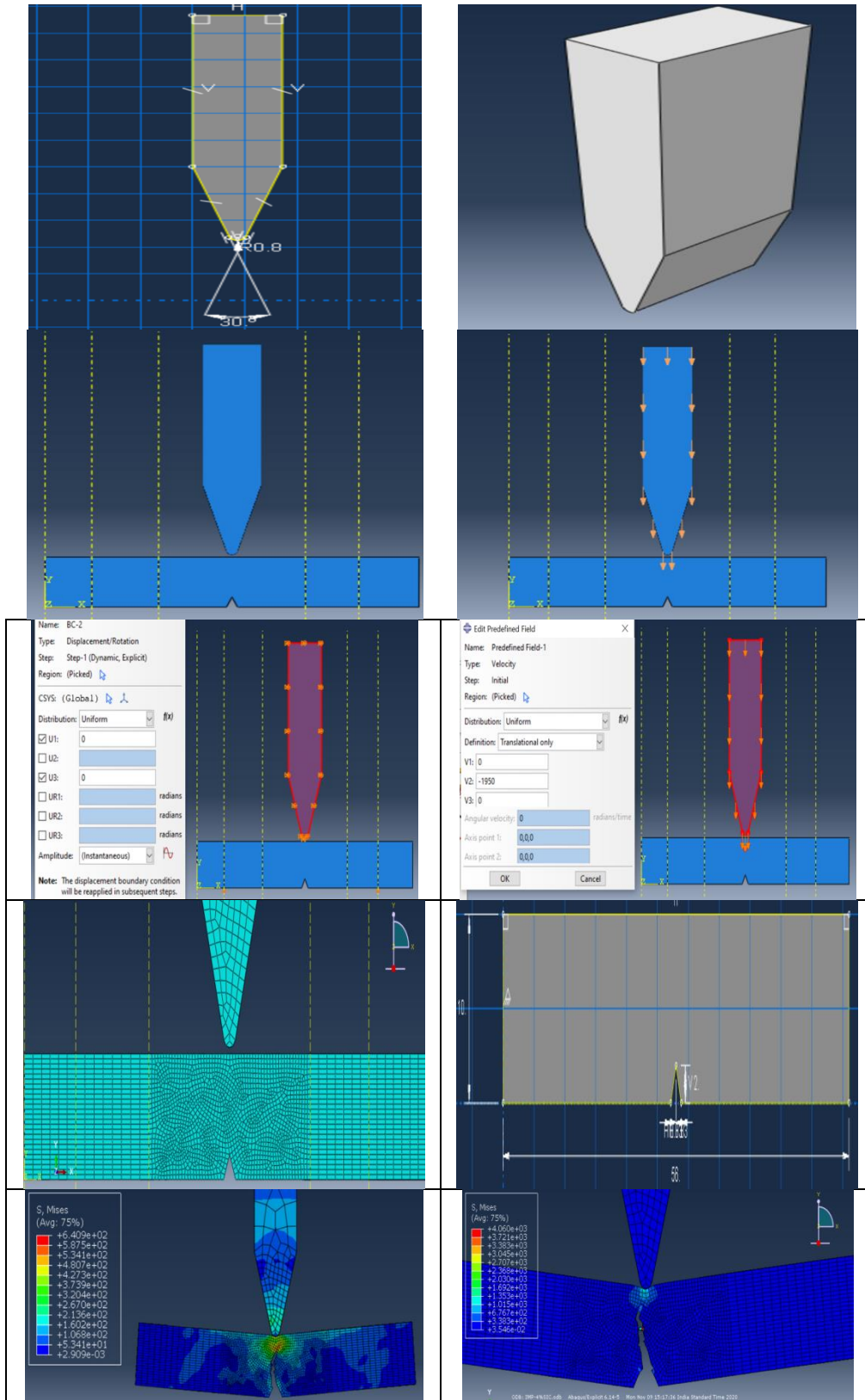
Using this all constants were obtained given in the Table.3

Table.3 Johnson cook Material constants

| %SiC | A | B | n | C |
|-------------|----------|-------------|----------|----------|
| 0% | 199.74 | 367.7855413 | 0.867 | 0.25 |
| 2% | 233.79 | 22879.58 | 1.9571 | 0.0625 |
| 4% | 252.8 | 32338.05535 | 2.0343 | 0.0625 |
| 6% | 274.14 | 63006.93 | 2.1366 | 0.0625 |
| 8% | 319.36 | 116308.3345 | 2.2168 | 0.0001 |

2.7 FEM analysis

Charpy impact test was carried out with Johnson cook material constants by using ABAQUS Impactor and the specimen model were created as per the ASTM standards and estimated young's modulus, Johnson cook material constants used to study the impact behavior. Fine Meshing was made near the Impactor Zone Hexagonal 8 Node (C3D8R) Brick elements used to mesh the model 60166 nodes were created and Total 65723 nodes were created all the details of FEM analysis shown in the below figures.



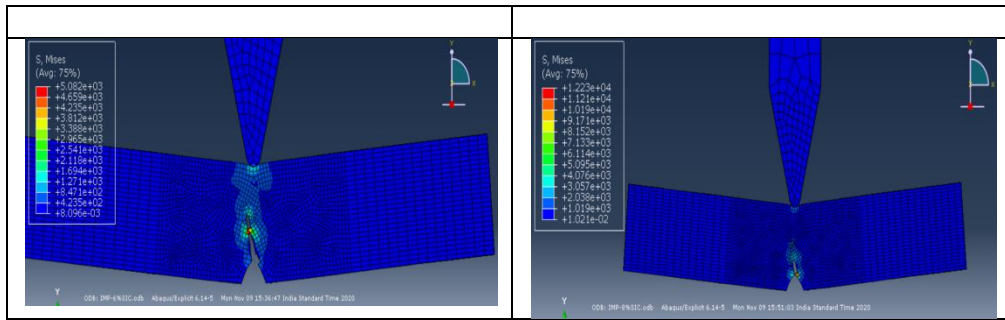


Fig.7 Meshed Model Boundary conditions FEM

2.8 Results & Discussions

Von mises stresses were obtained from the FEM results and the deformations, internal energy were also obtained which are given below.

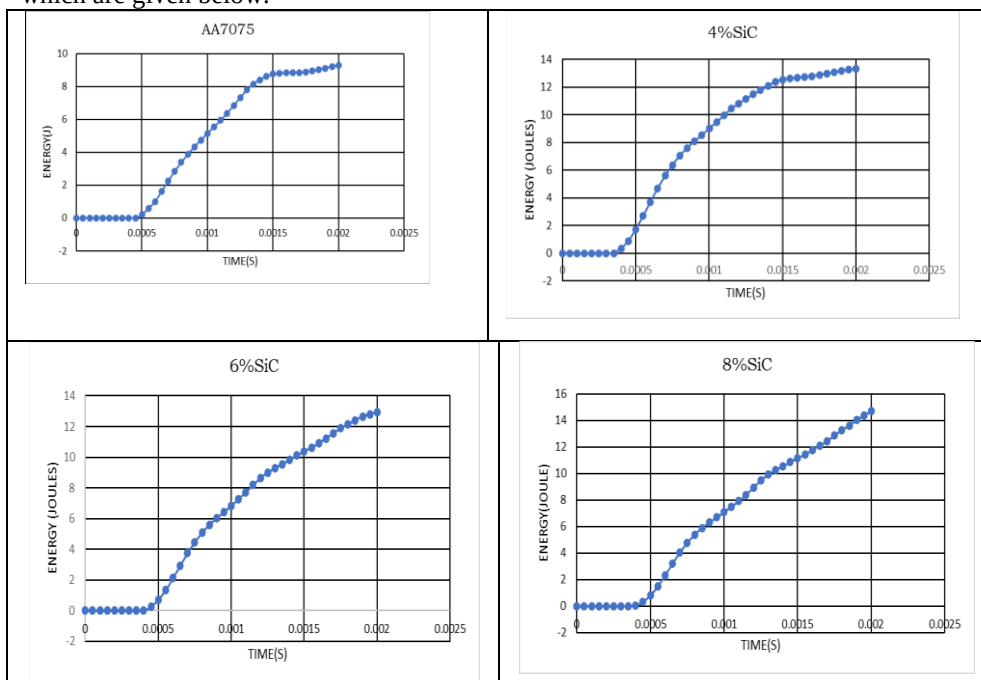


Fig.8 Energy Vs Time for all MMC's

2.8.1 Comparisons of FEM Results with Experiment results

Table.4 Result Comparison

| COMPOSITION | ENERGY(JOULE)-EXP | ENERGY(JOULE)-FEM |
|----------------|-------------------|-------------------|
| AA7075 as Cast | 9J | 9.29563 |
| 2%SiC | 10J | 11.0119 |
| 4%SiC | 13J | 13.3207 |
| 6%SiC | 13J | 12.9597 |
| 8%SiC | 14J | 14.6748 |

2.9 Conclusions

In this work Stir cast Samples of Nano SiC reinforced AA7075 metal matrix composites were fabricated and XRD peak positions, intensities confirmed the presence, crystal structure and crystal size of the silicon carbide. Impact testing experiments showed the increase in the energy for increase in weight percent of reinforcements. Young's modulus also increased with the addition of Silicon carbide and the FEM analysis was carried out using Johnson cook material constants and the impact behavior of MMCs with FEM was almost same as compared to the experimental results.

References

- [1]. Pharr, G. M & Oliver, W. C. (2004), "Measurement of Hardness and Elastic Modulus by Instrumented Indentation: Advances in Understanding and Refinements to Methodology," Journal of Materials Research,
- [2]. Sarkar, J., Kutty, T. R. G., Conlon, K. T., Wilkinson, D. S., Embury, J. D., and Lloyd, D. J. (2001), "Tensile and Bending Properties of AA5754 Aluminum Alloys," Materials Science and Engineering
- [3] L. Subramanian, C., Deus, R. and Yellup, J. M. (1997), "Dry Sliding Wear of Aluminum Composites—A Review," Composites Science and Technology
- [4] Prasad DS, Shoba C, Ramanaiah N. Investigations on mechanical properties aluminum hybrid composites. J Mater Res Technology 2014;3(1):79–85
- [5] Arulshri KP, Iyandurai N. Boopathi MM Evaluation of mechanical properties of aluminum alloy 2024 reinforced with silicon carbide and fly ash hybrid metal Matrix composites. Am J Appl Sci 2013; 10(3):219
- [6] Sharma RK, Priyadarshi D. Porosity in aluminum matrix composites: cause, Effect and defence. Mater Sci: Ind J 2016;14(4)
- [7] Ezatpour HR, Sajjadi SA, Sabzevar MH, Huang Y. Investigation of Microstructure and mechanical properties of Al6061-nanocomposite fabricated by stir casting. Mater Des 2014; 55:921–8
- [8] Mamun Al Rashed, ahman, H. M. "Characterization of silicon carbide reinforced aluminum matrix Composites"
- [9] Sun yun-ping, YAn Hong-ge, Chen Zhen-hua, Zhang Hao, "Effect of heat-treatment on microstructure and properties of SiC particulate-reinforced Aluminium matrix composite", Transactions Of Nonferrous Metals Society Of China, Vol.17, pg 318-321, 2007.
- [10] D N Drakshayani, Janardhana K, Dr. "Evaluation of Mechanical Properties of Retrogression and Reaged Al 7075 alloy reinforced with SiCp Composite Material", IJERT, Volume. 3, Issue. 09, 406-409, September - 2014

- [11] Xiang Zeng¹, Wei Liu, Ben Xu., Guogang Shu, and Qiulin Li, "Microstructure and Mechanical Properties of Al-SiC Nanocomposites Synthesized by Surface-Modified Aluminium Powder
- [12] Vamsi Krishna, Prasad Reddy, A.; P.; Narasimha Rao, R.; Murthy, N.V. Silicon carbide reinforced aluminium metal matrix nano composites— A review. *Mater. Today Proc.* 2017, 4, 3959–3971.
- [13] Shakoora, R.A., Penchal, M. "Enhanced performance of nano-sized SiC reinforced Al metal matrix nanocomposites synthesized through microwave sintering and hot extrusion techniques". *Prog. Nat. Sci. Mater. Int.* 2017, 27, 606–614.
- [14] Erol kilickap, Tamer, Ozben, Orhan Cakir :Investigation of mechanical and machinability properties of SiC particle reinforced AlMMC, *J. Mater. Process. Technol.*, Vol.198, No.1-3, pp.220-225, 2008.
- [15] Gao, H, Nix, W. D.: Indentation size effects in crystalline materials: a law for strain gradient plasticity. *J. Mech. Phys. Solids* 46, 411-425 (1998).
- [16] Chen Bo, Yuan Zhanwei, Li Fuguo, Zhang Peng, Xue Fengmei "Mechanical properties study of particles reinforced aluminum matrix composites by micro-indentation experiments".
- [17] Anilkumar S Kallimani, Chikkanna N, Suresha P, Hareesha G, "Enhancement of Fracture Toughness for Nano SiC reinforced AA7075 MMC's By Tensile tests and FEM analysis". et al 2021 IOP CONF.SER.MATER.SCI.ENG.1065 012037
- [17] Hareesha G, Chikkanna N, Saleemsab Doddamani, "Finite Element Simulation of fracture Toughness of Al6061 reinforced with SiC". et al 2021 IOP CONF.SER.MATER.SCI.ENG.1065 012036

Smart Freezing Technique Using Thermoacoustic Energy

Kaviarasu C¹, Barath M², Kavinkumar V S³, Santhosh B³

¹II Year, Mechanical Engineering, Bannari Amman Institute of Technology, Sathyamangalam, Erode, Tamil Nadu – 638 401.

²II Year, Electrical and Electronics Engineering, Bannari Amman Institute of Technology, Sathyamangalam, Erode, Tamil Nadu – 638 401.

³II Year, Biomedical Engineering, Bannari Amman Institute of Technology, Sathyamangalam, Erode, Tamil Nadu – 638 401.

³II Year, Biomedical Engineering, Bannari Amman Institute of Technology, Sathyamangalam, Erode, Tamil Nadu – 638 401.

Abstract

Preserving things to save money has become a major idea and it provoked to an invention called "refrigerator". Refrigeration process in those refrigerators involves some gases, they combine together and releases CFC which has a major impact on ozone layer. In order to protect ozone layer. A compact and safest model of refrigeration could be done using the Thermoacoustic refrigeration systems. In this modern era, using sound energy which involves the conversion of heat into cold is a kind of unique kind of technology. Acoustic sound waves while getting oscillates it absorbs and releases heat. In the refrigeration system, the sound waves transfer the heat away from the system. This phenomenon is called the cooling effect. In this paper review, we incepted the history of evolution of thermo acoustic freezing system and concluded with the application of the thermo acoustic system.

Keywords: *Refrigeration, Acoustic sound waves, Cooling effect.*

1. Introduction:

In the Primitive times of the Century 500 BC, the earliest forms of refrigeration were called an Ice House. From the nearby lakes and rivers, the ice is cut down and stored in these ice houses throughout the year. By the years passed, in 1802, Thomas Moore, an American businessman, done the Transportation of dairy products and this product is cooled by using his creation of Icebox. He called the ice box as "Refrigratory". Later he patented it as "Refrigerator" in 1803.

In 1834, the first step to modern refrigerator prototype was done by American inventor Jacob Perkins who lives in London. This refrigeration system is based on the vapor-compression, but it didn't succeed commercially. The refrigeration by using a liquefying gas [Ammonia] was patented by German engineering professor Carl von Linde. This Ammonia refrigeration becomes to end because of causing pollution and sewage dumping. Later In 1913, the first electric refrigeration was invented by American Fred W. Wolf. He invented it for domestic use only. So, he named it as **DOMELRE**, the **DOMestic ELelectric REfrigerator**.

In Continuation with the scientists, William C. Durant upgraded these refrigerators as including Compressors on the top of the cabinet and refrigerants as sulphur dioxide or methyl formate. Swedish inventors Baltzar von Platen and Carl Munters come up with the absorption refrigerator which is put into mass production.

2. Definition of Thermoacoustic Refrigeration:

Thermoacoustic refrigeration is a cooling device that is generally operated by using the high intensity of sound waves and a non-flammable inert gas like argon, helium, and air. The cooling effect in thermoacoustic refrigeration is done by using high intensity sound waves. This sound waves are produced by using high amplitude loud speaker in a certain frequency. A high intensity sound wave will cause a pressure pulsation. Stack, which is placed inside the resonator tube is in contact with the pressure pulsation. The sound waves will form a standing wave inside the resonator tube. The reflected wave and the original sound waves will cause

expansion and rarefaction in the resonator tube. It may cause a temperature difference in the resonator tube by the use of heat exchangers on the either side of the stack material, which will remove heat from the cold side and reject it at the hot side of the system.

3. Components used for the Setup:

For designing the Thermoacoustic refrigeration system setup, an acoustic driver, a resonator (closed cylinder), a stack (poriferous component) and a pair of heat exchange systems. **Inert gas** is used as a working medium in thermo acoustic refrigeration system. Depths of thermal penetration and the resonator's natural frequency depend on the selection of working fluid.

3.1. Acoustic Driver: Acoustic driver produces sound (acoustic) waves with high intensity and pressure. Diaphragm or flexible cone get vibrates which is made of metal, plastics or paper produces the sound waves. Sound is produced in the narrow end of the coil is attached to the voice coil. Permanent magnet and Electromagnet are the two type of magnets present in voice coil. Using the function generator, the sound waves are transmitted into the resonator.

3.2. Resonator: It is a closed cylinder component which consists working medium in its setup. It is of two types: half wavelength resonator and quarter wavelength resonator. Half wavelength resonator type consists open at one end and close at the end whereas in Quarter wavelength resonator one end is sealed. Construction of inner region of resonator tube is done by aluminium tubing with plastic tubing.

3.3. Stack: A porous medium which is considered as the heart of thermo acoustic refrigeration system setup. Little changes in the measurements of stack can undergo enormous distinctions in its display. The cooling power and the cooler productivity has opposite relation with each other, while the length of the stack get expands, the intensity of cooling of thermo acoustic fridge increases, however the proficiency get decreases.

3.4. Heat Exchange System: In thermo acoustic refrigeration setup, the heat exchange system is used to maintain the required temperature. Two heat exchangers are present where one is uses hot heat exchanger and the other one works as cold heat exchanger. The design of the stake is optimum which is necessary to get maximal difference in temperatures.

4. Working Principle and Construction:

4.1. Principle:

1. When the sound wave from the diaphragm is sent through a resonator, the pressure pulsation forms a standing wave.
2. This causes the oscillatory motion of the gas particles inside the resonator tube.
3. Combination of Pressure oscillation and oscillatory motion of gas causes heat transportation when the gas is in thermal contact with a stationary surface.
4. Due to the expansion and compression of gas particles by sound, cooling and heating occurs.

4.2. Construction:

Thermo-acoustic Refrigeration System mainly consist of a Function generator to generate different types of electrical waveforms such as sine wave, square wave, triangular waves and saw tooth waveforms over a wide range of frequencies. A loudspeaker is attached to an acoustic resonator (tube) filled with gas. In the resonator, a stack consisting of a number of parallel plates is fixed, which the most important component of this project is. The atoms at different temperature coefficient oscillates inside the stack which is needed for the refrigeration process. Two heat exchangers are installed at the two ends of stack where hot air and cold air is circulated. In Figure 4.1, the setup of Thermo-acoustic refrigeration system can be viewed.

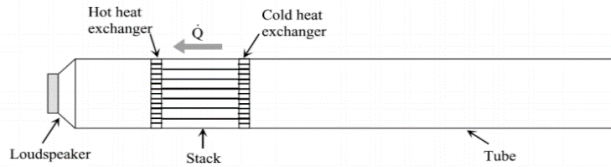


Fig 4.1 Thermo-acoustic refrigeration setup

5. Working:

The loudspeaker, which acts as the driver, sends a constant acoustic standing wave in the gas at the fundamental resonance frequency of the resonator. The acoustic standing wave displaces the gas in the channels of the stack while compressing and expanding respectively leading to heating and cooling of the gas. The gas, which is cooled due to expansion absorbs heat from the cold side of the stack and as it subsequently heats up due to compression while moving to the hot side, rejects the heat to the stack. Thus, the thermal interaction between the oscillating gas and the surface of the stack generates an acoustic heat pumping action from the cold side to the hot side. The heat exchangers exchange heat with the surroundings, at the cold and hot sides of the stack. Figure 5.1, shows the block diagram of the thermo-acoustic refrigeration system.

The heat exchangers are used so that heat interaction with the surrounding takes place. Heat is pumped from the cold end heat exchanger to the hot end heat exchanger. This exchange occurs rapidly and makes the system apt for refrigeration process. Figure 5.2, shows the distribution of temperature (heat and cold) in the heat and cold exchangers. The graph shows the temperature distribution, T_H and T_C .

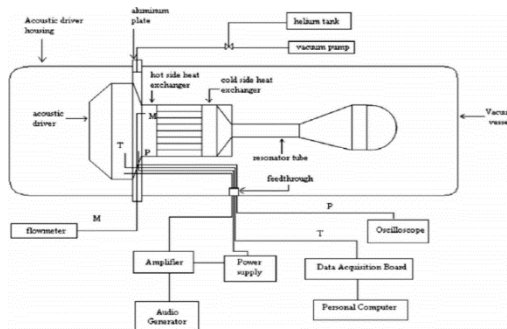


Fig 5.1 Block diagram of the system

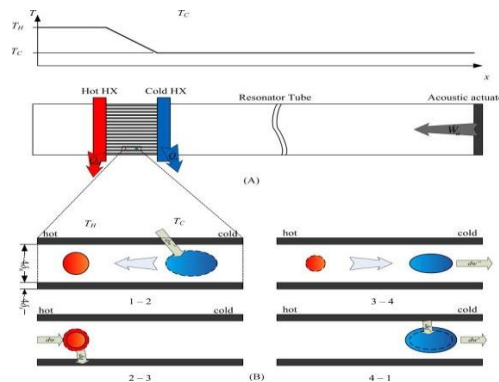


Fig 5.2 Distribution of temperature

6. Merits and Demerits of Thermoacoustic Refrigerator Setup:

6.1.Merits

- Simple working mechanism
- Weightless and conventional setup
- No harm to the atmosphere as it not emits the harmful chemicals such as Chlorofluorocarbons, Hydrofluorocarbons and Hydro chloro fluorocarbons.
- It has fewer moving parts, hence it is more stable

6.2. Demerits

- Implementation of components of these systems are cost.
- This system setup has lesser Coefficient of Performance.

7. Applications of Thermoacoustic Refrigeration:

1. Acoustic energy obtained by burning natural gas in thermo-acoustic engine, which liquefies the natural gases.
2. Most of our present works happens with electronic products, which works on chips and micro-controllers. The heat dissipated from the chip is cooled by Thermo-acoustic heat pump which increases efficiency in functioning of products.
3. Solar energy produces acoustic wave in acoustic engine, which is further used by motors to produce electricity.
4. By processing the industrial wastes in the thermo-acoustic engine produces the acoustic energy which upgrades the normal temperature to the finest required levels.
5. In submarines and ships, the electronic system cooling has a major step. In that means, the thermo-acoustic refrigeration stands good in efficient cooling of the systems.
6. It is mainly used for its mechanism of producing the low to high temperatures in harmless manner. It is used in freezing certain food items and ice creams.

8. Conclusion:

Thermo-acoustic refrigeration is a kind of specialized refrigeration technique which devoid of harmful substances. This setting is effective for industry purposes. Higher frequency gives up increased efficiency. Also, better efficiency is achieved by varying the placement of the stacks and altering the frequency. The variances can be fixed by trail and error method. Refrigeration with helium provides maximum cooling than other noble gases. To get greater efficiency in working and cost, the heat exchangers and stacks have to be developed accordingly. Standing wave thermos acoustic refrigeration can cool even high temperature ranges. Though it gives out lesser efficiency, but it overcome the defect by its user-friendly nature of working and simplicity. Implementation cost is high because of the materials used in the construction, while developing a suitable solution might make it popular than all other conventional refrigeration systems.

Acknowledgement

We are extending our gratefulness to every researchers and authors who had undergone and done esteemed works on the thermoacoustic refrigeration systems and all of your papers have assisted us to perform the review an overview of the kind, thermoacoustic refrigeration system setups.

References:

[1] G Bharadwaj, G Dilip Kumar, G Teja, G Surya, "Thermoacoustic Refrigeration", International Journal of Engineering Development and Research, Volume 7, Issue 4, ISSN: 2321-9939.

- [2] Bhansali P. S, Patunkar P.P, Gorade S.V, Adhav S.S, Botre S.S, "An Overview of Stack Design for A Thermoacoustic Refrigerator", International Journal of Research in Engineering and Technology, Volume: 04, Issue:06, June-2015, eISSN: 2319-1163, bpISSN: 2321-7308.
- [3] K. Augustine Babu, P. Sherjin, "A Critical Review on Thermoacoustic Refrigeration and its Significance", International Journal of ChemTech Research, 2017,10(7): 540-552.
- [4] Pranav Mahamuni, Pratik Bhansali, Nishank Shah, Yash Parikh, "A Study of Thermoacoustic Refrigeration System", International Journal of Innovative Research in Advanced Engineering (IJIRAE), Issue 2, Volume 2 (February 2015), ISSN: 2349-2163.
- [5] Vedhas A. Pathak, Dhruv G. Patel, Tushar Bora, "Thermoacoustic Refrigeration", International Conference on Emerging Trends in Engineering and Management Research, 23rd March 2016, ISBN: 978-81-932074-7-5

Data Analysis and Prediction of optimum process parameters for Cryo-cooled Near-dry WEDM Process

Boopathi Sampath¹, Sureshkumar Myilsamy²

¹*Department of Mechanical Engineering, Muthayammal Engineering College, Rasipuram-637408, Namakkal (Dt), India.*

²*Department of Mechanical Engineering, Bannari Amman Institute of Technology, Sathyamangalam, Erode. Tamil Nadu 638401 India.*

Abstract

In this paper, data analysis and prediction of best process parameters level for cryo-cooled near-dry wire-cut electrical discharge machining (WEDM) process for the machining of Inconel 718 alloy material. The Box-Behnken method is used to design the experiments to collect the response data from trial tests. The voltage, pulse-width, pulse-interval, and flow rate are the controllable variables for response characteristics such as rate of material removal and surface roughness. After data collection from experiments, the sequential sum of square tests was performed to predict the order of the models. The mathematical models for each response were developed using significant individual, interaction, and quadratic terms. Thus, the models have been evaluated by carried-out the lack-of-fit tests. The response surface plots for each response related to interacted terms of variables. Based on these plots, the variation of each control parameter on the response parameters has been analyzed. It was revealed that increasing voltage, and pulse-width, the material removal rate (M) and the surface roughness (Ra), and conversely, the pulse interval minimizes the MRR and Ra. The highest M and Ra are attained by the maximum flow rate of the dielectric medium. The desirability principles were applied to find the combination of process variable values for the best solution for satisfying both responses. The predicted combination of results has been validated by data that were collected from confirmation experiments.

Keywords: Box-Behnken, Design of experiments, Mathematical Models, Desirability, Data prediction

1. Introduction

The data analysis of manufacturing system is very essential for modern manufacturing industry. Based on the computation methods the machining parameters are analyzed. In the unconventional machining process, relationships between manufacturing parameters and environmental impact are developed to analyze the material removal mechanics, tool change, minimum rejections in production, and effects of cutting-fluid flow [1]. The environmental impact of machining processes should be analyzed for minimizing environmental impacts by modification of existing technology and the development of new manufacturing methods [2]. In these aspects, research on the modification of EDM and WEDM processes was developed to make the trade-off between machining performance and machining pollutions. The analytical relationship of EDM processes was developed to reveal the wear of the tool and workpiece, and the dielectric fluid flows, and the toxicity and flammability [2, 3]. The inferences of cooling electrode wear and surface roughness of the workpiece have been investigated by the change of process parameters such as voltage, pulse width, current, and pulse interval [4, 5]. The parametric analysis of dry electric discharge machining of mild steel was investigated and response models were developed by response surface methodology [6]. Generally, the machining performance of the dry EDM process is very low than the conventional process. It was revealed that the tool wear of the dry EDM process is significantly reduced by cryogenic cooling of electrode and workpiece [7]. The mechanism of the gas-liquid-powder mixture in EDM was investigated in both dry and near-dry processes to improve material erosions. It is found that cryogenically treated brass wire produces a 22.55% more material removal rate as compared to plain brass [8]. The parametric study was performed using a molybdenum wire tool and tool steel workpiece with an air dielectric medium to study the influence of air-mist pressure, voltage, pulse-off time, pulse-on time, and current on the MRR and Ra using the Taguchi technique [4, 9]. Later, the oxygen gas near-dry WEDM experiments have been conducted using Taguchi's L27 orthogonal array and Multi-objective artificial bee colony (MOABC) algorithm [10, 11, 15]. Some researches on cryo-treated wire electrode by using liquid nitrogen, zinc-coated brass wires were investigated to reduce tool wear rate for the green environment [3, 12–14]. However, it was found that no synchronized cryo-treated gas-liquid mixer in the near dry EDM and WEDM process.

In this research, the data was collected from 29 trials of cryo-cooled near-dry WEDM experiments. The collected data are used to predict the data for the better results of the WEDM process. The significant process parameters were identified to improve the quality of cutting processes.

2. Data Collection through Experiments

The cryo-cooled wire electrode setup was developed in numerically controlled (NC) wire-cut electrical discharge machining. The graphical layout representation of experimentation is shown in Figure 1. Liquid nitrogen was stored in dewar flask to maintain the cryo temperature. The molybdenum wire was cooled on both sides of electrode movements. The air and dielectric fluid mixture are used as a working medium in the reciprocating WEDM machine. Based on trial experiments, the input parameters and their significance levels are identified. The billet size of 718 is 50 mm × 50 mm × 5 mm Inconel 718 is used as work material for near dry WEDM machining processes. The experimental setup of cryo-cooled near-dry WEDM is shown in Figure 1. Below -150°C of Liquid nitrogen was stored and used to cool the molybdenum wire. Air and the dielectric fluid mixture are used as a working medium in reciprocating the WEDM machine. The surface roughness of WEDM was directly measured along with four different passes over the workpiece surface by the roughness tester. The material removal rate (MRR) can be calculated by the volume of materials removed concerning time using equations (1) and (2).

$$Kerf = \text{wire diameter} + 2 \times \text{times of parking gap} = 0.20\text{mm} \quad (1)$$

$$MRR = (\text{thickness} * Kerf * \text{length of cut}) / \text{time} \text{mm}^3/\text{min} \quad (2)$$

Based on pilot experiments, the input parameters and their significance levels are identified. The levels of each process variable are tabulated in Table 1. The experiments are conducted using the L9 orthogonal array Taguchi method[16] and the MRR and Ra values observed through the tests are shown in Table 2.

Box–Behnken method is used to conduct the experiments by design expert software. The Box-Behnken design is a self-determining quadratic design, which does not contain the partial factorial design. The designs have restricted capability related to the central composite designs. Five central points are repeated to avoid bias error. It uses 8 trails from (2 x 4 =8) two levels of k parameters, 16 trails of two factorial design (2⁴=16), and five repeated central points to calculate lack-of-fit. 29 sets of experiments were conducted and observed responses are tabulated in Table 4. Based on the analysis of the variance test, the significant individual and interaction and quadratic terms were identified [10]. In-significant terms are eliminated from the model. If response is 'f(x)', the independent variables are x1, x2, x3, x4, ..., xn, the response model is developed by following general equation (3).

$$f(x) = \beta_0 + \sum_{i=1}^k \beta_i x_i + \sum_{i=1}^k \sum_{j=1}^k \beta_{ij} x_i x_j + \dots + \phi \quad i < j \quad (3)$$

Where k is the number of process variables, β are the model coefficients, and φ is the statistical error, which represents variability by other noises.

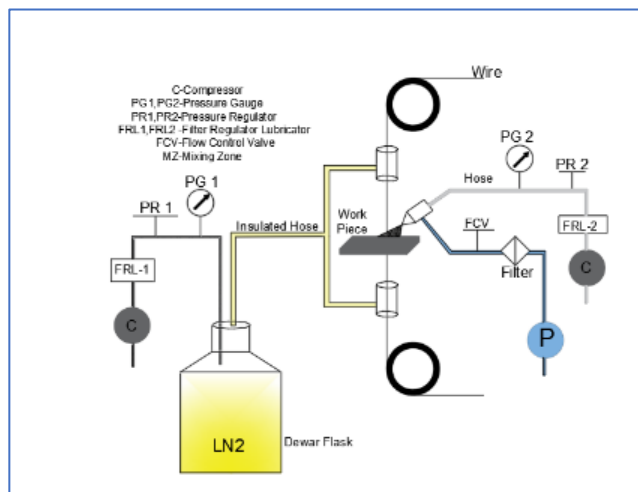


Figure 1: Collect the data from cryo-cooled near-dry WEDM Experimental Setup

Table 1: Parameter and Machine Setting level

| Factor | Parameter Name | Units | Low | High | Mean | Std. Deviation. |
|--------|----------------|-------|-----|------|------|-----------------|
| A | Current | A | 3 | 5 | 4 | 0.6433 |
| B | Pulse On | μs | 15 | 25 | 20 | 3.2163 |
| C | Pulse Off | μs | 45 | 75 | 60 | 9.6490 |

| | | | | | | |
|---|-----------|--------|----|----|----|--------|
| D | Flow Rate | ml/min | 10 | 20 | 15 | 3.2163 |
|---|-----------|--------|----|----|----|--------|

Table 2: Design of Experiments and observations using Box–Behnken method

| Exp. No. | C | PW | PI | F | MRR (mm ³ /min) | Ra (μm) |
|----------|---|----|----|----|----------------------------|---------|
| 1 | 3 | 20 | 75 | 15 | 6.13 | 1.72 |
| 2 | 5 | 20 | 75 | 15 | 9.45 | 2.32 |
| 3 | 4 | 15 | 60 | 20 | 8.38 | 2.38 |
| 4 | 4 | 20 | 45 | 10 | 9.28 | 3.68 |
| 5 | 4 | 25 | 60 | 10 | 9.57 | 3.41 |
| 6 | 4 | 20 | 60 | 15 | 9.12 | 2.9 |
| 7 | 4 | 20 | 60 | 15 | 9.09 | 2.68 |
| 8 | 4 | 15 | 75 | 15 | 7.12 | 1.57 |
| 9 | 5 | 20 | 60 | 20 | 10.9 | 3.07 |
| 10 | 3 | 25 | 60 | 15 | 8.51 | 3.2 |
| 11 | 3 | 20 | 60 | 10 | 6.58 | 2.76 |
| 12 | 4 | 25 | 45 | 15 | 10.91 | 3.67 |
| 13 | 4 | 20 | 75 | 10 | 7.78 | 2.35 |
| 14 | 3 | 20 | 45 | 15 | 7.76 | 3.14 |
| 15 | 4 | 15 | 60 | 10 | 7.38 | 2.84 |
| 16 | 4 | 15 | 45 | 15 | 8.67 | 3.41 |
| 17 | 4 | 20 | 75 | 20 | 8.74 | 1.77 |
| 18 | 5 | 20 | 45 | 15 | 10.87 | 3.89 |
| 19 | 5 | 20 | 60 | 10 | 9.44 | 3.46 |
| 20 | 4 | 25 | 75 | 15 | 9.38 | 2.48 |
| 21 | 5 | 25 | 60 | 15 | 10.77 | 3.23 |
| 22 | 4 | 20 | 45 | 20 | 10.29 | 3.35 |
| 23 | 5 | 15 | 60 | 15 | 9.47 | 3.38 |
| 24 | 4 | 20 | 60 | 15 | 9.12 | 2.88 |
| 25 | 4 | 20 | 60 | 15 | 9.11 | 2.89 |
| 26 | 4 | 25 | 60 | 20 | 10.63 | 2.99 |
| 27 | 4 | 20 | 60 | 15 | 8.77 | 2.86 |
| 28 | 3 | 15 | 60 | 15 | 6.02 | 1.86 |
| 29 | 3 | 20 | 60 | 20 | 7.24 | 2.3 |

3. Data Analysis and Discussion

The sequential sum of the square test was used to select the optimum model for the analysis. Initially, the linear model is selected. However, the model is not significant due to the R^2 value of MRR and Ra is very low (MRR $R^2 = 0.072$ and Ra $R^2 = 0.81$). The two factors interaction model (2FI) was also not fit with the solution due to the R^2 value of both models is minimum (MRR $R^2 = 0.608$ and Ra $R^2 = 0.075$). Then, the quadratic model of MRR was selected due to the R^2 value of 0.998 of both responses. The in-significant terms of the models were eliminated from quadratic models. The lack of fit of the model is in-significant, is acceptable. The cubic models of both responses were not selected due to more allies' terms in the models. The Lack of Fit tests of Ra and MRR were shown in Tables 3 and 4 respectively. The analysis of variations of MRR and Ra concerning process parameters are shown in Tables 5 and 6 respectively. The regression models of MRR and Ra were developed to identify the inference of process variables as shown in equations (4) and (5) respectively.

$$\text{MRR} = -8.241 + 5.335 \times C + 0.45 \times \text{PW} - 0.065 \times \text{PI} - 0.0575 \times F - 0.0595 \times C \times \text{PW} + 3.5 \times 10^{-3} \times C \times \text{PI} + 0.04 \times C \times F - 0.425 \times C^2 \quad (4)$$

$$R^2 = 99.40\% \quad \text{Adjusted } R^2 = 99.14\% \quad \text{Predicted } R^2 = 98.18\%$$

$$\text{Ra} = -1.958 + 1.8542 \times C + 0.227 \times \text{PW} - 0.0226 \times \text{PI} + 6 \times 10^{-3} \times F - 0.074500 \times C \times \text{PW} + 2.17 \times 10^{-3} \times \text{PW} \times \text{PI} - 8.3 \times 10^{-4} \times \text{PI} \times F - 4.821 \times 10^{-4} \times \text{PI}^2 \quad (5)$$

$$R^2 = 99.39\% \quad \text{Adjusted } R^2 = 99.15\% \quad \text{Predicted } R^2 = 99.04\%$$

The in-significant terms are eliminated from MRR and Ra regression models to improve the predicted R^2 and Adjusted R^2 . The regression models are used to plot the response surface between response and process variables. The influences of the interaction effects of process parameters have been studied by the response surfaces.

Table 3: Lack of Fit Test for surface roughness Model

| Source | Sum of Squares | Degree of Free- | Mean Square | F Value | p-value Prob> F | Comments |
|--------|----------------|-----------------|-------------|---------|-----------------|----------|
|--------|----------------|-----------------|-------------|---------|-----------------|----------|

| | | dom | | | | |
|------------------|--------------|-----------|--------------|--------------|--------------|------------------|
| Linear | 0.790 | 20 | 0.040 | 4.692 | 0.072 | insignificant |
| 2FI | 0.107 | 14 | 0.008 | 0.905 | 0.608 | insignificant |
| Quadratic | 0.009 | 10 | 0.001 | 0.102 | 0.998 | Suggested |
| Cubic | 0.001 | 2 | 0.001 | 0.069 | 0.935 | Aliased |
| Pure Error | 0.034 | 4 | 0.008 | - | - | - |

Table 4: Lack of Fit Test for material removal rate Model

| Source | Sum of Squares | Degree of Freedom | Mean Sum Square | F Value | p-value Prob> F | Comments |
|------------------|----------------|-------------------|-----------------|--------------|-----------------|------------------|
| Linear | 2.040 | 20 | 0.102 | 4.383 | 0.081 | insignificant |
| 2FI | 1.513 | 14 | 0.108 | 4.644 | 0.075 | insignificant |
| Quadratic | 0.215 | 10 | 0.022 | 0.924 | 0.584 | Suggested |
| Cubic | 0.036 | 2 | 0.018 | 0.775 | 0.520 | Aliased |
| Pure Error | 0.093 | 4 | 0.023 | - | - | - |

Table 5: Data analysis of material removal rate

| Source | Sum of Squares | Degree of Freedom | Mean Square | F Value | p-Value Prob.>F | Remarks |
|------------------|----------------|-------------------|-------------|----------|-----------------|--|
| Model | 54.491 | 8 | 6.811 | 404.036 | < 0.0001 | significant |
| A-Current | 29.016 | 1 | 29.016 | 1721.184 | < 0.0001 | significant |
| B-Pulse-width | 13.504 | 1 | 13.504 | 801.052 | < 0.0001 | significant |
| C-pulse-interval | 7.023 | 1 | 7.023 | 416.571 | < 0.0001 | significant |
| D-Flow rate | 3.152 | 1 | 3.152 | 186.962 | < 0.0001 | significant |
| AB | 0.354 | 1 | 0.354 | 21.000 | 0.0002 | significant |
| AC | 0.011 | 1 | 0.011 | 0.654 | 0.4282* | not significant Included for interaction analysis |
| AD | 0.160 | 1 | 0.160 | 9.491 | 0.0059 | significant |
| A ² | 1.271 | 1 | 1.271 | 75.369 | < 0.0001 | significant |
| Residual | 0.337 | 20 | 0.017 | - | - | - |
| Lack of Fit | 0.244 | 16 | 0.015 | 0.656 | 0.7580 | not significant |
| Pure Error | 0.093 | 4 | 0.023 | - | - | - |
| Cor Total | 54.8281 | 28 | - | - | - | - |

Table 6: Data analysis of Surface Roughness

| Source | Sum of Squares | Degree of Freedom | Mean Square | F Value | p-value Prob> F | Remarks |
|------------------|----------------|-------------------|-------------|----------|-----------------|-------------|
| Model | 10.621 | 8 | 1.328 | 409.723 | < 0.0001 | significant |
| A-Current | 1.591 | 1 | 1.591 | 491.131 | < 0.0001 | significant |
| B-Pulse-width | 1.044 | 1 | 1.044 | 322.286 | < 0.0001 | significant |
| C-pulse-interval | 6.645 | 1 | 6.645 | 2050.866 | < 0.0001 | significant |
| D-Flow rate | 0.581 | 1 | 0.581 | 179.243 | < 0.0001 | significant |
| AB | 0.555 | 1 | 0.555 | 171.288 | < 0.0001 | significant |

| | | | | | | | |
|----------------|--------|----|-------|--------|---|--------|-----------------|
| BC | 0.106 | 1 | 0.106 | 32.597 | < | 0.0001 | significant |
| CD | 0.016 | 1 | 0.016 | 4.822 | < | 0.0401 | significant |
| C ² | 0.083 | 1 | 0.083 | 25.548 | < | 0.0001 | significant |
| Residual | 0.065 | 20 | 0.003 | - | - | - | - |
| Lack of Fit | 0.031 | 16 | 0.002 | 0.231 | > | 0.9854 | not significant |
| Pure Error | 0.034 | 4 | 0.008 | - | - | - | - |
| Cor Total | 10.686 | 28 | - | - | - | - | - |

The response surface of MRR for Flow rate and current is shown in Figure 2. It is also significantly enhanced by increasing the flushing flow rate due to the quick disposal of debris from the cutting zone. Figure 3 shows that the response surface of MRR by the pulse width vs current. The MRR is improved by the increase in spark current between work materials and wire due to high spark strength [9,11]. It was observed that the large increase in MRR is seen from low pulse width to high value by enhancing spark strength as shown in Figure 4 [9,11]. However, the MRR is increased by reducing pulse interval due to an increase in spark ideal time.

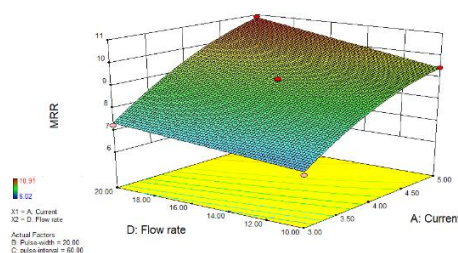


Figure 2: Response surface for MRR concerning Flow rate and current

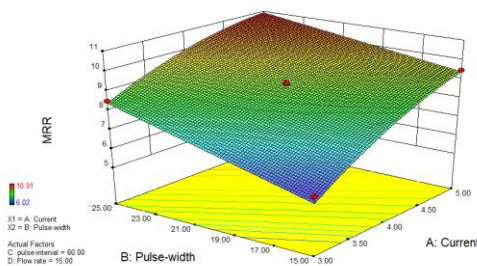


Figure 3: Response surface for MRR concerning Pulse width and current

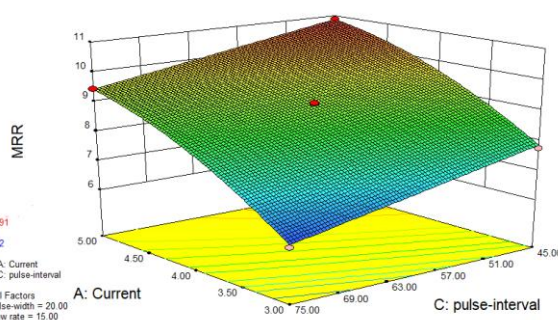


Figure 4: Response surface for MRR concerning current and pulse interval

The minimization of surface roughness is one of the goals of this study. The Ra is minimum at the low value of pulse interval and pulse width due to fine and soft spark in the cutting zone as shown in Figure 5. While the increase in pulse width, the spark strength is significantly increased with material removal rate and reduces the Ra. The increase in pulse interval is increasing the Ra due to high spark pause time[9]. Figure 6 shows the interaction effects of pulse width and current on Ra. While increasing the spark current, the Ra value is exploiting due to heave spark intensity [11]. Similarly, the Ra value is also slowly increased due to the growing MRR by fast flushing debris as shown in Figure 7.

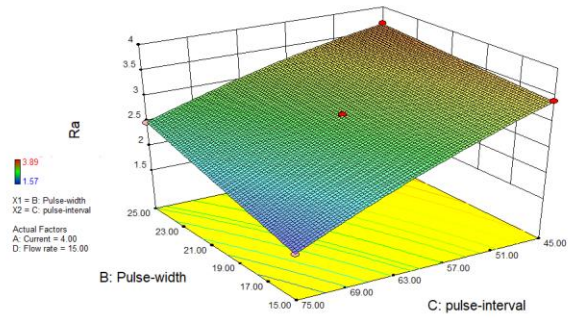


Figure 5: Response surface for Ra concerning Pulse width and pulse interval

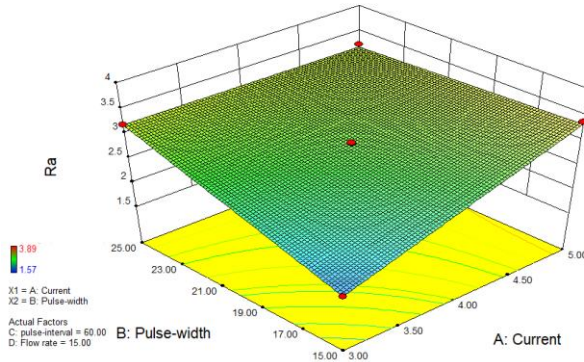


Figure 6: Response surface for Ra concerning Pulse width and current

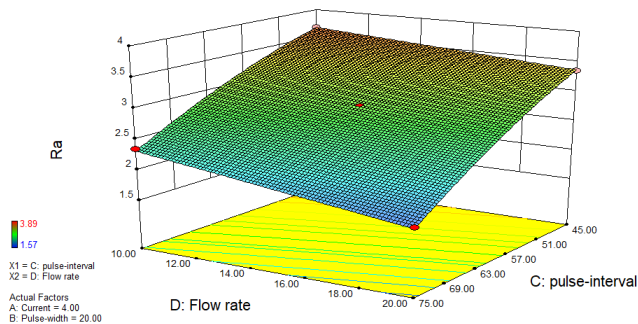


Figure 7: Response surface for Ra concerning Flow rate and pulse interval

4. Desirability Analysis and Data Evaluation

In this stage, predicts the combination of experimental parameters along with their responses based on the standard ranges defined for the responses. Thus, optimization based on the desirability function approach was used to predict the best results of both responses. It detects a point that maximizes the desirability function. For validating the models, some solutions were selected randomly. The predicted values of the responses were related to experimentally obtained values. The combination of variables that presents the overall optimum desirability (100%) of response and contour plots are displayed in Figures 8 and 9 respectively. Considering all quality attributes and using the optimization method which quality parameters were put into standard ranges (MRR and Ra), formulation one consisting of 25µs pulse width, 75µs Pulse interval, 5A current, and 20ml/min flow rate was selected as having the maximum desirability. The combined optimizing responses are predicted as 10.91mm³/min of material removal rate, and 2.20µm of surface roughness.

The confirmation tests were conducted to validate the predicted optimum process parameters for best MRR and Ra as shown in Table 8. The multi-optimization results were confirmed by the mean observed values of the test. The current 5 Ampere, pulse width 25µs, pulse interval 75µs, and 20ml/min flow rate gives 11 mm³/min of MRR and 2.3µm of Ra.

Table 8: Predicted Results from desirability and validation by confirmation experiments

| S.No. | C | PW | PI | F | MRR | Ra | Description |
|-------|---|----|----|----|-------|------|-----------------------|
| 1. | 5 | 25 | 75 | 20 | 10.91 | 2.20 | Desirability Approach |
| 2. | 5 | 25 | 75 | 20 | 11.00 | 2.3 | Experimental |

5. Conclusions

In this research, the data was collected from the experiments of cryo-cooled wire near-dry WEDM were carried-out to maintain enough temperature in the cutting zone to cut the Inconel 718 alloy material. The Lack of fit test was conducted to select the fitted model for the responses. The data analysis was done by the analysis of variance test. The optimum input parameters are predicted to maximize the material removal rate and surface finish by response surface methodology. The electrical conductivity of molybdenum was significantly increased by mixing liquid nitrogen with air. It was observed that pulse-width, pulse-interval, current, and flow rate are significant parameters on the material removal rate and surface roughness. The current and pulse width are the most important factors for material removal rate. Increasing the current and pulse width, the material removal rate was increasing and same time decreasing the surface roughness. While increasing pulse-interval from 45 μ s to 75 μ s, both the material removal rate and surface roughness were decreased. The surface finish has been significantly improved at the dielectric fluid flow rate of 20 ml/min. Thus, the optimum process parameters were obtained for the cryo-cooled molybdenum wire electrode used in the near dry wire-cut electrical discharge machining process. The desirability technique was used to find the best solution among the conflict behavior of MRR and Ra. It was observed that the behavior of the parameters against response variables is the same as the response surface method. The current 5 Ampere, pulse width 25 μ s, pulse interval 75 μ s, and 20ml/min flow rate gives 10.97mm³/min of MRR and 2.2 μ m of Ra. The multi-optimization results were validated by the mean observation value of confirmation experiments.

REFERENCES

1. A. A. Munoz, and P. Sheng, "An analytical approach for determining the environmental impact of machining processes," *Journal of Materials Processing Technology*, Vol. 53, pp.736–758,1994.
2. S. H. Yeo, H. C. Tan, and A. K. New, "Assessment of waste streams in electric-discharge machining for environmental impact analysis," *Proceedings of the Institution of Mechanical Engineers , Part B : Journal of Engineering Manufacture*, Vol. 212, pp.393–401, 1998.
3. M. S. Hewidy, T. A. El-Taweel, and M. F. El-Safty, "Modelling the machining parameters of wire electrical discharge machining of Inconel 601 using RSM," *Journal of Materials Processing Technology*, Vol. 169, pp.328–336, 2005.
4. S. Boopathi, and K. Sivakumar, "Optimal parameter prediction of oxygen-mist near-dry wire-cut EDM," *Int. J. Manufacturing Technology and Management*, Vol. 30, pp.164–178,2016.
5. S. Abdulkareem, and A. A. Khan, "Reducing electrode wear ratio using cryogenic cooling during electrical discharge machining," *Int. J. Adv. Manuf Technol*, pp.1146–1151,2009.
6. Sourabh K Saha, and S K Choudhury, "Experimental investigation and empirical modeling of the dry electric discharge machining process," *International Journal of Machine Tools & Manufacture*, Vol. 49,pp.297–308,2009.
7. Z. Jiang, H. Zhang, and J. W. Sutherland, "Development of an environmental performance assessment method for manufacturing process plans," *International Journal of Advanced Manufacturing Technology*, Vol. 58, pp.783–790,2012.
8. X. Bai, Q. H. Zhang, T. Y. Yang, and J. H. Zhang, "Research on material removal rate of powder mixed near dry electrical discharge machining," *International Journal of Advanced Manufacturing Technology*, Vol. 68, pp.1757–1766, 2013.
9. S. Boopathi, and K. Sivakumar, "Experimental investigation and parameter optimization of near-dry wire-cut electrical discharge machining using multi-objective evolutionary algorithm," *Int J Adv Manuf Technol*, pp.2639–2655, 2013.
10. S. Boopathi, "Experimental Comparative Study of Near-Dry Wire-Cut Electrical Discharge Machining (WEDM)," *European Journal of Scientific Research*, Vol. 75, pp.472–481,2012.
11. S. Boopathi, and K. Sivakumar, "Study of water assisted dry wire-cut electrical discharge machining," *Indian Journal of Engineering & Materials Sciences*, Vol. 21, pp.75–82, 2014.
12. G. Rajyalakshmi, and P. V. Ramaiah, "Multiple process parameter optimization of wire electrical discharge machining on Inconel 825 using Taguchi grey relational analysis," *Int J Adv Manuf Technol.*,Vol 69,pp. 1249-1262, 2013.
13. M. P. Garg, A. Kumar, and C. K. Sahu, "Mathematical modeling and analysis of WEDM machining

- parameters of nickel-based super alloy using response surface methodology,” *Sadhana - Academy Proceedings in Engineering Sciences*, Vol. 42, pp.981–1005,2017.
14. B. B. Nayak, and S. S. Mahapatra, “Optimization of WEDM process parameters using deep cryo-treated Inconel 718 as work material,” *Engineering Science and Technology, an International Journal*, Vol. 19, pp.161–170, 2016.
 15. Jenn-long liu, chung-chih L, "An Improved Artificial Bee Colony Algorithm Applied to Engineering Optimization Problems” *journal of information science and engineering*, Vol. 32, pp. 863-886,2016.
 16. S. Boopathi, “Experimental investigation and parameter analysis of LPG refrigeration system using Taguchi method,” *SN Applied Sciences*, Vol. 1, pp.892, 2019.

A Study of Electro Discharge Coating and Characteristics

Mr.K.Shanmuga Elango, K.Lakshminarasiman.,
st. Annes college of engineering and technology

Abstract

Applications of coated surface are swiftly increasing in present industrial context. Recently, the electro-discharge route is being explored for surface modification in terms of alloying and layer deposition. Electro-discharge machining parameters and response to surface deposition is of the research interest in electro-discharge coating. In this regard, electro-discharged surface modifications have been characterized in the present investigations. The effect of relevant EDM parameters (current, Pulse duration, duty factor, density of electrode material) on various surface alloying responses such as surface micro hardness, chemical composition of the alloying surface, surface deposition layer thickness has been studied. The EDM electrode is specially made of tungsten die sulphide powder by semi-sintering process. Negative or reverse polarity is used for better results of layer deposition of electrode material of tungsten die sulphide powder and carbon particles within the dielectric liquid used for machining. Considering ample of general applications in engineering, work piece is of low carbon steel/HSS has been identified. It is observed that tungsten carbide layer has been deposited on the work piece which shows better functional characteristics for the applications. Low to medium current (2–5 A), Low density of electrode material (7.15–8.03 kg/cm³) and low duty factor (3–5) are favourable conditions for better deposition of the layer.

Keywords: *electro discharge coating, deposition, tungsten powder, coating characteristics*

Introduction

Electro discharge machining (EDM) is a widely accepted non-traditional machining process primarily used for machining of hard material or those which are difficult to machine by the conventional machining process. It is also referred as spark machining, spark eroding and die sinking manufacturing process whereby a desired shape is obtained using electrical discharges(sparks).The material is removed from the work piece by a series of rapidly recurring current discharges between anode and cathode, separated by a dielectric liquid and subjected to electric voltage. EDM typically used for the electrically conductive but hard materials like alloy steel, Ti alloy, to cut very intricate shapes and contours or cavities. The EDM process is most widely used in mould making tools, dies, automobile and aerospace industries.

Under precise machining condition, when the electric sparks generated, the material from the tool-electrode is eroded and deposited on the work piece surface being machined by melting and vaporization process occurred at high temperature. During each spark, the material of the work piece gets solidified by a quenching process (rapid cooling) due to a low temperature of the dielectric medium. So, the transferred material from the tool-electrode can create a coating over the machined surface under suitable machining condition in EDM. This process for surface modification by the electric discharge is popularly known as Electrical discharge coating (EDC).

Surface modification is a very common feature of electric discharge machining that is developed in recent years. Surface modification by EDC can be done by different ways as described below.

1. Surface modification using conventional electrode
2. Surface modification by powder metallurgy electrodes

3. Surface modification by a powder-mixed dielectric

4. Surface modification by some other processes like EDT (Electrical Discharge Texturing)

In EDC, hard carbides are coated on the work piece material which mainly produced by the chemical reaction of the transferred tool material and the carbon particles decomposed from the dielectric fluid due to the high temperature of spark. It is necessary to keep the tool as anode and work piece as the cathode (reverse polarity) in this process. The material carbide is piled up on the work piece surface and produces a hard layer. This deposition improves the surface properties like hardness, wear resistance, oxidation and corrosion resistance of the substrate. At present, different surface enhancing techniques are used including laser coating ,chemical /physical vapour deposition(CVD / PVD), electroplating and plasma arcs praying.

1.1 Different types of coating methods

1.1.1 Laser coating

Laser coating is an advanced coating technique also referred as “laser cladding” or “laser spraying”, which is used for improving the surface properties of various components. It can be used to produce hard surfaces on a wide variety of engineering materials. In this technique, hard ceramic powders like tungsten carbide, titanium carbide and chromium carbide is coated on the work piece surface. Laser coating is surface modification technique, which gives extremely dense, crack-free and non-porous structure. These types of coatings show excellent metallurgical bonding to the base material having uniform composition and coating thickness. Since, the process occurs at high speed, a slight distortion and residual stresses (compressive) are left on the surface due to high temperature. However, along with such advantages some distinctive challenges related to the implementation laser coating technology have been identified.

1. This process has high equipment and running costs.
2. Poor acceptance of a potential reduction in manpower in this technology.
3. A need for retraining is required. 4. It has unexplored technical difficulties.

1.1.2. Physical Vapour Deposition (PVD)

Physical Vapour Deposition (PVD) comprises a group of surface coating technologies used for deposition of this coating, mainly in cutting tool coating, and other engineering coating applications. It describes the deposition method that is carried out in a vacuum, to deposit thin films of desired coating material in the vaporized form by condensation on a variety of work piece surfaces. This coating method involves entirely physical processes such as high temperature vacuum evaporation with subsequent condensation, or plasma sputter bombardment rather than involving a chemical reaction at the surface to be coated as in chemical vapour deposition. Physical vapour deposition is currently being used to improve a number of products, including automotive parts like wheels and pistons, surgical tools, drill bits, and guns .But there are some difficulties with this technique:

1. High capital cost

2. Some processes operate at high vacuums and because of high-temperature complicated control system required.
3. The rate of coating deposition is usually quite slow.

1.1.3. Chemical Vapour Deposition (CVD)

Chemical vapour deposition (CVD) is an extensively coating technology used to create high quality, high-performance, coating that produce by chemical reaction of vapours and deposition on substrate. The majority of its applications involve applying solid thin-film coatings to surfaces. Coatings obtained by CVD are usually thicker than those obtained via PVD. In this method, a very complicated coating environment is to be maintained, more precisely an inert gas atmosphere. Further, this process is limited to small size parts only .Chemical and safety hazards caused by the use of toxic, corrosive, flammable and explosive precursor gases and the requirement of sophisticated reactor or vacuum system restrict its application for common industrial use.

1.1.4. Electroplating

Electroplating is the application of a metal coating on a metallic surface by an electrochemical process. The work piece to be plate disconnected to cathode and metal to be coated kept as anode. From the anode , metal ions are discharged under the potential from the external source of electricity and then combine with the electrolyte ions and deposited on the cathode (work-piece).Besides the benefits, some drawbacks of the process make its restricted use in industry. It is a slow process and can be applied to certain types of materials only. Further adhesion of the coating material with the substrate also not high enough to overcome the limitations of the above-mentioned coating processes, different new coating techniques These limitations. 5. Electrical Discharge Coating (EDC) Although EDM is fundamentally a material removal process, efforts have been made to use the process as a surface treatment method and/or an additive process. EDC is a type of coating technique in which tool electrode is prepared by powder metallurgy method used as anode and work-piece(on which coating material to be deposited) is selected as cathode in EDM. In the presence of dielectric fluid, the material is eroded from the tool electrode and deposited on the work piece surface. This process improves the surface properties like wear resistance, hardness, oxidation and corrosion resistance of different engineering material. 1.2 Basic Mechanism of Electro Discharge Coating

Electro Discharge Coating is a very important aspect of EDM. It means to improve the chemical and mechanical behavior of the work piece surface. This process is carried out in ordinary EDM machine but under precise machining condition. During the generation of electric sparks, material from the tool electrode gets deposited on the work piece surface by a melting and vaporization process occurring in a micro plasma channel in high temperature. During each electric spark, the material of the work piece gets solidified by a rapid cooling process (quenching) due to low temperature of the working medium (liquid dielectric).EDC has the potential to becoming a very useful and cheap alternative for surface

modification process.

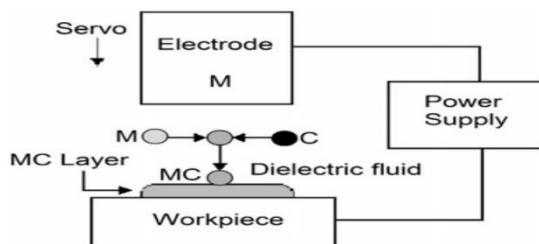


Fig.1: Basic principle of EDM

2. EDC by powder metallurgy tool electrode

In this method, powder metallurgy green compact or semi-sintered electrode is used as tool to transfer sufficient materials from tool to the work piece surface. Low bonding strength of the powders as compared to the fully dense material help to augment the metal transfer. The main advantage of the P/M tool is that, it can be easily fabricated by mixing powders of any composition and can be given different shapes with less effort. The properties of this kind of tool can be controlled by varying composition of the constituents, compaction pressure and the sintering temperature. With the use of PM tool electrodes, discharge energies to be used is higher than that of done with suspended powders, thus producing thicker recast layers and increased susceptibility to micro-cracking. Negative tool polarity is preferred for this method. PM materials used for EDM surface modification include different metal or combination of metals i.e., Al, Cr, Ti, TiC/Ni, WC/Co, Cr/Ni, Ni/Co, Ni/Mn, Ni/Fe, Ni/Si, Cu/W, Cu/Mn, Cu/Co and TiC/WC/Co etc..In this method usually the particle size ranges from 1 to 175 μ m with compacting pressures 100–540MPa and temperatures from 900 to 1300oC. When the sparks generated between the work piece and tool electrode with an appropriate condition, coating of hard carbide is produced on the work piece surface through the chemical reaction between the transferred material from the tool electrode and the carbon particles decomposed from the dielectric fluid under high temperature. The carbide is piled up on the work piece surface and produces a hard layer which provides better wear and corrosion resistance.

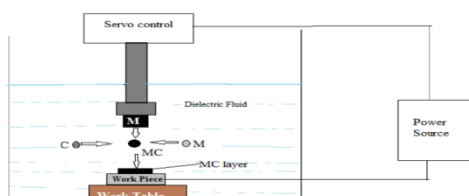


Fig.2: EDC by powder metallurgy tool electrode

3. Preparation of P/M compact tool electrode with powder mixture of Ws2 and Cu:

Electrode is prepared for electro discharge coating with the mixture of WS₂ and Cu powder. The electrode consists of a tool extension part made of mild steel for proper holding of the tool electrode in

the EDM tool holding collet, and a P/M compacted pellet that actually act as electrode. For making the pellets, Ws2 and copper powders were mixed properly by using mortar and pestle made of ceramic. Ws2 and copper powders were taken in the ratio of 60:40wt%. Then the mixture was compacted at compression pressure 300 MPa by using a compaction die of 15 mm diameter. The compaction pressure was selected based on the previous experiments performed by different research groups. Here, Cu powders act as binding agents. But the strength of the compact prepared is not strong enough since Ws2 is very brittle, and the possibility of bonding with other material is very less. So sintering was done at 900°C temperature. In order to prevent oxidation, inert (Ar) gas was provided during sintering from a separate cylinder. Detail of electrode preparation condition is depicted in table1. The pellet and tool extension part were then attached with the help of electrically conductive silver based epoxy glue. Fig.4 shows the Ws2-Cu tool electrodes prepared by P/M method after joining with mild steel tool extension.

Ws2-Cu tool electrodes prepared by P/M method after joining with mild steel tool extension

Table 1: Parameters of tool preparation by PM method

| | |
|-----------------------|-----------------------|
| Size of the pallets | 15mm dia.,10mm height |
| Powder composition | Ws2:Cu=60:40 wt% |
| Compaction Pressure | 300Mpa |
| Holding Time | 2 minutes |
| Sintering Temperature | 900°C |

4. Advantages of EDC

EDC has many advantages over some traditional coating techniques. Previously many techniques to enhance surface properties of materials has been described i.e. electro plating, plasma arc coating, laser coating and chemical/physical vapour deposition(CVD/PVD). But some of these methods require high investment cost and expensive equipments. EDC techniques can be used as an alternative approach to produce hard and wear resistant coating in different manufacturing sector. Some advantages of this method over the conventional method are listed below:

1. In EDC process, there is no need of any complicated equipment like vacuum apparatus.
2. Hard layers of different material composition can be easily created on the work piece surface using an ordinary EDM.
3. Coating layers can be produced in different parts of the work piece and the thickness of the coating can also control.
4. A large range of materials can be use in EDC method as per the requirement for different application on various workpiece surfaces.
5. EDC provides higher degree of hardness on the material surfaces, depending on the coating material used with strong metallurgical bonding.

5. Applications of EDC

Though EDM is fundamentally a material removal process, lot of efforts have been made to use this process as surface modification method. Many surface changes have been reported ever since the process established itself in the tool rooms of manufacturing industry. EDC is used very frequently due to its comparatively lower cost and lesser time. Some major applications of this process are listed below:

1. EDC can be used in different industrial applications like tool, die and mould manufacturing industries, to improve the wear, corrosion and oxidation resistance of these components.
2. It can be used in automobile and aerospace industries to improve the wear resistance of the light weight alloys used.
3. EDC can be used in the texturing of rolls (EDT) due to which hardness and the performance of the rolls increases and the coefficient of friction reduces.

6. Conclusion

From the present work following conclusions has been drawn:

1. It was observed that Ws₂ is successfully deposited on the Al7075 Aluminium alloy work piece.
2. Deposition rate of Ws₂ on the work piece was increasing up to 4 amp current, and after that for further increase in current deposition rate either decreased or remain same for different substrate materials.
3. Also, surface roughness increases with increase in peak current.
4. By XRD analysis it is found that, the coating contain Ws₂ and Cu, which indicate that, Ws₂ is transferred from tool electrode to the aluminium alloy substrates during EDC process. However, no specific change in composition of the coating with the change in peak current has been observed.
5. Substrate material i.e; different type of steel has significant effect on the deposition rate as well as on roughness value of the coating for different current condition.
6. In powder suspension method, further experimentation is required to deposit coating material on the substrate.

References:

- [1] Gangadhar, A., Shunmugam, M.S., Philip, P.K., 1991: Surface modification in electro discharge processing with powder compact tool electrode, *Wear* 143,45-55.
- [2] Shunmugam M.S., Philip, P.K., 1993: Improvement of wear resistance by EDM with tungsten carbide P/M electrode, *wear* 171, 1-5.
- [3] Zaw H. M, Fuh J. Y. H, 1999: Formation of a new EDM electrode material using sintering techniques, *Journal of Materials Processing Technology*, Vol. 89-90 pp.182-186.
- [4] Simao J., Aspinwall D., 2002: Surface alloying using PM composite electrode materials when electrical discharge texturing hardened AISI D2, *Journal of Materials Processing Technology* , Vol.127 pp. 211–216.
- [5] Wang Z.L, Y Fang, P.N Wu, W.S Zhao, K.Cheng, 2002 : Surface modification process by electrical discharge machining with a titanium powder green compact electrode, *Journal of Material Processing Technology*, Vol.129, pp. 139-142.
- [6] Lee H.G., Simao, J., Aspinwall, D.K., Dewes, R.C., Voice, W., 2004: Electrical discharge surface alloying, *Journal of Material Processing Technology*, 149,334-340.
- [7] Ho S.K., Aspinwall D.K., 2007: Use of powder metallurgy (PM) compacted electrodes for electrical discharge surface alloying/modification of Ti–6Al–4V alloy, *Journal of Materials Processing Technology* , Vol.191, pp.123–126.

- [8] Pichai , Apiwat 2012: Surface modification of tungsten carbide by electrical discharge coating (EDC) using a titanium powder suspension, *Journal of Applied Surface Science*, Vol. 258, pp. 7255– 7265.
- [9] Kumar S., Batra U., 2011 :Surface modification of die steel materials by EDM method using tungsten powder-mixed dielectric, Vol.14, pp. 35-40.
- [10] Furutani K., A. Saneto, H. Takezawa, N. Mohri, H. Miyake: Accretion of titanium carbide by electrical discharge machining with powder suspended in working fluid. *Precision Engineering* 25(2001),134-144.
- [11] Patowari, P.K., Mishra, U.K., Saha, P.,Mishra, P.K., 2006: Surface modification of C40 Steel using WC-Cu P/M green compact electrodes in EDM.AIMTDR Conference, IIT Roorkee, India ,pp. 875-879.
- [12] Masanta M., Shariff S.M, Choudhary A, 2011: comparative study of the tribological performances of laser clad TiB₂-TiC-Al₂O₃ composite coatings on AISI 1020 and AISI 304 substrates.
- [13] Hiroyuki, Mitsutoshi, 2006: Development of coating and cladding technology, MS coating, Vol .39.1.
- [14] Samuel M.P., Philip P.K., 1997: Powder metallurgy tool electrodes for electrical discharge machining, *Journal of Mach. Tools manufacturing*, Vol. 37-11, pp. 16251633.
- [15] Das A., Mishra J.P., 2012: Experimental investigation on surface modification of Aluminium by electric discharge coating process using TiC/Cu green compact tool electrode, *Journal of Machining science and technology*, Vol.16-4, pp.601-623.
- [16] Hwang Y, Kuo C, Hwang S, 2009: The coating of TiC layer on the surface of nickel by electric discharge coating (EDC) with a multi-layer electrode, *Journal of Materials Processing Technology*, Vol. 210, pp. 642–652. [

Prediction of Tool life on CNC Turning of Aluminium alloy 6063 using Tungsten Carbide Tools

R.Arokiadass^{a*}, D. Kaviyaran^b, N. Kumaran^c, P.Prakash^d, B. Balraj^e

^aProfessor, St.Anne's College of Engineering and Technology, Panruti, Tamil Nadu, India.
^{b,c,d,e} UG Scholar, St.Anne's College of Engineering and Technology, Panruti, Tamil Nadu, India.

Abstract

In the present study, investigate the influence of spindle speed (N), feed rate (f) and depth of cut (d) on tool life during CNC Turning of Aluminium alloy 6063 using Carbide Tools. Experiments were conducted through the Taguchi's Design of Experiments (DOE). Statistical model based on second order polynomial equation was developed for tool life. Analysis of variance (ANOVA) was carried out to identify the significant factors affecting the tool life. The surface plots were generated to study the effect of process parameters as well as their interactions.

Keywords: CNC turning, Carbide tool, Tool Life, Taguchi method, Mathematical model, Anova.

1. Introduction

Traditionally, the machinability of materials involves tool life, cutting forces, productivity or chip formation, with less attention paid to particle emission. Turning is one such machining process which is most commonly used in industry because of its ability to have faster material removal at the same time produces reasonably good surface finish quality. During turning process, higher values of cutting parameters offer opportunities for increasing output but it also involves a greater risk of deterioration of surface quality and tool life, therefore cutting speed and feed rate are two very important parameters to achieve optimum cutting conditions [1].

V. Devkumaret et.al., [2] investigated the optimal cutting conditions for attaining the better surface roughness using the mathematical modeling and analysis of machining response and tool wear in the turning of aluminum alloy 6061. There was process parameters such as spindle speed, depth of cut and feed rate used to determine the quality of surface roughness. chandra shekar et al [3] optimized the machining parameters speed, feed, depth of cut, nose radius in turning of Al 6063 T6 in CNC machine through design of experiments by taguchi method. P. Jayaraman et.al., [4] researched on multi response optimization of machining parameters such as cutting speed, feed rate, and depth of cut in turning of AA 6063 T6 using grey relational analysis in Taguchi method.

H.M. Samashekara [5] has developed regression model during machining of Al 6351-T6 Aluminium alloy with the help of uncoated carbide insert to analyze the combination of machining parameter(speed, feed, depth of cut) for better performance within selected range of machining parameter. Himanshuborade et al.,[6] optimizing the process parameter in CNC turning of Aluminium 7068 alloy using the Taguchi method with the use of multi-response criteria for grey relational analysis. B.Radhakrishnan et al.,[7] optimizing the surface roughness obtained by turning process in CNC machine using various parameters.

In this work, effects of process parameters on tool life in CNC turning of aluminium alloy 6063 by carbide tools are evaluated. A second order quadratic model is developed for predicting the tool life in CNC Turning of

aluminium alloy 6063 by response surface methodology. The predicted and measured values are fairly close to each other. Their proximity to each other indicates that the developed model can be effectively used to predict the tool life in CNC Turning of aluminium alloy 6063.

2. Experimental Details

The experiments were planned using Taguchi's orthogonal array in the design of experiments (DoE), which helps in reducing the number of experiments. The three process parameters selected in the present investigation were spindle speed, feed rate and depth of cut.

Table.1 Chemical composition of the aluminium alloy 6063

| Element | Si (%) | Fe (%) | Cu (%) | Mn (%) | Mg (%) | Zn (%) | Ti (%) | Cr (%) | Aluminium |
|---------|---------|----------|----------|----------|----------|---------|---------|--------|-----------|
| Weights | 0.2-0.6 | 0.0-0.35 | 0.0-0.10 | 0.0-0.10 | 0.45-0.9 | 0.0-0.1 | 0.0-0.1 | 0.1max | balance |

Table.2 Experimental parameters and their levels

| No | Factor | Unit | Notation | Levels | | |
|----|---------------|--------|----------|--------|------|------|
| | | | | (-1) | 0 | (+1) |
| 1 | Spindle speed | RPM | N | 1000 | 1500 | 2000 |
| 2 | Feed rate | mm/rev | f | 0.1 | 0.15 | 0.2 |
| 3 | Depth of cut | mm | d | 0.5 | 1 | 1.5 |

The machining was done on "LOKESH TL20" CNC turning machine using carbide tool. The parameters and their levels were selected is given in the Table.2. The dimension of work specimen was 25 mm diameter and 100 mm length. Experimental design using L_{27} orthogonal array and results are listed in Table 3.

Table.3 Experimental design using L_{27} orthogonal array and results

| Sl.No. | Spindle speed (N), RPM | Feed rate (f), mm/rev | Depth of cut (d), mm | Tool Life (T), mins |
|--------|------------------------|-----------------------|----------------------|---------------------|
| 1 | 1000 | 0.1 | 0.5 | 95.48 |
| 2 | 1000 | 0.1 | 1 | 69.68 |
| 3 | 1000 | 0.1 | 1.5 | 57.95 |
| 4 | 1000 | 0.15 | 0.5 | 44.68 |
| 5 | 1000 | 0.15 | 1 | 33.34 |
| 6 | 1000 | 0.15 | 1.5 | 27.73 |
| 7 | 1000 | 0.2 | 0.5 | 27.08 |
| 8 | 1000 | 0.2 | 1 | 19.76 |
| 9 | 1000 | 0.2 | 1.5 | 16.43 |
| 10 | 1500 | 0.1 | 0.5 | 27.95 |
| 11 | 1500 | 0.1 | 1 | 20.39 |
| 12 | 1500 | 0.1 | 1.5 | 16.96 |
| 13 | 1500 | 0.15 | 0.5 | 13.37 |
| 14 | 1500 | 0.15 | 1 | 9.76 |
| 15 | 1500 | 0.15 | 1.5 | 8.11 |

| | | | | |
|----|------|------|-----|-------|
| 16 | 1500 | 0.2 | 0.5 | 7.92 |
| 17 | 1500 | 0.2 | 1 | 5.78 |
| 18 | 1500 | 0.2 | 1.5 | 4.81 |
| 19 | 2000 | 0.1 | 0.5 | 11.69 |
| 20 | 2000 | 0.1 | 1 | 8.53 |
| 21 | 2000 | 0.1 | 1.5 | 7.09 |
| 22 | 2000 | 0.15 | 0.5 | 5.59 |
| 23 | 2000 | 0.15 | 1 | 4.08 |
| 24 | 2000 | 0.15 | 1.5 | 3.39 |
| 25 | 2000 | 0.2 | 0.5 | 3.31 |
| 26 | 2000 | 0.2 | 1 | 2.42 |
| 27 | 2000 | 0.2 | 1.5 | 2.01 |

The tool life was calculated using the formulae.

$$\text{Tool life} = \left(\frac{80}{V \times f^{n1} \times d^{n2}} \right)^{\frac{1}{n}} \text{ in mins} \text{-----(2)}$$

Where,

V = Cutting speed in m/min

f = Feed in mm/rev

d = Depth of cut in mm

T = Tool life in min

n = Tool constant for Tungsten carbide– 0.33(from toolmanufacturer's data book)

n1= feed exponent constant – 0.6 (from toolmanufacturer's data book)

n2 =depth of cut exponent constant- 0.15 (from toolmanufacturer's data book)

C= constant- 80 (from tool manufacturer's databook)

3. Results and Discussion

Tool life plays a predominant role in determining the machining accuracy and control the machining cost. The study of tool life characteristics of aluminium alloy 6063 dependent on many factors, it is more influenced by the process parameters like spindle speed, feed rate and depth of cut, etc., for a given machine tool and work piece set-up. The influence of different process parameters in CNC Turning of aluminium alloy 6063 can be studied by using response graph and response table. The influence of process parameters on surfaces roughness is shown in Figure 1.

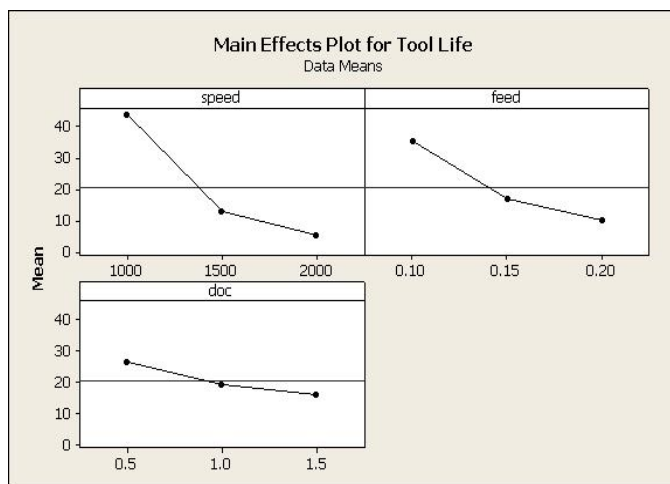


FIG1: Effect plot for Tool life.

The observed tool life increases at low spindle speed as compared to the high spindle speed. Also, tool life increases at low feed rate when compared to the high feed rate. The effect of depth of cut on CNC turning of aluminium alloy 6063 is less on tool life. The response table for tool life shows the effect of different process parameters, which is shown in Table. 4. From the table, it can be found that the spindle speed is the main parameters which affect the tool life followed by feed rate and depth of cut.

Table.4 Response table for Tool life

| Level | Spindle speed, N (RPM) | Feed rate, f (mm/rev) | Depth of cut, d (mm) |
|-------------|------------------------|-------------------------|----------------------|
| 1 | 31.46 | 27.60 | 24.18 |
| 2 | 20.78 | 21.20 | 21.44 |
| 3 | 13.21 | 16.66 | 19.84 |
| Delta | 18.24 | 10.95 | 4.34 |
| Rank | 1 | 2 | 3 |

The experimental values are analyzed using response surface analysis and the following relation has been established for Tool life in uncoded units as:

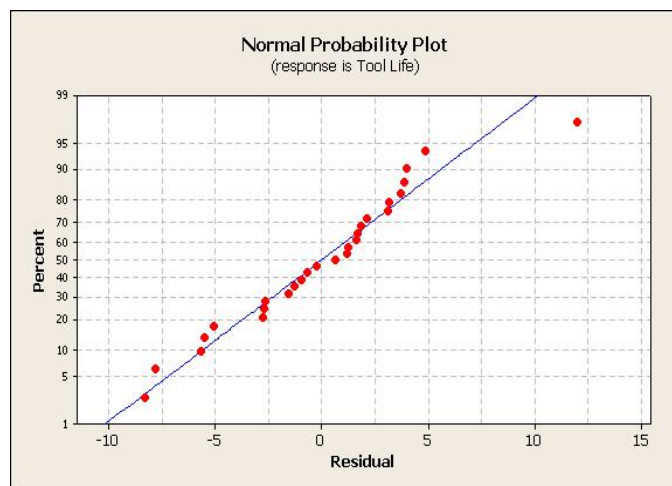
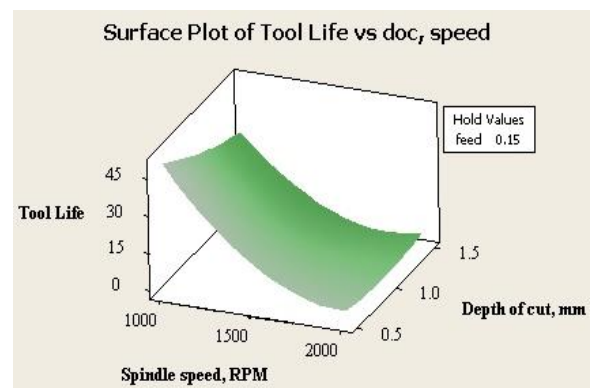
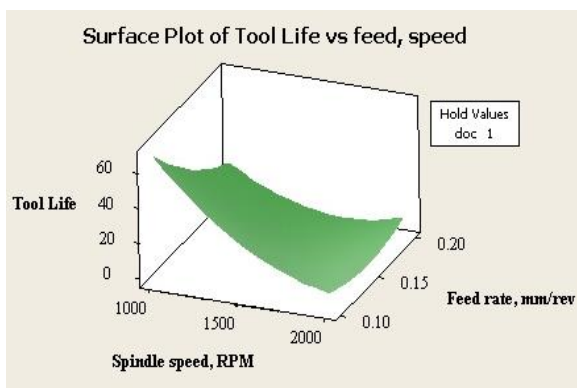
$$\begin{aligned}
 \text{tool life} = & 431.4 - 0.2686 \text{ speed} - 1767 \text{ feed} - 74.0 \text{ depth} + 0.000047 \text{ speed} * \text{speed} \\
 & + 2292 \text{ feed} * \text{feed} + 7.80 \text{ depth} * \text{depth} + 0.4676 \text{ speed} * \text{feed} + 0.01935 \text{ speed} * \text{depth} \\
 & + 126.8 \text{ feed} * \text{depth} \text{ -----(1)}
 \end{aligned}$$

A result of ANOVA for the response function Tool life is presented in Table 5. This analysis is carried out for a level of significance of 5% i.e., for a level of confidence of 95%. From the table, it is apparent that, the F calculated value is greater than the F-table value ($F_{0.05, 9, 17} = 2.49$) and hence the second order response function developed is quite adequate.

Table 5: ANOVA for the response function of the Tool life

| Source of variation | Degree of freedom | Sum of squares | Mean sum of squares | F value | p value |
|---------------------|-------------------|----------------|---------------------|---------|---------|
| Regression | 9 | 12969.2 | 1441.02 | 49.53 | 0.000 |
| Residual Error | 17 | 494.6 | 29.09 | | |
| Total | 26 | 13463.8 | | | |

The plot of normal probability of the residual, the plots of the residuals versus the fitted values for tool life is shown in figure. 2. From figure 2, it is evident that the data are spread roughly along the straight line. Hence it is concluded that the data are normally distributed. Hence, the developed model is significant & adequate.

**FIG 2: Normal Probability plot for Tool life**

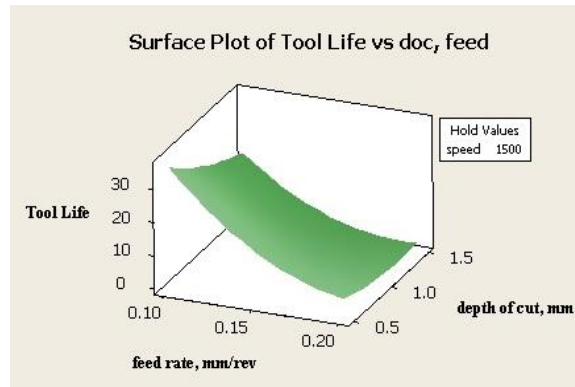


FIG: 3 Surface plots for Tool life (T), mins

Surface plots were drawn for different combination of process parameters, which is shown in figure. 3. These response surfaces can help in the prediction of the toll life at any zone of the experimental domain. It is clear from these figures that the tool life increases with the decrease of spindle speed and it decreases with the decreases of feed rate. Figure 3 shows the experimental values and their corresponding predicted values through Eq. (1). From the analysis of figure, it can be observed that the predicted values were very close to the experimental results.

4. Conclusions

The tool life in the CNC turning process has been measured for machining of aluminium alloy 6063 under different cutting conditions with a carbide tools using L_{27} Taguchi's orthogonal array. Based on the experimental and analytical results the following conclusions are drawn.

1. The developed second-order response surface model can be used to calculate the tool life of tungsten carbide tool at different cutting conditions with the chosen range with 95% confidence intervals. Using such model, one can obtain remarkable savings in time and cost.
2. From the results, it can be asserted that low spindle speed, low feed rate and moderate depth of cut are preferred for machining of aluminium alloy 6063.
3. The Spindle speed is the dominant parameter which affects the tool life of aluminium alloy 6063 followed by feed rate. Depth of cut shows a minimal effect on surface roughness compared to other process parameters.
4. From the developed mathematical model, the optimal machining parametric combination, i.e., spindle speed (N) 1000 rpm, feed rate (f) 0.10 mm/rev and depth of cut (d) 0.50 mm was found out to achieve the maximum tool life as 95.48 mins.

References

- [1] Rosemar B. da Silva a,*, Álisson R. Machado, “Tool life and wear mechanisms in high speed machining of Ti–6Al–4V alloy with PCD tools under various coolant pressures”, *Journal of Materials Processing Technology* 213, 2013, pp.1459– 1464.
- [2] V. Devkumar, e. Sreedhar, m.p. Prabakaran , optimization of machining parameters on al 6061alloy using response surface methodology , 2015, pp. 01-04
- [3] Chandra shekar, n b d pattar, y vijaya kumar, optimization of machining parameters in turning of al6063t6 through design of experiments , *international journal of mechanical engineering and technology*, 2016, pp.96–104.
- [4] P. Jayaraman, l. Mahesh kumar, multi-response optimization of machining parameters of turning aa6063 t6 aluminium alloy using grey relational analysis in taguchi method, *procedia engineering* 97, 2014, pp.197 –204.
- [5] H. M. Somashekara, “Optimizing Surface Roughness in Turning Operation Using Taguchi Technique and ANOVA”, *International Journal of Engineering Science and Technology*, 2012, pp. 1967-1973.
- [6] Himanshuborade, Amit Telang and Sanjay soni, Multi objective optimization of process parameters in turning of aluminium 7068 using taguchi based grey relational analysis, *International Journal of Mechanical and Production Engineering Research and Development*, 2020, pp.263–274.
- [7] B.Radhakrishnan, S.Tharun Kumar, P.Sankarlal, P.Ramakrishnan and S.Sarankumar, optimization of cnc machining parameters for surface roughness in turning of aluminium 6063 T6 with response surface methodology, *International journal of Mechanical Engineering*, 2017, pp.23-31.

A Comparative Account of Antioxidants Activity of Ethyl Acetate, Methanolic and Aquaous Extract of Leaves and Bark of *Baccaurea Ramiflora* (Lour.) by Synthesis of Gold Nanoparticles and Other Method

Mehebab Ali Khan, Ismail Sk*, Md. Akhtarul Alam*

Department of Chemistry, Aliah University, IIA/27, Action Area II, Newtown, Kolkata-700160

Corresponding authors: alam_iitg@yahoo.com, sk.ismail10@gmail.com

Abstract

In this work we have find out the antioxidants activity of the ethyl acetate, methanolic and aquaous extract of leaves and bark of *Baccaurea ramiflora* (Lour.). The antioxidant activity of the extracts was measured by in vitro chemical analyses involving the assays of (1) Au nanoparticle formation potential (2) 1,1-diphenyl-2-picrylhydrazyl (DPPH) radical scavenging activity (3) ferric ion reducing power and (4) ferrous ion chelating activity. A simpler method has been created based on Au nanoparticles formation to assess the antioxidant activity of any plant extract. It was for the assessment of the antioxidant activity of all the extract of leaves and bark of *Baccaurea ramiflora* (Lour.). In all the assays, methanolic extract of leaves of *Baccaurea ramiflora* (MEBRL) and methanolic extract of bark of *Baccaurea ramiflora* (MEBRB) showed significantly greater activity over other extracts. This work provides a scientific support for the high antioxidant activity of this plant and thus it may find potential applications in the treatment of the diseases caused by ROS.

Keywords: Antioxidants, *Baccaurea ramiflora* (Lour.), DPPH, Gold Nanoparticles(AuNps), MEBRL, MEBRB

1. Introduction

Free radicals, e.g. various reactive oxygen species (ROS), are allways produced during cellular metabolism in living systems and them because a number of oxidative stresses related disorders in human beings, such as atherosclerosis, ageing, cancer and cardiovascular diseases [1-4]. Natural antioxidants put a wall against the damages of the cellular organelles caused by free radical induced oxidative stress [5]. Apart from this, antioxidants also control the nutritional quality of the foods by reducing the nutritional loss and preventing the formation of harmful substances during the storage of the food. Various studies also suggest that a predominantly plant based diet reduces the risk of free radical induced diseases [6]. So, the scientist found it challenging to screen the plants on the basis of their antioxidant activity. Large numbers of medicinal plants have been registered for their antioxidant activities and the results proves that either their raw extracts or their individual chemical constituents are more effective antioxidants (in vitro) than the synthetic antioxidants, e.g. butylated hydroxyl anisole (BHA), butylated hydroxyl toluene (BHT) or vitamin E [7-9]. Moreover, these synthetic antioxidants, e.g. butylated hydroxyl anisole (BHA), butylated hydroxyl toluene (BHT) etc., may have carcinogenic and other harmful effects on the lungs and livers [10-12]. So, scientists are continuously involved to find out naturally occurring potential and non-toxic antioxidants, which could prevent this free radical related disorders in human beings and also can replace the harmful synthetic antioxidants[10-12].The Indian medicinal plants which are traditionally used as an integral part of Indian Ayurveda, can be the potential sources for various naturally occurring non-toxic antioxidants.

In our experiments we have found out the antioxidants activity of the ethyl acetate, methanolic and aqua extract of leaves and bark of *Baccaurea ramiflora* (Lour.). *Baccaurea ramiflora* (Lour.), (family: Euphorbiaceae) is a tree that grows slowly and evergreen could reach up to the height of 25 m, has spreading crown and thin bark. The fruit of *B. ramiflora* is yellow to red in color. We can find this tree in the Southeast Asian region and it also grows wild as well as under cultivation in Nepal, India, Myanmar, South China, Indo-China, Thailand, the Andaman Islands and Peninsular Malaysia. It mainly grows in evergreen forests. Latkan or Bhubi (Bengali), Leteku (Hindi), Mafai (Thai) and Burmese grape (English)[13-14] are the common names of this tree. In the traditional Chinese Dai medicine, the whole plant of *B. ramiflora* is used as an antiphlogistic and anodyne against rheumatoid arthritis, cellulitis, and abscesses and to treat injuries [15]. In Northern Thailand the plant is also used as medicine by hill-tribes [16]. Young leaves of *B. ramiflora* are used as vegetable, flavoring agent with curries and minced meat in Bangladesh [17]. In India, fresh bark is chewed or juice is used orally for constipation. That is why; we have chosen the leaf and bark of *B. ramiflora* as our research work.

The objective of the present study is to explore the antioxidant activity of the ethyl acetate, methanolic and aqua extract of leaves and bark of *Baccaurea ramiflora* (Lour.). *Baccaurea ramiflora* (Lour.), (family: Euphorbiaceae). The leaves and bark of this plant is selected because it is easily available throughout the year and the collection of the leaves and bark do not destroy the parent plant. Here we have used four different in vitro chemical assays (1) gold (Au) nanoparticle formation potential assay (2)1,1- diphenyl-2-picrylhydrazyl

(DPPH) radical scavenging activity assay (3) ferric ion reducing antioxidant power assay and (4) ferrous ion chelating activity assay. We have found in our work a detailed assay of the antioxidant activity of two parts of different extracts of this plant. We also used a simple method to assess the antioxidant activity of any plant extract by its ability to form Au nanoparticles and this method is exploited to estimate the antioxidant activity of the ethyl acetate, methanolic and aqua extract of leaves and bark of *Baccaurea ramiflora* (Lour.) The total polyphenol and flavonoid contents of the ethyl acetate, methanolic and aqua extract of leaves and bark of *Baccaurea ramiflora* (Lour.) were also measured according to the standard methods [18-21] and these values were correlated to the antioxidant activity of these extracts. cellular metabolism in living systems and them because a number of oxidative stresses related disorders in human beings, such as atherosclerosis, ageing, cancer and cardiovascular diseases [1-4]. Natural antioxidants put a wall against the damages of the cellular organelles caused by free radical induced oxidative stress [5]. Apart from this, antioxidants also control the nutritional quality of the foods by reducing the nutritional loss and preventing the formation of harmful substances during the storage of the food. Various studies also suggest that a predominantly plant based diet reduces the risk of free radical induced diseases [6]. So, the scientist found it challenging to screen the plants on the basis of their antioxidant activity. Large numbers of medicinal plants have been registered for their antioxidant activities and the results proves that either their raw extracts or their individual chemical constituents are more effective antioxidants (in vitro) than the synthetic antioxidants, e.g. butylated hydroxyl anisole (BHA), butylated hydroxyl toluene (BHT) or vitamin E [7-9]. Moreover, these synthetic antioxidants, e.g. butylated hydroxyl anisole (BHA), butylated hydroxyl toluene (BHT) etc., may have carcinogenic and other harmful effects on the lungs and livers [10-12]. So, scientists are continuously involved to find out naturally occurring potential and non-toxic antioxidants, which could prevent this free radical related disorders in human beings and also can replace the harmful synthetic antioxidants [10-12]. The Indian medicinal plants which are traditionally used as an integral part of Indian Ayurveda, can be the potential sources for various naturally occurring non-toxic antioxidants.

In our experiments we have found out the antioxidants activity of the ethyl acetate, methanolic and aqua extract of leaves and bark of *Baccaurea ramiflora* (Lour.). *Baccaurea ramiflora* (Lour.), (family: Euphorbiaceae) is a tree that grows slowly and evergreen could reach up to the height of 25 m, has spreading crown and thin bark. The fruit of *B. ramiflora* is yellow to red in color. We can find this tree in the Southeast Asian region and it also grows wild as well as under cultivation in Nepal, India, Myanmar, South China, Indo-China, Thailand, the Andaman Islands and Peninsular Malaysia. It mainly grows in evergreen forests. Latkan or Bhubi (Bengali), Leteku (Hindi), Mafai (Thai) and Burmese grape (English) [13-14] are the common names of this tree. In the traditional Chinese Dai medicine, the whole plant of *B. ramiflora* is used as an antiphlogistic and anodyne against rheumatoid arthritis, cellulitis, and abscesses and to treat injuries [15]. In Northern Thailand the plant is also used as medicine by hill-tribes [16]. Young leaves of *B. ramiflora* are used as vegetable, flavoring agent with curries and minced meat in Bangladesh [17]. In India, fresh bark is chewed or juice is used orally for constipation. That is why; we have chosen the leaf and bark of *B. ramiflora* as our research work.

The objective of the present study is to explore the antioxidant activity of the ethyl acetate, methanolic and aqua extract of leaves and bark of *Baccaurea ramiflora* (Lour.). *Baccaurea ramiflora* (Lour.), (family: Euphorbiaceae). The leaves and bark of this plant is selected because it is easily available throughout the year and the collection of the leaves and bark do not destroy the parent plant. Here we have used four different in vitro chemical assays (1) gold (Au) nanoparticle formation potential assay (2) 1,1-diphenyl-2-picrylhydrazyl (DPPH) radical scavenging activity assay (3) ferric ion reducing antioxidant power assay and (4) ferrous ion chelating activity assay. We have found in our work a detailed assay of the antioxidant activity of two parts of different extracts of this plant. We also used a simple method to assess the antioxidant activity of any plant extract by its ability to form Au nanoparticles and this method is exploited to estimate the antioxidant activity of the ethyl acetate, methanolic and aqua extract of leaves and bark of *Baccaurea ramiflora* (Lour.) The total polyphenol and flavonoid contents of the ethyl acetate, methanolic and aqua extract of leaves and bark of *Baccaurea ramiflora* (Lour.) were also measured according to the standard methods [18-21] and these values were correlated to the antioxidant activity of these extracts.

2. Materials and Methods

2.1 Chemicals

Folin–Ciocalteu reagent, gallic acid, quercetin, DPPH, trichloroacetic acid, ascorbic acid, methanol and ethyl acetate have been purchased from Sigma Aldrich. All other chemicals used for the study were of analytical grade and obtained from MERK, India. Double distilled water has been used for all the analyses. Chloroauric

acid (HAuCl₄) (Sigma Aldrich,) have been used as the source of Au (III) ions required for the synthesis of Au nanoparticles.

2.2 Collection and preparation for stock

At first, Leaves and bark of *Baccaurea ramiflora* (Lour.) have been collected from local area of Alipuarduar, West Bengal, India. Then these are washed with distilled water and dried under shade. Next, the dry leaves and the barks have been grinded and stored into an air tight container for further use. All chemicals/reagents we have used in the study were of analytical grade and have been purchased from Merck and Sigma-Aldrich Chemical Company. All reagents and spectroscopic grade solvents have been used as we have received from commercial sources without further purification. Aqueous medium experiments have been done in deionized water.

2.3 Preparation of leaf and bark extract

The leaves and barks extract have been prepared using the dried leaves and bark of *Baccaurea ramiflora* (Lour.). About 100 gm of each dried leaves and bark have been taken into a 1 litre round bottom flask and about 300ml of deionized water, 300ml of methanol and 300ml of ethyl acetate have been added and refluxed for 8 hr. The insoluble materials have been filtered off. The filtrate was then made to freeze-dry and a semi-solid was obtained from it. The semi-solid mass was stored at 4 °C for further use.

3. Results and Discussion

3.1 Estimation of total phenols and flavonoid content

The method we have used for the determination of total phenols using Folin Ciocalteu reagent and gallic acid as standard using the reported procedure. Total phenol values are expressed as gallic acid equivalents per gram of dry mass. The aluminum chloride colorimetric method was used for flavonoid content determination of leaves and bark of *Baccaurea ramiflora* (Lour.) extract quercetin (standard) solutions by following the reported procedure [22]. The total flavonoid content in these extracts was expressed in terms of milligram of quercetin equivalent per gram of dry mass. Interestingly, MEBRL and MEBRB have higher polyphenol flavonoid content.

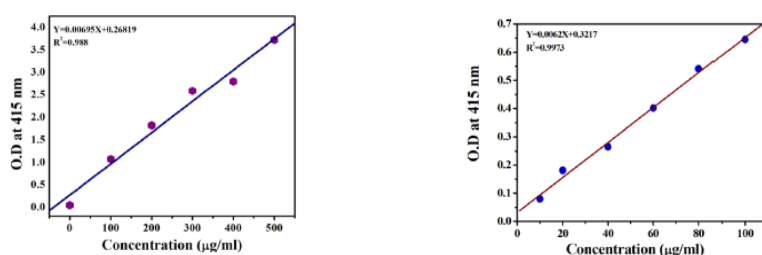


Figure 1: Calibration curve of (a) polyphenol content (Gallic Acid) and (b) flavonoid content (Quercetin)

Table 1: Polyphenol and Flavonoid content of the all Extracts

| sample | EEBRL | MEBRL | AEBRL | EERBB | MEBRB | AEBRB |
|---|------------|------------|------------|------------|------------|------------|
| Polyphenol content (mg GAE g ⁻¹) | 37.33±0.27 | 58.69±0.14 | 48.86±0.15 | 25.63±0.12 | 49.62±0.18 | 38.93±0.22 |
| Flavonoid content (mg QE g ⁻¹) | 18.14±0.16 | 33.32±0.21 | 4.14±0.28 | 12.83±0.22 | 27.33±0.26 | 2.40±0.25 |

3.2 Au nanoparticles formation potential based antioxidant assays

The antioxidant activity of the extracts has been measured from their ability to generate and stabilize Au nanoparticles. Here we have simplified the methods of Scampiccho et al. and Wang et al. [23-24]. Sample solutions of different concentrations ($100\mu\text{g ml}^{-1}$ to $800\mu\text{g ml}^{-1}$) have been prepared separately by dissolving the appropriate quantities of gummy masses obtained from the extracts in distilled water. To 10ml of this sample solution, $250\mu\text{L}$ of $0.1\text{ M aq. H AuCl}_4$ solution have been added followed by continuous stirring and heating at 45°C for 10 minutes; whereby a pink coloration was observed which is the indication of the onset of formation of Au nanoparticles. The progress of the reaction was monitored by measuring the absorbance of the solution in the range of 500-700 nm at regular interval of time. For the calibration of the standard, aqueous extract of amla (AEA) of the same concentration range have been used. The results are expressed as the milligram of AEA per gram of dry mass of the sample extracts.

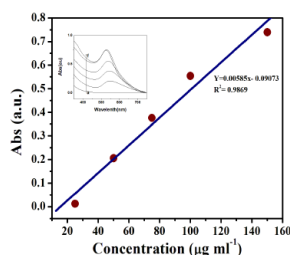


Figure 2: Calibration curve of the standard compound of aqueous extract of amla (AEA).

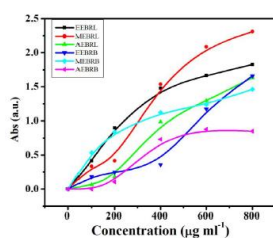


Figure 3: Plotting of absorbance maxima vs. different concentrations. of Au nanoparticle solutions formed after a 10-min reaction at 45°C .

Table 2: AuNps formation potential of the all Extracts

| Sample | AuNps formation potential (mg AEA/gm) |
|--------|---------------------------------------|
| EEERL | 449.475 ± 6.350 |
| MEERL | 596.329 ± 7.456 |
| AEERL | 379.286 ± 5.382 |
| EEERB | 341.899 ± 6.341 |
| MEERB | 479.023 ± 5.842 |
| AEERB | 238.710 ± 4.564 |

3.3 DPPH radical scavenging activity

The free radical scavenging activities of the all extracts have been evaluated through their ability to quench the synthetic DPPH radical. DPPH has been used to determine free radical scavenging activities of the all extracts by using standard method[25]. DPPH is a stable free radical and accepts an electron or hydrogen radical to become a stable diamagnetic molecule. The methodology involves reaction of specific compound or extract with DPPH in methanol solution. In the presence of hydrogen donors, DPPH is reduced and a free radical is formed from the scavenger. The reaction of DPPH is monitored by measuring the decrease of the absorbance of its radical at 517 nm. Upon reduction of this radical by an antioxidant, the absorbance at 517 nm disappears.

IC₅₀ value of MEBRL was 68.32µg ml⁻¹ while that of MEBRB is 47.61µg ml⁻¹. Both of these two values are comparable with the IC₅₀ value of the standard compound, Gallic acid; which has been found to be 15.98µg ml⁻¹. Thus MEBRL and MEBRB showed higher radical scavenging activity than that of other extracts. Moreover, both of these two values are significantly lower than that of some Indian green leafy vegetables [26].

Table 3: IC₅₀ value of all the extracts and standard compound

| Sample | EEBR L | MEBR L | AEBRL | EEBRB | MEBRB | AEBR B | Gallic Acid |
|--|-------------|-------------|-------------|-------------|-------------|-------------|----------------|
| DPPH Scavenging Ability (IC ₅₀ , µg/ml) | 37.38 ±2.68 | 68.32± 2.28 | 41.21±1 .63 | 29.06±2. 03 | 47.61±2 .21 | 43.19± 2.74 | 15.98± 3.65 |

The higher activity of MEBRL and MEBRB was probably due to its higher polyphenol content and also due to the better solubility of its polyphenol constituents in methanol. The difference in antioxidant activities of these extracts can be attributed to the presence of different types of flavonoids compounds for showing antioxidant activity [27]

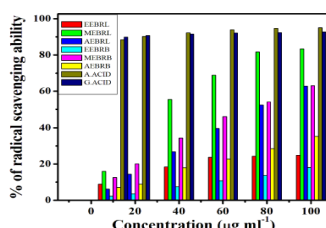


Figure 4: DPPH radical scavenging activities of all extracts, ascorbic acid and gallic acid (standard) solutions at different concentrations. All data are reported as mean± S.D. (n=3).

3.4 Ferric reducing antioxidant power assay

Reducing power of a compound is also a supporting feature for its antioxidant activity. Reducing power characteristics of the all extracts and ascorbic acid (standard compound) are given in Fig.5. The concentration dependent reducing power followed the order of: ascorbic acid > MEBRB > other. At lower concentration region, MEBRL showed slightly higher reducing power, but as a whole MEBRB had higher reducing activity. This may be due to the higher polyphenol content of this extract. Because being good electron donor, phenolic compounds have the ability to convert Fe³⁺ to Fe²⁺ and hence show higher reducing activity.

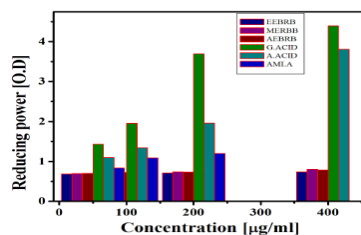


Figure 5: Reducing power of all extracts, galic acid and ascorbic acid (standard) solutions at different concentrations (0 to 400µg ml⁻¹).

Table 4: EC₅₀ value of all extracts

| Sample | EEBRL | MEBRL | AEBRL | EEERB | MEERB | AEERB |
|---------------------------------------|------------------|-------------------|------------------|-------------------|-------------------|------------------|
| FRAP (EC ₅₀ , µg/ml) | 469.222 ±8.22 | 1017.50 5±8.76 | 712.281±8 .32 | 1369.497± 7.01 | 1512.424 ±7.94 | 748.892± 5.33 |

3.5 Ferrous ion chelating activity assay

Fe²⁺ ions are abundant in foods and it is a well known and effective pro-oxidant which catalyses various oxidation reactions in biological systems [28]. Ferrous ion chelating activity assay of any extract or any compound actually measures the capacity of that extract or that compound to bind the Fe²⁺ ion. 1, 10-phenanthroline can quantitatively bind with Fe²⁺ to form a stable complex which is colored red and has the absorbance maximum at 510 nm. The absorbance of this complex at 510 nm steadily decreases with the increase of the chelating activity of chelating agents.

In our case, a concentration dependant chelating activity was noticed for all the extracts and also for the EDTA (standard) solutions as shown in fig.6. The chelating activity of EDTA is significantly higher than that of all the extracts. *T-Test* revealed that chelating activity of MEERB is significantly higher than that of others (*P*=0.00).

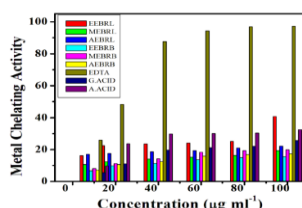


Figure 6: Fe²⁺ion chelating activities of all extracts, galic acid, ascorbic acid and EDTA (standard) solutions at different concentrations (10-100 µg ml⁻¹). All data are reported as mean± S.D. (n=3).

4. Conclusions

In all the assay systems, it was found that methanolic extract of leaves (MEBRL) and bark of *Baccaurea ramiflora*(MEERB) showed higher antioxidant activity over other extracts. But both these high polyphenol and flavonoid contents than those of others. So in addition to polyphenol and flavonoids, there must be some other non-phenolic components (may be reducing sugars) present in these extracts which also are responsible for its antioxidant activity. Our observations may enhance the potential application of methanolic extract of leaves and bark of *Baccaurea ramiflora*(L.)as antioxidant in various pharmaceutical products.

Moreover, this extract is always more bio-friendly than any other organic solvent extracts. So MEBRL and MEBRB may be a well substitute of other and can be explored for its applications in the prevention of free radical related diseases. Moreover, the high antioxidant activity of these plant extracts may be explored in controlling the nutritional quality of the foods by reducing the nutritional loss and preventing the formation of harmful substances during the storage of the food.

Acknowledgement

MAK likes to thank UGC for MANF. MAA likes to thank DST. Govt. of West Bengal, India (project No.376(Sanc.)/ST/P/S&T/9G-16/2013) for financial support.

References

- [1] B.A. Freeman, Biological sites and mechanism of free radical production. In: Free radicals in molecular biology aging and disease, New York, USA:Raven Press, pp. 43–52, 1984.
- [2] M. R. Moein, S. Moein, S. Ahmadizadeh, Radical scavenging and reducing power of *Salvia mirzayanii* subfractions, *Molecules*, vol. 13, pp. 2804–2813, 2008.
- [3] A.Singh, Physicochemical and physiological aspects. In: CRC handbook of free radicals and antioxidants in biomedicine Boca Raton, Florida, USA: CRC Press Inc, vol. 1, pp. 123–126, 1989
- [4] G. L. Squadrito, W. A. Pryor, Oxidative chemistry of nitric oxide: The roles of superoxide, peroxynitrite, and carbon dioxide, *Free Radical Biology and Medicine*, vol. 25, pp. 392–403, 1998.
- [5] Y. Quinming, P. Xianhui, K. Weibao, Y. Hong, S. Yidan, Li. Zhang, Antioxidant activities of malt extract from barley (*Hordeum vulgare* L.) towards various oxidative stress in-vitro and in-vivo, *Food Chemistry*, vol. 118, pp. 84–89. 2010.
- [6] S. L. Halvorsen, K. Holte, M. C. W. Muhrstand, I. Barikmo, E. Hvattum, S.F. Remberg, Systematic screening of total antioxidants in dietary plants, *Journal of Nutrition*, vol. 132, pp. 461–471, 2002.
- [7] M. H.Gordon, X. C.Weng, Antioxidant properties of extracts from Tanshen (*Salvia miltiorrhiza* Bunge), *Food Chemistry*, vol. 44, pp. 119–122, 1992.
- [8] L. W. Gu, X. C. Weng, Antioxidant activity and components of *Salvia plebeia* R. Br. – a Chinese herb, *Food Chemistry*, vol. 73, pp. 299–305, 2001.
- [9] Y. H. Pyo, T. C. Lee, L. Logendrac, R. T. Rosen, Antioxidant activity and phenolic compounds of Swiss chard (*Beta vulgaris* subspecies *Cyca*) extracts, *Food Chemistry*, vol. pp. 85, 19–26, 2004.
- [10] A.L. Branen, Toxicology and biochemistry of butylated hydroxyanisole and butylated hydroxytoluene, *Journal American Oil Chemists' Society*, vol. 52, pp. 59–63, 1975.
- [11] H. C. Grice, Safety evaluation of butylated hydroxytoluene (BHT) in the liver, lung and gastrointestinal tract, *Food and Chemical Toxicology*, vol. 24, pp. 1127–1130, 1986.
- [12] H. P. Wichi, Enhanced tumor development by butylated hydroxyanisole (BHA) from the perspective of effect on forestomach and oesophageal squamous epithelium. *Food and Chemical Toxicology*, vol. 26, pp. 717–723, 1988.
- [13] B. Khan, Encyclopedia of Flora and Fauna of Bangladesh. Asiatic Society of Bangladesh, Dhaka, Edition1, Vol. 7, pp. 392-393, 2008
- [14] SV. Hoang, B. Pieter, PJA. Keßler, Uses and Conservation of Plant Species in a National Park- A Case Study of Ben En, Vietnam. *Economic Botany*, vol. 62(4) pp. 574–593, 2008.
- [15] YF. Lin, Z. Yi, YH. Zhao, Chinese Dai Medicine Colorful Illustrations. Yunnan Nationality Press, First Edition, 2003.
- [16] XW.Yang, JS.Wang, YL.Ma, HT. Xiao, YQ. Zuo, H. Lin, HP.He, L.Li, XJ. Hao, Bioactive Phenols from the Leaves of *Baccaurea ramiflora*. *Planta Medica*, vol. 73 pp. 1415-1417, 2007.
- [17] SMR. Hasan, MM.Hossain, R. Akter, M. Jamila, MEH. Mazumder, S. Rahman, DPPH free radical scavenging activity of some Bangladeshi medicinal plants, *Journal of Medicinal Plants Research*, vol. 3(11) pp. 875-879, 2009.
- [18] C. Chang, M. Yang, H. Wen, J. Chern, Estimation of total flavonoid content in propolis by two complementary colorimetric methods, *Journal of Food and Drug Analysis*, vol. 10, pp. 178–182, 2002.
- [19] S. Mcdonald, P. D. Prenzler, M. Autolovich, K. Robards, Phenolic content and antioxidant activity of olive extracts, *Food Chemistry*, vol. 73, pp. 73–84, 2001.
- [20] R. A. Laskar, I. Sk, N. Roy, N. A.Begum, Antioxidant activity of Indian propolis and its chemical constituents, *Food Chemistry*, vol. 122, pp. 233–237, 2010.
- [21] N.Roy, S.Mondal, R. A. Laskar, S. Basu, D. Mandal, N. A. Begum, Biogenic synthesis of Au and Ag nanoparticles by Indian propolis and its constituents, *Colloids and Surfaces B: Biointerfaces*, vol.76, pp.317–325, 2010.

- [22] C. Chang, M. Yang, H. Wen, J. Chern, Estimation of total flavonoid content in propolis by two complementary colorimetric methods, *J. Food and Drug Analysis*, vol.10, pp. 178-182, 2002.
- [23] M. Scampicchio, J. Wang, A.J. Blasco, A.S. Arribas, S. Mannino, A. Escarpa, Nanoparticle-based assays of antioxidant activity, *Analytical Chem*, vol. 78, pp. 2060-2063, 2006.
- [24] J. Wang, N. Zhou, Z. Zhu, J. Huang, G. Li, Detection of flavonoids and assay for their antioxidant activity based on enlargement of gold nanoparticles, *Analytical and Bioanalytical Chemistry*, vol. 388, pp.1199-1205, 2007.
- [25] I.I.Koleva, T. A. van Beek, J. P. H. Linssen, A. De Groot, L. N. Evstatieva, Screening of plant extracts for antioxidant activity:A comparative study on three testing methods, *Phytochemical Analysis*, vol.13, pp.8-17, 2002.
- [26] S. Gupta, J. Prakash, Studies on Indian green leafy vegetables for their antioxidant activity, *Plant foods and Human Nutrition*, vol. 64 pp. 39-45, 2009.
- [27] D. Zielinska, D. Szawara-Nowak, A. Ornatowska, W. Wiczkowski, Use of Cyclic Voltammetry, Photochemiluminescence, and Spectrophotometric Methods for the Measurement of the Antioxidant Capacity of Buckwheat Sprouts, *J. Agric. Food Chem*, vol. 55, pp.9891–9898, 2007.
- [28] M.Y. Shon, S.D. Choi, G.G. Kahng, S.H. Nam, N.J. Sung, Antimutagenic, antioxidant and free radical scavenging activity of ethyl acetate extracts from white, yellow and red onions, *Food and Chemical Toxicology*, vol.42 659–666, 2004.

Correlation Studies in Fibre Reinforced Medium Strength Concrete

Regina Mary.I¹, Dr.Bhagavathy Pushpa.T²

¹Assistant Professor, Department of Civil Engineering, Mount Zion College of Engineering & Technology, Pudukkottai, Tamil Nadu.

²Assistant Professor, Department of Civil Engineering, University College of Engineering, Ramanathapuram, TamilNadu.

Abstract

Concrete is very strong in compression but weak in tension. To make up the tensile stresses steel is reinforced in concrete. As such fibre reinforced concrete directly enhances the usage of fibres randomly in concrete emerged as a rapid trend. Lot of researches have been done in steel fibre reinforced concrete. In this paper an attempt has been made to study the usage of lathe scrap in medium strength concrete. The fresh and hardened properties of concrete reinforced with 0%,0.5%,1%,1.5% and 2% of lathe scrap were studied. Based on the test results of mechanical properties of Fibre Reinforced Concrete the strength increases upto 1.5% addition of lathe scrap. The empirical relation between split tensile strength and compressive strength of Fibre Reinforced Concrete (FRC) was derived and the relation was compared with the predicted equation of previous literatures. The results predicted from the correlation studies coincides with the models obtained from various author works and the percentage of discrepancies fall below 5%.

Keywords: *Lathe scrap, fibre reinforced concrete, correlation, split tensile strength, compressive strength.*

1 Introduction

With the increase in population demands and needs of the population increase. The increase in the demands for construction industry many new materials are emerging as an alternative in the building sector. Lot of experiments and researches have been performed in fibre reinforced concrete. Several attempts and innovations find the fibre reinforced concrete a growing trend. In this paper an attempt has been done to use the industrial waste material in concrete as an effective manner. Several small scale industries are situated around Pudukkottai district. Scraps of 7.5 kg to 12 kg from lathe are dumped in soil daily. The ground water gets polluted and contaminated due to the dumping of scraps. As already known concrete is strong in compression and weak in tension, the tensile strength can be taken by steel. By referring the literature it has found that the flexural strength increases due to filling of cracks using fibres. The impact test and energy absorption characteristics also increases. This paper deals with the experimental work of using lathe scrap in concrete. Target has been made to achieve medium strength concrete. Correlation studies and model prediction has been done in this paper. Ali Behnood et.al (2015) studied the relation between split tensile strength and compressive strength using Non-linear regression, neural network, model tree, and support vector machine algorithms and given a positive result. Ganesan et.al (2013) studied the fresh and hardened properties of steel fibre reinforced concrete and predicted a model between the mechanical properties of concrete reinforced with steel fibres. Vijayakumaret.al (2012) studied the impact energy absorption characteristics of lathe fibre reinforced concrete and concluded that the addition of lathe scrap up to 1.5% addition enhances the compressive strength. Ozcan et.al (2009) carried out the finite element analysis study on fibre reinforced concrete. Srinivas et.al (2019) studied the behaviour of hooked end steel fibres in geo polymer concrete on different molarity and found out the modified binder index. Abdul Rahman et.al (2017) studied the performance of steel fibres in concrete containing M-sand and concluded that 1 % of lathe scrap addition gives good result. Shrivastava et.al (2014) and Xu & Shi (2009) concluded that the addition of fibres increase the crack resistance, reduces the crack propagation and increases the toughness of concrete. Sahaya Ruban et.al (2020) concluded that aramid fibres can be used for strengthening of reinforced concrete beams.

2. Materials

OPC of 43 grade cement was used with a specific gravity of 2.91. Fine aggregates having specific gravity 2.56 and fineness modulus 2.412 conforming to zone III was used. Coarse aggregates having fineness modulus 8.51 and specific gravity as 2.74 was incorporated in this study. Steel fibre from lathe (scrap) was added as 0.5 %, 1 %, 1.5 % and 2 % to the mix. The workability reduced due to the usage of fibres in concrete. The mix design ratio for M30 concrete was arrived as 1:1.43:2.56:0.45. To make the slump value fall between 100-125 mm a naphthalene based super plasticizer namely conplast SP 430 was used to improve the workability of fibre reinforced concrete.

Table: 2.1 Concrete Proportions

| Specification | Kg/m ³ |
|-------------------|------------------------------------|
| Cement | 420 |
| Fine Aggregate | 600 |
| Coarse aggregate | 1078.55 |
| Water | 189 |
| Super plasticizer | 1% for conventional concrete |
| Lathe scrap | 0.5 %, 1 %,1.5 % and 2 % by volume |

Table: 2.2 Properties of lathe scrap

| Name | Diameter (mm) | Length (mm) | Aspect ratio | Modulus of Elasticity(Mpa) | Density (kg/cm ³) |
|-------------|---------------|-------------|--------------|----------------------------|-------------------------------|
| Lathe scrap | 0.3-0.5 | 15-20 | 40-50 | 210 | 7850 |

Various types of fibres can be added in concrete like steel fibres, polypropylene fibres, jute fibres etc. The fibres may be naturally available, extracted in industry or it may be manufactured. The size and shape of the fibres also plays an important role. Fibres are available in different forms such as hooked end, deformed, mesh type, fabric type etc. In this study the waste scrap from lathe industry is used as an additive material in concrete. All the fibres used are more or less a straight one with aspect ratio ranging from 40-50.

3. Experimental Program

The experimental program includes the investigation of mechanical properties like compressive strength and split tensile strength for conventional and steel reinforced by 0.5 %, 1 %, 1.5 % and 2 % by volume (lathe scrap) of concrete and predicting a model by various proposed equation. The physical properties of lathe scrap are listed above.

3.1 Fresh properties of concrete:

The workability of lathe scrap reinforced concrete was found out by conducting slump test. By the addition of fibres the workability gets reduced and it became a dry mix. Hence super plasticizer was added in concrete to make up the slump value between 100 to 125mm. This is due to increase in water demand. To overcome this water demand super plasticizer was added 18% to 20%.

3.2 Hardened properties of concrete:

The hardened properties taken in the study was compressive strength and split tensile strength. Cylindrical specimen of length 300 mm and diameter 150 mm was used for both the studies as per ASTM C 39 and ASTM C 496 for both conventional and lathe scrap reinforced concrete. They were water cured and tested in a compression testing machine of 400 KN capacity and the results are listed in the table. The properties of lathe scrap is listed in the above table 2.2.

4. Results and Discussion

4.1 Workability Test

Tests were carried out on each mix to evaluate the workability characteristics. As the results the workability of conventional concrete, the slump value was 100 mm. The slump value gradually decreases with the addition of Lathe Waste scrap. To overcome this super plasticizer was added to maintain the workability.

4.2 Compressive strength test

Tests were carried out on each mix to evaluate the cube compressive strength of concrete. From the result the strength attained by the control concrete after 7 days was calculated as 29.79 N/mm² and the strength after 28 days for control concrete was 31.97 N/mm². The concrete obtained the maximum compressive strength at 1.5% addition of lathe scrap. From the results it has been identified clearly that the compressive strength increases with the addition of lathe scrap. The compressive strength increases upto 1.5 % addition of lathe scrap, after that the addition of 2% scrap causes a reduction in strength. The reason is that the workability gets reduced due to more absorption of water and the strength gets reduced.

Table: 4.1 Average compressive strength

| Lathe Waste Scrap in % | Average 7 days compressive strength (N/mm ²) | Average 28 days compressive strength (N/mm ²) |
|------------------------|--|---|
| 0 | 29.79 | 31.97 |
| 0.5 | 31.68 | 33.14 |
| 1 | 32.58 | 39.56 |
| 1.5 | 34.15 | 43.24 |
| 2 | 33.72 | 42.68 |

4.3 Split Tensile Strength Test

Tests were carried out on each mix to evaluate the characteristic split tensile strength of concrete. From the result it is clear that the split tensile strength of nominal concrete at 28 days was found to be increasing as the percentage of scrap goes on increasing. According to our result the maximum value was found to be 3.38 N/mm². The reason is the fibres increases the ultimate load thereby bridging the cracks and forms a dense matrix. The compressive strength and split tensile strength increases with the addition of fibres in concrete. From the below table it has been inferred that the split tensile strength increases with the increase in fibre addition upto 1.5% of lathe scrap. After that due to the addition of 2% scrap, the strength starts decreasing gradually. The addition of fibres can also be added an opportunity in producing light weight concrete thereby reducing the density of concrete. FRC leads to reduced shrinkage, reduced width of cracks and increases water-cement ratio.



Fig: 4.1(a) lathe scrap

Fig: 4.1(b) Compressive strength test

Table: 4.2 Average split tensile strength

| Lathe Waste Scrap in % | Average 7 days split tensile strength (N/mm ²) | Average 28 days split tensile strength (N/mm ²) |
|------------------------|--|---|
| 0 | 2.26 | 2.78 |
| 0.5 | 2.32 | 2.96 |
| 1 | 2.68 | 3.15 |
| 1.5 | 2.85 | 3.38 |
| 2 | 2.92 | 3.30 |

4.4 Prediction of Split Tensile strength from compressive strength

To derive a relation between compressive strength and split tensile strength the following models were collected from literature. An equation is arrived to predict the Split Tensile strength from compressive strength test results. The statistical model created by incorporating the results between split tensile strength and compressive strength is shown below. The model is predicted by comparing the split tensile strength and compressive strength of cylinder of size 100 mm x 300 mm by adding lathe waste in concrete.

Table: 4.3 Predicted model from literature

| S.No | Empirical relation | Model predicted from literature |
|------|-----------------------------|---------------------------------|
| 1 | $f_{spt} = 0.59f_c^{0.5}$ | ACI 363R-92[11] |
| 2 | $f_{spt} = 0.56f_c^{0.5}$ | ACI318-99[12] |
| 3 | $f_{spt} = 0.3f_c^{0.7}$ | CEB-FIB[13] |
| 4 | $f_{spt} = 0.387f_c^{0.63}$ | Ariolu.et.al[10] |
| 5 | $f_{spt} = 0.21f_c^{0.83}$ | Xu&Shi[14] |

The above relation had been taken from various literature studies and the results obtained from this experimental study have been matched with the predicted models. Table 4.4 represents the correlation equation and the corresponding results obtained from this study.

Table 4.4 Evaluation of split tensile strength for various models

| % of lathe scrap | $f_{spt} = 0.59f_c^{0.5}$ | $f_{spt} = 0.56f_c^{0.5}$ | $f_{spt} = 0.3f_c^{0.7}$ | $f_{spt} = 0.387f_c^{0.63}$ | $f_{spt} = 0.21f_c^{0.83}$ |
|------------------|---------------------------|---------------------------|--------------------------|-----------------------------|----------------------------|
| 0 | 3.33 | 3.17 | 3.39 | 3.43 | 3.73 |
| 0.5 | 3.39 | 3.22 | 3.48 | 3.51 | 3.84 |
| 1 | 3.71 | 3.52 | 3.94 | 3.93 | 4.44 |

| | | | | | |
|-----|------|------|------|------|------|
| 1.5 | 3.99 | 3.78 | 4.35 | 4.30 | 4.99 |
| 2 | 3.88 | 3.68 | 4.19 | 4.15 | 4.79 |

The model has been taken from ACI,CEB-FIB, Ariolu et.al and Xu&Shi. To compare the results obtained from this study and to make a coincidence done from experimentally and predicted value the results have been given in table. Here f_{spt} represents split tensile strength and f_c represents the compressive strength of concrete. It is clear that the model predicted from ACI318-99 is in good agreement with this study result. The value predicted by comparing the above model overestimates in CEB-FIB Ariolu.et.al and Xu& Shi model whereas it is comparable to ACI model.

4.5 Empirical Relation between split tensile strength and compressive strength

Figure 4.2 shows the relation between relation between split tensile strength and compressive strength test results. The predicted equation is shown in figure.

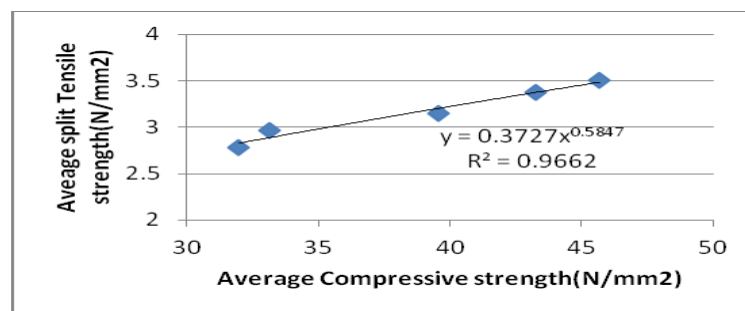


Fig: 4.2 Relation between split tensile strength and compressive strength

From the results obtained an empirical relation has been derived. The equation obtained is $y = 0.3727x^{0.5847}$. The Regression value is $R^2 = 0.9662$. It shows that the correlation between these two properties is good. From the comparison between experimental and predicted the discrepancy is below 5% only which is well agreed.

Table: 4.5 Comparison of results from the predicted model

| Lathe Waste Scrap in % | Split tensile strength – Experimental(N/mm ²) | Split tensile strength –Predicted(N/mm ²) | Difference(%) |
|------------------------|---|---|---------------|
| 0 | 2.78 | 2.83 | 1.80 |
| 0.5 | 2.96 | 2.89 | 2.36 |
| 1 | 3.15 | 3.20 | 1.50 |
| 1.5 | 3.38 | 3.37 | 0.30 |
| 2 | 3.30 | 3.28 | 0.60 |

5. Conclusion

Based on the results obtained in this investigation the following conclusions were drawn with respect to different volume of cast iron scrap on the structural behaviour of Industrial Lathe Scrap concrete.

- The highest increase in compressive strength was observed in mixes with 1.5% of Lathe Waste Scrap 21.80% higher strength than conventional plain cement concrete.

- The highest increase in split tensile strength was observed in mixes with 1.5% of Lathe Waste Scrap 20.55% higher strength than conventional plain cement concrete.
- We conclude from our experimental analysis and investigation that Lathe Waste Scrap up to 1.5 % can be effectively used for making concrete importing inherent capacity of compressive, tensile strength as well as flexural structures of concrete.
- It is possible to make Concrete with good strength-to-weight by adding Lathe Waste Scrap. Since the Lathe Waste Scrap in Concrete is better than that of plain concrete in terms of strength and cost, it can be used for the construction of structures subjected to seismic, impact, dynamic loadings, etc.
- Adding of lathe waste scrap reduces the workability of concrete and this can be improved by adding super plasticizers.
- Since a large quantity of lathe wastes is generated from industrial lathes (up to 10 kg/lathe/day), dumping of lathe waste is a problem hence by using it in concrete works, the disposal of waste will be reduced.
- The relation between split tensile strength and compressive strength shows good correlation. The model predicted from this study is in agreement with ACI 318-99 model. The error between experimental and predicted is also very less.

References

- [1] Abdul Rahman, Syed Mustafa Ali, Syed Azeemuddin, "Performance Analysis of Steel Scrap in Structural Concrete", IOSR Journal of Mechanical and Civil Engineering (IOSR-JMCE) Volume 14, Issue 2 Ver. VII PP 42-47, 2017.
- [2] ACI Committee 318, "Building Code Requirements for Structural Concrete (ACI 318 - 99) and Commentary (318R - 99)," American Concrete Institute, Farmington Hills, Mich., pp. 391, 1999.
- [3] ACI Committee 363, "State - of - the - Art Report on High - Strength Concrete (ACI 363R - 92)," American Concrete Institute, Farmington Hills, Mich., pp. 55, 1992.
- [4] Ali Behnood Pin Verian, MahsaModiriGharehveran, "Evaluation of the splitting tensile strength in plain and steel fiber-reinforced concrete based on the compressive strength" *Construction and Building Materials* 98, 519–529, 2015.
- [5] CEB - FIP Model Code for Concrete Structures,, "Evaluation of the Time Dependent Behaviour of Concrete," Bulletin d'Information No. 199, Comite European du Béton/FédérationInternationale de la Precontrainte, Lausanne, pp. 201, 1991.
- [6] GanesanN, P.V. Indira and AnjanaSanthakumar, "Engineering properties of steel fibre reinforced geopolymer concrete" *Advances in Concrete Construction*, Vol. 1, No. 4, 305-318, 2013.
- [7] IS: 383-1970, Specifications for coarse and fine aggregates from natural sources for concrete, Bureau of Indian Standards, New Delhi, India.
- [8] IS: 10262-1982, recommended guidelines for concrete mix design, Bureau of Indian Standards, New Delhi, India.
- [9] NihalArioglu, Z. CananGirgin, and ErginArioglu., "Evaluation of Ratio between Splitting Tensile strength and Compressive Strength for Concretes up to 120 MPa and its Application in Strength Criterion," *ACI Materials Journal*., 103 91), pp19 - 24, 2006.
- [10] Ozcan D M, Bayraktar A, SahinA, Haktanir T and Turker T, "Experimental and Finite Element Analysis on the Steel fiber reinforced Concrete Beams- Ultimate Behaviour", *Construction and Building Materials*, Vol. 23, No. 2, pp. 1064-1077, 2009.
- [11] Sahaya Ruben J, Murugan M, Prakash Arul Jose J, "The Effect of Aramid Fibre Reinforced Polymer Composites for Strengthening RC Beams", *Journal of Fiber Science Technology*, 76(10), 343-350, 2020.
- [12] Shrivastavaa, P, Joshib, Y.P, "Reuse of Lathe Waste Steel Scrap in Concrete Pavements", *Journal of Engineering Research and Applications*, Vol. 4, Issue 12(Part 4), pp.45-54, 2014.
- [13] Srinivas J, SessaSreenivas B, Rama Seshu D, "The effect of Molarity and Steel fibers on Compressive strength of Fiber Reinforced Geopolymer Concrete" *International Journal of Engineering and Advanced Technology* , Volume-8 Issue-4, April, 2019.
- [14] Vijayakumar G, SenthilNathan P, Pandurangan K and Ramakrishna, G, "Impact and energy absorption characteristics of lathe scrap reinforced concrete", *International Journal of Structural & Civil Engineering Research*. Vol. 1, No. 1, November 2012.
- [15] Xu B W and Shi H S, "Correlations among mechanical properties of steel fiber reinforced concrete", *Construction building materials*, 23, pp 3468-3474, 2009.

Study of Parametric Strength of Coconut Shell and Coir Fibres using Slump Test

, Jyoti Prasad Ganthia^{1*}, Paresh Biswal²

¹M.Tech Scholar, ²Assistant Professor

Department of Civil Engineering, GIET University,

Gunupur, Odisha, India, 765022

*jyotiprasadganthia007@gmail.com

Abstract

Recent days natural fibres and natural products are more in use as construction materials. Coconut fibre is one of the best choices among all natural fibres. This is freely available at all tropical reasons. Coconut shell as a natural fibre is effectively used in construction materials. It is helpful for enhancing strength of the matrix mix. As it is freely available as a raw materials, it can be used using fly ash, cement and can be used in tropical reasons. This is an eco-friendly material. This can change the matrix mix by strengthening its holding capacity to the material mix. This can create a environment friendly materials for the construction. In this paper Slump test is carried out to study the effectiveness and strength of the material mix. This can be better and sustainable product for the industrial as well as domestic work. This paper highlights the flexural strength and compressive strength of the coconut shell as a raw material for cementitious product. This material makes very much economical for utilizations in constructions.

Keywords: *Coconut shell, Coir fibre, Flexural Strength., Slump test, Tensile strength.*

1 Introduction

Concrete is the most versatile concrete material of use next to water. [1][2]The simplest reason for its extensive use in the construction of almost all civil engineering works is that the properties can be controlled within a wide range by using appropriate ingredients and by special mechanical, physical and chemical processing techniques. [3][4] Concrete is a composite material which essentially consists of cement, coarse aggregate (CA), Fine aggregate (FA) and water. Coarse aggregate gives the volume to the concrete and fine aggregate makes the concrete denser by filling the voids of coarse aggregate. [5] Water hydrates and sets the cement which thus acts as a binder of all ingredient particles of concrete. It is held together by a binder of cementitious paste that hardens over times. [6] The cementitious paste is typically made up of Portland cement and water and may also contain supplementary cementing materials, such as fly ash, slag cement (ground granulated blast-furnace slag), rice husk, silica fume and metakaolin. [7]

2 Coconut Fibres

Coir fibre is the natural fibre that is derived from cocoa husk. The thickest and most resistant coir fibre is all commercial fibres. The main benefits in manufacturing durable goods are the low decomposition rate. The high strength of the coir fibre is the key cause of the development of seams. Two forms commonly exist. One is brown cocoa fibre mature and, after 10 months, is fine white fibre from immature green cocoa. [8] Coir fibre is one of the finest natural fibres of lignin. Brown fibres are dense, durable and resistant to abrasion. The white fibres are also weaker, smoother and finer. The brown and white coir are fibres of 4-12 inch thickness. [9]

3 Coir Fibres

We have divided this section into three subsections. In the first subsection, we have discussed the various microarray datasets adopted in this study. The second and third subsection presents the experimental procedure and detail analysis of the metrics considered for the study of the purposed model. [10]

a. Properties of coir fibre

Coir fibre is available between skin and shell through husking. These are multi-cellular, heavy, very rough and rigid natural fruit fibre lignocelluloses.

Table 1. Coir fibre (Chemical composition)

| | |
|-----------------------------|--------|
| Lignin | 45.84% |
| Cellulose | 43.44% |
| Hemi-Cellulose | 00.255 |
| Pectin's & related compound | 03.005 |
| Water soluble | 05.25% |
| Ash | 02.22% |

Table 2. Coir fibre (Physical Properties)

| | |
|----------------------|-----------------------------|
| Length | 6-8 |
| Density | 1.40 |
| Tendency | 10.0 |
| Breaking elongation% | 30% |
| Diameter in mm | 0.1 to 1.5 |
| Rigidity of Modulus | 1.8924 dyne/cm ² |
| Swelling in water | 5% |
| Moisture at 65% RH | 10.50 |



Figure 1. Coconut Fibre

4 Slump Test

The most widely used method of measuring concrete consistency is the Slump Test. It is easily used as a control test and provides an impression of concrete's uniformity. By studying the way in which concrete slumps, additional knowledge on the workability and consistency of concrete can be obtained. The apparatus for the slump test consists essentially of metallic mould in the form of a cone frustum with internal dimensions of 20 cm bottom diameter, 10 cm top diameter and 30 cm height, as shown in Figure 2.



Figure 2 Slump Cone

5 Experimental Results

a. Compressive strength

A total of 6 cubes of size (150× 150× 150) mm were casted and tested for 7days and 28 days compressive test of three specimens each as per IS 516:1959.the results are shown below.

Table 3 Compressive strength of conventional concrete

| SAMPLE NO | STRENGTH | |
|-----------|----------|---------|
| | 7 DAYS | 28 DAYS |
| 1 | 19.85 | 26.16 |
| 2 | 20.57 | 29.64 |
| 3 | 22.65 | 31.13 |
| Average | 21.02 | 28.98 |

b. Splitting Tensile Strength

A total no of 6 cylinders of Diameter 150mm and height 300mm were casted and tested for 7days and 28 days split tensile test of 3 specimens each as per IS:516:1959.The results are shown below.

Table 4 Split tensile strength of conventional concrete

| SAMPLE NO | STRENGTH | |
|-----------|----------|---------|
| | 7 DAYS | 28 DAYS |
| 1 | 2.43 | 2.83 |
| 2 | 2.22 | 2.68 |
| 3 | 2.59 | 3.05 |
| Average | 2.41 | 2.85 |

c. Flexural strength

A total no of 3 prismatic bars of size 500×100×100mm were casted and tested for 28days compressive test of 3 specimen each as per IS:516:1959.The results are shown below.

Table 5 Flexural strength of conventional concrete

| SAMPLE | STRENGTH(N/mm2) 28 DAYS |
|----------------|----------------------------|
| 1 | 3.9 |
| 2 | 3.6 |
| 3 | 4.1 |
| Average | 3.86 |

In below figure 3 the compressive strength of the matrix mix studied for 7 days. It is found in average that the strength is increased with time durations.

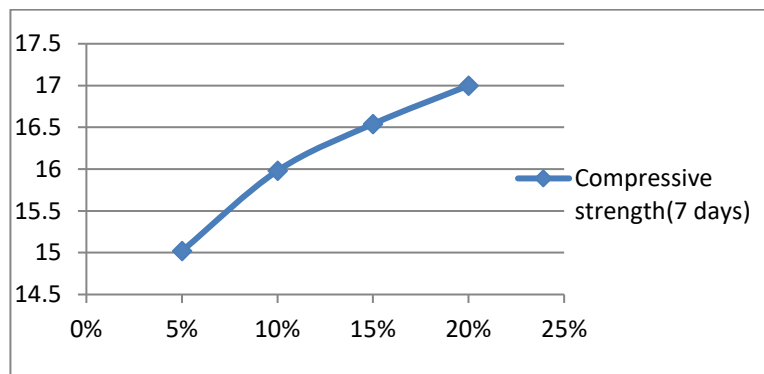


Figure 3. Compressive strength of 7 days mix with C.S

In below figure 4 the flexural strength of the matrix mix studied for 28 days. It is found in average that the strength is increased with time durations.

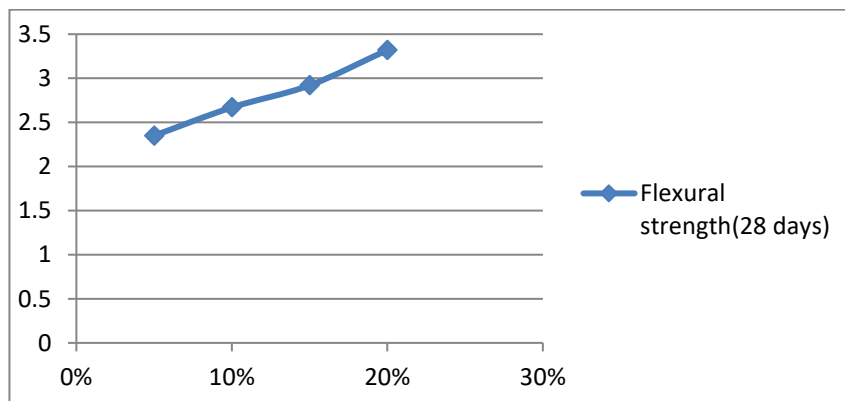


Figure 4. Flexural strength of 28 days mix with C.S

6 Conclusion

The slump test results shown above figure 3 and figure 4 illustrates that the strengths of the coconut shell as composite material can give better results. This can be useful by using as holding materials for concrete mix. This experimental work can give better results as raw materials for cements, concrete manufacturing in road and constructions. This can be used for both domestic and industrial uses. The proper concentrations of coconut shell powder give higher strength for the constructions. The matrix materials can be highly usable because of eco-friendly and economic point of view. This paper can be helpful for the researchers to use these materials in their studies to get better composite material manufacturing.

References

- [1] Majid Ali, Nawawi Chouw, “Experimental investigations on coconut-fibre rope tensile strength and pullout from coconut fibre reinforced concrete”, *Construction and Building Materials*, Vol. 41, pp. 681–690, 2012.
- [2] P Nibasumba, X L Liu, “Recent developments in fibre reinforced concrete and their effect on concrete columns analysis”, *Construction and Building Materials*, Vol. **18**(7), pp. 49–58, 2011.
- [3] Majib Ali, Anthony Liu, HouSou, Nawawi Chouw, “Mechanical and dynamic properties of coconut fibre reinforced concrete” *Construction and Building Materials* 30 (2011) 814 – 825, 2011.
- [4] Kullkarni V.P, Kumar. S, “Comparative study on coconut shell aggregate with conventional concrete”, Vol.2, Issue 12, pp 67-70, 2013.
- [5] P. Kumar Mehta, High-performance, high-volume fly ash concrete for sustainable Development, International Workshop on Sustainable Development and Concrete Technology, Beijing, May 20-21, 2004.
- [6] Yash Shrivastava and Ketan Bajaj, Performance of Fly Ash and High Volume Fly Ash Concrete in Pavement Design, International Proceedings of Computer Sciences and Information Technology, Singapore, Vol.28, 2012.
- [7] Neelesh Kumar Singh, Prerit saxena, Rishabh Sharma, Rohit Kumar Shakya, A Comparative Study on Partial Replacement of Cement with Fly ash & Granite Powder , *IOSR Journal of Mechanical and Civil Engineering*, volume 13.
- [8] Amarnath Yeramala, Ramchandrudu. C, “Properties of concrete with coconut shell as aggregate replacement”, *International Journal of Engineering Inventions*, Vol.1, Issue 6, pp 21-31, 2012.
- [9] R. Nagalakshmi, “Experimental Study on Strength Characteristics on M25 Concrete with Partial Replacement of Cement with Fly Ash and Coarse Aggregate with Coconut Shell”, *International Journal of Science & Engineering Research*, Vol. 4, Issue 1, 2013.
- [10] J.P. Ries, J.Speck, “Lightweight Aggregate Optimizes the Sustainability of Concrete Sustainability Conference, National Ready Mixed concrete Association, 2010.

Steady-State Analysis of an $M/M/2$ Queueing System Operating in A Multi-Phase Random Environment Subject To Disaster and Repair

D. Piriadarshani,

Department of Mathematics, Hindustan Institute of Technology & Science, Padur,
Chennai, Tamil Nadu 603 103, India

S. Narasimhan

Department of Mathematics, KCG College of Technology, Karapakkam,
Chennai, Tamil Nadu 600097, India

Abstract

An $M/M/2$ queueing system operating in a multi-phase random environment subject to disaster and repair is studied. The random environment has N phases and the k -th phase is exponentially distributed with mean $\frac{1}{\eta_k}$, $k = 1, 2, \dots, N$. The queueing system behaves like $M(\lambda_k)/M(\mu_k)/2$ while in the k -th phase. At the end of the k -th phase, a disaster occurs wiping out all customers in the system and the servers are taken for repair. Both the servers are repaired jointly and the repair time is exponentially distributed with mean $\frac{1}{\eta_0}$. Immediately after the repair completions the system moves to phase k_k with probability q_k . Customers are allowed to join the queueing system during repair time. The probabilistic behaviour of the system is studied in steady state by using probability generating function technique. Some performance measures are also obtained.

Keywords: $M/M/2$ queueing system, disaster, wash-out, repair, random environment, steady-state analysis.

1. INTRODUCTION

Several researchers have studied many-server queueing systems (see, for example Karlin and McGregor [5], Takacs [14], Kleinrock [6], Natarajan [12], Krishnamoorthy and Sreenivasan [11], and Dharmaraja and Rakesh Kumar [4]). A few researchers have obtained transient solution of many-server queueing systems (see Parthasarathy and Sharafali [13], Krishna Kumar and Arivudainambi [7], Krishna Kumar and Madheswari [9], Al-Seedy et al. [1], Krishna Kumar et al. [8] and Ammar [2]). On the other hand, many authors have paid their attention to study some special class of queueing systems subject to impatience of customers and/or randomly occurring disasters (see for example, Chakravarthy [3], Krishna Kumar et al. [10], Paz and Yechiali [15], Sengupta [16], Sudhesh [17], Udayabaskaran and Dora Pravina [18]) and Yechiali [19]. The steady-state behaviour of an $M/M/1$ queue operating in random environment subject to disasters have been analysed by Paz and Yechiali [15] in their paper, where the underlying environment is described by a n -phase continuous-time Markov chain. Udayabaskaran and Dora Pravina [18] have analysed the time-dependent behaviour of the model of Paz and Yechiali [15]. However, to the best of our knowledge, $M/M/2$ queue systems operating in a random environment subject to disasters and repair have not been studied so far in literature. In the present paper, we fill this gap by obtaining a steady-state analysis of a $M/M/2$ queueing system operating in a random environment subject to disasters and repairs. The sections of the research paper are sorted out the following manner: Section 2 elaborately describes the model. In section 3, we write down the integral equations for the time-dependent probabilities of the system. Section 4 we obtain explicit expressions for the steady-state probabilities of the queueing system.

2. MODEL DESCRIPTION

We consider a two server queueing system operating in a random environment. We assume that the environment is in any one of the $m + 1$ states $0, 1, 2, \dots, N$. The environmental state corresponds to the state that the servers are jointly undergoing repair. The repair time is random which is exponentially distributed with mean $1/\eta_0$. During the repair time, customers join the a random interval of time which is exponentially distributed with mean $1/\eta_k$ and at the end of the residing period (that is, at the occurrence of a disaster in phase k), all customers in the system are washed out and the system moves to phase 0. When the environment is in phase k , the system behaves like an $M(\lambda_k)/M(\mu_k)/2$ queue with arrival rate λ_k and service rate μ_k .

a random interval of time which is exponentially distributed with mean $1/\eta_k$ and at the end of the residing period (that is, at the occurrence of a disaster in phase k), all customers in the system are washed out and the system moves to phase 0. When the environment is in phase k , the system behaves like an $M(\lambda_k)/M(\mu_k)/2$ queue with arrival rate λ_k and service rate μ_k .

At time $t = 0$, we assume that a catastrophe has just occurred so that the system is in phase 0 (repair state). Let $E(t)$ be the phase of the environment at time t and let $X(t)$ denote the number of customers in the queueing system at time t . Then the joint process $\{(X(t), E(t)) | t \geq 0\}$ is a continuous time parameter Markov process whose state space is

$$\{(j, k) | j = 0, 1, 2, \dots; k = 0, 1, 2, \dots, N\}.$$

We define the state probability as follows:

$$p(j, k, t) = Pr[X(t) = j, E(t) = k | X(0) = 0, E(0) = 0], k = 0, 1, 2, \dots, N; j = 0, 1, 2, \dots \tag{1}$$

In the next section, we derive the integral equations for $p(j, k, t)$.

3. STEADY-STATE SOLUTION FOR THE SYSTEM

The steady-state probabilities are defined by

$$\pi(j, k) = \lim_{t \rightarrow \infty} p(j, k, t) \tag{8}$$

Applying the final value theorem of Laplace transform, equation (8) gives

$$\pi(j, k) = \lim_{s \rightarrow 0} sp^*(j, k, s) \tag{9}$$

where $p^*(j, k, s)$ is the Laplace transform of $p(j, k, t)$. Taking Laplace transform on both sides of equations (3)-(7), we obtain

Multiplying both sides of equations (10)-(14) with s and applying equation (9), we obtain

The system of equations (16)-(19) together with the total probability law can be explicitly solved. The result is given in the following theorem:

The product of the roots of equation (29) is $\alpha_k \beta_k = \frac{2\mu_k}{\lambda_k}$. For stable solution, we assume that $2\mu_k > \lambda_k$. Then, $2\mu_k + \eta_k > 2\mu_k > \lambda_k$. It is easy to establish that $0 < \beta_k < 1$. Further, we find that $\alpha_k > 1$. Using the roots α_k and β_k , equation (24) leads to

$$G(\theta) = \frac{\eta_0 q_k \theta [G_0(\theta) + \pi(0, 0)(1 - \theta)] - \pi(0, k)(1 - \theta)[(\lambda_k + \eta_k)\theta + 2\mu_k]}{k}, k = 1, 2, \dots, N. \tag{32}$$

Using table 1, we obtain the following table of mean values:

$$E[L_0] = 0.0111, E[L_1] = 0.1091, E[L_2] = 0.1173, E[L_3] = 0.2743, \\ E[L_4] = 0.1455, E[L_5] = 0.0444, E[L] = 0.7017, E[C] = 0.0149.$$

4. CONCLUSION

State analysis of an $M/M/2$ queueing system operating in a multi-phase random environment subject to disaster and repair is discussed and its steady state probability is obtained. Further, we find the characteristic of $M/M/2$ queueing system operating in a multi-phase random environment subject to disaster and repair.

5. REFERENCES

- [1] R. O. Al-Seedy, A. A. El-Sherbiny S. A. El-Shehawy S. I. Ammar, Transient solution of the $M/M/c$ queue with balking and reneging, Computers and Mathematics with Applications, vol. 57 , 1280-1285,2009.
- [2] S. I. Ammar, Transient analysis of a two-heterogeneous servers queue with impatient behavior, J. Egypt. Math. Soc. Vol. 22 , 90–95,2014.
- [3] S. R. Chakravarthy, “A disaster queue with Markovian arrivals and impatient customers,” Applied Mathematics and Computation, 214 , 48-59,2009.
- [4] S. Dharmaraja and Rakesh Kumar, Transient solution of a Markovian queuing model with heterogeneous servers and catastrophes, OPSEARCH, vol. 52 , 810-826,2015.
- [5] S. Karlin and J. McGregor, Many server queueing processes with Poisson input and exponential service times, Pacific Journal of Mathematics, vol. 8 , 87-118,1958.
- [6] L. Kleinrock, Queueing Systems: Volume I – Theory. New York: Wiley Interscience, 1975.
- [7] B. Krishna Kumar and D. Arivudainambi, Transient solution of an $M/M/c$ queue with heterogeneous servers and balking, Int. J. Inf. Manag. Sci., vol. 12 , 15-27,2001.
- [8] B. Krishna Kumar, S. P. Madheshwari and K. S. Venkatakrishanan, Transient solution of an $M/M/2$ queue with heterogeneous servers subject to catastrophes, Int. J. Inf. Manag. Sci., vol. 18 , 63–80,2007.
- [9] B. Krishna Kumar, S. Pavai Madheswari, Transient behaviour of the $m/m/2$ queue with catastrophes, Statistica, vol. LXII , 129-136,2002.
- [10] B. Krishna Kumar, A. Vijayakumar, and S. Sophia, “Transient analysis of a Markovian queue with chain sequence rates and total catastrophes,” International Journal of Operational Research, 5 , 375-391,2009.
- [11] A. Krishnamoorthy and C. Sreenivasan, An $M/M/2$ queueing system with heterogeneous servers including one with working vacation, International Journal of Stochastic Analysis, vol. 2012 , Article ID 145867, 16 pages,2012.
- [12] G. Natarajan, Analysis of Queues: Methods and Application, CRC Press, 2012.
- [13] P. R. Parthasarathy and M. Sharafali, Transient solution to many server Poisson queue: A simple approach, Journal of Applied Probability, 26 , 584-594 ,1986.
- [14] L. Takacs, Introduction to the theory of queues, Oxford University Press, New York, 1962.
- [15] N. Paz, and U. Yechiali, “An $M/M/1$ queue in random environment with disasters,” Asia Pacific J. Oper. Res. 31 , 1450016-12 pages,2014.
- [16] B. Sengupta, “A Queue with Service Interruptions in an alternating random environment,” Operations Research, 38 , 308-318,1990.
- [17] R. Sudhesh, “Transient analysis of a queue with system disasters and customer impatience,” Queueing Systems, 66 , 95-105,2010.
- [18] S. Udayabaskaran, and C. T. Dora Pravina, “Transient analysis of an $M/M/1$ queue in a random environment subject to disasters,” Far East Journal of Mathematical Sciences (FJMS), 91 , 157-167,2014.
- [19] U. Yechiali, “Queues with system disasters and impatient customers when system is down,” Queueing Systems, 56 , 195-202,2006.

Conservation of Natural Aggregate by Identifying Alternatives in Coarse Aggregate

Anne Mary Janarthanan¹ and Janardhanan Ganga Tulasi²

¹Research Scholar, Faculty of Civil Engineering, Anna University, Chennai.

²Associate Professor, National Institute of Technical Teachers Training and Research, Chennai.

Abstract

In recent days, one of the key fields of researchers' concern has been the development of innovative waste management strategies. This is due to the need for the products to be reused to prevent exhausting renewable resources that are abundantly exhausted by the increasing population. This waste materials will be used in the building industry for manufacturing artificial concrete as the use of natural aggregates has become a serious concern, leading to the over use of these materials in this developing infrastructure. The use of plastic has been growing day by day in recent years. Several efforts have been taken to limit the use of plastic because it poses one of the biggest environmental issues, since plastic waste is non-biodegradable. Waste plastic as a concrete aggregate provides a good way to lowering material costs and addressing some of the environmental challenges of solid waste management. Apart from plastic waste many industrial by products are also been disposed in environment which cause severe problem in environment. These materials can be effectively used in construction industry. This research work deals about the manufacturing of an alternative coarse aggregate for concrete.

Keywords: *Alternative Construction Material, Energy Conservation, Reuse*

1 Introduction

Global concern is to save the energy and conserve the resources effectively, efficient recycling of all these solid wastes requires extensive R&D work towards exploring newer applications and maximizing use of existing technologies for a sustainable and environmentally sound management^[1]. There has been a significant rise in the population that require huge natural building materials in enormous scale for construction. The large consumption of construction materials lead to think about alternate method, which will develop a better construction material. As concrete is the most widely used construction material it can be modified using new technologies. The annual consumption of plastic material is around 5 million tons in 1950 to nearly 100 million tons in recent time. Since the reason behind this plastic is disposal, as the disposal for this type of waste plastic takes more than 500 years. Recent development in the field of construction has shown one of the developments of new waste material i.e.. The need to manage these resources is a challenge, which requires innovative idea and a specified action to prevent these waste generations. It is a daring task for contractors and others in the construction industry to use recycled plastic in concrete. Artificial lightweight aggregate is manufactured with Copper slag, vermiculite, waste plastic, broken tiles and sisal fibre.

2 Materials Used For Manufacturing ACA

The following materials were used to manufacture the artificial coarse aggregate: copper slag, plastic waste, waste ceramic and vermiculite.

2.1 Copper Slag

Copper slag is a by-product obtained during matte smelting and refining of copper. Many researchers have investigated the use of copper slag in the production of cement, mortar and concrete as raw materials for clinker, cement replacement, coarse and fine aggregates^[5]. Copper slag, which is produced during Pyro-metallurgical production of copper from copper ores, contains material such as alumina, calcium oxide, silica etc. The physical properties and chemical properties of copper slag are given in table 1 and in table 2 as per Shahu et al (2017)^[6].

Table 1. Chemical Properties of Copper Slag

| Physical Properties | Remarks |
|--------------------------------|------------------|
| Shape | Irregular |
| Appearance | Black and Glassy |
| Specific Gravity | 2.8 - 3.8 |
| Finess Modulus | 3.28 |
| Bulk Density | 1.40-1.65 g/cc |
| Water Absorption | 0.17 % |
| Moisture Content | 0.1% |
| Coefficient of uniformity (Cu) | 2.50 |
| Coefficient of curvature (Cc) | 1.74 |
| IS classification | SP |
| Ph | <5.7 |

Table 2. Physical Properties of Copper Slag

| Chemical Properties | % of Composition |
|--------------------------------|------------------|
| Fe ₂ O ₃ | 50 - 60 |
| SiO ₂ | 25 – 35 |
| Al ₂ O ₃ | 02 – 05 |
| CaO | 01 - 05 |
| K ₂ O | 01 – 02 |

2.2 Plastic Waste

In the recent study, various form of coarse aggregate is being prepared using the waste product, which has a substantial property. Plastic waste for example polypropylene (PP), polyethylene (PE) and polyethylene terephthalate (PET) can be used in concrete as coarse aggregate to reduce the density of the concrete. Compare to low-density polyethylene (LDPE) and high-density polyethylene (HDPE). HDPE is stiffer, higher in tensile strength, and better in heat resistance, whereas LDPE is more flexible. The mechanical properties of HDPE and LDPE, including elongation and tensile strength, have also been reported. Construction materials will blended with LDPE and HDPE well compare to other type of plastics.

Plastic characteristic that is unable to absorb water, hampering cement hydration reaction, as there is limitation of water movement. The physical of LDPE is given in table 3as per Heruet al (2017)_[3]

Table 3. Physical Properties of LDPE

| Physical Properties | Remarks |
|---------------------|-----------------------|
| Colour | Transparent* |
| Specific Gravity | 0.78 |
| Flash point | 36 |
| Water Absorption | <0.01% |
| Solent Resistance | Resistance below 60°C |
| Alkaline Resistance | Resistant |
| Acid Resistance | Oxidizing oxides |
| Melting | 98 -115°C |
| Colour of Flame | Blue & Yellow |
| Speed of Burning | Slow |
| Odour | Paraffin |
| Impact Strength | High Impact Strength |

2.3 Ceramic Waste

Ceramic industries produce ceramic waste about 15 – 20 % in production stage because once broken cannot be used. Ceramic products are used worldwide the mass production and use of ceramic materials causes increased wastes, which may results in serious environmental problems[2]. The ceramic waste used for manufacturing artificial coarse aggregate is collected from nearby demolished building contains broken tiles and ceramic wastes. As per Correia et al (2006) the physical and chemical properties of ceramic waste are given below as tabulated in table: 4 & 5.[4]

Table 4. Physical Properties of Ceramic

| Physical Properties | Values |
|---------------------|------------------------|
| Appearance | White – Brown |
| Specific Gravity | 2.6 |
| Bulk Density | 1410 kg/m ³ |
| Water Absorption | 0.2% |
| Shape | Angular |
| Fineness Modulus | 3.29 |
| Surface Texture | Smooth |

Table 5. Chemical Properties of Copper Slag

| Chemical Properties | % of Composition |
|--------------------------------|------------------|
| Fe ₂ O ₃ | 4 |
| SiO ₂ | 68 |
| Al ₂ O ₃ | 18 |
| CaO | 1.5 |
| K ₂ O | 1.6 |
| Na ₂ O | 2 |
| MnO | 0.078 |
| P ₂ O ₅ | 0.034 |

Ceramic waste is a porous material, which acts as a wet curing medium for the hydration of cement paste and reduces autogenous shrinkage that ultimately results in the increase in its mechanical strength.

2.4 Vermiculite

The vermiculite aggregates used in this research have a bulk density ranging from 65 to 80 kg/m³ that is, exfoliated vermiculite procured from Hemalight Product PVT Ltd, Chennai. Vermiculite is a hydrous phyllosilicate mineral. It undergoes significant expansion when heated. Vermiculite is chosen to replace fine aggregates in concrete because of its specific properties such as it is lighter in weight, improved workability, improved fire resistance, improved resistance to cracking and shrinkage and mainly inert chemical nature.

Table 6. Physical Properties of vermiculite

| Physical Properties | Values |
|---------------------|------------------------|
| Appearance | Brownish Yellow |
| Specific Gravity | 2.7 |
| Bulk Density | 1410 kg/m ³ |
| Hardness | 1 – 2 |
| Melting Point | 1330°C |
| pH | 6-9 |
| Surface Texture | Mosaic |

Table 7. Chemical Properties of vermiculite

| Chemical Properties | % of Composition |
|--------------------------------|------------------|
| SiO ₂ | 39.6 |
| MgO | 23.5 |
| Al ₂ O ₃ | 9.2 |
| K ₂ O | 6.1 |
| Fe ₂ O ₃ | 7.9 |
| CaO | 2.1 |
| TiO ₂ | 1 |
| F | 0.6 |

The physical and chemical properties of the vermiculite listed in the table 6 & 7 as per Divya et al (2016). Vermiculite is generally used to reduce the dead weight of the structure as well as to reduce the risk of seismic damage to a structure.

3 Manufacturing Process

The ingredients were collected in the required form and the lightweight artificial coarse aggregate is manufactured. The manufacturing stages explained in fig 1.



Fig 1: Stages in manufacturing

The ingredients were added in the above order to manufacture an artificial coarse aggregate. The preparation process mainly in the following stages collection, segregation, melting, coating, dusting and curing. In collection stage all the ingredients collected from the source point and stored. The collected sample is then segregated in required form, first ceramic waste is crushed to 12 mm size, then the vermiculite and copper slag is sieved in 4.75mm sieve. Different forms of plastics were collected which is LDPE type and melted until it becomes liquid. The ceramic waste is crushed sieved and the granules are mixed with plastic, vermiculite and copper slag. The prepared aggregates are cooled at room temperature for a period of 60 days.

4 Experimental Investigation

The artificial lightweight aggregate was tested as per IS 383: 2016. The test was carried out for the manufactured aggregate as well as for natural coarse aggregate and the results were compared with the code provision. The aggregate is brownish black. The following tests were carried out for the sample: impact test, crushing test, water absorption, abrasion test, angularity number, soundness test and specific gravity. The aggregate was air cured for 60 days and the sample was tested. The aggregate manufactured is of 12.5 mm size.

4.1 Impact Test

This test is conducted to analyse the toughness of the aggregate, which is tested in Aggregate Impact Testing Machine (AITM). The aggregate taken in the cylinder is compacted by giving 25 gentle blows by tamping rod in three layers, levelled the cylinder and measured the weight of the cylinder.

Table 8: Aggregate Impact Strength Results

| Trial No | Natural Aggregate (A) | Artificial Aggregate (B) |
|---------------------|-----------------------|--------------------------|
| 1 | 15.62 | 13.09 |
| 2 | 14.06 | 12.6 |
| 3 | 14.75 | 12.56 |
| Impact Strength (%) | 14.81 | 12.75 |

The impact strength of coarse aggregate for non-wearing surface is 45% as per IS 383: 2016. The impact strength for artificial aggregate is higher than the natural aggregate.

4.2 Crushing Strength

The test conducted to analyse the aggregate crushing strength of an aggregate. The sample is taken in the crushing cylinder is compacted by giving 25 gentle blows by tamping rod in three layers, levelled the cylinder and measured the weight of the cylinder.

Table 9: Aggregate Crushing Strength Results

| Trial No | Natural Aggregate (A) | Artificial Aggregate (B) |
|-----------------------|-----------------------|--------------------------|
| 1 | 17.86 | 14.87 |
| 2 | 17.79 | 15.96 |
| 3 | 17.63 | 14.97 |
| Crushing Strength (%) | 17.76 | 15.26 |

The crushing strength value of coarse aggregate for non-wearing surface is 45% as per IS 383: 2016. The crushing strength for artificial aggregate is higher than the natural aggregate.

4.3 Abrasion Value

The test was conducted to analyse the hardness properties of an aggregate. The sample, which pass through 20mm size, retain in 12.5mm sieve of 2.5kg, and sample passed through 12.5mm and retained on 10mm sieve of 2.5 kg taken, sample is oven dried for 110°C and cooled for 4 hours. The sample and eleven steel balls are placed in Los Angeles Abrasion Testing Machine and allowed to rotate about 500 revolutions at a speed of 20 - 33 rev/min. then the sample is sieved in 1.70 mm the weight of total aggregate (W1) and retained (W2) are noted. The abrasion value is $(W1 - W2) / W1 \times 100$ the test results are tabulated in table 10.

Table 10: Aggregate Abrasion Strength Results

| Trial No | Natural Aggregate (A) | Artificial Aggregate (B) |
|-------------------------|-----------------------|--------------------------|
| 1 | 26.56 | 22.48 |
| 2 | 27.08 | 23.56 |
| 3 | 26.43 | 22.68 |
| Abrasion Resistance (%) | 26.69 | 22.90 |

The abrasion strength value of coarse aggregate for non-wearing surface is 50% as per IS 383: 2016. The crushing strength for artificial aggregate is higher than the natural aggregate.

4.4 Water Absorption Test

The test done to identify the amount of water absorbed by the sample. In order to identify the water absorption 1kg of aggregate is taken (W1) and soaked for 24 hours in water. Then the sample is wipe and oven dried and weighted (W2). The water absorption is $W2/W1 \times 100$ the test results tabulated in table 11.

Table 11: Aggregate Water Absorption Results

| Trial No | Natural Aggregate (A) | Artificial Aggregate (B) |
|----------------------|-----------------------|--------------------------|
| 1 | 1.56 | 0.50 |
| 2 | 1.75 | 0.65 |
| 3 | 1.83 | 0.58 |
| Water Absorption (%) | 1.71 | 0.57 |

The water absorption of coarse aggregate is 2.5 to 3. The water absorption for artificial aggregate is lower than the natural aggregate.

4.5 Specific Gravity Test

It is a measure of the strength or a quality of the aggregate. The test is performed by taking required readings as per the procedure of IS 2386: 1963 – Part (3). The specific gravity of the aggregate is calculated and tabulated in table 12.

Table 12: Specific Gravity of Aggregate

| Trial No | Natural Aggregate (A) | Artificial Aggregate (B) |
|------------------|-----------------------|--------------------------|
| 1 | 2.64 | 2.10 |
| 2 | 2.36 | 2.01 |
| 3 | 2.7 | 1.93 |
| Specific Gravity | 2.6 | 2.01 |

The water absorption of coarse aggregate is 2.5 to 3. The water absorption for artificial aggregate is lower than the natural aggregate.

4.6 Size and Shape Test

The size of the aggregate manufactured is of 12.5 mm according to the aggregate grading as per IS 2386: 1963 (Part 1) and shape of the aggregate is angular. As the shape of the aggregate plays, the major role in construction there is a need to test the samples for elongation flakiness and angularity.

Table 13: Elongation and Flakiness test of Aggregate

| Trial No | Natural Aggregate (A) | Artificial Aggregate (B) |
|----------------|-----------------------|--------------------------|
| 1 | 21.87 | 27.54 |
| 2 | 22.54 | 27.89 |
| 3 | 21.75 | 28.56 |
| Elongation (%) | 22.05 | 27.99 |
| 1 | 31.67 | 22.46 |
| 2 | 32.06 | 21.86 |
| 3 | 32.56 | 21.54 |
| Flakiness (%) | 32.09 | 21.95 |

The elongation and flakiness test conducted with the help of elongation gauge and flakiness gauge for natural aggregate and for artificial aggregate. The test results were tabulated in table 14. The combined flakiness and elongation should not exceed 30% for road works.

4. Result

The aggregate is tested for impact strength, crushing strength, water absorption, abrasion resistance, angularity, soundness and specific gravity then the result is compared with the natural aggregate are tabulated in table 15. The results were found satisfactory as per Indian standard codal recommendation. The aggregate can be use in concrete and well as in concrete pavement.

Table 14: Test Results of Aggregate

| Properties | Natural Aggregate (A) | Artificial Aggregate (B) |
|-------------------------|-----------------------|--------------------------|
| Size and Shape | 12.5mm & Angular | 12.5mm & Angular |
| Impact Strength (%) | 14.81 | 12.75 |
| Crushing Strength (%) | 17.76 | 15.26 |
| Water Absorption (%) | 1.71 | 0.57 |
| Abrasion Resistance (%) | 26.69 | 22.90 |
| Specific Gravity | 2.6 | 2.01 |
| Elongation Index (%) | 22.05 | 27.99 |
| Flakiness Index (%) | 32.09 | 21.95 |
| Angularity Number | 7 | 9 |

The concrete is prepared with different percentage of replacement and its tested in fresh and hardened state. The test results are tabulated in table no.16 and 17

Table 16: Test Results of Fresh Concrete

| Mix No | Different % of Replacement of aggregate | Slump (mm) | Compaction Factor (%) | Vee Bee (Sec) | Flow (%) |
|--------|---|------------|-----------------------|---------------|----------|
| 1 | Conventional Concrete | 85 | 0.9 | 9.54 | 40 |
| 2 | 10% of Artificial Coarse Aggregate | 82 | 0.86 | 9.25 | 42 |
| 3 | 20% of Artificial Coarse Aggregate | 77 | 0.87 | 8.57 | 43 |
| 4 | 30% of Artificial Coarse Aggregate | 79 | 0.83 | 8.48 | 45 |
| 5 | 40% of Artificial Coarse Aggregate | 78 | 0.85 | 8.36 | 48 |
| 6 | 50% of Artificial Coarse Aggregate | 78 | 0.85 | 8.35 | 48 |
| 7 | 60% of Artificial Coarse Aggregate | 78 | 0.85 | 8.30 | 48 |

Table 17 : Test Results of Hardened Concrete

| Mix no | Compression Test (N/mm ²) | Days | | | |
|--------|---------------------------------------|------|-------|-------|-------|
| | | 3 | 7 | 14 | 28 |
| 1 | Coventional Cube | 8.76 | 12.58 | 19.10 | 22.86 |
| 2 | 10% Artificial Coarse Aggregate | 8.80 | 12.60 | 21.08 | 22.97 |

| | | | | | | | |
|---|-----|----------------------|--------|------|-------|-------|-------|
| 3 | 20% | Artificial Aggregate | Coarse | 9.14 | 13.26 | 21.56 | 23.27 |
| 4 | 30% | Artificial Aggregate | Coarse | 8.67 | 12.56 | 19.05 | 22.67 |
| 5 | 40% | Artificial Aggregate | Coarse | 7.54 | 11.56 | 18.36 | 21.46 |
| 6 | 50% | Artificial Aggregate | Coarse | 6.46 | 10.57 | 17.56 | 20.86 |
| 7 | 60% | Artificial Aggregate | Coarse | 6.20 | 10.02 | 17.32 | 18.99 |

5 Conclusions

Many researchers identified many materials that can replace coarse aggregate. An artificial coarse aggregate is manufactured and compared with natural coarse aggregate.

This manufactured coarse aggregate has similar properties of natural coarse aggregates per the IS codes. The tested aggregate is then replaced in different replacement from 10% to 60% in concrete. Fresh and hardened concrete properties analysed and found satisfactory results as per Codal recommendation. In that 20% replacement gives highest compression strength. This manufactured artificial aggregate can be substituted for natural coarse aggregate which will reduce the natural aggregate content in manufacturing concrete. This leads to conserve the natural resource and effectively utilize natural aggregate_[10].

Reference

- [1] C. Albano, N. Camacho, M. Hernandez, A. Matheus, A. Guti rre, "Influence of content and particle size of waste pet bottles on concrete behavior at different w/c ratios" *Waste Management*, vol. 29, pp.07–16, 2009.
- [2] J.S. Correia, A.S. Pereira, A. Brito, "Concrete made with ceramic recycled aggregates. Experimental campaign performed at IST (in Portuguese)", Report ICIST DTC No. 5/02, IST, Lisbon. 2002.
- [3] HeruPurnomo, GandjarPamudji and MadsuriSatim "Influence of uncoated and coated plastic waste coarse aggregates to concrete compressive strength MATEC Web of Conferences, pp 1-5, 2017.
- [4] H. Higashiyama, M. Sappakittipakorn, M. Sano and F. Yagishita, F, "Chloride ion penetration into mortar containing ceramic waste aggregate." *Construction Building Materials*, vol. 33(8), pp 48–54, 2012.
- [5] C. Madheswaran, P. S. Ambily, and J.K. Dattatreya, "Studies on use of Copper Slag as Replacement Material for River Sand in Building Constructions *Journal of The Institution of Engineers (India): Series A*, vol. 95, Issue 3, pp 169–177, 2014.
- [6] J.T. Shahu and S. Patel and A. Senapati, "Engineering Properties of Copper Slag–Fly Ash–Dolime Mix and Its Utilization in the Base Course of Flexible Pavements" *Journal of Material Civil Engineering*, vol. 25(12), pp 1871-1879, 2013.
- [7] M.R. Divya, M.Rajalingam and Sunilaa George, "Study on Concrete with Replacement of Fine Aggregates by Vermiculite" *International Journal of New Technology and Research*, vol. 2(5), pp 87-89, 2016.
- [8] IS 10262-2009, 'Guidelines for concrete mix design proportioning', Bureau of Indian Standards, New Delhi, India.
- [9] IS 383-1970, 'Specification for coarse and fine aggregates from natural sources for concrete', Bureau of Indian Standards, New Delhi, India.
- [10] J. Anne Mary & G. Janardhanan, "Manufacturing of Artificial Coarse Aggregate with Copper Slag, Vermiculite, Waste Plastic and Waste Ceramic" *Indian Patent 356441*, 2021.

Mind Mapping: The Best Selective Tool for Learning and Teaching

Mr. Ramu Yarlagadda¹, Dr. Mantri Venkata Raghu Ram²

1. Assistant Professor, Dept. of Science & Humanities, KKR & KSR Institute of Technology and Sciences (KITS), GUNTUR, AP.

Mail ID: ramuphd2014@gmail.com

2. Professor & Head, Dept. of Basic Sciences & Humanities, Vasireddy Venkatadri Institute of Technology (VVIT), GUNTUR, AP.

Abstract

The present world scenario of learning and teaching community runs on MOOCs due to COVID-19 but the methods for learning and teaching have been progressively depending on the IQ of everyone who wants to become a master of his / her own interested area of knowledge. Among a many number of learning and teaching methods since antiquity, one of the best pioneering methods is Mind Mapping which has been proven as the zenith method in the lives of world great personals in diverse fields to make the entire world rich and smart through generation by generation by inventing and discovering the worlds innovatively to generate the lives of humans smooth and smart.

Mind Map is one of the best ways for learning and teaching of one's ideas or thoughts to produce any kind of presentation successfully. It plays a pivotal role especially in the lives student community to learn any subject of their interest with proper ideology. An idea can be structuralized in the form of a diagram or a chart in any variety of models rolling around the central concept or subject to build an intuitive design or framework with words, tasks, concepts, items and so on.

Key Words: *Mind Map, MOOCs, area of knowledge, learning and teaching methods, ideology, tasks, framework or diagram, central concept or subject etc.,*

1. Introduction

A Mind Map has been successfully a progressive and easy method for learning and teaching of brainstorm ideas or thoughts by using diagrams that visually "Map" information in pictorial methods which record knowledge of a long history in learning, memory, visual thinking and problem solving by educators, psychologists, engineers and others since its inception as it was familiarized by British psychology author Tony Buzan and organically having no worry about its order and framework. We are availed to visually structuralize our ideas to come with analysis and recall our thoughts.

Tony Buzan had claimed that he has won an authentication for the origin of the Mind Map. His specific approach towards the term "Mind Map" has arisen during a 1974 BBC TV series hosted and called Use Your Head. In this show and companion book series, his conception of radial tree and diagramming key words in a colourful, radiant, tree-like structure were promoted. In his opinion, the readers scan the information from left to right and top to bottom whereas human brain's natural preference is to scan the whole page in a non-linear fashion. For his credit he has a lot of registered trademarks on Mind Mapping and it is brought into the light to promote the exclusive use of Mind Mapping over other forms of learning and teaching methods.

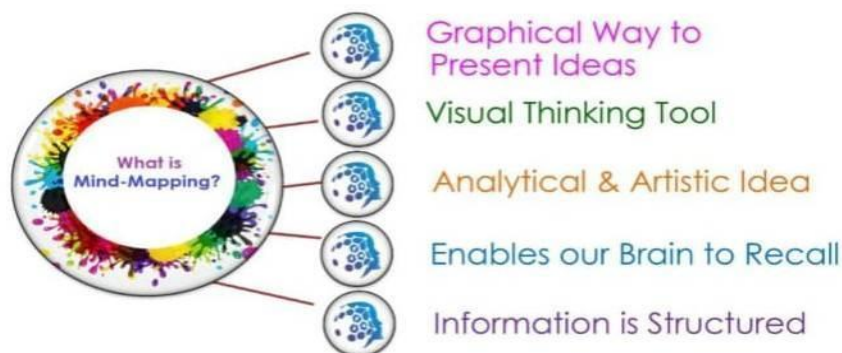


Fig.1

A Mind-Map is a tool that can change full length information into a simple, colourful, memorable and a highly structured diagram which works in an order with the brain's natural flow of functioning thoughts or ideas and is useful to entice, stimulate, delight and challenge everyone who wishes to discover the facts about an idea and its functions.

1.1 The General Structure of Mind-Mapping.

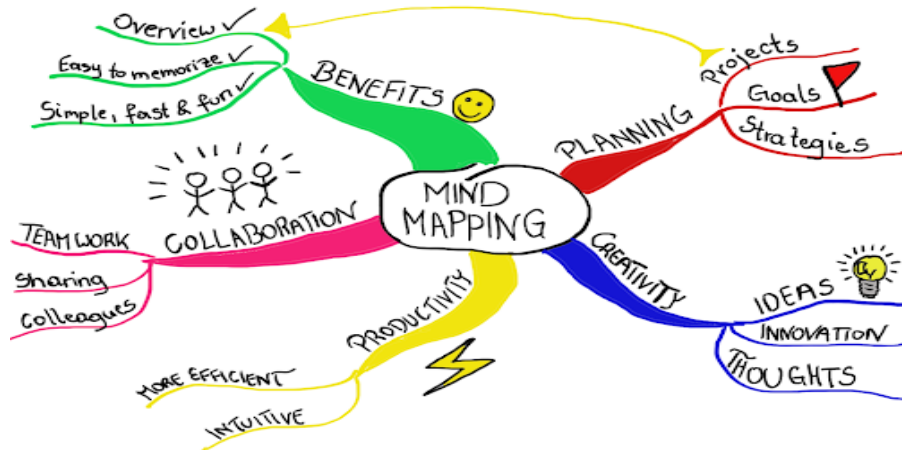


Fig.2

2. Importance and Exploitation of the Power of Human Brain

A Mind Map is an exclusive effective way of collecting information in and out of human brain. It is a creative and logical means of note-taking and not-making that literally maps-out human brain. When it is studied the functionality and the memory system of our brain, we should realize the extraordinary extent of its capacity and potential. It also has a natural organizational structure that radiates from the centre and use lines, symbols, words, colour and images according to simple, brain-friendly concepts.

In view of Dr. Roger Sperry, a Nobel Prize winner, it is confirmed that the evolutionarily most recent part of the brain, the “thinking cap” of the intellectual Cortex, has two major hemispheres those performed a comprehensive range of intellectual tasks named cortical skills which includes: Logic, Rhythm, Lines, Colour, Lists, Daydreaming, Numbers, Imagination, Words etc,. In his research, it is confirmed that when we plan Mind Map, we should practice and exercise the fundamental memory powers and information processing and also using our entire range of cortical skills. The Mind Map is made even more powerful by the use of all the left and right brain-thinking tools which enhance the clarity, structure and organization of our thinking. So it can be considered that the Mind Map is the ultimate thinking tool which incorporates all the significant and potent ways of thinking into its own structure.

It ...

- ✓ Explores and visualizes new ideas and concepts
- ✓ Activates our thoughts to flow freely and directly to the central concept
- ✓ Focuses on keywords and ideas
- ✓ Gathers brainstorm ideas
- ✓ Memorizes information, retention
- ✓ Creates presentations by connecting the pieces of the whole
- ✓ Executes group projects as an image in the centre
- ✓ Increases creativity and productivity
- ✓ Improves writing and thinking capability
- ✓ Makes learning interesting to summarize information in a very systematic way

2.1 Sample Structure of Mind-Mapping

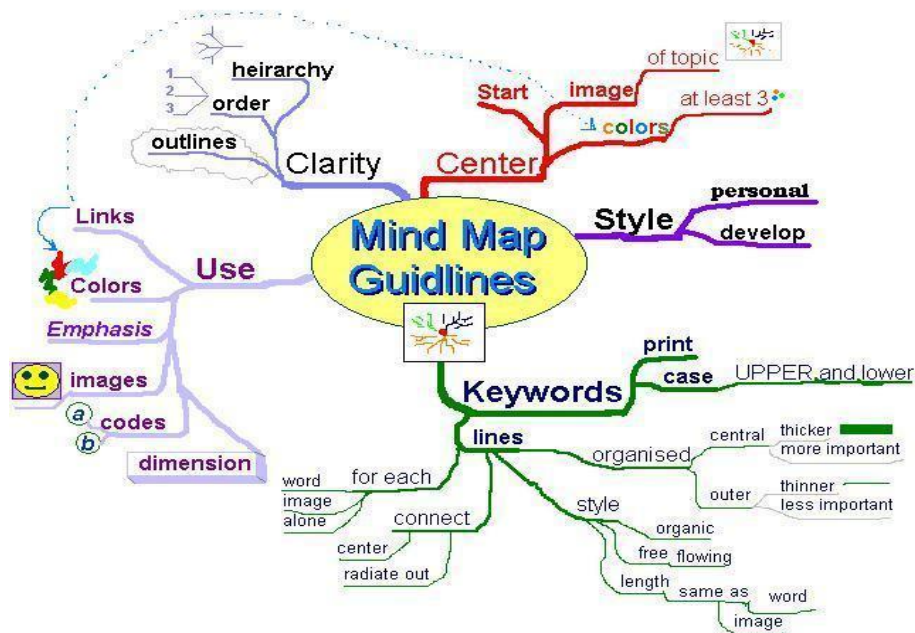


Fig.3

The only simple method to understand the Mind-Map is by the use of all the left and right brain thinking tools that explore clarity, structure and organization of human thinking because it constructively uses the tools of imagination, association and location as well as the tools of the left and right brain and it can be considered the ultimate thinking tool that incorporates all the significant and potent ways of thinking into its own structure.

3. The Best Five Characteristic Features of Mind Mapping

- ❖ The main idea, subject or focus is crystallized in a central image
- ❖ The main themes radiate from the central image as 'branches'
- ❖ The branches comprise a key image or key word drawn or printed on its associated line
- ❖ Topics of lesser importance are represented as 'twigs' of the relevant branch
- ❖ The branches form a connected nodal structure

3.1 A Picture is Worth a Thousand Words (The Power of Images)

As Ralph Haber's research noted in Scientific American magazine in 1970 that every individual has the accuracy in recognizing the images because they make use of a wide range of everyone's cortical skills and imagination. Images can be more redolent than words, more accurate and powerful in triggering a broad range of associations, thereby enhancing innovative thinking and memory. These findings support the argument so that the Mind Map is a uniquely appropriate tool.

In visualizing the impact of words through Mind Map is exemplified below as shown in the image of the thumbnail – How to Mind Map.

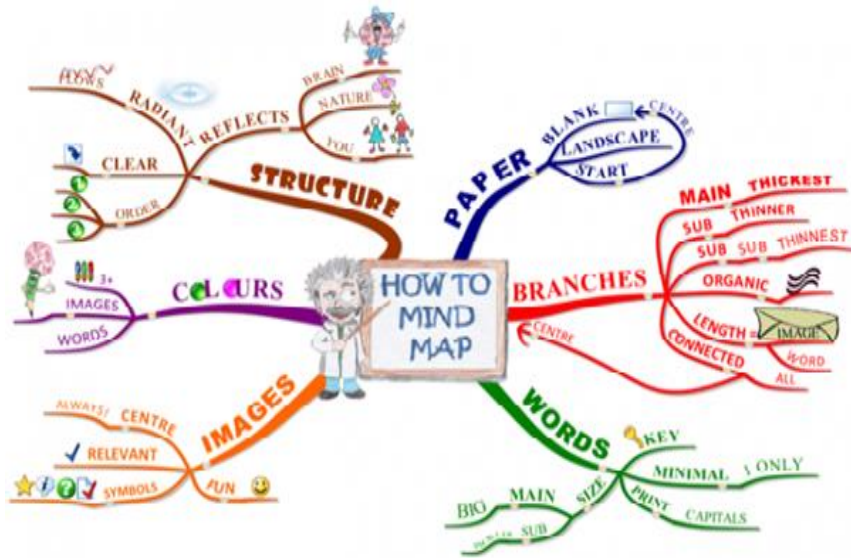


Fig.4

4. Mind Mapping - A Powerful Approach for student community to attempt exams

It is also proven that Mind Mapping is helpful for dyslexics and autistic students to better understand concepts and strategies. In fact, The British Dyslexia Association states that "Dyslexics struggle with their spoken and/or written language, following instructions, poor concentration and carrying out analytical or logical tasks. Strategies such as Mind Mapping are recognized as valuable learning tools." As Johns Hopkins study indicated that the student community who utilize Mind Mapping has increased their grades by 12%.

Mind Mapping is a useful technique that supports student community in learning, improves information recording, shows how different facts and ideas are related, and enhances creative problem solving. As Tony Buzan opined that student community uses a two dimensional structure, instead of a list format traditionally used to take notes which makes information easier to remember, recall and quick to review.

4.1 Dimensional Structure of Mind-Mapping During The Time of Exam



Fig.5

A good Mind Map shows the "shape" of the subject, the relative importance of individual points, and the ways in which facts relate to one another. It is shown that Research is of particular benefit when dealing with complex information, such as during business planning and strategy development. And further these are more compact than conventional notes which help us to make associations and to generate new ideas. Mind Mapping can also help us to break down large projects or topics into manageable chunks, so that we can plan effectively without getting overwhelmed and without forgetting something important.

5. Mind-Map: The Best Knowledge Recollecting Tool for Teachers

Mind Maps are also good for refreshing information in the mind of a teacher. When the teacher commits the shape and structure of a Mind Map to memory, he/she can often get the cues what he/she needs to remember the information that contains just by glancing quickly at the Map. Studies have shown that this makes them highly valuable when the teacher is learning a language. For example a teacher can really get inventive ideas with Mind Maps then he/she is great for boosting creativity when he/she includes colours, images or drawings what he/she can even resemble a work of art.

To draw a perfect Mind Map, the following five steps are most preferable to explore an idea of any area of the subject or project.

- Write the title of the subject or project that we explore in the centre of a page and draw a circle around it.
- Draw lines out from this circle as we think of subheadings of the topic or important facts or tasks that relate to our subject and label these lines with subheadings.
- Dive deeper into the subject to uncover the next level of information such as related to sub-topics or tasks or facts then link these to the relevant subheadings.
- Repeat the process for the next level of facts, tasks, and ideas. Draw lines out from the appropriate headings and label them aptly.
- As we discover new information or think of additional tasks, add them to our Mind Map in the appropriate places.

5.1 A Common Structure of Mind-Mapping in the Classroom



Fig.6

A complete Mind Map has its central point like a trunk which is surrounded by many radiating lines with sub-topics forking off like branches and twigs from the trunk of a tree. So everybody has an ideology to produce it with a unique structure which evolves of its own accord.

6. Tips for effective Mind Map

- ✳ **Use Single Words or Uncomplicated Phrases** – Keep things simple. In Mind Maps, single strong words and short, meaningful phrases can convey the same meaning more potently.
- ✳ **Use Colour to Separate Different Ideas** – Colour can help to show the organization of the subject. It can also make our Mind Map a more appealing document, and help us to visualize the different sections of our Mind Map for future recall.
- ✳ **Use Symbols and Images** – Pictures can help us to remember information more effectively than words, so use symbols or pictures that mean something to use it.
- ✳ **Using Cross-Linkages** – Information in one part of a Mind Map may relate to another part, so draw lines to show these cross-linkages. This will help us to see how one part of the subject affects another.

Mind Mapping is a powerful note-taking method. Mind Maps not only highlight important facts, but also show the overall structure of a subject and the relative importance of individual parts of it. They are great when we need to think creatively, and can help us to make new connections between ideas.

7. Conclusion

Creating a future mind map is easy and fun, whether we are artistically inclined or not. Think of it as an extended doodle and visually map out and plan our future, if it is wanted. Mind mapping is one modern day approach that draws on associations and imagination to create an overview of lots of seemingly separate pieces of information to find and clarify pathways, solutions and to organize issues. It uses words, colours and images to convey meaning. Mind mapping is a way of organizing our thoughts. Therefore, let our inner light shine when we create a mind map. Let our mind map express our innermost essence.

Eventually, Mind Mapping can improve study skills quickly and easily. Our brain responds to Mind Mapping as it replicates the natural thinking process, so we shall find our ideas simply flow onto the page, making the studying more enjoyable and more fun. In developing our career plan, Mind Mapping is a titanic tool to organize the skills and knowledge what we would like to develop.

References

- [1] Buzan, Tony, Use Your Head. London: BBC Books, 1974.
- [2] "Roots of visual mapping - The mind-mapping.org Blog". *Mind- mapping.org*. 2004-05-23. Retrieved 2013-07-10.
- [3] "Who invented mind mapping". *Mind-mapping.org*. Retrieved 2013-07-10.
- [4] "Buzan claims mind mapping his invention in interview". Knowledge Board. Archived from the original on 2010-02-13.
- [5] "Roots of visual mapping - The mind-mapping.org Blog". *Mind-mapping.org*. 2004-05-23. Retrieved 2013-07-10.
- [6] <https://www.mindmapping.com/mind-map>
- [7] <https://involve.co.uk/the-power-of-mindmaps>

Analyses of Plant Diversity in a Sacred Grove of Ariyalur District, Tamil Nadu, India

Rajkumar, G¹, Ravipaul, S²

^{1,2}P.G. & Research Dept. of Botany, Government Arts College, Ariyalur- 621713
(Affiliated to Bharathidasan University Tiruchirappalli-620024)
rajcumarguna83@gmail.com

Abstract

Assessment on the plant diversity in Karuppusamy sacred grove near Thathanur in the Ariyalur district of Tamil Nadu, India, was carried out during 2019-2020. In the study, a total of 121 plant species were recorded belonged to 104 genera distributed among 50 families, are Angiosperms. Fabaceae (8 species) is a dominant family followed by Asclepiadaceae, Mimosaceae (7 species), Euphorbiaceae, (6 species), and 5 species each from Rubiaceae and Poaceae. The diversity indices namely the Shannon -Weiner index, Simpson index, evenness index, etc., were analyzed.

Keywords: Sacred groves, Angiosperms, Diversity indices

1. Introduction

Biodiversity is the dissimilarity of life forms within a given ecosystem, biome, or for the whole earth. This entirety in the origin of species and ecosystems provide the basis of life on earth. (Reid and Miller *et al.*, 1989). Biodiversity is the “Totality of genes, species, and ecosystem of a region”. It plays a significant role in maintaining the entire earth. Besides this significant contribution, it also provides a socio-economic and monetary asset to the nation. Biodiversity is often used as a measure of the health of the biological system. The only means to rectify the loss is to achieve conservation of biological diversity, as in the case of protected areas wherein the aspect deals with reintroducing some species, restore the ecosystem, and managing or to eradicating previously introduced plants and animals. Biodiversity is the very basis of human survival and economic well-being and encompassed all life forms, ecosystems, and ecological processes, acknowledging the hierarchy at genetic, taxon, and ecosystem levels (McNeely *et al.*, 1990). Apart from the ethical and aesthetics, biodiversity provides to humankind enormous direct economic benefits in the form of timber, food, fibre, industrial enzymes, food flavours, fragrances, cosmetics, emulsifiers, dyes, plant growth regulators, and pesticides Mannion (1995); (Costanza *et al.*, 1997).

Sacred groves are temple forests or patches of national climax forests preserved as a product of above described beliefs by the local people. (Gadgil and vartak, *et al.*, 1975). Declaring a scrap of forest near the villages as sacred and protecting it on the grounds of spiritual and cultural beliefs is an venerable practice with the ethnic community in the northeastern hill region of India. Thousands of sacred groves are found in India. They occur chiefly in Andhra Pradesh, Assam, Bihar, Karnataka, Kerala, Madhya Pradesh, Maharashtra, Rajasthan, and Tamil Nadu. (Britto *et al.*, 2001).

These sacred groves during reality in the area since time immemorial and are considered to be the relic of the original forest vegetation of the region. These are among the few least disturbed forest patches in the region serving as the original treasure house of biodiversity. The sacred groves are extremely rich in floral and faunal elements. The species satisfied in these sacred groves is incredibly high. The sacred groves contain several valuable medicinal and other economically important plants. One of the most significant conventional uses of sacred groves was that it acted as a repository for a variety of Ayurvedic medicines.

The groves are often associated with ponds and streams and meet water requirements of local communities they sometimes help in recharging aquifers as well. The many of the groves are looked upon as abode of Hindu gods. In the recent past a number of them been partially cleared for construction of shrines and temples. A large number of distinct local art forms and folk traditions are associated with the deities of sacred

groves and are an important cultural aspect closely associated with sacred traditions. The sacred groves in India can basically be classified under three categories.

2. Material and Methods

2. 1. Study Area

The study area karuppusamy kovil Thathanur village, located at udayarpalayam taluk, Ariyalur district, Tamilnadu. Located at a distance of 310 km from the state capital Chennai. It is bounded on the north by cuddalore, south by Thanjavur and west by Perambalur and Tiruchirappalli districts. Its geographical limit is 11.1360°N Latitude, 79.2352°E longitude, with elevation ranging 83m altitude above mean sea level an inland district without any coastline. The district has Velar River in the north Kollidam River in the south. In spite of the human activity within its premises the site is well protected and conserved since it is revered as sacred.

2. 2. Methodology

The sacred grove is spread over 2 ha with the Karuppusamy kovil in the midst. The patch was randomly sampled with 10 (10x10) m workable quadrates. Within each quadrate all individuals' species of trees (with girth \geq 30cm) and shrubs GBH (girth at breast height) were measured and noted in field note. Herbs and seedlings were studied in 1x1m quadrates. The data are documented in a field note. The segments which were visited repeatedly. The collected specimens were identified and systematic enumeration was made with available monographs, relevant literatures and taxonomic revisions (Gamble 1935; Mathew, 1982). For phytosociological studies, the parameters like density, relative density, abundance, percentage frequency, relative frequency, relative basal area and importance value index (IVI) were estimated by using standard procedures (Magurran, 1988; Gopikumar *et al.*, 2005). Plant species associations were found out by using following formulae:

Total number of individuals of a species in all quadrates

$$1. \text{ Density} = \frac{\text{Total number of individuals of a species in all quadrates}}{\text{Total number of quadrates studied}}$$

Total number of quadrates studied

Number of quadrates in which the species occurred

$$2. \text{ Frequency (\%)} = \frac{\text{Number of quadrates in which the species occurred}}{\text{Total number of quadrates studied}} \times 100$$

Total number of quadrates studied

Total number of individuals of a species in all quadrates

$$3. \text{ Abundance} = \frac{\text{Total number of individuals of a species in all quadrates}}{\text{Total number of quadrates in which the species occurred}}$$

Total number of quadrates in which the species occurred

The number of individuals of the species

$$4. \text{ Relative density} = \frac{\text{The number of individuals of the species}}{\text{The number of individuals of all the quadrates}} \times 100$$

The number of individuals of all the quadrates

The number of occurrences of the species

$$5. \text{ Relative frequency} = \frac{\text{The number of occurrences of the species}}{\text{The number of individuals of all the species}} \times 100$$

The number of individuals of all the species

- The total basal area of the species
6. Relative dominance = $\frac{\text{The total basal area of the species}}{\text{The total basal area of all the species}} \times 100$
- The total basal area of all the species
7. Basal Area (BA) = $(P^2 \times 4\pi) \times 10,000 \text{ m}^2$
8. The species richness was calculated by 'Margalefs Index of richness' (D_{mg}) (Magurran, 1988)
9. Shannon wiener index (H) = $-\sum P_i \times \log_2 \text{ of } P_i$.
10. Simpson's index (λ) = $\sum P_i^2$
11. Evenness index (E) (pielou 1966) = $E = H/\log S$
11. Important value index (IVI) = $R.D+R.F+R.BA$

3. Results and Discussions

3. 1. Floristic Composition

The data collected during the field sampling are tabulated and consolidated separately for trees, Shrubs, Herbs and climbers. (Tables-1to3). In the present study of 121 species were recorded belonging to 104 genera distributed among 50 families belong to the angiosperms. The present study showed more number of plant species than the phyto-sociological studies of sacred groves, in Pudukottai district, Tamilnadu India (Vinoth-Kumar *et al.*, 2011). Among them, Fabaceae (8 spp.) is a dominant family followed by Asclepiadiaceae (7 spp.), Mimosaceae (7 spp.), Asteraceae, Amaranthaceae and Euphorbiaceae (6 spp each.), Poaceae, and Rubiaceae, (5 spp. each). Caesalpiniaceae, Cucurbitaceae, Lamiaceae, and Malvaceae (4 spp. each). The remaining families contribute a single species each. This study shows about 22% (27) tree species, 19% (23) shrub species and 41% (49) herbaceous species and 18% (22) climbers (Fig.2). This number of individual is relatively equal when compare to the floristic composition on the selected sacred groves of Perambalur district (Rajkumar *et al.*, 2014). In a similar study, Parthasarathy *et al.* (2008) enumerated 102 trees and 47 lianas from 75 groves in Pudukkottai district itself. Floristic study of vegetation is important to determine the distribution of food plants for wildlife (Ejtehadi *et al.*, 2005). Several studies with respect to floristic inventory were reported includes 260 species in 176 genera and 62 families from malliganatham (John Britto *et al.*, 2001). Thus, floristic diversity assessment is significant at local and regional levels to understand the present status and to make effective management strategies for conservation (Jain *et al.*, 1976).

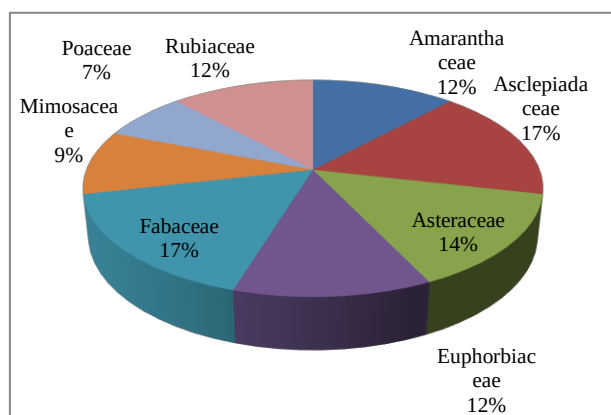


Figure 1: Predominant family-wise distribution of species in Thathanur village sacred grove

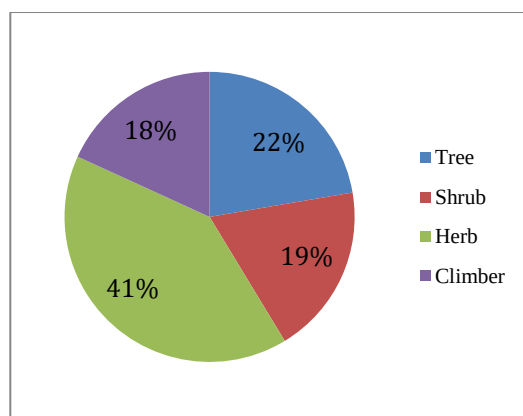


Figure 2: Habit-wise percentage of plants species in Thathanur village sacred grove.

3. 2. Phyto-sociological studies

Density, Frequency, Abundance, and Basal area

The sacred grove is mostly covered by deciduous species whose *Ailanthus excelsa* (1.30) had the highest density. The other frequency and abundance values are *Ailanthus excelsa* (50), *Cassia fistula* (40), *Alangium salvifolium*, *Albizia amara* (each 30), and the small tree *Atalantia racemosa* (10) have contributed the highest frequency values. The abundant tree species encountered in the study area are *Prosopiss juliflora* (4.0) followed by *Alangium salviifolium* (3.0) and the six species *Azadirachta india*, *Strychnos nux-vomica*, *Tamarindus indica*, *Wattakaka volubilis*, *Derris scandens* and *Ziziphus mauritina* contributed the medium abundance value (2.0) of the study area. A similar report made a study on woody vegetation structure in a sacred grove of Pudukkottai district (Muthukumar *et al.*, 2005).

The other tree species contributed the lowest abundance value 1.0 to 1.5. Species contribution to the total basal area 4.446 m² (109 indiv.) is shown in the table. *Ailanthus excels* (1.22 m²) is the highest contributor followed by *Tamarindus indica* (0.63m²) (Plate – 5) and *Alangium salvifolium* (0.531m²) *Albizia amara* community proposed for dry evergreen forest type by (Meher Homji, 1973) is applicable. It was low compared to the basal area contribution of Pondicherry, where the total basal area was 4.09 (Ramanujam *et al.*, 2003).

. In the shrub (23) species *Abutilon indicum* (2.4) and *Abutilon hirtum*, *Lantana camara* (1.2) (Plate – 9) contributed the highest density values followed by *Benkara malabarica* and *Capparis divaricata* showed the dense value (0.9) respectively. *Abutilon indicum*, *Capparis divaricata* (50) followed by *Benkara malabarica* (40), *Abutilon hirtum*, *Carrissa spinarum*, *Jatropha curcus*, *Lantana camara*, and *Sida acuta* (each 30) contributed the highest frequency value.

Among the herbaceous 49 species covered by the sacred grove, were *Anisomeles indica* (5.40) followed by *Aristida adscensionis* (4.70) and *Aerva lanata* (4.30) have showed highest density values. *Achyranthes aspera* (100) followed by *Croton bonplandianus* (80), *Anisomeles indica*, *Chloris virgata*, (90) and *Aerva lanata* (70) contributed the highest frequency value.

The climber 22 species like *Cardiospermum halicacabum* (1.50), *Citrullus colocynthis* (0.20), and *Mukia maderaspatana* (1.10) having high density and lowest value *Solena amplexiculis* (0.10). *Cardiospermum halicacabum*, *Citrullus colocynthis*, and *Hemidesmus indicus* (40) contributed the highest frequency.

3. 3. Important Value Index (IVI) Analysis

Among the tree species *Ailanthus excels* had (48.13) important value index (IVI) was very high followed by *Alangium salviifolium* (25.46) and *Borassus flabellifer* (23.39) (Table – 4). Ariyalur district. The important value index (IVI) combines relative frequency, relative density and relative dominance and this measure can be used to indicate the ecological influence of each species in the forest (Khamyong *et al.*, 2004).

Table 1: Structural diversity aspects of tree species in sacred grove of thathanur village,

| Species Name | AB | DEN | RD | FQ | RF | BA | RDO | IVI |
|--|------|------|-------|----|-------|--------|---------|-------|
| <i>Acacia leucophloea</i> (Roxb.) Willd. | 1.00 | 0.10 | 0.92 | 10 | 1.754 | 0.0306 | 0.6882 | 3.36 |
| <i>Acacia nilotica</i> (L.) Willd. | 1.50 | 0.30 | 2.75 | 20 | 3.509 | 0.0019 | 0.0427 | 6.30 |
| <i>Ailanthus excelsa</i> Roxb. | 2.60 | 1.30 | 11.93 | 50 | 8.772 | 1.22 | 27.4361 | 48.13 |
| <i>Alangium salviifolium</i> (L.f.) Wang. | 3.00 | 0.90 | 8.26 | 30 | 5.263 | 0.531 | 11.9414 | 25.46 |
| <i>Albizia amara</i> (Roxb.) Boivin | 1.67 | 0.50 | 4.59 | 30 | 5.263 | 0.0484 | 1.0884 | 10.94 |
| <i>Albizia lebbeck</i> (L.) Benth. | 1.00 | 0.20 | 1.83 | 20 | 3.509 | 0.062 | 1.3943 | 6.74 |
| <i>Atalantia monophylla</i> (L.) Correa | 1.00 | 0.10 | 0.92 | 10 | 1.754 | 0.028 | 0.6297 | 3.30 |
| <i>Azadirachta indica</i> Adr.Juss. | 2.00 | 0.40 | 3.67 | 20 | 3.509 | 0.0245 | 0.5510 | 7.73 |
| <i>Borassus flabellifer</i> L. | 2.33 | 0.70 | 6.42 | 30 | 5.263 | 0.5206 | 11.7076 | 23.39 |
| <i>Cassia fistula</i> L. | 1.50 | 0.60 | 5.50 | 40 | 7.018 | 0.0261 | 0.5870 | 13.11 |
| <i>Cassine glauca</i> (Rottb.) Kuntze | 1.50 | 0.30 | 2.75 | 20 | 3.509 | 0.023 | 0.5172 | 6.78 |
| <i>Chloroxylon swietenia</i> DC. | 2.00 | 0.40 | 3.67 | 20 | 3.509 | 0.0345 | 0.7759 | 7.95 |
| <i>Derris scandens</i> (Roxb.) Benth. | 2.00 | 0.20 | 1.83 | 10 | 1.754 | 0.0023 | 0.0517 | 3.64 |
| <i>Euphorbia antiquorum</i> L | 2.00 | 0.40 | 3.67 | 20 | 3.509 | 0.0389 | 0.8748 | 8.05 |
| <i>Ficus benghalensis</i> L. | 1.00 | 0.10 | 0.92 | 10 | 1.754 | 0.24 | 5.3973 | 8.07 |
| <i>Lannea coromandelica</i> (Houtt.) Merr. | 1.00 | 0.20 | 1.83 | 20 | 3.509 | 0.0129 | 0.2901 | 5.63 |
| <i>Madhuca longifolia</i> (L.) Macbr. | 1.00 | 0.10 | 0.92 | 10 | 1.754 | 0.0063 | 0.1417 | 2.81 |
| <i>Morinda pubescens</i> Smith. | 2.33 | 0.70 | 6.42 | 30 | 5.263 | 0.0071 | 0.1597 | 11.84 |
| <i>Pithecellobium dulce</i> (Roxb.) Benth. | 1.00 | 0.10 | 0.92 | 10 | 1.754 | 0.0666 | 1.4977 | 4.17 |
| <i>Prosopis juliflora</i> (Sw.) DC. | 4.00 | 1.20 | 11.01 | 30 | 5.263 | 0.24 | 5.3973 | 21.67 |
| <i>Strychnos nux-vomica</i> L. | 2.00 | 0.60 | 5.50 | 30 | 5.263 | 0.12 | 2.6986 | 13.47 |
| <i>Syzygium cumini</i> (L.) Skeels | 1.00 | 0.20 | 1.83 | 20 | 3.509 | 0.1151 | 2.5884 | 7.93 |
| <i>Tamarindus indica</i> L. | 2.00 | 0.20 | 1.83 | 10 | 1.754 | 0.63 | 14.1678 | 17.76 |
| <i>Tectona grandis</i> L.f. | 1.33 | 0.40 | 3.67 | 30 | 5.263 | 0.0965 | 2.1701 | 11.10 |
| <i>Thespesia populnea</i> (L.) Sol.ex Corr.Serr. | 1.00 | 0.10 | 0.92 | 10 | 1.754 | 0.3075 | 6.9152 | 9.59 |
| <i>Wattakaka volubilis</i> (L.f.) Stapf | 2.00 | 0.20 | 1.83 | 10 | 1.754 | 0.0061 | 0.1372 | 3.73 |
| <i>Ziziphus mauritiana</i> Lam. | 2.00 | 0.40 | 3.67 | 20 | 3.509 | 0.0068 | 0.1529 | 7.33 |

Table 2: Structural diversity aspects of shrub species in sacred grove of Thathanur village, Ariyalur district.

| Species Name | AB | DE | RD | FQ | RF |
|---|------|------|-------|----|-------|
| <i>Abutilon hirtum</i> (Lam.) Sweet | 4.00 | 1.20 | 9.02 | 30 | 5.882 |
| <i>Abutilon indicum</i> (L.) Sweet | 4.80 | 2.40 | 18.05 | 50 | 9.804 |
| <i>Adhatoda zeylanica</i> Medic. | 2.00 | 0.20 | 1.50 | 10 | 1.961 |
| <i>Allophylus serratus</i> (Roxb.)Kurz | 2.50 | 0.50 | 3.76 | 20 | 3.922 |
| <i>Benkara malabarica</i> (Lam.)Tirv. | 2.25 | 0.90 | 6.77 | 40 | 7.843 |
| <i>Cadaba fruticosa</i> (L.) Druce | 2.00 | 0.40 | 3.01 | 20 | 3.922 |
| <i>Calotropis gigantea</i> , (L.) R.Br. | 1.50 | 0.30 | 2.26 | 20 | 3.922 |
| <i>Canthium coromandelicum</i> (Burm.f) Alst. | 4.00 | 0.80 | 6.02 | 20 | 3.922 |
| <i>Capparis divaricata</i> Lam. | 1.80 | 0.90 | 6.77 | 50 | 9.804 |
| <i>Carrissa carandas</i> L. | 1.50 | 0.30 | 2.26 | 20 | 3.922 |

| | | | | | |
|---|------|------|------|----|-------|
| <i>Carrissa spinarum</i> L. | 1.67 | 0.50 | 3.76 | 30 | 5.882 |
| <i>Cassia auriculata</i> L. | 2.50 | 0.50 | 3.76 | 20 | 3.922 |
| <i>Catunaregam spinosa</i> (Thunb.)Tirveng. | 1.00 | 0.10 | 0.75 | 10 | 1.961 |
| <i>Clausena dentata</i> (Willd.)Roemer | 2.00 | 0.20 | 1.50 | 10 | 1.961 |
| <i>Euphorbia tirucalli</i> L. | 4.00 | 0.40 | 3.01 | 10 | 1.961 |
| <i>Flueggea leucopyrus</i> Willd. | 2.50 | 0.50 | 3.76 | 20 | 3.922 |
| <i>Grewia abutilifolia</i> Vent.ex Juss. | 3.00 | 0.30 | 2.26 | 10 | 1.961 |
| <i>Jatropha curcus</i> L. | 2.00 | 0.60 | 4.51 | 30 | 5.882 |
| <i>Lantana camara</i> L. | 4.00 | 1.20 | 9.02 | 30 | 5.882 |
| <i>Nerium oleander</i> L. | 1.00 | 0.10 | 0.75 | 10 | 1.961 |
| <i>Opuntia stricta</i> Haw. | 2.00 | 0.20 | 1.50 | 10 | 1.961 |
| <i>Sida acuta</i> Burm.f | 2.33 | 0.70 | 5.26 | 30 | 5.882 |
| <i>Vitex trifolia</i> L. | 1.00 | 0.10 | 0.75 | 10 | 1.961 |

Table 3: Structural diversity aspects of herb species in sacred grove of Thathanur village, Ariyalur district.

| Species Name | AB | DE | RD | FQ | RF |
|--|-------|------|------|-----|-------|
| <i>Acalypha indica</i> L. | 4.00 | 1.20 | 1.78 | 30 | 2.344 |
| <i>Acanthospermum hispidum</i> DC. | 4.83 | 2.90 | 4.31 | 60 | 4.688 |
| <i>Achyranthes aspera</i> L. | 3.80 | 3.80 | 5.65 | 100 | 7.813 |
| <i>Aerva lanata</i> (L.) Juss. | 6.14 | 4.30 | 6.39 | 70 | 5.469 |
| <i>Aeschynomene aspera</i> L. | 2.00 | 0.20 | 0.30 | 10 | 0.781 |
| <i>Ageratum conyzoides</i> L. | 2.00 | 0.40 | 0.59 | 20 | 1.563 |
| <i>Allmania nodiflora</i> (L.)R. Br. | 6.00 | 1.20 | 1.78 | 20 | 1.563 |
| <i>Alternanthera sessilis</i> (L.) R.Br. | 5.67 | 3.40 | 5.05 | 60 | 4.688 |
| <i>Alysicarpus bupleurifolius</i> (L.) DC. | 2.00 | 0.20 | 0.30 | 10 | 0.781 |
| <i>Amaranthus spinosus</i> L. | 4.67 | 1.40 | 2.08 | 30 | 2.344 |
| <i>Amaranthus viridis</i> L. | 4.00 | 0.40 | 0.59 | 10 | 0.781 |
| <i>Ammannia baccifera</i> L. | 6.67 | 2.00 | 2.97 | 30 | 2.344 |
| <i>Anisomeles indica</i> (L.) O.Kuntze | 7.71 | 5.40 | 8.02 | 70 | 5.469 |
| <i>Anisomeles malabarica</i> R.Br. ex Sims | 6.00 | 1.20 | 1.78 | 20 | 1.563 |
| <i>Argemone mexicana</i> L. | 2.00 | 0.20 | 0.30 | 10 | 0.781 |
| <i>Aristida adscensionis</i> L. | 15.67 | 4.70 | 6.98 | 30 | 2.344 |
| <i>Aristida hystrix</i> L.f. | 12.00 | 1.20 | 1.78 | 10 | 0.781 |
| <i>Asclepias curassavica</i> L. | 2.00 | 0.20 | 0.30 | 10 | 0.781 |
| <i>Bacopa monnieri</i> (L) Pennell | 6.00 | 0.60 | 0.89 | 10 | 0.781 |
| <i>Barleria prionitis</i> L. | 2.00 | 0.20 | 0.30 | 10 | 0.781 |
| <i>Blepharis maderaspatensis</i> (L.) Roth | 3.50 | 0.70 | 1.04 | 20 | 1.563 |
| <i>Boerhavia diffusa</i> L. | 23.00 | 2.30 | 3.42 | 10 | 0.781 |
| <i>Caralluma adscendens</i> (Roxb.) Haw. | 1.00 | 0.10 | 0.15 | 10 | 0.781 |
| <i>Cassia tora</i> L. | 9.00 | 0.90 | 1.34 | 10 | 0.781 |
| <i>Chloris barbata</i> Sw. | 7.25 | 2.90 | 4.31 | 40 | 3.125 |
| <i>Chloris virgata</i> L. | 4.29 | 3.00 | 4.46 | 70 | 5.469 |
| <i>Cleome viscosa</i> L. | 3.75 | 1.50 | 2.23 | 40 | 3.125 |

| | | | | | |
|---|-------|------|------|----|-------|
| <i>Commelina benghalensis</i> L. | 5.50 | 1.10 | 1.63 | 20 | 1.563 |
| <i>Corchorus aestuans</i> L. | 2.00 | 0.20 | 0.30 | 10 | 0.781 |
| <i>Corchorus trilocularis</i> L. | 3.00 | 0.30 | 0.45 | 10 | 0.781 |
| <i>Croton bonplandianus</i> Baillon | 4.13 | 3.30 | 4.90 | 80 | 6.250 |
| <i>Cynodon dactylon</i> (L.) Pers. | 4.25 | 1.70 | 2.53 | 40 | 3.125 |
| <i>Cyperus rotundus</i> L. | 10.00 | 1.00 | 1.49 | 10 | 0.781 |
| <i>Datura metel</i> L. | 2.00 | 0.20 | 0.30 | 10 | 0.781 |
| <i>Enicostema axillare</i> (Lam.) A. Raynal | 9.00 | 0.90 | 1.34 | 10 | 0.781 |
| <i>Evolvulus alsinoides</i> (L.) L. | 2.00 | 0.20 | 0.30 | 10 | 0.781 |
| <i>Heliotropium supinum</i> L. | 4.00 | 0.40 | 0.59 | 10 | 0.781 |
| <i>Hyptis suaveolens</i> (L.) Poit. | 6.75 | 2.70 | 4.01 | 40 | 3.125 |
| <i>Indigofera tinctoria</i> L. | 2.00 | 0.20 | 0.30 | 10 | 0.781 |
| <i>Leucas aspera</i> (Willd.) Link. | 3.25 | 1.30 | 1.93 | 40 | 3.125 |
| <i>Oldenlandia umbellata</i> L. | 2.00 | 0.20 | 0.30 | 10 | 0.781 |
| <i>Parthenium hysterophorus</i> L. | 11.00 | 1.10 | 1.63 | 10 | 0.781 |
| <i>Plumbago zeylanica</i> L. | 2.00 | 0.20 | 0.30 | 10 | 0.781 |
| <i>Polycarpha corymbosa</i> (L.) Lam. | 6.00 | 1.20 | 1.78 | 20 | 1.563 |
| <i>Sphaeranthus indicus</i> L. | 2.00 | 0.20 | 0.30 | 10 | 0.781 |
| <i>Tephrosia purpurea</i> (L.) Pers. | 4.00 | 0.40 | 0.59 | 10 | 0.781 |
| <i>Tribulus terrestris</i> L. | 5.25 | 2.10 | 3.12 | 40 | 3.125 |
| <i>Tridax procumbens</i> L. | 4.25 | 1.70 | 2.53 | 40 | 3.125 |
| <i>Xanthium indicum</i> Koen. | 2.00 | 0.20 | 0.30 | 10 | 0.781 |

Table 4: Structural diversity aspects of climber species in sacred grove of Thathanur village, Ariyalur district.

| Species Name | AB | DE | RD | FQ | RF |
|---|------|------|-------|----|--------|
| <i>Abrus precatorius</i> L. | 2.00 | 0.40 | 3.36 | 20 | 5.000 |
| <i>Acacia caesia</i> (L.) Willd. | 1.00 | 0.30 | 2.52 | 30 | 7.500 |
| <i>Aristolochia indica</i> L. | 2.00 | 0.20 | 1.68 | 10 | 2.500 |
| <i>Cansjera rheedii</i> J.F. Gmel. | 2.00 | 0.20 | 1.68 | 10 | 2.500 |
| <i>Capparis zeylanica</i> L. | 2.50 | 0.50 | 4.20 | 20 | 5.000 |
| <i>Cardiospermum halicacabum</i> L. | 3.75 | 1.50 | 12.61 | 40 | 10.000 |
| <i>Ceropegia juncea</i> Roxb. | 2.00 | 0.20 | 1.68 | 10 | 2.500 |
| <i>Cissus quadrangularis</i> L. | 9.00 | 0.90 | 7.56 | 10 | 2.500 |
| <i>Citrullus colocynthis</i> (L.) Schrad. | 2.00 | 0.20 | 1.68 | 10 | 2.500 |
| <i>Clitoria ternatea</i> L. | 3.00 | 1.20 | 10.08 | 40 | 10.000 |
| <i>Coccinia grandis</i> (L.) J. Voigt. | 3.00 | 0.90 | 7.56 | 30 | 7.500 |
| <i>Cocculus hirsutus</i> (L.) Diels | 7.00 | 0.70 | 5.88 | 10 | 2.500 |
| <i>Cuscuta reflexa</i> Roxb. | 2.00 | 0.20 | 1.68 | 10 | 2.500 |
| <i>Hemidesmus indicus</i> (L.) R.Br. | 2.50 | 1.00 | 8.40 | 40 | 10.000 |
| <i>Ipomoea cairica</i> (L.) Sweet. | 2.00 | 0.20 | 1.68 | 10 | 2.500 |
| <i>Mukia maderaspatana</i> (L.) Roemer | 3.67 | 1.10 | 9.24 | 30 | 7.500 |
| <i>Passiflora foetida</i> L. | 4.00 | 0.40 | 3.36 | 10 | 2.500 |
| <i>Pergularia daemia</i> (Forssk.) Chiov. | 2.00 | 0.20 | 1.68 | 10 | 2.500 |

| | | | | | |
|--|------|------|------|----|-------|
| <i>Solanum trilobatum</i> L. | 3.00 | 0.30 | 2.52 | 10 | 2.500 |
| <i>Solena amplexiculis</i> Lam. | 1.00 | 0.10 | 0.84 | 10 | 2.500 |
| <i>Tinospora cordifolia</i> (Willd.) Hook. | 5.00 | 1.00 | 8.40 | 20 | 5.000 |
| <i>Ziziphus oenoplia</i> (L.) Mill. | 2.00 | 0.20 | 1.68 | 10 | 2.500 |

3. 4. Diversity Indices Analysis

The tree population comprises the number of species (27) with genera (21) and families (17). The diversity indices showed Shannon – Wiener index value (3.08), evenness index (0.75), species richness index (43.6), Simpson index (0.93), and the dominance concentration of the tree species (0.060). The dominance concentration (Cd) was highest compare to the sacred grove in Konjikuppam village of Cuddalore district (Nithyadevi and Sivakumar 2015). Among the shrub populations number of species (23), Shannon-Wiener index (H') was (2.83) higher than Konjikuppam sacred grove (Nithyadevi and Sivakumar, 2015). Species richness index (5.542) tree species of the present study. The other diversity indices showed the Simpson index (0.091), the evenness index (1.22) and concentration dominance (0.112). In the present study, shrubs (23) with genera (21) and families (13). Population diversity indices showed Shannon Wiener index (2.832), Simpson index (0.9237), evenness index (0.738), species richness index (4.499), and the species dominance concentration (0.076). 2 are higher than a sample -1 which showed very least vegetation. The herb population comprises the number of species (49), with genera (43) and families (24). Population diversity indices showed the Shannon Wiener index (3.461), Simpson index (0.9604), evenness index (0.738), species richness index (7.371) and the species dominance concentration (0.6497). 22 Climber species with 24 genera and 15 families present in the study sites, diversity indices showed Shannon Wiener index (2.822), Simpson index (0.9287), evenness index (0.7644), species richness index (4.394) and the species dominance concentration (0.6497). Visalakshi (1995) the value of the concentration of dominance for tropical forests of India varies from 0.21 to 0.92. A similar type of results was observed in the present study. High diversity and low Simpson index of dominance in different sides due to variation in anthropogenic pressure. Less species diversity (Shannon–Wiener index (H') in Southside which was less protected, maybe due to decreased resource availability (Sagar *et al.*, 2003). The poor species diversity is due to indiscriminate logging in these areas and poor site conditions. The findings of local interviews on sacred grove biodiversity indicated that very few people having awareness of biodiversity. Similar types of observations were reported by Kellert (1991) among Japanese people. A society which is having environmental awareness called as ideal society (Saheb *et al.*, 2012). This survey suggests that general awareness and perception about sacred grove biodiversity is useful for the successful implementation of a conservation strategy to improve biodiversity in the study area by involving local inhabitants.

4. Conclusions

The present study was done in a sacred grove situated in Thathanur village of Ariyalur district. A total of 121 plant species were recorded under 104 genera and 50 families. The family Fabaceae comprises 8 species followed by Asclepiadaceae, Mimosaceae (8 Species), Amaranthaceae, Asteraceae, and Malvaceae (6 species each) and the other families contributed (1 to 5 species each). The total basal area 4.446 m² (109 indiv.). *Ailanthus excels* (1.22 m²) is the highest contributor followed by *Tamarindus indica* (0.63m²) and *Alangium salvifolium* (0.531m²), *Albizia amara* showed the highest frequency in the study area. In the present study area conservation status except making broad path around the temple and sacred grove is good by restricting to cut trees or woods for fuel and furniture and also the unknown new people are restricted to enter the grove without permission of the local community people. Further study is needed to quantify the data and suggests plans for the conservation of the area.

References

- [1] Costanza, R., The Value of the World's Ecosystem Services and Natural Capital *Nature*, **387**, 253-260, 1997.

- [2] Dhanasekar S, Muthukumar B, and Soosairaj S., Analyses of plant diversity in a sacred grove of Pudukkottai District, Tamil Nadu, India. *International Journal of Research and Analytical Reviews* vol.5 (4):433-458, 2018.
- [3] Ejtehadi, H., Amini, T., and Zare, H. Importance of vegetation studies in conservation of wildlife: A case study in Miankaleh wildlife refuge, Mazandran province. *Iran Environ Sci.* **9**:53-58, 2005.
- [4] Gadgil.M. and Vartak,V.D. Sacred Groves in India. A plea for continued conservation. *Jl. Bombay.Nat. Hist. Soc.* **72**(2) pp 315-320, 1975.
- [5] Gamble J S., and Fischer CEC., Flora of Presidency of Madras. Vols. 1-3 Adlard & Sons Ltd., London, 1935.
- [6] Gopikumar, K., Carmel Rani, Luckins Babu, C. and Peethambaran,C.K., Phytosociological studies of a sacred grove at Manarashala, Kerala. In: Kunhikannan and Gurudev Singh (Ed.) Strategy for conservation of sacred groves, IFGTB (ICFRE) Coimbatore, India. Pp. 65-71, 2005.
- [7] Jain, S.K., and Rao, R.R., A Handbook of field and herbarium methods. Today and tomorrow printers and publishers, New Delhi, 1976.
- [8] John Britto, S., Balaguru, B., Soosairaj, S., and Arockiasamy, DI., Diversity of plants in a sacred grove of Pudukottai District in Tamil Nadu. *J Eco Taxon Bot.* **25**:58-62, 2001.
- [9] Kellert SR., Japanese Perception of Wildlife, *Conservation Biology*, **5**(3), 297-308, 1991.
- [10] Khamyong S., Lykke A.M., Seramethakun D. and Barfod A.S., Species composition and vegetation structure of an upper montane forest at the summit of Mt Doi Inthanon, Thailand. *Nord J. Not.* **23**, 83-97, 2004.
- [11] Magurran, A.E., *Ecological diversity and its measurement*. Princeton University Press, New Jersey, 1988.
- [12] Mannion, A.M., *Env. Conserv.* **22**,201-210, 1995.
- [13] Margalef, R. Perspective in Ecological theory. University of Chicago Press, 1958.
- [14] Matthew K M., Flora of the Tamil Nadu Carnatic. Rapinat Herbarium, Tiruchirappalli. Vol.1-3, 1982.
- [15] McNeely, G. A., Miller, K. R., Reid, W. V., Mittermeie, R.A. and Werner, T. R. Conserving the world's biological diversity, IUCN, Gland, 1990.
- [16] Meher-Homji, V.M., A Phytosociological study of the Albizzia amara Biological Community of India, *Phytosociologia.* **1**:114-129, 1973.
- [17] Muthukumar, B., Dhanasekar,S., Soosairaj, S., Nagamurugan, N. and Balaguru, B. Woody vegetation structure in a sacred grove of Pudukottai District, Tamilnadu, South India. *Indian J. Environ. &Ecoplan.***10**(2) : 409-412, 2005.
- [18] Nithyadevi, J. and Sivakumar, R. Phytosociological and ethnomedicinal studies of sacred groves in Konjikuppam village, Cuddalore district, Tamil Nadu. *International letters of Natural Sciences.***32**: 77-91, 2015.
- [19] Parthasarathy, N., Selwyn M.A. and Udayakumar, M. Tropical dry evergreen forests of peninsular India: ecology and conservation significance. *Tropical Conservation Science.* **2**:89-110, 2008.
- [20] Pielou, E.C. Species Diversity and Pattern diversity in the study of ecological; succession. *Jour. of theoretical Biology.* **10**:370-383, 1966.
- [21] Rajkumar, G., Ravipaul, S., Sivasamy, A., and RiyasMohmaed., Floristic composition and practices on the selected sacred gives of Perambalur district, TamilNadu. *Int.J.Modn. Revs.***2**(11):486-491, 2014.
- [22] Ramanujam, M.P., and Praveenkumar, C. Woody Species Diversity of four sacred groves in the Pondicherry region South India. *Biodiversity and Conservation.* **12**:289-299, 2003.
- [23] Reid and Miller, In Singh, M.P., and Vinita Vishwakarma, Forest environment & biodiversity, pp. 354, 1989.
- [24] Sagar, R Raghubansi A.S. and Singh, J.S. Tree species composition, dispersion and diversity along a disturbance gradient in a dry tropical forest region of India, *Forest Ecology Management*, **186**, 61-71, 2003.
- [25] Saheb SU, Sessaiah S. and Viswanath B., Environment and Their Legal Issues in India, *Int. Res. J. environment Sci*, **1**(3), 44-51, 2012.
- [26] Shannon, C.E and Wiener, W. The Mathametical Theory of Communication, University Illinois Press, Urban, 1963.
- [27] Vinothkumar, D., Murugacelh, S. and KethsyPrabavathy, A. Phytosociological and Ethnobotanical studies of sacred groves in pudukottai District, Tamil Nadu, India. *Asian J.Exp.Biol.Sci.***2**(2):306-315, 2011.
- [28] Visalakshi, N., Vegetation analysis of two tropical dry evergreen forest in southern India, *Tropical Ecology*, **36**:117-127, 1995.

A Review on Applications of AHP and Fuzzy AHP in Geographical Information System

Dr. G. Mahender Reddy¹ Dr. P. Kousalya²

¹Guru Nanak Institutions Technical Campus, Hyderabad, Telangana, India

² Indian Institute Of Information Technology Design And Manufacturing, Kurnool, Andhra Pradesh, India
Email: mahender1563@yahoo.co.in Kousalya29@Yahoo.Com

Abstract

Analytical Hierarchy Process (AHP) is one of the frequently used techniques in multi criteria decision making methods and has been attracting researchers in solving spatial decision making problems. It deals with crisp numbers to compare the decision criteria. Later on it was modified and adopted to consider fuzzy numbers instead of crisp numbers. Extent analysis method on fuzzy AHP using triangular Fuzzy Numbers was applied in many problems of decision making in Geographical Information System (GIS). In literature, applications of AHP and GIS were found in Land slide susceptibility mapping, Site Selection for artificial groundwater recharge, Water Reservoirs, Municipal Solid Waste Landfill, Solar Energy Sites etc. A review was done and various applications of AHP and Fuzzy AHP in GIS were presented as a table. Also the importance of Extent analysis method on Fuzzy AHP using Trapezoidal fuzzy numbers was discussed.

Key Words: *Multi Criteria Decision Making, AHP, FAHP, Extent Analysis method on Fuzzy AHP, GIS*

1. Introduction

Analytical Hierarchy process was introduced by Saaty T. L [16]. It is a multi criteria decision making method in which we form matrices by comparing different criteria in terms of alternatives. Extent Analysis method on Fuzzy AHP [4] using Triangular fuzzy Numbers was introduced by Chang D.Y in 1996. It attracted many researchers and this method was applied on various problems in multi criteria decision making context. This method allows only Triangular Fuzzy Numbers, so Kousalya et.al. (2015) [7] employed Trapezoidal in Extent analysis method on Fuzzy AHP and applied on some multi criteria decision making problems of real life situations.

The integration of GIS and Multi criteria decision making methods have started from 1990's. Spatial decision problems generally involve large set of alternatives and multiple conflicting criteria. Many researchers employed multi criteria decision making methods especially Analytical Hierarchy Process in site selection, flood risk assessment, landslide Vulnerability assessment, etc. .

2. Application areas

Givi A. A. et. al. (2015) [8] applied Fuzzy AHP and GIS to select park site selection in Tehran municipality. The importance of various factors affecting the selection of park site was studied. Ahid Monjezi (2013) used fuzzy AHP method and GIS for selecting the site for artificial ground water recharge. Extent analysis method on fuzzy AHP was applied to find the weights of thematic layers. By combining the weights of each criteria Site selection for artificial groundwater recharge was determined. [Bayes Ahmed](#)(2014)[1], by combining Artificial Hierarchy Process (AHP), Ordered Weighted Average (OWA), GIS based Multi criteria decision making methods, Landslide susceptibility mapping has done in Chittagong Metropolitan Area, Bangladesh, and -were applied to scientifically assess the landslide susceptible areas.

[Biswajeet Pradhan](#) (2009)[2] identified nine factors that influence land slide occurrence. For this he combined the GIS, a data driven model and a knowledge derived model. Then for land slide hazard mapping, fuzzy membership functions and fuzzy arithmetic operators were applied. Farhad Hosseinali(2008)[6] applied three knowledge driven methods like Analytical Hierarchy Process(AHP), Ratio estimation, Delphi technique methods and three data driven methods like Artificial neural network(ANN), eight of evidence, Logistic regression in finding the characteristics of 26 copper boreholes. Numerical experimentations showed that

Artificial neural network (ANN) in data driven models gave accurate results whereas Analytical Hierarchy Process(AHP) is the most successful method in knowledge driven class.

Hamidreza Mehrabi(2012)[9] applied AHP to find the weights of criteria like rain fall, soil, lithology, slope, land use and were used for selection of artificial recharge in Silakhor of Iran. Keyvan Yousefi Sangani (2014) applied Fuzzy AHP method and GIS for evaluation of ground water potential zones. Based on available physiographical, climate data, hydro geological, structural and using Satellite images the maps of different layers were converted using Fuzzy membership functions and AHP, then ground water potential zones were prepared. The applications of AHP, Fuzzy AHP in different areas by authors and other methods which are integrated were discussed in Table.1.

Table-1: Applications of AHP, FAHP in GIS

| Author(s) | Specific area | Combined or compared with other methods |
|--|---|--|
| Bakhtiar Feizizadeh, Piotr Jankowski and Thomas Blaschke(2013) | Landslide susceptibility mapping | Analytical Hierarchical Process (AHP) and Ordered Weighted Averaging (OWA) |
| Ziari Y. A., Yazdanpanah S.(2011) | Locating Fire stations using AHP in GIS environment | AHP, Geographical Information System |
| Khalid Eldrandaly(2013) | GIS-Based MCE Site Selection Tool in ArcGIS Using COM Technology | GIS and Multi Criteria Evaluation techniques |
| A. Elahi and H. Samadyar(2014) | Municipal Solid Waste Landfill Site Selection Using Analytic Hierarchy Process Method | Analytic Hierarchy Process, GIS |
| Mahnaz Eskandari, Mehdi Homae, Shahla Mahmoodi, Ebrahim Pazira(2013) | Municipal Solid Waste Landfill Site Selection | Analytic Hierarchy Process, GIS |
| Dr. Le Canh Dinh, Dr. Tran Trong Duc | Land evaluation | Extent analysis on fuzzy AHP, GIS |
| E. H. Ibrahim, S. E. Mohamed, A. A. Atwan(2011) | Selecting best location for waste water lift station | Fuzzy AHP, GIS |
| A. Asakereh, M. Omid, R. Alimardani and F. Sarmadian(2014) | Selecting Solar Energy Sites in Shodirwan Region in Iran | Fuzzy AHP, GIS |

| | | |
|--|---|---|
| Mehrdad Hadipour and Maryam Kishani(2014) | Environmental Location Planning Of Industrial Zones | AHP and GIS |
| Jirattinart Thungngern , Saowanee Wijitkosum , Thavivongse Sriburi, Chaoyuth Sukhsri(2015) | Water Resource Management in Thailand | AHP, SWOT analysis |
| Rodney G. Tsiko and Tesfalem S. Haile(2011) | Modelling Optimum Sites for Locating Water Reservoirs | GIS, Fuzzy Logic and AHP |
| Ratchaphon Samphutthanon, Nitin Kumar Tripathi, Sarawut Ninsawat , Raphael Duboz(2014) | Generate hand,foot and mouth disease hazard zonation (hfmd-hz) model in Thailand | GIS with AHP and Fuzzy AHP |
| Mukhtar Elaalem, Alexis Comber and Pete Fisher(2010) | Land Evaluation Techniques Comparison | Fuzzy AHP withTOPSIS |
| Generino P. Siddayao, Sony E. Valdez, and Proceso L. Fernandez(2014) | Spatial Modeling for Floodplain Risk Assessment | AHP, Decision support system, GIS |
| Yunliang Meng, Jacek Malczewski, Soheil Boroushaki(2011) | Mapping Accessibility Patterns of Housing Development Sites | AHP-OWA Procedures, GIS |
| P. Tirkey, A. K. Gorai, J. Iqbal(2013) | Groundwater Vulnerability to Pollution Assessment | AHP, GIS |
| Nahid Monjezi , Kazem Rangzan , Ayoub Taghizadec, Ahmad Neyamadpour(2013) | Site selection for artificial groundwater recharge | Extent analysis on fuzzy AHP, GIS |
| Bakhtyar Ali Ahmad, Himan Shahabi and Baharin Bin Ahmad(2015) | Site Selection of Water Reservoirs | AHP, GIS |
| Amin Ahmadi Givi, Saeed Karimi, Negar Foroughi, Yasser Moarab, Vahid Nikzad(2015) | Parks Site Selection in Urban Environment | Geographic information systems (GIS); FAHP |
| Kordi, M., & Brandt, S.A. (2012) | Effects of increasing fuzziness on analytic hierarchy process for spatial multicriteria decision analysis | AHP, Fuzzy logic, Sensitivity analysis, GIS |
| Mehdi Ziaei, Fateme Hajizade | Approach for evaluation/selection of planning and design | Fuzzy Analytical Hierarchy process |

| | | |
|--|---|---|
| | alternatives | (FAHP), GIS |
| 1.H. Vahidniaa, A. Alesheikhb, A. Alimohammadic, A. Bassiri(2008) | FAHP applications in GIS | Fuzzy AHP, GIS, α -cut Based Method |
| Nang-Fei Pan(2008) | Fuzzy AHP approach for selecting the suitable bridge construction method | FAHP in Bridge construction |
| Esmail Tazik a., Zahra Jahantab b, Mohsen Bakhtiari a, Abdolali Rezaei a, Seyed Kazem Alavipanah a | Landslide susceptibility mapping by combining three methods in Dozain basin | Fuzzy Logic, Frequency Ratio and Analytical Hierarchy Process |
| S ehnaz S ener a, Erhan S ener b, Bilgehan Nas c, Remzi Karagüzel e(2010) | landfill site selection | AHP, GIS |
| Yuyue Xua,b, Jiulin Suna, Jinqu Zhanga , Yong Xuc , Mingwu Zhangd and Xiuying Liaoa(2012) | Evaluation of environmental suitability for living | AHP, GIS |
| Huang Li-Jeng(2015) | Debris-Flow Hazards Risk Assessment | FAHP, Trapezoidal fuzzy Numbers, GIS |
| M.Vetrivel Sezhan, C.Muralidharan, T.Nambirajans.G.Deshmukh(2011) | Performance measurement in a public sector passenger bus transport company | Fuzzy TOPSIS; Fuzzy AHP, ANOVA. |
| K. P. Anagnostopoulos, M Gratziou, A.P. Vavatsikos(2007) | Waste water facilities selection | FAHP, Triangular Fuzzy Numbers |
| Zeinab Mansouri1, Naser Hafezi Moghaddas, Behnaz Dahrazma(2013) | Wastewater treatment plant site selection | AHP, GIS |
| Mohammed A. Hajeesh | Water Desalination Plants Selection | FAHP, GIS |
| MaryamKordia S. AndersBrandt | GIS-based decision-making problem of locating a dam in Costa Rica | Analytic hierarchy process, Fuzzy logic |

3. Conclusion and Future Scope

In many practical problems AHP and Fuzzy AHP were widely applied in GIS environment to find the weights of criteria in ranking the alternatives. Qualitative and quantitative data can be handled by this method. The Trapezoidal Fuzzy Numbers can be employed in Fuzzy AHP, since Trapezoidal Fuzzy Numbers are more general form than Triangular Fuzzy Numbers. The Analytic Hierarchy Process can be integrated with other methods like TOPSIS in finding ranks of alternatives.

References

- [1] Bayes Ahmed. Landslide susceptibility mapping using multi-criteria evaluation techniques in Chittagong Metropolitan Area, Bangladesh, *Landslides*, 12:1077–1095, 2015.
- [2] Biswajeet Pradhan, Saro Lee, Manfred F. Buchroithner. Use of geospatial data and fuzzy algebraic operators to landslide-hazard mapping, *Applied Geomatics*, 3-15,2009.
- [3] D.Thirumalaivasan, Dr.M.Karmegam, Aquifer Vulnerability Assessment Using Analytical Hierarchy Process and GIS for Upper Palar Watershed, *Proceedings of 22nd Asian Conference on Remote sensing*, pp. 5-9,2001.
- [4] D.-Y. Chang, Applications of Extent Analysis method On Fuzzy AHP, *European Journal of Operational Research* 95 , 649-655,1996.
- [5] EunnyeongHeo, Jinsoo Kim, Kyung -Jin Boo, Analysis of the Assessment Factors for Renewable Energy Dissimilation Program Evaluation Using Fuzzy AHP, *Renewable and Sustainable Energy Reviews* 14, 2214-2220,2010.
- [6] Farhad Hosseinali and Ali Asghar Alesheikh, Weighting Spatial Information in GIS for Copper Mining Exploration, *American Journal of Applied Sciences* 5 (9): 1187-1198, 2008.
- [7] G. Mahender Reddy, P. Kousalya, A note on FAHP Extent Analysis Method for Determining Weights Using Trapezoidal Fuzzy Numbers in Selection of a Computer System, *Global Journal of Pure and Applied Mathematics*, Vol. 11, No. 2, pp. 76-82,2015.
- [8] Givi A. A, Karimi S, Foroughi N, Moarab Y, Nikzad V. Using Fuzzy Logic Analysis in GIS and FAHP Method for Parks Site Selection in Urban Environment (Case Study: Region 7, Tehran Municipality). *Curr World Environ* 10(2), 2015.
- [9] Hamidreza MehrabiA, Hossein ZeinivandB, Moslem HadidiC , Site Selection for Groundwater Artificial Recharge in Silakhor Rangelands Using GIS Technique *Journal of Rangeland Science*, Vol. 2, No. 4,2012.
- [10] Hossein Safari, Alireza Faghhih and Mohammad Reza Fathi, Fuzzy multi-criteria decision making method for facility location selection, *African Journal of Business Management* Vol. 6(1), 206-212,2012.
- [11] Huang Li-Jeng, Application of FAHP to Debris-Flow Hazards Risk Assessment Using Trapezoidal Fuzzy Numbers, *International Journal of Emerging Technology and Advanced Engineering*, Vol. No. 5(4), pp. 462-471,2015.
- [12] Huang Li-Jeng. Application of FAHP to Debris-Flow Hazards Risk Assessment Using Trapezoidal Fuzzy Numbers, *International Journal of Emerging Technology and Advanced Engineering*, Volume 5, Issue 4, 462-471,2015.
- [13] Kousalya P, Mahender Reddy G. On Some Mathematical Aspects of Fuzzy Analytic Hierarchy Process, *Mathematical Sciences International Research Journal (MS-IRJ)*.Vol.1,No.2,Page No.579,2012.
- [14] Maryam Kordi and S. Anders Brandt, , Effects of increasing fuzziness on analytic hierarchy process for spatial multicriteria decision analysis, *Computers, Environment and Urban Systems*, Volume 36, Issue 1, Pages 43–53,2012.
- [15] Nang Fei Pan, Fuzzy AHP Approach for Selecting the Suitable Bridge Construction Method, *Automation in Construction*, Vol. No. 17(8), pp. 958-965,2008.
- [16] T. L. Saaty, *The analytic hierarchy process*. McGraw-Hill, New York, 1980.
- [17] Wang, Y. M., & Elhag, T. M. S. On the Normalization of Interval and Fuzzy Weights. *Fuzzy Sets and Systems*, 157, 2456–2471,2006.
- [18] Zahedi, F., *The Analytic Hierarchy Process – A Survey of the Method and its Applications*, *Interfaces*, Vol. No. 16, pp. 96-108,1986.

Preparation and Investigation on Phosphor Materials

A John Peter
Professor

Department of Science and Humanities
St. Anne's College of Engineering and Technology,
Panruti

Abstract

The nanostructured $\text{NaY}(\text{WO}_4)_2:\text{Pr}^{3+}$ phosphor was rapidly synthesized at room temperature by mechanochemically assisted solid state meta-thesis reaction method. The as-synthesized Nanophosphor possess scheelite tetragonal crystal structure with space group $I4_1/a$. Photoluminescent studies revealed that under the excitation of blue light (448 nm), a strong emission in the red region was observed at 647 nm due to the transition from populated $^3\text{P}_0$ level to the $^3\text{F}_3$ lower level of Pr^{3+} ions. The Nanostructured $\text{NaY}(\text{WO}_4)_2:\text{Pr}^{3+}$ material could serve as excellent red phosphor candidate for solid state lighting applications.

Keywords- Phosphor, Solid meta-thesis reaction, Scheelite structure, WLED.

1 Introduction

Currently, researchers are engaged toward the synthesis of new class of micro/Nano structured luminescent phosphors to improve its lumen efficacy for white light emitting diodes (WLEDs) applications. Because, WLEDs are considered as promising next generation solid state lighting devices and play a major role by virtue of its high permanence, high efficiency, low-cost, energy saving, prolongation, environmental friendly, etc. WLEDs have number of prospective applications and used in fluorescent lamps, indicators, back lights, automobile light, traffic signals, etc. The ultimate and hopeful method to attain high quality phosphor-converted WLEDs is by pumping tricolor phosphors with UV InGaN chip or blue GaN chip. However, the commercially available white LED have lack of red emission component results in high correlated color temperature, low lumen efficiency of radiation, and low color-rendering index limits their applications to some extent. Hence, special attention is needed to find out an alternative novel red phosphor material must possess thermally and chemically stable and show better luminous efficiency with low-cost. Many reports were reported on scheelite type tungstates or tungstates with tetragonal structure due to their feasible luminescence applications in various fields such as laser host materials, fiber optics, WLEDs, scintillation detector, etc. The conventional method of preparation of tricolor phosphor typically requires high temperature and eats a lot of power and time. Whereas, the solid state meta-thesis reaction method (SSM) is an outstanding method does not requires high temperature and external high electrical energy. Using SSM one can synthesize the phosphor with homogeneous, pure and well crystallized powders at room temperature rapidly.

Pr^{3+} activated $\text{NaY}(\text{WO}_4)_2$ phosphor was synthesized by mechanochemically assisted solid state meta-thesis method at room temperature. All the starting materials were of analytical grade and used without any purification. The appropriate amount of $\text{Na}_2\text{WO}_4 \cdot 2\text{H}_2\text{O}$, $\text{YCl}_3 \cdot 7\text{H}_2\text{O}$, $\text{PrCl}_3 \cdot 7\text{H}_2\text{O}$ were mixed together and pulverized for a period of three hours in a planetary ball mill pulverisette 7 (FRITSCH). Two grinding vials of 15 cm volume with balls with diameter of 12 mm made of tungsten carbide materials were used to pulverize the mixer. The number of grinding balls and the speed of rotation of mill device were kept constant. The final product were washed and centrifuged with double distilled water several times for purification then it was dried at 60-80°C for 2 h in a muffle furnace in air.

2 Results and Discussion

Figure 1 shows the XRD pattern of $\text{NaY}(\text{WO}_4)_2$ doped with Pr^{3+} . From the XRD pattern, it is observed that the samples are pure and possess scheelite tetragonal crystal phase. All the peaks are indexed and matches well with the JCPDS card no. 25-0828 of $(\text{Na}_{0.5}\text{Y}_{0.5})\text{WO}_4$ structure. No other extra peaks of

impurity were detected. Moreover, it can be noticed an enhanced intensity of peak at (112) about 28.52° . Fig. 2 shows the FESEM image of the sample which clearly depicts that the average particle size was found to be approximately 100 nm.

FIGURE 1. XRD pattern of Pr^{3+} activated $\text{NaY}(\text{WO}_4)_2$

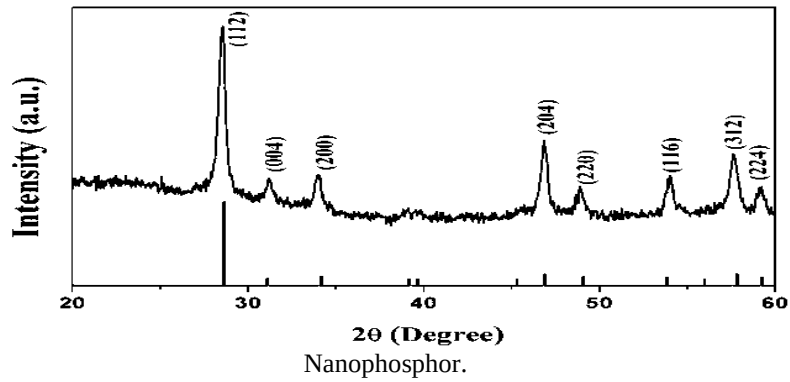


Fig. 3 shows the photoluminescence excitation spectra of $\text{NaY}(\text{WO}_4)_2$ doped with Pr^{3+} sample which consist of three intense and sharp absorption bands observed at 448 nm, 474 nm, 488 nm corresponding to the transitions from unexcited $^3\text{H}_4$ level to excited $^3\text{P}_2$, $^3\text{P}_1$, and $^3\text{P}_0$, levels respectively.

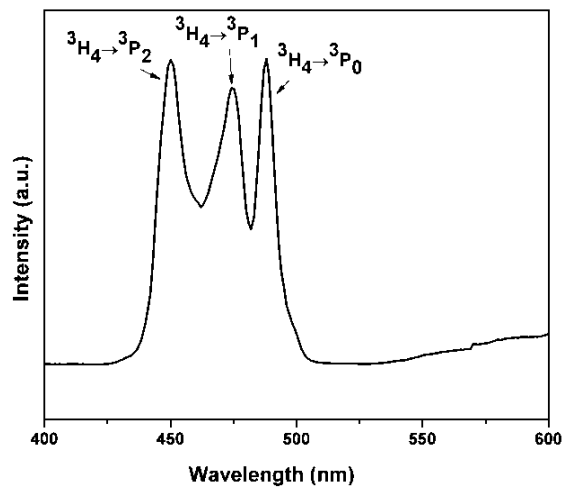


FIGURE 3. PL excitation spectrum of Pr^{3+} activated $\text{NaY}(\text{WO}_4)_2$ Nanophosphor Wntored at 647 nm.

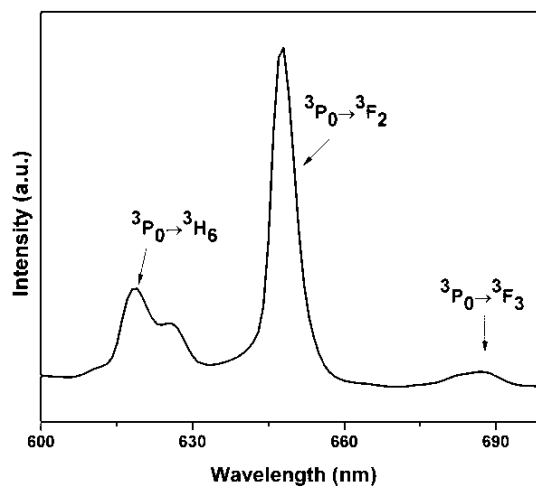


FIGURE 4. PL emission spectrum of NaY(WO₄)₂: Pr³⁺ excited at $\lambda_{ex} = 448$ nm.

Fig. 4 shows the room temperature PL emission spectra of NaY(WO₄)₂ doped with Pr³⁺ phosphor. Under the excitation of 448 nm blue light, the emission spectra were governed by the characteristic red luminescence primarily originated due to the transition from excited ³P₀ level to the ³F₂ lower level noticed at 647 nm. Also, the transitions observed at 3P₀ → 3H₆, 3P₀ → 3F₃ at 619 nm and 687 nm are relatively weak. Fig. 5 shows the corresponding Commission Internationale de l'Éclairage (CIE) diagram and color chromaticity coordinates was found to be x = 0.6989 and y = 0.3010 and occupy red part of the CIE diagram which are very close to the NTSC standard value. Thus, the obtained results suggesting that the material NaY(WO₄)₂: Pr³⁺ synthesized by solid state meta-thesis route might be useful for promising red phosphor candidate for WLEDs.

3 CONCLUSION

The Nano phosphor NaY(WO₄)₂ doped with Pr³⁺ has been rapidly synthesized by solid state meta-thesis reaction technique at room temperature. The phase purity of the crystal structure was identified by XRD pattern. FESEM image of the sample clearly depicts the mean particle size was found to be approximately 100 nm. The photoluminescence investigation suggesting that under blue light excitation, Pr³⁺ doped NaY(WO₄)₂ Nanophosphor shows the strong emission in the red region observed at 647 nm due to the ³P₀ → ³F₂. In summary, the as-obtained Nanophosphor could find the potential applications in solid state lighting applications and red phosphor for W-LED applications.

References

- [1] Xu Q, Xu D, and Sun J, "Preparation and luminescence properties of Orange-red Ba₃Y(PO₄)₃:Sm³⁺ phosphors", *Optical Materials*, Vol.42, pp 210-214, 2015.
- [2] Pawade V. B, and Dhoble S. J, "Blue emission in Eu²⁺ and Ce³⁺ activated novel aluminates based phosphors", *Journal of Luminescence*, Vol. 135, pp. 318-322, 2013.
- [3] Matsunaga T, Takeshita S, and Isobe T, "Synthesis, photoluminescence, and photostability of Y₂O₃:Bi³⁺, Eu³⁺ Nanosheets", *Journal of Luminescence*, Vol.165, pp.62-67, 2015.
- [4] Wei S, Yu L, Na F, Sun J, and Na S, "Photoluminescent properties of Eu³⁺-doped alkaline earth metal aluminates red phosphors with high quenching concentration", *Ceramics International*, Vol. 41, pp.1093- 1100, 2015

A Novel Method for Biosynthesis of Cadmium Sulphide

J. Joaquine Arokia Mary,
Assistant Professor,
St. Anne's College Of Engineering And Technology,
Panruti

Abstract

Nanoparticles are of great importance because of their unique physical, thermodynamic and chemical properties, which are different from bulk materials. Nanostructure sulfides have been studied extensively with a view to establish a relationship among size, structure and optical properties. Currently, many workers have focused on cadmium sulphide because of several important properties. Size dependant properties are exhibited by CdS nanoparticles because of high surface to volume ratio. It also possessed high photosensitivity which enables them useful for optoelectronic devices and various other biological applications and because of these applications various part of plants are used in the bulk production of CdS nanoparticles.

Keywords: CdS, UV-Visible, XRD, FT-IR and Antimicrobial activity.

1. Introduction

The field of nanotechnology has witnessed impressive advances in various aspects such as the synthesis of nanoscale matter and understanding/utilizing their exotic physicochemical and optoelectronic properties. Nano sized colloids are characterized by excellent electrical, thermal, optical and catalytic properties. As such, they have attracted a considerable degree of attention over the recent past owing to their various potential applications as conductors, catalysts and chemical sensors [1–5]. It has therefore become necessary to attempt to synthesise small-size and narrow distribution colloidal metal dispersions. Of the various techniques explored to obtain such metal nano particles, at present, there is a greater need to develop safe, reliable, clean and eco friendly methods for the preparation of these nanoparticles. Although many synthetic technologies are well documented, the search for suitable biomaterials for the biosynthesis of nanoparticles continues among researchers worldwide.

2. Experimental Methods

2.1 Materials

Cadmium Nitrate $4 \text{ H}_2\text{O}$, sodium sulphide, Phthalic acid, Succinic Acid was used as the introductory material was supplied by Sigma-Aldrich chemicals. A fresh leaf of *Calotropis gigantea* Flower was washed thoroughly with double distilled water, ground and was filtered through Whatmann filter paper was used for further studies. Then the Flower was nicely crushed in mortar pestle, after that was transferred into a centrifuge tube and centrifuged (Optima L-100XP Ultracentrifuge at a speed of 10000 -11000 rpm for 10 min at 4 to 5°C). After centrifugation, the supernatant was filtered using Whatmann paper and the filtrate was used for the synthesis of CdS.

3. Result and Discussion

3.1. UV-VIS Spectroscopy

The UV-vis absorption spectra of the cadmium sulfide nanoparticles solution were measured with Shimadzu 1800 UV-vis spectrophotometer shows Figure 1 & 2. Figure 1 shows the UV-vis absorption spectra of the Precursor product after centrifugation at 12000 rpm. Figure 2 shows the sharp peak at the wavelength of 405 nm [20] proves the presence of bio CdS nanoparticles. This lambda maximum (λ_{max}) is then further used for finding the band gap of CdS NPs synthesized from Phthalic Acid and Succinic acid. Optical excitation of electrons across the band gap happens, and causes an abrupt increase in absorptivity at the wavelength associated to the gap energy. This feature in the optical spectrum is called optical absorption edge [21].

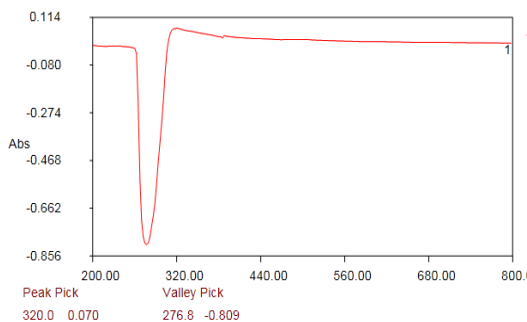


Figure – 1 UV-Visible Spectra for Cd(OH)₂ compound P1 & P4

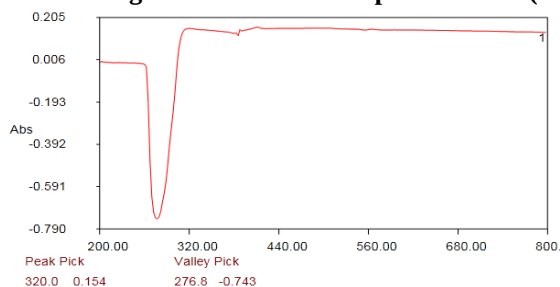


Figure - 2 UV-Visible Spectra of CdS nanoparticles N1 & N4

Concentration dependent reaction shows that 5*10⁻³mM concentration is the best option concentration for the synthesis of cadmium sulfide nanoparticles. The change in color occurs with the occurrence of the following reaction ($\text{CdNO}_2 + \text{Plant} + \text{NaS} \rightarrow \text{CdS} + 2\text{NaCl}$).

4. Conclusion

The present study demonstrates the green synthesis of cadmium sulfide (CdS) nanoparticles using the bacteria *Bacillus licheniformis* and the effect of varying ratios of cadmium chloride on nanoparticle formation. The synthesized nanoparticles proved to be stable for more than three months in water. The morphological and structural studies showed the nanoparticles were face centered crystals with a lattice plane spacing (d) of 50 nm. The FTIR results showed that the proteins might have played an important role as capping agents in stabilizing the CdS nanoparticles. Using varied ratios of cadmium chloride and sodium sulfide showed changes in the formation of functional groups of the nanoparticles which can act beneficial for CdS capping.

References

- [1] Alvarez-Peral F J., Zaragoza O., Pedreno Y., and Arguelles J C., "Protective role of trehalose during severe oxidative stress caused by hydrogen peroxide and the adaptive oxidative stress response in *Candida albicans*", *Microbiology.*, 148. 2599-2606. Aug. 2002.
- [2] Bai H, Zhang Z., Guo Y., and Jia W., "Biological synthesis of size-controlled cadmium sulfide nanoparticles using immobilized *Rhodobacter sphaeroides*" *Nanoscale Research Letters.*, 4. 717-723. Apr. 2009.
- [3] Bai H J., Zhang Z M., Guo Y., and Yang G E., "Biosynthesis of cadmium sulfide nanoparticles by photosynthetic bacteria *Rhodospseudomonas palustris*", *Colloids and Surfaces B: Biointerfaces.*, 70. 142-146. Apr. 2009.
- [4] Bhadwal A S., Tripathi R M., Gupta R K., Kumar N., Singh R P., and Shrivastav A., "Biogenic synthesis and photocatalytic activity of CdS nanoparticles", *RSC Advances.*, 4. 9484-9490. Dec. 2013.
- [5] Chen G., Yi B., Zeng G., Niu Q., Yan M., Chen A., Du J., Huang J., and Zhang Q., "Facile green extracellular biosynthesis of CdS quantum dots by white rot fungus *Phanerochaete chrysosporium*", *Colloids and Surfaces B: Biointerfaces.*, 117. 199-205. May. 2014.
- [6] Fernandez C A., and Wai C M., "Continuous tuning of cadmium sulfide and zinc sulfide nanoparticle size in a water-in-supercritical carbon dioxide microemulsion", *Chemistry- A European Journal*, 13(20). 5838-5844. Apr. 2007.
- [7] Ghows N and Entezari MH., "A novel method for the synthesis of cds nanoparticles without surfactant", *Ultrason Sonochem*, 18(1). 269-275. Jan 2011.

- [8] Giertsen E., "Effects of mouth rinses with triclosan, zinc ions, copolymer and sodium lauryl sulphate combined with fluoride on acid formation by dental plaque *invivo*", *Caries research.*, 38. 430-435. Oct. 2004.

An Analysis of Obesity in School Children during the Pandemic COVID-19 using Plithogenic Single Valued Fuzzy Sets

S.P. Priyadharshini* and F. Nirmala Irudayam
 Dept. of Mathematics, Nirmala College for Women, India.
 *priyadharshini125@gmail.com, nirmalairudayam@ymail.com

Abstract

The objectives of this research is to examine the perception that school children with obesity, when excluded from organised academic performance and constrained to their residences during the coronavirus epidemic 2019 will reveal negative consequences in health behaviours. To meet the objective, the concept of Plithogenic Single valued fuzzy sets (PSFS) and its aggregation operators were introduced. Based on the proposed theory, an analysis is presented with the case study to highlight its practicality and preciseness.

Keywords: Fuzzy set, Plithogenic Set, Plithogenic Single valued fuzzy set (PSFS), PSFS Operators.

1. Introduction

Global health analysts predict that school closures had worsen the epidemic of childhood obesity rates due to the COVID-19 pandemic. Analysts believe that school shutdown associated with COVID-19 will double out-of-school time for several children in world-wide previous year and could increase hazard factors involved with summer break for gaining weight.

Plithogenic set (PS) was introduced by Smarandache and he is the one who implemented contradictory degree and the dominant value of the attribute for this set. Every field where plithogenic set is being used in accordance with the implementation to elucidate, the newly introduced degrees will certainly help us to get the accurate results. Moreover, it is the generalisation of Crisp, Fuzzy, Intuitionistic fuzzy and Neutrosophic set.

In this research work we study how the Plithogenic Single valued fuzzy sets (PSFS) and its aggregation operators helps in analysing the main factors for increase in obesity among school children during the pandemic COVID-19 lock down with the analyst's fuzzy degree.

The uniqueness of this technique is its effectiveness, as the learner does not have to engage with complex operators based on lengthy calculations. The proposed method also has a realistic approach to the need for a broad spectrum that can penetrate alterations according to the need for the social structure provided.

2. Preliminaries

The preliminary concepts and definitions of Plithogenic sets and its operators have referred from [4], [5], [6] which helps to carried out our research work in a successful way.

3. Plithogenic Single valued fuzzy sets (PSFS) and its Operators

Definition 3.1: Let U be a universal set and P is the subset and $x \in P$ be an element. P is called a Plithogenic set which has the form $(P, A, \Lambda, D_F, C_F)$ where A is the attribute Values, Λ is the set of all attributes values that helps in solving an application, D_F is the degree of appurtenance and C_F is the dissimilarity degree.

Let us assume two Analyst A & B each evaluating the PSFS degree of appurtenance of Λ of x to the Plithogenic set P with some given constraints

$$D^F_A(\lambda) = \alpha \in [0,1] \text{ and } D^F_B(\lambda) = \beta \in [0,1]$$

Also \wedge_f be the fuzzy τ_{norm} and \vee_f be the fuzzy τ_{conorm} correspondingly

3.1.1 PSFS Intersection

$$\alpha \wedge_p \beta = C_O * (\alpha \vee_f \beta) + (1 - C_O) * (\alpha \wedge_f \beta) \quad (1)$$

3.1.2 PSFS Union

$$\alpha \vee_p \beta = C_O * (\alpha \wedge_f \beta) + (1 - C_O) * (\alpha \vee_f \beta) \quad (2)$$

Remarks:

(i) When more emphasis is allocated to $\tau_{norm}(\alpha, \beta) = \alpha \wedge_f \beta$ when compared to $\tau_{conorm}(\alpha, \beta) = \alpha \vee_f \beta$ for $C(\lambda_d, \lambda) = C_O \in [0, 0.5]$ is called an accurate plithogenic intersection.

(ii) When more emphasis is allocated to $\tau_{conorm}(\alpha, \beta) = \alpha \vee_f \beta$ when compared to $\tau_{norm}(\alpha, \beta) = \alpha \wedge_f \beta$ for $C(\lambda_d, \lambda) = C_O \in [0, 0.5]$ is called an accurate plithogenic union.

(iii) When more emphasis is allocated to $\tau_{norm}(\alpha, \beta) = \alpha \wedge_f \beta$ when compared to $\tau_{conorm}(\alpha, \beta) = \alpha \vee_f \beta$ for $C(\lambda_d, \lambda) = C_O \in (0.5, 1]$ is called an inaccurate plithogenic union.

(iv) When more emphasis is allocated to $\tau_{conorm}(\alpha, \beta) = \alpha \vee_f \beta$ when compared to $\tau_{norm}(\alpha, \beta) = \alpha \wedge_f \beta$ for $C(\lambda_d, \lambda) = C_O \in (0.5, 1]$ is called an inaccurate plithogenic intersection.

(v) $\tau_{conorm}(\alpha, \beta) = \alpha \wedge_f \beta$ and $\tau_{norm}(\alpha, \beta) = \alpha \vee_f \beta$ has allocated the same emphasis 0.5 for $C(\lambda_d, \lambda) = C_O \in 0.5$.

3.1.3 PSFS Negation

Denying the attribute Value

$$\neg_p(\lambda) = anti(\lambda), \text{ i.e. the opposite of } \lambda, \text{ where } anti(\lambda) \in \Lambda \text{ or } anti(\lambda) \in \text{Refined } \Lambda (\text{refined set of } \Lambda).$$

So we get $D^f_X(anti(\lambda)) = x$.

Denying the attribute value degree

$$\neg_p(x) = 1 - x, \text{ or } \neg_p D^f_X(\lambda) = 1 - x.$$

$$\begin{pmatrix} \lambda \\ x \end{pmatrix} \xrightarrow{\text{complement}} \begin{pmatrix} anti(\lambda) \\ x \end{pmatrix} \text{ or } \begin{pmatrix} \lambda \\ 1-x \end{pmatrix}.$$

4. Proposed Method to Find the Optimum Solution Using PSFS Operators.

Step 1: Classify the problem with the attributes and its corresponding values of attribute.

Step 2: Find the dissimilarity degree according to the Experts X and Y fuzzy degrees.

Step 3: Compute the UASPSFS optimum solution using Equation (1).

Note: We have used the intersection operator. But the alternative is free for the reader to work with other operators also.

5. Case Study

Consider the primary attribute "Reason for obesity in school children during lockdown" which has the attribute values

Food Habits- whose refined values are- less Vegetable intake, Sugary drinks, Junk food and Meat consumption which is represented by $\{g_1, g_2, g_3, g_4\}$

Screen time - whose refined values are-Mobile, Television and Computer which is symbolized by $\{t_1, t_2, t_3\}$

Sleeping pattern - whose refined values are- Increase in Day time sleep and Decrease in Night time sleep which is denoted by $\{h_1, h_2\}$

Sports- whose refined values are- More Indoor games and lack of Outdoor games which is signified by $\{r_1, r_2\}$

The multi attribute of dimension 4 is,

$$R_4 = \{g_i, t_j, h_k, r_l\}, \text{ for all } 1 \leq i \leq 4, 1 \leq j \leq 3, 1 \leq k \leq 2, 1 \leq l \leq 2\}$$

The dominant attribute values are g_3, t_1, h_1, r_2 respectively for each corresponding uni-dimensional attribute.

The unit dimensional attribute contradiction degrees are:

$$C(g_1, g_2) = \frac{1}{3}, C(g_2, g_3) = \frac{2}{3}, C(g_1, g_3) = 1,$$

$$C(t_1, t_2) = \frac{1}{2}, C(t_1, t_3) = 1$$

$$C(h_1, h_2) = 1 \text{ and } C(l_1, l_2) = 1 .$$

Let us use $\text{fuzzy } \tau_{norm} = a \wedge_F b = ab$ & $\text{fuzzy } \tau_{conorm} = a \vee_F b = a + b - ab$.

Four-dimensional PSFS Intersection

Let $x_A = \{d_A(x, g_i, t_j, h_k, r_l) \text{ for all } 1 \leq i \leq 4, 1 \leq j \leq 3, 1 \leq k \leq 2, 1 \leq l \leq 2\}$

and $x_B = \{d_B(x, g_i, t_j, h_k, r_l) \text{ for all } 1 \leq i \leq 4, 1 \leq j \leq 3, 1 \leq k \leq 2, 1 \leq l \leq 2\}$

Then

$$\begin{aligned} & x_A(g_i, t_j, h_k, r_l) \wedge_P x_B(g_i, t_j, h_k, r_l) = \\ & \{c(g_D, g_i) * [d_A(x, g_D) \vee_f d_B(x, g_i) + (1 - c(g_D, g_i)) * [d_A(x, g_D) \wedge_f d_B(x, g_i)]] \\ & \text{for } 1 \leq i \leq 4; \\ & c(t_D, t_j) * [d_A(x, t_D) \vee_f d_B(x, t_j) + (1 - c(t_D, t_j)) * [d_A(x, t_D) \wedge_f d_B(x, t_j)]] \\ & \text{for } 1 \leq j \leq 3; \\ & c(h_D, h_k) * [d_A(x, h_D) \vee_f d_B(x, h_k) + (1 - c(h_D, h_k)) * [d_A(x, h_D) \wedge_f d_B(x, h_k)]] \\ & \text{for } 1 \leq k \leq 2; \\ & c(r_D, r_l) * [d_A(x, r_D) \vee_f d_B(x, r_l) + (1 - c(r_D, r_l)) * [d_A(x, r_D) \wedge_f d_B(x, r_l)]] \\ & \text{for } 1 \leq l \leq 2\}. \end{aligned}$$

According to Analyst (A & B) fuzzy degrees the following table and the bar chart represents the Optimum solution.

Table 1. Analysis Table for obesity in school children during pandemic Covid-19 lockdown using PSFS

| Attribute | Food Habits | | | | Screen time | | | Sleeping Pattern | | Sports | |
|------------------------|--------------------------|---------------|-----------|------------------|-------------|------------|----------|---------------------|-----------------------|----------------------|-----------------------|
| values of Attribute | Lack of Vegetable intake | Sugary drinks | Junk food | Meat consumption | Mobile | Television | Computer | More Day time sleep | Less Night time sleep | More of Indoor games | Lack of Outdoor games |
| Dissimilarity degree | 0 | 1/3 | 2/3 | 1 | 0 | 1/2 | 1 | 0 | 1 | 0 | 1 |
| Analyst A Fuzzy degree | 0.4 | 0.4 | 0.8 | 0.6 | 0.8 | 0.6 | 0.5 | 0.7 | 0.8 | 0.3 | 0.8 |
| Analyst B Fuzzy degree | 0.5 | 0.7 | 0.9 | 0.7 | 0.6 | 0.5 | 0.7 | 0.6 | 0.7 | 0.4 | 0.9 |
| $x_A \wedge_p x_B$ | 0.7 | 0.7 | 0.8 | 0.4 | 0.9 | 0.6 | 0.4 | 0.9 | 0.6 | 0.6 | 0.7 |

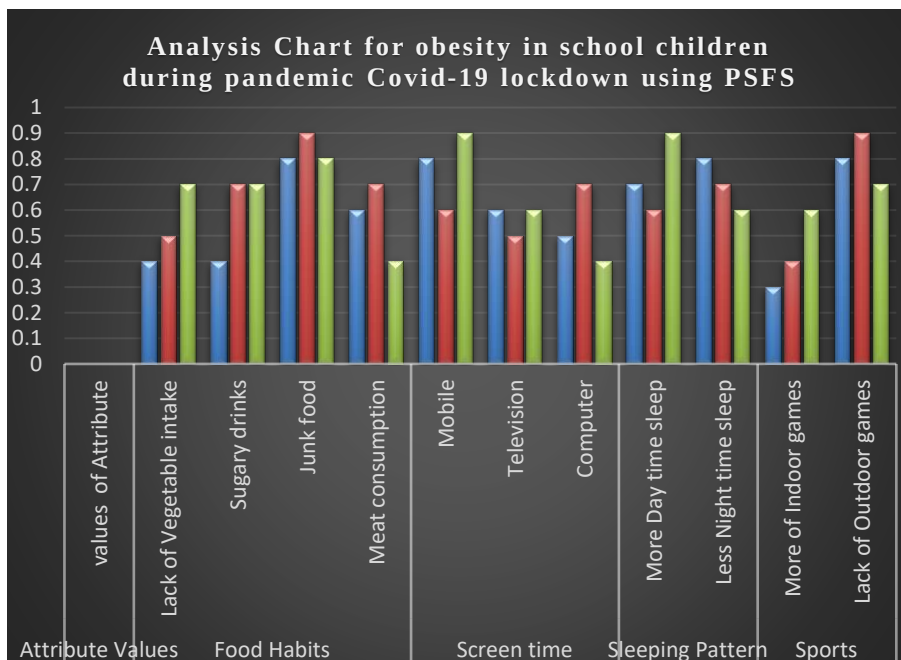


Fig 1. Analysis Chart

6. Conclusion & Future work

Based on the fuzzy degrees of Analyst’s (A & B) it is clearly shown that the major reasons for the obesity in children during COVID 19 lockdown is the Consumption of more junk food and the time spending on using mobile phones, more day time sleep along with the lack of Outdoor sports which reduces all their physical activities and in turn results in the obesity. In future we can extend this PSFS concept to interval valued and also learn its applications in decision making.

References

- [1] N. Martin and F. Smarandache, “Plithogenic Cognitive Maps in Decision Making”, International Journal of Neutrosophic Science (IJNS), vol..9, pp.09-21, 2020.
- [2] P.K. Singh, “Plithogenic set for multi-variable data analysis”, International Journal of Neutrosophic Science (IJNS), vol. 1, pp. 81-89, 2020.
- [3] F. Smarandache, “Plithogenic set, an extension of Crisp, Fuzzy, Intuitionistic Fuzzy, and Neutrosophicsets-Revisited”, Neutrosophic Sets and Systems, vol.21, pp.153-166, 2018. <http://doi.org/10.5281/zenodo.1408740>.
- [4] F. Smarandache, “Physical Plithogenic sets”, 71st Annual Gaseous Electronics conference, Session LW1, Oregon Convention Center Room, Portland, Oregon, USA, November,5-9, 2018; <http://meetings.aps.org/Meeting/GEC18/Session/LW1.110>
- [5] F. Smarandache, “Plithogeny, PlithogenicSet, Logic,Probability, and Statistics”, 141 pages, Pons Editions,Brussels,Belgium,2017, arXiv.org (Cornell University), ComputerScience-Artificial IntelligenceADS: http://adsabs.harvard.edu/cgi-bin/bib_query?arXiv:1808.03948.
- [6] Y. Deng, F.T. Chan, Y. Wu and D. Wang, “A new linguistic MCDM method based on multiple-criteria data fusion” Expert systems with Applications, vol.38, pp.6985-6993, 2011.

Tutoring Grammar in Professional Institutions

Dr. D. Sampath Kumar,
Assistant Professor,
Department of Science and Humanities,
Panruti.

Abstract

The aim of grammar instruction is to enable students to enhance their communication purposes. This goal has three implications: Students need clear instruction that connects grammar points with larger communication contexts. Students do not need to master every aspect of each grammar point, only those that are relevant to the day-to-day communication task. Error correction is not always the instructor's first responsibility.

Keywords: English grammar, communication, Games, etc...

1 Introduction

English grammar is notoriously difficult to learn for both native and second-language speakers. There are so many intricacies, obscure rules, and exceptions that it comes as no surprise that different generations of teachers have used various approaches to teaching grammar to train literate English writers. In the past, memorization-based techniques that relied on repetition slowly gave way to more creative methods. Today, we live in a society that prizes literacy and is willing to adapt to more effective methods to achieve the best results in teaching grammar, that illustrates the grammatical relationships between words. More recently, diagramming sentences has had small pop-culture resurgence in prints of famous opening sentences and websites that allow you to diagram to your heart's content

2 Simple Techniques

Songs

Repetition is key to mastering grammar as it helps the brain remembering patterns. Using songs is therefore a wonderful tool to practice grammar. Music conveys feelings, emotions and by singing the lyrics students learn a lot without even noticing it. You need to choose your song carefully according to what you want to teach. You want to work on the daily routine and the present tense for ESL students. Have a worksheet ready to give to your students. Depending on the level of your class you may have a filling gap activity, a matching up or lyrics to reorder. Wait before you hand out the worksheet; get your students to listen to the beat, to sing if they know the song. Only then do you give them the worksheet. After that you can quiz them on the tense used in the song. You could even try to change the tense and to have your students to sing! Songs are usually great fun and a wonderful way to practice grammar while avoiding boredom.

Games

Games have a strong motivational impact on learning and if you can instill some competition that is even better to stimulate your students' minds. Not only will games stimulate your students it will also create and reinforce a feeling of community.

3 Types

Traditional: grammar for grammar's sake

- Teach the regular *-ED* form with its two pronunciation variants
- Teach the doubling rule for verbs that end in *D* (for example, *WED-WEDDED*)
- Hand out a list of irregular verbs that students must memorize
 - Do pattern practice drills for *-ED*
 - Do substitution drills for irregular verbs

Communicative competence: grammar for communication's sake

- Distribute two short narratives about recent experiences or events, each one to half of the class
- Teach the regular *-ED* form, using verbs that occur in the texts as examples. Teach the pronunciation and doubling rules if those forms occur in the texts.
- • Teach the irregular verbs that occur in the texts. Students read the narratives, ask questions about points they don't understand.
- • Students work in pairs in which one member has read Story A and the other Story B. Students interview one another; using the information from the interview, they then write up or orally repeat the

story they have not read.

4 Traditional System

Inductive Teaching

This method of teaching grammar involves presenting several examples that illustrate a specific concept and expecting students to notice how the concept works from these examples. No explanation of the concept is given beforehand, and the expectation is that students learn to recognize the rules of grammar in a more natural way during their own reading and writing. Discovering grammar and visualizing how these rules work in a sentence allows for easier retention of the concept that the students were given an explanation that was disconnected from examples of the concept. The main goal of the inductive teaching method is the retention of grammar concepts, with teachers using techniques that are known to work cognitively and make an impression on students' contextual memory.

5 Modern System

Deductive Teaching

The deductive method of teaching grammar is an approach that focuses on instruction before practice. A teacher gives students an in-depth explanation of a grammatical concept before they encounter the same grammatical concept in their own writing. After the lesson, students are expected to practice what they have just been shown in a mechanical way, through worksheets and exercises. This type of teaching, though common, has many people—including teachers—rethinking such methods, as more post-secondary level students are revealing sub-par literacy skills in adulthood. Deductive teaching methods drive many students away from writing because of the tediousness of rote learning and teacher-centered approaches.

Interactive Teaching

Another method of teaching grammar is to incorporate interactivity into lessons. Using games to teach grammar not only engages students but also helps them to remember what they've learned. This method allows teachers to tailor their lessons to the different learning styles of students.

For instance, each student can be given a large flashcard with a word on it, and the students must physically arrange themselves into a proper sentence. Other games can include word puzzles or fun online quizzes.

6 Conclusion

Over the years, many methods have been developed for teaching grammar and have been built upon, abandoned, or combined, all with the same goal in mind—teaching students how to communicate effectively and understand how to use the English language. Because of the grammatical complexity of English, each method has its pros and cons. Some lessons are less likely to be remembered, while others may require more in-depth explanation and practice. Regardless of how grammar is taught, a well-rounded understanding of English grammar is the most important factor in improving the literacy of students.

7 References

- [1] A. James, *Learning Another Language Through Actions: The Complete Teacher's Guidebook*, Los Gatos, CA: Sly Oaks Productions, 1977. See also <http://www.tpr-world.com/>.
- [2] B. H. Douglas, *Teaching by Principles: An Interactive Approach to Language Pedagogy*, Prentice Hall, 1994.
- [3] F. Mary, B. Christopher, *The Functional-Notional Approach: From Theory to Practice*. Oxford University Press, 1983.
- [4] D. K. Stephen, D. T. Tracy, *The Natural Approach: Language Acquisition in the Classroom*, Pergamon Press, 1983. See also *Bilingual Education: Arguments For and (Bogus) Arguments Against*, *Theory of Second Language Acquisition, A Summary of Stephen Krashen's "Principles and Practice in Second Language Acquisition"*, *Why Bilingual Education?*.
- [5] L-F. Dianne, *Techniques and Principles in Language Teaching*. New York: Oxford University Press, 1986.
- [6] N. David, *Language Teaching Methodology: A Textbook for Teachers*, Prentice Hall, 1991. See also <http://ec.hku.hk/dcnunan/>
- [7] H. P. Clifford, C-M. Marianne, "An outline of language teaching approaches", in Celce-Murcia, Marianne & McIntosh, Lois (Ed.), *Teaching English as a Second or Foreign Language*, Newbury House, 1979.
- [8] R. Jack, R. Theodore, *Approaches and Methods in Language Teaching*, New York: Cambridge University Press, 1986.

Generalisation of Statistical Convergence in Cone Metric Space

Dr. Sonia Rani

Assistant Professor in Mathematics
BabuAnant Ram Janta College Kaul,(Kaithal) Haryana
e-mail:sonia10jan89@gmail.com

Abstract

Cone metric spaces are one of many generalizations of metric spaces. Every Metric Space is Cone Metric Space and Topological Metric Space. In this Paper, We introduce and discuss about the Statistical Convergence and its main Generalisation which are I-Convergence and I*-Convergence. The concept of I-Convergence is very important generalisation of Statistical Convergence. We introduce the idea of I-Cauchy and I*-Cauchy Sequence in cone Metric Spaces and study their properties

Key words: Cone Metric Space, Statistical Convergence, I-Convergence, I*-Convergence, ICauchy and I*-Cauchy Condition, Condition (AP).

1. Cone Metric Space

Cone Metric Space play an important role in fixed point theory, computer science, and some other research areas as well as in general topology. Cone metric spaces have been actually defined many years ago by several authors and appeared in the literature under different names. Dj. Kurepa was the first who introduced such spaces in 1934 under the name “espaces pseudo-distenci’es” [1]. In this paper, we shall introduce and investigate the convergence in cone metric spaces, discuss statistically convergence and I convergence of cone metric spaces. The paper is organized so that introduction is followed by three sections. In Section 2 we familiarize the reader with the basic notions concerning statistical convergence in cone metric spaces and give some topological natures of this convergence. In Section 3 we study about the I-Convergence and I*-Convergence and idea of I-Cauchy and I*-Cauchy Sequence in cone Metric Spaces and study their properties .Throughout this paper, the set of positive integers is denoted by N , the set of real numbers with the standard topology is denoted by R Let us we recall some basic concepts which will be needed throughout the paper.

Definition Let E be the Real Banach space and Let P be a subset of E . Then P is called a cone if and only if: (i) P is closed, nonempty and $P \neq \{0\}$; (ii) $a, b \in R, a, b \geq 0$ and $x_1, x_2 \in P \rightarrow ax_1 + bx_2 \in P$; (iii) $x \in P$ and $-x \in P$ implies $x = \{0\}$.

Let Given a cone $P \subset E$, we have a partial ordering \leq with respect to P is defined as $x_1 \leq x_2$ if and only if $x_2 - x_1 \in P$. We shall write $x_1 < x_2$ to indicate that $x_1 \leq x_2$ but $x_1 \neq x_2$, while

$x_1 \ll x_2$ Will stand for $x_2 - x_1 \in \text{int } P$ where $\text{int } P$ stands for interior of P . In this paper we always assume that $\text{int } P \neq \emptyset$ and $E^+ = \{c \in E : 0 \ll c\}$ [2]

Definition The Cone P is called normal if there is a number $K > 0$ such that for all $x_1, x_2 \in E$,

$0 \leq x_1 \leq x_2$, we have $\|x_1\| \leq K\|x_2\|$. The least positive number K is called the normal constant of P

The Cone P is called regular if every increasing (decreasing) sequence which is bounded from above (below) is convergent. A regular cone is a normal cone.

Definition Let (E, P) is a cone space and X be a non-empty set. Let $d : X \times X \rightarrow E$ be a mapping which satisfies the following conditions: Then d is called a cone metric on X and (X, E, P, d) a cone metric space

$0 \leq d(x, y)$ for all $x, y \in X$ and $d(x, y) = 0 \Leftrightarrow x = y$;

$$d(x, y) = d(y, x) \text{ for all } x, y \in X$$

$$d(x, y) \leq d(x, z) + d(z, y) \text{ for all } x, y, z \in X$$

Then d is called a cone metric on X and (X, E, P, d) a cone metric space.

*We can write simply (X, d) a cone metric space in place of (X, E, P, d) is a cone metric space.

Example of Cone Metric Space

Let $E = \mathbb{R}^2$ and $P = \{(x_1, x_2) \in E : x_1, x_2 \geq 0\} \subset \mathbb{R}^2, X = \mathbb{R}$. The Mapping $d: X \times X \rightarrow E$ is given by

$$d(x_1, x_2) = (|x_2 - x_1|, \gamma|x_2 - x_1|), \text{ where } \gamma \geq 0 \text{ is a constant. Then } (X, d) \text{ is clearly a Cone Metric Space.}$$

1.1 Asymptotic Density

Definition Let $A \subset \mathbb{N}$, put $A(n) = \{a \in A : a \leq n\}, \forall n \in \mathbb{N}$. Then $\underline{\delta}(A) = \liminf_{n \rightarrow \infty} \frac{|A(n)|}{n}$ and

$\bar{\delta}(A) = \limsup_{n \rightarrow \infty} \frac{|A(n)|}{n}$ are called *lower and upper asymptotic density* of the set A respectively.

$\underline{\delta}(A) = \bar{\delta}(A)$, then

$$\delta(A) = \lim_{n \rightarrow \infty} \frac{|A(n)|}{n}$$

is called an *asymptotic (or natural) density* of the set A .

All the three densities, if they exist, are in $[0, 1]$. A subset A of \mathbb{N} is said to be statistically dense if $\delta(A) = 1$. It is easy to see that $\delta(\mathbb{N} - A) = 1 - \delta(A)$ for each $A \subset \mathbb{N}$. [3]

1.2 Admissible Ideal

Definition A family $I \subset 2^U$ of subsets of a non-empty set U is said to be an ideal in U if

- (i) $A, B \in I$ implies $A \cup B \in I$;
- (ii) $A \in I, B \subset A$ implies $B \in I$;

While an admissible ideal I of U further satisfies $\{x\} \in I$ for each $x \in U$. If I is a proper ideal in U (i.e. U does not belong to $I, U \neq \phi$)

Then the family of sets $F(I) = \{M \subset U : \text{there exists } A \in I : M = U \setminus A\}$ is a filter in U . It is called the filter associated with the ideal I . Throughout the paper I will denote an admissible ideal of N . [4]

1.3 Condition (AP)

An admissible ideal $I \subset 2^N$ is said to satisfy the **condition (AP)** if for any sequence $\{A_1, A_2, \dots\}$ of mutually disjoint sets in I , there is a sequence $\{B_1, B_2, \dots\}$ of subsets of N such that $A_i \Delta B_i (i = 1, 2, 3, \dots)$ is finite and $B = \bigcup_{j \in \mathbb{N}} B_j \in I$.

2. Statistical Convergence in Cone Metric Space

In this section firstly we recall the convergence of sequences in cone metric space and then we introduce the concept of statistical convergence in cone

2.1 Statistically Convergence

Definition A sequence $\{a_n\}$ in R is said to be *statistically convergent* to a point $a \in R$ if for each

$$\varepsilon > 0, \lim_{n \rightarrow \infty} \frac{1}{n} |\{m \leq n : |a_m - a| \geq \varepsilon\}| = 0, \text{ i.e., } \lim_{n \rightarrow \infty} \frac{1}{n} |\{m \leq n : |a_m - a| \leq \varepsilon\}| = 1.$$

Definition Let (X, d) be a cone metric space.

(1) Let $\{x_n\}$ be a sequence in X and $x \in X$. If for each $c \in E^+ = \text{int } P$, there is $n_0 \in N$ such that for all $n > n_0$, $d(x_n, x) \ll c$, then $\{x_n\}$ is said to be convergent and $\{x_n\}$ converges to x .

(2) Let $\{x_n\}$ be a sequence in X . If for each $c \in E^+$, there is $n_0 \in N$ such that for all $n, m > n_0$, $d(x_n, x_m) \ll c$, then $\{x_n\}$ is called a Cauchy sequence in X .

(3) (X, d) is said to be *complete* if every Cauchy sequence in X is convergent in X . [5]

According to the sequential convergence and completeness of metric spaces, we give the following definition about cone metric space.

Definition Let (X, d) be a cone metric space, and $\{x_n\}$ a sequence in X . Then

- (1) $\{x_n\}$ is said to be statistically convergent to a point $x \in X$, if for each $c \in E^+$, we have $\delta\{n \in N : d(x_n, x) \leq c\} = 1$. This is denoted by $\text{st-}\lim_{n \rightarrow \infty} x_n = x$
- (2) $\{x_n\}$ is called a statistical Cauchy sequence in X , if for each $c \in E^+$, there is $n_0 \in N$ such that $\delta\{n \in N : d(x_n, x_{n_0}) \leq c\} = 1$.
- (3) (X, d) is said to be statistically complete if every statistical Cauchy sequence in X is statistically convergent. [6]

Corollary The statistical convergence of sequences in a cone metric space is a natural generalization of the usual convergence. But converse is not true in general.

Let $\{x_n\}$ be a sequence in a cone metric space (X, d) . If $\lim_{n \rightarrow \infty} x_n = x \in X$ then for each $c \in E^+$, There is $n_0 \in N$ such that $d(x_n, x) \leq c, \forall n > n_0$. Thus $\forall n > n_0$

$$|A(n)| = |\{k \leq n : d(x_k, x) \leq c\}| \geq n - n_0$$

$$\text{And } \lim_{n \rightarrow \infty} \frac{|A(n)|}{n} = 1$$

Thus $\text{st-}\lim_{n \rightarrow \infty} x_n = x$. Therefore every convergent sequence is statistical convergent in a cone metric space.

But converse is not true

Example Let $E = R^2$ and $P = \{(x_1, x_2) \in E : x_1, x_2 \geq 0\} \subset R^2, X = R$. The Mapping $d : X \times X \rightarrow E$ is given by $d(x_1, x_2) = (|x_2 - x_1|, \gamma|x_2 - x_1|)$, where $\gamma > 0$ is a constant. Then (X, d) is clearly a Cone Metric Space.

Consider a sequence $\{x_n\}$ in X defined by

$$x_n = \begin{cases} 1/n, & n \neq m^2 \\ n, & n = m^2 \end{cases} \text{ Where } m \in N$$

For $x = 0$, we have $d(x_n, x) = (1/n, \gamma/n)$, if $n \neq m^2$ and $d(x_n, x) = (n, \gamma n)$ if $n = m^2$, and $m \in N$. for each $c \in E^+$, we have

$$A(n) = \{k \leq n : d(x_k, x) \leq c\} \supset \{k \leq n : k > n_c, k \neq m^2, m \in N\}$$

for some $n_c \in N$. Then

$$\delta\{n \in N : d(x_k, x) \leq c\} \geq \delta\{n \in N : n > n_c, k \neq m^2, m \in N\} = 1$$

Consequently, $\text{st-}\lim_{n \rightarrow \infty} x_n = x$, but the sequence $\{x_n\}$ is not convergent.

Example Let $E = \mathbb{R}^2$ and $P = \{(x_1, x_2) \in E: x_1, x_2 \geq 0\}$, $X = \mathbb{R}$ and $d: X \times X \rightarrow E$ defined by

$$d(x_1, x_2) = \left(\left| \frac{x_1}{1+|x_1|} - \frac{x_2}{1+|x_2|} \right|, \sqrt{3} \left| \frac{x_1}{1+|x_1|} - \frac{x_2}{1+|x_2|} \right| \right)$$

It is easy to verify that it is a cone metric space. Consider a sequence $\{x_n\}$ in X defined by

$$x_n = \begin{cases} 1/n, & n \neq m^2 \\ n, & n = m^2 \end{cases} \text{ Where } m \in \mathbb{N}$$

Then we check whether $\{x_n\}$ is a statistical Cauchy sequence or not in X ,

For each $c \in E^+$, there exists $n_0 \in \mathbb{N}$ such that $n_0 \neq m^2$ for each $m \in \mathbb{N}$ and $2/n_0 < \|c\|$. If $n > n_0$ and $n \neq m^2$ for each $m \in \mathbb{N}$, then

$$\begin{aligned} \|d(x_n, x_{n_0})\| &= \left\| \left(\left| \frac{n}{1+n} - \frac{n_0}{1+n_0} \right|, \sqrt{3} \left| \frac{n}{1+n} - \frac{n_0}{1+n_0} \right| \right) \right\| \\ &= 2 \frac{n-n_0}{(1+n)(1-n_0)} < \frac{2}{n_0} \end{aligned}$$

Thus $A(n) = \{k \leq n: d(x_k, x_{n_0}) \leq c\} \supset \{k \leq n: k > n_0, k \neq m^2, m \in \mathbb{N}\}$

for some $n_c \in \mathbb{N}$. Then

$$\delta\{n \in \mathbb{N}: d(x_k, x_{n_0}) \leq c\} \geq \delta\{n \in \mathbb{N}: n > n_c, k \neq m^2, m \in \mathbb{N}\} = 1$$

Hence sequence $\{x_n\}$ is a statistical Cauchy sequence in X .

Lemma. Let $\{x_n\}$ and $\{y_n\}$ be two sequence in a cone metric space (X, d) .

(i) If $\text{st-}\lim_{n \rightarrow \infty} x_n = x$ and $\text{st-}\lim_{n \rightarrow \infty} x_n = x_1$ then $x = x_1$.

i.e. The limit of a statistically convergent sequence is unique in cone metric space (X, d) .

(ii) $\text{st-}\lim_{n \rightarrow \infty} x_n = x$ if and only if $\text{st-}\lim_{n \rightarrow \infty} d(x_n, x) = 0$.

(iii) If $\text{st-}\lim_{n \rightarrow \infty} x_n = x$ and $\text{st-}\lim_{n \rightarrow \infty} y_n = y$, then $\text{st-}\lim_{n \rightarrow \infty} d(x_n, y_n) = d(x, y)$

Theorem Let $\{x_n\}$ and $\{y_n\}$ be two sequence in a cone metric space (X, d) . If $\text{st-}\lim_{n \rightarrow \infty} y_n = a$ and

$d(x_n, a) \leq d(y_n, a)$ for each $n \in \mathbb{N}$ then $\text{st-}\lim_{n \rightarrow \infty} x_n = a$.

Proof Let $\text{st-}\lim_{n \rightarrow \infty} y_n = a$ then we have $\text{st-}\lim_{n \rightarrow \infty} d(y_n, a) = 0$ (by using Lemma above)

So for each $c \in E^+$ and $n \in \mathbb{N}$, we have $\{k \leq n: d(x_k, a) \leq c\} \supset \{k \leq n: d(y_k, a) \leq c\}$ and

$$\delta\{k \leq n: d(x_k, a) \leq c\} \geq \delta\{k \leq n: d(y_k, a) \leq c\} = 1$$

Thus $\text{st-}\lim_{n \rightarrow \infty} d(x_n, a) = 0$, i.e. $\text{st-}\lim_{n \rightarrow \infty} x_n = a$

2.2 Statistically Dense

Definition A subsequence $\{x_{n_k}\}$ of a sequence $\{x_n\}$ is *statistically dense* in $\{x_n\}$ if the index set $\{n_k : \in N\}$ is a statistically dense subset of N , i.e., $\delta \{n_k : \in N\} = 1$.

Theorem Let $\{x_n\}$ be a sequence in a cone metric space (X, d) . Then the following are equivalent:

- (1) $\{x_n\}$ is statistically convergent in (X, d) ;
- (2) There is a convergent sequence $\{y_n\}$ in X such that $x_n = y_n$ for almost all $n \in N$;
- (3) There is a statistically dense subsequence $\{x_{n_k}\}$ of the sequence $\{x_n\}$ such that the sequence $\{x_{n_k}\}$ is convergent;
- (4) There is a statistically dense subsequence $\{x_{n_k}\}$ of the sequence $\{x_n\}$ such that the sequence $\{x_{n_k}\}$ is statistically convergent. [6]

Corollary Every statistically convergent sequence has a convergent subsequence in a cone metric space.

The converse of above Corollary is not hold, i.e., there is a non-statistically convergent sequence in a cone metric space such that it has a convergent subsequence. In fact, the sequence $\{x_n\}$ in Example

Let $E = R^2$ and $P = \{(x_1, x_2) \in E : x_1, x_2 \geq 0\}$, $X = R$ and $d : X \times X \rightarrow E$ defined by

$$d(x_1, x_2) = \left(\left| \frac{x_1}{1+|x_1|} - \frac{x_2}{1+|x_2|} \right|, \sqrt{3} \left| \frac{x_1}{1+|x_1|} - \frac{x_2}{1+|x_2|} \right| \right)$$

Has the convergent subsequence $\{x_{m^2}\}$, but the $\{x_n\}$ is not statistically convergent.

3. I-Convergence and I*-Convergence on cone metric space

3.1 I-Convergence and I*-Convergence

Definition Let (X, d) be a cone metric space. Let $\{x_n\}_{n \in N}$ be a sequence in X and let $x \in X$. If for every $c \in E$ with $0 \ll c$ there is $K \in N$ such that for all $n > K$, $d(x_n, x) \ll c$, then $\{x_n\}_{n \in N}$ is said to be convergent to x and x is called the limit of the sequence $\{x_n\}_{n \in N}$. We denote this by

$$\lim_{n \rightarrow \infty} x_n = x. [2]$$

Definition Let (X, d) be a cone metric space. Let $\{x_n\}_{n \in N}$ be a sequence in X and let $x \in X$. If for every $c \in E$ with $0 \ll c$ (i.e. $c - 0 \in \text{int}P$) the set $\{n \in N : c - d(x_n, x) \notin \text{int}P\} \in I$, then $\{x_n\}_{n \in N}$ is said to be *I* – Convergent to x and we write it as $I - \lim_{n \rightarrow \infty} x_n = x$

Definition A sequence $\{x_n\}_{n \in N}$ in X is said to be *I** – convergent to $x \in X$ if and only if \exists a set $M \in F(I)$, $M = \{m_1 < m_2 < \dots < m_k < \dots\}$ such that $\lim_{n \rightarrow \infty} x_{m_k} = x$ i.e.

for every $c \in E$ with $0 \ll c$, there exist $t \in N$ such that $c - d(x_{m_k}, x) \in \text{int}P$ for all $k \geq t$

The cone metric space is First Hausdorft topological space with the topology induced by the open ball defined naturally for each element x in X and for each c in $\text{int}P$.

Also we can show that *I** – convergence always implies *I* – convergence but the converse is not true. The two concepts are equivalent if and if the ideal *I* has condition (AP). ([8],[9])

Here we consider cone metric space X with normal cone P and it is also known that

$$\text{For } a, b, c \in X, a \leq b, b \ll c \Rightarrow a \ll c$$

3.2 I and I* – Cauchy Conditions in Cone Metric Spaces

Definition The sequence $\{x_n\}_{n \in N}$ in X is said to be $I - Cauchy$ if for every $c \in E$ with $0 \ll c$ there exists J such that the set $\{n \in N: c - d(x_n, x_j) \notin \text{int}P\} \in I$.

Definition A sequence $\{x_n\}_{n \in N}$ in X is said to be $I^* - Cauchy$ sequence if there exists a set $M \in F(I)$, $M = \{m_1 < m_2 < \dots < m_k < \dots\} \subset N$ such that $\{x_{m_k}\}_{k \in N}$ is an ordinary Cauchy sequence in X .

Theorem Let I be an arbitrary admissible ideal. Then $I - \lim_{n \rightarrow \infty} x_n = \xi$, implies that $\{x_n\}_{n \in N}$ is an $I - Cauchy$ sequence.

Proof Let $I - \lim_{n \rightarrow \infty} x_n = \xi$. Then for each $c \in E$ with $0 \ll c$, we have $A(c) = \{n \in N: c - d(x_n, \xi) \notin \text{int}P\} \in I$. Since I is an admissible ideal, there exists $n_0 \in N$ such that $n_0 \in A(c)$. Let us put $B(c) = \{n \in N: 2c \leq d(x_n, x_{n_0})\}$. Then if $n \in B(c)$ it follows that $d(x_n, \xi) + d(x_{n_0}, \xi) \geq d(x_n, x_{n_0}) \geq 2c$ and $d(x_{n_0}, \xi) \ll c$ and so we must have $d(x_n, \xi) \geq c$. This implies $c - d(x_n, \xi) \notin \text{int}P$. Hence $n \in A(c)$. Thus $B(c) \subset A(c) \in I$, for each $0 \ll c$. Therefore it follows that $B(c) \in I$ and consequently $\{x_n\}_{n \in N}$ is an $I - Cauchy$ sequence.

Theorem Let (X, d) be a cone metric space and let I be an admissible ideal of N . If $\{x_n\}_{n \in N}$ is an $I^* - Cauchy$ sequence in X then it is an $I - Cauchy$ Sequence.

Proof is omitted [4].

Lemma Let $\{A_j\}_{j \in N}$ be a countable family of subsets of N such that $A_j \in F(I)$ for each j where $F(I)$ is the filter associated with an admissible ideal I with the property (AP) . Then there is a set

$A \subset N$ Such that $A \in F(I)$ and the sets $A \setminus A_j$ is finite for all j .

Theorem If I has property (AP) then the concepts of I and $I^* - Cauchy$ conditions coincide.

Proof: Let $\{x_n\}_{n \in N}$ be an $I - Cauchy$ sequence in X . Then from the definition there exists an $J = J(c)$ such that the set $A(c) = \{n \in N: c - d(x_n, x_j) \notin \text{int}P\} \in I$ for every $c \in E$ with $0 \ll c$. Let $x \in P$ with $x \neq 0$. Now define $A_j = \{n \in N: d(x_n, x_{m_j}) < \frac{x}{j}\}$, $j = 1, 2, 3 \dots$ where $m_j = J(\frac{x}{j})$. It is clear that $A_j \in F(I)$ for $j = 1, 2, \dots$. Since I has the property (AP) there exists a set $Q \subset N$ such that $Q \in F(I)$ and $Q \setminus A_j$ is finite for all j . Let $c \in E$ with $0 \ll c$ and let $i \in N$ be such that $\frac{2x}{i} \ll c$. As $Q \setminus A_i$ is finite, there exists $k = k(i)$ such that for all $m, n \in A_i$, we have $m, n > k(i)$.

Therefore $d(x_n, x_{m_i}) < \frac{x}{i}$ and $d(x_m, x_{m_i}) < \frac{x}{i}$ for all $m, n > k(i)$. Then it follows that

$$d(x_n, x_m) = d(x_n, x_{m_i}) + d(x_m, x_{m_i}) \ll c \text{ for } m, n > k(i).$$

Thus $\{x_n\}_{n \in Q}$ is an ordinary Cauchy Sequence.

The following example shows that in general $I - Cauchy$ condition does not imply $I^* - Cauchy$ condition.

Example Let (X, d) be a cone metric space. $\{x_n\}_{n \in N}$ be a Cauchy sequence of distinct elements. Let $N = \cup_{j \in N} \Delta_j$ be a decomposition of N such that each Δ_j is finite and $\Delta_i \cap \Delta_j = \emptyset$ for $i \neq j$. Let I be the class of all those subsets A of N which intersects only finite number of Δ_j 's. Then I is a non trivial admissible ideal of N .

Define a sequence $\{z_n\}_{n \in N}$ as $z_n = x_j$ if $n \in \Delta_j$. Then clearly $\{z_n\}_{n \in N}$ is an $I - Cauchy$ sequence. If possible assume that $\{z_n\}_{n \in N}$ is also $I^* - Cauchy$. Then there is an $A \in F(I)$ such that $\{z_n\}_{n \in A}$ is a Cauchy sequence. As $N \setminus A \in I$ so there exists $I \in N$ such that $N \setminus A \subset \Delta_1 \cup \Delta_2 \cup \dots \cup \Delta_t$. Let us put $d(x_{t+1}, x_{t+2}) = \epsilon_0$. Then $0 < \epsilon_0$. From the construction of Δ_j 's it clearly follows that for any given $k \in N$ there are $m \in \Delta_{t+1}$ and $n \in \Delta_{t+2}$ such that $m, n \geq k$. Hence we can see that there is no $k \in N$ such that whenever $m, n \in A$ with $m, n \geq k$ then $d(z_m, z_n) \ll \epsilon$ where $\epsilon = \epsilon_0 / 2$, this contradicts the fact that $\{z_n\}_{n \in A}$ is Cauchy.

Theorem Let (X, d) be a cone metric space containing at least one accumulation point. If for every sequence $\{x_n\}_{n \in \mathbb{N}}$ in X , I – Cauchy condition implies I^* – Cauchy condition then I satisfy the condition (AP) .

Proof is omitted [4].

4. Conclusions

In this paper we discussed about the Statistical Convergence and its main Generalisation which are I -Convergence and I^* -Convergence. Every convergent sequence is statistical convergent in a cone metric space. But converse is not true. The statistical convergence of sequences in a cone metric space is a natural generalization of the usual convergence. But converse is not true in general. The concept of I -Convergence is very important generalisation of Statistical Convergence. If ideal I has property (AP) then the concepts of I and I^* – Cauchy conditions coincide.

Acknowledgements

The authors would like to thank the reviewer for the detail list of correction, suggestion to the paper and all her/his efforts to improve the paper.

References

- [1] Z.P. Mamuzić, Introduction to General Topology, P. Noordhoff, Ltd., The Netherlands, 1963.
- [2] H. Long-Guang and Z. Xian, Cone metric spaces and fixed point theorems of contractive mappings, J. Math. Anal. Appl., 332, 1468–1476, 2007.
- [3] H. Fast, Sur la convergence statistique, Colloq. Math. 2, 241–244, 1951.
- [4] Sudip, Ekrem, Huseyin, I -Convergence on Cone Metric Spaces, Sarajevo Journal of Mathematics, 85-93, 2013.
- [5] L.G. Huang, X. Zhang, Cone metric spaces and fixed point theorems of contractive mappings, J. Math. Anal. Appl. 332 (2), 1467–1475, 2007.
- [6] K.Li et al./Topology and its applications 196, 641-651, 2015.
- [7] G. Di Maio, Lj.D.R. Kočinac, Statistical convergence in topology, Topol. Appl., 156, 28–45, 2008.
- [8] D.Turkoglu and M. Abuloha, Cone metric spaces and fixed point theorems in diametrically contractive mappings, to appear in Acta Math. Sin.
- [9] B. K. Lahiri and Pratulananda Das, I and I^* -convergence in topological spaces, Math. Bohemica, 130 (2), 153–160, 2005.
- [10] H. Çakalli, A study on statistical convergence, Funct. Anal. Approx. Comput. 1 (2), 19–24, 2009.
- [11] K.P. Chi, T.V. An, Dugundji's theorem for cone metric spaces, Appl. Math. Lett. 24, 387–390, 2011.

Adsorption and Filtration Techniques on the Pollutants from Different Waste Water

Karthick S¹, Mithunkumar M², Akash B³, Gobinathan S⁴

¹UG Student, Department of civil Engineering

²UG Student, Department of Electronics and Communication Engineering

³UG Student, Department of Automobile Engineering

⁴UG Student, Department of civil Engineering

Bannari Amman Institute of Technology, Alathukombai (Post), Sathyamangalam-638401, Erode Dt, Tamil Nadu.

Email: karthick.ce19@bitsathy.ac.in mithunkumar.ec19@bitsathy.ac.in gobinathan.au19@bitsathy.ac.in akash.ce19@bitsathy.ac.in

Abstract

The problem of water pollution is of a great concern. Adsorption is one of the most efficient techniques for removing noxious heavy metal from the solvent phase. Present study focuses on the detailed information and review on the purification of heavy metal ion, dye from the factories and pharmaceutical waste from the water by nano membrane technology and various adsorbents i.e., conventional (activated carbon, clays, biosorbent). The purification of waste water using nano membranes are mainly depends upon the pressure, temperature, permeate flow, pH, TDS, salt concentration of water. In this review, the technical feasibility of various low-cost adsorbents for removal of heavy metals(like pb,Ar,Hg,Cr,etc...) from the waste waters has been discussed. The adsorptive properties of this material are a result of its high specific surface area and some of the functional groups acquired during the chemical activation. These activated carbon have proven highly effective in the removal of textile dyes in aqueous solutions and waste water. They can also be prepared from low-cost easily attainable raw-materials in INDIA. The properties of activated carbon such as its large specific surface area and its chemical stability make this material an interesting substrate for the preparation of different composite materials. As a result of extensive review, we found, the flux rate of water through the membrane unit and pore size of adsorbent is trivial to optimize in water treatment plants. So we carried out our research on design of coloumn upflow reactor with optimized operational parameters for waste water treatment.

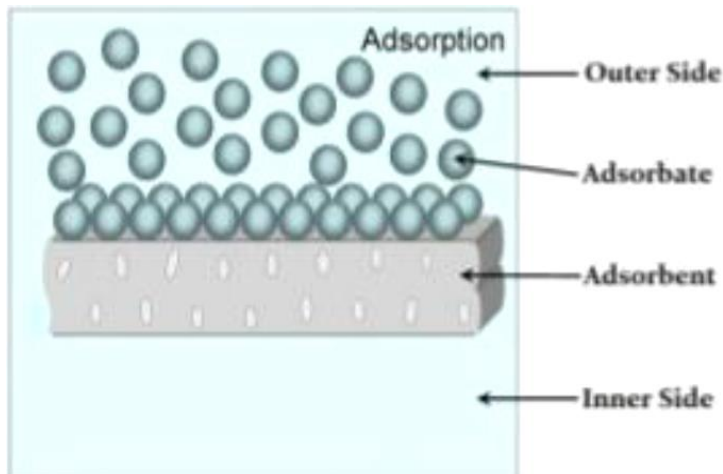
Keywords: *Adsorption, nanofiltration, review, industrial wastewater, coloumn reactor.*

1 Introduction

Water is a most essential thing in our living world. Now a days water pollution had gone worse. So we designed an product which can purify different types of chemicals and heavy metals. Adsorption play a huge in the purification heavy metals from unpurified water. Also membrane technology is used to purify various types of chemicals and harmful organism

2. Adsorption & adsorbents

Water is an essential element for the survival of all living organisms. Nowadays, the water sources contaminated by a wide variety of pollutants coming from industrial effluents are a subject of several researchers An adsorbent is a solid substance used to collect solute molecules from a **liquid** or **gas**. Adsorption is often used to extract **pollutants** by causing them to be attached to adsorbents such as **activated carbon** or **silica gel**.



Adsorption is a wastewater purification technique for removing a wide range of compounds from **industrial wastewater**. Adsorption takes place when molecules in a liquid bind themselves to the surface of a solid substance. Adsorbents have a very high internal surface area that permits adsorption.

Granulated Activated Carbon (GAC) is one of the most commonly used treatment processes for the removal of organic compounds from water.

Rice husk is an easily available product also this rice husk playing a huge role in removal of heavy metals in wastewater like **cadmium**.

3. Filtration

Filtration is a process that removes particles from suspension in water.


The methods used include physical processes such as **filtration, sedimentation, and distillation, biological processes** such as slow sand filters or biologically active carbon; chemical processes such as flocculation and chlorination; and the use of electromagnetic radiation such as ultraviolet light.




Flocculation is a type of wastewater treatment using filtration method. This is a process where colloids come out of suspension in the form of **floc** either spontaneously or due to the addition of a clarifying agent. Particle filtration is a physical or mechanical process that separates solids from fluids. Particle filtration typically is defined as the filtration of particles larger than 1 micron and is used as one of the first filtration steps in industrial wastewater treatment.

3.1 Membrane filtration

Membranes are screen filters that remove particles generally in the sub-micron range. These are used for both filtration and enumeration of particles and microorganisms.

Membranes used in laboratory analysis are cast membranes (mixed ester of cellulose used commonly for coliform colony counting) or sieve-like track-etch membranes. In water analysis membranes are used for capturing and analyzing microorganisms on the surface of the filter.

| s.no | Heavy metals In waste water. | Adsorbents. |
|------|------------------------------------|--|
| 1 | Cadmium | Rice husk  |
| 2 | Copper | Coconut coir  |
| 3 | Chromium(iv) | Peanut shell  |
| 4 | Nickel | Sawdust of pine tree |

| | | |
|---|---------|--|
| | |  |
| 5 | Lead | Rubber ash of waste tire  |
| 6 | Arsenic | Rice husk  |

4. Removal of toxicity from textile wastewater

The dyes released from the textile industry have high toxicity. The BOD *values* of wastewater samples were found **185 mg/L** and **174 mg/L**. These dyes have an ability to cause “**contact dermatitis and respiratory diseases, allergic reaction in eyes, skin irritation, and irritation to mucous membrane and the upper respiratory tract**”. Chemicals released from the textile industry in the form of dyes are listed below **nonyphenols, phthalates, chlorinated and brominated flame retardants, chlorobenzenes**. The membrane pore size required to filter the various chemical in dye is 0.3-0.2micron(approx.). The activated carbon derived from **neem tree** is playing an important role in removal of toxicants in the textile dyes. And also several activated carbon which extract **several heavy metal**

5. Pharmaceutical wastewater

Pharmaceuticals and personal care products (PCP) are used to cure humans and animals. This industry consumes a huge amount of water during their manufacturing process. The **wastewater** discharged from it is contaminated by organic and inorganic matters which can be toxic to the ecosystem. The PH value of the pharmaceutical wastewater is 6.65-7.40. The chemicals in pharmaceutical wastewater are **chlorides(3900-4100mg/L), sulphates(400-650mg/L) and phosphates(<98mg/L)**.

The pharmaceutical waste discharged from the industry is highly reactive and it has a tendency to cause different type of **chronic disease**. Thus the wastewater should be filtered using nano membrane layer technology and the pore size required is 0.2-0.4(in nm). The drug contain several chemicals which can cause a several disease and that chemicals **alkkoxyphenol, naproxen, salicylic acid , acetaminophen**.

6. Sewage waste water treatment

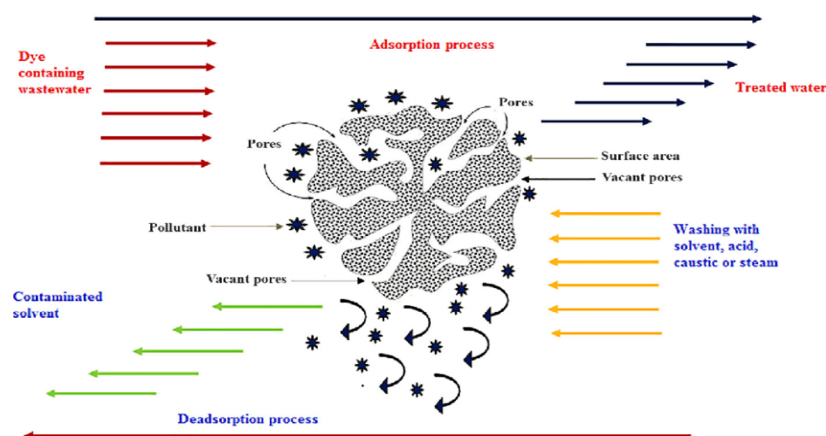
6.1 Sewage water treatment by adsorption

There are two basic type of wastewater filters: Particulate filters & adsorptive and reactive filter

Particulate filters exclude particles by size, and adsorptive/reactive filters contain a material (medium) that either adsorbs or reacts with a contaminant in water.

The principles of adsorptive activated carbon filtration are the same as those of any other adsorption material. The contaminant is attracted to and held (adsorbed) on the surface of the carbon particles.

The characteristics of the carbon material (particle and pore size, surface area, surface chemistry, etc.) influence the efficiency of adsorption.



Mostly all type of activated carbon are highly reactive towards several heavy metals and certain chemical compounds. Activated carbon units are commonly used to remove organics (odours, micropollutants) from drinking water at centralised and decentralised level.

Installation costs are moderate but additional technical equipment is required. Operating costs are usually limited to filter replacement. Depending on the type and concentration of the contaminant being removed, some carbon filters may require special hazardous waste handling and disposal, which can be costly. The activated carbon are prepared by eco-friendly in nature.

6.2 Sewage water treatment by filtration

Basically, sewage waters are highly reactive towards nature. It contain several contaminants which can cause a different type of diseases

Comparatively filtration method process of sewage water is more easier than the filtering by adsorption. The membrane technology is an emerging technology which is most efficient and used abroadly by the researchers, and also heavy metals are dissolved in water are in the size of 0.4-0.8nm(approx.)

Membranes allow certain molecules or ions to pass through by diffusion and sometimes by specialised 'facilitated diffusion'. The rate of passage depends on the pressure, concentration and temperature of the molecules or solutes on either side of the membrane, as well as the permeability of the membrane to each solute. This depends on solute size, solubility properties, or chemistry. we prefer a membrane layer in the size of lesser than one nm i.e (<1nm) approx. since the bacteria and viruses are in the size of 0.1-0.65micron(approx.)

7. Conclusions

A view on adsorption and filtration on the removal of pollutants from different industrial wastewater. The several harmful ion which is present in the wastewater are removed using Membrane technology.

Reference

- <https://doi.org/10.1016/j.ecoenv.2017.11.034>
- <https://doi.org/10.1016/j.cherd.2018.10.008> <https://doi.org/10.1016/j.cej.2019.122372>
- <https://doi.org/10.1016/j.ecoenv.2017.11.034>
- <https://doi.org/10.1016/j.ultsonch.2018.09.010>
- <https://doi.org/10.1016/j.seppur.2015.03.043>
- <https://doi.org/10.1016/j.wasman.2019.02.019>
- <https://doi.org/10.1016/j.jwpe.2016.10.007>
- <https://doi.org/10.1016/j.envres.2018.10.017>
- <https://doi.org/10.1016/j.chemosphere.2018.09.098>
- <https://doi.org/10.1016/j.jenvman.2019.04.004>
- <https://doi.org/10.1016/j.jenvman.2019.04.004>
- <https://doi.org/10.1016/j.jenvman.2019.01.012>
- <https://doi.org/10.1016/j.jece.2019.103183>
- <https://doi.org/10.1016/j.watres.2018.11.005>
- <https://doi.org/10.1016/j.envres.2019.01.055>
- <https://doi.org/10.1016/j.chemosphere.2018.05.124>
- <https://doi.org/10.1016/j.cej.2019.122607>
- <https://doi.org/10.1016/j.cej.2019.122607>
- <https://doi.org/10.1016/j.pce.2018.02.005>
- <https://doi.org/10.1016/j.jece.2018.10.014>
- <https://doi.org/10.1016/j.jece.2018.10.014>

<https://doi.org/10.1016/j.ecoenv.2017.10.025>

<https://doi.org/10.1016/j.ecoenv.2017.10.025>

<https://doi.org/10.1016/j.jcis.2017.01.031>

<https://doi.org/10.1016/j.jcis.2017.01.031>

<https://doi.org/10.1016/j.jclepro.2018.09.114>

<https://doi.org/10.1016/j.jtice.2016.03.030>

Customer Service Automation among Small and Medium Enterprises: An Empirical Examination

Dr. Sridevi. K. B
Professor – School of Management,
Sri Krishna College of Engineering and Technology,
Coimbatore, Tamilnadu, India
sridevikb@skcet.ac.in

Abstract

‘Customer Service Automation’ is emerging as the needful transformation in the present juncture for all the entrepreneurs in all the sectors. Comparatively large conglomerates are equipped enough for the implementation of customer service automation, but the small and medium enterprises (SMEs) have their unique constraints and bottlenecks in the implementation of customer service automation. In spite of all the constraints, SMEs aim to implement emerging customer service automation through self-service technologies and analytic capabilities to attain the desirable outcomes such as integrated application of Customer data, increase the effectiveness of the sales training, enhancing trust through transparency, profitable customer retention, fulfilling On-demand services, empower service and support activities and finally, WEB based Customer interaction management. Hence, the researcher has taken an attempt to analyze the gaps prevailing in the implementation of customer service automation among the SMEs in Tamilnadu State by investigating the respondents’ demographic and organizational variables. The research findings depict about the perception of SMEs towards customer service automation, readiness towards customer service automation and the expected benefits. This research would present the prevailing scenario of customer service automation and also facilitate for better customer service automation among the target group.

Keywords: *Customer Service Automation, Self Service Technologies, SMEs, WEB based Customer Interaction Management*

1. Introduction

‘Customer Service Automation’ is emerging as the needful transformation in the present juncture for all the entrepreneurs in all the sectors. Comparatively large conglomerates are equipped enough for the implementation of customer service automation, but the small and medium enterprises (SMEs) have their unique constraints and bottlenecks in the implementation of customer service automation. In spite of all the constraints, SMEs aim to implement emerging customer service automation through self-service technologies and analytic capabilities to attain the desirable outcomes such as integrated application of Customer data, increase the effectiveness of the sales training, enhancing trust through transparency, profitable customer retention, fulfilling On-demand services, empower service and support activities and finally, WEB based Customer interaction management.

2. Significance of Customer Service Automation

Automation has forced the entrepreneurs for restructuring their marketing functions and it has also influenced the entrepreneurs to implement new technologies and analytic capabilities to attain the desirable outcomes with an optimal cost.

One major trend relates to the migration of marketing spend from high-cost channels like TV and print to low-cost channels like auto generated email leads to more cost-effective marketing and could also be more regularly monitored and measured using analytics, which is vital from a performance management perspective.

Delivering superior customer service and support is critical to any business, but it has to be achieved at a reasonable cost. Additionally, wider reach of customers is easily attained through such self-service technologies at anytime from anywhere. Also, the self-service technologies are enabling SMEs to strengthen customer relationship economically while delivering win - win model of customer service. IDC has predicted that by the year 2023, most of the organizations (95%) will transform their traditional business approaches to automated approach by implementing digital KPIs, innovation management, data analytics, digital exposure and experience of their personnel and digital economy[1].

3. Benefits of Customer Service Automation

3.1. Self-service technologies

In the earlier context, enterprises were employing exclusive team of customer support and service personnel for delivering customer service, right from answering a simple query to a complex technical support. This traditional and manual method of customer support and services are characterized by stretched queues, more waiting time, inefficient customer service due to manual errors and ultimately inferior quality of customer service. Whereas, the modern era customers are more tech savvy and they lack patience and tolerance for all the flaws happening in support and services activities. They expect everything very instantly and that too at their easy reach. Innovative way of self-service technologies enables marketers to understand and communicate their brands through auto generated information sharing options such as portals with self-service knowledge bases, FAQs(frequently asked questions), interactive forums and self-service resources, the marketers are facilitated to ensure the delivery of right service at right time.

3.2. Integrated application of Customer data

Big Data is the trend across the industries which create lots of operational confusions and difficulties; it creates a challenge for the efficiency level of customer support and service activities. But, the integrated approach of data management pools the entire data and creates as a common database which could be accessed for multiple data requirements. Handling this bulk volume of data is possible by employing automated analytic software. Automation facilitates the service personnel right from data collection to outcomes generation, by which they strengthen up the market intelligence system [2]. Also, such integrated application of data minimizes the unnecessary duplication of work and saves time for more productive works.

3.3. Condense training process

The manual way of customer service demands professionalism among the customer service personnel and to fine tune the proficiency, a greater number of training programs need to be organized and this will involve a large amount of time and money. For SMEs, the affordability for such a heavy budget for training is not possible and at the same time, they cannot compromise on the service quality also. Customer service automation would considerably reduce the training expenses, but improves the customer service quality.

3.4. Enhance trust through transparency

Customer service automation eliminates all the discrepancies and it ensures complete trust among the customers. Best transparency is followed by the SMEs and customers across the market trust the information shared by the marketer. As trust is the very fundamental concept of customer relationship, it cannot be compromised for cost reduction. The facts are shared to all the target customers without any discrimination and deviation. The marketers are also keen in avoiding misleading information; fake assurances hide and seek approaches with the fear of cyber law regulations.

3.5. Profitable customer retention

Customer service automation provides a platform for improving the personalized customer care. The knowledgebase should act as a delivery vehicle for all pertinent support and service information, patches and fixes, downloads, manuals, etc. as well as comprehensive information on products and services. Through customer service automation, the target customers can easily identify the appropriate solutions for their requirements. The customer service automation facilitates data driven approach to understand and satisfy the customers [3]. The cost-effective approach leads to the continuous monitoring of customer behavior and hence, it could easily sense the changing preferences of the buyers and discover new products or services that may improve their affinity with the marketer.

3.6. Leasing On -demand services

Customer service automation simplifies the investment burden of the SMEs by being more focused in specifying the real requirements of the customers. Hence, the SMEs need not invest on the general services; instead they could lease the services.

3.7. Empower service and support activities

Customer service automation takes care of continuous follow up of the quality of customer service by conducting virtual surveys from the end users. The value less repetitive and routine services is just wasting the organizations financial wealth and hence automation may replace such services into value added services matching with the customers' expectations [4]. This regular follow ups will uplift the quality of customer service and support. A complete transformation of service and support will take place with the implementation of customer service automation. The SMEs could reach further heights by uplifting the quality of service and support.

3.8. Online Customer interaction management

A successful customer relationship needs continuous Customer interaction at any time and from anywhere. Customer service automation extends a convenient channel for extending the contact points between the buyer and seller. Web 2.0 has supported the two-way interaction by the social and business networks like blogs, wikis, and podcasts, and share their thoughts and experiences with a potentially immense audience.

4. Significance of The Study

The customer service automation is tremendously emerging in the Indian industry. Comparatively large conglomerates are equipped enough for the implementation of customer service automation, but the small and medium enterprises (SMEs) have their unique constraints and bottlenecks in the implementation of customer service automation. In spite of all the constraints, SMEs aim to implement emerging customer service automation through self-service technologies and analytic capabilities to attain the desirable outcomes such as integrated application of Customer data, increase the effectiveness of the sales training, enhancing trust through transparency, profitable customer retention, fulfilling On-demand services, empower service and support activities and finally, WEB based Customer interaction management. Service automation was predicted as the futuristic scenario of automation [5].

Hence, the researcher has taken an attempt to analyze the gaps prevailing in the implementation of customer service automation among the SMEs in Tamilnadu State by investigating the respondents' demographic and organizational variables. The research findings depict about the perception of SMEs towards customer service automation, readiness towards customer service automation and the expected benefits. This research would present the prevailing scenario of customer service automation and also facilitate for better customer service automation among the target group.

5. Objectives of The Study

- [1] To study the gaps in the SMEs' preferences towards the manual customer service and automated customer service.
- [2] To evaluate the interest for customer support automation among the SMEs.
- [3] To identify the influence of SMEs' demographic variables in the implementation of customer service automation.
- [4] To analyze the benefits expected by SMEs in shifting to automated customer service.

6. Research Methodology

In order to analyze the gaps prevailing among SMEs' readiness towards customer service automation, the research area selected for the study is Tamilnadu, the researcher has randomly selected 383 registered Small and Medium Enterprises (SMEs) in Tamilnadu as respondents and collected data through survey method with the help of a questionnaire. The collected data has been analyzed and findings are interpreted.

7. Analysis and Interpretation

7.1. Age

The age of the entrepreneur represents his or her experience in business and it also determines their expectations and perceptions on various aspects of digitization. In general, the aged entrepreneurs may have more experience and they may prefer conventional approach. At the same time, the youngsters may be aware of the innovative services offered by the digitalization approach and they may prefer automated approach. Hence, the age of the entrepreneurs is considered as one of the important profile variables of the entrepreneurs. In the present study, the age of the entrepreneurs is confined to less than 25 years, 25 to 35 years, 35 to 45 years, 45 to 55 years and more than 55 years. The age among the entrepreneurs is presented in Table 1.

Table 1: Age wise distribution of the respondents and their preferred customer service approach

| Sl. No. | Age (years) of the respondents | Manual approach(195) | | Automated approach(188) | | Total (383) | |
|---------|--------------------------------|----------------------|------|-------------------------|------|-------------|------|
| | | F | % | F | % | F | % |
| 1. | Less than 25 | 3 | 0.8 | 4 | 1.0 | 7 | 1.8 |
| 2. | 25-35 | 69 | 18.0 | 80 | 20.9 | 149 | 38.9 |
| 3. | 35-45 | 77 | 20.1 | 68 | 17.8 | 145 | 37.9 |
| 4. | 45-55 | 46 | 12.0 | 28 | 7.3 | 74 | 19.3 |
| 5. | More than 55 | 8 | 2.1 | 0 | 0 | 8 | 2.1 |
| | Total | 195 | 50.9 | 188 | 49.1 | 383 | 100 |

Source: Primary Data F – Frequency, % - Percentage

The first two major age groups among the entrepreneurs in the present study are 25 to 35 years and 35 to 45 years, which constitute 38.9 and 37.9 Per cent to the total. The most important age group among the manual approach preferred entrepreneurs is 35 to 45 years with 20.1 Percent of the total and it is followed by 25 to 35 years with 18 Percent of the total. In the case of automated approach, the leading age group of the entrepreneurs is 25 to 35 years, which constitutes 20.9 Percent of the total and it is followed by the age group 35 to 45 years with 17.8 Percent of the total. The entrepreneurs aged above 55 years constitute only 2.1 and 0 per cent of the total, in manual approach and automated approach respectively. To test whether there is any association between the entrepreneurs' age and their preference towards automated approach, Chi-square test is computed in order to test the null hypothesis H_0 . It is hypothesized that there is no significant association between the entrepreneurs' age and their preference towards automated approach. The result of the Chi-square test is given in Table 2.

Table 2: Chi - Square Test for Independency

| Calculated value of χ^2 | Table value of χ^2 | Inference |
|------------------------------|-------------------------|-------------------|
| 13.769 * | 9.49 | H_0 is rejected |

d.f. =4, $p < 0.05$, significant, d.f.: Degrees of freedom, *indicates that the χ^2 value is significant at 5 per cent level with 4 degrees of freedom.

The results of Table 2 reveal that the null hypothesis is rejected, since the calculated value is more than the Chi square Table value. Therefore, there exist statistically significant association between the entrepreneurs' age and their preference towards automated approach.

7.2. Gender

Since the gender of the entrepreneurs has its own impact on the level of estimation and perception on customer service automation, it is included as one of the profile variables. The nature of expectation and perception towards digitalization may completely differ from male to female. The gender of the entrepreneurs is illustrated in Table 3.

Table 3: Gender wise distribution of the respondents and their preferred customer service approach

| Sl.No | Gender of the respondents | Manual approach (195) | | Automated approach (188) | | Total (383) | |
|-------|---------------------------|-----------------------|------|--------------------------|------|-------------|------|
| | | F | % | F | % | F | % |
| 1. | Male | 162 | 42.3 | 164 | 42.8 | 326 | 85.1 |
| 2. | Female | 33 | 8.6 | 24 | 6.3 | 57 | 14.9 |
| | Total | 195 | 50.9 | 188 | 49.1 | 383 | 100 |

Source: Primary Data, F – Frequency, % - Percentage

Table 3 shows that 85.1 Per cent of the total entrepreneurs are males whereas the remaining 14.9 Per cent of the total entrepreneurs are females. The dominant gender of both the preferred customer service approaches is male. In manual approach preferred group, the male entrepreneurs constitute 42.3 Per cent of the total. In digital approach preferred group, the male entrepreneurs constitute 42.8 Per cent of the total. In manual approach preferred group, the female entrepreneurs segment constitutes 8.6 Per cent of the total and in automated approach preferred group they constitute 6.3 Per cent of the total. To test whether there is any association between the entrepreneurs' gender and their preference towards the customer service automation, Chi-square test is computed in order to test the null hypothesis H_0 . It is hypothesized that there is no significant association between the entrepreneurs' gender and their preference towards the automated approach. The result of the Chi-square test is given in Table 4.

Table 4: Chi - Square Test for Independency

| Calculated value of χ^2 | Table value of χ^2 | Inference |
|------------------------------|-------------------------|-------------------|
| 1.306 * | 3.841 | H_0 is accepted |

d.f. =1, $p > 0.05$, not significant, d.f.: Degrees of freedom, * indicates that the χ^2 value is not significant at 5 per cent level with 1 degree of freedom.

The results of Table 4 reveal that the null hypothesis is accepted, since the calculated value is less than the Chi square Table value. Therefore, there is no statistically significant association between the entrepreneurs' gender and their preference towards automated approach.

7.3. Educational qualification

The level of education provides more awareness on customer service automation to the entrepreneurs and exposure on the benefits of automated approach. The educated entrepreneurs may have more awareness and exposure on these aspects in general. Hence, the education may have its impact on the entrepreneurs' perceptions and preferences about digitalization. So, the level of education is included as one of the profile variables in the present study. It is confined to school level education, diploma, graduation, post-graduation and professional. The level of education among the entrepreneurs is shown in Table 5.

Table 5: Educational qualification wise distribution of the respondents and their preferred customer service approach

| Sl. No. | Educational qualification of the respondents | Manual approach (195) | | Automated approach (188) | | Total (383) | |
|---------|--|-----------------------|------|--------------------------|------|-------------|------|
| | | F | % | F | % | F | % |
| 1. | Professional | 9 | 2.3 | 0 | 0.0 | 9 | 2.3 |
| 2. | Post graduate | 46 | 12.0 | 40 | 10.4 | 86 | 22.5 |
| 3. | Graduate | 95 | 24.8 | 116 | 30.3 | 211 | 55.1 |
| 4. | Diploma | 24 | 6.3 | 20 | 5.2 | 44 | 11.5 |
| 5. | Schooling | 21 | 5.5 | 12 | 3.1 | 33 | 8.6 |
| | Total | 195 | 50.9 | 188 | 49.1 | 383 | 100 |

Source: Primary Data, F – Frequency, % - Percentage

Table 5 shows that the level of education among 55.1 percent of the total entrepreneurs is graduation and it is followed by post-graduation with 22.5 Percent of the total entrepreneurs. In the manual approach preferred group,

24.8 Percent of the entrepreneurs have completed graduation and 12 Percent have post-graduation. Whereas in case of the automated approach preferred group, 30.3 Percent have graduation and 10.4 Percent have post-graduation. Professionally educated entrepreneurs are very less in number in both the preferred groups; they constitute 2.3 Percent and 0 Percent, respectively. To test whether there is any association between the entrepreneurs' qualification and their preference towards customer service automation, Chi-square test is computed in order to test the null hypothesis H_0 . It is hypothesized that there is no significant association between the entrepreneurs' educational qualification and their preference towards automated approach. The result of the Chi-square test is given in Table 6.

Table 6: Chi - Square Test for Independency

| <i>Calculated value of χ^2</i> | <i>Table value of χ^2</i> | <i>Inference</i> |
|--|---|-------------------|
| 14.204 * | 9.49 | H_0 is rejected |

d.f.=4, $p < 0.05$, significant, d.f.: Degrees of freedom, * indicates that the χ^2 value is significant at 5 per cent level with 4 degrees of freedom.

The results of Table 6 reveal that the null hypothesis is rejected, since the calculated value is greater than the Chi square Table value. Therefore, there exist statistically significant association between the entrepreneurs' educational qualification and their preference towards automated approach.

7.4. Organization size

The size of the organization is considered as a vital factor for influencing the entrepreneurs' perception towards customer service automation. The small and medium level entrepreneurs differ in their requirements, expectations, preferences and perceptions based on their level of investment. Hence the study has included the size of the organization as an important variable in influencing the SME entrepreneurs' perception towards customer service automation and it is confined to small and medium size of the organization. The distribution of the respondents based on the organizational size is depicted in Table 7.

Table 7: Organization size wise distribution of the respondents and their preferred customer service approach

| Sl. No. | Organization size | Manual approach (195) | | Automated approach (188) | | Total (383) | |
|---------|-------------------|-----------------------|------|--------------------------|------|-------------|-------|
| | | F | % | F | % | F | % |
| 1. | Small | 136 | 35.5 | 156 | 40.7 | 292 | 76.2 |
| 2. | Medium | 59 | 15.4 | 32 | 8.4 | 91 | 23.8 |
| | Total | 195 | 50.9 | 188 | 49.1 | 383 | 100.0 |

Source: Primary Data F – Frequency, % - Percentage

Table 7 reveals that 76.2 Per cent of the total entrepreneurs belong to small level organization and the remaining 23.8 Per cent of the entrepreneurs belong to medium level organization. Small level organizations are found to prefer manual approach and automated approach in 35.5 Per cent and 40.7 Per cent respectively. Medium level organizations are found to prefer manual approach and automated approach in 15.4 Per cent and 8.4 Per cent respectively.

To test whether there is any association between the entrepreneurs' size of the organization and their preference towards customer service automation, Chi-square test is computed in order to test the null hypothesis H_0 . It is hypothesized that there is no significant association between the SME entrepreneurs' size of the organization and their preference towards automated approach. The result of the Chi-square test is given in Table 8.

Table 8: Chi - Square Test for Independency

| <i>Calculated value of χ^2</i> | <i>Table value of χ^2</i> | <i>Inference</i> |
|--|---|-------------------|
| 9.256* | 3.841 | H_0 is rejected |

d.f. = 1, $p < 0.05$, significant, d.f.: Degrees of freedom, * indicates that the χ^2 value is significant at 5 per cent level with 1 degrees of freedom.

The results of Table 8 reveal that the null hypothesis is rejected, since the calculated value is greater than the Chi square Table value. Therefore, there is statistically significant association between the SME entrepreneurs' organization size and their preference towards automated approach.

7.5. Location

Location is the place where the respondent is situated and it is having an influence in the exposure level of the entrepreneurs towards the customer service automation and its requirements. The study includes Rural, suburban and urban areas of the entrepreneurs' location and distribution of the respondents based on their location is exhibited in Table 9.

Table 9: Location wise distribution of the respondents and their preferred customer service approach

| Sl.No. | Location | Manual approach (195) | | Automated approach (188) | | Total (383) | |
|--------|----------|-----------------------|------|--------------------------|------|-------------|-------|
| | | F | % | F | % | F | % |
| 1. | Rural | 56 | 14.6 | 40 | 10.4 | 96 | 25.1 |
| 2. | Suburban | 28 | 7.3 | 48 | 12.5 | 76 | 19.9 |
| 3. | Urban | 111 | 29.0 | 100 | 26.1 | 211 | 55.1 |
| | Total | 195 | 50.9 | 188 | 49.1 | 383 | 100.0 |

Source: Primary data, F – Frequency, % - Percentage

Table 9 reveals that, 55.1 Per cent of the SME entrepreneurs are located in urban area and it is followed by 25.1 Per cent of the entrepreneurs, who are located in rural area. In the manual approach preferred group, 29.0 Per cent of the entrepreneurs are located in urban area and 14.6 Per cent of them are located in rural area. In the case of automated approach preferred group, 26.1 Per cent of them belong to urban area and 12.5 Per cent are located in suburban. To test whether there is any association between the SME entrepreneurs' location and their preference towards customer service automation, Chi-square test is computed in order to test the null hypothesis H_0 . It is hypothesized that there is no significant association between the SME entrepreneurs' location and their preference towards automated approach. The result of the Chi-square test is given in Table 10.

Table 10: Chi - Square Test for Independency

| Calculated value of χ^2 | Table value of χ^2 | Inference |
|------------------------------|-------------------------|-------------------|
| 11.347* | 5.991 | H_0 is rejected |

d.f. =2 p < 0.05, significant

d.f.: Degrees of freedom, * indicates that the χ^2 value is significant at 5 per cent level with 2 degrees of freedom.

The results of Table 10 reveal that the null hypothesis is rejected, since the calculated value is greater than Table value. Therefore, there exist statistically significant association between the SME entrepreneurs' location and their preference towards automated approach.

7.6. Benefits expected from customer service automation by the SME entrepreneurs and their organization size

Customer service automation is ultimately aimed to bring more benefits to the entrepreneurs. The significant benefits of customer service automation are identified as self- service technologies, integrated application of Customer data, increase the effectiveness of the sales training, enhancing trust through transparency, profitable customer retention, fulfilling On-demand services, empower service and support activities and finally, WEB based Customer interaction management. It is imperative to analyze the expectations of the SME entrepreneurs towards the benefits out of customer service automation and tabulation for this is presented in Table 11.

Table 11: SME entrepreneurs' expectation towards the benefits from customer service automation

| S.No | Benefits from Customer Service Automation | Yes | | No | |
|------|--|-----|------|-----|------|
| | | F | % | F | % |
| 1 | Self- service technologies | 281 | 73.4 | 102 | 26.6 |
| 2 | Integrated application of Customer data | 235 | 61.4 | 148 | 38.6 |
| 3 | Increase the effectiveness of the sales training | 193 | 50.4 | 190 | 49.6 |
| 4 | Enhancing trust through transparency | 129 | 33.7 | 254 | 66.3 |
| 5 | Profitable customer retention | 96 | 25.1 | 287 | 74.9 |

| | | | | | |
|---|--|-----|------|-----|------|
| 6 | Fulfilling On-demand services | 86 | 22.5 | 297 | 77.5 |
| 7 | Empower service and support activities and finally | 128 | 33.4 | 255 | 66.6 |
| 8 | WEB based Customer interaction management | 96 | 25.1 | 287 | 74.9 |

Source: Primary data, F – Frequency, % - Percentage

Table 11 reveals that out of the total SME entrepreneurs, 73.4 Per cent of them perceive that self- service technologies will be the top most benefit due to customer service automation and it is followed by the benefit integrated application of Customer data with 61.4 Per cent and then by increase the effectiveness of the sales training with 50.4 Per cent. Whereas, only 22.5 Per cent of the respondents perceive that fulfilling On-demand services will be a benefit.

8. Suggestions

1. The study has identified that majority of the respondents prefer the manual approach and automated approach to customer service is yet to be fully preferred by the SME entrepreneurs. Hence, training programs and campaigns are to be well designed for educating and convincing the SMEs for automation.
2. The respondents' age and educational qualifications are identified as associated influencing factors for their preference for customer service automation. Hence, adequate technical based training programmes could be provided to the young entrepreneurs to improve their interest for customer service automation.
3. The SMEs' location and their organization size are significantly associated with their preference for automation, special campaigns and training programmes could be exclusively planned by targeting the rural and small players in SME sector to motivate their transformation.
4. Self-service technologies and Integrated application of data are more expected by the respondents as the major benefits from customer service automation. Intensive training workshops could be extended for smoothening up the process of customer service automation.

9. Conclusion

The study is a humble effort taken by the researcher to analyze the customer service automation of the SME entrepreneurs in Tamilnadu and the findings have revealed that the need for customer service automation is realized by the respondents. Based on analyzing the demographic and organizational variables, it is found that rural and small players need a better focused training workshops for smooth implementation of customer service automation. Based on the research findings, it is obvious that the vision of customer service automation is going to be achieved very soon in India.

References

- [1] Nicastro, S, "Experience will be Everything in 2019—Starting with your Customer", IDC, 2019.
- [2] Laurent, P., Chollet, T., & Herzberg, E, "Intelligent Automation Entering the Business World", Deloitte, 2018.
- [3] Connatty, S, "Consumers are embracing AI and will reward organizations that offer more humanlike AI experiences", Capgemini, 2018.
- [4] Willcocks. P. L, "Service Automation - Robots and The Future of Work", Ashford, UK: Steve Brookes Publishing, 2016.
- [5] Middelburg. J.-W, "Service Automation Framework" Zaltbommel, The Netherlands: VanHaren Publishing, 2017.

Regular and Totally Regular Fuzzy Graphs

Mr. R. Viswalingam
Assistant Professor
Department of Mathematics
St. Anne's College of Engineering and Technology, Panruti

Mr. V. Prakash
Associate Professor
Department of Mathematics
St. Anne's College of Engineering and Technology, Panruti

Abstract

In this paper, neighbourly irregular fuzzy graphs, neighbourly total irregular fuzzy graphs, highly irregular fuzzy graphs and highly total irregular fuzzy graphs are introduced. A necessary and sufficient condition under which neighbourly irregular and highly irregular fuzzy graphs are equivalent is provided. Some results on neighbourly irregular fuzzy graphs are established

Keywords: degree of fuzzy graph, regular fuzzy graph, irregular fuzzy graph, highly irregular fuzzy graph

1. INTRODUCTION

Rosenfeld[7] considered fuzzy relations on fuzzy sets and developed the theory of fuzzy graphs in 1975. Nagoor Gani and Radha[6] introduced regular fuzzy graphs, total degree and totally regular fuzzy graphs. Gnaana Bhargava and Ayyaswamy[4] suggested a method to construct a neighbourly irregular graph of order n and also discussed some properties on neighbourly irregular graph. Yousef Alavi, et al., [9] introduced k -path irregular graph and studied some properties on k -path irregular graphs. In this paper, neighbourly irregular fuzzy graphs, neighbourly total irregular fuzzy graphs, highly irregular fuzzy graphs and highly total irregular fuzzy graphs are introduced. A comparative study between neighbourly irregular and highly irregular fuzzy graphs is made. Also some results on neighbourly irregular fuzzy graphs are studied. Throughout this paper only undirected fuzzy graphs are considered. We review briefly some definitions which can be found in [1] – [9].

DEFINITION: 1

Let $G = (\sigma, \mu)$ be a fuzzy graph on $G^* : (V, E)$. If $d_G(v) = k$ for all $v \in V$, (i.e) if each vertex has same degree k , then G is said to be a regular fuzzy graph of degree k or a k -regular fuzzy graph. This is analogous to the definition of regular graphs in crisp graph theory.

EXAMPLE: 1 Any connected fuzzy graph with two vertices is regular.

Remark: G is a k -regular fuzzy graph iff $\sum_{v \in V} d_G(v) = \Delta = k$.

Remark: In crisp graph theory, any complete graph is regular. But this result does not carry over to the fuzzy case.

A complete fuzzy graph need not be regular.

EXAMPLE: 2

Consider $G^* : (V, E)$ where $V = \{u, v, w\}$ and $E = \{uv, vw, wu\}$.

Define $G : (\sigma, \mu)$ by $\sigma(u) = 0.5$, $\sigma(v) = 0.7$, $\sigma(w) = 0.6$ and $\mu(uv) = 0.5$,

$\mu(vw) = 0.6$, $\mu(wu) = 0.5$. Then G is a complete fuzzy graph.

But $d(u) = \mu(uv) + \mu(wu) = 0.5 + 0.5 = 1$ and $d(v) = d(w) = 1.1$. So G is not regular.

DEFINITION: 2

Let $G: (\sigma, \mu)$ be a fuzzy graph in G^* . The total degree of a vertex

$u \in V$ is defined by

$$td_G(u) = \sum_{u \neq v} \mu(uv) + \sigma(u) = \sum_{uv \in E} \mu(uv) + \sigma(u) = d_G(u) + \sigma(u).$$

If each vertex of G has the same total degree k , then G is said to be a totally regular fuzzy graph of total degree k or a k – totally regular fuzzy graph.

EXAMPLE: 3

Consider $G^* : (V, E)$ where $V = \{v_1, v_2, v_3, v_4\}$ and $E = \{v_1v_2, v_2v_3, v_3v_4, v_4v_1\}$. Define $G : (\sigma, \mu)$ by $\sigma(v_1) = 0.5$, $\sigma(v_2) = 0.4$, $\sigma(v_3) = 0.7$, $\sigma(v_4) = 0.5$ and $\mu(v_1v_2) = 0.2$, $\mu(v_2v_3) = 0.4$, $\mu(v_3v_4) = 0.2$, $\mu(v_4v_1) = 0.4$. Then $d(v_i) = 0.6$ for all $i = 1, 2, 3, 4$. So G is a regular fuzzy graph. But $td(v_1) = 1.1 \neq 1 = td(v_2)$.

So G is not totally regular.

EXAMPLE: 4 Consider $G^* : (V, E)$ where $V = \{v_1, v_2, v_3\}$ and $E = \{v_1v_2, v_1v_3\}$.

Define $G : (\sigma, \mu)$ by $\sigma(v_1) = 0.4$, $\sigma(v_2) = 0.8$, $\sigma(v_3) = 0.7$, $\mu(v_1v_2) = 0.3$, $\mu(v_1v_3) = 0.4$. Then $td(v_i) = 1.1$ for all $i = 1, 2, 3$. So G is a totally regular fuzzy graph. But $d(v_1) = 0.7 \neq 0.3 = d(v_2)$. So G is not regular.

EXAMPLE: 5

Consider $G^* : (V, E)$ where $V = \{v_1, v_2, v_3\}$ and

$E = \{v_1v_2, v_2v_3, v_3v_1\}$. Define $G : (\sigma, \mu)$ by $\sigma(v_1) = \sigma(v_2) = \sigma(v_3) = 0.4$, and $\mu(v_1v_2) = 0.3$, $\mu(v_2v_3) = \mu(v_3v_1) = 0.3$.

Then $d(v_i) = 0.6$ for all $i = 1, 2, 3$. So G is a regular fuzzy graph. Also $td(v_i) = 1$ for all $i = 1, 2, 3$. Hence G is also a totally regular fuzzy graph.

EXAMPLE: 6

Consider $G^* : (V, E)$ where $V = \{v_1, v_2, v_3\}$ and $E = \{v_1v_2, v_1v_3\}$.

Define $G : (\sigma, \mu)$ by $\sigma(v_1) = 0.3$, $\sigma(v_2) = \sigma(v_3) = 0.4$, and $\mu(v_1v_2) = 0.1$,

$\mu(v_1v_3) = 0.2$. Then $d(v_1) = 0.3 \neq 0.1 = d(v_2)$. So G is not a regular fuzzy graph. Also $td(v_1) = 0.6 \neq 0.5 = td(v_2)$. So

G is not totally regular.

Remark:

From the above examples, it is clear that in general there does not exist any relationship between regular fuzzy graphs and totally regular fuzzy graphs. However, a necessary and sufficient condition under which these two types of fuzzy graphs are equivalent is provided in the following theorem.

THEOREM: 1

Let $G : (\sigma, \mu)$ be a fuzzy graph on $G^* : (V, E)$. Then σ is a constant function if and only if the following are equivalent: 1. G is a regular fuzzy graph. 2. G is a totally regular fuzzy graph.

Proof: Suppose that σ is a constant function. **To Prove:** (1) and (2) are equivalent

Let $\sigma(u) = c$, a constant, for all $u \in V$.

Assume that G is a k_1 – regular fuzzy graph.

Then $d(u) = k_1$, for all $u \in V$.

So $td(u) = d(u) + \sigma(u)$, for all $u \in V$.

$\Rightarrow td(u) = k_1 + c$, for all $u \in V$.

Hence G is a totally regular fuzzy graph. Thus (1) \Rightarrow (2) is proved.

Now, suppose that G is a k_2 – totally regular fuzzy graph.

Then $td(u) = k_2$, for all $u \in V$.

$\Rightarrow d(u) + \sigma(u) = k_2$, for all $u \in V$.

$\Rightarrow d(u) + c = k_2$, for all $u \in V$.

$\Rightarrow d(u) = k_2 - c$, for all $u \in V$.

So G is a regular fuzzy graph. Thus (2) \Rightarrow (1) is proved.

Hence (1) and (2) are equivalent.

Conversely, assume that (1) and (2) are equivalent.

(i.e) G is regular if and only if G is totally regular.

To prove: σ is a constant function.

Suppose σ is not a constant function. Then $\sigma(u) \neq \sigma(w)$ for at least one pair of vertices $u, w \in V$.

Let G be a k – regular fuzzy graph. Then $d(u) = d(w) = k$

So $td(u) = d(u) + \sigma(u) = k + \sigma(u)$ and $td(w) = d(w) + \sigma(w) = k + \sigma(w)$

Since $\sigma(u) \neq \sigma(w)$, we have $td(u) \neq td(w)$.

So G is not totally regular which is a contradiction to our assumption.

Now Let G be a totally regular fuzzy graph.

Then $td(u) = td(w) \Rightarrow d(u) + \sigma(u) = d(w) + \sigma(w)$

$$\Rightarrow d(u) - d(w) = \sigma(w) - \sigma(u) \neq 0$$

$$\Rightarrow d(u) \neq d(w).$$

So G is not regular which is a contradiction to our assumption.

Hence σ is a constant function.

THEOREM: 2

If a fuzzy graph G is both regular and totally regular, then σ is a constant function.

Proof: Let G be a k_1 – regular and k_2 – totally regular fuzzy graph.

So $d(u) = k_1$, for all $u \in V$ and $td(u) = k_2$, for all $u \in V$.

Now $td(u) = k_2$, for all $u \in V$

$$\Rightarrow d(u) + \sigma(u) = k_2, \quad \text{for all } u \in V$$

$$\Rightarrow k_1 + \sigma(u) = k_2, \quad \text{for all } u \in V$$

$$\Rightarrow \sigma(u) = k_2 - k_1, \text{ for all } u \in V.$$

Hence σ is a constant function.

Remark: Converse of theorem 5.12 need not be true.

For example, consider $G^* : (V, E)$ where $V = \{v_1, v_2, v_3\}$ and

$E = \{v_1v_2, v_1v_3\}$. Define $G : (\sigma, \mu)$ by $\sigma(v_i) = 0.5, i = 1, 2, 3$ and

$\mu(v_1v_2) = 0.1, \mu(v_1v_3) = 0.2$. Then σ is a constant function. But

$d(v_2) = 0.1 \neq 0.2 = d(v_3)$. Also $td(v_2) = 0.6 \neq 0.7 = td(v_3)$. So G is neither regular nor totally regular.

THEOREM: 3

Let $G : (\sigma, \mu)$ be a fuzzy graph where $G^* : (V, E)$ is an odd cycle. Then G is regular iff μ is a constant function.

Proof: Assume that μ is a constant function.

To Prove: G is regular.

If μ is a constant function, say $\mu(uv) = c$, for all $uv \in E$, then $d(v) = 2c$, for every $v \in V$.

So G is regular.

Conversely, Assume that G is regular.

To prove: μ is a constant function.

Suppose that G is a k -regular fuzzy graph. Let $e_1, e_2, e_3, \dots, e_{2n+1}$ be the edges of G^* in that order.

Let $\mu(e_1) = k_1$. Since G is k -regular,

$$\mu(e_2) = k - k_1$$

$$\mu(e_3) = k - (k - k_1) = k_1$$

$$\mu(e_4) = k - k_1$$

and so on.

$$\text{Therefore } \mu(e_i) = \begin{cases} k_1, & \text{if } i \text{ is odd} \\ k - k_1, & \text{if } i \text{ is even} \end{cases}$$

$$\text{Hence } \mu(e_1) = \mu(e_{2n+1}) = k_1.$$

So if e_1 and e_{2n+1} incident at a vertex u , then $d(u) = k$.

$$\text{So } d(e_1) + d(e_{2n+1}) = k$$

$$\Rightarrow k_1 + k_1 = k$$

$$\Rightarrow 2k_1 = k$$

$$\Rightarrow k_1 = k/2$$

Hence $k - k_1 = k/2$. So $\mu(e_i) = k/2$, for all i . Hence μ is a constant function.

Remark: The above theorem does not hold for totally regular fuzzy graphs.

For example, Consider the cycle $G^* : (V, E)$ where $V = \{v_1, v_2, v_3\}$ and

$E = \{v_1v_2, v_2v_3, v_3v_1\}$. Define $G : (\sigma, \mu)$ by $\sigma(v_1) = 0.5$, $\sigma(v_2) = 0.6$,

$\sigma(v_3) = 0.4$, and $\mu(v_1v_2) = 0.1$, $\mu(v_2v_3) = 0.2$, $\mu(v_3v_1) = 0.3$. Then

$d(v_i) = 0.9$ for all $i=1, 2, 3$.

Hence G is a totally regular fuzzy graph. But μ is not a constant function.

THEOREM: 4 Let $G: (\sigma, \mu)$ be a fuzzy graph where G^* is an even cycle. Then G is regular iff either μ is a constant function or alternate edges have same membership values.

Proof:

Given: Let $G: (\sigma, \mu)$ be a fuzzy graph where G^* is an even cycle. If either μ is constant function or alternate edges have same membership values, then G is regular fuzzy graph.

Conversely, Assume that G graph is regular.

To prove: μ is a constant function

(i.e) Alternate edges have same membership values.

Suppose G graph is a k – regular fuzzy graph. Let e_1, e_2, \dots, e_{2n} be the edges of the even cycle G^* in that order.

Proceeding as we know that,

Let $G: (\sigma, \mu)$ be a fuzzy graph where $G^* : (V, E)$ is an odd cycle. Then G is regular iff μ is a constant function.

$$\mu(e_i) = \begin{cases} k_1, & \text{if } i \text{ is odd} \\ k - k_1, & \text{if } i \text{ is even} \end{cases}$$

If $k_1 = k - k_1$, then μ is a constant function.

If $k_1 \neq k - k_1$, then alternate edges have same membership values.

Remark: The above theorem does not hold for totally regular fuzzy graphs

For example, Consider $G^* : (V, E)$ where $V = \{v_1, v_2, v_3, v_4\}$ and

$E = \{v_1v_2, v_2v_3, v_3v_4, v_4v_1\}$ Define $G : (\sigma, \mu)$ by $\sigma(v_1) = 0.9, \sigma(v_2) = 0.7,$

$\sigma(v_3) = 0.5, \sigma(v_4) = 0.7$ and $\mu(v_1v_2) = 0.2, \mu(v_2v_3) = 0.5, \mu(v_3v_4) = 0.4,$

$\mu(v_4v_1) = 0.3$. Then $td(v_i) = 1.4$ for all $i = 1, 2, 3, 4$. So G is a totally regular. But in G , neither μ is a constant nor alternate edges have the same μ - values.

THEOREM: 5

The size of a k – regular fuzzy graph $G: (\sigma, \mu)$ on $G^* : (V, E)$ is $\frac{pk}{2}$ where $p = |V|$.

Proof: The size of G is $S(G) = \sum_{uv \in E} \mu(uv)$.

Since G is k – regular, $d_G(v) = k$, for all $v \in V$.

We have $\sum_{v \in V} d_G(v) = 2 \sum_{uv \in E} \mu(uv) = 2 S(G)$.

So $2S(G) = \sum_{v \in V} d_G(v) = \sum_{u \in V} k = pk$.

Hence $S(G) = \frac{pk}{2}$.

THEOREM: 6

If $G: (\sigma, \mu)$ is a r -totally regular fuzzy graph, then $2S(G) + O(G) = pr$ where $p = |V|$.

Proof: Since G is r -totally regular fuzzy graph.

$R = td(v) = d(v) + \sigma(v)$ for all $v \in V$.

So $\sum_{v \in V} r = \sum_{v \in V} d_G(v) + \sum_{v \in V} d_G \sigma(u)$

$\Rightarrow pr = 2S(G) + O(G)$.

THEOREM: 7

If G is a k -regular and a r -totally regular fuzzy graph, then

$O(G) = p(r-k)$.

Proof:

To prove : The size of a k -regular fuzzy graph $G: (\sigma, \mu)$ on $G^* : (V, E)$ is $\frac{pk}{2}$ where $p = |V|$. i.e The size of G is

$S(G) = \sum_{uv \in E} \mu(uv)$. Since G is k -regular, $d_G(v) = k$, for all $v \in V$.

We have $\sum_{v \in V} d_G(v) = 2 \sum_{uv \in E} \mu(uv) = 2 S(G)$. So $2S(G) = \sum_{v \in V} d_G(v) = \sum_{u \in V} k = pk$ Hence $S(G) = \frac{pk}{2}$.

Next we prove: If $G: (\sigma, \mu)$ is a r -totally regular fuzzy graph, then

$2S(G) + O(G) = pr$ where $p = |V|$.

i.e since G is r -totally regular fuzzy graph.

$R = td(v) = d(v) + \sigma(v)$ for all $v \in V$.

So $\sum_{v \in V} r = \sum_{v \in V} d_G(v) + \sum_{v \in V} d_G \sigma(u)$

$\Rightarrow pr = 2S(G) + O(G)$.

$$\text{So } O(G) = pr - 2S(G)$$

$$= pr - pk$$

$$O(G) = p(r - k).$$

Therefore If G is a k – regular fuzzy graph and r- totally regular fuzzy graph then order of G is $p(r - k)$.

CONCLUSION

The neighbourly irregular fuzzy graphs, neighbourly total irregular fuzzy graphs, highly irregular fuzzy graphs and highly total irregular fuzzy graphs were introduced. A necessary and sufficient condition under which neighbourly irregular and highly irregular fuzzy graphs are equivalent is provided with adequate graphs. Some results on neighbourly irregular fuzzy graphs were established with the use of fuzzy classifieds.

REFERENCES

- [1] R.Balakrishnan and A.Selvam, k-neighbourhood regular graphs, Proceedings of the National Seminar on Graph Theory, 1996, pp. 35-45.
- [2] Devadoss Acharya and E.Sampathkumar, Indian J. Pure Appl. Maths., 18(10)(1987), 882-90.
- [3] Frank Harary, Graph Theory, Narosa / Addison Wesley, Indian Student Edition, 1988.



St. Anne's College of Engineering and Technology,

Panruti Taluk, Cuddalore District,

Tamilnadu, India - 607 106.

Email : stannescet@gmail.com

Website : www.stannescet.ac.in